Copyright **© ECMS2012**

Printed: ISBN: 978-0-9564944-4-3 **European Council for Modelling**

CD: ISBN: 978-0-9564944-5-0 **and Simulation**

Coverpicture **© Koblenz-Touristik**

printed by **Digitaldruck Pirrot GmbH**

66125 Sbr.-Dudweiler, Germany

PROCEEDINGS
26th European Conference on Modelling and Simulation ECMS 2012

May 29th – June 1st, 2012
Koblenz, Germany

Edited by:
Klaus G. Troitzsch
Michael Möhring
Ulf Lotzmann

Organized by:
ECMS - European Council for Modelling and Simulation

Hosted by:
University of Koblenz-Landau

Sponsored by:
University of Koblenz-Landau

International Co-Sponsors:
IEEE - Institute of Electrical and Electronics Engineers
ASIM - German Speaking Simulation Society
EUROSIM - Federation of European Simulation Societies
PTSK - Polish Society of Computer Simulation
LSS - Latvian Simulation Society

ECMS 2012 ORGANIZATION

General Conference Chair

Klaus G. Troitzsch

University of Koblenz-Landau

Germany

Conference Co-Chair

Michael Möhring

University of Koblenz-Landau

Germany

Programme Chair

Klaus G. Troitzsch

University of Koblenz-Landau

Germany

Programme Co- Chair

Ulf Lotzmann

University of Koblenz-Landau

Germany

President of European Council for Modelling and Simulation

Andrzej Bargiela

The University of Nottingham

United Kingdom

Managing Editor

Martina-Maria Seidel

St. Ingbert

Germany

INTERNATIONAL PROGRAMME COMMITTEE

Agent-Based Simulation

Track Chair: **Michael Möhring**
University of Koblenz-Landau, Germany

Co-Chair: **Ulf Lotzmann**
University of Koblenz-Landau, Germany

Simulation in Industry, Business and Services

Track Chair: **Alessandra Orsoni**
University of Kingston, United Kingdom

Co-Chair: **Serhiy Kovela**
University of Kingston, United Kingdom

Simulation of Intelligent Systems

Track Chair: **Zuzana Oplatková**
Tomas Bata University of Zlín, Czech Republic

Co-Chair: **Roman Senkerik**
Tomas Bata University of Zlín, Czech Republic

Finance, Economics and Social Science

Track Chair: **Javier Otamendi**
University of Rey Juan Carlos Madrid, Spain

Co-Chair: **Barbara Dömötör**
Corvinius University of Budapest, Hungary

Simulation of Complex Systems & Methodologies

Track Chair: **Krzysztof Amborski**
Warsaw University of Technology, Poland

Co-Chair: **Jaroslav Sklenar**
University of Malta, Malta

Simulation, Experimental Science and Engineering

Track Chair: **Jan Amborski**
KMB - Continuing Airworthiness Management Organisation, Modlin Poland

Co-Chair: **Rafal Kajka**
Institute of Aviation, Poland

Simulation and Visualization for Training and Education

Track Chair: **Webjørn Rekdalsbakken**
Aalesund University College, Norway

Co-Chair: **Robin T. Bye**
Aalesund University College, Norway

Modelling, Simulation and Control of Technological Processes

Track Chair: **Jiři Vojtěšek**
Tomas Bata University in Zlín, Czech Republic

Co-Chair: **Petr Dostál**
Tomas Bata University in Zlín, Czech Republic

Co-Chair: **František Gazdoš**
Tomas Bata University in Zlín, Czech Republic

Electrical and Electromechanical Engineering

Track Chair: **Sergiu Ivanov**
University of Craiova, Romania

Co-Chair: **Francis Labrique**
Catholic University of Louvain, Belgium

Co-Chair: **Maria José Resende**
Technical University of Lisbon, Portugal

Discrete Event Modelling and Simulation in Logistics, Transport and Supply Chain Management

Track Chair: **Gaby Neumann**
Technical University of Applied Sciences Wildau, Germany

Co-Chair: **Edward J. Williams**
University of Michigan-Dearborn, USA

High Performance Modelling and Simulation

Track Chair: **Joanna Kolodziej**
University of Bielsko-Biala, Poland

Co-Chair: **Philip Moore**
Birmingham City University, United Kingdom

Co-Chair: **Hai V. Pham**
Ritsumeikan University, Kusatsu, Shiga, Japan

Co-Chair: **Horacio Gonzalez-Velez**
Robert Gordon University Aberdeen, United Kingdom

Simulation-Based Business Research

Track Chair: **Matthias Meyer**
Hamburg University of Technology, Germany

Co-Chair: **Iris Lorscheid**
Hamburg University of Technology, Germany

Policy Modelling

Track Chair: **Maria Wimmer**
University of Koblenz-Landau, Germany

Programme Chair: **Scott Moss**
University of Koblenz-Landau, Germany
Visiting Professor

Social Dynamics and Collective Behaviour

Track Chair: **Flaminio Squazzoni**
University of Brescia, Italy

IPC Members in Alphabetical Order

Petra Ahrweiler, University College Dublin, Ireland
Marco Aldinucci, University of Torino, Italy
Frédéric Amblard, University of Toulouse, France
Monika Bakošová, Slovak University of Technology in Bratislava, Slovakia
Frøy Birthe Bjørneset, Rolls-Royce, Norway
Anna Boczkowská, Warsaw University of Technology, Poland
Pawel Borowski, Warsaw University of Technology, Poland
Fabian Böttinger, Fraunhofer Institute Stuttgart, Germany
Giangiacomo Bravo, University of Torino, Italy
Thomas Brenner, Fraunhofer Institute Stuttgart, Germany
David Broster, IPTS Seville, Spain
Juan C. Burguillo-Rial, University of Vigo, Spain
Aleksander Byrski, AGH Univ. of Science and Technology, Poland
Piers Campbell, University of United Arab Emirate, Arab Emirate
Ester Camiña Centeno, Complutense University Madrid, Spain
Krzysztof Cetnarowicz, AGH Univ. of Science and Technology, Poland
Petr Chalupa, Tomas Bata University in Zlín, Czech Republic
Edmund Chattoe-Brown, University of Leicester, United Kingdom
Ron Cörvers, Maastricht University, The Netherlands
Péter Csóka, Corvinus University of Budapest, Hungary
Peter Davis, University of Auckland, New Zealand
Peter De Smedt, Research Center of the Flemish Government, Belgium
Bruno Dehez, Catholic University of Louvain, Belgium
Andrea Del Pizzo, University of Naples Federico II, Italy
Ángel Díaz Chao, Rey Juan Carlos University, Spain
Ciprian Dobre, Polithechnical University of Bucharest, Romania
Luis Miguel Doncel Pedrera, University Rey Juan Carlos Madrid, Spain
Bernabé Dorronsoro, University of Luxembourg, Luxembourg
František Dušek, University of Pardubice, Czech Republic
Andrzej Dzielinski, Warsaw University of Technology, Poland
Tomoya Enokido, Rissho University, Japan
Cain Evans, Birmingham City University, United Kingdom

Miroslav Fikar, Slovak University of Technology, Slovakia

Cesar Garcia-Diaz, University of the Andes, Colombia

Charlotte Gerritsen, VU University of Amsterdam, The Netherlands

Nigel Gilbert, University of Surrey, United Kingdom

Pilar Grau-Carles, University Rey Juan Carlos Madrid, Spain

Dag Sverre Grønmyr, Rolls-Royce, Norway

Antoni Guasch, University Politècnica of Catalunya, Spain

Peter Haddaway, United Nations University Macau, China

Jana Hájková, University of West Bohemia, Czech Republic

Dániel Havran, Corvinius University of Budapest, Hungary

Hans Petter Hildre, Aalesund University College, Norway

Daniel Honc, University of Pardubice, Czech Republic

Mark Hoogendorn, VU University of Amsterdam, The Netherlands

Martin Ihrig, University of Pennsylvania, United States

Teruaki Ito, University of Tokushima, Japan

Martin G. Jaatun, SINTEF, Norway

Mike Jackson, Birmingham City University, United Kingdom

Wander Jager, University of Groningen, The Netherlands

Marco Janssen, Arizona State University, United States

Nikolaos Karadimas, National Technical University, Greece

Eugène Kerckhoffs, Delft University of Technology, The Netherlands

Sashidharan Komandur, Aalesund University College, Norway

Petia Koprinkova-Hristova, Bulgarian Academy of Sciences, Bulgaria

Igor Kotenko, St. Petersburg Institute, Russia

Martina Kotyrba, University of Ostrava, Czech Republic

Marek Kubalcik, Tomas Bata University in Zlín, Czech Republic

Jun-Ichi Kushida, Ritsumeikan University, Japan

Kamila Kustroń, Warsaw University of Technology, Poland

Thomas Lancaster, Birmingham City University, United Kingdom

Ramon Laplana, CEMAGREF, France

Roberto Legaspi, Osaka University, Japan

Ahmad Lotfi, Nottingham Trent University, United Kingdom

Thanasis Loukopoulos, Technological Edu. Institute (TEI) of Lamia, Greece

Dorin Lucache, Technical University of Lasi, Romania

Susan Lysecky, University of Arizona, United States
Radek Matoušek, Brno University of Technology, Czech Republic
Radek Matušů, Tomas Bata University in Zlín, Czech Republic
Nicolas Meseth, University of Osnabrück, Germany
Hermann Meuth, University of Applied Science, Germany
Dan Mihai, University of Craiova, Romania
Michaela Milano, University of Bologna, Italy
Marek Miller, Institute of Aviation, Poland
Yuri Misnikov, University of Leeds, United Kingdom
José Luis Montes, University of Rey Juan Carlos, Spain
Christian Müller, TH Wildau, Germany
Pavel Nahodil, Czech Technical University of Prague, Czech Republic
Edward Nawarecki, AGH Univ. of Science and Technology, Poland
Libero Nigro, University of Calabria, Italy
Jakub Novák, Tomas Bata University in Zlín, Czech Republic
Ilie Nuca, Technical University of Moldava, Republic of Moldava
Paul Ormerod, Volterra, United Kingdom
Ottar L. Osen, Aalesund University College, Norway
Teodor Pana, Technical University Cluj-Napoca, Romania
Johnatan E. Pecero, University of Luxembourg, Luxembourg
Arne Petermann, Berlin University for Professional Studies, Germany
Tuan Phung-Duc, Kyoto University, Japan
Jeremy Pitt, Imperial College, United Kingdom
Sabri Pllana, University of Vienna, Austria
Matthijs Pontier, VU University of Amsterdam, The Netherlands
Gary Polhill, James Hutton Institute Aberdeen Scotland, United Kingdom
Florian Pop, Polithechnical University of Bucharest, Romania
Ioan Popa, University of Craiova, Romania
Martyn Ratcliff, Birmingham City University, United Kingdom
Napoleon H. Reyes, Massey University, New Zealand
Young Ro, University of Michigan-Dearborn, United States
Boris Rohal-Ilkiv, Technical University of Bratislava, Slovakia
Toni Ruohonen, University of Jyväskylä, Finland
Hans Georg Schaathun, Aalesund University College, Norway

Sabrina Scherer, University of Koblenz-Landau, Germany
Thomas Schulze, Otto-von-Guericke University Magdeburg, Germany
Mamadou Seck, Delft University of Technology, The Netherlands
Abhijit Sengupta, UNILEVER, United Kingdom
Andrzej Sluzek, Nanyang Technological University, Singapore
Jan Spitzner, C21 Consulting GmbH, Germany
Arne Styve, Offsim, Norway
Claudiu Valentin Suciu, Fukuoka Inst. of Technology, Japan
Loránd Szabó, Technical University Cluj-Napoca, Romania
Károly Takács, Corvinius University of Budapest, Hungary
Elena Tanfani, University of Genova, Italy
Alexandru Adrian Tantar, University of Luxembourg, Luxembourg
Emilia Tantar, University of Luxembourg, Luxembourg
Tsubasa Tobiishi, Fukuoka Inst. of Technology, Japan
Duc-Khan Tran, Hanoi University of Science and Technology, Vietnam
Khang D. Tran, Hanoi University of Science and Technology, Vietnam
Peter Trkman, University of Ljubliana, Slovakia
Christopher Tubb, University of Wales Newport, United Kingdom
Anne van der Veen, University of Twente, The Netherlands
Alexey A. Voinov, University of Twente, The Netherlands
Rune Volden, Ulsteingroup, Norway
Eva Volna, University of Ostrava, Czech Republic
Stephan M. Wagner, ETH Zurich, Switzerland
Vishanth Weerakkody, Brunel University, United Kingdom
Bogdan Werth, Oliver Wyman, Germany
Roland Wertz, Fraunhofer IPA Stuttgart, Germany
Emilia Wolwiec, University of Lodz, Poland
Ivan Yatchev, Technical University Sofia, Bulgaria
Harald Yndestad, Aalesund University College, Norway
Jianwei Zhang, University of Hamburg, Germnay
Houxiang Zhang, Aalesund University College, Norway
Marcello Zottolo, Lee Memorial Health System, United States

PREFACE

The natural and the artificial environment of mankind is of enormous complexity, and our means of understanding this complex environment are restricted unless we make use of simplified (but not oversimplified) dynamical models with the help of which we can explicate and communicate what we have understood in order to discuss among ourselves how to re-shape reality according to what our simulation models make us believe to be possible. Being both a science and an art, modelling and simulation is still one of the core tools of extended thought experiments, and its use is still spreading into new application areas, particularly as the increasing availability of massive computational resources allows for simulating more and more complex target systems.

In the early summer of 2012, the 26th European Conference on Modelling and Simulation (ECMS) once again brings together the best experts and scientists in the field to present their ideas and research, and to discuss new challenges and directions for the field.

The 2012 edition of ECMS includes three new tracks, namely Simulation-Based Business Research, Policy Modelling and Social Dynamics and Collective Behaviour, and extended the classical Finance and Economics track with Social Science. It attracted more than 110 papers, 125 participants from 21 countries and backgrounds ranging from electrical engineering to sociology.

This book was inspired by the event, and it was prepared to compile the most recent concepts, advances, challenges and ideas associated with modelling and computer simulation. It contains all papers carefully selected from the large number of submissions by the programme committee for presentation during the conference and is organised according to the still growing number tracks which shaped the event. The book is complemented by two invited pieces from other experts that discussed an emerging approach to modelling and a specialised application.

We hope these proceedings will serve as a reference to researchers and practitioners in the ever growing field as well as an inspiration to newcomers to the area of modelling and computer simulation. The editors are honoured and proud to present you with this carefully compiled selection of topics and publications in the field.

Klaus G. Troitzsch	Michael Möhring	Ulf Lotzmann
General Conference Chair and Programme Chair	Conference Co-Chair	Programme Co- Chair

TABLE OF CONTENTS

Plenary Talks

Agent-Based Simulation

Simulation of Complex Systems and Methodologies

Electrical and Electromechanical Engineering

Simulation, Experimental Science and Engineering

Simulation and Visualization for Training and Education

Finance, Economics and Social Science

Simulation in Industry, Business and Services

Simulation of Intelligent Systems

Modelling, Simulation and Control of Technological Processes

High Performance Modelling and Simulation

Discrete Event Modelling and Simulation in Logistics, Transport and Supply Chain Management

Policy Modelling

Social Dynamics and Collective Behaviour

ECMS 2012
SCIENTIFIC PROGRAM

Plenary Talks

What's the good of agent-based modelling?

Nigel Gilbert

University of Surrey
Center for Research in Social Simulation

Agent-based modelling (ABM) has grown enormously in popularity over the last decade. It seems to be applied nowadays to every topic one can imagine. In this talk, I shall first present what I see as the essence of ABM for those not familiar with this approach, and then review a number of examples, taken from the disciplines of computer science, ecology, sociology, economics, geography, and business, both to show how ABM can be applied and to identify appropriate and inappropriate uses.

On the Utility of Simulation in Autonomous and Assisted Driving

Dieter Zoebel

University of Koblenz-Landau
Research Group Real-Time Systems (Institute for Software Technology)

Developments in the scope of autonomous and assisted driving are innovative, safety critical and costly. Particularly, universitary institutes are dependent on simulations to get the foot into the door of vehicular research, in our case with special emphasis on commercial vehicles. To be a successful player in this application scope we designed a layered software architecture to support the seamless development from simulated to physical applications.

Agent-Based Simulation

VARIANCE IN SYSTEM DYNAMICS AND AGENT BASED MODELLING USING THE SIR MODEL OF INFECTIOUS DISEASE

Aslam Ahmed, Julie Greensmith, Uwe Aickelin
Intelligent Modelling and Analysis Research Group
University of Nottingham
Nottingham, NG8 1BB, United Kingdom
E-mail:{awa, jqg, uxa} @cs.nott.ac.uk

KEYWORDS
System Dynamics, Agent Based Modelling, SIR, Uncertainty, Variance.

ABSTRACT

Classical deterministic simulations of epidemiological processes, such as those based on System Dynamics, produce a single result based on a fixed set of input parameters with no variance between simulations. Input parameters are subsequently modified on these simulations using Monte-Carlo methods, to understand how changes in the input parameters affect the spread of results for the simulation. Agent Based simulations are able to produce different output results on each run based on knowledge of the local interactions of the underlying agents and without making any changes to the input parameters. In this paper we compare the influence and effect of variation within these two distinct simulation paradigms and show that the Agent Based simulation of the epidemiological SIR (Susceptible, Infectious, and Recovered) model is more effective at capturing the natural variation within SIR compared to an equivalent model using System Dynamics with Monte-Carlo simulation. To demonstrate this effect, the SIR model is implemented using both System Dynamics (with Monte-Carlo simulation) and Agent Based Modelling based on previously published empirical data.

INTRODUCTION

Models of infectious diseases can be useful for understanding the spread of infection of the diseases within a population over time. However, within a given population, diseases can spread at different rates over time due to the natural random nature of contact between individuals in the population. If a simulation can incorporate this kind variation, the extra information can be used to determine the spread of uptake of infection in worst case and best case scenarios for a given population.

Currently, for classical System Dynamics (SD) models (Forrester, 1961) based on ordinary differential equations, the random contact between individuals is aggregated to fixed rates of contact and the output has no variation. Assuming the same parameter values are supplied to the System Dynamics simulation, on each run, the same results are produced. Subsequently, in order to understand the spread of output values, the simulations are repeated with different input parameters by applying Monte Carlo simulation (Stan, 1987). In this approach, multiple experiments are performed and the parameter values taken from a probability density function representing the input parameter range. In Agent Based Models (ABM), uncertainty or variance can be inherent within the model so that the simulations from the models produce non-deterministic results directly without input parameter variation.

In this paper, the two approaches are examined by generating an SD model with Monte-Carlo and an ABM and comparing the spread of output values against published data for a defined population. Simulations from modelling paradigms such as Agent Based Modelling, which can include variance, help to bridge the gap between raw data and simulation data and also help answer the issue of validation in simulation - assessing the degree to which a model is an accurate representation of the real world (Oberkampf et al., 2002). Both System Dynamics and Agent Based Models are able to capture overall variance but unlike simulations from SD models, a single simulation run from an Agent Based Model is able to capture the 'typical' outcome from a single simulation experiment.

Unlike System Dynamics which uses a top-down approach to model the system as a whole, in Agent Based simulations, the system is 'brought about' by carrying out the lower level interactions between the agents. For this reason, ABM is beginning to be used in a range of fields including biological simulations and social sciences representing people as interacting agents in environments (Zellner, 2008)(Siebers et al., 2010).

VARIANCE IN EPIDEMIOLOGICAL SYSTEMS

Early Mathematical models for epidemiology such as those by Bernoulli in 1766 (Dietz and Heesterbeek, 2002) were useful deterministic models that could be used to determine 'what-if' scenarios such as the change in life expectancy following the introduction of inoculation against smallpox. Further models followed including those for SIR proposed by Kermack and McKendrick which were stochastic (McKendrick, 1926) and deterministic (Kermack and McKendrick, 1927).

Early opinions for mathematical modelling of epidemic models were that deterministic models gave an

Proceedings 26th European Conference on Modelling and Simulation ©ECMS Klaus G. Troitzsch, Michael Möhring, Ulf Lotzmann (Editors)
ISBN: 978-0-9564944-4-3 / ISBN: 978-0-9564944-5-0 (CD)

average outcome of a corresponding stochastic model and that for large populations, it was the average that mattered. A more recent understanding is that both deterministic and stochastic models have their strengths and weaknesses.

Traditional deterministic models of epidemiology assume heterogeneity of mixing. It is assumed that individuals have the same rate of contact with others and recovery from infection takes the same time. In reality, contact rate is affected by transport networks and individual lifestyle and recovery from infection can depend on age and other factors so these are not take into account. Sometimes this data is difficult to ascertain but in smaller population sizes it may be possible to obtain this information and build a model that is a closer representation to reality.

One of the underlying reasons why epidemiological systems exhibit variation is due to the complex way that the individuals in a population have contact with each other. Infection levels can coincide with transport networks such as road and rail so individuals in areas with high levels of such transport links are more susceptible to catching infection. At a much lower level, random variation exists due to Brownian motion of the interaction between molecules (Gaspard, 2005).

AGENT BASED MODELLING AND SYSTEM DYNAMICS

Agent Based Modelling (Macal and North, 2008) is a more recent addition to the set of tools for simulations compared to classical mathematical models. ABM uses agents, which are discrete autonomous entities containing characteristics and rules which govern their behaviour and interaction with other agents. Agents can be programmed to adapt and learn from previous interactions. An ABM can have closer affinity with the system being modelled as the notable entities and their significant properties can be captured making the simulation more intuitive and closely resembling the real system. In System Dynamics (Sterman, 2004), complex non-linear systems are represented using feedback loops and delays by creating stocks which represent quantities over time, flows which measure the transition from stock to stock and factors which influence the values of the flows.

VARIANCE EXPERIMENT FOR ABM AND SD

In order to show how the variance differs in ABM and SD, two models are built. One using SD with Monte Carlo simulation (to drive variation) and one using ABM which has variance built into the design. A basic Susceptible-Infected-Recovered (SIR) model, originally proposed by Kermack and McKendrick is used for both types of modelling paradigms. The SIR model is a simple but effective model of infection that has been used to represent a wide range of epidemics including influenza, tuberculosis, chicken pox, rubella and measles (Enns, 2011).

In the basic SIR model, each person is in a state of:

- Susceptible
- Infected
- Recovered

A person who is susceptible has never been infected. As soon as they are infected by way of contact with an infected individual, they are set to the Infected state. After a period of time, during which the immune system is able to recover from the infection, an individual moves from the Infected to the Recovered state. Once in a Recovered state, the individual is immune to further infections.

SIR Data

The experimental data used in this paper is obtained from the Russian Influenza epidemic in Sweden between 1889 and 1890 (Skog, 2008). After the outbreak of Russian Flu in Sweden, questionnaires were sent to Swedish physicians to determine ascertain information about the flu in their region. Answers were received by 398 physicians for over 32,600 individuals. The information returned from the postcard included the following for each district:

- Date of first influenza case detected
- Peak of epidemic
- Percentage affected

The information returned from the questionnaire included the following for each household:

- Number of infected persons
- Gender
- Age

Some of the important findings are used as the parameter values. This included the duration of the disease which was found to be between 2.3 and 9.4 days and affected 61% of the population. For the purpose of the experiment, a single area, Österlövsta, was chosen for analysis. This area has a profile which shows a typical raise and decline of infection population counts over a period of 15 weeks. The complete data for Sweden can also be used but this will extend the ABM simulation time. The data obtained is shown in Figure 1.

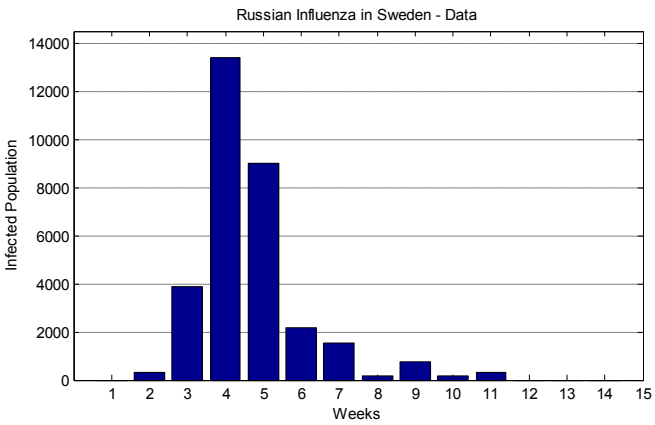

Figure 1: Russian Influenza in Sweden – Data

Data was taken from parishes surrounding one of the regions, Österlövsta, based on original work by Linroth over a period of 15 weeks. The total population size is 52910 and is used in the experiments. The other parameters for the models are based on the main findings of the study with the illness duration set to 4.2 and the probability of infection set to 0.065. This produced a best fit for the selected region of Österlövsta.

System Dynamics Model

The SD model is based on the original SIR model proposed by Kermack and Kendrick (Kermack and McKendrick, 1927). The model captures the spread of a contagious disease in a closed population over time. Three coupled, ordinary differential equations are used to represent the rate of change of the three different states of the people in a given population. The equations in the model are shown with the rate of change for each of the components of SIR.

$$\frac{dS}{dt} = -aSI$$
$$\frac{dI}{dt} = aSI - bI$$
$$\frac{dR}{dt} = bI \qquad (1)$$

The meaning of the parameters is shown in Table 1.

Table 1: Parameter Description for SIR Equations

Parameter	Description
a	Infection rate
b	Recovery rate
S	Susceptible population
I	Infected population
R	Recovered population

From the equations, a System Dynamics model is built in AnyLogic with stocks labelled as Susceptible, Infectious and Recovered and flows labelled as Infection Rate and Recovery Rate as shown in Figure 2.

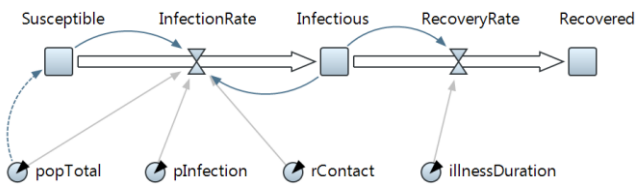

Figure 2: Stocks and Flows for the System Dynamics Model

The System Dynamics model produces the results shown in Figure 3.

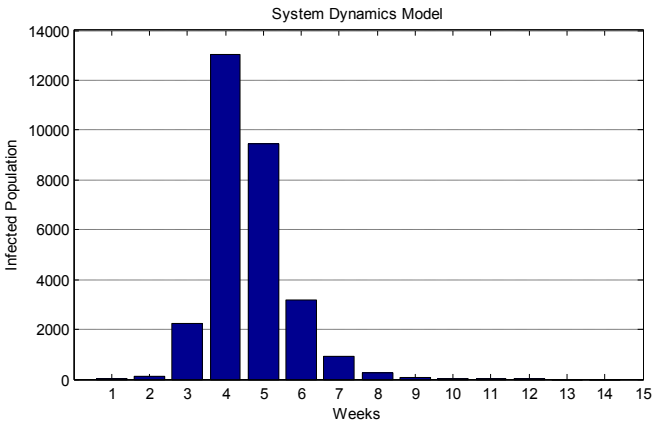

Figure 3: Results for the System Dynamics Model

Agent Based Model

In the ABM model, each person is in a state of **Susceptible**, **Infectious** or **Recovered**. A person in the **Susceptible** state moves to the **Infectious** state on receipt of a message representing the transfer of the infection from one person to another.

The infection is passed from one agent to another randomly connected agent in the network to another at a fixed contact rate and an individual recovers from the infection using a recovery rate. A state chart is used to model the state of the agent as shown in Figure 4.

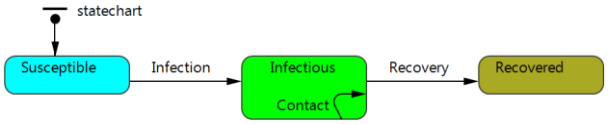

Figure 4: State Chart for the Agent Based Model

As per the System Dynamics model, a population count of 52910 is used in the model based on the Russian Influenza epidemic in Sweden. Individuals (agents) are connected using a small world (Watts and Strogatz, 1998) network topology. This is chosen as it represented a suitable route of transmission of the infection with many close connections in the network coupled with distant connections. The distant connections may be perceived as transportation links such as those by rail or sea. The small world network has been used in epidemiology (da Gama and Nunes 2006) with a number of studies using it as part of the models (Boots and Sasaki, 1999). A single randomly connected agent is chosen to kick-start the spread of infection.

A feasibility study is carried out for the modelling software and AnyLogic by XJ Technologies chosen as a suitable choice for modelling SIR in System Dynamics and Agent Based Modelling. One of the features of AnyLogic is that it has inherent support for combining different modelling paradigms into a single model.

In total, 100 experiments are carried out in AnyLogic. The experiments are carried out on a PC running Windows 7 with 3GB memory and an Intel Core 2 P8700 microprocessor. Output from the experiments is imported into MatLab to generate the box plots. The result for the ABM is shown in Figure 5.

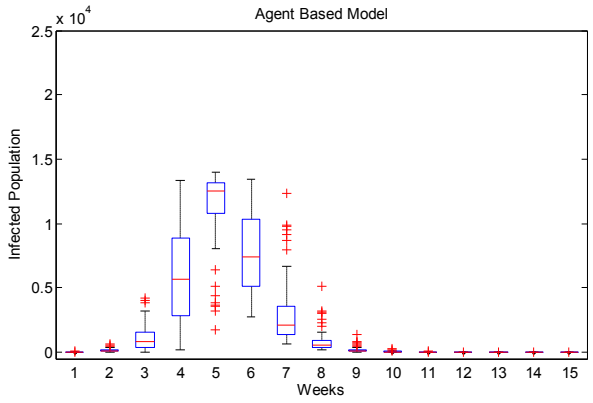

Figure 5: Agent Based Model Results

As per the SD model, the AB model is also validated against the data from the Influenza epidemic. The ABM simulation takes a total of 13 hours to complete.

SD Monte Carlo Simulation

The Monte Carlo simulations are used to determine how infected population counts change when the input parameters to the SD model are varied. Monte Carlo simulation uses repetitions of random sampling of the input parameters to determine the result. The randomness is applied 'outside' of the internal workings of the system as it is the parameters to the system being sampled.

One of the limitations of using the Monte Carlo method applied to simulations is the time taken to perform the simulation over a very large number of iterations. Therefore in areas such as Probability Sensitivity Analysis, the Monte Carlo solution is not always a viable method for complex models such as those for healthcare, involving thousands of patients (O'Hagan et al., 2007).

Monte Carlo simulations are carried out using the SD model to see the effect of varying each parameter and the effect of varying all parameters. In total, 100 simulations are carried out for each experiment to match the ABM. Parameter variation is carried out by randomly selecting values for each of the parameters taken from a standard normal distribution based on the mean value.

The following Monte Carlo simulations are carried out:

- Illness Duration variation
- Contact rate variation
- Infection rate variation
- Illness duration, contact and infection rate variation

Each SD experiment, comprising 100 simulations, takes a total of 9 seconds. The box plot for the SD Monte Carlo model with illness duration variation is shown in Figure 6. The infected population peaks at 21,442.

In the case where the contact rate is varied, the result is shown in Figure 7. In this case, the inter-quartile range is larger than the simulation where the illness rate is varied and clearly visible in weeks 3 to 7 inclusive.

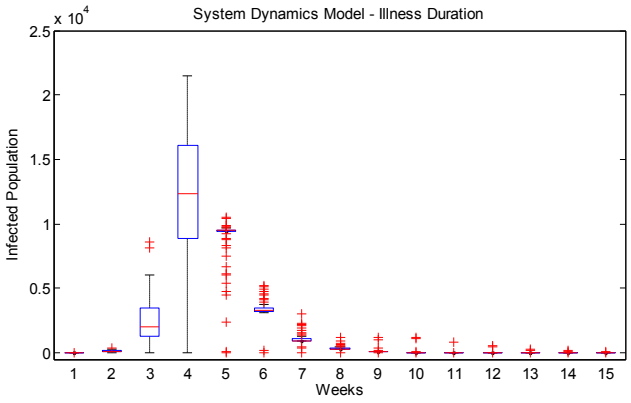

Figure 6: System Dynamics Model - Illness Duration Variation

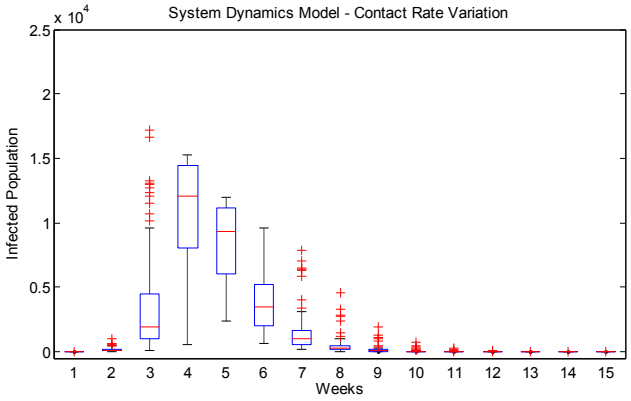

Figure 7: System Dynamics Model - Contact Rate Variation

The SD Monte Carlo model where the infection rate is varied is shown in the box plot in Figure 8.

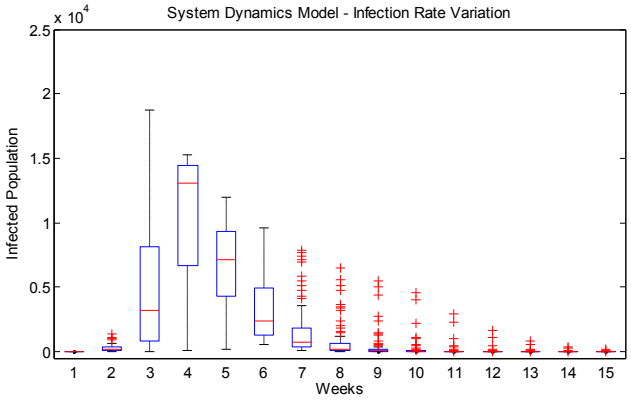

Figure 8: System Dynamics Model - Infection Rate Variation

The box plot for the experiment where multiple parameters are varied is shown in Figure 9. The results show that with multiple parameters being varied, the infected population peaks at 24,725 which is a substantial increase compared with the SD version without Monte Carlo simulation which peaks at 13,025. Therefore, compared with experiments where variations of contact rate and infection rate are altered to introduce randomness, the variation of multiple parameters has the undesired effect of scaling up the infected population counts.

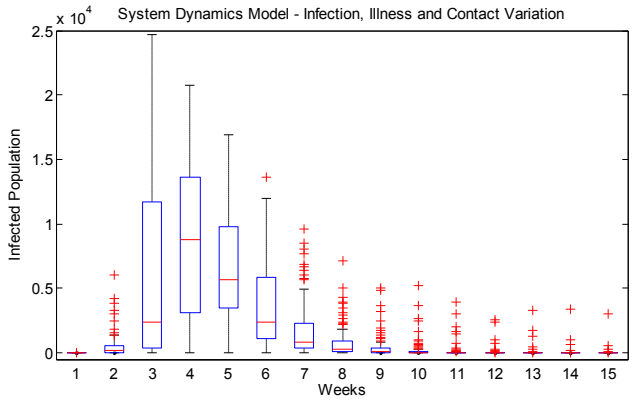

Figure 9: System Dynamics Model - Infection, Illness and Contact Rate Variation

Validation against Influenza data

The Wilcoxon signed rank test (Wilcoxon, 1945) is used to compare the simulation results against the Influenza data. This is a non-parametric paired test that tests the null hypothesis that the means for the two data sets are the same versus the means from the two data sets differ. The SD result without any Monte Carlo simulation is compared directly against the Influenza data. For ABM and SD with Monte Carlo, the median values for each experiment are obtained for each week.

The Wilcoxon rank sum test for the experiment is calculated using MatLab version R2010b. The results are summarized in Table 2. A 5% significance level is used.

Table 2: Wilcoxon Signed Rank Test for experiments

Simulation	p Value
SD	0.3013
ABM	0.4648
SD – Vary illness duration	0.2661
SD – Vary contact rate	0.2036
SD – Vary infection rate	0.0244
SD – Vary illness, contact, infection rate	0.0269

The h value for the tests is 0 and the p values of 0.0244 and 0.0269 indicate that the null hypothesis can be rejected for the experiment where infection rate is varied and for the version in which combined parameters are varied.

The Wilcoxon rank sum tests show that the SD without Monte Carlo and the ABM has equivalent overall fits with the experimental data. The ABM experiment, with natural variation between different simulations, due to the contacts between the agents, is in agreement with the Influenza data.

When the Monte Carlo simulation is applied to the SD model, the overall results of the simulation are in agreement with the Influenza data for illness duration variation and contact variation but for variations of infection rate and the combined variation the results are no longer in agreement. The last, combined Monte Carlo simulation, has the overall effect of scaling up the median values overall.

Variance in ABM and SD Experiments

Variance for each of the Monte Carlo experiments are taken from the box plots and compared against the variance of the ABM experiment. In order to compare the variances, the inter-quartile range (IQR) is calculated using the MatLab for the ABM experiment and SD Monte Carlo experiments. The IQR for the ABM is shown in Figure 10. The ABM experiment produces a broadly symmetric result reflecting variations of the uptake of the infection which occurs at different times in the simulations but producing the same shape of the infection curve.

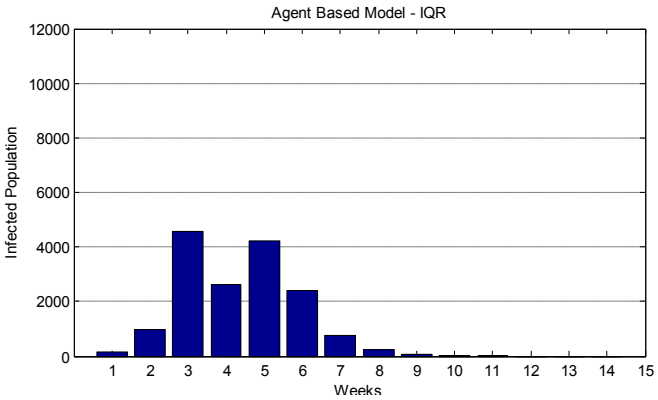

Figure 10: Agent Based Model - IQR

The IQR for the SD Monte Carlo simulation with variations in the illness duration is shown in Figure 11. The chart shows that there is less variation at the height or peak of infections. This is because the variation is created by the random connections that the individuals have in the simulations and critical parameters such as infection rate and illness are kept constant.

The results show that ABM is able to maintain stable peak infection values whilst at the same time exhibiting the type of randomness one may expect between different populations.

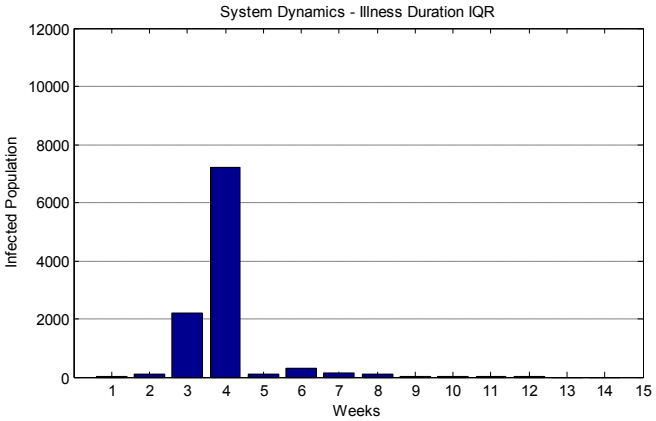

Figure 11: System Dynamics Model – Illness Duration IQR

The chart in Figure 12 shows the IQR where the Contact

Rate is varied in the SD Monte Carlo simulation.

The chart shows that the counts at the height of infection vary significantly between simulations compared to the ABM. In the ABM experiment, the contact rate is constant among the simulations and therefore in those simulations there is less difference of the counts at the height of infection.

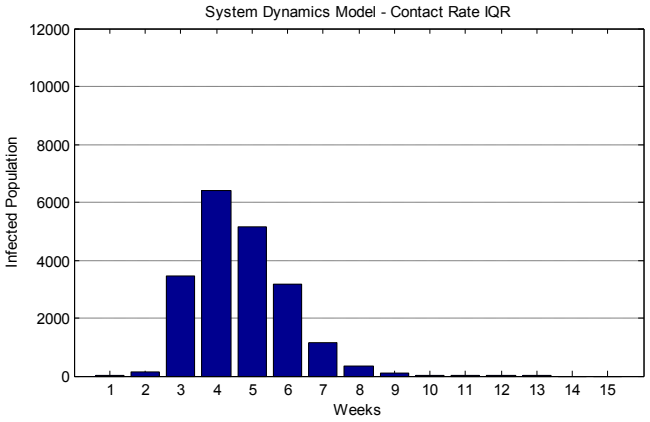

Figure 12: System Dynamics Model – Contact Rate IQR

The chart for the IQR for the infection rate variation for the SD Monte Carlo simulation is shown in Figure 13.

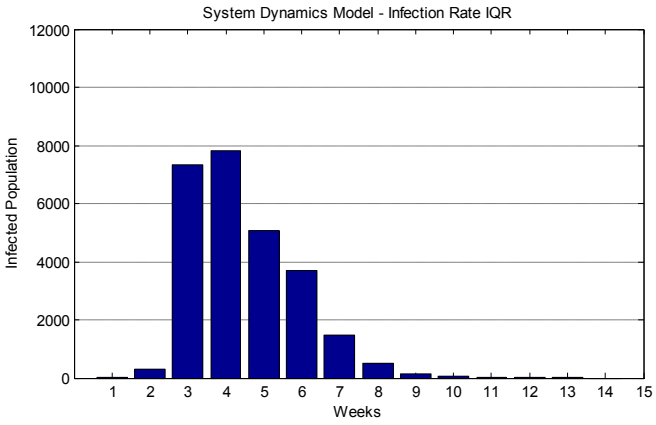

Figure 13: System Dynamics Model - Infection Rate IQR

The chart for the IQR in the case where multiple parameters are varied in the SD Monte Carlo simulation is shown in Figure 14.

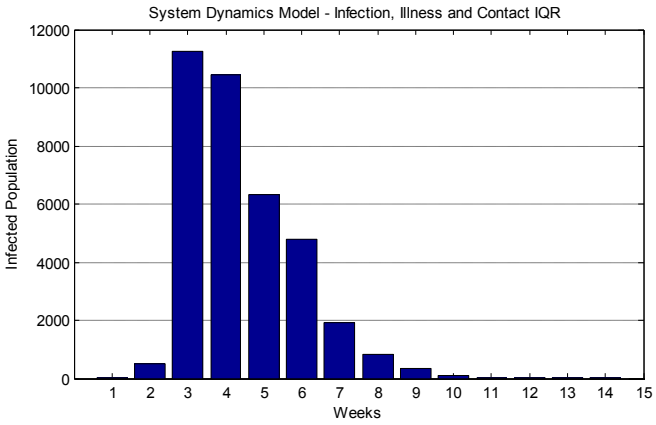

Figure 14: System Dynamics Model - Infection, Illness and Contact IQR

Unlike the Monte Carlo simulations where a single parameter is varied, in this case, with multiple parameter variations, there is an overall significant increase in the variation. Table 3 shows the total variation (the sum of IQR values) for the different experiments.

Table 3: Total variation for the SIR experiments

Simulation	Total Variation
ABM	16050
SD – Vary illness duration	10223
SD – Vary contact rate	19956
SD – Vary infection rate	26452
SD – Vary illness, contact, infection rate	36569

The least total variation for the simulation is obtained for the Monte Carlo experiment where the illness duration is varied. The Monte Carlo experiment where combined parameters are varied has more than twice the total variation of the ABM experiment.

Results from the ABM simulation showed that the overall peak total infection remained stable between simulations. The shape of the output curve for each simulation has a closer fit with the curve for the empirical data. The ABM simulations only differed with the initial delay before the uptake of infection which may also arise due to natural variation of the contact rate between individuals and their transport networks.

In contrast, for the SD model, the effect on the variation of the parameters has the effect of altering the rate at which the infection spread within the population.

DISCUSSION AND CONCLUSION

Although variations of SD models exist which are able to integrate random elements (Tuckwell and Williams, 2007)(Volz and Meyers, 2007) they produce a different kind of variation compared to ABM. Whereas in stochastic models there is a random element applied to the equations, in ABM the randomness is inherent and more natural, following the rules of the underlying system being modelled.

The ABM and SD experiments for the SIR data show that ABM is able to capture natural variation without recourse to modification of any parameters for a simulation. The classic SD model has no variation. The SD with Monte Carlo simulation has variation but it is very sensitive to parameter changes and in the case where multiple parameters are varied, it produces variation and infected population counts which no longer match up against the experimental data. Therefore an ABM of SIR with built-in randomness is able to capture the natural variation in SIR better than a classic SD model with Monte Carlo simulation. The source of variation for the ABM is the contact between the agents between the different experiments.

Several comparative studies between ABM and SD have been undertaken (Jaffry and Treur 2008). Some notable discussions in these studies include the issue of computing power and control. In this study, it also the case that the ABM is computationally expensive compared to the classical mathematical model although this may be overcome in future by highly parallel computing architectures (Tang et al., 2008). Traditional continuous models are generally easier to implement but many aspects of biological systems are intrinsically stochastic in nature (Wilkinson, 2009) so the ABM could be viewed as a more 'faithful' interpretation of the processes being modelled.

As the ABM is built using autonomous individuals, it could be extended to include connections between individuals across different regions to understand the effect of disrupting the spread of the epidemic by shutting down major transport links for example. Further work could include the effect of the use of different network topologies.

The use of ABM with its inherent and intuitive representation of natural variation and interaction among components can help to bridge the gap between computer simulation and biological systems and provide insight of how local level interactions bring about global system outcomes.

REFERENCES

Boots, M. and Sasaki, A. 1999. "Small worlds' and the evolution of virulence: infection occurs locally and at a distance." *Proc. R. Soc.* 266, 1933-38.

da Gama, M.M.T. and Nunes, A. 2006. "Epidemics in small world networks." *Eur. Phys. J.* 50, 205-208.

Dietz, K. and Heesterbeek, J.A.P. 2002. "Daniel Bernoulli's epidemiological model revisited." *Mathematical Biosciences* 180, 1–21.

Enns, R.H. 2011. "It's a Nonlinear World." Springer, ISBN 9780387753386.

Forrester, J.W. 1961. "Industrial Dynamics." Pegasus Communications, ISBN 1883823366.

Gaspard, P. 2005. "Brownian motion, dynamical randomness, and irreversibility." *New Journal of Physics* 7, 77.

Jaffry, S.W. and Treur, J. 2008. "Agent-Based and Population-Based Simulation: A Comparative Case Study for Epidemics." *Proceedings of the 22nd European Conference on Modelling and Simulation 2008*, 123-130.

Kermack, W. and McKendrick, A.G. 1927. "A Contribution to the Mathematical Theory of Epidemics." *Proc. Royal Soc. London* 115(772), 700–721.

Macal, C.M. and North, M.J. 2008. "Agent-based modeling and simulation: ABMS examples." *Proceedings of Winter Simulation Conference* 2008, 101-112.

McKendrick, A. G. 1926. "Applications of mathematics to medical problems." *Proceedings of the Edinburgh Mathematical Society* 44, 98–130.

Oberkampf, W.L., Trucano T.G., and Hirsch C. 2002. "Verification and Validation for Modeling and Simulation in Computational Science and Engineering Applications." *Foundations for Verification and Validation in the 21st Century Workshop, Maryland*.

O'Hagan, A., Stevenson, M., and Madan, J. 2007. "Monte Carlo probabilistic sensitivity analysis for patient level simulation models: efficient estimation of mean and variance using ANOVA." *Health Economics* 10(10), 1009-23.

Siebers P.O., Macal C.M., Garnett J., Buxton D., Pidd M. 2010. "Discrete-Event Simulation is Dead, Long Live Agent-Based Simulation!"' *Journal of Simulation* 4(3), 204-210.

Skog, L., Hauska, H., and Linde, A. 2008. "The Russian influenza in Sweden in 1889-90: an example of Geographic Information System analysis." *Eurosurveillance* 13, 49.

Stan, U. 1987. "John Von Neumann and the Monte Carlo method." *Los Alamos Science* 15, 131-136.

Sterman, J.D. 2004. "System dynamics modeling: Tools for learning in a complex world." *California management review* 43(4), 8–25.

Tang, W., Bennett D.A., and Wang, S. 2008. "A Parallel Agent-Based Model of Land Use Opinions." *Land Use Science* 6(2), 121-135.

Tuckwell, H.C. and Williams R.J. 2007. "Some Properties of a Simple Stochastic Epidemic Model of SIR Type." *Mathematical Biosciences* 208(1), 76-97.

Volz, E. and Meyers, L.A. 2007. "Susceptible-infected-recovered epidemics in dynamic contact networks." Proceedings of the *Royal Society* 274, 2925-2934.

Watts, D.J. and Strogatz, S.H. 1998. "Collective dynamics of 'small world' networks." *Nature* 393, 440-442.

Wilcoxon, F. 1945. "Individual Comparisons by Ranking Methods." *Biometrics Bulletin* 1(6), 80-83.

Wilkinson, D.J. 2009. "Stochastic modelling for quantitative description of heterogeneous biological systems." *Nature Reviews Genetics* 10, 122-133.

Zellner, M. 2008. "Embracing Complexity and Uncertainty: The Potential of Agent-Based Modeling for Environmental Planning and Policy." *Planning Theory & Practice* 9(4), 437-457.

AUTHOR BIOGRAPHIES

Aslam Ahmed is a PhD student in the Intelligent Modelling and Analysis Group at the University of Nottingham. His interests include the role of System Dynamics and Agent Based Modelling in areas of the immune system.

Julie Greensmith is a lecturer in the School of Computer Science at the University of Nottingham. Her interests include artificial immune systems and a wide range of application areas including computer security, affective computing and wearable biosensing.

Uwe Aickelin is an EPSRC Advanced Research Fellow and Professor of Computer Science at The University of Nottingham, where he is also the Director of Research in the School of Computer Science and leads one of its four research groups: Intelligent Modelling & Analysis (IMA).

AN AGENT BASED MODEL OF FIRMS SELLING AND SOURCING INTERNATIONAL DECISIONS WITH FLEXIBILITY TO DEMAND AND SUPPLY SHOCKS

Ermanno Catullo
University of Turin
Email: ermanno.catullo@gmail.com

KEYWORDS

Agent Based Model, International trade, Outsourcing.

ABSTRACT

The increasingly global fragmentation of production is a central topic of the international trade economics research agenda. The agent based model presented in this paper tries to combine in a unique coherent schema two usually distinct fields of internationalization analysis: from one side firms' selling decisions (i.e., the choice to export or to invest directly abroad) and from the other side firms' sourcing decisions (i.e., the choice to outsource or to produce directly intermediate goods). Therefore, assuming the presence of fixed and variable costs to export and to import, the model is able to reproduce both the exporters and importers firm better performance empirical evidence. Moreover, assuming that production flexibility to shocks is higher with lower capital intensity and it increases when firms outsource their intermediate goods, the model replicates the positive empirical relationship between sectoral capital intensity and imports of intermediate goods from foreign affiliates. The simultaneous study of selling and sourcing decisions might offer useful tools to understand economic processes and gives the opportunity to test the effects of different combinations of trade and industrial policy measures on international division of labor and welfare.

INTRODUCTION

International fragmentation of production is a central aspect of globalization processes, reshaping national and regional sectoral specializations with a strong impact on employment and welfare. From both an empirical and a theoretical approach international trade economics is trying to understand and analyze the reasons and the conditions that, from one side, determine firms' selling decisions, leading firms to export or to integrate horizontally (i.e., conceiving horizontal integration as the firm's choice to not export in a foreign country but producing directly in this country the products the firm want to sell) and, from the other side, delineate sourcing strategies: outsourcing the intermediate goods or vertical integrate their production in the home country or abroad (i.e., assuming firms need intermediate goods, vertical integration is the choice to not buy intermediate goods from an other firm but producing the intermediate good directly in the same plant or in an affiliate factory at home or abroad).

In the US there is a consistent empirical evidence according to which vertical integration abroad is stronger in sectors where capital intensity is higher: in these sectors firms prefer to import intermediate goods from affiliate companies abroad than buy them from not affiliate firms (intra-firm import) (Antràs, 2003). The Antràs 2003 model is able to replicate this stylized fact assuming the presence of transaction costs, modeling property right effects on appropriability of final goods and hold-on problems. In fact, conceiving capital intensity as a proxy for the relevance of headquarter services in the final good production, in the Antràs 2003 model firms with higher capital intensity have stronger incentives to produce by themselves intermediate goods. Moreover, the Antràs and Helpman model (Antràs et al., 2004) considers also firm heterogeneity in productivity as a determinant of sourcing decisions.

At the same time, firm heterogeneity (in the form of a given distribution of productivity) and the presence of fixed and variable costs to export are crucial elements of the Melitz model (Melitz, 2003), that is aimed to explain the reasons why exporters have a better performance than firms that do not export, besides this model has also been enlarged to deal with horizontal integration (Helpman et al., 2004).

However, in standard economic analysis is not easy to model at the same time firms' selling decisions and sourcing choices, moreover endogenizing technological change with firms heterogeneity is not so immediate. Thanks to the opportunities offered by agent based simulation to design a simple structure of firms decision processes and firms interactions, the model described in this paper aims to integrate the analysis of internationalization choices in serving markets and in sourcing. Moreover, the model assumes bounded rationality of agents : firms' decisions are the result of a basic reinforcement learning process based on the Tesfatsion 2005 model, which determines the dynamic of the simulation and permits to endogenize in a stylized way technological change as the effect of the choice to invest in innovation.

The model reproduces as emergent results the exporter and importer premia. In fact, exporters better performance (and in first instance the higher productivity of exporters) is the result of a stronger innovative effort, that

Proceedings 26th European Conference on Modelling and Simulation ©ECMS Klaus G. Troitzsch, Michael Möhring, Ulf Lotzmann (Editors)
ISBN: 978-0-9564944-4-3 / ISBN: 978-0-9564944-5-0 (CD)

allow firms to overcome the obstacles represented by the fixed costs to enter foreign markets. After a firm enters foreign markets, it gains more resources that could be used to foster the same good competitive decisions that allowed the firm to become an exporter or to produce directly abroad. At the same time considering sourcing choices, the model is able to replicate the importer premia empirical evidence, according to which also importer firms present a better performance than not importers.

The model reproduces also the capital intensive firms preference for vertical integration abroad, assuming the presence of both demand and supply shocks. The sourcing choice relies on a simple configuration of transaction cost that permit to focus the analysis on the reactions to demand and supply negative shocks. As in standard economics, production is made using a fixed factor (capital), that can not be modified in the short run, combined with a variable factor (labor) that can react faster to shocks, therefore capital intensity is conceived as a proxy for the intensity of the short run invariable factor. The nature of the shocks considered is twofold: demand negative shocks when firm's demand is lower than its productive capacity and supply shocks when, in reason of imperfect information and contract incompleteness, outsourcers do not provide the requested quantity of intermediate goods. The first shock is endogenous because it is the result of firms' and consumers' decisions, the second one is exogenous, in fact according to model's hypothesis there is an exogenous fixed probability that an intermediate good is not supplied.

The model is based on basic assumptions on negative shocks flexibility: in first instance firms with lower capital intensity are more reactive to negative shocks, because they can shift a larger part of the lost to the variable input (reducing the expenditure for the variable input), moreover firms can shift the burden of demand shocks to outsourcing firms (buying a minor quantity of the intermediate good). However outsourcing the intermediate good production lead to supply shocks.

The structure of the paper is divided in four parts. The first part illustrates the model, the second describes the simulation result regarding outsourcing and vertical integration, the third is focused on the exporter and importer premia, the fourth concludes.

THE MODEL

The model is made using the Phyton-SLAPP protocol (Terna, 2011), it can be synthetically described focusing on five interconnected parts of its structure: the interaction structure, agents' properties, the selling choice, the sourcing decision and the simulation data analysis.

Interaction Structure

In the model there are two typology of agents: firms and consumers, initially in the same number in two countries (A,B). Firms' interactions are indirect through competition, in fact firms produce different varieties of the same good and compete through price decisions, besides firms that have a negative Net-Worth exit from the market (the Net-Worth is given by the sum of firm's liquidity reserves and the value of firm's capital)

Firms have three separate selling choices: they could choose to serve just the home market, to sell also in the other country (export) or to create another firm abroad to produce and sell directly in the foreign country their product (horizontal integration).

On the other side, firms need intermediate goods to produce the final ones, they have four separate options to obtain intermediate goods: they could buy the intermediate goods at home (home outsourcing) at a constant price, they could buy them abroad (abroad outsourcing), firms can produce directly the intermediate goods at home (vertical integration at home) or they could produce them abroad (vertical integration abroad), there are costs differences among these forms and, moreover, because of market imperfections outsourcing leads to the possibility that part of the quantity of the intermediate good needed will not be provided. When a firm outsources abroad or vertically integrate abroad this firm imports intermediate goods, consequently the model partially deals with the import side of firm activity.

It is assumed that in one country (B) the unit cost to produce or to outsource the intermediate good is cheaper in order to give a reason for importing it from the other country (A), for simplicity simulation data analysis is restricted to country A where is convenient to import the intermediate good.

Agents

Consumers have different variety preferences and they weight in a different way the importance of price and variety. Every consumer has a first choice variety of the final good: the far the goods offered are from the first choice the lower is the utility the consumer will extract from them, besides if goods offered are too different from the preferred variety consumers do not buy it. Every run in a random order consumers choose the good they buy, determining firms' individual supply.

Firms are profit oriented and at the beginning they have the same characteristics, they use two factor of production one fixed in the short run (K) and the other variable (L), the proportion between the two factor is constant ($0 < \nu < 1$). where y is the output:

$$\begin{cases} K = (1-\nu)y \\ L = \nu y \end{cases} \tag{1}$$

Every firm produces a different variety of the same final good and for every unit of the final good they produce they need a unit of the intermediate good. In order to increase their productive capacity they have to buy units of the fixed factor (K). Firms make basic choices: the offering price of the final good they produce, increasing or reducing the production capacity, selling and out-

sourcing options and they choose whether to invest in research permitting them to reduce the unit cost (equal to the marginal cost) at which they produce. All the decisions are taken using a simple reinforcement learning algorithm based on the Tesfatsion 2005 model, that derives from Roth and Erev experimental analysis (Roth et al., 1993), in this way firms learn to react to external stimuli and they could change their behavior adapting it to the modification of the environment, of course reactions are not immediate, we could think that firms follow routines that suffer for a certain degree of inertia. Moreover, selling and outsourcing choices last for a short period of time, which is needed to recuperate the starting fixed cost that might be implied by the different selling and sourcing options. In fact, it is possible to conceive selling and sourcing choices as not short time ones.

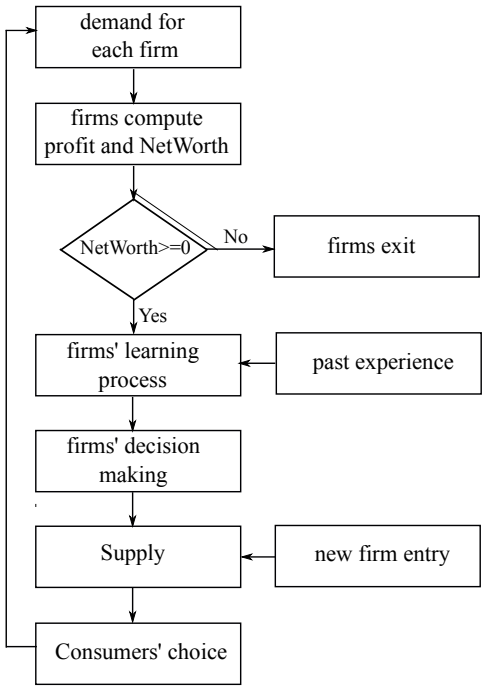

Figure 1: Simulation's Schema

Export/Horizontal Integration Choice
Selling in the foreign market increases firms' market opportunities, however if a firm chooses to export it incurs in an initial fixed cost (costs to build a commercial network abroad, to modify the good produced to match foreign standard and tastes etc..) and in higher variable costs (due to transport costs, export and import taxes, assurances etc..). On the other side, if a firm chooses to sell directly abroad building an affiliate firm in the foreign market (horizontal integration) it has to pay a fixed cost (start-up expenditure) but does not pay higher variable costs, because it has not to ship its products. The new firm created has the same characteristics of the mother firm as a clone: the same productivity capacity, unit cost level and final good variety. However, the foreign affiliate starts a semi-autonomous life, making its-own decision on sourcing, innovative effort and price setting, until the mother firm exits the market or chooses to disinvest. When the mother firm disinvests the value of capital and the liquidity of the affiliate is added to its liquidity. Finally, firms in order to export or to horizontally integrate need to have enough liquidity to pay the fixed costs to export or to invest abroad.

Outsourcing/Horizontal Integration Choice
Firms can buy the quantity of intermediate goods they need in the home market (home outsourcing) at a constant unit cost. If they buy it from abroad (outsourcing abroad) they pay a starting fixed cost and higher marginal costs (import costs). Similarly firms can make by themselves the intermediate goods they need, but if they want to integrate the production domestically (home vertical integration) they have to pay a fixed cost (start up cost) and they have to buy the needed capital to produce it, while the marginal cost is the same as in outsourcing. If a firm vertical integrates abroad both the starting fixed cost and the unit cost are higher (vertical outsourcing abroad). When a firm outsources for every unit of the intermediate good needed there is a constant probability ($p = 0.1$) that the good will not provided to the firm. Intermediate goods could not be provided for multiple reasons, for instance because of imperfect information and incomplete contracts some intermediate goods can not have the necessary characteristics or sufficient quality to be used. Therefore producing directly is more expensive but it is less dangerous (Antràs, 2003; Antràs et al., 2004).

Flexibility to negative demand and supply shocks
Flexibility to negative shocks is a crucial assumption of the model, starting from the idea that the firm structure in part is influenced by its capacity to react to shocks. For instance, outsourcing could be a way to shift demand shocks to provider firms. Moreover, a basic hypothesis of the model is that as in standard economics capital is conceived as a factor that can not be modified in the short run, consequently firms with higher capital intensity react in a slower way to negative shocks.

There are two crucial parameters in the simulation: flexibility to shocks (δf) and the capital intensity (ν). When a firm receives a demand that is lower than its productive capacity, it suffers a demand shock that could be in part absorbed employing a minor quantity of the variable input necessary to produce the final good at full productive capacity. Moreover, if the firm produces by itself the intermediate good it can reduce also the quantity of the variable input employed to produce it, otherwise if the firm outsources the intermediate good it could reduce by a fraction equal to δf the quantity of intermediate good it has to buy. Therefore, if a firm is vertical integrated producing directly at home or abroad the intermediate good it could reduce the expenditure just on

the variable factor by a fraction equal to δf, while if the firm outsources it could reduce all the excessive expenditure by δf. Consequently, if a firm outsources it could absorb a higher amount of a demand shock. On the other side if a firm outsources there is a constant probability for every intermediate good needed that the intermediate good will not be provided by the outsourcer, reducing the effective supply of the firm. However outsourcing is less expensive than integrate the intermediate good production.

Simulation Data Analysis

In every simulation firms are initially homogeneous, their heterogeneity (in productivity, productive capacities, international openness, prices) emerges as the results of individual firms' choices regarding innovative efforts, price setting, selling and outsourcing forms. While ν and δf are constant and equal for all the firms to compare different specification of the model and to cope with the empirical analysis based on sectoral differences (markets with different capital intensity ν) and not on individual heterogeneity. Simulation data are analyzed considering just the period of time (simulation cycles) in which the number of firms and the supply concentration stabilize, conceiving it as a quasi-equilibrium in a system that is intrinsically dynamic. Firms and time are the two dimensions used to implement Panel data econometric analysis, one panel is used to study integration processes (20 cycles) and a longer one for the exporter/importer premia (100 cycles).

The period of time used to analyze the exporter and the importer premia is longer than the one used to study production fragmentation processes, because the production fragmentation empirical evidence regards aggregate economic sectors differences, while the exporter and importer premia analysis is essentially microeconomic, therefore even if more computational demanding, using a longer micro dataset allows a more intensive exploration of firm individual characteristics.

PRODUCTION FRAGMENTATION RESULTS

Given the flexibility to shocks (δf), the higher the capital intensity the lower the firm capacity to reduce the effects of demand and supply shocks. Consequently, in simulations where firms have high capital intensity (lower ν) they could tend to outsource to limit the demand shock effects, however when they outsource they are hit by offer shocks. At the same time, in simulations with low capital intensity, demand shocks have a reduced effect on production, therefore the incentives to outsource are lower, but on the other side firms are more reactive to offer shocks due to outsourcing.

Running one hundred simulations for each of the four levels of the δf considered (ZF: $\delta f = 0$, LF: $\delta f = 0.2$, MF: $\delta f = 0.5$, HF $\delta f = 0.8$) and looking at the correlation between capital intensity and different integration indicators (ICm, INm, IQm are respectively the total cost, number and products from foreign integrate production divided by the total cost, number and intermediate products importation, while ICf, INf, IQf are respectively the total cost, number and products from integrate production divided by the total cost number and intermediate products made), it appears evident that firms with lower ν, therefore with higher capital intensity, in simulation with medium and high flexibility present an higher tendency to integrate vertically their production both domestically and abroad (table 1). Reproducing the empirical evidence ot the direct relationship between capital intensity and integration abroad.

Table 1: Production Fragmentation and Capital Intensity (Capital Intensity (ν) as independent variable)

	ZF	LF	MF	HF
ICm	0.013**	-0.004	-0.013**	-0.030**
	(0.0044)	(0.0055)	(0.0054)	(0.0058)
ICf	0.008**	-0.008**	-0.016**	-0.036**
	(0.0041)	(0.0038)	(0.0043)	(0.060)
INm	0.030**	0.011**	-0.009**	-0.029**
	0.0039	(0.0043)	(0.0043)	(0.0044)
INf	0.030**	0.008**	-0.007**	-0.033**
	(0.0036)	(0.0036)	(0.0037)	(0.0039)
IQm	0.016**	-0.002	-0.015**	-0.041**
	(0.0043)	(0.0055)	(0.0053)	(0.0051)
IQf	0.011**	-0.005	-0.018**	-0.039**
	(0.0039)	(0.004)	(0.0042)	(0.0053)
n	-53.761**	-58.27**	-11.69*	38.562**
	(8.2970)	(7.0403)	(6.6212)	(5.0830)
sim	100	100	100	100

Note: Standard error in parenthesis below the coefficients. Asterisks denote significance levels (**: $p < 5\%$; *: $p < 10\%$). All regressions include time dummies.

In figure 2 is represented the relation between ν and the percentage of intermediate goods expenditure that comes from foreign affiliate firms (vertical integration abroad) on the total of expenditure on intermediate goods from abroad (total of importations, therefore both from affiliated intermediate producers abroad and outsourcing from abroad). When ν decreases, capital intensity increases, and with high δf (MF and HF) vertical integration abroad augments. While for low level of flexibility the negative relation between ν and integration is not so relevant and it is reversed with zero flexibility.

To understand the micro processes that lead to the emergent sectoral distribution of sourcing integration, first of all it is possible to look at the macro patterns (table 1): in simulation with higher δf (MF and HF) there is a negative correlation between ν and the number of firms in the market, in fact with higher ν (less capital intensity) firms can easily increase their size because they have to buy a minor amount of the fixed factor to increase their productive capacity. When the demand is given, if firms are larger the total number of them has to decline. How-

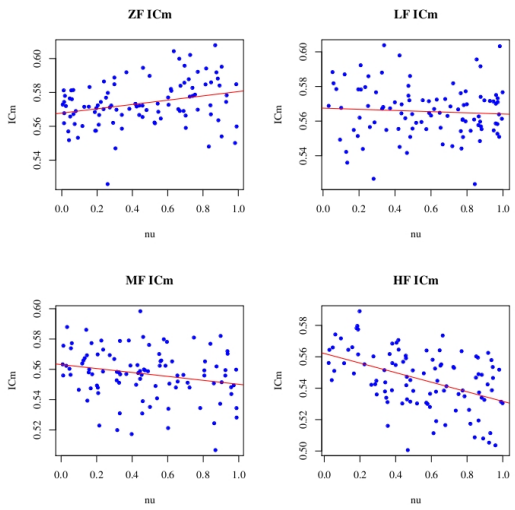

Figure 2: Intermediate Goods Imports Vertical Integration

ever, thanks to the higher flexibility in MF more firms are able to survive even if the average size increases, in fact the correlation between ν and n is less negative in MF than in LF simulations. Consequently, in MF simulations thanks to the higher possibility to compensate shocks more firms can survive, this leads to tougher competition, especially when capital intensity is lower as the stronger negative relationships between ν and p (prices) and between ν and uc (unit cost) shows in the case of medium flexibility (MF) with respect to LM simulations (table 2).

Table 2: Prices and Unit Costs (re panel regression)

	LF		MF	
	p	uc	p	uc
ν	-0.137**	-0.007**	-0.335**	-.0195**
	(0.01819)	(0.0044)	(0.0191)	(0.00439
pC	-0.0214**	-0.001**	-0.022**	-0.001**
	(0.0017)	(0.0001)	(0.0002)	(0.0001)
uc	-1.255**		-1.338**	
	(0.0220)		(0.0224)	
dexp	0.372**	-0.001**	0.369**	-0.001**
	(0.0069)	(0.0001)	(0.0071)	(0.0001)
dHorI	0.298**	-0.001**	0.266**	-0.001**
	(0.0144)	(0.0001)	(0.0140)	(0.0001)
firms	46,811		47,618	

Note: On the y axis independent variables. Standard error in parenthesis below the coefficients. Asterisks denote significance levels (**: $p < 5\%$; *: $p < 10\%$). All regressions include time dummies.

When capital intensity is lower (higher ν) and flexibility is higher (MF), the deriving tougher competitive environment leads to lower sales given the productive capacity, in fact looking at simulations with medium δf and higher ν (lower capital intensity) firms have lower sales (S) controlling for the level of productive capacity (pC). The lower level of sales results in stronger demand shocks as showed by the dhq indicator (dhq is the difference between productive capacity and sales divided by the productive capacity, it is a measure of plant underproduction), consequently the cost of an higher difference between sales and productive capacity could be more efficiently compensate through outsourcing, moreover a lower capital intensity allows firms to absorb in a greater extent supply shocks. While, when δf is lower the possibility to compensate demand shock becomes lower, therefore firms do not increase too much their productive capacity. In fact, the correlation between ν and sales is lower in the simulation with low δf and consequently also the correlation between ν and dqh is weaker, in fact the necessity to outsource to reduce demand shocks is lower and at the same time the capacity to absorb supply shocks is reduced (table 3).

Table 3: Supply and Demand Shocks (re panel regressions)

	LF		MF	
	dqh	S	dqh	S
ν	0.019**	-0.827**	0.045**	-2.138**
	(0.0012)	(0.0578)	(0.0013)	(0.0638)
pC	0.002**	0.819**	0.002*	0.804**
	(0.0001)	(0.0016)	(0.0001)	(0.0019)
p	0.014**	-0.617**	0.016**	-0.650**
	(0.0001)	(0.0075)	(0.0002)	(0.0078)
uc	0.142**	-3.331**	0.175**	-3.900**
	(0.0019)	(0.0561)	(0.0022)	(0.0644)
dExp	-0.081**	4.031**	-0.084**	4.187**
	(0.0008)	(0.0471)	(0.0008)	(0.0503)
dHorI	0.070**	-5.071**	0.065**	-4.760**
	(0.0018)	(0.1363)	(0.0018)	(0.1391)
firms	46,811		47,618	

Note: Standard error in parenthesis below the coefficients. Asterisks denote significance levels (**: $p < 5\%$; *: $p < 10\%$). All regressions include time dummies

On the other side changing δf the impact on integration is just partially relevant with lower and medium ν (respectively LN: $\nu = 0.2$, MN: $\nu = 0.5$), while the case of high ν (HN: $\nu = 0.8$) presents a significant negative relationship between all the integration indicators and δf. Therefore with high ν, so with low capital intensity, an increase of flexibility results in higher outsourcing, in fact low capital intensive firms can reduce demand shocks recurring to outsourcing and, at the same time, offer shocks could be easily absorbed (table 4).

EXPORTER AND IMPORTER PREMIA

There is a strong empirical evidence that in the same economic sector there are huge differences in productiv-

Table 4: Production Fragmentation and Flexibility (flexibility δf as independent variable)

	LN	MN	HN
ICm	0.001	-0.006	-0.015**
	(0.0043)	(0.0052)	(0.0054)
ICf	-0.001	-0.006	-0.018**
	(0.0038)	(0.0038)	(0.0041)
INm	-0.007**	-0.010**	-0.031**
	(0.0038)	(0.0043)	(0.0032)
INf	-0.009**	-0.016**	-0.032**
	(0.0032)	(0.0034)	(0.0032)
IQm	-0.012**	-0.015**	-0.020**
	(0.0042)	(0.0052)	(0.0053)
IQf	-0.013**	-0.017**	-0.023**
	(0.0035)	(0.0038)	(0.0040)
sim	100	100	100

Note: Standard error in parenthesis below the coefficients. Asterisks denote significance levels (**: $p < 5\%$; *: $p < 10\%$). All regressions include time dummies.

ity among firms, part of these differences are the consequence of: the better performance of exporter firms (the exporter premia), to the better performance of firms that invest abroad to produce and sell final products (horizontal integration) and in a minor extent to the importer premia, in fact importers present higher productivity than not importers (Bernard et al., 2001; Castellani et al., 2009; Feenstra, 2002). The model is able to replicate these empirical results endogenizing technological change and assuming the presence of fixed and variable cost to export, invest abroad and import (importing is equivalent to outsourcing or vertical integrate from abroad, in the last case we have intra-firm import). Exporters, importers and investors abroad present a better performance because from one side they have to increase their productivity to overcome the obstacle represented by the initial fixed cost to enter foreign markets (Melitz, 2003; Helpman et al., 2004). On the other side, entering the foreign market gives higher sales opportunities generating more resources that could be used to continue to follow the virtuous competitive policy, which allowed them to overcome the initial fixed costs. Consequently these difference in productivity are the consequence of an ex-ante self selection process and of an ex-post growth of productivity (Serti et al., 2008).

Productivity differences associated with selling and sourcing decisions could be detected by simple econometric analysis that are not aimed to find causal relationships. The econometric test is based on dummies associated with the status of exporter (dExport) or with the decision of horizontally integrated (dHorInt), controlling for the level of capital intensity of the sector and time dummies, eliminating in this way sectoral time and cohort effects, using both pooled and random effect analysis.

The correlations shows that unit costs are lower for exporters than for firms that do not integrate in both low and high flexibility simulation, moreover (as above) regressions underline the negative relation between unit cost and sectoral capital intensity (table 5).

Table 5: Exporter Premia, Pooled Regression (pr) and Fixed Effect Regression (fe)

	LF		MF	
	uc(pr)	uc(re)	uc(pr)	uc(re)
ν	-0.001**	0.007**	-0.014**	-0.012**
	(0.003)	(0.0042)	(0.0029)	(0.0041)
dExport	-0.097**	-0.001**	-0.099**	-0.001**
	(0.0012)	(0.0001)	(0.0012)	(0.0001)
dHorInt	-0.157**	-0.011**	-0.158**	-0.001**
	(0.0016)	(0.0001)	(0.0016)	(0.0001)
n. obs	59,126		60,348	

Note: Standard error in parenthesis below the coefficients. Significance levels **: $p < 5\%$; *: $p < 10\%$. Regressions include time dummies.

At the same time, in regressions with dummies for the outsourcing decisions: firms vertically integrated domestically (dIntHome), firms vertically integrated in the foreign country (dIntAbroad) and firms that outsource from abroad (dOutAbroad) present a better performance than firms that outsource from home (table 6).

Table 6: Importer Premia, Pooled Regression (pr) and Fixed Effect Regression (fe)

	LF		MF	
	uc(pr)	uc(re)	uc(pr)	uc(re)
ν	-0.007**	-0.007**	-0.016**	-0.012**
	(0.0031)	(0.0042)	(0.0030)	(0.0041)
dIntHome	-0.012**	-0.001**	-0.012**	-0.001**
	(0.0006)	(0.0001)	(0.0006)	(0.0001)
dIntAbroad	-0.020**	-0.001**	-0.021**	-0.001**
	(0.0006)	(0.0001)	(0.0006)	(0.0001)
dOutAbroad	-0.009**	-0.001**	-0.008**	-0.001**
	(0.0006)	(0.0001)	(0.0005)	(0.0001)
firms	59,126		60,348	

Note: Standard error in parenthesis below the coefficients. Significance levels **: $p < 5\%$; *: $p < 10\%$. Regressions include time dummies.

More in general importers have lower unit cost (higher productivity) thanks to the combined performance of firms that integrate vertically abroad and firms that outsource from abroad (dImpA), in fact importers performance slightly overcomes that of firms that integrate or outsource at home (table 7).

Table 7: Importer Premia, Pooled Regression (pr) and Fixed Effect Regression (fe)

	LF		MF	
	uc(pr)	uc(re)	uc(pr)	uc(re)
ν	-0.0071**	0.0071*	-0.0167**	-0.0124**
	(0.0031)	(0.0042)	(0.0030)	(0.0001)
dImpA	-0.0078**	-0.0002**	-0.0081**	-0.0002**
	(0.004)	(0.0001)	(0.0004)	(0.0001)
firms	59,126		60,348	

Note: Standard error in parenthesis below the coefficients. Significance levels **: $p < 5\%$; *: $p < 10\%$. Regressions include time dummies.

CONCLUSIONS

This agent based simulation model is an attempt to treat jointly two usually separated fields of research in international trade economics: international selling and sourcing decisions. Assuming that flexibility to demand and supply shocks could be an important factor in determining the choice to integrate or not the production of intermediate goods, the model is able to replicate the stylized fact according to which in sectors with higher capital intensity the percentage of intermediate goods import from foreign affiliate is higher. On the other side assuming fixed cost to export and endogenizing technological change (considering innovations as consequence of firms innovative efforts), the model replicates two micro stylized fact: the exporter and importer premia.

This model treats partially and in a very stylized way the problems of innovation efforts and firms structure in an international dimension, nevertheless the simplicity of the firm decision processes allow the model to be easily modified and used for different applications and topics (for instance the analysis of the ex-ante and ex-post characteristics of importers and exporters, or it could even be used to study the effect of asymmetries among countries deriving from differences in factor endowment or technological capabilities). It might be important to validate the micro-macro relationship emerging from the simulation, in fact even if the simulation approach has to deal with the complexity of the system reproduced, it might be useful to test the dynamic effects of different combinations of policy measures (as import and export taxes or incentives, flexibility to shocks tools etc..). Finally, a better understanding of the factors influencing export and import micro decisions might offer useful means to policy makers in different area of interest (for instance balance of payment policy effects or the reactivity to exchange rate variation). At the same time the analysis of the sectoral differences in firm's organization could give important suggestion on industrial policy interventions.

REFERENCES

Acemoglu, D. (2009). *Introduction to Modern Economic Growth*. Princeton University Press.

Alvarez, R., Lopez, R. (2005). Exporting and performance: Evidence from Chilean plant. *Canadian Journal of Economics*, 38 (4).

Antrás, P. (2003). Firms, Contracts, and Trade Structure. *Quarterly Journal of Economics*, 118(4).

Antràs, P. Helpman E. (2004). Global Sourcing. *Journal of Political Economy*, 112(3).

Antràs, P., Rossi-Hansberg E. (2009). Organizations and Trade. *Annual Review of Economics*, 1(1).

Bernard, A. B., Jensen, B. J., Redding, S. J. Schott, P. K. (2007). Firms in International Trade. *Journal of Economic Perspectives*, 21 (3).

Castellani, D., Serti, F.. Tomasi, C (2009). Firms in International Trade: Importers and Exporters Heterogeneity in the Italian Manufacturing Industry. *The World Economy*, 33, 424-457.

Feenstra, C. R. (2002). *Advanced International Trade: Theory and Evidence*.

Helpman E. H., Melitz M. J., Yeaple S. R., (2004). Export Versus FDI with Heterogeneous Firms. *American Economic Review*, 94(1).

Kirman, A. (2011). Learning in agent based models. *Grequam working paper*.

Melitz, M. J. (2003). The Impact of Trade on Intra-Industry Reallocations and Aggregate Industry Productivity. *Econometrica*, 71(6).

Serti, F., Tomasi, C. (2008). Self Selection and Post-Entry effects of Exports. Evidence from Italian Manufacturing Firms. *Review of World Economics*, 144(4).

Roth, A. E., Erev I. (1993) Learning in extensive form games: experimental data and simple dynamic models in the intermediate term *Games and Economic Behaviour*, 8.

Tesfatsion, L. (2005). Agent-Based Computational Economics:a Constructive Approach To Economic Theory, in L. Tesfatsion and K. L. Judd (ed.), *Handbook of Computational Economics 2*, North-Holland.

Terna, P. (2011). Slapp-Python Protocol. (http://eco83.econ.unito.it/terna/slapp/)

AUTHOR BIOGRAPHY

ERMANNO CATULLO is a PhD student in economics from University of Turin. I graduated in Development Economics in the University of Florence, I had a scholarship in the Italian Institute for International Trade. My mail is `ermanno.catullo@gmail.com`

A CRITIQUE OF AGENT-BASED SIMULATION IN ECOLOGY

Michael Hauhs Baltasar Trancón y Widemann
Ecological Modelling
University of Bayreuth
D-95440 Bayreuth
Email: {Michael.Hauhs,Baltasar.Trancon}@uni-bayreuth.de

KEYWORDS

Modelling Paradigm; Epistemic States; Ontic States; Category Theory; Coalgebra; Ecological modelling

ABSTRACT

Models link empirical observations with formal reasoning. If the computer plays an essential role in their functioning, it seems only fair to consider theoretical computer science as well as the discipline of application. We review some perennial philosophical problems about the nature of state and behaviour in models from that perspective. A mathematical framework for their explication and the unbiased choice of solutions is proposed. Agent-based models play an increasing role in ecological modelling. They are taken here as an example for demonstrating critical assumptions and dilemmas in integrating criteria of methodological rigour with practical relevance of models. Some possible solutions and their practical implications are outlined based on this new theoretical perspective.

INTRODUCTION

Models link observations from the empirical realm with formal systems. From the technological viewpoint, we restrict the discussion to those models which can be implemented and executed on a computer. From the application viewpoint, we consider the field of ecology, representative for a wide range of "complex system" science disciplines: Ecology studies the relationship between organisms and their environment. Development, application and testing of ecological models requires a correspondence to some selected empirical or theoretical aspects of these phenomena.

In ecology the empirical realm is characterized by data about the configuration and the behaviour of organisms, populations, or ecosystems. Organisms are the key notion of life sciences. Here we will focus predominantly on time series documenting the environmental relationships of organisms, i.e. their behaviour. Many key aspects of life are easily and naturally expressed as behaviour: living, surviving, reproducing, growing, etc.

The theoretical realm employs mathematics, i.e. axioms, theorems, and logic. The relationship between the empirical and the mathematical is not universal, but depends on context and observer perspective. In other words, models inevitably have a perspective, they are models of or for somebody, e.g. the meaning of their language is embedded into human cultures. At the same time computer models can be regarded as mathematical machines.

In ecology and other environmental sciences, it often seems that models can either be methodologically rigorous or practically relevant but rarely both (Peters, 1991). We shall refer to this situation as the *modeller's dilemma*. The puzzle why this is so can be posed in the form of four steps:

Theory in Ecology

Compared to other natural sciences ecological theory is relatively weak. Over the past years modelling has almost completely taken over from theory as a topic at ecological conferences. Some ecologists have even expressed their opinion that there can be no theory in ecology because systems which ecologists are dealing with are too complex and too poorly experimentally conditioned. The pragmatic interest of funding agencies have pushed modellers towards the empirical side.

Agent-Based Models in Ecology

The increasing importance of modelling and simulation in ecology is best exemplified by the ongoing proliferation of multi-agent models. This change is driven by technical progress in soft- and hardware rather than theory. In ecology these models have become known as "individual-based models" whereas in social sciences the term "agent-based models" is favoured. The two terms will be used synonymously and abbreviated as ABM.

Theoretical concepts behind Agent Based Models

ABMs as other simulation models run on mathematical machines. Thus there must be impliclit and inevitable assumptions about abstractions and interpretation of ecosystems built into these ecological models. Even if a modeller were convinced that ecosystems and ecology in general cannot have a theory, the mathematical machines they are using for analysing their data and for expressing ecological concepts have theories beneath their user interfaces. The pragmatic turn to applied research has only resulted in their hiding. Here we want to show that consultation of theoretical computing sci-

Proceedings 26th European Conference on Modelling and Simulation ©ECMS Klaus G. Troitzsch, Michael Möhring, Ulf Lotzmann (Editors)
ISBN: 978-0-9564944-4-3 / ISBN: 978-0-9564944-5-0 (CD)

ence will make some of these implicit assumptions behind models more explicit and transparent.

Mathematics of Agent Based Models

Physics has been the main and almost sole provider of scientific modelling prototypes, concepts, and paradigms. From the 19th century onwards these paradigms have been implicated in the formation and world views of other disciplines such as ecology, economy, or anthropology. Today computer science has emerged as a contestant in the field of modelling (especially interactive) behaviour. In this respect physical models have been weak, since they disregard the notions of choice and memory, i.e. subjective nondeterminism and dependence on history, that are so prominent in phenomena studied by life sciences. Physics has been named the science of simple systems, but whether or not a system is indeed simple, and in which respect, may lie in the eye of the modeller.

Theoretical computer science has studied formal behaviour (automata, process calculi) for a long time, and has recently come up with a unifying approach of formalizing behaviour of systems (Rutten, 2000). Since modeller's in ecology and especially users of ABMs often adopt a pragmatic perspective, they may overlook a mismatch between the physical modelling paradigms they are using conceptually and the computational tools they are employing technically. The following essay starts from the suspicion that a fundamental inconsistency may lay between *how* and *for what* ABMs are used in ecology, and potentially in social sciences as well.

We will use results of the new formal approach from computer science to discuss the implications for the interpretation of simulation models in ecology. They allow a new perspective at the modeller's dilemma in ecology, and ABMs in particular may take a key role in promoting this "interactive turn" in ecological modelling. The most important change is that these models allow for the formal representation of additional *empirical content*: i.e. interactive features in the behaviour of Life can formally be accounted for, whereas physical models inevitably abstract from such aspects. It is a separate question whether or nor living systems contain these features. Interactive models are expressive enough to allow testing of these hypotheses.

TERMS, DEFINITIONS

We use behaviour, as it is displayed at interfaces between organisms and ecosystems and their environments, as the prototype of an ecological data set. This type is exemplified by gas and energy exchange of plants or vegetation canopies, growth of biomass or changes in population size. Time series is the typical data format, especially with fairly static spatial coordinates, e.g. behaviour of plants.

Empirical Aspects

How can temporally ordered observations be expressed in mathematical language? From an empirical point of view the criterion is how to keep the key intuitions about living systems, while abstracting from the contingent details. Which attributes of a time series can be abstracted from, and on which one should the formalisation focus? One extreme attitude in this respect is simply to keep all attributes of a data set. This has been termed "petabyte science" and is the ultimate stance in data-driven research: "Petabytes allow us to say: 'Correlation is enough.' We can stop looking for models. We can analyse the data without hypotheses about what it might show. We can throw the numbers into the biggest computing clusters the world has ever seen and let statistical algorithms find patterns where science cannot." (Anderson, 2008) The following quote illustrates this pragmatic attitude further: "This is a world where massive amounts of data and applied mathematics replace every other tool that might be brought to bear. Out with every theory of human behaviour, from linguistics to sociology. Forget taxonomy, ontology, and psychology. Who knows why people do what they do? The point is they do it, and we can track and measure it with unprecedented fidelity. With enough data, the numbers speak for themselves." (Anderson, 2008)

Obviously, such approaches invoke applied rather than theoretical computer science, and constitute business plans rather than science. Even if the resulting description may again be termed models, they encode phenomenological and operational facts rather than hypothetical explanations. On the other hand, the same data can be treated with exact and logical methods without sacrificing the behavioural focus. From a theoretical perspective this approach turns away from explanation and prediction of states to classification and evaluation of behaviour.

In order to clarify the conceptual issues involved we need the notion of *streams*. A stream is a sequence of symbols from a finite alphabet where each symbol depicts an event at an interface. Attributes of streams are extensionally defined as the set of all streams which contain a respective property. Compiling all streams implies then capturing all attributes observed. However, the classification of behaviour into meaningful subsets and the assignment of appropriate and correlated labels remains a major task within this approach. Closely related is the theoretical question whether these sets of classes also have an *intensional* description as a formula. Such descriptions summarize the attributes in abstract notions of a mathematical language. Hence this results in the question which formal language is *expressive* enough for keeping the key intuitions about living systems? Which of these expressions are appropriate with respect to the empirical content?

Theoretical Aspects

In addition to the progress in computing power and storage capacities there is the theoretical side of computer science. The concepts formalising behaviour are phrased in terms of logical calculi. From this perspective one asks the perennial question of formal logics, namely whether valid formulas can be derived from an axiomatic system? Here *completeness* and *correctness* are the interesting properties: is there an axiomatic basis allowing for the deduction of all and only true/valid formulas, respectively?

Rosen (1991) proposed using *category* theory to formalise the modelling approach in biology and to specify how modelling relations of organisms differ from physical objects. This early introduction of categorial methods into life sciences provides the backdrop against which recent theoretical breakthroughs in computer science can be discussed below.

ONTIC AND EPISTEMIC STATES

We summarise the theoretical results in a non-formal manner. Two terms are used as the point of contact between empirical data and theoretical reasoning: *ontic* and *epistemic* states.

They stand behind one of the oldest and most important distinctions in western philosophy: between the world as it *is* and how it acts upon its observers, i.e. how a world *appears* to us or to other organisms. This distinction has been very useful for the systematic study of nature in a number of disciplines. In physics it has clarified the role of measurement and in mathematics the role of axioms and logic. Though none of these topics has been settled yet, the ability of distinguishing ontic from epistemic aspects is deeply implicated in the progress these disciplines took since the late 19th century. In ecology, however, this distinction has no prominent role today. Ecologist are typically pragmatically oriented, searching for empirical evidence in the form of field data and have little theory at the disposition to count on. Here we argue that the widespread neglect of the ontic–epistemic distinction can have severe consequences when judging models and the potential of new modelling techniques in ecology. We will take the implications of agent based models as an example how to represent, explain or evaluate behaviour of living systems.

Modern technology provides many examples of the difference between the way artefacts make their behavioural appearance in the world and their true internal state. Epistemically we perceive e.g. a red light on such machines when they display undesired behaviour, e.g. low battery, no coffee, or other malfunctions. Of course, the corresponding error states to this behaviour such as the red light are epistemic states and not the cause for the dysfunction. It rather signals an appropriate action to be taken by us, which in most cases does not involve at all the search for the true causal state of the problem. Neither does it help to distinguish proximate and ultimate causes. The degree to which we can ignore the causal states during the usage of these artefacts can be taken as a measure of a "ripeness" or robustness of technology. Computer science serves as the prime example here: It has become a design principle to impregnate a specified program behaviour against the various software and hardware options by which it can be implemented, often advertised as "compatibility". The behaviour of software is specified in a way which makes it general and abstracts from the details of implementations. This robustness is an explicit goal in human software design, and hence an ontic feature. It might be suspected that similar principles can be found behind the robustness of biological and ecological behaviour. As a sceptical scientist, one should then ask whether robustness of Life is ontic or epistemic.

The important point for the following discussion is distinguishing between the choice of access to a phenomenal realm and the choice of models which handle the transition between ontic and epistemic aspects, and the disappearance of the respective distinctions.

Historical Example: The Invention of Perspective

We start with a motivating example, albeit from a very different field: The historical change in the perception of space can be phrased in the ontic–epistemic distinction with respect to system states. From late antiquity up to the Gothic epoch there was no concept of space in the modern sense. Space without objects could only be talked about as emptiness, it had no properties. There was no abstract embedding of the painting of a scene as projecting from three to two dimensional patterns. Gothic painters had to focus on the ontic aspects, how people really are (and seen by God). People were placed into pictures due to the real size or due to their real importance and not how they appeared to us, due to their distance from the viewer. By contrast Renaissance painters used the epistemic states instead and mastered perspective as a technique of representation. They could distinguish between the real person and the model of it in the form of a painting.

They had a language in which the subjective (epistemic) impression of the observer of a scene could be handled objectively. This made the original (the real thing) and the impression in the eye of the observer congruent. The original could be replaced by the painting and the impression (from that point) would not change (see the instructions by Dürer how to do this). In other words they had a modelling language and praxis in which the change from ontic to epistemic could be controlled, while some aspects of the empirical realm remained invariant. This is also a fair description of modelling in physics: physical theory today is also a theory of the measurement process. This allows separation of concerns and a controlled transition between the two perspectives.

Actual Example: Simulators

The success of chess computers serves as a second example phrased in the ontic–epistemic distinction, but now with respect to system behaviour: These machines do not possess a winning strategy yet, but their performance has been boosted to world-champion level by improved evaluation abilities. Even for today's computer a typical prediction task from a midgame situation is unsolvable in general due to time constraints. That is why the ontic state, that is, the configuration of pieces on the chess board, cannot be linked effectively to the behavioral problems of interest: Who will be the winner? What is the final configuration of the game?

The epistemic state that both human and machine players act on consists of certain patterns of configuration that have been heuristically established. The machine representation of "behaviour space" is derived from already played games, preferably those between expert players. That is why modern chess computers can be regarded as local *representation* of the cultural memory in chess, while they remain unable to construct this memory autonomously from scratch.

The third example is checkers, where a winning strategy has indeed been discovered and implemented. The complete decision tree of this game has been annotated with corresponding potential final game configurations. In this case the configuration of checker pieces on the board is the effective ontic state, the behaviour can be reduced to a deterministic *function*. If white opens and plays a winning strategy the result is given. Black may remain ignorant about the fact the he will loose for most part of the game. In this case the choices made and human hopes experienced during such a game represent epistemic states only.

The above examples showed on the one hand the invention of a language expressive enough to characterize the distinction between epistemic and ontic states (typically by reflecting on the observation process and its limits). On the other hand the introduction of adequate models and formulas allows a smooth transition between them, ultimately obliterating the distinction: results from the formal derivation by (correct) model logic are the same as results from observations (phrased in an expressive language). In the perspective example this problem was posed for paintings: modelling of this process is successful when objects in represented abstract space appear indistinguishable from real space. In the gaming example the same problem was posed for choices: modelling of this process is successful when virtual choices and behaviour in represented (game) time appear indistinguishable from actual games (in real time). Note that in the first example temporal changes in objects are not important and can be abstracted from, while in the second example the inner state of players behind a game interface can be abstracted from.

Now we can turn to ecology and look there for corresponding cases. The key questions are: Firstly what attributes of the (empirical) world do we want to express in sufficiently expressive mathematical language?

- A behavioural, possible not locally decidable aspect, such as the ability to win a game, to master a situation in a simulator, the ability to have fertile offspring, or

- a configuration aspect, with possibly unforeseeable global consequences that appear as emergent behaviour, such as the reconstruction of local structure from simple building blocks.

Which of these aspects is more important in capturing intuitions about Life? There is no doubt that the mathematical tools will be different. And secondly how can we put the formulas (theorems) expressed in this language into a logical context? How do these theorems relate to formal deduction? Is there an axiomatic basis allowing to derive these formal expression as valid, in other words is there a theory available for a given realm? The advantage of category theory is that the theoretical possible answers to these questions can be derived within one framework and thus allowing to postpone the interpretation until after a modelling or simulation exercise. We will show below that current agent-based models, not only in ecology, come often hard-wired with an (extreme) implicit decision on these matters: ontic and epistemic descriptions are constructed as equivalent. In the remainder of this article, we shall argue that this decision is theoretically unnecessary, and empirically dubious.

Applied to Ecological Data

The behaviour of an organism is what is seen or experienced by human observers. Organisms cannot (yet?) be constructed from building blocks; they need to be taken out of one single (unique) context of natural history. That is why their behavioural aspects naturally dominate characterisations in ecology. Hence states of ecological systems come in the form of epistemic states. Corresponding ontic states (if they exist) need to be inferred (through a modelling exercise). Here we allow for the explicit possibility that organismic behaviour may include non-local attributes: for instance, the ability to eventually have fertile offspring is regarded as an adequate criterion for fitness.

In engineering problems, that is, in the design of system behaviour, similar non-local properties occur. They are often even necessary to rule out trivial, unproductive solutions; for instance, a computer program that guarantees never to answer incorrectly by simply not terminating, or a traffic light that prevents accidents by giving way to no one, or the prolonging of one's own lifespan by cryotechnology.

In theoretical computer science these features have been termed *liveness* properties. We suggest that the term carries more than metaphorical resemblance to its biological original, and that its mathematical explication can be re-imported backwards into theory of living systems. In

physical models these properties are not needed and typical models are designed to exclude them. In the modelling approaches discussed below, however, these possibilities are considered. Only in this more expressive language one is no longer forced to abstract from them before a quantitative modelling exercise is even started.

The typical definition of non-local properties in time series is extensional (the set of streams in which it occurs). The corresponding intensional abstract formulation can be provided by *modal/temporal logic*. From a theoretical viewpoint the empirically testable question is then whether or not liveness properties will turn out as helpful when coding the empirically intuitive aspects of living systems into simulation models. In order to test this, we select a mathematical approach which is unbiased in dealing with non-local properties.

The terminology introduced above allows a separation of the two following concerns:

Empirical grounding of models in local versus non-local features. This leaves open the decision whether or not non-local features such as liveness really exist in the world of living organisms; note that liveness is a technical term in computer science, while living organisms is a key concept in ecology.

Theoretical treatment of behaviour as a derived or fundamental feature (constructed by equational versus represented by modal logic, respectively). This leaves open the decision whether or not modal logic is indispensable in ecological theory, it leaves open the related question whether ecological systems may have a concise theoretical representation (in behaviour space) or whether this is impossible because their configuration is/appears as "too complex".

The first concern is addressed by decisions about the formal language for abstracting from data sets. The second concern is addressed by decisions about the formal tools for relating behavioural and configurational aspects in the model. This decision may reverse the relationship between fundamental and derived. In most physical models behaviour is reduced (simplified) to deterministic functions of changes in (ontic) states of the system. Here the characterisation of states is fundamental and the changes over time derived. In models of interactive games the fundamental role is taken by the space of possible behaviour while the (epistemic) states are reduced (simplified) to mere indicators of behavioural choices/classes at an interface. In current ABMs, as will be shown by a typical example from ecology, these details of the ontic–epistemic distinction are not left to the user, but already fixed tacitly by the software package.

EXAMPLE OF AN AGENT-BASED MODEL FROM ECOLOGY

The following case study describes a reinterpretation of an ecological model by Jovani and Grimm (2008), implemented on the popular ABM platform NetLogo (Wilensky, 1999). The model intends to explain the synchronicity of breeding behaviour in a bird colony in terms of the behaviour of individual birds. In its explanatory goal, as well as its numerical algorithm, the model resembles models in physics. The chosen model is regarded as a typical and pedagogical application of an ABM in ecology.[1] Our critique is aimedd at the mathematical structure of the model, which could be implemented in any ABM framework, not at the particular features of NetLogo. These models have become popular tools in social and life sciences mainly based on their pragmatic success in case studies. They allow the automated generation of global structural and behavioural patterns in a bottom-up manner, e.g. in self-organising systems from simple building blocks and their local interactions Gilbert (2008). Potentially they are powerful tools for generalising beyond case studies Grimm and Railsbeck (2005); Hauhs and Lange (2006).

As typical in ecology the case study starts with a characterisation of organismic behaviour. In a breeding colony birds show a wide range of interactive behaviour; they compete for space, defend nesting sites, attack neighbours, steal nesting material, fight and wound each other; but ultimately and almost miraculously they settle down calmly and begin breeding. In many environmental situations the synchrony in breeding is related to the overall reproduction success of a colony. Hence it is of interest for ecologists to understand the initiation and spread of behaviour which leads to synchrony. The goal of the ABM by Jovani and Grimm (2008) is reproducing and explaining the spatial breeding patterns in a bird colony from local interactions among neighbours.

Translated into an ABM

Characteristic features of the bird colony are translated into and simulated as an ABM. The *behaviour* of the neighbours of breeding birds is regarded as critical for the success of reproduction. The term *arousal* can be interpreted as an indicator whether a neighbour bird might for example tend to display aggressive or appeasing behaviour. Behaviour towards neighbour birds is the key observation (also for birds) to classify the "arousal state". Note that this classification of arousal as epistemic states for field ecologists, does not change with scale, or with proximate and ultimate "explanations". Even if field ecologists had mapped the DNA of successful and non-successfully reproducing birds from the colony that correlate with arousal these DNA states would still be epistemic states. Thus in the description of the ecological problem leading up to the design of an ABM it is clearly treated as an *epistemic* state identified by the corresponding behaviour.

In the subsequent modeling section of the article by

[1] We have used the code of the original model in student courses. It is used in a recent textbook on Individual Based Models Grimm and Railsback (2011) as one of the introductory examples into this modelling technique. It also appears as design on the associated web page.

Jovani and Grimm (2008) arousal becomes one of two *causal* state variables which characterise a bird in the ABM. The transition takes place in the sentence on page 2 when the authors state their hypothesis about a potential mechanism explaining synchronous behaviour: "If egg laying depends on ..." What could have continued as dealing with a classification of adaptive behaviour becomes from this point on a problem of searching for an explanatory mechanism of changes in an ontic state variable.

Within the subsequent sections on the ABM the arousal state is used as a typical causal (ontic) state from dynamical theory. Its use falls under the typical physical approach to modelling. The documentation scheme ODD (Overview, Design concepts and Details) for ABMs does not include nor require criteria which would allow distinguishing between causal (ontic) or epistemic states Grimm et al. (2006); Grimm and Railsback (2011). ODD intends to make the theoretical assumptions clearer such that the model is easier to reproduce Grimm and Railsback (2011). It does so by imposing a translation scheme into a dynamical system which closely matches physical models. This reflects the way in which many ecologists think about their system and the way in which most computer programs are developed in ecology. However, it restricts the running ABM computer codes to only one of the two possible interpretations, see below. This pre-selected abstraction and implicit model choice may even be the less-suited one as it is argued here the case of the breeding birds.

The article by Jovani and Grimm (2008) deals with epistemic states throughout the introduction. Then, in the section specifying the ABM only causal states are used, and with the first sentence of the discussion the reader is taken back to the perspective of epistemic states, when the relevance for synchronicity in breeding is discussed as adaptive behaviour or not.

Jovani and Grimm (2008) propose a number of field observations which can be predicted from their model. None of these takes the model out of the range of observations discussed in the introduction. It can be argued that the ABM can serve as a valuable tool for testing the consistency among different field observations. In this sense ABMs can be used as pragmatic communication tool about case studies; seemingly without much theoretical overhead. For physical models proper, by contrast, only predictions beyond the range of previous observations, so-called *nontrivial* predictions, count as a full validation.

DISCUSSION

Terminology such as "mechanism", "prediction" or "explanation" in the introduction and discussion of their paper is by no means unique for Jovani and Grimm. It reflects the general use of these terms in ecology, in particular in not distinguishing the two types of prediction. One advantage of the ABM is thus that it makes this terminology amenable to formalisation and critique by offering an alternate interpretation. There are several possibilities of deriving categorial formalisation of the breeding colony. Three of them will be presented and discussed informally.

Formalised as Bialgebra

A bialgebra is a mathematical form of models in which the complete possible behaviour is distributed stepwise over local (ontic, causal) states. A bialgebra implies two parallel decisions in the choices posed at the end of the preceding section: Behaviour cannot extend beyond deterministic functions (restricting observations to local properties) and is dependent on state changes (ontic states as fundamental to the dynamics). It has been shown that the mathematical structures underlying the ABM by Jovani and Grimm (2008) and many other typical and pedagogical examples, namely multidimensional cellular automata, can indeed be phrased as bialgebras (Trancón y Widemann and Hauhs, 2011). The analysis is mainly on the level of semantics, but for simple models such as the one of Jovani and Grimm (2008), the bialgebraic form directly yields a feasible algorithm for reimplementation and reproduction of results.

Such an approach implements the strongest possible assumptions about relationships between states and behaviour in the modelled realm. In a bialgebra epistemic states are set as congruent with ontic states and the complete behaviour can be set in a one-to-one mapping from these states. Thus behaviour can be predicted from the states, and these can be uniquely identified by observable behaviour in turn; the model is *fully abstract* in the jargon of theoretical computer science. Such models represent a maximal combination of constraints: behaviour has only locally observable attributes and system states can be constructed from attributes of building blocks. Philosophically this represent a modern form of Laplace's Demon or an "anti-holistic" modelling universe. Emergence in the sense of aggregate behaviour that is not *logically* determined by constituent behaviour is excluded in such a universe.

This new theoretical approach has the advantage that it separates the theoretical concerns and allows a second alternate (behavioural) interpretation in the ecological realm. In a categorial framework the decisions on interpretation and modelling paradigms can be separated from and made independently, even after the modelling! This is only possible because the change of perspective affects only the meta-level language of discussions about the model, but not the logics within the model, since by virtue of the bialgebraic structure, behaviour and states are fully equivalent in such a "reductionist's paradise".

The caveat of using a bialgebra is that it combines two drastic abstractions: In physical (functional) models one abstracts from non-local behaviour reducing any observed change to a deterministic function while retaining an advanced powerful concept of causal observable states. In interactive (game) models one abstracts

from causal (effective) states, while retaining an advanced powerful concept of non-local behavioural attributes (such as fairness, liveness, etc.). The two modelling approaches are categorical duals of each other (Hauhs and Trancón y Widemann, 2010), with their own respective testing criteria and blind spots. In the bialgebra approach, however, the two strong simplifying assumptions are made at the same time, by treating epistemic states as causal and interactive behaviour as functional. This puts a heavy load on the user arguing in favour of its plausibility. In addition it leaves this type of ABMs stranded between difficulties of testing against empirical data and difficult theoretical justifications.

Formalised as Course-of-Value Recursion

The next step towards a more powerful and expressive conceptual basis is dropping the identity of epistemic and ontic states on which the bialgebra was based. Instead of using the full-blown notion of ontic states with their implied causal power, only epistemic states are used, which are more readily supported by empirical data. Documented behaviour must be extended over time, that is why a more advanced instrument is needed than in the previous example for dealing with history. In a bialgebra one temporal slice of the system's state fixes future behaviour. Here epistemic states need to be recursively defined through past behaviour. This is not accommodated by the type of recursive relationship underlying state transitions in dynamical systems, which deal with instants only. A suitably generalized form of recursion has been formalized in the category-theoretic framework (Uustalu and Vene, 1999).

The resulting "historic space" is highly redundant, but models can be understood to operate on virtual states represented as equivalence classes of histories with undistinguishable future behaviour (Trancón y Widemann, 2012). The resulting models will resemble physical models and will still be able to construct trajectories. They could still seek explanation in the sense of traditional ABMs, but the assumption about accessible ontic states or the implicit identity between ontic and epistemic states is dropped. Hence models could allow a much more careful interpretation of observations, while keeping the (reductionist's) optimism about theory and explanations and predictions.

Formalised as Coalgebra

The fullest application of an alternate approach would use coalgebras as the fundamental level in an ABM. The coalgebraic approach subsumes a variety of high-level system models such as automata, graphs and networks, and behavioral differential equations (Jacobs and Rutten, 1997; Rutten, 2000), but is not recognized theoretically outside core computer science. Hence there is no real-world ecological example available today. Only a simple application to the logistic map following an idea due to Rutten (2000) has been made (Hauhs and Trancón y Widemann, 2010). The goal is to keep the model firmly in the behavioural perspective, while using only epistemic states as indicators of the undistinguishable classes in behaviour. At the same time a corresponding temporal logic could be applied and tested for the occurrance of non-local properties in the empirical data base. It is known that modal and temporal logic relate to coalgebraic models and theories in the same natural way as equations do to the algebraic models of physics (Cîrstea et al., 2008).

The "agents" in such a ABM could no longer be used in order to explain a phenomenon, but only to assess and evaluate the accumulated observations. Confer the famous "dining philosophers", a completely non-causal but nevertheless extremely illuminating model of resource contention. Applications of such models in ecology would resemble more the use of a flight simulator as a tool facilitating the communication within an expert group, rather than the use of non-trivially predictive simulators such as behind weather reports. A "flight simulator for foresters" in form of an interactive growth simulator of managed forests is another example of the former approach (Hauhs et al., 2003). In contrast to the case study discussed above, coalgebraic ABMs will clearly delineate the task of *evalulating* a given behaviour in given environment as adaptive, from the task of explaining or *predicting* this behaviour from observable states.

CONCLUSION

Here it is suggested that users of ABMs start looking at the mathematical structures beneath the friendly and versatile interfaces of their programs. This friendliness, as in the case study above, may come with a heavy philosophical load, of which many user may not be aware. With the help of theoretical computer science these structures can be unravelled and reversed, the implicit assumptions relaxed and other views at living systems may be opened for quantitative and formal assessment. There is a parallel move on the side of theoretical computer science where new formal tools for expressing behaviour and formalising choices are ready and searching for application in new fields. ABMs have the potential serving the role as an exchange between the empirical side of "complex system sciences" and the theoretical side of computer science. In order to develop this niche further, however, some of the now implicit assumptions in these models have to be lifted to the surface and put under control of their users.

The new approach provides a new perspective at typical problems in ecology: Models are not capable of providing non-trivial predictions. They need to be calibrated and are often more a concise summary of patterns in large, multidimensional datasets rather than an explanation of what goes on in an ecosystem. From the perspective of the categorial framework it is no longer necessary that these features are taken as characteristic of the ecosystem itself, e.g. because it must be supposed that living systems are inevitably complex ones. There is

a second reading of these modelling problems, they may directly result from inappropriate modelling approaches. To begin with, becoming more aware of these issues ecological modellers need to reflect on the ontic epistemic distinction when introducing state variables.

REFERENCES

Anderson, C. (2008). The end of theory: The data deluge makes the scientific method obsolete. *Wired Magazine*, 16.

Cîrstea, C., Kurz, A., Pattinson, D., Schröder, L., and Venema, Y. (2008). Modal logics are coalgebraic. In *BCS Visions in Computer Science*.

Gilbert, N. (2008). *Agent-Based Models*. Sage Publications, London.

Grimm, V., Berger, U., Bastiansen, F., Eliassen, S., Ginot, V., Giske, J., Goss-Custard, J., Grand, T., Heinz, S., Huse, G., Huth, A., Jepsen, J., Jørgensen, C., Mooij, W., Müller, B., Pe'er, G., Piou, C., Railsback, S., Robbins, A., Robbins, M., Rossmanith, E., Rüger, N., Strand, E., Souissi, S., Stillman, R., Vabø, R., Visser, U., and DeAngelis, D. (2006). A standard protocol for describing individual-based and agent-based models. *Ecological Modelling*, 198(1-2):115–126.

Grimm, V. and Railsback, S. F. (2011). *Agent-based and Individual-based Modeling: A Practical Introduction*. Princeton University Press.

Grimm, V. and Railsbeck, S. (2005). *Individual-based Modeling and Ecology*. Princeton University Press, Princeton.

Hauhs, M., Knauft, F.-J., and Lange, H. (2003). Algorithmic and interactive approaches to stand growth modelling. In Amaro, A. and Reed, D., editors, *Modelling Forest Systems*, pages 51–62. CABI Publishing, Wallingford, UK.

Hauhs, M. and Lange, H. (2006). Foundations for the simulation of ecosystems. In Lenhard, J., Küppers, G., and Shinn, T., editors, *Sociology of the Sciences Yearbook*, volume 25, pages 57–77. Kluwer Academic Publishers: Dordrecht, Bielefeld.

Hauhs, M. and Trancón y Widemann, B. (2010). Applications of algebra and coalgebra in scientific modelling, illustrated with the logistic map. *Electronic Notes in Theoretical Computer Science*, 264(2):105–123.

Jacobs, B. and Rutten, J. (1997). A tutorial on (co)algebras and (co)induction. *EATCS Bulletin*, 62:222–259.

Jovani, R. and Grimm, V. (2008). Breeding synchrony in colonial birds: from local stress to global harmony. *Proc. R. Soc. B*, 275:1557–1563.

Peters, R. H. (1991). *A critique for ecology*. Cambridge University Press.

Rosen, R. (1991). *Life Itself: A Comprehensive Inquiry into the Nature, Origin, and Fabrication of Life*. Columbia University Press, New York.

Rutten, J. (2000). Universal coalgebra: a theory of systems. *Theoretical Computer Science*, 249(1):3–80.

Trancón y Widemann, B. (2012). State-based simulation of linear course-of-value iteration. In *Draft Proceedings 11th International Workshop on Coalgebraic Methods in Computer Science (CMCS 2012)*. In review.

Trancón y Widemann, B. and Hauhs, M. (2011). Distributive-law semantics for cellular automata and agent-based models. In Corradini, A., Klin, B., and Cîrstea, C., editors, *Proceedings 4th International Conference on Algebra and Coalgebra (CALCO 2011)*, volume 6859 of *Lecture Notes in Computer Science*, pages 344–358. Springer.

Uustalu, T. and Vene, V. (1999). Primitive (co)recursion and course-of-value (co)iteration, categorically. *Informatica*, 10(1):5–26.

Wilensky, U. (1999). *NetLogo*. Center for Connected Learning and Computer-Based Modeling, Northwestern University, Evanston, IL.

AUTHOR BIOGRAPHIES

Michael HAUHS is Professor of Ecological Modelling at the University of Bayreuth, Germany. He teaches geoecology and environment informatics. He has published on water transport models, forest growth models, Artificial Life, and the theoretical basis of modelling. He holds a Diploma and a PhD from Göttingen University, Germany.

Baltasar TRANCÓN Y WIDEMANN is assistant professor at the chair of ecological modelling at the University of Bayreuth. He has studied computer science and received a PhD from the Technical University of Berlin. He has worked as postdoc in Limerick and has specialised on the semantics of computer languages, Coalgebra and functional programming.

AN AGENT-BASED MODEL FOR THE CONTROL OF MALARIA USING GENETICALLY MODIFIED VECTORS

Ana María Reyes, Hernando Díaz and Andrés Olarte
Department of Electrical and Electronic Engineering
Universidad Nacional de Colombia
Bogotá, Colombia
E-mail: amreyesp@unal.edu.co, hdiazmo@unal.edu.co, faolarted@unal.edu.co

KEYWORDS
Malaria, Agent Based Model, Population Dynamics, Epidemic Vectors, Transgenic Population, Fitness.

ABSTRACT

An agent-based model was developed to assess the use of Genetically Modified Mosquitoes (GMMs) as a control strategy for the Malaria epidemic. Mosquitoes responsible for the transmission of Malaria (vectors) have been modified genetically so that the probability of transmitting the parasite causing the disease when biting a human being is reduced with respect to wild type vectors. Our model represents the population dynamics of the introduction of a transgenic strain of malaria vectors of the species *Anopheles Gambiae*. In the model three different types of agents were included: wild type, homozygous and heterozygous transgenic mosquitoes. Each agent is characterized by a fitness parameter that represents a reproduction rate, relative to the wild type population. The model considers specific biological processes such as: gonotrophic cycle (the average interval between successive blood meals), egg maturation time and life cycle of the vector. Additionally, some spatial aspects such as: biting zones (human settlements) and water zones (breeding places) were included in the model to consider the influence of environmental conditions. Through simulations it was observed that the model represents adequately the dynamics of Malaria vectors. These results may be used to evaluate different control strategies considering spatial and environmental features.

INTRODUCTION

Malaria is one of the tropical diseases that have greater impact in terms of mortality and morbidity in the world. Annually, over a million people die due to this disease and almost 3200 million people in 107 countries and territories are in risk of developing it (WHO 2010). Currently, it is estimated that more than half of humanity is exposed to infection and unless new control measures are considered, the toll will be doubled in the next 20 years due to the effect of phenomena associated with climate change (Breman, 2001).

The disease is transmitted to humans by a mosquito of the genus Anopheles, when an infected female takes a blood meal. Traditional control measures for Malaria such as drug treatments, elimination or reduction of the vector's nesting places and the use of insecticides combined with bed nets, are not enough to control the spread of the disease. An effective vaccine is still far into the future (Ruiz et al. 2006).

In order to find more effective measures that can halt Malaria transmission, alternative strategies have been oriented to reduce or modify the vector population. In recent years, researchers have successfully developed genetically modified mosquitoes that are impaired for transmission of *Plasmodium berghei.* That seemed to reduce in an important level the transmission of the disease in controlled conditions (Ito et al., 2002). Later, it was established that GMMs had some fitness advantage over the wild type that could make them prevail (Gould et al., 2006). Therefore, a control strategy based on introducing GMMs into the wild mosquito population could be proposed.

On the other hand, literature on modeling of vector-borne disease spread, particularly Malaria, is abundant. There are many mathematical models that use ODEs (Ordinary Differential Equations) to represent interactions between humans and vectors as a function of time. Some of these models include environmental factors. Statistical models have also been proposed to predict the spatial distribution of vectors based on environmental variables. These models have showed the importance of combining spatial and temporal aspects of the spread of vector-borne diseases (Muller et al., 2004).

Boëte and Koella (2002) obtained a remarkable result from their stochastic model to study the spread of the refractory allele in the vector population. Their results show that if the refractoriness of transgenic vectors is not perfect (infectiousness equal to zero) then its effect on the epidemic will be totally insignificant.

Smith et al. (2006) developed an integrated dynamic mathematical model for predicting the economic and epidemiologic impact of a Malaria vaccine. This model is comprised of sub-models that were validated with data obtained from studies performed in Africa. One of the strengths of this modeling approach, is the possibility of consider many biological aspects in order to get a more realistic representation of the complex Malaria life cycle.

Proceedings 26th European Conference on Modelling and Simulation ©ECMS Klaus G. Troitzsch, Michael Möhring, Ulf Lotzmann (Editors)
ISBN: 978-0-9564944-4-3 / ISBN: 978-0-9564944-5-0 (CD)

A mathematical model was used to analyze conditions for sweeping the wild type by GMMs (Lambrechts et al. 2007). Results showed that the fitness advantage of Malaria refractoriness might be reduced by the cost associated with two copies of the allele in the homozygous population. Consequently, the epidemic cannot substantially be reduced unless the transgenic vectors sweep the wild type.

Diaz et al. (2011) implemented a differential equation-based model that represents mosquito population dynamics when genetically modified individuals are introduced into a wild type population. The model describes the dynamics of gene selection under sexual reproduction in a closed vector population, showing that the determinant parameter for a complete invasion is the fitness of the resulting heterozygous population. In order to determine how feasible would be to control a Malaria epidemic, they combined the vector population model with an epidemiological model.

As an alternative to mathematical models, Agent-Based Models (ABM) have been proposed to represent the determinant factors in disease transmitting and their interactions in a specific spatial environment. ABMs are stochastic models that are used to describe interactions among agents of a population. The behavior of these agents is established by a simple set of rules (Bousquet et al. 2004). Linard et al. (2008) developed multi-agent simulations to evaluate the risk of Malaria reemergence in the south of France. This model represents different agents (mosquitoes, people, animals and environment) that can influence the disease transmission. The model simulates temporal and spatial variations in the biting rate of mosquitoes. These variations depend on the distribution of humans and vectors, their behavior and interactions.

In this paper we present an agent based model that takes into account vector population dynamics and the introduction of a relatively small invading population of transgenic mosquitoes that are partially refractory to Malaria. GMMs reproduce sexually with the existing wild type and fitness conditions are analyzed by massive simulations. The model allowed establishing conditions for an invasion to be successful.

THE MODEL

In this section, the model is described following the standard ODD protocol (Overview, Design concepts, and Details) for individual-based and agent-based models (Grimm et al., 2006). The Unified Modeling Language (UML) is used for this description, including a class diagram (Booch et al., 2004).

Overview

The main phenomenon modeled in this ABM is the vector feeding cycle that involves mobile agents of the model (mosquitoes); this process is represented in figure 1. When new mosquitoes emerge from breeding sites, they mate and females search for a blood meal to complete the egg development. After the mosquito has found a host and has bitten it, it looks for a resting place where it can digest the blood. This process takes between two and three days in tropical areas. Then, the mosquito flies looking for a breeding site to lay the eggs. Finally, the mosquito lays the eggs and starts over again the feeding cycle seeking a host (Chitnis et al., 2010).

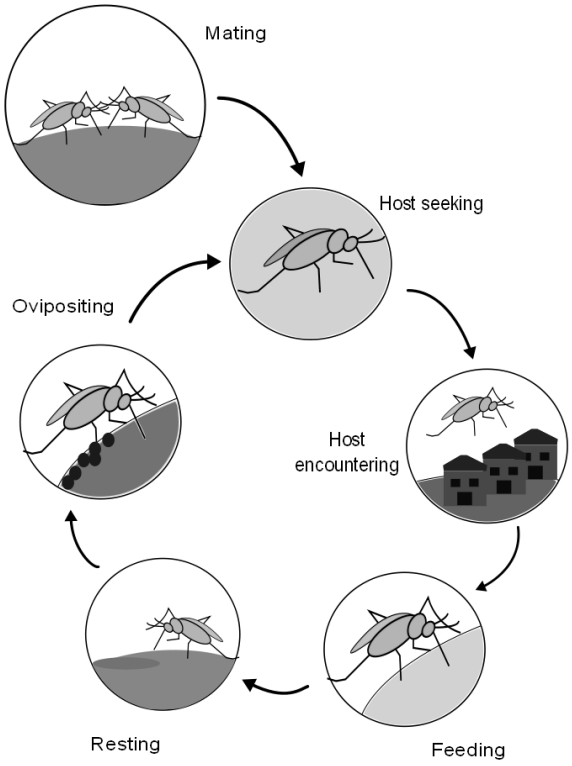

Figure 1: Mosquito feeding cycle.

Purpose

The purpose of the model is to simulate spatial and temporal variations of Malaria vectors including the transgenic population. The main objective is to understand the factors that control these variations and evaluate the possibility of using GMMs as a control strategy.

State Variables and Scales

The model focuses on *Anopheles Gambiae*, which is represented in the model by mobile agents. These agents have some attributes that lead them to interact with the environment, with other agents and that determine the dynamics of the entire population. The mosquito fitness is one of these attributes. In our model this condition is represented by a variation in the average number of eggs that a mosquito of a specific genotype can lay. In this way, a mosquito with a higher

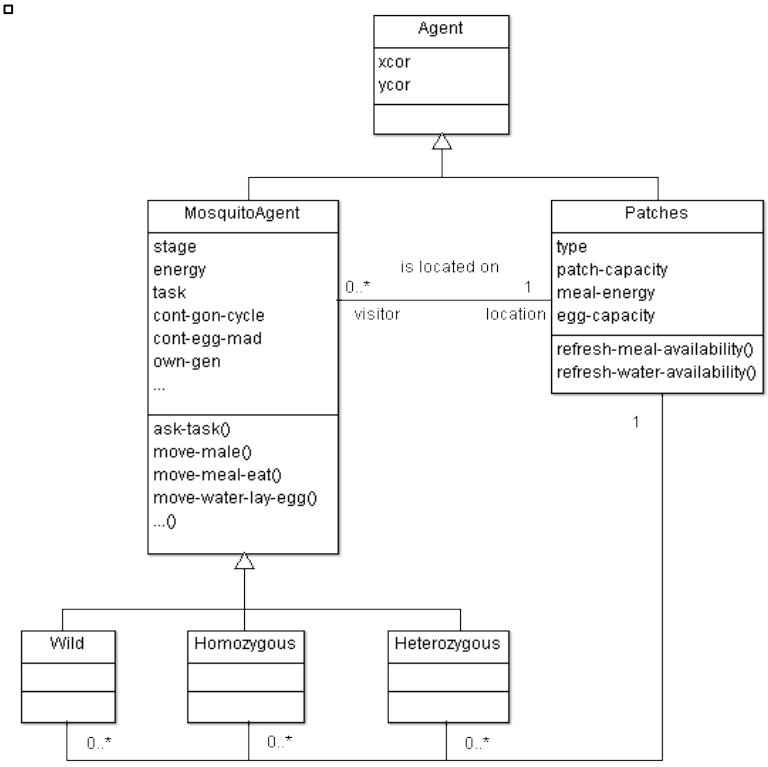

Figure 2: UML Class Diagram of the ABM.

fitness in relation with the wild type lays more eggs, whereas a mosquito with a lower fitness decreases the production of eggs. Fitness is an essential characteristic in the competition among populations of mosquitoes and a key factor for establishing conditions in which it is possible to use genetically modified vectors as a strategy to control the Malaria.

In the model, the landscape is represented by a grid that is formed by a group of cells (patches), which works as a spatial support for the movements and interactions among mosquitoes. In addition, patches have a set of attributes that can be sensed by the mosquitoes.

Figure 2 presents the UML class diagram of agents that compose the model. Rectangles in this diagram represent a set of objects (agents) that share the same attributes, operations, relationships and semantics. Each agent has a coordinate (xcor, ycor) that defines its location on the grid. Each patch of the grid is characterized mainly by four attributes: type, patch-capacity, meal-energyand egg-capacity.

The load capacity or patch capacity is related to the population of mosquitoes that each cell can support. The meal availability or meal-energy reflects the presence or absence of humans on each cell. This cell's attribute can be sensed by a mosquito and determine places where a mosquito can have a blood meal. A cell with nonzero meal availability implies that human settlements are located there and, therefore, a mosquito could have a blood meal on that cell. Finally, each cell belongs to one of three types of land: water-type, meal-type and land-type. This is an important attribute that determines cells where the mosquitoes are able to develop different activities such as laying eggs or biting a human.

Mobile agents have also a set of attributes that characterize them. Wild, homozygous and heterozygous mosquitoes are mobile agents that have the same attributes and operations described for mobile agents in Figure 2. Some of these attributes are: stage, energy, fitness, a counter of gonotrophic cycle and a counter of egg maturation. The stage is related with the level of maturation of the mosquito. Immature stage includes the egg, pupae and larvae stage, and the mature stage represents the adult mosquito. The energy is an important attribute that determines the capacity of the mosquito to perform an activity. This parameter decreases when the mosquito flies, lay eggs and mate, and increases when the mosquito gets a blood meal. The gonotrophic cycle counter establishes the time necessary to complete the cycle. The egg maturation counter determines the time elapsed before the mosquito can lay its eggs after a blood meal.

In addition, each type of agent (mosquitoes and patches) can perform a set of operations that determine its behavior and the way they react to external factors. Mosquitoes can develop the following activities: seek a

mate, move to a meal and eat, move to water and lay eggs. Patches have some other operations like refresh meal or water availability.
Time is modeled as discrete time steps. Each time step represents a time period of six hours.

Process Overview and Scheduling
At each time step, the same sequence of procedures is activated and always in the same order. Similarly, each procedure is either applied by an agent or by the scheduler level.

After updating global variables and setting up the model, each mosquito, at each time step, can perform one out of three possible activities: find a mate and reproduce (activity that is carried out by the mosquito only once in the model), find a concentration of humans and have a blood meal or find a breeding site and lay eggs. At the scheduler level in each time step, the availability of water and blood-meal sites is updated.

Changes in blood-meal availability depend on the time of the day. Since mosquitoes bite mostly from dusk to midnight, the attribute of each patch reflecting the presence of humans is only activated once every four time periods. Finally, population density is saved at the scheduler level.

Design Concepts

Observation
The user interface of the model displays spatial and temporal variations of the abundance of mosquitoes. It also shows the proportion of each genotype and the total number of mosquitoes in the immature and mature stage.

Sensing
Mosquitoes react to external environmental factors such as: temperature (affects biological aspects of the mosquitoes like the gonotrophic cycle and the development rate of the egg), blood-meal sites (presence of humans) and breeding sites (water reservoirs).

Interactions
The dynamics of the system is driven by interactions between mosquitoes and land. Mosquitoes seek other mosquitoes to reproduce, and then they search blood-meal sites to bite a human host and mature their eggs. Finally, once the egg is mature and mosquitoes are ready to oviposit, they look for a breeding site to lay their eggs.

The type of land defines the cells in which the mosquitoes can bite a human host or lay their eggs. Additionally, the number of breeding sites changes seasonally due to variations in rainfall. These changes in land influence the time required for the development of immature mosquitoes and also the gonotrophic cycle. Thus the vector population dynamics becomes affected.

Details

The model was implemented using NetLogo, a free programmable environment for the modeling of complex phenomena (Wilensky, 1999).

Initialization
Initial conditions of the model are mainly defined by the user or programmer. Parameters such as the initial number of wild, homozygous and heterozygous mosquitoes are established by the user, as well as the fitness of each type of mosquito. Initial number of patches associated with human concentrations and temperature value can also be defined for each simulation run. Finally, the location of mosquitoes, water patches and meal patches can be randomly established.

SIMULATION

This stage allows observing the behavior of the model. Then, a set of different setup conditions was tested to observe model's predictions. Simulations performed with the model were mainly done to determine conditions under which it is possible to use genetically modified vectors as a strategy to control the Malaria.

Given the stochastic elements in the model, we performed 100 simulations for each condition we analyzed. We tested the model in three different setup conditions mostly related with variations in the mosquito's fitness. One condition referred to the case where the heterozygous and homozygous are better adapted. Another one, where only the homozygous are the better adapted while the heterozygous are less adapted than the wild type. Finally, a third condition was studied, in which the heterozygous are much better adapted and the homozygous are less adapted. In all simulations, we consider the introduction of only 1% of GMMs on the total population of mosquitoes. A population of 5000 mosquitoes and a grid size that represents a landscape of one square kilometer was utilized in all simulations.

SIMULATION RESULTS

Results from simulations of the model in different setup conditions showed that fitness is the determinant parameter to establish strategy success. For all simulation cases, the dynamics of the population of mature mosquitoes were studied for ten years, the temperature value was 35 degrees Celsius, locations associated with human settlements corresponded to 1% of the environment simulated and the extension of water reservoirs varied seasonally between 0.5% and 1% of the number of patches.

As an example, simulation results of just one of the scenarios related with a particular setup condition are

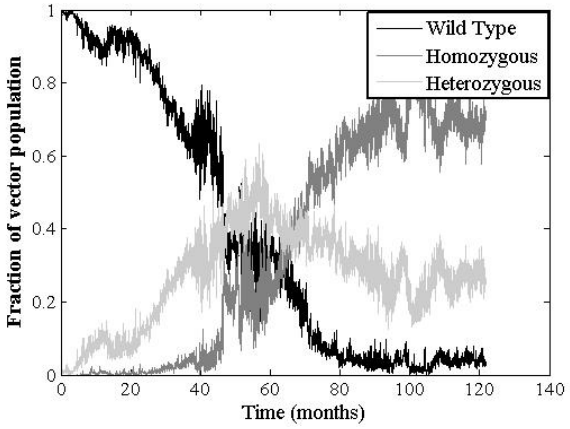

Figure 3: Time evolution of vector populations.
Heterozygous Fitness = 1.05.
Homozygous Fitness = 1.1.
Wild Fitness = 1.

presented. Figure 3 shows the time evolution of vector populations, when the heterozygous and homozygous are better adapted (heterozygous fitness = 1.05, homozygous fitness = 1.1, wild type = 1).

In this case, at the beginning most of the population corresponds to the wild type and the proportion of heterozygous and homozygous vectors is very low. After five years, the density of different populations of vectors is practically the same and thenceforth the proportion of homozygous and heterozygous mosquitoes increases. Finally, nine years after the invading process started, the wild type has been practically swept by the population of transgenic heterozygous and homozygous mosquitoes. Therefore, this could be a good scenario for Malaria control, since most of the vectors are less capable of transmitting the parasite. Results from the simulation experiment are consistent with the results reported with the Malaria vectors dynamic obtained by Díaz et al. (2011).

CONCLUSIONS

An agent-based model of the population effect of introducing transgenic mosquitoes into a wild type population was presented. The model was developed to simulate spatial-temporal variations in the populations of Malaria vectors. Using this model, different conditions can be analyzed to establish conditions when a small invasion of genetically modified mosquitoes has any chance of controlling a Malaria epidemic.

As a future work, other conditions will be assessed including not only the GMMs, but also environmental factors such as temperature and rainfall variations. Additionally, the model will be complemented by including a human population in order to represent the dynamics of a Malaria epidemic. Finally, we will use the model to evaluate different strategies for the Malaria control taking into account spatial aspects.

REFERENCES

Boete, C., Koella, J.C., 2002. A theoretical approach to predicting the success of genetic manipulation of malaria mosquitoes in malaria control.*Malaria J. 1, 3.*

Booch, G., Rumbaugh, J., Jacobson, I., 2004. *The Unified Modeling Language User Guide*. Addison-Wesley, Boston, USA, 482 pp.

Breman J., 2001. The ears of the hippopotamus: manifestations, determinants, and estimates of the malaria burden. *The American Journal of Tropical Medicine and Hygiene*, 64:1–11.

Bousquet F. and Le Pageb C., 2004. Multi-agent simulations and ecosystem management: a review. *Ecological Modeling,* 176:313–332.

Chitnis N., Schapira A., Smith T., Steketee R., 2010. Comparing the effectiveness of Malaria vector-control interventions through a mathematical model. Am. J. Trop. *Med. Hyg., 83(2),* 2010, pp. 230–240.

Depinay, J.M., Mbogo, C., Killen, G., Knols, B., Beier, J., Carlson, J., Dushoff, J., Bilingsley, P., Mwambi, H., Githure, J., Toure, A., McKenzie, E., 2004. A simulation model of African Anopheles ecology and population dynamics for the analysis of malaria transmission.*Biomed Central.* 3-29.

Diaz, H., Olarte, A., Ramirez, A., Clavijo, C., 2011. A model for the control of malaria using genetically modified vectors. *Journal of Theoretical Biology 276* (2011) 57-66.

Gould, F., Magori, K., Huang, Y., 2006.Genetic strategies for controlling mosquito-borne diseases.*Amer. Scien 94*, 238.

Grimm, V., Berger, U., Bastiansen, F., Eliassen, S., Ginot, V., Giske, J., Goss-Custard, J., Grand, T., Heinz, S.K., Huse, G., Huth, A., Jepsen, J.U., Jorgensen, C., Mooij, W.M., Muller, B., Pe'er, G., Piou, C., Railsback, S.F., Robbins, A.M., Robbins, M.M., Rossmanith, E., Ruger, N., Strand, E., Souissi, S., Stillman, R.A., Vabo, R., Visser, U., DeAngelis, D.L., 2006. A standard protocol for describing individual-based and agent-based models.*Ecol. Model. 198* (1–2), 115–126.

Harris, A., Matias-Arnéz, A., Hill, N., 2005. Biting time of Anopheles darlingi in the Bolivian Amazon and implications for control of malaria. *Transactions of the Royal Society of Tropical Medicine and Hygiene,* 100, 45-47.

Ito, J., Ghosh, A., Moreira, L.A., Wimmer, E.A., Jacobs-Lorena, M., 2002. Transgenic anophelinemosqitoes impaired in transmission of a malaria parasite. *Nature 417*, 452.

Lambrechts, L., Koella, J.C., Boete, C., 2007. Can transgenic mosquitoes afford the fitness cost?.*Trends Parasitol.* 24, 4.

Linard C., Poncon N., Fontenille D., Lambin E., 2008.A multi-agent simulation toassess the risk of malaria re-emergence in southern France.*Ecological Modeling*, 220:160–174.

Muller, G., Grébaut, P., Gouteux, J., 2004. An agent-based model of sleeping sickness: simulation trials of a forest focus in southern Cameroon. *C. R. Biol*. 327, 1–11.

Ruiz D., Poveda G., Velez I., Quiñones M., Rua G., Velasquez L., Zuluaga J., 2006. Modeling entomological-climatic interactions of Plasmodium falciparum malaria transmission in two Colombian endemic-regions: contributions to a National Malaria Early Warning System. *Malaria Journal* 2006, 5:66.

Smith T., Killen G., Maire N., Ross A., Molineaux L., Tediosi F., Hutton G., Utzinger J., Dietz K., Tanner M.,

2006. Mathematical Modeling of the Impact of Malaria Vaccines on the Clinical Epidemiology and Natural History of Plasmodium Falciparum Malaria: Overview. *Am. J. Trop. Med. Hyg.,*75(Suppl 2) , pp. 1–10.

Twonson, H., 2009. SIT for african malaria vectors: Epilogue. *Malaria J.8, S10.*

WHO (World Health Organization), 2010. Report on Malaria in the world. Available in: www.who.int/es/index.html .

Wilensky, U., 1999. NetLogo. Available in: http://ccl.northwestern.edu/netlogo/.

AUTHOR BIOGRAPHIES

ANA MARIA REYES was born in Bogotá, Colombia and went to the National University of Colombia, where she studied electronic engineering and obtained her degree in 2011. Actually, she is working in her master thesis in the program of Industrial Automation.
Her e-mail address is: amreyesp@unal.edu.co

HERNANDO DIAZ received a B.S. in Electrical Engineering from the National University of Colombia in 1978. He was awarded an M.S. Degree in Electric Power Engineering and a Ph. D. in Electrical Engineering from Rensselaer Polytechnic Institute, Troy, NY in 1984 and 1986, respectively. He has been with the Department of Electrical Engineering at the National University of Colombia, Bogota, where he is a Professor.
Prof. Diaz's main research interest is in modeling nonlinear dynamical systems with application to complex phenomena.
His e-mail address is: hdiazmo@unal.edu.co

ANDRES OLARTE received a B.S. in Electronics Engineering from the Universidad Distrital, Bogota, Colombia in 2005. He was awarded an M.S. Degree in Industrial Automation from National University of Colombia in 2007 and a Ph. D. in Electrical Engineering at the same institution.
Dr. Olarte's research interests are modeling of complex nonlinear systems and parameter estimation algorithms.
His e-mail address is: faolarted@unal.edu.co

SIMULATION OF ETHNIC CONFLICTS IN FORMER YUGOSLAVIA

Suvad Markisic
Inst. of Information Systems Research
University of Koblenz
Universitätsstr. 1, Koblenz 56070,
Germany
markisic@uni-koblenz.de

Martin Neumann
Institute for Sociology
RWTH Aachen University
Eilfschornsteinstr. 7, 52062 Aachen,
Germany
mneumann@soziologie.rwth-aachen.de

Ulf Lotzmann
Inst. of Information Systems Research
University of Koblenz
Universitätsstr. 1, Koblenz 56070,
Germany
ulf@uni-koblenz.de

KEYWORDS
Social dynamics and collective behaviour, Yugoslavia, Ethnic conflict, Ethnic norm, Norm innovation, Social simulation, Normative agents

ABSTRACT

The paper describes an agent-based model of the escalation of inner-state ethnic conflicts. Model assumptions are derived from the case of the former Yugoslavia. To comprehend the appearance of war crimes, the model refers to the concept of ethnic norms. The cognitive complexity of norm emergence is represented by using the simulation tool EMIL-S. The model consists of two agent classes: politicians, who enforce value orientations, and citizens, who form paramilitary militia. Simulation results confirm the feasibility of the theoretical approach.

INTRODUCTION

Twenty years ago, the phenomenon of war re-appeared in Europe. Unlike the peaceful secession of Czechoslovakia, for instance, the breakdown of Yugoslavia was extremely violent. The series of wars went hand in hand with serious crimes that captured the attention of the world community. On the one hand, attempts to recruit young Serbian men for the army where rather unsuccessful. On the other hand crimes where undertaken by civilians who were not part of organised armed forces.
The events in the former Yugoslavia had been a prime example for changing the focus of security studies from inter-state conflicts to inner-state societal security (Williams 2003). For instance, the term of so-called ”new wars” (Kaldor 1999) had been coined to characterise such conflicts as anomic conflict societies (Geller 2006). These are characterised by private and non-state actors, acting outside the rules of the Haager convention. However, these wars are not without any order or rules of expectation, respectively. For this reason, Bhavnani (2006) has introduced the notion of ethnic norms to model genocide that ”persuade members of an ethnic group to participate in violence against nominal rivals” (Bhavnani 2006: 122). Another theoretical framework that has been developed in the past decade is the theory of securitization (Buzan et al. 1997). This theory addresses the question of how security issues arise on a political agenda. Securitization is described as a speech act that declares an object of communication as being under threat. It describes a relation between a securitizing actor and its audience. However, the role of the audience (Balzacq 2005) and the mechanisms of the process of securitization (Guzzini 2011) are in need to be further explored. Thus a number of attempts exist to grasp the security situation and challenges in the time after the cold war, but a concise comprehension is not at sight. It still remains a puzzling question how people became attuned to commit crimes as they had to be observed in the former Yugoslavia.
To shed light on the mechanisms of the escalation of inner-state, ethnic violence an agent-based model has been developed. The unclear and controversial theoretical starting position suggests to rely on a descriptive, empirical approach (Edmonds and Moss 2005). The fact that the wars in the former Yugoslavia are well documented suggests to use this empirical example to derive the model assumptions. The paper proceeds as follows: first, the case of the conflicts in the former Yugoslavia is described and integrated into the framework of ethnic norms. Secondly, the framework for modelling is outlined. Here, cognitively complex agents are introduced. Subsequently model architecture and implementation is described. First simulation results are displayed and finally an outlook and conclusions are provided.

THE YUGOSLAVIA CASE

Yugoslavia was a multi-national federal republic, consisting of six republics. Each republic comprised one of Yugoslavia’s constituent nations. The territories of the republics were drawn along historically established borderlines. During the wars in the 1990s, Yugoslavia collapsed along these borderlines.
Soon after Tito’s death, nationalist movements emerged in the political landscape. The beginning of the conflict was triggered by a power struggle within the Yugoslavian Communist Party about Tito’s legacy. Formerly communist politicians took advantage of ethnic sentiments, allowing them to organise loyalty with an ethnic agenda. Milosevic was able to stimulate mass movements in Montenegro and the Vojvodina, bringing liegemen of Milosevic into power (Silber and Little 1997). The power struggles at the end of the 1980s still took place within the Yugoslavian Communist Party. However, the first free elections in the individual republics brought nationalist parties into power, albeit often with only marginal majorities. In April 1990, Franjo Tudjman won the first free elections in Croatia. Nevertheless, the degree of ethnic mobilisation in the population was rather small. Even in 1990, the results of opinion polls in Bosnia revealed that more than 90% considered

Proceedings 26th European Conference on Modelling and Simulation ©ECMS Klaus G. Troitzsch, Michael Möhring, Ulf Lotzmann (Editors)
ISBN: 978-0-9564944-4-3 / ISBN: 978-0-9564944-5-0 (CD)

ethnic relations in their neighbourhood to be good, even though there were already political tensions at the political level (Calic 1995).

Yet, very soon civilians were also becoming involved in the battles and, in particular, in war crimes. The violence was not accidental, but aimed at establishing ethnically homogeneous nations out of the former multi-ethnic country of Yugoslavia. The escalation of tensions into open conflict started after Croatia declared its independence in 1991. The Krajina region in south-west Croatia was inhabited by a majority of Serbs. As a reaction to the Croatian independence, the establishment of a Serbian autonomous province of Krajina was declared on 28 February 1991, provoking armed conflicts. A further stage was reached on 26/27 August 1991, when the first ethnic homogenisation took place in the small village of Kijevo, inhabited mainly by Croatians (Rathfelder 1999). After the village had been attacked by the Yugoslavian Army, a paramilitary militia of the Kraijna Serbs invaded the village and displaced the Croatian population. The militia consisted of the local Kraijna Serbs, civilians who were not integrated into the command structure of the Yugoslavian army. As characteristic for the militia's course of action, they prewarned the Serbian inhabitants of the village, who chose not to pass on the information to their Croatian neighbours. This modus operandi turned out to be a template for later ethnic homogenisation in Bosnia-Herzegovina (Rathfelder 1999). At this point, a stage was reached in which civilians were mobilised for participating in war crimes. This review of the escalation shows that both politicians and citizens where involved in the process. While politicians created a political atmosphere of ethnic fear and hatred, crimes where undertaken by citizens as well.

MODELLING AND COGNITIVE COMPLEXITY

The empirical case fits into the framework of ethnic norms as it had been developed by Bhavnani (2006), insofar as citizens where persuaded to voluntarily participate at war crimes. While ethnic homogenisation still remained an extraordinary event in Yugoslavia, it was not a prohibited type of action but, on the contrary, was a behaviour that was actively enforced by norm setting agencies. This refers to the two aspects of norms as described by the institutional theory of norms (Kelsen 1934, Andrighetto & Conte 2012), namely being an obligation that is prescribed by a normative authority. This leads to the role of politicians. Norms consist of both behaviour patterns as well as norm enforcing agencies. In the case of Yugoslavia, these had been politicians who enforced nationalistic chauvinism. Indeed, "... tacit knowledge structures .... may be used by ethnic entrepreneurs as motivating templates ..." (Bhavnani 2006: 125), as Bhavnani observes for the case of Rwanda. However, neither the Genocide in Rwanda nor ethnic homogenisation in Yugoslavia where enduring events. Thus the question arises how such a norm emerges in the first instance.

To develop a framework for modelling we have to start with the idea that for norms to emerge it will be necessary that agent societies must not consist of agents that are entirely lenient with respect to the behaviour of their fellow agents. Thus agents will have to be endowed with a set of goals which they do not necessarily share with all of their fellow agents. Thus the process of norm emergence or innovation in an artificial society of agents will have to start with actions arising from individual agents' goals. The process can be illustrated by an everyday example: *A* does not want to be exposed to the smoke of cigarettes. At this moment this is not yet a normative goal: to achieve the goal of living in a smoke-free world when the current environment contains a smoker, say *B*, a decision has to be taken which leads to one of several possible intentions which in turn lead to respective actions. One of the possible decisions *A* might take will be to demand from *B*, the smoker, to stop smoking. When *B* receives this message as a social input he will have to evaluate this message in the norm recognition procedure. If this event (*A* asks *B* not to smoke in her presence) is the first of this kind, *B* will not recognise a norm but store this message and the situation in which he received it as an event in his "event board". When an event like this is more often observed by *B* (but also by observers *C*, *D*, …) this kind of messages might be interpreted as a norm invocation, and a normative belief – "the belief that a given behaviour in a given context for a given set of agents is forbidden, obligatory, permitted, etc." (EMIL 2009) – is stored in all the recipients of the repeated message. If it turns out that the current state of the world does not conform to the normative goal, the decision maker generates a normative intention which in turn ends up in an action.

However, the normative authority plays a different role in the case of ethnic norms than in the example of non-smoking norms. No legal sanctions (e.g. such as a fine for smoking in restaurants) exist for not participating at genocide. To represent the informal character of ethnic norms, Bhavnani followed Axelrod (1986) by modelling the Rwanda case as a norms game, i.e. punishment for nonconforming in-group members by ethnic entrepreneurs. Additionally to this, the Yugoslavian case includes an even more intricate element. Speeches such as Milosevic's famous claim that 'nobody should beat you' or the 600 anniversary of the battle at Kosovo Polje are no direct requests such as normative sanctions for smoking in a restaurant. In this respect they differ from normative sanctions. Instead they provide a form of symbolic communication by appealing to symbols of (in this case) national pride. The symbolic (e.g. speech) speech acts appeal to social identities (Hogg & Abrams 1990, Cruz 2000), which then triggers an internal motivation to voluntarily participate at war crimes.

ARCHITECTURE OF EMIL-S

This form of communication can be represented by using the Simulation framework EMIL-S. It has been developed to model the cognitive complexity involved in norm innovation processes (Lotzmann 2010). In the case of symbolic communication it is of central interest to model the decisions of the politicians to which kind of value

orientation they should appeal. This in turn generates voluntary actions of citizens which are based on their respective value orientation.

Any multi-agent simulation system will have to be able to simulate the processes which go on within agents (recognition, memory, decision making), among agents (communication) and between agents and their environment (action). Mental processes within agents are thus separated from actions that agents take with respect to other agents (including communication) and their environment. Thus one of the central requirements for this kind of simulation is that agents do not communicate by mind-reading but by messages which have to be interpreted by the recipients of messages before they can have any effect on the recipient agent's behaviour. Decision making does not only concern observable actions, but also internal actions, such as one to form or not to form a given mental state. This is modelled in the framework EMIL-S. This module is the core of the simulation system which represents the "minds" of normative agents. Each agent must be equipped with a set of initial rules, which allows him to act in the simulation environment. Rules in EMIL-S are represented as so-called event-action trees, which is a kind of decision tree that represents the dependencies between events and actions (Figure 1 shows an example). For each event an arbitrary number of action groups are defined (G1 in the example). An action group represents a number of mutually exclusive actions (A1 to A4 in the example). The edges of the tree are attached to selection probabilities for the respective action groups or actions.

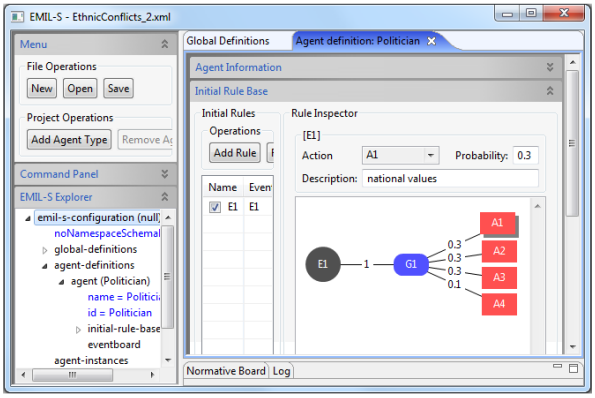

Figure 1: EMIL-S Agent Designer, displaying an event-action tree from the initial rule base

Based on perception of the environment, the decision tree generates some kind of action which in turn changes the state of the environment. Subsequently, the impact of the action must be evaluated in order to show modified (and preferably better in respect of goal achievement) behaviour at the next appearance of a similar environmental state. This process step is called valuation. The result of the evaluation from the previous step leads to an appropriate rule change, i.e. the actual rules must be adapted in some way. These steps are shown in Figure 2.

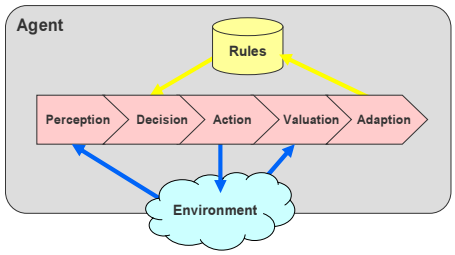

Figure 2: Generalized intra-agent process

MODEL DESIGN

In the following, it will be outlined how this agent design is integrated into the conflict escalation model. The model follows the KIDS principle (Edmonds & Moss 2005) to integrate as much empirical evidence in the architecture as possible. However, it has to be emphasised that only the processes of the early phases of conflict escalation will be considered, not the entire wars.

General design

The model consists of two types of agents: the political élite and the local population. However, the two types of actor are structurally coupled. On the one hand, politicians' careers are dependent on mass support; on the other hand, the mobilisation of mass support stimulates the mobilisation of individual value orientations and identities (Figure 3).

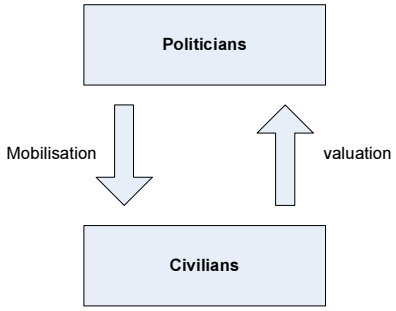

Figure 3: Relation of the two agent types of the model

Actor models

To represent the different motivation of citizens and politicians, the two agent classes are modelled using different actor models. Politicians act by holding speeches that either appeal to civil or nationalist values. Nationalist speeches can either be radical or moderate. Speeches represent the symbolic communication. While politicians are the norm enforcing actors for the society, their personal goals are represented by the rational actor model of the SEU (Subjective Expected Utility) theory. The goal of politicians is to make career advancements, by maximising their popularity. The strategic evaluation is undertaken in three dimensions:

- *Political atmosphere*
- *Credibility:* A politician is no longer credible if he or she changes the political agenda too frequently.

- *Exclusiveness:* It may be advantageous to opt for a type of agenda with fewer competitors, even if there is less overall support.

Learning arises from the fact, that all speeches are evaluated by the citizens. They form their own opinion and discuss with their neighbours. In dependence of that, they can take part on a pro or anti demonstration. All this goes in the evaluation process, so that the politician, who gave a speech, receives positive or negative feedback, i.e. sanctions in terms of EMIL-S. These sanctions cause the politician to continue to give speeches with the chosen type or to switch to another one.
Ethnographic accounts (Wilmer 2002) have described the involvement of the local population in war crimes as emotionally driven. This can be represented following the theory of the 'identity preserver', popularised by the German sociologist Uwe Schimank (Schimank 2000). Agents possess two value orientations: civil values and national identity. Individuals possess both types of value orientation. However, the strength of the respective value orientation may differ. This is illustrated in Figure 4, where the x axis represents the degree of civil values and the y axis represents the degree of national identity.

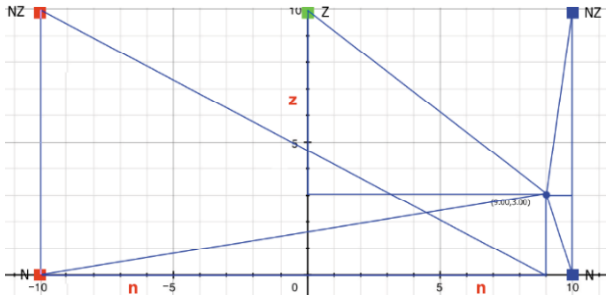

Figure 4: Evaluation of speeches

In this connection the orientation of an agent is a point in a two dimensional coordinate system limited by 10 in each axis. In Figure 4 the blue point with coordinates (9.00, 3.00) represents the civil and national values of a Croatian citizen. The speech types are represented as the maximum of each axis. In this connection a national speech of a Croatian politician is represented as the coordinate (10.00, 0.00). A moderate nationalist speech of a Croatian politician is represented as (10.00, 10.00). Finally a civil speech is represented as (0.00, 10.00). The national and civil-national speeches of non-Croatian politicians are represented as (-10.00, 0.00) and (-10.00, 10.00). Hence the evaluation of a speech is the distance between the coordinates of the agent and the coordinates of a particular speech. The smaller the distance, the better the evaluation is, e.g. in this case, the Croatian agent would rate a Croatian national speech with 3.16 and a Croatian civil speech with 11.40.

Scheduling

The overview of the scheduling (Figure 5) highlights the fact that the scheduling consists of two phases: a state of social order and an anomic state. In principle, the recursive feedback loop between politicians and citizens indicated by the two upward and downward bars may be maintained in the state of social order. This is a rather general mechanism, not specific to the Yugoslavian case. Namely, politicians hold speeches to organise support. Citizens discuss their evaluation of the speeches in friendship and neighbourhood networks. This represents the idea that the success of political campaigns is to become the topic of public debate. Support is signalled by participating in demonstrations in favour of the politician. This changes the value orientation of the citizens. The degree of support is observed by the politicians to evaluate which type of speech they should hold the next time.
Under certain circumstances the model may enter the anomic state. Following the KIDS principle (Edmonds & Moss 2005), the concrete mechanisms for the transition into the anomic state are specific for the Yugoslavian case. To abstract from this particular case, in the model an alarm function for the rise of a political conflict is activated if a nationalist politician gains support outside the territory of his or her home republic. This provides the opportunity for the emergence of paramilitary militia. Three conditions have to be fulfilled for their emergence:

- *Opportunities:* activation of the alarm function.
- *Motivation:* Militia consists of highly radicalised nationalists.
- *Complicity:* The militia planning to attack a certain village warned the inhabitants of their 'own' nationality. These could have warned their neighbours of different nationality, but they chose not to and often participated at the looting.

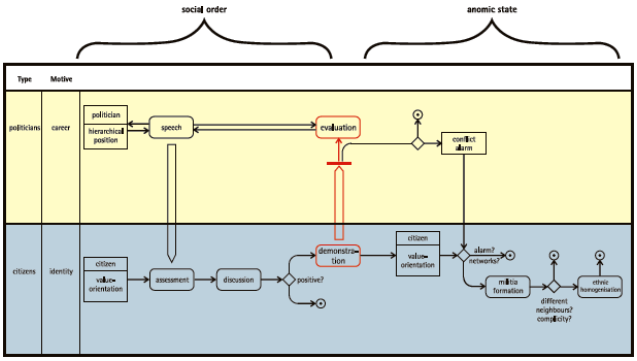

Figure 5: overview of the scheduling

MODEL IMPLEMENTATION

The implementation of the model (Marksic and Kilic 2012) is based on Repast Simphony (North et al. 2007). In addition, the normative behaviour of politicians is realised with the EMIL-S framework, and ArcGIS is used in order to create the geospatial data which is integrated into particular GIS projections.

Environment

To represent the boundaries or administrative districts with adequate precision, the geography has to be mod-

elled with a software like e.g. ArcGIS. The resulting geospatial data can then be loaded into GIS projections.

The environment is hierarchically structured from the state level to administrative areas. Each environmental context has an assigned shape file which holds information and whose records can be shown as objects. These objects are loaded into the specific context and displayed in the respective geographic projection (Figure 6). The three ethnic groups are distinguished by colours. The green dots are Bosniaks, the blue Croats and the red Serbs. These have three levels of intensity, depending on how strong the national identity of the agent is pronounced.

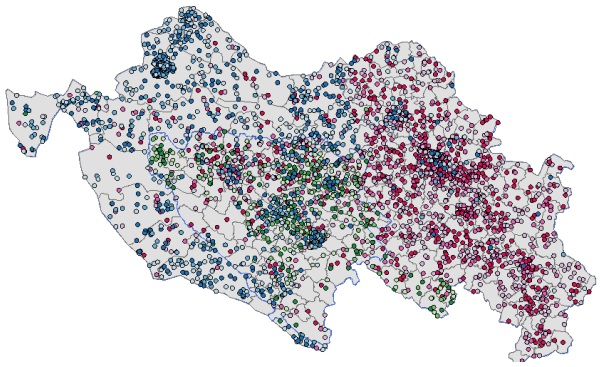

Figure 6: Initial Population distribution at the GIS Projection

Agents

- **Citizens:** Every shape file has an attribute table. Every modelled administrative district is handled as a record in that table. For each district the statistical data of population in former Yugoslavia of 1991 was used to fill the table. Every agent of each ethic group represents 5,000 residents of this ethic group.
- **Politicians:** The politicians have fixed coordinate points, so that each individual can be assigned clearly to a republic in which he operates. A politician of an ethnic group represents 100,000 residents of this ethnic group.

Time

Every tick in the simulation run represents a week in reality. In the model it is assumed, that a certain number of politicians can give only one speech every week. This means, that those politician agents executes an action every seven ticks. The citizen agents act within the seven-tick interval active. The simulation should cover a period of several years, namely the time before the disintegration of former Yugoslavia and subsequent wars.

Normative behaviour of politicians

The politician agent on the Repast layer has a mirror image on the EMIL Layer. This means that the same agent exists on two different levels. If an agent on the Repast layer wants to perform a certain action, then it triggers an event. In this case a politician would trigger the event to give a speech. This is the action of the triggered event. This event is then processed by the agent on the EMIL layer. The result in terms of an action is delivered back to the Repast agent. In the next step, the Repast agent would perform that action.

SIMULATION RESULTS

According to the Bayesian design of experiments, at initialization of the simulation it is assumed that the prior distributions between the citizens' value orientations and the probabilities between the three types of speeches are equal. The following sketches of a simulation run show how opinions develop according to the mechanisms of the model. After 2190 ticks - which equals 6 years - the average civil and national values of Bosniaks have evolved as displayed in Figure 7.

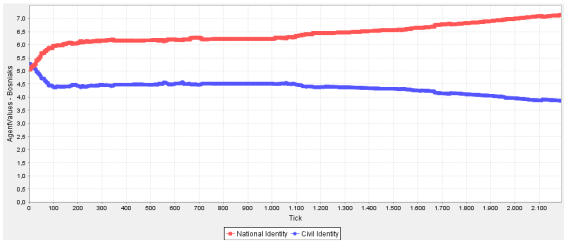

Figure 7: Bosniaks – Avg. civil and national values

The national values of Bosniaks showed a slight rise from the beginning up to middle of the simulation time interval. Also, the gap between the national and civil curve remained constant. This is caused by balanced acceptance of national and civil speeches. In the second half of the time interval the national values curve raised continuously. At the same time the civil values curve decreased also continuously. The reason for this is, that if an agent is displaced, then his national values rise up to the maximum. The logical outcome of this is the radicalisation of that agent, which also influences his new neighbourhood. Thus, in the progress of the simulation, the national speeches are going to be more accepted as the civil ones.

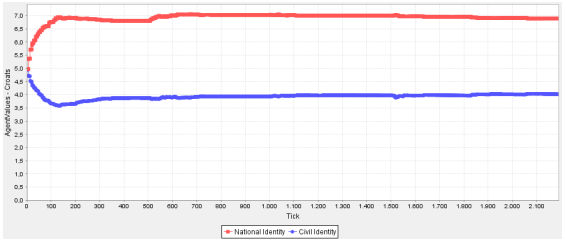

Figure 8: Croats – Avg. civil and national values

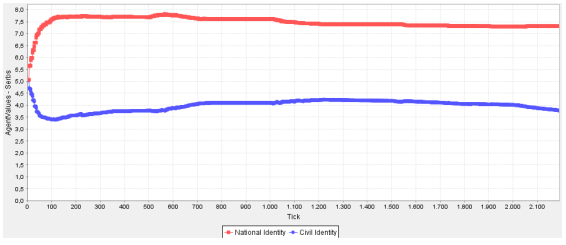

Figure 9: Serbs – Avg. civil and national values

From the beginning of the simulation the national values of Croats (Figure 8) and Serbs (Figure 9) have risen strongly. In this case, the politicians who held national speeches were more supported than the ones who held civil speeches. In consideration of this particular fact, the conflict was caused by the two ethnic groups which were directly radicalized. This can also be seen in the log file where the first militia was created by a part of the Serbian population.

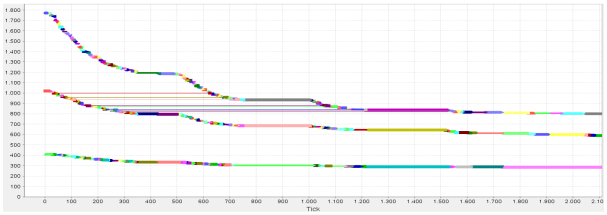

Figure 10: Population development

The curves in Figure 10 are labelling the population of the three ethnic groups during the simulation. From top to bottom the curves are standing for the number of Serbs, Croats and Bosniaks. It is clear that the two ethnic groups which were most rapidly radicalized, have suffered the highest numbers of victims.

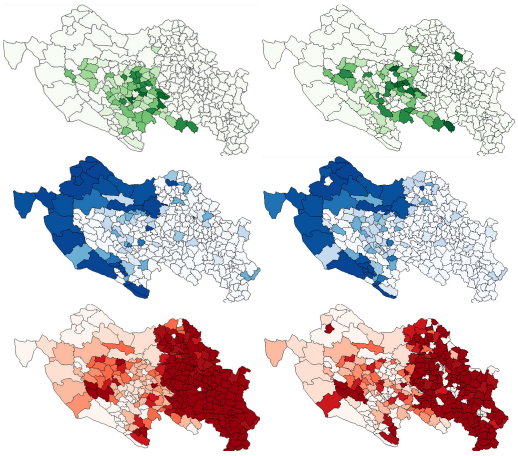

Figure 11: Intensity of ethnic groups (top: Bosniaks, centre: Croats, bottom: Serbs)

The choropleth maps on the left side in Figure 11 shows the state at the beginning of the simulation. The right side is the state at the end. The choropleth maps are showing the relative frequency of each ethnicity in a particular region, e.g. a dark blue region only says that there is a homogenous Croatian population. It can be determined, that all ethnic groups have defended their territory or have occupied adjacent territories.

Four types of actions can be undertaken by the politicians: holding a nationalist speech (A1), holding a civil speech (A2), holding a moderate nationalist speech (A3), and doing nothing (A4).

From the list of the politicians in Bosnia (Figure 12), it is evident that Bosniak politicians have kept their speeches fairly compensated. This confirms Figure 7 where the average national and civil values are quite balanced. However, because of displacement of Bosniaks and their concurrent radicalization, it can be expected that in further simulation ticks Bosniak politicians will become increasingly nationalist.

Bosnia

PolID	Ethnicity	NumSpeeches	STypes	Popularity	Avg
17	Serb	17	A1:2-A2:0-A3:0	114,00	6,71
11	Croat	20	A1:4-A2:2-A3:1	141,00	7,05
15	Serb	20	A1:0-A2:6-A3:0	145,00	7,25
6	Bosniak	20	A1:4-A2:4-A3:0	146,00	7,30
19	Serb	28	A1:2-A2:7-A3:1	206,00	7,36
2	Bosniak	19	A1:3-A2:1-A3:2	151,00	7,95

Figure 12: Six most acceptable politicians in Bosnia

On the two top places in all republics are Serb (Figure 14) and Croat (Figure 13) politicians, who have appealed especially to the citizen through national speeches. This confirms the rapid radicalization of these two ethnic groups by the high acceptance of these speeches.

Croatia

PolID	Ethnicity	NumSpeeches	STypes	Popularity	Avg
49	Croat	27	A1:9-A2:0-A3:0	65,00	2,41
46	Croat	32	A1:11-A2:0-A3:1	125,00	3,91
31	Croat	32	A1:0-A2:11-A3:0	183,00	5,72
38	Croat	21	A1:4-A2:0-A3:1	122,00	5,81
87	Croat	7	A1:2-A2:0-A3:1	44,00	6,29
37	Croat	30	A1:6-A2:2-A3:1	190,00	6,33

Figure 13: Six most acceptable politicians in Croatia

Serbia

PolID	Ethnicity	NumSpeeches	STypes	Popularity	Avg
90	Serb	8	A1:3-A2:0-A3:0	28,00	3,50
68	Serb	28	A1:7-A2:0-A3:2	137,00	4,89
71	Serb	29	A1:8-A2:3-A3:0	154,00	5,31
59	Serb	29	A1:8-A2:1-A3:1	157,00	5,41
79	Serb	27	A1:5-A2:0-A3:0	149,00	5,52
60	Serb	29	A1:8-A2:1-A3:3	162,00	5,59

Figure 14: Six most acceptable politicians in Serbia

Concerning the mechanisms of the escalation process an observation that was made during the simulation is the relationship between the parameters *avgOpinionMultiplicator* and *demoValueDivider*. If a speech has taken place, then each citizen evaluates it. However, there exists also a common opinion about that speech in the neighbourhood. The first parameter is used to give such a common opinion a particular weighting. Herewith it is possible to increase or decrease the influence of the neighbourhood on each citizen. This is the point where the citizen decides whether to go to a demonstration or not. The greater the *avgOpinionMultiplicator* is chosen, the more is he dragged by the crowd. The second parameter, *demoValueDivider,* is used to control the strength of influence of demonstrations on each participant. If a citizen decides to go to a demonstration, then the average orientation of all participants is used in order to update the orientation of each individual. The relation between the two parameters can be interpreted as follows: if the influence of the neighbourhood of an individual is small, the less he is directed to go to a demonstration. That means that the second parameter has no impact on the individual. In the case that the influence of the neighbourhood is high, then the second parameter determines the speed of the radicalization.

CONCLUSIONS AND FUTURE WORK

So far, the model is not calibrated but presents only theoretical results. Further empirical work would allow for a validation of an empirically calibrated model. This has to be left for future work. The good empirical data

basis of the Yugoslavian example provide a source for deeper empirical substantiation of the general framework developed in this model.

However, the results confirm that, following the KIDS principle, empirically derived assumptions allow to generate the process of conflict escalation. Moreover, this supports an approach from the theory of securitization. Ethnic conflict can be triggered through the political level. However, the citizens are not simply passive entities. This clarifies the role of the audience in the securitizing act. The success of mobilising attempts of politicians depend on the network structure of the citizens. Mobilisation is successful only when in the particular ethnic group people exist who are at the beginning highly nationalized and pursue their own goals. In addition, it is also necessary that there are people which can be easily manipulated. This result is substantiated by Horowitz's (2001) observation of the central role of rumours in the escalation of ethnic violence. These are transmitted through networks that are implemented in the model. Dissecting the mechanisms of the escalation of ethnic conflicts through simulation allows theoretical clarification that suggests further empirical work.

ACKNOWLEDGEMENTS

The authors would like to thank Prof. Dr. Klaus G. Troitzsch for enduring support in the process of the development of the model.

REFERENCES

Andrighetto, G. & Conte, R. (2012, forthcoming) Norms from the top-down. In Andrighetto, G. & Conte, R. *Minding Norms*. Oxford: Oxford University Press

Axelrod, R. (1986) An evolutionary approach to norms. *American political science review* **80**(4), 1095-1111.

Balzacq, T. (2005): The Three Faces of Securitization: Political Agency, Audience and Context. *European Journal of International Relations* 11(2): 171-201.

Bhavnani, R. (2006) Agent-based models in the study of ethnic violence. In Harrison, N. *Complexity in World Politics. Concepts and methods of a new paradigm.* Albani: State university of New York Press, pp. 121-136.

Bringa, T. & Christie, S. (1993) *We are all neighbours.* Granada TV.

Buzan, B., Waever, O., & de Wilde, J. (1997) *Security: a new framework for analysis.* Boulder: Lynne Rienner.

Calic, M. (1995) *Der Krieg in Bosnien-Herzegowina.* Frankfurt a.M.: Surkamp.

Cruz, C. (2000) Identity and Persuation. *World Politics* **52**(3), 275–312.

Edmonds, B. & Moss, S. (2005) From KISS to KIDS – an 'anti-simplistic' modelling approach. In Davidson, P. et al. *Multi Agent Based Simulation 2004.* Berlin: Springer. pp. 130 – 144.

EMIL (2009) Emergence in the Loop: Simulating the Two-Way Dynamics of Norm Innovation. *EMIL-T,* Deliverable 5.1.

Geller, A. (2006) *Macht, Ressourcen und Gewalt: Zur Komplexität zeitgenössischer Konflikte. Eine agenten-basierte Modellierung.* Zürich.

Guzzini, S. (2011): Securitization as a causal mechanism. *Security Dialogue* 42(4/5): 329-341.

Hogg, M. & Abrams, D. (1990) *Social Identifications. A social psychology of intergroup relations and group processes.* New York: Routledge.

Horowitz, D. (2001) *The deadly ethnic riot*. Berkley: University of California press

Kaldor, M. (1999) New and old wars. Organized violence in a global area. Stanford: Stanford: University Press.

Kelsen, H. (1934) *Reine Rechtslehre.* Wien: Deutscher Verlag.

Lotzmann, Ulf (2010) Enhancing Agents with Normative Capabilities. In Bargiela, A.; Ali, S.A.; Crowley, D.; Kerckhoffs, E.: *24th European Conference on Modelling and Simulation, ECMS 2010.* Kuala Lumpur: SCS Europe.

Markisic, S. & Kilic, S. (2012) Simulation ethnischer Konflikte. Koblenz: Diploma Thesis

Neumann, M. (2008). A classification of normative architectures. In *Proceedings of the 2nd WCSS.* Fairfax, VA.

North, M.J., Howe T.R., Collier N.T., & Vos J.R. (2007) A Declarative Model Assembly Infrastructure for Verification and Validation. In Takahashi S.; Sallach D.L.; Rouchier J.: *Advancing Social Simulation: The First World Congress*. Heidelberg: Springer.

Rathfelder, E. (1999) Der Krieg an seinen Schauplätzen. In Melcic, D., *Der Jugoslawien Krieg. Handbuch zu Vorgeschichte, Verlauf und Konsequenzen.* Opladen: Westdeutscher Verlag, pp. 344-361.

Schimank, U. (2000) *Handeln und Strukturen. Einführung in eine Akteurtheoretische Soziologie.*Munich: Juventa.

Silber, L. & Little A. (1997) *Yugoslavia: death of a nation.* New York: Penguin.

Williams, M. (2003) Words, Images, Enemies: Securitization and International Politics. *International Studies Quarterly* 47/4: 511-531.

Willmer, F. (2002) *The social construction of man, the state and war.* London: Routledge.

AUTHOR BIOGRAPHIES

SUVAD MARKISIC obtained his diploma degree in Computer Science from the University of Koblenz-Landau in 2012. His diploma thesis was about the simulation of ethnic conflicts which is handled in this paper. Currently he is also involved in the FP7 project OCOPOMO. His e-mail address is markisic@uni-koblenz.de.

MARTIN NEUMANN studied philosophy, mathematics and social science and obtained a PhD in Philosophy at the University of Osnabrueck in 2002. Subsequently he worked at the Institute for Philosophy at Bayreuth University in the EU funded project EMIL (Emergence in the loop). Currently he is at the department for social science at the RWTH Aachen University. His e-mail address is mneumann@soziologie.rwth-aachen.de.

ULF LOTZMANN obtained his diploma degree in Computer Science from the University of Koblenz-Landau in 2006. Since 2005 he has specialized in agent-based systems in the context of social simulations and is developer of simulation frameworks as for instance TRASS and EMIL-S. Currently he is involved in the FP7 project OCOPOMO (Open Collaboration for Policy Modelling) He is expected to take his PhD at the University of Koblenz-Landau in 2012. His e-mail address is ulf@uni-koblenz.de.

A SIMPLE AGENT-BASED MODEL OF THE TRAGEDY OF THE COMMONS

Julia Schindler
Center for Development Research
University of Bonn
Walter-Flex-Str. 3, 53113 Bonn, Germany
julia.schindler@uni-bonn.de

KEYWORDS:
Agent-based model, simple, Tragedy of the Commons, common-pool, simulation, social values

ABSTRACT

The Tragedy of the Commons by G. Hardin is a famous metaphor for social dilemmas in common-pool resource use. In his famous article from 1968 he argued for an abstract common-pool pasture that the pasture must become depleted as herdsmen have higher incentives to add cattle than to remove, due to the shared nature of the common. However, Hardin built his argument on the assumption of purely selfish and profit-oriented behavior of humans. For this article, we therefore hypothesized that the integration of other human values can lead to sustained use of the common. We test both of these questions via an implementation of Hardin's pasture as an agent-based model, which allowed us to simulate Hardin's pasture system over time. Simulation results verify both Hardin's argument and our hypothesis.

INTRODUCTION

In his article on the "Tragedy of the Commons", Hardin (1968) argued that an abstract common-pool pasture must become depleted if users are free to choose the number of cattle stocks. In specific, he based his argument on the observation that users are trapped in a social dilemma, where the cost of increased cattle stocks are shared among users while the benefit remains personal. Such biased payoffs, according to Hardin (1968) would deduce users to add more and more cattle, notwithstanding the observable but less-rated cost. Though, this argument was entirely based on the presupposition that the users are strictly profit-oriented. Other social values such as fairness, group welfare, institutions of remuneration and punishment, or more personal values such as risk aversion, were not considered. For this article, we therefore sought to validate Hardin's line of thought under the assumption of strict profit orientation, and to test if and under what conditions the common could be sustained when allowing social and personal non-profit values in addition. Since such social and personal values or dispositions influence and are influenced by others' and one's own past actions, we decided to implement Hardin's tragedy in an agent-based model, which allowed us to both implement feedback between the pasture and users, and social feedback between users.

In the next section, we present the model structure of a simple model of the Tragedy of the Commons, and describe the social and personal dispositions that are implemented and tested. In the subsequent section, we present simulations results. Simulation results verify the initial argument of Hardin when only the selfish disposition is active, and that the consideration of other dispositions can lead to a sustainable use, each in the way intuitively suggested.

MATERIALS AND METHODS

Agent-based modelling is an approach for modelling the actions and interactions of single entities called agents, with a view to testing their effects on the system as a whole. Thereby, agents can be spatial patches representing a gridded space, or mobile agents having the ability to move along space. Thus, agent-based modeling has the inherent capacity to model social and human-environment systems from the bottom-up in discrete time steps by specifying their constituent parts. Here, we implemented an abstract pasture close to the one described by Hardin (1968). Accordingly, in the model, human agents can decide in each time step to add or subtract their cattle stock by one cattle head, or leave it constant. Feedback between human agents and their biophysical environment consists of the effects of stocking rates on future grass growth, and of an integration of this cost in the stocking-rate choice. Social interactions are reflected in the stocking decision in terms of what stocks others have and what actions others have played in the previous round.

Model overview

The model that we developed was programmed in NetLogo (Wilensky 1999) and represents a square virtual pasture in a grid of 33 x 33 individual patches, a user-defined number of non-moving herdsman agents randomly located in space, and a user-defined number of moving agents representing cattle, each randomly assigned to a herdsman agent as owner. Over time, cattle graze, grass regrows, and agents update their stocks, forming an annual time loop. During the grazing routine, cattle move to the nearest grass patches and clear the grass cover of these patches. In order to

Proceedings 26th European Conference on Modelling and Simulation ©ECMS Klaus G. Troitzsch, Michael Möhring, Ulf Lotzmann (Editors)
ISBN: 978-0-9564944-4-3 / ISBN: 978-0-9564944-5-0 (CD)

Table 1: External parameters of the model

Parameters	Domain	Explanation
Cov	$[0, 100]$	Initial percentage of patches covered by grass
N	$\mathbb{N} \setminus \{0\}$	Total number of herdsman agents
C	$\mathbb{N} \setminus \{0\}$	Initial number of cattle agents
$rate_{growth}$	$\mathbb{R}^+ \setminus \{0\}$	Net relative grass growth rate near zero vegetation
P_{cow}	$\mathbb{N} \setminus \{0\}$	Cattle price
$requ_{cow}$	$\mathbb{N} \setminus \{0\}$	Annual forage requirement of cattle agents in patches
$rate_{learn}$	$\mathbb{N} \setminus \{0\}$	Total number of herdsman agents
$level_{self}$	$(0, 1)$	The tendency to favor actions that support personal financial benefit
$level_{coop}$	$(0, 1)$	The tendency to favor actions that support group financial benefit
$level_{fairself}$	$(0, 1)$	The tendency to refrain from actions that make the agent worse off than others
$level_{fairother}$	$(0, 1)$	The tendency to refrain from actions that make the agent better off than others
$level_{negrec}$	$(0, 1)$	The tendency to favor actions that penalize others
$level_{posrec}$	$(0, 1)$	The tendency to favor actions that reward others
$level_{conf}$	$(0, 1)$	The tendency to favor actions similar to the past behavior of the group
$level_{risk}$	$(0, 1)$	The tendency to favor actions that reduce financial risk

reflect the idea to integrate an environmental cost estimate in the stocking choice, we chose to represent subsequent grass growth by a logistic growth function that is dependent on the grass cover that remains after browsing. Finally, agents update their stocks.

In an earlier agent-based version of the Tragedy of the Commons (Schindler 2012), we assumed that during each time step, agents' actions converge to a Nash equilibrium. In this earlier version, we therefore identified the agents' actions by a random (Pareto-optimal) Nash equilibrium of the strategic game in the current time step, where payoffs were weighted by dispositions. The disadvantage of this version, however, was threefold: First, we believe using Nash equilibria does not realistically represent human behavior in the proposed setting, as we expect that herdsmen are not constantly engaged in a strategic game throughout the year but rather behave in a "trial and error" mode and revisit stocking decisions only once or twice a year. Second, the use of an extension to calculate Nash equilibria every time step was very costly in terms of computation speed. Third, the way how the dispositions influenced payoffs was complicated and not entirely intuitive. For this version, we therefore decided to straighten these shortcomings, i.e. build reactive instead of strategic agents, with a transparent and simple way to integrate social and personal dispositions.

These comprised eight dispositions, i.e. selfishness vs. cooperativeness, fairness concerning oneself vs. fairness concerning others, positive vs. negative reciprocity, conformity, and risk aversion (Table 1). The range of dispositions is inspired by Ebenhöh and Pahl-Wostl (2006). Accordingly, we identify selfishness and cooperativeness with the tendency to favor decisions that improve the agent's own or the entire group's financial benefit, respectively; fairness concerning oneself or others with the tendency to favor own decisions that reduce unfair cattle stock distributions towards the agent himself or towards others; positive and negative reciprocity with the tendency to factor own decisions that reward others' actions or punish others' actions, respectively; conformity with the level of favoring actions that are similar to others' past actions; and risk aversion with the tendency to avoid financial risks caused by the uncertainty of others' behavior.

Model details

Each herdsman agent i is endowed with an individual probability of adding one cattle to its stock ($prob_{add}$), and the corresponding counter-probability of subtracting one cattle ($prob_{subt}$). These probabilities are updated according to how the conditions induced by past actions match with the social and personal dispositions. According to these probabilities, a choice is made in each time step, denoted by x_i, while k_i denotes the current size of the cattle stock. The cattle agents are endowed with an owner variable indicating the owning herdsman agent ($owner \in \{1, \cdots, N\}$), and a feeding status ($feedstat \in \mathbb{N}$) indicating the number of patches browsed in the current time step. The patches are characterized by a variable ($cover \in \{no\ grass, grass\}$) indicating whether the patch is covered by grass or not, whereby the cover of a browsed patch is turned from grass to no grass.

User-defined parameters of the model comprise the settings for initialization (i.e. total number of herdsmen, initial total number of cows, and initial grass cover), one parameter for each of the time-loop procedures of grazing, grass regrowth, and taking action (the annual forage requirement of cattle in terms of number of

patches, the grass growth-rate near zero vegetation, the price per cattle), and factors determining the decision-making process, comprising the adaptation speed, i.e. how fast the agent responds to evaluations, and the eight social and personal dispositions (Table 1).

Cattle agent routine
Each cattle agent moves and browses patches: One-by-one each cattle agent tries to fulfill its demand of grass patches (i.e. $requ_{cow}$). In this process, the agent moves to the nearest grass patch and browses it, upon which the state of the patch is turned to "no grass". This procedure is repeated until a cattle's demand is fulfilled or cannot be fulfilled due to grass patch depletion. In this latter case, the cattle agent is automatically removed from the pasture. When this grass-patch search has terminated for a cattle agent, the search for a different cattle agent is initiated. Thus, one-by-one, all cattle agents sequentially try to fulfill their demand, while the sequence is random.

The removal of cattle due to grass depletion is automatic and thus is independent of the herdsman agent decision-making process. It is based on the assumption that insufficiently fed cattle can be sold in time, thus involving no cost for the herdsman agent, but simply reducing his cattle stock. This is based on the rationale that under normal market conditions herdsmen will not wait for their cattle to die but will and are able to take action.

Patch routine
Noy-Meir (1978) suggests that for the type of simplified pasture like the one that we assume here (i.e. a pasture consisting of one plant species grazed by a herbivore population with a constant physiological status of intake), the growth rate of green biomass can be described by a function which is dependent on the current available green biomass. thereby increasing at a low biomass level, and decreasing at a high level. Using such a function, the cost of degradation can be incorporated in the model. Noy-Meyr (1978) proposes four growth functions that fulfill these requirements, among them the logistic growth function that we used in MASTOC (see equation 1). However, different growth functions can theoretically be built into the model.

$$g(Veg) = Veg \cdot (1 + (rate \cdot Veg \cdot (1 - (Veg/Vegmax)))) \quad (1)$$

with Vegmax = 1089 (total number of patches). The cover variable of patches is updated by:

1. Update variable Veg
2. Ask (g(Veg) - Veg) patches with cover = no grass: set cover grass

Herdsman agent routine
The herdsman agent routine consists of the update of the cattle stocks. For that, first rewards for the dispositions are calculated, being either 1 or -1 for each disposition. Then, the total weighted reward is calculated. Finally, the choice probabilities are updated accordingly, and an action is chosen according to these probabilities.

Calculate disposition-oriented rewards

Selfishness and cooperativeness
We identify selfishness with the tendency to favor actions that are personally financially beneficial, where we denote $benefit^i_{self}$ with the financial benefit of the previous action of agent i, which is revenue minus cost caused by the action (equation 2). It is important to note that this benefit solely refers to the benefit caused by *changing* the cattle stock, and not of the entire cattle stock as such, since we are interested in calculating rewards for *actions*.

$$benefit_{self} = x_i \cdot P_{cow} - cost(K + \sum_{j \neq i} x_j, K + \sum_j x_j) \quad (2)$$

where P_{cow} is the cattle price, K the current total number of cattle on the pasture, and $cost(x, y)$ is the cost function, representing the financial loss of pasture potential in this time step caused by increased/reduced grazing pressure in the last time step:

$$\begin{aligned} cost(x,y) \quad &:= \Big[g(max(0, Veg - x \cdot Requ)) \\ &- g(max(0, Veg - (x+y) \cdot Requ))\Big] \cdot \tfrac{P}{Requ} \end{aligned} \quad (3)$$

where x is the previous number of total cattle agents, y the current number, and g the vegetation update function (equation 1). The reward of the past action is simply 1 if the benefit was positive, and -1 if the benefit was negative.

$$r_{self} = \begin{cases} 1 & if\ benefit_{self} > 0 \\ -1 & if\ benefit_{self} < 0 \end{cases} \quad (4)$$

Cooperativeness
Equivalently, cooperativeness is the tendency to favor group actions that are financially beneficial for the entire group, where we denote $benefit^i_{coop}$ with the the share of the group benefit for agent i. This share is the shared group action revenue minus cost caused by the group action (equation 5). Here again, the benefit solely refers to the benefit caused by the action, not of the entire cattle stock.

$$benefit_{coop} = (\sum_{j \neq i} x_j) \cdot \frac{P_{cow}}{N} - cost(K)(K + \sum_j x_j) \quad (5)$$

$$r_{coop} = \begin{cases} 1 & if\ benefit_{coop} > 0 \\ -1 & if\ benefit_{coop} < 0 \end{cases} \quad (6)$$

Fairness towards oneself and towards others
If fairness towards oneself is considered and an unfair situation existed for agent i in terms of cattle stocks, previous actions that increased the own cattle stock were rewarded, while a reduction was punished (equation 7).

For fairness towards others the procedure is equivalent (equation 8).

$$r_{fairself} = \begin{cases} 1 & if\ mean_{j\neq i}\ k_j > k_i\ and\ x_i = 1 \\ -1 & if\ mean_{j\neq i}\ k_j > k_i\ and\ x_i = -1 \end{cases} \tag{7}$$

$$r_{fairother} = \begin{cases} 1 & if\ mean_{j\neq i}\ k_j < k_i\ and\ x_i = -1 \\ -1 & if\ mean_{j\neq i}\ k_j < k_i\ and\ x_i = 1 \end{cases} \tag{8}$$

Positive and negative reciprocity

If the tendency for positive reciprocity is considered, i.e. non-zero, and the majority of actions was a reduction of cattle, the past action of agent i is rewarded if it was a deduction, too, and punished otherwise (equation 9). The procedure for negative reciprocity is equivalent (equation 10).

$$r_{posrec} = \begin{cases} 1 & if\ mean_{j\neq i}\ x_j < 0\ and\ x_i = -1 \\ -1 & if\ mean_{j\neq i}\ x_j < 0\ and\ x_i = 1 \end{cases} \tag{9}$$

$$r_{negrec} = \begin{cases} 1 & if\ mean_{j\neq i}\ x_j > 0\ and\ x_i = 1 \\ -1 & if\ mean_{j\neq i}\ x_j > 0\ and\ x_i = -1 \end{cases} \tag{10}$$

Conformity

Conformity works like an amplifier of others' actions: The agent's actions are rewarded if they are the same as the majority's past actions, and punished otherwise (equation 11).

$$r_{conf} = \begin{cases} 1 & if\ mean_{j\neq i}\ x_j < 0\ and\ x_i = -1 \\ 1 & if\ mean_{j\neq i}\ x_j > 0\ and\ x_i = 1 \\ -1 & if\ mean_{j\neq i}\ x_j < 0\ and\ x_i = 1 \\ -1 & if\ mean_{j\neq i}\ x_j > 0\ and\ x_i = -1 \end{cases} \tag{11}$$

Risk aversion

If risk aversion is non-zero and there was any financial risk for the agent due to the uncertainties of others' agents' actions, a reduction of the cattle stock is rewarded, and punished otherwise (equation 12).

$$r_{risk} = \begin{cases} 1 & if\ cost(K)(K+N) > P_{cow}\ and\ x_i = -1 \\ -1 & if\ cost(K)(K+N) > P_{cow}\ and\ x_i = 1 \end{cases} \tag{12}$$

Calculate total weighted reward Subsequently, the final weighted reward is calculated (equation 13).

$$\begin{aligned} &reward = \\ &= level_{self} \cdot r_{self} + level_{coop} \cdot r_{coop} \\ &+ level_{fairself} \cdot r_{fairself} + level_{fairother} \cdot r_{fairother} \\ &+ level_{posrec} \cdot r_{posrec} + level_{negrec} \cdot r_{negrec} \\ &+ level_{conf} \cdot r_{conf} + level_{risk} \cdot r_{risk} \end{aligned} \tag{13}$$

Update choice Probabilities and choose action

Finally, the probabilities are updated (equations 14), and according to the resulting probabilities, an action is chosen. If the reward compared to the previous time step is zero, the cattle stock remains the same.

$$\begin{aligned} &if\ reward > 0\ and\ x_i = 1: \\ &\quad Prob_{add} \mapsto Prob_{add} + (1 - Prob_{add}) \cdot rate_{learn} \\ &\quad Prob_{subt} \mapsto 1 - Prob_{add} \\ &if\ reward < 0\ and\ x_i = 1: \\ &\quad Prob_{add} \mapsto Prob_{add} \cdot (1 - rate_{learn}) \\ &\quad Prob_{subt} \mapsto 1 - Prob_{add} \\ &if\ reward > 0\ and\ x_i = -1: \\ &\quad Prob_{subt} \mapsto Prob_{subt} + (1 - Prob_{subt}) \cdot rate_{learn} \\ &\quad Prob_{add} \mapsto 1 - Prob_{subt} \\ &if\ reward < 0\ and\ x_i = -1: \\ &\quad Prob_{subt} \mapsto Prob_{subt} \cdot (1 - rate_{learn}) \\ &\quad Prob_{add} \mapsto 1 - Prob_{subt} \end{aligned} \tag{14}$$

RESULTS

We are mainly interested in the questions whether we can verify Hardin's line of thought via a simple and reasonably calibrated agent-based model, and how the consideration of dispositions as defined here influences the sustainability of the abstract common. To answer these questions, we varied the disposition values, while we selected reasonable values for the other six parameters as if it were a West-African rangeland. We chose the African case study just to be able to assign the parameters reasonable values - one could have equally chosen values from another region in the world. Doing so, we set the relative grass growth rate near zero ($rate_{growth}$) to 0.00496, which corresponds to a maximum annual grass growth factor of 2.2 as reported in Huffaker (1993), and set the forage requirement of 1205 $kgyear^{-1}$ (Ohiagu and Wood 1979) to one patch, one patch thus equalling 0.44 ha if we assume an annual grass production of 3157 $kgha^{-1}year^{-1}$ (Ohiagu and Wood 1979). The price was set to 133 US $ which corresponds largely to cattle prices in rural Ghana according to own data, and the initial grass cover was 100 %.

For testing Hardin's argument, we conducted 400 simulations with maximum selfishness, and all other dispositions set to zero. Number of herdsmen and number of initial cattle was thereby randomly varied between 2 and 20 and 0 and 500, respectively. Simulations verify Hardin's argument for more than 2 herdsmen agents and any cattle number. In each of these cases, the common broke down. However, in each of the cases where only two initial herdsmen agents were present, the common was always sustained.

For analyzing the second question, the number of herdsmen and initial cattle was varied within three scenarios (Table 2), while all dispositions were randomly set in units of 0.1. Correlation analysis showed that 7 of the 8 dispositions were significantly correlated with the sustainability of the common (Table 3), where a break-

Table 2: Parameter settings of selected scenarios

Parameters	Scenario 1	Scenario 2	Scenario 3
Initial percentage of patches covered by grass (Cov)	100	100	100
Total number of herdsman agents (N)	4	6	8
Initial number of cattle agents (C)	242	120	80
Net relative grass growth rate near zero ($rate_{growth}$)	0.00496	0.00496	0.00496
Cattle price (P_{cow}, \$)	133	133	133
Annual forage requirement in patches ($requ_{cow}$)	1	1	1
Total number of herdsman agents ($rate_{learn}$)	1.0	1.0	1.0

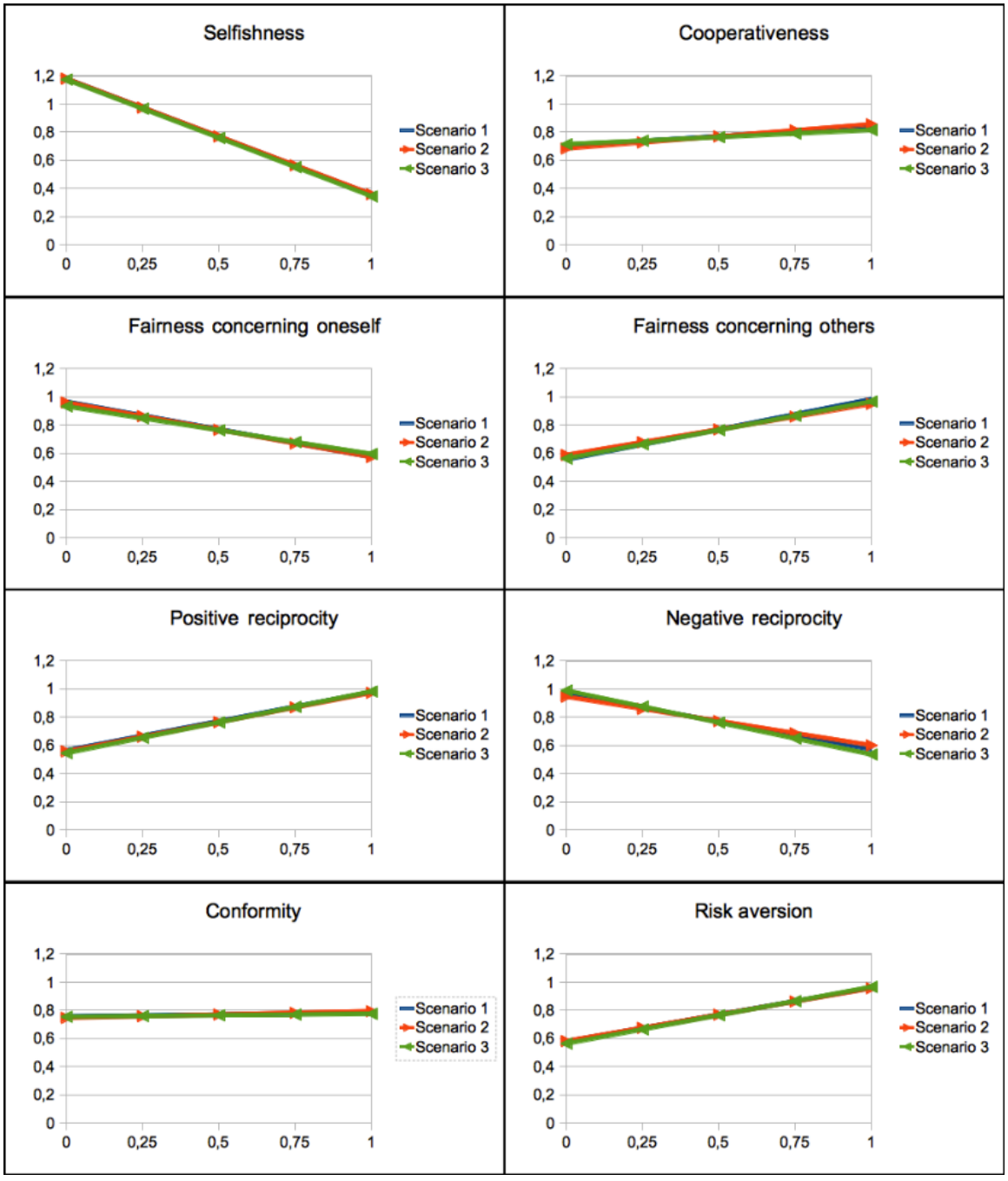

Figure 1: Simulation results of selected scenarios: Linear regression with sustainability value

Table 3: Simulation results of selected scenarios

Scenario	Selfish-ness	Coope rative-ness	Fairness towards oneself	Fairness towards others	Positive recip-rocity	Negative recip-rocity	Confor-mity	Risk aversion
Scenario 1								
Correlation	- 0.409	0.067	- 0.193	0.213	0.206	- 0.179	0.013	0.190
Significance	0.000	0.000	0.000	0.000	0.000	0.000	0.179	0.000
Scenario 2								
Correlation	- 0.411	0.085	- 0.192	0.180	0.208	- 0.172	0.023	0.188
Significance	0.000	0.000	0.000	0.000	0.000	0.000	0.120	0.000
Scenario 3								
Correlation	- 0.402	0.049	- 0.166	0.197	0.217	- 0.224	0.010	0.196
Significance	0.000	0.000	0.000	0.000	0.000	0.000	0.497	0.000

Table 4: Results of sensitivity analysis: Average sustained grass cover percentage for each disposition when set to values between 0 and 1 while other dispositions remain at their default values.

Value	Selfish-ness	Coope rative-ness	Fairness towards oneself	Fairness towards others	Positive recip-rocity	Negative recip-rocity	Confor-mity	Risk aversion
0.0	71	0	79	0	66	65	49	0
0.1	71	0	79	0	65	66	65	1
0.2	65	0	71	0	65	66	63	0
0.3	65	0	74	0	73	66	63	1
0.4	66	0	71	66	73	0	61	65
0.5	0	65	70	65	73	0	65	66
0.6	0	65	73	64	75	0	0	66
0.7	0	66	65	66	71	0	0	66
0.8	0	66	66	66	78	0	0	66
0.9	0	66	65	66	78	0	24	66
1.0	0	62	65	66	79	0	22	66

down was valued with 0, long-term sustainable use with 1, and removal of any cattle, i.e. exaggerated thoughtfulness, with 2. Only conformity did not show a significant correlation with the sustainability value, while all other dispositions behaved as intuitively suggested (Figure 1). While cooperativeness, fairness concerning others, positive reciprocity, and risk aversion significantly increased the sustainability level, selfishness, fairness towards oneself, and negative reciprocity decreased it, however, to different degrees. As such, a reduction in selfishness seems to have the greatest impact, while an increase in cooperativeness has only little. Identifying the reasons for these different degrees of impact is not straightforward, due to the complex interconnectivity of the dispositions' role in final action, therefore necessitating a simulation approach like the one conducted in this study.

Moreover, this complex nature has also other implications. If one is interested in management of a specific case study, it is necessary to look at the case-study dispositional values, which can cause behavior that violates the general statistical behavior of dispositions. To test this for a case study, we selected random disposition values using the scenario 2 (Table), which showed a sustainable system behavior. Then, we shifted each disposition in the respective direction that causes breakdown, until the system came to the point of breakdown. Starting with disposition values at this vulnerable point of breakdown, we conducted a sensitivity analysis, i.e. we separately shifted each value one-by one from 0 to 1 in steps of 0.1 and recorded the percentage of grass cover after as sufficient number of time steps (150). Each value combination was simulated 100 times. Results show that in this case study the increase of fairness towards oneself and the decrease of positive reciprocity did not lead to a breakdown of the system, but only to a reduction in the sustained grass cover (Table 4). In contrast, a shift of the other dispositions (apart from conformity) in their "negative" direction, i.e. the specific direction that leads to breakdown, caused a sudden switch from a sustained plateau to a system breakdown. For conformity, which does not have such a clear direction, we even obtained a significantly non-linear pattern of sustained grass cover. Moreover, in total, the land-cover levels seemed to cluster around two values of around 66 and 90 % (Figure), the reasons for which are not clear.

DISCUSSION

With this model, we found an easy way to validate

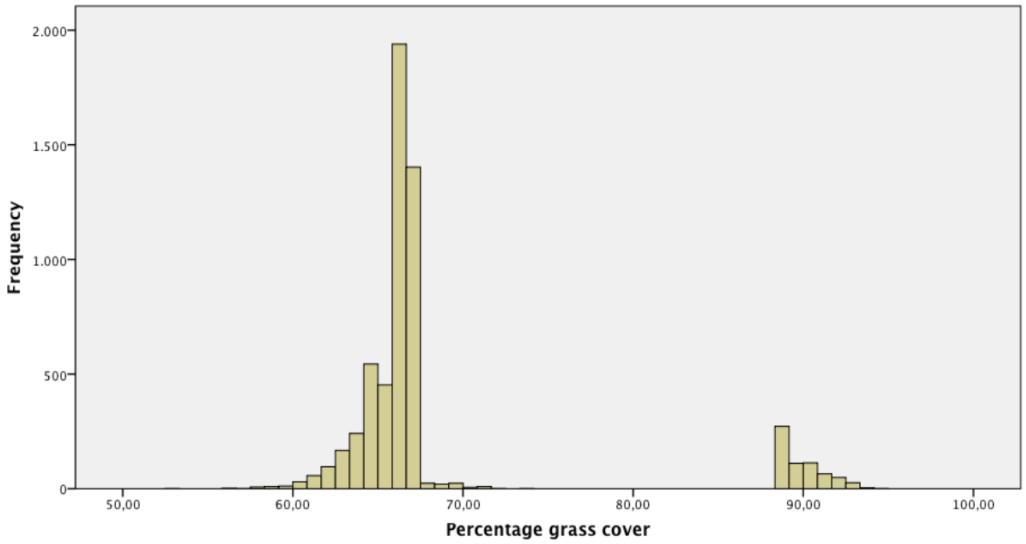

Figure 2: Frequencies of grass cover percentages of sustainable cases

Hardin's argument computationally, and validated the hypothesis that the consideration of other human values than pure profit orientation - as assumed by Hardin - can lead to sustained use of the common. We showed that statistically, these values or dispositions behave intuitively, but that this behavior can be counterintuitive and complex for specific case studies. This implies that when prosecuting to alter an existing endangered pasture system to a sustainable state, the specific behavior of this system should be studied via simulation. To do so, models with the ability to account for human behavior in human-environment interactions but with high computation speed are required. In contrast to a previous model version (Schindler 2012), which showed comparable results, this model fulfills this demand. While the computation load in the previous model version increased exponentially with increased herdsmen agent number, it increases here only linearly, which makes it suitable for real-world applications. This is due to the fact that this model calculates human behavior in a decentralized and reactive way, being the typical advantage of agent-based modeling, while the previous version used costly centralized calculation of equilibria to calculate human action. Having such a basic model may allow specification and adjustment to real-world applications, with the goal to strengthen those social norms that can make systems switch to sustainable states.

REFERENCES

Ebenhöh E. and C. Pahl-Wostl C. 2006. Agent-based modelling with boundedly rational agents. In J. P. Rennard, editor. Handbook of research on nature inspired computing for economy and management. Hershey-PA, USA.

Hardin G. 1968. The Tragedy of the Commons. Science 162:1243-1248.

Huffaker R.G. 1993. Optimal Management of Game and Forage Resources in a Private Fee-Hunting Enterprise. American Journal of Agricultural Economics, 75(3): 696-710.

Noy-Meir I. 1978. Stability in Simple Grazing Models: Effects of Explicit Functions. Journal of Theoretical Biology 71:347-380.

Ohiagu C.E. and T.G. Wood. 1979. Grass Production and Decomposition in Southern Guinea Savanna, Nigeria. Oecologia 40:155-165.

Schindler J. 2012. Rethinking the Tragedy of the Commons: The Integration of Socio-Psychological Dispositions. Journal of Artificial Societies and Social Simulation 15(1):4.

Wilensky U. 1999. NetLogo. http://ccl.northwestern.edu/netlogo. Center for Connected Learning and Computer-Based Modeling. Northwestern University, Evanston, Illinois.

JULIA SCHINDLER was born in Basel, Switzerland, grew up in Linz, Austria, and studied mathematics and geography at the University of Bonn. After her studies, she did her doctoral degree at the Center for Development Research in Bonn in geography. She has conducted research in Ghana and Uzbekistan, and her research interests are agent-based modeling of human-environment systems, psychology, and social simulation.

A NEW FRAMEWORK FOR COUPLING AGENT-BASED SIMULATION AND IMMERSIVE VISUALISATION

Athanasia Louloudi and Franziska Klügl
Modelling and Simulation Research Center
Örebro University, Sweden
Email: {athanasia.louloudi,franziska.klugl}@oru.se

KEYWORDS

Agent-based Simulation, Virtual Reality Systems, Representation Alignment

ABSTRACT

In this contribution, we are dealing with the problem of on-demand interfacing agent-based simulations with Virtual Reality (VR) systems. We focus on how to handle and relate information between the two systems and investigate a generic way for mapping the information which describes the state and context of a simulated agent to its 3D counterpart in the VR system. We provide details about the issues involved as well as propose generic representations and procedures that cope with the granularity discrepancies between the two systems. Finally, we present a first prototype and discuss aspects of its performance.

INTRODUCTION

In the field of agent-based modelling, visualisation plays an important role in communicating, analysing and debugging the behaviour of a model. As the technology advances, there is an increasing interest to use more realistic and complex environments such as 3D virtual worlds in order to improve the transparency, understandability and also attractiveness of the running simulation.

Advanced visualisation is particularly attractive for model evaluation. Especially for validation of a multi-agent simulation involving simulated humans, the lack of empirical data motivates searching for new validation methods such as the systematic usage of human experts checking the plausibility of a simulation (Klügl, 2008). Hereby, an immersive perspective - supported by 3D visualisation - is particulary important as the perspective during plausibility checks should be similar to the real-world perspective. A mere 3D visualisation might be useful for many simulations independent of the used paradigm; real immersion into the simulated system during simulation (as the high end of participatory simulation (Berland and Rand, 2009)) is particularly apt for agent-based simulations.

However, setting up and rendering a VR visualisation in addition to the actually intended simulation means additional effort for an addon to the simulation that is just relevant for plausibility checks (and selling the model), but not for the actual deployment runs. Thus, our vision is to create a generic component for connecting an agent-based simulation environment to a VR system which is able to control visualisation in an immersive virtual environment as the CAVE (Cave Automatic Virtual Environment) (Lee et al., 2010). In such a setup a human can observe the simulation's dynamics immersed in the simulation environment. Setting up a VR visualisation for a simulation model shall come at minimal costs. Ideally, all the necessary tasks for connecting a visualisation in a CAVE to an agent-based simulation shall be automated. Thus, a generic coupling between a simulation platform and a VR platform needs to be provided in a way that the simulation is not depending on the VR visualisation. The simulation shall mostly run without the VR platform, therefore embedding the simulation into a 3D environment with all the necessary visualisation overhead, does not make sense. The immersive component shall work as an add-on that is used when necessary, but still can be switched off for the deployment or other test simulation runs.

In the remainder of this paper, we will first give more details on the overall idea and the involved challenges. The next section gives an overview to the overall system setup and more specifically introduces the *MiddleLayerComponent*. Then we present the results from some initial performance tests of our prototype implementing the described setup. Then, we discuss upcoming challenges if a human interacts with the VR system. Finally, after a discussion of related work, the paper ends with a summary and an outlook to our planned next steps.

SYSTEM COUPLING

We consider the *Visualisation System* and *Simulator* as two different systems which represent the same multi-agent model, on different levels of temporal and representational granularities. The Simulator contains the more qualified representation assuming that it is built for validly reproducing the relevant features of the original system. It possesses refined object structures which aims to represent the relevant structural and especially behavioural aspects of the original system. Contrarily, the focus of the Visualisation System is on the realism and plausibility of the 3D object models and their animated behaviour. This means that it needs to display all details that a human observer would expect in the real world. In the following we will deal with particular aspects of the coupling that

Proceedings 26th European Conference on Modelling and Simulation ©ECMS Klaus G. Troitzsch, Michael Möhring, Ulf Lotzmann (Editors)
ISBN: 978-0-9564944-4-3 / ISBN: 978-0-9564944-5-0 (CD)

originate from this different objectives.

Mapping agents to object models Starting from a given multi-agent simulation model, every agent or passive entity in the Simulator has to be associated to a detailed 3D character in the Visualisation System. This entails information about the object model such as shape, size and scale in order to plausibly depict the simulated situation. All measurements must correspond.

Mapping agent behaviour to animations Displaying an agent's behaviour in a plausible way is more than connecting one action to one animation. There are several issues related to the way a character in the Visualisation System can change its appearance and displayed behaviour in runtime. For example, morphing operators can be used for changes in the shape (e.g. pregnancy) and movement of the object model. Animations can be combined in different ways and may have longer duration than what corresponds to a simulation step (that gives the frequency with which new data is arriving at the Visualisation System) yet the animations need to continue or to be connected in a smooth way.

Environmental dynamics A multi-agent simulation may contain global dynamics such as fog or raising temperature, but also discrete signals for example triggering evacuation. These dynamics cannot be assigned to one agent/object model, but should be visualised.

Interaction between the agents Apart from the individual dynamics of the characters, their interactions have to be visualised as well (e.g., characters that talk to each other, wave to each other etc.). Thus, the visualisation must be coordinated. Animations of different agents that the Visualisation System is independently informed about, cannot be independently displayed.

Synchronisation It is important to assure that for a given timestep t, both systems have matching situations/scenes. Yet, Simulator and Visualisation System have different time advance functions. The Visualisation System shall render in real-time whereas the Simulator updates the situation usually as fast as possible. The relation to real time may be varying depending on the numbers of agents or events to be treated. Thus, different time granularities are present and there is a clear need to buffer the relevant information while maintaining consistency between the two systems, as well as to interpolate or even extrapolate dynamics.

Interpolation of behaviour As we assume asynchronous operation modes for the two systems, there may be an update delay or insufficient information arrives at Visualisation System. To clarify this problem, consider the following example as illustrated in Fig. 1. At time $t_{Sim} = 0$ an agent A is at position $P_0 = \{x_0, y_0, z_0\}$.Given an action "$walk$", at time $t_{Sim} = 1$ he is at position $P_1 = \{x_1, y_1, z_1\}$. Between these two positions there is an obstacle that the agent has to avoid, yet it does not have the necessary information how to do as the more abstract Simulator just sent the position information to the Visualisation System. The latter has to maintain the needed realism. Therefore it becomes necessary to compensate this lack of information and estimate a reasonable movement between the given positions. A method which can be used to accomplish this is interpolation, for example using algorithms based on dead reckoning (Beauregard, 2007). The situation becomes critical, if the agent during its interpolated movement interacts with other entities not foreseen in the Simulator representation.

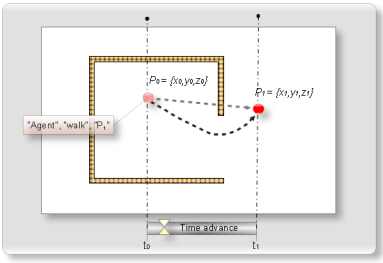

Figure 1: Graphical illustration of the behaviour's interpolation in a collision avoidance example.

VR world configuration In order to be able to render the scene in the Visualisation System, further configuration in addition to the actually simulated situation is necessary. Each scenario/scene may have specific demands on cameras and lighting. Their positioning in the scene is an important issue and can clearly affect the realism of the scene and therefore also the result of the immersive plausibility checks.

SYSTEM OVERVIEW

A general view of our proposed framework for coupling s Simulator and a Visualisation System is presented in Fig. 2.

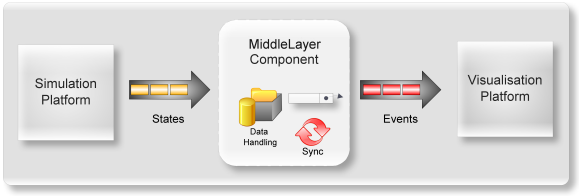

Figure 2: Graphical illustration of the overall framework.

We assume a time-stepped Simulator. In every time step, explicit information about the current situation is used to create a full snapshot. As the Visualisation System operates in an independent time regime, there is a need to use a component that buffers information from the Simulator and transfers the right information parts to the Visualisation System when needed. This is the *MiddleLayerComponent*. It constitutes the most important block in the framework because here the core data processing takes place. Its main responsibility is to buffer the different time and object granularities. It translates the incoming simulator data to specific event and actions at the appropriate time thus maintaining the consistency between the two platforms.

Data structures
Fig. 3 describes the data structure that forms the basic skeleton for all incoming data relevant for visualisation. A full snapshot `GameState` of the simulation at every tick is stored in a list of game states, the `GameStateList`. Every game state has a time-stamp, a list of objects that are populating the scene at that time, relevant information about the environment and information about the state of a human observer. The list of objects `ObjectList` is composed of information on all the entities currently existing in the scene; agents and passive entities (for example resources or obstacles). Both of them are `PhysicalObjects`, which means that they have an unique name, position and rotation information. We make a distinction between agents and passive entities: agents possess an additional attribute which denotes their state. This distinction facilitates mainly the generation of the scene due to fact that the 3D object model for the agents must hold animations that are controlled by the state. The classification agent/passive entity might be different in Simulation and Visualisation; in the later passive entities may appear to be active as well due to a more flexible and elaborated visualisation: A passive object may require an animation (e.g., opening/closing door). Also the environment may have a state which can trigger changes to the rendered scene (e.g., showing changes in day/night or displaying an evacuation signal).

This shared meta model allows the scene to be automatically generated from the Simulator. The modeller only needs to add pointers to the appropriate object models and animations. Based on this data buffer, the information stream from Simulator and the processes that access information for visualisation are decoupled. The memory needs are depending on the richness of the model. If the buffer size is restricted, problems may occur. Therefore we need to identify the actual requirements with respect to the simulated model.

Overall Process
There are two processes that need to be considered: The setup process that causes the main effort for the modeller and the run-time process connecting the two systems during simulation and visualisation. The modeller needs to execute the following tasks:

- Connect physical objects to 3D object models
- Connect animations / animation combinations to agent activities

We assume that the rest can be done automatically: The Simulator may full scene description. This scene describes the overall starting state of the Visualisation System and its configuration. This core material upon contains information about the size of the simulated world as well as the exact number and setups of agents and passive entities with their relevant initial positions as well as the assigned 3D object models. By default, cameras and lights are added following some generic heuristics about the size of the environment or the designation of a particular entity as the human user in the VR system/CAVE.

During simulation, agents execute particular actions or activities that are connected to combinations of animations or other operators. The high-level behaviour specification using activities is a speciality of the simulation platform that we used for the endeavour. The simulated agents are programmed using activity graphs. This structure facilitates the connection to animation combinations as the behaviour program is already structured. Due to this explicit information, the Simulator can generate the appropriate information for each agent and send this information for all agents to the *MiddleLayerComponent* where it is stored into buffering data structures. Triggered by rendering in VR system, the data structure is accessed and appropriate events are formed and sent for execution in the visualisation side. The execution of events is then completely handled by the Visualisation (e.g., *play animation*).

EXPERIMENTS

Prototype
We created a prototype for the *MiddleLayerComponent* connecting the two systems. This component connects SeSAm (Klügl, 2009), a general modelling and simulation platform and the Horde3D GameEngine (*http://hcm-lab.de/projects/GameEngine*) implementing the above introduced functionality. In addition, we developed an export function as a SeSAm plugin that generates a complete description of the scene in XML format. After minor configurations, it can be used as an initial scene description for Visualisation System. However, due to the absence of an automatic generation of geometries from the information in the simulation platform, this export is restricted as it assumes that the relevant object models are existing.

During the simulation, all the visible effects of the agents' actions, are transmitted via client/server communication. The protocol includes information as described above; position, orientation and activity (animation) of each entity in each update. In addition to this, information about environmental state changes or other events are also sent, as well as information the generation or removal of agents from the overall scene. The generation is handled with the same information used for the setup of the scene.

MiddleLayerComponent stores the incoming data in the above described buffer. The rendering process of Horde3D sends a request for the appropriate information to be rendered in the current frame. As an answer to this request, the *MiddleLayerComponent* generates all the necessary events so as to display the appropriate real-time scene.

Scenario
To evaluate the performance of our prototype, we used two testbed scenarios. The first one is an implementation of the well-known *Boids* model in 3D(Davison, 2005). The second, is a small evacuation scenario in

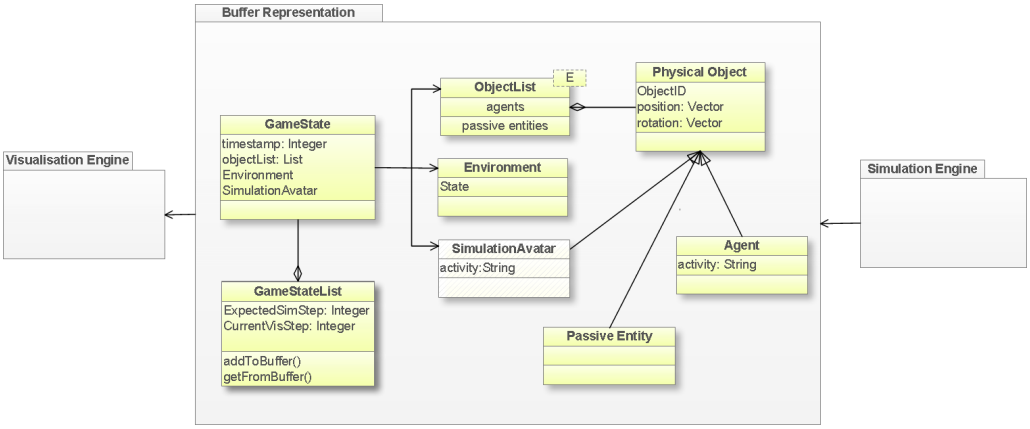

Figure 3: UML diagram of the data structures.

which agents randomly move around the environment, communicate/interact (e.g., talk, wave etc.) with other agents if they are nearer then a given distance. At a given time, there is an evacuation signal, which causes all agents to run towards the exit by avoiding collisions. Fig. 4 shows two snapshot pairs of the scenes in the two systems.

Performance in the Boids Scenario

Five situations of the same scenario are generated varying in the number of agents: 5, 20, 50, 100 and 500. A human observer is positioned as an obstacle. The agents are exhibiting flocking behaviour while avoiding the human observer/obstacle. The simulation ends after timestep 1000, running as fast as possible. At $t = 100$, 50 new agents are added, at $t = 500$, 50 randomly selected agents are deleted from the simulation for showing how the overall system reacts to generation and deletion of entities.

Fig. 5 gives our performance results. The graph in Fig. 6(a) shows the size of the buffer (`GameStateList`) depending on the number of agents in the scene in a simulation run of 1000 steps. The *Overall Buffer Size* shows the amount of data size the Simulator has sent to the *MiddleLayerComponent* (measurement of atomic information units) whereas the *Remaining Data* deals with the information that is pending to be executed by the Visualisation in the moment the simulator has ended. It is obvious that the memory consumption is linear, yet it appears that in all cases the Visualisation System can handle the load. From the observer's point of view, the animations' update and the overall performance in general was very smooth in all the five cases. Clearly, simulation speed reduced with higher numbers of agents but still it was fast enough to feed properly the Visualisation System.

In the following, we evaluate the time consumption of the several operations performed in the *MiddleLayerComponent*. We identify three main interesting values:

1. Transfer Time - It measures the time needed for the data from being sent by the Simulation to reach the socket in the *MiddleLayerComponent*.

2. Processing Time - It measures how much time it takes for the data to be processed and stored in the buffer.

3. Retrieval Time - It measures how much time it takes for the data to be retrieved for rendering.

We already described that during runtime, 50 agents are generated and the same number of agents is deleted after some time. The result of this operation is obvious in Fig. 6(c). At $t = 100$ the process time shows a significant increase which gradually is getting reduced and stabilises when the agents are deleted and no additional information is communicated apart from the agents' position, orientation and particular state. In Fig. 6(d) there is an interesting observation: The cases with 100 and 500 agents, do not really seem to be affected by the creation/deletion of agents but the time to retrieve the data from the buffer increases constantly. This is a result of an overall delay of the simulations update. The read/write process can be seen quite costly when a large amount of agents is involved. In the case of 500 the Visualisation System sometimes had to wait for the simulation to produce the state message. A more efficient simulation platform will replace SeSAm in our future work.

Performance in the Evacuation Scenario

In this test case, we demonstrate the generality of our framework. The evacuation scenario is a 2D agent-based simulation. Main difference to previous case is that we need to connect 2D shapes with fine grain object models as well as their relevant animations. Concerning the third dimension, it is not available in the 2D simulation, therefore it has to be given as additional information in visualisation. We have a variety of states/animations that need to be communicated as well as information triggered by the world such as the evacuation signal.

INTERACTION WITH HUMAN

The assumption that the human observer stays passive within the VR system when evaluating a simulation is not realistic. Thus, we must expect that the human observer

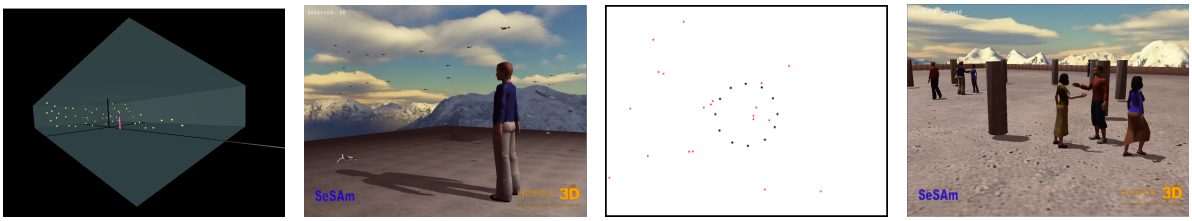

(a) SeSAm 3D (b) Horde3D and SeSAm 3D (c) SeSAm 2D (d) Horde3D and SeSAm 2D

Figure 4: Snapshots of the boids example in using the standard animation in SeSAm and the visualisation in Horde3D controlled by SeSAm.

Figure 5: Prototype's performance evaluation.

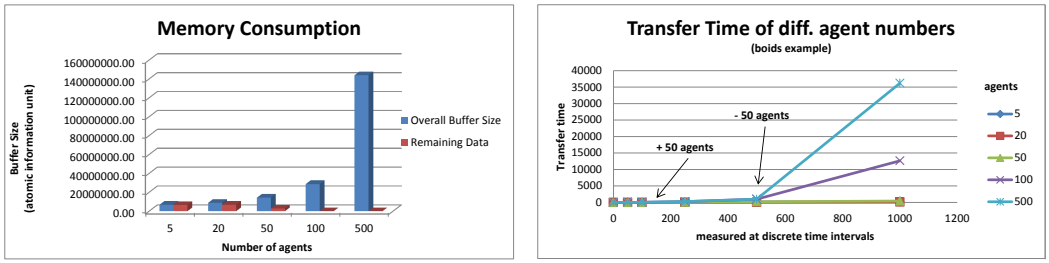

(a) Memory consumption (b) Transfer time

(c) Process time (d) Retrieval time

at least wants to move around in the overall scene or even interact with the simulated agents in a similar way as in real life. This was coined by (Pelechano et al., 2008b) as the necessity of "presence". Thus, for enabling a human to evaluate the simulation model dynamics, we must take the human immersion in our system serious. However, the overall complexity rises significantly as the behaviour of the human would affect the behaviour of simulated agents at a time when the simulation itself actually computes at a completely different time step. This would require that information flows back from the Visualisation System to the Simulator: In the prototype, the immersed human-avatar corresponds to a static obstacle from the other agents' point of view. The agents have to avoid the human by moving around him. Yet, if the human avatar interacts with other agents, then both his/her actions and their results have to be transferred back to the simulation. The agent in the simulation which is corresponding to the human then actually executes the actions induced by the human in the simulated timestamp corresponding to the time step that is currently displayed in the visualisation. This is a bidirectional coupling causing some challenges: An asynchronous operation of the two systems would basically imply the need to have a roll-back function in the simulation side. Imagine a case in which the Simulator is processing the agents' state in $t_{Sim} = 100$ while the user connected in the Visualisation platform, is changing the flow of actions in $t_{Vis} = 10$. The simulation has to adapt to this change and reset the simulated situation to $t_{Sim} = t_{Vis} = 10$ and restart again.

An alternative in some restricted cases might be based on a more intelligent *MiddleLayerComponent*. Instead of initiating a full roll-back on the Simulator side, the *MiddleLayerComponent* analyses and adapts all stored snapshots from the currently displayed time to the current simulation time. If there are not too extensive discrepancies, it might be possible to actively align the two representations starting with the human modifications in the Visualisation System. The *MiddleLayerComponent* calculates the effects and resulting delta in the next-to-render situation. If component possess enough knowledge about effects of actions, and the time difference between Simulator and Visualisation System is not too large, the effects of the human interaction might be isolated and the Simulator

might be just forced to restart from a time significantly later than the current visualisation time.

RELATED WORK

3D visualisation in multi-agent simulation made its first breakthrough with the seminal evolving creatures of (Sims, 1994). Despite the promising results, detailed 3D representations of simulated models could mostly be found until recently in domain specific applications such as in pedestrian simulation and 3D visualisation could not but be seriously considered. Recent developments in microscopic pedestrian simulation platforms yielded the need to increase visibility on generic multi-agent simulation and thus they include detailed 3D spatial representations in physically simulated 3D words. There is a number of agent simulation platforms specialized for 3D modelling; breve seems to be the most well known open source platform (*http://www.spiderland.org/breve*). Similarly, there is Repast (*http://repast.sourceforge.net/*) or MASON (*http://cs.gmu.edu/eclab/projects/mason/*) that embedded Java3D into their simulation platforms. However, a simple 3D visualisation is not always capable of increasing the understandability of the simulated situation so in a more complex scenario a finer visualisation is more desired leading to the creation of more complex 3D visual representations such as virtual worlds. The combination of virtual worlds and simulation is also prominent in crowd simulation (Pelechano et al., 2008a), (Thalmann and Musse, 2007). This endeavour often involves the use of game engines where apart from the agents' modelled environment, sensor data and action commands are available for communication between the simulation platform and the game engine (Norling, 2003). In our work we also consider the use of a game engine but as a means for visualising the simulated multi-agent model's dynamics. One of our main considerations is to provide a solution that is not application specific but rather generic.

In (Avouris, 1992) different multi-agent system architectures for identifying specific challenges are classified when designing interfaces to multiagent simulations but only cases restricted to top-down perspective (bird's eye view) are considered. In this area where visualisation for agent-based simulation is the main focus, there is also interesting work reported. Namely, (Kornhauser et al., 2009), give design guidelines for adapting general design principles and techniques (e.g., shapes/colours of the agents or use of entity groups) for visualising the dynamics of a multi-agent simulation. Their work involves the creation of 2D models implemented in Netlogo (`http://ccl.northwestern.edu/netlogo/`). Our research is related to some extent with the creation of interfaces for multi-agent systems but we are mainly interested in deploying the assets of a fine grain visualisation such as virtual reality.

There have been many uses of agent-based frameworks to create interactive simulation, (Vizzari et al., 2008) present in their work a framework for visualising crowd simulations based on interacting situation agents. They do not handle the synchronisation issue but they rather reduce the simulation's speed so as to visualise properly the simulation's dynamics and maintain consistency. Our framework presents similarities to the one of (Oijen et al., 2011), who consider the coupling of the two systems and not their embodiment. Nevertheless their vision is to use/include BDI agents in 3D game engines for building intelligent behaviour. The performance of this framework as well as others like (Gemrot et al., 2009) should be also tested in the context of our work that is mainly oriented towards the evaluation of the multiagent model.

Consistency plays a central role in our work. Thereby, a relation can be also found in the area of distributed interactive systems such as multiplayer network games, where consistency has to be assured for presenting the same situation to different users. Several techniques have been developed for avoiding or dealing with inconsistencies coming from latency and jitter (Diot and Gautier, 1999), (Delaney et al., 2006). In our case, we identify the major problems to be the different resolutions and synchronisation problems between two full representations of the same system, not a distributed representation. Nevertheless it is of worth to mention here that the interpolation of agent's behaviour has similarities with the consistency problem of distributed interactive systems.

SUMMARY AND FUTURE WORK

In this contribution we discussed the concept of adding a sophisticated visualisation to a multi-agent simulation using a generic *MiddleLayerComponent* for providing a way of easily setting up what is needed for plausibility checks by a human expert from the usual perspective. A first prototype of the overall system is available where a *MiddleLayerComponent* buffers information from the Simulator. It is accessed at the appropriate times by the Visualisation System. First performance measures show positive results indicating that the connection itself does not have critical performance problems.

However, in the current status just half of the problem is solved. A still critical one is how the overall system shall react on the human observer. The problem already starts with collision avoidance. Agents in the simulation might avoid the human observer but the question how the situation changes initiated by a mobile human in the Virtual World can be fed back into the simulation is not yet answered. This will be the major part of our future work.

Additionally, we will consider situations where the visualisation needs more and faster data than the Simulator and the *MiddleLayerComponent* can provide. Then, stops in the Visualisation System may hinder the objective of our endeavour; the human observer immersed into a virtual reality that cannot correspond to the real one just because of stops. It might be a good idea if there would be some extrapolation on the visualisation side, assuming that the simulation can later catch up again when e.g. the

number of agents has reduced and thus simulation speed has increased again. How then the state of the Visualisation System can be mapped back to the Simulator is a problem related to the interaction problem discussed above, yet it does not just affect the representation of the human in the simulation, but a number – in the worst case all – agents.

We currently have set up two test cases for the overall framework: the above used boids simulation and a small evacuation scenario. Clearly for showing the scalability of the system in terms of agent complexity and numbers, we need to use the system in several real simulation projects.

REFERENCES

Avouris, N. M. (1992). User interface design for DAI applications. In Avouris, N. M. and Gasser, L., editors, *Distributed Artificial Intelligence: Theory and Practice*, pages 141–162. Kluwer Academic Publisher.

Beauregard, S. (2007). Omnidirectional pedestrian navigation for first responders. In *Proceedings of the 4th Workshop on Positioning, Navigation and Communication (WPNC '07)*, pages 33–36.

Berland, M. and Rand, W. (2009). Participatory simulation as a tool for agent-based simulation. In *Proceedings of the 1st Int. Conference on Agents and Artificial Intelligence*, pages 553–7, Setubal, Portugal.

Davison, A. (2005). *Killer Game Programming in Java*. O'Reilly Media.

Delaney, D., Ward, T., and McLoone, S. (2006). On consistency and network latency in distributed interactive applications: a survey–part i. *Teleoperators and Virtual Environments*, 15:218–234.

Diot, C. and Gautier, L. (1999). A distributed architecture for multiplayer interactive applications on the internet. *Network, IEEE*, 13:6 –15.

Gemrot, J., Kadlec, R., Bída, M., Burkert, O., Píbil, R., Havlíček, J., Zemčák, L., Šimlovič, J., Vansa, R., Štolba, M., Plch, T., and Brom, C. (2009). Pogamut 3 can assist developers in building AI (Not only) for their videogame agents. In Dignum, F., Bradshaw, J., Silverman, B., and van Doesburg, W., editors, *Agents for Games and Simulations*, volume 5920 of *Lecture Notes in Computer Science*, pages 1–15. Springer Berlin / Heidelberg.

Klügl, F. (2008). A validation methodology for agentbased simulations. In Wainwright, R. L. and Haddad, H., editors, *Proceedings of the 2008 ACM Symposium on Applied Computing*, pages 39–43. ACM.

Klügl, F. (2009). Sesam : visual programming and participatory simulation for agent-based models. In Weyns, D. and Uhrmacher, A., editors, *Multi-agent systems : simulation and applications*, Computational analysis, synthesis, and design of dynamic models series, pages 477–508. CRC Press/Taylor and Francis.

Kornhauser, D., Wilensky, U., and Rand, W. (2009). Design guidelines for agent based model visualization. *Journal of Artificial Societies and Social Simulation*, 12(2).

Lee, H., Tateyama, Y., and Ogi, T. (2010). Realistic visual environment for immersive projection display system. In *Proceedings of the 16th Int. Conference on Virtual Systems and Multimedia (VSMM 2010)*, pages 128 –132.

Norling, E. (2003). Capturing the quake player: using a BDI agent to model human behaviour. In *Proccedings of the 2nd Int.Conference of Autonomous Agents and Multiagent Systems (AAMAS'03)*, pages 1080–1081, New York, NY, USA. ACM.

Oijen, J. v., Vanhee, L., and Dignum, F. (2011). CIGA: A middleware for intelligent agents in virtual environments. In *Proceedings of the 3rd International Workshop on Agents for Education, Games and Simulations, AAMAS'11 Taipei, Taiwan*.

Pelechano, N., Allbeck, J., and Badler, N. I. (2008a). *Virtual Crowds: Methods, Simulation, and Control*. Morgan and Claypool Publishers.

Pelechano, N., Stocker, C., Allbeck, J. M., and Badler, N. I. (2008b). Being a part of the crowd: towards validating VR crowds using presence. In *Proccedings of 7th Int.Conference of Autonomous Agents and Multiagent Systems (AAMAS 2008)*, pages 136–14. IFAAMAS.

Sims, K. (1994). Evolving 3d morphology and behavior by competition. In Brooks, R. A. and Maes, P., editors, *Artificial Life IV Proceedings*, pages 28–39.

Thalmann, D. and Musse, S. R. (2007). *Crowd Simulation*. Springer.

Vizzari, G., Pizzi, G., and da Silva, F. S. C. (2008). A framework for execution and 3d visualization of situated cellular agent based crowd simulations. In *SAC*, pages 18–22.

AUTHOR BIOGRAPHIES

ATHANASIA LOULOUDI is PhD student at the Modeling and Simulation Research Center of Örebro University. She holds a Master in Robotics and Intelligent Systems (Örebro University).

FRANZISKA KLÜGL is Professor in Information Technology at Örebro University, Modeling and Simulation Research Center. She holds a PhD in Computer Science and did her Habilitation with focus on Agent-based Simulation Engineering, all at the University of Würzburg in Germany. In 2008, she became Senior Lecturer at Örebro University, Sweden.

MODELLING LIFESTYLE ASPECTS INFLUENCING THE RESIDENTIAL LOAD-CURVE

Wolfgang Hauser
Stuttgart University
ZIRN
Seidenstr. 36, 70174 Stuttgart, Germany
wolfgang.hauser@sowi.uni-stuttgart.de

José Évora
University of Las Palmas de Gran Canaria
Parque Científico y Tecnológico
35017 Las Palmas de Gran Canaria, Spain
jose.evora@siani.es

Enrique Kremers
EIFER
Emmy-Noether-Str.11, 76131 Karlsruhe, Germany
enrique.kremers@eifer.uni-karlsruhe.de

KEYWORDS

ABS. Agent-based-model, residential energy consumption, load-curves, lifestyle.

ABSTRACT

Using the results of a representative survey for the city of Stuttgart, household load-curves are simulated through an agent-based modelling approach. Aggregated household load-curves for different lifestyle groups are presented and the effect of their corresponding behavioral profiles on the residential load-curve is evaluated.

INTRODUCTION

Residential consumption of electricity is influenced by a multitude of variables and shows big variance between households, even within the same society and geographic region: Lutzenhiser and Bender (2008) report differences of up to factor 40 between the measured electricity demands of 1 627 households in a Northern Californian sample Morley and Hazas (2011). Furthermore, electrical consumption for single household tasks vary greatly between households: ADEME et al. (2008) shows that electricity used for cooling devices differs by factor 10 between different households, the same applies to electricity used per person for dish-washers.

The rise of decentralized power supply raises the need for electricity demand forecasts of smaller areas. Simulations of household electricity demand are mostly based on mean values of the whole population (e.g. Paatero and Lund (2006)); for specific areas of interest this approach results in an ecological fallacy, because different kinds of households are not equally distributed in space: In Stuttgart the average number of persons per household differs from 1.56 to 2.18 for different city quarters. To reduce the ecological fallacy it is necessary to identify determinants of residential electricity consumption, which can be linked to geographic data or building types, e.g. the number of persons living in a household or lifestyle typologies.

For the planning of power grids, not only the overall quantity of electricity consumed is of importance, but it is also important to know at what time of day the electricity is demanded: it is the load curve that matters (a load curve visualizes the use of electrical energy over time, showing watts on the y-axis and time on the x-axis). Nevertheless, measured data about electricity demand on a household level is very hard to find, especially when looking for a random sample. To simulate load curves for different types of households, we connected a simulation converting weekly or daily probabilities of energy relevant household tasks, into start times of events with simulations of appliances‘ load curves.

METHODOLOGY

Based on the lifestyle typology developed by Otte (2005) usage rates and probabilities for the possession of different electrical appliances are compared between different groups of society, using data collected in a postal survey. In order to evaluate household energy consumption, the survey focused specifically on daily routines and appliance ownership, because direct data collection of household energy con-

Proceedings 26th European Conference on Modelling and Simulation ©ECMS Klaus G. Troitzsch, Michael Möhring, Ulf Lotzmann (Editors)
ISBN: 978-0-9564944-4-3 / ISBN: 978-0-9564944-5-0 (CD)

sumption through surveys faces a big problem regarding missing values (25-60% in most studies), which can not be expected to be distributed randomly. Usage rates, habits and probabilities for the possession of household equipment are transformed into household-agents with specific daily routines and specific household equipment, then the resulting load curves for each household are simulated in an agent based model and aggregated in different ways.

DATA

We get information about weekly and daily usage rates for different appliances from a postal survey conducted in the run of the European Centers and Laboratories for Energy Efficiency Research (ECLEER) Ph.D program. In Germany, 4 000 Stuttgart based households had been asked to fill out a questionnaire about household usage rates, sociodemographics and lifestyle issues; 769 filled out questionnaires have been sent back, equalling a return rate of 19.2 %. Results of the survey can be compared with a survey employing the same typology, conducted in 2008 by the *Statistisches Amt* of the city of Stuttgart, with a bigger sample and a better return rate Schwarz (2010). Our results are more or less in line with this survey, with the exception of a higher age average resulting in smaller proportions of modern lifestyles. The biggest differences are with regard to the proportion of *Conventionalists* and *Hedonists*. It seems plausible that younger people, spending less time at home, were less willing to take the time to answer our questionnaire, as it was substantially longer than the one used by Schwarz (2010), which also explains the lower overall return rate. A comparison of the results of both surveys is presented in Table 1.

SIMULATION MODEL

After the survey analysis, the information regarding the appliances usage for every social group is available. Now, the challenge is to build up a simulation where this information is integrated in order to calibrate an agent-based model. However, this task concerns external aspects which provide the agents environment. The environment is composed of two sides: the global and the local. The global regards the agent location within the world. This information arises when the agent is related to a concrete household of the scene and this is, in turn, related to a building. The first relation is due to a link and the second one is due to a contain relation. Finally, the building indicates the exact coordinates to locate itself in the world. On the other hand, the local environment consists of the appliances within the household as they are the elements with which the agent interacts.

Then, the simulation model describes agents, appliances, households and buildings. As described in Évora et al. (2011), the agents can be considered as intentional models and the appliances as design models. The agent model is described in section Household Model and represents parts of the behavior of a household, which have a big impact on consumption of electrical energy. The local environment of the agent is composed of many kinds of appliances which are switched by the agent. Then, the task to develop the local environment consists of modelling the many appliances that the agent uses. The appliances models consists in the description of how they work. For instance, the washing machine model works producing a non-consumption when switched off. When the agent turns the washing machine on, a three-cycle working mode starts up producing a non-zero consumption.

This model is represented using a bottom-up approach where the electrical grid consumption comes from the agents acts since they generate the appliances consumptions at switching them. The tool that we have used to model this experiment is Tafat (described in detail in Évora (2011)). This framework was used because, among other reasons, it allowed us developing the model fast since the appliances models reuse was possible. Another reason for choosing this framework was the performance as the intention is to model a huge scene where thousands of agents are running at the same time with their respective local and global environments.

Household Model

Each household is represented as an agent, having control over his electrical appliances; the probability to own a certain kind of appliance is derived from the distributions in the survey data and differs between the lifestyle groups (see section Survey Results). Each instance of an household draws randomly from the respective distribution, in order to determine if he owns a tumbler, washing machine, etc and what kind of cooling devices are to be found. In the same fashion, each household is assigned rates of using these appliances, as well as times of inactivity (sleep hours) and absence. Probabilities of

Table 1: Otte lifestyle groups in Stuttgart

Standard of consumption			
high	**Conservative well-off**	**Liberal well-off**	**Reflexives**
	4.82 (3) %	16.31 (15) %	4.68 (10) %
	Ø 66 (62) years	Ø 55 (50)years	Ø 45 (39) years
	Ø 2.12 pers.	Ø 2.46 pers.	Ø 2.28 pers.
medium	**Conventionalists**	**Success seekers**	**Hedonists**
	14.61(7) %	30.21 (27) %	6.52 (14) %
	Ø 64 (65) years	Ø 52 (48) years	Ø 42 (36) years
	Ø 2.21 pers.	Ø 2.43 pers.	Ø 2.09 pers.
low	**Traditional workers**	**Home-centered**	**Entertainment seekers**
	8.09 (7) %	12.20 (14) %	2.55 (5) %
	Ø 63 (65) years	Ø 50 (46) years	Ø 37 (33) years
	Ø 2.22 pers.	Ø 2.33 pers.	Ø 2.22 pers.
Modernity	low	medium	high

n = 705 (2138)

Results of the survey by Schwarz (2010) shown in parentheses for comparison

preparing a warm lunch or dinner and the time when these take place are also taken from the survey and differ between groups. Of course, the agent can not perform the household tasks in his time of absence or sleep. It is, however, able to start multiple devices at the same time, which will run for a predefined cycle (washing machine) or for a time that is, again, drawn from the distribution of the lifestyle group he belongs to. Lights are turned on automatically between 18:00 and 7:00 if the agent is not absent or sleeping; however, we added a normally distributed error component to the start and stop time, in order to prevent an artificial peak to the aggregated load-curve. Cooling devices are running on a regular pulse. To generate a load-curve that averages the behavior of the households of interest and is robust towards random variation, 1 000 households are set up for each simulation run. The behavior model of the households is connected to the Tafat environment, controlling the start and stop times for the appliance models stored therein.

Appliance Models

Each household is equipped with a set of appliances. Besides the usage of the appliances, the electrical devices themselves have different types of consumption patterns – for example a lightning bulb will run most of the time at a constant power, whereas a washing machine will consume more power during the heating cycle than during the washing period. The consumption depends on the type of electrical consumer and on its internal mechanisms of operation. High power devices such as ovens or stoves will usually operate in an intermittent mode, causing high power peaks, separated by almost zero consumption periods.

For simulating the different types of devices, the *European Institute for Energy Research* (EIFER) and the *University College of Engineering at the University of the Basque Country* (EUI/UPV) have developed a set of appliance models which allow to represent the load curves of individual devices. Parametering the devices is also possible, in order to represent different efficient appliances of the same type, e.g. characterized by their EU energy label or size. The device models can be switched on and off in simulation time, as if they would be a *real* device, and generate a load which is aggregated to the household load.

RESULTS

Survey Results

Regarding the ownership of electrical appliances and daily routines, there are significant differences between lifestyle groups. *Conservative well-off* and

Entertainment seekers appear to be specially suited for a direct comparison, as they are on the opposing ends of the lifestyle dimensions and show the biggest differences in appliance possession and usage rates. For this reason, these groups have been chosen for the simulation runs. A detailed analysis of all variables can not be presented in the scope if this article, so only the most striking differences will be presented.

In regard to the number of cooling devices to be found in households, *Conservative well-off* own on average 1.9 devices, meaning that almost every household owns two devices, while only one in three *Entertainment seekers* households has a second cooling device. A Welch t-test between the group shows that this difference between the two groups is significant on the 99.9%-level. Furthermore, we find significant differences regarding the percentage of household owning a of dish-washer (85 % vs. 39 %) or a tumble dryer (53 % vs. 11 %). Regarding daily routines, the two groups differ significantly in the number of times they are cooking per week (8.0 vs. 5.5) and in regard to their absence from home (see Figure 1).

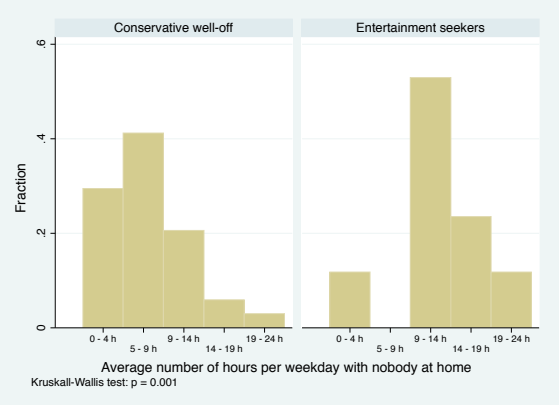

Figure 1: Absence from home on weekdays

Simulation Runs

Data about measured load-curves of different household is very sparse and not publicly available. This was one of the motivations for our approach. Unfortunately, this prevents a good verification of our results with measured data. Therefore, we compare the simulated load-curves (cumulatedSIM) with a standard household load-profile scaled to the electrical energy consumption of the simulation (weightedSLP). To evaluate the effect of the different lifestyles on the residential load-curve, we present results of three simulation runs: one with the share of the different lifestyle groups as found in the survey, one where all the households are set to the behavior and appliance ownership of the group of the *conservative well-off* and a last one with all households set to values found for the group of the *entertainment-seekers*.

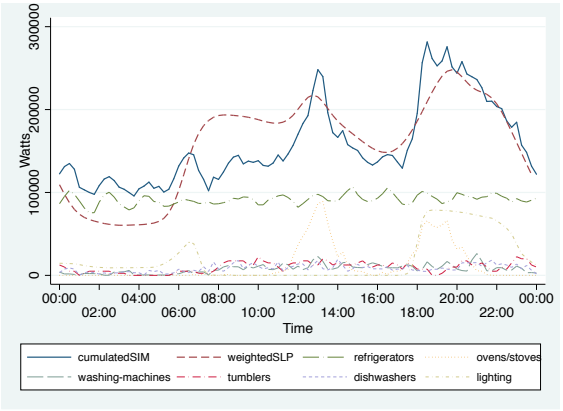

Figure 2: Simulated load-curve for 1 000 households with lifestyle groups distributed according to their share in the survey

With lifestyles represented in the simulation with the same shares as in our sample (Figure 2), we see that the noon and evening peaks are more accentuated than in the standard household load profile (SLP). One reason for this seems to be, that we model only a relatively small number of appliances by now and therefore the effect of stoves and ovens could be overestimated. Another reason - which applies especially to the evening peak - might be that employment figures in Stuttgart are very high, so that more consumption than on average in Germany is shifted towards the evening hours. A third reason might be, that we underestimated the variation in lunch and dinner preparation and should introduce a bigger error component to this decision.

Another difference in comparison to the SLP is that the simulated load curve does not decline as deep in the night hours and rises less sharply in the morning. With the small number of devices which can be simulated at the moment, cooling devices - which produce a continuous pulse - make up a big part of the electricity consumption in our simulation; even though refrigerators and freezers have a significant impact on the electricity consumption of

a household, their smoothing effect on the simulated load curve might be exaggerated here. However, our aim was to present the opportunities of a simulation model based solely on survey data and theoretical considerations, before extensive calibration and the simulated load curve shows a clear resemblance towards the SPL.

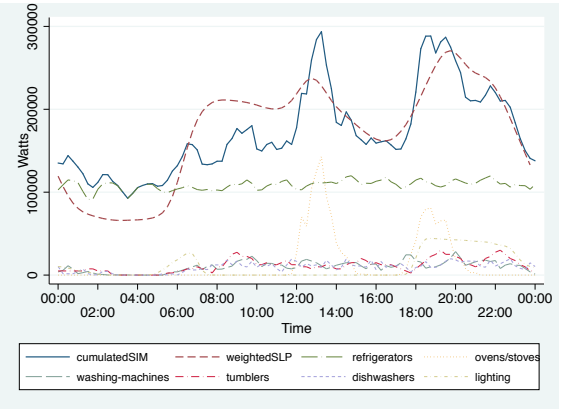

Figure 3: Simulated load-curve for 1 000 households with the profile of the *conservative well-off*

When we compare the load-curve of the *conservative well-off* (Figure 3) with the standard load profile or with the load curves of the other simulation runs, the most striking difference is the very pronounced peak at the middle of the day. In this group we find more elderly people than in the other groups, which explains why they spend more time at home, giving them the opportunity to consume more electricity during work hours. The share of people having a warm lunch at home is bigger than in the other groups which raises the peak at the middle of the day to a higher level than in any other group. At the same time, the percentage of people having a cold meal for dinner is rather high in this group, which explains why the evening peak is relatively small here. Overall their load-curve is on a higher level than the others, because they live in more spacious apartments/houses and own more electrical appliances than i.e. the entertainment-seekers (see section Survey Results). Their ownership of many cooling devices and the habit of having a warm meal for lunch reported clearly shows in the simulated load curve.

The load-curve of the *entertainment-seekers* (Figure 4) is characterized by the absence of the peak in the middle of the day and by a lower level than

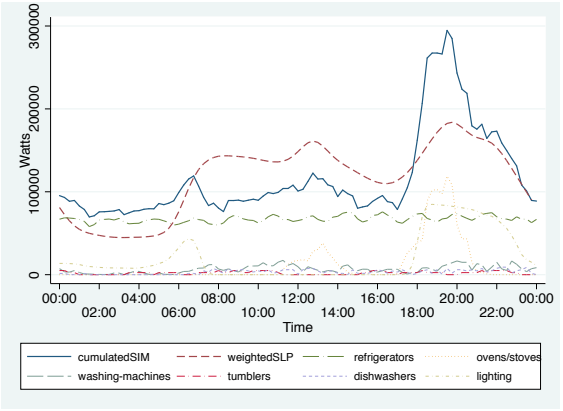

Figure 4: Simulated load-curve for 1 000 households with the profile of the *entertainment seekers*

the other load-curves. Households belonging to this group are rather young and there are less retired persons to be found in this group than amongst the conservative well-off, which is one reason why they spend more time out of home than other groups. Their consumption is therefore shifted to the evening hours, where they create a larger peak than the other groups. They have relatively few household appliances like dishwashers, tumble dryers and washing machines which decreases their energy consumption significantly.

CONCLUSIONS AND OUTLOOK

The simulation shows that the different lifestyles clearly produce different load-curves, which correspond to their behavior and ownership of appliances, even though not all the survey results and all appliances to be found in a household could be modelled by now. We expect the differences between the lifestyle groups to rise with the progressing inclusion of further appliances, e.g. water heaters and further entertainment electronics. As lifestyles are not equally distributed in space, this fact is important when planning power grids, especially when thinking about decentralized power supply. The smaller the area which is supplied by a single power source, the more important these differences become. The ecological fallacy of assuming a standard average load-profile for all households inside a specific region could lead to a wrong estimation not only of the level of electricity demand, but also of the shape of the load-curve.

ACKNOWLEDGEMENTS

The Tafat simulation framework is developed by the *Instituto Universitario de Sistemas Inteligentes y Aplicaciones Numéricas en Ingeniería* (SIANI). As a simulation framework, it joins many different simulation models by different authors and profited from advice of many colleagues at EIFER, SIANI and ZIRN, too numerous to name them all. Nevertheless, we want to thank at least some persons, without whom this article would not have been possible: we gratefully acknowledge the advice and insights from Oscar Barambones, Jose María Gonzalez de Durana, José Juan Hernández, Mario Hernández, Pablo Viejo and Wolfgang Weimer-Jehle.

REFERENCES

ADEME, ENERTECH, and EDF (2008). Campagne de mesures des appareils de production de froid et des appareils de lavage dans 100 logements. Technical report.

Lutzenhiser, L. and Bender, S. (2008). The "Average American" unmasked: Social structure and differences in household energy use and carbon emissions. In *2008 ACEEE Summer Study on Energy Efficiency in Buildings*.

Morley, J. and Hazas, M. (2011). The significance of difference: Understanding variation in household energy consumption. In *ECEEE 2011 summer study. Energy efficiency first: the foundation of a low carbon society*.

Otte, G. (2005). Entwicklung und Test einer integrativen Typologie der Lebensführung für die Bundesrepublik Deutschland. Construction and test of an integrative lifestyle-typology for germany. *Zeitschrift für Soziologie*, 34(6):442–467.

Paatero, J. and Lund, P. (2006). A model for generating household electricity load profiles. *International Journal of Energy Research*, 30(5):273–290.

Schwarz, T. (2010). Lebensstile und Wählerverhalten in Stuttgart. Ergebnisse der Stuttgarter Lebensstilbefragung 2008. *Statistik und Informationsmanagement*, (7).

Évora, J. (2011). Tafat-Profiler: una herramienta para la generación automática de modelos de simulación a partir de perfiles. Technical report.

Évora, J., Kremers, E., Cueva, S., Hernández, M., Hernández, J., and Viejo, P. (2011). Agent-based modelling of electrical load at household level. In Stepney, S., Welch, P. H., and Andrews, P. S., editors, *ECAL 2011: CoSMoS - Proceedings of the 2011 Workshop on Complex Systems Modelling and Simulation*, page 15, Paris.

AUTHOR BIOGRAPHIES

WOLFGANG HAUSER graduated in sociology at the University of Bamberg, Germany. During his studies he has been working at the Institute for Employment Research, Nuremberg. In 2008 he joined the Interdisciplinary Research Unit on Risk Governance and Sustainable Technology Development (ZIRN) at Stuttgart University, where he is working on a Ph.D.-thesis inside the framework of the European Centre and Laboratories for Energy Efficiency Research (ECLEER) and on an agent-based simulation of the german electricity market (AMIRIS).

JOSE ÉVORA graduated in computer engineering at the University of Las Palmas de Gran Canaria, Spain in 2010. He started his research in energy efficiency and sustainability at SIANI in 2010. On April 2011, he received a grant from the *Canary Agency of Researching, Innovation and Society Information* to develop his Ph.D. On June 2011, he finished the master degree in Intelligent Systems and Numeric Applications in the Engineering at SIANI. From 2010 until now, he has been involved in several projects at SIANI and EIFER.

ENRIQUE KREMERS received his diploma in electrical engineering from the University of Karlsruhe (now: Karlsruhe Institute for Technology), Germany in 2008. Since then he has been working as a researcher at the European Institute for Energy Research in Karlsruhe in the field of modelling and simulation of energy systems. His main research focus is on agent-based modelling of complex energy systems, by developing new, integrative and bottom-up simulation approaches. He has contributed to several smart grid projects and is currently in charge of the agent-based modelling activities of the geo-simulation group in EIFER.

INVESTIGATING ABSORPTIVE CAPACITY STRATEGIES VIA SIMULATION

Paolo Aversa
Martin Ihrig
The Sol C. Snider Entrepreneurial Research Center
The Wharton School of the University of Pennsylvania
Vance Hall 4th Floor, 3733 Spruce Street, Philadelphia, PA 19104, USA

KEYWORDS

Agent-based simulation, absorptive capacity, strategic management, organizational learning, knowledge, I-Space, SimISpace2, performance.

ABSTRACT

Absorptive capacity, defined as the organizational capability to identify, absorb and exploit knowledge, is one of the most discussed topics in the management literature. Yet, its complex nature makes it almost impossible to empirically test it. This paper develops SimAC, an agent-based simulation tool that enables studying and comparing different absorptive capacity strategies, their related financial payoffs, and their knowledge creation potential through time.

INTRODUCTION

Absorptive capacity (Cohen and Levinthal, 1990) – hereafter AC—is one of the most discussed and advanced concepts in management theory, and still one of the less empirically tested (Lane, Koka and Pathak, 2006). Absorptive capacity is traditionally defined as the organizational capability to identify relevant external knowledge, assimilate it and exploit it for commercial ends (Cohen & Levinthal, 1990: 128). Although scholars have advanced complex and detailed theoretical models about organizational skills in knowledge identification, absorption, and exploitation (Lane *et al.*, 2006; Todorova and Durisin, 2007; Zahra and George, 2002), empirical studies that test the entire AC process are rare, partial, and sometimes misleading. The reason is that knowledge acquisition involves several intervening variables that could be frustratingly difficult to retrieve and observe (Lim, 2009). Furthermore, the abstract nature of knowledge does not allow a direct observation of the phenomenon, forcing scholars to identify proxies to measure AC development. Knowledge is an intangible asset, which has distinctive characteristics when compared to physical assets. For this reason, in order to deeply understand the processes underpinning AC, research needs to be grounded in a solid theory of knowledge evolution.

In this paper, we aim to improve the understanding of diverse AC strategies by developing SimAC, a simulation model, which helps scholars to study the effect of diverse approaches to organizational learning on firm performance. Our work is based on *SimISpace2*, an agent-based graphical simulation environment designed to model strategic knowledge management processes, in particular knowledge flows and knowledge-based agent interactions. The simulation is based on Max Boisot's Information Space (or I-Space), a conceptual framework, which helps analyze knowledge flows in populations of agents (Boisot, 1995, 1998). Within the I-Space framework, the Social Learning Cycle provides a process interpretation of the dynamic evolution of knowledge, its structuring, and sharing. The process interpretation of organizational learning and its sub-phases makes the I-Space a suitable framework to advance the understanding of AC strategies (Aversa, 2011).

ABSORPTIVE CAPACITY STRATEGIES

According to the traditional definition of AC by Cohen and Levinthal (1990) and the more recent reconceptualization by Zahra and George (2002), AC can be summarized into a four-step process. In the first phase, the organization *identifies* bundles of external useful knowledge to *acquire*. The knowledge identified is usually very concrete, and embodied in artifacts that belong to other agents, or more in general to the external environment. Once identified and acquired, knowledge must be structured in order to be replicable and exploitable. Firms *transform* the practical and tacit knowledge embodied in the artifacts (e.g. products, technologies, machineries) into abstract and codified knowledge (e.g. formulas, scientific and technical principles etc.): the more structured knowledge is, the easier it becomes to share and exploit (Boisot, 1998; Nonaka, 1994). In the third phase, structured knowledge is diffused among the members of the organization and embedded in concrete practices aimed at develop artifacts, organizational rules, procedures and behavioral patterns (*impact* phase). The organization economically *exploits* the new knowledge, creating and commercializing new products, services, and knowledge assets. Therefore, according to the social learning cycle concept (Boisot, 1998), knowledge completes a full "cycle", since firms obtain it in an unstructured form, they structure it and then exploit it by embedding it in products, processes and artifacts. AC leads to superior performance and competitive advantage. To protect their competitive advantage, organizations can *patent* the knowledge they possess. However, while firms that have superior skills only in knowledge acquisition and transformation (called potential AC) obtain only part of

Proceedings 26th European Conference on Modelling and Simulation ©ECMS Klaus G. Troitzsch, Michael Möhring, Ulf Lotzmann (Editors)
ISBN: 978-0-9564944-4-3 / ISBN: 978-0-9564944-5-0 (CD)

the benefits, firms skilled in knowledge development and exploitation (called realized AC) are able to maximize their economic performance and develop, in a complete form, the entire AC potential (Jansen, Van den Bosch and Volberda, 2005; Zahra and George, 2002).
Literature shows that companies need different types of knowledge to develop innovation and increase performance. In this paper we follow the Lim (2009: 1252) three-type knowledge classification, complementing it with a fourth group we consider important: (1) *Disciplinary knowledge*, such as general scientific knowledge; (2) *Domain Specific Knowledge*, such as solutions specific to technical projects; (3) *Encoded knowledge*, such as knowledge embedded in tools and processes, and (4) *Market knowledge*, such as knowledge about commercial opportunities and market characteristics. Firms can concentrate on acquiring particular types of knowledge assets, for example focusing their investments on one kind, or on a mix of two or more. For this study, we decided to test the impact of five different types of AC strategies on financial performance. We simulated the competitive behavior of five different agent groups, each pursuing one specific AC strategy:

- Agent group 1 - **Research Firm**: These kinds of agents focus their AC strategy on *scanning knowledge*;
- Agent group 2 - **Managerial Firm**: These kinds of agents focus their AC strategy on *abstracting knowledge*;
- Agent group 3 - **Manufacturing Firm**: These kinds of agents focus their AC strategy on *impacting knowledge*;
- Agent group 4 - **Marketing Firm**: These kinds of agents focus their AC strategy on *exploiting knowledge*.
- Agent group 5 – **Balanced Firm**: These kinds of agents focus their AC strategy on pursuing a balanced mix of *all the possible actions.*

In addition, every agent group can protect the knowledge possessed via *patenting*.
According to our theoretical premises, our parameterization will distinguish between the different strategies in the simulation environment, and thus enables us to dynamically analyze micro and macro effects of AC strategies on firm performance. In particular, we are interested in comparing the payoffs of the five AC strategies. We expect to determine distinctive knowledge evolution and financial performance profiles for each firm (agent) type.

USING SIMISPACE2 TO MODEL AC STRATEGIES

SimISpace2 is an agent-based graphical simulation environment designed to simulate strategic knowledge management processes, in particular knowledge flows and knowledge-based agent interactions. The simulation engine's conceptual foundation is provided by Boisot's I-Space (1995, 1998). Recent studies have used the *SimISpace2* simulation suite to investigate knowledge evolution in complex systems (Ihrig, MacMillan, Knyphausen-Aufsess and Boisot, 2010).

Basic Parameterization of SimISpace2

Ihrig and Abrahams (2007) offer a rich and detailed description of the structure and technicalities of the *SimISpace2* simulation environment. Due to the wide set of modeling opportunities that this suite offers, we will limit our description to the set of features that will be used for our purposes. However, for readers that are not familiar with this simulation framework, we will briefly introduce some of the main *SimISpace2* principles, paying attention to the way knowledge is represented and processed by the agents. The following description is adapted from Ihrig (2010):

Two major forms of entities can be modeled with *SimISpace2*: agents and knowledge items/assets. When setting up the simulation, the user defines agent groups and knowledge groups with distinct properties. Individually definable distributions can be assigned to each property of each group (uniform, normal, triangular, exponential, or constant distribution). The simulation then assigns to the individual group members (agents and knowledge items) characteristics in accordance with the group they belong. Knowledge in the simulation environment is represented through *knowledge items*. Based on the *knowledge group* they belong to, those knowledge items have certain characteristics. All knowledge items together make up the *knowledge ocean:* a global pool of knowledge. Agents can access the knowledge ocean, pick up knowledge items, and deposit them in knowledge stores through the *scanning* action. A knowledge store is an agent's personal storage place for a knowledge item. Each knowledge store is local to an agent, i.e. possessed by a single agent. As containers, knowledge stores *hold* knowledge items as their contents. Stores and their items together constitute *knowledge assets*. Examples of knowledge stores include books, files, tools, diskettes, and sections of a person's brain. There is only one knowledge item per knowledge store, i.e. each knowledge item that an agent possesses has its own knowledge store. If an agent gets a new knowledge item (whether directly from the knowledge ocean or from other agents' knowledge stores), a new knowledge store for that item is generated to hold it.
The concept of a knowledge item has been separated from the concept of a knowledge store to render knowledge traceable. If knowledge items are drawn from a common pool and stored in the knowledge stores of different agents, it becomes possible to see when two (or more) agents possess the same knowledge, a useful property for tracking the diffusion of knowledge. The separation between a global pool of knowledge items and local knowledge stores is particularly important when agents *structure* knowledge (which only applies to knowledge stores, not to knowledge items). Multiple agents hold knowledge items, and one agent's investment in *structuring knowledge* does not influence

the codification and abstraction level of the same knowledge item held by another agent. Agents possess knowledge stores that can have different degrees of structure. If the agent structures its knowledge, the properties of the knowledge item itself – i.e., its *contents* – are not changed, but it gets moved to a new knowledge store with higher degrees of structure – i.e., its *form* changes.

SimISpace2 also features a special kind of knowledge. A DTI (knowledge *Discovered Through Investment*) is a composite knowledge item that is discovered by integrating the knowledge items that make it up into a coherent pattern. DTIs cannot be discovered through scanning from the global pool of knowledge items. The user determines knowledge items to act as the constituent components of a DTI. The only way for an agent to discover a DTI is to successfully scan and appropriate its constituent components and then *structure* them beyond user-specified threshold values in order to achieve the required level of integration and abstraction. Once these values are reached, the agent automatically obtains the DTI (the discover occurrence is triggered in the simulation). Investing in its constituent components – i.e. scanning and abstracting them – is the primary means of discovering a DTI. By specifying the values of different DTIs, the user can indirectly determine the values of the networks of knowledge items that produce DTIs. Such networks represent more complex forms of knowledge. Once an agent has discovered a DTI item, it is treated like a regular knowledge item, i.e. other agents are then able to scan it from the agent that possesses it.

Specific *SimISpace2* Parameterization to Model AC Strategies

Similar to Ihrig (2010) we decided to keep our model as parsimonious as possible, thus using only six out of the twenty actions available in the *SimISpace2* suite: *1. Scan, 2. Abstract, 3. Impact, 4. Learn, 5. Exploit*, and *6. Patent.* Each agent's goal is to scan knowledge items (either from the *ocean* or from others), *abstracting* the new knowledge (which correspond to structuring it). Once knowledge has reached a certain level of structure, it is diffused in practices and routines among and across the organization (*impact*), and absorbed within the organization (*learn*). Through the commercialization of products and services developed based on the newly acquired knowledge assets, the agent *exploits* the knowledge potential, and thus increases its financial performance. Simply put, superior capabilities in managing this process of knowledge development and exploitation correspond to higher AC. Higher levels of AC lead to superior financial funds. The higher the financial funds obtained following a specific AC strategy, the more successful we will consider that specific AC strategy.

Within the *SimISpace2* environment we use specific actions to model the agent groups' focus on a particular set of learning strategies AG1: Research firm (*scanning* from the ocean and from others); AG2: Managerial firm (*abstracting*); AG3: Manufacturing firm (*impacting* and *learning*); AG4: Marketing firm (*exploiting*); AG5: Balanced firm (*an distributed mix of all the actions*). In addition, all the AGs have an equal propensity to protect their knowledge through *patenting*. An agent can patent knowledge for a certain duration and with a specific strength. The agent can patent only the knowledge it possesses, and only if it holds the knowledge in a knowledge store that has an abstraction level above a user set-level. In other words, patenting is valid only if performed after abstraction. Also, when the knowledge is possessed by a user-set number of other agents, it becomes public domain and it cannot be patented. In our simulation, the patent protection lasts for the entire 2,000 rounds, and has a strength of 0.5, which means that the patented knowledge has a likelihood of 50% to be effectively protected. Our patent abstraction threshold has a value of 0, which means that any kind of knowledge can be patented. Finally, when all the 50 agents possess a specific knowledge item, nobody can *patent* it as we consider it "public domain."

In order to compete in the market, each firm needs to have at least a minimum propensity in pursuing each type of these actions, which are mandatory for any kind of innovation development. Yet, as mentioned above, focusing on specific sets of actions corresponds to different AC strategies.

We have also created four groups of knowledge items, corresponding to the classification we previously explained. For each group we assigned a base value of 20 and an abstraction and codification increment of 0.1. Also, for each knowledge group we assigned a starting value of codification and abstraction. The more *structured* knowledge is, the higher will be the codification and abstraction level we assigned.

- Knowledge group 1: *Disciplinary knowledge*
  Codification: 1.0
  Abstraction: 1.0
- Knowledge group 2: *Domain specific knowledge*
  Codification: 0.8
  Abstraction: 0.8
- Knowledge group 3: *Encoded knowledge*
  Codification: 0.5
  Abstraction: 0.5
- Knowledge group 4: *Market knowledge*
  Codification: 0.3
  Abstraction: 0.3

To develop innovations, firms need to acquire all four types of knowledge items. To simulate this knowledge acquisition, development, and exploitation scenario, we have given a fixed budget of 9 "chips" to each agent per round. The nine chips correspond to the different activities that each agent can theoretically pursue in each round, in order to develop innovation. The chips are distributed based on the actions that define their learning strategy. One of these chips is dedicated to patenting their knowledge. For example, overall *research firms* will spend 5 chips out of 9 in *scanning*, because their strategy is focused on that kind of activity. The remaining 3 chips are equally distributed for the

other actions, and 1 chip will be used for *patenting*. Table 1 shows the resource distribution for each agent group.

Table 1: Parameterization of the 5 strategies

Action	AG 1. Balanced Firm	AG 2. Research Firm	AG 3. Managerial Firm	AG 4. Manufacturing Firm	AG5. Marketing Firm
1.Scan*	2.0	5.0	1.0	1.0	1.0
2.Abstract	2.0	1.0	5.0	1.0	1.0
3.Impact	1.0	0.5	0.5	2.5	0.5
Learn	1.0	0.5	0.5	2.5	0.5
4.Exploit	2.0	1.0	1.0	1.0	5.0
5.Patent	1.0	1.0	1.0	1.0	1.0
Total	9.0	9.0	9.0	9.0	9.0

*From the ocean and from others.

For each round, the agents perform their actions in knowledge acquisition, transformation, and exploitation. The agents gain a DTI, the knowledge we model innovation with, when they obtain a specific set of knowledge items. Agents increase their financial funds by capitalizing on the knowledge they possess, especially DTIs. The financial funds accumulated by an agent are the measure of its performance and success. Agents with financial funds of zero die.

Following the definition of potential and realized AC (Zahra and George, 2002), we developed two different kinds of DTIs: *scientific DTI* and *technical DTI*. The scientific DTI represents the potential AC (i.e. abstract knowledge, that has no practical application yet), and agents obtain it when they get a scientific knowledge item plus a managerial knowledge item. The technical DTI, which leads to higher financial return than the scientific one, represents the realized AC (i.e. concrete and applied knowledge), and agents obtain it when they get a *scientific DTI* plus a *manufacturing knowledge* item and a *market knowledge* item. Table 2 describes the knowledge items needed for agents to collect DTIs.

Table 2: Knowledge items and DTIs in *SimAC*

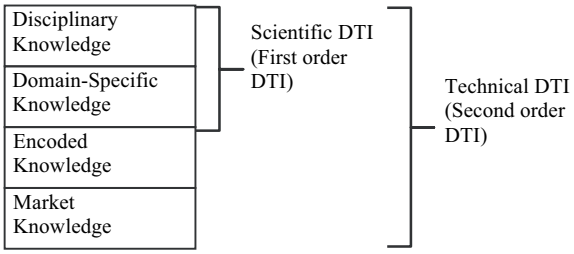

SIMULATION AND RESULTS WITH *SIMAC*

We have conducted *SimISpace2* virtual experiments with the *SimAC model,* aimed at exploring the impact of different AC strategies on firm performance. We ran the simulation 20 times, and each run lasted 2000 periods. We created 10 participants for each of the five agent groups (50 agents in total) and 10 knowledge items per type (40 knowledge times in total). All graphs show the average across all runs.

Simulating Financial Performance with SimAC

The first graph we present (Figure 1) shows the different financial performance profiles measured in funds accumulation, derived from the five different strategies. Based on distinct AC strategies of the five firm types, we can clearly distinguish five different groups.

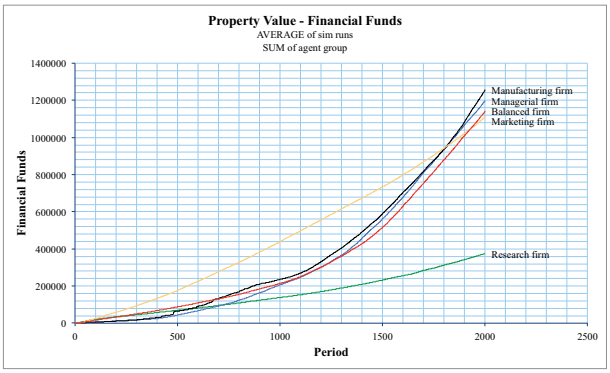

Figure 1: Financial Funds (Longitudinal Report)

Insight 1: The financial performance of the five AC strategies – *research, managerial, manufacturing, marketing,* and *balanced* – will have distinct profiles, as a result of the differences in their knowledge appropriation and knowledge development behaviors.

The *SimAC* results are consistent with management theory. Research firms are strongly dedicated to knowledge identification and *scanning*, and therefore are not able to exploit the commercial value of their knowledge. *Marketing firms*, on the contrary, are mainly dedicated to knowledge *exploitation* (*exploit* activity set to five), but do not widely develop the first phases of AC processes. As a result in the long run they perform as the second worst, despite being the best performing AG for the first 1750 periods. At the end, the manufacturing firms, which focus on *impacting* and *learning*, are the best performers of all the groups.

All of this highlights distinct simulation and modeling capabilities of *SimAC*, which can be summarized as follows.

Simulation & Modeling Capability 1*: *SimAC enables simulating the different AC strategies and their respective financial payoffs for different agent groups.

Simulating Potential AC with SimAC

The first insight shed light on the impact of strategies on financial performance. However, money is not the only way to measure the outcomes of organizational learning. Innovation is also an important aspect that we have to take into consideration in this context. Innovation performance in *SimAC* is measured via the accumulation of DTIs. The first type of DTI is the

scientific DTI, which stands for the *potential AC* (Zahra and George, 2002). This kind of DTI corresponds to possessing and combining *disciplinary* and *domain specific knowledge.* The agent groups have access to a maximum of 100 DTIs in the simulation environment. Figure 2 represents the appropriation of scientific DTI across the agent population (maximum 100 DTIs – 10 DTIs, 10 agents in a group). In Figure 2, we can distinguish how different AC strategies require different timing to obtain the 100 scientific DTIs.

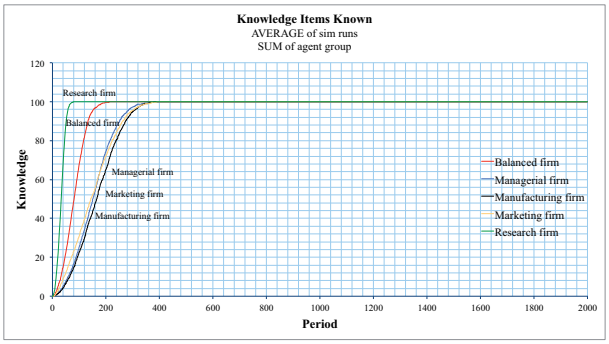

Figure 2: Scientific DTIs (Longitudinal Report)

Insight 2*:* The five AC strategies – *research, managerial, manufacturing, marketing,* and *balanced* – lead to distinct results *in potential AC*, due to the agents' knowledge appropriation and knowledge development behaviors.

Again, *SimAC* demonstrates results that are consistent with management theory. *Research firms*, whose main intent is focused on scanning new knowledge, are the first ones to obtain the totality of 100 *scientific DTIs,* followed by *balanced firms*. *Managerial, marketing and manufacturing firms*, whose main attempt is not collecting new knowledge, but maximizing the processing and exploitation of the available knowledge, are the slowest in reaching the 100 *scientific DTIs.* Specifically they are more than 4 times slower than the best performers since they obtain the 100 DTIs at around period 400, while *research firms*—the best in class—get them at around period 70. This evidence leads us to define the second *SimAC* capability.

Simulation & Modeling Capability 2**:** *SimAC* enables simulating the different AC strategies and their respective innovation payoffs of *potential AC*, for different agent groups.

Simulating Realized AC with SimAC

The second type of DTI is the *technical DTI,* which in our scenario corresponds to the *realized AC* (Zahra and George, 2002). This kind of DTI is obtained when an agent gets a *scientific DTI* plus an *encoded* and *marketing knowledge item.* The agent groups can access a maximum of 100 DTIs in the simulation environment. The *technical DTIs* represent knowledge that is more structured and easy to exploit, thus leading to superior financial performance for the agents that obtain them. Figure 3 depicts the distribution of scientific DTIs across the agent population. We can distinguish how different AC strategies lead to different timings to obtain the 100 scientific DTIs.

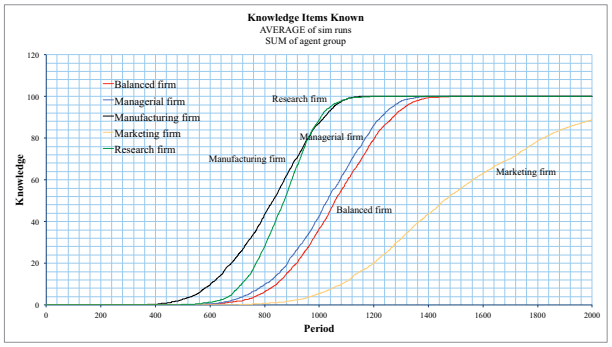

Figure 3: Technical DTIs (Longitudinal Report)

Insight 3*:* The five AC strategies – *research, managerial, manufacturing, marketing,* and *balanced* – lead to distinct results in *realized AC*, due to the agents' knowledge appropriation and knowledge development behaviors.

The *SimAC* report shows how *research firms* are still the first to obtain the 10 technical DTIs, leveraging their time advantage in reaching the *scientific DTIs,* which are a mandatory requirement to get to the second order DTIs. In fact, in the real world firms need to develop general structured knowledge before developing it in innovative products and services, thus being able to exploit them. *Manufacturing firms*, due to their focus on the *impact/learn* activities, manage to be first together with the *research firm*, despite being the slowest at obtaining the *scientific DTIs*. *Managerial firms* and *balanced firms* follow the same curve, but the *managerial firm* is slightly faster than the *balanced one*. The slowest is the marketing firm, which at the end of the 2000 run is not able to obtain all the 100 *technical DTIs.* This said, we can advance another possibility offered by *SimAC*.

Simulation & Modeling Capability 3**:** *SimAC* enables simulating the different AC strategies and their respective innovation payoffs of *realized AC*, for different agent groups.

Simulating Knowledge Storage with SimAC

Another way to measure knowledge outcomes, is considering in how many "locations" knowledge is stored. Firms embed innovations into documents, objects, artifacts, and locations. For example, the same technical innovation can be contained in a patent, in two types of products, and in the personal knowledge of the five engineers. Thus, we can affirm that the same knowledge is contained into eight *knowledge stores.* Knowledge stores allow us to trace the diffusion of knowledge among diverse agents, which can hold the

same knowledge item in different stores at the same time. Accordingly, literature has underlined how knowledge is an asset that can be shared without implying ownership (Boisot, 1998). For example, while a physical object is either in one place or in another, several people can share the exact same knowledge without affecting its structure or nature.

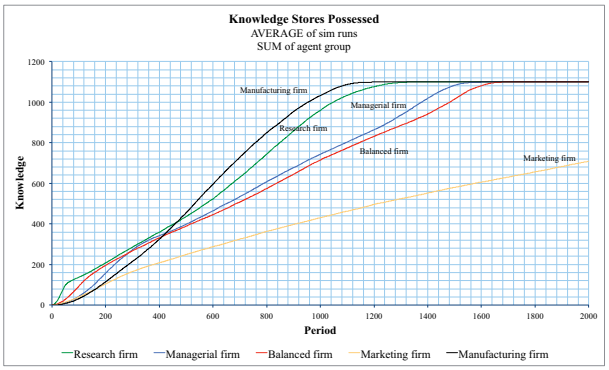

Figure 4: Scientific DTI Knowledge Stores

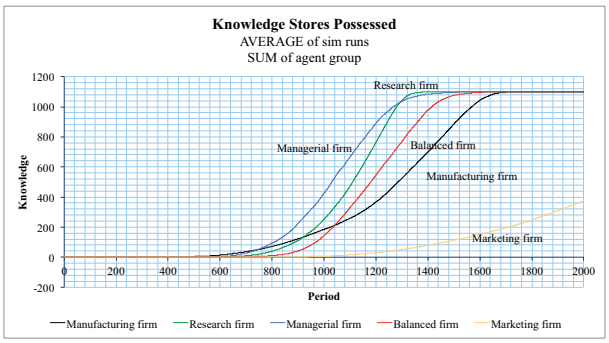

Figure 5: Technical DTI Knowledge Stores

Insight 4*:* The five knowledge AC strategies – *research, managerial, manufacturing, marketing,* and *balanced* – lead to different knowledge store trajectories, as a result of the differences in the agents' knowledge appropriation and knowledge development behaviors.

SimAC consistently reflects the nature of knowledge by allowing knowledge stores to be more numerous than knowledge items. Figure 4 shows the development of knowledge stores for scientific DTIs among the five agent groups, while figure 5 shows the development of knowledge stores for technical DTIs. The vertical axis shows that the number of knowledge stores is higher than the DTIs obtained. For example, the *manufacturing firms* present around 1100 knowledge stores for *scientific and technical DTIs*. Yet, while manufacturing firms are the fastest at obtaining knowledge stores for *scientific DTIs,* they are the second slowest to obtain the knowledge store for *technical DTIs.* This confirms that the skills in knowledge allocation are independent from knowledge creation, and develop clearly different outcomes depending on the strategy adopted. This leads us to the last reflection on the *SimAC* tool capability.

Simulation & Modeling Capability 4**:** *SimAC* enables simulating the different AC strategies and their respective innovation payoffs related to knowledge storage, for different agent groups.

CONCLUSION

SimAC is a powerful tool to conduct virtual experiments for exploring the effects of different AC strategies on financial and innovation performance. Being based on the I-Space framework (Boisot, 1995, 1998), the tool offers a consistent integration of AC theory with fine-grained insights about knowledge evolution in populations of agents. Processes of knowledge identification, acquisition, transformation and exploitation can be observed in detail. In this paper we displayed only a limited set of the several reports that the suite *SimISpace2* offers. However, the results we presented in this article already offer opportunities to develop new research questions that can be addressed using the *SimAC* application. For example, in our simulation we have explored a possible scenario where an arbitrary set of 50 firms compete. In our new experiments, we are taking care of simulating environments with significantly higher number of competitors. Also, to compare the outcome of basic AC approaches, this first SimAC simulation models the competition between four strategies focused on one single objective (i.e. AG2, AG3, AG4, AG5) and one strategy that engages in a balanced tradeoff between all the other possible strategies (i.e. AG1). We are aware that in real life firm strategies might be more complex than in our experiments, but our parameterization of SimISpace2 shows that it is possible to simulate competitive situations with more diverse and realistic characteristics, and it is in our future plans providing analysis of these kinds of environments.

ACKNOWLEDGEMENTS

This research was supported by the Snider Entrepreneurial Research Center at the Wharton School of the University of Pennsylvania, the I-Space Institute, and Technogel US Inc. The authors would like to thank Ian MacMillan and Max Boisot for their help in formulating the theoretical foundations of the *SimAC* simulation model.

REFERENCES

Aversa P. 2011. Understanding the Absorptive Capacity through the Social Learning Cycle, *31 Strategic Management Society Conference*: Miami, USA.

Boisot M. 1995. *Information space: A framework for learning in organizations, institutions and culture*. Thomson Learning Emea.

Boisot M. 1998. *Knowledge assets: Securing competitive advantage in the information economy*. Oxford University Press, USA.

Cohen WM, Levinthal DA. 1990. Absorptive Capacity:

A New Perspective on Learning and Innovation. *Administrative Science Quarterly* **35**(1): 128-152.
Ihrig M. 2010. Investigating entrepreneurial strategies via simulation, *24th European Conference on Modelling and Simulation (ECMS)*: Kuala Lumpur, Malaysia.
Ihrig M, Abrahams AS. 2007. Breaking new ground in simulating knowledge management processes: SimISpace2, *21st European Conference on Modelling and Simulation (ECMS)*: Prague, Czech Republic.
Ihrig M, MacMillan I, Knyphausen-Aufsess Dz, Boisot M. 2010. Knowledge-based Opportunity Recognition Strategies: A Simulation Approach, *30° Strategic Management Society Annual Meeting*: Rome.
Jansen JJP, Van den Bosch FAJ, Volberda HW. 2005. Managing potential and realized absorptive capacity: How do organizational antecedents matter? *Academy of Management Journal* **48**(6): 999-1015.
Lane P, Koka B, Pathak S. 2006. The reification of absorptive capacity: a critical review and rejuvenation of the construct. *The Academy of Management Review* **31**(4): 833-863.
Lim K. 2009. The many faces of absorptive capacity: spillovers of copper interconnect technology for semiconductor chips. *Industrial and Corporate Change* **18**(6): 1249-1284.
Nonaka I. 1994. A Dynamic Theory of Organizational Knowledge Creation. *Organization Science* **5**(1): 14-37.
Todorova G, Durisin B. 2007. Absorptive capacity: valuing a reconceptualization. *Academy of Management Review* **32**(3): 774-786.
Zahra SA, George G. 2002. Absorptive Capacity: A Review, Reconceptualization, and Extension. *Academy of Management Review* **27**(2): 185-203.

AUTHOR BIOGRAPHIES

PAOLO AVERSA is Post-Doctoral Research Fellow at the Management Department of the *Wharton School*, *University of Pennsylvania*, and Marie Curie Fellow at the *Cass Business School*, London. He holds a Ph.D. in management at the University of Bologna, an MBA at the CUOA Foundation (Vicenza), and an MA in Communication at University of Padova. In 2011 he was awarded with the 1st Prize for the Best Ph.D. Paper of the European Academy of Management.

Since 2009 he has worked at the *Sol C. Snider Entrepreneurial Center, Wharton School*. His current research interests are related to firm networks, strategic peripheries and absorptive capacity. He has been teaching and tutoring at the University of Pennsylvania, University of Bologna, and University of Padova.

His e-mail address is paversa@wharton.upenn.edu.

MARTIN IHRIG is President of *I-Space Institute, LLC* (USA) and Adjunct Assistant Professor at the *Wharton School* of the *University of Pennsylvania* (USA). He holds a Master of Business Studies from *UCD Michael Smurfit School of Business* (Ireland) and a Doctor of Business Administration from *Technische Universität Berlin* (Germany).

The research initiative he manages at Wharton's *Snider Entrepreneurial Research Center* focuses on the strategic and entrepreneurial management of knowledge. In his simulation research, he is studying entrepreneurial opportunity recognition strategies with the help of agent-based models.

His e-mail address is ihrig@wharton.upenn.edu.

EXPLORING OPEN INNOVATION STRATEGIES: A SIMULATION APPROACH

Irina Savitskaya
Lappeenranta University of Technology
Faculty of Technology Management
Prikaatintie, 9
45100, Kouvola, Finland

Martin Ihrig
The Wharton School
University of Pennsylvania
418 Vance Hall, 3733 Spruce Street
Philadelphia, PA 19104, USA

KEYWORDS

Agent-based modeling, simulation research, open innovation, strategic management, knowledge assets.

ABSTRACT

This paper presents an agent-based simulation tool that allows researchers to model innovation strategies with different degrees of openness in their R&D and commercialization processes. It implements the micro-foundations of open innovation and can be used to explore innovation strategies and their associated financial performance and their knowledge creation potentials in different market environments.

INTRODUCTION

Recent research on innovation management has been preoccupied with the challenges of openness of innovation processes, with the discussion primarily built upon Chesbrough's *Open Innovation* concept (Chesbrough 2003) and further extensions to it (e.g. Gassmann and Enkel 2004). The concept refers to the process of innovation management when a company provides internally produced knowledge for the market and lets external knowledge flow in for maximizing the value for the company. It can also be described as "both a set of practices for profiting from innovation and a cognitive model for creating, interpreting and researching those practices" (West et al, 2006 p. 286).

Being introduced in 2003, open innovation was first developed as a result of a set of in-depth case studies (Chesbrough 2003) and then further investigated in quantitative research (Gassman and Enkel 2004), suggesting a difference in the open innovation process between inbound and outbound open innovation. Currently, open innovation research is conducted through a multitude of methods and tools. However, there is not yet agreement on what method is more suitable for the study of the open innovation phenomenon and currently used methods do not resolve the main question of whether open innovation is superior to closed innovation (Trott and Hartmann, 2009; Almirall and Casadesus-Masanell 2010). To resolve this dilemma, we suggest conducting virtual experiments modeling the behavior of agents following four innovation strategies. To achieve our goal, we use a unique simulation tool which has already proved its efficiency in strategy simulations (Ihrig and Abrahams 2007; Ihrig 2010, 2011).

THE CONCEPTUAL BACKGROUND

Open Innovation

Although innovation is recognized as a key driver of firms' competitive advantage and growth, and collaborative innovation as a source of competitiveness of entire ecosystems (Almirall and Casadesus-Masanell, 2010), there is still no consensus on how to reach the optimal level of openness in collaboration for innovation. The open innovation approach suggests that opening up company borders for inflows and outflows of knowledge is a feasible option, even in lean times (Chesbrough and Garman, 2009). The literature discusses the potential practical implications of such an approach, but it still remains unclear how to manage the internal knowledge under different levels of openness in co-innovation. While open innovation clearly provides several benefits and opportunities for companies – and is therefore often being touted as superior to a closed innovation model (Laursen & Salter, 2006; Chesbrough et al., 2006 and others) – the theoretical grounds of it still stay undefined. The question whether open innovation is a winning strategy has been previously addressed by some researchers (Trott and Hartmann, 2009; Almirall and Casadesus-Masanell 2010), however, there is still no definitive answer to it.

At the same time, if we look back at the definition of the concept of open innovation, knowledge flows are at the center of open innovation transactions, and we can use them to formulate knowledge-based innovation strategies. This approach allows us to view open innovation through the lense of the I-Space framework (Boisot, 1995, 1998) that describes knowledge-flows in different populations of agents. The Information Space or *I-Space* is a conceptual framework which relates the degree of structure of knowledge (i.e. its codification and abstraction) to its diffusibility as that knowledge develops. As will be described below, we draw on this in our simulation modeling.

Most commonly, the innovation process is considered to follow one of four strategies of openness (Figure 1):

Proceedings 26th European Conference on Modelling and Simulation ©ECMS Klaus G. Troitzsch, Michael Möhring, Ulf Lotzmann (Editors)
ISBN: 978-0-9564944-4-3 / ISBN: 978-0-9564944-5-0 (CD)

Closed Innovation (or pure in-house development). Referred to as closed innovation by Chesbrough (2003), it is also known as traditional innovation. The literature shows, that the innovation process has hardly ever been completely closed (besides strategic industries such as the military) and has encompassed to a high extent the cooperation on horizontal and vertical levels. However, in order to cover all the possible strategic options for this research, we include pure in-house development and commercialization of innovation as an extreme case.

Outbound Open Innovation (Outbound OI). This strategy encompasses in-house product development and profits from external exploitation of knowledge. Companies using this strategy are major sources of innovation solutions to the market for technology, as they exploit a big share of their technological discoveries outside the company. Of course they do not sell their core knowledge in order to maintain core competences and the ability to produce innovation.

Inbound Open Innovation (*Inbound OI)*. This strategy sees knowledge acquisition as the important contribution to the internal innovation process. Firms purchase technologies and other knowledge in order to complement own developments, to save resources and costs on in-house R&D, and to shorten the time-to-market.

Open Innovation. It is the combination of the two aforementioned strategies – Inbound and Outbound OI. Open innovators invest a share of their efforts into in-house development, complement it with knowledge acquisition from the market, and sell and/or license out their intellectual property (IP) in order to accumulate more funds for internal R&D and other activities.

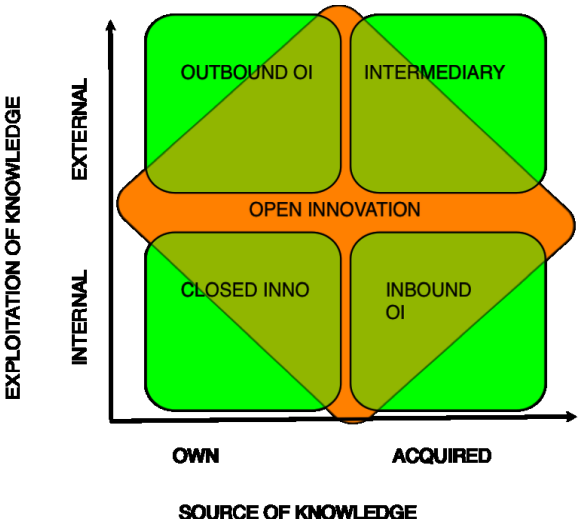

Figure 1: Knowledge-based innovation strategies

These strategies, described through the knowledge lense, constitute the basis of the simulation model presented below. Although we illustrate five potential knowledge-based innovation strategies in the matrix (Figure 1), we exclude the intermediary strategy from the simulation model. The intermediary in this case is buying and selling knowledge as a broker without having its own innovation process, which reflects a different business model, not matching the scope of this research. However, for clarity sake, the intermediary strategy is reflected in the matrix.

THE SIMULATION SOFTWARE *SIMISPACE2*

Ihrig and Abrahams (2007) offer a comprehensive description of the entire *SimISpace2* environment and explain the technical details. Before discussing the simulation model built in this paper, we must review some of the basics of the *SimISpace2* simulation software.

Two major forms of entities can be modeled with *SimISpace2*: agents and knowledge items/assets. When setting up the simulation, the user defines agent groups and knowledge groups with distinct properties. Individually definable distributions can be assigned to each property of each group. When the simulation runs, the individual group members (agents and knowledge items) are assigned characteristics in accordance with the distribution specified for the corresponding property for the group of which they are a member.

Knowledge in the simulation environment is defined as a 'global proposition'. The basic entities are *knowledge items*. Based on the *knowledge group* they belong to, those knowledge items have certain characteristics. All knowledge items together make up the *knowledge ocean* – a global pool of knowledge. Agents access the knowledge ocean, pick up knowledge items, and deposit them in knowledge stores. A knowledge store is an agent's personal storage place for a knowledge item. Each knowledge store is local to an agent, i.e. possessed by a single agent. Knowledge stores as containers *hold* knowledge items as their contents. This happens after agents obtain a knowledge item. Examples of a knowledge store include books, files, tools, diskettes, and sections of an agent's brain. There is only one knowledge item per knowledge store, i.e. each knowledge item that an agent possesses has its own knowledge store. If an agent gets a new knowledge item (whether directly from the knowledge ocean or from other agents' knowledge stores), a new knowledge store for that item is generated to hold it. The knowledge item is held at a certain level of abstraction and codification in that knowledge store. Knowledge stores are about the *form*, knowledge items about the *content* of knowledge.

Discovered Through Investment (DTI) Knowledge. DTI knowledge is a special kind of knowledge, which is discovered through investing in related (child) knowledge. DTI knowledge items cannot be discovered through scanning the knowledge ocean. The user chooses a set of knowledge items to be children of a DTI knowledge item (DTI network; separate from linked knowledge). The only way for an agent to discover DTI items is to successfully scan the children

and then to codify and abstract (or absorb and impact) them above (or below) a certain user-set value. Once the specified codification and abstraction levels are reached, the agent automatically obtains the DTI knowledge item. Investing in the child items, i.e. scanning, codifying and abstracting them, is the primary means of getting DTI knowledge. Once an agent has discovered a DTI item, it is treated like a regular knowledge item, i.e. other agents are then able to scan it from the agent that possesses it. By specifying the value characteristics of the DTI knowledge item, the user can indirectly determine the value of the respective DTI network.

The agents in the simulation are able to perform various *actions* and thereby to adopt different role types. Actions are assumed to have zero duration, start and end in the same period and are purposefully taken by agents.

The state of the world as well as that of the agent (and the knowledge) changes after an action is successfully undertaken.

What follows next is a description of each action-type. When deciding what to do in a period, agents pick from this list of actions.

Scanning (storing). An agent can scan knowledge. Scanning means picking up a random knowledge item, whether from the knowledge ocean or from other agents' knowledge stores. The probability of scanning from the knowledge ocean is specified by the agent-group-level property 'Propensity To Scan From Ocean'. An agent can scan any knowledge item in the knowledge ocean, but can only scan knowledge items in knowledge stores within its vision. Vision determines how far the agent can see spatially. An agent's vision is a certain radius from its current location within which it can *scan* and call for *meetings*. Thereby, it establishes the size of the market within which the agent operates. Some will be village markets and some will be global markets. An agent can scan knowledge possessed or owned (patented or copyrighted) by other agents within its vision. Agents only try to pick up knowledge items that they do not already possess at that level of abstraction and codification. If a knowledge item is successfully scanned, it starts off in a new knowledge store possessed (but not owned) by the agent. Depending on the origin of the knowledge item, the new knowledge store picks up the level of codification and abstraction from the knowledge group the knowledge item belongs to (knowledge item from knowledge ocean) or from the knowledge store it found the item in (knowledge item from other agent). If the agent fails to find a store he does not already know (has a store with the same codification level and abstraction level) then the action will fail and the agent will lose his turn.

Once an agent has scanned all the child items of a DTI knowledge item and has codified and abstracted them up to a certain level, then the agent automatically gets the DTI knowledge item associated with that DTI network. The action that is triggered if all the conditions for obtaining a particular DTI are met (set of knowledge items, codification and abstraction threshold) is called *discover*.

Codifying. An agent can codify knowledge. Codification only occurs on knowledge stores (form), not on knowledge items (content). The agent must possess the knowledge store to carry out codification. Each codification action creates a new string-of-pearl store with an increased level of codification. Codification of the new knowledge store increases by the codification increment specified for the knowledge item in the store. The level of codification cannot exceed one.

Patenting. An agent can patent knowledge for a certain duration and with a specific strength. An agent can only patent a knowledge item it possesses, and only if it holds the knowledge item in a knowledge store that has an abstraction and a codification level above a user-set level. That is, an agent can usually only invest in patenting after it has invested in codifying and abstracting.

Each patent has a particular strength and duration. The user can assign a distribution for both characteristics (general setting for all knowledge). The user can set the number of periods a patent lasts and specify the strength of it. The strength of a patent has an influence on whether agents who possess but not own a particular knowledge item can exploit it. The value for strength should be between zero and one. It influences an agent's effectiveness of exploiting knowledge that has been patented or copyrighted. Agents that do not have the patent for a particular knowledge item should be less likely to succeed in exploiting the knowledge.

Once an agent patents an item, it owns that item. Consequently, all of the agent's knowledge stores that hold the newly patented knowledge item are then eligible for the actions that require ownership (e.g., trading).

An agent may not patent a knowledge item that is already possessed by a user-defined number of other agents (diffusion threshold). This is because knowledge that is in the public domain cannot be patented or copyrighted. 'In the public domain' is defined as follows. First, 'in the public domain' means that other agents also possess the knowledge item in question. Knowledge that is widely diffused cannot be patented or copyrighted, and it is up to the user to specify what widely diffused means by setting an appropriate level of absolute diffusion. Once a patent or copyright is requested for a knowledge item that has surpassed the diffusion threshold, that knowledge item will permanently be in the public domain, i.e. the knowledge item is no longer available for copyright or patent protection. The threshold is specified as the minimum number of agents that must hold the knowledge item in order for it to be considered public domain. Second, all knowledge items with expired copyrights or patents automatically become public

domain. Third, the user can opt to put all knowledge items of a group into the public domain. This means, from period one on, these knowledge items will be in the public domain and cannot be patented or copyrighted during the simulation.

Learning. An agent can learn, i.e. register, existing knowledge. Learning enables agents to exploit the knowledge items they learned of. This means that before knowledge items can be exploited, learning has to take place. Agents can only learn from a knowledge store they possess. The more string-of-pearl knowledge stores an agent possesses for a particular knowledge item, the more probable it is that this knowledge item will be learned first. An agent's chance of successfully learning is higher for more codified knowledge.

Exploiting. An agent can exploit knowledge to gain value. Exploitation means capitalizing on internalized knowledge. This means that an agent must register the knowledge prior to exploiting it, i.e. perform the learning action on the knowledge item. The financial funds of the exploiter agent are increased by the value of the exploiting. Exploiting increases the financial funds of the agent by the intrinsic *base value* of the knowledge item multiplied by the *exploit revenue multiplier*. The level of codification and abstraction, the degree of diffusion, and obsolescence are also taken into account.

Meeting. An agent can meet with another agent. Only agents who have initiated the meeting (initiator) and those who have responded positively (responder) are allowed to attend. An agent can only initiate a meeting with agents within its vision. Meeting is a prerequisite for a trade.

Buying knowledge and selling knowledge (trading). An agent can buy (sell) knowledge from (to) another agent for a certain price (sale amount). In contrast to scanning, buying only targets knowledge that is owned by other agents. Meeting is a prerequisite for trading, and mutual consensus is necessary. Agents can only sell knowledge stores that they own, i.e. knowledge stores with a knowledge item that is copyrighted or patented. The buyer acquires ownership and the seller loses ownership. This means that the patent or copyright for the underlying knowledge item is terminated for the seller, and the rest of the patent or copyright (remaining time) is transferred to the buyer. Note that the seller still possesses the knowledge and is still in a position to learn and to exploit it.

Only knowledge that the acquiring agent has not previously owned will be traded. The financial funds of the seller agent are increased by the sale value for the trade, and the financial funds of the buyer agent are decreased by the sale value for the trade.

THE SIMULATION MODEL *KnOISim*

After explaining the simulation software, we can now proceed with describing the *KnOISim* model, designed for open innovation strategy simulations, as well as its properties, agents, and knowledge groups.

Agents

Following the conceptual framework, we have introduced four groups of agents, each corresponding to the innovation strategy of a different level of openness (Figure 1). Strategies in the model are differentiated by the ability of agents to perform certain actions. Two major distinguishing categories are source and exploitation of knowledge. 'Own' source of knowledge is implemented by the activity of knowledge *scanning.* Agents can either scan from the ocean (which is own ideation of the agent – coming up with the insight by themselves) or from other agents, or both. The scanning is mediated by vision – some agents will have better vision than others, hence they can see more other agents with potentially useful knowledge. Additionally, some agents can also buy knowledge from other agents.

When it comes to exploitation of knowledge, all agents use the *exploit* action, and all agents protect their knowledge through patenting (all knowledge can be patented with a patent duration of 1000 periods, for details see section on Knowledge). However, only some agents are able to sell knowledge.

In order to develop an initial idea into knowledge about an innovation and to successfully capitalize on it, agents can *codify* and *learn.* Knowledge can only be learned after it has been obtained, and only exploited after it has been learned. For agent to capitalize on certain knowledge, this knowledge should reach a certain level of codification.

The differences of agent groups in their actions and the propensity to perform these actions are reflected in Table 1.

Table 1: Agent groups' actions

Agent Action Properties:	**Closed**	**Outbound**	**Inbound**	**Open**
Propensity				
Scanning	1	1	1	1
Learning	1	1	1	1
Codifying	1	1	1	1
Patenting	1	1	1	1
Exploiting	1	1	1	1
Propensity Scan from Ocean	1	1	0.5	0.5
Meeting (Initiator)	0	1	1	1
Buying (Initiator)	0	0	1	1
Selling (Initiator)	0	1	0	1
Vision	Small	All	All	All

It should also be noted that in order to buy or sell knowledge, agents have to first meet. Additionally,

depending on the strategy, agents can also initiate and/or respond to certain actions.

There are ten agents in each agent group. All agents start with financial funds of 100. Open Innovators, Closed Innovators, Inbound OI'ers and Outbound OI'ers are randomly spread in the SimWorld (uniform distribution 0-100 for x and y location)

Knowledge

We use both basic knowledge and the higher-level DTI knowledge in *KnOISim*. There are three basic knowledge groups *Business Knowledge, Engineering Private Knowledge*, and *Engineering Public Knowledge.* In the beginning, all agents only have Engineering Private Knowledge and Business Knowledge, but no Engineering Public Knowledge.

Business Knowledge represents the general understanding of companies of how to do business. This knowledge is required for managing innovation processes, being able to learn new things and to capitalize on innovation. It starts at low levels of codification and abstraction (0.4) since it is primarily the tacit knowledge of business managers and has a base value of 10. This knowledge has an abstraction and codification increment of 0.1.

Engineering Private Knowledge represents the technical skills of personnel responsible for innovation (corresponding to R&D scientists, engineers etc.). This is the basis for innovation to emerge and be developed and exploited by the company (here – agent). This knowledge starts at codification and abstraction levels of 0.5 as it is both tacit knowledge of engineering staff and some more codified technical knowledge. It has a codification and abstraction increment of 0.1 and a base value of 15.

Engineering Public Knowledge is the commonly available technical knowledge in a very structured form. It can be available in the market both as public good – prior knowledge in the forms of manuals, instructions, process descriptions, etc. – and as the engineering knowledge offered for sale by other agents. As this knowledge is more structured, its codification and abstraction level is 0.8. However, the increment is lower than for other knowledge groups – 0.05 – to account for the additional effort needed when integrating external knowledge into own processes. Engineering Public Knowledge has a base value of 10, and it starts in the public domain and hence cannot be patented by the agents without combining it with other knowledge.

There are ten knowledge items in each knowledge group, all groups have obsolescence rates of zero and no per period gain or cost.

Innovations

We use DTI knowledge to model innovations. Once an agent possesses an item each from Business Knowledge, Engineering Private Knowledge and Engineering Public Knowledge in knowledge stores with codification levels greater than 0.7 it obtains the corresponding DTI, i.e. the agent 'discovers' an innovation. There are 20 DTIs each of them being based on the combination of the n-th item of each basic knowledge group (e.g., required knowledge items for DTI 1 are knowledge item 1 of Business Knowledge, knowledge item 1 of Engineering Private Knowledge and knowledge item 1 of Engineering Public Knowledge). DTI knowledge items have a high starting level of codification and abstraction (0.8), a high base value of 2500, an obsolescence rate of zero, a codification and abstraction increment of 0.1, and no per period carrying gain or cost.

Agents obtain innovations in different ways: (1) they can achieve innovation through internal development, by combining all underlying knowledge items, codifying them up to the necessary threshold and hence 'discovering' the innovation as a reward. The missing knowledge items can be obtained directly from the knowledge ocean or from knowledge stores of others. Agents can also trade the missing knowledge items. (2) Alternatively, agents can scan DTIs from other agents. However, since knowledge above a codification and abstraction threshold of 0.6 can be patented, agents might have to get into a trade to acquire and exploit DTIs.

VIRTUAL EXPERIMENTS

The simulation originally included 40 runs, each 2000 periods. Because of the complexity of our simulation, the data storage and processing capacities required are extremely high. So for being able to analyze the outcomes in full scale, we had to limit the simulation to 10 runs to maintain the 2000 periods, allowing us to follow certain trajectories and the extended full set of required actions. We compared results received from 40 runs with results received from 10 runs and did not discover apparent difference between the results. Hence, we used the 10 runs simulation to construct the results graphs below.

One period of the simulation run is expected to correspond to a particular period in a real-life environment. This will be however industry dependent and can for example be calculated by observing the trends in the industry and approximating the amount of time needed to come up with innovation in a particular sector.

Figure 3 displays the financial funds results of our four agent groups. The graph shows the average across all runs and also demonstrates the standard deviation (black bands). We can clearly see the outcomes of the groups following different innovation strategies. The financial performance profiles differ in early periods and later periods: Outbound OI and Closed Innovation show higher profits in the *short-term*, when they are

focused on exploiting their innovations. Since they do not have any intake of fresh ideas other than own resources however, they run out of innovations to exploit in the *longer-term*, whereas the Inbound OI and Open Innovator make profits from commercializing knowledge they have acquired earlier. As profit maximization is one of the most important targets of companies, we can indeed support the claim that openness is the preferred long-term strategy.

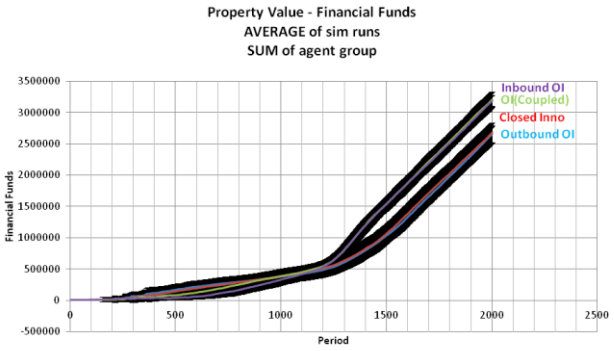

Figure 3: Financial Funds, four agent groups

Insight 1: Open innovation is a beneficial long-term strategy. However, there is indication that the Inbound side of it is more profitable than the Outbound side or pure OI.

Figure 4 shows how the different agent groups discover innovations. In order to create innovations, our agents have to accumulate all three types of knowledge described in the simulation settings. As we see, inbound and open innovators discover innovations faster, which goes in line with one of the main arguments in open innovation theory – companies open up in order to optimize their time to market. However, in the longer term, once the R&D process of in-house innovators produce new knowledge, they come up with more innovations in absolute terms, and this advantage looks sustainable for one fourth of our simulation time (periods 1400 to 2000). Apparently, open innovators and inbound innovators are missing certain in-house R&D intensity to catch up or are simply too busy operating at technology markets. However, this lagging in terms of innovativeness is compensated by monetizing the existing innovations (as demonstrated by financial performance in Figure 3).

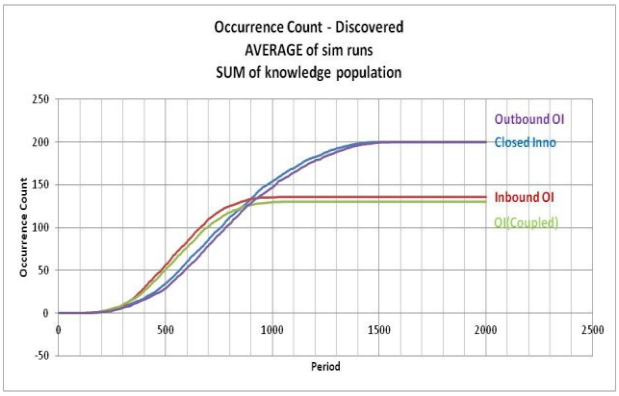

Figure 4: Discovered Innovations

Insight 2: Inbound OI and Open Innovation are indeed faster strategies for creating innovations. However, once agents are actively engaged in knowledge exchange and scanning activities, Outbound OI and Closed Innovators, who stick to in-house R&D, discover more innovations. Hence, they have potentially a higher probability to come up with radical innovations.

Figure 5 shows the patterns of knowledge trade by those agents that are involved in trading knowledge. One can see how trading behaviors are changing through the periods, starting with the trade of originally proprietary knowledge and coming to the trade with new innovative knowledge (DTIs). Once Open Innovators and Inbound Innovators are trying to maximize their profits by acquiring existing innovations from the market, the closed and outbound innovators continue to generate innovations and, in the end, discover all possible innovations (DTIs) as we can see looking back at Figure 3. Hence, one can conclude, that the time spent for activities at the markets for technology is taken from the other important activities in the company, e.g. R&D.

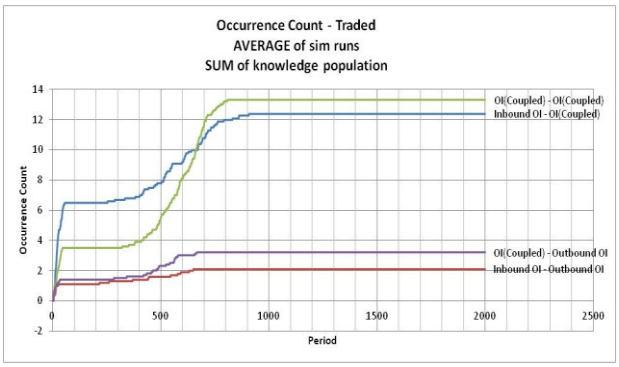

Figure 5: Knowledge Trade

Of course we model a 'perfect' scenario in the sense that agents (or companies) do not differ in their resource base from one another and are only differentiated by important activities in the company, e.g. R&D actions they perform, but this allows us to

isolate the performance effects of the four distinct competitive strategies.

Insight 3: The resources spent for knowledge acquisition are shifted from the common resource base of the company and hence the in-house development gets fewer resources allocated, thus, endangering the innovative output of the company.

CONCLUSION

In this paper, we used the *SimISpace2* simulation software to model knowledge-based innovation strategies and to measure financial pay-offs of different innovation strategies and general innovation-related performance of agents.
The simulation model allowed for comparing the performances of different strategies and, on a practical level, to get a deeper understanding of the strategic choices in the orientation of a company, either on innovativeness (aiming at radical innovation) or on profit-making, which would define the selection of a particular innovation strategy at a specific point in time.
Hence, the application of such a model (and its further development) for analyzing strategic innovation decisions of companies is very promising. It allows for observing the influences of pure strategic decisions under the conditions of no external interferences. Additionally, by adding external factors to the next versions of the model we expect to be able to simulate the innovation strategies' performance in diverse environments.
Moreover, our insights will have to be further tested, by increasing the level of complexity of the model and observing if the assumptions still hold. We suggest further extensions of the simulation model to encompass less pure strategies, to include more actions (e.g. in addition to trading knowledge, add the licensing aspects of the trade), and to test the replication of those in different environments, simulating for example developed versus developing markets.

REFERENCES

Almiral E, Casadesus-Masanell R. 2010. Open versus closed innovation: a model of discovery and divergence, *Academy of Management Review,* **25**(1): 27-47

Boisot MH. 1995. *Information space: a framework for learning in organizations, institutions and culture,* Routledge: London

Boisot MH. 1998. *Knowledge assets – securing competitive advantage in the information economy.* Oxford University Press: New York

Chesbrough HW. 2003. *Open Innovation: the new imperative for creating and profiting from technology.* Harvard Business Press Boston, MA.

Chesbrough, H. and Garman A. 2009. How Open Innovation Can Help You Cope in Lean Times. *Harvard Business Review*; 87(12): 68-76

Ihrig M, Abrahams AS. 2007. Breaking new ground in simulation knowledge management processes: SimISpace2. In I Zelinka, Z Oplatkova, A Orsoni (Eds.), *21st European Conference on Modelling and Simulation (ECMS 2007):* Prague

Trott, P. & Hartmann, D. 2009. Why "open innovation" is old wine in new bottles. *International Journal of Innovation Management,* 13(4): 715-736.

West J, Vanhaverbeke W, Chesbrough H. 2006. Open Innovation: a research agenda, In: Chesbrough H, Vanhaverbeke W., West J. (Eds) *Open innovation: researching a new paradigm,* Oxford University Press, New York, NY

AUTHOR BIOGRAPHIES

Irina Savitskaya, Dr.Sc. (Technology), is a project researcher at Lappeenranta University of Technology, Kouvola research unit, Finland. Her main research focus is on open innovation paradigm, and more specifically on the external to firm barriers towards its implementation in diverse cultural contexts. Additional research interests include regional and national innovation systems, open innovation, and specifically outbound open innovation and cultural aspect of its implementation. The results of her research have been presented at scientific conferences (ECEI, IAMOT, ISPIM) and published in academic journals (IJIBR, JOTMI and others).
Her e-mail address is irina.savitskaya@lut.fi.

Martin Ihrig is an Adjunct Assistant Professor at the *Wharton School* of the *University of Pennsylvania* (USA), a Visiting Professor at *Lappeenranta University of Technology* (Finland), and President of *I-Space Institute, LLC* (USA). He holds a Master of Business Studies from *UCD Michael Smurfit School of Business* (Ireland) and a Doctor of Business Administration from *Technische Universität Berlin* (Germany).
The research initiative he manages at Wharton's *Snider Entrepreneurial Research Center* focuses on the strategic and entrepreneurial management of knowledge. In his simulation research, he is studying entrepreneurial opportunity recognition strategies with the help of agent-based models.
His e-mail address is ihrig@wharton.upenn.edu.

AGENTS OVER THE GRID: AN EXPERIENCE USING THE GLOBUS TOOLKIT 4

Franco Cicirelli, Angelo Furfaro, Libero Nigro, Francesco Pupo
Laboratorio di Ingegneria del Software
Dipartimento di Elettronica Informatica e Sistemistica
Università della Calabria
87036 Rende (CS) – Italy
Email: {f.cicirelli,a.furfaro}@deis.unical.it, {l.nigro,f.pupo}@unical.it

KEYWORDS
M&S, complex systems, agent-based computing, grid computing, actors, Globus, Java.

ABSTRACT

This paper describes an experience of porting the THEATRE agent architecture on top of the grid. The agent architecture consists of light-weight actors and computational theatres which have been proven to be well suited for modeling and simulation of complex systems. THEATRE nodes act as agencies that provide common services of message scheduling and dispatching to mobile actors. THEATRE is currently implemented in Java and can work with different transport layers and middleware. In the last years it was successfully interfaced to HLA/RTI, Terracotta, Java Sockets and Java RMI. The work described in this paper aims at experimenting with THEATRE over the grid, using in particular the Globus toolkit. The goal is to open THEATRE to the exploitation of virtual organizations of computing resources with secure communications, and to favor simulation interoperability through grid services. The paper summarizes THEATRE, describes a design and prototype implementation of THEATRE on top of the Globus Toolkit 4 (GT4), and demonstrates its practical use by means of a modeling example.

INTRODUCTION

Grid computing (Foster *et al*., 2001) enables hardware/software resources belonging to distinct organizations/institutions to be shared globally along with a concept of a Virtual Organization (VO) with an associated secure communication model. A grid infrastructure is founded on the service-oriented paradigm, where grid services are deployed, advertised, discovered and ultimately exploited by typically large distributed applications. A grid service is a (stateless) web service plus a (stateful) resource. A well-known software toolkit supporting grid computing is Globus (Globus, on-line)(Sotomayor & Childers, 2006).

In the last years, the research theme emerged of integrating agents with computational grids, which has been tackled by different researchers with different goals. In (Fukuda & Smith, 2006) the mobile agent system UWAgents is used as a technology starting point for building a grid infrastructure, e.g. enabling search of computing resources by agent navigational autonomy, exploiting migrating agent status for remote job submission and result collection etc. In (Moreau, 2002)(Avila-Rosas *et al*., 2002) an integration of the SoFAR agent system with web services (WS) is developed, where agents are created, deployed and published as WSs, with the goal of opening grid computing to agent-based applications.

In this work an original approach is proposed which uses a Globus grid as a middleware for supporting the Java-based THEATRE agent infrastructure (Cicirelli *et al*., 2009). The realization purposely embeds mobile agents in the grid and delivers an effective framework for modelling and executing large, high-performance, decentralized, VO based THEATRE multi-agent systems. A key difference from the above mentioned agent systems is that THEATRE agents are thread-less actors that execute in computing nodes -*theatres*- which act as *agencies* which furnish basic message scheduling/dispatching, migration, communication and time management services to local actors. Theatres can coordinate to one another e.g. for global time management or to ensure termination conditions in untimed applications. Actor behaviour is modelled as a finite state machine or through a statechart (Cicirelli *et al*., 2011b). Agents can migrate from a theatre to another at runtime, e.g. for functional requirements or for load balancing. Being light-weight in character, a huge number of actors can be created to populate a complex distributed model (Cicirelli *et al*., 2009)(Cicirelli *et al*., 2011a). In the proposed approach, only theatres are exposed as grid services. Actors remain transparent to the grid. All of this favours interoperability, e.g. theatre services could be implemented in different languages and grid services could permit integrating legacy services e.g. devoted to visualization. THEATRE is currently interfaced and can also work with HLA/RTI, Terracotta, Java Sockets and Java RMI.

The rest of this paper is structured as follows. In the next section basic concepts of THEATRE are summarized. Then the software engineering design process underlying the proposed mapping of Theatre on top of GT4 is highlighted. After that, as a testbed, a scalable distributed computing example is presented, which is

Proceedings 26th European Conference on Modelling and Simulation ©ECMS Klaus G. Troitzsch, Michael Möhring, Ulf Lotzmann (Editors)
ISBN: 978-0-9564944-4-3 / ISBN: 978-0-9564944-5-0 (CD)

based on a variant of the Minority Game (Cicirelli *et al*., 2011c)(Challet & Zhang, 1997)(Challet *et al*., 2005). Finally, conclusions are given with an indication of on-going and future work.

CONCEPTS OF THEATRE

Features of the THEATRE infrastructure (Cicirelli *et al*., 2009) are logically split between (a) the *execution platforms*, i.e. theatres, which provide the environmental services supporting actor execution, migration and interactions. Services are made available to actors through a suitable API; (b) *actor components*, i.e. the basic building blocks which are programmed in Java and capture the application logic. Basic components in a theatre platform (see also Fig. 1) are (i) an instance of the Java Virtual Machine (JVM), (ii) a Control Machine (CM), (iii) the Transport Layer (TL); (iv) the Local Actor Table (LAT) (v) a Network Class Loader (NCL). The Control Machine hosts the runtime executive of the theatre, i.e. it offers basic services of message scheduling/dispatching which regulate local actors. CM organizes all pending (i.e., scheduled) messages in one or multiple message queues. During the basic *control loop*, a pending message is selected (e.g., the or one of most imminent in time) and dispatched to its destination agent by activating the relevant handler() method. At the handler() termination, the control loop is re-entered, it schedules new sent messages of last activated agent and, finally, starts its next cycle. The Transport Layer furnishes the services for sending/receiving network messages and migrating agents. Concretizations of TL refer to Java Sockets or Java RMI, HLA/RTI (Cicirelli *et al*., 2009) or Terracotta (Cicirelli *et al*., 2010). In this work TL depends on the services of the Globus Toolkit 4 (GT4). The Local Actor Table contains references to local agents of the theatre. The Network Class Loader is in charge of getting dynamically and automatically the class of an object (e.g. a migrated agent) from a network Code Server.

Actors are *reactive objects* which encapsulate a data state and communicate to one another by asynchronous message passing. Messages are typed objects. Actors are at rest until a message arrives. Message processing is atomic and constitutes the unit of scheduling and dispatching for a theatre. The dynamic behaviour of an actor is modelled as a finite state machine or a distilled statechart (Cicirelli *et al*., 2011b) which is programmed in the *handler(message)* method which receives the message to process as a parameter. Responding to a message causes in general the following reactions: (i) new actors are (possibly) created (ii) some messages are sent to known actors (*acquaintances*). For proactive behaviour, an actor can send to itself one or more messages (iii) the actor migrates to a different theatre (iv) current state of the actor is changed (*become* operation). User-defined actor classes extend the Actor abstract base class. Message classes are derived from the Message abstract base class. Actors do not have internal threads. As a consequence, message handling naturally extends the control thread of the theatre within which the agent runs. Being thread-less, a huge number of application actors can be created, with very limited demand on the underlying operating system resources. All of this improves model scalability and ensures the achievement of good execution performance (Cicirelli *et al*., 2009, 2010, 2011a). Theatres and actors are assumed to have unique names (string). At its creation, the Java reference of an actor is stored in the Local Actor Table. Subsequently, the agent can decide to move to another theatre etc. The Java reference, though, of an agent persists despite migration. After migration, in the Local Actor Table of the source theatre the agent reference is kept but now refers to a *proxy* version of the agent, which behaves as a forwarder. The proxy keeps the network information about the destination theatre where the agent migrated. Dispatching a message to a proxy actor automatically generates a network message to the destination theatre. In general, a certain number of hops can be required before reaching an agent.

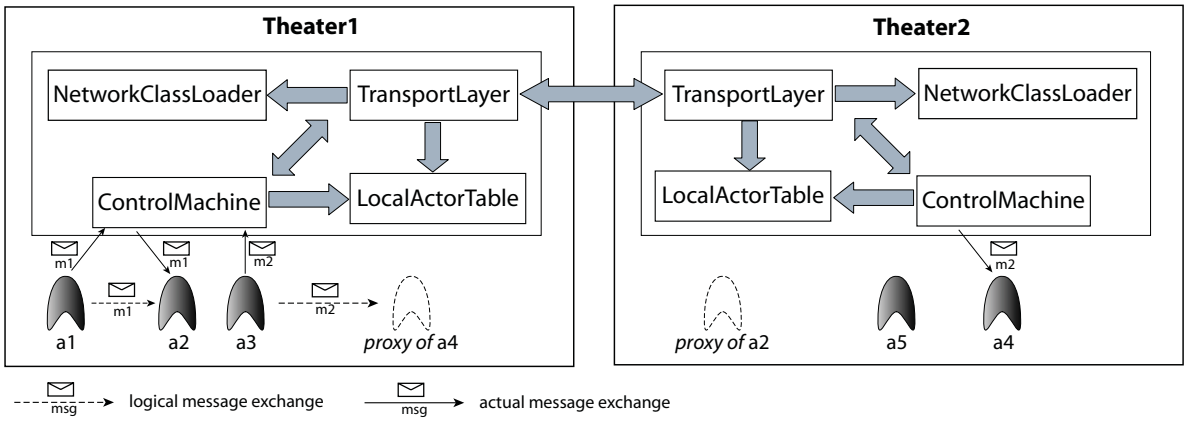

Figure 1. A THEATRE system

Of course, an agent can come back to a theatre where a proxy of itself exists. In this case, the proxy is replaced by a normal version of the actor which gets its state updated from that of the arrived agent. Agent migration

implies the relation proxy/normal of its acquaintances to be updated according to the viewpoint of the destination theatre. Some acquaintances become proxies because the corresponding actors reside in a remote theatre. Other acquaintance references can change from proxy to normal in the case the referred actor is local to the reached theatre. The update operation relies on the Local Actor Table information and the location data carried by the migrated actor. For efficiency of communications, a network message actually counts the number of hops realized for reaching its destination and automatically asks for an update of the addressing information in the proxy agent in the originating theatre.

PROTOTYPING THEATRE ON TOP OF THE GLOBUS TOOLKIT 4

The Globus Toolkit (Globus, on-line) is a de facto standard software package for developing grid systems. It includes several high-level services (for resource monitoring, service discovery, job submission infrastructure, security infrastructure, data management) useful for building grid applications. GT4, in particular, meets the requirements of the Open Grid Service Architecture (OGSA) and implements the specifications of the Web Service Resource Framework (WSRF), i.e. WS-ResourceProperties, WS-ResourceLifetime, WS-ServiceGroup, WS-BaseFaults, and related specifications of WS-Notification and WS-Addressing. In this work the Java version of GT4 was chosen for building grid services (Sotomayor & Childers, 2006), in particular Java WS Core version 4.0.8. Grid services are achieved by combining (stateless) web services with (stateful) resources according to some common design patterns. Grid service communications are based on SOAP XML-based messages which can be transported by different transport protocols (e.g. HTTP). The runtime infrastructure is the Java Web Service *container* which combines a SOAP engine, an application server and HTTP server. The container is responsible of making a grid service available to its clients.
Theatres map naturally on grid services. Fig. 2 portrays the structure of a theatre service based on GT4.

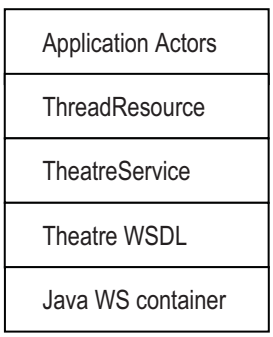

Figure 2. Design of a GT4 based theatre

Each theatre service runs on a distinct container allocated on a distinct computing node. The glue of a GT4 federation of theatres is Globus and SOAP. Each container is supposed to listen about incoming connection requests on a distinct port (8080 is the default port). TheatreService is a Java class implementing the service. The service itself is formalized through a WSDL (Web Service Description Language) file which specifies each operation the service can accept and the parameter types and return type of each operation. The WSDL also declares which SOAP messages will accompany each operation request.
As discussed in (Sotomayor & Childers, 2006), status information can be added to a stateless web service through the design of one or multiple resource instances. In this work only one resource instance is associated with a given theatre service, according to the *singleton* design pattern (Gamma *et al*., 1994) which is directly supported by Globus. TheatreResource implements in Java the internal organization of a theatre (see Fig. 1) which gives support to the execution of a collection of local application actors.
The interface of TheatreService is described in a WSDL XML file (Theatre.wsdl) which logically corresponds to the following Java interface:

```
interface Theatre{
    String getName();
    void setName( String theatreName );
    void receive( String obj );
    void start();
    void launch( String starterClass );
    void stop();
    void pause();
    void resume();
    void reset();
}//Theatre
```

As a design principle, the service interface only makes public the admitted operations (methods), i.e. it does not expose resource properties (RPs). RPs are hidden in the implementation class TheatreResource and can only be queried/modified by invoking the service operations. All the methods in TheatreServices are synchronized for concurrency control, can throw RemoteException and delegates to the actual methods of TheatreResource for the implementation aspects.
The *receive(String object)* method/operation transmits to the target theatre service an XML serialized object (actually a message or an actor). The object is first XML deserialized. Then if it is an *application message*, it gets scheduled in the control machine message queues. In the case of a *control message*, i.e. one which coordinates control machines to one another e.g. for time management, it is directly interpreted by the receiving theatre. If the object is a migrating actor, it is handled so as to update the proxy/normal relationship of the actors in the target theatre.
The *start()* method configures the target theatre so as to bootstrap its internal data structures and starts the

control thread of the control machine (note that initially there is no pending message therefore the control thread immediately blocks as it starts. The control thread will awake as soon as some message arrives).
The effective execution of a theatre federation begins by invoking the *launch(starterClass)* method on a given theatre service. This method receives the name of a starter class which gets loaded and then it is responsible of creating and initializing a first actor (e.g. a master or model actor) by sending to it an init message, on the target theatre. The master can then create further actors and send them messages thus spreading the execution.
The methods *stop(), pause(), resume()* control the execution of the theatre control machine. *reset()* resets all the theatre data structures, e.g. message queues of the control machine.

A critical point in the design framework of theatres as GT4 services, is the process of XML serialization/deserialization of messages and actors. From this point of view, the internal data component of such an object can be saved/restored into/from an associated Java bean. In addition, to each message/actor class is tied an XMLEncoder class (provided by Java) which gets the bean of the class and transforms it into standard terms of XML serialization. The encoding phase is in general complicated by the fact that a message or an actor can have acquaintance actors as internal fields and so forth recursively. The XML serialization process is capable of distinguishing the proxy/normal status of an actor in a given theatre, and generating the XML accordingly. In the case of a proxy actor, only grid service location information are generated during the serialization. The XML deserialization process in a destination theatre is the responsibility, after a minimal recourse to Java reflection, of the XMLDecoder class which does not necessitate of any adaptation.
After defining the WSDL of the service, and having implemented the TheatreService and TheatreResource classes, the operational lifecycle of GT4 grid services continues by specifying the deployment phase. A deployment descriptor file (deploy-server.wsdd) is prepared which tells the Java WS container how it should publish the theatre service. Deployment information is completed by an JNDI (Java Naming and Directory Interface) file (deploy-jndi-config.xml) which specifies, e.g., the class to be used for supporting the singleton pattern adopted by TheatreService. Java WS core improves the process of publishing a grid service by requiring a GAR (Grid ARchive) file to be created from the WSDL, the Java service+resource classes and wsdd+jndi files plus files from the Globus library. The creation of the GAR file (assisted by Apache Ant+Phyton) also compiles and generates all the *stub* classes (e.g. associated to operations parameters and return types, classes for the addressing/location of a service dynamically etc.) accompanying the given service. A Globus *deploy* command can then unpack the GAR and actually publish the service on to the container.
A federation of theatre grid services is put into execution by a client application which e.g. invokes the launch method upon a theatre service by passing to it a suitable starter class.

A DISTRIBUTED MODEL BASED ON MINORITY GAME

The prototype implementation of THEATRE on top of GT4 outlined in the previous section, was tested experimentally in a significant case using a distributed simulation of a model based on the Dynamic Sociality Minority Game (DSMG) (Cicirelli *et al*., 2011c). DMSG is a novel variant of the classical Minority Game (MG) (Challet & Zhang, 1997). In MG a fixed number of people have to decide about making use of a shared resource e.g. a bar. Since the space in the bar is limited (finite resource), the sojourn is considered enjoyable only if the number of attendances remains under a specified threshold. MG considers N (supposed odd) players that make a choice between the two options at each turn, i.e. attending the bar or stay at home. Winners are those that belong to the minority side, which is chosen by at most (n-1)/2 players. Each player gets initially a fixed and randomly chosen set of strategies that it may use to determine its next choice on the basis only of the past outcomes of the game. MG generalizes to the study of how many individuals, competing in a resource constrained environment, may reach a collective solution to a problem under adaptation of each one's expectation about the future without resorting to cooperation strategies.
DSMG assumes that information about the outcome of the previously played game step is only known to players that really attended the bar (Lustosa & Cajueiro, 2010), and that a dynamically established acquaintance relationship is available to propagate such information to non-attendant players. DSMG argues, in particular, that the capability of exploiting dynamic sociality behavior can be a key issue for modeling realistic scenarios of daily life. Consider, for instance, a player which can move on a territory. Situations can occur where acquaintances depend on the specific position owned by a player during a game step. In addition, the number of acquaintances may vary with time and can also be related to the ability of a player to establish (or maintain) social relations with other people in its nearness.
As a concrete DSMG modeling example, a road traffic scenario is considered where a single road (shared and constrained resource) connects a city and a resort, and people have to decide if to go on holyday or returning home avoiding traffic.
As in MG, N (supposed odd) players make a binary choice attempting to be in the minority side. Each player is initially fed with a randomly chosen set S of strategies that it uses to calculate its next choice on the basis only of the past M outcomes of the game. Since

there are only two possible outcomes, *M* is also the number of bits needed to store the history of the game. The number of possible histories is of course $P=2^M$, strategies are numerable and their number is 2^P. Players rank their own strategies on the basis of their respective ability to predict the winner side. Every player associates each strategy with a virtual score which is incremented every time the strategy, if applied, would have predicted the minority side. A penalty is instead assigned to bad behaving strategies. At each game step, a player uses the first ranked strategy. When there is a tie among possible strategies, the player chooses randomly among them. Classical MG supposes that information about the last game step is publicly available. As a consequence, the same history exists for all players.

At each game step, DSMG partitions players in three categories named *participant* (PA), *informed* (IN) and *non-informed* (NI). PA contains players that really attended "the bar" and directly know the game outcome. IN represents players that although not went to the bar they indirectly know the game outcome through their social network. NI denotes non-attendant players which remain unaware of the last game outcome. NI players are not able to update their strategies nor their history. As a consequence, players in the DSMG may accumulate a different history and may have a different view about the whole game status.

Formal definitions of DSMG

Let $O=\{-1,+1\}$ be the set of possible outcomes of the game, PL be the set of players and I be a subset of natural numbers corresponding to the game steps. Let $h: PL\times I \to O^M$ be a function modeling the history of a player, i.e. $h(p,i)$ returns the last M outcomes of the game of player *p,* preceding a given game step *i*; $h(p,0)$ is randomly set for each player. Let $S=\{S_1,...,S_n\}$ be the set of all the allowed strategies and $S_j: O^M \to O$ be a strategy function which guesses the next winner side by looking at the game history. Let $str: PL\times I \to N$ be the function which returns the index of the strategy used by player *p* at the game step *i*. The outcome of a player *p* at game step *i* is given by $S^{h(p,i)}_{str(p,i)}$. Once all players have determined their choice at step *i*, the sum of these choices defines the outcome *A(i)* of that step: $A(i)=\sum_{p\in PL} S^{h(p,i)}_{str(p,i)}$. Let $Acq: PL\times I \to 2^{PL}$ be a function determining the set of acquaintances of player *p* at game step *i*, and $Cat: PL\times I \to \{PA, IN, NI\}$ be a function which determines the category of player *p* at game step *i*:

$$Cat(p,i)=\begin{cases} PA & if \quad S^{h(p,i)}_{str(p,i)}=+1 \\ IN & if \quad S^{h(p,i)}_{str(p,i)}=-1 \wedge \exists p' \in Acq(p,i): Cat(p',i)=PA \\ NI & otherwise \end{cases}$$

Let $V_{Sj}: PL\times I \to \mathrm{Z}$, where Z is the set of integers, be the virtual score assigned by player *p* to strategy *Sj* at game step *i*. $V_{Sj}(p,0)=0$ for each strategy and for each player. Virtual scores are updated according to the following rule:

$$V_{Sj}(p,i+1)=\begin{cases} V_{Sj}(p,i) & if \quad Cat(p,i)=NI \\ V_{Sj}(p,i)-S^{h(p,i)}_{str(p,i)}A(i) & otherwise \end{cases}$$

Similarly, the history function of player *p* at game step *i* is not updated in the case $Cat(p,i)=NI$.

In this paper, the observable measures of the game are the *average of the game outcomes* $M_A=\frac{1}{T}\sum_{i=1}^{T}A(i)$, where T is the number of played game steps, and the fundamental variable for MG games in general which is the *per-capita fluctuation* of the game outcomes σ^2/N, where N is the number of players and $\sigma^2=\frac{1}{T}\sum_{i=1}^{T}(A(i)-M_A)^2$. The per-capita fluctuation is an important observable tied to player coordination. More precisely, a smaller value implies a better level of coordination among players (Sysi-Aho, 2005).

Modeling the road traffic example using THEATRE

The modeling example is split between two theatres running on two distinct network nodes (see Fig. 3). Two Win7 workstations, Pentium 4, 3.4GHz, 1GB Ram, interconnected by a 1Gbit Ethernet switch, were used for the experiments.

An odd number of players are randomly split between the two theatres. At every game step, a player who is in the city (resort) side has to decide whether to make a trip toward the resort (city) or to avoid traveling. Since the road has a limited traffic capacity, the enjoyable choice is that done by the minority of players. A player having +1 as outcome in a game step decides to make the trip. A player having -1 as outcome does not make use of the road. A player which does not make the travel may ask other players in the same place, i.e. its acquaintances, about traffic news. Due to departures and arrivals, the identity and the number of players in a place changes with time.

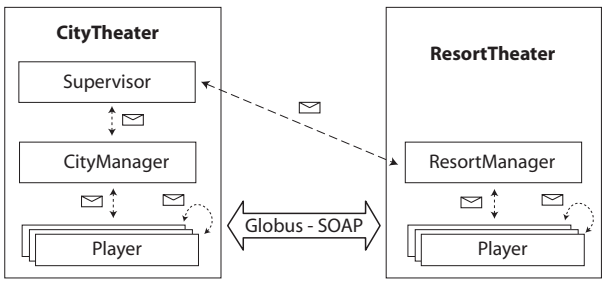

Figure 3. Theatre organization of the traffic road modeling example

Players are instances of a Player actor class. In each theatre there is a manager actor who controls the

realization of each game step by interacting with players through message exchanges. A Supervisor actor, supposed allocated to the CityTheatre, synchronizes the behavior of the two managers by signaling when the next step of the overall game can be started. The supervisor also collects statistics information about the game behavior.

Player agents which decide to move to the other side, leave a proxy version of themselves on their originating theatre and exploit the migration mechanism to transfer and operate in the partner theatre.

Fig. 4 portrays a sequence diagram about the messages exchanged during a game step. The supervisor starts the protocol by sending a StepMSG message to both managers which react to it by transmitting a StepMSG to the collection of managed players. Every player replies its own decision about the on-going game step to its manager through a ResultMSG message. Upon collecting all the replies from the relevant players, the manager replies in its turn to the supervisor with the player outcomes by another ResultMSG message. On receiving the two ResultMSGs, the supervisor first evaluates the winner side of the game (i.e. the minority side) and then sends an OutcomeMSG to the managers containing the current game outcome. After that, the managers broadcast the outcome to its managed players which update their local strategies/history. Then players reply to managers with a StepEndMSG message. Upon collecting all the required StepEndMSGs, the managers communicate to the supervisor a StepEndMSG which will allow updating the statistics in the supervisor and preparing for the next game step. For simplicity, Fig. 4 does not include the social interactions among players nor the action of migration of minority players to the other theatre.

Simulation experiments

Some simulation experiments were carried out with a fixed number of $N = 101$ players and $T = 5000$ game steps. Different configurations of the game were achieved by varying (a) the number of acquaintances that a player may contact at each game step, (b) the history size M and (c) the number of strategies assigned to players. The parameter values were chosen so as to reveal more detailed behavior hidden in the preliminary experiments documented in (Cicirelli *et al*., 2011c). In these first experiments, the number of acquaintances of a player was varied from 1 to 51, with a cutoff of behavior emerging when $|Acq|$=11. In particular, the average of game outcomes tends to be the same as for standard MG regardless both the number of strategies and history size assigned to each player. Moreover, the per-capita fluctuation of the game outcomes tends to be the same as for MG in the case M=8 whereas in the case M=2 this observable reaches its minimum to a smaller value than that obtained for the MG in the same configuration.

As the number of acquaintances reaches the value of 11, the number of *non-informed* players tends to zero, and the categories tend to become only *participant* and *informed*. As a consequence, the new experiments were planned with the following parameter values:

$M \in \{2,8\}$, $|Acq| \in \{1,3,5,7,9,11\}$, $\#strategies \in \{2,6\}$.

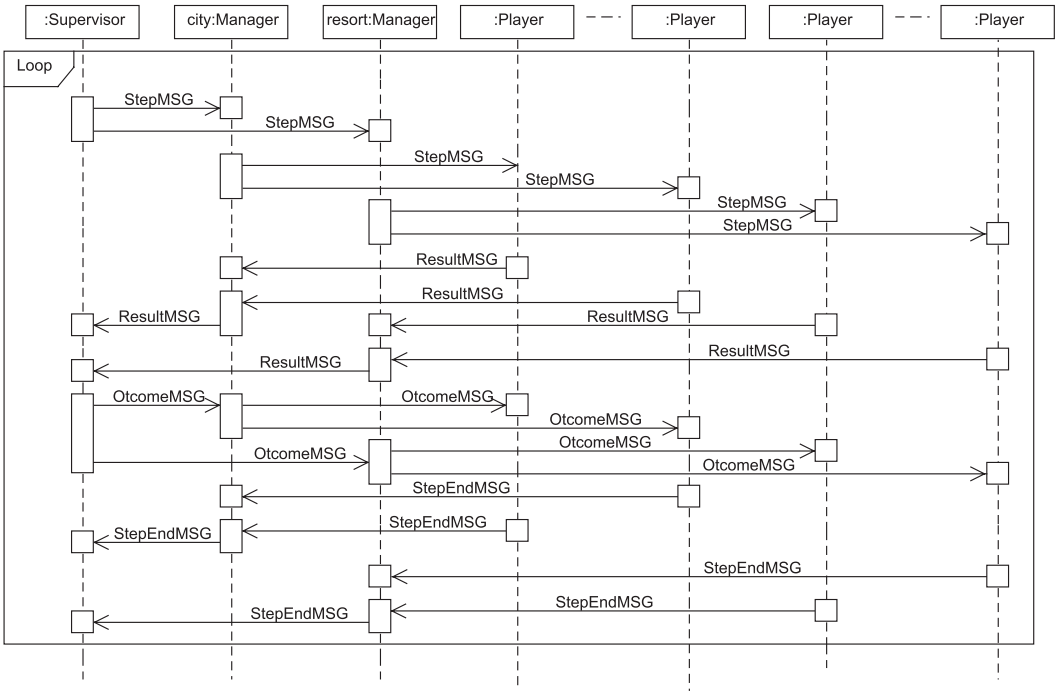

Figure 4. Message protocol at each game step

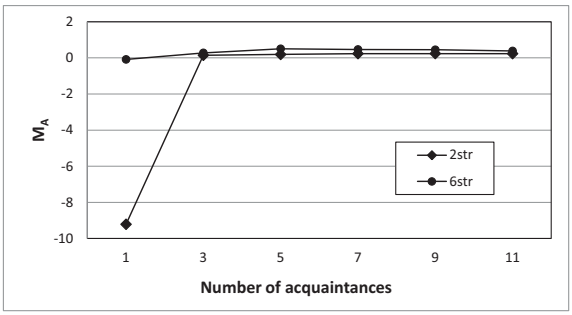

Figure 5. Average game outcomes, M=2

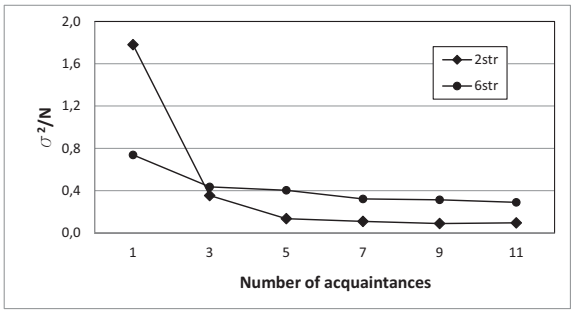

Figure 6. Per-capita fluctuation of game outcomes, M=2

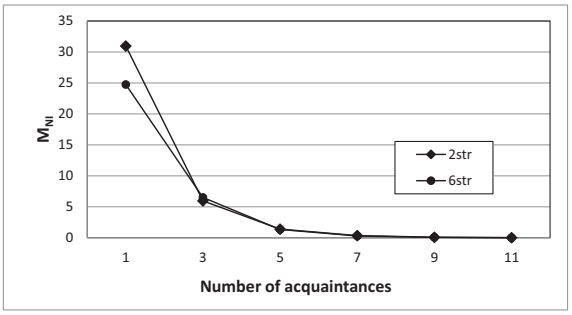

Figure 7. Average number of non-informed, M=2

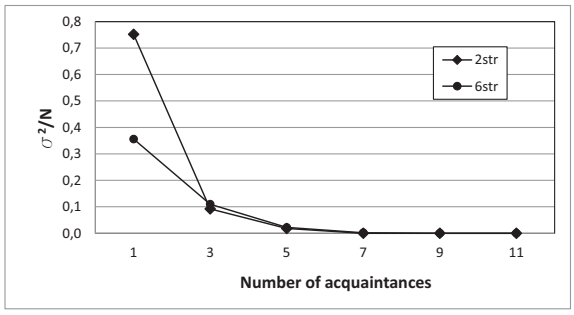

Figure 8. Per-capita fluctuation of number of non-informed, M=2

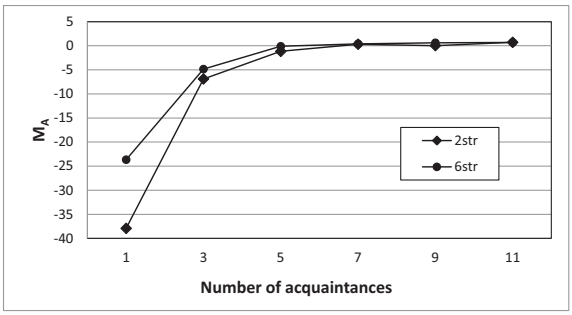

Figure 9. Average of game outcomes, M=8

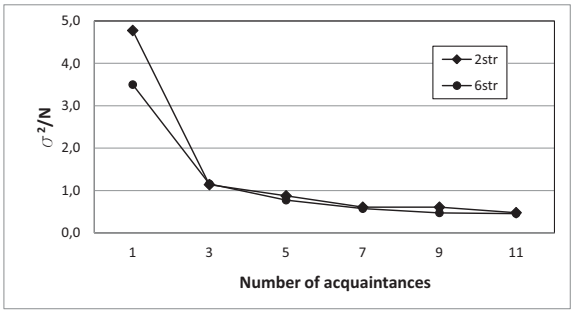

Figure 10. Per-capita fluctuation of game outcomes, M=8

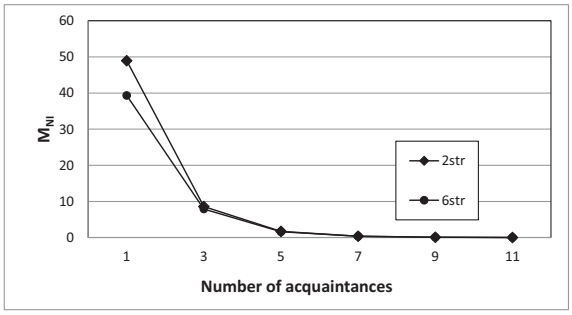

Figure 11. Average number of non-informed, M=8

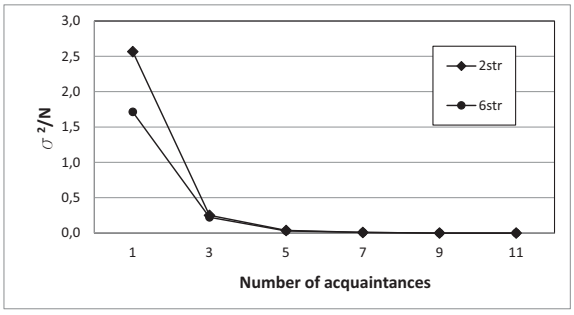

Figure 12. Per-capita fluctuation of number of non-informed, M=8

Each point in the figures from 5 to 12 was derived as the mean of five runs. Fig. 5 and Fig. 6 show respectively the average of game outcomes and the per-capita fluctuation of game outcomes when M=2. As one can see, as the number of acquaintances increases toward 11, a saturation phenomenon occurs and M_A tends to zero whereas σ^2/N reaches its minimum value. Moreover, as Fig. 6 witnesses, the case S=2 performs better than that S=6.

Fig. 7 and Fig. 8 confirm that by increasing the acquaintances number from 1 to 11, the behavior of the non-informed players tends to disappear definitely from the game because the number of non-informed players tends to zero. The same behavioral character is exhibited by the Fig. 9 to Fig. 12 which are concerned with the case M=8. In this scenario, though, as one can see from Fig. 10, the per-capita fluctuation is greater than that for M=2, for both S=2 and S=6. From the experiments seem to emerge that there is no benefit to

have a deeper history (i.e. M>2) with DSMG. Rather, it is more convenient to exploit a minimal social network (e.g. a number of acquaintances about $|Acq|=5$).

Scaling Issues

The chosen DSMG model used for the experiments is very challenging: after each game step about an half of the existing agents migrates to the other side of the road, making the model almost communication bound. Model scalability was studied by varying the number of players (from 11 to 100001) and measuring the amount of wallclock time (WCT) required by each game step. Fig. 13 shows the Normalized WCT (that is the ratio between the WCT and the number T of simulation game steps) vs. the number of players. Variables on both axes are reported in logarithmic scale. As Fig. 13 witnesses, the model seems to scale very well, thus talking about scalability of the whole Theatre/GT4 approach.

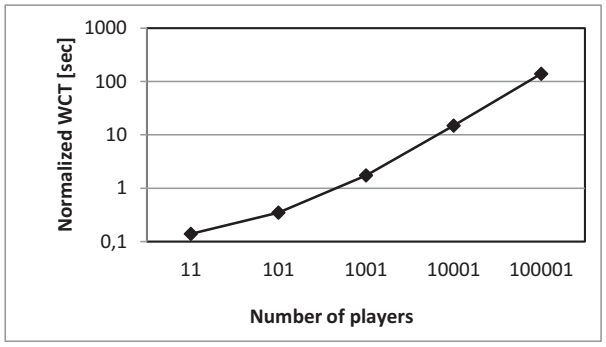

Figure 13. DSMG model scalability

CONCLUSIONS

This paper describes a novel approach and prototype implementation of using the THEATRE agent architecture (Cicirelli *et al*., 2009) on top of the Globus Toolkit 4 (Sotomayor & Childers, 2006), which aims at experimenting with grid computing in the M&S of complex multi-agent systems. The realization favors interoperability and opens to an exploitation of virtual organizations of computing resources and secure communications. A practical application of the proposed approach is demonstrated by a distributed simulation of an agent-based model which depends on the Dynamic Sociality Minority Game (Cicirelli *et al*., 2011c).

Future and on-going work is directed at:

- Improving the grid service implementation of theatres.
- Extending THEATRE/GT4 so as to give support to general time-management scenarios e.g. as described in (Cicirelli *et al*., 2009, 2010) which are based on a distributed conservative algorithm.
- Experimenting with THEATRE/GT4 in the M&S of large and scalable situated multi-agent systems (Cicirelli *et al*., 2011a) which relies on a composite time notion.
- Applying Dynamic Sociality Minority Game to more complex applicative scenarios.

REFERENCES

Avila-Rosas A., L. Moreau, V. Dialani, S. Miles, X. Liu. 2002. Agents for the Grid: a comparison with web services (Part II: Service Discovery). *Proc. of Workshop Challenges in Open Agent Environments*, pp. 52-56.

Cicirelli F., A. Furfaro, L. Nigro. 2009. An agent infrastructure over HLA for distributed simulation of reconfigurable systems and its application to UAV coordination. *SIMULATION - Transactions of the Society for Modeling and Simulation International*, vol. 85/1, pp. 17-32, SAGE.

Cicirelli F., A. Furfaro, A. Giordano, L. Nigro. 2010. Parallel Simulation of multi-agent systems using Terracotta. *Proc. of 14th IEEE/ACM International Symposium on Distributed Simulation and Real Time Applications (DSRT2010)*, pp. 219-222.

Cicirelli F., A. Giordano, L. Nigro. 2011a. Distributed simulation of situated multi-agent systems. *Proc. of IEEE/ACM International Symposium on Distributed Simulation and Real Time Applications (DSRT2011)*, September 4 - 7, Manchester, UK, pp. 28-35.

Cicirelli F., A. Furfaro, L. Nigro. 2011b. Modeling and simulation of complex manufacturing systems using statechart-based actors. *Simulation Modeling Practice and Theory* 19/2, pp. 685-703, Elsevier.

Cicirelli F., A. Furfaro, L. Nigro, F. Pupo. 2011c. Dynamic Sociality Minority Game. *Proc. of European Conference on Modelling and Simulation*, 7-10 June, Krakow, pp. 27-33.

Challet D., Y.C. Zhang. 1997. Emergence of cooperation and organization in an evolutionary game. *Physica A: Statistical and Theoretical Physics*, 246(3-4):407–418.

Challet D., M. Marsili, Y. Zhang. 2005. *Minority games*. Oxford University Press.

Foster I., C. Kesselman, S. Tuecke. 2001. The anatomy of the Grid: Enabling scalable virtual organizations. *International J. of Supercomputer Applications*, 15(3).

Fukuda M., D. Smith. 2006. UWAgents: a mobile agent system optimized for grid computing. *Proc. of GCA'2006*, pp. 107-113.

Gamma E., R. Helm, R. Johnson, J. Vlissides. 1994. *Design Patterns: Elements of reusable object-oriented software*. Addison-Wesley Prof.

Globus, on-line: http://www.globus.org.

Lustosa B.C., D.O. Cajueiro. 2010. Constrained information minority game: How was the night at El Farol?. *Physica A: Statistical Mechanics and its Applications*, Vol. 389, Issue 6, pp. 1230-1238.

Moreau L. 2002. Agents for the Grid: a comparison with web services (Part I: Transport Layer). *Proc. of 2nd IEEE/ACM Int. Symposium on Cluster Computing and the Grid*, pp. 220-228.

Sotomayor B., L. Childers. 2006. *Globus Toolkit 4 – Programming Java Services*. Morgan Kaufmann, Elsevier.

Sysi-Aho M. 2005. *A Game Perspective to Complex Adaptive Systems*. Ph.D. Thesis, Department of Electrical and Communications Engineering, Helsinki University of Technology, Espoo, Finland.

Simulation of Complex Systems and Methodologies

Cascade Simulation on Optimized Networks

Takanori Komatsu
Department of computer science,
National Defense Academy,
Yokosuka, Japan
Email: ed10004@nda.ac.jp

Akira Namatame
Department of computer science,
National Defense Academy,
Yokosuka, Japan
Email: nama@nda.ac.jp

KEYWORDS

Cascade Phenomena, Evolutionary Optimization, Genetic Algorithm, Network Topology, Diffusion of innovation

ABSTRACT

Cascade phenomena, which are sequences of adoption by agents, are the important driven forces for the society to make a successful diffusion of innovation. Cascade phenomena on complex networks occur under a range of conditions (or known as cascade windows) defined by both the average degree of the underlying network topology and the threshold of each agents(or nodes). In this paper, we obtain optimal networks for good cascade using generic algorithm (GA). In order to obtain the optimal network for good cascade, the network should have a sufficient number of vulnerable nodes and hub nodes of medium sizes, in other words, the degree distribution of the optimal network should follow a linear combination of Poisson and uniform distribution.

Introduction

Why does new fashion craze every year in the world? Why can one of software company succeed to deploy the operating system markets of the personal computers? Why was Arab Spring able to begin in the Arab world suddenly on Saturday, 18 December 2010 after the dictatorship lasted for many years? These phenomena can be considered as results of coordination, agreements, and information cascade on the underlying network topologies. One of common features of these phenomena is they start from the small fraction of agents on the network and the impact of it spreads into the entire networks with self-reinforcement mechanism. The phenomena with these features are called cascade phenomena and is also called snow ball effects. The cascade consists of good cascade and bad cascade. In the former case, cascade phenomena, which are sequences of adoption by agents, are the important driven forces for the society to make a success of the diffusion of innovation or new products. Many people are also easy to get concert on the wrong decision or choice, and this is an example bad cascade.

The network topology is the most fundamental network structure to consider the performance for cascade phenomena on many networked-systems (for example, Internet, sensor networks, social networks and financial networks). From the high point of view, an agent on each node can denote the human on social network, the router or the terminal on computer network and the company on financial network and each agent are connected by links which denotes there are communications or interactions between agents. The topology, which describe links between them, defines the frequency of interaction and has a certain influence on the dynamics of the application on it. Each agent also has threshold value, which is based on the proportion of the sate of neighbors, to change the own state. If the threshold of the agents is large, it is difficult for external effect to change the state of the agents, but it is easily affected when the threshold is small. In this paper, we study about changing the dynamics of the cascade phenomena using the underlying topology, which needs not to change in other parameters (the number of agents and links and the threshold of agents).

The approach we do in this paper is based on the concept of the dynamic network topology. In some networked systems, it is not easy to change the network topology, in which the network topology is defined by physical layer, but the development of information communication technology allows us to change the topology more easily. For examples, the logical over-lay network is effective to change the topology of the P2P network, the sensor network and the cloud computing network, and the social media (Facebook(Facebook, 2011) or Twitter(Java et al., 2007)) makes the information flow in society faster and more widely. While it is basic and common problem of cascade phenomena to design or find the optimal network topology for good cascade, it becomes difficult when we have large number of nodes and links, because the situation calls on us to check the performance of huge combinations of networks. Then, we need to develop new network design method which has enough scalability compared with human-centric network design. Then, we propose evolutionary optimization by genetic algorithm (GA) to obtain the optimal network for good cascade. The evolutionary optimization is based on the accumulation of heuristic improvements and it also has three key aspects to find optimal networks for good cascade; first, the formulation of the problem requirements; second, understanding and modeling essential properties of optimized network by GA; and finally simulating cascade phenomena on optimized networks to

Proceedings 26th European Conference on Modelling and Simulation ©ECMS Klaus G. Troitzsch, Michael Möhring, Ulf Lotzmann (Editors)
ISBN: 978-0-9564944-4-3 / ISBN: 978-0-9564944-5-0 (CD)

Table 1: Payoff matrix

i \ j	1	0
1	a, a	0, 0
0	0, 0	b, b

confirm those performances. Especially the second is effective to understand the relationship between the topology and the performance. We show the network with a linear combination of Poisson and uniform degree distribution is evolutionary optimal for good cascade, on which cascade phenomena can occur under a wide range of conditions. The overall objective of the research presented in this paper is to change the dynamics of the network application on demand exploiting the underlying topology.

The rest of this paper is organized as follows. Section 2 defines a cascade model on networks. Section 3 describes the proposed evolutionary network optimization by genetic algorithms and presents some results. Section 4 simulates cascade phenomena on optimized networks, which are compared with scale-free networks and random networks. Section 5 shows the topology obtained by the evolutionary optimization. Section 6 presents a summary.

A cascade model on networks

Let the given networked system have N agents (nodes) and L links and the state of all agents is 0 as the initial state. We change the state of a few agents from 0 to 1 as a trigger of cascade and observe the spread of the state 1 into the entire network. At each time step, all agents select own state from the space $S = \{0, 1\}$ based on the proportion of the state of neighboring agents at previous time step, to be more exact, agents play a 2×2 coordination game with each neighbor and revise the state using a deterministic myopic-best response to maximize his current payoff given the proportion of neighbors choosing each action in the population. In this framework, selecting 0 or 1 means, for example, selecting product A or product B, adopting old regime or new regime, and accept or reject. Then, this cascade model has the locality and the decision rule based on the proportion, and thanks to this simplicity, the model can be applied on many situations, on which each agent make a binary decision. The payoff of each state for agents is summarized in symmetric matrix (see Table 1).

Let s_i represent the state of agent i and $j \in N_i$ is the set of neighboring agents of agent i. Networks can be directed or undirected. Here, to simplify matters, we consider undirected networks. This implies that neighboring agents mutually affect each other. In addition, let $U(s_i, s_{j \in N_i})$ be the total payoff after a 2×2 coordination game with neighboring agents, which is denoted using the summation of the payoff of each coordination game $u(s_i, s_j)$.

$$U(s_i, s_{j \in N_i}) = \sum_{j \in N_i} u(s_i, s_j) \tag{1}$$

The best response of each agents depends on the proportion of neighbors choosing 1. If the proportion p is larger than the threshold ϕ, then $i's$ best response is to choose 1. Otherwise i choose 0. The dynamics of the choosing state by agents is summarized in Eq. (2).

$$s_i \quad = \quad \begin{cases} 1 & p > \phi \quad (\phi = b/(a+b)) \\ 0 & p < \phi \end{cases} \tag{2}$$

Watts showed there exist some cascade area in term of the threshold ϕ and the average degree(the average number of neighboring agents) Z, where cascade may occur. They define this area as cascade window (Watts, 2002).

Fig.1 shows the example of the cascade window on networks using the cascade condition by Watts(Watts, 2002) (see Eq. (3)). In the cascade window, an initial trigger can make the cascade on the entire network, but on the outside the trigger have only a limited effect and it cannot make the cascade.

$$\sum_{k=0}^{\lfloor 1/\phi \rfloor} k(k-1)P(k) = z \tag{3}$$

where $P(k)$ represents the degree distribution of the network.

It is very interesting that even if the network with same average degree Z, the network with different degree distribution has different the size of cascade window. This implies us that we can change the dynamics of the cascade phenomena exploiting the underlying topology.

Young modeled the diffusion of innovation using cascade model and studied the cascade condition on the lattice network(Young, 2010, 2009, 1993) and Watts showed the importance of the agent with small degree to maximize cascade window(Watts and Dodds, 2007). From their results, it is important there exist a large cluster which consists of agents with a small number of links (connections). López used the technique (mean-filed approximation) of modeling the cascade phenomena and said that a network with an intermediate variance in term of degree (the number of connection) of agents maximizes the size of cascade window because the limitation make a network have a cluster as Yong and Watts introduce. López also showed the following relationship between the topology and the size of cascade window that the exponential network has larger cascade window than the scale free network(López-Pintado, 2006), which is

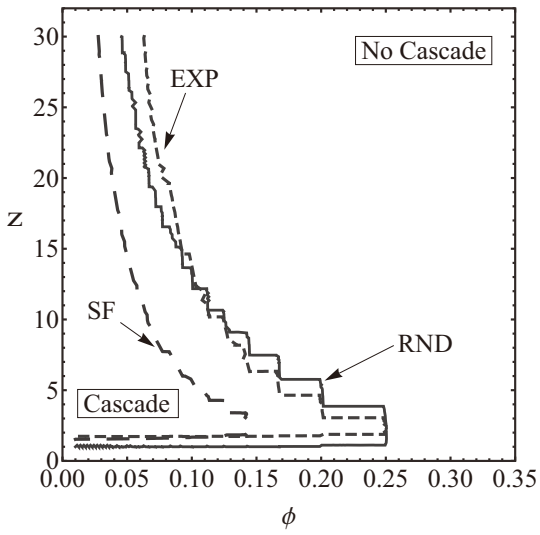

Figure 1: The cascade window as a function of the threshold value and the networks in different network topologies: Scale-Free network(SF), Random network(RND), and Exponential network(EXP).

the best topology for spreading a disease(Pastor-Satorras and Vespignani, 2002).

$$\phi^*_{\mathrm{SF}} < \phi^*_{\mathrm{EXP}} \tag{4}$$

As a result, we have simple questions "Is the exponential network the optimal network to maximize the cascade window?" or "How do we get the network which meets our requirements on the size of cascade window?" Answering these questions is the first step to change the cascade dynamics using the network topology. Then, in this paper, we consider the maximizing the cascade window for good cascade as an example problem.

Evolutionary optimization

We propose evolutionary network optimization method by genetic algorithm (GA) to obtain the optimal network, which maximize the cascade window, for good cascade. We assume all agents have same threshold ϕ and only consider connected networks, in other words, the one giant cluster should include all nodes.

Chromosome

The network topology, which consists of N nodes, are completely described by the $N \times N$ adjacency matrix $\boldsymbol{A}$. For the simplicity, we use undirected networks, then the element $a_{ij} = a_{ji} = 1$ denotes there is the interaction between agent i and agent j. The sequence of elements of adjacency matrix is the chromosome of genetic algorithm (see Fig.2). In order to generate new networks from two parents networks, we apply uniform crossover into chromosome of them.

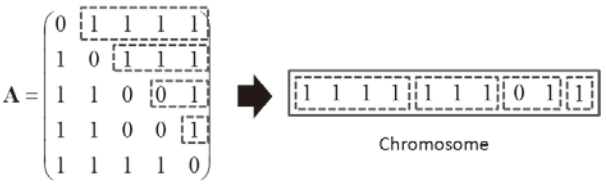

Figure 2: The chromosome of the network topology in genetic algorithms

Fitness function

According to the mean-field analysis of cascade phenomena by Lopez(López-Pintado, 2006), we can estimate cascade window size ϕ^*

$$\phi^* = \arg \min_{\phi \in [0,1]} \sum_{k \geq 1}^{\lfloor 1/\phi \rfloor} k^2 P(k) \tag{5}$$
$$\text{s.t.} \sum_{k \geq 1}^{\lfloor 1/\phi \rfloor} k^2 P(k) > 1$$

In order to maximize cascade window for good cascade, we need to find the network which has the largest ϕ^* and then we use ϕ^* as a fitness function for genetic algorithm.

Procedures

The approach we propose in this section consists of three steps (see Fig.3). First steps is generating initial population by random network and scale free network. Second step is picking up two network as parents from population randomly and generating new networks as children using uniform crossover. Third step is selecting two elite networks based on fitness value to insert them into population and the next step will start from the first step again. The approach we propose do this optimization cycle until the fitness value attain required value or there is no improvement for long time. In addition, we apply programming tips not to change the number of links and isolate no node from the giant cluster after uniform crossover. This implies uniform crossover just change connected-network topology.

Experiments and outputs

Table 2 shows the detail of settings of evolutionary network optimization by GA. The accumulation of improvement by optimization cycle outputs the network which has lager fitness value along the evaluation number is growing (see Fig. 4). We summarize the results of each experiment on Fig.5. As described previously, the exponential network is most suitable to maximize cascade window, but the approach we proposed can find more optimal network which has larger cascade window.

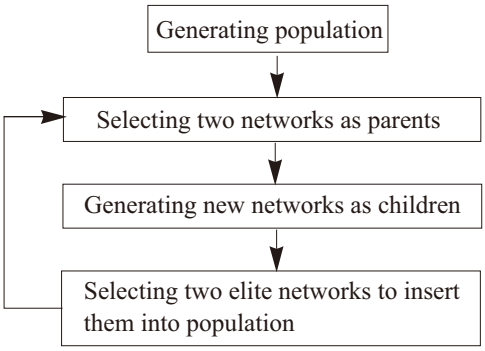

Figure 3: The procedures of evolutionary optimization by genetic algorithms

Table 2: Parameters for genetic algorithm

Genetic algorithm model	Minimum Generation Gap model(H.Sato et al., 1997)
Initial population size	20
” Child ” population size	20
Fitness function	see Eq.(6)
Crossover	Uniform crossover
Mutation	Not used
Selection	An elite selection strategy
The number of evaluations	Over 20000

Cascade Simulation on Evolutionary Optimized Networks

In this section, we present a set of simulation results. The simulations are conducted to confirm the optimal networks by GA have the largest cascade window, compared with scale-free network, random network and exponential network, especially, the exponential network is considered to have the largest cascade window(López-Pintado, 2006).

Simulation scenario

The fitness function (Eq.(6)) is directly derived from mean-filed theory, which can technically apply to the network which has no loop and degree correlation. They are not tiny assumptions, and then we need to confirm the properties of the optimal network by numerical simulations. We use three type (SF:scale-free network, RND:random network, EXP:exponential network) networks, which has 500 nodes, to compare with the optimal network by GA. Initially, all nodes have the state 0 and we change the state of only one node from 0 to 1. We run same simulation 1000 times and observe the average final proportion of agents choosing 1.

Simulation results

We plot border point, on which we observe the cascade which spreads into the entire network at least one time

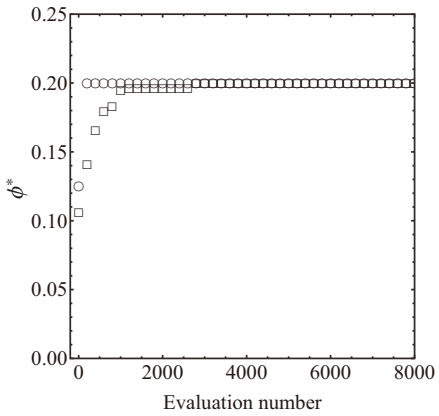

(a) $\langle k \rangle = 10$

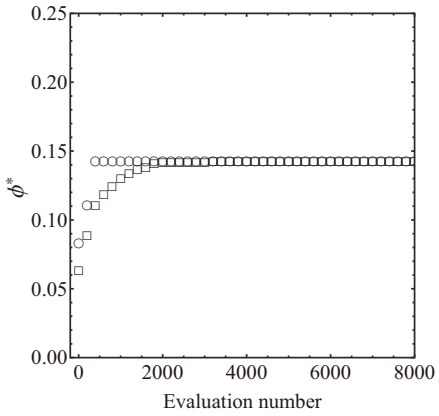

(b) $\langle k \rangle = 20$

Figure 4: The fitness value of the network as a function of the evaluation number: ○:largest fitness value, □:average fitness value

out of 1,000 trials (see Fig.6). It is very clear that the optimal network by GA has the largest cascade window compared with other network topologies. The results on all networks reflect the trend of the theoretical cascade window. We summarize these results with same manner of López as

$$\phi^*_{\mathrm{SF}} < \phi^*_{\mathrm{EXP}} < \phi^*_{\mathrm{GA}} \tag{6}$$

Topology of evolutionary optimized networks

The degree distribution of evolutionary optimized networks(GA networks) show that the network has a wide range of nodes in terms of degree(see Fig.7(a), Fig.8(a)). Note that, in the degree distributions, not merely a large proportion of nodes having small degree is to be found, but also hub nodes with a certain size are to be found.

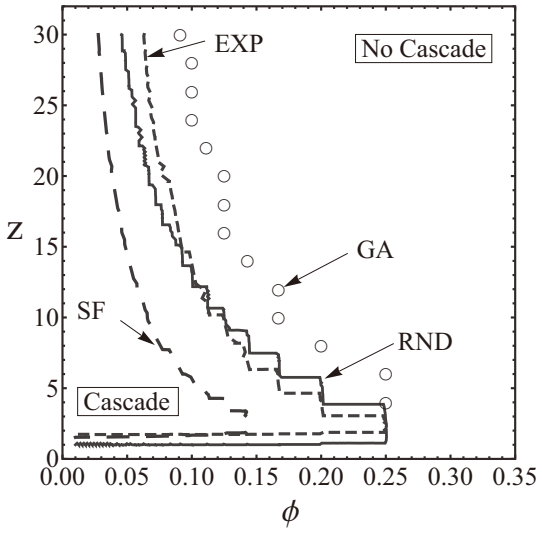

Figure 5: The cascade window of evolutionary optimal network for good cascade as a function of average degree Z and the threshold value ϕ of the agents

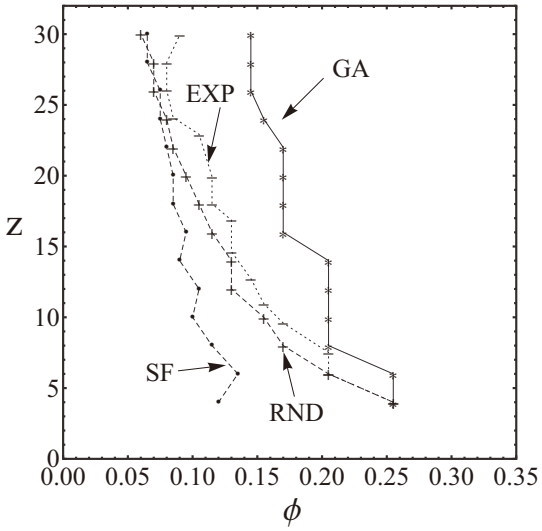

Figure 6: The cascade window by numerical simulations as a function of average degree Z and the threshold value ϕ of the agents

Fig.9 and Fig.10 shows how nodes in exponential and GA networks are connected to others. More preciously, we plot each point on (d_i, d_j) when node i with degree d_i and node j with degree d_j are connected. The diameter of each point is also proportional to the logarithm of the frequency of the cases. After that, the figure is converted to be symmetry for the only visualization. Although in the exponential networks, we found one big cluster and the center of it is near from $(\langle k \rangle, \langle k \rangle)$, in the GA networks, we found two cluster and the center of the cluster in the circle is located on (k_c, k_c) where $k_c < \langle k \rangle$. The nodes of the cluster in the circle have small number of links and the cumulative fraction of those nodes is about $80 - 90\%$ which can percolate the almost entire network(see Fig.7(b) and Fig.8(b)). These topological properties of the GA networks imply that the cascade occurs more easily on GA networks compared with the exponential network.

We also try to model the degree distribution of the GA networks by using a linear combination of two different degree distributions, because each cluster of GA networks may have a different degree distribution. From results of preliminary experiments(they are not included in this paper), we use Poisson and uniform distribution to model the degree distribution of each cluster in GA networks. The model is shown as:

$$p(k) = \frac{1}{A}\frac{\lambda^k e^{-\lambda}}{k!} + B \tag{7}$$

where A and B are controlling parameters for the network design.

We plot the degree distribution and complementary cumulative distribution function of the model on Fig.7 and Fig.8 where each coefficient was adjusted heuristically in this case. These distributions of the model fit the distributions of GA networks very well.

From the results obtained, the GA networks have a degree distribution which follows a linear combination of Poisson and uniform degree distribution and the distribution enables the network has a sufficiently large cluster, of which nodes have relatively small number of links and facilitate cascade phenomena.

Then, we obtain the relationship of the threshold of each network for cascade as:

$$\phi^*_{\text{SF}} < \phi^*_{\text{EXP}} < \phi^*_{\text{Poisson-Uniform}} \tag{8}$$

Conclusion

In this paper, we study changing the behavior of the application on networks exploiting the underlying network topology and, as an example problem, maximize cascade in terms of a region of cascade conditions, which is important driven forces for the diffusion of the innovation. Instead of a human-centric method, which is creative but not scalable, we propose evolutionary network optimization by genetic algorithm to obtain a network required. The approach we propose can find that networks with a linear combination of Poisson and uniform distribution have largest cascade window compared with exponential networks, random networks and scale free networks by the accumulation of the improvements.

REFERENCES

Facebook (2011). Statistcs. *http://www.facebook.com/press/info.php?statistics*.

H.Sato, O.Isao, and K.Shigenobu (1997). A new generation alternation model of genetic algorithms and its assessment. *Journal of Japanese Society for Artificial Intellligence*, 12(5):734–744.

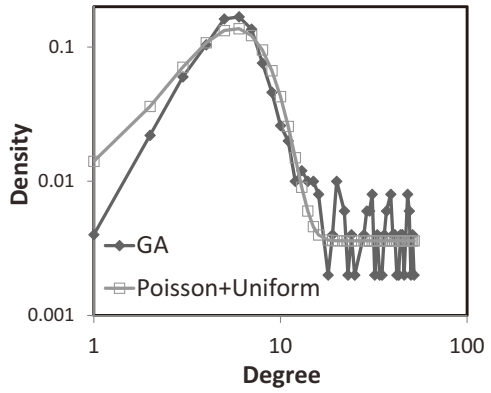

(a) Degree distribution

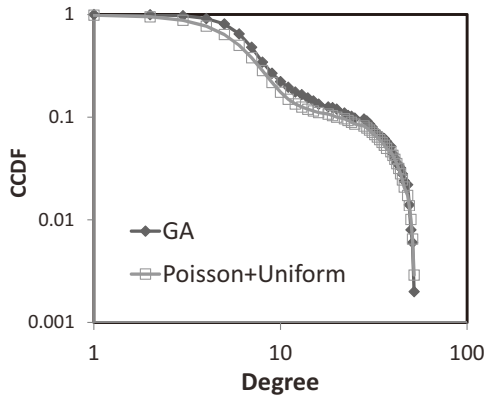

(b) Complementary cumulative distribution function

Figure 7: The density and the complementary cumulative distribution function of the degree of the evolutionary optimal network(GA) and the combination distribution of Poisson and uniform distribution($A = 1.2$, $B = 0.0036$ in Eq.(7)) as a function of degree k on logarithmic scale:Both of these distribution have same average degree $\langle k \rangle = 10$

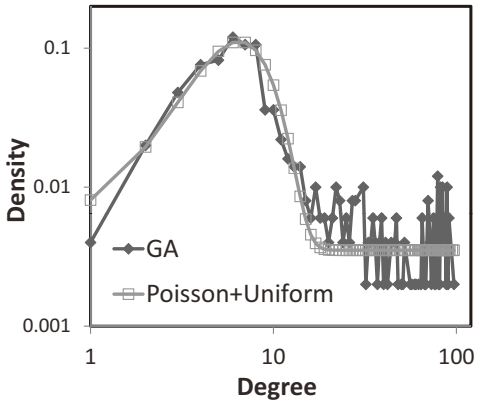

(a) Degree distribution

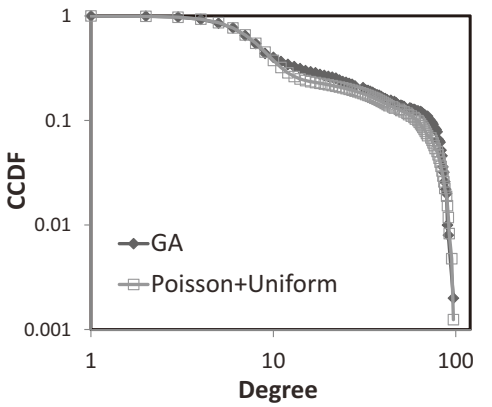

(b) Complementary cumulative distribution function

Figure 8: The density and the complementary cumulative distribution function of the degree of the evolutionary optimal network(GA) and the combination distribution of Poisson and uniform distribution($A = 1.4$, $B = 0.0035$ in Eq.(7)) as a function of degree k on logarithmic scale:Both of these distribution have same average degree $\langle k \rangle = 20$

Java, A., Finin, T., Song, X., and Tseng, B. (2007). Why we twitter: Understanding microblogging usage and communities. *The Joint 9th WEBKDD and 1st SNA-KDD Workshop*.

López-Pintado, D. (2006). Contagion and coordination in random networks. *International Journal of Game Theory*, 34(3):371–381.

Pastor-Satorras, R. and Vespignani, A. (2002). Epidemic dynamics in finite size scale-free networks. *Physical Review E*, 65(3):035108+.

Watts, D. and Dodds, P. (2007). Influentials, networks, and public opinion formation. *Journal of Consumer Research*, 34:441–458.

Watts, D. J. (2002). A simple model of global cascades on random networks. *Proceedings of the National Academy of Sciences*, 99(9):5766–5771.

Young, H. (1993). The evolution of conventions. *Econometrica*, 61:57–84.

Young, H. P. (2009). Innovation diffusion in heterogeneous populations: Contagion, social influence, and social learning. *American Economic Review*, 99(5):1899–1924.

Young, H. P. (2010). The dynamics of social innovation. Department of Economics, University of Warwick, Economic Theory Workshop.

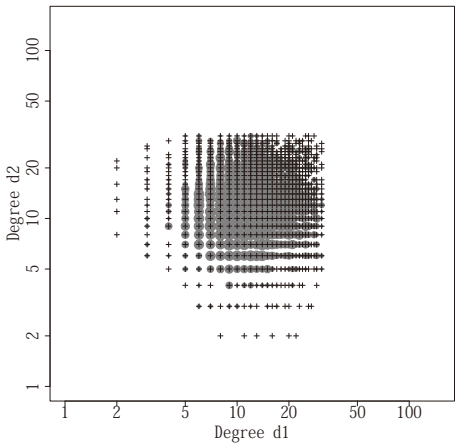

(a) Exponential network

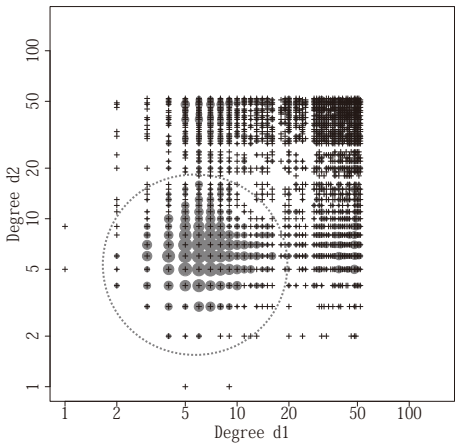

(b) GA network

Figure 9: This map shows the relationship of degrees between nodes, which are connected by links. The average degree of each network is $\langle k \rangle = 10$. The diameter of each point on the map is proportional to the logarithm of the frequency.

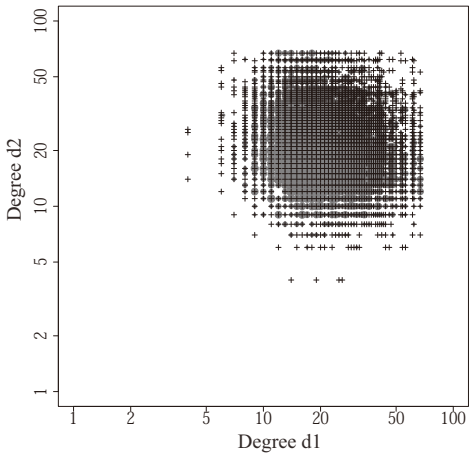

(a) Exponential network

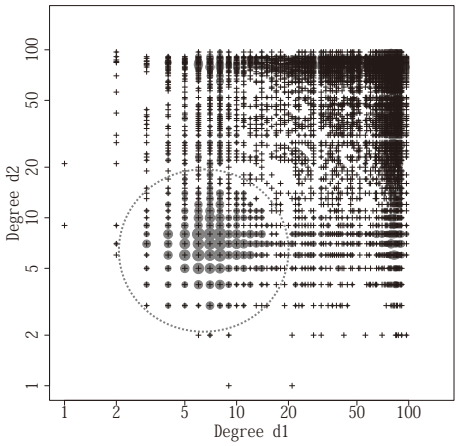

(b) GA network

Figure 10: This map shows the relationship of degrees between nodes, which are connected by links. The average degree of each network is $\langle k \rangle = 20$. The diameter of each point on the map is proportional to the logarithm of the frequency.

AUTHOR BIOGRAPHIES

Takanori Komatsu holds the bachelor's degree of Science in Electrical and Electronic Engineering at Tokyo University of Agriculture and Technology in Japan and master's degree of Science in Computer Science and Engineering at National Defense Academy of Japan. Currently he is doing his PhD in Computer Science at National Defense Academy of Japan. His research interests include network design, network security and Multi-agents. His email is ed10004@nda.ac.jp and his personal webpage at http://www.nda.ac.jp/~hsato/taka/.

Akira Namatame is professor of Dept. of Computer Science National Defense Academy of Japan. He holds the degrees of Engineering in Applied Physics from National Defense Academy, Master of Science in Operations Research and Ph.D. in Engineering-Economic System from Stanford University. His research interests include Multi-agents, Game Theory, Evolution and Learning, Complex Networks, Economic Sciences with Interaction Agents and A Science of Collectives. He is a member of the AAAI, the IEEE, the SICE. His email is nama@nda.ac.jp and her personal webpage at http://www.nda.ac.jp/~nama.

PREDICTION AND MODELLING OF LIGAND-BINDING SITES USING AN INTEGRATED VOXEL METHOD

Ling Wei Lee
School of Computer Science
The University of Nottingham Malaysia Campus
Jalan Broga, 43500 Semenyih
Selangor Darul Ehsan, Malaysia

Andrzej Bargiela
School of Computer Science
The University of Nottingham Jubilee Campus
Wollaton Road,
Nottingham NG8 1BB, UK.

KEYWORDS
Ligand-Binding Sites, Voxelisation, Voxel-Based Analysis, Grid-Based Method, Binding Site Residues

ABSTRACT

The interaction between proteins and their binding agents take place on surfaces and involve factors such as chemical and shape complementarity. It was shown in past studies that protein-protein interactions involve flatter regions whereas protein-ligand bindings are associated with crevices. Many approaches have been implemented which focus on the identification of such sites using various measures. Here we present an integrated method based on the use of voxels and computer-vision in the search for ligand-binding areas. Each identified site is modeled and analysed in 2D with the corresponding residues listed out. We carried out our experiment on a set of 3 FK506-bound proteins and 2 heme-bound proteins and showed that the integrated method is capable of identifying correctly the sites of interest.

INTRODUCTION

Proteins are made up of combinations of amino acids and they carry out binding to external agents usually on their surfaces. A host of factors contribute to the reactivity of a site of interest including hydrophobicity, electronegativity, chemical composition, shape complementarity etc (Fisher et al, 1993; Cheng and Weng, 2003; Venkatachalam, 2003; Kellenberger et al, 2004; Nayal and Honig, 2006; Weisel et al, 2009). Bind site characteristics can be attributed to the arrangement of atoms therefore leading to the activation and deactivation of certain atoms and thereby giving the protein its unique set of functions. Protein surface analysis is capable of returning better exterior information compared to sequential or structural studies. Via et al (2000) stated that "protein surface comparison is a hard computational challenge and evaluated methods allowing the comparison of protein surfaces are difficult to find". One of the properties which allow a group of proteins to bind to the same ligand is the probable conservation of features within the dock sites indicating the proteins may be descended from the same family. However in the event of mutations non-related proteins may carry similar features as well (Kinnings and Jackson, 2009).

Many attempts have been undertaken in the past to study protein surfaces and identify potential dock sites. Some of the earliest programs available include POCKET (Levitt and Banaszak, 1992) and LIGSITE (Hendlich, Rippmann and Barnickel, 1997). The former uses an experimental sphere of a specified radius to examine protein surfaces for pockets in a 3-dimensional grid space, although the algorithm is still exposed to orientation-related problems. The latter identified this issue and introduced rigorous scannings to reduce the severity of the problem. From a 3-directional check the scan is increased to 7, the additional directions being the 4 diagonals.

Jones and Thornton (1997) proposed the use of surface patches for the detection of interaction sites on a protein. A series of parameters are calculated for each patch including the solvation potential, hydrophobicity, planarity, accessible surface area etc with the patch rankings determined based on these parameters. Bogan and Thorn (1998) presented the concept of 'hot spots' which correlates to active sites. The authors found that binding energy does not distribute evenly across the surface of a protein but tend to be highly concentrated on dock areas. In a work by Fernandez-Recio et al (2005) the Optimal Docking Area (ODA) method was presented focusing on hot spots. ODA identifies patches through experimentations of different atomic solvation parameters. It was also found that larger interfaces generally consist of multiple patches with at least a pair of patches equivalent in size to a single patch interface (Chakrabati and Janin, 2002).

Understanding of the factors contributing to an active site is vital for successful detection of such areas. Most grid-based approaches prioritise shape complementarity in the search for potential sites. A crevice has to be sufficiently large to accommodate a ligand for interaction to take place. In our approach we present an integrated method using a combination of computer-vision techniques and voxel-based environment for the identification and modeling of potential binding sites. All associated atoms and corresponding residues are extracted as well.

Proceedings 26th European Conference on Modelling and Simulation ©ECMS Klaus G. Troitzsch, Michael Möhring, Ulf Lotzmann (Editors)
ISBN: 978-0-9564944-4-3 / ISBN: 978-0-9564944-5-0 (CD)

BACKGROUND

The surface of a protein is an interesting landscape of concave and convex areas. Each protein has its own set of defined functionalities. The use of grid spaces or voxels in protein studies is no longer a new paradigm as demonstrated in programs like POCKET and LIGSITE. The grid space offers a fast and robust solution to many applications. In our implementation we introduce a cubic grid-space for the identification of potential dock sites based on computer vision-inspired techniques.

A cubic grid-space is first constructed large enough to contain within it the entire protein. The experimental space is then tessellated into smaller units, with each unit having a size of 4 Å (the size of a voxel which fully encapsulates most atoms). All data sources for the test proteins are obtained from the RCSB Protein Data Bank in PDB format. We then extract all required information from the files including the spatial coordinates of all the atoms, the atom types and included the van der Waals radii for the atoms. These information are compiled into a new file that will be used as input for the algorithm.

We have chosen well-tested proteins for the study. The first set consists of FK506-bound proteins [PDB: 1FKF, 1BKF, 1YAT] which are molecules having a single active binding site each for one substrate. The protein 1FKF has been experimentally determined through a wet lab approach (Van Duyne et al, 1993) and attempted as well using a geometrically-based search coupled with geometric hashing (Peters, Fauck and Frommel, 1996). With proven results this protein serves as a good test subject. The second set consists of heme-bound proteins [PDB: 4HHB, 4MBN]. All input proteins are first projected into the 3D grid environment and tessellation of the space is carried out. As the 3D space induces a higher complexity compared to 2D processing, as such a 'slicing' process is carried out which converts the 3D environment into a series of 2D images by selection of a chosen dimension for conversion (Lee and Bargiela, 2009). This is conceptually similar to the Z-buffer algorithm in 3D graphics.

Each obtained image is processed using simple image processing techniques to identify voxels related to the protein. Surface voxels are then identified such that a list of surface atoms can be obtained (Lee and Bargiela, 2010). As each protein is encapsulated in a grid space, one is only able to obtain 6 views of the protein based on the characteristics of the cube. In a visual sense, crevices on the protein can be discerned through a sense of depth and clarity. We attempt to identify potential dock sites based on the depth attribute. A cuboid is first grown within the protein until it hits a plateau in each of the 6 faces. This defines the starting plane of visual projections executed from within to the surface. A depth count is then carried out and any area in which the count is smaller than the surface average or a user-specified

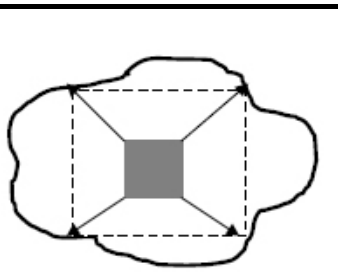

Figure 1. The construction of a cuboid beginning from the center of the protein. The algorithm terminates when the largest fully-filled cuboid has been obtained.

threshold is defined as a potential dock site. Finally all associated atoms and residues are projected for the sites.

THE ALGORITHM

The human vision is capable of perceiving areas protruding from the protein and 'valleys' of which binding agents of matching shape and chemical configurations may bind to. However to translate this into a simulated system is computationally challenging. As such most algorithms seek to minimise complexities and represent the problem in simpler domains. In our implementation, the protein is first enclosed in a grid space. By translating the human view to the 6 faces of the grid space (since the grid space is made up of voxels and each voxel has only 6 faces) one can then obtain 6 views of the protein.

For each of these 6 faces, we proceed to locate the crevices within the viewing boundary of each face. The 'starting plane' for each face is first defined by identifying the largest cuboid beginning from the averaged center of the protein. The algorithm terminates when a perfect plane (one in which the plane is fully occupied by voxels) in any axis is no longer encountered. A 2D visualisation of this approach is given in Figure 1. The surfaces of this inner cuboid become the 'starting planes' for all analyses working outwards beginning from the voxels situated on the plane. Each higher level of the voxels builds on the previous level, therefore rendering some voxels on the lower levels hidden to the external environment. Such a move is capable of determining potential sites if deeper clefts are found and are externally exposed. Due to the inside-out numbering of the levels binding sites have smaller depth-level values and outermost regions have larger numbers.

A breakdown of the cuboid-growing process is given below.

1. All identified surface voxels and surface atoms are first loaded and stored into memory.
2. The full list of voxels defining the protein – including both internal and surface voxels – is accessed.

3. Identify the largest possible cuboid constructed from voxels from the center of the protein. the process begins with the initiation of an ‘infant cube’ in the from of an equilateral cuboid. The rule is such that the cuboid must not contain any parts devoid of voxels.
4. Once the ‘infant cube’ has been created, the method then proceeds to stretch all sides of the cube until the largest possible cuboid is attained that is completely filled with voxels.

Following that a color grid map is created with different levels of voxels distinctly color-marked based on the depth level. A matrix is instantiated alongside this grid map for the checking of potential sites. A rule-based 3x3 window is designed for use in the scans. Figure 2(a) shows how the internal cuboid provides a ‘starting plane’ for internal-to-external voxel layering with the color map for the arrow-designated face presented in Figure 2(b). The matrix for the color map is given in Figure 3 – all 0s represent blank spaces, 1 for the deepest levels, 2 for a level higher and so on.

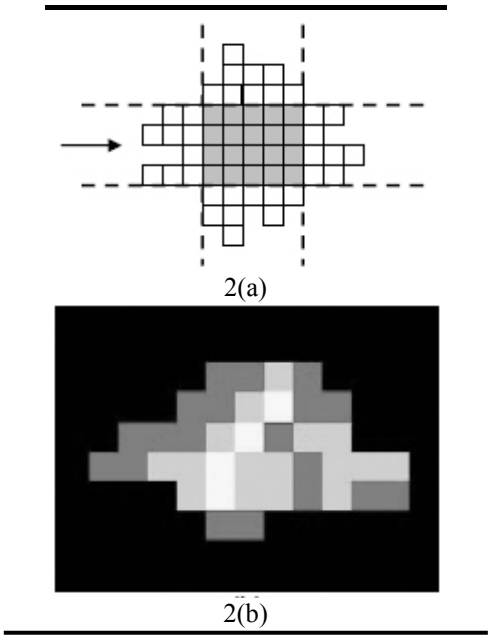

2(a)

2(b)

Figure 2. (a) The cuboid acting as a starting plane for internal-to-external visualisation of the voxels for all faces. (b) The color-map projection of the tessellated protein from the view specified by the arrow in (a). Different colors indicate different depth levels. The image has been converted to grayscale.

0	0	0	0	0	0	0	0	0	0	0	0	0
0	0	0	0	0	0	0	0	0	0	0	0	0
0	0	0	0	0	1	1	2	1	0	0	0	0
0	0	0	0	1	1	2	3	1	1	0	0	0
0	0	1	1	1	2	3	1	2	2	0	0	0
0	1	1	2	2	3	2	2	1	2	2	2	0
0	0	0	0	2	3	2	2	1	2	1	1	0
0	0	0	0	0	1	1	0	0	0	0	0	0
0	0	0	0	0	0	0	0	0	0	0	0	0
0	0	0	0	0	0	0	0	0	0	0	0	0

Figure 3. The resulting matrix for the color-map presented in Fig. 2(b).

The 3x3 window is then used to filter the matrix for the sites. The purpose of this matrix is to reduce the computation time of processing a face from the voxel. Scanning of the color-map takes longer time as each voxel has 1600 pixels (40x40) and there are many voxels in a face. With the use of a matrix the computation time is effectively reduced – only an integer array of NxN dimensions is involved. This is many times faster than processing of the color-map. The filter-window is dependent on the threshold value defined by the user. In most cases a value equivalent to the average of all depth levels suffices. However should the user wished to obtain a larger or smaller model of the dock site, the threshold value may be adjusted accordingly.

The final step in the process is to check all surface atoms against the selected range of dock site voxels. The atoms are shortlisted if they are found to be partially or wholly contained within the voxels. A list of residues associated with the identified atoms is compiled and compared against visualisations from the RCSB PDB and for the case of protein 1FKF, comparisons are made against both the documented wet lab and geometric hashing results.

RESULTS

The results obtained for this study are divided into two sections. The first section presents the output for the FK506-bound proteins, with extra comparisons carried out for the protein 1FKF to published results, and the second section gives the output for the heme-bound proteins. The identified sites of each protein is presented in image-form and compared to screenshots from the RCSB PDB. Note that all screen shots from the PDB include solvent molecules whereas these molecules have been omitted in the implementation.

(A) FK506-Bound Proteins

Protein 1FKF

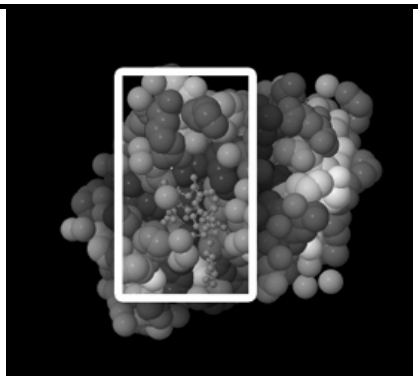

(a)

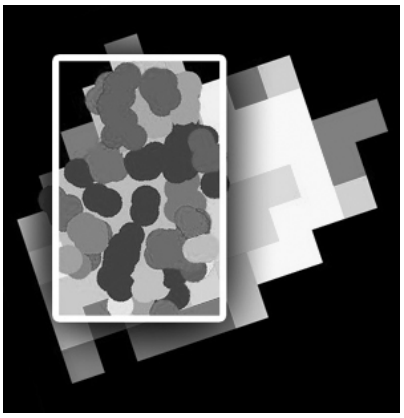

(b)

Figure 4. Protein 1FKF. (a) Visualisation from RCSB PDB. (b) Dock site identification from voxel-based integrated approach.

Table 1. Comparison of extracted residues from a wet lab experimentation, a geometric hashing-based approach and the implemented method for protein 1FKF.

	Residue	WL*	GH**	Voxel
1	TYR26	Y	Y	Y
2	PHE36	Y	Y	Y
3	PHE46	Y	Y	Y
4	VAL55	Y	Y	Y
5	ILE56	Y	Y	Y
6	ARG57	-	Y	Y
7	TRP59	Y	Y	Y
8	ALA81	Y	Y	Y
9	TYR82	Y	Y	Y
10	PHE99	Y	Y	Y
11	ASP37	Y	-	Y
12	ARG42	Y	-	Y
13	GLU54	Y	-	Y
14	HIS87	Y	-	Y
15	ILE91	Y	-	Y

* WH – Wet Lab
** GH – Geometric Hashing

Based on the results from the table it can be seen that the integrated voxel-based method correctly extracts all the residues involved in the binding site. However the number of excess residues obtained is high as well – although this can be considered a small problem as there are bound to be atoms from unconcerned residues contained within the identified dock site voxels. This is a compromise that has to be made due to the use of a lower level representation of the protein in voxel units. the excess residues are listed as ILE90, TYR80, PRO45, ASP79, ARG40, GLN53, PRO78, ASP41, PHE48, ASN43, GLY58, SER39, GLY83, LYS44, PRO88, HIS25 and LYS47.

Protein 1BKF

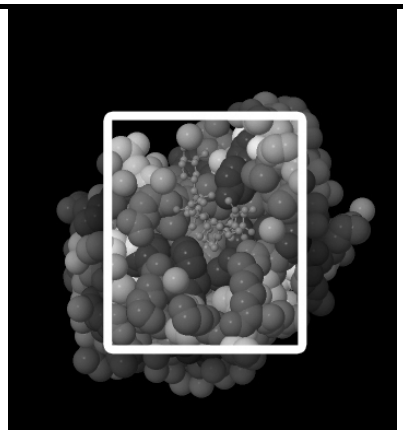

(a)

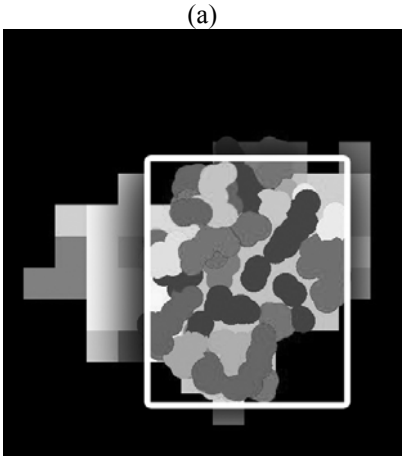

(b)

Figure 5. Protein 1BKF. (a) Visualisation from RCSB PDB. (b) Dock site identification from voxel-based integrated approach.

Protein 1YAT

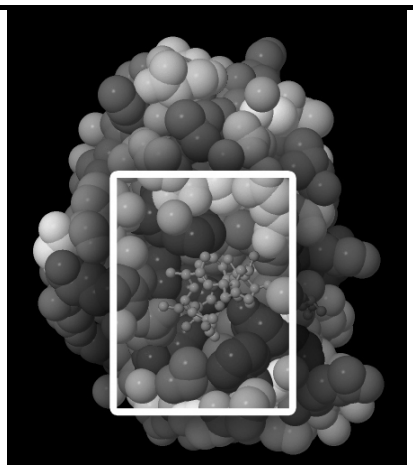

(a)

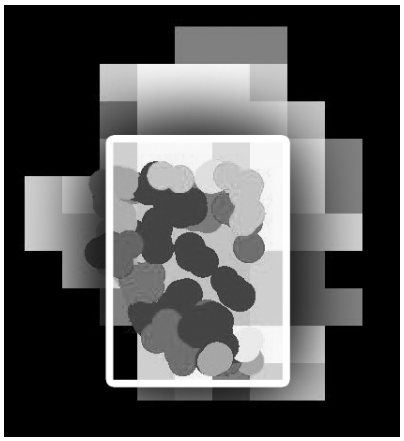

(b)

Figure 6. Protein 1YAT. (a) Visualisation from RCSB PDB. (b) Dock site identification from voxel-based integrated approach.

(B) Heme-Bound Proteins

Protein 4HHB

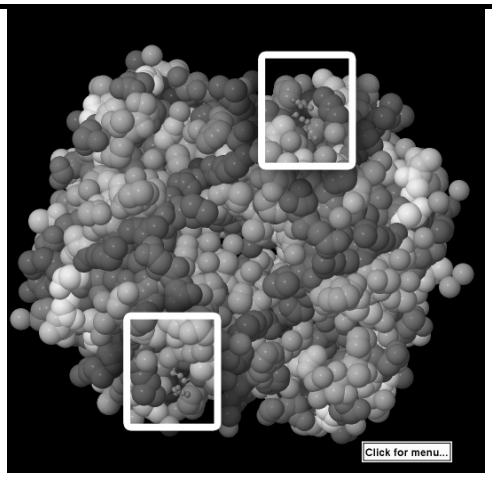

(a)

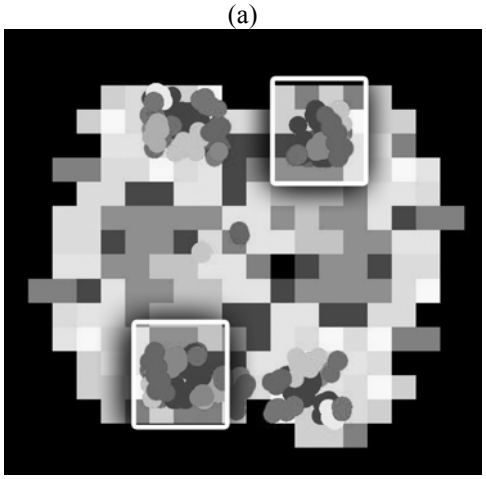

(b)

Figure 7. Protein 4HHB. (a) Visualisation from RCSB PDB. (b) Dock site identification from voxel-based integrated approach.

Protein 4MBN

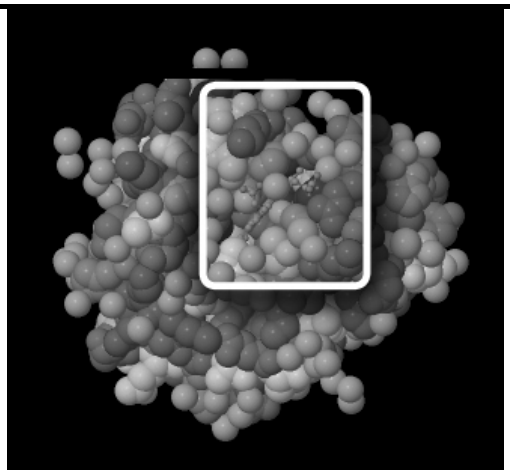

(a)

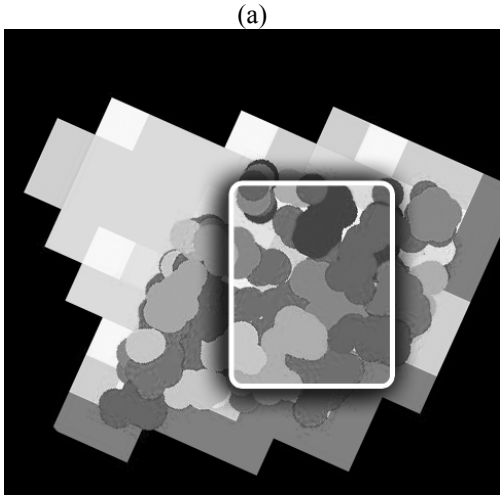

(b)

Figure 8. Protein 4MBN. (a) Visualisation from RCSB PDB. (b) Dock site identification from voxel-based integrated approach.

DISCUSSION

The results reported above show that a voxel-based approach integrated with some visuals understanding is capable of identifying potential dock sites on the surfaces of proteins. The algorithm correctly identifies the residues contributing to the dock site, and is reasonably efficient computationally. A protein with ready datasets of surface voxels and atoms requires approximately 10 seconds of processing time on a standard PC to identify and output potential dock sites from all 6 viewing platforms, although the time is largely dependent on the size of the protein as well. The areas and depth of all 6 faces are contributing factors to the computational complexity of the method. A larger and deeper area results in a higher number of voxels being processed starting with the identification and arrangement of the voxels in generating the levels and color-map to the filtering of the corresponding matrix in the search for potential regions. As the matrix is composed of a set of numbers therefore the filtering process is fast with a complexity of O(n).

However as with most algorithms the method has its limitations as well. The algorithm works well when potential binding sites are located parallel to any of the 6 faces of the voxel. The contradiction comes in the form of a site located on any edge and is split between any two (or more) faces. This calls for further enhancements for tackling of such issues.

The proposed method is simple to implement and is effective in identifying potential dock sites. Due to the representations of the protein in voxels terms which effectively reduces the resolution, the probability of each voxel containing atoms belonging to several residues is high. This explains the excess residues obtained from the identified dock sites for the proteins, and is listed in comparison for protein 1FKF. Despite that the excess residues are mostly neighbouring entries which help indicate the location of the site of interest although they do not contribute directly to the site.

CONCLUSION

An integrated approach based on a voxelisation method equipped with understanding of visuals is presented here for the identification and modeling of potential dock sites on proteins. The experiment was carried out on 2 sets of proteins (FK506-bound proteins and heme-bound proteins) with the dock sites correctly identified. Compilation of the list of residues for the site of protein 1FKF showed successful extractions comparable to both the wet-lab and geometric hashing approaches. Dock sites were identified using a 'depth-level' scanning with potential regions targeted at areas having lowest numbers. Once all site-related voxels have been identified, the algorithm lists all atoms and residues associated with the site. Although excess extractions were obtained, the method remains a promising solution based on the quality of the results obtained.

REFERENCES

Bogan, A.A., Thorn, K.S. (1998) "Anatomy of Hot Spots in Protein Surfaces." J. Mol. Biol. 280, 1 – 9.

Chakrabati, P., Janin, J. (2002) "Dissecting Protein-Protein Recognition Sites." Proteins 47, 334 – 343.

Cheng, R., Weng, Z. (2003) "A Novel Shape Complementarity Scoring Function for Protein-Protein Docking" Proteins 51, 397 – 408.

Fernandez-Recio, J., Totrov, M., Skorodumov, C., Abagyan, R. (2005) "Optimal Docking Area: A New Method for Predicting Protein-Protein Interaction Sites." Proteins 58, 134 – 143.

Fisher, D., Norel, R., Wolfson, H., Nussinov, R. (1993) "Surface Motifs by A Computer Vision Technique: Searches, Detections, and Implications for Protein-Ligand Recogniton." Proteins 16, 278 – 292.

Hendlich, M., Rippmann, F., Barnickel, G. (1997) "LIGSITE: Automatic and Efficient Detection of Potential Small Molecule-Binding Sites in Proteins." J. Mol. Graph. Model. 15, 359 – 363.

Jones, J., Thornton, J.M. (1997) "Analysis of Protein-Protein Interaction Sites using Surface Patches." J. Mol. Biol. 272, 121 – 132.

Kellenberger, E., Rodrigo, J., Muller, P., Rognan, D. (2004) "Comparative Evaluation of Eight Docking Tools for Docking and Virtual Screening Accuracy" Proteins 57, 225 – 242.

Kinnings, S.L., Jackson, R.M. (2009) "Binding Site Similarity Analysis for the Functional Classification of the Protein Kinase Family." J. Chem. Inf. Model., 49, 318 – 329.

Lee L.W., Bargiela A. (2009) "Space-Partition Based Identification of Protein Docksites." Proceedings of the 23rd European Conference on Modelling and Simulation (ECMS 2009), 848 – 854.

Lee L.W., Bargiela A. (2010) "Statistical Extraction of Protein Surface Atoms based on A Voxelisation Method." Proceedings of the 24th European Conference on Modelling and Simulation (ECMS 2010), 344 – 349.

Levitt, D.G., Banaszak, L.J. (1992) "POCKET: A Computer Graphics Method for Identifying and Displaying Protein Cavities and Their Surrounding Amino Acids." J. Mol. Graph., 10, 229 – 234.

Nayal, M., Honig, B. (2006) "On the Nature of Cavities on Protein Surfaces: Application to the Identification of Drug-Binding Sites." Proteins 63, 892 – 906.

Peters, K.P., Fauck, J., Frommel, C. (1996) "The Automatic Search for Ligand Binding Sites in Proteins of Known Three-Dimensional Structure Using only Geometric Criteria." J. Mol. Bio. 256, 201 – 213.

Weisel, M., Proschak, E., Kriegl, J.M., Schneider, G. (2009) "Form follows Function: Shape Analysis of Protein Cavities for Receptor-based Drug Design" Proteomics 9, 451 – 459.

Van Duyne, G.D., Standaert, R.F., Karplus, P.A., Schreiber, S.L., Clardy, J. (1993) "Atomic Structures of the Human Immunophilin FKBP-12 Complexes with FK506 and Rapamycin." J. Mol. Biol. 229, 105 – 124.

Venkatachalam, C.M., Jiang X., Oldfield, T., Waldman, M. (2003) "LigandFit: A Novel Method for the Shape-Directed Rapid Docking of Ligands to Protein Active Sites" J. Mol. Graph. Model. 21, 289 – 307.

Via A., Ferre F., Brannetti B., Helmer-Citterich M. (2000) "Protein Surface Similarities: A Survey of Methods to Describe and Compare Protein Surfaces." Cell. Mol. Life Sci. 57, 1970-1977.

AUTHOR BIOGRAPHIES

LING WEI LEE was born in Kuala Lumpur and studied at the University of Nottingham Malaysia Campus where she took up Computer Science and obtained her honours degree in 2007. She worked for about a year as an analyst programmer with a local company before deciding to pursue her postgraduate studies. Her current research focuses on the use of multiresolution and computational methods in the area of proteins. She is currently in her final year of completion. She can be reached at leelingwei@yahoo.co.uk.

ANDRZEJ BARGIELA is Professor in the School of Computer Science at the University of Nottingham, UK. He served as Director of the School of Computer Science at the Malaysia Campus of the University of Nottingham from 2007 to 2010. He is currently President of the European Council for Modelling and Simulation and serves as Associate Editor of the IEEE Transactions on Systems Man and Cybernetics and Associate Editor of the Information Sciences. His research involves investigation into Granular Computing, human-centred information processing as a methodological approach to solving large-scale data mining and system complexity problems. He can be reached at Andrzej.Bargiela@nottingham.ac.uk.

Genetic algorithm for process optimization in hospitals

Matthias Kühn
System and Software Engineering
Technical University Ilmenau
Ehrenbergstraße 29,
Ilmenau 98693, Germany
E-Mail: matthias.kuehn@stud.tu-ilmenau.de

Tommy Baumann
Andato GmbH & Co. KG
Ehrenbergstraße 11,
Ilmenau 98693, Germany
E-Mail: tommy.baumann@andato.com

Horst Salzwedel
MLDesign Technologies
2230 Saint Francis Drive
Palo Alto, CA 94303
E-Mail: horst@mldesigner.com

KEYWORDS

Business process, process modeling, process optimization, process simulation, hospital process performance, work flow optimization, hospital logistics, scheduling

ABSTRACT

In 2004 new reimbursement policies for hospitals based on Diagnosis Related Groups (DRGs) were introduced in Germany. These force hospitals to minimize the cost of treatment and improve quality of care, in order to attract more patients and become more competitive. To achieve these goals hospital processes need to be optimized and compared with processes in competing hospitals. Regarding this, the scheduling of patient treatment poses a huge challenge. For purpose of analysis, optimization and validation of hospital processes - especially interaction of processes and effects of interconnection - it is necessary to develop validated and executable models. In (Salzwedel et. al. 2007) the processes of a cancer treatment center were modeled and optimized. This paper describes our developments toward automatically optimizing scheduling of patients, reducing processing time and optimizing resource usage in a cancer center using genetic algorithms.

1. INTRODUCTION

Health care costs in Germany have been rising continuously. They increased by 34.2% to 278.3 billion Euros within 1999 and 2009 and became the highest in Europe (Statistisches Bundesamt 2012). To overcome this problem, in 2004 a new reimbursement system for hospital services based on disease patterns was enacted by the German government. Following these new reimbursement rules, hospitals are no longer reimbursed according to the number of days a patient is cared for, based on Diagnosis Related Groups (DRGs), independent of the actual treatment time. Now hospitals have to reduce processing time and resources for patient treatment, in order to reduce costs. In this context the income of hospitals can be defined as:

Income = (DRG-payment – treatment costs) x number of Patients treated.

If treatment costs are reduced and the number of patients treated is increased, income and profit of hospitals grow. Treatment costs are strongly related to processing time and the number of hospital resources used for treatment. Processing time for patients can be defined as:

Processing time (hospital residence time) = treatment time + waiting time.

Measurement of processing time is a common instrument. By optimizing and reducing processing time, hospital resources can be used to treat more patients and so increase income. The mean hospital residence time in Germany is 20% higher than in comparable European countries (Statistisches Bundesamt 2011). Hence, there is a potential for optimizing processing time to reduce treatment costs.

Kühn showed that scheduling of patient treatment has a large influence on reducing processing time and increasing efficient usage of hospital resources (Kühn 2006). Rixen and Hackl demonstrated that genetic algorithms can optimize complex scheduling problems of production processes (Rixen 1997; Hackl 2000).

This paper describes the application of a genetic algorithm for optimizing patient scheduling processes in hospitals for an example of a cancer treatment center utilizing computer simulation. For modeling, simulation, validation and optimization the SW tool MLDesigner is used (Mission Level Design Inc. 2011). Section 2 points out the benefits of using genetic algorithms instead of other heuristics or other mathematic methods. Section 3 represents the current developments in scheduling patients in hospitals. Section 4 describes the development and structure of the genetic algorithm utilized. Furthermore, this section shows how the algorithm is linked to the model of the cancer treatment center. Section 5 summarizes the results.

Proceedings 26th European Conference on Modelling and Simulation ©ECMS Klaus G. Troitzsch, Michael Möhring, Ulf Lotzmann (Editors)
ISBN: 978-0-9564944-4-3 / ISBN: 978-0-9564944-5-0 (CD)

2. GENETIC ALGORITHM

A genetic algorithm is a modern search algorithm for optimization based on the mechanisms of natural evolution. It avoids getting stuck at a local maximum of a search space and can move very flexibly in it. Genetic algorithms belong to the group of meta heuristics. Heuristics are search methods for approximate solutions. Meta heuristics are generic principles and schemata for diverse, basically unspecified problems. They can optimize complex, non-calculable or non-mathematically describable problems and there aren't any restrictions regarding their target function (Nissen 1997, p.248). Genetic algorithms use nature approved methods – evolution – the creation of individuals that perfectly match their environment. Especially reproduction, mutation, recombination and selection in combination are the natural optimizers (Nissen 1997, p.34 ff.; p.164 ff.).

3. CURRENT STAGE OF DEVELOPEMENT

The use of genetic algorithms for scheduling problems in different practical industrial cases is shown by Rixen (Rixen 1997) and Hackl (Hackl 2000). Furthermore, Werber demonstrates the use of genetic algorithm for optimizing visual data of medical applications in hospitals (Werber 2010).

Concerning the scheduling of patients in hospitals a cooperation of the Fraunhofer Institute and a hospital formed a workgroup for Supply Chain Services (SCS) and made advances in modeling and planning patient flow (Kriegel et. al. 2009). Starting point was the assumption that a patient can be located in a hospital during the entire processing time. Based on this, an algorithm was developed that is able to optimize the status in real time. As a result of this optimization, patients get information on where to go next in the clinic process chain. The developed algorithm is based on software agents, which represent supplier and customer of a service. Market mechanisms were implemented and used to reach an optimum. Expense factors and processing time are set up as target functions (Niemann 2006). The algorithm has been tested against a simulation with real data but not implemented in a real system. A forecast and planning of patient flow up front has also not been carried out. The focus was on optimization of the dynamic and continuously changing system status.

Moreover, an experiment in the use of genetic algorithms for scheduling patients in hospitals was carried out for scheduling surgery. This project was set up with HELIOS Kliniken GmbH to test the usage of genetic algorithm and particle swarm optimization in a clinical environment. Surgery planning was defined as a highly dynamic multi criteria optimization problem. Up to now there has been no follow up on this approach.

4. DEVELOPEMENT OF GENETIC ALGORITHM USED

Starting point was the developed executable model of a cancer treatment center, shown in figure 1 (Kühn 2006, Salzwedel et. al. 2007).

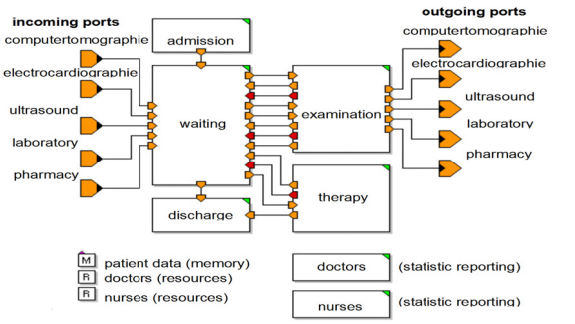

Figure 1: Level 2 Model of cancer treatment center

For purposes of model development and validation real system data were collected. The real data database was split up in two parts. One part was used to develop the simulation model and the other to validate it and to quantify the model error probability. The Model deviation was measured by scheduling time and waiting time for all simulated patients in a defined number of simulation runs. Scheduling time deviated in average -0.7% and waiting time -4.0% compared to the data collected in real system (Kuehn 2006, p.71). Simulation of the existing process clearly shows underutilization of all resources. Analyzing potential improvements showed the greatest potential in scheduling patients based on expected treatment time.

Until now determination of the best scheduling of patient treatment relied just on experience and interpretation of simulation results. This paper shows how a process can be automatically optimized using a genetic algorithm. The development of genetic algorithm and adjustment to the specific problems of a hospital environment is described in the following for an example of a cancer treatment center. Figure 2 shows the general sequence of action for a genetic algorithm.

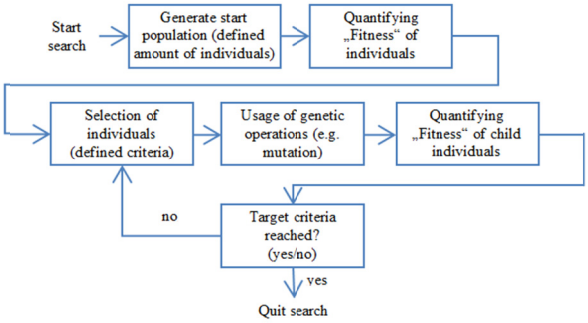

Figure 2: general sequence of action for a genetic algorithm (Pohlheim 2000, p.9)

First, a startup population with a defined number of individuals is generated (parent individuals). In this case 5 individuals are generated randomly. Each individual contains a number of 34 patients with associated treatment plan. This number equals the average of patients treated each day in the cancer center. Every patient has an identification number and an appointment time when he is planned to be treated at the cancer center. In analogy to biology, animals and plants have chromosomes in their cells, which contain genetic material (Gene). Different species can have different numbers of chromosomes. But, for each species the number of chromosomes is the same in every cell. In this example, the cells of each individual contain one chromosome with 34 genes (equals 34 patients). This was implemented as a vector as shown in figure 3.

appointed time	7:30	7:38	7:45	8:14	8:38	9:17 … 11:27	12:17
patient-ID	9	21	33	14	34	10 … 1	34

Figure 3: Layout of an individual

Genes itself contain genetic information (Allele). Within the meaning of optimizing processing time, the appointed time is defined as genetic information. Each gene is labeled with the patient identifier (Patient-ID).

In the next step the fitness function (target function) quantifies the fitness of each parent individual. Therefore every individual is sent through the simulation model of the cancer center. At the end, key properties for each individual are calculated, such as total processing time of the patients and average waiting time per patient. To compare the individuals the fitness function was designed to calculate a benchmark value for each individual. The result is a fitness value for the quality of each individual in order to reduce the processing time and the waiting time of patients. In every fitness test, the best fitness value computed at that time is compared with the current fitness value. If the current fitness value is better than the values reached, the individual and the current fitness value are saved in a file as shown in figure 6.

The fitness function is designed as follows:

Collection of required data

- Calculation of accumulated waiting time of all patients of an individual: (begin taking blood sample – end of admission) + (begin of examination – end of taking blood sample) + (begin of therapy – end of examination) + (discharge – end of therapy is calculated).
- Calculation of accumulated processing time of all patients of an individual: discharge – arrival time is calculated.
- Calculation of processing time fitness:
  (1000 - accumulated processing time / number of patients) / 1000
- Calculation of waiting time fitness:
  (500 - accumulated waiting time / number of patients) / 500)

Calculation of individual fitness

- Calculation fitness of an individual: processing time fitness x processing time loading (= 0.5) + waiting time fitness x waiting time loading (= 0.5)
- If discharging last patient of the individual is at a simulation time (minutes passed from opening of cancer center) less than 250 the fitness value is set to 0.
- If discharging last patient of an individual is at a simulation time greater than 540 the fitness value is multiplied by 0.1.

So fitness values can be between 0 and 1. Best individual values between 0.45 and 0.87 were documented.

Following the general sequence in Figure 2, the next step is to select parent individuals based on their fitness value (Selection). One child is generated out of two parent individuals. Selection is a genetic operator, which controls the search direction in the search room. It determines which parents can pass their genetic attributes to a child. Individuals with better genetic material (higher fitness value) are more likely selected. During several iterations, the children population converges to an optimum. To prevent stagnation at a local optimum, it is important to keep population variety sufficient and genetic material diverse. Therefore, parent individuals with low fitness value also need to be selectable. This keeps the population "alive".
In our algorithm, this is realized through normalization of fitness values of each individual of a parent population. Based on this, individuals are selected randomly. Thus, individuals with high fitness are more likely selected and individuals with low fitness can also be selected.

Furthermore, a parent individual can be used as child individual without any genetic changes. In the current case this is related to the so called "Reproduction". Reproduction rate defines the likelihood that a parent individual is used as child individual.

In addition, children individuals can be an output of a genetic operator "Recombination". Within evolution theory Recombination (Crossover) of genetic information is located between Selection and Mutation regarding to its contribution to achieving the optimum. Recombination means exchanging selected genes of two individuals. Thus genetic information is being passed. In order to do this, a crossover point for both individuals is selected randomly, as shown in figure 4a (vertical line). At the selected point the parent individuals are split into two parts.

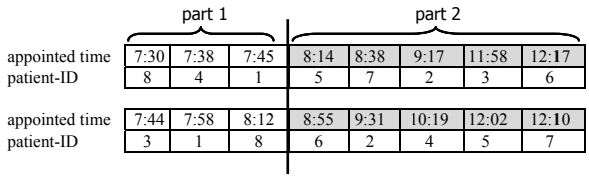

Figure 4a: Genetic operation ”Crossover“ - parents

Crossover here relates to alleles (appointed time). Thus the areas to the right of the vertical line of each parent individual are exchanged. The grey marked areas are the areas of exchange. Out of these two child individuals are formed as shown in figure 4b. This form of Crossover is called “Shuffle Crossover” (Nissen 1997, p. 54-56). One outcome can be that the appointed time of two patients is the same after crossover. For example the appointed time of Patient 1 and Patient 3 is 8:12 a.m. This is the case when two or more patients arrive at the same time in a clinic or the appointed time is the same, because of different treatments.

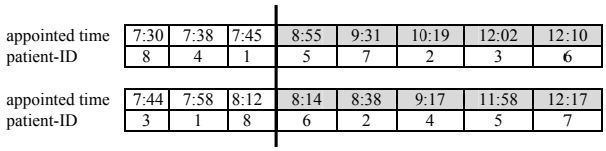

Figure 4b: Genetic operation ”Crossover“ - children

Mutation, which is used as third genetic operator, is an undirected process. It is used to get new genetic information. Totally new individuals can be created, which Crossover can’t provide. This causes the population variety to increase. New variants and so eventually better individuals and better solutions for the focused problem are possible, which may otherwise never come out of existing populations. This method is also used to overcome local maxima and prevent a stop in a search for a maximum, like it is the case in “Hillclimbing“ (Gerdes et. al. 2004, p.25).
For the example of a cancer center, mutation means: A randomly selected new value between opening hours and closing time of the cancer center is set as new appointed time for an patient of an individual, as shown in figure 5.

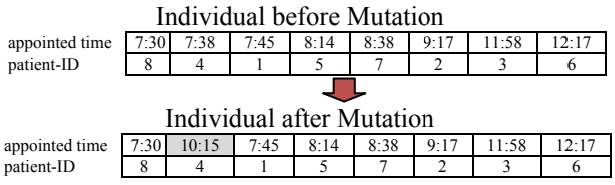

Figure 5: Genetic operation „Mutation“

The grey marked area with value of 10:15 a.m. is set as the new appointed time instead of 7:38 as it was before.

So far, several genetic operations are mentioned. Each operation has its own variable that can be changed by a user and gives an input to the model regarding its likeliness to be processed. For the optimization of the cancer center, the following probabilities produced the best optimization results:

- Crossover: 0.3
- Reproduction: 0.7
- Mutation: 0.4

This looks like a high mutation rate. However, only one gene is mutated in this case. This is necessary to produce new appointed times of patients and achieve the necessary flexibility of the algorithm.

After all child individuals have been generated, they are rated by the fitness function, as described before.
The simulation loop will be executed until an exit criteria is reached. This can be a number of loops, elapsed time or a specific value of fitness. In our example the simulation time is limited to 12 hours (overnight run). In this timeframe more than 1000000 loops where done in each run.

The optimization loop, the data link for interaction between genetic algorithm and the model of the cancer center are shown in figure 6.

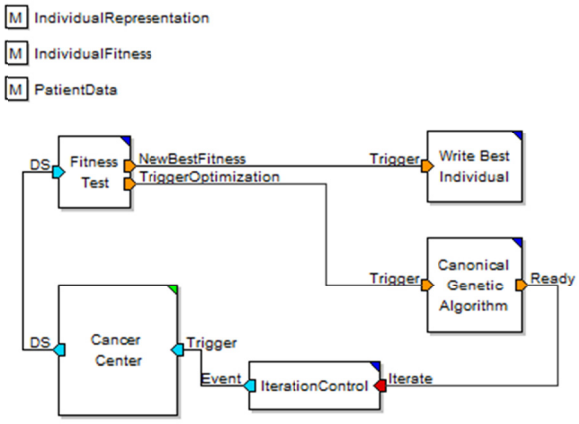

Figure 6: Optimization loop

By doing so the hospital process model becomes a component of this new model as well as the optimization algorithm and fitness function.

5. SUMMARY AND OUTLOOK

It was shown how genetic algorithms can be applied to optimize processes in hospitals. For an example of a cancer treatment center the waiting time was reduced up to 40%. By analyzing the simulation results, a group of patients was identified and summoned in order to be treated at early opening hours of the cancer center. For another group of patients the optimization model planned the treatment between the times of 11:00 a.m. and 01:30 p.m. In addition this group was planned in remaining time slots in the morning until 11:00 a.m. This automated optimization utilizing genetic algorithms confirmed the results in (Kühn 2006) made by expert analysis of simulation results. Thus the applicability of genetic algorithms for optimization of hospital processes could be validated. The optimization results were translated into handling instructions for the cancer center and realized in daily work. These handling instructions lead to nearly equivalent results in practical use as simulated in advance. Currently, this work is extended to scheduling of patients in multi department hospital processes.

REFERENCES

Gerdes, I., Klawonn, F., Kruse, R.: Evolutionäre Algorithmen: Genetische Algorithmen - Strategien und Optimierungsverfahren – Beispielanwendungen, 2004.

Hackl, R.: Optimierung von Reihenfolgeproblemen mit Hilfe Genetischer Algorithmen, Dissertation, Regensburg 2000.

Kriegel, J., Jehle, F., Seitz, M.: Arbeitsgruppe für Supply Chain Services SCS: Der schnelle Patient - Innovationen für die Patientenlogistik in Krankenhäusern, Stuttgart 2009.

Kühn, M.: Simulation und Optimierung einer Tagesklinik - Simulationsstudie mit dem MLDesigner -, Diplomarbeit, Ilmenau 2006, URL: http://www.tu-ilmenau.de/fakia/fileadmin/template/startIA/sst/Diplomarbeiten/2006/Diplom2006_MatthiasKuehn.pdf.

Mission Level Design Inc.: User's Manual, URL: http://www.mldesigner.com, 2011.

Niemann, C.: Softwareagenten in der Krankenhauslogistik - Ein Ansatz zur effizienten Ressourcenallokation (mit Torsten Eymann), in: HMD - Praxis der Wirtschaftsinformatik, Nr. 251, dpunkt Verlag, Heidelberg 2006.

Nissen, V.: Einführung in evolutionäre Algorithmen: Optimierung nach dem Vorbild der Evolution, Braunschweig, Wiesbaden 1997.

Pohlheim, H.: Evolutionäre Algorithmen – Verfahren, Operatoren und Hinweise für die Praxis, Berlin u.a. 2000.

Rixen, I.: Maschinenbelegungsplanung mit Evolutionären Algorithmen, Wiesbaden 1997.

Salzwedel, H., Richter, F., Kühn, M.: Standardized Modeling and Simulation of Hospital Processes - Optimization of Cancer Treatment Center at International Conference on Health Sciences Simulation, HSS '07, 14.-18. January 2007, San Diego, California. URL: http://wcms1.rz.tu-ilmenau.de/fakia/fileadmin/template/startIA/sst/Veroffentlichungen/2007/HospitalOptimization_HSS2007.pdf.

Statistisches Bundesamt, call of website: 05.06.2011, URL: http://www.gbe-bund.de/gbe10/ergebnisse.prc_tab?fid=9144&suchstring=Gesundheitsausgaben&query_id=&sprache=D&fund_typ=TAB&methode=2&vt=1&verwandte=1&page_ret=0&seite=&p_lfd_nr=6&p_news=&p_sprachkz=D&p_uid=gast&p_aid=11039905&hlp_nr=3&p_janein=J.

Statistisches Bundesamt, call of website 17.01.2012, URL: http://www.gbe-bund.de/oowa921-install/servlet/oowa/aw92/dboowasys921.xwdevkit/xwd_init?gbe.isgbetol/xs_start_neu/&p_aid=i&p_aid=93552860&nummer=322&p_sprache=D&p_indsp=-&p_aid=41989013.

Werber, A.: Optimierung medizinischer Bilddatensätze mittels eines iterativen Verfahrens auf Basis genetischer Algorithmen, Dissertation, Universität Freiburg 2010.

AUTHOR BIOGRAPHIES

MATTHIAS KÜHN graduated in Business Informatics at the Technical University of Ilmenau, where he obtained his degree in 2006. He gained experiences at Dräger Medical (Germany, USA) and several projects in hospitals. He started as doctoral student in 2007 at the Technical Univeristy of Ilmenau. His e-mail address is: matthias.kuehn@stud.tu-ilmenau.de

TOMMY BAUMANN studied computer sciences at Technical University of Ilmenau and obtained his degree in 2004. Afterwards he became a doctoral student at Technical University of Ilmenau and Stanford University. In 2009 he completed his doctoral thesis on automation of early design stages of distributed systems. Today he is managing director of the software development company Andato, specialized in the development of customized modeling and simulation solutions. His e-mail address is tommy.baumann@andato.com.

HORST SALZWEDEL received his Diploma from Technical University Munich and got his Ph.D. in Aeronautical and Astronautical Sciences from Stanford University. From 1978 to 1992 he was Senior Scientist at Science Applications International (SAIC) and Professor at Stanford University. From 1992 to 2001 he was Senior Architect in system design at Cadence Design Systems. Since 2001 he has been CTO at MLDesign Technologies and Prof. in System Design at Technical University Ilmenau. His research concentrates on development of methods and tools for complex system developments. His e-mail address is horst@mldesigner.com

ADDER: A PROPOSAL FOR AN IMPROVED MODEL FOR STUDYING TECHNOLOGICAL EVOLUTION

Janne M. Korhonen and Julia Kasmire

School of Economics / Aalto Design Factory and TU Delft Faculty of Technology, Policy and Management

Betonimiehenkuja 5, 02150 Espoo, Finland and Jaffalaan 5, 2628BX, Delft, The Netherlands

E-mail: janne.m.korhonen@aalto.fi and j.kasmire@tudelft.nl

ABSTRACT

Computer simulations are increasingly used to study the development, adoption, and evolution of technologies. However, existing models suffer from various drawbacks that may not be easily corrected, among them lack of internal structure in technologies, static environments and practical difficulties of introducing rational or semi-rational search for solutions. This paper discusses the theoretical background and rationale for an improved model, the Adder, and sketches out the model's main features.

INTRODUCTION

For the last two decades, researchers studying various aspects of change and evolution in organizations, strategy and technology have increasingly turned to computer simulations to better understand the dynamic and often complex interactions that are inherent in their fields of study. Much of this research has been undertaken using only few basic types of simulation models, resulting to the emergence of "dominant designs" that effectually serve as benchmarks against which novel contributions are evaluated. In particular, the NK and percolation frameworks have seen broad use in the social sciences, with a number of papers appearing in top journals over the last 15 years (e.g. Levinthal 1997, Frenken, 2001, 2006; Auerswald et al, 2000; Ethiraj and Levinthal, 2004; Rivkin 2000; Almirall and Casadesus-Masanell, 2010).

Although these model frameworks continue to be useful, they also suffer from certain limitations. First, NK and percolation frameworks have difficulties simulating endogenous situations, i.e. where attributes of solution space change over time (Ganco and Hoetker 2009).

Second, they ignore the internal structure of technologies. Although many authors who have used simulations to study technological evolution (such as Murmann and Frenken 2006 and Frenken 2006) do specifically argue that technologies have a hierarchical structure and consist of systems, subsystems and sub-subsystems (etc.), the current models do not easily allow for this. Thus, individual technologies are independent of each other, instead of existing in an interdependent ecosystem of combinatory possibility. Furthermore, the lack of internal structure makes the improvement of existing technologies through improvements in their components - a feature visible in any case study of technology - clearly impossible.

Third, introducing more rational or goal-seeking behavior is difficult in the existing models. While implementing advanced AI algorithms to search for solutions in the NK solution space or within percolation lattice is certainly possible, programming these algorithms is non-trivial for most researchers. Furthermore, complex AI algorithms pose their own challenges when applied to models that are intended to be simple and easily understandable “toy models” of innovation and technological change.

These limitations are particularly visible when the goal is to model a co-evolutionary system that evolves on several different levels simultaneously, a system whose complexity changes over time, or the influence of more or less rational actors. Obviously, these types of systems are of interest to many researchers from fields such as organization science, studies of science and technology, or management of innovations, to name just a few. Developing model frameworks that answer better to their requirements thus remains a challenge for simulation community.

Proceedings 26th European Conference on Modelling and Simulation ©ECMS Klaus G. Troitzsch, Michael Möhring, Ulf Lotzmann (Editors)
ISBN: 978-0-9564944-4-3 / ISBN: 978-0-9564944-5-0 (CD)

THEORETICAL BACKGROUND

The notion that technologies "evolve" is not new. For example, Basalla's seminal work (1989) notes that the earliest attempts linking technology and evolution explicitly date from the 19th century. In addition to Basalla's work, the evolutionary processes have been explored by authors such as Frenken (2001, 2006) and Arthur (2009). All broadly agree that while technologies exhibit evolutionary features, strict 1:1 mapping of biological metaphors to technological evolution is not appropriate. Instead, technological evolution should be understood as an instance of "Universal Darwinism" (UD) as introduced by Dennett (1995). In principle, UD states anything that displays variation, selection and heredity will evolve through natural selection, whether or not it would be classified as "alive" in any traditional sense. This universal definition of evolution does not specify *how* variation, selection and heredity work; the sources of variation and the mechanisms of selection may result either from unconscious environmental pressures and random events, or from deliberate "tinkering" and rational selection. Similarly, heredity can operate through biological mechanisms such as DNA, or it can operate through information codified in drawings, patents, and operating manuals. In fact, all technologies are seen to descend in some way from technologies that preceded them (Arthur 2009:18).

However, Arthur (2009) emphasizes the need to consider *combinatorial evolution,* where novel technologies can arise by combination of existing technologies, in addition to incremental change. He finds this particularly useful when explaining developments such as jet engines or radar, that appear to be radical departures from the existing technologies (Arthur 2009:17). Arthur proposes a mechanism of *combinatorial evolution* where novel technologies can arise by combination of existing technologies. Combinatorial evolution (CE) does not abandon incremental variation, selection and retention: it acknowledges that these, too, have an important role to play. Rather, CE proposes an additional mechanism to explain how radical departures from existing technology might happen.

The idea of technologies being recombinations of existing technologies has been long accepted by scholars such as Gilfillan (1935), Schumpeter (1939), and Usher (1954), among others, who describe production or inventions as combinations of materials and forces (Schumpeter) or "new combinations of prior art" (Gilfillan). In Arthur's formulation, a CE mechanism for the evolution of technology would work as follows (Arthur 2009:21-24):

1. Early technologies form using existing primitive technologies as components.

2. These new technologies in time become possible components, or building blocks, for the construction of further new technologies.

3. This implies that technologies have an internal structure, a hierarchy of subsystems and sub-subsystems.

4. The complex technologies form using simpler ones as components.

5. The overall collection of technologies bootstraps itself upward from the few to the many and from the simple to the complex.

Furthermore, it is notable that few modelers have tried to test alternative assumptions of rationality, preferring to assume relatively myopic search (taking into account only one decision at any given time) in the technology landscape. However, solution search by humans is usually assumed to have some overarching direction, even though it is clearly "boundedly rational" (e.g. Simon 1982). I therefore argue that any model of technological evolution should accommodate both essentially random events - "mutations" - and non-random, somewhat directed but boundedly rational search for new technologies. Thus,

6. The evolution of technology happens both as a result of essentially random events and boundedly rational search for and evaluation of new solutions.

It should be noted that most scholars of technology are in a broad agreement that "technologies" should be understood to mean not just material artefacts, but also nonmaterial methods, processes and devices that are means to fulfill a human purpose (e.g. Arthur 2009:28). This broader definition of technology thus includes fields such as management practices and strategies.

TOWARDS A BETTER MODEL: THE "ADDER" SUGGESTION

Given the drawbacks of the NK and percolation models, some scholars have introduced alternative models of technological evolution. Of particular interest is a model introduced by Arthur and Polak (2006) and latter used by Arthur (2007, 2009) to illustrate his formulation of the CE framework, as well as by scholars from other fields (e.g. White 2008). In their model, technological build-out begins from simple "primitive" technologies. These technologies are randomly combined to result to more complex technologies, which themselves are then potential components in future technologies. The system includes concrete needs instead of abstract fitness values, and technologies that better satisfy these needs or have fewer components - i.e. are cheaper - than their alternatives supersede older technologies.

The model is implemented using simple logic circuits (NAND gates in the most common version) as

primitive technologies. Needs include simple logical functions, such as 2-bit adders. New technologies are evaluated against how closely they fulfill a need's truth table, and how few primitive components they use in doing so.

This model successfully captures the interlinked build-out of technologies from simpler components, and replicates stylized facts such as avalanches of "creative destruction" when a significant innovation suddenly makes obsolete many old technologies. However, the model is still relatively fixed, with no easy way to add many more needs than simple logical functions (e.g. NOT, IMPLY, *n*-way-or, 2-bit adder, 8-bit adder and so on) present in the original implementation. This limitation creates difficulties for studying settings where more or less every technology might fulfill *some* need.

In addition, introducing bounded rationality is – again – difficult. As a result, even Arthur and Polak (2006) are reduced to arguing that their model of random combinations *can* be representative of search through solution space, given certain assumptions. While this may be true, one would very much like to test how the assumption affects this otherwise excellent model.

A possible solution is the Adder model detailed in this paper. The Adder simplifies Arthur and Polak's model by replacing logic circuits and Boolean arithmetic with real numbers and arithmetical expressions. Each experiment starts with elementary components (primitives) and arithmetical operators, usually with number 1 and operators plus (+) and minus (-).

During each time step of the experiment, developer agent(s) alter existing "technologies" by adding or removing components, hence the name of the model. The resultant technologies are then evaluated against goals and added to the repertoire of possible components. The objective of the system is to satisfy a certain set of needs or goals, expressed as real numbers. These needs can be thought to represent the needs that drive technology evolution, and as simplifications of logical operator needs used by Arthur and Polak (2006). The numbers can be either drawn randomly or according to some distribution pattern. Compared to a relatively fixed set of goals in the original model, this allows for certain flexibility in studying different technological landscapes (some landscapes might have feasible technologies more clustered in design space than others, for example).

As an example, let us assume that one of the goals is "10," that this is the first step and therefore the available component is "1" and operators plus and minus, and that the selected method of alteration is random draw of 0 to 12 components and operators. A possible draw could be

$$1+1-1+1+1-1+1+1 \qquad (1)$$

"producing" the value "4." Although this technology did not fulfil the goal in itself, it is now added to the repertoire of possible components and is therefore available for use in the next step. Suppose that the next draw gets the components

$$-4-1-1+4+4+4 \qquad (2)$$

that produce "10" and thus satisfy the first goal. The process continues until desired set of conditions is reached, for example, when all the goals are satisfied or the simulation has progressed for a predetermined time.

Evaluation by Cost and Fitness

The "goodness" or "fitness" of these technologies can be evaluated in a variety of ways, depending on the requirement of particular experiment.

One important evaluation criteria is the "cost" of the technology. In its simplest form, the cost is determined by counting the number of primitive elements required for the technology. To continue the above example, the primitive components (1's) have a cost of 1. Component technologies, such as technology "4" above, have a cost equal to the cost of primitives within it. Thus, the above technology "4" would cost 8.

It is evident that such costing schemes neatly capture one of the important mechanisms in the evolution of technologies: that many technologies, when first developed, are very expensive, but become cheaper as R&D efforts are made towards improving the efficiency and manufacturing processes, for example. The "technologies" encapsulated in the model can be thought of as simplified idealisations of production recipes or assembly instructions, subject to improvements as more streamlined processes are found.

For example, the technology "4" in the model could be superseded by several generations of more efficient technologies, with the ultimate limit of efficiency being

$$1+1+1+1 \qquad (3)$$

with a cost of 4. Determining the efficiency limits and the most efficient technology possible is always trivial (i.e. when Cost = Product).

Another possible evaluation criteria is the fitness-for-purpose, that is, how close the technology gets to the target. For example, the model may accept only those new technologies that are either i) closer to the target value than existing technologies or ii) cheaper than existing technologies.

Obsoleted Technologies

The Adder can model the obsolescence of technologies through basic mechanisms described above. If a new technology proves to be either fitter or

cheaper than existing technologies, it takes their place in the repertoire of technologies that are used as a pool of possible components in the future. If the new technology is simply a cheaper version of already existing technology, the technologies currently using the old version are updated. As their costs are updated in turn, it is possible that a development of a new component triggers an avalanche of replacements. The size-frequency distribution of these avalanches (see Fig. 1) shows hints of power law distribution, indicative of self-organized criticality (Pak and Wiesenfeld 1988)

This obsolescence does not, however, necessarily obsolete other technologies that are already using the now-obsoleted technology. This allows for "legacy" technologies, where otherwise obsoleted components remain in use as parts of older systems. As an example, suppose that a target "10" is reached, while there exist technologies that use the tech 9 as a component. Although future technologies will not use tech 9 any longer, any technologies that have tech 9 as a component will retain it. It is even possible that tech 9 is incrementally developed towards a cheaper version, resulting to decreased costs for technologies that use it.

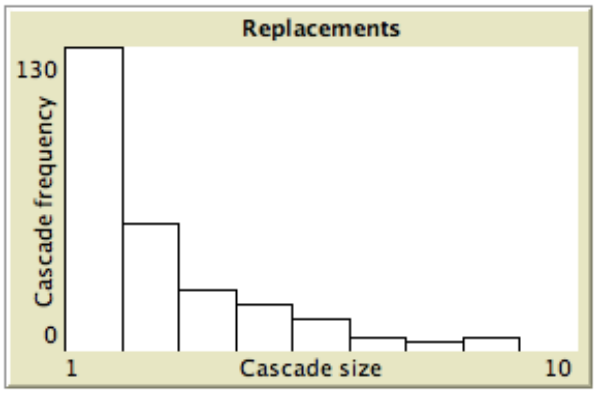

Figure 1: Sample Distribution of "Replacement Cascades"

Bounded Rationality

It is easy to see that implementing even fully rational agents is nearly trivial in this model. For example, it's easy to have the agents determine the optimum components they'd need in order to reach a certain target. One can easily go further and implement bounded rationality (Simon 1982) by e.g. introducing random uncertainty into the calculation. Thus, studying the effects of bounded rationality in the product development process becomes possible.

Tuneable Difficulty of Search

The description above assumes that all technologies – all real numbers - are possible. This, however, is hardly the case in reality: one can imagine products such as chocolate coffee pots that may be feasible, but unviable.

A simple way of tuning the difficulty of the search in this landscape is the addition of "anti-targets" or "valleys." These are simply numbers that are either not allowed or that incur some kind of a penalty. The density of these anti-targets can be easily adjusted, and thus different technological landscapes can be explored using the Adder model. It should be noted that these anti-targets correspond roughly to sites that are impossible to realize in the lattice percolation model described above.

An example of how the density of targets and anti-targets may be used to tune the difficulty of search for new technologies is shown below in Figure 2, where the y axis reports the highest technology reached at the moment of time.

Keystone technologies

Key variables of the model – the density and spread of targets and anti-targets – can be set to replicate an important finding of Arthur and Polak's model, namely, that without early low-level needs, more advanced needs are difficult or impossible to satisfy. In other words, certain technologies may serve as "keystone" technologies, enabling further technological development. However, as the Adder is far more tuneable than the original, I have also found that these results depend on the setting of the variables in question. If (nearly) all technologies are feasible (no anti-targets), the lack of early needs does not stop the progress towards more complex technologies.

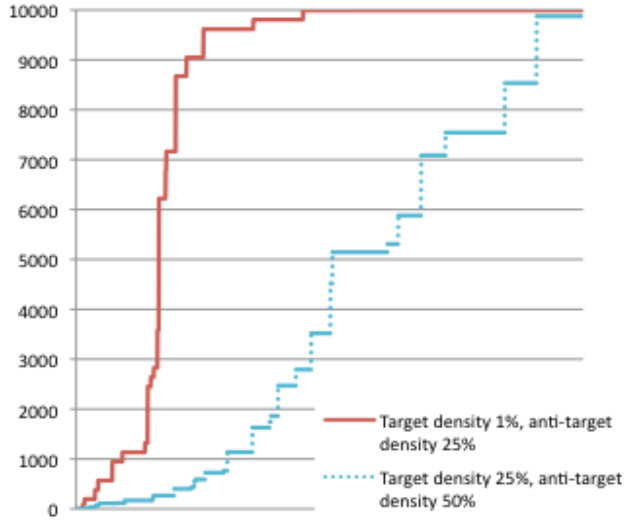

Figure 2: Differences in Performance With Two Different Target/Valley Ratios'

Incremental versus Radical Innovation

The Adder can be used to model either incremental improvement of existing technologies or radical departures from the existing state-of-the-art, or both at the same time. Both incremental and radical improvement may take place by either randomly redrawing components and operators for existing technologies, or by more "rational" methods.

Multi-agent Industrial Ecosystems

The Adder can serve as a basis for a multi-agent simulation where agents have different search strategies. An industrial ecosystem can be modelled in this manner; for example, the Adder can model the division of labour between component producers and original design manufacturers. Features such as patents and knowledge sharing are possible to implement as well.

EXAMPLE CASE: RATIONAL AGENTS AND (UN)CERTAIN NEEDS

As an example demonstrating the Adder's basic flexibility, I will briefly detail a somewhat modified, work-in-progress version of the basic Adder model. The goal of the following model is to study how the understanding of technological possibilities and user needs may affect technological development, and how fully rational agents would develop new technologies.

In a review of evolutionary theories of technological change, Nelson (2005) notes that two key variables – the strength of technological understanding and the knowledge of user needs - seem to control the rate and direction of technological advance. If both are very strong, technological advance can almost be planned.

To test this theory, I have coded a model where technologies are developed in a goal-seeking manner, instead of myopic or random searches of previous models. The developer has a perception (possibly incorrect) of user needs, i.e. target values, and a variable understanding of technologies it can use. In each turn of the simulation, a single developer agent attempts to satisfy a single perceived need by combining together available components. When developing a technology, the agent evaluates the expressions

$$T \pm U_t - P \pm U_p \qquad (3)$$

and

$$T \pm U_t - C \pm U_c \qquad (4)$$

where T is the target, P the product of the technology under development, C the contribution of a component under evaluation, and U_t, U_p and U_c associated uncertainties. If a component is found that brings the new combination closer to target T, it is added to the combination (so that $P_{t+1} = P_t + C$), and the evaluation round starts again.

The goal of the agent is to get as close to the perceived target as possible using the technologies available at the time, using as few components as possible. The target T is selected from a space of adjacent possible targets. This non-monotonically increasing two-dimensional space is simply the space of those target values that neighbour already discovered target values, but have not been yet discovered (i.e. $T = P$). This represents in a stylized form the observation made by e.g. Arthur (2009) that technological "frontier" advances over time, as new technologies open new combinatory possibilities and create new needs.

The search for new technologies is made more difficult by introducing a variable density of "valleys." These valleys represent combinations that are unfeasible for any reason. At no point in the development of technology can the combination's real value, P, equal any valley value. However, the valleys can be "leapfrogged" by adding sufficiently "large" components. (For example, if "3" is a valley value but "4" is not, combinations 2+1 and 2+1+1 are not viable, but a combination 2+2 is.) Viable technologies are added to the repertoire of technologies and can be used as components in the following turns.

As the agent tests different components and repeatedly tries to satisfy a given target, it gains experience of both technology and the needs, enabling it to make more accurate assessments of what components are needed to satisfy a given need. The uncertainty associated with both technologies and needs diminishes according to a standard learning curve model,

$$U = U_i (x+1)^{\log_2 b} \qquad (5)$$

where U_i is the initial uncertainty, x the number of times a technology has been used as a component, and b the learning percentage.

Results

The simulation was run with varying parameter values for initial uncertainty and target and valley densities. All the simulations had learning percentage set to 80%, and one primitive component, "1," and (+) operator were used. The plots of two representative simulation runs ($n = 5$) are displayed below:

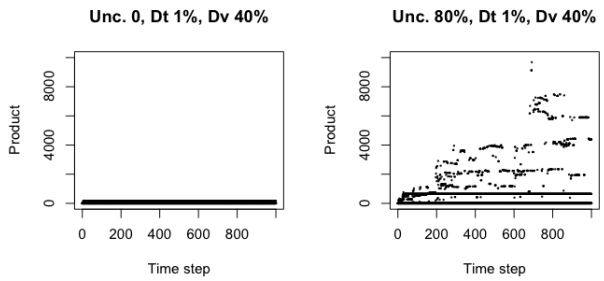

Figure 3: Representative Simulation Results, 5 Runs For Each Setting

On the left panel, the agent has perfect knowledge of user needs and technologies. On the right, it starts with an 80% initial uncertainty about target values and technology performance. In both simulations, the density of target values is 1% and the density of valleys or infeasible technologies 40% out of all the possible technologies. The results are robust to these parameters.

As the sample plots show, surprisingly, uncertainty seems to be a requirement for technological progress. When the agents have perfect knowledge of the needs and the performance of their technologies, they do not make mistakes that help them overcome technological barriers (valleys). Instead, they get stuck after a few non-primitive technologies, at most, are developed.

The preliminary results from this and other test runs indicate that the overall behavior of the model seems to be in line with stylized facts broadly used in other simulations of technological development, e.g. Silverberg and Verspagen (2005). For example, the technological development in the model often displays self-organized criticality and bursts of technological development: usually, the technological development is very slow over a number of turns, until a major valley is bypassed. After that, the speed of development may increase exponentially, until another large valley blocks development – for a while.

Although this example details a simple model, it is easy to see how a more complex model could be developed. For example, the model could be easily extended to *n* dimensions, and agents with different development strategies and differing knowledge can be added to compete with the single agent of above simulations. As the Adder's basic premise – numbers and +/- operators – is so simple, the modeler is free to quickly test out variations.

DISCUSSION

In this paper, I have presented an alternative to the two simulation frameworks most commonly used to study technological evolution. The Adder model is designed to be a streamlined version of an alternative model. Being easy to understand, implement, and modify, I believe it has potential to help researchers interested in the evolution of technologies to study settings hitherto unreachable with existing model frameworks.

Of course, the Adder is not meant to be everything for everyone. NK models are still very well suited for studying complex interactions in a relatively static environment. Similarly, percolation models are perfectly adequate for studying the spread of technologies or concepts over time. A benefit of these simpler models is that they are largely parameterized by a single variable – the K in NK models and the density of available sites in the percolation model. Such simplicity makes for parsimonious models, a desirable feature in most cases. However, the parsimony can also lead to too abstract models, and I believe that unmodified NK and percolation models are not very good fit for studying the evolution of "ideas" over time and in a dynamic environment, i.e. where the ideas themselves have an effect on the selection environment.

The basic framework of using real numbers and arithmetical operators to study technological evolution is extremely flexible and very easily extendable. Thus, it lends itself well to further research. In addition to some of the possibilities outlined above, the model can be used in e.g. studying the effects of constraints on technological development, the effect of different product development strategies, and perhaps even the workings of a broader, interlinked economy of technology-developing organizations. Simpler modifications, such as random mutations, are even easier to implement.

I will explore some of these promising avenues in further publications, and welcome any researcher to join in the effort.

REFERENCES

Almirall, E., Casadesus-Masanell, R., 2010. Open versus closed innovation: A model of discovery and divergence. *Academy of Management Review* 35, 27-47.

Altenberg, L., 1997. NK fitness landscapes, in: Back, T., Fogel, D., Michalewicz, Z. (Eds.), *The Handbook of Evolutionary Computation*. Oxford University Press, Oxford.

Anderson, P.W., 1983. Suggested mode for prebiotic evolution: The use of chaos. *Proceedings of the National Academy of Sciences of the United States of America* 80, 3386.

Arthur, B.W., 2009. *The Nature of Technology: What it is and how it evolves*. Free Press, New York.

Arthur, W.B., Polak, W., 2006. The evolution of technology within a simple computer model. *Complexity* 11, 23-31.
Auerswald, P., Kauffman, S.A., Lobo, J., Shell, K., 2000. The production recipes approach to modeling technological innovation: An application to learning by doing. *Journal of Economic Dynamics and Control* 24, 389-450.
Bak, P., Wiesenfeld, K., 1988. Self-Organized Criticality: An Explanation for 1/f Noise. *Physical Review A* 38, 364.
Basalla, G., 1989. *The Evolution of Technology*. Cambridge University Press, Cambridge, UK.
Dennett, D.C., 1995. *Darwin's Dangerous Idea: Evolution and the meanings of life*. Simon & Schuster, New York.
Ethiraj, S.K., Levinthal, D.A., 2004. Modularity and innovation in complex systems. *Management Science* 50, 159-173.
Frenken, K., 2001. *Understanding Product Innovation using Complex Systems Theory*. PhD thesis, Faculty of Social and Behavioral Sciences, University of Amsterdam.
Frenken, K., 2006. *Innovation, Evolution and Complexity Theory*. Edward Elgar, Cheltenham and Northampton.
Ganco, M., Hoetker, G., 2009. NK Modeling Methodology in the Strategy Literature: Bounded Search on a Rugged Landscape, in: Ketchen, D., Bergh, D. (Eds.), *Research Methodology in Strategy and Management Volume 5*. Emerald, pp. 237-268.
Gilfillan, S.C., 1935. *The Sociology of Invention*. Follett Publishing, Chicago.
Grebel, T., 2004. *Entrepreneurship: A New Perspective*. Routledge, London & New York.
Kauffman, S.A., 1993. *The Origins of Order. Self-Organization and Selection in Evolution*. Oxford University Press, New York and Oxford.
Kauffman, S.A., Macready, W.G., 1995. Technological evolution and adaptive organizations. *Complexity* 1, 26-43.
Levinthal, D.A., 1997. Adaptation on Rugged Landscapes. *Management Science* 43, 934-950.
Murmann, J., Frenken, K., 2006. Toward a systematic framework for research on dominant designs, technological innovations, and industrial change. *Research Policy* 35, 925-952.
Nelson, R. R. 2005. Perspectives on technological evolution. In K. Dopfer, ed. *The Evolutionary Foundation of Economics*. Cambridge: Cambridge University Press, 461-471.
Rivkin, J.W., 2000. Imitation of complex strategies. *Management Science* 46, 824-844.
Schumpeter, J.A., 1939. *Business Cycles*. McGraw-Hill, New York.
Silverberg, G., Verspagen, B., 2005. A percolation model of innovation in complex technology spaces. *Journal of Economic Dynamics and Control* 29, 225-244.
Simon, H.A., 1982. Reply: Surrogates for Uncertain Decision Problems, in: *Models of Bounded Rationality, Volume 1*. MIT Press, Cambridge, Mass., pp. 235-244.
Stauffer, D., Aharony, A., 1994. *Introduction to Percolation Theory*. Taylor and Francis, London.
Usher, A.P., 1954. *A History of Mechanical Inventions*. Harvard University Press, Cambridge, Mass.
Valente, M., 2008. Pseudo-NK: an Enhanced Model of Complexity. LEM Working Paper 2008/26, Università dell'Aquila.
White, A.A., 2008. A developmental perspective on technological change. *WORLD ARCHAEOLOGY* 40, 597-608.

AUTHOR BIOGRAPHIES

JANNE M. KORHONEN is a doctoral student at Aalto University School of Economics in Helsinki. His thesis explores the role of constraints on innovation and inventiveness. Prior to PhD studies, he was a partner in an industrial design consultancy Seos Design. He also has a M.Sc. degree from Helsinki University of Technology. He can be reached from janne.m.korhonen@aalto.fi or via jmkorhonen.net.

JULIA KASMIRE studied linguistics in Santa Cruz, California and Barcelona, Spain before starting an MSc in Edinburgh on the evolution of language and cognition. There she studied how agent based models and simulations can be used to disentangle some of the many interdependent factors in the evolution of complex systems of interacting agents. She is currently working towards a PhD in the Delft University of Technology.

INTEGRATED PLANNING OF ACTIVE MOBILE OBJECTS CONTROL SYSTEM WITH ALLOWANCE OF UNCERTAINTY FACTORS

Sergey V.Kokorin, Semyon A.Potrasaev,
Boris V.Sokolov, Viacheslav A. Zelentsov
Laboratory of Information Technologies in
Systems Analysis and Modeling
St. Petersburg Institute for Informatics and
Automation of RAS (SPIIRAS)
37 14-ja liniya V.O., Saint-Petersburg
199178, Russia
E-mail: **sokolov_boris@mail.ru**
kokorins@yandex.ru, sokol@iias.spb.su

Yuri A.Merkuryev
Department of Modelling and Simulation
1 Kalku Street, Riga LV-1658, Latvia
E-Mail: merkur@itl.rtu.lv

KEYWORDS
Integrated planning and scheduling, active mobile objects, combined methods of modeling and optimization.

ABSTRACT

The Active Mobile Objects Control System (AMO CS) is the main object of an investigation in the proposed paper. An integrated structure and dynamic models of AMO CS functioning, and combined methods and algorithms of planning and scheduling in the system, are developed. The general advantage of suggested models methods and algorithms is related with comprehensive consideration main constraints of investigation area on the base of integrated approach.

INTRODUCTION

Analysis of the main trends for modern complex organizational-technical systems (COTS) indicates their peculiarities such as: multiple aspects and uncertainty of behavior, hierarchy, structure similarity and surplus for main elements and subsystems of COTS, interrelations, variety of control functions relevant to each COTS level, territory distribution of COTS components.

The preliminary investigations confirm that the most convenient concept for the formalization of COTS control processes is the concept of an active mobile objects (AMO). In general case, it is an artificial object (a complex of devices) moving in space and interacting (by means of information, energy, or material flows) with other AMO and objects-in service [7, 8].

At the conceptual level, the process of AMO functioning can be described as a process of operation execution, while each operation can be regarded as a transition from one state to another one. Meanwhile, it is convenient to characterize the AMO state by the parameters of operations.

The particular control models are based on the dynamic and structural interpretation of operations and the previously developed particular dynamic models of AMO functioning.

In accordance with the proposed conceptual model of AMO control system (AMO CS), let us introduce the following basic sets and structures.

VERBAL DESCRIPTION OF A SCHEDULING AND RESOURCE ALLOCATION PROBLEM

Let $A = \{A_i, i \in N\}, N = \{1, \ldots, n\}$ be a set of active mobile objects, elements of COTS. Let us introduce a set $B = \{B_j, j \in M\}, M = \{1, \ldots, m\}$ of resources and two more sets: a set of interaction operations $D^{(i)} = \{D_\kappa^{(i)}, \kappa \in \Phi\}, \Phi = \{1, \ldots, s_i\}$ and a set of flows $E^{(i)} = \{E_\rho^{(i)}, \rho \in \widetilde{R}\}, \widetilde{R} = \{1, \ldots, \pi_i\}$. These sets will be used in formal statement of the considered scheduling problem.

The presented considerations permit the following verbal description of the scheduling problem: it is necessary to find such allowable program (a plan of functioning) for activities of AMO that all operations of AMO technological control cycles (TCC) are executed in time and completely, and the quality of support meets the requirements. In addition, if several allowable programs of AMO control are available, the best one would be selected according to the optimality criteria.

DYNAMIC MODELS OF OPERATIONS PLANNING FOR AMO

The formal statement of the scheduling problem will be produced, as it was noted in the introduction, via dynamic interpretation of operation execution processes (Athans, and Falb, 1966; Sokolov, and Kalinin, 1985; Zimin, and Ivanilov, 1971).

Models for program control of interaction operations and channels

a) Models of processes:

Proceedings 26th European Conference on Modelling and Simulation ©ECMS Klaus G. Troitzsch, Michael Möhring, Ulf Lotzmann (Editors)
ISBN: 978-0-9564944-4-3 / ISBN: 978-0-9564944-5-0 (CD)

$$\dot{x}_{i\kappa}^{(o)} = \sum_{j=1}^{m} \varepsilon_{ij}(t) \cdot \Theta_{i\kappa j} \cdot u_{i\kappa j}^{(o)}, \quad (1)$$

$$\dot{x}_{j}^{(k,1)} = \sum_{i=1}^{n} \sum_{\kappa=1}^{s_j} u_{i\kappa j}^{(o)}, \quad (2)$$

$$\dot{x}_{i\kappa j}^{(\pi)} = u_{i\kappa j}^{(\pi)}(t), i = 1,\ldots,n; \kappa = 1,\ldots s_i. \quad (3)$$

b) Constraints

$$\sum_{j=1}^{n} u_{i\kappa j}^{(o)} \cdot \left(a_{i(\kappa\text{-}1)}^{(o)} - x_{i(\kappa\text{-}1)}^{(o)}\right) = 0, \quad (4)$$

$$\sum_{j=1}^{n} u_{i\kappa j}^{(o)}(t) \le 1,\ u_{i\kappa j}^{(o)}(t) \in \{0,1\}, \quad (5)$$

$$\sum_{i=1}^{n} \sum_{\kappa=1}^{s_i} u_{i\kappa j}^{(\pi)}(t) \le R_j^{(\pi)}, \quad (6)$$

$$i = 1,\ldots,n; \kappa = 1,\ldots s_i; j = 1,\ldots,m.$$

c) End conditions

For the initial time $t = t_0$:

$$x_{i\kappa}^{(o)}(t_0) = d_{i\kappa}^{(o)};\ x_{j\kappa}^{(\pi)}(t_0) = d_{j\kappa}^{(\pi)};\ x_j^{(k)}(t_0) = d_j^{(k)}. \quad (7)$$

For the end point $t = t_f$:

$$x_{i\kappa}^{(o)}(t_f) = a_{i\kappa}^{(o)};\ x_{i\kappa}^{(\pi)}(t_f) = a_{i\kappa}^{(\pi)};\ x_j^{(k)}(t_f) \in \mathbf{R}^1. \quad (8)$$

d) Quality measures of schedule for AMO operation

$$J_1^{(o)} = \frac{1}{2} \sum_{i=1}^{n} \sum_{\kappa=1}^{s_i} \left(a_{i\kappa}^{(o)} - x_{i\kappa}^{(o)}\right)^2 \Bigg|_{t=t_f}; \quad (9)$$

$$J_2^{(o)} = \sum_{i=1}^{n} \sum_{j=1}^{m} \sum_{\kappa=1}^{s_i} \int_{t_0}^{t_f} \alpha_{i\kappa}(\tau) u_{i\kappa j}^{(o)}(\tau) d\tau; \quad (10)$$

$$J_3^{(\kappa)} = \frac{1}{2} \sum_{j=1}^{m} \left(T - x_j^{(k)}(t_f)\right)^2, \quad (11)$$

$$J_4^{(\pi)} = \frac{1}{2} \sum_{i=1}^{n} \sum_{\kappa=1}^{s_i} \left(a_{i\kappa}^{(\pi)} - x_{i\kappa}^{(\pi)}\right)^2 \Bigg|_{t=t_f}, \quad (12)$$

where $x_{i\kappa}^{(o)}$ is a variable characterizing the state of operation $D_\kappa^{(i)}$. Here we interpret the state of operation as an actual amount of work done by a specified time; $\varepsilon_{ij}(t)$ is a preset matrix time function of time-spatial constraints for interaction between AMO A_i and resource B_j, here $\varepsilon_{ij}(t) = 1$ if A_i falls within the interaction zone of B_j, $\varepsilon_{ij}(t) = 0$ if not; $\Theta_{i\kappa j}$ is a preset matrix that characterizes structure of operation execution, here $\Theta_{i\kappa j} = 1$ if the interaction operation $D_\kappa^{(i)}$ can be executed on resource B_j and $\Theta_{i\kappa j} = 0$ if not; $x_j^{(k)}$ is a variable equal to joint activity duration of resource B_j by the time t; $u_{i\kappa j}^{(o)}(t)$ is a control input that is equal to 1 if the operation $D_\kappa^{(i)}$ involving AMO A_i is being executed on resource B_j and equal to 0 if not.

The constraints (4) set a sequence of operations of AMO CS. These equations prohibit the execution of operation $D_\kappa^{(i)}$ until the previous operation $D_{(\kappa-1)}^{(i)}$ is completed, i.e., $x_{i(\kappa-1)}^{(o)} = a_{i(\kappa-1)}^{(o)}$. Here $a_{i(\kappa-1)}^{(o)}$ is known (preset) value. $x_{i\kappa j}^{(\pi)}$ is a variable that is equal to actual amount of information was processed (transmitted) during the operation $D_\kappa^{(i)}$ on resource B_j.

To simplify the expressions describing AMO TCC it was assumed that the operations of TCC are strictly ordered and are executed one after another. The expression (5) is actual for non-separable operations. These constraints mean that at a fixed time each resource B_j can execute at most one operation $D_\kappa^{(i)}$.

The constraint (6) sets maximum total intensity of process execution by resource B_j.

End conditions (7), (8) specify the values of variables at the beginning and the end of scheduling period. Here $d_{i\kappa}^{(o)}$, $d_{j\kappa}^{(k,1)}$, $d_j^{(k)}$, $a_{i\kappa}^{(o)}$ are given values, $\mathbf{R}^1 = [0,\infty)$.

The measure (9) of program control quality characterizes the accuracy of end conditions accomplishment or expresses extent of losses caused by disparity. The functional (10) lets specify preferable time gaps for execution of operation $D_\kappa^{(i)}$. The quality measure (11) helps to estimate the uniformity of channels use by the end point $t = t_f$ of planning period.

Now the scheduling problem can be formulated as a following problem of dynamic system (1)–(3), program control: it is necessary to find an allowable control $\vec{u}(t), t \in (t_0, t_f]$, that meets the requirements (4)–(6) and guides the dynamic system (1)–(3) from the initial state (7) to the specified final state (8). If there are several allowable control (schedules) then the best one (optimal) should be selected in order to maximize (minimize) the quality measures of program control (9)–(12). The components of the program-control vector $\vec{u}(t)$ possess Boolean values and specify time intervals for works of the appropriate AMO.

Formal problem statement

Also we can present the multiple-model multi-criteria description of AMO program control problem:

$$\vec{J}\left(\vec{x}(t), \vec{u}(t), \vec{\beta}, t\right) \to \underset{\vec{u}(t) \in \Delta}{\text{extr}}, \quad (13)$$

$$\Delta = \left\{ \begin{array}{l} \vec{u}(t) \mid \vec{x}(t) = \vec{\varphi}\left(t_0, \vec{x}(t_0), \vec{x}(t), \vec{u}(t), \vec{\beta}, \vec{\xi}(t), t\right), \\ \vec{y}(t) = \vec{\psi}\left(\vec{x}(t), \vec{u}(t), \vec{\beta}, \vec{\xi}(t), t\right), \\ \vec{x}(t_0) \in X_0\left(\vec{\beta}\right), \quad \vec{x}(t_f) \in X_f\left(\vec{\beta}\right) \end{array} \right\},$$

The formulas define a dynamic system describing AMO control processes. Here $\vec{x}(t)$ is a general state vector of the AMO CS, $\vec{y}(t)$ is a general vector of output characteristics. $\vec{u}(t)$, control vector, represents AMO control programs (plans of AMO CS functioning). The vector $\vec{\beta}$ is a general vector of AMO CS parameters. The vector $\vec{\xi}(t)$ is a general vector of uncertainty factors. The vector of AMO CS effectiveness measures is described:

$$\vec{J}\left(\vec{x}(t),\vec{u}(t),\vec{\beta},t\right)=\left\|\vec{J}^{(\mathrm{o})\mathrm{T}},\vec{J}^{(\mathrm{k})\mathrm{T}},\vec{J}^{(\pi)\mathrm{T}}\right\|^{\mathrm{T}}. \qquad (14)$$

The indices «o», «k», «π» corresponds to the following models: models of operations control; models of resources control; models of flows control. Expression (16) determines end conditions for the AMO state vector $\vec{x}(t)$ at time $t=t_0$ and $t=t_f$ (t_0 is the initial time of a time interval the AMO CS is being investigated at, and t_f is the final time of the interval).

STRUCTURAL MODEL OF AMO WITH ALLOWANCE OF INCERTANT ENVIRONMENT

Structural representation of AMO can explicitly define the sequence of operations and determine the spatial relationships, technical and technological limitations of various elements of the AMO CS. The structural model has a different interpretation of the dynamic model parameters. The processes are interpreted as a finite set of predefined orders of different types in the sense of queueing theory (QT); $\vec{p}$ are parameters of the distribution of productivity of the resource, which is of stochastic nature, not deterministic as in case of dynamic models; Θ_{ikj} determines the structure of operations, as described in (1); ζ_{ik} corresponds to static priorities of processes: $\zeta_{ik}=\psi_{i\kappa}(t_0), i=1,\ldots,n;\kappa=1,\ldots,s_i$, where $\vec{\psi}(t)$ has been defined in (13) . The higher ζ_{ik} the higher the priority of a process; all other parameters are interpreted the same way as in dynamic model.

The simulation of structural model allows approximate the quality measures of schedule for AMO operations (Kokorin, Sokolov 2010, 2011) defined, as a means of values of multiple realization of a process, which will be defined as $\bar{f}\left(q_0\left(\vec{\zeta},\vec{p}\right)\right)$.

THE METHOD OF RESOLVING THE PLANNING AND RESOURCE ALLOCATION TASKS

We pose the problem of optimizing $J_G=\sum_{i=1}^{4}\lambda_i J_i, \lambda_i\geq 0, \sum_{i=1}^{4}\lambda_i=1$ as a function of static priorities of operations and the maximum limit of resources productivity rates: $J_G=f\left(q_0\left(\vec{\zeta},\vec{p}\ \right)\right)\to\min\limits_{\mathrm{Z},\Omega}$, where $q_0(\cdot)$ determines the all other fixed parameters of the formal model, Z is a set of possible priorities, and Ω is a set of possible rates or resources productivity. In this formulation, the use of unlimited resources allow arbitrarily close to the global optimum J_G. Therefore, it is proposed to add constraints of the form:

$$\begin{aligned}&\vec{p}\ =\left(R_1^{(\pi)},\ldots,R_m^{(\pi)}\right)^{\mathrm{T}}, \qquad (1)\\ &\vec{c}^{\,\mathrm{T}}\vec{p}\ \leq C,\end{aligned}$$

where $\vec{c}=\left(c_j\right)^{\mathrm{T}}, j\in M$ – factors determining the cost of one unit of resources productivity maintenance and C is a limit to the total cost of resource maintenance. The uncertainty of dynamic mode $\vec{\xi}(t)$ is included in structural model as a stochastic model of resource allocation, set as an exponential distribution function with a variable parameters $\vec{p}$.

Priorities $\vec{\zeta}$ represent ordinal values, while the maximum intensity of the resources $\vec{p}$ are continuous and nonnegative. The mixed optimization problems are difficult to solve. We propose to consider the scheme of ν successive iterations in this paper, where iteration consists of two steps and it starts with $\nu=0$ and $\vec{\zeta}^{(0)}=\vec{\zeta}_g$, where $\vec{\zeta}_g$ – fixed vector of initial priorities, e.g. equal values consider the FIFO discipline.

Phase 1. Optimization of resource allocation for data transmission and processing using a structural model:

$$\bar{f}\left(q_0\left(\vec{\zeta}^{(\nu)},\vec{p}\right)\right)\to\min_{\vec{p}\in\Omega}, \qquad (2)$$

Phase 2. Dynamic scheduling with fixed vector of resources productivity distribution $\vec{p}_\nu$ obtained from previous step:

$$f\left(q_0\left(\vec{\zeta},\vec{p}_\nu\right)\right)\to\min_{\vec{\zeta}\in\mathrm{Z}}. \qquad (3)$$

For the stopping criteria of the iteration procedure we propose to use one of the following approaches:

- any time algorithm;
- achievement of level $\tilde{e}$ of a difference values of successive iterations, that is,

$$\min\left\{\nu:\left|f\left(q_0\left(\vec{\zeta}^{(\nu)},\vec{p}_\nu\right)\right)-f\left(q_0\left(\vec{\zeta}^{(\nu-1)},\vec{p}_\nu\right)\right)\right|<\tilde{e}\right\}$$

- the value is close (vicinity $\tilde{\tilde{e}}$) to the global extreme, for the case then convergence could not be met:

$$\min\left\{\nu: f\left(q_0\left(\vec{\zeta}^{(\nu)},\vec{p}_\nu\right)\right)<\tilde{\tilde{e}}\right\}.$$

RESOURCE ALLOCATION OPTIMIZATION ALGORITHM

We are going to investigate the influence of the structure of a CTS network.

Two methods are used for optimization of the target function, described earlier in the paper: global search method – the method of psi-transform (CHichinadze 1983), and a method of numerical optimization without calculating derivatives – the method of principal axes of Brent (Brent 1973).

The method of psi-conversion is a method for searching the global extremum of the objective function. It is not critical to the choice of an initial approximation, but requires of significant computational resources in the case when the dimension of parameters to be optimized is increasing. We chose a probability measure on the set of modifiable parameters which the value of a given objective function above a predetermined levels as a psi-function at. Thus, the problem of optimization reduces to finding a solution to the equation with many variables (parameters to be optimized). Using this method as an independent method of optimization often yields results of the very low accuracy.

The algorithm of the global optimization (Algorithm #1):

Step 1.1. The estimation of the spread of values of the objective function by the random test.

Step 1.2. Choose of the value levels $f\left(q\left(\vec{\zeta}^{*}, \vec{p}^{(\pi)}\right)\right) \geq \sigma_l, \quad l \in \{1,..., L\}$.

Step 1.3. Define the $\Delta_l = \left\{\vec{p}: \bar{f}\left(q\left(\vec{\zeta}^{*}, \vec{p}\right)\right) \geq \sigma_l\right\}$

Step 1.4. Calculation of mean values of the objective function for each level by the means of the random test.

$$\Psi_l = 1/S \sum_{\Delta_l} \left(\bar{f}\left(q\left(\vec{\zeta}^{*}, \vec{p}\right)\right) - \sigma_l\right), \qquad (21)$$

S – number of random generations, $\vec{p}_k$ – parameters of the k-th iteration, $l \in \{1,..., L\}$.

Step 1.5. Calculation of the mean values for optimizing parameters for each level.

$$\bar{p}_{il} = S / \Psi_l \sum_{\Delta_l} \vec{p}_i \left(\bar{f}\left(q\left(\vec{\zeta}^{*}, \vec{p}\right)\right) - \sigma_l\right)^{\alpha}. \qquad (22)$$

Step 1.6. The parabolic approximation of Ψ_l and the extrapolation to the level 0 and search for optimal parameters.

Because of the high computational complexity of the method of psi-transformation and its lack of the precision while solving problems of large dimensions are proposed the method of principal axes of Brent. This method focuses on local optimization of functions of several variables without calculating derivatives. In practice, the method proved effective in the solving problems of optimization of network structure, including, for the case when the parameters' space has a large dimension and fairly tight restrictions, the introduction of possible restrictions will be described below. The main drawback of the algorithm, it implements, is the need to specify the initial approximations, which should be calculated for an each task separately. In this case, the algorithm is characterized by two main parameters: the index of accuracy of the target function and the magnitude of step changes in parameters to be optimized. The first of these determines the moment to stop the iterative process; the second determines the rate of convergence of the algorithm.

The algorithm of the local optimization (Algorithm #2):

Step 2.1. Calculation of initial approximation $\vec{p}_0$, which is the final solution of the global optimization algorithm (see the step 5 of previous algorithm).

Step 2.2. The initial directions is defining $U^{(0)} = \left\{(u_i)^{(0)}\right\}_{i=1}^{m} = I$, where I – the identity matrix of the given dimension.

Step 2.3. Alternately, the optimal value is searched along each direction.

Step 2.4. The direction vector with minimal index is dropped and new vector is substituted in the end of direction matrix $\vec{p}_m - \vec{p}_0$.

Step 2.5. After a complete change of a set of directional vectors U^m, a set of directional vectors is replacing with the orthogonal matrix that approximates the Hessian of the objective function in the point of current value.

Step 2.6. Steps 2.3 – 2.5 is repeating till the achieving the given factor of preciseness: $\left|\bar{f}_r\left(q\left(\vec{\zeta}, \vec{p}\right)\right) - \bar{f}_{r-1}\left(q\left(\vec{\zeta}, \vec{p}\right)\right)\right| \leq \hat{e}$, where r is index of successive iterations and $\hat{e}$ – parameter for convergence level.

It proposed to use global optimization method for initial estimation of a local one. Such combination allows achieve a fast convergence for a given task.

The method is proven to converge in case of double continuously differentiable functions, and numerical experiments shows good convergence for wider class of target functions. Same time the method of a global optimization could be adopted to define the maximal possible distance from checked points to the global optimum by setting its parameters.

DYNAMIC SCHEDULING ALGORITHM

Computational scheme of the scheduling algorithm (Algorithm #3) is as follows.

Step 3.1. Setting the rough decision (any valid plan) $\vec{u}_g(t), t \in (t_0, t_f]$. In the special case empty plan ($\vec{u}_g(t) \equiv \vec{0}$) can be selected.

Step 3.2. Integrating basic system of equations (1)–(3) with initial conditions (7) and the $\vec{u} = \vec{u}_g(t)$. Vector $\vec{x}_{(0)}(t)$ obtained as a result of integration. In addition, determine $\vec{J} = \left\|J_1, J_2, J_3, J_4\right\|$ at $t = t_f$, which is taken as a record. Calculating the transversality condition which could be found in […].

Step 3.3. Integrating the conjugate system of equations

$$\dot{\psi}_l = -\frac{\partial H}{\partial x_l} + \sum_{\alpha=1}^{I_1} \eta_\alpha(t) \frac{\partial q_\alpha^{(1)}(\vec{x}(t),\vec{u}(t))}{\partial x_l} + \\ + \sum_{\rho=1}^{I_2} \rho_\beta(t) \frac{\partial q_\beta^{(2)}(\vec{x}(t),\vec{u}(t))}{\partial x_l}, l = 1,\ldots,\tilde{n} \quad (18)$$

where H – Hamiltonian […], η_α and ρ_β could be found from

$$\rho_\beta(t) q_\beta^{(2)}(\vec{x}(t),\vec{u}(t)) \equiv 0, \beta = 1,\ldots,I_2,$$

$$grad_{\vec{u}} H(\vec{x}(t),\vec{u}(t),\vec{\psi}(t)) =$$

$$\sum_{\alpha=1}^{I_1} \eta_\alpha(t) grad_{\vec{u}} q_\alpha^{(1)}(\vec{x}(t),\vec{u}(t)) +$$

$$\sum_{\beta=1}^{I_2} \rho_\beta(t) grad_{\vec{u}} q_\beta^{(2)}(\vec{x}(t),\vec{u}(t)),$$

where $\vec{\psi}(t)$ is a general vector of the conjugate system of equations, $q_\alpha^{(1)}(\vec{x}(t),\vec{u}(t))$ and $q_\beta^{(2)}(\vec{x}(t),\vec{u}(t))$ – components of given system of constraints, from $t = t_f$ to $t = t_0$ with $\vec{u} = \vec{u}_g(t)$. At $t = t_0$ we get a first approximation of $\vec{\psi}_i(t_0)$. This completes the iteration $r = 0$.

Step 3.4. From the moment t_0 control $\vec{u}^{(r+1)}(t)$ is sought (r = 0,1,2,... – number of iterations) based on the maximization of the Hamiltonian $H\left(\vec{x}^*(t),\vec{u}^*(t),\vec{\psi}^*(t)\right)$ […]. Simultaneously the main system of equations is integrated. Thus at any given time there is a dynamic decomposition of the main tasks for several mathematical programming problems: linear programming, assignment problems.

The iterative optimization process ends when the following conditions are satisfied: $\left|J^{(r+1)} - J^{(r)}\right| \le \varepsilon$.

Thus $\vec{\psi}(t_0)$ defines vector of associative values of static priority $\vec{\zeta}$ for each operation $D_\kappa^{(i)}$.

CONCLUSION

As a result of the research, the multi-stage procedure for an integrated planning of the AMO CS has been developed. One of its main advantages is a combination of different types of restrictions related to the operation of AMO CS and uncertainties affecting the stability of worked-out plans. The originality of the developed models of planning bases on the fact that each of them takes into accounts the limitations and characteristics of planning procedures that are within each of these structurally formalized. Studies have shown that the basic space-time, technical and technological constraints related to the operation of AMO CS best described by using a previously developed by the authors, models, software operations management and resources. Uncertainty and structural factors were taken into account in the static model. It is shown (Krasnoshokov) that the proposed resource allocation algorithms provide theoretical and practical convergence and obtaining the planning results in a finite number of steps. The results of computer experiments have confirmed this convergence.

ACKNOWLEDGMENTS

This research is supported by project 2.1/ELRI - 184/2011/14:

«Integrated Intelligent Platform for Monitoring the Cross-Border Natural-Technological Systems» as a part of «Estonia-Latvia-Russia cross border cooperation Programme within European Neighborhood and Partnership instrument 2007-2013».

REFERENCES

Ackoff, R.L. (1978). *The Art of Problem Solving*. Wiley-Interscience, New York.

Athaus, M. and P.L. Falb (1966). *Optimal control: An Introduction to the Theory and Its Applications*. McGrow-Hill Book Company. New York, San Francisco, Sidney.

Klir, G.J. (1985). *Architecture of Systems Problem Solving*. Plenum Press, New York.

Sokolov, B.V. and V.N Kalinin (1995). Multi-model Approach to the Description of the Air-Space Facilities Control Process. *Control Theory and process*, N 1, pp.149-156 (in Russian).

Sokolov, B.V. and V.N Kalinin (1985). A Dynamic Model and an Optimal Scheduling Algorithm for Activities with Bans of Interrupts. *Automation and Telechanics*, N 1, pp.106-114 (in Russian).

Ivanov D., Sokolov B. (2010a), Adaptive supply chain management, Springer, London at al.

Ohtilev, M., Sokolov, B., Yusupov, R. (2006). Intelligent technologies of monitoring and control. Moscow, Nauka (in Russian).

Zimin, I.N. and Yu.,P. Ivanilov (1971). Solving of network planning problems via a reduction to optimal control problems. Journal of Calculus Mathematics and Mathematical Physics, Vol. 11, N 3, pp.632-631 (in Russian).

Kreipl, S., Pinedo, M. (2004). Planning and scheduling in supply chains: an overview of issues in practice. Production and Operations Management. 13(1) 77-92.

Ivanov, D., Sokolov, B. (2010). Dynamic sypply chain scheduling. Journal of scheduling, DOI: 10.1007/s10951-010-0189-6.

G. Bolch; S. Greiner; H. De Meer; K. S. Trivedi (2006) Queuing Networks and Markov Chains Modeling and Performance Evaluation with Computer Science Applications, *A Wiley-Interscience publication*.

Brent, R. P. (1973) Algorithms for minimization without derivatives. *USA, NJ: Prentice-Hall Inc.,* pp 195.

Medhi, J., Stochastic Models in Queueing Theory, Boston: Academic Press, 1972.

Чичинадзе, В.К. (1983) Решение невыпуклых нелинейных задач оптимизации. Метод пси-преобразования. *М.: Наука*.

Kokorin S.V., Sokolov B.V., Ryzhikov Yu.I. Model And Algorithm For Combinational Optimization Of Information System Bandwidth Proceedings 25th European.

Kokorin S.V., Sokolov B.V. Miroslav Snorek, Zdenek Buk, M. C. J. D. (Ed.) Numerical Methods of Structure Optimization of Homogeneous Queuing Networks Proceeding.

Краснощёков П.С., Морозов В.В., Фёдоров В.В. Декомпозиция в задачах проектирования. Изв. АН СССР. Техн. Кибернетика, 1979. 2 7-18.

AUTHOR BIOGRAPHIES

BORIS V. SOKOLOV is a deputy director at the Russian Academy of Science, Saint Petersburg Institute of Informatics and Automation. Professor Sokolov is the author of a new scientific lead: optimal control theory for structure dynamics of complex systems. Research interests: basic and applied research in mathematical modeling and mathematical methods in scientific research, optimal control theory, mathematical models and methods of support and decision making in complex organization-technical systems under uncertainties and multicriteria. He is the author and co-author of five books on systems and control theory and of more than 270 scientific papers. Professor B. Sokolov supervised more over 50 research and engineering projects. Professor B. Sokolov supervised more over 50 research and engineering projects. *Homepage: www.spiiras-grom.ru.*

SEMYON A. POTRYASAEV is PhD research fellow at the Russian Academy of Science, Saint Petersburg Institute of Informatics and Automation. He graduated from the Baltic State Technical University "VOENMEH" with a degree of control systems engineer and Moscow Institute of International Economic Relations as an economist in finance and credit.
Research interests: applied research in mathematical modeling, optimal control theory, mathematical models and methods of support and decision making in complex organization-technical systems under uncertainties and multicriteria. *Homepage: www.spiiras-grom.ru.*

SERGEY V. KOKORIN Ph.d.-student. Professional Interests: numerical methods, queueing theory, mathematical statistics. 8 scientific papers.

VIACHESLAV A. ZELENTSOV Leading researcher, Laboratory for Information Technologies in Systems Analysis and Modeling, Head of Research Consulting Center for Space Information Technologies and Systems at St. Petersburg Institute of Informatics and Automation of the RAS (SPIIRAS), professor and Director of Research and Education Center "AeroSpaceInfo" in St Petersburg State University of Aerospace Instrumentation. More than 180 scientific papers, more over 50 research and engineering projects, 5 teaching books.

YURI MERKURYEV is professor, head of the department of Modelling and Simulation of Riga Technical University. He earned the Dr.sc.ing. degree in 1984 in systems identification, and Dr.habil.sc.ing. degree in 1997 in systems simulation, both from Riga Technical University, Latvia. His professional interests include methodology of discrete-event simulation, supply chain simulation and management, as well as education in the areas of simulation and logistics management. Professor Merkuryev is a corresponding member of the Latvian Academy of Sciences, president of Latvian Simulation Society, Board member of the Federation of European Simulation Societies (EUROSIM), senior member of the Society for Modelling and Simulation International (SCS), and Chartered Fellow of British Computer Society.

ONE-DIMENSIONAL MODELLING OF A CARBON NANOTUBE-BASED BIOSENSOR

Karolis Petrauskas
Faculty of Mathematics and Informatics
Vilnius University
Naugarduko str. 24, LT-03225, Vilnius, Lithuania
Email: karolis.petrauskas@mif.vu.lt

Romas Baronas
Faculty of Mathematics and Informatics
Vilnius University
Naugarduko str. 24, LT-03225, Vilnius, Lithuania
Email: romas.baronas@mif.vu.lt

KEYWORDS

Modelling, reaction-diffusion, biosensor, carbon nanotube.

ABSTRACT

This paper presents a one-dimensional-in-space mathematical model of an amperometric biosensor based on a carbon nanotube electrode deposited on a perforated membrane. The developed model is based on nonlinear reaction-diffusion equations. The conditions at which the one-dimensional mathematical model can be applied to an accurate simulation of the biosensor response are investigated. The accuracy of the response simulated by using one-dimensional model is evaluated by the response simulated by the corresponding two-dimensional model. The mathematical model and the numerical solution are also validated by an experimental data. The obtained agreement between the simulation results and experimental data is admissible for different configurations of the biosensor operation. The numerical simulation was carried out using the finite difference technique.

INTRODUCTION

Biosensors are analytical devices mainly used to measure concentrations of substances (Turner et al., 1987; Scheller and Schubert, 1992). They are relatively cheap and widely used in environment monitoring, drug detection and food industry (Wollenberger et al., 1997). Main parts composing a biosensor are: a biochemically active material, usually an enzyme, selectively detecting a target analyte (substrate), and a transducer. The transducer converts the biological recognition event into an electrical signal. The latter is then processed and displayed to an end user of the device.

Since carbon nanotubes (CNT) were discovered (Iijima, 1991), they were used in various applications. Because of their unique properties, carbon nanotubes are also used to build highly sensitive biosensors (Ahammad et al., 2009; Balasubramanian and Burghard, 2006).

A development of new biosensors is a rather expensive process requiring to perform a lot of experiments. In order to reduce the cost, a part of the experiments can be replaced by a computer simulation (Amatore et al., 2006). The action of practical biosensors is often modelled by a non-linear reaction-diffusion system (Schulmeister, 1990; Baronas et al., 2010). A CNT-based biosensor was mathematically modelled by Lyons (Lyons, 2009). A two-compartment mathematical model involving the mass transport and the enzyme kinetics was formulated in a one-dimensional domain, and the corresponding problem was solved analytically assuming the steady state conditions. More advanced biosensors than the modelled one are usually covered by outer porous or perforated membranes (Turner et al., 1987; Scheller and Schubert, 1992; Wollenberger et al., 1997).

Recently, a novel biosensor based on a carbon nanotube enzyme-loaded electrode deposited on a perforated polycarbonate membrane was developed (Razumienė et al., 2009), and a mathematical model of the biosensor was proposed (Baronas et al., 2011). The model has been formulated in a two-dimensional domain, and therefore the simulation was time and resource consuming. This is especially important when investigating numerically peculiarities of the biosensor response in wide ranges of the model parameters. The multifold numerical simulation of the biosensor response based on the one-dimensional model is much more efficient than the simulation based on the corresponding two-dimensional model.

In this paper, a corresponding one-dimensional-in-space model for the biosensor based on a CNT enzyme-loaded electrode deposited on a perforated membrane is proposed. The mathematical model and the numerical solution are validated by the experimental data (Razumienė et al., 2009; Baronas et al., 2011). The obtained agreement between the simulation results and experimental data is admissible for different configurations of the biosensor operation.

The conditions at which the one-dimensional mathematical model can be applied to accurate simulation of the biosensor action are investigated in this paper. The accuracy of the biosensor response simulated by using one-dimensional model is evaluated by the response simulated by the corresponding two-dimensional model. The numerical simulation was carried out using the finite difference technique.

PRINCIPAL STRUCTURE OF THE BIOSENSOR

The investigated biosensor has a layered structure (Razumienė et al., 2009). The biosensor was built by bind-

Proceedings 26th European Conference on Modelling and Simulation ©ECMS Klaus G. Troitzsch, Michael Möhring, Ulf Lotzmann (Editors)
ISBN: 978-0-9564944-4-3 / ISBN: 978-0-9564944-5-0 (CD)

ing the carbon nanotubes to the perforated membrane. Some of the carbon nanotubes are sinked into holes of the membrane during the preparation process. The membrane-CNT film was loaded with an enzyme and covered with an insulating film. Part of the enzyme was left outside of the CNT mesh and formed a layer between the CNTs and a insulating film. The principal structure of the active surface of the biosensor is shown in figure 1.

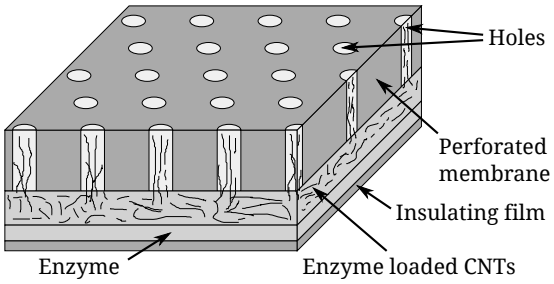

Figure 1: Principal structure of the active surface of the biosensor. The figure is not to scale

The following enzymatic reactions take place in the enzyme-loaded layers of the biosensor:

$$\mathrm{E_o} + \mathrm{S} \xrightarrow{k_1} \mathrm{E_r} + \mathrm{P}, \tag{1}$$

$$\mathrm{E_r} + \mathrm{M_o} \xrightarrow{k_2} \mathrm{E_o} + \mathrm{M_r}, \tag{2}$$

where k_1 and k_2 are the rate coefficients of the corresponding reactions. In reaction (1) the enzyme in the oxidized form ($\mathrm{E_o}$) detects the target substrate (S) and is reduced ($\mathrm{E_r}$). The other product (P) of the reaction has no impact on the biosensor response, and therefore is omitted in the following model. The reduced enzyme is re-oxidized in reaction (2) by converting a mediator from its oxidized form ($\mathrm{M_o}$) to the reduced one ($\mathrm{M_r}$). In the layer of enzyme-loaded carbon nanotubes, the reduced mediator participates in the following electrochemical reaction:

$$\mathrm{M_r} \longrightarrow \mathrm{M_o} + n_\mathrm{e}\mathrm{e}^-. \tag{3}$$

In reaction (3) the mediator is re-oxidized and electrons forming the response current are emitted. Here n_e stands for a number of electrons emitted per one reaction event. Reaction (3) is considered to be very fast. Such assumption is a common when modelling amperometric biosensors (Scheller and Schubert, 1992).

MATHEMATICAL MODEL

The model is formulated as a system of non-linear reaction-diffusion equations with initial and bounary conditions. Applying the homogenization process to the perforated membrane allows to formulate the mathematical model of the considered biosensor in a one-dimensional domain, on a line perpendicular to the surface of the biosensor (Bakhvalov and Panasenko, 1989). The surface of the insulating film is assumed to be zero point in the space interval. The model of the biosensor involves four layers (Ω_i) with different properties,

$$\begin{aligned} &\Omega_i \equiv (x_{i-1}, x_i), \quad x_0 = 0,\ x_i = x_{i-1} + d_i, \\ &\qquad \Gamma_0 \equiv \{0\},\ \Gamma_i \equiv \{x_i\}, \quad i = 1,2,3,4, \end{aligned} \tag{4}$$

where d_1 is the thickness of the enzyme layer, d_2 – the thickness of the enzyme-loaded CNT mesh, d_3 – the thickness of the perforated membrane, and d_4 stands for the thickness of the Nernst diffusion layer forming on the surface of the perforated membrane.

Governing Equations

Due to the enzyme immobilization in the CNT mesh, no mass transport of the enzyme is considered. The dynamics of the enzyme concentration is only impacted by biochemical reactions (1) and (2),

$$\begin{aligned} \frac{\partial E_{\mathrm{o},i}}{\partial t} &= -k_1 E_{\mathrm{o},i} S_i + k_2 M_{\mathrm{o},i} E_{\mathrm{r},i}, \\ \frac{\partial E_{\mathrm{r},i}}{\partial t} &= k_1 E_{\mathrm{o},i} S_i - k_2 M_{\mathrm{o},i} E_{\mathrm{r},i}, \\ &\qquad x \in \Omega_i,\ i = 1,2,\ t > 0, \end{aligned} \tag{5}$$

where x and t stand for space and time, respectively. $U_i = U_i(x,t),\ U_i \in \{E_\mathrm{o}, E_\mathrm{r}, S, M_\mathrm{o}\}$ are concentrations of the corresponding species in i^{th} layer (Ω_i) of the biosensor.

The substrate is affected by the diffusion in all layers of the biosensor. Additionally, in the layers filled with the enzyme the substrate participates in the reaction (1),

$$\begin{aligned} \frac{\partial S_i}{\partial t} &= D_{\mathrm{S}_i} \frac{\partial^2 S_i}{\partial x^2} - k_1 E_{\mathrm{o},i} S_i, \quad i = 1,2, \\ \frac{\partial S_i}{\partial t} &= D_{\mathrm{S}_i} \frac{\partial^2 S_i}{\partial x^2}, \qquad\qquad\quad i = 3,4, \\ &\qquad\qquad x \in \Omega_i,\ t > 0, \end{aligned} \tag{6}$$

where D_{S_i} ($i = 1,4$) is the diffusion coefficient of the substrate in the corresponding layer, and $D_{\mathrm{S},i}$ ($i = 2,3$) is the effective diffusion coefficient of the substrate in the CNTs and the perforated membrane.

The mediator in the oxidized form is affected by the diffusion in the entire biosensor and the Nernst diffusion layer. In the layer of the enzyme-loaded CNTs (Ω_2), the mediator is consumed in the reaction (2) and immediately regenerated in the reaction (3). The reactions compensate each other in terms of the mediator concentration. No electrochemical reaction occurs in the layer entirely filled with the enzyme Ω_1. Therefore, the mediator is consumed in reaction (2) without regeneration. The dynamics of the concentration of the oxidized mediator is described by the following equations ($t > 0$):

$$\begin{aligned} \frac{\partial M_{\mathrm{o},i}}{\partial t} &= D_{\mathrm{M}_{\mathrm{o},i}} \frac{\partial^2 M_{\mathrm{o},i}}{\partial x^2} - k_2 M_{\mathrm{o},i} E_{\mathrm{r},i}, \quad i = 1, \\ \frac{\partial M_{\mathrm{o},i}}{\partial t} &= D_{\mathrm{M}_{\mathrm{o},i}} \frac{\partial^2 M_{\mathrm{o},i}}{\partial x^2}, \quad i = 2,3,4, \quad x \in \Omega_i, \end{aligned} \tag{7}$$

where $D_{\mathrm{M}_{\mathrm{o},i}}$ is the diffusion coefficient of the oxidized mediator in the corresponding region, $i = 1,4$. $D_{\mathrm{M}_{\mathrm{o},2}}$ is

the effective diffusion coefficient of $\mathrm{M_o}$ in the enzyme-loaded CNTs (Ω_2), and $D_{\mathrm{M_{o,3}}}$ is the corresponding coefficient for the perforated membrane.

Because of very high rate of the electrochemical reaction (3), the reduced mediator resides only in the enzyme layer (Ω_1), where it diffuses and is generated in the reaction (3),

$$\frac{\partial M_{\mathrm{r},1}}{\partial t} = D_{\mathrm{M_{r,1}}} \frac{\partial^2 M_{\mathrm{r},1}}{\partial x^2} + k_2 M_{\mathrm{o},1} E_{\mathrm{r},1}, \tag{8}$$

where $M_{\mathrm{r},1} = M_{\mathrm{r},1}(x,t)$ is the concentration of the reduced mediator in Ω_1, and $D_{\mathrm{M_{r,1}}}$ is the diffusion coefficient of $\mathrm{M_r}$ in the enzyme layer.

Boundary Conditions

The modelled experiments were performed by intensively mixing the solution to be analysed (Razumienė et al., 2009). This leads to constant concentrations of the species above the Nernst diffusion layer,

$$S_4(x_4,t) = S_0, \quad M_{\mathrm{o},4}(x_4,t) = M_0, \tag{9}$$

where S_0 is the substrate and M_0 is the mediator concentrations in the bulk solution.

At the surface of the insulating film ($x = 0$), the non-leakage boundary conditions are applied for all the diffusive substances,

$$\left.\frac{\partial U}{\partial x}\right|_{\Gamma_0} = 0, \quad U \in \{S_1, M_{\mathrm{o},1}, M_{\mathrm{r},1}\},\ t > 0. \tag{10}$$

The matching conditions are applied on all the boundaries between adjacent regions,

$$D_{U_i} \left.\frac{\partial U_i}{\partial x}\right|_{\Gamma_i} = D_{U_{i+1}} \left.\frac{\partial U_{i+1}}{\partial x}\right|_{\Gamma_i}, \qquad U_i|_{\Gamma_i} = U_{i+1}|_{\Gamma_i}, \tag{11}$$

for $U_i = S_i,\ i = 1,2,3$ and $U_i = M_{\mathrm{o},i},\ i = 2,3$.

Due to the electrochemical reaction (3) taking place on the boundary Γ_1 between the enzyme layer and the enzyme-loaded CNTs, the concentration of $\mathrm{M_r}$ is permanently reduced to zero,

$$M_{\mathrm{r},1}|_{\Gamma_1} = 0, \quad t > 0. \tag{12}$$

All the reduced mediator is immediately re-oxidized on this boundary,

$$D_{\mathrm{M_{o,2}}} \left.\frac{\partial M_{\mathrm{o},2}}{\partial x}\right|_{\Gamma_1} = D_{\mathrm{M_{o,1}}} \left.\frac{\partial M_{\mathrm{o},1}}{\partial x}\right|_{\Gamma_1} + D_{\mathrm{M_{r,1}}} \left.\frac{\partial M_{\mathrm{r},1}}{\partial x}\right|_{\Gamma_1}, \qquad M_{\mathrm{o},1}|_{\Gamma_1} = M_{\mathrm{o},2}|_{\Gamma_1}. \tag{13}$$

Initial Conditions

The numerical simulation of an experiment starts at the moment $t = 0$, when the substrate and the mediator are poured into the buffer solution and reaches the external boundary of the Nernst diffusion layer,

$$S_4|_{\Gamma_4} = S_0, \quad M_{\mathrm{o},4}|_{\Gamma_4} = M_0. \tag{14}$$

Simultaneously ($t = 0$), the substrate and the mediator are absent elsewhere,

$$S_i = M_{\mathrm{o},i} = 0, \quad x \in \overline{\Omega}_i \setminus \Gamma_4,\ i = 1,2,3,4. \tag{15}$$

All the enzyme is assumed to be in the oxidized form at the beginning of the experiment,

$$E_{\mathrm{o},1} = E_0, \quad E_{\mathrm{r},1} = 0, \quad x \in \Omega_1,\ t = 0, \tag{16}$$

where E_0 is the total concentration of the enzyme in the enzyme layer (Ω_1). The layer of the carbon nanotubes is assumed to be only partially filled with the enzyme,

$$E_{\mathrm{o},2} = \eta E_0, \quad x \in \Omega_2,\ t = 0, \tag{17}$$

where $0 \le \eta < 1$ is the ratio of enzyme concentration in CNTs to its concentration in Ω_1.

Output of the Biosensor

The output current of the biosensor is generated due to the electrochemical reaction (3) taking place in the region Ω_2 of the CNT electrode. The reaction (3) was assumed so fast that all the mediator in the reduced form is immediately oxidized. The reduced mediator $\mathrm{M_r}$ arises in the region Ω_2 due to the enzymatic reaction (2) as well as the diffusion from the adjacent region Ω_1 through the boundary Γ_1. The latter part of the reduced mediator is completely oxidized in (3). Taking into account these two sources of $\mathrm{M_r}$ for the electrochemical reaction (3) leads the total output current $j(t)$ of the biosensor,

$$j(t) = n_{\mathrm{e}} F \times \left(k_2 \int_{x_1}^{x_2} E_{\mathrm{r},2} M_{\mathrm{o},2}\, dx - D_{\mathrm{M_{r,1}}} \left.\frac{\partial M_{\mathrm{r},1}}{\partial x}\right|_{\Gamma_1} \right), \tag{18}$$

where F is the Faraday constant.

When using practical biosensors the saturated output current is commonly used as a response of the biosensor. The steady state current density J of the considered biosensor is defined as follows:

$$J = \lim_{t \to \infty} j(t). \tag{19}$$

Effective Diffusion Coefficients

In order to reduce the number of the model parameters, the species S, $\mathrm{M_o}$ and $\mathrm{M_r}$ are assumed to have the same diffusion coefficients in a certain medium. The enzyme

and Nernst diffusion layers are assumed to be homogeneous, therefore diffusion coefficients for the species are expressed as

$$\begin{aligned} D_U &= D_\mathrm{e}, \qquad U \in \{\mathrm{S}_1, \mathrm{M}_{\mathrm{o},1}, \mathrm{M}_{\mathrm{r},1}\}, \\ D_U &= D_\mathrm{n}, \qquad U \in \{\mathrm{S}_4, \mathrm{M}_{\mathrm{o},4}\}, \end{aligned} \tag{20}$$

where D_e is the diffusion coefficient of the species in the enzyme, and D_n is the corresponding diffusion coefficient in the diffusion layer.

The CNT layer as well as the perforated membrane are really non-homogeneous mediums. Assuming these layers as the periodic media and applying the volume averaging approach to them lead to the effective diffusion coefficients for these mediums (Whitaker, 1999; Bakhvalov and Panasenko, 1989). The CNT layer (Ω_2) is considered as a composite of three compartments: the carbon nanotubes, the enzyme and the bulk solution. The perforated membrane (Ω_3) was treated as a composite of non-permeable material, and the bulk solution together with carbon nanotubes in the holes of the membrane. Assuming low volume of the CNTs the effective diffusion coefficients can be expressed in terms of the volume fractions, the tortuosity and the diffusion coefficients for the corresponding compartments,

$$\begin{aligned} D_U &= \theta_2 \left(\eta D_\mathrm{e} + (1-\eta) D_\mathrm{n}\right), \quad U \in \{\mathrm{S}_2, \mathrm{M}_{\mathrm{o},2}\}, \\ D_U &= \theta_3 \rho D_\mathrm{n}, \qquad\qquad\qquad\quad U \in \{\mathrm{S}_3, \mathrm{M}_{\mathrm{o},3}\}, \end{aligned} \tag{21}$$

where ρ stands for the perforation level of the membrane expressed as the volume fraction of the holes, θ_2 and θ_3 are the tortuosities defining the structural properties of the corresponding media.

Similar approach for estimating the effective diffusion coefficients was also applied to formulating the two-dimensional model of the considered biosensor (Baronas et al., 2011) and to modelling the biosensor with the perforated membrane in the one-dimensional space (Petrauskas and Baronas, 2009).

NUMERICAL SIMULATION

The proposed mathematical model was formulated as an initial boundary value problem with PDEs containing non-linear terms representing reactions. Analytical solutions of this type of systems are known in very special cases only, therefore numerical methods are usually used to get approximate solutions in wide ranges of the model parameters (Schulmeister, 1990; Baronas et al., 2010). The method of finite differences was employed to solve numerically the equation system of the proposed model (Samarskii, 2001). The domain of the model was discretized by applying a regular mesh to each region Ω_i, $i = 1, 2, 3, 4$, and constant step was used to discretize the time during the simulations.

In simulation, the steady state was assumed already reached if the decay of the biosensor current over time becomes small enough,

$$T_\mathrm{R} = \min_{j(t)>0} \left\{ t : \frac{d\, j(t)}{d\, t} \times \frac{t}{j(t)} < \varepsilon \right\}. \tag{22}$$

The dimensionless decay rate $\varepsilon = 0.01$ was used in the simulations presented in this paper. The current density $j(T_\mathrm{R})$ was assumed as the steady state biosensor response.

The following values of the model parameters were used as a basic configuration of the considered biosensor and were kept constant in all the simulations:

$$\begin{gathered} d_1 = 10^{-7}\,\mathrm{m}, \;\; d_2 = 4 \times 10^{-7}\,\mathrm{m}, \;\; d_4 = 1.5 \times 10^{-4}\,\mathrm{m}, \\ E_0 = 4.55 \times 10^{-2}\,\mathrm{mol\,m^{-3}}, \;\; n_\mathrm{e} = 2, \;\; \eta = 0.5, \\ D_\mathrm{e} = 3 \times 10^{-10}\,\mathrm{m^2 s^{-1}}, \;\; D_\mathrm{n} = 2D_\mathrm{e}, \;\; \theta_2 = 1/3, \\ k_1 = 6.9 \times 10^{2}\,\mathrm{m^3 mol^{-1} s^{-1}}, \\ k_2 = 6.9 \times 10^{4}\,\mathrm{m^3 mol^{-1} s^{-1}}. \end{gathered} \tag{23}$$

The adequateness of the proposed model was evaluated by comparing the simulated responses with the responses of the corresponding physical experiments. The results of the comparison are shown in figure 2.

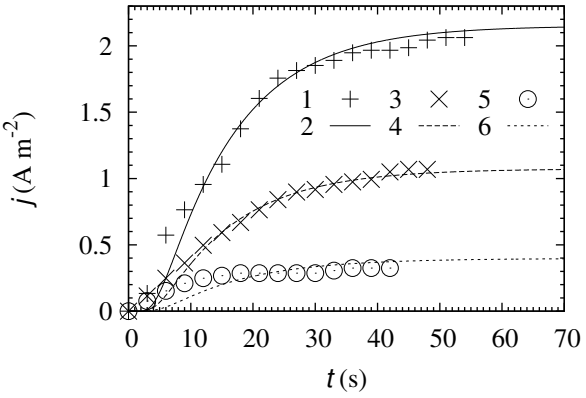

Figure 2: Biosensor current densities obtained experimentally (1, 3, 5) and numerically (2, 4, 6) at $\rho = 0.0625$, $\theta_3 = 0.5$, $d_3 = 10^{-5}$ m and the following concentrations of the substrate and the mediator: $M_0 = 0.2$, $S_0 = 9.9$ (1, 2), $M_0 = 0.05$, $S_0 = 4.98$ (3, 4), $M_0 = 0.005$, $S_0 = 1.99\,\mathrm{mol\,m^{-3}}$ (5, 6). The other parameters were as defined in (23)

As one can see in figure 2, the simulated responses of the biosensor are close to the results of the corresponding physical experiments. When approaching the steady state, the corresponding current densities differ not more than 10%. Similar accuracy of the simulation was observed when simulating operation of the considered biosensor using the two-dimensional model (Baronas et al., 2011). However, the two-dimensional model is much more computational resource consuming. An individual numerical simulation runs approximately 25 hours using the two-dimensional model and approximately 5 minutes using the corresponding one-dimensional model for the biosensor configurations employed in the experiments presented in figure 2. The simulations were performed on a computer with Intel® Core™ i5-540M (2.53 GHz) CPUs, each simulation running on one CPU only.

The two-dimensional model takes into consideration the geometry of the perforated membrane, while the perforation topology is approximated by introducing the effective diffusion coefficients in the one-dimensional model. Therefore, the one-dimensional model can be considered as an approximation of the corresponding two-dimensional one. The two-dimensional model was reduced by introducing two perforation parameters: the perforation ratio ρ and the tortuosity θ_3.

In order to investigate the conditions under which the one-dimensional mathematical model can be applied to an accurate simulation of the biosensor response, a number of simulations was performed and the modelling error of the one-dimensional model was calculated, assuming the two-dimensional model as a precise one,

$$\nu = \frac{J - J_{2\mathrm{D}}}{J_{2\mathrm{D}}}, \tag{24}$$

where $J_{2\mathrm{D}}$ is the density of the steady state current obtained by using the two-dimensional model formulated in (Baronas et al., 2011). A similar approach to a comparison of one and two-dimensional models was also used in (Petrauskas and Baronas, 2009).

RESULTS AND DISCUSSION

The accuracy of the proposed one-dimensional model (6)–(19) was evaluated for different values of the parameters of the geometry of the perforated membrane. The biosensor response was simulated and the modelling error ν was calculated at different values of the perforation ratio ρ, the tortuosity θ_3 and the thickness d_3.

Impact of the Perforation Level

The dimensionless perforation level ρ depends on the topology and the form of the holes in the membrane. In the case of two-dimensional modelling, the holes were modelled by right cylinders of uniform diameter and spacing, forming a regular hexagonal pattern. The corresponding one-dimensional modelling treats the membrane as a homogeneous medium with the corresponding effective (averaged) diffusion coefficients. In order to investigate the impact of the perforation geometry on the modelling error ν, the numerical simulations were performed using the one and two-dimensional models at various levels of the membrane perforation. The simulations of the biosensor response were repeated for the same concentrations of the substrate and the mediator as in the physical experiments depicted in figure 2. Figure 3 shows the calculated values of the one-dimensional modelling error ν.

As one can see in figure 3, the absolute value $|\nu|$ of the modelling error is less than 10% when the perforation level ρ is greater than 0.002. The real biosensor was modelled at the perforation level $\rho = 0.0625$ (see figure 2). At this value of the level ρ the modelling error ν is approximately equal to 0.075. Similar modelling errors

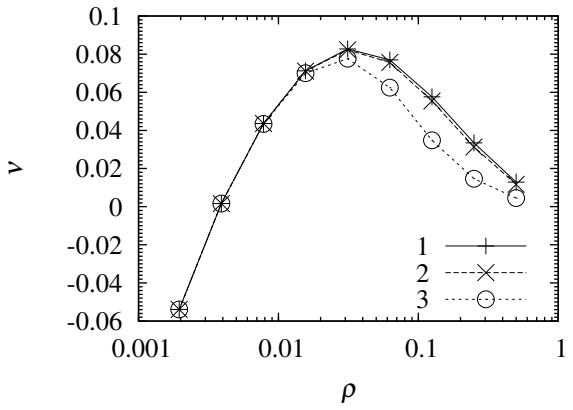

Figure 3: The dependence of the one-dimensional modelling error ν on the membrane perforation level ρ at the tortuosity $\theta_3 = 0.5$, the thickness $d_3 = 10^{-5}$ m and the following concentrations of the substrate and the mediator: $M_0 = 0.2,\ S_0 = 9.9$ (1), $M_0 = 0.05,\ S_0 = 4.98$ (2), $M_0 = 0.005,\ S_0 = 1.99\,\mathrm{mol\,m^{-3}}$ (3). Values of other parameters are defined in (23)

are usually admissible for an investigation of the peculiarities of the biosensor response (Baronas et al., 2010). When the perforation level ρ decreases below 0.002, the error escalates.

Impact of the Tortuosity in the Perforated Membrane

The tortuosity θ_3 of the perforated membrane varies due to the structural properties of the carbon nanotubes sinked into the holes. The tortuosity impacts the effective diffusion coefficient of the substances in the perforated membrane. In order to investigate the impact of the tortuosity on the accuracy of the one-dimensional model, multiple numerical experiments were performed using both models, and the relative error ν of the one-dimensional modelling was calculated. The simulation results are shown in figure 4.

As one can see in figure 4, the error ν of the one-dimensional modelling decreases with decreasing the tortuosity θ_3. The maximum error reaches at the theoretical maximum tortuosity $\theta_3 = 1$. Although the error ν is quite high ($\nu \approx 0.12$) at $\theta_3 = 1$, it is still at the level allowing one to use the one-dimensional model for approximate estimations of the biosensor behaviour.

Impact of the Perforated Membrane Thickness

The thickness of the perforated membrane influences the flux of the substrate and the mediator from the bulk to the active region of the biosensor. The role of the effective diffusion coefficients in the perforated membrane increases with increasing the thickness d_3. In order to investigate the impact of the thickness d_3 of the perforated membrane on the one-dimensional modelling error ν, multiple numerical simulations were performed by changing the thickness d_3 from $0.1\,\mu\mathrm{m}$ up to $0.1\,\mathrm{mm}$. Figure 5 presents the calculated values of the error ν.

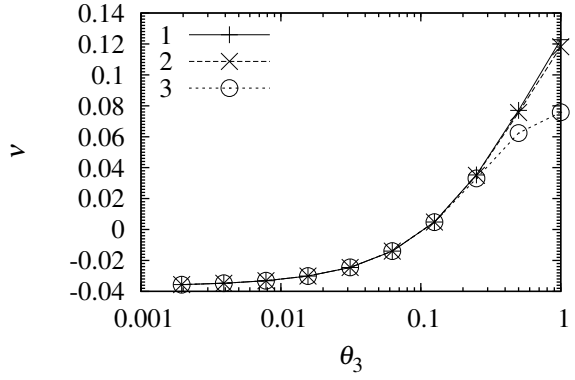

Figure 4: The modelling error ν versus the membrane tortuosity θ_3 calculated at the perforation level $\rho = 0.0625$ and the thickness $d_3 = 10^{-5}\,\mathrm{m}$. The other parameters and the notation are the same as in figure 3

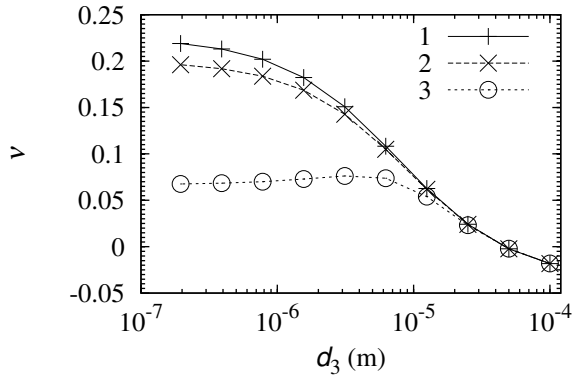

Figure 5: The modelling error ν versus the membrane thickness d_3 calculated at the perforation level $\rho = 0.0625$ and the tortuosity $\theta_3 = 0.5$. The other parameters and the notation are the same as in figure 3

One can see in figure 5 that the modelling error ν is a monotonous decreasing function of thickness d_3 for the higher concentrations of the substrate and the mediator (curves 1 and 2) and is a non-monotonous function in the case of the low concentrations (curve 3). However, the corresponding absolute value $|\nu|$ is a non-monotonous function of d_3 for all the considered concentrations. Only when the perforated membranes is relatively tick ($d_3 > 5\,\mu\mathrm{m}$), the proposed one-dimensional model can be successfully applied to predicting the biosensor response.

CONCLUSIONS

The proposed one-dimensional mathematical model (6)–(19) can be successfully used to simulate the response of the biosensor based on the carbon nanotube electrode at practical configurations of the biosensor operation (figure 2).

The accuracy of the simulated response considerably depends of the geometry of the outer perforated membrane. The mathematical model (6)–(19) accurately describes the biosensor action for relatively thick ($d_3 > 5\,\mu\mathrm{m}$, figure 5) perforated membranes of moderate as well as high perforation level ρ ($\rho > 0.002$, figure 3). Otherwise, the corresponding two-dimensional mathematical model should be used (Baronas et al., 2011), though computational resource consuming.

ACKNOWLEDGEMENTS

This research is funded by the European Social Fund under the Global Grant Measure, Project No. VP1-3.1-ŠMM-07-K-01-073/MTDS-110000-583.

The authors are grateful to Dr. J. Razumienė for the experimental data and Prof. J. Kulys for valuable discussions as well as his contribution to modelling of biosensors.

REFERENCES

Ahammad, A. J. S., Lee, J.-J., and Rahman, M. A. (2009). Electrochemical sensors based on carbon nanotubes. *Sensors*, 9(4):2289–2319.

Amatore, C., Oleinick, A., Svir, I., da Mota, N., and Thouin, L. (2006). Theoretical modeling and optimization of the detection performance: a new concept for electrochemical detection of proteins in microfluidic channels. *Nonlinear Analysis: Modelling and Control*, 11(4):345–365.

Bakhvalov, N. and Panasenko, G. (1989). *Homogenisation: Averaging Processes in Periodic Media*, volume 36 of *Mathematics and its Applications*. Kluwer Academic Publishers, Dordrecht.

Balasubramanian, K. and Burghard, M. (2006). Biosensors based on carbon nanotubes. *Analytical and Bioanalytical Chemistry*, 385(3):452–468.

Baronas, R., Ivanauskas, F., and Kulys, J. (2010). *Mathematical Modeling of Biosensors*, volume 9 of *Springer Series on Chemical Sensors and Biosensors*. Springer, Dordrecht.

Baronas, R., Kulys, J., Petrauskas, K., and Razumiene, J. (2011). Modelling carbon nanotube based biosensor. *Journal of Mathematical Chemistry*, 49:995–1010.

Iijima, S. (1991). Helical microtubules of graphitic carbon. *Nature*, 354:56–58.

Lyons, M. E. (2009). Transport and kinetics at carbon nanotube – redox enzyme composite modified electrode biosensors. *International Journal of Electrochemical Science*, 4(1):77–103.

Petrauskas, K. and Baronas, R. (2009). Computational modelling of biosensors with an outer perforated membrane. *Nonlinear Analysis: Modelling and Control*, 14(1):85–102.

Razumienė, J., Gurevičienė, V., Barkauskas, J., Bukauskas, V., and Šetkus, A. (2009). Novel combined template for amperometric biosensors with changeable selectivity. In *Biodevices 2009: Proceedings of the international conference on biomedical electronics and devices*, pages 448–452.

Samarskii, A. A. (2001). *The Theory of Difference Schemes*. Marcel Dekker, New York-Basel.

Scheller, F. and Schubert, F. (1992). *Biosensors*. Elsevier, Amsterdam.

Schulmeister, T. (1990). Mathematical modelling of the dynamic behaviour of amperometric enzyme electrodes. *Selective Electrode Reviews*, 12:203–260.

Turner, A. P. F., Karube, I., and Wilson, G. S. (1987). *Biosensors: Fundamentals and Applications*. Oxford University Press, Oxford.

Whitaker, S. (1999). *The Method of Volume Averaging*, volume 13 of *Theory and Applications of Transport in Porous Media*. Kluwer Academic Publishers, Boston.

Wollenberger, U., Lisdat, F., and Scheller, F. W. (1997). *Frontiers in Biosensorics 2, Practical Applications*. Birkhauser Verlag, Basel.

AUTHOR BIOGRAPHIES

KAROLIS PETRAUSKAS was born in 1981 in Vilnius. He is a lecturer at Vilnius University, Department of Software Engineering. Petrauskas obtained his MSc degree in 2006 and his PhD degree in Computer Science in 2011 from the Vilnius University. His research interests are in computational modelling of biosensors. His e-mail address is `karolis.petrauskas@mif.vu.lt`.

ROMAS BARONAS was born in 1959 in Kybartai, Lithuania. He is a professor and serves as chair of the Department of Software Engineering at Vilnius University. Prof. Baronas received his MSc degree in Applied Mathematics in 1982 and then obtained his PhD degree in Computer Science in 2000 from the Vilnius University. His teaching and research interests lie in the areas of database systems and computational modelling of biochemical processes. His e-mail address is: `romas.baronas@mif.vu.lt` and his personal web-page can be found at `http://www.mif.vu.lt/~baronas`.

eRAMZES – NOVEL APPROACH FOR SIMULATION OF REACTIVE MOLDING PROCESS

Lukasz Matysiak, Robert Platek, Michal Banas and Robert Sekula
ABB Corporate Research
Starowislna 13A Street, Krakow 31-038, Poland
E-mail: lukasz.matysiak@pl.abb.com

KEYWORDS
Reactive molding, Computational Fluid Dynamics, Finite Element Method, Automated meshing, Web-based computations.

ABSTRACT

This paper describes a unique multiphysics simulation tool allowing one to analyze and optimize reactive molding process used for the production of electrical insulation (in the form of epoxy resin embedding) in many power products. The presented methodology differs from the standard approach, since it excludes the requirement for high end-user's knowledge and experience in the area of CFD (Computational Fluid Dynamics) and mechanical simulations. The role of the tool user is limited only to the definition of CAD geometry and process parameters via user-friendly Website. The remaining operations involved in numerical computations, including CAD geometry analysis and discretization, solving and post-processing, are executed automatically and the simulation results are published online. In this way the presented tool gives engineers an opportunity to verify the product/mold design and manufacturing process prior to the production launching or to improve the existing solutions without time-consuming and expensive experimental trials. In addition, the time needed to perform simulation (especially to prepare numerical mesh) is significantly shortened.

INTRODUCTION

Reactive molding process is an excellent area where advanced computer simulations can be utilized to design, optimize and visualize products digitally and evaluate different design concepts before incurring the cost of physical prototypes. This is a typical virtual prototyping approach (De Paolis et al. 2007) that on the one hand leads to the cost decrease and on the other hand provides useful information about highly complex phenomena taking place during reactive molding process. This, in turn, allows one to detect technological problems such as premature gelation, undesired weld-line locations, air traps or cracks (Wang et al. 1991, Macosko 1989, Grindling and Gehrig 1998) even prior to the mold manufacturing.
In the traditional approach to the analysis of the reactive molding process (Sekula et al. 2000) all design stages are executed manually by engineers utilizing different autonomous computer programs that are not directly linked to each other. These operations are time-consuming and require from the user a specialized expertise in many areas connected with numerical modeling. In the meantime, taking into consideration the industrial scale and complexity of products geometries and complicated physical phenomena taking place during the described technological process it is expected, especially by business units often located far away from Research & Development or Technical Centers, to possess an access to automated method (including generation of Finite Volume Method and Finite Element Method meshes, CFD and mechanical computations, reporting) providing high quality and reliable numerical simulations of the reactive molding process.
As a consequence, a new Web-based and automated tool linking several state of the art numerical software, called eRAMZES, has been developed to give engineers, even not familiarized with computer-aided-engineering problems, an online and, hence, unlimited access to advanced reactive molding simulations (Rajca et al. 2010a, Rajca et al. 2010b, Rajca et al. 2011). This opened totally new horizons for the analysis and optimization of the products manufactured in reactive molding technology.

BASIC PRINCIPLES OF THE REACTIVE MOLDING PROCESS

The mentioned automated simulation tool is dedicated to the analysis of products manufactured in APG (Automated Pressure Gelation) process, which is one of the leading reactive molding technologies (Sekula et al. 2003). In this process, which is presented schematically in Figure 1, two or more liquid reactants with additional components are mixed in the first step. Then, after homogenization and degassing, the mixture is introduced by injection system into the heated mold (filling stage). Polymerization of the resinous material (curing stage) results in its phase change from the liquid form to the solid body (final product shape). Afterwards, de-molding stage occurs and product is placed most often in a tunnel furnace (Ashmad et al. 2006) (post-curing stage) in order to finish the curing process and finally to release thermal and chemical stresses applying gradual product cooling.

Proceedings 26th European Conference on Modelling and Simulation ©ECMS Klaus G. Troitzsch, Michael Möhring, Ulf Lotzmann (Editors)
ISBN: 978-0-9564944-4-3 / ISBN: 978-0-9564944-5-0 (CD)

MATHEMATICAL MODELING OF THE REACTIVE MOLDING PROCESS

The complexity of the reactive molding process is presented in Figure 2 illustrating different phenomena taking place during all stages involved in APG technology, i.e. filling, curing and post-curing. Each phenomenon is reflected in an appropriate mathematical model implemented in the developed simulation tool. In the case of CFD analysis (run in a commercial CFD software ANSYS FLUENT) one have to deal not only with numerically unstable multiphase flow calculations, but also with the kinetics of curing reaction and conjugate heat transfer. Additionally, because of the dynamics of the chemical reaction and complexity of the resulting thermal effect, an accurate modeling of the stresses and deformations during mechanical analysis (run by using another commercial application dedicated to structural analyses, i.e. ABAQUS) is not an easy task.

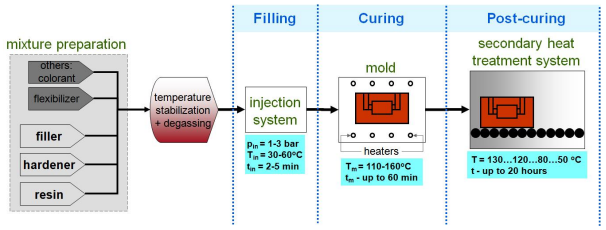

Figure 1: Scheme of the reactive molding process

One can find in the following part of this paper a brief description of models used in fluid mechanics, thermal and mechanical calculations offered by the presented tool as well as in materials characterization (Sekula et al. 2003).

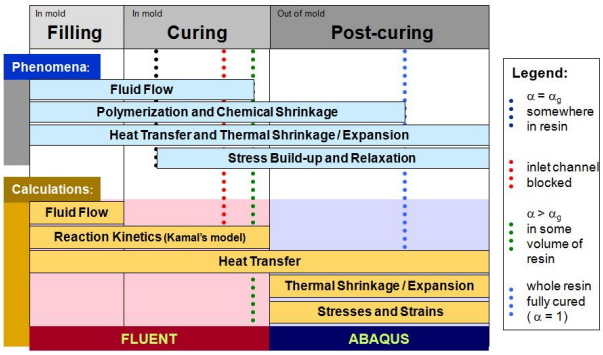

Figure 2: Complex nature of the APG process

CFD simulations

Because of the principle of the conservation of material the solution must satisfy the continuity equation:

$$\frac{\partial \rho}{\partial t} + \nabla \cdot (\rho u) = 0 \qquad (1)$$

where t is time, ρ is density and u velocity of the fluid. From Newton's second law one can obtain the dynamical equation describing the fluid motion, namely the momentum equation:

$$\rho \frac{Du}{Dt} = \nabla \cdot (\tau) - \nabla p - \rho g \qquad (2)$$

where p is pressure, τ is the stress tensor (whose components are the function of viscosity η and spatial derivatives of u), g is acceleration due to the gravity and Du/Dt term is the substantial (or particle) derivative of the velocity computed by following a particle in the flowing substance.

Due to the presence of two different fluids during the mold filling stage (epoxy resin and air) volume of fluid method (VOF) is used to predict accurately the location of the interface between both phases. In the VOF approach the volume fraction of the resin a in each cell is solved from the conservation equation:

$$\frac{\partial a}{\partial t} + \nabla \cdot (au) = 0 \qquad (3)$$

where $a = 0$ means no epoxy resin in the cell, $0 < a < 1$ means partly filled cell, $a = 1$ means cell filled totally with epoxy resin and the volume fraction of air b is the complement of a (i.e. $b = 1\text{-}a$).

The nature of the reactive molding process causes that it is important to monitor the course of polymerization reaction of thermosetting epoxy resin. For this purpose curing kinetics model in the form of Kamal-Sourour equation is applied (Kamal and Sourour 1973, Kamal et al. 1973) and implemented in ANSYS FLUENT by using User Defined Function and User Defined Scalar functionalities (ANSYS Help 2010). According to this model degree of curing α at time t is defined as:

$$\alpha = \frac{H(t)}{H_{\Sigma}} \qquad (4)$$

where $H(t)$ is the heat of reaction released until time t and H_{Σ} is the total heat of reaction.

The progress of the curing phenomenon is linked to the mass conservation and thus the degree of curing α is governed by its own un-steady state conservation equation:

$$\frac{\partial (\rho \alpha)}{\partial t} + \nabla \cdot (\rho u \alpha) = S_a \qquad (5)$$

where S_a is the source term of degree of curing based on the mentioned Kamal-Sourour model expressed by the equation below:

$$S_a = \rho (k_1 + k_2 \alpha^m)(1 - \alpha)^n \qquad (6)$$

where m and n are the model constants, whereas k_1 and k_2 are the reaction rate constants calculated as follows:

$$k_i = A_i e\left(\frac{-E_i}{RT}\right) \quad (7)$$

where i = 1 or 2, A_i is the pre-exponential factor, E_i is the activation energy, R is the universal gas constant and T is the absolute temperature. It is worth stressing that all parameters of Kamal-Sourour model are determined experimentally, usually by using Differential Scanning Calorimetric technique, and their values are characteristic for each epoxy resin.
Conservation of energy is guaranteed by the energy equation in the form:

$$\rho c_p\left(\frac{\partial T}{\partial t} + u \cdot \nabla T\right) = \nabla \cdot (k \nabla T) - p \nabla \cdot u + \nabla \cdot (\tau \cdot u) + S_T \quad (8)$$

where c_p is the specific heat capacity, k is the thermal conductivity and the source term of thermal energy is calculated as $S_T = S_a H_\Sigma$.

Data transfer between CFD and mechanical stage

As soon as the CFD calculations are completed, the results (temperature and degree of curing) have to be transferred from CFD mesh (Finite Volume Method) into structural mesh (Finite Element Method) for mechanical calculations. Since no adequate direct data transfer codes are available on the market, an external data transfer procedure called MapMesh was developed in the course of this study and successfully implemented to perform the solution mapping between CFD and structural numerical models. More detailed description of the CFD simulation approach and the data transfer mechanism is provided in Isotalo et al. 2001.

Mechanical simulations

The structural results are obtained in a transient and coupled thermal and stress analyses conducted sequentially as presented in Figure 3. In the first step the effects related to the heat transfer are determined and then chemically driven deformations are calculated in the static analysis. Finally, this leads to the definition of the strains and stresses as a function of the process time.

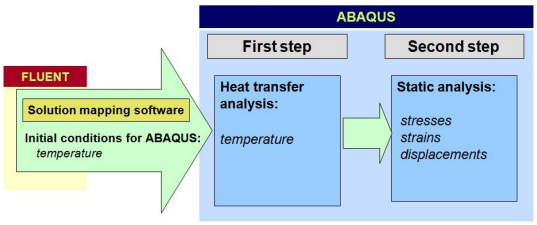

Figure 3: Sequential calculations in ANSYS FLUENT and ABAQUS

The chemical shrinkage model was developed based on the assumption that the total strain increment $\Delta\varepsilon^{\text{Total}}$ (in each time-step) can be expressed as a sum of mechanical $\Delta\varepsilon^{\text{Mechanical}}$ and thermal $\Delta\varepsilon^{\text{Thermal}}$ components:

$$\Delta\varepsilon^{\text{Total}} = \Delta\varepsilon^{\text{Mechanical}} + \Delta\varepsilon^{\text{Thermal}} \quad (9)$$

ABAQUS software allows defining thermal component by applying a user-defined subroutine (UEXPAN). This component covers both chemical and thermal effects influencing the material density:

$$\Delta\varepsilon^{\text{Thermal}} = \sqrt[3]{\frac{\rho}{\rho'}} - 1 \quad (10)$$

where ρ' means actual density and ρ is the value of density from the previous time-step. It is worth stressing that in order to realize that stage of calculations it was necessary to apply the dependence of temperature and degree of curing on density. This correlation was derived based on the experimental measurements. More information about the modeling of epoxy resin shrinkage can be found in Isotalo et al. 2004.

WEB-BASED TOOL FOR AUTOMATED REACTIVE MOLDING SIMULATIONS

The architecture of eRAMZES tool

eRAMZES tool is controlled by a dedicated multifunctional Web platform linking a number of applications interacting between each other. Among them one can find software available on commercial conditions (CAD software, pre-processors, processors and post-processors) and developed specially for the purpose of simulations automation, which are fully customizable.
The general workflow of eRAMZES tool is presented schematically in Figure 4. Green boxes illustrate steps that require interaction with user, while violet boxes indicate fully automated operation of the tool. One can notice that engineer is obliged only to define the geometrical model and planned process parameters, while the remaining computational steps are executed in an automated manner. When the simulation finishes and results are visualized, the user decides whether the analyzed product and process fulfills requirements or further optimization is needed. In this way the developed approach allows engineers to design reactively molded products in an automated way by using advanced CFD and mechanical methods without expert's knowledge related to numerical modeling.

The automation applied in the presented tool is based on the concept of developed Watcher and Launcher programs. In general, Watcher software observes the progress of each task executed by the tool by analyzing the task status ('ready to start', 'work in progress' or 'finished') and controls the availability ('busy' or 'free to run' status) and operation of Launchers performing three specific tasks, namely:

- 'Pre' – preparation of the starting directory for the specific program (e.g. pre-processor or solver) maintained by a given Launcher;
- 'Launch' – launching the program;
- 'Post' – cleanup and file management after termination of the program operation.

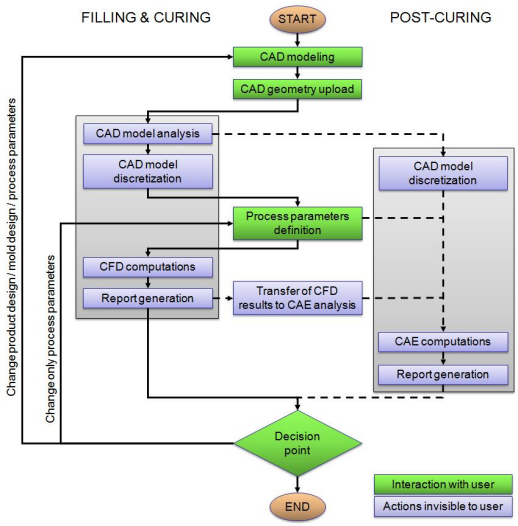

Figure 4: Architecture of the presented approach

CAD modeling

The very first step of the analysis that must be taken by user is CAD modeling, preferably in advanced CAD system like for example SolidWorks. This is a crucial operation, since engineer decides at this stage about the geometrical components, their features and possible simplifications, which will be taken into consideration during computations. Due to a big significance of this analysis step several recommendations have been worked out to guide users in the preparation of geometrical models. This concerns among others proper labeling of the geometrical parts, since only regions starting with "fluid" or "solid" prefixes are included in further simulation steps (e.g. fluid_cavity, solid_mold, solid_insert_steel etc.). In addition to that, all regions must be represented as solid bodies without Boolean operations performed on them (see Figure 5), geometry should be properly positioned in Cartesian coordinate system (e.g. symmetry plane along YZ plane for X = 0) and the prepared model has to be exported to STEP file.

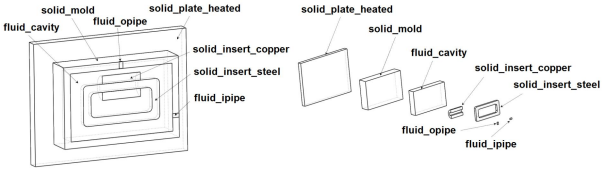

Figure 5: Proper labeling (left) and structure (right) of geometrical parts

Case creation

In the consecutive step the simulation case must be created by user via the mentioned Web platform as presented in Figure 6. This requires connection and login to the eRAMZES Website, choice of the file with the CAD geometry prepared in the previous step and activation (if applicable) of the model symmetry option and mechanical calculations.

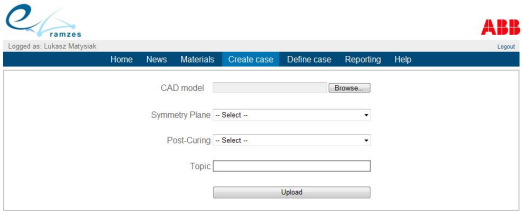

Figure 6: Case creation Web page

CAD model analysis

The uploaded CAD geometry is then analyzed automatically to detect parts included in the model and marked by user with "fluid" and "solid" prefixes at the CAD modeling stage. CAD model analysis is extremely important, because the gathered data is used further during the meshing and solving operations. Additionally, based on these information an individual Website is generated to allow user to enter the process parameters.

Numerical model preparation

Geometry discretization is the next fully automated step executed by eRAMZES, however it should be stressed that this stage was recognized as the most challenging part of the tool development, mainly due to high complexity and variety of the geometries of products manufactured in the reactive molding technology. Additionally, the mentioned differences in CFD and mechanical calculations made it necessary to perform the meshing operations in different meshing software, i.e. HyperMesh and ABAQUS for CFD and mechanical module respectively.

In the proposed approach, the mentioned Launchers initiate and control the discretization procedure in each of the mentioned pre-processors. The process

automation is ensured by scripts including a sequence of commands. In this way specific orders are given to the meshing software like import CAD geometry, clean and repair geometry (removal of holes, fillets, intersections, overlapping surfaces, etc.), discretize geometry (different mesh topologies can be used and consequently either non-structural or structural mesh can be generated), define CFD (e.g. inlet, outlet, convection etc.) and mechanical (e.g. constraints, interactions etc.) boundary conditions, export output file in CAS and INP formats for ANSYS FLUENT and ABAQUS solvers respectively.

One can find below two exemplary geometries of medium-voltage products that were analyzed by using eRAMZES tool. Figure 7 depicts the geometrical model of outdoor embedded pole and the CFD mesh generated, while Figure 8 illustrates the geometrical model of current transformer and the mechanical mesh prepared. It can be seen that high quality mesh was created automatically in both cases in spite of the complexity of components included in both geometries.

An additional and simultaneously one of the biggest benefits coming with the meshing automation is the time needed to generate numerical grids. eRAMZES tool spent only 30 minutes to decompose the current transformer geometry into almost 3 million of CFD mesh elements and 300 thousand of mechanical mesh elements (by using PC computer equipped with two 2.5 GHz dual-core CPUs and 8 GB RAM), while it takes usually days or sometimes even weeks for CAE engineers to generate manually the numerical mesh for such complex geometries. This allows eRAMZES users to focus on solving engineering problems rather than spending time on models discretization.

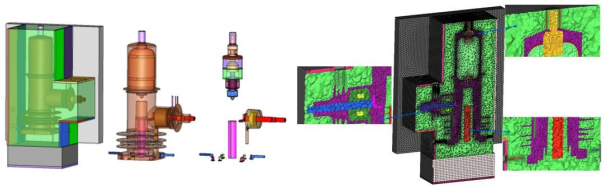

Figure 7: Geometry of outdoor pole (left) and its discretization in HyperMesh (right)

Figure 8: Geometry of current transformer (left) and its discretization in ABAQUS (right)

Process parameters definition

Definition of the process parameters is another step of the reactive molding analysis with the eRAMZES tool that requires input from the user side. The Web application uses information gathered during the CAD model analysis and creates dynamically a dedicated Website (as shown in Figure 9) allowing user to enter all parameters required to configure the simulation. At this stage both the process parameters, material properties, materials assignment to product parts and finally, numerical parameters related to mechanical computations are selected. Among the process parameters one can find injection parameters (e.g. filling time or injection velocity), thermal parameters (e.g. temperature of injected material, temperature of heaters, initial temperatures before injection), ambient conditions (e.g. air temperature or air convection intensity), post-curing procedure (time and temperature of each cooling stage). All these settings are saved by the tool in the case folder and the automated computations can be started.

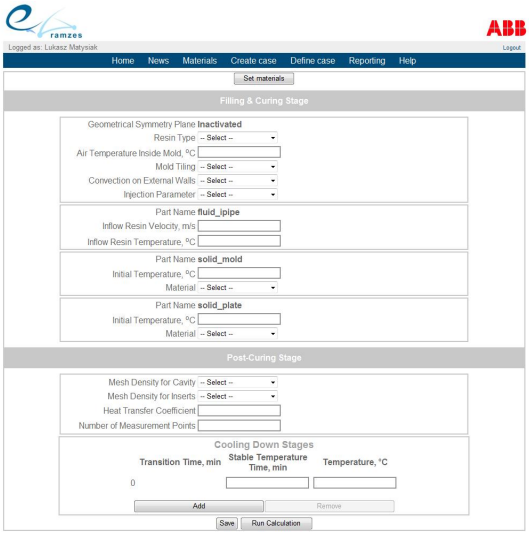

Figure 9: Definition of the process parameters

Computations

Processing (or solving) is the subsequent fully automated stage of the simulation process, executed by using scripts generated automatically and individually for each simulation case. Processors controlled again by Launchers operate in a batch mode to shorten the computational time remaining one of the critical issues reported by users.

At the very beginning of the solving step the discretized geometry is imported into the CFD processor – ANSYS FLUENT. Next, information provided by user during CAD modeling stage and process parameters definition are assigned to the numerical model to specify material for each geometrical component and to define initial conditions, boundary conditions, operating conditions and materials properties. Additionally, the solver

configuration is performed including the choice of mathematical models used in the reactive molding simulation (both built-in models like e.g. turbulence model, flow model etc. as well as additionally implemented models like curing kinetics model) and numerical parameters to ensure reliable and accurate solution of these models. In the consecutive step the transient numerical computations for filling and curing stage are conducted and, once done, results are generated and exported.

The computations can be continued if user decided to include post-curing simulation. In such case temperature results obtained for the end of curing stage are translated by using the mentioned MapMesh software and transferred to the mechanical solver ABAQUS to constitute the starting point for post-curing computations.

The first step taken by ABAQUS software is the geometrical model import and repair (if needed). Next, material properties are assigned to the geometrical parts and the analysis steps and time are specified according to the user input provided during CAD modeling and process parameters definition. In the subsequent stage boundary conditions (the mentioned data from ANSYS FLUENT, constrains, etc.) and interactions between geometrical parts are set and the mesh is generated based on the information about the mesh density specified earlier by user. Finally, the input file is prepared and submitted to solver for computations and, once finished, results are generated and exported.

It is worth noticing that the solution convergence is monitored and controlled automatically, what was recognized as one of the biggest challenges during the tool development and became one of the most significant achievements. The reason for this is that the reactive molding simulation is known as numerically instable, even in case of manual approach, due to the complexity of phenomena involved in the process. In the meantime, eRAMZES ensures excellent solution stability without any user actions.

Results visualization

Post-processing is the last step of the automated reactive molding analysis with eRAMZES tool. The simulation results are further processed in a batch-mode in ANSYS CFD-Post and built-in ABAQUS post-processor controlled by Launchers. For this purpose master macros, recorded for each post-processor individually, are executed for each simulation case making the results visualization process automated and repeatable irrespective of the product under consideration.

In the next step, the obtained results are presented to user in different forms like movies, pictures and charts via the Website or as a printable *PDF* document. It is worth stressing that the way of results visualization can be modified to meet the user expectations, what constitutes another advantage of the presented approach. Exemplary results generated for CFD and mechanical analysis are presented in Figure 10 and Figure 11 respectively.

The developed way of results visualization allows users to observe in details the course of the reactive molding process and capture effects inside the mold and product, which cannot be detected in a normal production process or in an experimental way. This includes information about the flow pattern of epoxy resin during the filling stage, distribution of temperature in time during all process stages, distribution of degree of curing in time during the filling and the curing stage, distribution of deformations, stresses and strains during the post-curing stage.

The acquired knowledge is then used by engineer to decide whether further process and product optimization is needed or not. In the first case two options are possible, namely modification of the process parameters for the same product and mold geometry (CAD model upload, analysis and discretization is not repeated) or redesign of the product and/or mold (analysis process starts from the very beginning).

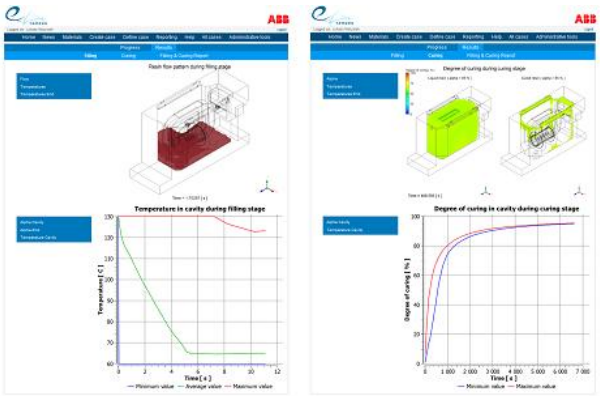

Figure 10: Results generated for filling stage (left) and curing stage (right)

Figure 11: Results generated for post-curing stage

SUMMARY

The presented novel Web-based tool combining CFD and mechanical simulations can be successfully utilized both for the design of new and optimization of the existing products manufactured in the reactive molding technology. The tool allows users to observe the influence of changes in the product and/or mold design as well as in the configuration of the process parameters without any interference in the real production process. This was achieved by high quality simulation results presenting details about the process course.

The described automation of meshing and solving operations executed during CFD and mechanical computations allowed one to shorten significantly the total computational time and eliminate the requirement for high user knowledge and experience in the field of numerical simulations. Among the other tool advantages one can notice its user-friendliness, unlimited online access to the tool and the repeatability of the simulation process resulting in manual-error resistance.

All aspects mentioned above lead, on the one hand, to shorter development time of new products manufactured in the reactive molding technology and, on the second hand, to improved quality of the epoxy based components. Moreover, the presented approach can be adapted to provide the possibility to analyze also other manufacturing processes and, consequently, benefit in faster development and optimization of much wider group of power products, not only limited to reactively molded ones.

REFERENCES

De Paolis L.T., A. Agrimi, A. Zocco and G. Aloisio, 2007, *A Feasibility Study on the Use of a Remote Supercomputer in a Collaborative Virtual Environment with Force Feedback*, Proceedings of the 11th WSEAS International Conference on Computers, Agios Nikolaos, Crete Island, Greece, July 26-28.

Wang V.W. and L.S. Turng, 1991, *Simulation of Injection Mold Filling and Curing with Reactive Materials*, SPE Technical Papers, 37.

Macosko C.W., 1989, *Fundamentals of Reaction Injection Molding*, Hanser Verlag.

Grindling J. and M. Gehrig, 1998, *Introduction to FEM Based Computer Simulation to Assist Molding and Casting Processes*, CIBA Speciality Chemicals Inc., Basel.

Sekula R., P. Saj, T. Nowak and K. Kaczmarek, 2000, *3D Computer Simulations of Thermosetting Materials Molding*, SGI Conference, Krakow, Poland.

Rajca R., L. Matysiak, M. Banas and R. Sekula, 2010, *A Novel Simulation Approach for Analyzing Reactive Molding Process*, International Journal of Mathematics and Computers In Simulation, Vol. 4, Issue 4.

Rajca R., L. Matysiak, M. Banas and R. Sekula, 2010, *Web-Based Tool for the Automated 3-D Reactive Molding Simulations*, 2nd International Conference on Manufacturing Engineering, Quality and Production Systems (MEQAPS'10), Constantza, Romania, September 3-5.

Rajca R., L. Matysiak, M. Banas and R. Sekula, 2011, *Industrial Application Of A New CFD Simulation Approach*, 25th European Conference on Modelling and Simulation, Krakow, Poland, June 7-10.

Sekula R., P. Saj, T. Nowak and K. Kaczmarek, 2003, *3-D Modeling of Reactive Moulding Processes: From Tool Development to Industrial Application*, Advances in Polymer Technology, Vol. 22, No. 1.

Kamal M.R. and S. Sourour, 1973, *Kinetics and Thermal Characterization of Thermoset Resin*, Polymer Engineering and Science.

Kamal M.R., S. Sourour and M. Ryan, 1973, *Integrated Therm-rheological Analysis of the Cure of Thermosets*, Proceedings of the 31st Annual Technical Conference, pp. 187-191, Quebec.

ANSYS Help, 2010, ANSYS Inc..

Sekula R., K. Kaczmarek, D. Bednarowski and P. Piekarski, 2002, *Manufacturing of Voltage Transformer Enhanced by 3-D Computer Simulation Tools*, Advances in Polymer Technology, Vol. 25, No. 2, pp. 138-144.

Isotalo P., D. Bednarowski and K. Forsman, 2001, *ABB Internal Report No. AFX01-236*, Vaasa, Finland.

Isotalo P., T. Nowak and D. Bednarowski, 2004, *Reactive Moulding process Modeling: Structural Analysis of Thermoset Insulated Electrical Components*, International Journal of Materials and Product Technology, Vol. 20, No. 4.

AUTHOR BIOGRAPHIES

LUKASZ MATYSIAK graduated in 2007 from the Silesian University of Technology in Gliwice, Poland, where he studied computational methods in thermal engineering. Since then he has been working in ABB Corporate Research Krakow, where he participates in research projects in the area of heat and mass transfer, processing of silicones, epoxy resins and thermoplastics, thermal and CFD simulations. His e-mail address is: lukasz.matysiak@pl.abb.com.

ROBERT PLATEK graduated in 2003 from the University of Technology in Krakow, Poland. He has been working in ABB Corporate Research Center in Krakow since 2004. He works as a scientist and his work is focused on multiphysics simulations (fluid-structure interaction, seismic calculations) and development of the simulation tool for thermal calculations. Mr. Platek has M.Sc. degree. He has authored and co-authored several scientific papers and technical reports. His e-mail address is: robert.platek@pl.abb.com.

MICHAL BANAS graduated in 2000 from Technical University in Kielce (Poland), where he studied Computer

Science. Since then he worked in ABB as an Industrial Research Scientist in Information Technologies in areas of Engineering Collaboration, Transformer Design Automation, ABB Simulation Toolbox System development, Design Visualization, Web Technologies and Thermal Network tools. Moreover he acquired some experience in dielectric analyses of electrical apparatus. His e-mail address is: michal.banas@pl.abb.com.

ROBERT SEKULA graduated in 1990 from the University of Mining and Metallurgy in Krakow, Poland. In 1996 he received Ph.D. in the field of heat engineering and environmental protection. From 1990 to 1996 he was lecturer and scientist at that university. Since 1997 he has been working at the ABB Corporate Research in Krakow as a research scientist. His special fields of interest include environmental science, heat transfer, waste management, as well as polymers processing modeling. He leads the Manufacturing, Mechanics and Material Science group. His e-mail address is: robert.sekula@pl.abb.com.

TOWARDS A MULTI-DIMENSIONAL MODELLING OF COMPLEX SOCIAL SYSTEMS USING DATA MINING AND TYPE-2 NEURO-FUZZY SYSTEM: RELIGIOUS AFFILIATION CASE OF STUDY

Manuel Castañón–Puga, Carelia Gaxiola–Pacheco and Juan Ramón Castro
Facultad de Ciencias Químicas e Ingeniería
Universidad Autónoma de Baja California
Tijuana, Baja California, México.
Email: {puga,cgaxiola,jrcastro}@uabc.edu.mx

Dora–Luz Flores
Facultad de Ingeniería, Arquitectura y Diseño
Universidad Autónoma de Baja California
Ensenada, Baja California, México.
Email: dflores@uabc.edu.mx

Ramiro Jaimes–Martínez
Instituto de Investigaciones Históricas
Universidad Autónoma de Baja California
Tijuana, Baja California, México.
Email: rjaimes@uabc.edu.mx

KEYWORDS

FUZZY AGENTS, DATA MINING, SOCIAL COMPLEXITY, RELIGION AFFILIATION

ABSTRACT

The purpose of this paper is, to describe a work-in process for application of distributed agency methodology to multi-dimensional preference model into a complex social system. This paper shows a study case focused on a modeling system for decision-making on cognitive structure religious affiliation preference. A type-2 neuro-fuzzy approach is used to configure cognitive rules into an agent to build a multi-agent model for social simulation.

INTRODUCTION

The social systems are complex entities that represent a whole that cannot be understood by looking at its parts independently Yolles (2006). Another characteristic is the interdependence of the parts conforming the whole: a change to one of the components in the system may potentially affect all others. Boulding (1956).

The main goal of this part of our research is to develop a computational model of change in religious affiliation that incorporates available mathematical and computational theories that have not been appropriately considered in models of complex social phenomena. Even though applications of Multi-Agent Systems (MAS) have been developed for the social sciences, MAS have been widely considered in some areas such as Artificial Intelligence (AI) Gilbert (2007). The state-of-the-art in computational capabilities has been incorporated in multiple areas Russell and Norvig (2004), particularly as it refers to distributed systems and distributed agencies López et al. (2002).

Previous and Related Work

There are some related work on oriented simulation methodology for modelling complex problems. In Suarez et al. (2008), is proposed "fuzzy agents" to represent agencies that can not be modelled with specific actors. Then, in Suarez and Castanon-Puga (2010) is proposed "distributed agency" as a simulation language for describing social phenomena.

In Suarez et al. (2010) shows an approach to decision-making system based on type-2 fuzzy inference system in order to implement fuzziness on cognitive agents. This model introduces subjectivity and uncertainty in agent perceptions and preferences levels, were decision-making system are influenced by different agencies. Preferences for choosing one option competing with each other, but also were influenced by endogenous and exogenous variables that could affect the levels of uncertainty and, therefore, affect the way the agents interpret the messages.

In Márquez et al. (2011b), a methodology is proposed based on neuro-fuzzy technique, where a data mining procedure based on a neural network are applied to a real data to configure a type-2 fuzzy inference system into an agent.

Some other important work related to these approaches is presented in Mendel and Wu (2010) where we find an example of the application of type-2 fuzzy logic to model a subjective decision-making system or perception.

Data Mining and Neuro–Fuzzy System

An Interval Type-2 Fuzzy Neural Network (IT2FNN) are used for automatically generate the necessary rules. The phase of data mining using Interval Type-2 Fuzzy Logic Systems (IT2FLS) Castillo et al. (2010); Castro et al. (2010) becomes complicated, as there are enough rules to determine which variables one should take into account. The search method of back-propagation and hybrid learning (BP+RLS) is more efficient in other methods, such as

Proceedings 26th European Conference on Modelling and Simulation ©ECMS Klaus G. Troitzsch, Michael Möhring, Ulf Lotzmann (Editors)
ISBN: 978-0-9564944-4-3 / ISBN: 978-0-9564944-5-0 (CD)

genetic algorithms Rantala and Koivisto (2002); Castro et al. (2008).

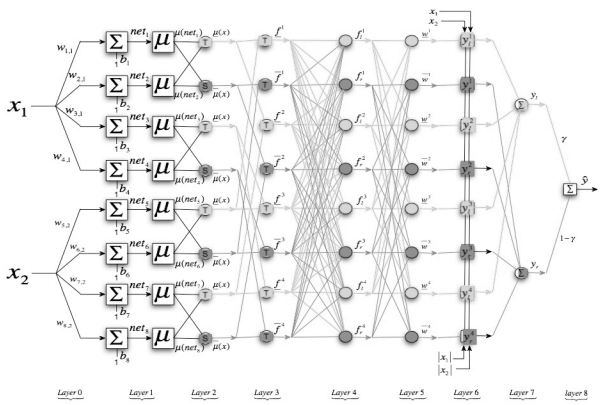

Figure 1: Generation of the necessary rules using an Interval Type–2 Fuzzy Neural Network (IT2FNN).

Since the IT2FNN method seems to produce more accurate models with fewer rules is widely used as a numerical method to minimize an objective function in a multidimensional space, find the approximate global optimal solution to a problem with N variables, which minimize the function varies smoothly Stefanescu (2007).

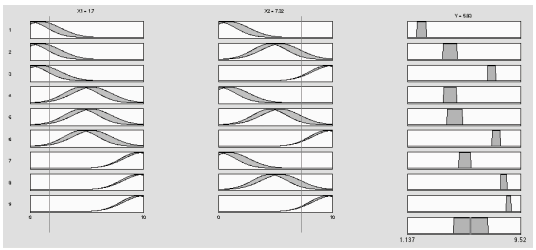

Figure 2: Rules on a Type-2 Fuzzy Inference System.

With the application of this grouping algorithm we obtain the rules, the agent receives input data from its environment and choose an action in an autonomous and flexible way to fulfill its function Peng et al. (2008).

Religious Affiliation

When literature talks about of religious change, usually refers to the attachment or religion affiliation Ortiz (2006). Although some authors have argued that the concept can not be limited to this dimension, membership is one of the most important variables to study the religious phenomena Fortuny (1999).

The religious field is conformed by several dynamics systems. For example, we can identify some organizational entities:

- institutional
- socio-demographic groups
- individual

Within these multiple dimensions interrelated complex processes are occurring, such changes of allegiance, change in commitment and participation, socialization and subjectivity of standards (through doctrines, values, practices), reformulation and affirming traditions. These multiple dimensions shape the religious field, and generically is known as religious change.

Religious Affiliation in México

In México, religious affiliation has undergone major changes since the 1950's until today. Based on population censuses, the growth rates of the evangelical population has been higher than the total Catholic population [1] Jaimes-Martínez (2007).

Baja California has one of the percentages of highest evangelical population of Northern states [2].

CASE OF STUDY

Tijuana is a city located in north-western of México. Belongs to the state of Baja California, and is one of the fastest growing city in the country due to high migration rates. The population is mainly composed by migrants from southern of the country. They came to the border to further job opportunities, or looking to migrate to the United States, staying in the city long time.

Tijuana's multi-cultural and religious complexity

Tijuana is an example of social and religious change. Its boundary condition has been one factor that has become a city in full development and expansion, not only by the strength of the Southern California economy, but by the early efforts to boost manufacturing by the federal government.

These factors, combined with growing internal and international migration, have transformed a town of Tijuana from a town with 12,181 inhabitants in 1930 to one with 1.2 million in 2000[3] Alegría and Ordónez (2002). It was so from NAFTA, Tijuana was consolidated as a major call centres maquiladora industry, with an evident increase in employment and production, but not productivity or living standards and welfare Arias (2008).

According to some authors, the economic balance, social and cultural development of these global processes, regional and local has had complex effects on Tijuana's society, where stands the reconfiguration of identities and new forms of social and cultural reproduction Jiménez (2006).

[1] The evangelical population has experienced rates of 8.90, between 1970 and 1980, while the total population was 3.16. Although at present growth rate 2.46 points, it is still higher than that of the population is Catholic and total population.

[2] Baja California has 7.90% and evangelical population, surpassed only by one of the first entities to which the Protestant missionaries arrived in the nineteenth century, Tamaulipas, to 8.65%. Nationally, the percentage of evangelicals is 5.20%.

[3] Tito Alegría and Gerardo Ordóñez consider the growth process of Tijuana covers from 1930 to 2000, thanks mainly to the economic expansion of Southern California.

In this sense, the religious sphere in Tijuana has a great religious diversification as a result of different waves of migration that have shaped their society. Therefore, religious affiliation is also an indicator to study these processes of reconfiguration and realignment[4] Jaimes-Martínez (2007).

Preference for religious affiliation in Tijuana

The city has a great diversity of faiths and religious traditions. Although more numerous the Christian (Catholic, Protestant, evangelical non-biblical), there are Buddhists, Muslims, Jews and a variety of groups and beliefs generically known as New Age[5].

Considering this, we can say that every group or social stratum in Tijuana has a wide range of choice, or affinity, in the religious field in the city. Each of them is not only an expression of traditions, customs and religious practices of different groups have brought to Tijuana from their places of origin, but the dynamic formulation of these beliefs in the new environment.

Importance of modelling Tijuana habitants religious affiliation

Qualitative tools are used mainly by social scientists to analyze religious change. This preference is justified by explanatory depth they are able to work on the meaning of the action of the subject. However, its explanatory power is limited to the subjects observed, without looking at a larger scale or level, for which we assume a similar behavior.

For larger scales of analysis is necessary to use quantitative tools, which have a greater ability to generalize, but is constrained to observe the direction and motivation for action. Therefore, tools such as computational modeling are an alternative to unite both fields.

METHODOLOGY FOR THE MODELLING OF COMPLEX SOCIAL SYSTEM USING NEURO-FUZZY AND DISTRIBUTED AGENCIES

To build the model of change of religious affiliation will follow the distributed agency methodological steps Márquez et al. (2011a):

1. Determining the levels of agency and their implicit relationships
2. Data mining
3. Generating a rule-set
4. Multi-Agent Modelling (Implementation on a agent based simulation tool)
5. Validating the model
6. A simulation and optimization experiment
7. Analysing the outputs

Although the methodology covers the entire life-cycle of a research process, on this paper we are describing the data mining and generating rule set steps. We are focused on the neuro-fuzzy approach in order to set up a rule set into agents.

MODELLING TIJUANA CITY

The principal difference between MAS and our proposed approach is that in our methodology the space includes transformations performed by a higher level of agency. This upper-level agent is composed of lower-level subcomponents the may enjoy agency in their own right. It is the responsibility of this intermediate agent to present its subcomponents with individual phase-spaces that are tailored to induce the desired behaviour from the lower-level agents which inhabit it, when it chooses according to its own objective function.

Therefore, for our proposed work-in-progress case study, if we consider a municipality an agent, this upper-level agent is composed by subcomponents, which in our case study of the city of Tijuana, Mexico, will be represented by the AGEBS that compose this city. AGEBS is the terminology used to describe the different areas of the city that are in turn are composed of neighbourhoods.

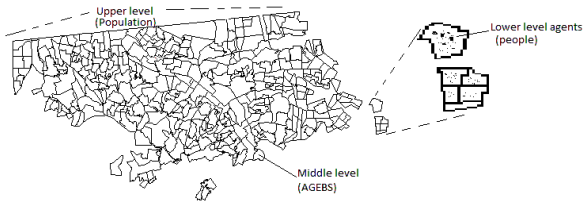

Figure 3: Levels of agents represented on the social system.

Levels of agency

In our study we use three levels of agency: the upper-level agent is represented by the religion groups or organizations, the intermediate agents are represented by the AGEBS and the lower level agents are the individual inhabitants of the city.

Using a recent census of the reunion sites distribution of the different religious organizations operating in the city, we know the exact places where they carry out activities of proselytizing. This information gives us hints of the influence of the presence of organizations in its environment and its impact on socio-demographic variables.

We are looking for relationships between demographic and economic factors (subtracted from AGEBS) and distribution of meeting places of religious organizations. We believe that factors such as poverty, marginalization

[4]Between 1990 and 2000 Tijuana just recorded a growth rate of 8.94 evangelical population, while at the national level was 2.46.

[5]Syncretic movements oriental religions such as Buddhism, introducing ideas of self-motivation, personal growth, alternative medicine, psychology, etc.

and other characteristics related to socio-demographic issues influencing the decision-making system of individuals in a complex and distributed way. Similarly, religious organizations act as agents who are influenced by other agencies distributed.

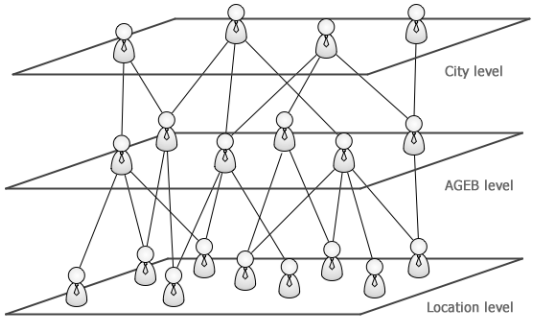

Figure 4: Multiple layers of agents represented on the social system.

Data sets

In the particular case of the city of Tijuana, the data set used came from the Instituto Nacional de Estadistica y Geografia (INEGI), the Mexican governmental organization in charge of gathering data at a federal level including aspects that are geographical, socio-demographic and economical. The data set of the city of Tijuana is divided into 363 areas, known as AGEBS. "The urban AGEB encompass a part or the totality of a community with a population of 2500 inhabitants or more... in sets that generally are distributed in 25 to 50 blocks"INEGI (2006).

The data sets for this case study were originally compiled in an information system that is intrinsically geographical. These systems helped in the generation, classification and formatting of the required data—a fact which facilitates the edition of the different thematic layers of information, in which one can quantify the spatial structure to visualize and interpret the areas and different spatial patterns in Tijuana.

For this paper, we going to use de following variables to exemplify the proposed approach using information from 2010 population census in México INEGI (2010).

- P15YMAS = Population over 15 years old on locations.
- P15YMSE = Population over 15 years old on locations without education.
- GRAPROES = Education.
- PEA = Working population.
- PEINAC = Non working population.
- PCATOLICA = Catholic population on locations.
- PNCATOLICA = Non catholic population on locations.

Neuro-fuzzy inference system

Using the neuro-fuzzy system for the automatic generation of rules, this phase of the data extraction from the data may become complicated, as the process needs to appropriately establish the number of sufficient norms and variables that the study needs to take into account.

Using this grouping algorithm, we obtain the appropriate rule-set assigned to each agent representing an AGEB or a inhabitant of it, the agent receives inputs from its geographical environment and in turn much choose an action in an autonomous and flexible fashion Gilbert (2007); Drennan (2005); Wooldridge and Jennings (1995).

The purpose of this structure without central control is to garner agents that are created with the least amount of exogenous rules and to observe the behavior of the global system through the interactions of its existing interactions, such that the system, by itself, generates an intelligent behavior that is not necessarily planned in advance or defined within the agents themselves; in other words, creating a system with truly emergent behavior Botti and Julian (2003); Russell and Norvig (2004).

From the 2010 census information, we create a Type-2 Fuzzy Inference System as how we could represent different agencies as a decision-making system into agents.

City level Type-2 Fuzzy Inference Systems

The figure 5 shows a type-2 fuzzy inference system for Tijuana city. It depicts a set of input-output variables and a rule set. Output variables are catholic and non-catholic as a response of the system. We could use the difference between both values to make decisions into an agent as a preference decision-making system.

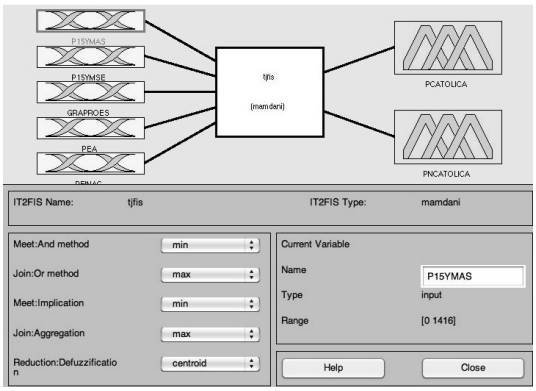

Figure 5: Fuzzy Inference System for Tijuana City.

The Figure 6 depicts the resolution example of the rules by the fuzzy inference system. Different quantitative input values could be introduced and the system resolve creating different responses. Depending of the combination of inputs, we can expect different responses of the system. An agent will use this inference system as a decision-making system to show different behaviours depending of the situation.

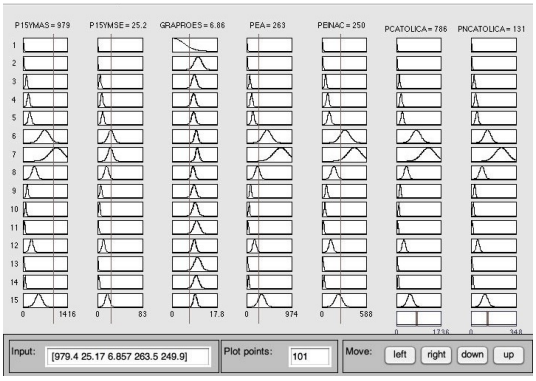

Figure 6: Fuzzy Inference System Rule Set Evaluation for Tijuana City.

The Figure 7 represents the response of the system to catholic preference, and the Figure 8 for non-catholic preference. We can see that there are response differences, so we can us it to make decisions.

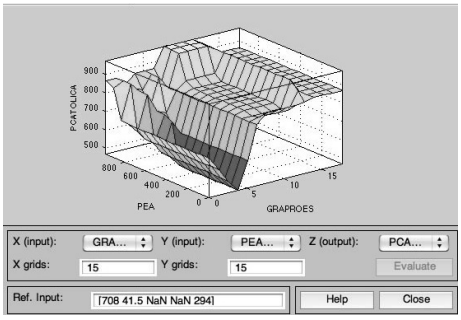

Figure 7: PEA vs. GRAPROES Type-Reduced Surface View for Tijuana City PCATOLICA output.

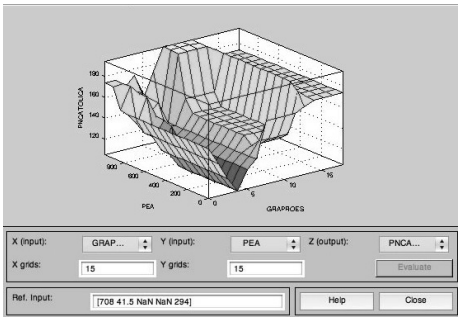

Figure 8: PEA vs. GRAPROES Type-Reduced Surface View for Tijuana City PNCATOLICA output.

Distributed agents do not necessarily define agents in lower-levels of description, but rather consider all levels of agency that are interconnected in a type of organism that spreads throughout the system Suarez et al. (2008); Suarez and Castanon-Puga (2010); Gilbert (2007).

AGEB level Type-2 Fuzzy Inference Systems

On AGEB layer, we can build fuzzy inference systems for agents that represents locations. Figure 9 and Figure 10 depicts the FIS response for different locations into the same AGEB. As we can see, there are differences between AGEB agents. At this level, we could be representing AGEB agents into a city context.

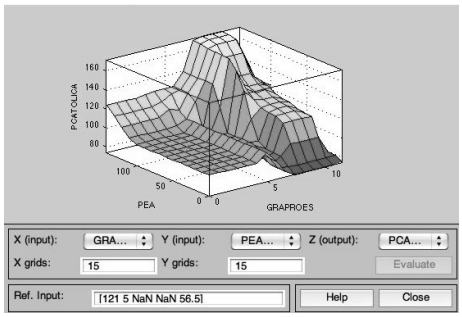

Figure 9: PEA vs. GRAPROES Type-Reduced Surface View for AGEB 32 PCATOLICA output.

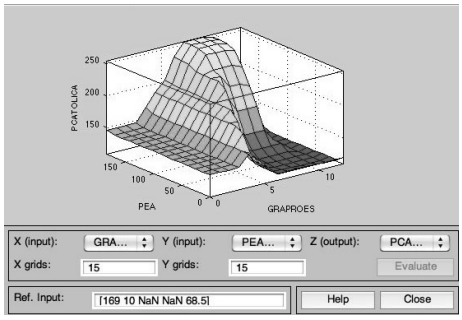

Figure 10: PEA vs. GRAPROES Type-Reduced Surface View for AGEB 51 PCATOLICA output.

Location level Type-2 Fuzzy Inference Systems

On location layer, we can build fuzzy inference systems for agents that represents locations. Figure 11 and Figure 12 depicts the FIS response for different locations into the same AGEB. As we can see, there are differences between locations agents. At this level, we could be representing locations agents into a AGEB context.

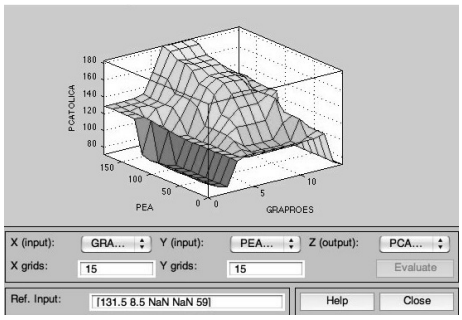

Figure 11: PEA vs. GRAPROES Type-Reduced Surface View for Location 187 PCATOLICA output.

Testing Religion Affiliation Type-2 Fuzzy Inference System in NetLogo

With the use of a NetLogo extension of a type-2 fuzzy inference machine, we can test the fuzzy inference sys-

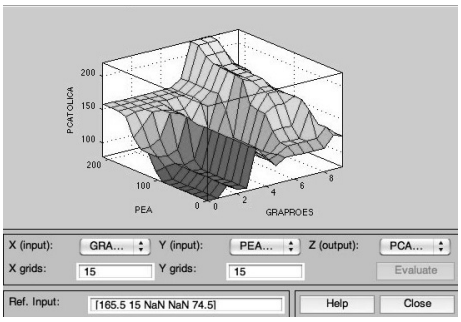

Figure 12: PEA vs. GRAPROES Type-Reduced Surface View for Location 283 PCATOLICA output.

tem for catholic population and the non-catholic population of Tijuana city. Figure 13 shows an screen shot of the test in NetLogo with the extension mentioned before. The test include a set of 100 agents with their initial attributes. The test consist in the evaluation of all agents inside of a type-2 fuzzy inference system, representative of each city. The result was a different response of each agent, according of the city in wich was evaluated.

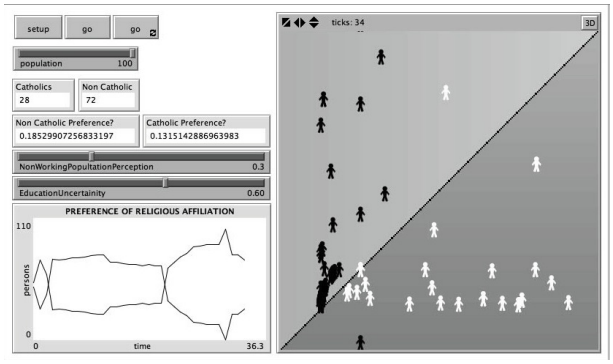

Figure 13: Screen Shot of Religion Affiliation Type-2 Fuzzy Inference System in NetLogo test prototipe.

The test evaluates variations in the limits of some input variables' membership functions, simulating a perception variation of the individuals in their respective context (their city). The result of this is a variation in the choice of religious afiliation in response of variations of the perception values.

Finally, the test evaluates changes in uncertainty values of input variables' membership functions, simulating a variation on the security of individuals regarding the risk or doubt. The result is that if we make changes in the uncertainty values, the response is a change in the choice of religious affiliation.

CONCLUSIONS

The development of a general methodology for the description and analysis of complex systems remains an open research task for computer scientists and all other scholars interested in the subject matter. Naturally, such a vast language will imply the use of different techniques and theories, given that the perspectives of each scientific discipline-and ultimately of each researcher-may vary greatly.

The religious affiliation can be modelled with Fuzzy Inference Systems. Establishing different layers of interaction between agents and analysing their influence on decision-making system of agents in each level, we can represent the complexity of the phenomenon of individual preference to a religious affiliation.

We use the case study of the city of Tijuana, as it has an updated census of the distribution of meeting places of religious organizations in the city and their respective socio-demographic information.

We use a neural-fuzzy approach to develop a computational model of the decision-making system of agents in order to build a multi-agent system. We represent different levels of agency with different cognitive agents. Each agent in the system are a fuzzy cognitive agent that can choose religion options based on preferences.

ACKNOWLEDGEMENTS

We would like to thank the Mexican National Council for Science and Technology (Consejo Nacional de Ciencia y Tecnología, CONACYT) and Universidad Autónoma de Baja California for the economic support granted for this research.

REFERENCES

Alegría, T. and Ordónez, G. (2002). Regularización de la tenencia de la tierra y consolidación urbana en tijuana, b.c. Research report, El Colegio de la Frontera Norte, México.

Arias, A. L. (2008). Cambio regional del empleo y productividad manufacturera en méxico, el caso de la frontera y las grandes ciudades,1970-2004. *Frontera Norte*, 20(40):79–103.

Botti, V. and Julian, V. (2003). Estudio de métodos de desarrollo de sistemas multiagente. *Inteligencia Artificial, Revista Iberoamericana de Inteligencia Artificial*, 18.

Boulding, K. (1956). General systems theory the skeleton of science. *Management Science*, 6(3):127–139.

Castillo, O., Melin, P., and Castro, J. R. (2010). Computational intelligence software for interval type–2 fuzzy logic. *Journal Computer Applications in Engineering Education*.

Castro, J. R., Castillo, O., Melin, P., Mendoza, O., and Rodríguez-Díaz, A. (2010). An interval type–2 fuzzy neural network for chaotic time series prediction with cross–validation and akaike test. *Soft Computing for Intelligent Control and Mobile Robotics*, 318:269–285.

Castro, J. R., Castillo, O., Melin, P., and Rodríguez-Díaz, A. (2008). A hybrid learning algorithm for a class of interval type–2 fuzzy neural networks. *Journal of Information Sciences*, 179(13):2175–2193.

Drennan, M. (2005). The human science of simulation: a robust hermeneutics for artificial societies. *Journal of Artificial Societies and Social Simulation*, 8(1).

Fortuny, P. (1999). *Creyentes y creencias en Guadalajara*. CIESAS, México.

Gilbert, N. (2007). *Computational social science: Agent-based social simulation*, pages 115–134. Bardwell, Oxford.

INEGI (2006). Segundo conteo de población y vivienda 2005. instituto nacional de estadística geografía e informática.

INEGI (2010). Censo de población y vivienda 2010. instituto nacional de estadística geografía e informática.

Jaimes-Martínez, R. (2007). *La paradoja neopentecostal. Una expresión del cambio religioso fronterizo en Tijuana, Baja California*. PhD thesis, El Colegio de la Frontera Norte, México.

Jiménez, G. (2006). Cultura, identidad y metropolitanismo global. Online.

López, A., Hernández, C., Pajares, J., and Aguilera, A. (2002). Sistemas multiagente en ingeniería de organización. técnicas computacionales de simulación de sistemas complejos.

Márquez, B. Y., Castañón Puga, M., Castro, J. R., and Suarez, E. D. (2011a). Methodology for the Modeling of Complex Social System Using neuro-Fuzzy and Distributed Agencies. *Journal of Selected Areas in Software Engineering (JSSE)*, March:1–8.

Márquez, B. Y., Castanon-Puga, M., Castro, J. R., and Suarez, E. D. (2011b). A distributed agency methodology applied to complex social system, a multi-dimensional approach. In Zhang, R., Cordeiro, J., Li, X., Zhang, Z., and Zhang, J., editors, *Proceedings of the 13th International Conference on Enterprise Information Systems, Volume 1, Beijing, China, 8-11 June, 2011.*, pages 204–209. SciTe Press.

Mendel, J. M. and Wu, D. (2010). *Perceptual Computing, Aiding People in Making Subjective Judgments*. IEEPress.

Ortiz, O. O. (2006). Cambio religioso en la frontera norte. aportes al estudio de la migración y las relaciones transfronterizas como factores de cambio. *Frontera Norte*, 18(35):111–134.

Peng, Y., Kou, G., Shi, Y., and Chen, Z. (2008). A descriptive framework for the field of data mining and knowledge discovery. *International Journal of Information Technology and Decision Making*, 7:639–682.

Rantala, J. and Koivisto, H. (2002). Optimised subtractive clustering for neuro-fuzzy models.

Russell, S. and Norvig, P. (2004). *Inteligencia Artificial. Un Enfoque Moderno*. Pearson Prentice Hall, 2 edition.

Stefanescu, S. (2007). Applying nelder mead's optimization algorithm for multiple global minima. *Romanian Journal of Economic Forecasting.*, pages 97–103.

Suarez, E. D. and Castanon-Puga, M. (2010). Distributed agency, a simulation language for describing social phenomena. In *IV Edition of Epistemological Perspectives on Simulation*, Hamburg, Germany. The European Social Simulation Association.

Suarez, E. D., Castanon-Puga, M., Flores, D.-L., Rodriguez-Diaz, A., Castro, J. R., Gaxiola-Pacheco, C., and Gonzalez-Fuentes, M. (2010). A multi-layered agency analysis of voting models. In *The 3rd World Congress on Social Simulation WCSS2010*, Kassel, Germany.

Suarez, E. D., Rodriguez-Diaz, A., and Castanon-Puga, M. (2008). *Soft Computing for Hybrid Intelligent Systems*, volume 154, chapter Fuzzy Agents, pages 269–293. Springer.

Wooldridge, M. and Jennings, N. (1995). Intelligent agents: Theory and practice. *Knowledge Engineering Review*.

Yolles, M. (2006). Organizations as complex systems, an introduction to knowledge cybernetics.

AUTHOR BIOGRAPHIES

MANUEL CASTAÑÓN PUGA was born in Tijuana, Baja Califonria, México. Dr. Castañón-Puga is a full time Professor at Chemistry Sciences and Engineering Faculty of Baja California Autónomus University. Currently is leader of the "Complexity and computation" research group. His email is `puga@uabc.edu.mx` and his personal webpage at `http://cyc.tij.uabc.mx/puga`.

CARELIA GAXIOLA PACHECO was born in Sinaloa, México. Dr. Gaxiola-Pacheco is a full time Professor at Chemistry Sciences and Engineering Faculty of Baja California Autónomus University. Currently is member of the "Complexity and computation" research group. Her email is `cgaxiola@uabc.edu.mx` and her personal webpage at `http://cyc.tij.uabc.mx/gaxiola`.

DORA-LUZ FLORES was born in Tijuana, Baja California, México. Dr. Flores is a full time Professor at Engineering, Architecture and Design Faculty of Baja California Autónomus University. Currently is member of the "Complexity and computation" research group. Her email is `dflores@uabc.edu.mx` and her personal webpage at `http://cyc.tij.uabc.mx/flores`.

RAMIRO JAIMES MARTÍNEZ was born in México. Dr. Jaimes-Martínez is a full time Researcher at Historical Research Institute of Baja California Autónomus University. Currently is leader of the "History and society" research group. His email is `rjaimes@uabc.edu.mx`

JUAN RAMÓN CASTRO was born in Tijuana, Baja California, México. Dr. Castro is a full time Professor at Chemistry Sciences and Engineering Faculty of Baja California Autónomus University. Currently is member of the "Computational intelligence" research group. His email is `jrcastro@uabc.edu.mx`

COENOME MODEL: ELEMENTARY ECOLOGICAL CYCLE AS A DYNAMICAL UNIT

Serge V. Chernyshenko
Faculty of Informatics
University of Koblenz-Landau
D-56070, Koblenz, Germany
E-mail: svc@a-teleport.com

KEY WORDS

Ecosystem, mathematical ecology, succession, hypercycle, coenome.

ABSTRACT

A general approach to modelling of ecosystem dynamic is considered. The special term "coenome" is proposed for basic dynamic element of biogeocoenoses. The coenome is an association of populations which have complementary properties (up to symbioses) or united by trophical links. Each succession stage is characterised by a major dominant coenome. The succession process is considered as a process of step-by-step changing dominating coenome. Sketch models of the coenome are considered. The application of M. Eigen's hypercycle for modelling of ecosystem successions is proposed. The model describes a specific interaction between coenomes, which are similar, but not equivalent to the competition and "host-parasite" relations. As a result of the interaction, a redistribution of ecological resources may take place. During several steps of the succession process, the ecosystem "selects" its optimal dimension and complexity. Succession process is considered as reaching optimal complexity of ecosystems.

COENOME AS A UNIT OF ECOSYSTEM DYNAMIC STRUCTURE

The method of mathematical modelling become a traditional tool of ecology. The modern approach to theoretical ecology modelling is founded by the famous monographs of A. Lotka (1925) and V. Volterra (1931). The chief purpose of this kind of modelling is not an exact quantitative simulation of natural ecosystems, but determining and formal description of main properties of ecosystems' behaviour. In the nature there is no pair of populations absolutely corresponding to the Volterra's "predator-pray" style of relations, as well as there is no "material points" in real physical systems. At the same time such abstract objects are extremely useful as elements of complex mathematical models. Within voluminous literature on the dynamical analysis in ecology one can mention classical monographs of E.P. Maynard Smith (1974), Yu.M. Svirezhev and D.O. Logofet (1978), E.C. Pielou (1977).

Let's concentrate on some aspects of long-term ecosystem dynamics and consider the succession phenomenon as a result of ecosystem property of self-recovery (or homeostasis). The traditional succession models (Horn 1976; Lepš 1988; Perry and Millington 2007) are based on using stochastic models and such parameter as "a probability of transition" between different ecosystem states. The parameter is considered as external one, and, as a result, the model structure does not reflect adaptive nature of the succession process (Begon et al. 1986). Modelling of ecosystem transforming on the base of adaptation approach looks more interesting from theoretical point of view. The idea is to describe changes of ecosystem structure as a result of changing ecological conditions determined by internal and external factors.

The phenomenon of homeostasis is not determined directly by complexity of real ecosystems. Mathematical modelling shows that, in general, growth of complexity leads to reduction of ecosystem stability, or does not influence it (May, 1973). Stability of real ecosystems is a result of very special character of interaction between their elements. It is not only trophic and topic relations between populations or individuals. Another kind of dynamical units should be found to describe this aspect of ecosystem dynamics (Chernyshenko 1996).

Let's consider "succession generations" (intermediate dominate ecosystems) as units, interaction between which is a driving force of successions. Each succession generation is identified by an unequal association of species with complementary ecological properties (up to symbioses) or united by trophical links. We propose a special term "coenome" for such associations. "Coenomes" are considered as main elements of forest ecosystem (or biogeocoenosis) useful for purposes of modelling long-term dynamic processes. Each succession stage is characterised by main dominant coenome. The succession process is considered as a process of step-by-step changing dominant coenome.

An association of species, forming coenome, includes populations of producers, consumers, and reducers. The central position of producers in coenome is determined by their role as an energy source for the whole ecosystem. The role of consumers is not such important, although there are situations, when activity of consumers determines a tendency of succession (Begon et al., 1986). An energetic role of reducers consists in restoring some biomass to biota by detrital trophic webs, but their major importance for biogeocoenose is explained by the necessity "to close" biogeochemical cycles. The simplest artificial stable ecosystems, functioned in closed flasks, included populations of producers (unicellular algae) and reducers (fungus) (Lappo, 1987).

Proceedings 26th European Conference on Modelling and Simulation ©ECMS Klaus G. Troitzsch, Michael Möhring, Ulf Lotzmann (Editors)
ISBN: 978-0-9564944-4-3 / ISBN: 978-0-9564944-5-0 (CD)

Theoretically, it is possible to envision producers, independently realising the function of decomposition regarding own biomass. But this possibility is not realised in reality. If the hypotheses of E. Odum (1971) about origin of heterotrophs before phototrophs is correct, first producers had no problems with utilisation of died biomass and products of metabolism, and there were no evolutionary reasons for forming "self-sufficient" organisms.

Stable biogeochemical cycles were formed gradually, during the process of co-adaptation of producers and reducers. The formation of a first stable "producers-reducers" cycle meant origin of a first ecosystem. The cyclic character of ecological stability creates an analogy between the beginnings of ecosystems and first organisms in accordance with the "hypercyclic" model of M. Eigen (1979).

We propose a special term "coenome" for the elementary biogeocoenotic cyclic element. The coenome includes one or several populations of producers (as a source of energy and a kernel of the association); reducers, which "close" biogeochemical cycles; and consumers, which stimulate energetic processes in the system (Chernyshenko 2008a). Naturally, the areas of the ecological optimum of coenome species must have common parts. Coenome species are characterised by some level of co-adaptation. The main features of cross-population relations in a coenome are the following: a) a low level of competition, as a result of effective separation of niches; b) a high level of mutualism, especially, in pairs "producer-reducer"; c) an optimal (energetically determined) level of trophic relationship.

The coenome closely corresponds to the sinusia of 3-rd order of H. Gams (1918). The "stable" group of populations forms a dominant coenome, the "regressive" populations represent previous coenomes (succession generations), the "progressive" populations reflect forming a next coenome. Interaction of producers from the different groups is very important for the course of succession. It can not be described by the traditional schemes like "++" or "--", and need in more detailed analysis.

A principal scheme of matter and energy flows in coenome (without consumers) is represented in Fig.1. The symbols *x, y, p, q* denote contents of some chemical elements, correspondingly: in the biomass of producers; in the biomass of reducers; in the dead biomass; in the inorganic matter, accessible for producers. Characteristic intensity of the element cycling is symbolised by *M*. The coefficient α ($0<\alpha<1$) determines a part of the element, escaping the populations of producers as an organic matter, and λ ($0<\lambda<1$) determines the same for populations of reducers.

MATTER, ENERGY, AND INFORMATION FLOWS IN COENOMES

The simplest model of matter cycling in coenome (the unbroken lines in Fig.1) can be designing on the base of the Lotka-Volterra model (Lotka, 1925; Volterra, 1931).

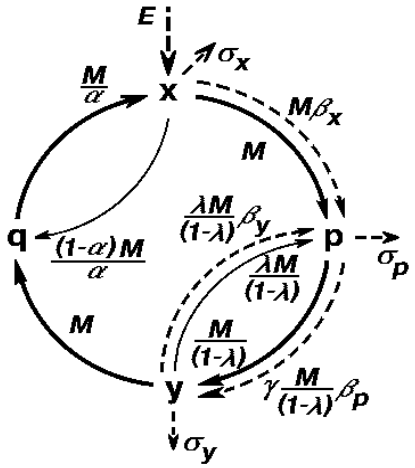

Figure 1: Matter and energy flows in a coenome

In the case without effects of saturation and self-limitation of populations, it can be written as

$$\begin{aligned} dx/dt &= a\,q\,x - b\,x \\ dp/dt &= \alpha\,b\,x + \lambda\,s\,y - r\,y\,p \\ dy/dt &= r\,p\,y - s\,y \\ dq/dt &= (1-\alpha)\,b\,x + (1-\lambda)\,s\,y - a\,x\,q \end{aligned} \qquad (1)$$

The coefficients b and s are coefficients of mortality of producers and reducers; a and r estimate a rate of the use of, correspondingly, inorganic matter by producers and dead biomass by consumers. The model (1) can be considered as a modification of the model of V.V. Alekseev (1976). The value M for the model is equal to αbx, that is to say, it is determined by the intensity of the element transferring from producer populations to the dead biomass.

Although the model (1) is only a sketchy model, it is characterised by some special features. The concentration of the element in inorganic matter, accessible for producers ("in soil"), is determined in the steady-state by the ratio of the coefficient of producer mortality to the rate of producer absorption of the element: $q_{st}= b/a$. Similarly, but on the base of ecological features of reducers, the stable level of the element concentration in the dead biomass ("in litter") is found from the equation $p_{st}= s/r$. The model does not determine the stable values of x and y, but only their ratio: $x/y = (1-\lambda)s/\alpha b$. It is explicable both from mathematical point of view (the sum of the right-hand sides of the equations equals to zero, and the sum $(x+y+p+q)$ is not changed during the process), and from biological reasons (the model describe closed circulation of the element, its amount in the cycle have to be determined by some external factors). The system (1) is not asymptotically stable, but under natural assumptions that $A>b$, $R>s$, the own numbers of the linearised system have negative real parts (except one, which equals zero).

A more realistic model of the coenome is arrived by the use of equations with Michaelis-Menten functions in the right-hand sides (Thornley 1976):

$$\frac{dx}{dt} = A\left(\frac{X}{x+X} - \frac{b}{A}\right)x \qquad (2)$$

where X means the concentration of semisaturation, which is proportional to the concentration of controlling factor. The equation (1) assumes the form:

$$\begin{cases} \dfrac{dx}{dt} = A\left(\dfrac{cq}{x+cq} - \dfrac{b}{A}\right)x \\ \dfrac{dp}{dt} = \alpha bx + \lambda sy - R\dfrac{hp}{y+hp}y \\ \dfrac{dy}{dt} = R\left(\dfrac{hp}{y+hp} - \dfrac{s}{R}\right)y \\ \dfrac{dq}{dt} = (1-\alpha)bx + (1-\lambda)sy - A\dfrac{cq}{x+cq}x \end{cases} \qquad (3)$$

The system (3) dictates the same parameter $M = \alpha bx$ and the same ratio between biomass of populations, as the model (1). However, the quantities p and q depend on populations' sizes in this case by the following way:

$$y = \frac{\alpha b}{(1-\lambda)s}x, \qquad q = \frac{b}{c(A-b)}x$$
$$p = \frac{s}{h(R-s)}y = \frac{\alpha b}{(1-\lambda)h(R-s)}x, \qquad (4)$$

In the vicinity of an arbitrary equilibrium point the characteristic equation for the own numbers have the form:

$$\Lambda^4 + (\Phi+\Psi)\Lambda^3 + (\Phi\Psi+\Gamma+\Xi)\Lambda^2 + (\Phi\Gamma+\Psi\Xi)\Lambda = 0,$$

where $\Phi = (A-b)(b+c(A-b))/A$, $\Psi = (R-s)(s+h(R-s))$, $\Gamma = \alpha bc(A-b)^2/A$, $\Xi = (1-\lambda)sh(R-s)^2/R$. One of the eigenvalues is equal to zero, but others have negative real parts. In the vicinity of any equilibrium points of the system (3) there are an infinite number of other equilibrium points, and any of them is not asymptotically stable. At the same time the set of the equilibrium points (as a whole) is a global attractor. The fact is confirmed by numerical experiments.

Let us consider energetic flows in coenome (the dotted lines in the Fig. 1). On the base of the model (3) it is possible to write the following system:

$$\begin{cases} \dfrac{de_x}{dt} = (E - \alpha b - \sigma_x)e_x \\ \dfrac{de_p}{dt} = \alpha b e_x + \lambda s e_y - R\dfrac{he_p}{e_y + he_p}e_y - \sigma_p e_p \\ \dfrac{de_y}{dt} = \left(\gamma R\dfrac{he_p}{e_y + he_p} - \lambda s - \sigma_y\right)e_y \end{cases} \qquad (5)$$

where e_x, e_y, e_p - the variables, which estimate, correspondingly, the energy amount in biomass of producers, reducers, and dead biomass; $\sigma_x e_x$, $\sigma_y e_y$, $\sigma_p e_p$ - the losses of energy for each of this groups; $E e_x$ - the intensity of energy flow into populations of producers; $\gamma(0<\gamma<1)$ - the part of energy of the dead biomass, which passes to energy of the biomass of reducers.

As it is easy to see, the first equation of the system (5) does not depend on the other. The condition of existing a stationary nonzero value of e_x is $\sigma_x = E - \alpha b$. The stationary value of e_x is depend on initial conditions, as well as the variation x in the model (3). With the natural supposition of s_p=0 (the role of abiotic degrading the dead biomass is not essential) the stationary values for other co-ordinates are determined by the equations:

$$e_y = \frac{\gamma\alpha b}{(1-\gamma)\lambda s + \sigma_y}e_x; \quad e_p = \frac{(\lambda s + \sigma_y)}{h(\gamma R - \lambda s - \sigma_y)}e_y = \qquad (6)$$
$$= \frac{\gamma(\lambda s + \sigma_y)\alpha b}{h((1-\gamma)\lambda s + \sigma_y)(\gamma R - \lambda s - \sigma_y)}e_x.$$

The conditions of positivity of the steady-state are the following: $\gamma > \lambda s / R, \sigma_y < \gamma R - \lambda S$. If they assert, the steady-state (6) is stable.

Let's consider the problem of the interplay of the matter and energy flows in the coenome. Let β_x, β_y, β_p be the measure of energy per the biomass unit of, correspondingly, producers, reducers, and dead biomass. Then $e_x=\beta_x x$, $e_y=\beta_y y$, $\beta_p=\beta_p p$. Let us substitute to (6) the values x, y, p from the model (3) and arrive:

$$\beta_y = \frac{\gamma(1-\lambda)s}{(1-\gamma)\lambda s + \sigma_y}\beta_x; \beta_p = \frac{(R-s)(\lambda s + \sigma_y)}{s(\gamma R - \lambda s - \sigma_y)}\beta_y = \qquad (7)$$
$$= \frac{\gamma(1-\lambda)(R-s)(\lambda s + \sigma_y)}{((1-\gamma)\lambda s + \sigma_y)(\gamma R - \lambda s - \sigma_y)}\beta_x.$$

The formulas (7) supposedly describe more realistic relationship between energy concentration in biomass of different groups, than the equations, derived on the base of the quadratic model (Ulanowicz 1972).

From equations (3), (5) one can obtain the system, describing the dynamics of variables β_x,β_y, β_p :

$$\begin{cases} \dfrac{d\beta_x}{dt} = A\left(E + (1-\alpha)b - A\dfrac{c}{x_q + c} - \sigma_x\right)\beta_x \\ \dfrac{d\beta_p}{dt} = \alpha b x_p \beta_x + \left(\lambda s - R\dfrac{h\beta_p}{y_p\beta_y + h\beta_p}\right)y_p\beta_y + \\ \qquad + \left(R\dfrac{h}{y_p + h} - \alpha bx - \lambda sy - \sigma_p\right)\beta_p \\ \dfrac{d\beta_y}{dt} = \left(\gamma R\left(\dfrac{h\beta_p}{\beta_y y_p + h\beta_p} - \dfrac{h}{y_p + h}\right) + (1-\lambda)s - \sigma_y\right)\beta_y \\ \dfrac{dx_p}{dt} = \left(A\dfrac{c}{x_q + c} - b - \alpha bx_p - \lambda s y_p + R\dfrac{h}{y_p + h}y_p\right)x_p \\ \dfrac{dy_p}{dt} = \left(R\dfrac{h}{y_p + h} - s - \alpha bx_p - \lambda s y_p + R\dfrac{h}{y_p + h}y_p\right)y_p \\ \dfrac{dx_q}{dt} = \left(A\dfrac{c}{x_q + c} - b - (1-\alpha)bx_q + (1-\lambda)sy_q - A\dfrac{c}{x_q + c}x_q\right)x_q \\ \dfrac{dy_q}{dt} = \left(R\dfrac{h}{y_p + h} - s - (1-\alpha)bx_q + (1-\lambda)sy_q - A\dfrac{c}{x_q + c}x_q\right)y_q \end{cases} \qquad (8)$$

Here the co-ordinates are defined as $x_p=x/p$, $y_p=y/p$, $x_q=x/q$, $y_q=y/q$. Their dynamics is not depend on β_x, β_p,

β_y , and they may be described in the vicinity of the equilibrium point by the first three equations from (8), where the values of biomass from (4) are used:

$$\begin{cases} \dfrac{d\beta_x}{dt} = (E - \alpha b - \sigma_x)\beta_x \\ \dfrac{d\beta_p}{dt} = h(R-s)(1-\lambda)\beta_x + h(R-s)\left(\lambda - R\dfrac{\beta_p}{(R-S)\beta_y + s\beta_p}\right)\beta_y \\ \dfrac{d\beta_y}{dt} = \left(\gamma R\dfrac{s\beta_p}{(R-s)\beta_y + s\beta_p} - \lambda s - \sigma_y\right)\beta_y \end{cases} \quad (9)$$

The steady-state is specified by equation (7) and it is stable. The variables β_x , β_p , β_y can be used as a measure of the level of organisation (or thermodynamic instability) of population biomass. It is possible to interpret the system (9) as the model of information transformation in the coenome, if to use the term "information" as a synonym of negentropy.

The flows of matter, energy, and information, describing by the models (3),(5),(9), are ultimately determined by producer activity. The variables x, e_x , and β_x are external parameters of the models in some sense. Particularly, it is evident from formulas (4), (6), (7), where other coordinates of the steady-state are expressed by these variables. It is reasonable to use models (3), (5), (9) without first equations, and to consider variables x, e_x, β_x as external parameters, describing by some additional equations.

The value of e_x is determined by the energetic potential of producers. The stable value e^* can be derived from a model of productivity (Thornley 1976; Berezovkaya et al. 1991). Particularly, it is possible to use models of such type as (2):

$$\frac{de_x}{dt} = \left(A\frac{E(u_s,u_c,u_h,u_t)}{e_x + E(u_s,u_c,u_h,u_t)} - b(u_t)\right)e_x . \quad (10)$$

The variables E (the intensity of the flow of physiologically accessible energy) and b (the intensity of energy spending in the course of vital activity) depends on such parameters as u_s (the intensity of the flow of solar energy), u_c (the concentration of accessible carbonic acid gas), u_h (the concentration of accessible water), u_t (the temperature), and other factors, which can be included in the model too. For the model (10) one can obtain:

$$e^* = E(u_s,u_c,u_h,u_t)\left(\frac{A}{b(u_t)} - 1\right)$$

The energy flow to the coenome can be limited by scantiness in the environment of some chemical elements or substances in accessible forms. Besides carbonic acid gas and water it can be such elements as N, P, K, microelements, etc. Each i-th critical element or substance can be characterise by two indices. The first one, $x_i^{(\min)}$ is a physiologically necessary concentration of the element in the producer biomass. If $x_i < x_i^{(\min)}$, the productivity of the producer decreases proportionally to x_i. The second index, $x_i^{(\mathrm{nom})}$ ($x_i^{(\mathrm{nom})} > x_i^{(\min)}$) is a physiologically optimal concentration of the element. Let $X_i^{(c)}$ be a general amount of the element in the coenome. Than, in accordance with (6), its amount in the producers biomass will be

$$x^{(c)} = \left(\frac{cA-(c-1)b}{c(A-b)} + \frac{hR-(h-1)s}{h(R-s)}\frac{\alpha b}{(1-\lambda)s}\right)^{-1} X^{(c)}$$

The value of x_i^* and the corresponding value of e_{xi} can be defined by the following formulas:

$$\begin{array}{ll} x_i^* = x_i^{(\mathrm{nom})},\ e_{xi} = e^*, & \text{when } x_i^{(c)} > x_i^{(\mathrm{nom})} \\ x_i^* = x_i^{(c)},\ e_{xi} = e^*, & \text{when } x_i^{(\min)} < x_i^{(c)} < x_i^{(\mathrm{nom})} \\ x_i^* = x_i^{(c)},\ e_{xi} = e^* x_i^{(c)}/x_i^{(\min)}, & \text{when } x_i^{(c)} < x_i^{(\min)} \end{array} \quad (11)$$

In accordance with the principle of minimum of J. Liebig (1847) the productivity of a plant is determined by the amount of a substance, which is physiologically minimal. Consequently, the final value of the intensity of stable energy flow in a coenome can be defined as

$$e_x^* = \min_i e_{xi}.$$

In the case, when the energy flow is limited by climatic factors only, $e_x^* = e^*$. In the opposite case, $e_x^* < e^*$.

The variable β_x appears to be determined physiologically, and only slightly ecologically. It is confirmed by the wide variation of energy concentration in biomass of different producers. For example, it has a minimal value for trees, which are characterised by high development of support organs, and it is essentially higher for phytoplankton. In accordance with the definition, $\beta_x^* = e_x^*/x^*$. Based on (11), one can suppose that the energy concentration in biomass have to be higher in a condition of deficiency of necessary substances. However, this is not correct always, particularly, as a result of variation of the substance concentration during year and effects of accumulation.

THE MODEL OF DIRECT INTER-COENOME RELATIONS

Let us consider the direct inter-coenome relations, without taking into account their mutual influence by the way of changing environmental conditions. It is possible to recognise two components in this relation: competition and facilitation.

By the Lotka-Volterra equation, the competition between two populations can be describing as

$$\frac{dx_i}{dt} = x_i\left(a_i - b_i\sum_{j=1}^{n} d_{ij}x_j\right), \quad i = \overline{1,n}$$

After some generalisation it can be written as

$$\frac{dx_i}{dt} = \Gamma_i(x) - b_i x_i \sum_{j=1}^{n}\Gamma_j(x), \quad i = \overline{1,n}. \quad (12)$$

The system (12) has some special features, when b_i do not depend on i. This is a case, when the competition oppresses equally all interacting coenomes (an analogue of third Newton's law is true). The system assumes the following form:

$$\frac{dx_i}{dt} = \Gamma_i(x) - \frac{x_i}{C_0}\sum_{j=1}^{n}\Gamma_j(x), \quad i = \overline{1,n}. \qquad (13)$$

Models of the form (13) have been used by M. Eigen (Eigen and Schuster 1979) for describing the evolutionary process of self-organisation of organic macromolecules. The functions $\Gamma_i(x)$ have been decided as:

$$\begin{aligned} &\Gamma_1(x) = k_1 x_1, \\ &\Gamma_i(x) = x_i(k'_{i-1}x_{i-1} + k'_i x_i), \quad i = \overline{2,n} \end{aligned} \qquad (14)$$

The functions (14) describe limitless increase of sizes of isolated populations and their mutual stimulation (with simultaneous competition for ecological resources in accordance with structure of the equation (13)). In the case of self-restriction of the populations the "functions of growth" $\Gamma_i(x)$ (Allen 1976) can be written in the following form:

$$\begin{aligned} &\Gamma_1(x) = x_1(N - x_1), \\ &\Gamma_i(x) = x_i(a_{i-1}x_{i-1} - x_i), \quad i = \overline{2,n} \end{aligned} \qquad (15)$$

The parameters C_0 , a_i , and N are presumed positive. Initial conditions are supposed positive and essentially less than the parameters N and C_0 . The modification (13), (15) of the M. Eigen's model was proposed in the article (Chernyshenko, 1995). Equilibrium points of the system (13) can be classified for two groups. The first one is defined by the following formulas:

$$\sum x_i = C_0, \qquad \frac{x_i}{\Gamma_i(x)} = const \quad \text{for all } i, \qquad (16)$$

and for the second group it is true

$$\Gamma(x_1,...,x_n) = 0, \qquad i = \overline{1,n}. \qquad (17)$$

The level of the competition between the coenomes varies in inverse proportion to the value of C_0 . Considering that by (16) a limiting value of the total biomass of all coenomes is equal to C_0 (for the case (17) it does not exceed this value too) it is possible to interpret the parameter C_0 as a "environmental capacity", which limits a maximal total biomass of the ecosystem.

The system (13), (15) has

$$n + 2 + \sum_{i=1}^{n/2+1} C_n^i$$

equilibrium points, with $(n+1)$ points X_k can be stable:

$$\begin{cases} X_k = \{x_k^{(1)}, x_k^{(2)}, ..., x_k^{(k)}, 0, ...\}, & k = \overline{1,n} \\ X_{n+1} = \{N, a_1 N, ..., a_1 ... a_{n-1} N\}, \end{cases} \qquad (18)$$

The variables $x_k^{(i)}$ are defined by the following equations:

$$x_k^{(i)} = \left(R_i^{(k)} N + B_i^{(0)} C_0\right) / \sum_{j=1}^{k} B_j^{(0)}, \qquad i = \overline{1,k},$$

$$R_i^{(k)} = \prod_{j=1}^{i-1} a_j \sum_{j=1}^{k-i} B_j^{(i)} - \sum_{j=1}^{i-1}\left(B_{i-j}^{(j)} \prod_{l=0}^{j-1} a_l\right), \qquad a_0 = 1,$$

The variables $B_j^{(i)}$ can be obtained from the recurrent formula of the Fibonacci type:

$$B_0^{(i)} = 0, \quad B_1^{(i)} = 1, \quad B_j^{(i)} = (a_{i+j-1} + 1)B_{j-1}^{(i)} - a_{i+j-2}B_{j-2}^{(i)}.$$

It is true that for any k:

$$\sum_{i=1}^{k} R_i^{k)} = 0, \ \sum_{i=1}^{k} x_k^{(i)} = C_o \ .$$

A concrete value of k for the steady-state (its dimension) is determined by values of the parameters C_0 , a_i , and N . The value of k increases simultaneously with growth of the parameter C_0 . The dimension of the system in a steady-state (or the number of succession steps before a climax stage) increases simultaneously with increasing "environmental capacity".

Let us consider the two-dimensional system:

$$\begin{cases} \dfrac{dx_1}{dt} = \Gamma_1(x_1, x_2) - \dfrac{x_1}{C_0}\sum_{i=1}^{2}\Gamma_i(x_1, x_2) \\ \dfrac{dx_2}{dt} = \Gamma_2(x_1, x_2) - \dfrac{x_2}{C_0}\sum_{i=1}^{2}\Gamma_i(x_1, x_2) \end{cases}. \qquad (19)$$

There are three (excluding the infinity) potentially steady equilibrium points:

$$\begin{cases} X_1^{(1)} = C_0 \\ X_1^{(2)} = 0 \end{cases}, \quad \begin{cases} X_2^{(1)} = \dfrac{C_0 + N}{a_1 + 2} \\ X_2^{(2)} = \dfrac{(a_1 + 2)C_0 - N}{a_1 + 2} \end{cases}, \quad \begin{cases} X_3^{(1)} = N \\ X_3^{(2)} = a_1 N \end{cases},$$

For fixed values of the parameters of the system there is only one steady-state. The state X_1 is steady when

$$C_0 < \frac{N}{a_1 + 1}, \qquad (20)$$

the state X_2 is steady under the condition

$$\frac{N}{a_1 + 1} < C_0 < (a_1 + 1)N, \qquad (21)$$

and the state X_3 is steady if

$$C_0 > (a_1 + 1)N. \qquad (22)$$

All steady equilibrium points are nodes, unsteady points are nodes or saddles. The system has no focal equilibrium points under any vales of the parameters. Oscillatory regimes are not possible in the model. In the bifurcation points $N/(a_1+1)$ and $(a_1+1)N$ a change of steady-states takes place. Under the critical values of C_0 two equilibrium points are merged into a point of the "saddle-node" type.

The cases (20)-(22) determine different scenarios of the system development. Under small value of C_0 ("environmental capacity") the second coenome can not develop and its biomass x_2 in the steady-state is equal zero. Under middle values of C_0 (the case (21)) the second coenome has possibility of growth after attainment by the first coenome of some level of development. In this case both coenomes share the resources ($x_2^*>0$, $x_1^*+x_2^*=C_0$). Finally, for large values of C_0 the coe-

nomes progress to the maximal possible values and do not exhaust the capacity of the environment.

The qualitative graphic representation of the system's dynamics in the case (21) is shown in the Fig.2. The initial conditions are perceived to be small. On the first interval $[t_0,t_1]$ the progressive increasing x_1 take place. When the critical value x_1^* is reached, the development of the second coenome starts, with x_1 begins to decrease. Then the dynamics of the system is gradually stabilised. In (Chernyshenko, 1995) it is shown for the model (19) that under the condition

$$\frac{N}{a_1+1} < C_0 < \frac{N}{a_1}$$

an "internal catastrophe" take place. If this take place, the value of x_1^* equals $N\text{-}a_1C_0$.

In the Fig. 3-6 phase-portraits of the system (19) are represented. One can see that in the different cases an area of attraction of an finite steady-state includes the neighbourhood of the origin of co-ordinates. The dynamics of the system in this area is in agreement with ecological reasons. In the same time the each phase-portrait includes an area of attraction of the infinite equilibrium point. This fact illustrates that for large values of the co-ordinates the model is not correctly describe a succession process.

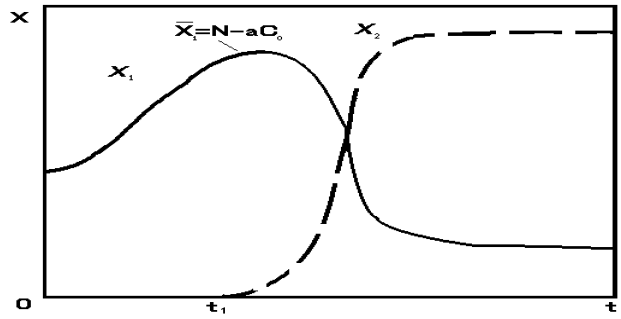

Fig.2: Biomass dynamics in the succession model (19).

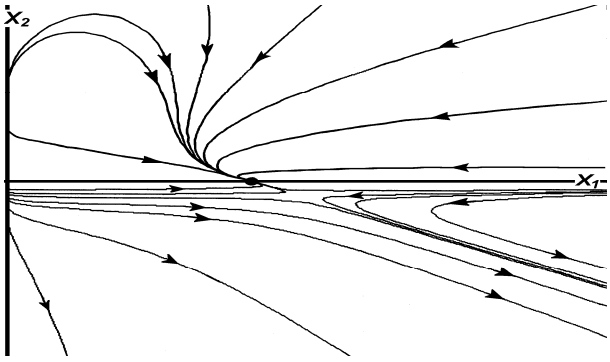

Fig. 3: The phase portrait of the model (19). The case (20) (a=3, N=1, C_0=0.2). A neighbourhood of the origin of co-ordinates.

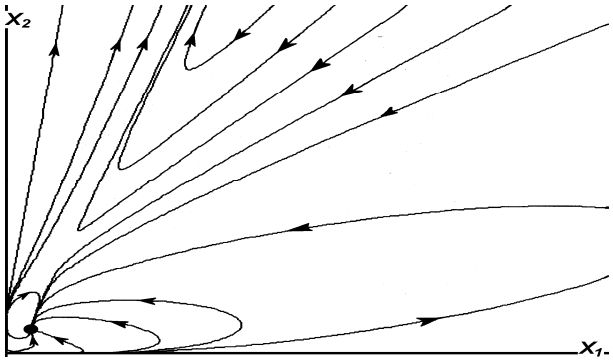

Fig. 4. The phase portrait of the model (19). The case (21) (a=3, N=1, C_0=1).

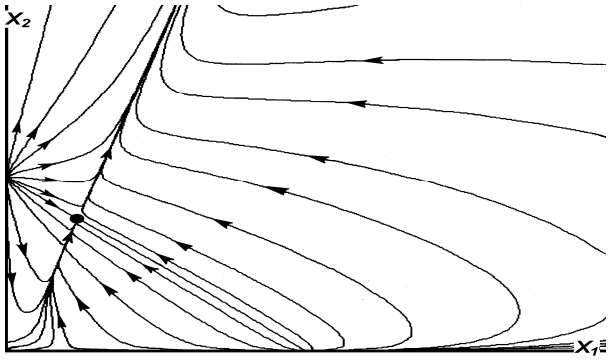

Fig. 5. The phase portrait of the model (19). The degenerate case (21),(22) when $C_0=(a_1+1)N$ (a=3, N=1, C_0=4). The equilibrium point of the "saddle-node" type.

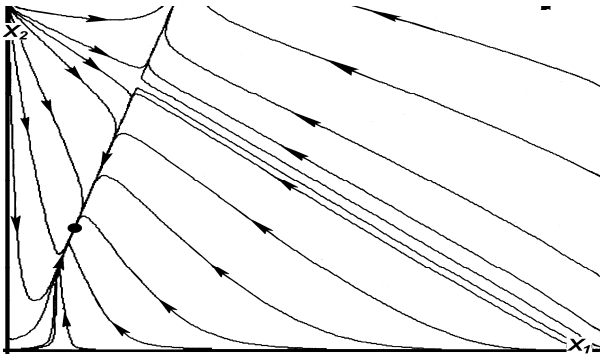

Fig. 6. The phase portrait of the model (19). The case (22) (a=3, N=1, C_0=10).

CONCLUSION

The model (13),(15) describes the succession process as a result of ecosystem ability of self-recovery and homeostasis. Coenome is considered as a major dynamic element of ecosystems in long-term dynamic processes. It is an association of species which have complementary properties (up to symbioses) or united by trophical links. Each succession stage is characterised by a main dominant coenome. The succession process is considered as a process of step-by-step changing the dominant coenome.

The model is an "open" modification of M. Eigen's hypercycle. The model describes a specific intercoenomes interaction, which are similar, but are not equivalent to the competition and "host-parasite" relations. As a result of the interaction and redistribution of ecological resources, several "succession steps" may take place (Fig.2). The number of the steps depends on the major system bifurcation parameter C_0, which is determined by accessible energetic resources. During the succession process the ecosystem "selects" own optimal dimension and complexity. Additional coordinates appear as a result of "technological innovations" in the ecosystem, which increase the flow of accessible energy. Succession process is the process of recreation of optimal complexity level.

In the framework of the model (13), (15) succession process is explained by a low level of the solar energy utilisation by first "undemanding" succession stages. They leave "energetic space" for the development of next, more effective coenomes. The evolution of biogeocoenose proceeds in the direction of a maximal utilisation of the solar energy. The succession process is a process of producing information, if the information is understood as the evaluation of system complexity or complexity of system response to variations of environmental conditions (Eigen and Schuster 1979). A information measure peaks in a climax state. Correspondingly, the entropy decreases during successions. This statement is in agreement with modern ecological conceptions (Brooks and Wiley 1988; Chernyshenko 2008b). The model (13), (15) describes the process of entropy decrease and its characteristic properties: discrete nature of the process and the limitation of the information growth by amount of the energy, accessible for the system.

REFERENCES

Alekseev V.V. 1976 "Dynamic models of water biogeocoenosis" // *Humanity and biosphere*. No. 1, 3-137 (Rus.).

Allen P.M. 1976 "Evolution, Population Dynamics and Stability" *Proceedings of the National Academy of Sciences of the USA*, 73, No. 3, 665-668.

Begon M.; J.L. Harper and C.R. Townsend 1986 *Ecology. Individuals, populations and communities*. Blackwell Scientific Publications, Oxford.

Berezovkaya F.S., G.P. Karev and A.Z. Shvidenko 1991 *Modelling of forest dynamic*. VNII Lesresurs Press, Moscow (Rus.)

Brooks D.R. and E.O. Wiley 1988 *Evolution as entropy: toward a unified theory of biology*. The University of Chicago Press, Chicago and London.

Chernyshenko S.V. 1995 "Qualitative analysis of two-dimensional modification of the M. Eigen's hypercycle and internal catastrophes" *Problems of applied mathematics and mathematical modelling*. Dniepropetrovsk University Press, 129-134 (Rus.).

Chernyshenko S.V. 1996 "System approach to modelling of succession processes in phytocoenoses" *Problems of the forestry and forest recultivation*. Dniepropetrovsk University Press, 70-77 (Rus.).

Chernyshenko S.V. 2008a "Matter and matter flows in the biosphere" *Encyclopedia of Ecology*, Vol. 3 Oxford: Elsevier, 2279-2292.

Chernyshenko S.V. 2008b "Structure and history of life" *Encyclopedia of Ecology,* Vol. 4. Oxford: Elsevier, 3403-3416.

Eigen M. and P. Schuster 1979 *The Hypercycle. A principle of natural self-organization*. Springer-Verlag, Berlin, Heidelberg, New York.

Gams H. 1918 "Prinzipienfragen der Vegetationsforschung" *Vierteljahrschr. Naturforsch. Gesellsch* Bd. 63, 293-493.

Horn H.S. 1976 "Succession" *Theoretical ecology*. Blackwell, 187-204.

Lappo A.V. 1987 *Signs of past biospheres*. Znanie, Moscow (Rus.).

Lepš Jan 1988 "Mathematical Modelling of Ecological Succession: A Review" *Folia Geobotanica & Phytotaxonomica,* Vol. 23, No. 1, 79-94

Liebig J. 1847 *Chemistry in its application to agriculture and physiology*. Taylor & Walton, London.

Lotka A.J. 1925 *Elements of physical biology*. Williams and Wilkins, Baltimore.

May R.M. 1973 *Stability and complexity in model ecosystems*. Princeton University Press, Princeton.

Maynard Smith J. 1974 *Models in ecology*. Cambridge University Press, Cambridge.

Odum E.P. 1971 *Fundamentals of ecology*. Saunders, Philadelphia.

Perry G.L.W. and J.D.A. Millington 2008 "Spatial modelling of succession-disturbance dynamics in forest ecosystems: Concepts and examples" P*erspectives in Plant Ecology, Evolution and Systematics*, No. 9, 191–210

Pielou E.C. 1977 *Mathematical ecology.* Wiley and Sons, N.Y.

Svirezhev Yu.M. and D.O. Logofet 1978 *Stability of biological societies*. Nauka, Moscow (Rus.).

Thornley J.H. 1976 *Mathematical models in plant physiology*. Academic Press, London.

Ulanowicz R.E. 1972 "Mass and energy flow in closed ecosystems" J.Theor.Biol., V. 34, 1014-1029

Volterra V. 1931 *Theorie mathematique de la lutte pour la vie*. Paris.

AUTHOR BIOGRAPHY

SERGE V. CHERNYSHENKO was born in Dnipropetrovsk, Ukraine and graduated from the Dnipropetrovsk State University. After obtaining PhD degree on computing in 1986, was, successively, head of Laboratory of Mathematical Modeling in Biology, head of Computer Science Department, dean of Applied Mathematics Faculty at Dnipropetrovsk National University. He was a supervisor of several Ukrainian national projects on mathematical modeling. From 2009 he is a visiting professor of Koblenz-Landau University, Faculty of Informatics. His e-mail address is svc@a-teleport.com and his website can be found at www.uni-koblenz.de/~svc

HIERARCHICAL HETEROGENITY OF POPULATIONS: MODELING BY THE OPEN EIGEN HYPERCYCLE

Vasiliy Ye. Belozyorov
Faculty of Applied Mathematics
O. Gonchara Dnipropetrovsk National University
49010, Dnipropetrovsk, Ukraine
Email: belozvye@mail.ru

Serge V. Chernyshenko
Faculty of Informatics
University of Koblenz-Landau
D-56070, Koblenz, Germany
Email: svc@a-teleport.com

Vsevolod S. Chernyshenko
Computer Software Department
National Mining University
49600, Dnipropetrovsk, Ukraine
Email: VseVsevolod@hotmail.com

KEYWORDS

System of ordinary quadratic differential equations, asymptotic stability, biological population.

ABSTRACT

The case of a biological population, which consists of several sub-populations (different kinds of the population "social" groups: families, bevies, etc.), has been considered. For description of non-trivial interactions between these groups, a model of "open the Eigen hypercycle" has been proposed. Its bifurcation analysis for 3-dimension case has been carried out. Ecological interpretation of the results has been discussed.

INTRODUCTION

A huge number of mathematical models of ecological population structure (for example, (Allen 1974; Austin 1990; Billik and Case 1994; Chernyshenko 1995; Maurer 1999; Williamson 1990)) are designed for the description of population dynamics while taking into account different kinds of physiological differences between specimens (of age, sex, size, etc.) At the same time it is known (Breder 1959; Urich 1938) another form of population heterogeneity, based on the "social" population structure.Contrary to sex difference, specimens can change their group membership (though this changes are not as mechanistic as change of age). The main feature of social groups is an hierarchical character of the "social structure" and dependence of the existance of higher groups on the proper functionality of the lower ones. Big populations of relatively "intellectual" animals form new levels of population organization. The most bright example is the row "specimen – family – bevy" and, correspondingly, different kind of specimens (ordinary specimen, head of family, bevy leader) (Manteyfel 1992).

In the famous hypercycle model, proposed by Eigen and Shuster (Eigen and Schuster 1979; May 1991), similar relationship between system elements is described. At the same time, relations between "social groups" are not cyclic, and worsening of life conditions of the populations leads to elimination of higher levels while keeping lower ones. That gives an idea to use an open modification of the hypercycle model, which was proposed initially for the description of ecological successions and some social processes (Sole and Bascompte 2006; Ellner and Rees 2006).

The open hypercycle model is based on a matrix representation, which is non-linear (it is natural for a model of "social self-organization" of the population). In the article we focus on a continuous case, although the results may be used for discrete versions also. The model shows dependence of a complexity of population "social structure" from the size of its niche. Population "chooses" its complexity (or dimension) itself. We show it exactly for 3-dimension case (as well as for 2-dimension earlier (Chernyshenko 2005); generalization for N-dimension case is matter of further research.

1. OPEN HYPERCYCLE MODEL.

Let's consider the dynamic behavior of the heterogeneous biological population $\mathbf{x}(t) = (x_1(t), ..., x_n(t))^T$, which describing by Eigen's model hypercycle (here and further symbol T signifies transposition)

$$\begin{cases} \dot{x}_1(t) = x_1(t)\left(F_1(t) - \dfrac{1}{S_0}\displaystyle\sum_{j=1}^{n} x_j(t)F_j(t)\right), \\ \cdots\cdots\cdots\cdots\cdots\cdots, \\ \dot{x}_n(t) = x_n(t)\left(F_n(t) - \dfrac{1}{S_0}\displaystyle\sum_{j=1}^{n} x_j(t)F_j(t)\right), \end{cases} \tag{1}$$

Proceedings 26th European Conference on Modelling and Simulation ©ECMS Klaus G. Troitzsch, Michael Möhring, Ulf Lotzmann (Editors)
ISBN: 978-0-9564944-4-3 / ISBN: 978-0-9564944-5-0 (CD)

(here $S_0 > 0$). The population consists of n subpopulations $x_i(t), i = 1, ..., n,$, which represent different levels of "social" hierarchy. The vector of initial values is $\mathbf{x}^T(0) = (x_{10}, ..., x_{n0})$.

We will consider that $F_1(t) = N - x_1(t), F_i(t) = a_{i-1}x_{i-1}(t) - x_i(t); i = 2, ..., n,$ where $N, a_1, ..., a_{n-1}$ are positive numbers. (The functions $F_1(t), ..., F_n(t)$ are called as Allen's functions (Allen 1974).)

These functions determine very special interaction between the sub-populations, whene each of them depends on all the previous ones. Contrary to Eigen's hypercycle, the dependence has no cyclic character, so we can call this model as 'open' hypercycle.

2. THE EQUILIBRIUM POINTS OF THE SYSTEM (1).

Let's investigate analytically main features of the model dynamics.

Let's define as $i_1, ..., i_k$ $(k \leq n)$ permutations of any k symbols $1, 2, ..., n$, for which the condition

$$1 \leq i_1 < ... < i_k \leq n$$

is fulfilled.

Assume that $x_{i_1} \neq 0, ..., x_{i_k} \neq 0$ and $x_{i_{k+1}} = 0, ..., x_{i_n} = 0$. Then the system of equations that define equilibriums has the form

$$\begin{pmatrix} 1 - \frac{x_{i_1}}{S_0} & -\frac{x_{i_2}}{S_0} & \cdots & -\frac{x_{i_k}}{S_0} \\ -\frac{x_{i_1}}{S_0} & 1 - \frac{x_{i_2}}{S_0} & \cdots & -\frac{x_{i_k}}{S_0} \\ \vdots & \vdots & \ddots & \vdots \\ -\frac{x_{i_1}}{S_0} & -\frac{x_{i_2}}{S_0} & \cdots & 1 - \frac{x_{i_k}}{S_0} \end{pmatrix} \cdot \begin{pmatrix} F_{i_1} \\ F_{i_2} \\ \vdots \\ F_{i_k} \end{pmatrix} = 0,$$

$$x_{i_{k+1}} = ... = x_{i_n} = 0. \qquad (2)$$

A determinant of the first k equations of system (2) may be presented as:

$$\det \begin{pmatrix} 1 - \frac{x_{i_1}}{S_0} & -\frac{x_{i_2}}{S_0} & \cdots & -\frac{x_{i_k}}{S_0} \\ -\frac{x_{i_1}}{S_0} & 1 - \frac{x_{i_2}}{S_0} & \cdots & -\frac{x_{i_k}}{S_0} \\ \vdots & \vdots & \ddots & \vdots \\ -\frac{x_{i_1}}{S_0} & -\frac{x_{i_2}}{S_0} & \cdots & 1 - \frac{x_{i_k}}{S_0} \end{pmatrix} =$$

$$= 1 - \frac{x_{i_1} + ... + x_{i_k}}{S_0}.$$

Here we may face two cases: 1)$1 - \frac{x_{i_1} + ... + x_{i_k}}{S_0} \neq 0$ and 2)$1 - \frac{x_{i_1} + ... + x_{i_k}}{S_0} = 0$.

2.1. Determinant of the first k equations of the system (1) is not equal to zero.

In this case, according to (2) we get that $F_{i_1} = ... = F_{i_k} = x_{i_{k+1}} = ... = x_{i_n} = 0$. Condition $F_{i_1} = 0$ leads to $x_1 \neq 0$, then $x_1 = N, x_2 = a_1 N, x_3 = a_1 a_2 N, ..., x_n = a_1 \cdot ... \cdot a_{n-1} N$; in this case the condition

$$S_0 \neq N(1 + a_1 + a_1 a_2 + ... + a_1 \cdot ... \cdot a_{n-1})$$

has to be fulfilled.

Let $x_1 \neq 0, x_2 = 0$. Then $x_3 = ... = x_n = 0$. Assume $x_1 \neq 0, F_2 = 0$. Then $x_1 = N, x_2 = a_1 N, x_3 = ... = x_n = 0$.

It is easy to find out that in this case we have $n + 1$ equilibriums:

$$E_1 = \begin{pmatrix} 0 \\ 0 \\ \vdots \\ 0 \end{pmatrix}, ..., E_{k+1} = \begin{pmatrix} 1 \\ a_1 \\ \vdots \\ a_1 \cdot ... \cdot a_{k-1} \\ 0 \\ \vdots \\ 0 \end{pmatrix} N, ...,$$

$$E_{n+1} = \begin{pmatrix} 1 \\ a_1 \\ \vdots \\ a_1 \cdot ... \cdot a_{n-1} \end{pmatrix} N \in \mathbb{R}^n.$$

2.2. Determinant of the first k equations of the system (1) is equal to zero.

Here, we have $x_{i_k} = S_0 - x_{i_1} - ... - x_{i_{k-1}}$. Substituting the last formula in the system (2) we derive $F_{i_1} = F_{i_2} = ... = F_{i_k} = F$, where F is a nonzero function. Taking into account the last equations, system (2) may be presented as

$$\begin{cases} x_{i_1}(a_{i_1 - 1}x_{i_1 - 1} - x_{i_1} - F) = 0, \\ \cdots\cdots, \\ x_{i_k}(a_{i_k - 1}x_{i_k - 1} - x_{i_k} - F) = 0, \\ x_1 + ... + x_n = S_0, \\ x_{i_{k+1}} = 0, \\ \cdots\cdots, \\ x_{i_n} = 0, \end{cases} \qquad (3)$$

where $F \neq F_{i_{k+1}}, ..., F \neq F_{i_n}$.

From this system we derive that $x_{i_1} \neq 0, ..., x_{i_k} \neq 0$. As $k = 1, 2, ..., n - 1$, we get $C_n^1 + C_n^2 + ... + C_n^{n-1} + C_n^n$ solutions. Here C_n^i is a number of combinations of k sets from n elements $(k < n)$.

Taking into account the case when determinant of the rst k equations of the system (1) is not equal to zero, we get for this system (1) $n + 1 + C_n^1 + ... + C_n^{n-1} + 1 = 2^n + n$ equilibriums.

2.3. Jacobian matrix building.
The Jacobi matrix for arbitrary n can be evaluated as $J = A + B + C$, where:

$$A = \begin{pmatrix} F_1 - \frac{1}{S_0}\sum_{j=1}^{n} x_j F_j & \cdots & 0 \\ \vdots & \ddots & \vdots \\ 0 & \cdots & F_n - \frac{1}{S_0}\sum_{j=1}^{n} x_j F_j \end{pmatrix};$$

$$B = \begin{pmatrix} -x_1 & 0 & 0 & \cdots & 0 \\ x_2 a_1 & -x_2 & 0 & \cdots & 0 \\ \vdots & \vdots & \ddots & \ddots & \vdots \\ 0 & 0 & \cdots & x_n a_{n-1} & -x_n \end{pmatrix};$$

$$C = -\frac{1}{S_0}\begin{pmatrix} x_1(N - 2x_1 + a_1 x_2) & \cdots & x_1(a_{n-1}x_{n-1} - 2x_n) \\ \vdots & \cdots & \vdots \\ x_n(N - 2x_1 + a_1 x_2) & \cdots & x_n(a_{n-1}x_{n-1} - 2x_n) \end{pmatrix}.$$

3. EIGENVALUES OF JACOBI MATRIX IN EQUILIBRIUM POINTS FOR n = 3.

Let $n = 3$ and $F_1(t) = N - x_1(t)$, $F_2(t) = a_1 x_1(t) - x_2(t)$,$F_3(t) = a_2 x_2(t) - x_3(t)$, where $N > 0, a_1 > 0, a_2 > 0$.

Here we come to two cases: 1)$x_1 + x_2 + x_3 \neq S_0$ and 2)$x_1 + x_2 + x_3 = S_0$.

In the first case $(x_1 + x_2 + x_3 \neq S_0)$ we have four equilibriums:

$$(0,0,0)^T, (N,0,0)^T, (N, a_1 N, 0)^T, (N, a_1 N, a_1 a_2 N)^T.$$

In the second case $(x_1 + x_2 + x_3 = S_0)$ we have seven systems of equations, watch (3), to determine additional seven equilibriums:

$$\begin{cases} a_1 x_1 - x_2 - F = 0 \\ a_2 x_2 - x_3 - F = 0 \\ x_1 + x_2 + x_3 = S_0 \\ x_1 = 0 \end{cases}, \begin{cases} N - x_1 - F = 0 \\ a_2 x_2 - x_3 - F = 0 \\ x_1 + x_2 + x_3 = S_0 \\ x_2 = 0 \end{cases},$$

$$\begin{cases} N - x_1 - F = 0 \\ a_1 x_1 - x_2 - F = 0 \\ x_1 + x_2 + x_3 = S_0 \\ x_3 = 0 \end{cases}, \begin{cases} a_2 x_2 - x_3 - F = 0 \\ x_1 + x_2 + x_3 = S_0 \\ x_1 = 0 \\ x_2 = 0 \end{cases},$$

$$\begin{cases} N - x_1 - F = 0 \\ x_1 + x_2 + x_3 = S_0 \\ x_2 = 0 \\ x_3 = 0 \end{cases}, \begin{cases} a_1 x_1 - x_2 - F = 0 \\ x_1 + x_2 + x_3 = S_0 \\ x_1 = 0 \\ x_3 = 0 \end{cases},$$

$$\begin{cases} N - x_1 - F = 0 \\ a_1 x_1 - x_2 - F = 0 \\ a_2 x_2 - x_3 - F = 0 \\ x_1 + x_2 + x_3 = S_0 \end{cases}.$$

(Indefinite form of function F doesn't affect the present analysis.)

So, for the system (1) where $n = 3$ we got following 11 equilibriums:

E_1 :
$$x_1 = 0, x_2 = 0, x_3 = 0.$$

E_2 :
$$x_1 = 0, x_2 = \frac{S_0}{a_2 + 2}, x_3 = \frac{(a_2 + 1)S_0}{a_2 + 2}.$$

E_3 :
$$x_1 = \frac{S_0 + N}{2}, x_2 = 0, x_3 = \frac{S_0 - N}{2}.$$

E_4 :
$$x_1 = \frac{S_0 + N}{a_1 + 2}, x_2 = \frac{(a_1 + 1)S_0 - N}{a_1 + 2}, x_3 = 0.$$

E_5 :
$$x_1 = N, x_2 = a_1 N, x_3 = 0.$$

E_6 :
$$x_1 = 0, x_2 = 0, x_3 = S_0.$$

E_7 :
$$x_1 = 0, x_2 = S_0, x_3 = 0.$$

E_8 :
$$x_1 = S_0, x_2 = 0, x_3 = 0.$$

E_9 :
$$x_1 = N, x_2 = 0, x_3 = 0.$$

E_{10} :
$$F_1 = F_2 = F_3 = 0;$$

in this case

$$x_1 = N, x_2 = a_1 N, x_3 = a_1 a_2 N.$$

E_{11} :
$$F_1 = F_2 = F_3 \neq 0, x_1 + x_2 + x_3 = S_0;$$

then

$$x_1 = \frac{S_0 + (a_2 + 2)N}{3 + a_1 + a_2 + a_1 a_2}, x_2 = \frac{(a_1 + 1)S_0 + (a_1 - 1)N}{3 + a_1 + a_2 + a_1 a_2},$$

$$x_3 = \frac{(1 + a_2 + a_1 a_2)S_0 - (a_1 + a_2 + 1)N}{3 + a_1 + a_2 + a_1 a_2}.$$

(It is easy to find that all equilibriums do exist in the first orthan, necessary and sufficient criteria are: $S_0 \geq N$ and $a_2 \geq 1$ will be fulfilled.)

Now we are going to find a positive invariant set of the system (1) in case $n = 3$. Sum of all equations of system (1) is equal to:

$$\frac{d(x_1 + x_2 + x_3 - S_0)}{dt} = (x_1 + x_2 + x_3 - S_0) *$$

$$* \frac{1}{S_0}(-Nx_1 - a_1x_1x_2 - a_2x_2x_3 + x_1^2 + x_2^2 + x_3^2). \quad (4)$$

The behavior of solutions of (7) is described by the matrix

$$\begin{pmatrix} 1 & -a_1/2 & 0 \\ -a_1/2 & 1 & -a_2/2 \\ 0 & -a_2/2 & 1 \end{pmatrix}.$$

As $x_1 \geq 0, x_2 \geq 0, x_2 \geq 0$, then it follows from the equation (7) that if $x_{10} + x_{20} + x_{30} \leq S_0$, in case $t \geq 0$, $x_1 + x_2 + x_3 \leq S_0$. Let's define by V a domain in the first orthant bounded by coordinate planes $x_1 = 0$, $x_2 = 0$, $x_2 = 0$ and $x_1 + x_2 + x_3 = S_0$.

Recasting the equation (7) by successively completing the squares, we obtain:

$$\frac{d(x_1 + x_2 + x_3 - S_0)}{dt} =$$

$$= (x_1 + x_2 + x_3 - S_0)\frac{1}{S_0}(-Nx_1 + (x_1 - 0.5a_1x_2)^2$$

$$+(x_3 - 0.5a_2x_2)^2 + (1 - 0.25a_1^2 - 0.25a_2^2)x_2^2) =$$

$$= (x_1 + x_2 + x_3 - S_0)\frac{1}{S_0}\Big[\Big(x_1 - \frac{a_1}{2}x_2 - \frac{N}{2}\Big)^2 +$$

$$+\frac{4 - a_1^2 - a_2^2}{4}\Big(x_2 - \frac{2a_1N}{4 - a_1^2 - a_2^2}\Big)^2 + \Big(x_3 - \frac{a_2}{2}x_2\Big)^2 -$$

$$-\frac{N^2}{4} - \frac{a_1^2N^2}{4 - a_1^2 - a_2^2}\Big].$$

Let $a_1^2 + a_2^2 < 4$. Define by W an ellipsoid with center in point

$$K\left(\frac{N}{2} + \frac{a_1^2N}{4 - a_1^2 - a_2^2}, \frac{2a_1N}{4 - a_1^2 - a_2^2}, \frac{a_1a_2N}{4 - a_1^2 - a_2^2}\right)$$

and product of semiaxes

$$\frac{N^3(4 + 3a_1^2 - a_2^2)^{3/2}}{4(4 - a_1^2 - a_2^2)^2}.$$

If $a_1^2 + a_2^2 < 4$, $x_{10} + x_{20} + x_{30} \geq S_0$ and $(x_{10}, x_{20}, x_{30})^T \in W$, then a vector $(x_1(t), x_2(t), x_3(t))^T \in W$, and the formula in big rectangular brackets is negative. Therefore $\lim\limits_{t\to\infty}(x_1(t), x_2(t), x_3(t))^T = E_{11}$. (Let $u = x_1(t) + x_2(t) + x_3(t) - S_0$. Then the equation (7) may be written in the form $\dot{u} = \xi(u)u$, where $\xi(u) < 0$; we derive the analog of a linear equation, the solution of which tends to zero.) Further we will consider the case $(x_{10}, x_{20}, x_{30})^T \in V$ only.

4. ANALYSIS OF THE EQUILIBRIUMS.

In all computations elements of Jacobian matrix divided on S_0 (so eigenvalue λ is replaced by the construction λ/S_0).

Let $\mu = N/S_0$. This value characterizes the ecological niche's size (it is inversely proportional the size). Let's analyse a behavior of the system (1) in the vicinity of all equilibriums.

Let's estimate all eigenvalues:

E_1. In this point eigenvalues $\lambda_1 = \mu, \lambda_2 = \lambda_3 = 0$. Equilibrium is a degenerative unstable node.

E_2. In this point eigenvalues

$$\lambda_1 = \mu + \frac{1}{a_2 + 2}, \lambda_2 = -\frac{a_2 + 1}{a_2 + 2}, \lambda_3 = \frac{1}{a_2 + 2}.$$

As $\mu > 0$, $a_2 \geq 0$ and $\lambda_2 \leq 0$, equilibrium is a saddle-node.

E_3. Here

$$\lambda_1 = \frac{\mu(a_1 - 1)}{2} + \frac{a_1 + 1}{2}, \lambda_2 = -\frac{1 - \mu^2}{2}, \lambda_3 = \frac{1 - \mu}{2}.$$

If $\mu \neq 1$, then from condition $\lambda_2\lambda_3 < 0$ it follows that this point is saddle-node. If $\mu = 1$, then

$$\lambda_1 = a_1, \lambda_2 = \lambda_3 = 0,$$

and we get a degenerative unstable node.

E_4. Here

$$\lambda_1 = -\frac{\mu(1 + a_1 + a_2)}{a_1 + 2} + \frac{1 + a_2 + a_1a_2}{a_1 + 2},$$

$$\lambda_2 = -\frac{\mu(1 + a_1)}{a_1 + 2} + \frac{1}{a_1 + 2}, \lambda_3 = \frac{(\mu + 1)(\mu - 1 - a_1)}{a_1 + 2}.$$

A simple analysis shows that if

$$\frac{1 + a_2 + a_1a_2}{1 + a_1 + a_2} < \mu < 1 + a_1, \quad (5)$$

then this point is a stable node. If $\mu > 1 + a_1$, then it is a saddle-node.

E_5. Here

$$\lambda_1 = a_2a_1\mu, \lambda_{2,3} = -\frac{\mu(a_1 + 1 - \mu)}{2} \pm$$

$$\pm\frac{\mu}{2}\sqrt{(a_1 + 1 - \mu)^2 + 4a_1(a_1\mu + \mu - 1)}.$$

As $\lambda_1 > 0$, then equilibrium is either a saddle or an unstable node.

E_6. Here $\lambda_1 = 1 + \mu, \lambda_{2,3} = 1$. Equilibrium is an unstable node.

E_7. Here $\lambda_1 = 1 + \mu, \lambda_2 = 1, \lambda_3 = a_2 + 1$. Equilibrium is an unstable node.

E_8. Here $\lambda_{1,2} = 1 - \mu, \lambda_3 = a_1 + 1 - \mu$. This point is either an unstable node or a stable node or a saddle-node.

E_9. Here $\lambda_1 = \mu(\mu-1), \lambda_2 = a_1\mu, \lambda_3 = 0$. This point is an unstable node or saddle.

E_{10}. It is clear that $N(1+a_1+a_1a_2) \le S_0$ or

$$\mu = \frac{S_0}{N} \le \frac{1}{1+a_1+a_1a_2} \qquad (6)$$

then $E_{10} \subset V$.

The Jacobi matrix in point E_{10} may be presented as:

$$J_{10}/S_0 = \mu \begin{pmatrix} -1 & 0 & 0 \\ a_1^2 & -a_1 & 0 \\ 0 & a_1a_2^2 & -a_1a_2 \end{pmatrix} +$$

$$+\mu^2 \left[\begin{pmatrix} 1 \\ a_1 \\ a_1a_2 \end{pmatrix} \cdot \begin{pmatrix} (1-a_1^2), a_1(1-a_2^2), a_1a_2 \end{pmatrix} \right].$$

A characteristic polynomial of the Jacobi matrix in point E_{10} is:

$$\det(\lambda I - J_{10}/S_0) = \lambda^3 + p_1\lambda^2 + p_2\lambda + p_3 =$$

$$= \lambda^3 + [\mu(1+a_1+a_1a_2) - \mu^2]\lambda^2 + [a_1(1+a_2+a_1a_2)\mu^2 -$$

$$-a_1(1+a_1+a_2)\mu^3]\lambda + a_1^2a_2[\mu^3 - (1+a_1+a_1a_2)\mu^4].$$

Let's assume that the condition (6) is satisfied. Then $E_{10} \subset V$. If $\mu \to 0$, then this point is asymptotic stable. In case when μ is increasing, but inequality (6) is satisfied, it easy to check that $p_1 > 0, p_2 > 0, p_3 > 0, p_1p_2 > p_3$. If $\mu = (1+a_1+a_1a_2)^{-1}$ (bifurcation point), then $\lambda_1 = 0$ and the point turns out to be unstable.

E_{11}. One of eigenvalues of the Jacobi matrix is

$$\lambda_1 = \frac{1-\mu(1+a_1+a_1a_2)}{3+a_1+a_2+a_1a_2}.$$

Therefore the inequality (6) is hold. So $\lambda_1 > 0$ and equilibrium E_{11} may be node or saddle.

If

$$\mu \approx \frac{1}{1+a_1+a_1a_2}$$

and

$$\mu > \frac{1}{1+a_1+a_1a_2},$$

then equilibrium is a stable node. Thus, if

$$\mu = \frac{1}{1+a_1+a_1a_2}$$

then points E_{10} and E_{11} are exchange.

Consider the case

$$\mu > \frac{1}{1+a_1+a_1a_2}.$$

It is clear that

$$\frac{1}{1+a_1+a_1a_2} \le \frac{1+a_2+a_1a_2}{1+a_1+a_2}.$$

Note, if

$$\mu = \frac{1}{1+a_1+a_1a_2}$$

then one of eigenvalues of the Jacobi matrix in the point E_{11} equal to zero; if

$$\mu = \frac{1+a_2+a_1a_2}{1+a_1+a_2},$$

then another eigenvalue of the Jacobi matrix equal to zero (other two eigenvalues have negative real parts).

If

$$\frac{1}{1+a_1+a_1a_2} < \mu < \frac{1+a_2+a_1a_2}{1+a_1+a_2},$$

then the point E_{11} is stable; if

$$\mu > \frac{1+a_2+a_1a_2}{1+a_1+a_2},$$

then the point E_{11} is unstable.

At last, if the condition (5) is fulfilled, then we have the stable equilibrium in E_4.

5. BIFURCATION POINTS.

Let's find a positive invariant set of the system (1) for $n = 3$. Add all equations of system (1):

$$\frac{d(x_1+x_2+x_3-S_0)}{dt} = (x_1+x_2+x_3-S_0)\frac{1}{S_0}(-Nx_1-$$

-a$_1x_1x_2 - a_2x_2x_3 + x_1^2 + x_2^2 + x_3^2$).(7)

Let's introduce a new variable $u(t) = x_1(t) + x_2(t) + x_3(t) - S_0$. Then equation (**??**) may be written as

$$\frac{du}{dt} = u\frac{1}{S_0}(-Nx_1 - a_1x_1x_2 - a_2x_2x_3 + x_1^2 + x_2^2 + x_3^2). \quad (8)$$

Theorem 1. *Any solution $u(t)$ (for any initial value $u_0 = u(0)$ and $\forall t \ge 0$) of equation (8) has the property: $u_0u(t) \ge 0$.*

Let $u_0 \le 0$. As $x_1 \ge 0, x_2 \ge 0, x_2 \ge 0$, then according to the Theorem 1 while $t \ge 0$, the function $u(t) = x_1(t) + x_2(t) + x_3(t) - S_0 \le 0$. We will define as V a domain in the first orthant, bounded by coordinate planes $x_1 = 0$, $x_2 = 0$, $x_2 = 0$ and $x_1 + x_2 + x_3 = S_0$. Then, we derive that V is an invariant set ($\forall t \ge 0$ from $x_{10}+x_{20}+x_{30} \le S_0$ it follows that $x_1(t) + x_2(t) + x_3(t) \le S_0$).

We will consider that $(x_{10}, x_{20}, x_{30})^T \in V$ is a vector of initial values. In this case we will have $\forall t > 0$ $(x_1(t), x_2(t), x_3(t))^T \in V$. Thus, V is a positive invariant set.

We suppose that $x_{10} > 0, x_{20} > 0, x_{30} > 0$. (If one initial value is zero, then we will come to a 2-D analysis.)

There are 4 different bifurcations points:

$$\mu_0 = 0, \mu_1 = \frac{1}{1 + a_1 + a_1 a_2}, \mu_2 = \frac{1 + a_2 + a_1 a_2}{1 + a_1 + a_2},$$

$$\mu_3 = 1 + a_1.$$

1.

$$0 < \mu < \frac{1}{1 + a_1 + a_1 a_2}.$$

The trajectory tends to the single equilibrium $E_{10} \in V$. Thus, for small μ (when the size of the ecological niche larger then the critical value: $S_0 > (1 + a_1 + a_1 a_2) \cdot N$), all sub-populations do exist and try to reach maximal possible size; on the other hand, their aggregate size is smaller then the size S_0 of the population niche.

2.

$$\frac{1}{1 + a_1 + a_1 a_2} < \mu < \frac{1 + a_2 + a_1 a_2}{1 + a_1 + a_2}.$$

The trajectory tends to the single equilibriums $E_{11} \in V$. With such a size of the ecological niche, all three subpopulations may be presented; they occupy whole ecological niche S_0 and are limited in size by the size of the niche.

3.

$$\frac{1 + a_2 + a_1 a_2}{1 + a_1 + a_2} < \mu < 1 + a_1.$$

The trajectory tends to the single equilibriums $E_4 \in V$. The niche size S_0 is so small that the third level of the subpopulation "social" organization (the third sub-population) can not come into existence. Two other populations occupy the entire ecological niche.

4. $1 + a_1 < \mu < \infty$.

In this case the trajectory tends to the point $E_8 \in V$. In the environment of such a small ecological niche only the first subpopulation is able to exist. So population is limited only by the size of niche. It has no internal structure; second and third sub-populations are absent.

6. CONCLUSION.

The analysis of results which were resulted above, leads to the several observations. In case of small values of p, only the first subpopulation survives. Second and third subpopulations survive just with growth of p. In addition, all surviving populations occupy whole ecological niche. Finally, if $p > p_3$ then an "era of abundance" comes, when all populations survive, and ecological niche is filled partially (all resources of the niche are used not completely).

One should also mention the following: parameters S_0, N, a_1, a_2 have different influence on a character of flowing processes. The most important of these parameters are S_0, N. Parameter S_0 determines the maximal volume of resources, that can be used while populations development. Parameter N shows that at any nonzero S_0 the first population always survives. This conclusion allows to assert that in case of the Eygen model, the biological association remains (what is possible thanks to the reduced structure). Parameters $a_1 and a_2$ specify only a quantitative influence of one population on others. In addition, these parameters do not change the type of bifurcation points and their ammount.

Analysis of the 3-D open Eigen's model allows to propose the following suggestion sfor n-dimension case.

There do exist $n + 1$ bifurcation points :

$$0 = \mu_0 < \mu_1 < \mu_2 < ... < \mu_n < \infty,$$

where

$$\mu_1 = \frac{1}{1 + a_1 + a_1 a_2 + ... + a_1 \cdot ... \cdot a_{n-1}}.$$

If

$$0 < \mu < \mu_1,$$

then all populations survive and occupy only part of ecological niche; a volume of this niche is $N(1 + a_1 + a_1 a_2 + ... + a_1 \cdot ... \cdot a_{n-1}) < S_0$.

If:

$$\mu_1 \leq \mu < \infty,$$

then populations (but not all) occupy whole ecological niche S_0; if

$$\mu_i < \mu < \mu_{i+1}, 1 \leq i \leq n - 1,$$

then populations $1, 2, ..., n - i + 1$ remain and populations $n - 1, n - 2, ..., i - 1$ die out ; when

$$\mu_n < \mu < \infty,$$

then only unique population survive and fill whole ecological niche S_0.

REFERENCES

[Ackleh and Allen 2003] Ackleh A. S., Allen L. J. S. 2003. *Competitive exclusion and coexistence for pathogens in an epidemic model with variable population size*. J. Math. Biol. Vol.47, 153-168.

[Allen 1974] Allen P. M. 1974. *"Evolution, population dynamics and stability"*. Proc. of the National Academy of Sciences of the USA. Vol. 73, No 3, 665-668.

[Austin 1990] Austin M. P. 1990. *Community theory and competition in vegetation . Perspectives on plant competition*. San Diego: Academic Press, 215-238.

[Billik and Case 1994] Billik I., Case T. J. 1994. *Higher order interactions in ecological communities: What are they and how can they be detected.* . Ecology. Vol. 75, 1529-1543.

[Breder 1959] Breder C. M. 1959. *Studies on social grouping in fishes*. –Bull. Amer. Mus. Natur. Hist. Vol. 117. No 6, 397-481.

[Caswell 2001] Caswell H. 2001. *Matrix population models:Constructions, Analisis, and Inerpretation*. 2nd. ed. Sinauer. Sunderland MA.

[Chernousenko et al. 1988] Chernousenko V. M., Chernenko I. V., Chernyshenko S. V. 1988. *Bifurcation in the modified Eigen hypercycle . Nonlinear and turbulent processes in physics*. Proc. of 3rd Intern. workshop. Kiev: Naukova Dumka. Vol. 2, 261-263.

[Chernyshenko 1995] Chernyshenko S. V. 1995. *The open Eigen Hypercycle and selforganization of ecological systems. Sustainable Development: Environmental Pollution and Ecological Safety*. Dniepropetrovsk: Dniepropetrovsk Univ. Press, 42-43.

[Chernyshenko 2005] Chernyshenko S.V. 2005. *Nonlinear analysis of forest ecosystems dynamics*. Dnipropetrovsk, Dnipropetrovsk University Press.

[Deng 2008] Deng B. 2008. *The time invariance principle, the absence of ecological chaos, and a fundamental pitfall of discrete modeling. Ecologicall Modelling. Vol.215, 287-292.*

[Easterling et al. 2000] Easterling M. R.,Ellner S. P., Dixon P. 2000. Size-specific sensitivity: applying a new structured population model. *Ecology. Vol.81, 964-708.*

[Eigen and Schuster 1979] Eigen M., Schuster P. 1979. The hypercycle: A principle of natural selforganization. *Spriger: Berlin.*

[Ellner and Rees 2006] Ellner S. P., Rees M. 2006. Integral projection models for species with complex demography. *American Naturalist. Vol.167, 410-428.*

[Levin 1997] Levin S. A. 1997. Models of population dispersal. *Differential Equations and Applications in Ecology, Epidemics, and Population Problems. New-York: L. Academic Press, 1-18.*

[Manteyfel 1992] Manteyfel B. P. 1992. Ecological and evolutional aspects of animal behaviour. *Moscow: Nauka.*

[Maurer 1999] Maurer B. A. 1999. Untangling ecological complexity. *Chicago : Univ. of Chicago Press.*

[May 1991] May R.M. 1991. Hypercycles spring to life. *Nature. Vol.353, 607-609.*

[Odum 1994] Odum H. T. 1994. Ecological and general systems and introduction to systems ecology. *Niwot: University Press of Colorado.*

[Roff 1974] Roff D. A. 1974. Spatial heterogenity and persistence of populations. *Ecologia. Vol. 15, 245-258.*

[Sole and Bascompte 2006] Sole R.V., Bascompte J. 2006. Self-Organization in Complex Ecosystems. Monograps in Population Biology. *Prinston University Press. Vol.42.*

[Urich 1938] Urich I. 1938. The social hierarchy in albino mice. *J. Comp. Psychol. Vol. 25., 373-413.*

[Williamson 1990] Williamson M. 1990. The analysis of biological populations. *L.: Academic Press.*

AUTHOR BIOGRAPHIES

VASILIY Ye. BELOZYOROV was born in Dnipropetrovsk, Ukraine graduated from the Dnipropetrovsk State University. Obtained PhD degree on mathematical system theory in 1986. From 1996 till 2009 was, successively, head of Applied Mathematics Department at Dnipropetrovsk National University. He is an Honoured Science Worker of Ukraine. In 2010 he became a professor of Computer Technologies Department, Dnipropetrovsk National University. His e-mail address is belozvye@mail.ru

SERGE V. CHERNYSHENKO was born in Dnipropetrovsk, Ukraine and graduated from the Dnipropetrovsk State Uni-versity. After obtaining PhD degree on computing in 1986, was, successively, head of Laboratory of Mathematical Modeling in Biology, head of Computer Science Department, dean of Applied Mathematics Faculty at Dnipropetrovsk National University. He was a supervisor of several Ukrainian national projects on mathematical modeling. From 2009 he is a visiting professor of Koblenz-Landau University, Faculty of Informatics. His e-mail address is svc@a-teleport.com and his web-site can be found at www.uni-koblenz.de/ svc.

VSEVOLOD S. CHERNYSHENKO was born in Dnipropetrovsk, Ukraine and graduated from the Dnipropetrovsk National University. Got PhD degree on Mathematical Modeling and Numerical Methods in 2009. Nowadays he is a docent at the Computer Software Department of the National Mining University of Ukraine. He is a member of editorial board of journals "Ecology and Noospherology", "Soil Science". His e-mail address is VseVsevolod@hotmail.com and his personal webpage at www.programmer.dp.ua/chernishenko.php.

DEVS GRAPH IN MODELICA FOR REAL-TIME SIMULATION

Alfonso Urquia, Carla Martin-Villalba
Departamento de Informática y Automática
Universidad Nacional de Educación a Distancia (UNED)
Juan del Rosal 16, 28040, Madrid, Spain
Email: {aurquia,carla}@dia.uned.es

Mohammad Moallemi, Gabriel A. Wainer
Department of Systems and Computer Engineering
Carleton University
1125 Colonel By Drive, Ottawa, ON, Canada
Email: gwainer@sce.carleton.ca

KEYWORDS

Modelica, DEVS, DEVS Graph, real-time simulation

ABSTRACT

Two new Modelica libraries are presented. The first library, named GGADLib, supports the DEVS graph notation in Modelica. The second Modelica library, named UDPLib, allows sending and receiving data using the User Datagram Protocol (UDP). GGADLib uses UDPLib. As a result, DEVS graph models composed using GGADLib can receive and send data (input and output events, according to DEVS terminology) using UDP. This feature allows Modelica DEVS graph models to communicate with hardware and with other models, e.g., with models developed using other languages and tools, and running in other computers. The implementation of UDPLib and GGADLib is discussed in this paper. Their use is illustrated by means of a case study: evaluating an obstacle avoidance controller for the e-puck mobile robot. The UDPLib and GGADLib Modelica libraries can be freely downloaded from http://www.euclides.dia.uned.es/

INTRODUCTION

The object-oriented modeling language Modelica facilitates describing the type of models commonly used in control engineering (Åström et al., 1998). This is, models of multi-domain physical systems (containing, e.g., electrical, mechanical, thermal, hydraulic or control subcomponents), which are mathematically described using differential and algebraic equations, and events. This type of model is known as hybrid-DAE model. The continuous-time part of the model can be described in Modelica using equations (non-causal modeling) and algorithms. In addition, Modelica includes functionalities for discrete-event management, such as *if* expressions to define changes in the structure of the model, and *when* expressions to define event conditions and the actions associated with the defined events (Otter et al., 1999).

In some cases, the application of a discrete-event modeling formalism facilitates the development and description of the discrete-event part of hybrid models. Modelica libraries have been developed for supporting different discrete-event modeling formalisms, including State Graphs (Otter et al., 2005), Petri nets (Mosterman et al., 1998) and DEVS (Sanz et al., 2010). These libraries can be used together with other Modelica libraries in order to compose multi-formalism hybrid models.

The DEVS (Discrete EVent Systems specification) formalism allows the modular and hierarchical specification of discrete-event systems (Zeigler, 1976). The Parallel DEVS formalism (Chow and Zeigler, 1994) is an extension of DEVS. DEVSLib (Sanz, 2010) is a full-fledged Modelica library that facilitates the description of discrete-event models according to the Parallel DEVS formalism and provides components to interface with continuous-time models, which can be composed using other Modelica libraries. DEVSLib can be freely downloaded from (Urquia et al., 2012).

DEVS graph (Zeigler et al., 1994) is a graphical notation for describing atomic DEVS models. Graph-based notations have the advantage of allowing the modeler to think about the problem in a more abstract way. For this reason, the use of the DEVS graph notation makes model behavior specification easier.

Two new Modelica libraries will be presented in this paper. The first library, GGADLib, supports the DEVS graph notation in Modelica. The second Modelica library, UDPLib, allows sending and receiving data using the User Datagram Protocol (UDP). GGADLib uses UDPLib. As a result, DEVS graph models composed using GGADLib can receive and send messages (input and output events, according to DEVS terminology) through the network using UDP. This feature allows Modelica DEVS graph models to communicate with hardware and with other models, e.g., with models developed using other languages and tools, and running in other computers.

The DEVS graph notation will be described in the following section. Next, the implementation and use of the UDPLib and GGADLib Modelica libraries will be discussed. Finally, these libraries are applied to assess an obstacle avoidance controller for the e-puck mobile robot (E-puck, 2012).

DEVS GRAPH NOTATION

A DEVS graph model is formally defined by the following tuple of seven elements (Wainer, 2009):

$$\text{GGAD} = \langle X, S, Y, \delta_{int}, \delta_{ext}, \lambda, ta \rangle \qquad (1)$$

Proceedings 26th European Conference on Modelling and Simulation ©ECMS Klaus G. Troitzsch, Michael Möhring, Ulf Lotzmann (Editors)
ISBN: 978-0-9564944-4-3 / ISBN: 978-0-9564944-5-0 (CD)

The model may have input and output ports to communicate with other models. The tuple elements

$$X = \{(pI, x) \mid pI \in IPorts, x \in X_p\} \quad (2)$$
$$Y = \{(pO, y) \mid pO \in OPorts, y \in Y_p\} \quad (3)$$

represent the set of input ports ($IPorts$) and values (X_p), and the set of output ports ($OPorts$) and values (Y_p), respectively. The set of sequential states is represented by S,

$$S = B \times P(V) \quad (4)$$

where B represents the set of model states, also known as model phases

$$B = \{b \mid b \in Bubbles\} \quad (5)$$

and V represents the intermediate state variables of the model and their values

$$V = \{(v, n) \mid v \in Variables, n \in \mathbb{R}_0\} \quad (6)$$

The internal (δ_{int}) and external (δ_{ext}) transition functions, and the output (λ) and time-advance (ta) functions have the same meaning as in DEVS models (Zeigler et al., 2000). At any time the system is in some state $s \in S$. If no external event occurs, the system will stay in state s for time $ta(s)$. When the $ta(s)$ time expires, the system outputs the value $\lambda(s)$ and changes to state $\delta_{int}(s)$. If an external event $x \in X_p$ occurs before the expiration time, $ta(s)$, then the system changes to state $\delta_{ext}(s, e, x)$, where e is the elapsed time since the last transition.

The model graphical description is composed of bubbles, arcs and labels. Bubbles represent model phases. Each bubble includes an identifier and a state lifetime. Arcs represent transitions between states: dotted lines represent internal transitions and full lines represent external transitions. Labels placed beside external transitions indicate the corresponding transition conditions, while labels placed beside internal transitions show the associated output events.

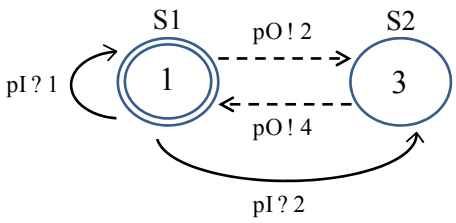

Figure 1: Atomic model defined as a DEVS graph.

The atomic model shown in Figure 1 illustrates this notation. The model has two phases: S1 and S2. The S1 bubble is composed of two concentric circumferences. This indicates that S1 is the initial phase, i.e., the model is in S1 when the simulation starts. The number written into each bubble is the corresponding phase lifetime.

The $p!v$ notation indicates that an output event of v value is generated through the p port. For instance, pO!2 means that an event with 2 value is sent through pO port.

Trigger conditions of external transitions are logical expressions. When the logical expression is evaluated to true, then the corresponding transition is executed. The $p?v$ expression is true when the v value is received in the p input port. In this model, if an event with 1 value is received in pI while in S1, an external transition to S1 is executed. If the event value is 2 while in S1, an external transition to S2 is executed.

THE UDPLib MODELICA LIBRARY

The UDPLib Modelica library is composed of two model classes, *inputUDPport* and *outputUDPport*, and two packages, *src* and *Examples* (see Figure 2a). The *src* package contains Modelica functions that are used by *inputUDPport* and *outputUDPport*. These functions are not intended to be used directly by the library users. The *Examples* package contains some use examples.

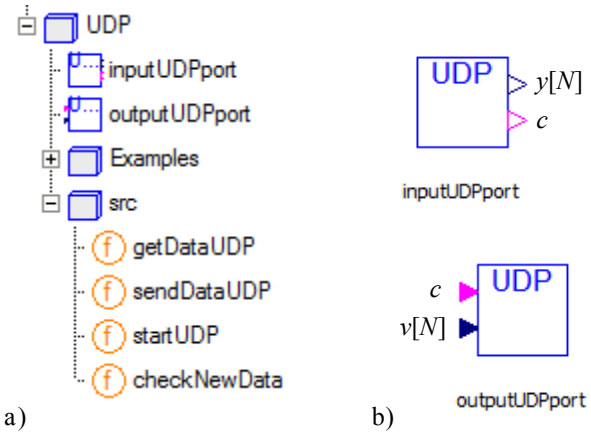

Figure 2: a) The UDPLib Modelica library; and b) *inputUDPport* and *outputUDPport* models.

The *outputUDPport* model allows to send data using the UDP protocol. The port number and IP address are model parameters, whose values can be modified when the model is instantiated. The model interface is composed of the following two connectors (see Figure 2b): an input Boolean variable, c, and an input array of N real variables, v, whose size (N) is a model parameter. When the value of c changes from false to true and vice versa, the N values of the v variable array are sent through the network to the designated IP address and port.

The *inputUDPport* model allows to receive data, using the UDP protocol, from a specified IP address and port number, which are model parameters. The model interface is composed of two connectors (see Figure 2b): an output array of N real variables, y, whose size (N) is a model parameter, and an output Boolean variable, c. The model checks for newly arrived data with a certain sampling period of simulated time, which is a model parameter (the default value is 0.01 seconds). When a new

data (an array of N real values) is received from the network, the value of the Boolean variable c is changed and the received data is assigned to the y array. Therefore, y is an array of N piecewise constant variables which contains the last received data. The changes in the value of c indicate the time instants when data have been received.

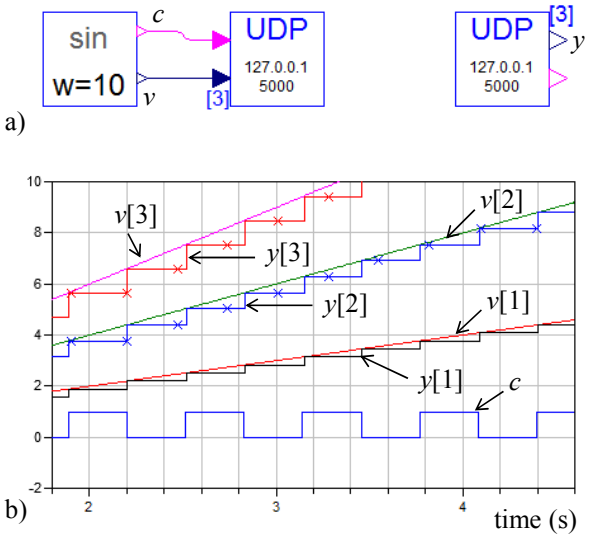

Figure 3: a) Model; and b) detail of simulation result.

The simple model shown in Figure 3a is used to illustrate the use of *inputUDPport* and *outputUDPport*. The left-most component sets the value of the c Boolean variable and the three elements ($N = 3$) of the v array as follows:

$$c = \sin(w \cdot time) > 0 \quad (7)$$

$$v = \{time, 2 \cdot time, 3 \cdot time\} \quad (8)$$

where the $time$ variable represents time and the value given to the w parameter is 10. When the value of c changes (from false to true and vice versa), the three values of the v array are sent to port number 5000, IP address 127.0.0.1.

The component of the *inputUDPport* class checks the port number 5000, IP address 127.0.0.1, for more incoming data every 0.01 seconds of simulated time. The received data are assigned to the y array. The simulated time is synchronized with real time. A detail of the simulation result is shown in Figure 3b.

In general, several instances of the *inputUDPport* and *outputUDPport* classes can be present in a model. Also, instances of these classes can be used to communicate several models running in the same and in different computers.

THE GGADLib MODELICA LIBRARY

The GGADLib library contains predefined Modelica components that facilitate to compose DEVS graphs models. These components include bubbles, to describe the model states, and internal and external transitions. The library is shown in Figure 4a. Ready-to-use components are placed at the higher hierarchical level of the library. These components inherit from the components included within the *src* package. The *Examples* package contains examples of use.

Model states are represented as bubbles in DEVS graph notation. To this end, two classes are provided in the library: *InitialState* and *State* (see Figure 4b). The *InitialState* class allows to specify the model state at the simulation start time. Therefore, a model has to contain one and only one instance of the *InitialState* class. The other model phases are described using instances of the *State* class. *InitialState* and *State* have the same superclass, *src.State*.

The *InitialState* and *State* classes have two parameters: an identifier, which stores the state name, and the state lifetime, whose default value is one second. A Boolean local variable, *active*, indicates whether the model is in the state (*active*=true) or not (*active*=false). The simulated time elapsed since the last transition is stored in the e local variable. This variable allows detecting when the state lifetime has been consumed.

InitialState and *State* have two connectors: one represented as a black filled triangle (*connectorA*) pointing toward the bubble, and another represented as a hollow triangle (*connectorB*) pointing outwards the bubble. Transitions to the state have to be connected to the first connector, while transitions from the state have to be connected to the second connector.

Components describing internal and external transitions are provided in the library. A transition takes place from an initial state to a final state. The *connectorB* of the initial state has to be connected to the *connectorB* of the transition component, and the *connectorA* of the final state has to be connected to the *connectorA* of the transition component. Common features to internal and external transitions are modeled in the *src.Transition* class, which is the superclass of the *InternalTransition* and *ExternalTransition* classes (see Figures 4c and 4d).

The *InternalTransition* class describes an internal transition and the generation of the output event associated to the transition. The internal transition is triggered when its initial state is active and the state lifetime has been consumed. The *send* and *data* connectors describe the output event generation (see Figure 4c). When the transition takes place, the value of the *send* Boolean variable changes and the *data* real variable is set to the event value. By default, the value of the output event is a component parameter (i.e., the output functions returns a single constant value). This by-default behavior can be easily modified, so that output event values can be evaluated from any Modelica function.

The *InternalTransitionUDP* class provides additional features. It sends the event value to a predefined port and IP address, using the UDP protocol. *InternalTransitionUDP* has been defined by connecting the *InternalTransition* and the *outputUDPport* classes. The icon and

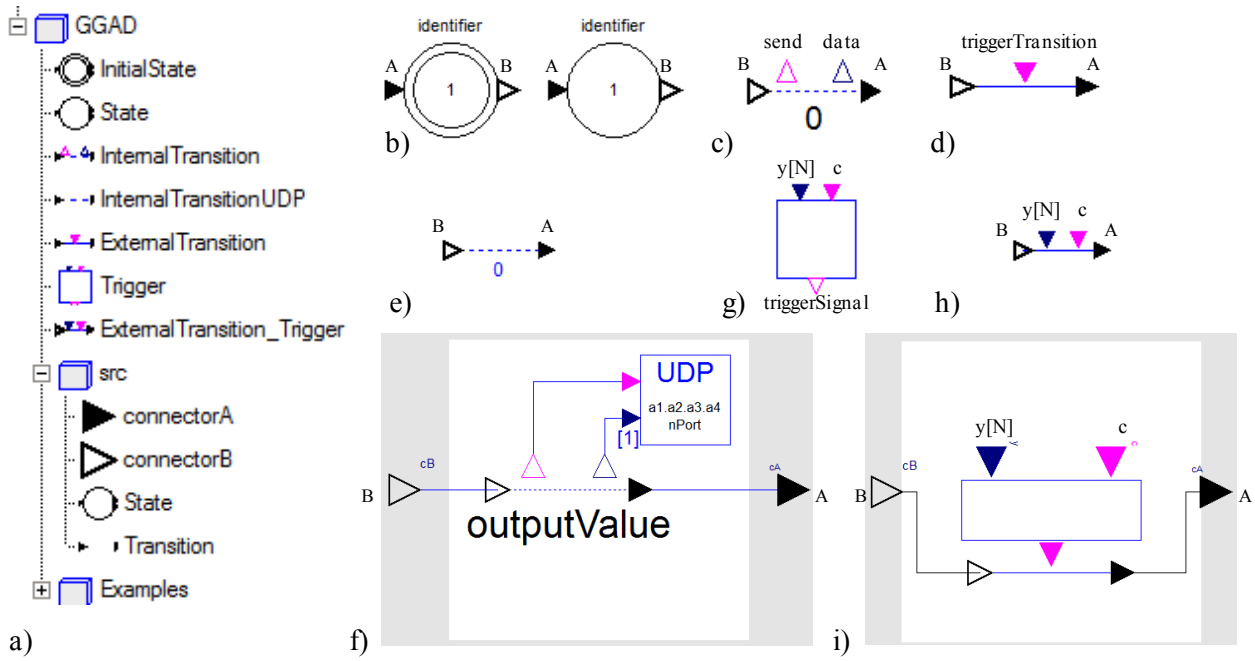

Figure 4: a) The GGADLib Modelica library; b) *InitialState* and *State* classes; c) *InternalTransition* class; d) *ExternalTransition* class; e) *InternalTransitionUDP* class; f) diagram of the *InternalTransitionUDP* class; g) *Trigger* class; h) *ExternalTransition_Trigger* class; and i) diagram of the *ExternalTransition_Trigger* class.

diagram of the *InternalTransitionUDP* class are shown in Figures 4e and 4f, respectively.

The *ExternalTransition* class facilitates describing external transitions. The transition is triggered when the Boolean value of the *triggerTransition* input connector changes (see Figure 4d) and the transition initial state is active.

Frequently, the trigger condition is the result of evaluating a logical expression. The *Trigger* partial class facilitates describing the trigger condition in these cases (see Figure 4g). The interface of this partial class is composed of an input Boolean variable (c), an array of input real variables (y) and an output Boolean variable (*triggerSignal*). When the c value changes, the value of *triggerSignal* is evaluated from an expression that depends on the y array. The expression is specified when the class is instantiated.

The *ExternalTransition_trigger* class is implemented by connecting the *Trigger* and *ExternalTransition* classes. The icon and diagram of *ExternalTransition_trigger* are shown in Figures 4h and 4i, respectively.

Several external transitions are allowed to have the same initial state. However, if two of these external transitions are triggered simultaneously, the final state is undefined. The instances of the *src.State* class check for this condition during the simulation run. When two external transitions with the same initial state are triggered simultaneously, an error message is logged out and the simulation execution aborts.

The number of internal transitions from a state can be zero or one. The *src.State* class checks that this condition is fulfilled. If it is not fulfilled, the corresponding error message is shown when the simulation starts. In case of confluence between an internal and an external transition, only the internal transition is executed.

EVALUATION OF AN OBSTACLE AVOIDANCE CONTROLLER FOR THE E-PUCK ROBOT

The simulation study discussed in this section illustrates the use of the UDPLib and GGADLib Modelica libraries. The study objective is evaluating an obstacle avoidance controller for the e-puck mobile robot (E-puck, 2012). To this end, Modelica models of the controller and the robot movement in an environment with obstacles have been developed. The communication between the real-time simulation of these models is accomplished using the UDP protocol.

Once the controller performance has been tested using simulation, the simulated robot has been substituted by the real robot. In this case, the real-time simulation of the controller is used to control the real e-puck. The communication is implemented via the UDP protocol, using ECD++ (Yu and Wainer, 2007; Moallemi and Wainer, 2010) to interface with the e-puck. The dynamic interfaces provided by ECD++ allow for integration of external entities with the real-time model which operates as a controller for the robot. Dymola 6.1 (Dynasim, 2008) is used to simulate the Modelica models.

A hybrid model of the e-puck has been developed. The model has one discrete-time state variable, $phase$, and three continuous-time state variables: the robot position, $\mathbf{r} = (x, y)$, and orientation, θ. The

$phase$ variable has the following four possible values: $\{Stop, TurnL, TurnR, Forward\}$.

The e-puck model has an input port: *motor*. Possible event values are: $\{1, 2, 3, 4, 5, 6\}$. These events, which are generated by the controller, trigger transitions between the model phases as shown in Figure 5.

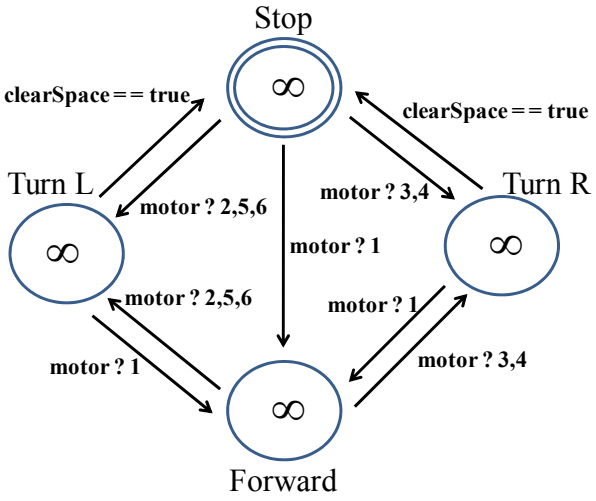

Figure 5: DEVS graph describing the phase transitions of the e-puck model.

The e-puck robot is equipped with a ring of 8 infrared proximity sensors (E-puck, 2012). The $IR[0]$, ..., $IR[7]$ readings from these sensors are the distance to obstacle measured in cm. These values are sent to the controller through an output port. In addition, the e-puck uses these readings to trigger the transition from the *TurnL* and *TurnR* phases to the *Stop* phase. The turning maneuvers stops when enough clear space is detected in front of the e-puck, i.e., when the *clearSpace* function

$$clearSpace = min(IR[0, 1, 6, 7]) > \delta \qquad (9)$$

returns true. The δ distance is a model parameter. The e-puck model calculates the sensor readings from its actual location and orientation, for a predefined environment. In this study, a $L \times H$ rectangular free space surrounded by a wall is assumed.

The e-puck position and orientation are calculated from its linear ($\mathbf{v}$) and angular (w) velocities:

$$\frac{d\mathbf{r}}{dt} = \mathbf{v}, \qquad \frac{d\theta}{dt} = w \qquad (10)$$

The velocity vector ($\mathbf{v}$) can be calculated from the velocity module (v) and the orientation (θ):

$$\mathbf{v} = |\mathbf{v}| \cdot \{\cos\theta, \sin\theta\} = v \cdot \{\cos\theta, \sin\theta\} \qquad (11)$$

The velocity module (v) and the angular velocity (w) depend on the robot phase. The velocity is zero while the e-puck is in the *Stop*, *TurnL* and *TurnR* phases. $v = V$ while *phase=Forward*. The angular velocity is $w = W$ and $w = -W$ while the e-puck is in the *TurnL* and *TurnR* phases, respectively, and $w = 0$ otherwise. The forward (V) and angular (W) velocities are model parameters.

The Modelica model of the e-puck moving in an environment with obstacles is shown in Figure 6. The *inputUDPport* component located in the upper-left corner of the figure represents the *motor* input port. It receives messages from the controller. The *sensors* component located in the lower-left corner calculates the sensor measurements from the actual position and orientation of the robot, and the obstacle position. The sensor data are sent to the controller through an output port, which is modelled using the *outputUDPport* component located in the lower-right corner of the figure. All the phase changes in this model are driven by external transitions. An arbitrary value is given to phase lifetimes: $1e10$.

The model describing the e-puck controller is shown in Figure 7. The *inputUDPport* component (upper-left corner) receives messages from the e-puck sensors. The y and c connectors of this *inputUDPport* component are connected to the y and c connectors of the *ExternalTransition_Trigger* components. For the sake of clarity, these connections are not shown in the diagram (i.e., they are drawn in white color). Components of the *InternalTransitionUDP* class are used to describe the internal transitions and the generation of output events. The output events are sent to the 5000 port of the local address.

In order to facilitate visualizing the simulation results and experimenting with the robot and controller models, an interactive graphic interface has been developed using the *Interactive* Modelica library (Martin-Villalba et al., 2012). The main window of the virtual-lab is shown in the left side of Figure 8. It contains an animated diagram of the e-puck location and orientation. The robot moves within an $L \times H$ rectangular area surrounded by walls. The length (L) and width (H) of this area can be changed interactively. Check boxes allow to show and hide plots of the robot location and orientation versus time, and the events generated by the controller and the sensors. The virtual-lab plot window displaying the time evolution of the robot position and orientation is shown in the right side of Figure 8.

CONCLUSIONS

Two new Modelica libraries have been presented: UDPLib and GGADLib. UDPLib facilitates sending and receiving arrays of real values using the UDP protocol. This feature allows communicating the Modelica models with hardware and with other models, e.g., with models developed using other languages and tools, and running in other computers. GGADLib supports the DEVS graph notation in Modelica. GGADLib uses UDPLib, facilitating the development of DEVS graph models that send and receive events using the UDP protocol. The UDPLib and GGADLib Modelica libraries can be freely downloaded from http://www.euclides.dia.uned.es/

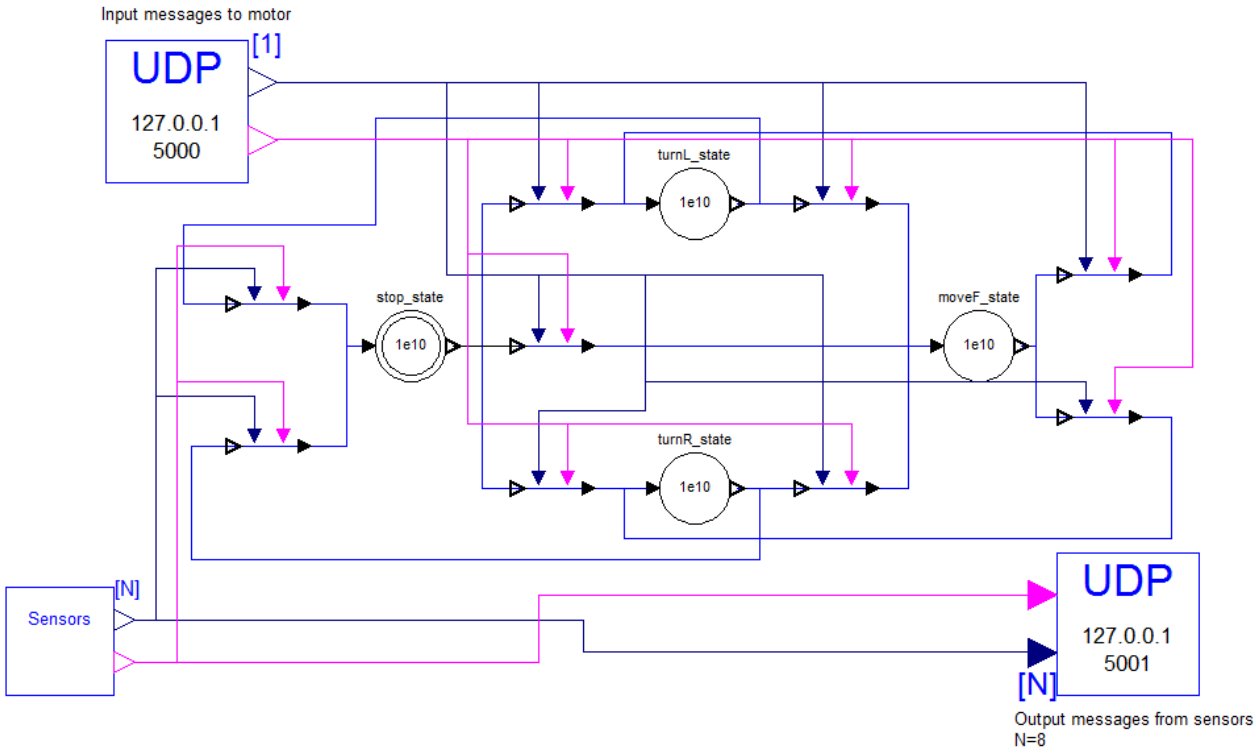

Figure 6: Model of the e-puck and its environment.

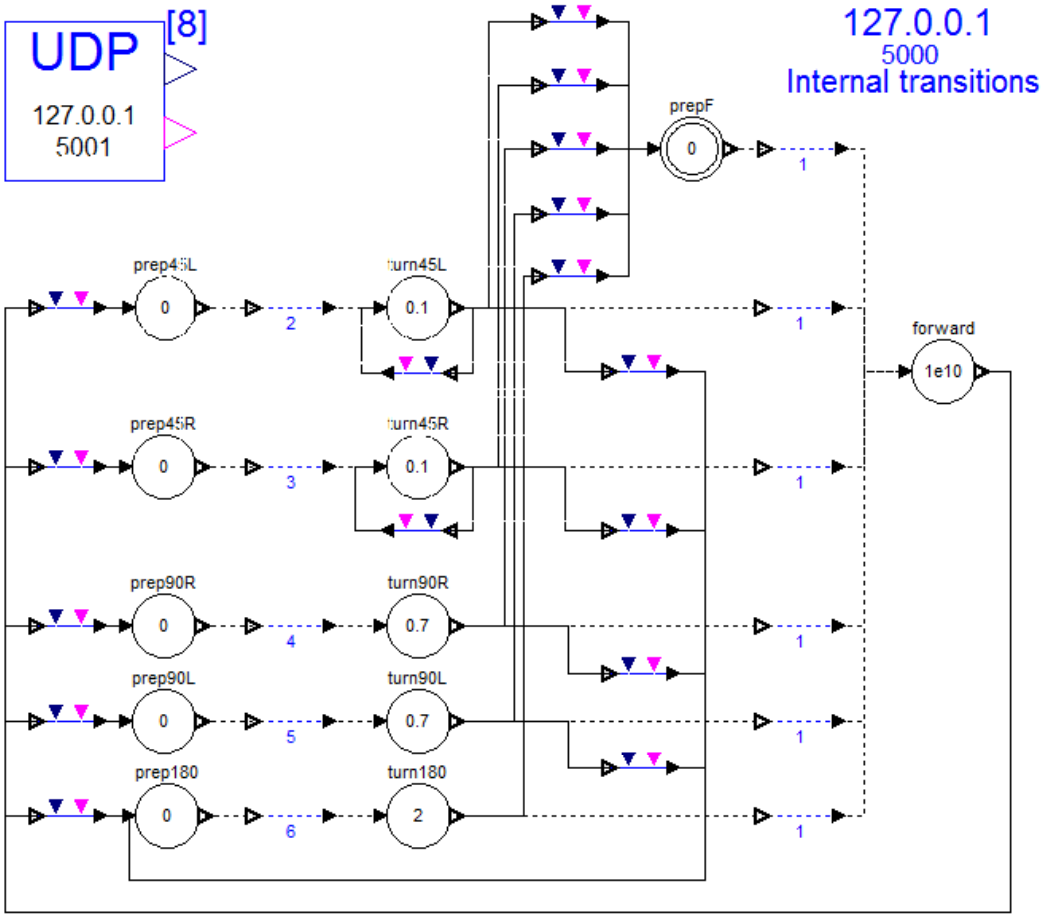

Figure 7: Model of the e-puck controller.

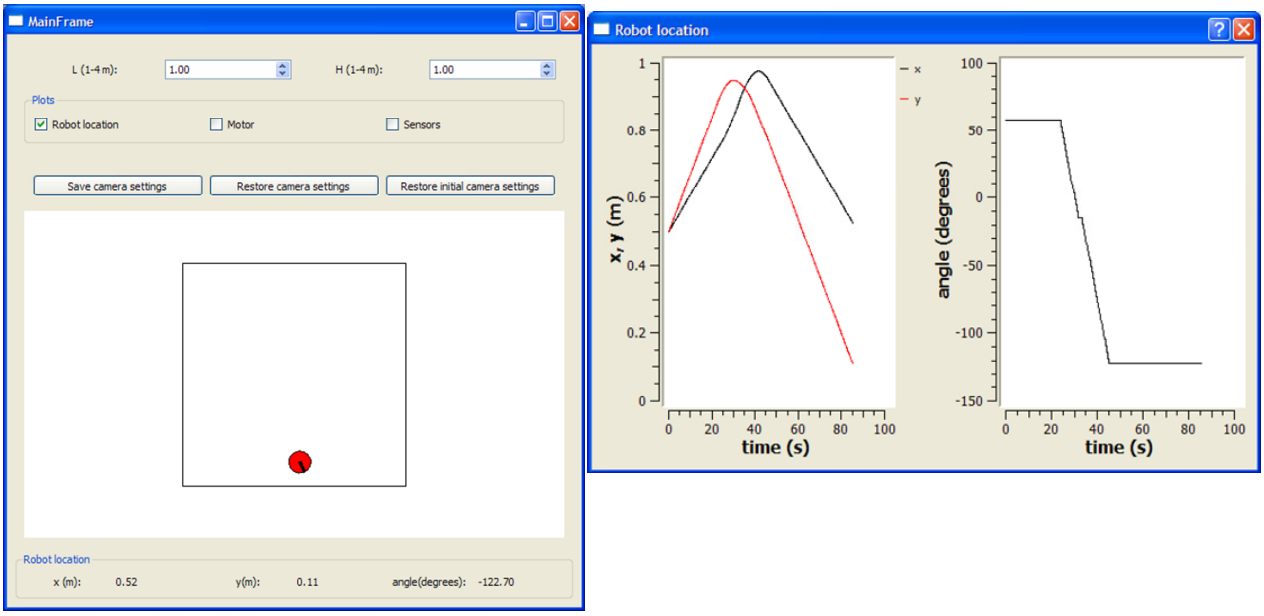

Figure 8: Main window of the virtual-lab for evaluating the e-puck controller (left). Virtual-lab plot window displaying the time evolution of the robot position and orientation (right).

ACKNOWLEDGEMENTS

This work has been supported by: Universidad Nacional de Educación a Distancia (UNED) under 2010V-PUNED/0001 grant; Programa Nacional de Movilidad de Recursos Humanos del Plan Nacional de I+D+i 2008-2011 del Ministerio de Ciencia e Innovación de España; and NSERC.

REFERENCES

Åström, K. J., Elmqvist, H., and Mattsson, S. E. (1998). Evolution of continuous-time modeling and simulation. In 12^{th} *European Simulation Multiconference*, Manchester, UK.

Chow, A. C. H. and Zeigler, B. P. (1994). Parallel DEVS: a parallel, hierarchical, modular, modeling formalism. In 26^{th} *Winter Simulation Conference*, San Diego, CA, USA.

Dynasim (2008). *Dymola - User's manual*. Dynasim AB, Lund, Sweden.

E-puck (2012). Website of EPFL education robot. http://www.e-puck.org/.

Martin-Villalba, C., Urquia, A., and Dormido, S. (2012). Development of virtual-labs for education in chemical process control using Modelica. *Computers and Chemical Engineering*, 39:170–178.

Moallemi, M. and Wainer, G. A. (2010). Designing an interface for real-time and embedded DEVS. In *2010 Spring Simulation Multiconference (SpringSim'10), DEVS Symposium*, Orlando, FL, USA.

Mosterman, P. J., Otter, M., and Elmqvist, H. (1998). Modelling Petri Nets as local constraint equations for hybrid systems using Modelica. In *Summer Computer Simulation Conference*, Reno, Nevada, USA.

Otter, M., Årzén, K.-E., and Dressler, I. (2005). StateGraph - A Modelica library for hierarchical state machines. In 4^{th} *Int'l Modelica Conference*, Hamburg-Harburg, Germany.

Otter, M., Elmqvist, H., and Mattsson, S. E. (1999). Hybrid Modeling in Modelica Based on the Synchronous Data Flow Principle. In 10^{th} *IEEE Int'l Symposium on Computer Aided Control System Design*, Hawaii, USA.

Sanz, V. (2010). *Hybrid System Modeling Using the Parallel DEVS Formalism and the Modelica Language*. PhD thesis, Dept. Informática y Automática, UNED, Madrid, Spain.

Sanz, V., Urquia, A., Cellier, F., and Dormido, S. (2010). System modeling using the parallel DEVS formalism and the modelica language. *Simulation Modelling Practice and Theory*, 18:998–1018.

Urquia, A., Martin-Villalba, C., Rubio, M., and Sanz, V. (2012). Some free modelling & simulation resources. http://www.euclides.dia.uned.es/.

Wainer, G. A. (2009). *Discrete-Event Modeling and Simulation: a Practitioner's Approach*. CRC Press, Taylor and Francis.

Yu, Y. H. and Wainer, G. A. (2007). ECD++: an engine for executing DEVS models in embedded platforms. In *2007 Summer Computer Simulation Conference (SCSC'07)*, San Diego, CA, USA.

Zeigler, B. P. (1976). *Theory of Modelling and Simulation*. John Wiley & Sons, Inc.

Zeigler, B. P., Praehofer, H., and Kim, T. G. (2000). *Theory of Modeling and Simulation*. Academic Press, Inc., Second edition.

Zeigler, B. P., Song, H. S., Kim, T. G., and Praehofer, H. (1994). DEVS framework for modelling, simulation, analysis, and design of hybrid systems. In *Hybrid Systems'94*.

INTEGRATED DELIVERY PLANNING AND SCHEDULING BUILT ON CLUSTER ANALYSIS AND SIMULATION OPTIMISATION

Galina Merkuryeva
Department of Modelling and Simulation
Riga Technical University
1 Kalku Street, Riga LV-1658, Latvia
E-mail: galina.merkurjeva@rtu.lv

KEYWORDS
Tactical planning, vehicle scheduling, cluster analysis, simulation, optimisation.

ABSTRACT

Integrated solutions for product delivery planning and scheduling in distribution centres are proposed and built on a cluster analysis and simulation optimisation methodology. A cluster analysis of product demand data of stores is used to identify typical dynamic demand patterns and product delivery tactical plans. Further, simulation optimisation techniques are applied to find optimal parameters of product transportation and vehicle delivery schedules. In the paper, a cluster analysis of the demand data by using the K-means clustering algorithm and silhouette plots mean values is performed, and an NBTree-based classification model is built. In order to define optimal parameters of vehicle schedules, a genetic algorithm is applied and interacts with a discrete-event simulation transportation model built in AnyLogic simulation environment. Integrated solutions are illustrated and adjusted to a specific business case.

INTRODUCTION

Product delivery planning and scheduling is a high commercial priority task in transport logistics. In real-life applications the problem has different stochastic performance criteria and conditions. Optimisation of transportation schedules itself is computationally time-consuming task which is based on the data from tactical planning of weekly deliveries. This research focuses on the methodology that will allow reducing the affect of the demand variation on the product delivery planning and scheduling, and avoid numerous time-consuming planning adjustments and high computational costs.

In the distribution centres (DC), this problem is related to deliveries of various types of goods to a net of stores, in predefined time windows, taking into account transportation costs and product demand variability. The problem has also a high number of decision variables, which complicates the problem solution process. Heuristic methods and commercial software that are usually applied could lead to non-effective solutions, high computational costs and high time consumption. In practice, product demand from stores is variable and not deterministic. As a result, the product delivery tactical plan that is further used for vehicle routing and scheduling has to be adjusted to real demand data, and product delivery re-planning supervised by a planner is often required. This task is very time-consuming and requires specific knowledge and experience of planning staff in this domain. Moreover, in practice a cluster analysis of the product demand data and potential tactical plans is not performed. But the most suitable delivery plan could be defined as a result of such an analysis that would ensure high quality solutions to schedule optimisation problem and reduce computational costs of the problem solution.

The paper presents an integrated approach to product delivery planning and scheduling built on a cluster analysis and simulation optimisation techniques. In the paper, a cluster analysis is performed by using the K-means clustering algorithm. To define an appropriate number of clusters, silhouettes plots are built and their mean values are estimated. As far as the demand is dynamic and variable, a classification model that assigns an appropriate demand cluster is presented by an NBTree, which induces a hybrid of decision-tree and Naive-Bayes classifiers. In order to find an on optimal grouping of stores into regions based on their geographical locations and aimed to leverage the total product demand over regions, a multiobjective optimisation algorithm NSGA-II is used in (Merkuryeva et al, 2011). In simulation optimisation of vehicle schedules, a genetic algorithm (GA) is designed to search for the best combination of schedule parameters. GA interacts with an AnyLogic-based simulation model which is used to simulate product transportation schedules and estimate their fitness values. All algorithms are applied to a specific business case.

INTEGRATED APPROACH

The methodology for integrated delivery planning and scheduling is aimed at selecting an effective product delivery tactical plan for the upcoming week and optimising product transportation routes and delivery schedules. The proposed methodology integrates a cluster analysis that defines typical product dynamic demand patterns, identifies an appropriate demand

Proceedings 26th European Conference on Modelling and Simulation ©ECMS Klaus G. Troitzsch, Michael Möhring, Ulf Lotzmann (Editors)
ISBN: 978-0-9564944-4-3 / ISBN: 978-0-9564944-5-0 (CD)

cluster and tactical weekly delivery plan; and simulation optimisation to optimise vehicle delivery schedules.

Moreover, vehicle routing and scheduling optimisation is based on the data from tactical planning for a week delivery. At the same time, a weekly delivery plan itself is dependent on the data about the number of goods to be delivered to stores in a particular day of a specific week and stores' geographical allocation. In practice, historical data of store demands shows that often the real demand can be very different from expected or average one, which is determined in the predefined or base plan. Thus, significant changes should be made in the base delivery plan for each new week. It seems reasonable to specify typical patterns of dynamic daily demand for different planning weeks and introduce several base plans each representing an appropriate product delivery time table for a specific demand pattern. This will reduce the work of adjusting a typical or base delivery plan to the current situation. Since there are now more typical delivery plans that are based on typical demand patterns, the work will be reduced to making a decision, which delivery plan should be used for the next week and small adjustments of it still may be required. In addition, selecting the most suitable delivery plan may ensure better scheduling solutions and reduce their computational costs.

The proposed scheme for an integrated solution (Fig. 1) includes the following tasks (Merkuryeva et al, 2011):

- Definition of typical dynamic demand patterns by clustering historical daily demand data available for different planning weeks;
- Grouping of stores based on their geographical locations to leverage the total product demand over regions.
- Tactical weekly delivery planning performed for each group of stores and each pattern demand by using combinatorial meta-heuristic optimisation techniques.
- Identification of a specific demand pattern based on the classification model created for typical dynamic demand patterns, and selection an appropriate tactical delivery plan for the new week.
- Adjustment of a selected tactical weekly delivery plan to a new or forecasted demand.
- Vehicle routing and scheduling by using scheduling optimisation meta-heuristics (Merkuryeva and Bolshakov, 2011).

CLUSTER ANALYSIS OF DYNAMIC DEMAND DATA

Here, a cluster analysis (Seber, 1984) is aimed: (1) to find a number of typical dynamic demand patterns and corresponding clusters of planning weeks; (2) to construct a classification model that for any week allows determining an appropriate demand pattern, allocating a specific week to one of previously defined clusters and determining correspondent product delivery plan. In the business case, the historical data on daily number of delivered products for 52 weeks are used and specified by weekly demand time-series each representing a sequence of points - daily number of the product deliveries for a specific week (see Fig. 2).

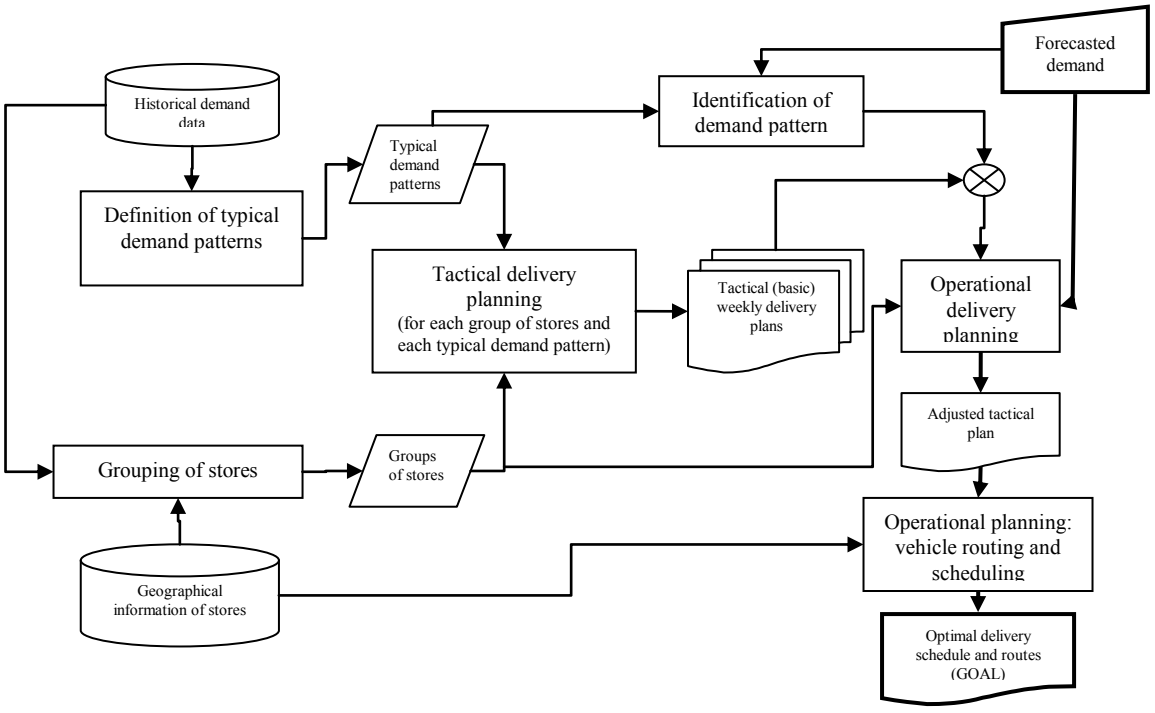

Figure 1: Scheme of Integrated Solution

Monday	Tuesday	Wednesday	Thursday	Friday	Saturday	Sunday
2885	3390	3891	4115	4612	4687	3371
2831	3553	3859	3785	4432	4899	3527
2763	3548	4067	4631	4838	5057	3511
2951	3820	3987	4360	5075	[illegible]	3345
[illegible]	2731	3101	2988	[illegible]	3524	2643
3150	3459	4339	4377	5187	4956	3545
2934	3229	3643	3693	4018	4411	3583

Figure 2: Sample Demand Data

Here, a cluster analysis of input data provides an opportunity to divide a variety of planning weeks into clusters and to find the number of clusters that represent weeks with specific demand patterns. It also gives information for a construction of the classification model in order to decide which weekly delivery plan would be preferable for next week.

The K-means clustering algorithm (MacQueen, 1967) is used in the paper. It is aims to divide n observations into a user-specified number k of clusters, in which each observation belongs to a cluster with the nearest mean representing a cluster centroid. The result is a set of clusters that are as compact and well-separated as possible. Here, an appropriate number of k clusters, or typical demand patterns is defined by using silhouette plots (Kaufman and Rousseeuw, 1990). In this method, a numerical measure of how close each point is to other points in its own cluster compared to points in the neighbouring cluster is defined as follows:

$$s_i = \frac{b_i - a_i}{\min(a_i, b_i)}, \qquad (1)$$

where s_i is a silhouette value for point i, a_i is an average dissimilarity of point i with the other points in its cluster, and b_i is the lowest average dissimilarity between point i and other points in another cluster. Higher mean values of silhouettes show better clustering results that determine better clusters giving the best choice for a number of clusters.

In the research, k-means clustering experiments have been performed for the number of clusters from 2 to 8. Then for each clustering experiment, silhouette plots have been built, and mean values of silhouettes per cluster have been calculated (Fig. 3). Analysis of silhouettes mean values leads to the conclusion that the best cluster separation could be done at k=4 with a silhouette mean value equal to 0.558. Clusters 1 to 3 seem to be appropriately clustered. However, silhouettes values for a cluster 4 are negative. Theoretically, weekly demands assigned to this cluster could be better allocated to another cluster. These weeks are unlike in the demand dynamics and in specific days, where demand peaks observed.

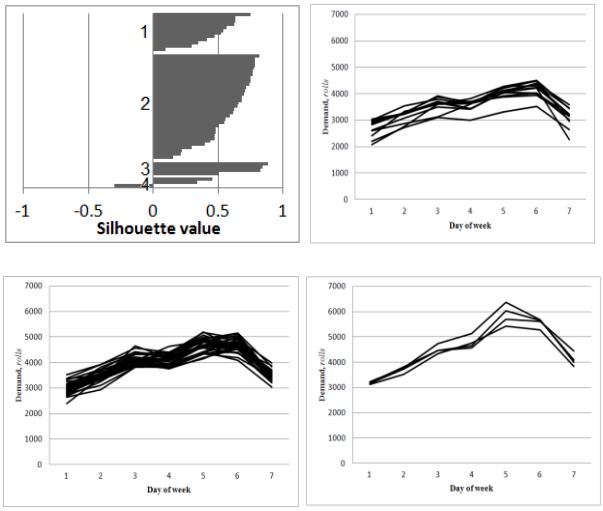

Figure 3: Silhouette plots for the number of clusters k=4 and demands patterns with a mean value greater than 0.5

Reallocation of 'unlike' weeks avoids receiving negative silhouette values (see Fig. 4). However, this does not provide an increase of the silhouette mean value as might be expected. In this case, 'unlike' weekly demands behave as a 'noise' in their 'native' clusters, decreasing silhouette values. Then, clustering experiments have been performed with 49 weeks, where three 'unlike' weeks have been excluded from a cluster analysis. This has allowed us to increase the silhouette mean value up to 0.5822 while getting the same groups of data clusters 1-3.

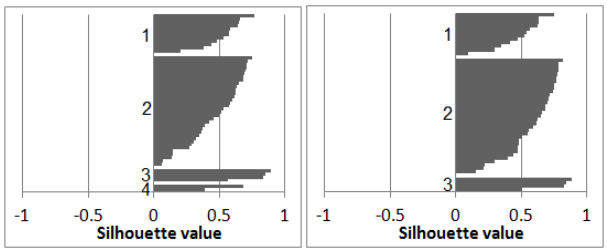

Figure 4: Silhouette plots for a number of clusters k=4 with reallocation of 'unlike' weeks and for the number of clusters k=3 and 49 sample weeks

As a result, the number of clusters is fixed and set to k=4. It is worth noting that a tactical weekly delivery base plan could be defined for a cluster with a silhouette mean value greater than 0.5. In this case, a tactical product delivery base plan is selected, adjusted or build for the first three clusters, and not analysed for the last one. Dynamic patterns received for clusters from 1 to 3 are presented in Fig. 3.

A classification model that assigns an appropriate demand cluster is presented by a NBTree, which induces a hybrid of decision-tree and Naive-Bayes classifiers. This algorithm is similar to classical recursive

partitioning schemes, except that leaf nodes created are Naive-Bayes categorizers instead of nodes predicting a single class (Seber, 1984).

For a specific week and demand time-series, a cluster is identified by determining a proper leaf number C according to the decision tree. When the leaf number is known, a cluster is estimated by a formula:

$$C = \arg\max_{c_j=C} P(c_j)\prod_{i=1}^{m} P(a_i \mid c_j), \qquad (2)$$

where $P(c_j)$ defines the probability that weekly demand belongs to cluster c_j, and $P(a_i / c_j)$ defines a conditional probability that demand in day a_i belong to cluster c_j. Probabilities $P(c_j)$ are calculated from clustering results, while $P(a_i / c_j)$ defined from the classifier according to the above determined leaf number.

To improve performance of the classification model, the number of weeks has been increased up to 156. Two demand time-series were generated for each planning week by uniformly changing its daily number of delivered products by ±5%. In a similar way, input data for another 52 weeks have been generated and used to validate a classification model itself. Built on this data the NBTree-based classification model with an example of the leaf Naive Bayes classifier is given in Fig. 5. In this case, 10-fold cross-validation showed that only eight weeks have not been classified correctly, which produced an error value of about 5%.

```
FRI <= 4294.5
|   TUE <= 3380.5: 1 cluster
|   TUE > 3380.5: Leaf Number 1
FRI > 4294.5
|   TUE <= 3700.5
|   |   MON <= 3062: 2 cluster
|   |   MON > 3062
|   |   |   THU <= 4368.5: Leaf Number 2
|   |   |   THU > 4368.5: Leaf Number 3
|   TUE > 3700.5: Leaf Number 4
```

Leaf Number: 4 Naive Bayes Classifier

Class	Monday	Tuesday	Wednesday			Thursday	
			(-∞-4406]	(4406-5152.5]	(5152.5-∞)	(-∞-5467.5]	(5467
2 0.348	1.000	1.000	0.727	0.182	0.091	0.900	
3 0.522	1.000	1.000	0.067	0.867	0.067	0.929	
4 0.130	1.000	1.000	0.167	0.167	0.667	0.200	

Figure 5: Detailed of NBTree Classification Model

For a specific week, an NBTree allows identifying an appropriate cluster and then choosing weekly tactical delivery base plan corresponding to this cluster. Then, selected weekly delivery plan is used for optimisation of parameters of vehicle schedules.

SIMULATION OPTIMISATION OF VEHICLE SCHEDULES

A vehicle schedule defines a schedule of deliveries of various types of goods from DC to a net of stores, in predefined time windows. All delivered goods are divided into three groups. Input data includes three data sets about stores, vehicles and trips. Each store is described with its daily demand and time windows for delivery of each group of goods. Vehicle capacities are limited and known. Each trip is determined by a sequence of stores (trip points) and average time intervals for vehicle moving between these points, loading and unloading processes and, and types of goods to be carried.

Decision variables are introduced to assign vehicles to trips and define a start time for each trip. The problem operational constraints include vehicle capacity constraints and delivery time constraints defined by time windows. The objective function is defined by the total idle time for all vehicles and is minimised. Idle time is the time between two sequential trips performed by a vehicle.

Express analysis shows that the problem could have many solutions not feasible within defined constraints. To increase optimisation efficiency all constraints are converted in soft constraints and fitness function is modified with penalties (Merkuryeva et al, 2010). In the paper, dimensions of the problem are 37 trips, 17 vehicles and 36 stores.

The vehicle schedule model (Fig. 6) is built as a discrete-event simulation model (Merkuryeva and Bolshakov, 2010). Each vehicle is modelled as an active object. Its behaviour is described by a state chart that defines vehicle states (e.g., parking, loading, moving and unloading) and transitions between them.

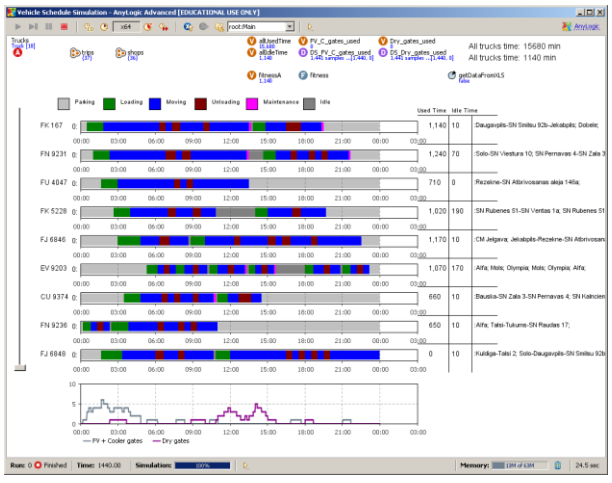

Figure 6: Vehicle Scheduling Model Gantt Chart

Input data are defined in MS Excel spreadsheets and transferred into the simulation model within its

initialisation. The vehicle schedule parameters are introduced as control variables in the model. During simulation, constraint violations are fixed.

For search of the best combination of vehicle schedule parameters, a genetic algorithm (GA) is applied. It is implemented as Java class and interacts with the simulation model via 'Parameter variation' experiment in AnyLogic (Merkuryeva and Bolshakov, 2011). GA chromosomes are implemented as strings of integer numbers that encode parameters of vehicle schedule, i.e. a vehicle number and start time for each trip. All genetic operators are customized for operating with the proposed structure of a chromosome. One-point crossover with rate of 75%; a mutation operator that changes on each iteration one random trip in the solution, with rate of 1%; and tournament selection with tournament size of two individuals are involved in the algorithm. The solution found allowed decreasing the total idle time for all vehicles comparing with the original delivery schedule in the business case. Better results have been achieved compared with ones received with a general-purpose optimiser OptQuest, which had stuck in local optima and could not find any solutions satisfied all constraints in the problem.

Further GA improvements through fitness landscape analysis are suggested in (Bolshakov et al, 2011). Here, a plug-in of the HeuristicLab optimisation framework (Wagner, 2009) has been implemented by maintaining the logic of the simulation model. Fitness landscape experiments has been performed to compare optimisation results for different GA operators with integer encoding of solutions, as well as to analyse the problem fitness landscapes for different types of solution representations and define most effective for the problem optimisation.

CONCLUSIONS

The proposed integrated approach to product delivery tactical planning and scheduling allows identifying typical dynamic demand patterns and corresponding product delivery tactical plans as well as finding the optimal parameters of product delivery schedules. This allows reducing the effect of product demand variation on the delivery planning process and avoids numerous time-consuming adjustments of the delivery tactical plans. Also, identifying demand pattern and an appropriate delivery plan ensure more qualitative solutions of the schedule optimisation task and cut down its computational costs.

REFERENCES

Bolshakov, V., Erik Pitzer, Michael Affenzeller, 2011. "Fitness Landscape Analysis of Simulation Optimisation Problems with HeuristicLab". *Proc. 2011 UKSim 5th European Symposium on Computer Modeling and Simulation*, p. 107-112.

Kaufman, L., Rousseeuw, P. J. 1990. *Finding Groups in Data: An Introduction to Cluster Analysis*. Hoboken, NJ: John Wiley & Sons, Inc.

MacQueen, J. B. 1967."Some Methods for Classification and Analysis of MultiVariate Observations" *Proc. of the 5th Berkeley Symposium on Math. Statistics and Probability,* Vol. 1, p. 281-297, 1967.

Merkuryeva, G., Bolshakovs, V. 2010. "Vehicle schedule simulation with AnyLogic," *Proc. of 12th Intl. Conf. on Computer Modelling and Simulation,* 2010, p. 169–174.

Merkuryeva, G., Merkuryev, Y., Bolshakov, V. 2010. Simulation-based fitness landscape analysis for vehicle scheduling problem. *Proc. of the 7th EUROSIM Congress on Modelling and Simulation. September 6-10, 2010, Prague, Czech Republic,*7 p.

Merkuryeva, G., Bolshakov, V. 2011 "Simulation-based Fitness Landscape Analysis and Optimisation for Vehicle Scheduling Problem," *Lecture Notes in Computer Science, EUROCAST 2011,* Part I, LNCS 6927, pp. 280–286, 2011.

Merkuryeva, G., Bolshakov, V., Kornevs, M. 2011. "An Integrated Approach to Product Delivery Planning and Scheduling". *Scientific Journal of Riga Technical University, Computer Science, Information Technology and Management Science,* p. 97-103.

Seber G. A. F., 1984. *Multivariate Observations*. Hoboken, NJ: John Wiley & Sons, Inc.

Wagner, S., 2009."Heuristic Optimization Software Systems - Modeling of Heuristic Optimization Algorithms in the HeuristicLab Software Environment", PhD Thesis, Institute for Formal Models and Verification, Johannes Kepler University Linz, Austria, 2009.

AUTHOR BIOGRAPHY

GALINA MERKURYEVA is a full professor at Riga Technical University, Department of Modelling and Simulation, Latvia. She has research interests and experiences in discrete-event simulation, simulation metamodelling and optimisation, decision support systems, supply chain simulation and management, and simulation-based training.

Electrical and Electromechanical Engineering

IMPROVED BRUSHLESS DC MOTOR CONTROL ALGORITHM FOR REDUCING SOURCE CURRENT HARMONICS. SIMULATION STUDY

George Adam, Alina G. Stan (Baciu) and Gheorghe Livinţ
Faculty of Electrical Engineering
Technical University Gheorghe Asachi of Iaşi
700050, Iaşi, Romania
E-mail: yojorj@yahoo.com

KEYWORDS
Active power filter, brushless DC motor, control, simulation

ABSTRACT

Recently, BLDC motors have become very popular in wide application areas. The BLDC motor does not have a mechanical commutation, and is, consequently, more reliable than the classic DC motor. In recent years, with the increasing number of nonlinear loads drawing nonsinusoidal current, power quality has become a serious problem; hence an optimal control scheme must ensure the desired motor behavior and an undistorted current waveform in the network. This paper presents a new simplified control scheme for the BLDC motor, eliminating the disadvantages of the classic control scheme, and in addition keeping the source currents waveforms near sinusoidal, according to the standards.

INTRODUCTION

Considering the wide range of different types of motors, the choice of a specific motor type for a particular application generally is determined by performance and cost. Of all these, the brushless DC (BLDC) motor is gaining widespread use in various consumer and industrial applications. The BLDC motor features high efficiency and good controllability due to their linear speed/torque characteristics, giving predictable speed regulation.

A BLDC motor is a rotating electric machine where the stator is a classic 3-phase wound stator, like that of an induction motor, and the rotor has surface-mounted permanent magnets. When the wound stator is energized by a 3-phase alternating current, it creates a rotating magnetic flux that causes the rotor to rotate synchronously with it.

In a BLDC motor, the position of the rotor (and hence its permanent magnetic field) is sensed with respect to the stator coils (phases), and the supply current is switched electronically (commutated) to the appropriate phases. BLDC motor control systems often incorporate either internal or external position sensors to sense the actual rotor position. Alternatively, the rotor position can be detected without sensors by measuring the back-EMF in each stator winding (Cyan Technology 2007).

The BLDC motor is driven by trapezoidal currents coupled with the given rotor position. They offer longer life and less maintenance than conventional brushed DC motors. Some other advantages over brushed DC motors and induction motors are: better speed versus torque characteristics, noiseless operation and higher speed ranges. In addition, the ratio of torque delivered to the size of the motor is higher, making them useful in applications where space and weight are critical factors.

In recent years, with the increasing number of nonlinear loads drawing nonsinusoidal currents, power quality distortion has become a serious problem in electrical power systems due to the increasing harmonics disturbance. These harmonics currents causes adverse effects in power systems such as overheating, perturbation of sensitive control and communication equipment, capacitor blowing, motor vibration, excessive neutral currents, resonances with the grid and low power factor (Maswood el al. 2002). Hence an optimal control scheme must ensure the desired motor behavior and an undistorted current waveform in the network.

This paper presents a new simplified control scheme for the BLDC motor, which eliminates the disadvantages of the classical control scheme, and in addition, also keeps the network current waveform sinusoidal. The new scheme is simulated using Matlab SimPowerSystems.

CLASSICAL BLDC CONTROL SCHEME

The classical BLDC control scheme is shown in figure 1. Typically it contains two power electronics bridges – first one is an uncontrolled rectifier with diodes and the second one is a three phase controlled PWM inverter. Usually, between the two bridges is a capacitor (King et al. 2008).

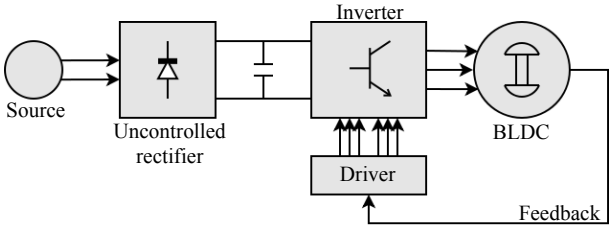

Figure 1: Classical BLDC Control Scheme

The torque and the speed of the BLDC motor depend on the magnetic field of the windings, consequently on the

Proceedings 26th European Conference on Modelling and Simulation ©ECMS Klaus G. Troitzsch, Michael Möhring, Ulf Lotzmann (Editors)
ISBN: 978-0-9564944-4-3 / ISBN: 978-0-9564944-5-0 (CD)

currents. Thus, for maintaining the torque and the speed constant at a desired value, one need to measure the current through the motor and generates the command for the PWM inverter. But, because of the uncontrolled rectifier, this type of control scheme draws from the network a nonsinusoidal current, thus distorting the current waveform, as seen in figure 2. The total harmonic distortion is 144.95%.

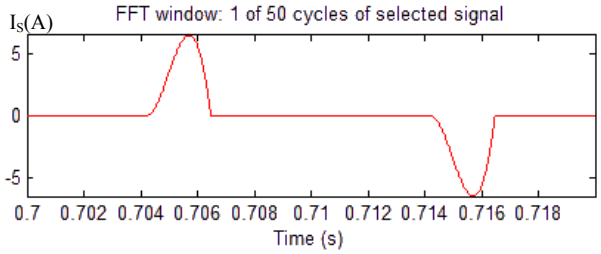

Figure 2: Source Current Waveform

PROPOSED BLDC CONTROL SCHEME

Figure 3 shows the proposed BLDC control scheme. The scheme contains two controlled power bridges, one PWM controlled inverter and one PWM controlled rectifier.

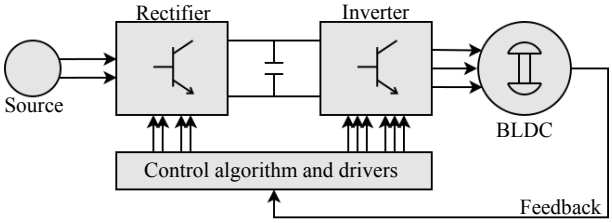

Figure 3: Proposed BLDC Control Scheme

The advantages of the proposed control scheme over the classical scheme are due to the introduction of the controlled rectifier over the uncontrolled rectifier, and are as follows:

- the current waveform of the source is kept near sinusoidal, due the controlled rectifier, in the range of the imposed (IEEE STD. 519-1992);
- the DC voltage on the capacitor is filtered and kept constant to the reference value provided by the regulated speed error;
- a quick response to load variations;
- robustness against uncertainties in component values and operations conditions;

The speed and the torque of the BLDC motor depend on the currents in the stator windings. To control the speed or the torque of the BLDC motor is sufficient to control the voltage of the inverter, possible by commanding the rectifier.

Figure 4 shows the Matlab Simulink model of the proposed BLDC control scheme, according to figure 3. The power supply is a single phase 220V/50Hz source and the BLDC motor has three phases, with the back EMF waveform sinusoidal and rotor type with salient poles. The mechanical input of the BLDC motor is the torque, set to 1 N·m. The reference of the system is the desired speed, ω^*, first set at 2000 r/min, then after 0.5s is set to 3000 r/min.

The inverter provides the commutation for the creation of the rotation field. For proper operation is necessary to keep the angle between the stator and rotor flux close to 90^0, thus the stator flux vector must be changed at a certain rotor position. The rotor position is sensed with Hall sensors, which generates three signals comprising six states, according to figure 5 (Musil 2006).

Using the correspondence between each of the Hall sensor states and stator flux vectors, a truth table can be assigned to control the each of the IGBT of the inverter, as shown in table 1.

Table 1: Truth Table for Inverter Command

Ha	Hb	Hc	Q1	Q2	Q3	Q4	Q5	Q6
0	0	1	0	0	0	1	1	0
0	1	0	0	1	1	0	0	0
0	1	1	0	1	0	0	1	0
1	0	0	1	0	0	0	0	1
1	0	1	1	0	0	1	0	0
1	1	0	0	0	1	0	0	1

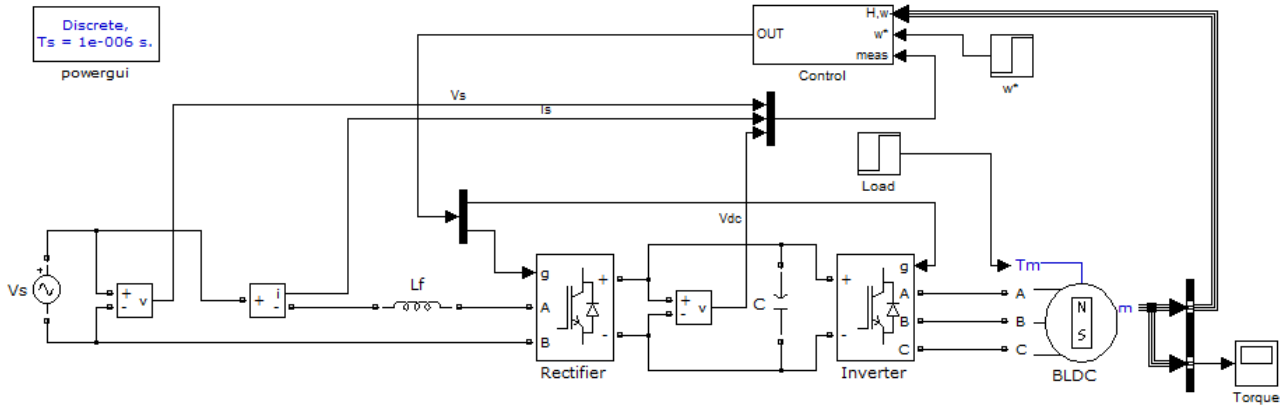

Figure 4: Matlab Simulink Model of the Proposed BLDC Control Scheme

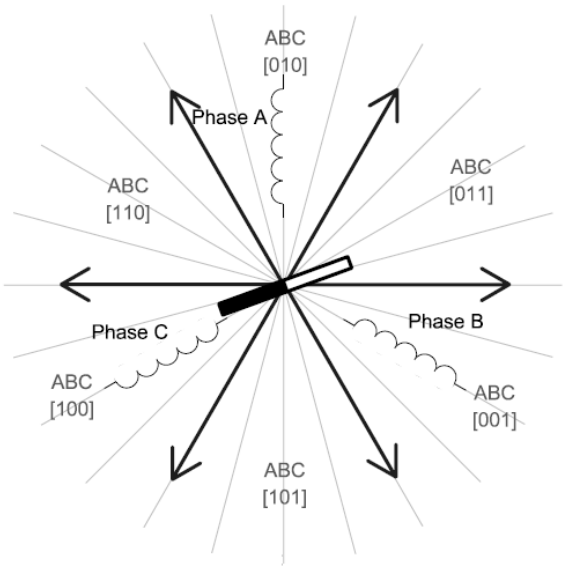

Figure 5: Stator Flux Vectors and Hall Sensors Output

While commutation ensures proper rotor rotation of the BLDC motor, the motor speed depends on the amplitude of the applied voltage. The amplitude of the applied voltage is adjusted by the controlled rectifier. The required speed and voltage are controlled by two PI controllers. The difference between the actual and required speed (and voltage) is the input of the PI controller. Using the difference, the PI controller control the duty cycle of PWM pulses fed to the controlled rectifier, corresponding to the voltage amplitude required to keep the desired speed. In addition, it needs to keep the source current harmonics free. The proposed control algorithm is presented in figure 6.

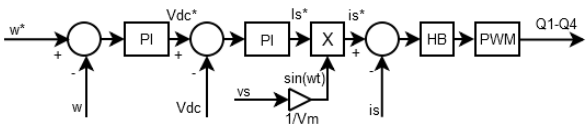

Figure 6: Proposed Algorithm for BLDC Control

SIMULATION RESULTS

The overall model of the proposed BLDC control is presented in figure 4 and the results were obtained using Matlab Simulink SimPowerSystems. The parameters of the chosen BLDC is seen in table 2.

Table 2: Motor parameters

Nominal voltage	220 V/50 Hz
Number of phases	3
Rotor type	Salient-pole
Back EMF waveform	Sinusoidal
Stator resistance	18.5 Ω
Inductances Ld and Lq	0.02682 H
Number of pole pairs	4

Figure 7 shows the reference and the obtained speed using the proposed BLDC control, under two reference speeds, 2000r/min and 3000r/min. It can be seen that the actual speed follows its reference speed very good, with a transient of 0.1s for the first reference, and with a transient of 0.05s for the second reference, thus proving the proposed BLDC control algorithm is very effective.

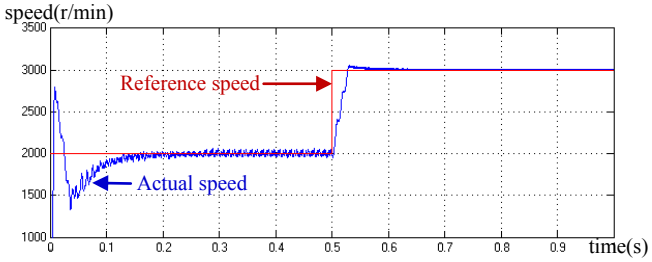

Figure 7: Reference and Actual Speed

Figure 8 shows the DC capacitor reference and actual voltage. Once the transient is over, the DC capacitor voltage is recovered to its reference value. It can be seen that its value follows up its reference, thus the objective of the proposed BLDC controller is achieved.

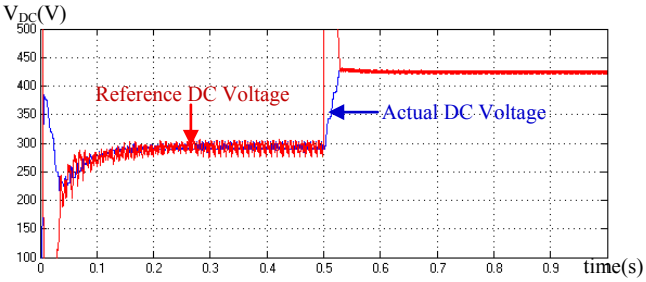

Figure 8: Reference and Actual DC Voltage

Figure 9 shows the simulation results of the source current obtained using the proposed BLDC control algorithm.

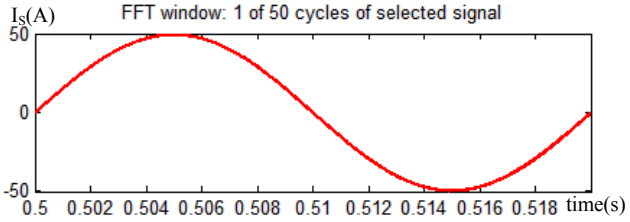

Figure 9: Source Current Waveform

Figure 10 shows the harmonic analysis of the source current. By using the proposed BLDC control algorithm, the source current has a total harmonic distortion of only 1.06%, thus meeting the limit of the harmonic standard of (IEEE STD. 519-1992).

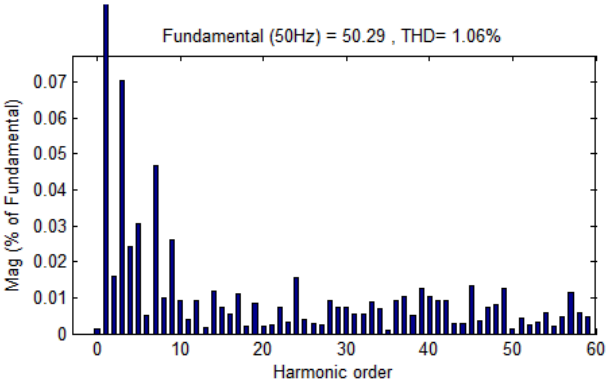

Figure 10: Harmonic Analysis of the Source Current

CONCLUSION

From the simulation results, it can be seen that the proposed BLDC control algorithm is a good alternative over the conventional BLDC control scheme, because not only that the motor operates as desired, but also the source current waveform is kept sinusoidal and with a harmonic distortion less than 5% according to the standards.

Still, this algorithm can be improved, by using it in threephased systems, so that the controlled rectifier can also provide the reactive power to the motor. In addition, it can act as a filter to the network, because it can balance unbalanced threephase systems.

REFERENCES

Cyan Technology, 2007, "3-Phase PMSM Control with Sensor Feedback – Version 1.0"

King K., Proctor R., Xu H. and Jani Y., 2008,"MCU Performance for Various Control Algorithms of BLDC Motors", Renesas Technology America, Inc.

IEEE STD. 519-1992, "IEEE Recommended Practices and Requirements for Harmonic Control in Electric Power Systems", *IEEE Industry Applications Society/Power Engineering Society*.

Maswood A. and Haque M.H., 2002, "Harmonics, Sources, Effects and Mitigation Techniques", *Second International Conference on Electrical and Computer Engineering.*

Musil J. 2006, "3-Phase BLDC Drive Using Variable DC Links Six-Step Inverter – Design Reference Manual", *Freescale Czech Systems Laboratories.*

ACKNOWLEDGEMENTS

This paper was realized with the support of POSDRU CUANTUMDOC "DOCTORAL STUDIES FOR EUROPEAN PERFORMANCES IN RESEARCH AND INOVATION" ID 79407 project funded by the European Social Found and Romanian Government.

AUTHOR BIOGRAPHIES

GEORGE ADAM was born in Romania in 1984. He received the B.S. and M.S. degrees in electrical engineering from Technical University of Iaşi, Romania in 2009 and 2010 respectively. He is currently a Ph.D. student under the supervising of Professor Gheorghe Livinţ. His research interests include power electronics, active power filters and hybrid vehicles. His e-mail address is: yojorj@yahoo.com.

ALINA GEORGIANA STAN (BACIU) was born in Romania in 1980. She received the B.S. and M.S. degrees in electrical engineering from Technical University of Iaşi, Romania in 2005 and 2010 respectively. She is currently a Ph.D. student under the supervising of Professor Gheorghe Livinţ. Her research interests include hybrid vehicles, power electronics and Fuzzy logic. Her e-mail address is: alinutza_222000@yahoo.com.

GHEORGHE LIVINŢ was born at 20 December 1949 in Vaslui, Romania. He is a Professor in Technical University of Iaşi, Romania, Faculty of Electrical Engineering since 1996, head of department since 2000 and Ph.D. mentor since 2004. His research interests include systems theory, automatic control, power electronics, electric motor control and hybrid vehicles. His e-mail address is: glivint@tuiasi.ro.

USING WAVELET TRANSFORM AND NEURAL NETWORK ALGORITHM FOR POWER DEMAND PREDICTION

Alina G. Stan (Baciu), George Adam and Gheorghe Livinț
Faculty of Electrical Engineering
Technical University "Gheorghe Asachi" of Iaşi
700050, Iaşi, Romania
E-mail: alinutza_222000@yahoo.com

KEYWORDS
Neural network, power demand, prediction, wavelet analysis

ABSTRACT

This paper presents a method for prediction short-term power demand of a vehicular power system. The forecasting of power demand is presented using wavelet decomposition and artificial neural network, a hybrid model which absorbs some merits of wavelet transform and neural network. The power demand time series is first decomposed into a certain number of levels with discreet wavelet transform and for each individual wavelet sub-series are created neural networks to predict future values. To form the aggregate prediction the individual wavelet sub-series forecasts are recombined utilizing the reconstruction property of wavelet transform. The results are conducted in Matlab software and the performance of this procedure is investigated.

INTRODUCTION

The aim of this work is to realize a short-term prediction model for the power demand of a vehicular system using wavelet analysis and neural-networks.
Wavelet analysis has become a research hot point; it has good time and frequency multi-resolution and can effectively diagnose signal's main frequency component and abstract local information of the time series. It has huge advances in signal processing, image compress, mode identification and nonlinear science fields (Wang et al. 2003).
Wavelet technology has been successfully employed in electrical power systems for transient process analysis. Wavelets were first applied precisely to analyze transients under the assumption that they could help detect the transient wave structure. By using discrete wavelet transform, Robertson studied the propagation of transients through switch capacitors (Zhang et al. 2011).
Artificial neural network is highly flexible function approximation that has self-learning and self-adaptive feature. Neural network is a powerful model in solving complex problems. Since the neural network has natural potential of solving nonlinear problem and can easily achieve the input-output mapping, it is perfect to use it for solving the predicting problem.

As it concern time series prediction, it means to predict value y(t+k) of future time t+k (t>0) on the basis of real history data of time series {y(t), y(t-1),… …, y(t-m+1)} and corresponding variance which influence the time series, that is to find, the relationship between future value y(t+k) and history data {y(t), y(t-1),… …, y(t-m+1)}.
As we told at the beginning we propose here the forecasting model based on neural networks and the wavelet decomposition of the power demand of a vehicular system. The measured signal is decomposed into wavelets and the prediction is performed for the wavelet coefficients (the detailed coefficients up to some level and the approximated coarse signal corresponding to the last level) in the original resolution. On the basis of these predicted values the reconstruction of the real value of the forecasted power demand is performed by simply summing up the predicted decomposition signals.

WAVELET ANALYSIS

The wavelet transform has been used for time series analysis in many papers in recent years. Much of this work has focused on periodogram or scalogram analysis of periodicities and cycles. Wavelet would appear to be very appropriate for analyzing non-stationary signals.
In this paper we used the undecimated Haar transform and the choice of it can be motivated by the fact that the wavelet coefficients are calculated only from data obtained previously in time and the aliasing problems are avoided (Renaud et al. 2003).

Wavelet Transform

Wavelet analysis is a multi-resolution analysis in time and frequency domain which projects a time series onto a collection of wavelets to produce a set of wavelet coefficients.
Wavelet faction $\Psi(t)$ is called mother wavelet and it can be defined as:

$$\int_{-\infty}^{+\infty} \Psi(t)\, dt = 0 \qquad (1)$$

The discreet wavelet transform (DWT) involves choosing scales and positions based on powers of two – so called dyadic scales and translation. The DWT algorithm is capable of producing coefficients of fine scales for capturing high frequency information and

Proceedings 26th European Conference on Modelling and Simulation ©ECMS Klaus G. Troitzsch, Michael Möhring, Ulf Lotzmann (Editors)
ISBN: 978-0-9564944-4-3 / ISBN: 978-0-9564944-5-0 (CD)

coefficients of coarse scales for capturing low frequency information (Hwa Loh R. 2003).
The DWT with respect to a mother wavelet, Ψ(t), is defined as:

$$F(t) = \sum_{k} c_{j0,k}\Phi_{j0,k}(t) + \sum_{j>j0}\sum_{k} w_{j,k}\,2^{\frac{j}{2}}\Psi(2^{j}t-k) \quad (2)$$

where j is the dilatation or level index, k is the translation or scaling index, $\Phi_{j0,k}$ is a scaling function or coarse scale coefficients and the functions $\Psi(2^{j}t-k)$ are all orthogonal to one another. $c_{j0,k}$, $w_{j,k}$ is the scaling function of detail coefficients. The coefficients $w_{j,k}$ conveys information about the behavior of the function F concentrating on effects of scale around 2^{-j} near time $kx2^{-j}$.
The output of a discreet wavelet transform can take various forms. Usually, a triangle is used to represent all that we have to consider in the sequence of resolution scales. Such a triangle comes about as a result of "decimation" or the retaining of one sample out of every two. Although it has a major advantage of keeping enough information which allow exact reconstruction of the input data, the decimated form of output not allow having shift invariance. This means that if we had deleted the first few values of our input time series then the output wavelet transformed, and decimated, data would not be the same as therefore. This problem can be solved by using a redundant or non-decimated wavelet transform.

The Algorithm of Wavelet Transform

A redundant transform based on an N-length input time series has an N length resolution scale for each of the resolution levels that we consider. In these conditions it is easy to relate information at each resolution scale for the same time point and we do have shift invariance.
The à trous wavelet transform decomposes a signal $F=(F_1,F_2,.....,F_N)$ as a superposition of the form:

$$F_t = c_{J,t} + \sum_{j=1}^{J} w_{j,t} \quad (3)$$

where, c_J is the smooth version of the original signal F and w_j represents the details of F at scale 2^{-j}.
In this paper we used for the decomposition the non-decimated Haar algorithm which is the same with à trous wavelet transform with the difference that Haar algorithm uses a simple filter $h=(1/2, 1/2)$.
Considering the first wavelet resolution level, we derive it from the input data by convolving the latter with h. Then:

$$c_{j+1,t} = \frac{1}{2}\left(c_{j,t-2j} + c_{j,t}\right) \quad (4)$$

and

$$w_{j+1,t} = c_{j,t} - c_{j+1,t} \quad (5)$$

This algorithm has the following advantages:

- It is easy to implement;
- The wavelet coefficients at any scale j of the signal $(F_1,\ldots..,F_t)$ are strictly equal to the first t wavelet coefficients at scale j of the signal $(F_1,\ldots.,F_N)$, N>t.

In figure 1 is shown the level-2 decomposition using this algorithm:

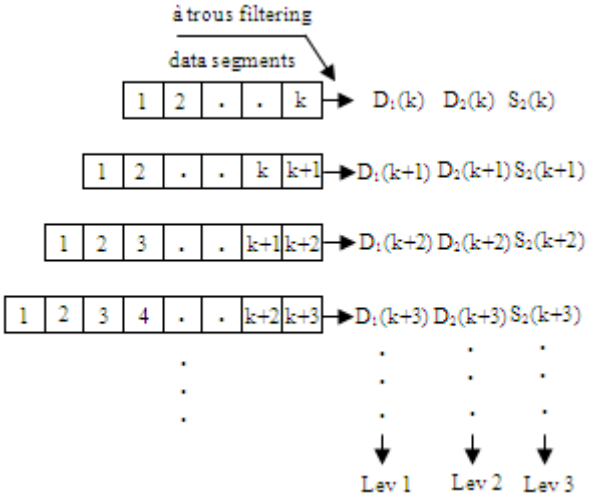

Figure 1: Procedure for Preparing Data for Prediction Using a Hybrid Method with Wavelet Transform and Neural Network (Ahmad et al. 2005)

The wavelet coefficients and scale coefficients of the power demand time series derived from wavelet decomposition algorithm are shown in figure 2. In this figure w1(t) and w2(t) denote wavelet coefficients at the resolution level 1 and 2 respectively and c2(t) denotes scale coefficients at resolution level 2.

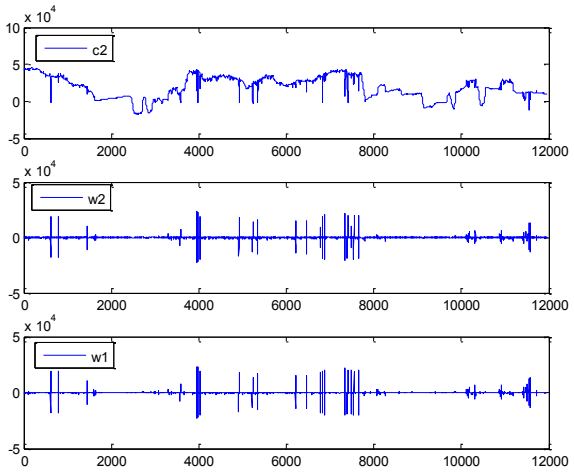

Figure 2: Wavelet Decomposition for Power Demand Time Series

ARTIFICIAL NEURAL NETWORK

Artificial neural networks have a large numbers of computational units neurons algorithms are based and do not require an explicit formulation of the mathematical or physical relationships of the handled problem (Ting et al. 2009).
Figure 3 is a typical neural network.

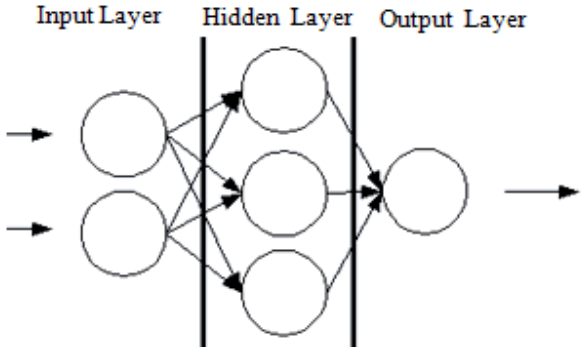

Figure 3: A Simple Neural Network

Feedforward neural networks are composed of layers of neurons in which the input layer of neurons is connected to the output layer of neurons through one or more layers of intermediate neurons. The training process of the neural network involves adjusting the weights till a desired input/output relationship is obtained. The majority of adaptation learning algorithms are based on the back-propagation algorithm.
Suppose we have the signal $F=(F_1, F_2,\ldots\ \ldots,F_N)$ and assume that F_{N+1} will be predicted. The main idea of neural network model is that, using coefficients that are found by the decomposition will predict F_{N+1} value with certain neural network architecture.
Feed Forward Neural Network architecture used to process the wavelet coefficients consists of one hidden layer with P neurons, which is mathematically written as (Hwa Loh R. 2003):

$$\hat{F}_{N+1}= \sum_{p=1}^{p} \widehat{b_p}\, g\left(\sum_{j=1}^{J}\sum_{k=1}^{Aj} \widehat{a_{j,kp}}\, w_{j,N-2^j(k-1)} + \sum_{k=1}^{Aj+1} a_{J+1,kp}\, \vartheta_{J,N-2^j(k-1)}\right) \quad (6)$$

where, j is the number of levels $\{j=1,2,3,\ldots\ \ldots,J\}$, A_j orders of model $(k=1,2,3,\ldots\ \ldots,A_j)$, $w_{j,t}$ is the wavelet coefficient value, $v_{j,t}$ is the scale coefficient value.
G is an activation function in hidden layer, which is usually sigmoid logistic, but in this architecture of neural network the activation function in output layer is linear.

RESULTS

Figure 4 illustrates the hybrid neuro-wavelet scheme for power demand prediction.

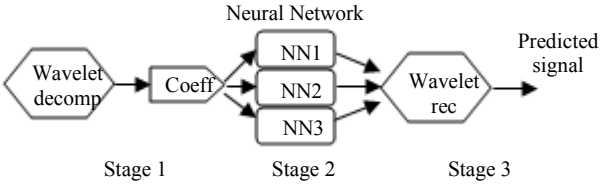

Figure 4: Prediction Model

The method basically involves three stages described as follows:
Stage 1: Data Pre-processing
Stage 2: Data Prediction
Stage 3: Data Post-processing

Stage 1: Data Pre-processing. The data used in this article is the power demand time-series for a vehicular system. Non-decimated Wavelet Transform is used as the data pre processor. The resolution level is defined as 2 and after decomposing the signal we have one approximation coefficient series with 2 number of detail coefficient series.
Stage 2: Data prediction. Neural networks are used for data prediction in the forecasted model. The number of neural networks needed for the model is determined by the number of wavelet coefficients signals at the output of the pre-processor. In this case we have 3 neural networks because for each wavelet coefficient signal one neural network is required to perform the corresponding prediction.
Stage 3: Data Post-processing. In this stage we used the same wavelet technique and resolution level as data pre-processing. The output from the neural networks is recombined to form the final predicted output.
We considered the power demand time series with 11962 data samples, on which we wish to carry out level 2 time based a trous transform. We can do this by implementing the scheme described in Fig. 1 by starting off with 11953 samples (k=11953). That is we simply carry out a level 2 wavelet transform on values F(1) to F(11953). The last values of the wavelet coefficients at time-point t=11953 are kept because they are the most useful ones for prediction. Then we repeated the same procedure at time point t=11954 (carry out level 2 wavelet transform on values F(1) to F(11954) and keep coefficients at t=11954) and so on until we reached 11962, the total number of samples in the original data.
In this way, we had wavelet decompositions for the time-series from t=11953 to t=11962.
In figure 5 is illustrated the power demand from t=11953 to t=11962, a total of 10 samples and the corresponding wavelet transform computed by the above method. From top to bottom the power demand, the wavelet "smooth", w_1 (D_1) and w_2 (D_2).

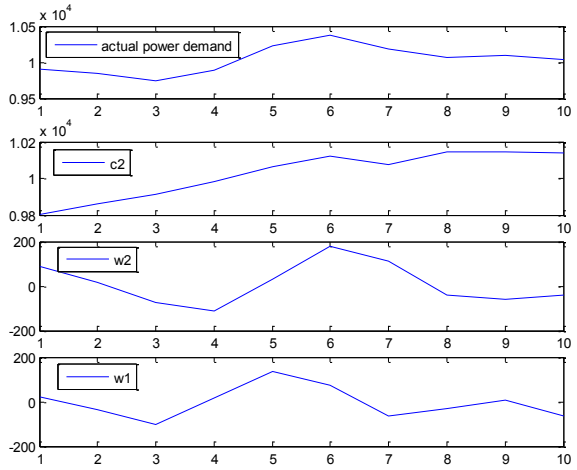

Figure 5: Illustration of the Wavelet Decomposition of Power Demand

In the second stage, separate neural networks models are created for each of the wavelet coefficients, approximation and details at level 1 and 2.
For the approximation time series we created a Feed forward neural network with three layers: input layer, hidden layer and output layer. The number of nodes in hidden layer is equal to 3 and the number of training is 1000. The results are shown in the figure 6.

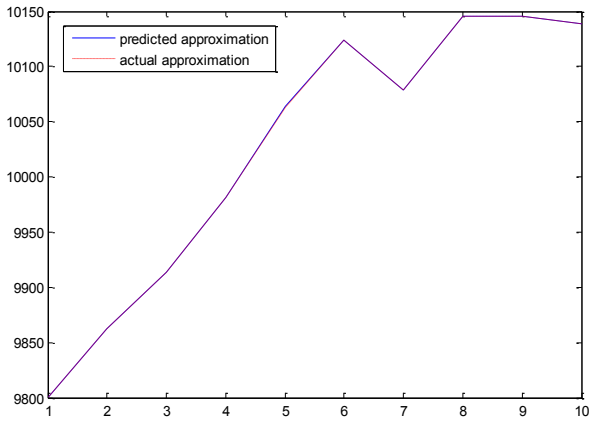

Figure 6: Actual (Red) and Predicted (Blue) Approximation for 10 Samples

For the detail at level 1 we used also a Feed forward neural network with three layers and the number of nodes in hidden layer was 5. The results are shown in figure 7.

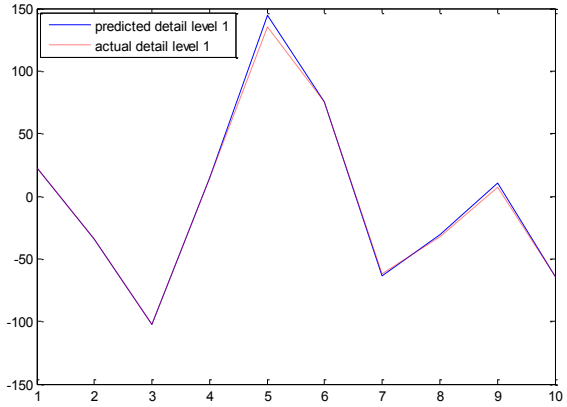

Figure 7: Actual (Red) and Predicted (Blue) Detail Level 1 for 10 Samples

In figure 8 are shown the results for the detail coefficients at level 2. The red color is for the actual detail signal at level 2 and the blue color is for the predicted one.

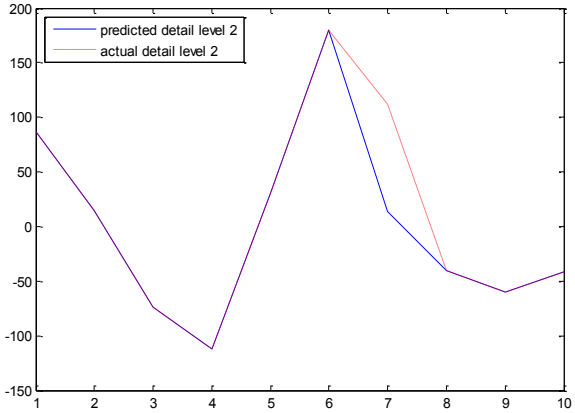

Figure 8: Actual (Red) and Predicted (Blue) Detail Level 2 for 10 Samples

Figure 9 illustrates the aggregate prediction (sum of the individual wavelet predictions) for the power demand series over a test set of 10 samples.

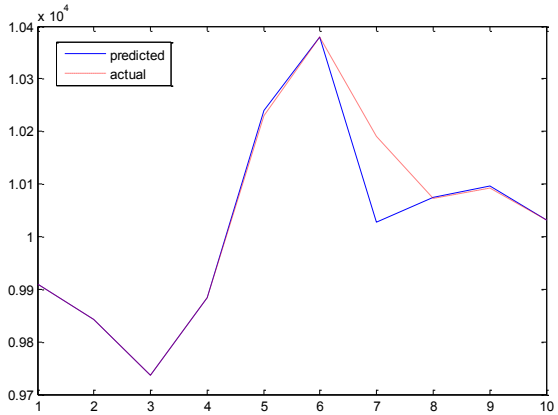

Figure 9: Actual (Red) and Predicted (Blue) Time Series of Power Demand for Next 10 Steps

CONCLUSION

This paper presented a method that combines a trous wavelet transform pre-processing with neural networks for short-term power demand prediction. The results show advantages of wavelet pre-processing for time series analysis and prediction. Also from results we can see that the model was capable of producing a reasonable accuracy in short-term prediction.

REFERENCES

Ahmad, S.; Popoola, A. and Ahmad, K. 2005. "Wavelet-based Multiresolution Forecasting.", UniS Technical Report (June 2005) *Department of Computing, University of Surrey* .

Hwa Loh, R. 2003. "Time Series Forecast with Neural Network and Wavelet Techniques", *Department of Electrical and Computer Engineering, University of Queensland*.

Renaud, O. and Starck, J-L. 2003. "Prediction Based on a Multiscale Decomposition", International Journal of Wavelets, Multiresolution and Information Processing.

Ting, X.; S. Xiaoduan; W. Yan; H. Yulong and X. Changrong. 2009. "Artificial Neural Network and Wavelet Analysis Application in Speed Forecast of Beijing Urban Freeway", Intelligent *Vehicles Symposium, 2009 IEEE*, 1004-1008.

Wang, W. and J. Jing. 2003. "Wavelet Network Model and its Application to the Prediction of Hydrology", *Nature and Science.* 1(1): 67-71.

Zhang, X. and C. Mi. 2011. "Vehicle Power Management", Springer-Verlag London 2011.

AUTHOR BIOGRAPHIES

ALINA GEORGIANA STAN (BACIU) was born in Romania in 1980. She received the B.S. and M.S. degrees in electrical engineering from Technical University of Iaşi, Romania in 2005 and 2010 respectively. She is currently a Ph.D. student under the supervising of Professor Gheorghe Livinț. Her research interests include hybrid vehicles, power electronics and Fuzzy logic. Her e-mail address is: alinutza_222000@yahoo.com.

GEORGE ADAM was born in Romania in 1984. He received the B.S. and M.S. degrees in electrical engineering from Technical University of Iaşi, Romania in 2009 and 2010 respectively. He is currently a Ph.D. student under the supervising of Professor Gheorghe Livinț. His research interests include power electronics, active power filters and hybrid vehicles. His e-mail address is: yojorj@yahoo.com.

GHEORGHE LIVINȚ was born at 20 December 1949 in Vaslui, Romania. He is a Professor in Technical University of Iaşi, Romania, Faculty of Electrical Engineering since 1996, head of department since 2000 and Ph.D. mentor since 2004. His research interests include systems theory, automatic control, power electronics, electric motor control and hybrid vehicles. His e-mail address is: glivint@tuiasi.ro.

LPV MODEL OF WIND TURBINES FROM GH BLADED'S LINEAR MODELS

Asier Díaz de Corcuera
Aron Pujana-Arrese
Jose M. Ezquerra
Edurne Segurola
Joseba Landaluze
IKERLAN-IK4 Technological Research Centre
Arizmendiarrieta, 2. E20500 Arrasate. Spain
E-mail: ADiazCorcuera@ikerlan.es

KEYWORDS

Linear Parameter Varying, LPV model, Wind turbine, GH Bladed, Linear model.

ABSTRACT

This paper shows a strategy to carry out a wind turbine LPV (Linear Parameter Varying) and MIMO (Multivariable Input and Multivariable Output) model from a family of LTI (Linear Time Invariant) models. The family of LTI models is obtained from a linearization process in different operational points of the wind turbine model in GH Bladed. The procedure is valid for any family of LTI models obtained from other simulation packages, as for instance, from FAST. The wind turbine model chosen is based on a 5 MW wind turbine defined in the *Upwind* European project. The LPV model is represented by the LFT (Linear Fractional Transformation) representation and its dynamics varies according to a selected parameter: blade pitch angle or wind speed. The MIMO LPV model has been developed in *Matlab/Simulink*. This model is validated analyzing some quality values in the frequency domain and in the time domain. These values determine the quality of the approximation of the LPV model to the family of LTI models.

INTRODUCTION

The incessant increase of the size of wind turbines in the last few years, due to the power production capacity, has led to new challenges in control strategies of wind turbines. Over the last few years, modern control techniques used to replace the classical PI controllers have been numerous. Ikerlan-IK4 has been working on the application of robust control techniques, especially H_∞ (Díaz de Corcuera et al. 2011), but H_∞ techniques often give controllers very conservatives in performance. A very interesting variation is to formulate the problem in terms of linear parameter varying system (LPV). This requires having a LPV model of the system.

The process used to adjust LPV models is described in (Salcedo and Martínez 2006) and it is used in other physical systems (Groot Wassink et al. 2003; Bodenheimer et al. 1995). In (Bianchi et al. 2007), the wind turbine LPV model is created from a reduced analytical model. There are several documents about the design of LPV controllers for wind turbines (Ostergaard 2008; Bobanac et al. 2010; Muhando el al. 2011), but in all of them LPV models are obtained from analytical models, and the identification of analytical models from real wind turbines is not an easy work. Most wind turbine manufactures use specialized modelling and simulation packages (for instance GH Bladed) to certificate their designs. Parameter adjustment of an analytical model according to a detailed model in GH Bladed is a very difficult task. It is easier to obtain linear models, which are often used to design the wind turbine controllers, classic controllers or based on applying modern control techniques. The process of obtaining a LPV model from a family of linear models is the main topic of this paper. The family of LTI models is obtained from a linearization process in different operational points of the wind turbine model in GH Bladed. The procedure is valid for any family of LTI models obtained from other simulation package, as for instance, from FAST. Therefore, the objective is to obtain from the family of linear models a system (1), whose dynamics depend on a time varying parameter p, which is valid for all operational points bounded by the family of linear models.

$$\begin{aligned} \dot{X}(t) &= A(p) \cdot X(t) + B(p) \cdot u(t) \\ y(t) &= C(p) \cdot X(t) + D(p) \cdot u(t) \end{aligned} \tag{1}$$

As stated, this paper shows the procedure to build a MIMO LPV model from a family of LTI models. The procedure has been applied to a wind turbine model based on a 5 MW wind turbine defined in the *Upwind* European project. MIMO LPV model is based on SISO LPV models. SISO LPV models are systems which dynamics vary according to a parameter *p*. In these models this parameter is the wind speed or the pitch angle of the blades.

This paper presents, initially, the reference wind turbine Upwind and the family of linear models extracted from GH Bladed. Then, a process to carry out a SISO LPV model is explained. The LPV models represented in LFT representation are discretized (Tóth et al. 2011)

Proceedings 26th European Conference on Modelling and Simulation ©ECMS Klaus G. Troitzsch, Michael Möhring, Ulf Lotzmann (Editors)
ISBN: 978-0-9564944-4-3 / ISBN: 978-0-9564944-5-0 (CD)

and validated in the frequency domain. After that, the paper explains the process to build a MIMO LPV model. Validation results of the LPV models are presented as well. Finally, the conclusions are stated.

LINEAR MODELS FROM GH BLADED

Non linear model

The *Upwind* wind turbine defined in the *Upwind* European project was modelled in GH Bladed and it is the reference non-linear model used in this paper. The *Upwind* model consists of a 5 MW offshore wind turbine (Jonkman et al. 2009) with a monopile structure in the foundation. It has three blades and each blade has an individual pitch actuator. The rotor diameter is 126 m, the hub height is 90 m, gear box ratio of 97, the rated wind speed is 11.3 m/s, the cut-out wind speed is 25 m/s and the rated rotational speed is 12.1 rpm.

Family of linear models

The non-linear wind turbine model developed in GH Bladed is linearized in seven operational points according to the wind speeds in the above rated power production zone. The operational points in the above rated control zone (Bossanyi 2009) are defined in Table I. The family of the seven linear models are used to obtain the LPV models. Extra linear models in other intermediate operation points could be obtained as well in order to use them during the validation process. After obtaining the family of linear models, a modal analysis has been done. This analysis is carried out to elaborate the Campbell diagram, where the frequency variations of the wind turbine modes can be clearly seen. The modes in the operational point of a wind of 11 m/s are showed in Table II. The linearized models (2) are represented by the state-space matrices A_x, B_u, B_w, C_x, D_u and D_w, and they have different inputs and outputs. The inputs are the control signals $u(t)$ of collective pitch angle $\beta(t)$ and generator torque $T(t)$ together with the output disturbance $w(t)$ caused by the wind speed. The outputs $y(t)$ are the sensorized measurements in the wind turbine and, in this paper, the considered outputs

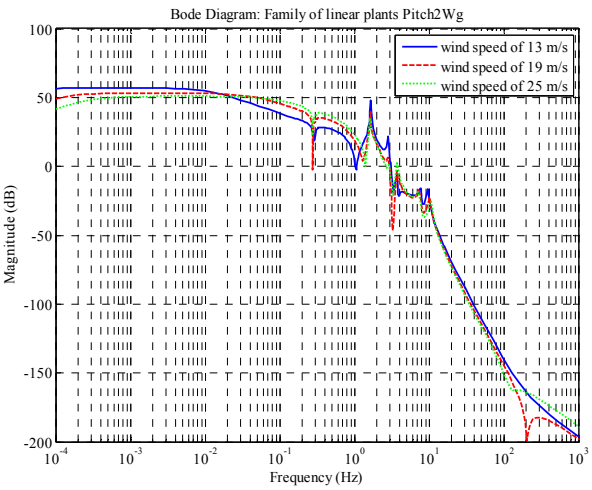

Figure 1: Family of Linear Plants *Pitch2Wg*

are the generator speed w_g, the tower top fore-aft acceleration a_{Tfa} and the tower top side-to-side acceleration a_{Tss}. Due to the non-linear model complexity, and the number of modes taken into account, the order of the linear models is 55. All the structural modes appear in them, but the non-structural modes of the wind turbine (1P, 3P, 6P…) do not appear in the linear models, so their influence will not be considered in the developed wind turbine LPV models.

$$\begin{aligned} \dot{X}(t) &= A_x \cdot X(t) + B_u \cdot u(t) + B_w \cdot w(t) \\ y(t) &= C_x \cdot X(t) + D_u \cdot u(t) + D_w \cdot w(t) \end{aligned} \quad (2)$$

SISO LPV MODELLING

This section explains the process to obtain a SISO LPV model of a wind turbine. Initially, the MIMO LPV model is reduced to a SISO problem and a MIMO LPV model can be constructed combining different SISO LPV models (see next section).

Table I: Operational Points

w (m/s)	*β (rad)*	*T (Nm)*	*w_g (rad/s)*	*a_{Tfa} (m/s^2)*	*a_{Tss} (m/s^2)*
13	0.11	43094	122.9	0	0
15	0.17	43094	122.9	0	0
17	0.23	43094	122.9	0	0
19	0.28	43094	122.9	0	0
21	0.32	43094	122.9	0	0
23	0.36	43094	122.9	0	0
25	0.40	43094	122.9	0	0

Table II: Modal Analysis of the *Upwind* model

Elem.	*Mode*	*Freq (Hz)*	*Abrev*
Rotor	In plane 1st	3.68	M_{R1ip}
	In plane 1st FW	1.31	M_{R1ipfw}
	In plane 1st BW	0.89	M_{R1ipbw}
	In plane 2st	7.85	M_{R2ip}
	In plane 2nd FW	4.30	M_{R2ipfw}
	In plane 2nd BW	3.88	M_{R2ipbw}
	Out of Plane 1st FW	0.93	M_{R1opfw}
	Out of Plane 1st	0.73	M_{R1op}
	Out of Plane 1st BW	0.52	M_{R1opbw}
	Out of Plane 2nd FW	2.20	M_{R2opfw}
	Out of Plane 2nd	2.00	M_{R2op}
	Out of Plane 2st BW	1.80	M_{R2opbw}
Drive Train	Drive Train	1.66	M_{DT}
Tower	1st tower side-to-side	0.28	M_{T1ss}
	1st tower fore-aft	0.28	M_{T1fa}
	2nd tower side-to-side	2.85	M_{T2ss}
	2nd tower fore-aft	3.05	M_{T2fa}
Non-str.	1P	0.2	*1P*
	3P	0.6	*3P*

BW : Backward whirl
FW: Forward whirl

SISO modelling process

The selected family of linear plants is the plant *Pitch2Wg*, whose input is the pitch angle and the output is the generator speed. The process to develop the LPV wind turbine model is divided into seven steps:

Step 1. To extract the family of linear models of the Upwind wind turbine non-linear model from GH Bladed. Figure 1 shows these linear models in three operational points.

Step 2. To represent the seven linear models of the family in seven state space systems in the canonical representation (3). *m* is the position of the operational point from 1 to 7. *m*=1 for the operational point with wind speed of 13 m/s and *m* is 7 for 25 m/s. *n* is the order of the linear models, so in this family of linear models *n*=55.

$$\begin{pmatrix} \dot{X}_{m1} \\ \dot{X}_{m2} \\ \dots \\ \dot{X}_{mn} \end{pmatrix} = \begin{pmatrix} -a_{m1} & -a_{m2} & \dots & -a_{mn} \\ 1 & 0 & 0 & 0 \\ 0 & 1 & 0 & 0 \\ \dots & \dots & \dots & \dots \\ 0 & 0 & 1 & 0 \end{pmatrix} \cdot \begin{pmatrix} X_{m1} \\ X_{m2} \\ X_{m3} \\ \dots \\ X_{mn} \end{pmatrix} + \begin{pmatrix} 1 \\ 0 \\ 0 \\ \dots \\ 0 \end{pmatrix} \cdot u$$
$$y = (c_{m1} \quad c_{m2} \quad \dots \quad c_{mn}) \cdot \begin{pmatrix} X_{m1} \\ X_{m2} \\ X_{m3} \\ \dots \\ X_{mn} \end{pmatrix} + 0 \cdot u \qquad (3)$$

Step 3. To create the component vectors $a_1, a_2 \dots a_n$ and $c_1, c_2 \dots c_n$. Each vector consists of the components of the seven canonical representations obtained in the first step. For example, the vector $a_1 = [a_{11}, a_{21}, a_{31}, a_{41}, a_{51}, a_{61}, a_{71}]$.

Step 4. To obtain the polynomial approximations of the component vectors to represent the family of linear model in a LPV representation (4) which varies according to a defined parameter *p* (wind speed). For example, $p_{a1}(p)$ is the polynomial approximation of the vector a_1. This polynomial approximation could be done using different orders. Figure 2 shows the polynomial approximations using different orders of the vector a_1 (*ord=[1,2,3,4,5]).*

$$\begin{pmatrix} \dot{X}_1 \\ \dot{X}_2 \\ \dots \\ X_n \end{pmatrix} = \begin{pmatrix} p_{a1}(p) & p_{a2}(p) & \dots & p_{an}(p) \\ 1 & 0 & 0 & 0 \\ 0 & 1 & 0 & 0 \\ \dots & \dots & \dots & \dots \\ 0 & 0 & 1 & 0 \end{pmatrix} \cdot \begin{pmatrix} X_1 \\ X_2 \\ X_3 \\ \dots \\ X_n \end{pmatrix} + \begin{pmatrix} 1 \\ 0 \\ 0 \\ \dots \\ 0 \end{pmatrix} \cdot u$$
$$y = (p_{c1}(p) \quad p_{c2}(p) \quad \dots \quad p_{cn}(p)) \cdot \begin{pmatrix} X_1 \\ X_2 \\ X_3 \\ \dots \\ X_n \end{pmatrix} + 0 \cdot u \qquad (4)$$

Step 5. To transform the LPV model based on polynomials to the upper LFT (linear fractional transformation) representation (see Figure 3). The LFT consists of a LPV system representation (5) with three input channels –$\dot{X}(t)$ is the derivated state vector, $w_d(t)$ the input occurrence vector and $u(t)$ the input vector– and three output channels –$X(t)$ is the state vector,

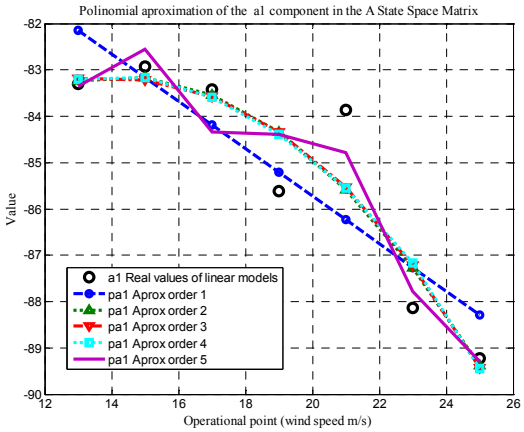

Figure 2: Polynomial Approximation of the Vector a_1

$z_d(t)$ is the output occurrence vector and $y(t)$ the output vector–. The Δ matrix is an identity square matrix with *nocc* size which is multiplied by the parameter *p*. In this SISO LPV model, the $u(t)$ is the pitch angle and $y(t)$ is the generator speed. The size of the state vector $X(t)$ and $\dot{X}(t)$ channels are defined by the order of the linear models, so for this LFT representation this channel size is 55. The size *nocc* of the occurrence vectors $z_d(t)$ and $w_d(t)$ varies according to the order of the polynomial approximation *ord* (6). For a fifth order polynomial approximation, the occurrence vector size is 30. The *p* parameter could be one of the changeable variables which define the operational points (see table I). So, the *p* parameter could be the wind speed or the pitch angle. In the presented LPV model the *p* parameter is the wind speed, but it can be easily carried out using the pitch angle in the blades.

$$\begin{cases} \dot{X}(t) = A \cdot X(t) + B_1 \cdot w_d(t) + B_2 \cdot u(t) \\ z_d(t) = C_1 \cdot X(t) + D_{11} \cdot w_d(t) + D_{12} \cdot u(t) \\ y(t) = C_2 \cdot X(t) + D_{21} \cdot w_d(t) + D_{22} \cdot u(t) \\ w_d(t) = \Delta \cdot z_d(t) \\ \Delta = p \cdot I \end{cases} \qquad (5)$$

$$nocc = ord(ord + 1) \qquad (6)$$

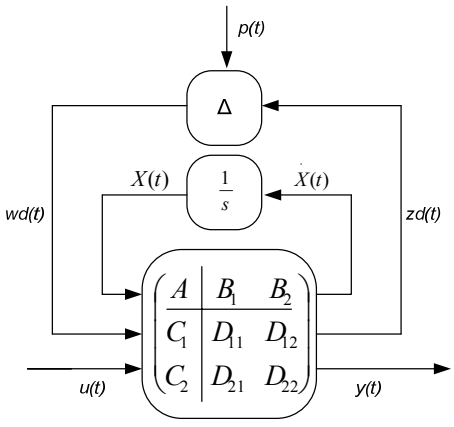

Figure 3: LPV Continuous Model in LFT Representation

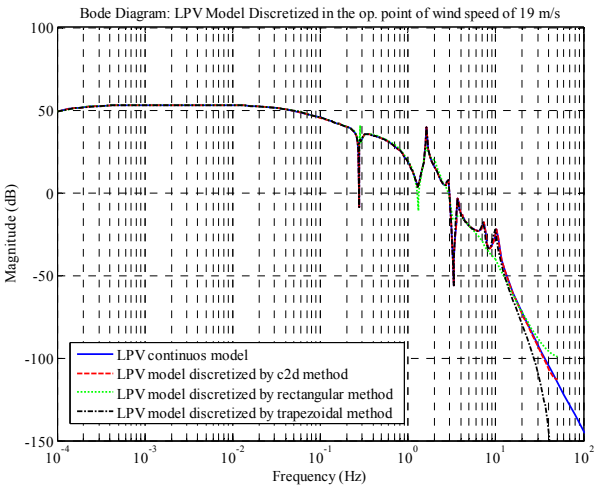

Figure 4: Discretized *Pitch2Wg* LPV Model in the Nominal Operational Point (Wind Speed 19 m/s)

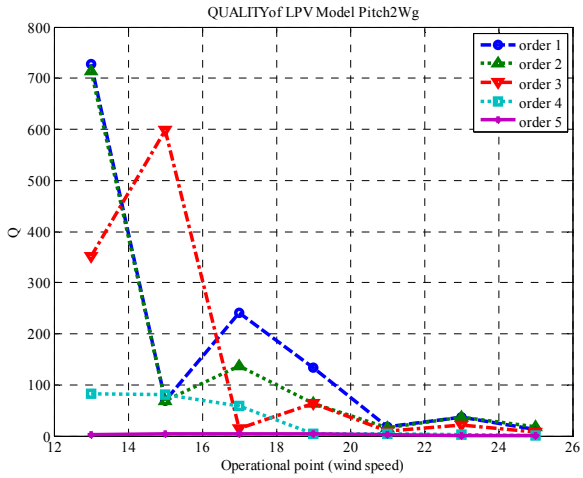

Figure 5: Quality *Q* of the SISO LPV Model *Pitch2Wg*

Step 6. Finally, the LPV model represented in LFT can be discretized. The selected sample time is 0.01 s and different discretization methods are used to discretize this model. The discretization of LFT systems has some level of complexity and the most common methods are the rectangular and the trapezoidal methods, where the size of the occurrence channel is maintained. Other methods like methods of Pade and Henselman, where the size of the occurrence channel is bigger to obtain a better discretization, are not used in this paper. For the *Pitch2Wg* LPV model, the used discretization methods are the classical *zoh,* the *rectangular* and the *trapezoidal* ones, and a result comparison is carried out. Figure 4 shows the discretized *Pitch2Wg* LFT system in the nominal operational point (wind speed of 19 m/s). The best results are obtained with the *zoh* method used in the Matlab function *c2d* to convert continuous time systems in discrete time.

Validation of SISO LPV model

A LPV model quality analysis has to be done to guarantee the validity of this model. The value *Q* (7) determines the LPV model quality compared to the family of linear model extracted from GH Bladed. The value *Q* is obtained in the seven operational points. Figure 5 shows the *Q* values for *Pitch2Wg* LPV model comparing the quality for different polynomial approximations.

$$Q = \left\| RealModel_{op} - LPVModel_{op} \right\|_{\infty} \qquad (7)$$

Table III: Quality of *Pitch2Wg* LPV Model

Pitch2Wg	***Polynomial aproximation order***				
	1	***2***	***3***	***4***	***5***
Qmean	176.91	150.82	152.20	33.15	2.79
Qmax	728.03	714.83	598.99	81.81	5.01

The values *Qmax* and *Qmean* are defined to show the quality for the LPV model in all operational points. Obviously, the best quality of the LPV model is obtained with small *Qmean* and *Qmax* values. *Qmax* is the maximum value of the *Q* values in all operational points (different values of the *p* parameter) and *Qmean* is the mean value of these *Q* values. For LPV model of the *Pitch2Wg* family of plants, Table III shows the quality values *Qmax* and *Qmean* for different polynomial approximation of the LPV model. The fifth order polynomial approximation gives the best quality for the *Pitch2Wg* LPV model.

MIMO LPV MODEL

Once the wind turbine *Pitch2Wg* SISO LPV model has been explained, the wind turbine MIMO LPV model is carried out in this section.

MIMO modelling process

The wind turbine MIMO model consists of different SISO models. The selected wind turbine LPV model has three inputs –wind *w(t)*, pitch angle *β(t)* and generator torque *T(t)*– and three outputs –generator speed $w_g(t)$, tower top fore-aft acceleration $a_{Tfa}(s)$ and top side-to-side acceleration $a_{Tss}(s)$–. This LPV model *MIMOLPV* (8) is formed by nine SISO LPV models defined in a 3x3 representation in the MIMO model. The nine SISO LPV models are generated using the process defined in last section to create the final *MIMOLPV* matrix.

$$\begin{pmatrix} w_g(t) \\ a_{Tfa}(t) \\ a_{Tss}(t) \end{pmatrix} = MIMOLPV \cdot \begin{pmatrix} Wind(t) \\ Pitch(t) \\ Torque(t) \end{pmatrix} \qquad (8)$$

$$MIMOLPV = \begin{pmatrix} Wind2w_gLPV & Pitch2w_gLPV & Torque2w_gLPV \\ Wind2a_{Tfa}LPV & Pitch2a_{Tfa}LPV & Torque2a_{Tfa}LPV \\ Wind2a_{Tss}LPV & Pitch2a_{Tss}LPV & Torque2a_{Tss}LPV \end{pmatrix}$$

Where $Wind2W_gLPV$, $Wind2a_{Tfa}LPV$ and $Wind2a_{Tss}LPV$ are the SISO LPV models which relate the wind speed input with the outputs generator speed, tower top fore-

aft acceleration and tower top side-to-side acceleration respectively. *Pitch2W$_g$LPV*, *Pitch2a$_{Tfa}$LPV* and *Pitch2a$_{Tss}$LPV* are the SISO LPV models which relate the input of collective pitch angle in the blades with the outputs generator speed, tower top fore-aft acceleration and tower top side-to-side acceleration respectively. *Torque2W$_g$LPV*, *Torque2a$_{Tfa}$LPV* and *Torque2a$_{Tss}$LPV* are the SISO LPV models which relate the input of generator torque with the outputs of generator speed, tower top fore-aft acceleration and tower top side-to-side acceleration respectively.

Validation of MIMO LPV model

Finally, a global quality analysis is done to show the MIMO LPV model approximation to the real family of plants extracted in GH Bladed. Table IV shows the *Qmean* value of the different LPV SISO plants of the *MIMOLPV* system. In this table, the *Qmean* values appear for different polynomial approximations. Furthermore, Table V shows the *Qmax* values in the different LPV SISO plants of the *MIMOLPV* system (8) for different polynomial of the LPV model. After analyzing the results, the best results for six SISO LPV

Table IV: Quality *Qmean* Value of MIMO LPV Model

Plant	***Polynomial aproximation order***				
	1	***2***	***3***	***4***	***5***
Wind2W$_g$	6,11E+00	5,27E+00	4,91E+00	1,07E+00	**1,08E-01**
Wind2a$_{Tfa}$	1,55E-02	9,87E-03	8,04E-03	6,62E-03	**4,79E-03**
Wind2a$_{Tss}$	2,13E-02	5,91E-03	5,05E-03	3,86E-03	**3,26E-03**
Pitch2W$_g$	1,77E+02	1,51E+02	1,52E+02	3,32E+01	**2,80E+00**
Pitch2a$_{Tfa}$	8,68E-01	5,75E-01	**1.97E-01**	2,00E-01	1,97E-01
Pitch2a$_{Tss}$	8,68E-01	3,94E-01	3,31E-01	3,47E-01	**1,91E-01**
Torque2W$_g$	8,14E-04	5,61E-04	4,80E-04	1,47E-04	**9,66E-05**
Torque2a$_{Tfa}$	1,48E-05	4,87E-06	**2,42E-06**	2,85E-06	4,13E-06
Torque2a$_{Tss}$	2,00E-05	4,87E-06	**2,42E-06**	2,85E-06	4,13E-06

Table V: Quality *Qmax* Value of MIMO LPV Model

Plant	***Polynomial aproximation order***				
	1	***2***	***3***	***4***	***5***
Wind2W$_g$	2,93E+01	2,86E+01	1,77E+01	3,31E+00	**2,27E-01**
Wind2a$_{Tfa}$	2,27E-02	1,65E-02	1,26E-02	1,24E-02	**7,73E-03**
Wind2a$_{Tss}$	4,75E-02	8,56E-03	8,30E-03	8,36E-03	**5,83E-03**
Pitch2W$_g$	7,28E+02	7,15E+02	5,99E+02	8,18E+01	**5,01E+00**
Pitch2a$_{Tfa}$	1,64E+00	6,73E-01	**3,94E-01**	4,10E-01	4,10E-01
Pitch2a$_{Tss}$	1,64E+00	6,72E-01	7,13E-01	7,10E-01	**3,95E-01**
Torque2W$_g$	2,94E-03	2,87E-03	1,64E-03	3,31E-04	**2,30E-04**
Torque2a$_{Tfa}$	3,15E-05	7,05E-06	**4,47E-06**	7,10E-06	1,21E-05
Torque2a$_{Tss}$	6,94E-05	7,05E-06	**4,47E-06**	7,10E-06	1,21E-05

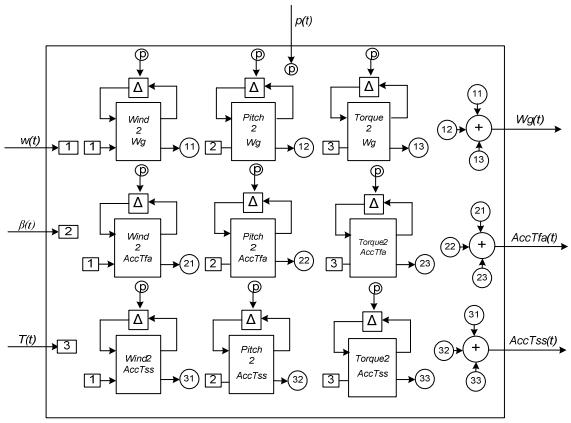

Figure 6: MIMO LPV Model

models (*Wind2Wg, Wind2AccTfa, Wind2AccTss, Pitch2Wg, Pitch2AccTss* and *Torque2Wg*) are obtained using the biggest order of the polynomial approximation of order five. However, three SISO LPV models (*Pitch2AccTfa, Torque2AccTfa, Torque2AccTss*) have the best quality values using a third order polynomial approximation. So, the *MIMOLPV* system has six SISO LPV models of fifth order polynomial approximation, and three SISO LPV models of third order polynomial approximation. The size of the occurrence channel of the MIMOLPV is *MIMOnocc* (9).

$$MIMOnocc = 6 \cdot \{5 \cdot (5+1)\} + 3 \cdot \{3 \cdot (3+1)\} \quad (9)$$
$$MIMOnocc = 216$$

The MIMO LPV model (see Figure 6) has been developed in *Matlab/Simulink*. Finally, to validate the LPV model in time domain, three simulations made in three operational points not explicitly defined by the linear models used to build the LPV models, are presented here. In these simulations, the response of the family of LTI plants is compared to the response of the MIMO LPV model. Figure 7 shows the inputs of these simulations to representing the response of the systems

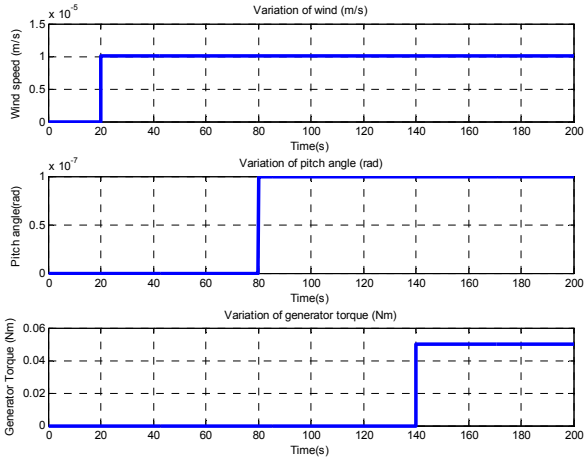

Figure 7: Input of Time Domain Simulations

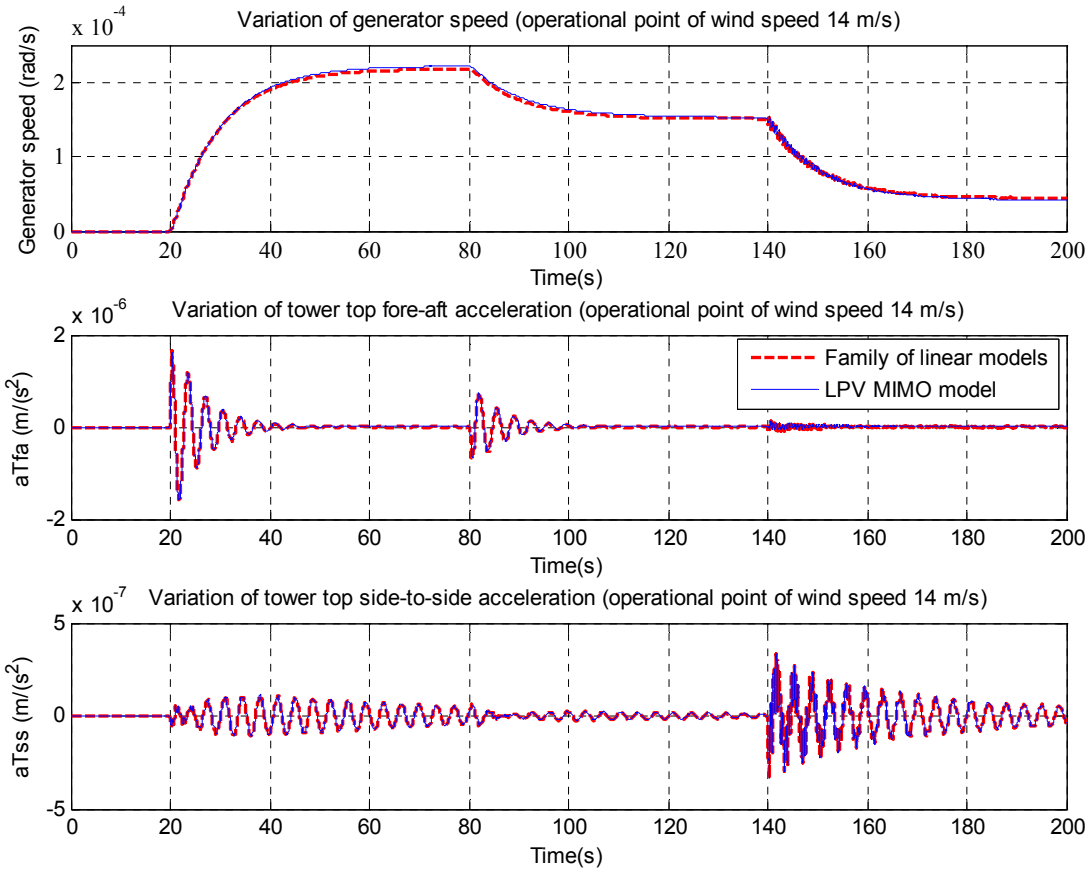

Figure 8: Simulation for Wind Operational Point of 14 m/s

near to the operational points. These inputs are a variation of wind speed step of 10^{-5} m/s at 20 s, a variation of pitch angle step of 10^{-7} rad at 80 s and a variation of generator torque step of 0.05 Nm at 140 s. The operational points used are wind speed of 14 m/s and 24 m/s, whose linear models were not used to generate the LPV model.

Figure 8 and 9 show the comparison of the variation of the outputs (w_g, a_{Tfa}, a_{Tss}) of the family of linear plants and the outputs of the LPV model in these operational points. Differences are negligible. These time domain simulations confirm the good frequency response previously calculated with the quality values *Qmean* and *Qmax*. In fact, for the operational points not considered in the LPV model design process (for instance, wind speeds of 14 m/s and 24 m/s in examples presented in the paper), the quality of the MIMO LPV is good due to the excellent approximation of the LPV model to the family of linear model extracted in GH Bladed.

CONCLUSIONS

Some conclusions are extracted from the work carried out and presented in this paper:

- In spite of the complexity of the wind turbine non-linear model, a wind turbine MIMO LPV model can be carried out using the method described in this paper. The number of calculations is very high, but it can be developed with mathematical software packages like *Matlab/Simulink*. The linear models extracted from GH Bladed are very reliable and they are commonly used by wind turbine manufacturer companies to design real wind turbines models.
- The MIMO LPV model is validated not only in frequency domain using the values *Qmax* and *Qmean*, but it is also validated in time domain due to the implementation of the LPV model represented in LFT representation in Simulink.
- The increasing of the polynomial approximation order makes the LPV model more complex. This complexity involves a bigger size of the occurrence channel and a bigger computational cost in the system. Generally, a high order of the polynomial approximations guarantees a better quality for the LPV model, but this is not absolutely true as it has been probed in this paper. For each system, the best quality of the LPV model could be obtained with a particular order of the polynomial approximation.
- Using LPV models, the uncertainties of the wind turbine are modelled. So, this uncertainly model can be taken into account to design LPV controllers which improve the closed loop performance of using LTI controllers.

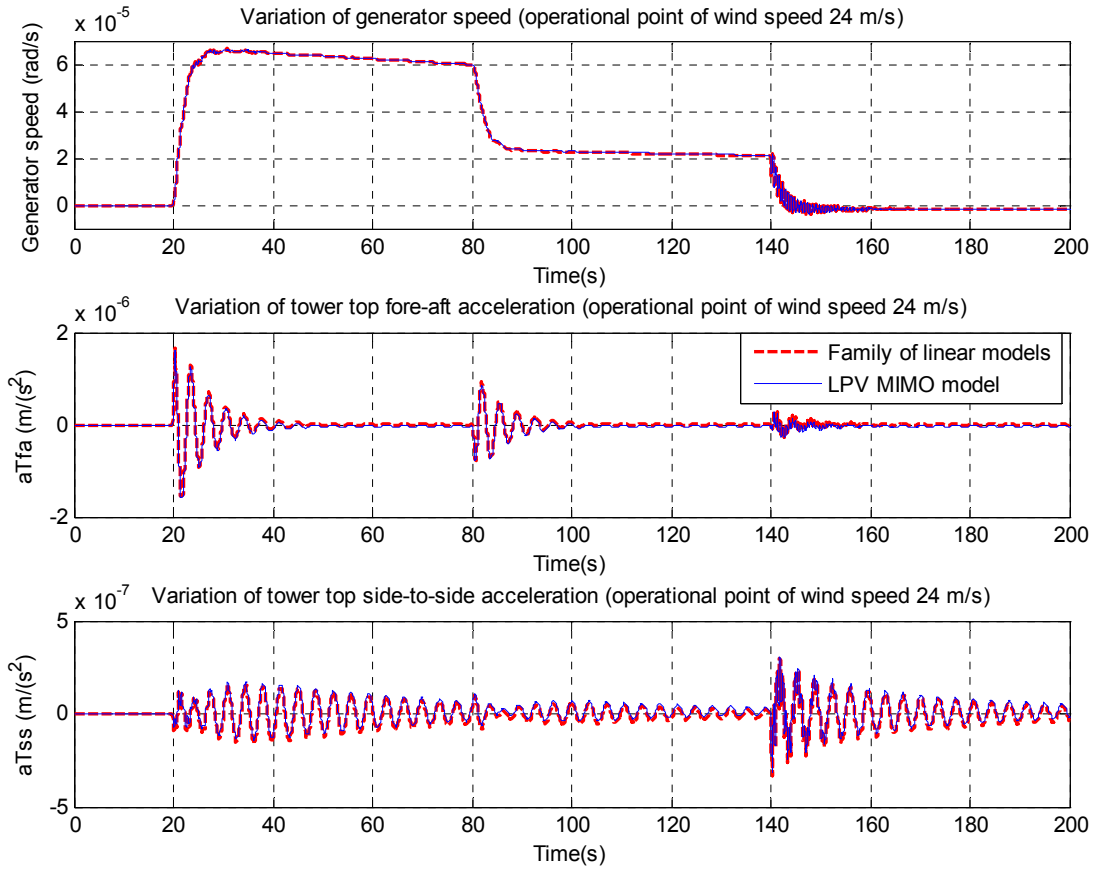

Figure 9: Simulation for Wind Operational Point of 24 m/s

REFERENCES

Bianchi, F.D., H. De Battista and R.J. Mantz. 2007. "Wind Turbine Control Systems. Principles, Modelling and Gain Scheluding Design". Advances in Industrial Control AIC. Springer.

Bobanac, V., M. Jelavic and N. Peric. 2010. "Linear Parameter Varying Approach to Wind Turbine Control". *14th International Power Electronics and Motion Control Conference*l, 6-8 September, Ohrid, Macedonia.

Bodenheimer, B., P. Bendotti, and M. Kantner. 1995. "Linear Parameter-Varying Control of a Ducted Fan Engine". *The Inter. Journal of Robust and Nonlinear Control,* Jan.

Bossanyi, E.A. 2009. "Controller for 5MW reference turbine". European Upwind Project Report, www.upwind.eu**.**

Díaz de Corcuera, A., A. Pujana-Arrese, S. Nourdine, H. Camblong, and J. Landaluze. 2011. "GH Bladed's linear models based H_∞ control for offshore wind turbines". *EWEA Offshore 2011,* November 29- December 1, Amsterdam.

Groot Wassink M., M. Van de Wal, C. Scherer and O. Bosgra. 2003. "LPV control for a water stage: beyond the theoretical solution". *Control Engin. Practice*. 231-245.

Jonkman, J., S. Butterfield, W. Musial and G. Scott. 2009. "Definition of a 5 MW Reference Wind Turbine for Offshore System Development. NREL*"*. Technical Report, NREL/TP-500-38060, Feb 2009.

Muhando, E. B. and S. B. Butterfield. 2011. "Gain- Scheluded H_∞ Control for WECS via LMI Techniques and Parametrically Dependent Feedback Part II. Controller Design and Implementation". *IEEE Transactions on Industrial electronics,* 58.

Ostergaard, K. Z. 2008. "Robust, Gain-Scheluded Control of Wind Turbines". Ph.D. Thesis. Aalborg University.

Salcedo, J.V. and M. Martínez. 2006. "Identificación de modelos LPV para el control de sistemas no lineales". *Revista Iberoamericana de Automática e Informática Industrial*. ISSN: 1697-7912. Vol. 3, Num. 3, pp. 92-107.

Tóth, R., M. Lovera, P.S.C. Heuberger and P.M.J. Van der Hof. 2011. "Discretization of Linear Fractional Representations of LPV Systems". *IEEE Transactions on Control Systems Technology.* ISNN: 1063-6536. Vol. Issue 99, pp 1-17.

AUTHOR BIOGRAPHIES

ASIER DIAZ DE CORCUERA, ARON PUJANA-ARRESE, JOSE M. EZQUERRA, EDURNE SEGUROLA and **JOSEBA LANDALUZE** are with the Control Engineering and Power Electronics department of Ikerlan-IK4, a Technological Research Centre located in the Basque Country (Spain). Their current research interests include design, modelling and control of complex mechatronic systems, modelling and control of wind turbines, and linear and non-linear robust control techniques. E-mail addresses are: ADiazCorcuera@ikerlan.es, APujana@ikerlan.es, JMEzquerra@ikerlan.es, MESegurola@ikerlan.es and JLandaluze@ikerlan.es.

LOSSELESS STARTING METHOD FOR THE WOUND ROTOR INDUCTION MOTOR

Sergiu Ivanov
University of Craiova, Romania
Faculty of Electrical Engineering
107, Decebal Blv., 200440 Craiova
E-mail: sivanov@em.ucv.ro

Mihai Rădulescu
INDA Craiova
30, Mărăşeşti Street
200494, Craiova, Romania
E-mail: mihai.radulescu@inda.ro

KEYWORDS
Induction motor, Wound rotor, Doubly fed, Start.

ABSTRACT

In heavy duty drives in the range of hundreds kW, like cement and minerals industries, wound rotor induction motors are used. Important users make use of hundred of such drives, summing hundreds of MW. This type of motors have technical capabilities to easily operate at variable speed. Despite this simple capability, the large amount of losses which occur at low speeds determine the users to use the facility given by the wound rotor only for starting. Even so, the losses specific to the additional rotor resistors are quite important, given the range of power. The paper describes the existing technologies involved in the variable speed drives based on wound rotor induction machines. Finally, it proposes a technique for starting which avoids the use of additional rotor resistors and consequently it eliminates the corresponding losses. The simulations confirm the viability of the technique.

INTRODUCTION

For high power (x 100 kW – MW) and heavy duty drives like pumps, fans, cement and minerals industries, hydro and wind generators, shaft generators for ships, wound rotor induction motors are generally used. In this range of power, generally, the stator windings are high voltage ones (6 kV). For such rated voltage the classical solution for variable speed drives which involves a controlled V/f source is difficult to be applied. Only few manufacturers are able to offer such solutions which cancel the necessity of a wound rotor machine, but the price is quite prohibitive.
For existing drives, the control on the rotor side is technically more accessible, knowing that the rated rotor voltage can be ten times smaller than the stator one. Thus, power electronic equipment is easily to be reached.
The paper proposes a solution for starting (and speed adjustment) high power heavy duty wound rotor asynchronous motors drives which would have a maximized efficiency thanks to the elimination of the losses specific to the additional resistors. The method, known as double feeding of the induction machine is presently used, as example, for speed adjustment of the asynchronous generators within the wind generators. The literature does not report the use of this method for starting the drives, knowing that the applications that use such type of motors need high starting torque. The literature (Vas 1998) signals technical difficulties in using this method for speed ranges around zero (i.e. starting). The paper proposes a solution for extending the speed range down to zero.
The proposed solution dramatically improves the energetic efficiency of the variable speed drives with wound rotor induction machines, mainly during the starting process, grace to elimination of the power dissipation in the additional rotor resistances. It maintains in the same time the drive performances in terms of torque capability.

EXISTING TECHNOLOGIES

In the present, for starting (and speed adjustment) of the heavy duty electric drives with wound rotor asynchronous motors, beside the classical solution which involves a variable three-phased additional resistor on the rotor side, two other solutions are used, both of them using additional resistors on the rotor side. Consequently, especially during the starting phase, but also during the speed adjustments mostly in the low speed range, important losses occur.
The first of the two technologies (Fig. 1) uses an uncontrolled rectifier supplied by the rotor winding. The load of this rectifier is an electronic variable resistor, by the way of a chopper.

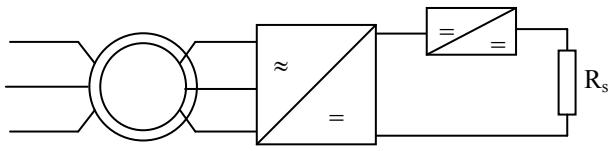

Figure 1: Technology with Uncontrolled Rectifier and Electronic Variable Resistor

The chopper can be avoided if, instead of an uncontrolled rectifier is used a controlled one on the ground of the second technology described below. The equivalent resistance in the rotor side can be thus adjusted by the fire angle of the rectifier. The practical technical difficulties lie in the control part of the rectifier, knowing that the frequency on the rotor side is

Proceedings 26th European Conference on Modelling and Simulation ©ECMS Klaus G. Troitzsch, Michael Möhring, Ulf Lotzmann (Editors)
ISBN: 978-0-9564944-4-3 / ISBN: 978-0-9564944-5-0 (CD)

permanently variable. Thus, the classical "phase control" of the fire angle cannot be used anymore.
The second technology (Fig. 2) involves a graduator on the rotor side. The fire angle of the semiconductors adjusts the equivalent additional resistance in the rotor circuit.

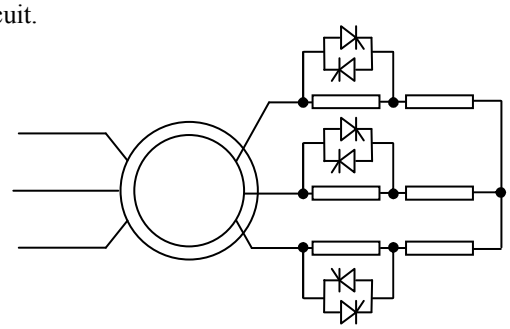

Figure 2: Technology with Graduator

Two elements are common to the technologies described above:

- the both involves the direct connection of the stator at the power grid; this aspect is mandatory due to the high rated voltage of the stator (6 kV). As was stated above, for this voltage, it is not impossible, but is difficult to apply the V/f control on the stator side;
- the both use additional resistors. Besides the disadvantages given by the necessity of the additional resistors themselves (size, occupied space), during the operation, inevitable additional losses occur. The amount of the losses is higher if the drive must perform speed adjustment, especially in the low speed range, as losses are proportional to the slip. The amount of losses is unacceptable for current exploitation purpose.

EXPLORED TECHNOLOGY

In the range of high and very high power, speed adjustment of the wound rotor asynchronous machines can be achieved by applying the double fed principle.
The typical applications of doubly fed induction machines are high power drives (pumps, fans, cement and minerals industries), hydro and wind generators, shaft generators for ships etc. where operating speed range is about ±30% of the synchronous one. Consequently, due to the fact that only the slip energy is circulated by the two converters, only small power is spread by the static converters chain. As example, for a speed range of D=3:1 (0.5÷1.5 n_N), the rated power of the rotor side converter can be just about 0.33 of the machine rated power. This is the main reason why this method is used only for speed adjustment in limited range. If the principle must be used for starting too, the rated power of the converters chain will rise to the rated power of the induction machine.
The classical technology of this principle is the sub synchronous cascade. It allows the regulation of the motor speed, as the name is saying, only below the synchronous speed and it consists in retrieving of the slip energy from the rotor and reinsertion of this energy either in the grid or, as mechanical energy, at the motor shaft.
The real doubly fed principle consists in supplying the rotor winding by a bidirectional converter, the stator being directly connected to the grid (Fig. 3). Even the principle diagram from Fig. 3 is similar to the static sub synchronous cascade, the control principle for the double fed induction machine is different.

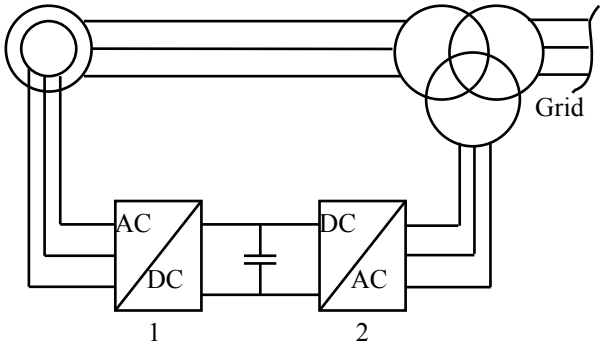

Figure 3: Speed Control by Double Feeding the Asynchronous Motor

Thus, in the case of the sub synchronous cascade, the static converter 1 connected to the rotor windings is an uncontrolled rectifier, the energy corresponding to the induction motor slip being reinserted into the grid by the inverter (converter 2).
For the double fed machine, the both converters are bidirectional ones. In fact the two are fully controlled bidirectional bridges, able to circulate the energy in both directions.
The most "in fashion" application of this technology is the speed control of the wind generators for achieving the MPP operation, thus the machine runs in generator mode around the rated speed. It is the most suited application, as it does not need to be started, because the wind is used to accelerate the machine up to the operating speed range (Ivanov 2004, Ivanov 2006).
As can be seen, the proposed solution is able to perform speed control on the both sides of the synchronous speed. This is another important facility of the solution, face to the classical sub synchronous cascade. Furthermore, the price of the converter can be more attractive than in the case of V/f converter on the stator side, taking into account the quite different values of the rated voltages on the two sides of the machine.
Another important advantage of this control technology is the short time maximum torque. For doubly fed asynchronous machine, this parameter is much higher than all other electric machines, including induction or permanent magnet machines. This is due to the fact that the increasing of the active current does not directly increase the air-gap flux and consequently the iron saturation. The active current is temporally limited only

by the thermal stress of the windings and by the current capability of the rotor side converter.

Continuing with the advantages of the control technology, it must be mentioned the very important facility to control the reactive power changed by the stator with the grid. The term "changed" was used because, with a proper control of the rotor side converter, it is possible not only to cancel the reactive power got by the stator from the grid (unity power factor), but even to inject reactive power into the grid. This is a quite important advantage, taking into account the size and number of such drives in the mining industry, for example.

For motor operation, several reasons are mentioned in the literature which limits the use of this technology only for speed adjustment, not for starting too:

- high rotor to stator winding turn ratio. This generates at low speeds (standstill) very high voltages in the rotor windings, much higher than the rated one;
- if the technology is used for starting and speed adjustment in the low speed range, the rated power of the static converter chain must be designed for the rated power of the motor;
- high instability of the control in the very low speed domain (around zero).

This last aspect is highlighted in the results of the simulation of the 2.2 kW doubly fed induction machine drive. The control was performed by considering stator flux oriented control on the rotor side of the doubly fed induction machine. The two components of the rotor voltage are obtained based on the rotor voltage equation written in the stator-flux-oriented frame:

$$\underline{u}_{r\Psi s} = \left(R_r + L_r' p\right)\underline{i}_{r\Psi s} + \frac{L_m^2}{L_s} p\left|\underline{i}_{ms}\right| + j\omega_{sl}\left[\frac{L_m^2}{L_s}\left|\underline{i}_{ms}\right| + L_r' \underline{i}_{r\Psi s}\right], \quad (1)$$

with ω_{sl} the angular slip frequency.

The projections of Equation (1) on the two orthogonal axes are:

$$T_r' \frac{di_{rx}}{dt} + i_{rx} = \frac{u_{rx}}{R_r} + \omega_{sl} T_r' i_{ry} - \left(T_r - T_r'\right)\frac{d\left|\underline{i}_{ms}\right|}{dt}, \quad (2)$$

$$T_r' \frac{di_{ry}}{dt} + i_{ry} = \frac{u_{ry}}{R_r} - \omega_{sl} T_r' i_{rx} - \omega_{sl}\left(T_r - T_r'\right)\left|\underline{i}_{ms}\right|. \quad (3)$$

By assuming constant stator flux operation, constant stator magnetizing current respectively and considering the imposed values of the currents, the decoupling components of the rotor voltage result:

$$u_{drx} = -\omega_{sl} L_r' i_{ry}^*, \quad (4)$$

$$u_{dry} = \omega_{sl} L_r' i_{rx}^* - \omega_{sl}\left(L_r - L_r'\right)\left|\underline{i}_{ms}^*\right|. \quad (5)$$

In equations (1)-(5), the term L_r' is the rotor transient inductance.

The complete simulation diagram results the one depicted in Fig. 4. For the rotor inverter was not considered any specific model because was assumed that, thanks to the high frequency switching, it can be considered that it acts as an ideal amplifier.

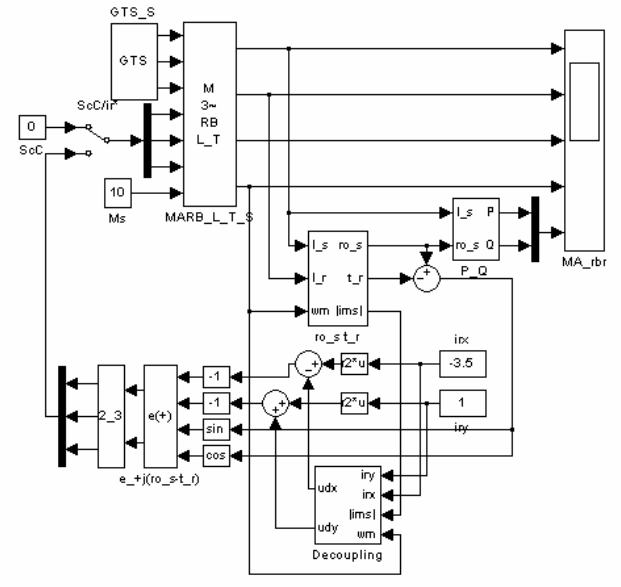

Figure 4: Doubly Fed Induction Machine Supplied by Voltage Source Inverter in the Rotor Side

The results of the simulation of the drive when the speed decreases to low values are plotted in Fig. 5.

The plot begins when the motor comes to be controlled in the rotor circuit, being supplied on the rotor side by a voltage source inverter. Until then the motor has the rotor in short circuit, being supplied in the stator by a constant frequency voltage (the grid) and loaded with a 10 Nm static torque. The stator continues to be connected to the grid after the control on the rotor side begins. The stator flux oriented vector control imposes constant active and reactive rotor currents. The reactive rotor current is greater than the rated one and the stator injects reactive power in the grid (plotted in the last window).

The active current is smaller than the one needed for balancing the static torque. Consequently, the speed constantly decreases. It can be seen that around 25 rad/sec the system became instable.

For the reasons pointed above, literature signals as starting method for this kind of drives the quite classical method with additional resistors in the rotor circuit. When speed arrives within the operating speed range, the resistors are disconnected and the frequency converter is connected to the rotor. Another possibility is to reverse the operation of the machine: short circuit the stator and supply the rotor by the static converters up to the necessary speed then switching the control types.

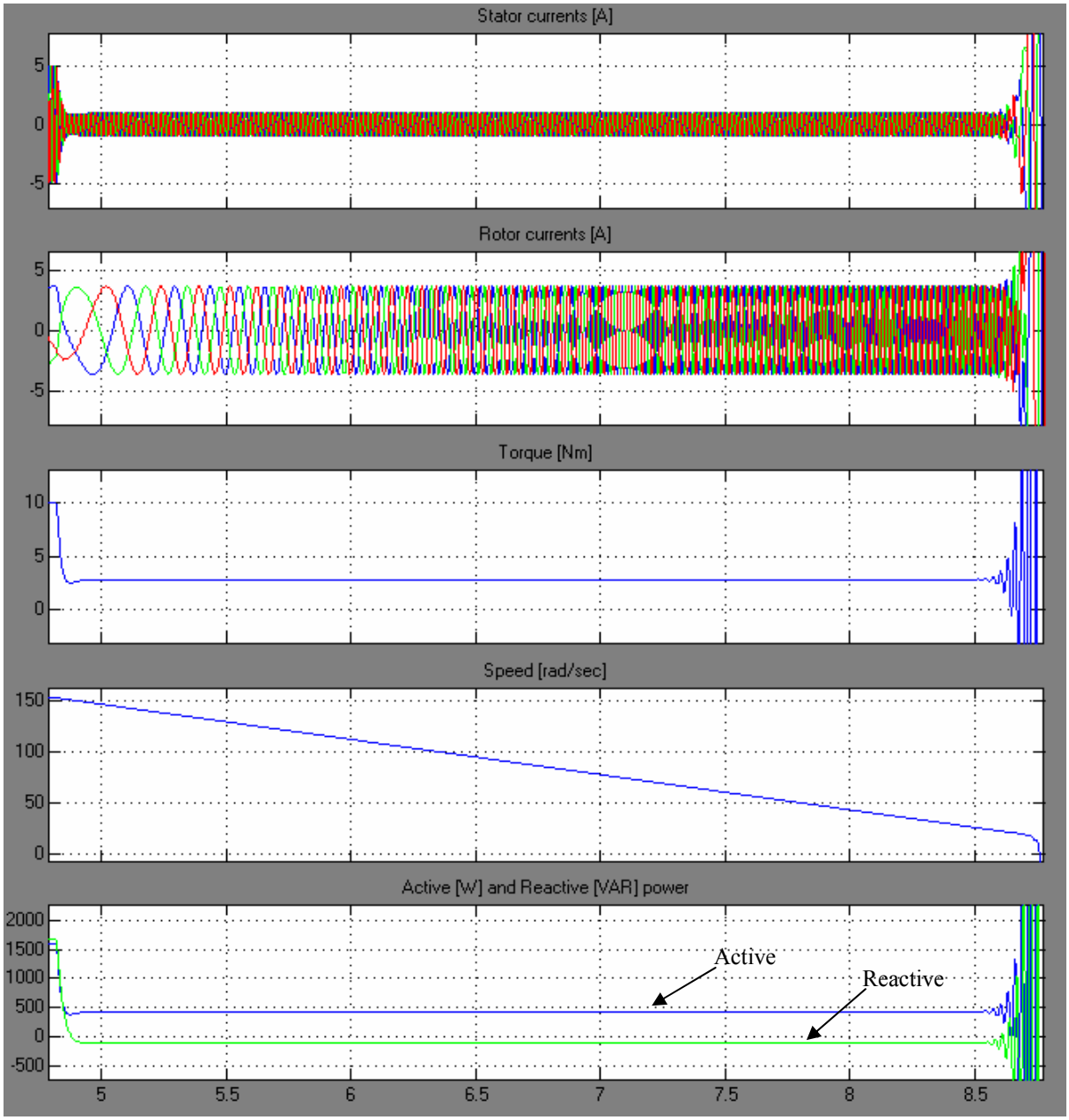

Figure 5: Behavior of the Doubly Fed Induction Machine in the Low Speed Range

In the case of wind generators the technology of rotor control is very well suited, as they are driven by the wind turbine. Consequently, they do not need to be started, because the wind is used to accelerate the machine up to the operating speed range, when the rotor control comes to manage the operation. For this type of application, the vector control is not the single possibility. Literature signals as possible alternative the Direct Torque Control on the rotor side (Gokhale et al. 2002). The experience of the authors (Ivanov 2010) shows that this type of control requires very high performances control hardware due to the fact that the sampling period of the control system is exactly the minimum duration of the pulse width modulation. Consequently, in order to be able to achieve high frequency modulation and low ripple currents, powerful (fast) control systems are necessary.

The technique we propose is simply to supply the rotor side of the induction motor by a preset currents inverter. The simulation diagram (Fig. 6) uses the model of a preset currents voltage source inverter (P3Htg) which injects the necessary currents in the rotor windings. The two orthogonal components of the rotor currents result as outputs of two continuous PI controllers: the direct component is the output of the reactive power controller and the quadrature component is the output of the speed controller.

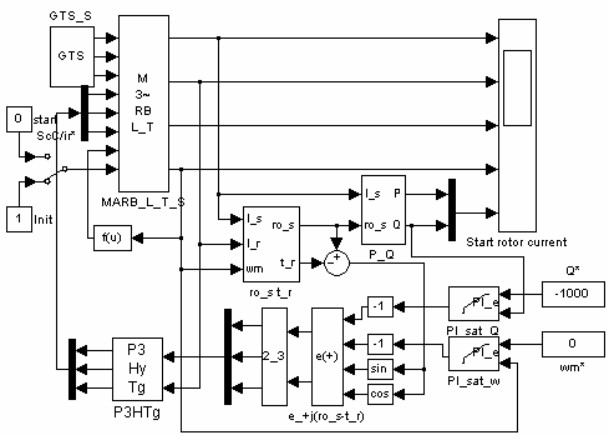

Figure 6: Doubly Fed Induction Machine Supplied by Preset Currents Voltage Source Inverter

Some results of the simulation of the system are plotted in Fig. 7. The torque applied to the motor shaft is proportional to the mechanical speed. It attains the rated value at the rated speed.

The start process is imposed to begin at 1 second after the beginning of the simulation. The preset speed of 150 rad/sec is achieved in about 1.2 seconds, the currents controllers being tuned to limit the maximum torque to double of the rated one.

No hesitation is present at the very beginning of the starting phase.

At 3 seconds from the beginning of the simulation, a negative 1000 VAR reactive power is imposed i.e. the motor would act as a reactive power generator (traced in the last plot).

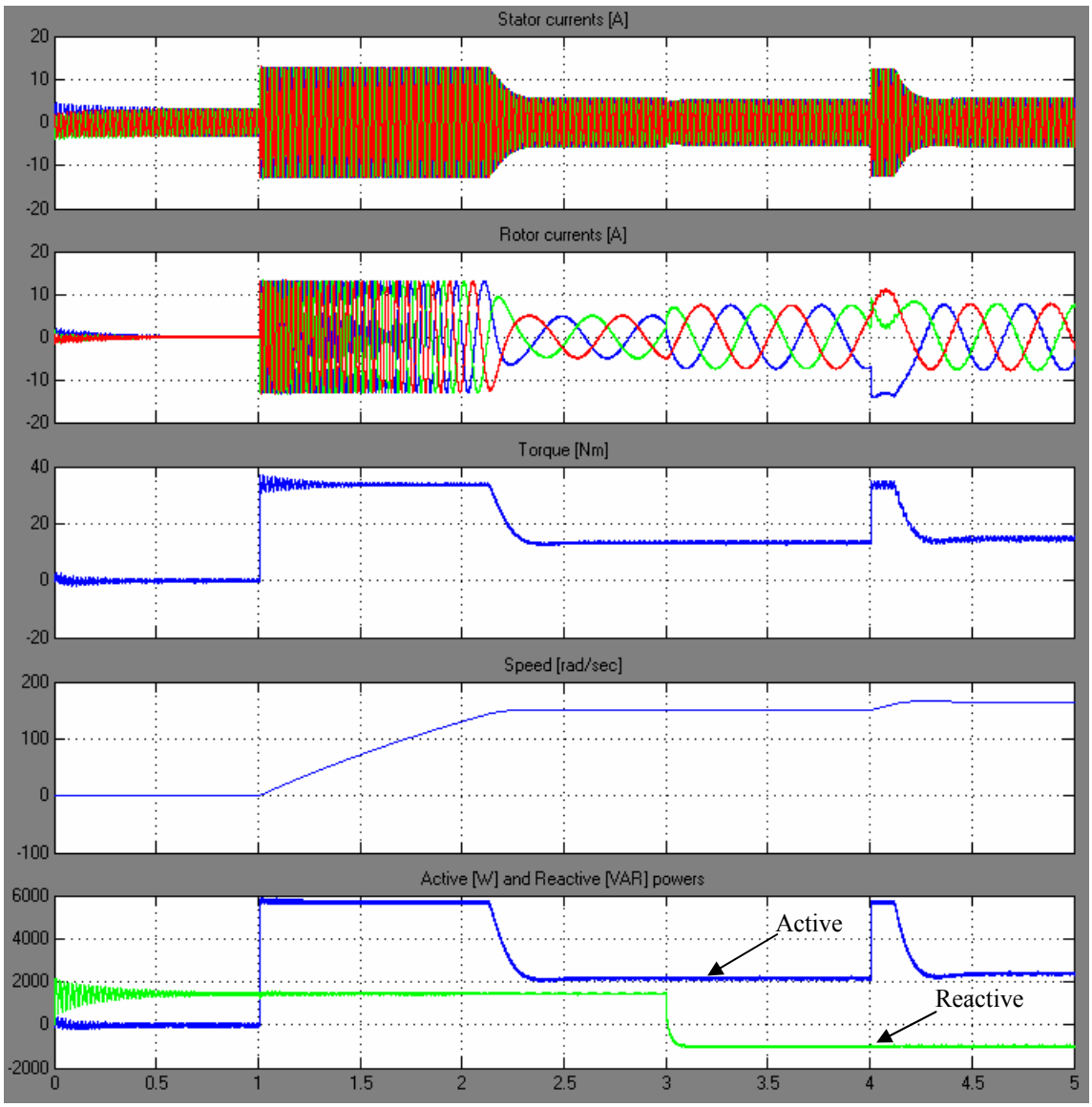

Figure 7: Behavior of the Doubly Fed Induction Machine Supplied by Preset Currents Voltage Source Inverter

The hyper-synchronous operation is imposed at 4 seconds after the beginning of the simulation, when the preset speed becomes 165 rad/sec, the synchronous one being 157 rad/sec.
It is notable the very good behavior of the drive during all the phases of the simulation.
The two reasons for using the double fed technology only for speed adjustment and not for starting too explained above are not always valid.
On one hand, the motors used in several existing applications have low (less than 1) rotor to stator winding turn ratio, i.e. the rated rotor voltage is much less than the stator voltage, up to 1 tenth. Consequently, the risk of over voltages on the rotor side there is not present anymore, with the price of quite important currents.
On the other hand, even for starting, the rated power of the motor is to be delivered by the rotor converter, does not imply severe technical problems because the technology is mature enough to be able to offer high power converters having the rated voltage in the range of 1 kV.
Besides the very truthfully behavior, an important disadvantage must be noted. It is the preset current modulation technology of the inverter. It is known that this type of modulation is specially suited for low power applications.
Another mentioned disadvantage of this modulation strategy is the variable switching frequency which has bad influence on the switching losses estimation in the designing phase.
The mentioned disadvantages could be minimized if the preset currents modulation would be used only for the very first moments of the starting process of the wound rotor induction machine. After the speed would arrive in the zone where it could be controlled by the way of a voltage source inverter (unstable at very low speed), the controlled would be switched. This subject, as well as the practical experimentation of the solution, are ideas for continuation of the research.

CONCLUSIONS

The paper discusses the existing technologies involved in the variable speed drives based on wound rotor induction machines and proposes a technique for starting which avoids the use of additional rotor resistors and consequently it eliminates the corresponding losses.
It implies the double fed of the induction machine and vector control of the currents injected in the rotor windings. It is shown by simulations that the voltage source inverters determine instability in the low range of the speed. The paper proposes the using of preset currents voltage source inverters which, even have known and notable disadvantages, are capable to truthfully control the drive, especially its start.
Further researches will focus on minimization of the disadvantages of the preset currents modulation strategy.

REFERENCES

Ivanov, S.; Bitoleanu, A.; Lincă, M., 2004. “Simulation of the doubly fed induction machine and voltage source inverter”. In *Proceedings of the International Conference on Applied and Theoretical Electrotechnics, ICATE'2004*, 234-239.

Ivanov, S.; Laridan, S.; Blondel, T.; Manolea, G.; Robyns, B.; Ivanov, V., 2006. “Simulation of a wind generator with doubly fed induction machine and preset currents voltage source inverter”. In *Bulletin of the Polytechnic Institute of Iaşi*, Tom LII(LVI), Fasc. 5A Electricity, Power systems, Electronics, 359-364.

Ivanov, S., 2010. “Continuous DTC of the Induction Motor”. In *Advances in Electrical and Computer Engineering*, vol. 10, no. 4, 149-154. (http://dx.doi.org/10.4316/AECE.2010.04024).

Vas, P., 1998. *Sensorless Vector and Direct Torque Control*, Clarendon Press, Oxford.

Gokhale, K.P.; Karraker, D.W.; Heikkila, S.J, 2002. “Controller for a wound rotor slip ring induction machine”. U.S. Patent 6,448,735 B1.

AUTHOR BIOGRAPHIES

SERGIU IVANOV was born in Hunedoara, Romania and went to the University of Craiova, where he studied electrical engineering. He obtained his degree in 1986. He worked for the Institute for Research in Motors, Transformers and Electrical Equipment Craiova before moving in 1991 to the University of Craiova. He obtained his PhD in 1998 with a topic in the field of the control of the electric drives systems. He is involved in modelling of the electromechanical systems.

MIHAI RĂDULESCU was born in Craiova, Romania and went to the University of Craiova, where he studied electrical engineering. He obtained his PhD in 2009 with a topic in the field of the electric traction. He is presently General manager of his own company, INDA Craiova.

EXPERT SYSTEM FOR POWER TRANSFORMER DIAGNOSIS

Virginia Ivanov Maria Brojboiu Sergiu Ivanov
University of Craiova
Faculty of Electrical Engineering
107 Decebal Blv., 200440, Romania
E-mail: vivanov@elth.ucv.ro E-mail: mbrojboiu@elth.ucv.ro E-mail: sivanov@em.ucv.ro

KEYWORDS
Diagnosis, the faults tree, power transformer.

ABSTRACT

The power transformers are essential equipment in all transport and distribution grids. Minor faults or defects of this equipment can lead to ravaging effects.
The most part of the monitoring and diagnosis systems are developed around expert systems. The expert systems regroup the methods based on analytical models and the ones based on knowledge on the system.
The paper deals with a diagnosis system dedicated to the power transformers. Based on the effects noted in the behavior of the power transformers, an expert system for the diagnosis and the functional testing was developed, by considering the abnormal comportments and the faults which determine these.
For building the inference mechanism, the faults tree method applied to the transformers was used. The database is comprehensive and takes into account the most frequent faults which occur during the transformers operation. The designed expert system was developed by using the CLIPS 6.0 programming medium.
The paper presents the results of the system running and the conclusions resulted after the expert system was executed.

INTRODUCTION

An expert system is a program which uses knowledge and inference procedures for solving quite difficult problems which normally require a human expert for finding the solution. On brief, the expert systems are software which stores dedicated knowledge programmed by the experts for solving problems difficult to be revealed manually.

Characteristics of the expert systems

The expert systems are often used when there are not available clear algorithmic solutions. The main characteristic is the presence of a knowledge database together with a searching algorithm proper with the reasoning type.
Often, the knowledge database is quite large. For this reason it is very important the way how the knowledge is represented.
The knowledge database must be separated by the software which at its turn must be as stable as possible.
The operations of these systems are then controlled by a simple procedure whose nature depends by the knowledge nature.
As different artificial intelligence software, when other techniques are not available, the searching method is used. The different expert systems differ from this point of view (Patterson 1999).

Structure of an expert system

The systems based on knowledge can be applied for any area of knowledge. Expert systems must contain three main modules (Figure 1):
a) The knowledge database is done from the sum of specific knowledge specified by the human expert. The knowledge loaded here is mainly the description of the objects and of the relations between them.
b) The inference devices consist in the sum of the algorithms for determining solutions for the expertise problems, similarly to the human expert.
c) The base of facts (Factual knowledge) contains a dynamic collection of information which changes itself during the call of the expert system. It depends on the practical expertise problem.
Besides these modules, an expert system contains also several modules which offer the ability to communicate with the user and the human expert.
The user interface is the one which performs the dialogue between the user and the system, by using a quasi-natural language. It generally contains the systems of menus and the graphical user interfaces specific to the men-machine communication.
Knowledge acquisition module performs the task of acquiring the specialized knowledge offered by the human expert or by the knowledge engineer. It verifies the validity of the knowledge and generates a knowledge base specific to the expert system.
Explanations module allows tracing the way followed during the ration activity by the expert system. It outputs arguments for the resulted solutions.

Proceedings 26th European Conference on Modelling and Simulation ©ECMS Klaus G. Troitzsch, Michael Möhring, Ulf Lotzmann (Editors)
ISBN: 978-0-9564944-4-3 / ISBN: 978-0-9564944-5-0 (CD)

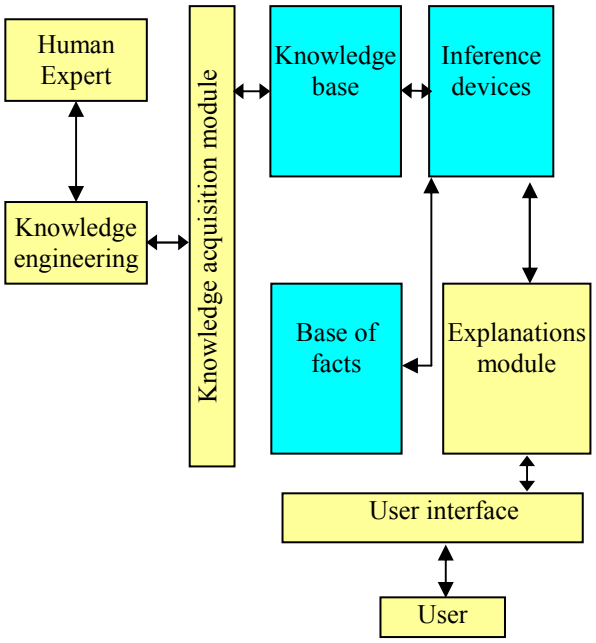

Figure 1: The general structure of an expert system

There are more the formalisms for knowledge representation, the most important being: the first order predicates logic formalism; the production rules formalism; the frames formalism.

In present, the production rules formalism is the most used method for knowledge representation. This formalism is based on the idea that most of the expert information has a structure which is like the natural language, as "if certain premises are fulfilled then some conclusions can be obtained".

A rule consists of an IF part and a THEN part (also called a condition and an action). The IF part, lists a set of conditions in some logical combination. The piece of knowledge represented by the production rule is relevant to the line of reasoning, being developed if the IF part of the rule is satisfied; consequently, the THEN part can be concluded, or its problem-solving action taken. Expert systems whose knowledge is represented in rule form are called rule-based systems.

For presenting the production rules formalism, an expert system from simplifying the truth table of a complex logical circuit was belt up. This is using the most frequently procedures of the language CLIPS. This application indicates how interesting can be integrated the procedures with the rules.

EXPERT SYSTEM FOR DIAGNOSIS OF A POWER TRANSFORMER

The power transformers are the subject of important electric and mechanic stresses during all the operation. These stresses reduce the dielectric rigidity of the insulation system of the transformer. The reduction of the electric rigidity evolves to thermal and electric faults which can determine defects and even transformer destruction. Still in the incipient faults, chemical and physical changes occur within the transformers. These changes can be analyzed in order to get a warning signal on the type of fault which evolves within the transformer. In this way, actions can be performed before the situation gets dangerous.

The expert system used for the diagnosis of the analyzed system is based on the faults tree method.

This method implies to fulfill several steps, as follows: defining the analyzed system; the development of the faults tree of the system; qualitative and quantitative evaluation of the faults tree.

For the proposed system, power transformer respectively, the different faults and their possible causes are analyzed (Popescu et al. 2002), as are presented.

The most five frequent symptoms which occur during the power transformers operations will be analyzed. They are:

a) Symptom S_1: Gases emanation

Causes:

S11: Short circuit between turns;

S12: Overloaded operation.

b) Symptom S_2: Abnormal noises

Causes:

S21: Screw assembling;

S22: Wrong positioning of the jokes on cores;

S23: Wrong fixation of the coils;

S24: Air in the tank and in coils;

S25(S11): Short circuit between turns;

S26: Static discharges or light breakdowns of the insulation.

c) Symptom S_3: Local or general heating

Causes:

S31 (S11): Increased current due to short circuit between turns;

S32: Increased current due to short circuit of the terminals;

S33: Increased current due to short circuit to the core;

S34: Weaken contacts;

S35: Oil saponification;

S36: Weaken magnetic core.

d) Symptom S_4: Protections tripping

Causes:

S41(S11): Short circuit between turns;

S42: Breakdown at one terminal;

S43: Ground fault in the grid;

S44: Short circuit in the grid.

e) Symptom S_5: Oil leakage

Causes:

S51: Points of welding;

S52: Sealing faults.

The development of the faults tree is a laborious step, when the human expert must demonstrate high ability in knowledge and understanding of the analyzed system. The faults tree is developed in a hierarchal manner, starting from the upper level towards the lower levels. The level of detail is given by the requested deep of the analysis.

The faults tree of the expert system corresponding to the power transformer, developed based on the faults and possible causes presented, is depicted in Figures 2 and 3.

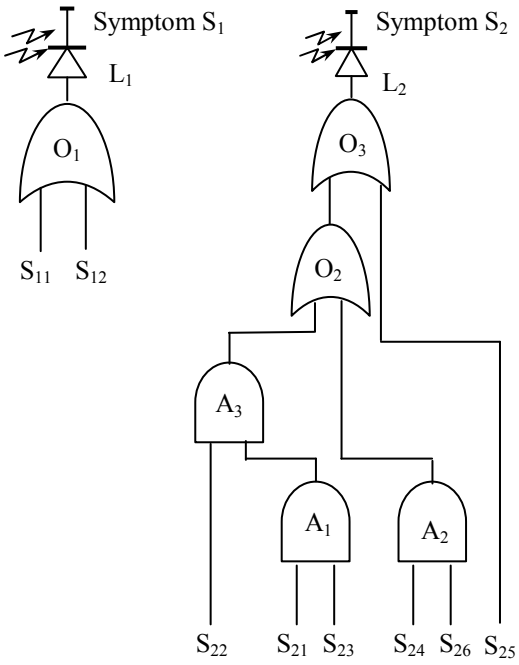

Figure 2: The faults and possible causes for the symptoms S_1 and S_2

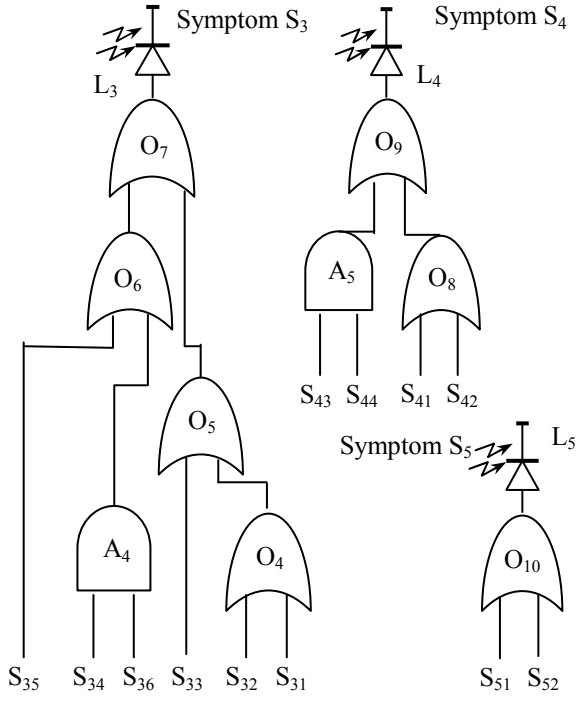

Figure 3: The faults and possible causes for the symptoms S_3, S_4 and S_5

It can be noticed that the same cause can produce different faults, with different symptoms. As example is the fault "Short circuit between turns".

The implementation of the faults tree is performed with logic gates.

Each possible fault which influences the considered critical event is represented by a source. The logic 1 of each source means existence of the corresponding fault.

In order to reduce the true table of the tree corresponding to the considered fault, an expert system was developed, by using the programming language CLIPS (Reference Manual CLIPS 1998).

The specific algorithm developed in CLIPS language simplifies the table of truth for a logical complex circuit with more inputs (sources) and outputs.

The simplification procedure implies the following steps:

- the connections between the circuit components are initialized;
- the response of the system when all sources are set to zero is determined;
- a single source is modified and the answer of the system is determined. By using the Gray code, all possible combinations of inputs are iterated. By using the Gray code, only one source is modified at each step, in order to determine the answer in the table of decisions (the use Gray code determines the minimization of the execution time);
- during the determination of the responses, a rule checks if two sets of inputs which are different by a single input determines the same answer. If YES, this single input can be replaced by „*" (it signifies that the value of that input has no importance for obtaining the same answer);
- once that all the answers and the simplifications were determined, the table of decisions of the circuit is printed.

This application exemplifies the use of most usual procedures available within CLIPS software and how interesting can be integrated with the rules.

Considering that the symptoms S1, S2 and S3 occur simultaneously, the causes which produced them can be identified by analyzing the results of the program as is shown in Figure 4.

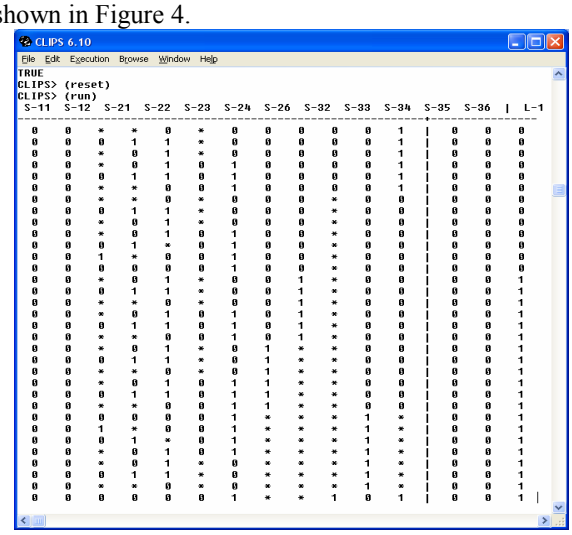

Figure 4: The results of the program running for simultaneously symptoms S_1, S_2 and S_3

The results of the program running highlight important simplification of the true table. The 2^{12} (4096) possible combinations are reduced to 160 distinct combinations. For the symptom S4 (Protections tripping) the causes can be identified by analyzing the results in Figure 5.

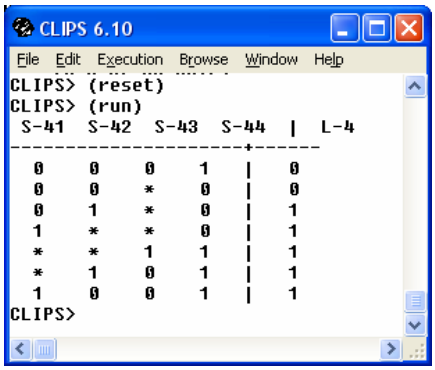

Figure 5: The results of the program running for symptom S_4

If two or more symptoms occur simultaneously, the developed Inference devices can identify very fast the causes which induced the fault. If the information within the Base of facts is considered, the causes can be identified even more precisely.

QUANTITATIVE ANALYSIS OF THE RELIABILITY OF THE POWER TRANSFORMER

The quantitative analysis of the fault tree is the last step in the methodology of reliability analysis of the systems by using the fault tree method. This impose to determine the probability of occurrence of the critical event analyzed, starting from the probabilities of occurrence of the events (faults) and taking into account their propagation ways through the logic gates of the tree.
This methodology imposes to write the structural logic function starting from the fault tree of the analyzed system as::

$$E_{cr} = \Phi_l\left(E_1, E_2, ..., E_i, ...E_n\right) \qquad (1)$$

where,
E_{cr} is the critical event of the system, expressed in terms of the primary events Ei (i=1, 2,…,n), considered as independent between them.
Starting from the logic function (1) it can be expressed the algebraic one

$$E_{cr} = \Phi_a\left(E_1, E_2, ..., E_i, ...E_n\right) \qquad (2)$$

By taking into account the transformations specified in Table 1, corresponding to the basic logic gates of the fault trees:

Table 1: The transformations of the basic logic gates

Logic gate	Relation	
	logical	Algebraic
AND	Ei ∩ Ej	Ei · Ej
OR	$E_i \cup E_j$	$E_i + E_j - E_i \cdot E_j$

Even the method described above is systematic, it is quite complex because it requires writing and processing the structural function corresponding to the fault tree of the analyzed system. In practice, in order to facilitate the quantitative evaluation, it is possible to avoid the writing of the structural function. In this case, the calculus will be done step by step, from down to up, starting from the basic levels corresponding to the primary events, to the critical event. Following will be presented the relations which allow to highlight the propagation of the tree events by the way of the fundamental logic gates (AND, OR).
For an AND gate with n inputs we have:

$$P(1 \cap 2 \cap ... \cap n) = P(1) \cdot P(2) \cdot ... \cdot P(n) \qquad (3)$$

For an OR gate with two inputs we have:

$$P(1 \cup 2) = P(1) + P(2) - P(1) \cdot P(2) \qquad (4)$$

For small enough fault probabilities (in practice $P<10^{-2}$, which is quite usual), it can be used the approximate expression:

$$P(1 \cup 2) = P(1) + P(2) \qquad (5)$$

The simplified expression (5) can be generalized for an OR gate with n inputs:

$$P(1 \cup 2 \cup ... \cup n) = P(1) + P(2) + ... + P(n) \qquad (6)$$

The faults for the symptoms S_4

The fault tree from Figure 4 will be quantitatively evaluated for the symptoms S_4. The probability of occurrence of the event E_{cr} will be estimated, starting from the probabilities of occurrence of the primary events S_{41}, S_{42}, S_{43}, S_{44}. A possible approach is to write the structural logic function corresponding to the tree:

$$E_{cr} = \left[\left(S_{41} \cup S_{42}\right) \cup \left(S_{43} \cap S_{44}\right)\right] \qquad (7)$$

For the presented example, thanks to the reduced complexity of the structural function, the probability of occurrence of the critical event can be expressed directly:

$$P(E_{cr}) = P\left\{\left[\left(S_{41} \cup S_{42}\right) \cup \left(S_{43} \cap S_{44}\right)\right]\right\} \qquad (8)$$

It results the algebraic expression corresponding to relation (8):

$$P(S_4) = \{[P(S_{41}) + P(S_{42})] + [P(S_{43}) \bullet P(S_{44})]\} \quad (9)$$

The faults for symptoms S_3

In order to quantitatively analyze the tree from Figure 3, it is better to avoid writing the structural logic function, because it would be too difficult to process it. The probability of occurrence of the critical event can be evaluated by computing step by step, considering the expressions (3), (5), (6).
This approach is exemplified in Figure 6, where is computed the probability of occurrence of the critical event, staring from the probabilities of occurrence of the primary events. The initial data for the probabilities of the primary events can be obtained from the datasheets of the components.

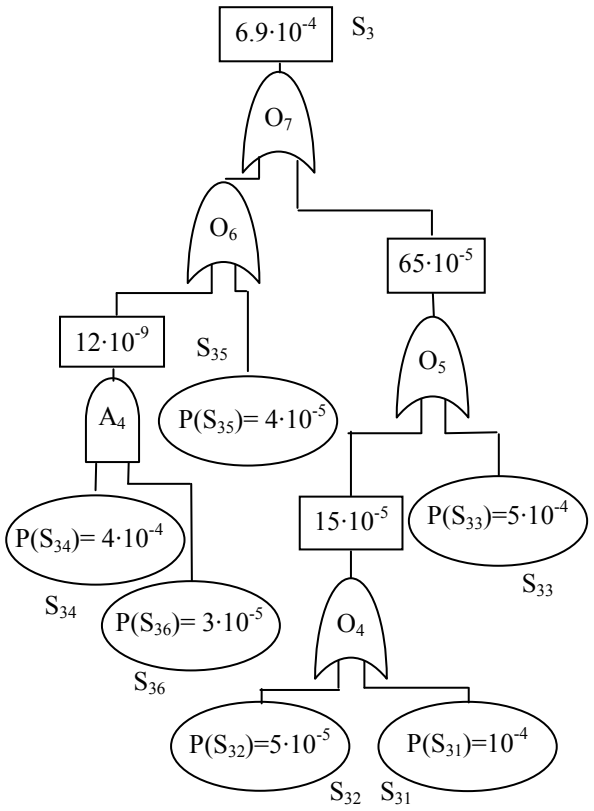

Figure 6: The probability of occurrence of the critical event S_3

CONCLUSIONS

This paper presents an application of the expert systems for the diagnosis of a power transformer. In order to achieve the results, the faults tree method is used.

Taking into account the great number of possible faults (12 sources), the total number of possible combinations being 2^{12} (4096), the expert system performs algorithms difficult to be done manually.
This example shows how the most usual procedures available in CLIPS can be used and how interesting they can be integrated with the rules.

REFERENCES

Patterson, D.W. Introduction to Artificial Intelligence and Expert Systems, Prentice-Hall International, 1999.

Popescu, M.O. Claudia Laurenţa Popescu, ş.a., Sisteme expert pentru diagnoza echipamentelor electrice, Electra, Bucureşti, 2002.

Reference Manual CLIPS, *Basic Programming Guide*, Volume I, Version 6.10, 1998.

AUTHORS BIOGRAPHIE

VIRGINIA IVANOV was born in Vela, Dolj, Romania, 1963. She was graduated in Electrical Engineering at University of Craiova, Romania, in 1986 and Doctor in Electrical Engineering in 2004. From 1986 to 1998 she worked as researcher with the Researching Institute for Motors, Transformers and Electric Equipment Craiova. In 1998 she joined the Faculty for Electrical Engineering, Department of Electrical Equipment and technologies.

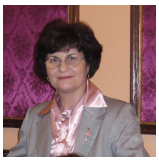

MARIA D. BROJBOIU was born in 1952 in the town Pucioasa Romania. She is currently working as Professor at the University of Craiova, Electrical Engineering Faculty, Department of Electrical Equipment and Technologies since 1981. Before that, she worked as design engineer at the Electroputere holding the Research and Development Center. She is Doctor in Science Technique – Electrical Engineering.

SERGIU IVANOV was born in Hunedoara, Romania and went to the University of Craiova, where he studied electrical engineering and obtained his degree in 1986. He worked for the Institute for Research in Motors, Transformers and Electrical Equipment Craiova before moving in 1991 to the University of Craiova. He obtained his PhD in 1998 with a topic in the field of the control of the electric drives systems. He is involved in modelling of the electromechanical systems.

CONCERNING THE NO LOAD HIGH VOLTAGE TRANSFORMERS DISCONNECTING

Maria D. Brojboiu and Virginia I. Ivanov
Faculty of Electrical engineering
University of Craiova
200440, 107 Decebal Blv, Craiova, Romania
E-mail: mbrojboiu@elth.ucv.ro, vivanov@elth.ucv.ro

KEYWORDS
no load transformer, overvoltage, Matlab

ABSTRACT

The computation program of the transient recovery voltages that appears across the terminals of a circuit breaker, after the low inductive current has been interrupted at the disconnecting no load high voltage transformers, using the routines set developed in Matlab is presented. The computation algorithm is based on the peculiarities of operation of the transformer. The computation program has been applied for transformers from the high voltage electric stations ST North Craiova and ST Urechesti. The computed level of the overvoltage amplitude allows the proper selection of the rated insulation level of the electrical equipment from the electric stations.

INTRODUCTION

The breaking of a low inductive current (around the 100 A value) causes overvoltages. The selection of the circuit breaker will be made so that the overvoltages that occurring do not damage the insulation of the consumers such as transformer or motors. The computation of the overvoltages that appear at the disconnection of a no load transformer (the current interrupted is the transformer magnetizing current) is deeply developed in the literature (Dragan et all, 1975). The evaluation methods of the overvoltages are also well developed, starting from analytical ones, based on a mathematical model of the system obtained using a simplified diagram and ending with the direct methods, based on direct test on the system. By the analytical methods, the integral transformation method and the Laplace transformation respectively, are most common. In this paper an automatic computation algorithm of the overvoltages due to the no load transformers disconnection, when appearing the cutting phenomena of the inductive current, is presented. The low inductive current cutting phenomena appears due to the electric arc instability.
From analysis of the experimental results (Gusa 2002), for the high voltage transformer having a large range of rated current, the value of the cutting current is approximately constant and depends mainly on the characteristics of power circuit breaker and less on the characteristics of the disconnected transformer. The computation of the overvoltages is made by means of the monophase equivalent diagram, Figure 1, neglecting of the electrical resistances of the electrical connections between high voltage source and transformer.

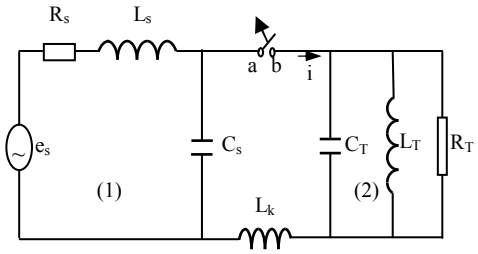

Figures 1: The monophase equivalent diagram of the low inductive current disconnecting

where: L_S is the equivalent inductivity, C_S is the equivalent capacity and R_S is the equivalent electric resistance of the high voltage source; L_T is the transformer magnetizing inductivity, C_T is the transformer equivalent capacity and R_T is the resistance corresponding to the core losses of the transformer; L_k is the inductivity of the electrical connection between voltage source and transformer. At the time when the circuit breaker contacts are opening, the electric current continues to pass through the electric arc formed between the contacts. Due to the intensive deionization, the quenching arc occurs before natural zero inductive current switching. Due to the energy stored in these two circuits, they begin to oscillate independently. The oscillations amplitude from the circuit (1) depends on the stored energy in the L_S inductivity. Therefore, after disconnection, the high frequency oscillations occur, having the small amplitude that overlap with the source voltage so that it may be considered that in the circuit (1) remains the sinusoidal voltage. Meanwhile, in the disconnected circuit (2) the oscillations pulsation ω_T is less than the oscillations pulsation ω_S and higher then industrial pulsation ω: $\omega_T = 1/\sqrt{L_T \cdot C_T}$, but the amplitude overvoltage is greater. The amplitude of the overvoltage in the disconnected circuit (2) is determined using the equation of the energy balance, taking into account the energy loss on the resistance circuit by introducing a subunit factor η (η=0,3÷0,5). If I_t is the current through the L_T inductivity and U_0 is the voltage over the C_T capacity at the time moment of the inductive

Proceedings 26th European Conference on Modelling and Simulation ©ECMS Klaus G. Troitzsch, Michael Möhring, Ulf Lotzmann (Editors)
ISBN: 978-0-9564944-4-3 / ISBN: 978-0-9564944-5-0 (CD)

current cutting, the equation of the energy balance is obtained:

$$\eta \cdot \left(\frac{L_T \cdot I_t^2}{2} + \frac{C_T \cdot U_0^2}{2} \right) = \frac{C_T \cdot U_{2\max}^2}{2} \qquad (1)$$

where U_{2max} is the amplitude value of the overvoltage. Neglecting the current through the R_T resistance the U_{2max} can be obtained:

$$U_{2\max} = \sqrt{\eta \cdot \left(U_{\max}^2 \cdot \cos^2 \alpha + \frac{L_T}{C_T} \cdot \frac{U_{\max}^2}{\omega^2 \cdot L_T^2} \cdot \sin^2 \alpha \right)} \qquad (2)$$

Where U_{max} is the amplitude of the voltage source *u(t)* and α is the current cutting angle $I_t = I_{o\max} \cdot \sin \alpha$. Considering the expressions of the pulsations it is obtained:

$$U_{2\max} = \sqrt{\eta} \cdot U_{\max} \cdot \sqrt{\left(\cos^2 \alpha + \left(\frac{f_T}{f} \right)^2 \cdot \sin^2 \alpha \right)} \qquad (3)$$

In Figure 2 the variations of the voltage source *u(t)*, the inductive current of the transformer *i(t)* and the recovery voltage $u_2(t)$ across the circuit breaker terminals at the moment of current cutting are shown.
Using the above presented formulas, the amplitude factor of the overvoltage can be computed:

$$\gamma = \frac{U_{2\max}}{U_{\max}} = \sqrt{\eta} \cdot \sqrt{\cos^2 \alpha + \left(\frac{f_T}{f} \right)^2 \cdot \sin^2 \alpha} \qquad (4)$$

Analyzing the last formula, can be observed that the worst disconnected case occurs when the cutting angle has the value $\alpha = \pi / 2$, that means the cutting current reaches the maximum value of the inductive current and the maximum value of the amplitude factor is obtained:

$$\gamma = \sqrt{\eta} \cdot \frac{f_T}{f} \qquad (5)$$

The variations of the source voltage, inductive current and transient recovery voltage $u(t), i(t), u_2(t)$ are shown in Figure 2.
From formula (5) it is noted that maximum value of the overvoltage depends on the ratio between the frequency of the overvoltage oscillations from the disconnected circuit (2) and the industrial frequency oscillations. Theoretically, this ratio can reach higher values (4 or 5, even more).

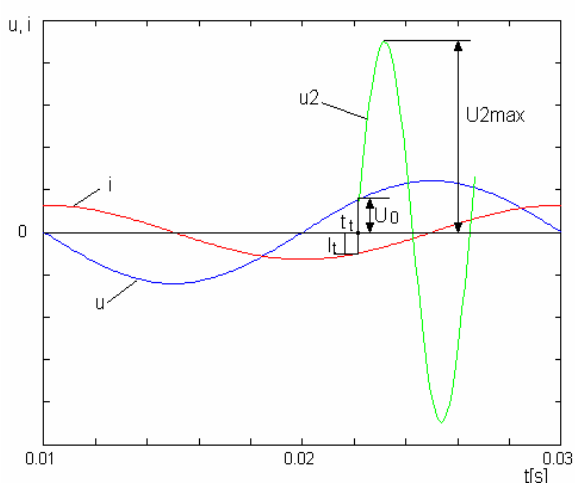

Figures 2: The variation of the $u(t), i(t), u_2(t)$

In reality, the phenomenon is influenced by the appearance of the arc reignition between contacts *a–b* of the circuit breaker. Taking into account the successive reignitions the variations of the $u(t), i(t), u_2(t)$ are shown in Figure 3.

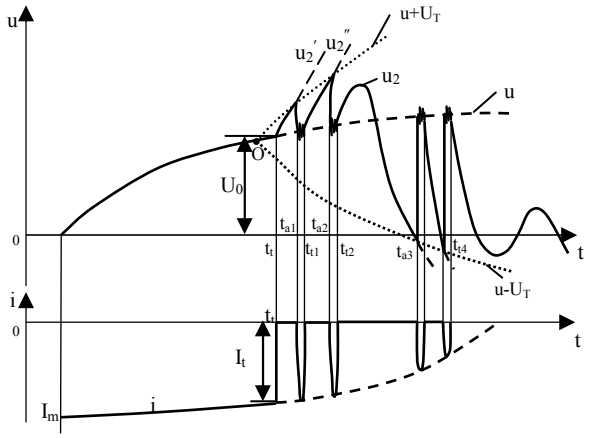

Figures 3: The variation in time of the *u(t)*, *i(t)* and $u_2(t)$ succesive reignitions

If the withstand voltage of the quenching medium of the circuit breaker is exceeded by the transient recovery voltage, then it happens that arc to reignite.
In the figure 3 are displayed the variation of the voltages and the current through the analyzed circuit, considering the successive reignitions of the arc between the contacts a-b of the circuit breakers.
The appearance of the successive reignitions leading to reduction of the transient recovery voltage.

THE COMPUTATION PROGRAM

The Matlab application has been developed in order to compute the electrical overvoltages which appear at the disconnection of the no load high voltage transformers from the high voltage electrical stations of the Oltenia district network, named ST North Craiova and ST

Urechesti. The parameters of the AT1 transformer from ST North Craiova are: rated power $S_n = 200MVA$, rated voltage $U_n = 220kV$, no load current $I_o = 3\%$, the capacity at the input terminals of the transformer $C_T = 10^{-9}F$. The parameters of the AT2 transformer from ST Urechesti are: rated power $S_n = 400MVA$, rated voltage $U_n = 400kV$, no load current $I_o = 19{,}6\%$, the capacity at the input terminals of the transformer $C_T = 10^{-9}F$. The program was developed in an interactive manner which allows the selection of the high voltage network (Brojboiu 2005). The main program runs routines that allow: the calculus of the parameters of the transient overvoltage for the selected transformer (the amplitude of the overvoltage, the amplitude factor and the frequency), the graphical analysis of the influence of cutting angle of the magnetization current on the transient overvoltage; graphical analysis of the influence of the source's power and voltage. The routines can run within the main program or independently. In Table 1 are presented the computed parameters applying the designed program, for electrical stations ST North Craiova and ST Urechesti.

Table 1 The Computed Parameters

Station	I_{omax} [A]	α [rad]	It [A]	U_{2max} [kV]	*k*
ST North Craiova AT1 Sn=200 MVA Un= 220 kV	22	π/6	11,5	320,70	1,58
		π/3	19	477,20	2,65
		π/2	22	498,50	2,77
ST Urechesti AT2 Sn=400 MVA Un= 400 kV	160	π/6	80	1061,7	3,25
		π/3	138	1738,8	5,32
		π/2	160	1911,5	5,82

The Matlab program has been applied to graphically observe the influence of cutting angle on the overvoltages values. By analyzing the computed data, was observed the increasing of the recovery transient overvoltage amplitude as well as the amplitude factor value, as the cutting angle of the inductive current increases. The graphical variations of the source voltage and the recovery transient voltage for the AT2 transformer from ST Urechesti, considering the different cutting angles of the inductive current are presented in Figure 4 ($\alpha = pi/6$) and Figure 5 ($\alpha = pi/2$).

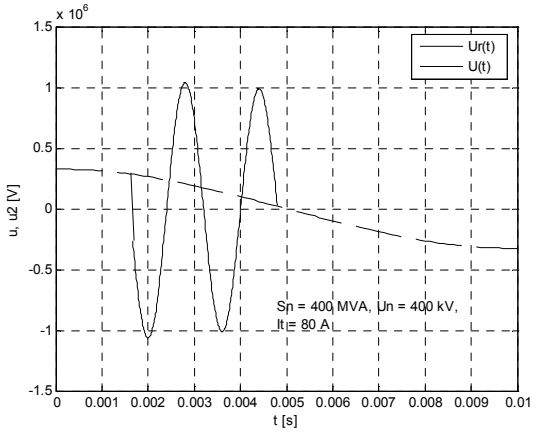

Figures 4: The recovery transient voltage variation $u_2(t)$ Sn=400MVA, Un=400kV, α=pi/6

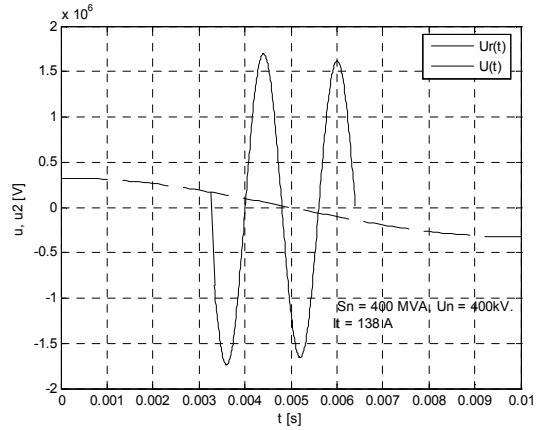

Figures 5: The recovery transient voltage variation $u_2(t)$ Sn=400MVA, Un=400kV, α=pi/3

From the mentioned figures can be noticed the increasing of the overvoltage amplitude value, as the cutting angle increases. The frequency of the overvoltage variation is constant f_T=*624Hz*, because the transformer parameters are constant, $C_T = 10^{-9}F$, $L_T = 6{,}49H$. The graphical variations of the source voltage and the recovery transient voltage for the AT1 transformer from ST North Craiova, considering the different cutting angles of the inductive current are presented in Figure 6 ($\alpha = pi/6$) and Figure 7 ($\alpha = pi/2$).

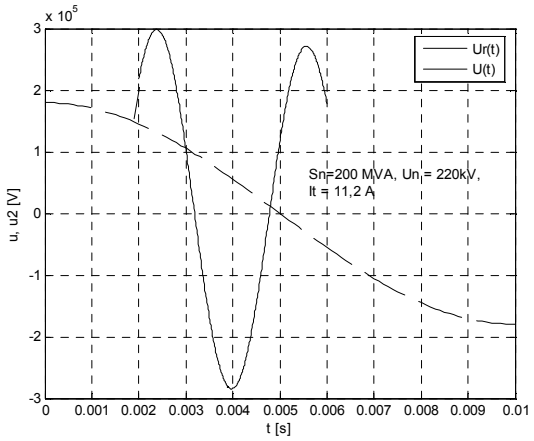

Figures 6: The recovery transient voltage variation Sn=200MVA, Un=220kV,α=pi/6

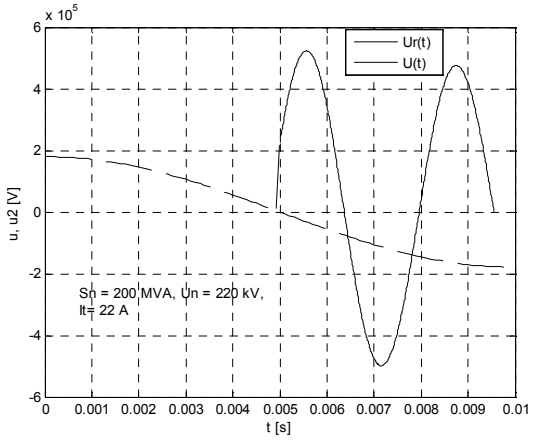

Figures 7: The recovery transient voltage variation Sn=200MVA, Un=220kV, α=pi/2

The frequency of the overvoltage oscillations is constant $f_T = 362Hz$, because the transformer parameters are constant, $C_T = 10^{-8} F$, $L_T = 25{,}7H$. Regarding the influence of the ratio $I_t / I_{o\max}$ on the amplitude factor for different values of the ratio, the graphical variations are shown in Figure 8.

As expected, the maximum values of the amplitude factor are obtained for the maximum value of the ratio, as result from (5) formula. In the same time, for the same value of the ratio, the amplitude factor increases as the cutting value of the inductive current increases; consequently, the cutting of the current at one value near the maximum value led to the higher value of the recovery transient overvoltage.

In the Figure 9, the variations of the amplitude factor depending on the cutting angle, as parameter are shown. From this figure, the same conclusion can be drown: the amplitude factor value increases as the cutting angle value increases for the same value of the ratio.

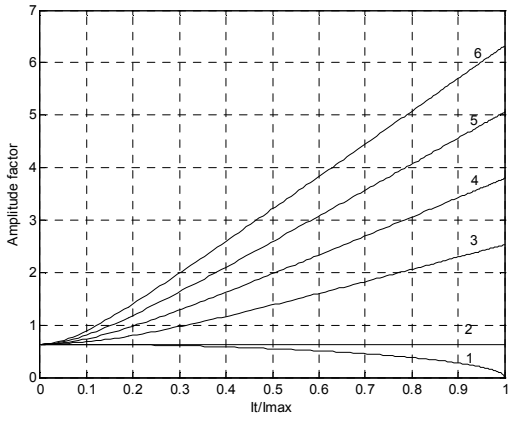

Figure 8 The variation of the amplitude factor vs $I_t / I_{o\max}$ ratio, ω_T / ω as parameter: 1 - $\omega_T / \omega = 0$, 2 - $\omega_T / \omega = 1$, 3 - $\omega_T / \omega = 4$, 4 - $\omega_T / \omega = 6$, 5- $\omega_T / \omega = 8$, 6 - $\omega_T / \omega = 10$

In the Figure 9, the variations of the amplitude factor depending on the cutting angle, as parameter are shown. From this figure, the same conclusion can be drown: the amplitude factor value increases as the cutting angle value increases for the same value of the ratio.

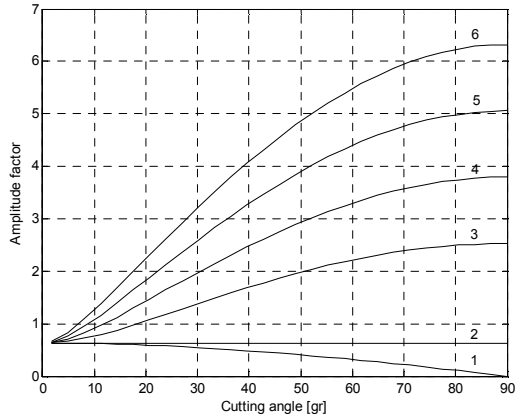

Figure 9 The variation of the amplitude factor vs cutting angle, ω_T / ω as parameter: 1 - $\omega_T / \omega = 0$, 2 - $\omega_T / \omega = 1$, 3 - $\omega_T / \omega = 4$, 4 - $\omega_T / \omega = 6$, 5- $\omega_T / \omega = 8$, 6 - $\omega_T / \omega = 10$

The maximum values of the recovery transient voltage have been computed without taking into account the limiting influence of the withstand voltage of the circuit breaker due to the speed of the recovery of the quenching dielectric medium rigidity (oil or SF_6). The diminishing of the overvoltage level can be also obtained by increasing of the input capacity of the transformer. The limiting of the dielectric stresses of the equipment can be done through the proper selection of the surge arresters parameters.

CONCLUSIONS

The Matlab computation program presented in this paper allows the evaluation of the maximum values of the recovery transient voltages appearing at the no-load high voltage transformer disconnecting. The influence of the cutting angle values of the inductive current on the overvoltage amplitude as well as the influence of the ratio ω_T / ω has been also studied. The program has been applied for the case of the high voltage transformers from ST North Craiova and ST Urechesti, for which the rated parameters are known. The computed level of the overvoltages can be compared with the withstand performances of the switching equipments within the stations. The analysis [Brojboiu, M., 2005] emphases the correctness of the chosen equipments of the station.

REFERENCES

Dragan, G. et all, 1975. *Switching surges in power systems*. Technical Ed., Bucureşti.

Gusa, M., 2002, *The transient regime of the network,* Gheorghe Asachi Ed, Iasi

Brojboiu, M., 2005. "*The computation of the electrical stresses in the high voltage network from the ST Craiova*". Research Report nr.35./2005, Beneficiary – Transelectrica SA Craiova.

Brojboiu, M.; Ivanov, V.; Leoveanu, M.S., 2005. "*Computation program for short-circuit current from Craiova substation*", Buletinul Institutului Politehnic Iaşi Tom 1 (LIV), Fasc. 5, Seria Electrotehnică, Energetică, Electronică.

AUTHOR BIOGRAPHIES

MARIA D. BROJBOIU was born in 1952 in the town Pucioasa Romania. She is currently working as Professor at the University of Craiova, Electrical Engineering Faculty, Department of Electrical Engineering since 1981. Before that, she worked as desing engineer at the Electroputere holding the Research and Development Center . She is Doctor in Science Technique – Electrical Engineering.

.

VIRGINIA IVANOV was born in Vela, Dolj, Romania, 1963. She was graduated in Electrical Engineering at University of Craiova, Romania, in 1986 and Doctor in Electrical Engineering in 2004. From 1986 to 1998 she worked as researcher with the Researching Institute for Motors, Transformers and Electric Equipment Craiova. In 1998 she joined the Faculty for Electrical Engineering, Department of Electrical Engineering

.

Simulation, Experimental Science and Engineering

EXPLORING ARTIFICIAL VISION FOR USE IN DEMANDING SHIP OPERATIONS

Webjørn Rekdalsbakken
Ottar L. Osen
Department of Information and Communication Technology
Aalesund University College
N-6025 Aalesund, Norway
E-mail: wr@hials.no

KEYWORDS

Augmented reality, inertial sensor technology, remote sensing.

ABSTRACT

Aalesund University College (AAUC) is situated in an area of industry companies developing the most advanced equipment and procedures for safe ship operations. AAUC has established a close cooperation with these private technology developers for the purpose of joint research and testing in this field. This work deals with the design of tomorrow's ship bridges. In the light of the bridge officer's situation of continuously growing information influence it has become mandatory to develop a new bridge concept in order to maintain and improve safety and efficiency in ship operations. The focus has been to explore the possibilities of modern vision technology in combination with dedicated systems for information extraction from large quantities of data. An important concept in this setting will be artificial sight and augmented reality. So far some interesting sensor and vision concepts have been tested and the results have shown to be promising. This research activity is supported by funding from the Norwegian Research Council (NFR).

INTRODUCTION

Aalesund University College (AAUC) has over a period of several years gained a broad and deep expertise in the design and building of nautical simulators and has in daily operation a number of full scale simulators. This development has taken place in close cooperation with Rolls Royce Marine Dept. AS (RRMD) and Offshore Simulation Centre AS (OSC), and the simulators are being continually upgraded and further developed. In addition to traditional nautical simulators, the collection includes full scale simulators for High Speed Craft (HSC), Dynamic Positioning (DP), anchor handling and winch operations, see (Rekdalsbakken 2005), (Kjerstad 2006), (Rekdalsbakken 2006) and (Rekdalsbakken and Styve 2008). The purpose of this simulator activity is to provide the most realistic operator training environment possible within state-of-the-art technology. Based on this knowledge research programs of mutual interest to industry and academia are taking place to develop the next generation of ship bridges. The prime concern of this research activity is security. The immense amount of information that the bridge officer is exposed to in stressed situations may pose a threat to safe ship operation. The central part of this research is to identify, extract and present the most adequate information to the ship officer at any time. This is a complex problem, but the focus in this work is limited to the use of the latest and most appropriate sensor technology and efficient extraction of relevant information from the large amount of data acquired in these situations. Part of this research is directed into the students' Bachelor and Master thesis, supervised by the professors involved in the respective research activities. The most prospective of these projects are followed up by the research staff and further developed. A most relevant topic in this setting is the utilization of sensor technology in combination with smart software that will enable extraction and presentation of crucial information to the ship officer. The working situation of the bridge officer is a context of monitors, lights, handles and joysticks, representing a severe amount of impressions. In this demanding setting the ship officer is expected to make the right decisions in the operation of the ship. In this context the concept of an augmented reality will come into particular interest. How should the officer perceive his world of extreme information load? How and when shall important messages manifest themselves to secure safe and economic ship operations? This is the superior aim of the research. On the way towards the target some topics of central interest have been chosen and investigated in cooperation between students and research staff. The effect of this initiative has been to provide realistic and motivating problem settings for the students, and challenging tasks of practical research to the scientist. Most of the projects have been realized through the design and building of small scale models, among which autonomous and remotely controlled model vehicles have become important tools for experiments and testing. This paper represents a survey of this broad activity, where three of these projects have been selected and elaborated. The projects represent a normative selection of the ideas and technologies which guide this research at the moment and concern the

Proceedings 26th European Conference on Modelling and Simulation ©ECMS Klaus G. Troitzsch, Michael Möhring, Ulf Lotzmann (Editors)
ISBN: 978-0-9564944-4-3 / ISBN: 978-0-9564944-5-0 (CD)

following topics; “Remote camera control by head movements” (Fjørtoft 2010), “Autonomous object tracking by a mobile camera” (Håheim 2010) and “Real time object recognition system for offshore operations” (XU 2011). In these projects modern sensor and vision technology and wireless communication systems are integrated into useful devices for search and tracking of selected objects. The idea is to make it possible to see and identify objects in areas otherwise hidden to the operator. Among the promising sensor technologies that have been explored here, is the advances in inertial measurements and gyro sensing devices (Håheim 2010). Vision devices like video glasses have also been examined. The experience gained from these projects represents a basis for further development of vision systems for surveillance of operations onboard and around a ship, especially in inaccessible areas and under high-risk conditions. A summary of the arrangements and results of each of these projects is presented in the next sections.

REMOTE CAMERA CONTROL BY HEAD MOVEMENTS

This project represents an experimental test of using video glasses in the field of visual surveillance and inspection. The video glasses were equipped with a tilt-compensated compass circuit, which includes a three-axis magneto resistive gyro and a three-axis accelerometer. With this equipment readings of the head’s pitch and yaw angles will be available at the appropriate time resolution to control the direction of sight of a remote camera in real time according to the movements of the head. In this way the field of view of the eyes will be extended through the lens of the camera. To the bridge officer the visual expression is very important in many operations, and the acquired information must be in synchronism with the actual operation in real time. Augmenting the officer’s sight through such glasses connected to cameras in strategic positions onboard the ship may be an important tool in improving his survey of all kinds of operations on deck and towards the surroundings of the ship. This kind of technology may also be extended by exploring new ways of projection of the visual information, for instance on the windows of the bridge.

Equipment and Connections

The system consists of two independent parts. The first part comprises a remotely controlled vehicle equipped with an Arduino Duemilanove microcontroller board (Arduino 2011), featuring an ATmega328 microcontroller from Atmel, and a motion stabilized platform with a Panasonic BL-C20 web camera. The second part is a control station with a PC and two Arduino Duemilanove (ATmega328) microcontroller boards. The microcontroller boards are furnished with appropriate Arduino shields to perform the necessary I/O functions. The interface shields are connected to the microcontroller boards through the general serial bus “Serial Peripheral Interface” (SPI) defined by Motorola (intersil 2007). The control station layout is shown in Figure 1. The PC receives the video signals from the remote camera over a local Wi-Fi network and processes each picture in the video stream. This communication is established by furnishing one of the Arduino microcontroller boards at the control station with an Arduino Ethernet shield that enables connection to a wired Ethernet. The connection to the local Wi-Fi network is obtained through a Nano WiiReach (ConnectOne 2011) wireless LAN bridge using the 802.11b/g standard. All of the communication to the remote vehicle takes place on this local Wi-Fi network. This microcontroller is also connected to an analog joystick and a tilt compensated compass device of the type HMC6343 (Honeywell 2011). This MEMS chip is mounted on the video glasses and uses a combination of gyro and accelerometer to monitor the pitch and yaw angles of the head. It is connected to the microcontroller by use of the serial Inter-Integrated Circuit bus (I^2C) (Philips 2007). The microcontroller uses the readings of the head angles from the compass device to position the onboard camera, and the joystick is used to manually control the remote operation of the vehicle. The second Arduino microcontroller board at the control station is used to control an On Screen Display (OSD) chip of the type Max7456 from Maxim (Maxim 2008). The OSD is connected to the microcontroller by use of the SPI bus, and is programmed by use of an own library for MAX7456 developed by Arduino. It takes as input the video signal from the PC and writes a text to selected images before forwarding the video stream to the video glasses. It is the ATmega328 on the basis of the input information that selects which pictures in the video stream to be written to, and chooses the position to write the informative text. In this way messages of importance to the operator may be projected to the visual field of the video glasses. The vehicle is also controlled by an Arduino Duemilanove microcontroller board (ATmega328). This board is connected to an Ethernet access point through an Ethernet shield. The onboard web camera is mounted on the motion stabilized platform and is connected to the access point by cable. It is configured to transmit its images over the Wi-Fi network independent of the microcontroller communication. The steering and speed of the vehicle are both controlled with PWM signals by a LM-406FB motor controller unit, commonly used in the hobby market. The camera angles are controlled by use of a Pololu servo controller (Pololu 2011) which is set up to control two DC servo motors. The ATmega328 communicates with the Pololu controller over a serial line. The Pololu is configured by sending it a string of 5 or 6 bytes. In this case the Pololu is programmed to control both speed and position of the servo motors by use of PWM signals. The connection diagram for the vehicle is shown in Figure 2.

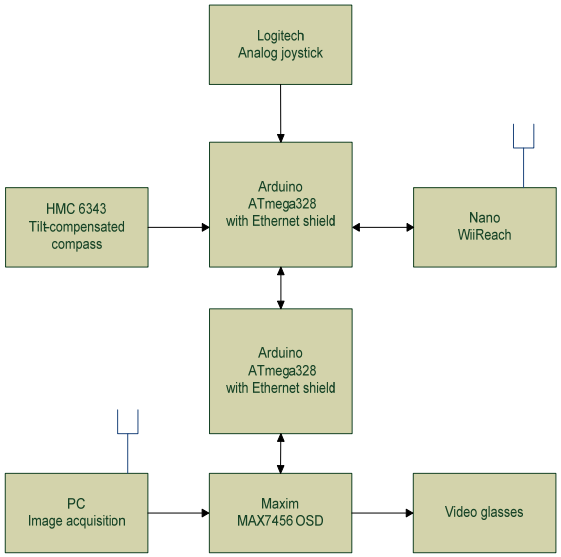

Figure 1: Control Station Diagram

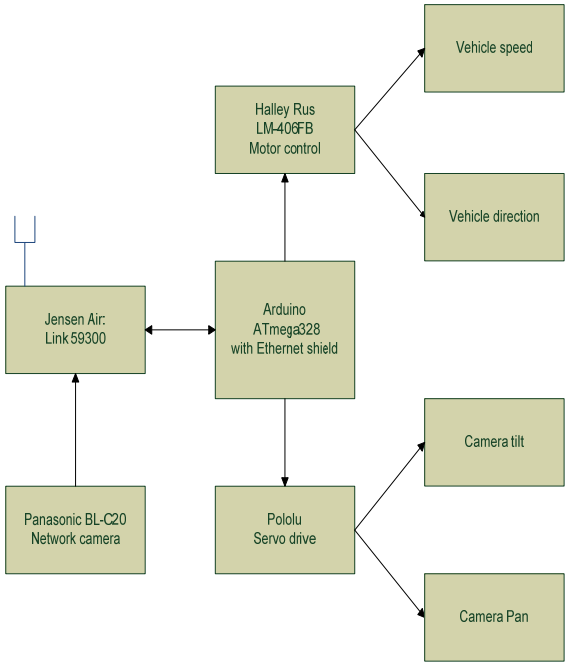

Figure 2: Vehicle Connection Diagram

Software and Communication

The application programs for the ATmega328 microcontrollers were developed in C++ by use of the Arduino IDE. The Arduino API is delivered with several libraries for controlling the different I/O ports, including the SPI bus, the I^2C bus and Ethernet communication. The wireless Ethernet communication is set up as a client/server connection with a simple telegram protocol described below. The vehicle is configured as the server, and both the PC and the ATmega328 at the control station are configured as clients. Permanent MAC and IP addresses are defined for both server and clients and the server listens to a predefined port number. This instantiation of the Ethernet communication is performed by use of the Ethernet Library from Arduino. To transmit the values of the control variables to the vehicle a simple telegram including 16 bytes of information was designed. The variables are heading and speed of the vehicle and pan and tilt of the camera. The video camera uses the compress method M-JPEG. This method compresses each picture in JPEG format before assembling them into a video film. This gives very good picture quality at low transfer rates. The speed is 15 images per second at the resolution 320x240 pixels. On the PC the video stream is received and presented by the program Active Webcam (Py software 2011). This is a very versatile program package for distribution of images from all kinds of video units. The program can be run with a full screen secondary monitor, which is used here to forward the pictures to the video glasses.

Programs for the Arduino Microcontrollers

The program applications for the control station and remote vehicle are quite extensive. The most important parts are the following procedures:

Managing the Ethernet communication

The Ethernet communication is based on the Ethernet library from Arduino. This library includes a data buffer that holds all the characters received from the net. To avoid corruption of data a telegram of a total of 20 bytes was designed to hold information and a simple synchronization protocol was implemented. When a complete telegram is received, it is immediately transferred to another buffer for processing. The telegram starts with the symbol "<" and ends with the symbol ">", and the variables of the telegram are separated by commas. The variables are extracted and converted from ASCII to integer representation and stored in their respective memory locations. When one complete telegram is processed, the variables are used to update the positions of the four servo motors of the vehicle. At last a message is returned to the client to inform that the server is ready to receive a new message.

I^2C communication with the compass unit and data extraction

The communication on the I^2C bus is performed by use of the Wire library from Arduino. This library contains all the routines necessary to establish the communication and transfer the data. The default slave address for the compass unit on the I^2C bus is 0x32. The procedure is to send a command asking for the values of the head's roll and pitch angles. After a delay of 1 msec. the values will be ready on the bus as three pairs of

bytes. Each pair of bytes is converted to a 16 bits integer. The head angles are referred to the north compass direction and will change from 0° to 360° at this point. The result of this is that the servo motors will be turned the wrong way. Therefore, when passing the north direction the angles have to be further processed by a routine that decides the correct direction of the servo drives.

SPI communication between Arduino and OSD

The On Screen Display hardware is implemented by the chip MAX7456 on an Arduino shield using the SPI bus. There has been developed a special software library for this chip by members of the Arduino forum. This library makes it straightforward to send a string of information to a given position at the image, and also to clear the information.

Instantiation and communication with the Pololu servo controller

With the demands set in this project for quick and smooth camera positioning the servo controller has to be configured for Pololu mode, which enables the servo to control both speed and position of the motors. Commands are sent to the servo controller as telegrams of 5 or 6 bytes over a serial line using the standard Arduino library.

AUTONOMOUS OBJECT TRACKING BY A REMOTE CAMERA

Among the many different activities in the operation of a ship, surveillance by use of lights and cameras are of crucial significance in many situations. Both in rescue operations and in the handling of cargo and equipment from the ship there is often a need for fast object recognition and following. The search equipment has to be mounted on motion platforms for compensation of the ship movements, and search algorithms have to be developed for accurate and precise detection of the object position. This type of operation depends on the interaction of a selection of quite complex hardware and software, and the close cooperation of several parallel activities. This is a field of growing importance and thus also an important research area.

Equipment and Assembly

In this experiment the search operation is realized by the building of a small scale autonomous model vehicle equipped with a web camera on a stabilized motion platform. Figure 3 shows a picture of the vehicle. Onboard are two independent control systems, one for the motion of the camera by the platform for the purpose of finding the object; the other for the control of the car to follow the object. Both control systems are run on a local Phidget microcontroller board (Phidgets 2011) programmed in Java. The purpose of the vehicle is to find and track a red ball moving on the ground. The tests were performed mainly inside the laboratory building on floors of fairly uniformly colored surfaces, but also on an outdoor parking area with rougher ground and a more diversely colored surface. Because of the substantial computational load of the image analysis the video stream from the camera was transferred as a sequence of still images over a Wi-Fi connection to a stationary PC. The PC performs the image analysis and recognizes the object. When the position of the ball is defined, its location relative to the vehicle is calculated, i. e. the distance and angle of direction. These variables are sent to the Phidget controller on the vehicle, where they are used to calculate the reference signals to control the vehicle and the camera. Altogether four control signals are determined, the speed and steering of the vehicle in addition to the yaw and pitch position of the platform holding the camera.

Hardware

The hardware is built around the Phidget SBC 1070 microcontroller development board. This is a very powerful and versatile controller including four general USB ports to connect a number of auxiliary components. On the vehicle these ports are used for a Logitech QuickCam Pro 5000 web camera and the LPR530AL 6DOF Razor inertial measurement unit (IMU) (STMicroelectronics 2009). The IMU includes a three-axis accelerometer chip ADXL335 from Analog Devices, a dual-axis gyroscope chip LY530AL (STMicroelectronics 2011a) and a single axis chip LY530ALH (ST Microelectronics 2011b). Included on the SBC 1070 board are also a Wi-Fi connection and the Phidget Advanced Servo Kit for controlling the four servo motors. All hardware was built into a solid cage to withstand rough treatment.

Stabilized Platform

The camera is mounted on a 2D stabilized motion platform, see Figure 4. The control of the motion platform has a twofold objective, to move the camera according to the reference positions given by the search algorithm, while synchronously keeping the platform compensated from the influence of the vehicle's roll and pitch angles caused by motion on an uneven ground. This last aspect is taken care of by use of the inputs from the Inertial Measurement Unit (IMU). The IMU combines the readings from accelerometers and gyroscopes to obtain precise measurements of angles. In this procedure a Kalman filter (Balchen and Mummé 1988) was used to extract the optimum information from the measurements. Depending on the noise in the accelerometer readings the Kalman filter will decide the weights put on the gyroscope measurements. In this way the camera motion pattern will be controlled independently of the random movements of the vehicle.

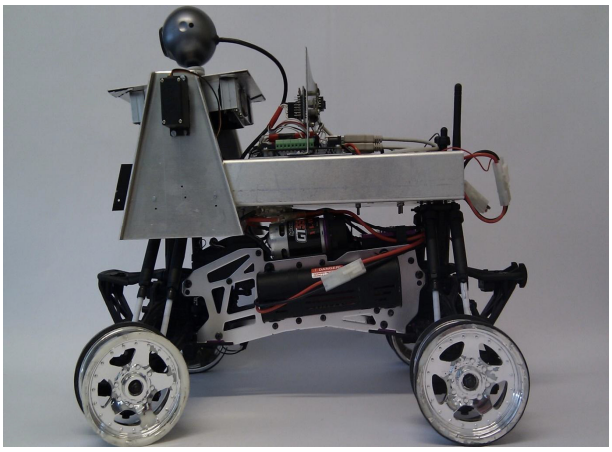

Figure 3: Autonomous Path Tracking Vehicle

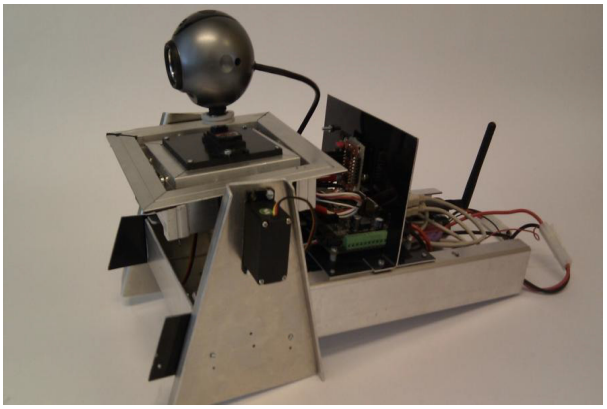

Figure 4: Stabilized Camera Platform

Image Analysis

Because of heavy computational load it was decided to perform the image analysis on a PC. The pictures are received from the web camera in real time and treated as single still images. For the analysis the Java Advanced Imaging (JAI) (Java.net 2011) package was used. Several basic algorithms were used in the search for the given object. First a threshold level was found to distinguish the ball from the background, and the image was transformed into a binary representation. Then morphology, in form of growing and erosion, was used to shape the images and remove structural elements smaller than a given limit. After these operations a labeling algorithm was used to identify the separate objects. Now the resulting image representation is ready for the identification of the ball. This was performed by a function finding the most circular object. The area and a representative radius of the object are used to estimate the value of π from the formula $\pi_e = A/r^2$. Then the objects in the image are tested for maximum roundness by the function:

$$e = \sqrt{\left(1 - \left(\frac{\pi}{\pi_e}\right)^2\right)^2} \qquad (1)$$

Once the roundest object in the image is found, the ball is supposed to have been localized and the coordinates of its center within the image is calculated.

Software

Java is used as the programming language for the software implementation of this project, and NetBeans has been used as the development environment. In addition to standard Java some auxiliary program libraries have been implemented. The most important ones are the Java Advanced Imaging library for use in the image analysis on the PC, and the proprietary Phidget library for implementation on the Phidget controller. This last library includes object classes with software drivers for all hardware ports on the Phidget SBC, including the classes for acquisition of images from the web camera and control of the Wi-Fi connection. The Phidget SBC is set up as a server and the PC as the client. A ServerSocket object on the Phidget listens to a network port with the method *serversocket.accept* until it gets contact with the PC, which returns its IP address and port number for the connection. The necessary streams for communication are then established on both server and client.

REAL TIME OBJECT RECOGNITION SYSTEM FOR OFFSHORE OPERATIONS

This is a research project to develop a vision system for real-time observation and presentation of human activities on a ship deck. The system aims to detect, recognize and follow objects entering the deck scene. The purpose is to help the bridge officer to command and schedule the working process on deck in a safe and efficient manner. The project uses methods and principles described in the above sections to simulate a realistic working environment on a ship deck. In demanding and potentially dangerous ship operations, like anchor handling, it is crucial that the leading officer is able to watch the whole operational scene. This may in some cases be difficult, even impossible by one person. In this work an arrangement of four cameras is used to cover the overall operation. A suitable graphical user interface (GUI) with well arranged camera fields and icons makes it easy for the officer to view any part of the scene from different directions. There are also substantial software applications to detect and recognize objects, and to track the movements of objects on the scene. By this arrangement the bridge officer will be able to follow all activities during the deck operation. A small scale test rig was built in accordance with the dimensions and layout of the deck scene. With this model it was possible to simulate deck operations with different kinds of objects on the deck. In this way the camera equipment and software applications could be tested, and image processing algorithms could be explored. See Figures 5 and 6 below.

Equipment and Software

The camera system consists of four USB cameras connected to a central computer through an USB hub. The cameras, of the model Logitech Webcam C270, are located at each corner of the deck so that they can survey the entire deck area. By use of the GUI the officer can choose which of the cameras to be active at any time, each camera view being presented on a separate screen window. He can also select one camera to cover the whole screen for closer inspection and image analysis. The application programs are developed in C++ by use of Microsoft Visual Studio 2008. The graphical user interface is developed by use of the Qt UI framework (Nokia 2011), implemented as the Qt - Visual Studio Integration. The image acquisition and analysis is performed with OpenCV (Open Source Computer Vision Library) (Willow Garage 2011), including the Intel IPP (Intel Integrated Performance Primitives) (Intel 2011). Object recognition and tracking is the central part of this project, so much effort has been laid down in developing effective algorithms for this part of the application. The OpenCV library contains all the basic algorithms for image analysis, and these are explored and combined to give secure methods for recognition and tracking of objects on deck.

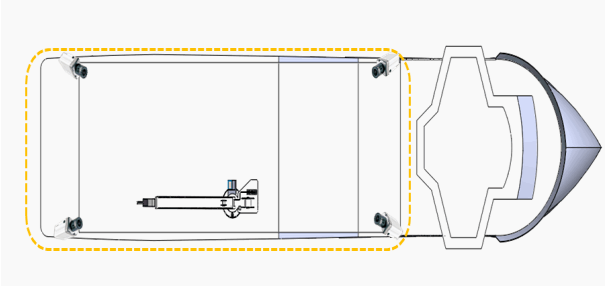

Figure 5: Camera Configuration on Deck

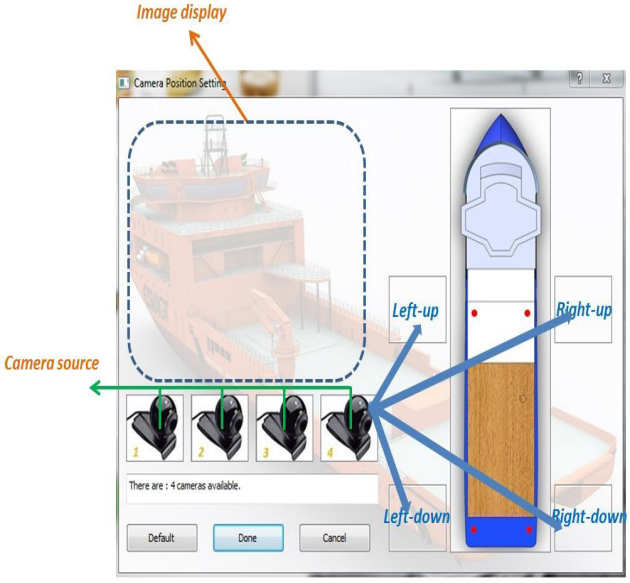

Figure 6: Graphical User Interface

Digital Image Processing

The video cameras record images at a rate of 20 images per second and save them to a disk as individual AVI files. The resolution is 320x240 pixels with the option of 640x480 when using only one camera. The saved images from simulations are used for later testing and experimenting with different kinds of image processing algorithms. Object recognition is done by the following procedure. First the image is converted to a grey scale and the static background is subtracted from the image. Then a dilation filter is used to reduce noise, and a threshold function is used to transform the image to black and white. After this an edge function is used to find the contours of objects in the image. Objects smaller than a given size, are removed as noise and the rest of the objects are bounded by minimum rectangles. The positions of these objects relative to the deck coordinates may now be accurately calculated based on corresponding images from multiple cameras. The objects and positions are saved to disk. A database of objects is maintained for later comparison and identification of new objects. To track objects they have to be compared from image to image. This is done by comparing the contours of the objects by the use of moments and histograms. In the OpenCV software there are three different algorithms for comparing contours by moments. However, this method gives only an approximate result working only for objects of quite different shapes. This is because the objects change with camera facing and lighting. The histogram matching is performed both on the grey scale images and on the corresponding color images. The algorithms used for histogram comparison are Correlation, Chiaquare, Intersection and Bhattacharyya. By using an EMD matching on the results of these three methods, a distance measure from the exact model is found, and a good match may be verified.

DISCUSSION

The primary goal of this work has been to investigate new trends in sensor and vision systems for possible integration of such technologies into the future ship bridge. As the operations on modern ships become increasingly more complex and demanding there is a need for exploring new sides of human machine interaction. Here the focus has been on the rich market of consumer electronics driven mainly by the cell phone and game industry, resulting in the development of advanced and low-cost sensor and vision technology. Experiments with selected equipment of this type have been performed on small scale physical models, mainly by building remotely controlled and autonomously operating ground vehicles. However, the aim is to find new technologies to be adapted into the context of the future ship bridge, and the vehicles represent an easy approach to testing equipment and methods in an adequate way for ship operations. The results of these

tests are documented through the fact that the different devices function well in the designed context, and that the vehicles perform their tasks in accordance with the plans. This is like an interactive trial and error process where components and methods are systematically selected and tested in practical experiments.

CONCLUSION

The underlying aim of this work has been to investigate some new products in the consumer technology market for possible future employment of such technologies in ship operations. This activity of practical testing of vision and sensor systems on small scale models has shown to represent a fertile way to reveal the potential for adapting this technology into the ship bridge. The surplus of new devices within wireless communication, vision systems and MEMS components available in the consumer market, driven by the cell phone and game industry, represent fantastic new possibilities in the integration an adaptation of advanced technology into more traditional fields, both in the production process and in the products. The experiments performed in this work have revealed that it may be highly beneficial to keep an eye on this market, and they encourage further work towards implementation and use of such technologies in real ship operations. In the testing of these devices and concepts the approach of building small scale models as test equipment has shown to be very efficient.

ACKNOWLEDGMENT

We would like to express our grateful thanks to our hard working and clever students participating in these projects.

REFERENCES

Arduino. 2011. Arduino Duemilanove microcontroller board Retrieved 2011-05-05, from http://arduino.cc/en/Main/ArduinoBoardDuemilanove

Balchen, J. G, Mummé, K. I. 1988. Process control : structures and applications. New York: Van Nostrand Reinhold.

ConnectOne. 2011. Nano WiReach Retrieved 2011-05-05, from http://www.connectone.com/products.asp?did=73&pid=80

Fjørtoft, V, Lund M. 2010. Kamerakontroll for mobil søkerobot. B.Sc. thesis, Aalesund University College, Aalesund.

Honeywell. 2011. HMC6343, from http://www51.honeywell.com/aero/common/documents/myaerospacecatalog-documents/Missiles-Munitions/HMC6343.pdf

Håheim Ø, Saure T, Siqveland M. 2010. Nettverkstyrt modellbil med stabilisert kamera. B.Sc. thesis, Aalesund University College, Aalesund.

Intel. 2011. IPP – Integrated Performance Primitives. Retrieved 2011-05-05, from http://software.intel.com/en-us/articles/intel-ipp/

Intersil. 2007. SPI (Serial to Peripheral Interface) bus Retrieved 2011-05-05, from http://www.intersil.com/data/an/an1340.pdf

Java.net. 2011. Java Advanced Imaging (JAI). Retrieved 2011-05-05, from http://java.net/projects/jai/

Kjerstad, N, Rekdalsbakken, W. 2006. "Low Cost Three Degrees of Freedom Motion Platform for High-Speed Craft Simulator." Proceedings of Marsim 2006.

Maxim. 2008. MAX7456 on Screen Display Chip. Retrieved 2011-05-05, from http://datasheets.maxim-ic.com/en/ds/MAX7456.pdf

Nokia. 2011. Qt – Cross-platform application and UI framework. Retrieved 2011-05-05, from http://qt.nokia.com/

Phidget. 2011. Phidget SBC. Retrieved 2011-05-05, from http://www.phidgets.com/products.php?category=21

Philips. 2011. I2C-bus specification. Retrieved 2011-05-05, from http://www.nxp.com/documents/user_manual/UM10204.pdf

Pololu. 2011. Pololu Servo Controller. Retrieved 2011-05-05, from http://www.pololu.com/catalog/product/207

Py Software. 2011. Active Web Cam. Retrieved 2011-05-05, from http://www.pysoft.com/ActiveWebCamMainpage.htm

Rekdalsbakken, W. 2005. "Design and Application of a Motion Platform in Three Degrees of Freedom." In Proceedings of SIMS 2005, the 46th Conference on Simulation and Modelling, pp 269-279, Tapir Academic Press, NO-7005 TRONDHEIM.

Rekdalsbakken, W. 2006. "Design and Application of a Motion Platform for a High-Speed Craft Simulator." In Proceedings of ICM 2006, IEEE 3rd International Conference on Mechatronics, pp. 38-43, IEEE Catalog Number of Printed Proceedings: 06EX1432.

Rekdalsbakken, W, Styve A. 2008. "Simulation of intelligent ship autopilots" Proceedings of ECMS 2008, the 22th European Conference on Modelling and Simulation. European Council for Modelling and Simulation, printed ISBN: 978-0-9553018-5-8, CD ISBN: 978-0-9553018-5-5.

STMicroelectronics. 2009. IMU LPR530AL 6DOF Razor. Retrieved 2011-05-05 from http://www.sparkfun.com/datasheets/Sensors/IMU/lpr530al.pdf

STMicroelectronics. 2011a. LY530AL - MEMS motion sensor Dual Axis Gyroscope. Retrieved 2011-05-05, from http://www.st.com/internet/com/TECHNICAL_RESOURCES/TECHNICAL_LITERATURE/DATASHEET/CD00208931.pdf

STMicroelectronics. 2011b. LY530ALH - MEMS motion sensor Single Axis Gyroscope. Retrieved 2011-05-05, from http://www.st.com/internet/com/TECHNICAL_RESOURCES/TECHNICAL_LITERATURE/DATASHEET/CD00237186.pdf

Xu, Q. 2011. Real Time Object Recognition System for Offshore operations. MSc. Thesis, Aalesund University College, Aalesund.

SOME MECHANICAL CHARACTERISTICS OF MATERIALS FOR DENTAL PROSTHETICS

Diana Cotoros, Anca Stanciu and Mihaela Baritz
Department of Product Design, Mechatronics and Environment
Transilvania University of Brasov
500036, Brasov, Romania
E-mail: dcotoros@unitbv.ro, ancastanciu77@yahoo.com, mbaritz@unitbv.ro

KEYWORDS
Molar modelling, finite element method, mechanical characteristics.

ABSTRACT

The paper presents some researches concerning the mechanical properties of composite materials used for prosthetic dental elements. After a short introduction concerning the general strains and loads that usually apply upon prosthetic works, the authors present the virtual model of a molar tooth subjected to the most common actions, using finite element method. Then the results are further shown by means of experimental methods and finally the conclusion concerning the possible use of fibre reinforced composite materials are presented.

INTRODUCTION

One of the most pressing issues concerning dental health is related to the use of materials for prosthetics and implant jobs. These materials should be suitable not only from the biocompatibility point of view but also their mechanical properties should be at least similar to those of the natural dentition, let alone the fact that we still need to meet the aesthetics requirements.
Prosthetic works either mobile or constructed upon an implant structure should be able to resist to all kind of loads and strains of various types, starting with mechanical actions, chemical attacks or temperature variation.
Usually the materials are included in the metal-acrylate or metal-ceramics family, each with corresponding benefits and risks. Roughly, we may say that metal-ceramics (with porcelain antagonists) are mostly preferred today due to their structure rigidity while acrylic works present the advantage of a better shock damping, but they are not resistant enough.
Another serious candidate seem to be fibre reinforced composite materials, including different types of fabric, like weft or warp fabric, each offering additional properties.
Of course, prosthetic works should be covered generally with porcelain or noble metals crowning and require extended preparations. These covers will protect at a certain extent the surface from chemical agents and moderate temperature variations, even from some types of mechanical actions. But still there is an obvious necessity that the prosthetic structure resists to the real mechanical strains involved in the everyday mastication process and also to some imperfections due to the lack of symmetry in antagonist teeth during occlusion.
The investigations done upon the occlusion forces clearly showed that the average bite force of a patient may reach 665N in molars and up to 220N in incisive teeth. Generally the bite force of women is a little smaller than the one applied by males.

FINITE ELEMENT METHOD APPLIED FOR A MOLAR MODELLING

Generally, the finite element method is the most suitable to predict the analysis parameters and the tendencies of the analyzed item.
There are several information to consider in order to determine the stress and deformations by help of finite elements method, like:
- number of nodes and discretization elements
- a numbering system required to identify every node and element
- elasticity modulus E and Poisson's coefficient for the materials associated to each element
- coordinates of every node
- type of constraints and boundary conditions
- values of forces applied in external nodes

The first step is simulating the 3D model of the molar using a virtual representation software, like CATIA V5 and the results were imported in the finite element software ABAQUS.
But still we needed to consider the fact that not always the teeth are symmetrically located, therefore during dental occlusion the compression force is very likely to act in an eccentric position, overloading only a certain part of the tooth. So the interaction between antagonist teeth might look like in fig.1.

Figure 1 Antagonist Teeth Interaction

Proceedings 26th European Conference on Modelling and Simulation ©ECMS Klaus G. Troitzsch, Michael Möhring, Ulf Lotzmann (Editors)
ISBN: 978-0-9564944-4-3 / ISBN: 978-0-9564944-5-0 (CD)

This is why it was necessary to consider two types of loads upon the composite material molar model: centric compression and eccentric compression using forces compatible to the normal human bite force.
If the load is applied at the center of the molar, which is an ideal situation, corresponding to a perfect symmetry of the anagonist teeth during occlusion, the values and distribution of the principal stress is shown in figure 2.

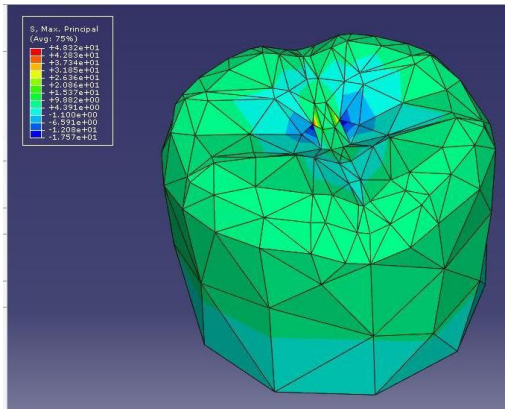

Figure 2: Principal Stress Distribution for a Centric Compression

For the second situation, which is also more encountered due to the imperfections in the occlusion of antagonist teeth, the principal stress distribution is presented in figure 3.

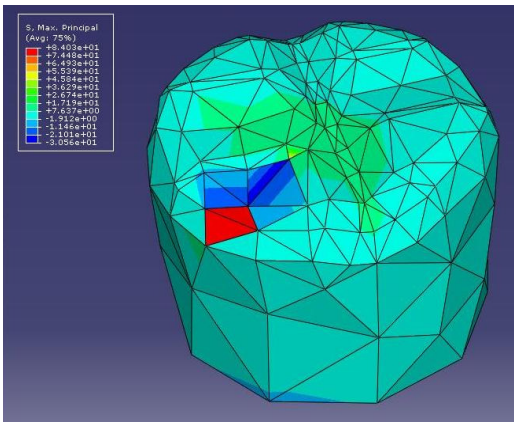

Figure 3: Principal Stress Distribution for an Eccentric Compression

The performed analytical study gives clues upon the stress distribution and values, deformations values in dental structures subjected to a known load and allows the choice of the optimum material and geometrical shape of the dental prosthetic works, according to real requirements.
Thus, the representation of the two types of strains clearly shows that the centric compression is uniformly distributed upon the tooth surface, leading to an almost uniform stress distribution, while the second type of strain, leads to a dangerous increase of the stress in the force action area, though the rest of the tooth remains in a comfortable strain zone.

For comparison we also performed models for other type of materials, usually used in dental prosthetics in order to estimate the opportunity of using composite materials, from mechanical point of view. The figure 4 presents the results obtained for an acrylate tooth subjected to an eccentric compression, which is obviously more likely to produce stress.

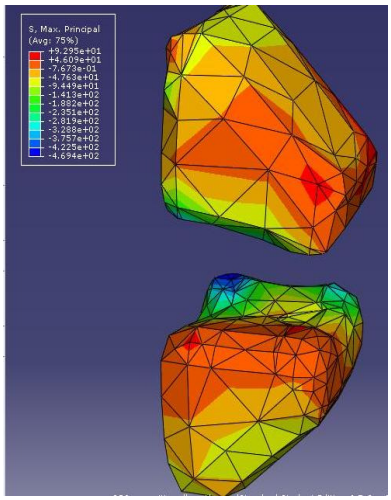

Figure 4: Principal Stress Distribution for an Acrylate Tooth Subjected to Eccentric Compression

The representations above confirm again that the stress is much higher in the area where the eccentric forces are acting and also the fact that the stress is considerably smaller and more uniform in the models designed of fibre reinforced composite materials.
We also were able to obtain the diagrams representing the force-displacement variation for both types of compression: centric (figure 5) and eccentric (figure 6).
Analyzing the diagrams we observe that the centric load leads to an almost uniform increase of the displacement with the force, while the eccentric one presents abrupt variations.

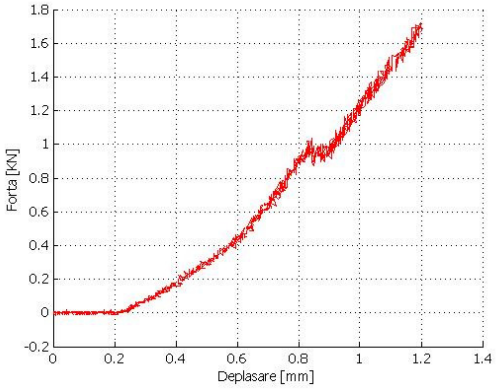

Figure 5: Force-Displacement Diagram for Centric Compression

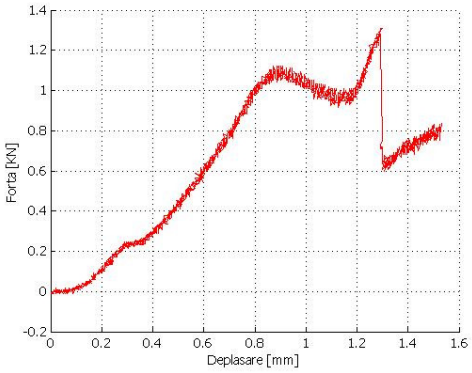

Figure 6: Force-Displacement Diagram for Eccentric Compression

EXPERIMENTAL RESULTS

The compression tests were performed using a Multipurpose Servohydraulic Universal Testing Machine, type LFV 50-HM. The maximum load force is ±50kN and the maximum stroke of the working head is up to 400mm.
The first tests were made for a centric compression as shown in figure 7.

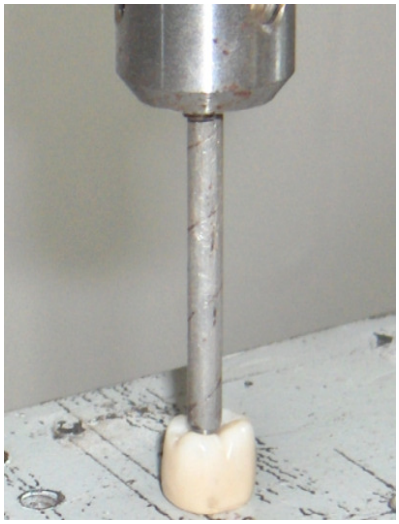

Figure 7: Centric compression of the composite material tooth sample

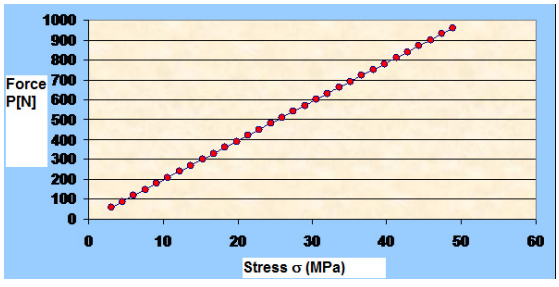

Figure 8: Value of stress depending on the applied centric compression force

Considering the compression force P, between 0 and 960N, the diagram in figure 8 was obtained for the corresponding stress during the experiment.
Further on the samples were subjected to an eccentric force placed as shown in figure 9.

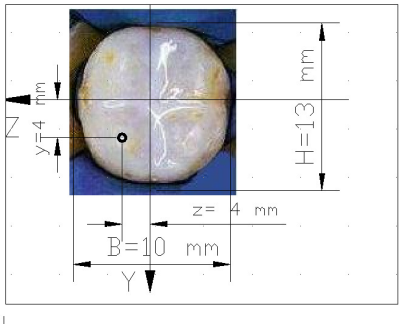

Figure 9: Location of the force point of application during the eccentric compression

Considering P between 300N and 990N to cover all the possibilities of bite forces, we are able to obtain the diagram of the stress depending on the force value, as shown in figure 10.

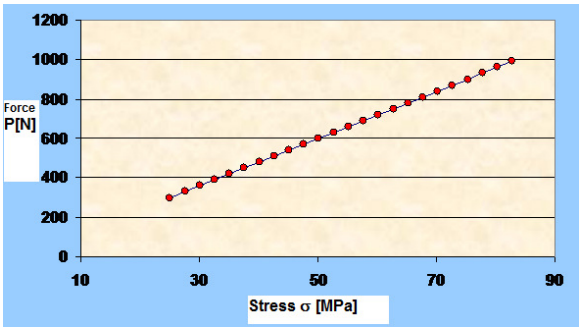

Figure 10: Value of stress depending on the applied eccentric compression force

Up to a certain value of the unit load the material behaves elastic, then it goes into plastic domain becoming unable to return to the initial size and shape. When the unit loading increases over the breaking strain value, the material deformation concentrates, a crack occurs leading to the sample break.
The experiments proved that the samples do not break up to 990N which is much higher than the bite force exerted by a human being.

CONCLUSIONS

The finite element analysis allows visualizing the areas where the principal stress appears in dental structures subjected to certain loads and creates the possibility of an accurate intervention in order to eliminate them.
Analyzing the principal stress, deformation and safety factors, we found that edges are most exposed so using corresponding methods to smooth surfaces becomes necessary.

The finite element analysis allows us to obtain enough data to determine the optimal shape and size of the dental prosthetic structures.
It will be also necessary to consider the fact that a small cross-section of the tooth (e.g. incisive or canine), leads to a bending tendency in horizontal plane so the rupture takes place horizontally.

REFERENCES

Cotoros, D. et al. 2009. "Aspects concerning impact tests on composites for rigid implants", *World Congress on Engineering, London England*, 1658-1661.

Stanciu, A.; D. Cotoros; M. Baritz; and M. Florescu. 2008. "Simulation of Mechanical Properties for Fibre Reinforced Composite Materials". *Theoretical and experimental aspects of continuum mechanics*, WSEAS Cambridge, 146-150.

Bratu, D. et al. 1994. "Materiale dentare-Materiale utilizate în cabinetul de stomatologie". Helicon Publishers. Bucharest, Romania.

Albrektsson, T. and Wennerberg, A. 2004. „Oral implant surfaces: part 1—review focusing on topographic and chemical properties of different surfaces and in vivo responses to them". Int. J. Prosthodont. 17, 536–543.

Regenio, M. et al. 2009. "Stress distribution of an internal connection implant prostheses set", Stomatologija, Baltic Dental and Maxillofacial Journal, 11, 55-59.

Baritz, M.; D. Cotoros; and L. Cristea. 2010. "Analysis of dental implants behavior in mobilizing prosthesis", The 12th Wseas International Conference on Mathematical and Computational Methods in Science and Engineering (MACMESE '10) Faro, Portugal, 141-145.

Cotoros, D. 2010. "Analysis of Skeletal Prosthesis Component Elements at Structural Level", Metalurgia International, No.7/2010, Bucharest, Romania (Jul).

AUTHOR BIOGRAPHIES

DIANA L. COTOROS was born in Brasov, Romania and went to the Transilvania University of Brasov, where she studied mechanical engineering and obtained her degree in 1986. She worked for five years for the Romanian Aircraft Company before moving in 1991 to Transilvania University of Brasov where she is now working with a research group in the field of simulation for biomechanical analysis and new implant materials identification. Her e-mail address is: `dcotoros@unitbv.ro` and her Web-page can be found at `http://www.unitbv.ro`.

ANCA E. STANCIU was born in Calarasi, Romania and went to the Transilvania University of Brasov, where she studied Technological Engineering and obtained her degree in 2005. She starts then as Ph.D. student in Transilvania University of Brasov and now is working as assistant professor. Her e-mail address is: `ancastanciu77@yahoo.com` and her Web-page can be found at `http://www.unitbv.ro`.

MIHAELA I. BARITZ was born in Bacau, Romania and went to Politehnica University of Bucharest, where she studied mechanical engineering and obtained her PhD degree in Fine Mechanics specialisation in 1997. She is now working in University Transilvania from Brasov in the field of optometry and biomechanical analysis for human behaviour. Her e-mail address is: `mbaritz@unitbv.ro` and her webpage can be found at `http://www.unitbv.ro`.

SIMULATION OF VISUAL ASSESSMENT FOR THE GIVEN DEPLOYMENT OF GRAPHICAL USER INTERFACE ELEMENTS

Daniel Skiera
Mark Hoenig
Juergen Hoetzel
Pawel Dabrowski*
Bosch Thermotechnik GmbH
Thermotechnology
Werk Lollar
Postfach 11 61
35453 Lollar, GERMANY
E-mail: Daniel.Skiera@de.bosch.com
E-mail: Mark.Hoenig@de.bosch.com
E-mail: Juergen.Hoetzel@de.bosch.com
E-mail: Pawel.Dabrowski@de.bosch.com

Slawomir Nikiel
Institute of Control and
Computation Engineering
University of Zielona Gora
Podgorna 50
65-246 Zielona Gora, POLAND
E-mail: S.Nikiel@issi.uz.zgora.pl

*Institute of Computer
Engineering and Electronics
University of Zielona Gora
Podgorna 50
65-246 Zielona Gora, POLAND
E-mail: P.Dabrowski@weit.uz.zgora.pl

KEYWORDS

Simulation, Graphical User Interface (GUI), Information Design, Algorithm

ABSTRACT

We observe a constant growth of methods and models enabling automated generation of graphical data, derived either from physical world or taken from simulations. Good information design is crucial for human-computer interface, improving productivity and enhancing human understanding. This paper proposes two novel algorithms to simulate the visual assessment of deployment of GUI elements. GUI elements are treated as the uniform rectangular blocks on the layout. Those blocks eventually are replaced by the system dependent object representations, e.g. visual metaphors of the heating system. The results returned by the algorithms were compared with results obtained by a survey. The proposed metrics can be used in visual evaluation of various simulation models, as long as they consist of logically separable elements. The paper discusses the theoretical background, the properties of proposed algorithms alongside with the sample application prototype outputs.

INTRODUCTION

Good information design requires an understanding of many things. Included are the perception of people: how we see, understand, and think (Winograd and Flores, 1986). It also includes how information must be displayed to enhance human acceptance and comprehension (Miller, 1955; Bodker, 1991). Good design must also consider the capabilities and limitations of the hardware and software of the human-computer interface (Wood, 1997; Teo et al., 2000). Information design, crucial for human-computer interaction (HCI) blends the results of visual design research, knowledge concerning people, knowledge about the hardware and software capabilities of the interfaces and artificial intelligence algorithms. Visual information may be obtained as a result of real-life data collection or as an output of numerical simulations. During the design process the individual elements are assigned visual metaphors. A logical flow of information needs also to be determined.

The next step is to organize and lay out individual elements clearly and meaningfully. Proper screen presentation and structure will encourage quick and correct information comprehension, the fastest possible execution of tasks and functions, and enhanced user acceptance (Gromke, 2007; Hoffmann et al., 2011). It is much harder to estimate numerically how a screen is organized and how its information is actually understood by user, there are some attempts to provide useful metrics (Gamberini et al., 2011). This paper will present the metrics for the redesigned layouts, and the rationale and reasoning that explains why they are useful in automated deployment of visual elements.

Proceedings 26th European Conference on Modelling and Simulation ©ECMS Klaus G. Troitzsch, Michael Möhring, Ulf Lotzmann (Editors)
ISBN: 978-0-9564944-4-3 / ISBN: 978-0-9564944-5-0 (CD)

LAYOUT ALIGNEMENT

Many researchers addressed interface and screen design from the users perspective, giving away hundreds of guidelines for good design in a clear and concise manner (Hartswood and Procter, 2000; Keppel and Wickens, 2004; Galitz, 2007). Generally fewer screen alignments reduce a screens complexity and make it more visually appealing, it is known as the rule of minimum design (Sirlin, 2009). Aligning elements will also make eye movement through the screen much more obvious and reduce the distance it must travel. Screen organization will also be more consistent and predictable. Alignment is achieved by creating vertical columns and horizontal rows of screen fields. Screen balance should be attained as much as possible. But how can we check whether the pattern created is consistent, predictable, and distinct? One of the solutions is the visual complexity measure related to the estimation of the even deployment layout of elements described in the following sections.

ESTIMATION OF EVEN DEPLOYMENT

The estimation of the even deployment can be used for selecting the best even deployments of GUI elements or for construction of a cost (objective) function for a deployment algorithm (Nikiel and Dabrowski, 2011). An example of GUI elements deployment can be seen in the Figure 1.

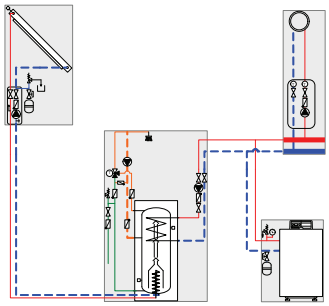

Figure 1: The GUI elements on example of heating system elements.

For the estimation of even deployment algorithms a simple representation of the GUI elements will be used. The elements will be replaced by the rectangles. The rectangles are shown in the Figure 1 (the grey rectangles). The connections between the GUI elements will not be considered in this paper.

Preconditions

Preconditions for the presented estimation of even deployment algorithm:

- the deployment area influences the return results,
- the GUI elements may not overlap,
- the GUI elements should be positioned vertically or horizontally on the given area,
- it's possible to compare the same GUI's with different GUI's where only the deployment of GUI elements is different (the deployment area, the amount and kind of GUI element should remain the same).

The Distances Algorithm

In this algorithm the elements are deployed on the grid (for example one pixel can be treated as a single cell). All distances (vertical and horizontal) between the element and another element or the edges are considered. Figure 2 illustrates the concept of vertical distances for given elements.

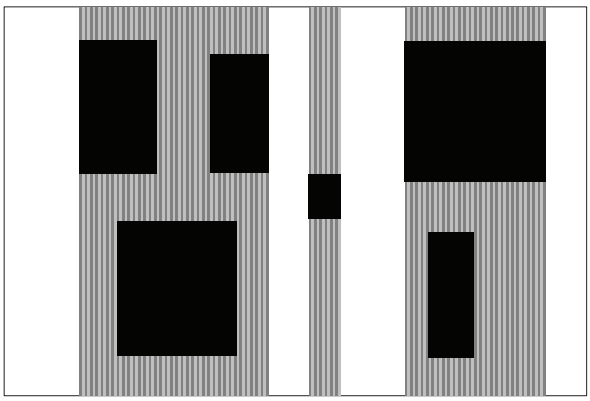

Figure 2: The elements with vertical distances (the length of the gray lines - vertical distances and the horizontal distances are considered).

The idea of this algorithm is based on the fact, that if all the distances have the same length, then the perfect even deployment of the GUI elements is obtained. A histogram of distances is presented in the Figure 3. This histogram was created for the example from Figure 2. The distances have to be determined in the vertical and horizontal direction.

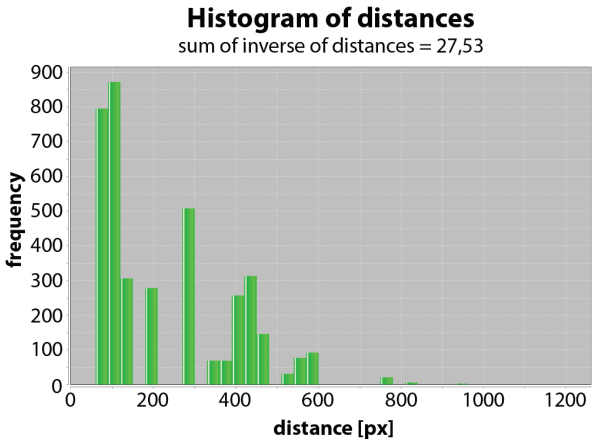

Figure 3: The histogram of distances for the example from Figure 2. The Figure 2 has dimension 1200x800 [px] and the grid cell is 1px.

The sum of squares of distances and the variance of distances were the first metrics used to determine the correctness of even deployment. During our research we compared the returned results by the algorithm for different deployments of the GUI elements on the given area. The smaller the return value of the algorithm, the better the given solution should be. It turned out that these measures classify well most of the deployment examples, but are not resistant to certain cases. En example is shown in the Figure 4.

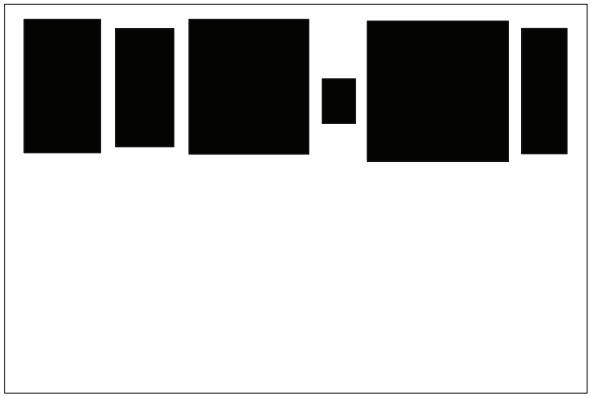

Figure 4: The uneven deployment of GUI elements.

In the situation of grouping of GUI elements the algorithm, which uses the sum of squares of distances or the variance of distances returns good results, despite the fact, that the given deployment is uneven in relation to the area in which the GUI elements have been deployed. This is because of the fact, that the small distances between the GUI elements and the edges are beginning to dominate and they affect the returned result of the algorithm greatly. Figure 5 shows a histogram with the distances for the example from Figure 4. The histogram shows that the short distances dominate.

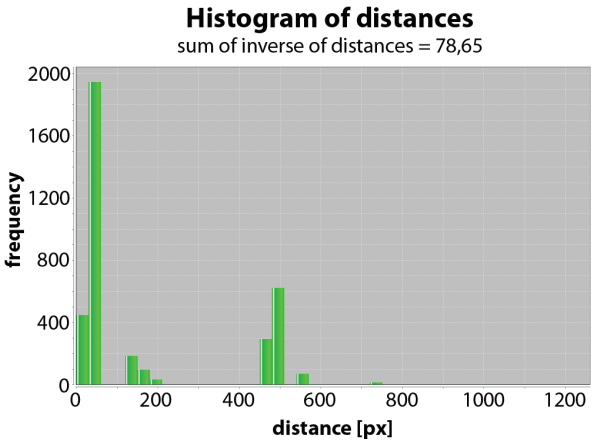

Figure 5: The histogram of distances for the example from Figure 4. The figure 4 has dimension 1200x800 [px] and the grid cell is 1px.

The sum of squares of distances favors short distances between the GUI elements and the edges.

When the elements are grouped, the short distances dominate and the sum of squares of distances is small. This fact should mean that the given deployment is good, but it is not. The solution to this problem would be the sum of the distances raised to more power. This would make the long distances more important than the short distances. However determination of the power is problematic, because it depends on the ratio of the long distances to the short distances. The ratio depends on the considered case.

A similar situation occurs in the variance of distances. If the short distances dominate, the value of the variance is small, because fewer long distances affect the return value non-significantly.

To prevent the above described cases, we should calculate the correctness of the deployment in such a way, that the long distances have to be favored and the short distances have to be "punished". In this case the estimation of simulated deployment of GUI elements have to be factual.

Based on the previous considerations a new approach was created, that sums the inverse of distances between the GUI elements and the edges. This methodology leads to favor the long distances and "punishes" the short distances. The returned value by the algorithm, which uses the sum of inverse of distances is smaller, the deployment of GUI elements on the given area is more even.

After testing, it turned out that this approach works well for estimation of the different configurations of deployments and is fast in cases, in which short distances dominate.

Finally to calculate the even deployment of GUI elements in a given area for the Distances Algorithm the sum of inverse of distances between the GUI elements and the edges is used (see Equation 1).

$$D = \sum_{i=1}^{n} \frac{1}{d_i} \tag{1}$$

where:
D - the sum of inverse of distances
n - the amount of distances between the rectangles and between the edges and rectangles
$i \in N \setminus \{0\}$
d_i - the length of i distance

In the Figure 3 and 5 you can compare the value of the sum of inverse of distances for the two cases.

The time complexity for the Distances Algorithm is equal to $\Theta(N)$.

The Energy Algorithm

The Energy Algorithm is based on the field potential. Some examples we can find in physics e.g.: the Newton's law of universal gravitation (Serway and Jewett, 2010)

or the Coulomb's law (Anaxos Inc. et al., 2009) (see the Equation 2).

$$F = \alpha \frac{o_1 o_2}{r^2} \tag{2}$$

where:
F - the force between the two objects
α - the constant (e.g.: gravitational or proportionality)
o_1 - the first object (e.g.: mass or charge)
o_2 - the second object (e.g.: mass or charge)
r - the distance between the centers of the two objects

For the physical models the objects are treated as a point with mass or charge. This means that for the model the objects do not have physical size and the dimension of the objects is not considered (Anaxos Inc. et al., 2009).

For the Energy Algorithm the constant can ignored, because for our algorithm the constant is not needed. The Energy Algorithm is based on the physical model, therefore we can observe the analogy presented in Table 1.

Table 1: Analogy to physical model

PHYSICAL MODEL	ENERGY ALGORITHM
force	energy
objects (with mass or charge)	GUI elements (width area)
distance between centers of masses or charges	distance between centers of GUI elements

The Energy Algorithm utilizes changes of the value of the power for the distance between centers of two GUI elements. The experiments have shown better results returned by the Energy Algorithm if the power was equal to 4. When the value of power was increased the short distances between the centers of GUI elements were "punished" in greater extent. The given deployment was better, when the associated energy was smaller. Finally the energy between two GUI elements is equal to the Equation 3.

$$E = \frac{a_1 a_2}{r^4} \tag{3}$$

where:
E - the energy between the centers of the GUI elements
a_1 - the area of the first GUI element
a_2 - the area of the second GUI element
r - the distance between the centers of the two GUI elements

The energy for the all given elements is calculated from the Equation 4:

$$E_d = E_e + E_m \tag{4}$$

where:
E_d - the energy for the given deployment of GUI elements
E_e - the energy to another elements, it is calculated from the formula 5
E_m - the energy to mirror elements, it is calculated from the formula 6. The mirror elements are shown in the Figure 6 for one GUI element.

$$E_e = \sum_{0<i<j}^{n} \frac{a_i a_j}{r_{ij}^4} \tag{5}$$

where:
n - the amount of GUI elements, $n \in N \setminus \{0\}$
$i, j \in N \setminus \{0\} \cap 0 < i < j$
a_i - the area of the i GUI element
a_j - the area of the j GUI element
r_{ij} - the distance between the centers of the GUI elements

$$E_m = \frac{1}{16} \sum_{i=1}^{n \in N} a_i^2 \left(\frac{1}{r_{li}^4} + \frac{1}{r_{ti}^4} + \frac{1}{r_{ri}^4} + \frac{1}{r_{bi}^4}\right) \tag{6}$$

where:
$i \in N \setminus \{0\}$
$r_{li}, r_{ti}, r_{ri}, r_{bi}$ - the distance between the center of element and the left, top, right, bottom edge of the area

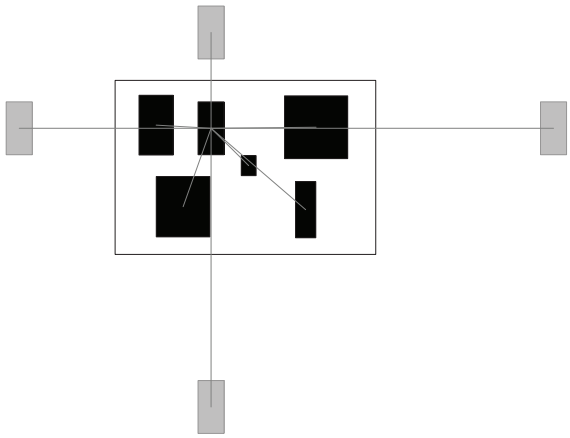

Figure 6: The GUI element with all distances (the gray lines) to another GUI elements and to mirror elements (the gray rectangles).

The mirror elements are used to keep suitable distances of the GUI elements to the edges of the deployment area.

The energy is dependent on the area of the rectangles with GUI elements. The estimation will be better, if the bigger rectangles will be located in longer distances from each other.

The Energy Algorithm unfortunately has some drawbacks, because the approach does not take into consideration the geometry of rectangles. A situation can occur

that for the same GUI elements, but only rotated, the energy will be the same or the distance between rectangles will be to small (see the Figure 7). This can happen, because the Energy Algorithm does not treat the GUI elements as rectangles but as points of mass.

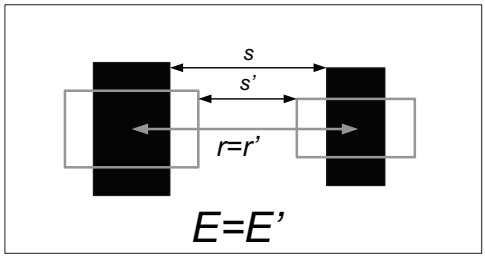

Figure 7: The same energy for two configuration (vertical and horizontal) of GUI elements.

The value of mass is equal to the area of the rectangle and can be treated as circle. The circle has the same area as the rectangle and the point of mass (see the Figure 8).

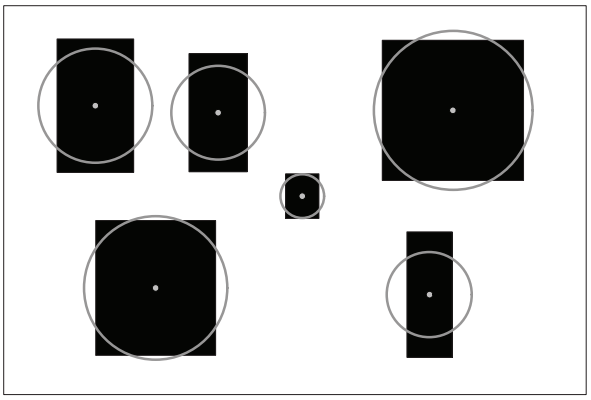

Figure 8: The Energy Algorithm considers the GUI elements as points of mass.

To minimize the above drawbacks we need to make some additional limitations for the Energy Algorithm:

- vertical or horizontal position of the GUI element should not be changed,
- the GUI elements should be represented by the square (in this case the rectangles have the biggest overlap with the circles).

The time complexity for the Energy Algorithm is equal to $\Theta(N^2)$.

Discussion

The disadvantage of the Energy Algorithm is that, it ignores the shape of the GUI elements. With a large amount of elements running time of the Energy Algorithm will rise dramatically, because its time complexity is equal to $\Theta(N^2)$.

The Distances Algorithm allows for the shape of the GUI elements and its time complexity is equal to $\Theta(N)$.

VERIFICATION

In an aim to verify the algorithms sample deployments of the GUI elements were created, which were sorted from good to bad by a group of fourteen people. The respondents received fourteen possibilities for deployment of GUI elements. The elements in all examples were the same. The deployments were printed on cards (an example of a deployment is shown in Figure 4). The cards are shuffled and the respondents sorted the cards from the best to the worst deployment of GUI elements. From the survey results were determined the order of the fourteen deployments. To compare the correctness of simulation of visual assessment the results returned by the described algorithm are presented in a chart. The chart in Figure 9 shows the results obtained from the survey to the results returned by the algorithms.

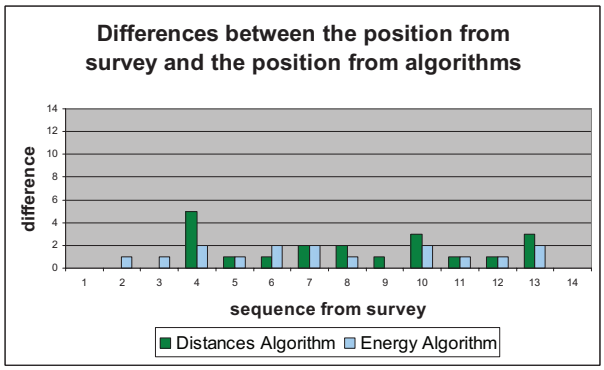

Figure 9: Results from the survey to the results returned by the algorithms.

For better understanding of the chart an example is presented:
For the ninth deployment (the x axis) the Energy Algorithm returned the same position as the position from survey (the difference (the y axis) is equal to zero). The Distances Algorithm returned one more or less position as the position from the survey (the difference is equal to one). This means that the algorithm returned position eight or ten for the deployment of GUI elements). In the best case the returned results by the algorithms should have the difference equal to zero. In this case the simulated visual assessment would be ideal.

As shown in the chart in Figure 9, both algorithms classify the best and the worst deployments of GUI elements in the same place. The differences occur in order of worse deployments, but they are relatively low.

The described algorithms simulate the visual assessment for the given deployment of GUI elements well.

CONCLUSION

Information design delivers constant challenges in the field of HCI. The paper proposes two novel algorithms for estimation of deployment of the visual elements in the given layout. GUI is treated as the output of simulation placing uniform rectangular blocks on the selected

area. The paper proposes alternative metrics of visual complexity, based on the Distances and the Energy techniques. The novel schemes utilize estimation of distances on the image grid to obtain a global goal - the optimization of layout. It is possible to greatly improve automated presentation of data. The authors plan to develop further the method in order to support more complex systems.

ACKNOWLEDGMENT

This study is supported by Bosch Thermotechnik GmbH, and the authors would like to thank the company for the cooperation and assistance rendered.

REFERENCES

Anaxos Inc., Brazell, B., Heckert, P., Nittler, J., Vannette, M., and Willis, M. (2009). *AP Physics B & C 2009*, chapter Coulomb's Law; Field and Potential of Point Charges, page 245. Kaplan Publishing, New York, USA.

Bodker, S. (1991). *Through the interface: a human activity approach to user interface design*. Lawrence Erlbaum Associates, Hillsdale.

Galitz, W. (2007). *The Essential Guide to User Interface Design*. Wiley.

Gamberini, L., Spagnolli, A., Prontu, L., Furlan, S., Martino, F., Solaz, B., Alcaniz, M., and Lozano, J. (2011). How natural is a natural interface? an evaluation procedure based on action breakdowns. *Personal and Ubiquitous Computing*, 5.

Gromke, G. (2007). Digital asset management - der effektive umgang mit mediendaten. *Proceedings, Intl. Conf. EVA 2007 Berlin*, pages 161–166.

Hartswood, M. and Procter, R. (2000). Design guidelines for dealing with breakdowns and repairs in collaborative work settings. *International Journal on Human Computer Studies*, 53:91–120.

Hoffmann, P., Lawo, M., and Kalkbrenner, G. (2011). Zur aesthetik interaktiver medien - hypervideo im spannungsfeld zwischen usability und design. *Proceedings, Intl. Conf. EVA 2007 Berlin*, pages 117–123.

Keppel, G. and Wickens, T. (2004). *Design and analysis: a researchers handbook*. Pearson/Prentice Hall, Upper Saddle River.

Miller, G. (1955). The magical number seven, plus or minus two - some limits on our capacity for processing information. *In: Psychological Review*, 101(2):343–352.

Nikiel, S. and Dabrowski, P. (2011). Deployment algorithm using simulated annealing. In *Methods and Models in Automation and Robotics - MMAR 2011 : 16th international conference*, pages 111–115, Miedzyzdroje, Poland.

Serway, R. and Jewett, J. (2010). *Physics for Scientists and Engineers*, volume 1, chapter Newton's Law of Universal Gravitation, page 375. Brooks Cole, Belmont, USA, 8 edition.

Sirlin, D. (2009). Subtractive design. *Game Developer*, pages 23–28.

Teo, L., Byrne, J., and Ngo, D. (2000). A method for determining the properties of multi-screen interfaces. *International Journal of Applied Mathematics and Computer Science*, 10(2):413–427.

Winograd, T. and Flores, F. (1986). *Understanding computers and cognition*. Ablex Publishing, Norwood.

Wood, L. (1997). *User Interface Design: Bridging the Gap from User Requirements to Design*. CRC Press.

AUTHOR BIOGRAPHIES

DANIEL SKIERA is currently working as a Software Architect at Bosch Thermotechnik GmbH, Lollar, Germany. He obtained a PhD in Physics at the University of Giessen, Germany. His scope of work included data analysis, image processing and system simulation. His e-mail is Daniel.Skiera@de.bosch.com.

MARK HOENIG is currently working as a group manager at Bosch Thermotechnik GmbH, Lollar, Germany. He graduated in Physics at the University of Goettingen and received a PhD from the University of Cologne. His work included data analysis and nonlinear optimization. His e-mail is Mark.Hoenig@de.bosch.com.

JUERGEN HOETZEL is currently working as manager at Bosch Thermotechnik GmbH, Lollar, Germany. He graduated in Electronics at the University of Darmstadt and received a PhD from the Technical University Berlin. His work included system architecture and Internet connectivity. His e-mail is Juergen.Hoetzel@de.bosch.com.

SLAWOMIR NIKIEL is currently the Professor at the Institute of Control and Computation Engineering, Department of Electrical Technology, Computer Science and Telecommunication, University Of Zielona Gora, Poland. His research interest include HCI, game programming and multimedia systems. His e-mail is S.Nikiel@issi.uz.zgora.pl.

PAWEL DABROWSKI is currently the PhD student at the Institute of Computer Engineering and Electronics, Faculty of Electrical Engineering, Computer Science and Telecommunications, University Of Zielona Gora, Poland. His dissertation is developing in cooperation with Bosch Thermotechnik GmbH, Lollar, Germany. His research interest include automatic deployment of GUI elements. His e-mail is P.Dabrowski@weit.uz.zgora.pl or Pawel.Dabrowski@de.bosch.com.

APPLICATION OF MOSEL-2 LANGUAGE IN PERFORMANCE AND MODELING OF CELLULAR WIRELESS NETWORKS

AYMEN I. ZREIKAT
Department of Information Technology, Mutah University, Mutah, Karak, Jordan, P.O. Box 7, (zip code:61710)
e-mail: siayzrei@yahoo.com

KEYWORDS
Application of MOSEL-2, Cellular Wireless Networks, Performance Analysis and Modeling, IGL.

ABSTRACT
Today's cellular wireless networks must meet increasing challenges of handling a larger demand for service without a loss of quality, by maximizing the spectral efficiency of the network. Therefore, performance evaluation and modeling of cellular wireless networks is considered to be an important issue to overcome the problem of limited resources of the network. MOSEL-2 (MOdelling Specification and Evaluation Language) offers the ability to evaluate complex systems in a straight, simple and very friendly environment. The old version of MOSEL offers only performance evaluation of complex systems with exponential distribution. However, by the new version of MOSEL (i.e. MOSEL2) with new constructs, it is possible to handle other behaviors with non-exponential distribution. In this paper, the application of MOSEL-2 in cellular wireless networks with mix service is presented. The main objective of the call admission control algorithm and the analysis is to obtain lower handover blocking probability over the new call blocking probability for both voice and data connections, which leads to minimum grade-of-service (i.e. < 0.01) over the whole cell. The numerical analysis of the suggested model with the associated interesting performance measures proves the effectiveness of this simulation in describing and solving this type of systems.

1. INTRODUCTION

1.1 Application of MOSEL-2 in the literature

The generation of mobile networks are evolving very fast starting from 1G, cellular concept based on the analog technology (i.e. only voice), then moving from analog to digital technology (i.e. 2G, GSM and EDGE, providing users with voice and data). The third generation supports broadband voice, data and multimedia services. Performance analysis of multi-service 3G networks plays a major role for mobile network providers, because of the W-CDMA technique used in these systems, which leads to an interference limited systems with a dynamic cell capacity and load dependent cell coverage (Smida et al 2002; Heiska et al 2002).
Performance, reliability modeling and evaluation plays an important role in the design, development, testing, and maintenance of many complex systems in different applications such as: communication systems, manufacturing systems, computer networks and many other. It has been an extensive use of the old version MOSEL (Al-Begain et al 2001) and the modified version of MOSEL with new constructs, MOSEL-2 (Wuechner 2003) ,in the literature in various applications. The old version of MOSEL has been used intensively for many years and most of these applications are in queueing networks, some of them are in (Zreikat and Bolch 2007; Al-Begain et al 2003; Zreikat et al 2003; Wüchner et al 2007;Gunter et al 2006; Wüchner et al 2005). However, MOSEL-2 language is also used in different applications to model 2G and 3G of mobile networks, some of these examples are in (Zreikat et al 2008; Wüchner et al 2004; Barner and Bolch 2003). Moreover, new work has been done recently to use MOSEL-2 in modeling and evaluation of the 4G of mobile networks (i.e. WIMAX/WIFI or even LTE) (Zreikat 2011). Performance and modeling of one cell of cellular wireless networks with mix service is presented in this paper to show the effectiveness of MOSEL-2 language to describe and solve different types of systems, especially in mobile communications applications.

The paper is organized as follows. In Section 1.2, a description of MOSEL-2 language and environment is given. Modeling of cellular wireless networks is presented in Section 2. In Section 2.1, the modeling assumptions are presented and in Section 2.2, the call admission control algorithm is presented, whereas in Section 2.3, the model solution by MOSEL-2 is presented. The numerical results are presented in Section 3, and finally followed by the conclusions and future work in Section 4.

1.2 Description of MOSEL-2 language and environment

The reliability modeling and evaluation process by MOSEL-2 language is described in Figure 1. There are six main steps that can be summarized as:

- Step 1. The real world system is described by the user via generating a high-level system description using the syntax of MOSEL-2 language. However, the following steps are done without the user interaction. The generated file is saved as filename.mos.
- Step 2 & 3: MOSEL-2 translates the model description into a specific tool and the appropriate tool (MOSES, SPNP or TimeNET) is invoked by

Proceedings 26th European Conference on Modelling and Simulation ©ECMS Klaus G. Troitzsch, Michael Möhring, Ulf Lotzmann (Editors)
ISBN: 978-0-9564944-4-3 / ISBN: 978-0-9564944-5-0 (CD)

MOSEL-2. This can be done by given an option in the command line. The MOSEL-2 environment is called from a shell using the following command line syntax:

>mosel2 options input-file.mos

The parameter input file is the name of MOSEL-2 file (for example: filename.mos), which has the suffix ".mos". This MOSEL-2 file is read in, parsed and checked for errors. The options are prefixed by a dash" –" followed by a single letter like "-o". Also multiple options can follow s single dash, like "-Ts", which has the same meanings as "-T -s". To see the list and description of all command options of MOSEL-2, call MOSEL-2 with option "-h" as:
>mosel2 -h
The option "-s" causes MOSEL-2 to start the selected tool, to read the results and create the result file and if the input file contains picture definitions, an igl file will also be generated, which will contain all the figures specified in the picture part of the file in a nice way. There are 3 additional options for MOSEL-2, usually they are written in association with the "-s" option in order to select the specific tool for evaluation: ("-c", for SPNP tool (Buetel 2003; Wüchner 2005)),("-T", for TimeNET tool (Buetel 2003; Zimmermann 2005)) or "-m" for MOSES tool (Bolch et al 1998).

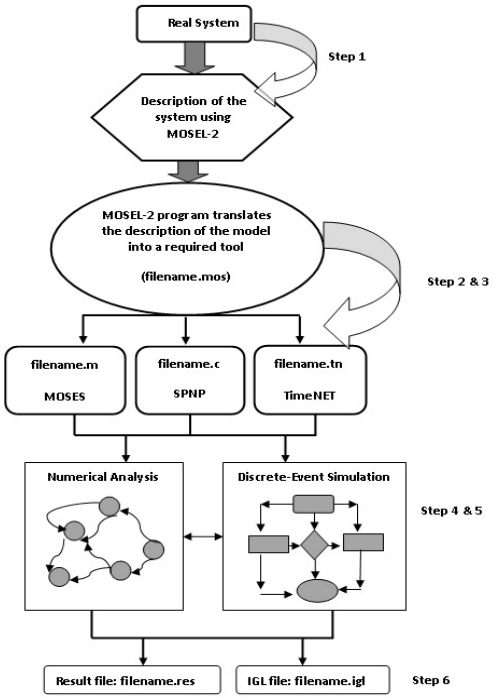

Figure 1: Modeling and Evaluation process in MOSEL-2

- Steps 4 & 5: The appropriate tool processes its input file in one of the two following ways (this can be done by different command line options in MOSEL-2):
  - Numerical analysis: out of the static model description, the whole state space of the model is generated by the tool according to the semantic rules of its modeling formalism. This semantic model is mapped onto a stochastic process. The stochastic process is solved by one of the standard numerical solution algorithms, which are part of the tool.
  - Simulation: the model is evaluated by the tool without building the whole state space, using discrete event simulation.

  The results of the numerical analysis or discrete event simulation are saved in a file with a tool specific structure.
- Step 6: The MOSEL-2 environment parses the tool specific output and generates a textual result file (i.e., filename.res) which contains the values of the performance and reliability measures according to the user description in the optional "RESULT" part of the program. Additionally, if the optional "PICTURE" part is specified, then the graphical representations of the results are generated by IGL utility in a file "filename.igl".

2. MODELLING OF CELLULAR WIRELESS NETWORKS BY MOSEL-2 LANGUAGE

2.1 Modelling Assumptions

- Only one cell is considered in the analysis and the arrival process over the whole cell is assumed to be Poisson process with {on and of} state for the voice calls.
- The number of mobile terminals in the cell is fixed and assumed to be M_Ter = 500.
- The number of available channels in the cell NO_CH is 64.
- The call duration or holding time is a random variable which is independent and exponentially distributed with mean $1/\mu_v$ for voice = $1/\mu_d$ = 100 seconds.
- The call duration for incoming handover to the cell is also assumed to be a random variable which is independent and exponentially distributed with mean $1/\mu_{hv}$ for voice = $1/\mu h_d$ = 80 seconds.
- The overall traffic over the cell area is λ. Two types of services are assumed in the analysis: voice and data with the following ratios:
  Voice = λ * 0.75, data = λ * 0.25.
- The maximum transmission rate of the ongoing data connection is assumed to be 16 (i.e. max_Trans_rate := 16).
- The minimum transmission rate of the ongoing connection is assumed to be 4
  (i.e. min_Trans_rate := 4). It is a threshold for accepting new handover calls.
- Transmission rate threshold is the threshold for accepting the new handover calls. It is assumed in the analysis to be a set of values: 4,7,10 and 13.
- Ideal free space propagation for the signal is assumed.
- No mobility is assumed in the analysis of this paper.

2.2 Call Admission Control

- For incoming calls, the priority is given to the voice calls over the data. All incoming voice connections are served normally as long as there are enough free channels in the cell after accepting a new person. One channel is used for a voice call and max_Trans_rate (i.e. maximum transmission rate) for the data connection (is given a value 16 in the code, which means that the data connection is considered to be a multiple of one radio channel). Therefore, the condition for accepting a new voice person will be: Number of voice calls after accepting a new connection < NO_CH – 1.
- In the case of incoming data connection, the call is accepted if there is a free channels but after we exclude the transmission threshold value (i.e. Trans_rate_thr) according to the following condition: Number of voice calls after accepting a new connection < NO_CH – Trans_rate_thr (is given a range of values in the program, 4-13 to be considered for the next analysis). However, the Trans_rate_thr should not be less than the minimum threshold value to admit the new connection. The min_Trans_rate (i.e. minimum transmission rate) in the program is given the value 4.
- In case of the incoming handover calls from the neighboring cells either voice or data are treated as a normal incoming call to the cell. The call is only rejected if there are no available channels in the cell after accepting the new call (i.e. 1 channel for the voice connection and max_Trans_rate for the data connection). This is why we considered minimum threshold value for accepting the handover calls, which is smaller than both the Trans_rate_thr and max_Trans_rate. Hence, in our model, the priority is given to the handover calls over the new calls as it is easy to reject a new call rather than stopping the ongoing connection.

2.3 The Model solution by MOSEL-2 language

MOSEL-2 model description of one cell cellular wireless networks is in Figure 2. There are line numbers used in Figure 2. However, there are no line numbers in MOSEL-2 code and the numbers in Figure 2 are used only for referencing. MOSEL-2 specification can be divided into six main parts:

1. The optional constant, parameter and enumerator definition part (Lines 1-14). In a "CONST" definition, the variable is given a floating point constant. In a "PARAMETER" definition, the variable is given a set of values, and the model is evaluated at each value. In "ENUM" definition, the variable is a given a set of constants between two brackets "{}".
2. The node definition part (Lines 15-17), where the nodes are defined. Nodes are used to describe the model's state, each node has a certain value ranges from 0 to a maximum value called the capacity of the node.
3. The optional function and condition part (Lines 18-23). Only function is used in Figure 2 with "FUNC". However, MOSEL-2 offers two types of functions: either the "FUNC", which yields to a numeric value, or the "COND", which is a placeholder of logical expression.
4. The rule part (Lines 24-31), which contains MOSEL-2 rules. Rules in MOSEL-2 is used to describe how the system may change from one state to another.
5. The optional result part (Lines 32-46). The computation of the required performance measures is done in this part.
6. The optional picture part (47-55). IGL (Intermediate Graphical Language) is a user-friendly tool, which is responsible for this part, to generate the graphical representation of the defined performance measures by the user, in a very nice way. IGL utility is associated with MOSEL-2, where the user can edit, modify and prepare the curves in a nice way. Moreover, the curves can be saved into an encapsulated postscript form (i.e. "figure.eps"), which can be easily viewed and modified in different operating systems. The following interesting performance measures are computed and studied in this paper:

[1] New call blocking probability: is the fraction of calls, from the new call requests, that are rejected (i.e. blocked) due to the shortages of the available channels.

[2] Handover blocking probability: is the fraction of handover calls that cannot be admitted due to the shortages of the available channels. This will cause the call request to be terminated.

[3] Grade-of-service for the data or voice service: is defined as a combination of the new call blocking probability and handover probability multiplied by a factor of 10:
Grade-of-service = new call blocking probability + handover probability *10;
The acceptable level of the grade-of-service is assumed to be <= 10%.

[4] Cell utilization: is defined as the average used channels in the cell divide by the total number of available channels in the cell.

[5] Average data rate: the average transmission rate of the data connection.

[6] Cell Throughput: is defined as the percentage of voice and data connection that have been successfully served in the cell.

3. NUMERICAL RESULTS

The numerical results are generated by the IGL utility, which is associated with MOSEL-2 language. Nine curves are generated (Figures 3-11) for different transmission rate threshold. This threshold is assumed to have a set of values (4, 7, 10 and 13). The main objective of the analysis is to achieve minimum grade-of-service of both voice and data (i.e. < 0.01) in the assumed cell as well as the whole network. MOSEL-2 model evaluation took only 5 seconds, whereas the same model evaluation by the old version of MOSEL took around 35 seconds. In Figure 3, the grade-of-service for the voice calls is presented. It can be seen that a minimum grade of service (< 0.01) can be achieved even at higher rate for threshold values of 4, 7 and 10.

```
//-----------CONSTANT AND PARAMETER PART-----------------------------------------
1 CONST  NO_CH:= 64; //NUMBER OF CHANNELS
2 CONST  M_Ter:= 500; // finite number of mobile terminals in the cell
3 CONST  max_Trans_rate := 16;//maximum transmission rate to the ongoing conection
4 CONST  min_Trans_rate := 4;//minimum transmission rate to the ongoing conection
5 PARAMETER Trans_rate_thr :=4..13 STEP 3;//transmission rate threshold:
   //(min_Trans_rate <= Trans_rate_thr <= max_Trans_rate)
6 PARAMETER  lambda := 0.10..0.50 STEP 0.10;//arrival rate
7 CONST      lambda_for_voice := lambda*0.75;
8 CONST      lambda_for_data  := lambda*0.25;
9 CONST      mue_handover_for_voice := 1.0/80;
10 CONST     mue_handover_for_data  := 1.0/80;
11 CONST     mue_for_voice          := 1.0/100;
12 CONST     mue_for_data      := 1.0/100;
13 CONST     data_max_capacity  := NO_CH/min_Trans_rate;
14 ENUM      on_off_queue:={on,off};
//-----------NODES PART-----------------------------------------------------------
15 NODE   voice_with_queue[on_off_queue] := on;
16 NODE   voice_con[NO_CH];
17 NODE   data_con[data_max_capacity];
//---------------FUNC PART-------------------------------------------------------
18 FUNC NO_of_occupied_CH := IF (voice_con+data_con*max_Trans_rate < NO_CH) THEN
   voice_con+data_con*max_Trans_rate ELSE NO_CH;//No. of accupied channels
19 FUNC  Handover_thr(x,y):= x+y*min_Trans_rate; //threshold for acceptance of
     handover calls
20 FUNC new_call_thr(x,y):= x+y*Trans_rate_thr;//threshold for acceptance of new calls
21 FUNC Actual_rate_data(x,y):= IF (NO_CH-x)/y >max_Trans_rate THEN max_Trans_rate
     ELSE (NO_CH-x)/y;//actual transmission rate for data connection,
22 FUNC    h(x,y):=(NO_CH - x)/y;
23 FUNC reward := IF data_con > 0 THEN h(voice_con,data_con) ELIF
   h(voice_con,data_con) > max_Trans_rate THEN max_Trans_rate ELSE 0; //reward function
//---------------RULE PART-------------------------------------------------------
//---NEW ARRIVAL---------------------------------------------------------------
24 IF  (new_call_thr(voice_con,data_con) <= NO_CH-1) AND (voice_with_queue == on) FROM
     EXTERN   TO   voice_con  RATE (M_Ter - (voice_con+data_con)) *
     (lambda_for_voice/M_Ter);
25 IF  (new_call_thr(voice_con,data_con) <= NO_CH- Trans_rate_thr)
     FROM  EXTERN   TO   data_con   RATE (M_Ter - (voice_con+data_con)) *
     (lambda_for_data/M_Ter);
//-------------------------------------------------------------------------------
26 FROM voice_with_queue[on]  TO voice_with_queue[off]    RATE   lambda_for_voice;
27 FROM voice_with_queue[off] TO voice_with_queue[on]     RATE    mue_for_voice;
//------NEW HANDOVER ARRIVAL---------------------------------------------------
28 IF (Handover_thr(voice_con,data_con) <= NO_CH-1) AND (voice_with_queue == on)
     FROM EXTERN   TO   voice_con   RATE    mue_handover_for_voice;
29 IF (Handover_thr(voice_con,data_con) <= NO_CH-min_Trans_rate)
     FROM EXTERN   TO   data_con    RATE    mue_handover_for_data;
//-------------------------------------------------------------------------------
//Termination of Call and Outgoing Handover Request
30 FROM  voice_con     RATE    voice_con*(mue_for_voice+mue_handover_for_voice);
31 FROM  data_con   RATE    data_con*((1.0*Actual_rate_data(voice_con,data_con)
     /max_Trans_rate)*mue_for_data + mue_handover_for_data);
//----------------RESULT PART------------------------------------------------
32 PRINT   MEAN_voice := MEAN(voice_con);
33 PRINT   MEAN_data  := MEAN(data_con);
34 PRINT   voice_blk  := PROB(new_call_thr(voice_con,data_con) > NO_CH-1);
35 PRINT   voice_hof  := PROB(Handover_thr(voice_con,data_con)> NO_CH-1);
36 PRINT   data_blk:= PROB(new_call_thr(voice_con,data_con)>NO_CH-  Trans_rate_thr);
37 PRINT   data_hof := PROB(Handover_thr(voice_con,data_con)>NO_CH- min_Trans_rate);
38 PRINT   data_com   := PROB(data_con > 0)
39 PRINT   result            := MEAN(reward);
40 PRINT   av_data_rate      := result/MEAN_data;
41 PRINT   GOS_voice         := voice_blk + voice_hof*10;
42 PRINT   GOS_data          := data_blk  + data_hof*10;
43 PRINT   utilization       := MEAN(NO_of_occupied_CH)/NO_CH;
44 PRINT   Throughput_data   := MEAN_data  * mue_for_data;
45 PRINT   Throughput_voice  := MEAN_voice * mue_for_voice;
46 PRINT   Throughput :=   Throughput_data +  Throughput_voice;
```

```
//------------------PICTURE PART-----------------------------------------------
47 PICTURE "Grade_of_service_voice"
   PARAMETER lambda
   XLABEL "lambda"
   YLABEL "Grade_of_service"
   CURVE  GOS_voice
48 PICTURE "Grade_of_service_data"
   PARAMETER lambda
   XLABEL "lambda"
   YLABEL "Grade_of_service"
   CURVE  GOS_data
49 PICTURE "utilization"
   PARAMETER lambda
   XLABEL "lambda"
   YLABEL "utilization"
   CURVE  utilization
50 PICTURE "AVG_DATA_RATE"
   PARAMETER lambda
   XLABEL "lambda"
   YLABEL "AVG_DATA_RATE"
   CURVE  av_data_rate
51 PICTURE "Blocking_voice"
   PARAMETER lambda
   XLABEL "lambda"
   YLABEL "Blocking"
   CURVE   voice_blk
52 PICTURE "Blocking_data"
   PARAMETER lambda
   XLABEL "lambda"
   YLABEL "Blocking"
   CURVE   data_blk
53 PICTURE "HO_Blocking_voice"
   PARAMETER lambda
   XLABEL "lambda"
   YLABEL "Blocking"
      CURVE   voice_hof
54 PICTURE "HO_Blocking_data"
   PARAMETER lambda
   XLABEL "lambda"
   YLABEL "Blocking"
   CURVE   data_hof
55 PICTURE "Throughput"
   PARAMETER lambda
   XLABEL "lambda"
   YLABEL "Throughput"
   CURVE   Throughput
```

Figure 2: MOSEL-2 model for one cell cellular wireless networks

However, at higher threshold value 13 only good quality of service can be achieved at low rate. This can be explained as: when the threshold value is high then the number of voice connections who are blocked will be high, because the number of available channels in the cell will be less for the benefit of data connections and therefore, the grade-of-service will then increase. The minimum the threshold value, the better the number of voice calls who are being served, then the better the grade-of-service. An interesting result can be noticed in Figure 3, where at high traffic load, the minimum value of threshold (i.e. 4), the grade-of-service becomes the worst. This can be explained that very small value of threshold has a negative effect on both the new call blocking probability and the handover blocking probability. Different behavior can be noticed in Figure 4, which indicates that the data calls suffer more from the increase of the threshold value.

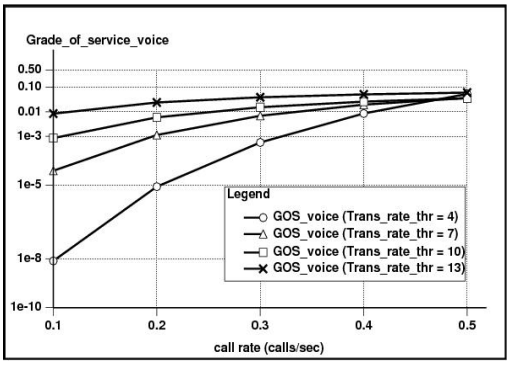

Figure 3:Grade-of-service against call rate for voice calls

This can be explained as: in Figure 3, at rate 0.20 and threshold value 10, the grade-of-service is less than 0.01. However, at the same rate and same threshold value in Figure 4, the grade-of-service is a round 0.09. From both Figures, it can be noticed that, the higher value of threshold has a negative effect on both new call blocking probability and handover blocking probability, which leads to a negative effect on the grade-of-service. In Figure 5, the utilization of the cell is shown, where it can be noticed that higher value of threshold has extremely affect the utilization of the cell at different traffic load. This is clear by looking at Figure 5 (the curve where the threshold value is 13), following the same explanation above. The average transmission rate of data connection is shown in Figure 6. It is clear that as the traffic load increases, the average data transmission rate is also increases. However, for high threshold value (i.e. 13), the average transmission rate is better. This is clear as the higher threshold value, the higher the number of channels who are reserved for the benefit of data connection.

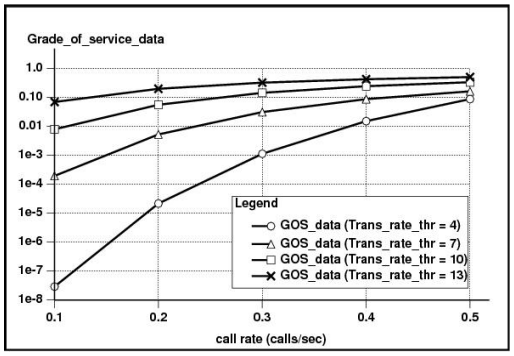

Figure 4: Grade-of-service against call rate for data calls

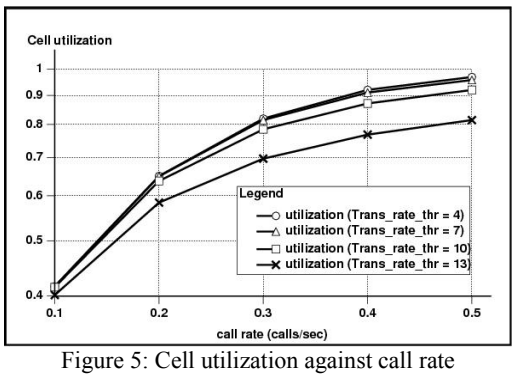

Figure 5: Cell utilization against call rate

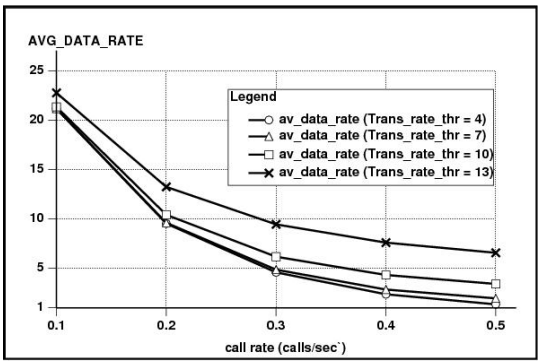

Figure 6: Average data transmission rate against call rate

In Figures 7 and 8, the call blocking probability is shown for both the voice and data connection. Whereas in Figure 9 and 10, the handover blocking probability is shown for both voice and data. In our model, the ongoing handover calls are given higher priority on new calls for both voice and data connection. Therefore, it can be noticed from Figures 7 that the voice calls are only suffering when the threshold value is high for the benefit of the data connection. On the other hand, the data connection almost suffers at different traffic load as they consumes the channels faster than the voice calls, this can be noticed from Figure 7 and 8, where for example: at traffic load 0.50 and threshold value 13, the voice blocking probability reaches a value less than 0.10, whereas the data blocking probability reaches a value close to 0.70.

The suggested model gives significant results in Figures 9 and 10 for both voice and data calls. It can be noticed that the main objective of this analysis has been achieved. The handover blocking probability of both voice and data connections gives lower values at different traffic load,

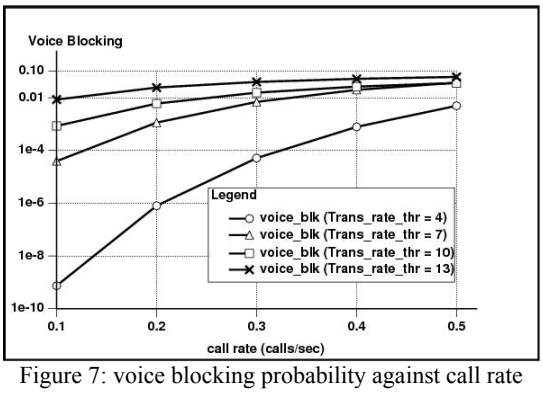

Figure 7: voice blocking probability against call rate

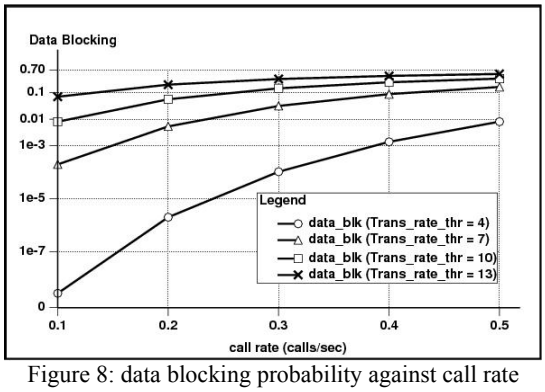

Figure 8: data blocking probability against call rate

however, this can be significantly noticed at lower value of the threshold. This can be explained that when the threshold value is low, more channels will be reserved in the cell, but only for the benefit of handover calls. At this lower rate of the threshold, the throughput of the cell will be increased significantly at different traffic load. This last behavior can be noticed by looking at Figure 11.

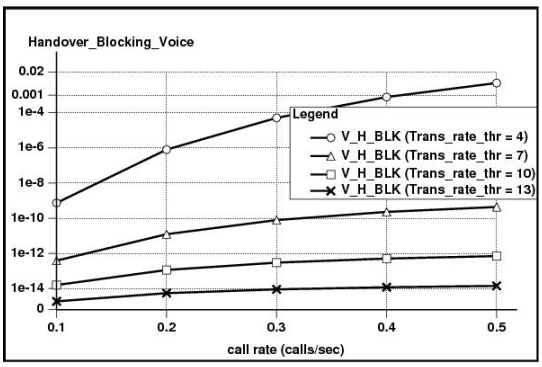

Figure 9: voice handover blocking against call rate

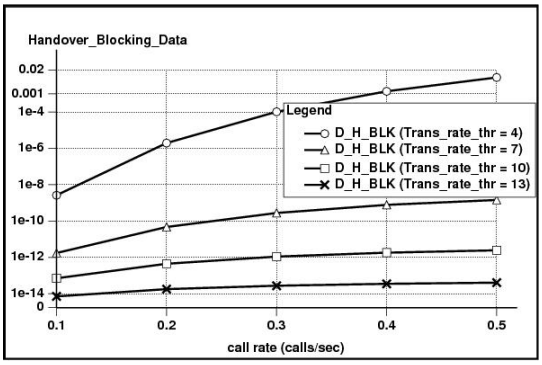

Figure 10: data handover blocking against call rate

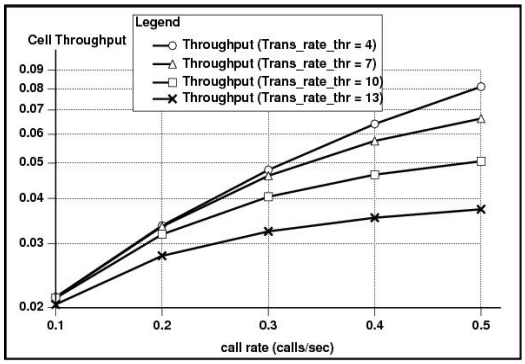

Figure 11: cell Throughput against call rate

4. CONCLUSIONS AND FUTURE WORK

The main objective of this work is to show the effectiveness of MOSEL-2 simulation in the performance modeling of cellular wireless networks by introducing an example. Firstly, the main features and environment of MOSEL-2 is presented. Secondly, the suggested model in this paper has been solved using MOSEL-2 language. The numerical results show two things: firstly, the effectiveness of MOSEL-2 in performance and modeling of cellular wireless networks in a very nice and friendly environment and secondly, the suggested model and its

call admission control algorithm are improving the handover blocking over the new call blocking for both voice and data connections. For model verification, it is shown that the model evaluation by MOSEL-2 takes less time than the model evaluation by the old version of MOSEL. In the future work, the work of this paper can be extended to show the efficiency of MOSEL-2 in the performance modeling and evaluation of different models of 2G (GSM/GPRS), 3G (UMTS), and even 4G (WiMAX/LTE) of mobile networks. Additionally, to improve the handover blocking probability over the new call blocking probability, a reservation policy of channels for handover calls can be suggested. Moreover, a queuing principle of the connection can also be suggested, where instead of directly blocking the connection when there is no free channels, the connection can wait for some time until the channel is available. This last suggestion will significantly improve both the new call blocking probability and the handover blocking probability.

REFERENCES

Smida, B., V. Sampath and P. Marinier, May 2002. "Capacity degradation due to coexistence between second generation and 3G/WCDMA systems," in Proc. IEEE Veh. Technol. Conference, vol. 1, pp. 95-99.

Heiska K., H. Posti, P. Muszynski, P. Aikio, J, Jan. 2002. Numminen and M. Hamalainen."Capacity Reduction of WCDMA Downlink in the Presence of Interference From Adjacent Narrow-Band System," IEEE Trans. on Veh. Technol., vol. 51, Issue 1, pp. 37-51.

Al-Begain, K., G., Bolch, H., Herold, , 2001. Practical Performance Modelling, Application of the MOSEL Language; Kluwer Academic Publishers, 409 pages.

Wuechner P., 2003. Performance Modeling of mobile networks using MOSEL-2, M.S. Thesis, Department of computer science, University of Erlangen, Germany.

Zreikat A. I., G. Bolch, 2007. "Performance Evaluation of Queuing Networks with Finite Capacity and non-exponential Distribution using MOSEL-2", Published in AMSE (Association for Modelling and Simulation in the Enterprises), Vol. 12, No. 4.

Al-Begain K., J. Barner, G. Bolch, A. I. Zreikat, 2003. The Performance and reliability modeling language MOSEL and its applications, International Journal in Simulation: Systems, Science and technology, Vol. 3, No. 3-4, pp. 66-80.

Zreikat A. I.,G. Bolch, J. Sztrik, 2003. Performance Modeling of Non-Homogeneous Unreliable Multi-Server systems using MOSEL, International Journal in Computers and Mathematics with Applications, Elsivier, Vol. 46, pp. 293-312.

Wüchner P., de Meer H., Bolch G., Roszik J., Sztrik J., 2007. Modeling Finite-Source Retrial Queueing Systems with Unreliable Heterogeneous Servers and Different Service Policies Using MOSEL, Proc. of ASMTA 2007 Conference, Prague, Czech Republic, June 4-6.

Gunter B., J. Roszik, J. Sztrik, P. Wüchner, November 2006. Modeling Finite-Source Retrial Queueing Systems with Unreliable Heterogeneous Servers and Different Service Policies Using MOSEL. Technical Report MIP-0611, University of Passau, Germany.

Wüchner P., H. de Meer, J. Barner, G. Bolch, 2005. MOSEL-2 - A Compact But Versatile Model Description Language And Its Evaluation Environment. Proc. of MMBnet'05 Workshop, University of Hamburg, Germany, September 8-9, pp. 51-59.

Zreikat A. I., S., Yerima, K., Al-Begain January, 2008. "Performance Evaluation and Resource Management of Heirarchical MACRO-/MICRO Cellular Networks Using MOSEL-2", Published in Wireless Personal Communications, Springer (USA), and Vol. 44, No. 2.

Wüchner P., K. Al-Begain, J. Barner, G. Bolch, May 2004. Modelling a single GSM/GPRS cell with delay tolerant voice calls using MOSEL-2, Proc. of UK Simulation Conference, Oxford, UK, pp. 88-94.

Barner, J. ; G. Bolch, 2003. MOSEL-2. Modeling, Specification and Evaluation Language, Revision 2 . In: Sanders, William (Hrsg.) : Proceedngs of the 13th International Conference on Modeling Techniques and Tools for Computer Performance Evaluation (Performance TOOLS 2003 Urbana-Champaign, Illinois, 2 - 5.9 2003)..

Zreikat A. I., Sep., 2011. "A new WIMAX/WI-FI Interoperability model and its performance Evaluation", submitted to Wireless Personal Communications, Springer (USA).

Buetel B. 2003."Integration of the Petri Net Analysator TimeNET into the Model Analysis Environment MOSEL," Technical Report, University of Erlangen-Nürnberg.

Wüchner P., 2005. "Extending the Interface Beetween the Modelling Language MOSEL and CSPL by Adding Simulation Constructs," Technical Report, University of Erlangen-Nürnberg.

Zimmermann A., 2005.TimeNET 3.0, User Manual, TU Berlin, 2001, available at: http://pdv.cs.tu-berlin.de/~timenet/TimeNET-UserManual30.ps.gz.

Bolch G., S. Greiner, H. De Meer, and K. Trivedi, 1998. "Queueing Nteworks and Markov Chains", John Wiley & Sons New York.

AUTHOR BIOGRAPHIES

AYMEN I. ZREIKAT is an Associate professor at the Information Technology Department, Mu'tah University, Jordan. He has obtained his B.Sc. in Computer Science from Yarmouk University, Jordan in 1990 and MSc in Computational Engineering from University of Erlangen, Germany in 2000. Additionally, he has obtained his Ph.D. from Bradford University, UK in 2003. In January, 2001, he has joint the Performance Modelling and Engineering Research Group at the Computing Department of Bradford University, UK. His area of research is in the Performance Evaluation and Resource Management of 3G Wireless Mobile Networks and beyond. He has published a set of international books, Journal and Conference papers in this field and he is responsible for reviewing a set of papers in this area of research in a very reputable Journals. Furthermore, he is a member of some national coordinating committees; (such as the coordinating committee for the management of Queen Rania Al-Abdullah center for Educational Technology, Jordan, April, 2009, also committee for Higher Education Accreditation Commission, May, 2009,…etc) and international organizations; i.e., MOSEL group. He has been appointed as an Assistant Dean at the Faculty of Science, Mutah University, Jordan, from 1/9/2008-1/9/2010. From 1/9/2010-1/9/2011, he has been appointed as the chairman of the IT in Mu'tah University. His e-mail address is: siayzrei@yahoo.com.

High-Precision, Robust Cascade Model for Closed-Loop Control of Ceramic Glow Plug Surface Temperature in a Diesel Engine

Ramita Suteekarn *
DTSquare GmbH
Nobelstraße 15,
70569 Stuttgart, Germany
rsuteekarn@borgwarner.com

Martin Sackmann,
Bernd Last,
BorgWarner BERU Systems GmbH
Mörikestraße 155,
71636 Ludwigsburg, Germany
msackmann@borgwarner.com

Clemens Gühmann
Chair of Electronic Measurement and Diagnostic Technology,
Technische Universität Berlin
Sekretariat EN13, Einsteinufer 17,
10587, Berlin, Germany
clemens.guehmann@tu-berlin.de

KEYWORD

Model-based control, system identification, glow plug

ABSTRACT

A closed-loop control of a glow plug in a diesel engine is a solution to replace a table-based regulation algorithm to minimise application effort and increase robustness. This paper proposes a method to develop a robust, real-time and accurate temperature model to be used with a model-based temperature controller. Analytical models provide *a priori* knowledge to the design and optimisation of steady-state temperature estimation for the nonlinear part of a Hammerstein-type dynamic model. Accuracy and robustness are improved compared to those of a classical multivariate nonlinear regression model and an artificial neural network model. Experimental results of a preliminary controller based on the developed model on a test bench and in a test vehicle show excellent dynamic accuracy.

INTRODUCTION

A modern glow plug system is equipped with a glow control unit (GCU), whose function is to regulate the glow voltage of the installed glow plugs, in order to satisfy the glow temperature demanded by the engine control unit (ECU). The importance of the glow temperature is not only in the cold start behaviour but also in the exhaust gas quality, (Last et al., 2008).

A current temperature control strategy is a lookup table-based voltage regulation (Houben et al., 2000), with the input variables of the current engine operating points and a desired glow temperature, and the output of a glow voltage to supply to the installed glow plugs. The lookup tables are predetermined during the development phase of the GCU, which involves comprehensive measurements on engine test benches and in test vehicles, to experimentally evaluate the required glow voltage for each desired temperature nouveau under almost all possible engine operating points. With every application variation, in the engine design or in the glow plug type, this tremendous effort, both time-consuming and expensive, must be undertaken again.

Another disadvantage of the current strategy is that it does not take into account the glow plug behaviour variation due to manufacturing tolerances between individual glow plugs. The production yield is consequently severely limited due to the imposed tolerance bandwidth on the product specification to ensure reliability.

PROPOSED SOLUTION

A closed-loop control of glow plug temperature is a solution to eliminate the rigidity of the table-based regulation strategy and the necessity of high development effort. The main requirement of the control loop in Figure 1 is the glow plug surface temperature estimation, due to the unavailability of a temperature signal in serial-production glow plugs.

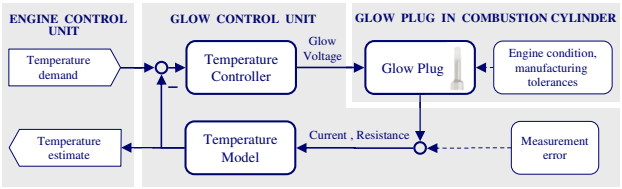

Figure 1: Closed-Looped Temperature Controller

By considering a glow plug as a system whose internal uncertainty is the manufacturing tolerances, affecting electrical and heat conduction, and energy conversion within the heating element; and whose external disturbances are the engine conditions, influencing the heat transfer between the glow plug surface and the surrounding, three crucial aspects in the development are as follows:

Aspect 1: Using the response of the installed glow plug as an indicator to evaluate the external influences, replacing the measurement signals of the engine operating condition and eliminating the dependency of the table-based algorithm thereof.

Aspect 2: Identifying individual glow plug characteristics to improve robustness against the manufacturing tolerances by adapting the controller accordingly.

Aspect 3: Designing for real-time application.

The third aspect imposes restriction on the computational complexity of the model. Existing glow plug simulation models, such as a finite-difference model (FDM) in (Formaggia et al., 2007) and FEM during the glow plug design phase, coupled with heat transfer analysis in a diesel combustion chamber, such

Proceedings 26th European Conference on Modelling and Simulation ©ECMS Klaus G. Troitzsch, Michael Möhring, Ulf Lotzmann (Editors)
ISBN: 978-0-9564944-4-3 / ISBN: 978-0-9564944-5-0 (CD)

as those reviewed in (Finol and Robinson, 2006), can offer detailed insights, but are invariably too computational intensive and not suitable for a system with unknown tolerances. On the other hand, artificial neural networks (ANN) can achieve high accuracy with adjustable complexity without requiring detailed knowledge of the system, but still require careful selection of the training regime, and can still result in complex computations of multiple nonlinear functions.

The most efficient model is thus a single-output temperature model based purely on the electrical behaviour with sufficiently high dynamic accuracy to simplify the control algorithm to a classical temperature controller. The structure of this paper follows the model development: Section 1 gives an overview of an analytical model of a BorgWarner ceramic glow plug, which presents an insight into the thermal-electrical behaviour; Section 2 lays a foundation of the temperature model by identifying the most influential electrical properties and their correlation to internal and external disturbances in sensitivity analyses based on the model in Section 1; and Section 3 bridges the gap between the analytical model and experimental data, gives a detailed procedure of temperature model optimisation with the consideration of application-related criteria, and presents the optimum temperature model structure to be used in closed-loop control.

1 Analytical Model of a Nominal Glow Plug

A ceramic glow plug can be modelled as a thermal-electrical system, whereby the specially designed, electrically conductive ceramic materials convert electrical power into heat production via the Joule effect. The electrical and thermal domains are further coupled by the temperature-dependant material properties.

The thermal-electrical behavioural model of an outer-heating ceramic glow plug by BorgWarner has been developed by BorgWarner. It is a two-dimensional FDM representing an axial-symmetric three-layer ceramic heating rod, protected by a steel outer sleeve and a steel body, as shown in Figure 2.

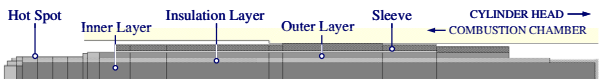

Figure 2: FDM Element Definition of an Outer-Heating Ceramic Glow Plug for Sensitivity Analysis

The thermal-electrical behaviour is described by a system of heat equations at each finite volume i:

$$\nabla q_i = I_{GP}^2 \left(\rho_{el,i} \frac{L_{el,i}}{A_{el,i}} \right) - \rho_i c_i \frac{dT_i}{dt}, \qquad (1)$$

where ∇q is the net heat flux output of the element; L_{el} and A_{el} the effective length and cross-sectional area with respect to electrical conductance; $\rho_{el}(T)$, $\rho(T)$, and $c(T)$ the temperature-dependent specific electrical resistance, density and heat capacity, respectively; and T the local temperature. Material properties were implemented as polynomial functions of temperature; for instance, heat capacity of a material m:

$$c_m = c_{o,m} + k_{c1,m}(T - T_o) + k_{c2,m}(T - T_o)^2, \qquad (2)$$

with the polynomial coefficients $\boldsymbol{c}_o \in \mathbf{R}^{1\times m}$ and $\boldsymbol{k}_c \in \mathbf{R}^{2\times m}$ determined using least-square method to fit literature tabular data, and T_o the reference temperature at 20°C. The net heat flux term is expanded by heat conduction to neighbouring elements and the cylinder head, and by convective and radiation heat transfer from surface elements to the surrounding. Surrounding condition under no external influence is modelled with free-convection. The electrical current I_{GP} is calculated from the glow voltage U_{GP} divided by the total resistance of the electrically-conductive elements, R_{GP}. The analytical model of a nominal glow plug under no external influence, that is, free convection, is referred to hereafter as the nominal model.

To simulate the dynamic behaviour, a discrete-time explicit calculation of the changes in temperature profile, material properties, and heat balance equations were carried out to yield time-variant temperature profile $\boldsymbol{T}(t)$ and resistance distribution $\boldsymbol{R}(t)$. Alternatively, by setting Dirichlet boundary conditions $\boldsymbol{T}(t=0)=T_{RT}$ and $\nabla \boldsymbol{q}_i - \boldsymbol{q}_{i,Joule}\ (t=t_{ss})=0$, the system of equations could be solved for the steady-state temperature profile $\boldsymbol{Tss}=[T_1 \ldots T_i]$ and electrical resistance distribution $\boldsymbol{Rss}=[R_1 \ldots R_i]$.

It is clear from Equations 1, 2, and higher-order temperature terms from radiation, that the glow plug is a highly nonlinear, dynamic system. However, most relevant to this work are the desired maximum surface temperature $T_{max} \in \boldsymbol{T}$, and the measurable total resistance R_{GP} and current I_{GP}.

2 Sensitivity Analyses

The aim of this phase is to analyse the glow plug behaviour to ascertain the correlation between the measurands I, R and the controlled variable T_{max}, the inputs and output of the temperature model, respectively. A theoretical approach was based on the nominal glow plug model with glow plug's ideal geometry and material properties, as detailed in the previous section. The system disturbances were introduced into the model as (a) raw material tolerances via temperature-dependent modification functions augmented to the polynomials in Equations 2; (b) geometrical tolerances in the critical areas via modification factors $\boldsymbol{k}_s$ multiplied to ideal geometric measures $\boldsymbol{s}$; and (c) external disturbances via a matrix of combined convective-and-radiation heat transfer coefficients $\boldsymbol{\alpha}_{equiv}$ at the glow plug surface layer. A parallel experimental approach was based on test-bench measurement data, with (a,b) tolerance uncertainties among 79 glow plugs from 14 different manufacturing batches, and (c) disturbances by means of pressurised air stream with adjustable flow rate directed head-on at the glow plug.

The experimental setup on a test bench allows the surface temperature to be measured by a pyrometer, and the total electrical resistance and current by a shunt.

In analysing the internal influences, Spearman rank- and Pearson product-moment correlation coefficients (ρ_S, ρ_P) were averaged from individual {$\boldsymbol{\alpha}_{equiv}$ | Flow rate} scenarios; whereas in analysing the external influences, the coefficients were averaged from individual {model's (a, b) configuration | glow plug} cases. In most cases, the coefficients (ρ_S, ρ_P) resulted in an identical ranking of influences. Table 1 and 2 show the top three main effects' ranking from the model-based and the experiment-based sensitivity analyses against internal and external disturbances, respectively. The suffix *nom* denotes the nominal value specified as reference points for voltage at 5.6V, and temperature at 1200°C*; HS*, denotes the simulated value at the element where the maximum temperature occurs. The symbol > is used in place where the influence rankings of the left-hand side has marginally more effect; while = is for equal influence. The symbol Δ stands for the difference between the scenario's simulated result and the result of the nominal model excited by the same voltage. By exciting a nominal glow plug under no external influence, or simulating the nominal model, with two voltages [U_{nom} U_{nom}+dU], the additional *reference resistance* $R_f = R_{GP}(U_{nom})$ and the *reference resistance gradient* $g_R = dR/dU$ can be calculated. The values were consequently independent of measured glow voltage U, and thus offered a bias-free glow plug characteristics.

Table 1: Sensitivity Analysis of Glow Plug Temperature Against Manufacturing Tolerances

Response	Main effects	
	Simulation	Experiment
Temperature	1. $I_{GP} > P_{HS} > P_{GP}$	1. $I_{GP} > P_{GP}$
T at nominal	2. R_{HS}	2. $R_f > g_R$
voltage U_{nom}	3. $R_f > g_R$	3. R_{GP}
Temperature	1. $R_{HS} > R_f$	1. R_f
gradient	2. I_{GP}	2. I_{GP}
dT/dU	3. g_R	3. g_R

Table 2: Sensitivity Analysis of Glow Plug Temperature Against External Disturbances

Response	Main effects	
	Simulation	Experiment
Temperature	1. $\Delta I_{GP} = \Delta R_{HS}$	1. I_{GP}
T at nominal	2. ΔR_{GP}	2. P_{GP}
voltage U_{nom}	3. P_{GP}	3. R_{GP}
Temperature	1. $\Delta I_{GP} = P_{GP}$	1. P_{GP}
gradient	2. I_{GP}	2. I_{GP}
dT/dU	3. ΔR_{HS}	3. R_{GP}

According to Table 1, the model-based and the experiment-based results show an agreement in that the steady-state maximum surface temperature of a glow plug has the largest correlation to the glow plug current, logically due to the thermal power being proportional to the electrical power $I_{GP}^2 R_{GP}$, then to the power, and the resistance. The second row predicts that the thermal response to the change in excitation voltage, at the same surrounding conditions, should be estimable from glow plug characteristic resistance measured at the nominal voltage, under no external influences.

From Table 2, the influence rankings between the simulation and the experimental data again were in good accord. Under variation of external influences, the most promising factors in determining the temperature at a nominal voltage $T(U_{nom})$ were the measured current, followed by the resistance and electrical power. The response of the temperature with respect to glow voltage, dT/dU was most correlated to the measured electric power P_{GP}. Mechanistic analyses by extracting changes of the current I_{GP} and power P_{GP} when compared to those of a nominal glow plug under no external influence offer even a better correlation. Analogous to the reference parameters from Table 1, these ΔI_{GP}, ΔP_{GP} and ΔR_{GP} *comparators* provide nearly glow plug-neutral behavioural indicators. The fact that neither the indicative $\boldsymbol{\alpha}_{equiv}$ nor the flow rate *FL* was in the top-three main effects was a positive sign that the external influence can indeed be deduced from the glow plug's electrical behaviour alone.

An advantage of the model-based sensitivity analysis is the complete transparency of the manufacturing tolerances' effects on the glow plug behaviour. While the results from both approaches agree that the measurable electrical signals (R_{GP}, I_{GP}) can be further utilised as indicator signals for the external disturbances and internal uncertainties, the simulation results make a step farther by ensuring that these signals are indeed good indicators regardless of the source or magnitude of manufacturing tolerances. The simulation model also offers a much quicker preliminary analysis of a new glow plug type, to predict whether the proposed model development procedure can be adapted successfully.

3 Procedure for Development of Cascade Temperature Model of Glow Plug in Engine

The previous phase demonstrates that both the intrinsic behaviour of a glow plug and the external influences by way of heat exchange behaviour with the surrounding can be estimated qualitatively from merely electrical resistance and current signals. This phase aim is to predict the temperature quantitatively using the available signals and *a priori* knowledge from the simulation models.

3.1 Structure of Cascade Model

The structure of the temperature model was selected as a Hammerstein-type nonlinear dynamic system, which generally offers a good behavioural approximation in many automotive systems (Kirschbaum et al., 2009). The inputs of the nonlinear static function are measurable electrical properties (R, I) of the installed

glow plug. By selecting its output to a steady-state temperature estimate, and designating the linear dynamic transfer function to describe the dynamic response of the system to the step response, from the current temperature estimate to the next as updated by the preceding nonlinear block, the modelling task was simplified by separately tackling the steady-state accuracy and the dynamic behaviour. By setting the discrete time step Δt to that of the sampling period of GCU at 30.5ms, one further simplification is to assume that during the short interval of Δt, the dynamic behaviour can be represented by a nominal transfer function regardless of the manufacturing tolerances or the engine conditions,

$$G(s) = \frac{K(\tau_N s + 1)}{(\tau_{P1} s + 1)(\tau_{P2} s + 1)}. \quad (3)$$

The time constants were identified with least-square method from experimental data of nominal glow plugs under no external influence with temperature step variations.

The main focus of this work is the identification of the nonlinear static part, beginning by first describing the nonlinear time-invariant function as a mixed effect model,

$$\hat{T} = f_{NL}(F, N, \Theta, T_o), \quad (4)$$

where $\boldsymbol{F}$ is a vector of glow plug-specific internal influences, $\boldsymbol{N}$ a vector of indicators to external disturbances, $\boldsymbol{\Theta}$ a weighting coefficient vector of influences and disturbances, and T_o the expected temperature of a given glow plug under no external influences. Equation 4 was then broken down into a cascade of effects

$$\hat{T} = f_{NL,L1}(N, \Theta_N, T_o), \text{ and} \quad (5)$$

$$[\Theta_N, T_o] = f_{NL,L3}(F, \varphi). \quad (6)$$

That is, Equation 5 predicts the steady-state temperature of a given glow plug based on the external influence indicators, $\boldsymbol{N}$, and an expected temperature of that glow plug under no external influence, T_o. Equation 6 then in turn describes how large the impact of the external influences has on the given glow plug, $\boldsymbol{\Theta_N}$, and its expected temperature, T_o, based on the glow plug intrinsic properties $\boldsymbol{F}$ and the model parameters, $\boldsymbol{\varphi}$.

Let vector $\boldsymbol{N}$ be a regression vector composed of measured electrical properties, their higher-order terms, their relation with respect to the simulated expected values, and the interaction thereof, then Equation 5 can be converted to a linear function

$$\hat{T} = \Theta_N \times N + T_o, \quad (7)$$

with $\boldsymbol{\Theta_N} \in \mathbf{R}^{1\times P}$, and $\boldsymbol{N} \in \mathbf{R}^{P\times 1}$ for P indicators. Let $\boldsymbol{F}$ be a regression vector of Q selected glow plug characteristic properties. Then equation 6 becomes

$$\begin{aligned} \Theta_N &= F \times \varphi_\Theta, \\ T_o &= F \times \varphi_{To} \end{aligned} \quad (8)$$

where $\boldsymbol{\varphi}_\Theta \in \mathbf{R}^{Q\times P}$, $\boldsymbol{\varphi}_{To} \in \mathbf{R}^{Q\times 1}$, and $\boldsymbol{F} \in \mathbf{R}^{1\times Q}$. From the above structure configuration, the system identification tasks were (i) the selection of external influence indicators $\boldsymbol{N}$; (ii) the selection of glow plug characteristic properties $\boldsymbol{F}$; and then (iii) the model parameter estimation.

Considering the three criteria of model development — namely, the accuracy of the temperature estimate, the robustness against the external and internal influences, and the real-time capability — the system identification tasks outlined above become intertwined with multiple objectives. An approach is to view them as multi-level optimisation, parallel to the cascade of effects. The procedure of evaluating the quality of a model structure with an arbitrary configuration $\{\boldsymbol{N_C}, \boldsymbol{F_C}\}$ based on measurement data of M glow plugs under D external influence conditions, excited by U levels of glow voltages, $(T, I, R) \in \mathbf{R}^{M\times D\times U}$, is then as follows:

Level 0: Define variables

$\boldsymbol{N_C} = [N_1 \ldots N_P]$ and $\boldsymbol{F_C} = [F_1 \ldots F_Q]$

Level 1: For each glow plug, at each level of external disturbance, solve for

$\Theta_{N,L1}\big|_{m,d} = \left[\Theta_{N1,L1} \ldots \Theta_{NP,L1}\right]_{m,d}$ and $T_{o,L1}\big|_{m,d}$ at

$$\min\left(rms\left(T_i - \left(\Theta_{N,L1,i} \times N_{c,i} + T_{o,L1}\right)\right)\right),$$

where i=1…U for glow voltage levels.

Level 2: For each glow plug under all conditions, find intermediate coefficients $\boldsymbol{c_\Theta}|_m = [c_{\Theta 1} \ldots c_{\Theta P}]|_m$ and $c_{To}|_m$ as functions of external influences $\boldsymbol{N_C}$ in

$$\begin{aligned} \Theta_{N,L2}\big|_m &= \left[c_{\Theta 1} \cdot N_1 \ldots c_{\Theta P} \cdot N_P\right]_{m,d=1\ldots D} \\ T_{o,L2}\big|_m &= \left(c_{To,1} \cdot N_1 + \ldots + c_{To,P} \cdot N_P\right)\big|_{m,d=1\ldots D} \end{aligned}, \text{ at}$$

$$\begin{aligned} &\min\left(rms\left(\Theta_{N,L1,j} - \Theta_{N,L2,j}\right)\right) \\ &\min\left(rms\left(T_{o,L1,j} - T_{o,L2,j}\right)\right) \end{aligned}$$

with j=1…D×U for voltage and disturbance levels.

Level 3: For all glow plugs, under all conditions, solve for the model parameters $[\boldsymbol{\varphi}_\Theta, \boldsymbol{\varphi}_{To}]$ to satisfy

$$\begin{aligned} &\min\left(rms\left(c_{\Theta,k} - F_k \times \varphi_\Theta\right)\right) \\ &\min\left(rms\left(c_{To,k} - F_k \times \varphi_{To}\right)\right) \end{aligned},$$

where k = 1… D×U×M.

Therefore, Level 3 yields the final model, with (P+1)×Q identified model parameters:

$$\hat{T} = F \times \varphi_\Theta \times N + F \times \varphi_{To}. \quad (9)$$

Notice that as the optimisation level goes higher, less specific information regarding the internal and external influences is available, and the model becomes more general. In Level 1, clear distinction of individual glow plugs must be known, as well as the level of external disturbances. The model parameters $\boldsymbol{\Theta}_{N,L1}$ and $T_{o,L1}$ only work with that specific glow plug under that known external disturbance level. In Level 2, still the identity of the glow plug must be known, but the intermediate model parameters, $\boldsymbol{c}_{\Theta}$ and $\boldsymbol{c}_{To}$, apply to that glow plug under any external disturbances. Lastly, in Level 3, the final model parameters, $\boldsymbol{\varphi}_{\Theta}$ and $\boldsymbol{\varphi}_{To}$, describe the behaviour of all glow plugs under all circumstances.

3.2 *Selection of Influence Indicators*

The challenge would be to optimise the accuracy and robustness of the final model in Level 3, while aiming for simplicity of the model with few but the most influential variables in $\boldsymbol{N}$ and $\boldsymbol{F}$.

Typically, the task of optimising the model structure in system identification begins with high complexity to capture the essence of the system. However, the analytical model as well as previous experimental data gave *a priori* knowledge of influential ranking to the glow plug behaviour, and thus reducing the initial complexity. From the sensitivity analyses in the preliminary phase, the temperature at a certain voltage $T(U_{nom})$, as well as the response to voltage change dT/dU, show strong correlations with electrical properties, as well as the comparators between the electrical behaviour of a glow plug under external influences and that of the same glow plug under no external influence. Hence, the logical choices for external influence indicators $\boldsymbol{N}$ are the variables I_{GP}, P_{GP}, and R_{GP}, their comparators, their nonlinear terms as well as interaction terms thereof. To reduce the computational complexity, the steady-state resistance and maximum surface temperature of the nominal model were approximated by polynomial functions, where NM signifies the results from a simplified model:

$$R_{\mathrm{NM}} = f_{NMU1}(U) = R_{NM,o}+a_{U1}U+a_{U2}U^2+a_{U3}U^3$$

$$T_{NM,U} = f_{NMU2}(U) = T_{NMR,o}+b_{U1}U+b_{U2}U^2+b_{U3}U^3, \quad (10)$$

and additional reverse models:

$$U_{\mathrm{NM}} = f_{NMR1}(R) = U_{NM,o}+a_{R1}R+a_{R2}R^2+a_{R3}R^3$$

$$T_{NM,\mathrm{R}} = f_{NMR2}(R) = T_{NMU,o}+b_{R1}R+b_{R2}R^2+b_{R3}R^3, \quad (11)$$

where the inputs U and R are the real-time measured values, and the coefficients a_U, a_R, b_U and b_R were determined from least-square fitting to the nominal model subjected to the voltage range 2…12V with ±0.5% accuracy. Therefore, the comparators $\Delta R_{GP,U}$, $\Delta I_{GP,U}$ and $\Delta P_{GP,U}$ are then calculated from:

$$\Delta R_{GP,U} = R_{GP,measured} - R_{\mathrm{NM}}(U_{GP,measured})$$

$$\Delta I_{GP,U} = I_{GP,measured} - U_{GP,measured}/R_{\mathrm{NM}}(U_{GP,measured}), \quad (12)$$

$$\Delta P_{GP,U} = P_{GP,measured} - U_{GP,measured}^2/R_{\mathrm{NM}}(U_{GP,measured})$$

Three augmented comparators, $\Delta U_{GP,R}$, $\Delta I_{GP,R}$ and $\Delta P_{GP,R}$, are also added using the reverse models.

Thus, an example of initial $\boldsymbol{N}$ vectors representing the external influence indicators is

$$\boldsymbol{N}_{initial} = [\Delta R_{GP,U} \;\; \Delta I_{GP,U} \;\; \Delta U_{GP,R} \;\; \Delta P_{GP,U}]^{\mathrm{T}} \quad (13)$$

On the other hand, based on *a priori* knowledge of the manufacturing tolerances' effect upon the change in the glow plugs' electrical properties, Table 2 illustrates that the summation of tolerances and individual glow plug characteristics under a fixed external influence can be captured by a set of bias-free reference parameters: the resistance at the nominal voltage and the resistance gradient measured at no external influence. Hence, a sample heuristic choice for the characteristic vector $\boldsymbol{F}$ is then:

$$\boldsymbol{F}_{initial} = [R_{f1} \;\; R_{f2} \;\; g_R \;\; R_{\mathrm{o}}]. \quad (14)$$

3.3 *Model Structure Optimisation Procedure*

The task of system identification and multi-level optimisation of the system matrix structure is summarised in Figure 3.

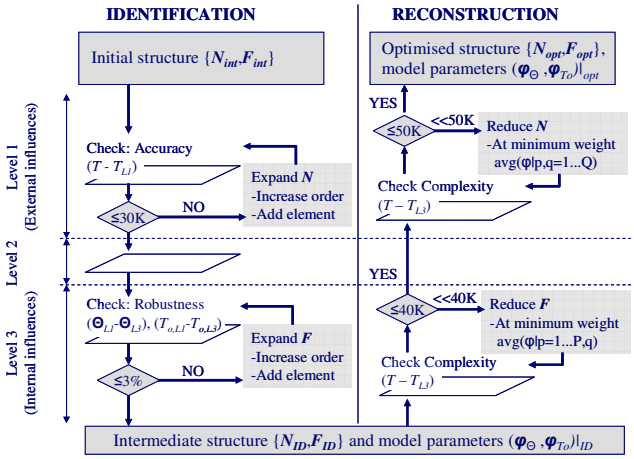

Figure 3: Optimisation Routine of Model Structure

From the guideline above, the optimal system matrices were found to be:

$$\boldsymbol{N}_{opt} = [\, I_{GP} \;\; R_{NM}^2/\Delta U_{GP,R} \;\; R_{NM}\,]^{\mathrm{T}} \quad (15)$$

$$\boldsymbol{F}_{opt} = [R_{f1} \;\; g_R \;\; 1/g_R], \quad (16)$$

with 12 model parameters ($\boldsymbol{\varphi}_{\Theta}$, $\boldsymbol{\varphi}_{To}$). The determination of each level's coefficients was with least-square method, requiring the amount of available measurement data in each case at least equal to the degree of freedom, as summarised in Table 3.

The relaxing accuracy thresholds from 30K to 50K reduce computational complexity at the cost of accuracy. The thresholds can be increased further for a loose control strategy with emphasis on hardware limitation, or conversely tightened in high-precision control. Likewise, the 3% limit imposed at Level 3 can be adjusted to change the level of robustness against internal uncertainties.

For instance, if the manufacturing tolerances can be improved to result in smaller variance between glow plugs, or if the model parameters are allowed to be identified and utilised within each manufacturing batch, the percentage as low as 1% can be achieved sufficiently by setting $\boldsymbol{F}$ to merely R_{f1} to distinguish one glow plug from another.

Table 3: Requirement of Measurement Data Set for System Identification

Level	Specificity		Degree of Freedom	
	# Glow Plug	# Disturb. Level	Identified Parameters	Minimum # training data points
1	1	1	$\boldsymbol{\Theta_{N,LI}}$, $\boldsymbol{T_{o,LI}}$	P + 1
2	1	D	$c_{\boldsymbol{\Theta}}$, $\boldsymbol{c_{To}}$	(P+1)·P
3	M	D	$\boldsymbol{\varphi}_{\Theta}$, $\boldsymbol{\varphi}_{To}$	(P+1)·Q

Another application-oriented approach to configure the optimisation routine is to aim for maximum number of glow plugs with acceptable maximum error. An additional residual analysis at Level 3 can also illuminate how the failed glow plugs can be identified from their reference values $\boldsymbol{F}_{fail}$, when compared to those of the passed glow plugs, $\boldsymbol{F}_{pass}$. Consequently, a glow plug that is potentially extreme in behaviour, lying outside the identified model's reliability domain, can be discarded as early as the end of production by means of reference parameter range check, or to be sorted to use with another set of model parameters $(\boldsymbol{\varphi}_{\Theta}, \boldsymbol{\varphi}_{To})|_{\#2}$ identified specifically for this glow plug subtype.

Initialisation Routine

The objectives of the initialisation routine are to identify a glow plug characteristic $\boldsymbol{F}$, and to harvest the basis of external influence indicator $\boldsymbol{N}$, at known engine condition $\mathbf{BP_o}$. The routine algorithm is to excite the installed glow plugs, measure the electrical properties, calculate and then save the resulting $\boldsymbol{F}_{BPo}$ and $\boldsymbol{N}_{BPo}$ in the glow control unit's memory. The excitation profile $U_{INIT}(t)$ is defined by the model's $\boldsymbol{N}$ and $\boldsymbol{F}$. Further details on initialisation routine can be referred in (Last et al., 2012).

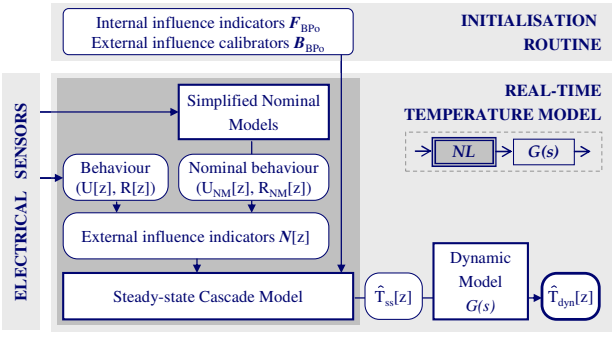

Figure 4: Dynamic Cascade Model of Glow Plug Surface Temperature

RESULTS

Simulation Results and Model Comparison

Table 4 shows a comparison of steady-state temperature accuracy, when all measurements had been used in the identification phase, among (1:CM) the cascade temperature model developed from the proposed method; (2:ANN) an artificial neural network of [*U*,*I*,*R*,*P*] inputs with one hidden-layer, 12 hidden nodes, and *tanh* activation functions, and (3:NLR) a multivariate nonlinear regression model of the electrical properties $[I^n, R^n, P^n]$ | n=[-1, 0, 1, 2]. The measurement data for both system identification and validation were obtained from 79 glow plugs, subjected to varying test bench conditions that represent more than 80% of full engine operating range. The model complexity was quantitatively considered in three areas: (P) number of model parameters, (M) number of multiplications, and (A) number of additions

Table 4: Steady-State Accuracy Comparison with the Complexity of Steady-State Temperature Models

Model	Model Complexity		Accuracy at 100% Training	
	P M , A	Type	RMS(εT)% MAX(εT)%	% Glow Plug with MAX|εT|±3%
1	20 31 , 20	CM	2.1 14.4	89.9
2	72 - , -	ANN	4.8 19.0	40.7
3	10 13 , 9	NLR	4.8 18.5	34.2

The accuracy of the proposed Model (1) was superior to those of classical Models (2) and (3), using the criteria of overall model accuracy as well as the model applicability coverage within ±3% error threshold. However, in real application, it is not possible to measure every glow plug at the end of manufacturing and update the model parameters accordingly.

To validate the robustness against manufacturing tolerances, the identification phases of Models (1) and (2) and the training phase of Model (3) were additionally conducted with incomplete sets of measurement data. To represent the scalability of the model robustness, the percentage of a number of glow plugs used for model training versus the total number of glow plugs range from 15% to 100%. For example, at 15% training selection, the measurement data of 12 randomly selected glow plugs out of the total 79 glow plugs were used to identify Model (1) parameters, then the same data were used for the identification of Model (2) and the training of Model (3). This selecting and training procedure was carried out 100 times with different random glow plug sets, in order to compensate the dependency of artificial neural network models on randomised initial weights and also to neutralise the overall dependency on which glow plugs were selected

in a training set. Each point in Figure 5 is the average value of the model results of 100 different model parameter sets. The dashed lines represent the robustness perceived during the training phase when validated with only the selected glow plugs for training, while the solid lines represent the real robustness across all 79 glow plugs.

The limitation of the training percentage represents the real challenge in application, where only a small sample of glow plugs are available in the development phase of the simulation model to be implemented in GCUs prior to online usage. From Figure 5, the proposed cascade model's robustness is higher than those in ANN and NLR, as shown that even with reduced percentage of training data available, the temperature errors are still lower and the applicability coverage still higher.

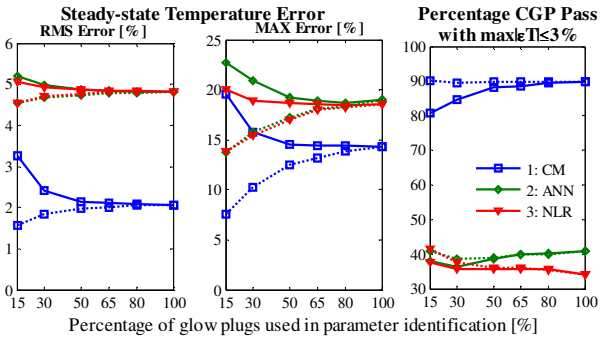

Figure 5: Robustness Comparison

Experimental Results

The developed dynamic temperature model was implemented in a rapid-prototyping system to test the closed-loop control strategy. The algorithm of the temperature model and controller was built in MATLAB/Simulink and transferred to an Autobox unit. The real maximum surface temperature was measured by a pyrometer on a test bench, and calculated as a function of internal glow plug temperature in an engine using a special-type glow plug with an internal thermocouple near the hot spot. The controller was a PI/PT_1 type. Further boundary conditions and bench specifications are discussed in more details in (Last et al., 2012).

The model robustness against external disturbances was tested with the thermocouple glow plug on a test bench with varying air flow rate directed head-on and parallel to a glow plug, and in a test vehicle driven at high dynamic range covering city driving cycle. The dynamic temperature model achieved very high precision accuracy on the test bench at ±1.7% maximum temperature error during 225-second cycle, and in the engine at ±4% calculated maximum error during a 800-second cycle. The closed-loop controller accuracy to maintain the desired glow plug temperature at T_{nom} under all conditions was excellent with 2% RMS error on test bench and 1.5% RMS error in engine. The compensation between delayed controlled voltage and over-nervous temperature estimator contributed to the disparity in model and controller accuracy in the engine.

CONCLUSION

The proposed method of model development with the aim for model-based control using *a priori* knowledge and experimental data has yielded a dynamic cascade model. The approach to model a cascade of effects, with the initial selection of physically-meaningful internal variables based on sensitivity analyses, and an integrated model structure optimisation and parameter identification procedure with configurable objectives led to a good balance between robustness, accuracy, and real-time capability. Rapid-prototype implementation on the test bench and in the test vehicle shows extremely accurate real-time dynamic temperature estimate and excellent control accuracy.

REFERENCES

B. Last, H. Houben, M. Rottner, Stotz, 2008. "Influence of modern diesel cold start systems on the cold start, warm-up and emissions of diesel engines". *8th International Stuttgarter Symposium*

H. Houben, G. Uhl, H. Schmitz, M. Endler, 2000. "Instant Start System (ISS) - The electronically controlled glow system for diesel engines". *MTZ* 61/2000

L. Formaggia, S. Micheletti, R. Sacco, A. Veneziani, 2007. "Mathematical modelling and numerical simulation of a glow-plug". *Applied Numerical Mathematics* 57/2007

C. A. Finol, K. Robinson, 2006. "Thermal modelling of modern engines: a review of empirical correlations to estimate the in-cylinder heat transfer coefficient". *Proceedings of the Institution of Mechanical Engineers, Part D: Journal of Automobile Engineering*

F. Kirschbaum, D. Boja, R. Sauermann, 2009. "Model Based Controller Calibration on Powertrains". *Design of Experiments (DoE) in Engine Development.* Expert Verlag

B. Last, M. Eberhardt, M. Sackmann, I. Demirdelen, F. Puente, R. Suteekarn, S. Schmauder, 2012. "Closed Loop Control Strategies for Glow Plug Surface Temperature". *12th International Stuttgarter Symposium*

AUTHORS

RAMITA SUTEEKARN studied Master Programme in Automotive System Engineering at RWTH Aachen. She is employed by DTSquare GmbH to work in a BorgWarner BERU Systems GmbH advanced research project to develop a controller for ceramic glow plugs.

Dr.-Ing. MARTIN SACKMANN is Manager of the Modeling, Analysis and Reliability Test Department in Global Engineering of Cold Start and Ignition Systems at BorgWarner BERU Systems GmbH.

Dr.-Ing. BERND LAST is Director of Cold Start and Ignition Engineering Department at BorgWarner BERU Systems GmbH.

Prof. Dr.-Ing. CLEMENS GÜHMANN is Head of Chair Electronic Measurement and Diagnostic Technology, Department of Energy and Automation Technology at Technische Universität Berlin.

VEHICLE NAVIGATION SYSTEM

Camelia Avram
Adina Aştilean
Dan Radu
Automation Department
Technical University of Cluj Napoca
Ge. Bariţiu street, no. 26 – 28, Cluj – Napoca, Romania
E-mail: camelia.avram@aut.utcluj.ro
adina.astilean@aut.utcluj.ro
dan.radu@aut.utcluj.ro

KEYWORDS
RSSI, VANET, road traffic concestion, wireless communication, vehicle to vehicle communication.

ABSTRACT

The paper proposes a vehicle flux estimator, based on Received Signal Strength Indicator measurements in order to prevent the road traffic congestions. Successive RSSI intensity determinations and the corresponding time values were used to estimate the vehicle flux in various conditions. A hierarchical network model, including a simulation module and experimental data, was implemented. In order to estimate the current traffic state, a new strategy in which a special attention was given to information collected from the converging streets near the main crossroads was elaborated. The updated information was used by a road traffic simulator in order to improve the traffic flow.
The proposed solution could contribute to the improvement of the performances obtained using other existing traffic control and monitoring systems.

INTRODUCTION

The main cause of congested traffic is that the vehicle volume is closing to the maximum capacity of the roads network. As the cities evolve one of the problem that rise is traffic congestion.
Congestion involves queuing, slower speeds and increased travel times, which impose costs on the economy and generate multiple impacts on urban regions and their inhabitants. Congestion also has a range of indirect impacts including the marginal environmental causes, impacts on quality of life, stress, safety as well as impacts on non-vehicular road space users such as the users of sidewalks and road frontage properties.
Strategic action to reduce traffic volume to a level where conditions do not vary too much from day to day and practical measures to provide good alternatives for freight and passenger movements, which reduce the intensity of use of scarce road space in congested conditions, are proposed by Goodwin (2004) to solve the traffic congestions.

Several authors present a system that allows vehicles to cooperate in order to reduce the traffic congestion. The proposed vision explores the concept of dynamic time space corridor that can be negotiated between cooperating vehicles to guarantee congestion-free journeys from departure to arrival (Sivaharan et al 2004, Morla 2005).
Mayor (2009) investigates the feasibility of a distributed traffic information system based on Inter-Vehicle Communication (IVC) technology. In IVC-based ATIS (Advanced Transportation Information Systems), vehicles are envisioned to exchange precise position information from satellite navigation data (GPS) via IVC at low cost to optimize traffic flows and provide valuable, real-time traffic information to the drivers.
Another approach developing a new tool for simulation which integrates inter-vehicular communications, Traffic and Network Simulation Environment (TraNS) links and two open-source simulators: a traffic simulator, SUMO, and a network simulator, ns2 is presented by Yang et al 2005.

The proposed paper presents a navigation system that receives real time road traffic information, transmitted in a Wi-Fi based VANET network, in order to detect and estimate possible traffic congestions. A new strategy in which a special attention was given to information collected from the converging streets near the main crossroads was elaborated in order to estimate the current traffic state. The updated information is used by a complex road traffic simulator in order to improve the traffic flow.
The information exchange, regarding congestions and traffic light queues, among the servers placed in the main crossroads and a central control station is performed using a dedicated wired network. In parallel, several vehicles, with Wi-Fi capabilities, form an ad-hoc network in order to transmit warnings. The vehicles send messages, including current speed and other specific zone information to a local server. Based on the received signal strength, the server can determine the position of the vehicle and can approximate if it is in a moving or waiting state. The correlation of these data is

Proceedings 26th European Conference on Modelling and Simulation ©ECMS Klaus G. Troitzsch, Michael Möhring, Ulf Lotzmann (Editors)
ISBN: 978-0-9564944-4-3 / ISBN: 978-0-9564944-5-0 (CD)

used to obtain the needed updated information about the current queues length for each crossroad.
The paper is structured in four sections: after the presentation of the early work in the field, the second section describes the vehicle flux estimator based on Received Signal Strength Indicator measurements, the system architecture of the navigation system is presented in the third section; some experiments, tests and simulation results are discussed in the fourth section, the main conclusions and directions of the future being presented in the fifth section.

VEHICLE FLUX ESTIMATION

The paper proposes a vehicle flux estimation stategy based on RSSI measurements as follows.
The time required to cover the distance between two crossroads is used to determine the road traffic volume at different moments. Successive RSSI intensity and corresponding time values measurements are performed in order to estimate the moments in which a vehicle is in the closest position to an Access Point (AP). Three sets of measurements, the first two for AP situated near the origin crossroad (the crossroad corresponding to the origin of a road segment) and the third for an AP pertaining to the destination intersection (the end of the crossroad segment) are needed to calculate the travel time for the corresponding road segment. The three AP correspond to the entering and leave of the origin intersection, and the third to the entering in the next intersection (the end of the segment).
The distributed traffic control units assigned for each crossroad allow the temporary storing and the processing of the data transmitted from vehicles and from neighbor intersections.
Taking into account the temporary data registered, there are two categories of vehicles: cars that enter for the first time in a crossroad and the others, present in the network. In the moment in which the first frame transmitted by a vehicle, which travels on a road segment (street) to an intersection, is received via the corresponding AP, the system verifies if other frames, having the same id, were transmitted from the neighbor crossroads. For each vehicle which travels to and from an access point, successive values, representing the RSSI measured intensity, are compared in order to determine the maximum value, obtained in the closest point from the AP. When the maximum value is found, it is stored and all the others values are deleted. The time moment corresponding to the found maximum value is also registered. For each vehicle crossing the intersections, the moments corresponding to the entrance and leave of that intersection are stored. Based on the correlation between the identity of each access point and its position in intersection, the movement direction of the vehicle (next crossroad) is determined. So, it is possible to transmit the identity data of vehicles to the next crossroads they enter, before their arrival.

SYSTEM ARCHITECTURE

The conceptual network model of the Navigation System is presented in Figure 1.
In the network model, the city map is divided into several, less complex networks. The resulting hierarchical routing network consists of the higher, abstract level, where each area (sector) is represented as a node and the detailed level, consisting of all corresponding areas.
The Simulation Nodes (SN) are represented by computers or virtual machines (running on application servers) used to simulate the traffic behaviour (their main functions are to collect data, to change the control algorithms and to initiate different scenarios).
Taking into account the information exchange initiator, the messages can be local messages (from the road traffic simulator, related to data acquisition, routing system etc.) and inter-zones messages, sent by a different PC, and having a unique or several receivers (broadcast messages). Each node serves several access points which receive/broadcast messages from/to vehicles. The SN is a multi-thread Wi-Fi server which waits for incoming client connections in order to collect traffic information from the vehicles. The Wi-Fi client module is located in the moving vehicle and it initiates an ad-hoc network connection to the server as soon as it enters in the radio range of the server. Then, the client computes the RSSI value of the Wi-Fi server and periodically sends this value to the server.

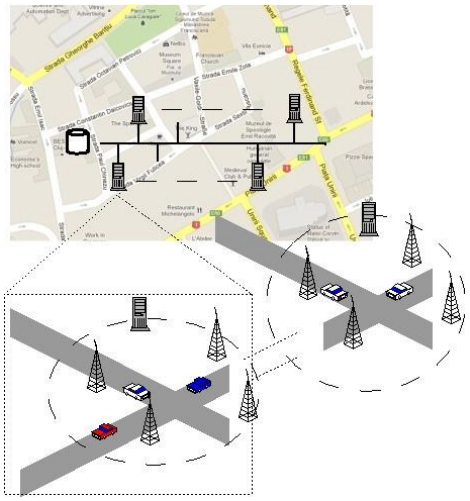

Figure 1: Conceptual network model used for simulation

The software architecture of the system is presented in Figure 2.

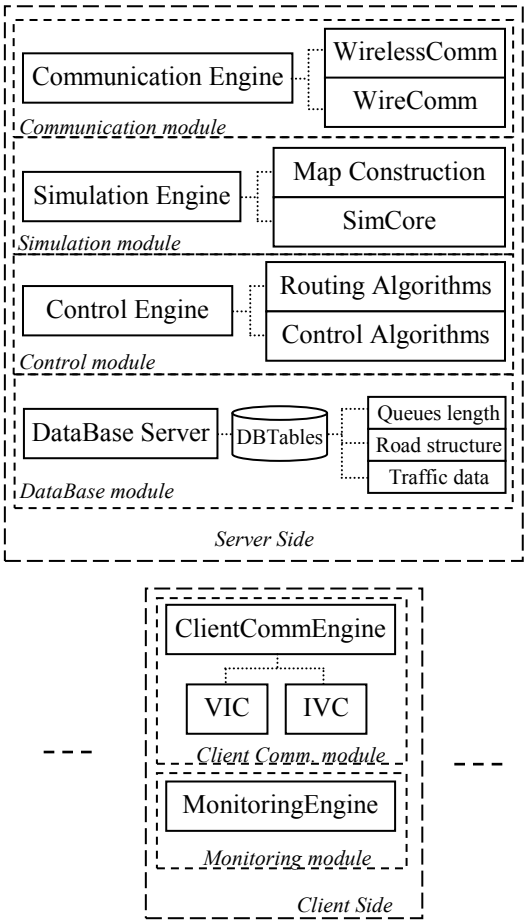

Figure 2: The Software Architecture

Communication Module performes:

- Wireless communication – for the data exchange from traffic (vehicles and infrastructure), to the WiFi AP;
- Wired communication – for the data exchange among different SNs.

Simulation module generates a virtual map for each zone. This module will utilize a virtual representation of the entire system (vehicles, roads structure and communication) and will detect the vehicles movement.

The **Simulation Engine** (SE) reads the information contained in the simulated map from xml files which describe the map and the initial state. The map file contains information about the length of the segment, traffic light, next segment, no. of lanes and type of the segment. The initial state file contains information for each segment regarding the number of vehicles and the time they need to pass through the segment. During the simulation, the program can start several clients all acting in the same manner: first, the client initiate a connection; after this is established, the server sends the initial data (several xml files) to start the simulation; an acknowledgement message is sent in the case in which all the files are successfully transmmited. Then the communication channel is closed.

The **Vehicle Movement Detection** module (VMD) is used to determine the trajectory of the vehicle within a traffic zone based on RSSI. This tool was developed and implemented in Java, using a client-server architecture and Java socket programming in an ad-hoc network. The proposed method is usefull to identify the congested traffic zones.

The Control Module is responsible with the setting up of the control strategies and the routing algorithms (Hierarchical Routing System - HRS).

The HRS calculates the best routes based on the last traffic information. It offers dynamic route guidance, alerting the driver regarding the congested roads and consists of two parts: the Global Routing System (GRS) and the Area Routing Systems (ARS).

The GRS determines the zones with a normal, usual, traffic flow; inside these zones the ARS updates the optimum routes. Finally, the recommended trajectory is composed by the concatenation of the best routes computed for each component area.

In accordance with the distributed approach a hierarchical Dijkstra algorithm is used to determine the best route in both cases (GRS and ARS). Probability values are assigned for possible alternatives inside the routing procedure. The probability tables contain only local information related to the best routes. The final route is composed of a list of nodes constituting the recommended trajectory.

Data Base Server realizes the connection to the data base tables'. The queues length, road structure and traffic data are stored in these tables.

The Client Comm. Module implements the communication functions for clients which are vehicles or traffic signs.

A Vehicle to Vehicle (V2V) communication based scenario was analyzed and tested.

Two different types of communication were taken into account:

- Inter Vehicle Communication (IVC);
- Vehicle to Infrastructure Communication (VIC).

V2V communication can be applied into several scenarios from which can be mentioned danger warnings (inter vehicle) or communication with *traffic signals* (vehicle to infrastructure communication).

Vehicles are able to communicate, to sense their environment, to control their speed and direction, and in general to cooperate with each other. Numerous objects from the urban landscape are also able to communicate and sense their environment (communicating and sensing signposts, sidewalks, and street lamps).

V2V communication system must fulfill some major requirements, like: everywhere availability, utilization of existing technology and low operating costs. As a solution to these problems, this paper proposes a V2V communication based on WiFi technology (available on each computer), the information being sent using ad-hoc networks.

The Monitoring Module displays the received traffic information from traffic signs, other vehicle or from a server, regarding congestions, road closure and the best routes to follow.

SIMULATION AND TESTING

All the experiments took place in Cluj-Napoca city. The RSSI values were experimentaly determined transmitting data between two WiFi equipments in a client-server configuration in real road traffic conditions. Other results were obtained in different simulation scenarios.

The testing scenario for the VMS simulation was developed based on the following hardware architecture:

Wi-Fi Server: Intel Core 2 Duo Laptop, with 2 GHz CPU, 2 GB RAM and Intel Wi-Fi Link 5300 AGN supporting 802.11 b/g/n;

Wi-Fi Client: Intel Core i7 Laptop, with 1.6 GHz CPU, 4 GB RAM and Intel Wi-Fi Link 5300 AGN supporting 802.11 b/g/n. The Graphical Interface for WiFi Client and WiFi Server are presented in figure 3.

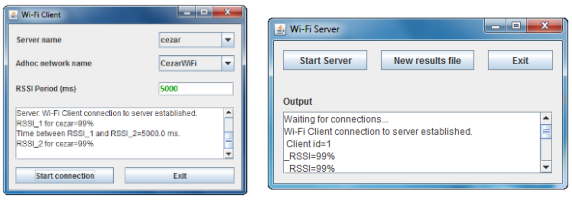

a) b)

Figure 3: a)Wi-Fi Client Java applications; b) Wi-Fi Server Java applications

Figure 4 details the setup of the experiment with two cars (Wi-Fi Client) and one Access Point (Wi-Fi Server) connected in an ad-hoc network.

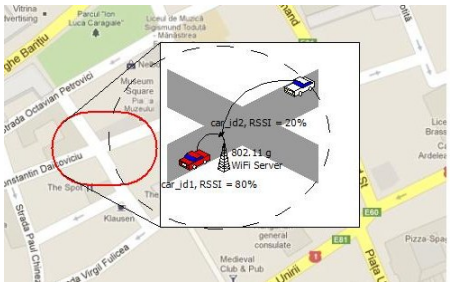

Figure 4: Vehicle movement detection scenario (speed=40 km, time interval=6 s)

For checking out the feasibility of Wi-Fi VMD module, many relevant experiments were initiated, some average values of the obtained results being presented below.

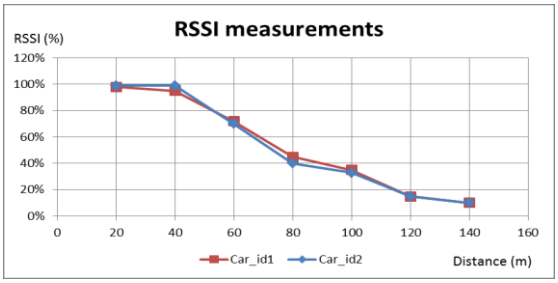

Figure 5: Measurement of RSSI value at different distances from the AP

In the first case, two cars moved and the client RSSI values were measured at different distances from the access point. Figure 5 represents the corresponding variations of RSSI values with the distance.

In figure 6, the presented RSSI values were computed by the Wi-Fi client and transmitted to the server, during a time intervals of 6 s, at speeds up to 45 km/h.

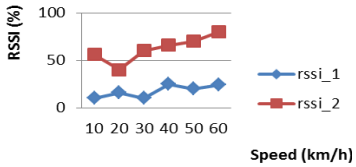

Figure 6: Received RSSI Values from a Moving Vehicle During a Time Interval of 6 s

The VMD module can be successfully used to determine the movement of vehicles within a traffic zone.

The communication between vehicles was simulated and tested using the GloMoSim environment and the mobility of the nodes was implemented using the VanetMobiSim simulator. Inter vehicle communication (IVC), both via hopping among vehicles in the same direction of traffic flow, as well as via cross transmission of information for vehicles moving in the opposite direction, is modelled in figure 7.

For this scenario a part of the Cluj-Napoca city map was considered, the square being zoomed in. All the vehicles with Wi-Fi capabilities are represented with their covered transmission area. The communication on a road segment was established using a single Wi-Fi AP. All the vehicles form a VANET, the whole related traffic information being shared among them.

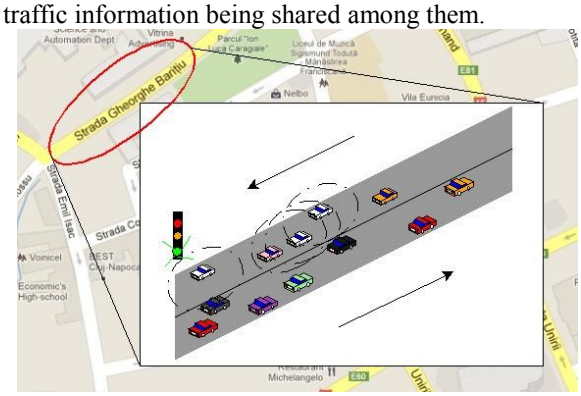

Figure 7: The communication between vehicles

The registration of a queue length during 1000 simulation steps is represented in figure 8. The duration of each simulation step is variable and can be set up at the beginning of the simulation scenario.

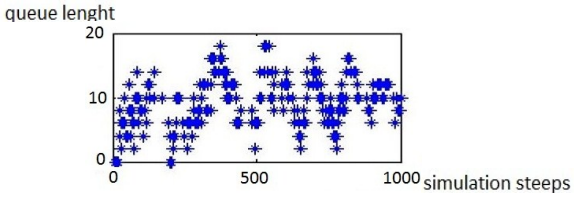

Figure 8: Variation of the queue length

CONCLUSIONS

Successive RSSI intensity measurements and the corresponding time values were used to determine the vehicle flux in various conditions. The permanent updated information was utilised in a simulation system to determine the best routes and to prevent road congestions. The data considered in the simulation network represent the result of experiments conducted in real traffic conditions. The performances can be improved extending the number of AP and modifying their locations in order to complete the needed real time traffic information. The proposed solution could contribute to the improvements of the performances in of other existing traffic control and monitoring systems.

ACKNOWLEDGMENTS

This work was technical and material supported by the project: "Development and support of multidisciplinary postdoctoral programs in major technical areas of national strategy of Research - Development - Innovation" 4D-POSTDOC, contract no. POSDRU/89/1.5/S/52603, project co-funded by the European Social Fund through Sectorial Operational Program Human Resources Development 2007-2013.
and laboratory resources supported by:
"Doctoral studies in engineering sciences for developing the knowledge based society-SIDOC" contract no. POSDRU/88/1.5/S/60078, project co-funded by the European Social Fund through Sectorial Operational Program Human Resources Development 2007-2013.

REFERENCES

Goodwin, P. 2004. "The Economic Costs of Road Traffic Congestion", *Rail Freight Group*.

Sivaharan, T., Blair, G, Friday, A., Wu, M., Duran-Limon, H., Okanda, P., and Srrensen., C.R. 2004. "Cooperating Sentient Vehicles for Next Generation Automobiles." *Proceedings of the 1st International Workshop on Applications of Mobile Embedded Systems*, Boston.

Morla, R. 2005."Vision of Congestion-Free Road Traffic and Cooperating Objects". *The Sentient Future Competition book chapter,*Germany.

Mayor, K. 2005. "Time is Money: An Enquiry into the Effectiveness of Road Traffic Management Schemes and Congestion Charges", *Managing Urban Traffic Congenstion*.

Yang, X. and Recker, W. 2005. "Simulation studies of information propagation in a self-organizing distributed traffic information system", *Transportation Research Part C 13*, 370–390, Elsevier Publisher.

Piorkowski, M., Raya, M., Lezama Lugo, A., Papadimitratos, P., Grossglauser M. and Hubaux, J.P. 2008. "TraNS: Realistic Joint Traffic and Network Simulator for VANETs", *Proceedings of the 11th communications and networking simulation symposium*.

Online: http://sumo.sourceforge.net/

Padron, F.M. 2009. "Traffic Congestion Detection Using VANET". *Master thesis*.

Cassias, I. and Kun, A. L. 2007. "Vehicle Telematics: A Literature Review" . *Technical Report ECE*.P54.2007.9.

Pathak, S.N. and Shrawankar U. 2009. "Secured Communication in Real Time VANET". *Second International Conference on Emerging Trends in Engineering and Technology*, pp. 1151-1155, Nagpur, India.

Tufail, A., Fraser, M., Hammad, A., Ki, H.K. and Yoo, S.W. 2008. "An Empirical Study to Analyze the Feasibility of WiFi VANETs", *Proceedings of the 12th International Conference on Computer Supported Cooperative Work in Design*, pp. 555-558, IEEE.

Saricks C. Belella P., Koppelman F., Schofer J. and Sen A. 2006. Formal Evaluation of the ADVANCE Targeted Deployment.

Wang, C.Y., Hwang, R.H. and Ting, C.K. 2010. "UbiPaPaGo: Context-Aware Planning", Article in Press, Elsevier.

Thangavelul, A., Bhuvaneswari, K, Kumarl, K., Kumar, S. and Sivanandam, S.N. 2007. "Location Identification and Vehicle Tracking using VANET (VETRAC) ", *IEEE-ICSCN*, pp. 112-116, MIT Campusm Anna University, Chennai, India.

Maekawa, M. 2004. "ITS (Intelligent Transportation Systems) Solutions". *Journal of Advance Technolgy*, Special Issue on Advanced Technologies and Solutions toward Ubiquitous Network Society.

ECMT. 2007. "Managing Urban Traffic Congestion". http://www.internationaltransportforum.org/jtrc/CongestionSummary.pdf.

AUTHOR BIOGRAPHIES

AVRAM, CAMELIA, PhD, is assistant professor at Technical University of Cluj Napoca, Automation Department, Romania. Her research interest: designing and implementing of Real Time applications, Discrete Events Systems and Data Communication.

ASTILEAN, ADINA, PhD, is Professor in the Department of Automation at the Technical University of Cluj Napoca. She is author of 7 books, of most than 110 conference and journal publications and a member in various committees promoting research. Her research interests cover the areas: Discrete Event Systems, Data Communication, Artificial Intelligence and Distributed Control Systems. Her current research focus includes Healthcare Telematics.

Simulation and Visualization for Training and Education

FLEXIBLE MODULAR ROBOTIC SIMULATION ENVIRONMENT FOR RESEARCH AND EDUCATION

Dennis Krupke*, Guoyuan Li and Jianwei Zhang
Department of Computer Science
University of Hamburg
Email: {3krupke, li, zhang}@informatik.uni-hamburg.de

Houxiang Zhang and Hans Petter Hildre
Faculty of Maritime Technology and Operations
Aalesund University College
Email: {hozh, hh}@hials.no

*corresponding author

KEYWORDS

Modular robots control, educational software, OpenRAVE, interactive simulation

ABSTRACT

In this paper a novel GUI for a modular robots simulation environment is introduced. The GUI is intended to be used by unexperienced users that take part in an educational workshop as well as by experienced researchers who want to work on the topic of control algorithms of modular robots with the help of a framework. It offers two modes for the two kinds of users. Each mode makes it possible to configure everything needed with a graphical interface and stores configurations in XML files. Furthermore, the GUI not only supports importing the user's control algorithms, but also provides online modulation for these algorithms. Some learning techniques such as genetic algorithms and reinforcement learning are also integrated into the GUI for locomotion optimization. Thus, its easy to use, and its scalability makes it suitable for research and education.

INTRODUCTION

Robotics is one of the best ways to motivate young people to work with new technologies. As explained in (Daidié et al., 2007) especially modular robots are very popular among students. Simulative robotic systems are usually developed to help them to get familiar with robotics. On the other hand, these simulative systems are also good testbeds for research. Experienced people can save time by using the functions of the proposed framework and focus on the development of new algorithms.

A lot of robot simulation software has been developed. There are general purpose simulators for mobile robots in 2D, 2.5D and 3D, like Player/Stage (2D), Gazebo (2.5D) from the *player-project*, described in (Player-Project, 2008), and Webots (3D) that can be found in (Michel, 1998). All of them offer so much freedom to the users that it is hard for them to start immediately with a simulation according to current needs. There are also special purpose simulators for grasping like GraspIt! (Miller et al., 2004) and OpenGRASP (León et al., 2010) that are based on OpenRAVE. But to the best of our knowledge there is no special purpose simulation software for modular robots that allows for fast and easy creation of a simulation setup while being easy to use and easy to understand.

A modular robot GUI has been developed that enables the user to focus on robotics while most of the programming part is hidden. This idea is also described in (Zhang et al., 2006). In contrast to other powerful systems only few rules have to be learned for proper use of our system. Motivation is the most important aspect for people who have just begun with something new to proceed and succeed. The GUI enables the user to get results very quickly because only some basic knowledge about the application space of modular robotics is needed. This makes the simulation system suitable for educational purposes with hard time restrictions, typical for a workshop or project. The research-related user also benefits from these properties. In research an expert configuration interface can be used to create several simulations. Some parts in the hierarchy of a complete configuration, for example the robot or the environment, can be reused to save time and to make different control algorithms comparable. To compare different control algorithms in a reliable way, an abstract base class has been developed that is used to implement several locomotion algorithms published by different institutions. It has been tested with arbitrary algorithms like the MTRAN-CPG (Murata et al., 2002), different networks of CPGs based on spiking/bursting-neurons, described by (Herrero-Carrón et al., 2010), and many more. The extension of the library with control algorithms can be performed with the help of software development patterns described in (Gamma et al., 2005) and (Beveridge, 1998). Methods to analyze the kinematics, described in (Hirose et al., 1990) and (Hirose, 1993) can be added and the results passed to special data handlers. These handlers are needed to visualize the data and to write it to the disk.

In the following a short introduction to the modular robots GUI and its components that has been developed is given. It is followed by a detailed description of several parts of the software and an example that shows how the system can be used, before the final section presents the paper's conclusion and raises possible future work.

Proceedings 26th European Conference on Modelling and Simulation ©ECMS Klaus G. Troitzsch, Michael Möhring, Ulf Lotzmann (Editors)
ISBN: 978-0-9564944-4-3 / ISBN: 978-0-9564944-5-0 (CD)

INTRODUCTION TO THE MODULAR ROBOTS GUI

For achieving realistic and reasonable simulations, the simulated world should look and behave as close to the real world as possible; therefore a system using a physics-engine and a 3D-viewer is needed. OpenRAVE (Diankov, 2010) offers calculation of the physics and three-dimensional visualization of the running simulation. It is a controlling and planning software that is developed as a general robotics simulation and control system. It can be extended easily to fulfill the demands of the user. In our simulation system many components of OpenRAVE have been applied:

- 3D-viewer interface and implementation of Coin3D
- Physics engine interface and implementation of ODE
- XML- and COLLADA readers
- Abstract sensor interface and implementations of several sensors

ODE (Smith, 2006) works as a physics engine to calculate realistic behaviour of the rigid bodies. After the robot has been assembled, sensors can be attached to the robot and the configuration can be stored in an XML-file. With another XML-file the user is able to describe a world. Concepts like *cloning* allow us to run a copy of a simulation. This is ideal to run copies of simulation in parallel or to start an identic simulation again with only a small change in the configuration of the control algorithms. OpenRAVE has become very popular because of its modules that calculate the inverse kinematics for several industrial robot arms. It is under intense development and the support using the user-list is very fast. Many institutes from different countries are currently working with OpenRAVE. That makes it an ideal base for our ideas. By now, OpenRAVE offers a package for the Ubuntu Linux operating system that enables the automatic installation of all needed dependencies including Coin3D, SoQt, ODE and many more. In this way, it is very comfortable to install OpenRAVE on a standard Ubuntu system.

A plugin for OpenRAVE (Gonzalez-Gomez, 2010) the *OpenMR-plugin* has been written by Juan Gonzalez-Gomez. It implements a servo controller as shown in Fig.1. In modular robotics these are used to drive robots. The controllers have been applied to our system as well as the 3D-model of a modular robot prototype included by the plugin. The robot model that has been used in our experiments is described in (Gonzalez-Gomez et al., 2006).

To access the core simulation system including the physics-engine and the 3D-viewer and the robot models, *graphical user interfaces* for comfortable handling have been implemented. In addition *I/O-classes* and a *kernel for control algorithms* used in our *simulation container* have been added.

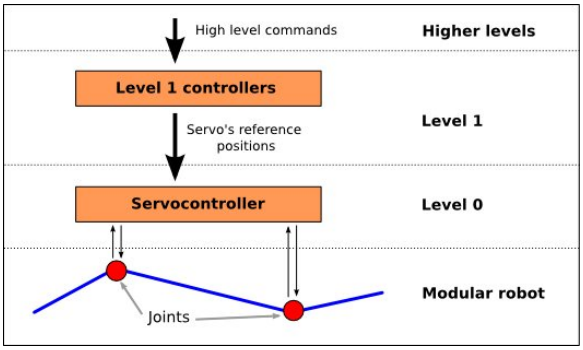

Figure 1: Concept of the used servo controller (Figure is taken from (Gonzalez-Gomez, 2010)). As level 1 controllers several algorithms has been implemented using the abstract interface for actuation modules.

The GUI elements and many classes, extending the standard library of C++, are taken from *Qt*, *Boost* and *QWT*. One of the main features is that the user can easily create his own algorithm for joint control. This can be a locomotion algorithm or an adaptive algorithm to adjust the shape of the robot. Another feature is that all parameters of this new algorithm can be accessed and changed while the simulation is already running. This makes it possible to experiment with different values to gain a better understanding of the algorithm. It also allows us to implement online-optimization methods to find good sets of values for the parameters for different purposes. The GUI is divided into two main parts, the *configuration-* and the *control-GUI*. The configuration part permits the setting up of everything that is neccessary to run a certain simulation while the control GUI offers online control over the control algorithms and supervision of the robot within its world. Additionally it is possible to see certain live plots of different data.

To enable the user to configure simulations, a **configuration GUI** with two different modes has been implemented. One interface for a user at the *beginner level* and one for an *intermediate or experienced user*. A level of detail has been found that is complex enough for reasonable usage. Beginners get in touch with a *configuration-wizard* that guides them step by step through the process of configuration. Clear instructions explain the current task and the meaning of the information that needs to be filled in. The user is not asked for filenames as everything gets stored automatically. The filenames are generated automatically at predefined places within the project folder. The *expert-configuration-dialog* makes very flexible configurations possible. Both configuration interfaces allow the user to create and *extend the user-library* of control algorithms for robot-joint-actuation during the runtime of the program. OpenRAVE utilizes XML-format to define robots with its sensors, physical properties and the environments the simulation is set in. This property has been extended with actuation-configuration files to assign control algorithms to the robot very easily.

In this way, as many control algorithms as needed can be assigned to many different groups of joints. Each group must consist of at least one joint. Overlapping groups are allowed. Complex architectures can be built from basic building blocks.
The function of the **control GUI** is to supervise the simulation with the help of several visualizations and to adjust everything just in time while the simulation is running. This can be used to do experiments in an explorative way, manually by a user or automatically by an optimization-process. To supervise the control algorithms and the robot, applied to the current simulation, a monitoring system has been included. It allows us to select and combine several data plots to show them on the screen. These are *live-plots*, used to see the current state of the simulation. This combined with the possibility to adjust the parameters of the locomotion algorithms on-line makes the GUI a powerful system for interactive experiments and automated optimization.
To record all of the calculated data of interest, a *data file writer* has been developed that stores everything to an XML-file. Special readers for this file format are able to extract a single series of data. Data series can be exported into separate files for later usage.

DETAILED SYSTEM DESCRIPTION

Our software consists of the following parts.

- Configuration GUI
- Control GUI
- Simulation container
  - CPG kernel
  - Data handlers
  - OpenRAVE as core simulation system
- Several I/O-classes

The structure of the simulator is also shown in Fig.2.

Configuration GUI

The configuration GUI can be started in two different modes. One is a *wizard* for simple usage that guides the user through all steps that are neccessary to set up and start a simulation. The *expert mode* allows us to configure only the neccessary steps seperately. It can be used to generate configuration files for only a single step of the whole configuration process and to reuse configured parts that were already defined.
The *configuration wizard* is made for people who are not familiar with this software or are just starting with modular robots. Without knowledge about the simulator and some basics about C++ it should be possible to create a robot, to define the behaviour of its joints and to create a world, the workspace of the robot. Only a few ideas about locomotion principles of modular robots in chain configuration will be needed to fullfill this task. This also

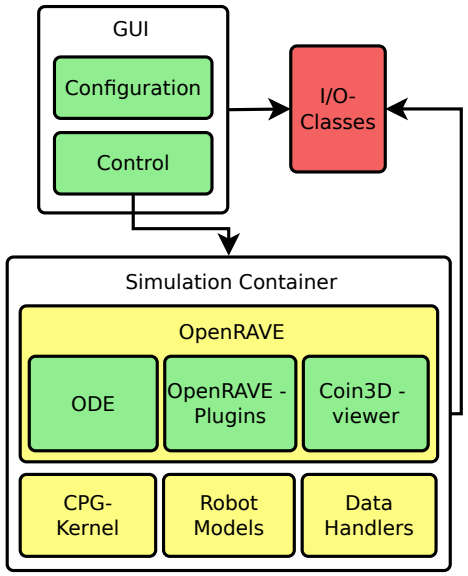

Figure 2: The architecture of the simulator.

means that everybody dealing with computer science is able to implement a simple locomotion algorithm after a short introduction to the locomotion principles of modular robots.
The *expert mode* is intended for the experienced user who wants to create different simulation set-ups to compare the results for qualitative analysis. The expert mode is useful because the configuration of a whole simulation consists of many parts and it is possible to reuse some of them for another simulation set-up to save time and avoid monotonic work. A simulation configuration file containes three parts:

- the *robot configuration* file with all of the physical parts of the robot and the sensors
- a configuration for the *joint actuation* of a specific robot
- the definition file of the *environment*

Complex environments, suitable for tasks of a robot described in (Granosik et al., 2005), can be built by using the integrated environment editor. Additionally, there are some global options that can be adjusted to determine the simulation mode and some other properties.

Control GUI

The control GUI offers different tabs to give structured access to the different components. It communicates with the core of the simulator with the help of the *Signals and Slots principle* used by Qt. In this way the delay between two simulation steps of the discrete simulation can be changed. When the simulation is started and the user has configured the simulator to store the calculated data, all of the data gets stored to a temporary file after a

certain period. The user can store this data to a file any time.
One tab is for the *data live-plots* and enables the addition of several plot widgets that can contain any combination of the available data type. To select the desired combination of plots a GUI element with checkboxes, one for each avilable data series, has been created. It is possible to change the sampling rate, the refreshing rate, as well as the size of the buffer containing the data. The GUI elements used for the plotting are taken from the *QWT* library. QWT supports a lot of features that can help to display data on the screen in a clean and clear way. As a data buffer for the plots the *circular buffer* from the *Boost-library* has been used. It is easy to handle and very efficient because the single entries in the circular buffer are contiguous in the memory. Resizing of this circular buffer has been proved to be very stable in our experiments.
Another tab offers access to the used *sensors* in the current robot. It is possible to change the state of the single sensors, e.g. sensors can be switched on and off.
With the help of the *data*-tab, recorded simulation data of the currently running or already past simulations can be loaded. It is possible to select one or more graphs to plot it on the screen. These plots can be exported to portable network graphics (*.png) or into a gnuplot file for later, more differentiated usage. After loading a data file, all contained types can be selected. In case of a specific value type the number of the joints is an additional criterium that must be chosen.
The last tab contains the *Coin3D-viewer* taken from OpenRAVE to visualize the simulation running in the core module with OpenGL. It supports all features from the original OpenRAVE software and can be used as described in the OpenRAVE documentation. The viewer uses very simple shading mechanisms to achieve high performance even on slower systems. Tests with an EeePC 1000H netbook have revealed that our software works on such slow systems. With the viewer the pose of the camera can be changed according to the needs of the user and videos of the simulation can be recorded. It is possible to manipulate displayed objects. Objects can be moved and joint-angles can be adjusted.

Simulation Container
The container, where the core of the simulator is running, is a class inherited from *QThread*. The thread calls all neccessary step-functions of the OpenRAVE environment and the CPG-Kernel and emits certain signals. For example, one signal is emitted after one calculation step has been completed. The speed of the simulation depends on the machine where the program is running. To achieve a short time of response in the system, an adjustable delay between the calculation steps has been added. In this way the speed of the simulation and the CPU load can be controlled.
The container can run without the graphical components. This is useful for longtime- or remote-runs of the program, for example when a parameter or an algorithm for locomotion needs to be optimized. In these cases graphical output is not needed and computational effort can be saved.

CPG-Kernel
The most important part of the work was to create an abstract interface that fulfills the needs of any general central pattern generator or other locomotion algorithms. Our interface facilitates the creation of new control-algorithms. It has been tested for arbitrary algorithms from scientific publications which can be evaluated, optimized or combined in several ways. Even distributed control algorithms that have been described in (Conradt et al., 2003) can be implemented. To integrate as much functionality as possible in the Control-GUI and to allow for further extension of the program, it has been realized as an abstract base interface that holds only the most common features of a control algorithm. To provide enough flexibility for future implementations of several locomotion or actuation algorithms it has been kept simple. But it offers some basic functionality like parameter-modulation, data-handling and supervising of the current state.

I/O-Classes And Data Handlers
There are many XML-readers and -writers to store and read all of the needed information for specifying a simulation in detail. To overcome this complexity, arbitrary classes for each category have been created. Access to these classes using a graphical interface hides the syntax needed to build valid configurations and makes the process of configuring parts of a simulation very fast, easy and robust.

- Robot-configuration-writer
- Sensor-configuration-writer
- Actuation-configuration-writer and -reader
- Environment-configuration-writer
- Simulation-configuration-writer and -reader
- Simulation-data-writer and -reader

There are three different kinds of *simulation-data* occuring in a running simulation. For each type a data handler has been implemented to manage the values.

- CPG-/locomotion-algorithm data
- Robot data
- Sensor data

For each type the values are computed after the global step-function is called. It is the same for the physics engine and the OpenRAVE-core as for our simulator- and CPG-core. A reader and a writer have been implemented to access and generate these files. The data format makes it possible to acquire specific data-series from the file even if different files contain different types of data.

EXAMPLE — HOW TO USE THE SYSTEM

In the following the complete process to create a proper simulation is described. It includes how a new locomotion algorithm can be defined using the beginner's *configuration wizard* of the simulator and how the simulation can be started.

Starting The Simulator

After the program has been started from the command-line a dialog is shown. A button with *'Start Wizard'* has to be used to start the wizard.

Creating A Robot

The first page of the current version of the wizard, shown in Fig. 3, is intended to create a robot. It is neccessary that a reasonable name is given to the robot. It will be used for the filename-generation of the configuration file describing the robot. Because the interface is built to create robots in a chain-like configuration it is recommended to select the needed topology. To create a robot with three-dimensional locomotion capabilities the *'Pitch-Yaw'* connection type has to be selected. The size of the robot can be changed by selecting a reasonable number of modules, e.g. five. The preview in the lower right corner gets updated if anything has been changed. For simplicity no sensors have to be added this time. That is enough for a simple robot and the *'Next'* button can be clicked.

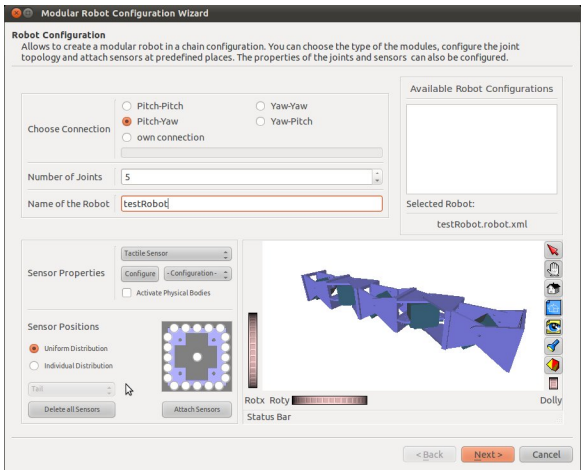

Figure 3: With the robot creation page robot description files can be created in a simple way without any knowledge about the OpenRAVE XML tags.

Creating A User-Defined Locomotion Module

A new dialog page will appear for creating a new control algorithm. With this interface all neccessary properties of the new algorithm can be declared and applied with initial values. To create a new control module that generates sinusoidal output, a name for the new module must be given first. This name will be used for the new class. To have access to the hidden functionality of the actuation modules, like plotting and storing of data, as well as live modulation of the output, some properties of the new module must be declared. All parameters must be registered one after the other and initial values must be given to initialize the new module. In this example, four parameters including amplitude, frequency, phase-difference and stepsize are typed as neccessary parameters. Using the *sine* function to calculate the output angles, an input will be needed. That is the reason why a value type called *'time'* must be added. It is related to the parameter *stepsize*. Both together will be used to generate a slowly increasing value as input for the oscillating sine function. By clicking the button *'Next'*, a header- and an implementation-file will be generated. For this simple actuation module only the *'CalculateAngles'*-function must be implemented in the implementation window of the next dialog page. A single loop that calculates the output for each joint has to be added for this purpose:

```
1   for (int m=0; m<_numOfConnectedJoints; m++)
2   {
3     *current_time(m) = *old_time(m) + *Stepsize;
4
5     *current_angle(m) = *Amplitude
6                 * sin(2*M_PI**Frequency**current_time(m)
7                 +m**PhaseDifference*M_PI/180);
8
9     SetAngle(m, *current_angle(m));
10  }
```

A click on the *'Compile'* button causes the new module to get compiled to the user library.

Defining The Behaviour Of The Robot

Functionality can be added to the joints with a grouping-interface. Users can select desired joints as a group and perform them with a common control method. In this example, by clicking the button *'Add Group'*, only the pitching joints are added as a group. The newly developed control method is then applied to this group.

Creating An Environment

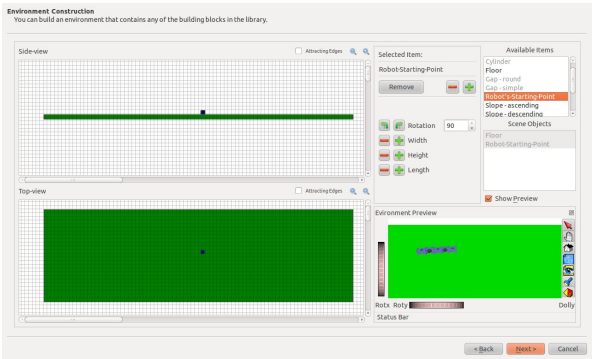

Figure 4: A very simple environment containing the robot and one floor has been constructed with the integrated environment-editor.

Arbitrary *'Available Items'* can be added to the currently empty environment with the help of *drag-and-drop* into one of the two editor views. The previously defined robot will be placed with the help of the representative object for its pose. In this way the pose of the robot can be changed. To change the position of any object it can be dragged in one of the views. To change the x- and the z-coordinate the *side-view* can be used, for x- and y-coordinate the *top-view*. The size and the orientation relative to the z-axis can be changed after the current object has been double-clicked. The selected item can be resized and rotated with the help of the buttons. To fit the created objects in the two views the zooming-buttons should be used. The preview, as shown in Fig. 4, can be eanbled by selecting the checkbox labeled with *'Show Preview'*. Each object, except the robot's position object, can be right-clicked to adjust the frictional coefficient that has a range between zero and one. In this way a slippery ground can be simulated as well as a very sticky floor.

Setting-Up The Global Simulation Properties

At the bottom of the last wizard-page the full paths of the recently created configuration files are summarized. With the upper part the *simulation mode* and some properties can be changed. *'Single Run Simulation'* must be selected to create a simple simulation that keeps running until it gets stopped by the user. With the *sampling rate* the computational effort of the simulation and its relative to the steps of the OpenRAVE-core is determined. A value of 30 means that every 30th physics-engine-step one step of our sensors and actuation modules will be computed. For the physics-engine-step size a standard value of 0.001 is recommended. Storing of the calculated data can be deactivated, if needed. After hitting *'Finish'* a master configuration file will be stored that contains the names of all other files and the newly added simulation properties. This file will be passed to the simulator that gets initialized with the information from this file.

Starting The Simulation And Using The Control GUI

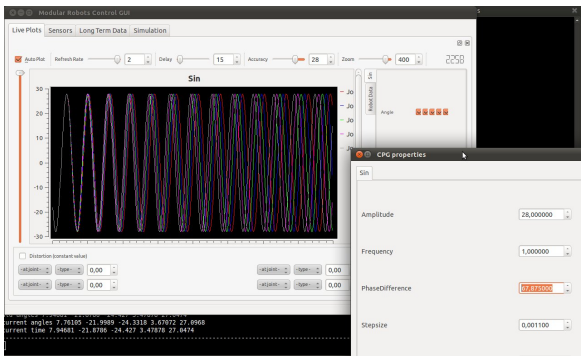

Figure 5: Example of online-modulation of the phase difference between neighboring modules.

To start the simulation the *'Play'*-button, located at the toolbar of the control GUI, must be pressed. It can also be used to pause the simulation.With the *properties dialog* all control parameters of the currently applied actuation modules can be modulated online. As shown in Fig. 5 for example the phase can easily be changed using the properties dialog. To visualize the calculated data the checkboxes of the *plot-selector*-element of the control GUI can be used to add arbitrary data-lines to a new plot. The live-plot will be created after the button, labled with *'Add'*, has been pushed.

CONCLUSION

A new graphical user interface to create and control simulations for modular robots in an easy and flexible way has been introduced. The software focusses on modular robotics and their control algorithms. It tries to hide the programming part as well as possible behind the GUI. In this way even beginners with very limited time are able to use the software with only basic knowledge in writing C++ functions and little idea of modular robotics. It enables beginners to get in contact with modular robotics and intermediate users will benefit from a decrease in time for implementing their own ideas. The software fulfills two tasks. On the one hand it can be used as an educational framework to introduce somebody to modular robotics in an explorative way and on the other hand it can be used in research to get results from optimization methods. Studies and improvements of control algorithms can be done with reduced time effort. To the best of our knowlegde this is very new and offers a framework to achieve good results from the simulation of control algorithms that can be applied to real modular robots.

FUTURE WORK

Considerable works remains to be done, e.g. in extending existing parts. To reduce the restrictions in building modular robots another page to create new *modules* will be added to the configuration interface. Simple geometric objects or 3D-data of a single link will be used to create a new module available in the robot-construction page of the configuration-GUI. More *sensors* with adjustable properties will be implemented. The placing of the sensors needs to become more flexible. Creation of actuation modules using sensor information via the configuration-GUIs will be implemented. The library of objects for creation of the *environment* should also be extended to build a world suitable for more complicated tasks. More simulation modes that support the user in getting good results from the simulations will be implemented. These will include *optimization methods*, especially learning mechanisms, that improve a single parameter or a whole feature vector of a certain actuation module.

REFERENCES

Beveridge, J. (1998). *Self-Registering Objects in C++*. Dr. Dobb's Journal, Vol. 23, Issue 8, pp. 38-41, August 1998.

Conradt, J., Varshavskaya, P. (2003). *Distributed central pattern generator control for a serpentine robot*. ICANN 2003.

Daidié, D., Barbey, O., et al. (2007). *The DoF-Box Project: An Educational Kit for Configurable Robots*. Switzerland, ETH Zurich, Proceeding of AIM 2007, 4 - 7 Sept., 2007.

Diankov, R. (2010). *Automated Construction of Robotic Manipulation Programs*. Carnegie Mellon University, Robotics Institute, 2010.

Gamma, E., Helm, R., Johnson, R., Vlissides, J., Booch, G. (2005). *Design Patterns: Elements of Reusable Object-Oriented Software*. Addison-Wesley, Reading, Massachusetts, 2005.

Gonzalez-Gomez, J., Zhang, H., Boemo, E., Zhang, J. (2006). *Locomotion Capabilities of a Modular Robot with Eight Pitch-Yaw-Connecting Modules*. Proceeding of CLAWAR 2006, Brussels, Belgium, September 12-14, 2006.

Gonzalez-Gomez, J. (2010). *OpenMR: Modular Robots plug-in for Openrave*. http://www.ieearobotics.com/wiki/index.php?title=OpenMR:_Modular_Robots_plug-in_for_Openrave, 2010, (last access in March 2012).

Granosik, G., Hansen, M. G., Borenstein, J. (2005). *The Omnitread Serpentine Robot for Industrial Inspection and Surveillance*. Industrial Robot: An International Journal, Vol.32, No.2, pp.139-148, 2005.

Herrero-Carrón, F. and Rodríguez, F. B. and Varona, P. (2010). *Study and application of Central Pattern Generator circuits to the control of a modular robot*. Escuela Politécnica Superior, Universidad Autónoma de Madrid, 2010.

Hirose, S., Morishima, A. (1990). *Design and control of a mobile robot with an articulated body*. The International Journal of Robotics Research, Vol. 9 No. 2, pp. 99-113, 1990.

Hirose, S. (1993). *Biologically inspired robots (snake-like locomotor and manipulator)*. Oxford University Press, 1993.

León, B., Ulbrich, S. Diankov, R.,Puche, G.,Przybylski, M.,Morales, A.,Asfour, T.,Moisio, S.,Bohg, J., Kuffner, J., Dillmann, R. (2010). *OpenGRASP: A Toolkit for Robot Grasping Simulation*. Berlin, Heidelberg: Springer Berlin Heidelberg, 2010.

Michel, O. (1998). *Webots*. http://www.cyberbotics.com, 1998, (last access in March 2012).

Miller, A., Allen, P. K. (2004). *Graspit!: A Versatile Simulator for Robotic Grasping*. IEEE Robotics and Automation Magazine, Vol. 11 No. 4, Dec. 2004, pp. 110-122, 2004.

Murata, S., Yoshida, E., Kamimura, A. , Kurokawa, H., Tomita, K., Kokaji, S. (2002). *M-TRAN: self reconfigurable modular robotic system*. IEEE(ASME) Transactions on Mechatronics, December 2002.

Smith, R. (2006). *Open Dynamics Engine*. http://www.ode.org, 2006, (last access in March 2012).

The Player Project (2008). *The Player Project*. http://www.playerstage.sourceforge.net, 2008, (last access in March 2012).

Wall, M. (2007). *Matthew's Genetic Algorithm Library* http://lancet.mit.edu/ga/, 2007, (last access in March 2012).

Zhang, H., Baier, T., Zhang, J. , Wang, W., Liu, R., Li, D., Zong, G. (2006). *Building and Understanding Robotics — a Practical Course for Different Levels Education*. Proceedings of the 2006 IEEE, International Conference on Robotics and Biomimetics, Kunming, China, December 17-20, 2006.

AUTHOR BIOGRAPHIES

DENNIS KRUPKE is student assistant at TAMS, Department of Informatics, University of Hamburg, Germany. His research interests are simulative systems and control of modular robots.

GUOYUAN LI is PhD student at TAMS, Department of Informatics, University of Hamburg, Germany. His research interests lie in locomotion control and CPG model design.

JIANWEI ZHANG is professor and head of TAMS, Department of Informatics, University of Hamburg, Germany. His research interests are multimodal information systems, novel sensing devices, cognitive robotics and human-computer communication.

HOUXIANG ZHANG joined the Department of Technology and Nautical Sciences, Aalesund University College, Norway in April 2011 where he is a Professor on Robotics and Cybernetics. The focus of his research lies on mobile robotics, especially on climbing robots and urban search and rescue robots, modular robotics, and nonlinear control algorithms.

HANS PETTER HILDRE is professor at the Faculty of Maritime Technology and Operations, Aalesund University College, Norway.

ACKNOWLEDGEMENT

This work has been supported by the BICCA project, which is a DFG project concerning the development of a biologically inspired climbing caterpillar.

Finance, Economics and Social Science

ON BIOLOGICALLY INSPIRED PREDICTIONS OF THE GLOBAL FINANCIAL CRISIS

Peter Sarlin
Turku Centre for Computer Science - TUCS
Department of Information Technologies
Åbo Akademi University
FIN-20520, Turku, Finland
E-mail: psarlin@abo.fi

KEYWORDS
financial crises, early warning system, neural networks, genetic algorithms, neuro-genetic model.

ABSTRACT

This paper evaluates the performance of biologically inspired early warning systems (EWS) for systemic financial crises. We create three EWSs: a logit model, a standard back-propagation neural network (NN) and a neuro-genetic (NG) model that uses a genetic algorithm for choosing the optimal NN configuration. The performance of the NN-based models are compared with the benchmark logit in terms of utility for policymakers. For creating the NN-based EWSs, we use two training schemes for parsimonious and generalized models and advocate adopting to the EWS literature the scheme using validation sets for better generalization of data-driven models. The performance evaluation shows that NN-based models, in general, outperform the logit model. The key finding is, however, that NG models not only provide largest utility for policymakers as an EWS, but also in form of decreased expertise and labor needed for, and uncertainty caused by, manual calibration of a NN.

INTRODUCTION

The first wave of the ongoing global financial crisis, while being a self-evident truth in ex post predictions, has demonstrated the importance of ex ante identification of elevated risks that may lead to a systemic financial crisis. Early warning systems (EWSs) have generally treated the task of giving signals of a crisis as a binary-choice problem; however, the modeling techniques have evolved over the years. In the very early days of financial stability surveillance, data were analyzed by hand (e.g. Ramser and Foster, 1931). To the turn of the century, most commonly applied methods have been conventional statistical techniques: discriminant analysis (DA) (e.g. Frank and Cline, 1971), signaling approach (e.g. Kaminsky et al., 1998) and different forms of generalized linear models (GLM), such as logit and probit analysis (e.g. Demirgüc-Kunt and Detragiache, 2000). These methods, however, suffer from assumptions violated more often than not, such as normality of the indicators, distributional assumptions on the relationship between the indicators and the response, and the absence of interactions between indicators. For instance, Lo Duca and Peltonen (2011) show that crisis probabilities increase non-linearly with the increase of vulnerabilities. In past years, some non-parametric, oftentimes distribution-free and non-linear, techniques have been introduced to financial stability surveillance. The key methods in non-parametric EWSs have so far been based upon biologically inspired computing in general and artificial neural networks (NNs) in particular.[1] NNs are effective data-driven non-linear function approximators, but alas they are no panacea for binary-choice classification. To fully benefit from capabilities of NNs, they need to be provided with their computational demands (i.e. large samples and computing power) and specific training schemes for generalization.

Recently, circumstances for financial stability surveillance have changed. While the degree of financial integration and connectivity, and its interplay with the stability of the system, has increased, the soar in data availability and computing power has been remarkable. The former factor advocates further research on early warning modeling whereas the latter enables data-driven modeling of complex relationships. Even though non-parametric methods have produced some promising results in crisis prediction, they have seldom been implemented for financial stability surveillance in practice.[2] One reason might be the complexity of setting up a non-parametric model, not the least a NN. While there exist a large number of "rules-of-thumbs" for parameterization of NNs, manual calibration is still an expertise-demanding and laborious task as well as increases the risk of being trapped in a suboptimum. To this end, Sarlin and Marghescu (2012)

[1] NNs have been implemented as EWSs in, for instance, Nag and Mitra (1999), Franck and Schmied (2004), Peltonen (2006), Aminian *et al*. (2006), Fioramanti (2008), Sarlin and Marghescu (2011) and Sarlin and Peltonen (2011).

[2] For instance, recent work at the European Central Bank, such as Alessi and Detken (2011), Lo Duca and Peltonen (2011) and Hollo *et al*. (2012), includes little computational intelligence.

Proceedings 26th European Conference on Modelling and Simulation ©ECMS Klaus G. Troitzsch, Michael Möhring, Ulf Lotzmann (Editors)
ISBN: 978-0-9564944-4-3 / ISBN: 978-0-9564944-5-0 (CD)

used genetic algorithms (GAs) for finding an optimum model configuration for a NN in currency crisis prediction. Another obstacle for financial stability surveillance might be the problem of parsimonious and generalized modeling; the analyst should know how to avoid overfitting. While NN-based EWSs have generally applied early stopping at the level of performance of a benchmark statistical model (e.g. Fioramanti, 2008; Sarlin and Marghescu, 2012), there is still room for improving accuracy with a balance between complexity and generalization power. What is missing from the EWS literature is using a third dataset, a validation set, for optimizing generalization of a model, something common already in the early NN literature (e.g. Ripley, 1994; Hagan et al., 1996).

This paper tests the usefulness of NN-based models for predicting systemic financial crises. First, we test a wide range of manually calibrated configurations for standard NNs. Second, we apply a standard GA for finding the optimal configuration of the NN – and coin it a neuro-genetic (NG) model. The rationale for this is to test whether NN-based models are better than logit models and the effect of automated calibration of the NG model. For parsimonious models, we implement two training schemes. First, we test whether NN-based models that perform equally well as a logit model on in-sample data perform better on out-of-sample data. Second, we train NN-based models by optimizing utility for policymakers on a third dataset, a validation set. This indicates how much better, if at all, the NN-based models performs when attempting optimal generalization.

METHODOLOGY

This section introduces biologically inspired computing, the underlying data and the evaluation framework. Biologically inspired computing involves processing data in ways that imitate how nature works. While NNs attempt to mimic the functioning of biological neurons in human brains, GAs imitate natural biological evolution dynamics. The dataset consists of two parts: macro-financial indicators and dates of financial crises. And the evaluation framework attempts to measure utility for policymakers by incorporating preferences between type I and type II errors.

Neural networks and genetic algorithms

NNs are data-driven non-linear function approximators composed of a system of units, which are interconnected by weighted links. Units of a NN are ordered into three layers: input, hidden and output layers. Through learning, the weights between units are set to find the best possible approximation of a function f that maps input data x to output values y, i.e. $y=f(x)$. The learning of the back-propagation algorithm can be thought of as a two-step process. First, it evaluates the derivative of the error function with respect to the weights. Then, the obtained derivatives are used for optimal adjustment of the weights.

The NN used in this paper is the very basic multi-layer perceptron with back-propagation learning.[3] The outputs of units U_j are transformed to an output of the NN Y_j as follows:

$$U_j = \sum (X_i * w_{ij}) \quad (1)$$

$$Y_j = f_{th}(U_j + t_j) \quad (2)$$

where U_j equals the sum of inputs X_i multiplied by weights w_{ij} and output Y_j is the sum of the internal values U_j and a bias t_j transformed by an activation function f_{th} into [0,1] and by a threshold *th* into {0,1}. In this paper, we test the following functions f_{th} for a mapping into [0,1]: sigmoidal, hyperbolic, gaussian and linear.

The back-propagation algorithm functions in two steps. It starts at the output layer by computing first the error term e_j and then the weight w_{ij}:

$$e_j = Y_j * (1 - Y_j) * \left(d_j - Y_j\right) \quad (3)$$

$$w_{ij} = w'_{ij} + (1 - M) * \alpha * e_j * (X_i + \varepsilon) + M * (w'_{ij} - w''_{ij}) \quad (4)$$

where the error term e_j equals the product of the output Y_j, its complement $1 - Y_j$, and the difference between the desired output d_j and the output Y_j. Then, weight w_{ij} is determined by the previous weight w'_{ij}; the product of the complement of the momentum factor $1 - M$, learning rate α, the error term e_j, and the input X_i and its input noise ε; and the momentum factor multiplied by the difference between the previous and next to previous weights w'_{ij} and w''_{ij}. On the next layer, while the adjustment proceeds as in Eq. (4), e_j is determined by a modified version of Eq. (3):

$$e_j = Y_j * (1 - Y_j) * \sum (e_k * w'_{jk}) \quad (5)$$

where the sum of the error terms e_k for each neuron k in the succeeding layer multiplied by the respective

[3] The model specification follows, but extends, that in Sarlin and Marghescu (2012). For more detailed presentations of the algorithms, see for example Hagan *et al.* (1996), Haykin (1998) and Bishop (2007).

weights from the previous epoch w'_{ij} replaces the difference between the desired and actual output in Eq. (3). Eq. (5) is applied to each hidden layer. This procedure iterates until fulfilment of a specified stopping criterion or after a specified number of epochs.

An obvious feature of this types of standard NN frameworks is that several parameters need to be specified. These include the learning rate α, momentum factor M, input noise ε, and the number of hidden layers and hidden units per layer. Learning rate sets the extent of adjustment to the old weight, while momentum allows a change to the weights to persist for a number of epochs. Input noise is a small random variation to each input that prevents learning of exact input values and increases thus generalization. In addition, the input-output mapping $f_{th} \in [0,1]$ performed by the activation function can take various forms. Another delicate question for NN modeling is the number and optimum combination of input indicators included in a model. Supervision of an expert analyst is required for obtaining a final, but still subjective, model. User-specified parameterization is not only time-consuming, but also has the drawback of using personal, possibly biased, experience in setting parameters that might overlook optimal solutions. As manual repetition obviously does not ensure even local convergence, it increases the risk of the NN being trapped in a suboptimum.

The choice of indicators, NN parameters and NN architecture can be resolved by a GA (Holland, 1975). GAs can be thought of as stochastic search methods for solving an optimization problem (for instance, maximize utility for a policymaker of an EWS over different NN configurations):

$$\max\{g(s)|s \in \Omega\} \quad (6)$$

where s is a candidate binary string solution to function g that belongs to the solution set Ω. In biological terms this translates to 'individuals' (candidate solutions) represented by 'structures' of genetic information (genotypes) and the 'population' (solution set Ω). The population evolves by genetic operators, such as the weakest structures replacing, by some 'reproduction', the best structures, and by random variation. 'Crossovers' determine the intermingling of features on the same string (or reproduction), where a one-point crossover creates interchanged offspring of the two parent solutions at a randomly chosen point, and 'mutations' determine a random change in a structure. On the candidate solutions, a crossover is performed on the best solutions and a mutation on the rest. Hence, specifying a parameter value for the mutation rate also sets the crossover rate. We specify each candidate solution to have a structure composed of three strings: one for input indicators, one for the NN architecture and one for the NN parameters. This gives the option to only optimize parts of the NN configuration. Let us exemplify the functioning with a simple example. For five inputs, three solutions could be, for instance: s_1={1,1,1,0,1}, s_2={0,0,1,1,1} and s_3={1,0,1,1,1}, where s_1 includes inputs 1-3 and 5, s_2 only inputs 3-5 and s_3 inputs 1 and 3-5, and the performance of $s_1 > s_3 > s_2$. Then, a mutation rate of 0.4 would introduce a random mutation to s_2, such that s_2={0,0,0,1,1}, for instance. If s_1 is read first and crossed over with s_3 after the second element, the offspring would be {1,1,1,1,1}, i.e. inclusion of all inputs 1-5.

Data

The dataset is an extended version of that in Lo Duca and Peltonen (2011) consisting of macro-financial indicators and the occurrence of a systemic financial crisis. The sample includes 28 countries, 10 advanced and 18 emerging economies, from 1990:1–2011:2. The macro-financial indicators consist of 14 quarterly country-specific vulnerabilities that proxy asset price developments and valuations, credit developments and leverage as well as traditional macroeconomic measures. The indicators, and their properties, are shown in Table 1. The statistical properties show that they are skewed and non-mesokurtic, and hence not exhibiting normal distributions. Each indicator is normalized into historic country-specific percentiles to control for cross-country differences, as is common in the EWS literature.

Table 1: The indicatiors and their statistical properties

No.	Variable	Abbreviation	Mean	SD	Min.	Max.	Skew.	Kurt.	KSL	AD
1	Inflation[a]	Inflation	0.89	5.17	-10.15	42.53	4.80	26.72	0.29	263.90
2	Real GDP[b]	Real GDP growth	3.73	3.76	-17.54	14.13	-0.86	3.16	0.06	11.34
3	Real equity prices[b]	Real equity growth	5.93	33.01	-84.40	257.04	0.99	4.31	0.05	7.28
4	Credit to private sector to GDP[a]	Leverage	3.48	51.64	-62.78	1673.04	22.76	673.35	0.29	Inf
5	Stock market capitalisation to GDP[a]	Equity valuation	3.90	28.32	-62.79	201.55	0.77	2.41	0.03	3.86
6	Government deficit to GDP[c]	Government deficit	0.01	0.05	-0.19	0.22	-1.09	3.46	0.09	35.90
7	Global Inflation[a]	Global inflation	0.03	0.64	-1.33	2.29	0.71	1.28	0.08	12.12
8	Global real equity prices[b]	Global real equity growth	2.31	19.08	-40.62	37.77	-0.57	-0.68	0.15	41.90
9	Global stock market capitalisation to GDP[a]	Global equity valuation	0.89	17.41	-40.54	27.46	-0.50	-0.43	0.09	19.11
10	Real credit to private sector to GDP[b]	Real credit growth	234.07	4724.00	-69.42	101870.34	20.76	429.59	0.51	Inf
11	Current account deficit to GDP[c]	CA deficit	-0.02	0.07	-0.27	0.10	-0.98	0.73	0.09	33.12
12	Global real GDP[b]	Global real GDP growth	1.84	1.59	-6.34	4.09	-3.02	11.74	0.20	122.16
13	Global real credit to private sector to GDP[b]	Global real credit growth	3.87	1.68	-0.23	7.20	-0.21	-0.31	0.07	8.82
14	Global credit to private sector to GDP[a]	Global leverage	1.15	2.79	-2.79	11.21	1.84	3.40	0.22	105.26

Note: Transformations: [a], deviation from trend; [b], annual change; [c], level. KSL: Lilliefors' adaption of the Kolmogorov-Smirnov normality test. AD: the standard Anderson-Darling normality test. All normality tests are significant on a 1% level.

Using the financial stress index (FSI) in Lo Duca and Peltonen (2011), we have an objective criterion to date financial crises.[4] The FSI is transformed to an ideal leading indicator that perfectly signals a systemic financial crisis before the event (i.e. the predicted variable) by first defining crisis periods as those when the FSI moves above the 90th percentile of a country-specific distribution, and then by setting the pre-crisis dummy to '1' in the 18 months preceding the systemic financial crisis, and to '0' in all other periods. While the NN and GA methodology is flexible for different forms of input data, the rationale behind using a dataset previously introduced in the literature is to test performance on objective data rather than those that fit the model (i.e. data dredging). To objectively test model performance on the global financial crisis that started in 2007, the sample is split into two sets: the in-sample set (1990:4–2005:1) and out-of-sample set (2005:2–2009:2).

Performance evaluation

In this paper, performance of EWSs is evaluated by computing a goodness-of-fit measure that incorporates policymakers preferences. As is common in the literature, the EWSs issue signals when the estimated probability of a crisis is above a specified threshold. The outcomes are classified into a contingency matrix, including true positives (TP), true negatives (TN), false positives (FP) and false negatives (FN). We follow the approach employed in Demirgüc-Kunt and Detragiache (2000) and Alessi and Detken (2011) by calibrating an optimal model and threshold for policy action that maximizes the utility for a policymaker with specific preferences about giving false alarms (type I errors) and missing crises (type II errors). The policymaker has the following loss function:

$$L(\mu) = \mu(FN/(FN+TP)) + (1-\mu)(FP/(FP+TN)) \quad (7)$$

where the parameter μ represents the relative preference of the policymaker between FNs and FPs. Given differences in class size, the policymaker is equally concerned of missing crises and issuing false signals for a value of $\mu = 0.5$, less concerned of issuing false signals when $\mu > 0.5$, and less concerned of missing crises when $\mu < 0.5$. Hence, the utility of one specific threshold is given by subtracting from the expected value of a best-guess with those preferences:

$$U = Min(\mu, 1-\mu) - L(\mu) \quad (8)$$

The performance of a model is solicited by choosing a threshold on the probability of a crisis such that utility U is maximized.

BIOLOGICALLY INSPIRED PREDICTIONS OF THE GLOBAL FINANCIAL CRISIS

To evaluate the NN and NG models, it is necessary to compare them with a benchmark, such as conventional statistical techniques from previous EWS literature. These methods (e.g. DA and logit/probit analysis) can in fact be related to very simple NNs; in particular, NNs with no hidden layer, single-layer perceptrons, with a threshold activation function and logistic activation function (Ripley, 1994; Sarle, 1994). The obvious problem with most statistical methods is that all assumptions on data properties are seldom met. As methods from the GLM family have less restrictive assumptions (e.g. normality of the indicators), we turn to logit analysis. It is preferred over probit analysis as its more fat-tailed nature corresponds better to the rarity of crises.

[4] The FSI consists of five components: the spread of the 3-month interbank rate over the rate of the 3-month government bill; quarterly equity returns; realized volatility of a main equity index; realized volatility of the exchange rate; and realized volatility of the yield on the 3-month government bill.

Even very simple NNs have been shown to be universal approximators by following any continuous function to any desired accuracy (Hornik et al., 1989). This said, the focus of data-driven NN applications in real-world settings should rather be on parsimonity and generalization than on fitting models to all non-linearities and complexities in data. Another common concern is the extent of data dredging when conducting data-driven analysis. To this end, we build NN-based EWSs using two objective training, or early stopping, schemes:

- Scheme 1: Training is performed until in-sample performance of a conventional benchmark model has been reached.
- Scheme 2: Data is divided into three datasets: train, validation and test sets. Models are trained on the train set and the one with optimal validation performance is chosen.

The in-sample dataset is used for estimating a logit model. The estimates of the model are then used to solicit the probability of a crisis and further the utility for policy action. In training scheme 1, the in-sample utility of the logit model for policy action, U=0.25, is used as a benchmark (stopping criterion) when training the NNs. The rationale behind this is twofold: it attempts to prevent overfitting and enables testing whether a NN that is equally good on the in-sample performs better on out-of-sample data. We manually test the performance of NN configurations over a wide set of possibilities as well as of the automated NG model. In training scheme 2, the in-sample dataset is randomly split as follows: 80% train set and 20% validation set. This gives us three datasets: train (in-sample, 80%), validation (in-sample, 20%) and test (out-of-sample) sets. Then we train NN and NG models by optimizing utility for policymakers on the validation set. In practice, we train models for 200 epochs, evaluate them at each epoch and choose the one that maximizes utility on the validation set. This allows testing how much better, if at all, the NN and NG models perform when attempting an optimal model. As NNs are sensitive to initial conditions of the weights, the training of NN and NG models is repeated ten times with randomized starting weights and biases, and then the one with the fastest convergence (least epochs) is chosen. Robustness of GA parameters is tested by varying generation count, population size and mutation rate. The number of crossovers and the fitness criterion are kept fixed because of the shortness of the strings and the aim of the GA training (i.e. utility for policymakers), respectively.

We assume a benchmark policymaker to be equally concerned of missing crises and giving false alarms (μ=0.5), but also show model performance for those with other preferences (μ={0.4,0.6}). For all models using training scheme 1 (in-sample U=0.25), the final NN elements and GA parameters, as well as their out-of-sample utility for policymakers, are shown in Table 2.[5] The results clearly depict differences in model performance (best models per μ are bold). The NN-based models, while having similar in-sample performance by definition, show consequently better out-of-sample performance than the benchmark logit model. Best overall performance is shown by the NG model and the best NN model (NN1) follows parameterization practices common in the literature (see e.g. Peltonen, 2006; Fioramanti, 2008). Most notably, the optimal GA configuration uses only 9 indicators (bold in Table 2). When examining differences in performance for different policymakers' preferences, one can observe that the logit model fails for those emphasizing the share of correctly called crises (U=0), the NN results are somewhat mixed and the NG model brings utility for all types of policymakers (U={0.10,0.19,0.08} for μ={0.4,0.5,0.6}). While NNs are heuristic in nature, the consistency in the slight superiority is likely to be a result of the parsimonious training scheme.

Training scheme 2 attempts better generalization by being less restrictive in terms of parsimonity but still preventing overfitting. Table 3 summarizes in-sample (includes both train and validation sets), validation and out-of-sample performance of the logit model, the best-performing NN model (NN1) and the NG model using training scheme 2. The table shows that, in principle, when allowing for longer training, and thus also a better fit to data, model performance improves on all datasets (best performing model per μ and dataset is bold). This is obvious when it comes to in-sample data, but the validation as well as out-of-sample data still need sufficient parsimonity for decent performance. Compared to training scheme 1, while there is only a small increase in out-of-sample utility of NN1 (from 0.18 to 0.19), the performance of the NG model increases significantly (from 0.19 to 0.22). Out-of-sample utility of the NG model is 70% better than that of the logit model and 17% better than that of the model from training scheme 1.

[5] Model robustness has been tested with respect to different forecast horizons. In general, for longer horizons (e.g. 24 months) there is a slight increase in utility and for shorter (e.g. 6 and 12 months) a slight decrease. However, the relative performance is similar to the benchmark results with a horizon of 18 months.

Table 2: The Configuration of the Models as well as Their Utility for Policymakers using Training Scheme 1

	Logit	*NN1*	*NN2*	*NN3*	*NN4*	*NN5*	*NN6*	*NN7*	*NN8*	*NN9*	*NG*
NN configuration											
No. of nodes in the input layer:	-	14	14	14	14	14	14	14	14	14	9
No. of nodes in the output layer:	-	1	1	1	1	1	1	1	1	1	1
Number of hidden layers:	-	1	1	1	2	2	1	1	1	2	1
No. of nodes in layer 1:	-	2	2	8	2	8	2	2	2	20	4
No. of nodes in layer 2:	-	0	0	0	2	8	0	0	0	20	0
Activation function:	-	Sigmoid	Sigmoid	Sigmoid	Sigmoid	Sigmoid	Gaussian	Hyperbolic	Linear	Sigmoid	Sigmoid
No. of training epochs:	-	15	11	9	22	11	21	13	12	5	6
Learning rate α:	-	0.9	0.8	0.95	0.9	0.9	0.9	0.9	0.9	0.9	0.97
Momentum m:	-	0.9	0.2	0.8	0.9	0.9	0.9	0.9	0.9	0.9	0.15
Input noise ε:	-	0.01	0	0	0.01	0.01	0.01	0.01	0.01	0.01	0.01
GA configuration											
Generation count:	-	-	-	-	-	-	-	-	-	-	10
Population size Ω:	-	-	-	-	-	-	-	-	-	-	3
No. of crossovers:	-	-	-	-	-	-	-	-	-	-	1
Mutation rate:	-	-	-	-	-	-	-	-	-	-	0.10
Fitness criterion:	-	-	-	-	-	-	-	-	-	-	train error
Out-of-sample utility											
μ=0.4	0.07	0.08	0.06	0.07	0.06	0.08	0.06	0.07	0.08	0.08	**0.10**
μ=0.5	0.13	0.18	0.15	0.16	0.16	0.16	0.14	0.14	0.17	0.16	**0.19**
μ=0.6	0.00	**0.08**	0.04	0.05	0.06	0.04	0.02	0.01	0.07	0.05	**0.08**

Table 3: The Utility for Policymakers of Models on In-sample, Validation and Out-of-sample Data using Training Scheme 2

Model	**Epochs**	**In-sample**			**Validation set**			**Out-of-sample**		
		μ=0.4	*μ=0.5*	*μ=0.6*	*μ=0.4*	*μ=0.5*	*μ=0.6*	*μ=0.4*	*μ=0.5*	*μ=0.6*
Logit	-	0.16	0.25	0.14	-	-	-	0.07	0.13	0.00
NN1	36	0.19	0.29	0.19	0.09	0.19	0.10	0.09	0.19	0.09
NG	17	**0.20**	**0.30**	**0.21**	**0.13**	**0.22**	**0.12**	**0.13**	**0.22**	**0.11**

CONCLUSIONS

This paper compared the utility for policymakers of a NN and NG model with that of a conventional logit model. Given similar in-sample performance, we have shown that the NN-based, in particular NG, models outperform the conventional statistical model. The introduction of an early stopping method using a third dataset, a validation set, further increases the difference in utility. Hence, the main finding is that NG models not only provide more utility for policymakers in terms of predictive capabilities, but also in form of decreased expertise and labor needed for, and uncertainty caused by, manual calibration of a NN. The paper also motivates adoption of validation sets for increased generalization of data-driven EWSs.

ACKNOWLEDGMENTS

The author wants to thank Barbro Back, Marco Lo Duca and Tuomas Peltonen, as well as seminar participants at the Data Mining and Knowledge Management Laboratory at Åbo Akademi University, for useful comments and discussions.

REFERENCES

Alessi, L. and C. Detken. 2011. "Quasi real time early warning indicators for costly asset price boom/bust cycles: a role for global liquidity." *European Journal of Political Economy* 27, No.3, 520–533.

Aminian, F.; E. Suarez; M. Aminian; and D. Walz. 2006. "Forecasting Economic Data with Neural Networks." *Computational Economics* 28, 71–88.

Bishop, C. 2007. *Pattern Recognition and Machine Learning*. Springer, Germany, Heidelberg.

Demirgüc-Kunt, A. and E. Detragiache. 2000. "Monitoring Banking Sector Fragility: A Multivariate Logit Approach." *World Bank Economic Review* 14, 287–307.

Fioramanti, M. 2008. "Predicting sovereign debt crises using artificial neural networks: a comparative approach." *Journal of Financial Stability* 4, No.2, 149–164.

Franck, R. and A. Schmied. 2003. "Predicting currency crisis contagion from East Asia to Russia and Brazil: an

artificial neural network approach." AMCB Working Paper No 2.
Frank, C. and W. Cline. 1971. "Measurement of Debt Servicing Capacity: An Application of Discriminant Analysis." *Journal of International Economics* 1, 327–344.
Hagan, M.T.; H.B. Demuth; and M. Beale. 1996. *Neural Networks Design*. PWS Publishing, Boston, MA.
Haykin, S. 1998. *Neural Networks: A Comprehensive Foundation*. Second Edition. Prentice Hall, New Jersey.
Holland, J. 1975. *Adaptation In Natural and Artificial Systems*. The University of Michigan Press, Ann Arbour.
Hollo, D.; M. Kremer; and M. Lo Duca. 2012. "CISS – A composite indicator of systemic stress in the financial system." ECB Working Paper, forthcoming.
Hornik, K.; M. Stinchcombe; and H. White. 1989. "Multilayer feedforward networks are universal approximators." *Neural Networks* 2, 359–366.
Kaminsky, G.; S. Lizondo; and C. Reinhart. 1998. "Leading indicators of currency crises." *IMF Staff Papers* 45, 1–48.
Lo Duca, M. and T. Peltonen. 2011. "Macro-Financial Vulnerabilities and Future Financial Stress – Assessing Systemic Risks and Predicting Systemic Events." ECB Working Paper, No. 1311.
Nag, A. and A. Mitra. 1999. "Neural networks and early warning indicators of currency crisis." Reserve Bank of India, Occasional Papers 20(2), 183–222.
Peltonen, T.A., 2006. "Are emerging market currency crises predictable? A test." ECB Working Paper, No. 571.
Ramser, J. and L. Foster. 1931. "A demonstration of ratio analysis." Bureau of Business Research, University of Illinois,Urbana, IL, Bulletin 40.
Ripley, B. 1994. "Neural Networks and Related Methods for Classification." *Journal of the Royal Statistical Society* 56, 409–456.
Sarle, W. 1994. "Neural Networks and Statistical Models". In *Proceedings of the Nineteenth Annual SAS Users Group International Conference*, Cary, NC: SAS Institute, 1538–1550.
Sarlin, P. and D. Marghescu. 2011. "Visual Predictions of Currency Crises using Self-Organizing Maps." *Intelligent Systems in Accounting, Finance and Management* 18(1), 15–38.
Sarlin, P. and D. Marghescu. 2012. "Neuro-Genetic Predictions of Currency Crises." *Intelligent Systems in Accounting, Finance and Management*, forthcoming.
Sarlin, P. and T.A. Peltonen. 2011. "Mapping the state of financial stability." ECB Working Paper No. 1382.

AUTHOR BIOGRAPHY

PETER SARLIN was born in Turku, Finland and obtained his MSc (Econ.) degree in 2009 from Åbo Akademi University. At the same university, he is currently pursuing a PhD degree in information systems with an emphasis on financial stability surveillance with computational intelligence. Peter has regularly also visited central banks, such as the European Central Bank and the Bank of Finland. His e-mail address is: `psarlin@abo.fi` and his Web-page can be found at `research.it.abo.fi/personnel/psarlin`.

CORPORATE VALUATION MODEL IN A STOCHASTIC FRAMEWORK

Barbara Dömötör, Péter Juhász, PhD, CFA
Department of Finance
Corvinus University of Budapest
1093, Budapest, Hungary
E-mail: barbara.domotor@uni-corvinus.hu

KEYWORDS
Corporate valuation, Business modeling, Financial simulation

ABSTRACT[1]

In this paper we present a corporate valuation model, which integrates the different approaches of various fields of finance in a single stochastic framework. We construct a stylized company, which has its explicit production, inventory, export and import activity. In our simulation we analyze the affect of the future volatility of three stochastic factors (production, inflation and exchange rate) and their correlations on the distribution of the current value of the firm. Furthermore we investigate the added value of the possibility of early termination of the project.

MOTIVATION

In corporate finance the immanent uncertainty of financial processes is treated generally by taking the expected value of a random variable – the elements of the future cash-flow – and the risk of the realization appears in the increased discount factor.[2]. As a consequence of this solution, on one hand the cash-flow of a firm is predicted on the base of the expected value of its projects and its financing, on the other hand the stock price movement is described with a distribution, pretending as if the risk of the equity was generated by the capital markets (the trading) only, and not even partly by the corporate operation itself. Moreover the classical present value calculation neglects the stochastics of the applied financial processes like inflation, money market returns and currency rates.

In the following analysis we present a corporate valuation model, which uses the distribution instead of the expected value of the stochastic processes. In our calculations the values of the stochastic factors are generated as a realization of correlated Ito processes. So the input parameters of the valuation model come from the random walk model used in derivative asset pricing in the financial markets.

Nevertheless this Monte Carlo simulation is not an alternative of the sensitivity, or scenario analysis. In case of sensitivity analysis our aim is to identify the factors the changes of which have a critical effect on the results (being either a distribution or an expected value), and which because of this need to be forecasted very carefully. The scenario analysis however investigates some special joint outcomes of the random variables. This kind of analysis can be carried out in our framework as well.

The structure of the paper is as follows. The next session introduces the theoretical background and then we present the assumptions of our model. The second part of the paper contains the results of the simulations: first we analyze the effect of the volatility of one stochastic factor on the distribution of the current value of the firm, then we model the corporate value taking all 3 factors volatile and finally the real option of terminating the project early is valued.

THEORETICAL BACKGROUND

Financial modeling uses several models to describe the time depending stochastic variables. The classic model assumes that the change in a stochastic parameter (market price) is independent of its past price movements (Markov property, due to market efficiency). The change in the price during a time of *dt* adds up from a deterministic and a stochastic part, where the random part is normally distributed. If this change is continuous both in time and value, the process is called Ito-process:

$$dS_t = x(S,t)dt + \sigma(S,t)dw_t \qquad (1)$$

Where dS_t is the change of process S during a period of dt, the length of which approaches to zero and x and σ are variables depending on S and the time (t); dw stands for the change of a Wiener process[3] during the same period, that is a normally distributed random variable with a mean of zero and variance of t.

In case of market traded assets, like foreign exchange rates, normality is a consequence of the market

1 The paper was supported by the European Union and co-financed by the European Social Fund in the framework of TÁMOP-4.2.2/B-10/1-2010-0023 project.

2 However the Gaussian distribution emerges when modeling the stock returns, and consequently the lognormality of stock prices is accepted, the corporate finance deals with constant figures.

3 See details in Hull (2009) and Medvegyev, Száz (2010).

Proceedings 26th European Conference on Modelling and Simulation ©ECMS Klaus G. Troitzsch, Michael Möhring, Ulf Lotzmann (Editors)
ISBN: 978-0-9564944-4-3 / ISBN: 978-0-9564944-5-0 (CD)

efficiency, namely that only a per definition random new information can affect the actual price.
We agreed to use the same process (with a slight modification) for the process of inflation and production. In the simulation the price can change only in discrete time, that's why we used the discrete version of equation (1):

$$\Delta S_t = x(S,t)\Delta t + \sigma(S,t)\Delta w_t \qquad (2)$$

This one-letter difference (the change in time is considered not in limit) has severe mathematical consequences, which exceeds the content of our paper. The most important consequence of the dicretization of the continuous model is the fact, that the risk cannot be perfectly eliminated – except for the binomial approach. In all other discrete cases (trinomial model, etc) the market is incomplete (Medvegyev, Száz 2007).
The random figures used for the simulation are calculated by weighting independent normal variables, where the weights are generated from the Cholesky factorization of the correlation matrix. The method is detailed among others in Bau and Trefethen (1997).

THE MODEL

The model we used for our calculations is not very much different to the standard present value calculus. In order to be able to analyze more complex problems in the future we built an MS Excel model that is more detailed and its parameters can be set more flexibly. So beside balance sheets and income statements it also contains a business cash flow and a discounted cash flow based business valuation model.
The explicit period is 20 years long, in the terminal value the invested capital can not generate a return in excess of the required level, so the value of the firm equals the invested capital. The firm produces only one type of product that is sold both locally and for export.
The invested assets and working capital needed for the production are invested at time zero. The useful lifetime of the invested assets is 10 years, the firm uses a linear depreciation and amortization model. In year 10 we need to replace the invested assets and the model extends until this replacement is completely used up again. In this paper – as some financial theories do - we assume, that financing is always available for good projects, so our model-company is financed exclusively from equity, we disregard the question of capital structure.
Both selling and purchasing prices and the cost of replacement for invested assets are affected by the inflation rate of the corresponding currency. Yet there is no difference made between consumer and industrial price index.
Among the expenses of the firm we have both fix (independent of the quantity produced) and variable items. The turnover days of inventory, receivables and payables can be set year-by-year individually, though in the models presented here those are all set to 30 days meaning those depend only upon the sales.
Our model calculates the tax due always based on the given years earnings so no deferred tax exists. We also took care of money not needed for the operation. If the extra money can not be redrawn as dividend because the maximum of that is the annual after tax earning, owners decrease capital (buy back shares).
Based on the cash flow of the 20 years predicted we determine the value of the firm (project) for the start of each year. For that we apply the APV method where the sum of the free cash flow (FCFF) and the tax shield (TS) generated by the annual interest payments on debt is to be discounted by the operative cost of capital (r_A) With a formula:

$$V_0 = \sum_{i=1}^{20} \frac{FCFF_i + TS_i}{\prod_{j=1}^{i}(1+r_{Aj})} + \frac{IC_{TV}}{\prod_{j=1}^{20}(1+r_{Aj})} \qquad (3)$$

where V stands for the value of the firm. As terminal value we used the invested capital value for the end of the 20th year in line with our assumption that after that year achieved and required return will equal. (For a detailed description of this model see Koller, Goedhart and Wessels (2010).)

In our model three stochastic processes appear. Probability variable describes for each of the 20 years the demand (and so the produced quantity) of the good (Q), the local inflation (Π) and the foreign exchange rate (S). The variables in contrast to the classic Monte Carlo simulation are not independent from each other but rather the correlation between them can be set by parameters.
The expected amount of annual quantity sold is given. The source of uncertainty here is a random variable following a normal distribution with an expected value of zero and a set standard deviation. This variable gives the difference in percentages between the actual and the expected annual quantity. The risk originating from this is somewhat limited: because of long term contracts the realized value may not be lower than *b* percent (60%) of the expected and due to the maximum capacity of the machines it may not exceed *a* percent (140%). (The expected value is 1 million pieces.)

$$Q_t = \max(\min(1+\sigma_q \Delta w_q; a); b) \qquad (4)$$

For the focus of our investigation we picked the uncertainty emerging associated with the local inflation whilst the change in the foreign price level is dealt with as an exogenous, well predictable variable. The changes of the local interest rates follow exactly the pattern of the local inflation (in other words the local real interest rate is constant) while the exchange rate (starting form 1 euro = 300 HUF) is linked to the inflation differences only as a trend with some volatility around that. We assume the foreign inflation to be constant and modest (2 percentage) compared to the local level.

$$\Delta\Pi_t = \sigma_I \Delta w_I \quad (5)$$

So while in case of the inflation and the production the expected value has an unchanged mean though the full time horizon of the model in case of the exchange rate we have a non-constant mean. This is because the mean of the later for a given year is the theoretical rate calculated from the previous year's rate based on the inflation differences.

$$\Delta S_t = (\Pi_0^{domestic} - \Pi_0^{foreign})S_t \Delta t + \sigma_S S_t \Delta w_S \quad (6)$$

The correlation matrix of the random parts of the stochastic processes (Δw_i) is predetermined and constant in time.

First our model calculates five thousand realizations for each combinations of starting parameters and then determines the base statistics for the distribution. We recorded not only the net present value of the project (that is the difference between the intrinsic value and the invested capital) but also the value of the firm and the present value of tax paid to the state and the probability of bankruptcy.

The starting point of our calculus is very similar to a formal paper of Száz [2007] on the Ho-Lee model. That model examined the long term equilibrium ratios using a stochastic interest rate. In our current model the stochastic inflation determines the change in interest rates and it explicitly shows at the changing risk involved in the exchange rates.

ANALYSIS OF THE DISTRIBUTION OF CORPORATE VALUE

First, we calculated the corporate value by switching all risks off by setting all standard deviations to zero. In this case there is no uncertainty, each and every parameter can be foreseen. In our theoretical example the value of the company is 1.497,62 million HUF, and it requires 1.360 million HUF invested capital. Therefore entering into that business has 137,62 million HUF net present value (Market Value Added), meaning the project is worth to finance.

We applied the same real operative (unlevered) cost of capital (r_A=12%) in every scenario, which is a constraint of our analysis, as the cost of capital may vary according to the fact whether the sales revenue derives from export or domestic market, or whether it is ensured by fixed quantity sold or it is random.

On the other hand the cost of capital is a function of numerous other factors (like macroeconomic environment, industry or labor force needs), so the systematic risk is considered identical in all cases. We assume that the volatility of the analyzed factors stem from individual and diversifiable risk, and consequently do not enhance the risk premium of the project.

Effect of the volatility of production

The increasing volatility of the production – corresponding to the relevant theory – increases the extent of the distribution, and so the probability of negative outcomes, but it reduces the expected value as well. Figure 1 depicts the probability distributions of the net corporate value in time 0, assuming different volatility of the annually produced quantity. Table 1 summarizes the statistics of the distributions.

Figure 1: Distribution of corporate value as a function of production volatility (HUF million)

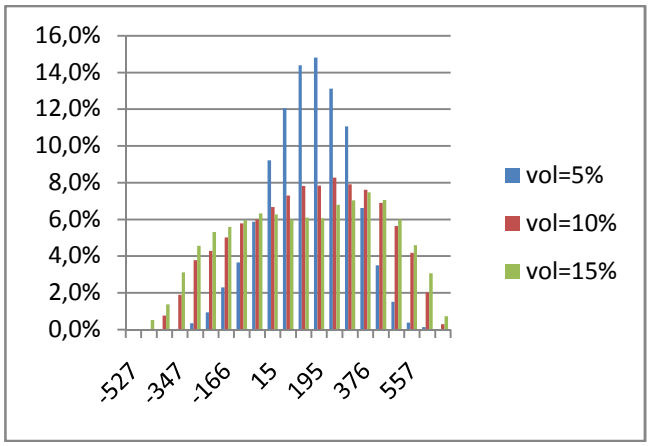

Table 1: Statistics of the distribution

HUF million	Volatility		
	5%	**10%**	**15%**
Mean	134	125	110
Standard deviation	157	254	282
St. Dev/Mean	117%	203%	255%
Maximum	598	659	677
Minimum	-439	-464	-527
Median	140	140	122
Quartile 1	28	-69	-120
Quartile 2	140	140	122
Quartile 3	247	330	348
Probability of default	20%	32%	37%

A slight volatility (5%) of the production results a negative net present value in 20% of the cases, meaning that the generated cash flow is not enough to cover the required cost of capital. In the worst case (1 realization out of 5000) the discounted value of the cash flow during the 20 years is only 68% of the invested capital. The increasing volatility causes trivially higher upside and downside deviations.

As the produced quantity can fluctuate in a +/-40% range around the mean, in the theoretical worst case the production is the fixed minimum (600 thousand pieces annually). In that case the firm value is -667 million HUF. The term "probability of default" refers not to a real default in our analysis, but the probability that the return fails to exceed the cost of capital, as we assume

that financing is always available, the project is to be continued in case of negative cash flow as well.

Exchange rate volatility

The other source of the dispersion of the corporate profit and so the corporate value derives from payments in foreign currency. In the example shown in this paper only the sales revenue (export) depends on foreign exchange rate, but of course any other items of the cash flow could contain similar risk. The sensitivity toward currency risk is determined by the net position in foreign currencies that can be reduced or even perfectly eliminated by natural hedge (matching foreign currency position of incoming and outgoing items: e.g. export revenue and foreign exchange loan) or financial derivatives.

According to our assumptions the expected change of the foreign exchange rate equals the difference of the inflation – the uncovered interest rate parity is held –, and the sales price follows the change of the price level, therefore if the exchange rate volatility is 0 percent, the denomination of the sales revenue has no affect on the results. Table 2 shows the statistics of the distribution of the corporate value by 50% and 100% export ratio (denominated and settled in euro) and different EUR/HUF exchange rate volatility. The expected value is the same almost in all cases, except for the scenario of full export and 15% currency rate volatility. Here we can see a drastic drop (by 33%) of the mean of the corporate value, which is to be explained by the fact that in contrast to the process of the production, we do not apply any constraint on the exchange rate fluctuation, so the appearance of extreme values has impressive effect. An exchange rate volatility of 15% – without any currency hedge – causes for an exporter company the risk of failing the project in half of the cases, and almost 150% of the invested capital can be lost (here we neglect the possibility of getting out of the project, so the owners meet their payment obligation even if the net present value of the project at the end of the year 10 is negative). It is remarkable, that the drift of the EUR/HUF exchange rate during the first decade of the 2000s, was not only less than the interest rate difference, but it was in most of the years negative, resulting a forint-appreciation.

Table 2: Corporate value in case of FX-risk

Export ratio	50%			100%		
HUF million	Volatility			Volatility		
	5%	10%	15%	5%	10%	15%
Mean	136	137	133	133	133	91
Standard deviation	125	252	386	251	526	838
St. Dev/Mean	92%	185%	289%	188%	396%	916%
Maximum	660	1 245	2 482	1 230	2 484	5 470
Minimum	-244	-600	-754	-812	-1 598	-2 052
Median	131	114	74	121	100	-1
Quartile 1	49	-43	-136	-36	-220	-487
Quartile 2	131	114	74	121	100	-1
Quartile 3	219	285	346	293	456	570
Probability of default	14%	31%	40%	30%	43%	50%

Stochastic inflation

In our model exclusively the domestic inflation is stochastic, we handle the foreign inflation to be constant. The price level affects both the revenue and the cost side, so the change of the inflation has a balanced influence on the profitability of the company. The inflation takes effect on the corporate value principally through the financing costs, as it is included in the nominal cost of capital. At a moderate inflation level (3%), volatility of inflation can be neglected, as even an extreme (50%) volatility causes just a modest range of corporate value fluctuation (table 3).

Volatility of inflation can cause negative net present value if the inflation exceeds 10%, with a larger volatility of 50%. In this extreme case the probability of default is 5%, but it is due to the higher cost of capital, and accordingly low expected value, the affect of the volatility is less significant.

Table 3: Affect of the price level and volatility of inflation on corporate value

Inflation	3%				10%			
HUF million	Volatility				Volatility			
	5%	10%	15%	50%	5%	10%	15%	50%
Mean	138	138	138	137	18	18	19	22
Standard deviation	1	1	2	7	1	3	4	14
St. Dev/Mean	0%	1%	2%	5%	8%	15%	22%	64%
Maximum	140	143	145	164	23	28	34	78
Minimum	135	132	128	105	13	7	4	-21
Median	138	138	138	137	18	18	18	21
Quartile 1	137	137	136	133	17	16	16	12
Quartile 2	138	138	138	137	18	18	18	21
Quartile 3	138	139	139	142	19	20	21	31
Probability of default	0%	0%	0%	0%	0%	0%	0%	5%

Three stochastic factors

Each of the simulations above present the effect of one stochastic factor on corporate value. Supposing all the three parameters to be stochastic, we have to model the joint distribution of the three risk factors. The factor volatilities used in the model are: 5% (production); 10% (inflation)[4]; 10% (exchange rate)[5].

We applied three correlation structure: independent factors (correlation coefficient: 0); perfect positive correlation – meaning an increase in the production is followed by increasing inflation and exchange rate; and a "real" correlation structure, which we intended to construct to be close to the real market circumstances. Consequently the correlation between inflation and exchange rate is strong (δ=0.8), as weakening of the forint usually causes higher inflation. We assume a weak, almost zero correlation between the production and the inflation (δ=0.1), because inflation has a two-sided effect on the produced quantity. The correlation of exchange rate and production is assumed to be positive, but not too strong (δ=0.4). Table 4 contains our results.

The higher correlation (economic predictability) enhances the corporate value. The same result was achieved by Csányi, Juhász and Megyik (1997) in their simulation of a corporate population. On the other hand the deterministic relationship excludes the possibility that the unfavorable market movements of the factors are balanced, the risks are less diversified, and so the confidence of the estimation.

Table 4: Affect of correlations of the stochastic factors

Export ratio	50%		
HUF million	correlation		
	real	0	1
Mean	145	131	165
Standard deviation	352	300	422
St. Dev/Mean	244%	229%	256%
Maximum	1 991	1 576	2 118
Minimum	-805	-767	-1 077
Median	111	105	122
Quartile 1	-98	-78	-125
Quartile 2	111	105	122
Quartile 3	342	313	412
Probability of default	37%	36%	38%

According to that the intervention of the state into the economy (for example the home currency is under pressure because of an extreme foreign debt) is value destroying. However the bias caused by the state can lead to less correlated affects of the economic factors.

As in such cases the link between different risk factors may be shifted some negative tendencies in the real economy may be counterbalanced by the weakening of the correlations. But as soon the distortions disappear (the increase of foreign debt slows) and the basic connections come again to dominate and the effect of the real economic tendencies (global and euro crisis) may influence the economy undimmed. The value of the projects would change in line with the basic tendencies end their risk will surely grow.

[4] The standard deviation of the annual consumer price indices between 2000-2011 was 2,2%, according to the data of the Hungarian Central Statistical Office.

[5] The annual EUR/HUF exchange rate volatility is 9,2% since 2000; the volatility of the last 5 years is 12,2% , based on the daily ECB fixings.

TERMINATION OF THE PRODUCTION

It is an important assumption of the above analysis, that the company will operate for 20 years after starting the project (entering into a contract about the annual delivery) and there is no chance to cease production even if the discounted cash-flow of the further years is negative.

The possibility of termination the project earlier can be considered as a real option. In case of arising financing need (negative cash flow), it is always worth to examine, whether the discounted cash flow of the further years can cover the new investments and otherwise abandon it.

We build this option in our model allowing the project owners to deny the additional capital investment at the end of the 10th year. In the absence of risky factors (all processes are deterministic), this option has of course no value. Using the volatility figures and the "real" correlation matrix of the previous section, the option of early termination enhances the initial corporate value by 11 million HUF, 7% of the total project value (table 5.).

The real option has no influence on the probability of default, but it moderates the extent of the losses in the negative outcomes.

Table 5: Distribution of the corporate value, with and without the possibility of early termination

Export ratio	**50%**	
HUF million	**Real option**	
	not available	**available**
Mean	145	156
Standard deviation	352	343
St. Dev/Mean	244%	220%
Maximum	1 991	1 962
Minimum	-805	-576
Median	111	110
Quartile 1	-98	-97
Quartile 2	111	110
Quartile 3	342	360
Probability of default	37%	37%

CONCLUSION

In this paper we presented the consequences of the uncertainty deriving from stochastic production and inflation in addition to the market risk of currency rates on the corporate value. We constructed a simplified corporate model, which includes production, investment, inventory, export and import. Our calculations confirm the more significant role of the fluctuation of foreign exchange rates on the corporate value volatility of an exporter company, than the volatility of production itself. The reason for this is the fact, that the lower income of a decreasing production is counterbalanced partly by the parallel reduction of the costs. The volatility of inflation proved to be less determining, as we provided, that inflation affects the similarly both the incoming and outgoing items of the profit and loss. Furthermore early termination of the project as a real option enhances the corporate value considerably.

The extent of these effects can be critical in corporate operation. We offered a framework that expands the usual corporate valuation models with the methods used in risk management and derivatives' pricing. Monte Carlo simulation is the most adequate tool for that.

We plan to develop further our research by releasing the assumption of perfect market liquidity (financing sources being always available), in order to investigate the effect of the capital structure, and the different types of loan.

REFERENCES

Bau III, D., Trefethen, L. N. (1997). *Numerical Linear Algebra*. Society for Industrial and Applied Mathematics, Philadelphia

Brealey, R. A., Myers, S. C., Allen, F. (2008): *Principles of Corporate Finance*, ninth edition, McGraw-Hill, New York

Csányi, T., Juhász, P., Megyik, L. (1997): From Shortage Economics to the Shortage of Market Economy, (in Hungarian: A hiánygazdaságtól a gazdaság hiányáig), *Élet és Irodalom*, 28 November 1997. pp. 5-6.

Damodaran, A. (2002): *Investment Valuation. Tools and Techniques for Determining the Value of Any Assets*. second edition, Jonh Wiley & Sons, Inc., New York

ECB Statistics: http://sdw.ecb.europa.eu/browseTable.do?node=2018794&CURRENCY=HUF&FREQ=D&sfl1=4&sfl3=4&DATASET=0&SERIES_KEY=120.EXR.D.HUF.EUR.SP00.A downloaded: 08.02.2012

Hull, J. C. (2009): *Options, Futures and other Derivatives*, seventh edition, Pearson/Prentice Hall

Koller, T., Goedhart, M., Wessels, D. (2010): *Valuation, Measuring and Managing the Value of Companies*, fifth edition, John Wiley & Sons, New York

KSH Statistics: http://statinfo.ksh.hu/Statinfo/haViewer.jsp; downloaded: 08.01.2012

Medvegyev, P., Száz, J. (2010): *The Nature of Continuous Surprices in the Financial Markets*. (in Hungarian: A meglepetések jellege a pénzügyi piacokon), Jet Set, Budapest

Ross, S., A., Westerfiled, R., W., Jordan, B., D. (2008): *Corporate Finance Fundamentals*, eight edition, McGraw-Hill, New York

Száz J. (2007): The Increase of the Corporate Capital and the Ho-Lee Model. (in Hungarian: A vállalati tőkeállomány bővülése és a Ho-Lee model), In: Pénzügy-politikai stratégiák a XXI. Század elején, Budapest, Akadémiai Kiadó

AUTHOR BIOGRAPHIES

BARBARA DÖMÖTÖR is an Assistant Professor of the Department of Finance at Corvinus University of Budapest. Before starting her PhD studies in 2008, she worked for several multinational banks' treasury in field of structuring currency and interest rate risk hedging products for corporate clients. She works now on her doctoral thesis about corporate hedging. She lectures Corporate Finance, Financial Risk Management and Investment Analysis, her main research areas are financial markets, financial risk management and corporate hedging. Her e-mail address is: barbara.domotor@uni-corvinus.hu

PÉTER JUHÁSZ, PhD, CFA is an Associate Professor of the Department of Finance at Corvinus University of Budapest. Besides teaching he also works as a trainer and management consultant mainly for SMEs and governmental entities. His field of research covers business valuation and planning, valuation of off-balance sheet items, corporate risk management and solving financial problems using VBA programming of MS Excel. His e-mail address is: peter.juhasz@uni-corvinus.hu

SIMULATING CAPACITY AUCTIONS WITH *econport*

F. Javier Otamendi[1]
Luis Miguel Doncel[1]
Pilar Grau[1]
Javier Ramos de Castro[2]
Universidad Rey Juan Carlos
[1]Departamento Economía Aplicada I
Paseo Artilleros s/n
28032 Madrid, Spain
[2]Departamento Ciencias de la Comunicación I
Camino Del Molino, s/n, 28943 Fuenlabrada, Madrid, Spain
E-mail: franciscojavier.otamendi@urjc.es

KEYWORDS
Auctions, On-line simulation, LNG capacity rights

ABSTRACT

A simulator environment to study and understand capacity auction has been developed based on the on-line web simulator *econport*. The goods to auction are unloading rights for ships that transport liquefied natural gas (LNG) into harbours. Experiments have been carried out at a company that will participate in the future capacity market. The efficiency of the auctions both for the auctioneer and the bidders is assessed.

INTRODUCTION

It is not easy to find an industry in Europe that goes through such drastic changes like the ones observed in utilities markets. The deregulation of the international energy markets means utility companies are facing completely new challenges, and these shifts will continue for several years to come.

The EU directives on the liberalization of the electricity and the gas markets require large capital investments as well as new management tools. However, both should be studied, analysed and designed in parallel.

One of these changes relates to the development of markets in every stage of the supply chain. Besides the utilities markets currently available for the products or commodities, the trend is to develop capacity markets, that is, the rights to move the product along the supply chain. In particular, this article focuses on the necessity to understand the rules that would govern the capacity auctions related to the rights to offload LNG from ships into harbour tanks. More specifically, time slots for offloading are to be auctioned by the corresponding governmental agency.

This type of auction is similar to the one carried to assign slots at airports. In Spain and LNG, the only auctions that are currently underway are those of the reservation of space at underground storages (CNE 2012).

There exists therefore the need to understand the dynamics of the capacity auction markets through the use of a simulator. Moreover, it is possible to test the simulator under different scenarios at a company that will be participating in the real capacity market when it will be developed by the Spanish authorities.

Auction simulators have been extensively used in research and teaching in computational and experimental economics (Kagel and Roth 2011), showing that these simulators might be particularized adhoc for the real situation. In that sense we employ, for the first time to our knowledge, an auction simulator which has been particularized to study capacity auctions in general and in the energy market in particular.

Out of the available options, we select *econport* due to its wide use and its functional interface (Chen et al. 2003; Cox et al. 2005), as well as its enormous parameterisation potential that favours its particularisation to capacity auctions.

Section 2 further defines the process to offload the LNG and the related capacity rights. Section 3 is devoted to *econport* and its options while Section 4 is used to parameterise the software to favour capacity auctions. Section 5 describes the experiment that has been carried out at a participating company. Section 6 is devoted to explain the restrictions of the software in its current state as well as the possibilities of the tool in teaching and research while Section 7 is used to conclude and to define new lines of research.

OFFLOADING OF LNG SHIPS AND AUCTION RIGHTS

Companies that wish to offload LNG at the harbour tanks have to reserve or buy capacity, since the resources are very much limited. The usage of the harbour facilities have been addressed in the literature using simulation (Bruzzone et al. 1998; or more

Proceedings 26th European Conference on Modelling and Simulation ©ECMS Klaus G. Troitzsch, Michael Möhring, Ulf Lotzmann (Editors)
ISBN: 978-0-9564944-4-3 / ISBN: 978-0-9564944-5-0 (CD)

recently, Gyoungwoo et al. 2009), including the problem when unloading ships that carry coal (Otamendi 2008) or the loads on LNG terminals (Rezende et al. 2007).

The procedures to reserve capacity are currently known by the players, but may be rapidly changed, according to the Spanish regulation set back in December of 2007. There is a trend to liberalize the markets by installing auctions at any of the supply chain stages. In addition to those available for the price of gas and LNG, markets will be also set for capacities, that is, for allocation of capacity slots at the harbours for offloading, at the plants for regasification, at the network for transportation or at the underground buffers for storage. In Spain, the auctions started in 2009 with the underground storage capacity auction (CNE 2012). It looks like the appropriate time for the companies to understand the new system and rules and develop platforms which will help in the new auction era.

Let's further define the offloading system. A company buys LNG that is transported by ship and must be offload at a harbour. Ships or tankers are usually large. The investments in LNG are therefore high and the price to pay for not offloading at the proper time is ever increasing with the delays. The size of the tankers will also force the company to buy just a few offloading rights over a long period of time. So timing is very important and bidding for the proper slots in critical.

The competitors should not be large in number. The value of offloading at the required time should also be similar for each competitor, and so should be the penalties for lack of timing. As of right now, a secondary market does not appear to be necessary, although over-the-counter (OTC) transaction should take place to trade rights.

Therefore, the companies that are going to to participate in the auction and buy offloading rights must learn how to proceed in this new situation and design strategies that will allow them to maximize their profit while maintaining the reliability of service. If a simulator existed that resembled the capacity auctions…

econport and CAPACITY AUCTIONS

econport was designed by the Experimental Economics Center of Georgia State University back in 2006 as an experimental tool to research in economics. It has one module that allows for simulating auctions. In particular, it has one routine that resembles one market in which one seller offers several goods to different bidders. This module could be used as the basis for simulating capacity auctions.

General Options and Use

To set an experiment, the auctioneer sets the following parameters:

- Number of goods or consecutive periods in which one good is auctioned at a time.
- Value of the goods, which might be individually set by hand or randomly assigned according to a uniform distribution
- Type of auction among four possibilities:
  a) Sealed-bid auctions: all the bidders submit simultaneously a single bid within the allotted time.
     1. First price: the good is awarded to the bidder who has submitted the highest bid.
     2. Vickrey or second highest price: the good is awarded to the bidder who has submitted the highest bid, but at the second highest price.
  b) Dynamic: the bids keeps on varying along time, which is limited by design.
     3. English or ascending: the bids keep on rising until time is over. The good is awarded to the bidder who has submitted the last bid.
     4. Dutch or descending: The price keeps decreasing following a preset clocked pattern until one bidder stops the proceedings by accepting and paying the current price.

The auctioneer posts then the experiment on the web and sends instructions to the bidders, including a password (Figure 1).

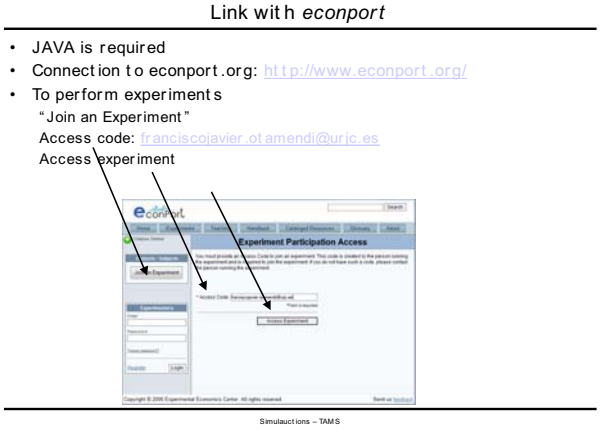

Figure 1. Platform access

Each bidder might then join the experiment and send a message to the auctioneer with the username (Figure 2). Once all the bidders have logged in and showed their intention to participate, the auctioneer starts the simulation.

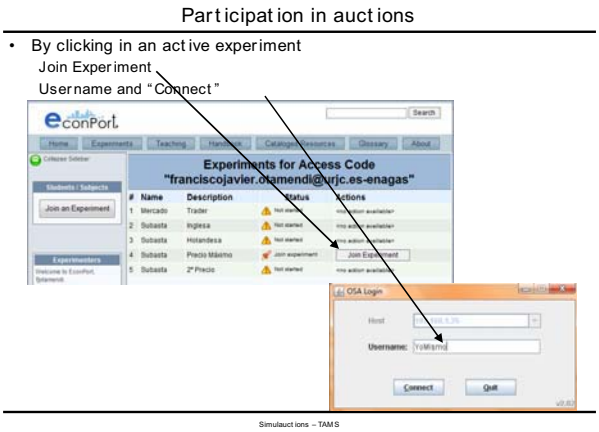

Figure 2. Intention to participate

The bidder must then place a bid if the good is of his interest. Each bidder knows his value for the good, the feasible values for the bids, as well as the number of competing bidders (Figure 3).

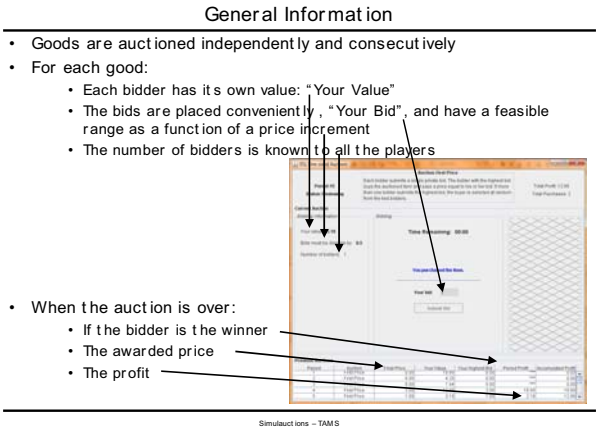

Figure 3. General information for the bidder

After a good is sold, each bidder knows the selling price, but not the name of the awarding bidder (bottom of Figure 3). He also gets information about his performance in terms of profit, calculated as the difference between value and bid. The profit accumulates after each good is sold. The auctioneer also gets information on a summary screen, which includes number of purchases and profits per bidder (Figure 4) and the relationship between values and bids (Figure 5).

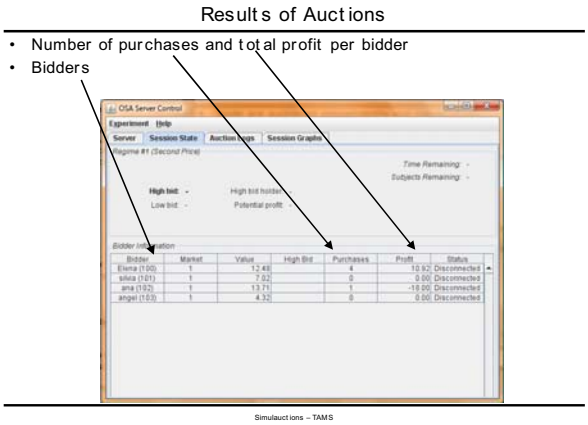

Figure 4. Auctioneer information about purchases and profits

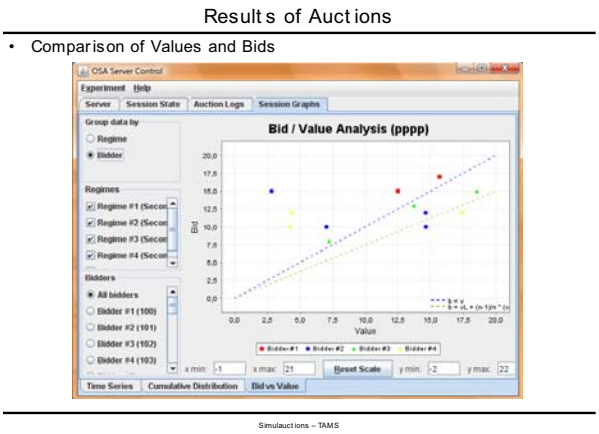

Figure 5. Auctioneer information about values and bids

Parameterisation for capacity auctions

econport must be parameterised to correctly represent the capacity auctions and for allowing for the comparison between types of auctions.

Since slots or rights are auctioned, the first decision is to determine the number of periods or goods to auction in each period. There are some markets, mainly commodity markets that offer all the goods at once, and the bids are for a certain number of rights (Capen et al. 1971; Iledare et al. 2004; Fitzgerald, 2010). Multiple rounds might be held until there is a match between supply and demand. Capacity auctions favour however one-right-at-a-time auctions due to the importance of the timing of the offloads. *econport* allows for the setting of different consecutive periods in which one good is individually auctioned.

The second decision is to determine the length of each of the auction periods. To allow for comparison across auction types, the same length should be set for each of them. While the time for sealed bid auctions (high price and Vickrey) is intuitively set, the pure English ascending price auctions do not have a time limit other than the one set by the auctioneer after a bid has been provided. *econport* allows also for a total time limit

which could be set for making the English auctions comparable to the sealed-bid auctions.

However, Dutch auctions are very different in nature. The time is set by the starting price set by the auctioneer as well as the price decrement between calls. If the starting price is high and the decrement is low, the auction time might be very long. These two decisions restrict the way the parameters are set across auction types.

The decrement should be set by the price units. The monetary units are cents, so 0.01 should be the decrement. The starting price sets then the maximum time that will be spent on the auction.

A total period length must then be set. It will be fixed for all the auctions other than the Dutch. For this auction the starting price will be set so that the auction does not last longer than the one fixed for the first three types.

Then, the value of the right assigned to the bidders is of critical importance. The starting price should be somewhat higher than the value, but close to it so that the auction price gets close to the bidder values soon.

TESTING THE SIMULATOR

General rules

Several experiments were carried out to validate the simulator and test its virtues to explain auction concepts and study strategies both for bidders and auctioneers within the capacity markets in general and LNG offloading rights in particular.

For any experiment, the simulation period was divided in 5 slots or rights, so up to 5 tankers are liable to be offloaded. Each auction period lasted 65 seconds: 5 to read the instructions and prepare the strategy and 60 to participate in the auction and bid. Each experiment was going to be tested under the rules of each of the four auction types (4 scenarios per experiment).

Almost all the experiments were set so that the average market value of the right (V*) is the same for all the bidders, although the individual values might be stochastically varied even between periods.

The session at a participating company was held on March 29th, 2011. Four teams of two people freely bid on the following auctions:

- The values were sampled from a distribution of values (V dist) that follows a Uniform distribution that ranges between 0 and 20, U(0,20).
- The values were basically constant, "common values", and sampled from a distribution of values (V dist) that follows a Uniform distribution that ranges between 9.9 and 10.1, U(9.9,10.1).
- The values were constant, "common values", but varying between periods (10, 10, 12, 8, 10).

The results that were successfully stored in *econport* are shown on Figure 6. All the 12 combinations (3 values * 4 types of auctions) were performed but some of the results were lost as they have to be stored in separate files in the system by the auctioneer (instead of by the system itself). Over-writing of files was not known at the time of the experiment.

The main result of the profits were calculated for each period or right as (Value-Bid), and averaged over the 5 rights. It is striking to see that the bids are very similar to the values, which corresponds to players that are professionally related to the field of study.

Profit (Average)

			Auction Type				
Date	V dist	Name	First Price	Vickrey	English	Dutch	Total general
29/03/2011	U (0,20)	A	0.20		2.08	0.68	0.99
		B	0.00		0.00	0.09	0.03
		C	0.66		1.44	0.00	0.70
		D	0.04		-1.34	0.22	-0.36
	Total U (0,20)		0.22		0.55	0.25	0.34
	U (9.9, 10.1)	A			0.00		0.00
		B			0.23		0.23
		C			0.09		0.09
		D			-0.39		-0.39
	Total U (9.9, 10.1)				-0.02		-0.02
	Common but not fixed (10,10,12, 8, 10)	A				0.00	0.00
		B				0.00	0.00
		C				-0.10	-0.10
		D				0.00	0.00
	Total Common but not fixed (10,10,12, 8, 10)					-0.03	-0.03
	U (9.9-10.1; 9.9-10.1; 7.9 -8.1; 5-15; 14-16)	A		-1.98			-1.98
		B		0.00			0.00
		C		-0.61			-0.61
		D		0.07			0.07
	Total U (9.9-10.1; 9.9-10.1; 7.9 -8.1; 5-15; 14-16)			-0.63			-0.63
Total 29/03/2011			0.22	-0.63	0.26	0.11	0.06
Total general			0.22	-0.63	0.26	0.11	0.06

Figure 6. Auction results

From the financial point of view, and just using descriptive statistics, it looks like "common" values call for lower profits due to the increased competition and that First Price and Dutch obtain lower prices (Kagel and Levin 1986; Turocy et al. 2007), and English auctions might rise the price more (Levin et al. 1996). More experiments are however necessary to perform a more robust inferential study and confirm these results.

Discussion

Regarding teaching, the experiments showed the potential to study concepts like:

- The importance of perfect information as provided by the common values
- The possibility of monopoly, by raising the bids and not earning profits
- The entry barriers: just by assigning low values to the same player throughout one experiment.
- The technological restrictions and advantages: some computers have better connections to the internet than others.

In terms of research, the use of the simulator demonstrated the possibility of designing a full, consistent set of experiments, whose results could shed new light on how to set a market or submit bids. Besides, the experiments could resemble the real system; role playing case studies (Myron 1971; Holt 1996; Asker et al. 2004) should be set accordingly.

Finally, *econport* has proved to be a simple tool to learn easy general concepts about auctions but somewhat rigid up to our knowledge when:

- Setting rules across periods, since the values must be set before hand.
- Analysing and comparing the results across experiments, since the values must be copy-pasted into the spreadsheet.

CONCLUSIONS

It is feasible to use *econport* to learn about capacity auctions, which will be used ever more across Europe and specifically in Spain.

The experimental simulator has been tested in a business with success. However, it appears the need to develop more "realistic" scenarios to be used as the basis for the experiments.

There also exists the possibility of performing on-line sessions. *econport* should however be integrated with other on-line tools to facilitate the communication between bidders and the auctioneer. These on-line groups might be bigger and would increase the possibility of repetitive experimentation to help in teaching and research.

ACKNOWLEDGEMENTS

This research has been partly funded by the Universidad Rey Juan Carlos by an Educational Innovation Project.

REFERENCES

Asker, J.; B. Grosskopf; C.N. McKinney; M. Niederle; A.E. Roth and G. Weizsäcker. 2004. "Teaching auction strategy using experiments administered via the Internet." *Journal of Economics Education* 35, No 4, 330-342.

Bruzzone A.G.; R. Musca; P.D. Esposti; S. Vacante and A. Carbone. 1998. "Distributed development of simulation models for harbour processes." *Computational methods in water resources* 5, 145-154.

Capen E.C.; R.V. Clapp and W.M. Campbell. 1971. "Selection bias, demographic effects and ability effects in common value auction experiments." *American Economic Review* 97, 1278-1304.

Chen H.; D. Zeng; R. Kalla; H. Zan; J.C. Cox and J.T. Swarthout. 2003. "EconPort: a digital library for Microeconomics education." In *Proceedings Joint Conference on Digital Libraries*.

Comisión Nacional de la Energía (CNE). 2012. *Analysis of Cross Border Transmission Gas Tariffs between Portugal and Spain*. Ocassional working paper.

Cox J.C. and J.T. Swarthout. 2005. *EconPort: Creating and Maintaining a Knowledge Commons*. Andrew Young School of Policy Studies Research Paper No. 06-38 (Dec).

Fitzgerald T. 2010. "Evaluating Split Estates in Oil and Gas Leasing." *Land Economics* 86, No 2, 294-312.

Gyoungwoo L.; S Svendran; and K. Sang-Hyun. 2009. "Algorithms to control the moving ship during harbor entry." *Applied Mathematical Modelling* 33, No 5, 2474-2490.

Holt C.A. 1996. "Classroom games: Trading in a pit Market." *Journal of Economic Perspectives*10, No 1, 193-203.

Iledare O.O.; A.G. Pulsupher; W.O. Olatubi and Mesyan. 2002. "An empirical analysis of the determinants and value of highs bonus bids for petroleum leases in the US Outer Continental Shelf (OCS)." *Energy Economics* 26, No2, 239-259.

Kagel J.H. and D. Levin. 1986. "The winner's curse and public information in common value auctions." *American Economic Review*76, 894-920.

Kagel, J.H, and A. E. Roth. 2011. *The Handbook of Experimental Economics* (Eds.). Princenton University Press.

Levin D.; J.H. Kagel and J.F. Richard. 1996. "Revenue effects and information processing in English common value auctions." *American Economic Review* 86, 442-460.

Myron, J. 1971. "Pricing in a perfectly competitive market." In *Projects and role playing in teaching economics* 1971, C.T. Sandford and M.S. Bradbury (Eds.). Macmillan, London, 69-73.

Otamendi, J (2008). "Visualization and Scheduling Of Jetty Operations In Harbours". In *Proceedings of the Sixth International Conference on Simulation in Industry and Services*. Public University of Navarre, 31-52.

Rezende F.; L. Xin and C. Xiao-Bo. 2007. "Second order loads on LNG terminals in multi-directional sea in water

of finite depth." In *Proceedings of the 26th International Conference on Offshore Mechanics and Artic Engineering* 1, 259-266.

Turocy T.L.; E. Watson and R.C. Battalio. 2007. "Framing the first-price auction." *Experimental Economics* 10, 37-52.

AUTHOR BIOGRAPHIES

F. JAVIER OTAMENDI received the B.S. and M.S. degrees in Industrial Engineering at Oklahoma State University, where he developed his interests in Simulation and Total Quality Management. Back in his home country of Spain, he received a B.S. in Business Administration and a Ph.D. in Industrial Engineering. He is currently a simulation and statistics consultant and university professor at the Rey Juan Carlos University in Madrid.

LUIS MIGUEL DONCEL obtained a BS in Economics, from University Complutense of Madrid. Later he attended University of York achieving a Master in Economics and Finance. Back to Spain he got a Ph.D. in Economics from the Rey Juan Carlos University with a research about foreign exchange rates and simulation. Currently he is a lecturer at Rey Juan Carlos University. He has been an external consultant for monetary affairs for the EU in Bulgaria and Dominican Republic. His research focuses on financial markets and Simulation. His e-mail address is: luismiguel.doncel@urjc.es

PILAR GRAU received a BS in Economics at University Complutense of Madrid. Later on she got a Ph.D. in Economics from the same university with a research about nonlinearites and chaos in financial markets. Currently she is a lecturer at Rey Juan Carlos University. Her research focuses on computational finance and stochastic modeling of financial time series. Her e-mail address is: pilar.grau@urjc.es

JAVIER RAMOS is Lecturer in "Multimedia Communication" at the Rey Juan Carlos University. He also coordinates the Virtual Campus of that University. He holds a graduate degree in Audiovisual Communication, an MSc in "Communication and sociocultural problems", and a Technical degree in Image Treatment. He is completing his PhD research at the same university, together with participating in various research projects. He is responsible of the Ada-Madrid project at URJC, member of the "Committee of quality, follow-up and pedagogical support" of that project, and a member of the editorial board of the electronic journal "Relada".

LINEAR MODELLING AND SIMULATION OF AN ENDOGENOUS GROWTH MODEL WITH HETEROGENEOUS ENTREPRENEURS

Félix-Fernando Muñoz[1], F. Javier Otamendi[2]
[1]Universidad Autónoma de Madrid
Departamento de Análisis Económico: Teoría Económica e Historia Económica
Francisco Tomás y Valiente 5
28049 Madrid, Spain
E-mail: felix.munoz@uam.es
[2]Universidad Rey Juan Carlos, Campus Vicálvaro
Departamento Economía Aplicada I
Paseo Artilleros s/n
28032 Madrid, Spain
E-mail: franciscojavier.otamendi@urjc.es

KEYWORDS
entrepreneurship, heterogeneity, endogenous growth

ABSTRACT

The lack of 'true' entrepreneurs is often blamed for the failure of international aid and expansionary internal economic policy. Experience attempts to solve this question by responding that "we must create entrepreneurs", or "it is necessary to stimulate entrepreneurial activity." In this paper, we present an economic model of endogenous growth based on the Rivera-Batiz & Romer (1991) model that can explain how changes in the structure of payoffs of the economy can affect the rate of growth of output via the rate of change of the number of innovations. Different characterizations of heterogeneous entrepreneurs in an economy are modelled as well as their intention to innovate. We solve the entrepreneur problem using both analytical equations and simulation, and compare the solutions of a simplified linear problem in terms of future developments and applications.

INTRODUCTION

Why is it that over economies with apparently similar growth possibilities we observe large differences in growth rates? Why is it that the lack of entrepreneurs (or in the negative case, the abundance of speculators) is often blamed for the failure of international aid and expansionary internal economic policy? Why is it more difficult to organise production in some countries than in others? Why are some economies more innovative than others? These are all questions present in public debates, and that frequently appear in relation to economic policy. Experience attempts to solve these questions by responding that "we must create entrepreneurs", "it is necessary to stimulate entrepreneurial activity".

These questions, and their alleged solutions, are evidence of the relationship that necessarily exists between the actions or decisions of entrepreneurs and the economic performance of a society as measured, for example, by the rate of change of *per capita* output, γ_y (Figure 1) in terms of the innovation quantities.

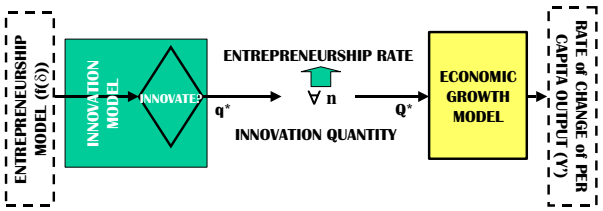

Figure 1. Entrepreneurship and per capita output

This relationship has been studied by economists, with greater or lesser intensity, ever since Economics was born as an independent science. The answers that modern economic theory has given have been rather varied, but it is only recently that they have been formally integrated in the type of mainstream model that attempts to explain economic processes; models of endogenous growth that formally incorporate the intentional actions of entrepreneurs in the explanation of how the rate of growth is determined (Romer, 1994).

However, a closer examination of these models reveals that the above mentioned intuition is only partial. One of the reasons for this type of limitation in these models can be found in the definition of entrepreneur that is used, since the models only take into account a particular case, that of the entrepreneur as an innovator. The models understand *entrepreneurship* as a unique and homogeneous function, and therefore it is rather difficult to apply the theory to questions of endogenous growth that were mentioned above (unless it is done with *ad hoc* models).

The paper explores how an extension of the concept of entrepreneur within a model of endogenous growth, can generate a wider range of explained phenomena than can be obtained in traditional models. Section 2 is devoted to model the entrepreneurs while Section 3 and Section 4 are used to explain the proposed models of innovation and economic growth. In Section 5, all the

Proceedings 26th European Conference on Modelling and Simulation ©ECMS Klaus G. Troitzsch, Michael Möhring, Ulf Lotzmann (Editors)
ISBN: 978-0-9564944-4-3 / ISBN: 978-0-9564944-5-0 (CD)

models are integrated into a full model, which might be solved both analytically and via simulation. A linear example is solved in Section 6. Section 7 compares both solution techniques and discusses about further research possibilities.

MODELLING ENTREPRENEURS

Conceptualisation of entrepreneurs.
In a letter to F.A. Walker, Léon Walras recognised that the definition of entrepreneur was, under his point of view, «le nœud de totut l'économique» (Jaffé, 1965) Indeed, this concept plays a fundamental role in the explanation of many economic facts —like economic growth—, but at the same time there must exist few central economic theory concepts that have been understood and applied in such a diverse manner (Casson 1982). The main function of the entrepreneur within the economy, from the point of view of the contribution to economic growth, is to increase the productivity of the system, or to create added value, through a -generally understood- process of innovation. The immediate consequence of innovation is the introduction of certain new aspects of the productive process, or of (new) types of more productive capital goods, or consumption goods with greater added value, and the corresponding resource reallocations that this implies. The introduction of innovations in the productive process increases the productivity of the system, thereby providing the impulse for economic growth.

From mainstream economics we can identify at least three different kinds of entrepreneurship: (1) the entrepreneur-producer, (2) the entrepreneur-innovator and (3) the entrepreneur-rent seeker. Obviously, real-life entrepreneurs share characteristics of these three ideal types, although with different degrees of intensity of each type. In this paper we are primarily interested in considering the two most opposing stereotypes as far as their consequences for economic growth are concerned: innovative entrepreneurial activity and rent seeking. We shall leave the entrepreneur-producer type aside, since in endogenous growth models this type is secondary (although important).

Given this simplification of entrepreneurial activity, we hypothesise that: (a) the maximum potential growth is associated with the use of the greatest part of the existing entrepreneurial capacity, and consequentially, of available resources, in activities that result in an increase in productivity; while on the other hand, (b) the allocation of all of the existing entrepreneurial capacity to rent seeking activities generates a lower economic performance in terms of *per capita* output growth -and, as a limit case, may degenerate into a contractive economy).

In short, the behaviour of the economy depends on how entrepreneurs carry out their entrepreneurial functions, which in turn is set by the internal evolution of the social dynamics that determine the distribution of entrepreneurs between the two extreme types. So, different social structures of payoffs (Baumol, 1993) will result in different economic performances (in terms of growth of output, for example) through different distributions of heterogeneous entrepreneurs between innovators and rent seekers.

The entrepreneurial density function.
A simple way to determine the distribution of entrepreneurs between the two extreme types –the innovator and the rent seeker entrepreneur- consists of assuming that each entrepreneur in the economy establishes the relative value of each of the two extreme types together with the restrictions that impinge upon these values; thus we can define an *entrepreneurial density function* between the two extremes. Moreover, since each extreme type implies different resource allocations, depending on whether there is a greater density of one type or the other in the economy we observe different rates of growth due to the fundamental link that determines γ_y in endogenous growth models. This entrepreneurial density function reflects the *hypothesis of heterogeneity* of entrepreneurs.

We characterise entrepreneurs as follows: we distribute the objectives and activities of economic agents between two extreme types, denoted by type 0 — associated with pure innovative activities — and type 1 — agents whose underlying (and unique) objective is the search for the maximum possible source of earning in the economy. Any given type of entrepreneur that is characterised by some type of mixture of the two extremes can be defined by his relative position, denoted by δ. Assuming a continuum of entrepreneurial types, $\delta \in [0,1]$, by construction we can interpret δ as the "psychological distance" of any given entrepreneur from the extreme type 0, and consequentially, $(1-\delta)$ is the "psychological distance" from type 1.

With each type of entrepreneur, we associate a "density" and a "distribution", respectively denoted by $f(\delta)$ and $F(\delta)$. In an abstract model, this functions could be *any* random variable at all, and so in principle, each economy is characterised by a given "density" of entrepreneurs of each feasible type.

MODELLING INNOVATION

The objective of a given entrepreneur δ will be defined in terms of a *subjective utility function* that defines the degree to which he will take part in activities of type 0 and of type 1, depending on his own δ. We denote by $q(\delta)$ the amount of innovation that an entrepreneur of type δ will generate under the assumption that an invention is available to him. The entrepreneur can decide between:

(a) producing a positive quantity of that good, $q(\delta)>0$
(b) obtaining a "guaranteed" income, denoted by E (expressed in units of account), by carrying out other activities in some other sector of the economy thereby generating $q(\delta)=0$.

We assume that the utility gains from each alternative are compared using the values $q(\delta)$; that is, the entrepreneur first decides how much of the innovative good he would like to produce should he decide to produce it at all, and then decides which activity he will finally opt for. Of course, even if he decides in favour of the innovative alternative (which we denote as E), he will always search for an earning that at least is equal to the cost of innovating, α_0, should he decide to repeat his plan in future periods. The entrepreneur will then compare this earning, from his position δ, with his other option, E.

The objective function of an entrepreneur δ.
In this context, the objective function of a heterogeneous entrepreneur might be defined as:

$$J(\delta,q)=(1-\delta)\ u(q)+\delta\ v(\pi(q)) \qquad (1)$$

It can really be thought of as a special type of utility function in which the first term, u(q), represents the *average earnings in utility terms* that the entrepreneur can obtain by innovating, which depends directly on the amount of the innovative good that is introduced into the economy. On the other hand, the second term, $\pi(q)$, is the profit associated with a given amount of the innovative good q and $v(\pi(q))$ is the utility gains that this profit produces. It is this second term that allows entrepreneur δ to compare the profits associated with this activity with the profit that can be obtained by alternative uses of his entrepreneurial capacity; the first term, however, always refers to the utility obtained from innovating. In this way, each entrepreneur has two ways of obtaining "subjective gains": via pure innovation; and via economic profit, which may be obtained either innovating or by alternative short run means. How each entrepreneur weighs exactly each method of improving his personal situation is described in the model by a relative position (δ) in the entrepreneurial density function, $f(\delta)$.

The entrepreneur's restriction.
No entrepreneur would want to become bankrupt by carrying out the activity that he values most; rather he would attempt to obtain the best possible position from among those available that are associated with his plan: he will attempt to obtain the maximum profit (or yield) associated with his decision. However, we are assuming that this *profit is subjective* — and so it is written in terms of a *utility* function — and is only a *minimal condition* that must be satisfied; that is, a restriction on a more general entrepreneur.

If the *economic profit* is defined as:
$\pi(q)\equiv(p(q)-c)q \qquad (2)$

where $\pi(q)$ is the profit associated with the innovative good, q; $p(q)$ is the "demand function" for the innovative good; and c is the average cost associated with the production of an additional unit of q, then we can define this minimal condition as follows:
$(p(q)-c)q\geq\alpha(\bullet) \qquad (3)$

where $\alpha(\bullet)$ is a function that sets the minimum yield that the plan of each type δ entrepreneur must obtain.

The function $\alpha(\bullet)$ has the following arguments: (1) the position of the entrepreneur in $f(\delta)$, which determines the subjective evaluation of the yield associated with the decision to innovate in relation to (2) the cost of introducing an innovation α_0; and (3) the yield that can be obtained in other sectors of the economy, E.

The (necessary) condition to innovate.
Each type δ entrepreneur compares the (potential) earnings associated with each innovative plan — the amount that he would prefer to produce of the innovative good — with E. Then, for $q(\delta)>0$, it must happen that: $\pi_\delta(q)\geq\alpha(\delta)$, $\forall\delta\in[0,1]$, for certain values of α_0 and E. If this *minimum condition* is not satisfied, the entrepreneur opts for the activity that produces the result E, thereby producing $q(\delta)=0$ new goods.

The entrepreneur's problem (EP).
Therefore, we may set-up the entrepreneur's problem (EP) at a given moment of time, as follows:

$$(EP)\quad \begin{cases} \underset{q\geq 0}{\text{Max}}\ J(\delta,q)=(1-\delta)\ u(q)+\delta\ v(\pi(q)) \\ \text{s.t.:}\ \ \pi(q)\equiv(p(q)-c)q\geq\alpha(\delta,\alpha_0,\$) \end{cases} \qquad (4)$$

For greater simplicity, we set α_0 and E to equal constants for each entrepreneur, that are identical for all types of inventions/innovations, and $E\geq\alpha_0$. The same assumptions can be applied to the average costs of production of an additional unit of the new good, c.[1] [2]

[1] A very common assumption in the endogenous growth literature (as well as the assumptions of symmetry and a constant initial cost of innovating -η in Romer's (1990) model-, etc.) In a certain way, these assumptions replace the functions of production of new goods in the cost functions.
[2] A very different problem, although of significant theoretical interest, is the consideration of the demand function for the new goods, p(q); on this point, we simply adopt a construction of the Grossman-Helpman (1991) type.

Solution of (EP). The continuity of the utility function $J(\delta,q)$ and the fact that the feasible set is closed and bounded guarantees that there *exists a global maximum* (Weierstrass Theorem). Moreover, since $J(\delta,q)$ is strictly concave and the feasible set is convex, the Fundamental Theorem of Convex Programming guarantees that the global maximum of (EP) is unique. We shall denote this maximum by q_δ^*.

Therefore, the amount of the innovative good that each type δ entrepreneur, q_δ, will be a function of the following variables:

$$q_\delta^* = q(\alpha_0, E, c, p, \delta) \quad (5)$$

The quantity of innovation goods will be higher:

- the lower the minimum profit claimed by entrepreneurs in innovative activities, α_0;
- the lower the alternative sources of gains, E;
- the lower the cost of (re)producing innovations, c;
- the higher the price of innovations, p;
- the higher the propensity of society to innovation — the "higher" the density of entrepreneur capacity towards innovation, $f(\delta)$.

The shape of this last variable will drastically differ between economies — between different economies at the same time or inside the "same" economy at different times.

Aggregate solution of (EP).
Since the "*average*" value of q_ε for the economy as a whole must be determined, and using the concept of the density function of entrepreneurial capacity, $f(\delta)$, we add the individual quantities across entrepreneurs:

$$q_\varepsilon = \int_0^1 q(\delta) f(\delta) d\delta \quad (6)$$

The rate of entrepreneurs (δ_0)
An additional output indicator of the (EP) is the rate of entrepreneurs of a given economy. Referred as δ_0, its value is calculated after solving the following equation:

$$\pi_{max} = \alpha(E,\delta_0) \quad (7)$$

Those entrepreneurs with $0 \leq \delta \leq \delta_0$ will innovate and those with higher values of δ will not.

MODELLING ECONOMIC GROWTH

Due to its simplicity, we use an adapted version of Rivera-Batiz & Romer, endogenous growth model for evaluating the evolution of γ_y over time. Thus, we assume the following definition of capital:

$$K(t) = A(t)\, q_\varepsilon(t) \quad (8)$$

where $K(t)$ is the accumulated amount of goods that have been incorporated in the production process, and $A(t)$ is the number of varieties of new production goods that have been generated up to the moment of time t. That is to say, at each moment t, the amount of varieties that can be used in the production of output is given by the amount (and number) of innovative goods of previous periods, as well as those that are introduced at moment t. Hence, the introduction of new goods will imply an increase (change) in $A(t)$ equal to $A'(t)$; and $A(t)$ will depend on both the dynamics of inventions and the dynamics of innovations.

In the Rivera-Batiz and Romer model, changes in A are denoted as: $A' = \tau HA$; that is, the rate of growth of A is proportional to the human capital in the system, H, and a parameter that measures the productivity of this capital, τ. In these types of model, it also turns out that all inventions are introduced into the economic system as innovations. In our case, things do not happen with such a high degree of automation, since the entrepreneurs, from the problem (EP) and their relative types, δ, will determine the amount of each invention (variety) that will be produced, where a possible solution is that no positive amount at all is produced, i.e.: an invention is not transformed into an innovation.

The rate of change of innovations according to the constant growth RBR model is:

$$\gamma_A(t) \equiv \frac{\dot{A}(t)}{A(t)} = \frac{(1-\mu)\beta q_\varepsilon(t) - \dot{q}_\varepsilon(t) c(t)}{q_\varepsilon(t) c(t) + \alpha_0(t)} \quad (9)$$

where we also assume a consumption function with a constant marginal propensity to consume $C = \mu Y$, with $0 < \mu < 1$, and β is the productivity of the innovation.

It is easy to show that this rate of change is increasing in q_ε and decreasing in $\dot{q}_\varepsilon$. That is to say, the rate of growth of the number of new goods is directly proportional to investment in the introduction of new goods — and the proportion is the productivity of new goods —, and is inversely proportional to the cost of developing and producing them, and in the production of existing goods.

If we use a constant growth model independent of time, then, the rate of change of innovations is:

$$\gamma_y = \frac{A'}{A} = \frac{(1-\mu)\beta q_\varepsilon}{q_\varepsilon c + \alpha_0} \quad (10)$$

MODELLING ECONOMIC GROWTH BASED ON ENTREPRENEUR ACTIVITY

Figure 2 depicts the combination of the models into an endogenous growth model based on the new categorization of entrepreneurs. Given f(δ), it is possible to compute innovation quantities for each entrepreneur, and then for the Economy. This aggregate quantity $Q^*=q_\varepsilon$ is used then as the input to the RBR constant growth model.

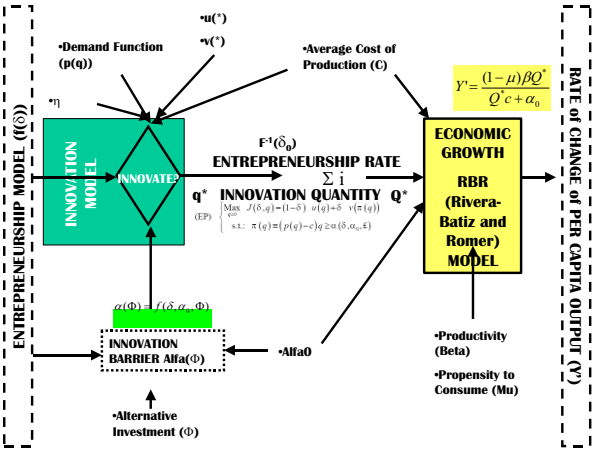

Figure 2. The proposed integrated model

In terms of computation, the model is usually difficult to solve analytically. The steps of calculating the quantities using the (EP) and the aggregate q_ε using integration could take too long to compute. That is why a simulation approach might be preferred.

SIMULATING ECONOMIC GROWTH BASED ON ENTREPRENEUR ACTIVITY

Instead of integrating over δ to calculate the quantity q_ε, it is possible to simulate for any f(δ). What follows is the pseudocode that has been designed to summarize the process of estimating γ_y:

Input data: f(δ), E, α_0
Input data: p(q), c, u(q), v(•), π(•)
Input data: μ, β
For each simulation s
    For each entrepreneur i
        Generate δ
        Compute α(E), π(•)
        If π(•)>α(E), calculate q* by solving EP
    Compute indicators
        Q as the sum of q*'s
        δ_0
        Rate of entrepreneurship as $F^{-1}(\delta_0)$
    Compute

This type of modelling facilitates the use of higher-order functions as well as modifications over time if needed.

SIMPLIFIED EXAMPLE: LINEAR FUNCTIONS

In this simple example, the functions that we use are linear so that the problem is readily solvable both analytically and via simulation:

- p(q)=a-bq with a,b>0, so π(q)=(a-bq-c)q
- u(q)=ηq; v(x)=x
- α(δ, α_0, E) = (1-δ) α_0 + δE
- f(δ) follows a Uniform distribution, U(0,1)

Therefore, the entrepreneur problem is:

$$(EP)\quad \begin{cases} \max\limits_{q\geq 0} J(\delta,q)=(1-\delta)u(q)+\delta v(\pi(q)) \\ \text{s.t.}: \pi(q)\geq \alpha(\delta,\alpha_0,E) \\ \alpha(\delta,\alpha_0,E)=(1-\delta)\alpha_0+\delta E \end{cases} \qquad (12)$$

Analytically, the solution for each individual entrepreneur is given by:

$$q^*(\delta,\alpha_0,E)=\begin{cases} \min\{q_1(\delta,E),q_2(\delta,E)\} & \text{if } \alpha(\delta,E)\leq \dfrac{(a-c)^2}{4b} \\ 0 & \text{if } \alpha(\delta,E)> \dfrac{(a-c)^2}{4b} \end{cases} \qquad (13)$$

where:

$$q_1=\frac{(a-c)}{2b}+\frac{\sqrt{(a-c)^2-4b\alpha(\Phi)}}{2b}$$
$$q_2=\frac{(a-c-\eta)}{2b}+\frac{\eta}{2b\delta} \qquad (14)$$

The rate of entrepreneurs (δ_0) follows:

$$\delta_0=\frac{\dfrac{(a-c)^2}{4b}-\alpha_0}{\Phi-\alpha_0} \qquad (15)$$

However, and even in this simple case, it is complicated to calculate q_ε; it will be very complex to integrate q* due to the existence (at least a priori) of non-linearities and the shape of f(δ).

For the sake of validating the simulation model, the following example has been used:

- f(δ): Uniform (0,1); E = 0.5; α_0 = 0.01
- p(q) = 1-1 q; c = 0.5; u(q) = 1 q
- μ = 0.8; β = 1.5

The results for N = 100 entrepreneurs after theoretically calculating the analytical values are Q* = 4.3152 and δ_0 = 10.7143%. If S = 50 simulations are run:

- The goods in the Economy, Q*, lie between 2.3307 and 7.0562 with an average of 4.2390
- The rate of entrepreneurship, δ_0, lies between 6% and 18% with and average of 10.4694%.
- The rate of change of *per capita* output, lies between 59.4895% and 59.8304% with an average of 59.7009%.

CONCLUSIONS

The model analysed in this paper is a simple example of how widening the content of the concept of entrepreneur –allowing him to carry out heterogeneous tasks within his entrepreneurial capacity formalised in this model by (EP), allow us to give more meaningful answers to the questions posed at the very beginning of this paper.

From (EP) we have been able of establish the relationship between variables such as minimum profit threshold, opportunity of gains in other sectors of the economy, the cost of innovation, etc., and the quantity of innovation finally produced depending on the attitude of entrepreneurs themselves and society in general towards innovation effort — defined by f(□)— , and the consequences of all this in the rate of growth of output.

The innovation-growth model is solvable using simulation techniques. Therefore, it is our aim to keep on improving the simulation model to be able to increase its applicability. In particular, we are already addressing the possibility of incorporating non-linearities in the functions as well as incorporating other growth models. Moreover, we are trying to develop rules to vary all the parameters and functions over time.

The potential of the model for policy making must also be investigated. On that regard, we are aware of the limitations of the proposed macroeconomic growth model "as-of-today", limitations that would also be easier to avoid if simulation modelling is used to solve the entrepreneur's problem (EP).

ACKNOWLEDGEMENTS

This research has been partly funded by the IIES Francisco de Vitoria.

REFERENCES

Baumol, W. (1993). Entrepreneurship, Management and the Structure of Payoffs. MIT Press, Cambridge, Mass.

Billari Francesco C., Thomas Fent, Alexia Prskawetz & Jürgen Scheffran (eds.) Agent-Based Computational Modelling. Applications in Demography, Social, Economic and Environmental Sciences. Physica-Verlag, Heidelberg, 2006.

Grossman, G. and E. Helpman (1991). Innovation and Growth in the Global Economy. MIT Press.

Casson, M. (1982). The Entrepreneur: an Economic Theory. Oxford, Martin Robertson.

Dosi, G., Fagiolo, G. Roventini, A. (2010) Schumpeter me etnia Keynes. A policy-friendly model of endogenous growth and business cycles. Journal of Economic Dynamics and Control, 34, pp. 1748-1767

Jaffé, W. (ed.) (1965) The correspondence of Léon Walras. L 800. North Holland.

Rivera-Batiz, L.A. and P.M. Romer (1991). "Economic Integration and Endogenous Growth." Quarterly Journal of Economics, 106(2) May, 531-555.

Romer, P.M. (1994). "The Origins of Endogenous Growth". The Journal of Economic Perspectives, Vol. 8, No. 1. (Winter), pp. 3-22.

AUTHOR BIOGRAPHIES

FÉLIX-FERNANDO MUÑOZ is PhD. in Economics (Economic Theory) at Universidad Autónoma de Madrid (UAM). His research areas of interest are Endogenous Growth Theory, Evolutionary Economics and Economic Methodology. He is director of the Master in International Economics program at UAM.

JAVIER OTAMENDI received the B.S. and M.S. degrees in Industrial Engineering at Oklahoma State University, where he developed his interests in Simulation and Total Quality Management. Back in his home country of Spain, he received a B.S. in Business Administration and a Ph.D. in Industrial Engineering. He is currently a simulation and statistics consultant and university professor at the Rey Juan Carlos University in Madrid.

AN EXHAUSTIVE APPROACHMENT TO THE INNOVATION EFFICIENCY IN SPAIN

María Rocío Guede
María Auxiliadora de Vicente
Desiré García Lázaro
Department of Financial Economy and Accounting II
José Javier Fernández
Department of Management and Business Organization
Rey Juan Carlos University
E-mail: rocio.guede@urjc.es

KEYWORDS
Innovation, efficiency, productivity, Data Envelopment Analysis, Electre TRI.

ABSTRACT

The objective for this article is to analyze the innovation efficiency in Spain by activity branch. To this end we will work with the 2009 data from the INE (Spanish National Institute of Statistics) innovation and R&D activities surveys. To this aim, we will use the following methodology for the efficiency analysis: the one based on output oriented DEA (Data Envelopment Analysis) with constant returns to scale and weight restrictions.
This technique will be completed in three aspects. Firstly with the introduction of more inputs and outputs without causing an increment of efficient units. Secondly, we will use the Principal Component Analysis to extract the idea to implement the weight restrictions in the DEA. Thirdly, the analysis will be completed with a robustness Analysis of the efficient activity branches to improve the DEA discrimination capacity.

MOTIVATION OF THE RESEARCH AND LITERATURE SURVEY

The structure of the Spanish economy is suffering nowadays some very significant changes marked by a double crisis at the same time. On one hand the serious international crisis, and on the other hand a national crisis product of a long term growth model based on exhausted activity branches: construction and tourism.
It has been pointed out within the new strategic goals for this decade set at the Lisbon European Council, in march 2000, that the European Union will become one of the most competitive and dynamic knowledge-based economies in the world, capable of sustainable economic growth with more and better jobs and greater social cohesion. Achieving these goals requires an overall strategy aimed at preparing the transition to a knowledge-based economy and society by better policies for the information society and R&D, as well as by stepping up the process of structural reform for competitiveness and innovation and by completing the internal market. (Lisbon European Council, 2000).
Spain should add value to the European Union, and became more competitive and efficient, with a dynamic economy based on the knowledge, such as education, innovation, research and development.
In that point, we would need to know which is the role of the innovation in the transformation of the economic structure of Spain and which activity branches of the Spanish economy are the most efficient ones.
These key questions will be studied throughout the present paper to understand the current structure of the Spanish economy and to be able to offer information to economic politics decision makers. Structural transformations needed to the economic growth and increase of the rent per capita imply changes of certain relevance in the structure of the production, in the role of the trade and in the public sector weight. (García and Myro, 2008).
These changes leaded by the upward tendency of some activity branches and the decline of others, alter the structure of the whole economy. The research, development and innovation, all of them focused on the increase of productivity, are needed to lead these significant structure changes. Throughout the base of a balanced and sustainable Economic growth based on innovation must be designed the nowadays Spanish economy structure change.
There are two motivations in this paper. Firstly, we want to answer the previous key questions related to the Spanish economy. Secondly, we want to propose a new methodological approach to improve the Data Envelopment Analysis, looking for improving one previous research developed in this field (De Vicente *et al*, 2009), (Guede *et al*, 2011).
Although there has been carried out very interesting researches on this topic (Buesa *et al*, 2006), (Galende del Canto 2008), (Gómez and Zabala 2008), (De Vicente *et al*, 2009), (Guede *et al*, 2011), the solution proposed in this paper has not been applied in this field previously, and it's new in the application of the most advanced DEA research methods too. (Cooper *et al.* 2004), (Doyle and Green, 1994), (Dyson *et al,* 2001),

Proceedings 26th European Conference on Modelling and Simulation ©ECMS Klaus G. Troitzsch, Michael Möhring, Ulf Lotzmann (Editors)
ISBN: 978-0-9564944-4-3 / ISBN: 978-0-9564944-5-0 (CD)

(Lugones *et al,* 2003), (Madlener *et al,* 2006), (Maystre *et al,* 1994), (Raftery, 1993), (Roy and Bouyssou, 1993), (Zhu and Cook, 2007).
In order to follow the most authorized data analysis methodology it has been developed the study under the Oslo Manual framework and in concordance with the the INNO-policy reports, INNO Metrics (2007) and the European regional innovation scoreboard report (2009).

METHODOLOGY

This paper intends to analyze the relationship between efficiency and innovation activity in Spanish activity branches. The methodology includes three levels of analysis.
We will apply a Data Envelopment Analysis (DEA), a non-parametric technique, to a set of several inputs and outputs associated to economic and financial data.
The practical application of Data Envelopment Analysis presents a range of procedural issues to be examined and resolved including those relating to the homogeneity of the units under assessment, the input/output set selected, the measurement of those selected variables and the weights attributed to them (Dyson *et al,* 2001).
Each of these issues can present difficulties in practice. In this work we will try to highlight some of the pitfalls related with this case, and to improve the DEA's discrimination capability.
There are two main pitfalls detected in this analysis. In first place, if there are many inputs and outputs the number of efficient DMUs increases. To obtain a more realistic result, we will apply Principal Components Analysis (PCA) over the set of inputs and, separately, over the set of outputs. This was made to reduce the number of inputs and outputs, increasing the discrimination power of the DEA.
We will use the following methodology for the efficiency analysis: the one based on output oriented DEA (Data Envelopment Analysis) with variable returns to scale.
The other main pitfall detected is related to the application of a DEA without priori information about weights, because it allows DMUs with unrealistic behaviour could be efficient.
DEA allows each decision making unit (DMU, branches in our study) to specify its own weights so as to obtain a maximum efficiency score for itself. Without the possibility of introducing weight restrictions, complete weight flexibility is allowed. This may result in identifying a Decision Making Unit with an unrealistic weighting behaviour to be efficient.
Problems arising from the total flexibility of weights in DEA model are often dealt incorporating weight restrictions. Nevertheless, weight restrictions must be meaningful and justified. Consequently, this poses a new problem to the analyst who should be able to explain why particular weights restrictions were used, especially when there is no full cooperation with the stakeholders or there is a lack of information. Moreover, weight restrictions can pose as well technical and computational problems in some cases. For example, it is necessary to look for a compromise unique weight bounds suitable for all the units.
Due to these problems, we propose to take a different approach. We will introduce weight restrictions over the set of factors obtained from the PCA. The first factor from the set of inputs explains more variance than the second, the second explains more variance than the third, and the third factor explains more than the fourth factor. In that way, weight restrictions for the inputs are the next:

$$p_1 \geq p_2 \geq p_3 \geq p_4 \quad (1)$$

with p_1 as the first factor's weight (1).
The same idea is applied to the set of factors obtained from PCA for the outputs.
With the application of Data Envelopment Analysis, we can obtain two groups of units. The non efficient ones will be classified and we could build a ranking, but the efficient ones will be in the same group without possibility of discrimination. In this point, we would like to know which units are robust efficient DMUs.
For this aim, we are going to use Multicriteria Decision Aid to increase the discriminating power of DEA for the efficient branches.
The multicriteria Decision Aid method chosen will be Electre Tri. Electre Tri is a non compensatory, outranking relations based method and deals with the issue relating to classifying each alternative into a predefined category. Reference alternatives are used to segment criteria into categories: each category is limited below and above by two reference alternatives and each reference alternative thus serves as a border for the two categories, one upper and the other one lower.
Electre Tri is therefore a method of assigning action (regions) to pre-defined categories (hypothetical reference regions). The assigning of an action (region) "a" results from the comparing of "a" to the profiles (action – regions- reference) that define the limits of categories. Electre Tri will be applied to the crossefficiency matrix of the DEA-efficient DMUs/branches.
Efficient branches will be classified into two groups: those branches that are efficient or reach good enough efficiency values over the different set of weights for DMUs, and those ones that are efficient with their optimal weights but that reach bad efficiency values with the rest of weights for the others DMUs. We could also name these classes as the robust efficient branches and the non robust efficient branches.
To this end we will work with the 2009 data from the Spanish National Institute of Statistics innovation and R&D activities surveys.
This identification of the most innovative efficiency Spanish economy activity branches will be carried out in three levels:

First level
Firstly, we will obtain the principal components of the inputs and, separately, of the outputs.
Second level
Secondly, it will be identified the efficient and the non efficient activity branches obtained by a DEA applied over the new variables precedent from the principal components analysis. We will use an output oriented DEA, with variable returns to scale and with weight restrictions extracted from the PCA Analysis.
Third level
In third place, we will apply an Electre Tri over the DEA efficient activity branches, in order to be able of distinguee robust efficient and non-robust efficient activity branches. This Electre Tri creates two groups, fourteen robust efficient activity branches and ten non-robust efficient activity branches.

IDENTIFICATION OF THE MOST INNOVATIVE EFFICIENCY SPANISH ECONOMY ACTIVITY BRANCHES IN THREE LEVELS

First of all it must be introduced the activity branches in which of research is focused on. How to separate or distinguish the different activity branches from the whole economy it is itself an interesting topic of research. We follow the international main stream activity branches division, leaded by the OECD Oslo Manual from 1995, improved in 2005. This reference gives the main international standard guidelines, followed as well by the INE (Spanish national institute of statistic).

Data source and specification
The basic data of our research is from the survey of technological innovation in the companies in 2009 organized per activity branches, published by the INE. This survey offers main indicators of technological innovation in 2009.

The selection of input and output variables
In our study of innovation efficiency, we use the indicators mention above as reference, with the combination of the availability of data, we finally choose twelve input variables and twelve output variables.
The input variables are:
• Total of innovative companies.
• Expenses in innovation: total in thousands of Euros.
• Expenses in innovation: R&D (internal and external) (%).
• Expenses in innovation: other innovative activities (%).
• Percentage of companies with innovative activities in 2009 over the total number of companies.
• Percentage of companies with innovative activities with internal R&D.
• Percentage of companies with innovative activities with external acquisition of R&D.
• Percentage of companies with innovative activities with acquisition of machinery, tools and software.
• Percentage of companies with innovative activities with acquisition of external knowledge.
• Percentage of companies with formative innovative activities.
• Percentage of companies with innovative activities with introduction of innovation in the market.
• Percentage of companies with innovative activities in design and other applications to production and/or distribution.
On the other hand, the output variables are:
• Intensity of innovation of the total companies.
• Intensity of innovation of the companies with innovation activities.
• Intensity of innovation of the companies with R&D activities.
• Percentage of companies with innovation in product (improvement of goods or services).
• Percentage of companies with innovation in the processes.
• Percentage of companies with innovation in product and processes.
• Percentage of companies that have introduced products that were a novelty only for the company.
• Percentage of companies that have introduced products that were a novelty for the market.
• Percentage of the company figure of business in 2009 consequence of the goods and/or services that were a novelty only for the company.
• Percentage of the company figure of business in 2009 consequence of the goods and/or services that were a novelty for the market.
• Percentage of the company figure of business in 2009 consequence of the goods and/or services that were a novelty only for the company in companies with innovations in course or not successful.
• Percentage of the company figure of business in 2009 consequence of the goods and/or services that were a novelty for the market in companies with innovations in course or not successful.

FIRST LEVEL
Principal Component Analysis

Firstly, we will obtain the principal components of the inputs and, separately, of the outputs, using the Principal Component Analysis.
Referring to the inputs, It has been identified four main factors over the inputs, which have a global variance explanation power of 82,685%. The explained variance of each component in 2009 could be observed in the following table**.**

Table 1: Inputs' explained total variance

INPUTS		
Component	Variance percentage	Accumulated %
1	33,308	33,308
2	20,562	53,87
3	16,945	70,815
4	11,87	82,685

Extraction method: Principal Component Analysis.

Once applied the matrix of rotated component weights, using the rotated method of Varimax normalization with Kaiser, it has been obtained four main factors that explains the most of the variance and oppose some variables to another.

Referring to the outputs, it has been identified as well four main factors over the outputs, which have bigger global variance explanation power. All the four factors explain the 93,181% of the variance. The explained variance of each component in 2009 could be observed in the following table**.**

Explained total variance: outputs

OUTPUTS		
Component	Variance percentage	Accumulated %
1	36,543	36,543
2	28,15	64,693
3	17,328	82,021
4	11,16	93,181

Extraction method: Principal Component Analysis.

As it has been previously done in the inputs case, here it has been as well applied the matrix of rotated component weights, using the rotated method of Varimax normalization with Kaiser, and it has been obtained four main factors that explains the most of the variance and oppose some variables to another.

SECOND LEVEL
Data Envelopment Analysis

Secondly it has been identified the efficient activity branches obtained by an output oriented DEA over the principal components of the inputs and of the outputs. By using this technique it is possible to identify which activity branches are efficient and which are not efficient.

DEA with weight restrictions
On a next step, we will introduce weight restrictions over the set of factors obtained from the PCA. The first factor from the set of inputs explains more variance than the second, the second explains more variance than the third, and the third factor explains more than the fourth factor. In that way, weight restrictions for the inputs are the next:

$$p_1 \geq p_2 \geq p_3 \geq p_4 \qquad (1)$$

with p_1 as the first factor's weight (1).
The same idea is applied to the set of factors obtained from PCA for the outputs.
The weights restrictions applied in this case are detailed in the next table.

Weights

	Minimun	Maximun
input 1	0	100
input 2	0	61,73
input 3	0	50,87
input 4	0	35,64
output 1	0	100
output 2	0	77,03
output 3	0	47,42
output 4	0	30,54

Carrying out an output oriented DEA with variable returns to scale with these restrictions; we obtained twenty three efficient activity branches. By specifying the weights' value, the DEA eliminates possible efficient DMUs with unrealistic data. The next tables show the results of this DEA.

Efficient Activity Branches
Transport and storage
Textile
Cardboard and paper
Feeding, drinks and tobacco
Edition, impression and reproduction
Recycled
Mail and telecommunications
Other manufactures
Naval
Making and furrier
Leather and footwear
Non strong metals
Coke, petroleum and nuclear fuel
Automobiles
Office, calculation and computer machines
Other computer activities
Strong metals
Electric machines

Aerospace
Computer programs
Other material of transport
Electronic components
R&D services

Twenty three efficient activity branches

Non Efficient Activity Branches	Efficiency
Agriculture	98,51
Optic instruments and watch-make	97,33
Rubber and plastic	96,22
Machinery and mechanical machines	94,77
Radio, TV and Communication devices	94,25
Chemistry (except pharmacy)	93,44
Construction	92,82
Non Metallica minerals	92,34
Wood and cork (except furniture)	91,80
Furniture	90,83
Pharmacy	87,73
Financial services	84,58
Metallica manufactures	76,77
Trade and hostelry	76,50
Extractive	75,33
Public, social and collective se	75,00
Services to companies	74,36
Electricity, gas and water	68,23

Eighteen non efficient activity branches

THIRD LEVEL

Electre Tri

Once the previous analysis has been carried out, the final and most significance add value of this research has been completed by improving the capacity of discrimination of the DEA method by carrying out Electre Tri over the cross-efficiency matrix of the efficient activity branches when weight restrictions are considered.

We will consider the next parameters, trying to build two classes:

Indifference threshold	5
Preference threshold	10
Veto threshold	40
Profile	75

Working with these values, we obtained two classes, the first class with fourteen robust efficient activity branches, and the second class with nine activity branches.

Results are the following:

First class group: robust efficient activity branches

- Cardboard and paper
- Edition, impression and reproduction
- Making and furrier
- Leather and footwear
- Non strong metals
- Coke, petroleum and nuclear fuel
- Automobiles
- Office, calculation and computer machines
- Strong metals
- Electric machines
- Aerospace
- Computer programs
- Another material of transport
- Electronic components

Second class group: non robust efficient activity branches

- Transport and storage
- Textile
- Feeding, drinks and tobacco
- Recycled
- Mail and telecommunications
- Another manufactures
- Naval
- Other computer activities
- R&D Services

We may consider that if we work with a profile of 50% the program is not able to make a good discrimination. Nevertheless, if we improve this profile till 75% we obtain two groups, even without thresholds and veto. It suggests that we could try, for example, to build three different groups.

CONCLUSIONS

As it has been explained the three main conclusions obtained in this paper are:

1. Methodologically it is possible to introduce weight restrictions in DEA by considering the importance of the main factors obtained with Principal Component Analysis. It is possible to obtain a more realistic classification using DEA with weight restrictions.

2. Economic investment is not directly related with eficiency in innovation. It is the way of managing resourses what really supposes a wider efficiency level.

3. To be able to classify the activity branches in three groups: non efficient activity branches, non robust efficient activity branches and robust efficient activity branches, by using both DEA and Multicriteria Decision Aid methods.

REFERENCES

Buesa, M., J. Heijs, M. Martínez Pellitero, and T. Baumert. 2006. Regional systems of innovation and the knowledge production function: The spanish case. *eat* 26, (4): 463-72.

Cooper WW., Seiford LM., Zhu J. (eds.) (2004). Handbook of Data Envelopment Analysis. Kluwer Academic Publishers.

De Vicente, M., Guede, R., Blanco, F.J., Romero, A. (2010). "Innovation Efficiency in Spain: An Analysis by activity branch". Otamendi, J., Bargiela, A., Montes, J. L. y Doncel, L. M. (2010). En *23rd European Conference on Modelling and Simulation*. Dudweiler, Germany.

Directorate-General, E. INNO-policy TrendChartpolicy trends and appraisal report.

Doyle J., Green R., (1994). Efficiency and Crossefficiency in DEA: Derivations, Meanings and Uses. *Journal of the Operational Research Society.* Vol 45, No. 5, pp. 567-578.

Dyson, R.G. *et al* (2001). Pitfalls and Protocols in DEA. *European Journal of Operational Research* 132 (2001) 245-259.

Galende del Canto, J. 2008. La organización del proceso de innovación en la empresa española. *Economía Industrial*(368): 169-85.

Gómez Uranga, M., and J. M. Zabala Iturriagagoitia. 2008. Panorámica de la innovación en españa a través de la evolución de indicadores regionales. *Economía Industrial*(368): 125-39.

Guede, R., De Vicente, M., Manera, J. y Romero, A. (2010). "Innovation Efficiency and Open Innovation: An Application to Activity Branches in Spain", in Pablos, C. y López, D. (2010). *Open Innovation in Firms and Public Administrations: Technologies for Value Creation*. IGI Global, Herchey PA.

Hollanders, H. 2009. 2009 Regional innovation scoreboard (2009 RIS). *MERIT,Maastricht*.

Hollanders, H., and F. Celikel-Esser. 2007. Measuring innovation efficiency. *INNO Metrics*.

Lugones, G., F. Peirano, M. Giudicatti, and J. Raffo. 2003. Indicadores de innovación tecnológica. *Centro De Estudios Sobre Ciencia, Desarrollo y Educación Superior (REDES), Argentina*.

Madlener R., Henggeler Antunes C., Dias L.C., (2006). Multi-Criteria versus Data Envelopment Analysis for Assesing the Performance of Biogas Plants. *CEPE Working Paper No.* 49, ETH Zurich.

Maystre, L., Pictet, J. and Simos, J.(1994). *"Méthodes Multicritères ELECTRE"*. Presses Polytechniques et Universitaires Romandes.

Raftery, A. (1993). Bayesian model selection in structural equation models. In K. Bollen & J. Long (Eds.), Testing structural equation models (pp. 163-180): Newbury Park, California.

Roy, B. y Bouyssou, D. (1993). *"Aide Multicritère à la Décision: Méthodes et Cas"*. Economica

Zhu, J. and Cook, W.D. (2007). *Modeling Data Irregularities and Structural Complexities in Data Envelopment Analysis.* Springer.

AUTHOR BIOGRAPHIES

MARÍA ROCÍO GUEDE studied Industrial Engineering, specializing in business organization at University of Vigo, Spain, and she is Phd by Rey Juan Carlos University. She worked for four years for several private sector companies and then, in 2005, she moved to the Rey Juan Carlos University, as a lecturer. She is now researching about efficiency in technology transfer and innovation topics. Her e-mail address is: rocio.guede@urjc.es

MARÍA AUXILIADORA DE VICENTE studied mathematics in the Complutense University of Madrid (UCM) where she obtained her degree in 1991 and her P.H.D. in Economics in 1999. She began to work Teaching statistics in the CESSJ Ramón Carande, an institution depending from UCM. She is professor in the University Rey Juan Carlos since 1998 where she has been doing research in multicriteria decision making and multivariate analysis. In the last years she has been applying the results of her theoretical research to innovation and technology transfer's topics. Her email address is: maria.devicente@urjc.es

DESIRÉ GARCÍA was born in Madrid, Spain and has a Minor in Business Science, Bachelor in both Business Administration and Management and Market Research and Technique. She also has a Masters Degree in Business Management. She has a wide experience in the private sector, where she has worked for more than five years. Since 2007, she has been a lecturer at Universidad Rey Juan Carlos, where she currently teaches Corporate Mathematics, Financial Mathematics, Corporate Statistics, Computer Science Applied to Corporations and Corporate Decision Methods. Her e-mail address is: desire.garcia@urjc.es

JOSÉ JAVIER FERNÁNDEZ was born in Madrid, Spain and has a Minor in Business Science, Bachelor in Business Administration and he also has a Masters Degree in Business Management. He worked in several private companies and then he moved to Rey Juan Carlos University as a lecturer, where he teaches strategic management and business policy. He is now researching about ecoefficiency and environmental management systems. His e-mail address is: josejavier.fernandez.rodriguez@urjc.es

LIQUIDITY TRADING ON STOCK MARKETS: DETERMINANTS OF THE HUMPED SHAPE OF THE ORDER BOOK

Dániel Havran, István Margitai and Balázs Árpád Szűcs
Department of Finance*
Corvinus University of Budapest
1093, Budapest, Fővám tér 8, Hungary
E-mail: balazsarpad.szucs@uni-corvinus.hu

April 17, 2012

KEYWORDS

Market liquidity, market microstructure, order book simulation, genetic algorithm

ABSTRACT

In this paper we examine pure limit order markets in order to find out how different trading strategies affect the shape of the order book. We concentrate on liquidity trading, which implies that any new information that would influence the fundamental value of the traded asset is excluded. The humped shape of the order book is a stylized fact studied in the literature. We build a simulation model to explain the position of this hump in a setting where liquidity takers and providers submit buy and sell orders to complete their exogenous trading needs. We show that under the above assumptions the exogenous impatience factor of liquidity traders determines the position of the hump.

1 INTRODUCTION

On electronic stock markets, market actors submit buy or sell orders into the order book. The limit order volume structures of the offered/asked prices form a humped shape. An example is shown in Figure 1.1. We model market microstructure in order to explore the determinants of stock exchange order book shapes.

The order book itself is the collection of specific buy and sell *limit* orders, submitted by patient market players, defined as Liquidity Providers (LP). The other type of market players are the impatient Liquidity Takers (LT), who are submitting buy and sell *market* orders. Transactions always consist of a market and a limit order matched to one another. The two types of players are making money on the expense of each other: transactions close to the mid-price (the average of the best bid and ask prices) favour LTs, whereas transactions far from the mid-price favour LPs. It follows that there is a trade-off between trading immediately (i.e. being impatient) and reaching a better price, which trade-off is often referred to as price impact or market impact (for a precise definition of market impact, where order volume is also included, see Bouchaud et al. (2002)).

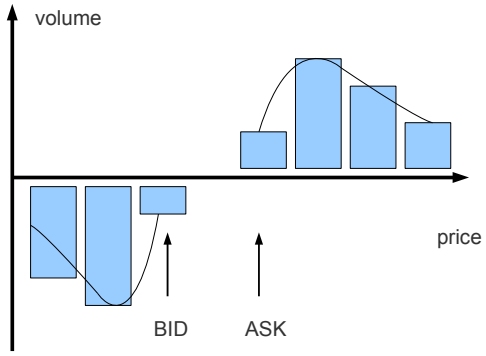

Figure 1.1: Humped shape of the order book

The limit order market literature is fairly recent, it has less than two decades of history. The most comprehensive work that introduces the limit order markets and connects liquidity to the economic literature is Parlour and Seppi (2007). The most commonly known statistical analysis is provided by Bouchaud et al. (2002), where the shape of the average order book is described. This shape has already been tested on different markets. For example, Gu et al. (2008) investigates the shape of the order book on Chinese stock markets in their empirical study. With a limit order market model, Rosu (2009) explains how the humped shape is formulated by liquidity takers and providers. He also makes suggestions to price formation. Our contribution is related to his results, we also suppose symmetric information relations among the market players. In contrast to Rosu (2009), we focus on the heterogeneity of impatience.

*This conference material was prepared with the support of the TÁMOP-4.2.2/B-10/1-2010-0023 project.

Proceedings 26th European Conference on Modelling and Simulation ©ECMS Klaus G. Troitzsch, Michael Möhring, Ulf Lotzmann (Editors)
ISBN: 978-0-9564944-4-3 / ISBN: 978-0-9564944-5-0 (CD)

We are reasoning that the humped shape of the order book can be derived from the liquidity takers' impatience, together with the heterogeneity of the liquidity providers' market expectations. In order to exclude the speculation on fundamental value, so that we could concentrate only on liquidity motives, we assume that there is no new information on asset values during the observed period. We suppose exogenously defined LTs, while the LPs' order strategies are continuously evolving over time according to a genetic algorithm.

So building on the stylized fact and the common behavioural patterns reported in the literature, we construct a model of market microstructure aiming to explain the dynamic evolution of the above mentioned hump shape in the order book. The following hypothesis will be tested in this paper.

Hypothesis: Assuming that LPs are following a genetic algorithm to adopt their strategies to the exogenous and fixed strategies of the LTs, then the position of the hump in the order book is determined by the aggregate strategy (through the impatience) of LTs.

The rest of the paper is organized as follows. The next chapter introduces the market players in detail. The third section investigates the simulation process. Section four describes our main results, while providing some further analyses based on our model. The last section concludes.

2 MARKET PLAYERS

We only model liquidity trading, therefore we must exclude all other motivations to trade, especially the arrival of new fundamental information on the asset. This results in a setting where all players stick to their initial plans concerning the direction of trades (buy or sell) as well as the overall amount they wish to trade during the simulation. As a result, there are four different types of players in our model, as shown in Table 1. Types 1 and 2 are LPs, who only submit limit orders, while types 3 and 4 are LTs, who only use market orders.

	Liquidity Provider	Liquidity Taker
Buy	1	3
Sell	2	4

Table 1: Player types

The core motivation of any player in this model (LPs and LTs alike) is the same: they wish to trade their full predefined volumes and reach the best possible volume weighted average prices while doing so. However the way they reach their goals is different. The following two subsections elaborate on the behaviour of LPs and LTs.

Liquidity Providers

Every LP has an idea (a forecast) on what is going to happen in terms of trades in the subsequent trading period. Namely they all have a guess on the price level that is furthest from the mid-price but still will be used. They base their limit order submission strategies on this forecast. On the one hand, if they expect this level to be close to the mid-price, they will also put their orders at closer price levels, because otherwise a considerable amount of their orders would remain unmatched. On the other hand, if they expect this price level to be further from the mid-price, they will then submit their orders at further levels, because they have a reason to believe these orders will still be matched. Thus they will have improved the volume weighted average price of their own trades.

The technical interpretation of this behaviour is the following. Initially every LP receives a random binary string that codes their unique expectations. This string is then converted into a scalar through equation 2.1 (similarly to Lettau (1997)) as follows:

$$\lambda = l\frac{\sum_{j=1}^{k} s_j 2^{j-1}}{2^k - 1}, \tag{2.1}$$

where λ is the above mentioned price level they are expecting, while l denotes the number of available price levels on one side, k is the length of the string, and s_j is the jth character of the string.

LPs then determine the volumes they submit on each price level using the following function form:

$$v_i(\lambda) = \frac{\frac{\lambda^i e^{-\lambda}}{i!}}{\sum_{i=1}^{l} \frac{\lambda^i e^{-\lambda}}{i!}} V, \tag{2.2}$$

where v_i denotes the volume submitted on the ith price level, and V is the latent need for transaction (inventory) of the LP. The λ is a scalar defined by equation 2.1.

Using this setup implies that each LP will submit some orders to all available price levels. The aggregate submissions of LPs shape up the order book.

Liquidity Takers

LTs differ in their levels of impatience/aggression, but they all base their market order submission strategies on the actual state of the order book. Their primary goal is also to trade, and depending on their level of impatience they are willing to clear more or less price levels, that is willing to bare more or less liquidity costs in exchange for quicker execution (although market orders are executed immediately, more aggressive players who clear more price levels trade larger volumes, hence fulfill their own trading need more quickly). Those who are very patient may sometimes choose not to trade at all in that cycle given the actual limit orders.

The technical interpretation of this behaviour is as follows. All LTs have an initial γ that is constant through-

out the simulation. This is their unique factor of impatience, that determines the worst volume weighted average price (VWAP) that they are willing to achieve while trading. Generally, if there are l price levels, for the ith LT $1 \leq VWAP_i \leq l$ holds. Each LT faces a limit of $VWAP_i \leq \gamma_i$, but if they have enough inventory left to trade, they will hit the γ limit. The smaller this γ value, the more patient the LT is, not willing to clear many price levels, being ready to wait instead. Larger γ means the LT urges the trade by letting the VWAP of their own trade go further away from the mid-price, that is clearing more price levels and thus trading the full amount in fewer rounds.

This strategy is obviously conditional on the actual state of the order book. The same γ may result in very different trading volumes depending on the depth of the book on each price level.

Note that LTs start trading at the best price levels and go towards worse ones as the better levels are cleared.

3 SIMULATION PROCESS

We used the Matlab/Octave environment to run our simulation. The simulation setup consists of cycles and phases as shown in Figure 3.1. The remaining of this section elaborates on this setup.

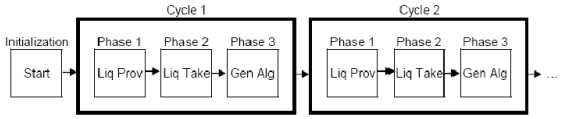

Figure 3.1: Structure of simulation

Initialization

This is the starting phase of each run that sets the initial parameters of the simulation. It is important to separate this phase from the cycles, because thus we are able to set the same initial parameters across different runs if necessary. The parameters that must be set are (1) the random strings for each LP (e.g. 1001101), (2) the random γ for each LT, (3) the number of each player type listed in Table 1, (4) the inventory of each player, which equals the latent volume they try to trade, and (5) the number of available price levels on each side of the mid-price.

Cycles

The series of cycles is the model of the trading period. Trading is continuous as the cycles follow each other. Any inventory that runs out is refilled at the beginning of the next cycle.

Phase 1 - Liquidity providers

This is the phase of the liquidity providers. When Phase 1 begins, there is an existing order book that remained from the previous cycle (except in Cycle 1). LPs are allowed to revise their previous quotes, that is they can cancel and replace those that were not matched in the previous cycle. It is achieved in model by starting Phase 1 with the cancellation of all previous orders, thus LPs face a blank order book in Phase 1.

Given that our goal is to model the evolution of the shape of the order book, it follows that the price formation falls beyond the scope of our interest in this model. This is why we continue Phase 1 by setting the mid-price to a constant. The bid-ask spread is also fixed, which means that the best prices are a constant distance away from the mid-price in both directions. All price levels beyond the best prices follow each other by one tick.

All LPs act simultaneously, which implies that their strategies exclude the response to the behaviour of each other. The result of their aggregate behaviour is the order book itself. We model this by making them all decide their submission strategies at the beginning of the phase, and then follow each other one by one in a random order (uniform distribution) ignoring the submissions of the other LPs in the same phase.

It is important to mention that the matching mechanism of the order book is First-In-First-Out (FIFO). This means that limit orders closer to the mid-price have priority when a market order arrives, and because limit orders have a timestamp, on the same price level those with an earlier timestamp have priority. This is why the random order is important in order to model the diversity in submission times.

By the end of Phase 1, the order book is built.

Phase 2 - Liquidity takers

This is the phase of the liquidity takers. They condition their order submission strategies on the actual state of the order book, in consideration of their own γ. They implicitly also consider the submissions of other LTs, given that the order book changes as a result of their actions. This is captured in our model in a way where within the same phase, they follow each other in a uniformly distributed random order. This implies that they do not face the full order book, only the remainders of it after the quicker LTs' trades.

Let us suppose for example an LT with $\gamma = 1$. This means that $VWAP = 1$ is the only acceptable scenario, hence no trade beyond the first price level is possible. In a situation where this LT is not within the first few ones to trade, it is highly probable that the first price level will be long gone by the time this LT takes its turn, it will therefore decide not to trade.

By the end of Phase 2, all transactions took place.

Phase 3 - Genetic algorithm

This is the phase of the genetic algorithm, and it is the LPs that evolve genetically. The strings of those LPs who had a better guess on the λ will survive with higher probabilities into the next cycle, because a better guess will clearly result in statistically more favorable volume weighted average prices. We use a fitness function to rank the LPs based on the success of their preliminary guesses as shown in equation 3.1.

$$f(\lambda, l, \Omega) = l - |\lambda - \sum_{i=1}^{l} \frac{\sum_j v^1_{i,j} - \sum_j v^2_{i,j}}{\sum_j v^1_{i,j}}|, \qquad (3.1)$$

where f is the fitness value of the LP (the higher, the better) and l is the number of price levels on one side of the book. i stands for price levels, j for LPs, v^1 and v^2 are the volumes in the book at the end of Phases 1 and 2. The fitness is the highest if they got the λ correctly, and gets smaller as their guess deteriorates.

The genetic algorithm itself has two stages: crossover and mutation. The first one is the crossover stage, where a random h number is selected, and the strings are cut after the hth character. Then the strings are mixed up in pairs along this h cutoff with probability p_c. The second stage is mutation, where random characters of random strings are changed with probability p_m. For illustration of the two stages of the genetic algorithm see figure 3.2. The LPs thus evolve, and those that are more successful survive with higher probabilities.

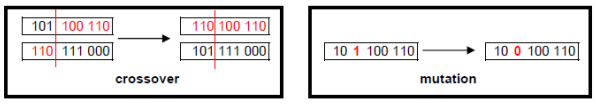

Figure 3.2: Genetic algorithm

For a better understanding of the mechanism behind the genetic algorithm driven LP behaviours, we tested the effects of LP mutations. The two factors of the evolution are the mutation and the crossover probabilities. When the crossover probability is high, there are big jumps in the time series of λ, until such a level is reached, where all strings are identical, hence mutation has no effect.

The mutation causes noisy changes. The mechanism of mutation is illustrated in Figure 3.3, where we plotted the average λ values of LPs against the simulation cycle count. The two graphs represent the zero and the positive (but small) probability cases of mutation.

4 RESULTS

First we set up three alternative simulation environments with different parameter sets regarding the LTs' impatience and the LPs' evolution. Second, we analyze the behaviour of the two kinds of players with random initial variables.

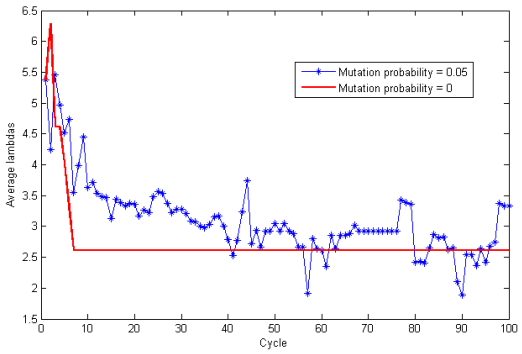

Figure 3.3: Mutation effects

We calibrated the model as follows. At the initial state, the λ of LPs is allocated from 0.5 to 9.5 in steps of one. We chose $l = 10$ as the number of price levels on one side. LPs are therefore inhomogeneous, each of them having different initial values. The setup so far corresponds to a very controlled environment with special assumptions on the initial λ parameters. The probability of the crossover in a given cycle is twenty percent, and the probability of mutation is five percent in each run.

The γ value of LTs, therefore their level of impatience is homogeneous in all the three runs, with values of 1.5 in the first run, 3.5 in the second and finally 5.5 in the third. For an overview of the different calibration setups, see Table 2.

Simulation	Liquidity Takers	Liquidity Providers		
	γ	λ_0	p_c	p_m
Run a)	1.5	0.5 ... 9.5	0.2	0.05
Run b)	3.5	0.5 ... 9.5	0.2	0.05
Run c)	5.5	0.5 ... 9.5	0.2	0.05

Table 2: Model calibrations

According to Run a)-c) the diversity of liquidity providers disappears with time, as the genetic algorithm in each running cycle improves their λ expectation. In case of Run a), after the cycle number 20, the peak of the curve is around the 1.5th price level, while in case of Run c) the hump in the order book locates around the 5th price level. In Run c) the LTs are much more aggressive as they are willing to trade at less favourable price. Hence, they clear approx. 5 price levels from the book. Figure 4.1 shows that the heterogeneous λ values are converging to the pre-defined and fix γ in each simulation.

We showed in special cases that the location of the hump in the order book is a result of a learning process of liquidity providers if liquidity takers are homogeneous. In Run a)-c) the humps after 20 cycles moved from the middle of the book to a price level of the LTs' γ.

Given that the above described results hold for arbitrary γ values, our hypothesis can be confirmed in the special setup of homogeneous LTs. Our next question was whether our hypothesis can also be confirmed for a

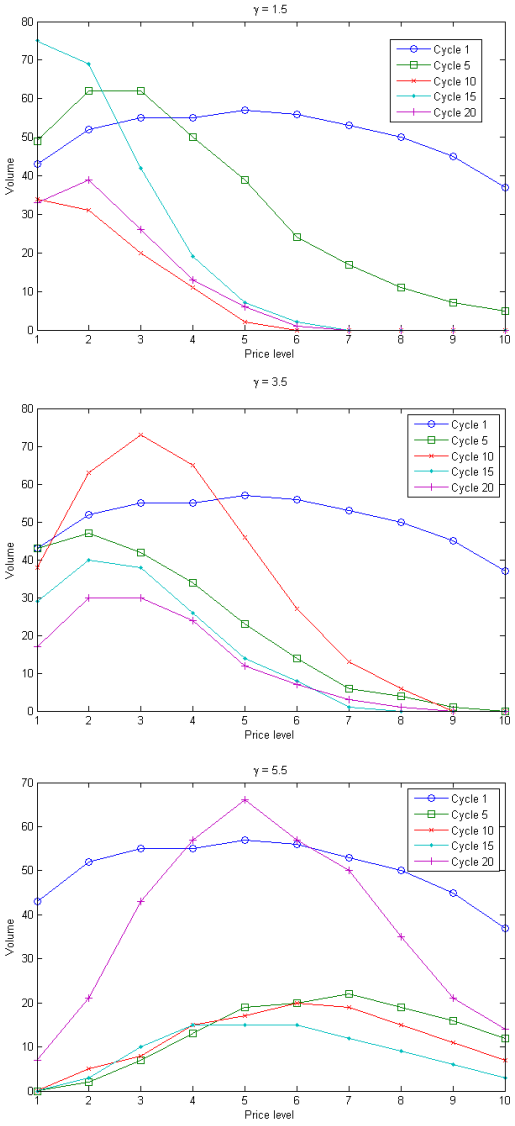

Figure 4.1: Runs a), b) and c)

more general case, where both LPs and LTs are heterogeneous.

In order to examine such a case, let each LT have a random γ impatience coefficient. After repeating the simulations 150 times, we plotted the result in Figure 4.2, which depicts how the LPs' expectations adjust to the LTs' impatience in random cases. Even after 30 running cycles in each simulation the average λ is close to the average impatience parameters of LTs. We note that the slope of the regression line on Figure 4.2 is close to one. The deviation of λ and γ points from the regression line can be reasoned by the mutation in the genetic algorithm. It can randomly improve or deteriorate the LPs' λ from the LTs' average γ in each cycle.

The deviation of the slope of regression line from one can be explained as follows. As the inventories of agents (the volume that the LTs and LPs intend to trade in a certain cycle) dynamically change, and both LTs and LPs are heterogeneous, it is not ensured that the number of

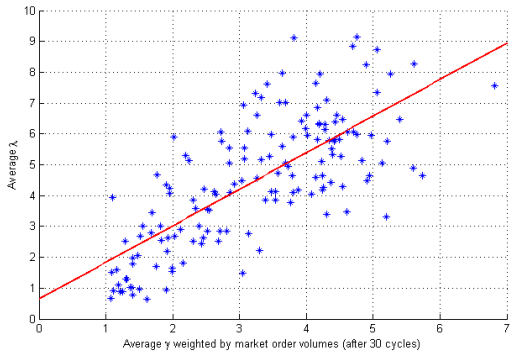

Figure 4.2: Average γ and λ

aggregately cleared price levels will be equal to the unweighted average of γ values. Hence, the LPs evolve in a way that they place the hump on a price level, which might be different from the average γ values. This is the reason why we plotted the evolved λ values against the *inventory weighted* average γ.

5 CONCLUSION

In this paper we model a pure limit order market with a heterogeneous set of players including liquidity takers and providers who buy and sell a single asset. The strategies of the liquidity takers are exogenous, whereas the strategies of the liquidity providers evolve according to a genetic algorithm that is conditioned on the behaviour of the liquidity takers. Knowing that such market microstructures tend to provide a humped shape order book, we run our simulations to show that within the above conditions, the position of the hump in the order book can be explained by the exogenous strategies (the impatience) of the liquidity takers.

The next step of further research could examine the determinants of the humped shape in a similar model, where the strategies of the liquidity takers are endogenous. Changing this single aspect may add interesting interactions to the model of the current paper.

REFERENCES

Bouchaud, J.-P., Mezard, M., and Potters, M. (2002). Statistical properties of stock order books: empirical results and models. Science & Finance (CFM) working paper archive 0203511, Science & Finance, Capital Fund Management.

Gu, G.-F., Chen, W., and Zhou, W.-X. (2008). Empirical shape function of limit-order books in the chinese stock market. *Physica A*, 387(21):5182–5188.

Lettau, M. (1997). Explaining the facts with adaptive agents: The case of mutual fund flows. *Journal of Economic Dynamics and Control*, 21:1117–1147.

Parlour, C. A. and Seppi, D. J. (2007). *Limit Order Markets: A Survey*. Handbook of Financial Intermediation & Banking.

Rosu, I. (2009). A dynamic model of the limit order book. *Review of Financial Studies*, 22(11):4601–4641.

AUTHOR BIOGRAPHIES

DÁNIEL HAVRAN holds an Assistant Professor position at the Department of Finance, Corvinus University of Budapest. He actively teaches Financial Markets, Corporate Finance and Credit Risk Management courses. His research interest is related to corporate financial flexibility, liquidity and credit risk. Earlier, he developed methodical tools and forecasting models for corporate liquidity and cash management systems. He obtained his PhD in Economics in 2011. His email is daniel.havran@uni-corvinus.hu.

ISTVÁN MARGITAI majored in Investments and Risk Management at the Corvinus University of Budapest. He currently works as an analyst at the Asset Liability Management Department of a Hungarian retail bank, where his main responsibility is strategic risk management. He joined the Liquidity Research Group of the Department of Finance, Corvinus University of Budapest in February 2011. His email is margitai.i@gmail.com

BALÁZS ÁRPÁD SZŰCS is a PhD candidate in Economics. He currently works as a Research Assistant at the Department of Finance, Corvinus University of Budapest. His research interest covers market microstructure, modeling and experimental games of financial microstructures. His email is balazsarpad.szucs@uni-corvinus.hu

COMPARATIVE STUDY OF TIME-FREQUENCY ANALYSIS APPROACHES WITH APPLICATION TO ECONOMIC INDICATORS

Jiří Blumenstein
Department of Radio electronics
Brno University of Technology
Purkyňova 118
612 00 Brno, Czech Republic
Email: xblume00@phd.feec.vutbr.cz

Jitka Poměnková
Department of Radio electronics
Brno University of Technology
Purkyňova 118
612 00 Brno, Czech Republic
Email: pomenkaj@feec.vutbr.cz

Roman Maršálek
Department of Radio electronics
Brno University of Technology
Purkyňova 118
612 00 Brno, Czech Republic
Email: marsaler@feec.vutbr.cz

KEYWORDS

time-frequency analysis, wavelets, multiple window method, AR process, periodogram

ABSTRACT

Presented paper deals with comparison of various methods for time-frequency representation of a signal with time-varying behavior. We choose methods such as wavelet analysis, multiple window method using Slepian sequences, time-frequency varying autoregressive process estimation and time-frequency Fourier transform representation (periodogram). We apply these methods first on the simple simulated artificial signal and we assess their performance. Then we proceed with application on the real data which is monthly data of the industry production index of European Union in the period 1990/M1-2011/M11. During the evaluation we focus on the results with respect to the time of global crisis. The results of the experiments are represented in the the graphical form and briefly discussed.

INTRODUCTION

The description of time-frequency structure of signal has wide range of usage. Its application can be seen in many scientific areas such as engineering (Xu et al., 2011), medicine (Xu et al., 1999), economy and many others. In last several years these techniques are in the front of economic researchers which analyze comovement of economic indicators. In this sense the papers of (Rua, 2010), (Yogo, 2008) or (Hallett and Richter, 2007) and many others were written. Estimation of spectrogram or scalogram of input signal or time series depends on used methods and their parameters. We investigate in this article four basic methods such as wavelet analysis (Jan, 2002), multiple window method using the slepian sequences (MWM) (Xu et al., 1999), time-frequency varying autoregressive (AR) process (Proakis et al., 2002) spectrum estimation and time-frequency Fourier transform estimation (periodogram) (Jan, 2002). On the basis of simulations on the artificial well-know signal we analyze behavior of each method and search for their advantages, disadvantages and recommendations for their usage. Consequently we compare obtained results with the aim to give recommendation for methods application. In order to practically demonstrate and evaluate the performance of the chosen methods we apply them to the analysis of the real data which is the monthly data of the industry production index of the European Union countries in the period 1990/M1-2011/M11.

The paper is organized as follows: In the section Methodical Background we describe chosen methods of time-frequency analysis. Consequently, in the section Data, we briefly describe data used both for the simulation as well as for the practical application. After that, in the section Simulation, we show results of an application of chosen methods on simulated artificial data. The section Application presents results of real data analysis of the industry production index of the European Union and its brief economic interpretation. In both later sections results are graphically represented. The paper ends up with the conclusion and the list of used references.

METHODICAL BACKGROUND

Let us have a signal (a time series) $y(n),\ n = 1, \ldots, N$. Under assumption that the time series contain a long-term trend, we can apply additive decomposition in the following form

$$y(n) = g(n) + s(n) + c(n) + \varepsilon(n),\ n = 1, \ldots, N, \quad (1)$$

where $g(n)$ denotes a long-term trend, $s(n)$ is the seasonal component, $c(n)$ is the cyclical component and $\varepsilon(n)$ is the irregular component (a random noise). Focusing on analysis of cyclical movements around its long-term trend it is necessary to remove the long-term trend applying some filtering methods. When the seasonally adjusted data are not available (in other words the analyzed series contains the seasonal component), the seasonality should be removed by applying some corresponding method.

The spectrum of the signal (time series) $y(n),\ n = 1, \ldots, N$ can be written as a Fourier sum (Hamilton, 1994)

$$S_y(f) = \frac{1}{2\pi} \sum_{j=-\infty}^{\infty} \gamma_j e^{-ifj}, \quad (2)$$

where $\gamma_j = cov(y(n)y(n+j))$ is autocovariance between $y(n)$ and $y(n+j)$, $i = \sqrt{-1},\ f = 2\pi/N$.

Proceedings 26th European Conference on Modelling and Simulation ©ECMS Klaus G. Troitzsch, Michael Möhring, Ulf Lotzmann (Editors)
ISBN: 978-0-9564944-4-3 / ISBN: 978-0-9564944-5-0 (CD)

Sample periodogram
Let N denotes an odd integer, $M = (N-1)/2$. Let $f_j = 2\pi j/N, j = 1,\dots,M$ and let $\mathbf{x}_n = [1\ cos(f_1(n-1))\ sin(f_1(n-1))\ \dots\ cos(f_M(n-1))\ sin(f_M(n-1))]'$. Then $\sum_{n=1}^{N}\mathbf{x}_n\mathbf{x}_n' = \begin{bmatrix} N & \mathbf{0}' \\ \mathbf{0}' & (N/2)\mathbf{I}_{N-1} \end{bmatrix}$. Furthermore, let $y(n), n = 1,\dots,N$ be any N numbers. Then the following holds:

1. The value $y(n)$ can be expressed as

$$y(n) = \hat{\mu} + \sum_{j=1}^{M} \hat{\alpha}_j cos(f_j n) + \hat{\delta}_j sin(f_j n), \quad (3)$$

with $\hat{\mu} = N^{-1}\sum_{n=1}^{N} y(n)$ and for $j = 1,\dots,M$ $\hat{\alpha}_j = (2/N)\sum_{j=1}^{N} y(j)cos(f_j(n-1))$, $\hat{\delta}_j = (2/N)\sum_{j=1}^{N} y(j)sin(f_j(n-1))$.

2. The sample variance of $y(n)$ can be expressed as

$$var(y) = \frac{1}{N}\sum_{n=1}^{N}(y(n)-\overline{y})^2 = \frac{1}{2}\sum_{j=1}^{M}\left(\hat{\alpha}_j^2 + \hat{\delta}_j^2\right) \quad (4)$$

end the portion of sample variance of y that can be attributed to the cycles of frequency f_j is given by $1/2\sum_{j=1}^{M}\left(\hat{\alpha}_j^2 + \hat{\delta}_j^2\right)$.

3. The portion of sample variance of y that can be attributed to the cycles of frequency f_j can equivalently be expressed as

$$1/2\sum_{j=1}^{M}\left(\hat{\alpha}_j^2 + \hat{\delta}_j^2\right) = \frac{4\pi}{N}\cdot\hat{S}_y(f_j), \quad (5)$$

where $\hat{S}_y(f_j)$ is the sample periodogram at frequency f_j.

Proof: (Hamilton, 1994).

Periodogram in time-frequency: Spectrogram
Practically, the periodogram is often estimated by the mean of a discrete Fourier transform

$$S_y(f) = \sum_{n=0}^{N-1} y(n)e^{-j2\pi fn}, \quad (6)$$

In the assumption that the time-varying signal have a locally periodical behaviour, the time-frequency representation - spectrogram can be constructed by the mean of the Short Time Fourier Transform (STFT, here defined in the discrete form) at time n:

$$S_y(n,f) = \sum_{m=-\infty}^{\infty} y(m)\theta(n-m)e^{-j2\pi fm}, \quad (7)$$

where $\theta()$ is the observation window with N_w nonzero elements. According to the application and desired properties, different window functions can be used as the rectangular, the Hanning, the Hamming or the flat-top. A window is then slided over the analyzed signal and corresponding values of the STFT are computed. The (squared) module of the STFT results is then plotted in the 2D graph.

Multiple window method (MWM)
Similar approach for construction of the spectrogram has been proposed in (Xu et al., 1999). According the author the Slepian sequences are the eigenvectors of the equation

$$\sum_{m=0}^{N-1}\frac{\sin 2\pi W(n-m)}{\pi(n-m)}\nu_m^{(k)}(V,W) = \quad (8)$$

$$= \lambda(N,M)\nu_m^{(k)}(V,W)$$

where N is the length of the eigenvectors (or data), and W is the half-bandwidth that defines a small local frequency band centered around frequency $f : |f - f'| \leq W$. Denote that Slepian sequences are orthogonal time-limited functions most concentrated in the frequency band $[-W, W]$.

The procedure how to compute the spectral estimate of $y(n)$ using the multiple window method written according to (Xu et al., 1999) consists from the following steps:

1. Specify N and W, where N is the number of data points, and W depends on desired time-bandwidth product (or frequency resolution) NW.

2. Use (8) to compute the λ_k's and ν_k's.

3. Apply ν_k to the entire length-N data $y(n)$ and take the discrete Fourier transform

$$y_k(f) = \sum_{n=0}^{N-1} y(n)\nu_m^{(k)}e^{-j2\pi fn}, \quad (9)$$

where $y_k(f)$ is called k-th eigencoefficient and $|y_k(f)|^2$ the k-th eigenspectrum.

4. Average the K eigenspectra (weighting by the reciprocal of the corresponding eigenvalues) to get an estimate of the spectrum

$$\hat{S}(f) = \frac{1}{K}\sum_{k=0}^{K-1}\frac{1}{\lambda_k}|y_k(f)|^2. \quad (10)$$

Since the first few eigenvalues are very close to one, (10) can be simplified to

$$\hat{S}(f) = \sum_{k=0}^{K-1}\frac{1}{\lambda_k}|y_k(f)|^2. \quad (11)$$

The concept of the multiple window method can be easily extended into the time-frequency domain analysis, similarly to the spectrogram construction. In case of

MWM in TFA the idea is to apply a set of sliding windows and then takes the average (Xu et al., 1999)

$$Y_{MW}(t,f) = \frac{1}{K}\sum_{k=0}^{K-1} |Y_k(t,f)|^2 \qquad (12)$$

where

$$Y_k(t,f) = \int y(\tau) h_k(\tau - t) e^{-j2\pi f n} d\tau \qquad (13)$$

$y(t)$ is the signal or time series to be analyzed. For the details you can see (Xu et al., 1999), (Frazer and Boashash, 1994). This equation stands for the time-frequency multiwindow analysis in the continuous time domain. The modification to the discrete form, similarly to eq. 7 is straightforward.

Time-frequency varying AR process

As the alternative to the above mentioned non-parametric approaches, the time-frequency analysis can be performed in the parametric way. In such a case we assume (according to the well-known concept of the whitening filter), that analyzed time series y can be considered as the output of linear time invariant filter $H(e^{j\omega})$ driven by a with noise w with the variance σ_w^2. Note that $\omega = 2\pi f$. The spectrum at the filter output is then $S_y(f) = \sigma_w^2 |H(e^{j\omega})|^2$. For this filter we can find so called whitening filter, on which output there is again a white noise. For the correctly designed whitening filter it holds $H_w(e^{j\omega}) = 1/H(e^{j\omega})$ (Jan, 2002).

The whitening filter can be implemented in the general form using the auto regressive moving average ($ARMA$) model. Its identification is not so simple, therefore moving average (MA) or auto regressive (AR) process are usually used. Using the AR process, the spectrum estimation can be done according to the formula (Proakis et al., 2002).

$$\hat{S}_y(\omega) = \frac{\sigma_\omega^2}{|1 - \sum_{i=1}^{p} a_i e^{-i\omega j}|^2}, \qquad (14)$$

where a_i are the coefficients of the AR process of the order p. An advantage of this approach is better frequency resolution. This depends on the order of the process which is smaller in comparison to the sample size N. Several methods can be used for the AR process coefficient estimation like the Burg, Yule-Walker (Proakis et al. (2002)) or modified covariance method that we used in our previous paper (Šebesta (2011)).

In order to easily extend the AR process spectrum estimation to the time-frequency representation, a sliding window of the length N_w was moved across the analyzed signal (series) $y(n)$. For each window shift, the AR process coefficients have been estimated and subsequently the spectrum has been computed and represented in the form of 2D plot.

Wavelet transform

Let us assume the time series is seasonally adjusted without the long-term trend. The continuous wavelet transform of the signal (the time series) $y(n)$ with respect to the mother wavelet $\psi_{a,\tau}(n)$ is defined as

$$S_{CTW}(a,t) = \int_{-\infty}^{\infty} y(t) \frac{1}{\sqrt{a}} \psi\left(\frac{n-\tau}{a}\right) dn, \qquad (15)$$

$$a > 0, \tau \in R,$$

where the mother wavelet takes the form $\psi_{a,\tau}(n) = \psi\left(\frac{n-\tau}{a}\right)$, τ is the time shift, a is the parameter of dilatation (scale), which is related to the Fourier frequency. The numerator of the fraction $\sqrt{a}$ ensures the conservation of energy (Jan, 2002).

To satisfy assumptions for the time-frequency analysis, wavelets must be compact in time as well as in the frequency representation. There exist a number of wavelets which can be used, such as Daubechie, Morlet, Haar or Gaussian wavelet (Gençay et al., 2002), (Adisson, 2002).

An inverse wavelet transformation is defined as

$$y(n) = \frac{1}{C_\psi} \int_{-\infty}^{\infty} \int_{-\infty}^{\infty} \psi_{a,\tau}(t) S_{CTW}(a,t) \frac{da d\tau}{a^2}, \quad (16)$$

where $\psi_{a,\tau}(n)$ is the mother wavelet and $S_{CTW}(a,n)$ is the continuous wavelet transform of time series $y(n)$ defined in relation (15). For C_ψ hold $0 < C_\psi = \int_0^\infty \frac{|\Psi(\omega)|^2}{\omega} d\omega < \infty$, $\Psi(\omega)$ is the Fourier transform of $\psi_{a,\tau}(n)$.

DATA

Artificial data

For the simulation purposes we used the following data. We assumed two sinusoidal waves with different periods which have been shifted and partially overlap in time. The resulting signal is given by following equation

$$y = w_1 \sin(2\pi n/T_1) + w_2 \sin(2\pi n/T_2), \qquad (17)$$

where $n = 1, \ldots 263$ is the time (in seconds, for the illustration),

$$w_1 = \begin{cases} 1 & n = 10, \ldots, 180, \\ 0 & \text{elsewhere,} \end{cases}$$

and

$$w_2 = \begin{cases} 1 & n = 100, \ldots, 249, \\ 0 & \text{elsewhere.} \end{cases}$$

are time windows of the two sinusoidal waves with period $T_1 = 4s.$ and $T_2 = 16s.$. The length of the artificial time series is chosen the same as the length of the real data (see next section). The time domain plot of the artificial signal is in Figure 1.

Figure 1: Simulated signal

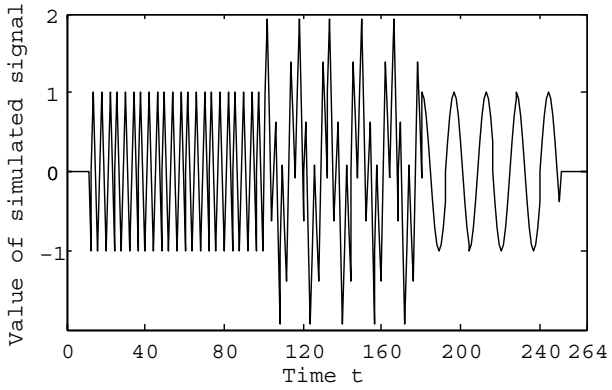

Real data

In order to demonstrate the performance of investigated methods in the real application, we used the data of the industry production index (IPI) of EU 27 in the period 1990/M1-2011/M11 ($n = 263$). Note that the length of this time series motivates our choice of the artificial signal length (see above). The monthly data are obtained from free database of Eurostat (Eurostat, 2011) and they are seasonally adjusted volume index of production, reference year 2005, mining and quarrying, manufacturing, electricity, gas, steam and air conditioning supply. Prior to the application of time-frequency analysis methods the input data of the industry production index is transformed by the natural logarithm and the long-term trend is removed with the use of Baxter-King filter (Guay, 2005).

SIMULATION

For simulation on the artificial data, the signals described in the preceding part in equation (17) were used. Let us remind that the simulated signal consists from two harmonic signals with periods of 4 and 16 seconds which partially overlap in time.

For the time frequency analysis (in figures denoted as TFA) - estimation of spectrogram we used time-frequency Fourier transform representation (periodogram) (Fig. 2), multiple window method (Fig. 3), time-frequency varying autoregressive process AR spectrum estimation with the lag order $p = 6$ (Fig. 4). For optimization of lag order we used the Akaike information criterion, for estimation of parameters of autoregressive process we used the Yulle Walker method (Green, 1997). We toke the sliding window of the length 64 moving through the time series with the one observation (sample) step. As the last method for time-frequency representation we used the continuous wavelet transform for scalogram (Fig. 5) computation. We took the Morlet wavelet as the mother wavelet and the maximum value of the scale parameter $a = 30$.

As the values of the spectrograms have been normalized, all figures has the same gray scale (Fig. 6). In the case of spectrogram plots (independently on the estimation method) we present the results in the whole normalized frequency range $(0, 1)$. Note that 1 here stands for the half of the sampling frequency and that there is a straightforward relationship between the normalized frequency and the cyclic component period T:

$$f_{normalized} = \frac{2}{T}. \tag{18}$$

Normalized frequencies of 0.5 and 0.125 thus correspond to the periods of the artificial harmonic components $T_1 = 4$ and $T_2 = 16$, respectively. For better visibility of scalogram (wavelet analysis) results we limit the frequency range to $(0, 0.81)$ as no other components above the normalized frequency 0.81 were observable.

Figure 2: TFA via periodogram

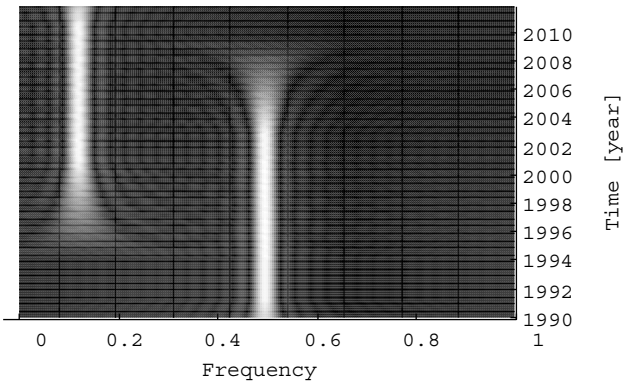

Figure 3: TFA via MWM

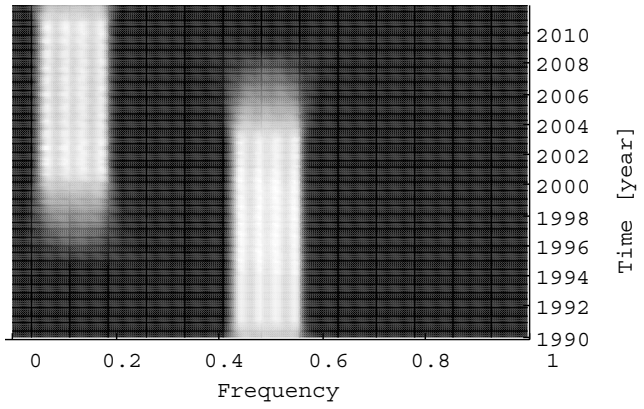

As we can see in the figures (2-5), we detect the simulated artificial components by all used methods. The highest frequency resolution is achieved by the AR process-based estimation, the lowest by the multiwindow and wavelet analysis. But the analysis results depend on the experiment setup and it is out of the scope of this paper to explore all the possible setups (e.g. the mother wavelet family) in order to generalize. In the case of wavelet analysis the results are by some reason slightly

Figure 4: TFA via $AR(6)$

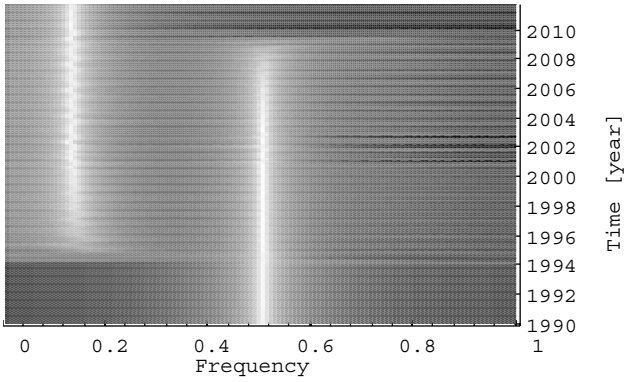

Figure 5: TFA via Wavelet analysis

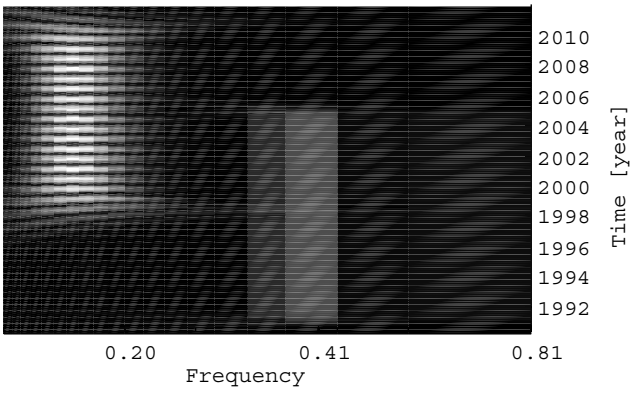

Figure 6: Scale

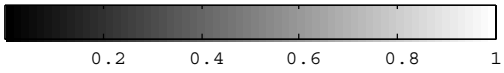

moved towards the longer periods and are not well localized. Note that in contrast to other analysis methods, the frequency axis is in the logarithmic scale.

Influence of noise

In order to assess the performance of the TFA methods and particularly the influence of noise we setup a simple experiment. The additive white gaussian noise was added to the above mentioned data and the analysis with autoregressive process and wavelet transform were performed. The signal to noise ratio (SNR) of 0 dB was used. Thus the power of the useful signal is the same as the power of the noise. The results are shown on figures 7 and 8. It is possible to see that for such noised data, one of the signal components almost disappears in the plot of the wavelet analysis results while the AR estimation method works still well.

Figure 7: TFA via $AR(6)$ on noised data

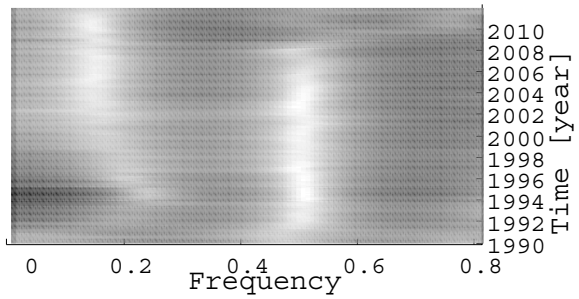

Figure 8: TFA via Wavelet analysis on noised data

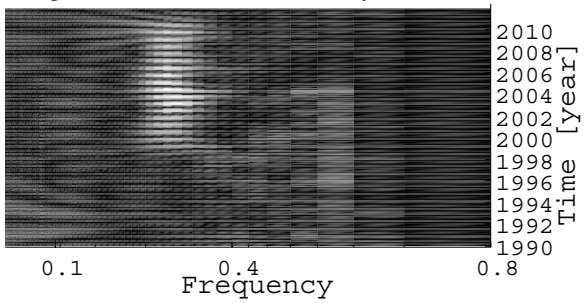

APPLICATION

Application was done on the real data described in the part "Data". Often there is no macroeconomic indicator with the long sample size, especially for small open economies. In most cases available data are quarterly data like in the case of gross domestic products (GDP), investment or consumption. The industry production index can be taken as an aggregated index containing the investments cycles, the household consumptions and production similar to GDP. It is available in monthly frequency. Therefore, with respect to the longer available sample size, we choose it for demonstration of discussed methods on the real data.

For time frequency analysis (TFA) of real data we used time-frequency Fourier transform representation (periodogram) (Fig. 9), multiple window method (Fig. 10), time-frequency changing autoregressive process AR with the lag order $p = 6$ (Fig. 11). For optimization of lag order we used Akaike information criterion, for estimation of parameters of autoregressive process we used Yulle Walker method. We toke the sliding window of the length 64 (Šebesta, 2011) moving through the time series about one observation. As the last method for the time-frequency representation we used the continuous wavelet transform for scalogram computation (Fig. 12). As in the previous case we took the Morlet mother wavelet and the maximum value of the scale $a = 30$.

As in the previous analysis of the artificial data, all figures have the same gray scale (Fig. 6). For better visibility, we limit the frequency range in all plots from the analysis of real data to the interval of $(0, 0.6)$ of normalized frequency. Remember again that 1 stands for the half of the sampling rate.

Figure 9: TFA via periodogram

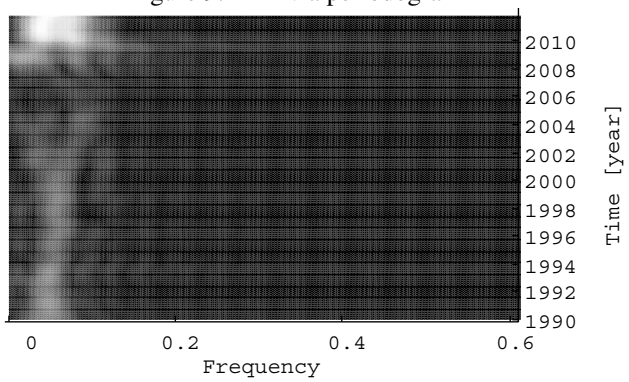

Figure 10: TFA via MWM

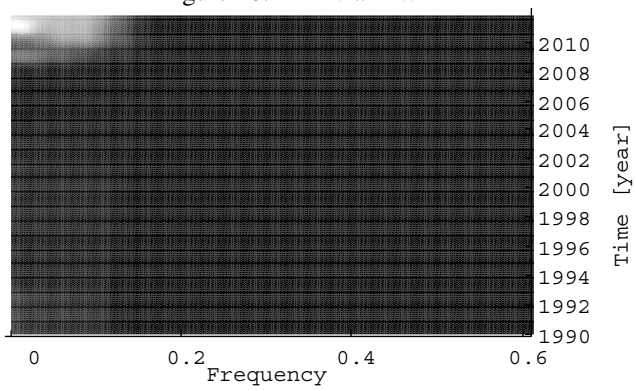

Figure 11: TFA via $AR(6)$

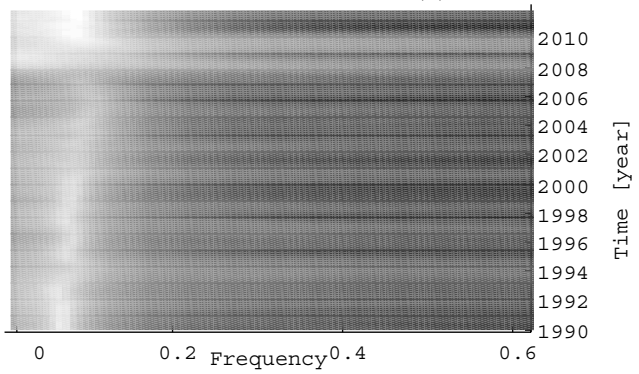

All presented figures identified two main exogenous shocks which affected not only short but also the long-term cycles in the economic activity of the Eurozone. The first, mortgage crisis began with collapse of price bubbles at the asset markets in the year 2007. The debt crisis followed two years after in the Eurozone. Both events were unique in its intensity in the last few decades. Obviously, the moving window approach (Fig. 10) identified only these two significant shocks and effects in long-term cyclical movements. Other previous changes in aggregate economic activity were obscured.

Figure 12: TFA via Wavelet analysis

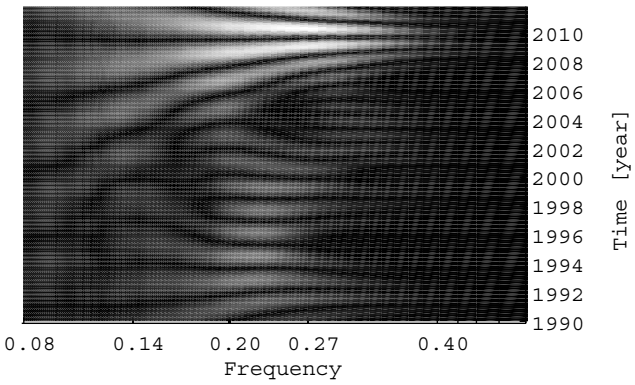

Figure 9 shows the contrast between the turbulent moving in low frequencies in the years 2007-2011 and cyclical movements during the nineties. The cyclical movements in the years 1997, 1998 and 1999 are sourced by low economic growth in Germany, Asian crisis and massive external imbalances at the capital accounts. The persistent effects of these imbalances were appeared at labor markets and investments (long-term cycles). Consumption changes were transmitted through decrease of credit money creation into the shorter waves (Kapounek, 2011). These two types of cyclical movements at different frequencies are evidently identified by wavelet analysis (Fig. 12).

Similar results, in comparison with wavelet analysis, provides time-frequency AR process, however there are not separated different types of cyclical movements between the years 2002 and 2006. As well, the mortgage and debt crisis consequences are slightly biased in the years 2008 and 2010.

CONCLUSION

In this paper we compared several methods for time-frequency analysis of given signal / time series. Chosen methods were time-frequency Fourier transform representation (periodogram), multiple window method using the slepian sequences, time-frequency varying AR process and the continuous wavelet transform. The methods have been first applied on the artificial data with the known structure, then we proceeded to the application on selected economic indicator. Note that the main limitation of the analysis is the short sample size of the analyzed data. At the final part of the paper, we tried to interpret the analysis results for the real data in the context of economic situation.

Estimation of time-frequency structure of simulated artificial data using all above discussed methods lead into similar results. In the case of wavelet analysis the identified spectrum makes impression to contain wider range of frequency components. A detailed look to the 3D representation of the chart would provide precise estimate of

the identified frequency components which is very close to the other simulated results and it will be presented during the conference.

To successfully apply the wavelet analysis, it is necessary to make a detailed analysis of mother wavelet choice. That will thus be the motivation for further research. In order to get the more realistic results of the time-frequency analysis of the economic indicators we therefore suggest to use two methods as minimum. We recommend to use the estimate of spectrogram (either periodogram, AR process based or multiwindow analysis) and to consult the results with the scalogram estimate obtained from the wavelet analysis.

In the case of multiwindow method the resultant time-frequency structure is estimated as the average over various used windows, so in this way we can cover area without any frequency by some average one and obtain spurious (or over-smoothed) result. Therefore we suggest for the work with real data to make a detailed look to the interconnection with field of the work (such in our case was economic situation) or to compare results with Fourier-transform based periodogram or wavelet analysis.

ACKNOWLEDGEMENT

The research described in the paper was supported by the Czech Science Foundation via grant n. P402/11/0570 with the title "Time-frequency approach for the Czech Republic business cycle dating" and by the project CZ.1.07/2.3.00/20.0007 WICOMT of the operational program Education for competitiveness. It was performed in the laboratories supported by the SIX project; the registration number CZ.1.05/2.1.00/03.0072, the operational program Research and Development for Innovation.

References

Adisson, P. (2002). *The illustrated wavelet transform handbook*. The Institute of Physics, London.

Eurostat (2011). Industry production index [online]. http://epp.eurostat.ec.europa.eu/statistics explained/index.php/Industrial p. [cit. 2012-02-02].

Frayer, G., Boashash, B. (1994). Multiple window spectrogram and time-frequencz distribution. *Proc. IEEE Int. Conf. Acoustic, Speach and Signal Processing-ICASSP'94* Vol. IV, pp. 293–296.

Gençay, R., Selçuk, F., Whitcher, B. (2002). *An introduction to wavelets and other filtering methods in finance and economics*. California: Academic Press, 359 pp., ISBN: 978-0-12-279670-8.

Green, W. H. (2002). *Econometric Analyses*. London: Prentice - Hall, 1076 pp. ISBN 0-13-7246659-5.

Guay, A., St-Amant, P. (2005). Do the Hodrick-Prescott and Baxter-King Filters Provide a Good Approximation of Business Cycles?. *Annales d'economie et de statistique, No. 77-2005*

Hallett, A. H., Richter, Ch. R. (2007). Time Varying Cyclical Analysis for Economies in Transition. *CASE Studies & Analyses* No. 334, Center for Social and Economic Research.

Hamilton, J. D. (1994). *Time Series Analysis*. Princeton University Press 790 pp., ISBN 0-691-04289-6

Jan, J. (2002). *Číslicová filtrace, analýza a restaurace signálu*. VUTIUM Brno, 427 pp., ISBN 80-214-2911-9.

Kapounek, S. (2011). Monetary Policy Implementation in the Eurozone - the Concept of Endogenous Money. *MENDELU Working Papers in Business and Economics* 2011-12.

Proakis, J. G., Rader, Ch. M, Ling, F. L., Nikias, Ch. L., Moonen, M., Proudler, J. K. (2002). *Algorithms for Statistical Signal Processing*. Prentice Hall, 567 pp., ISBN 0-13-062219-2.

Rua, A. (2010). Measuring comovement in the time-frequency space *Journal of Macroeconomics* Vol. 32, pp. 685–691.

Šebesta, V. V, Maršálek, R. (2011). A Cyclical Component Estimation using the AR Process and its Error an Application to Economic Time Series *Recent Research in Circuits, Systems, Communications & Computers*, Puerto De La Cruz, Spain, pp. 94-100

Xu, A., Haykin, S., Racine, R. J. (1999). Multiple Window Time-Frequency Distribution and Coherence of EEG Using Slepian Sequences and Hermite Function *IEEE Transactions of Biomedical Engineering* Vol. 46, No. 7, pp.861–866

Xu, Z., Bi, G., Li, X. (1999). On application of time-frequency analysis to communication signal detection and estimation *Proceedings of Control and Automation (ICCA), 2011 9th IEEE International Conference on* pp. 1044–1048

Yogo, M., (2008). Measuring business cycle. A wavelet analysis of economic time series. *Economics Letters*, Vol. 100, No. 2, pp. 208–212.

AUTHOR BIOGRAPHIES

JIŘÍ BLUMENSTEIN received his Master degree in electrical engineering from the Brno University of Technology in 2009. At present, he is a PhD student at the Department of Radio Electronics, Brno University of Technology. xblume00@phd.feec.vutbr.cz

JITKA POMĚNKOVÁ received the Ph.D. degree in applied mathematics at Ostrava University in 2005, the habilitation degree in Econometric and operational research at Mendelu in Brno in 2010. From 2011 she is the Senior researcher at Department of Radio electronics, Brno University of Technology. pomenkaj@feec.vutbr.cz.

ROMAN MARŠÁLEK received his Master degree in control and measurements in 1999 from the Brno University of Technology and the Ph.D. in electronics and signal processing from Universite de Marne la Vallee, France in 2003. marsaler@feec.vutbr.cz.

Simulation in Industry, Business and Services

GENERATION OF EPC BASED SIMULATION MODELS

Prof. Dr. Christian Müller
Department of Management and Business Computing
Technical University of Applied Sciences Wildau
Bahnhofstrasse
D-15745 Wildau, Germany
christian.mueller@th-wildau.de

ABSTRACT

Bflow is an Eclipse plugin for modeling business processes in event driven process chain (EPC) notation. A code generator and its integration into Bflow to build a DesmoJ simulation model is presented. Possibilities to extend the generated models are also presented.

INTRODUCTION

The analysis and simulation of business processes is an important way of process optimization [Oberweis (1999), Böhnlein(2004), Böhnlein(2010)]. In the area of business process modeling, Business Process Modeling Notation (BPMN) [Object Management Group (2011), Freud(2010)] and Event-Driven Process Chain (EPC) [Rump(1999), Scheer(2000)] are the most popular standard notations. On the market, there are a lot of business process modeling tools that support the BPMN and EPC Notation. Some of these tools have an extension for business process simulation [ARIS Business Simulator(2012), IYOPRO(2012), Kloos(2010)]. For these approaches, the business process model is extended with some simulation related data, for instance, data about process times and decision probabilities. These simple models assume that the probability distribution for a decision is independent. This assumption is not realistic because a lot of decisions depend on some other system-properties and some earlier decisions.

Another way to build simulation models is based on universal simulation frameworks, simulation languages. or GUI simulation tools [Kennington(2012), OR/MS Today(2012)]. With these tools, it is possible to construct simulation models with arbitrary level of detail. On the other hand, a normal business person is not able to write and read these models.

In this paper, we present a approach, where the business process is formulated in EPC notation with some extensions about simulation relevant data. For EPC modeling Bflow [Kern et. al.(2010) Nüttgens(2011)], an Eclipse [Eclipse(2012)] plugin, is used. From this EPC model we generate a DesmoJ [DesmoJ(2012), Page(2005), Müller(2012)] simulation model. A DesmoJ model contains a set of Java classes that use the DesmoJ simulation framework. Based on the Java programing language, the generated models can be extended in all directions. The generation mechanism is designed in such a way that the modeling extensions are not lost by regeneration.

In this approach, the main part of model building can be done by business persons. Only for model extensions, executing and analyzing simulation, experts are necessary.

The base technology of this approach, Bflow and DesmoJ, are both open source projects. Bflow runs under Eclipse License [Eclipse License(2004)] and DesmoJ under Apache License [Apache License(2004)]. It is planed to publish the devoloped code generator and model validator also on an open source licence.

CONCEPT

All parts of this EPC Simulator are running in an Eclipse IDE. These are:

- Bflow as EPC modeling tool
- the model validator
- the code generator and
- the generated DesmoJ simulation model

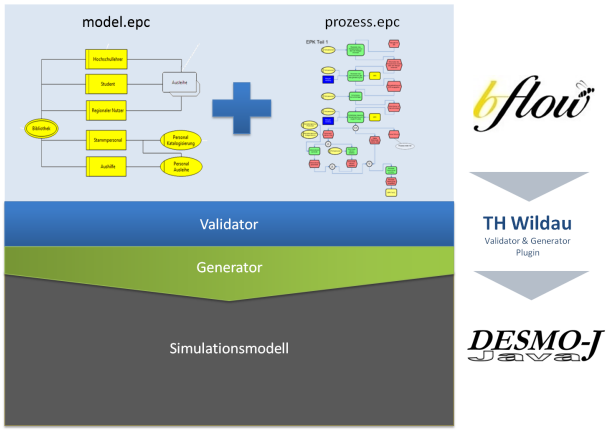

Figure 1:

Bflow is an Eclipse plugin that offers integration of external applications into Bflow. The model validator and code generator are developed as such kinds of

Proceedings 26th European Conference on Modelling and Simulation ©ECMS Klaus G. Troitzsch, Michael Möhring, Ulf Lotzmann (Editors)
ISBN: 978-0-9564944-4-3 / ISBN: 978-0-9564944-5-0 (CD)

integrated programs. The code generator writes the generated code directly into the source code areas of its workspace. The simulation model can be started directly from the Eclipse IDE.

In some circumstances it makes sense to extend the generated code by some manual implemented extensions. The code generator supports some features that ensure that no extensions are lost by code regeneration. This mechanism is described in section “model extensions”.

The simulation process model stored in Bflow contains two type of documents. One is a model file and the others are process files. The common simulation attributes with information about the master and slave entities are stored in the model file. The process files contain classical process information and some extensions about distributions of processing times and decision probabilities. The simulation process model is described in the next section.

All parts of the project can be found in [Müller(2012)]. It embraces the specification of simulation process model, the model validator, the code generator and a toolbox (SimTools.jar) with some DesmoJ extensions to simplify the generated code.

SIMULATION PROCESS MODEL

In terms of simulation data structures, this simulation process model is an application of a master slave waiting queue. [Page(2005) p.289]

There are master and slave entities. The masters are walking as active entities through the processes described by EPC. For some tasks, they require some resources, represented by slaves. All free slaves are waiting in a master slave waiting queue for a new task. When a master requires a slave, it looks in the waiting queue for appropriate slaves.

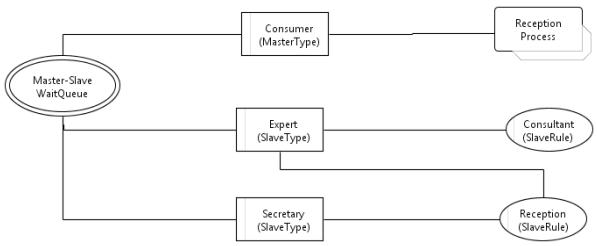

Figure 2: Model.epc

When no appropriate slaves are present, it waits for one. The master entities are grouped in different master types with special properties. For each master type, we have a master generator that produces master entities. The interarrival times are given by a random process. The distribution formulas of these processes can be different for different schedules of simulation time. Each master type has an unique associated EPC, that must be processed by the masters of this type. In a business process, the master types may represent customers with different visit frequency and different service requirements.

The slave entities are grouped in different slave types too. All slaves of a type have the same working time schedule and the same qualifications, represented as slave rules. When a master asks for a slave, it asks for slaves with special qualifications that are active in its working time schedule. When a slave has finished its job, it walks directly back to the waiting queue.

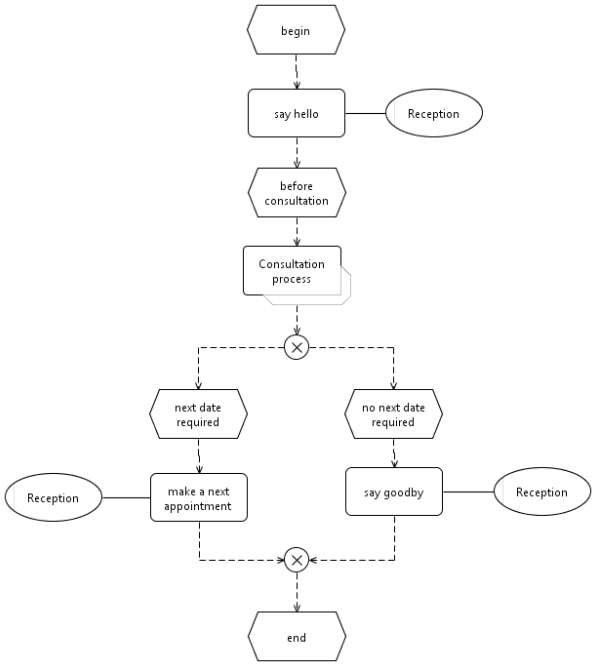

Figure 3: Reception.epc

In the given example (Figure 2), each customer starts in a reception process (Figure 3). In this process it needs a resource with qualification “Reception”. This can be satisfied from both slave types. Additionally, there is a process interface with a process link to a ”Consultation Process” (Figure 4). When the “Consultation Process” is finished, the process is continued according to the process interface in “Reception Process”. Each function has an individual random distribution of processing time.

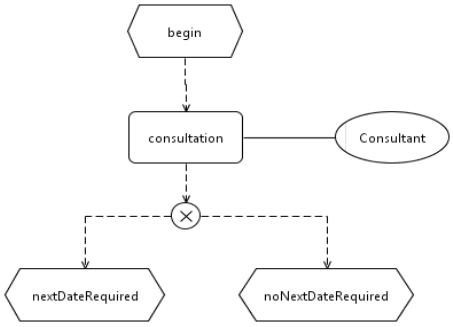

Figure 4: Consulting.epc

Both example processes (Figure 3 and 4) contain a XOR decision. This decisions can be driven by probabilities or by conditions. They are stored as additional data in the event-elements following the decision-element. Each master entity, that flows throw the process, stores the names of each passed event. One type of condition asks a master if it has passed a specified event. This technique is used in "Reception Process" to decide when a next date is required.

Besides XOR decisions, the EPC Simulator supports also OR decisions and AND splits. In these cases we get parallel working process lines. For each process line, a clone of the master entity is build. At the end of the parallel process lines, the clones are synchronized with its original master entity

SIMULATION CODE MODEL

The code generator transforms the simulation process model into a DesmoJ Simulation model. A DesmoJ simulation model is a Java Program which uses the DesmoJ Framework. The components of this framework can be divided in black- and white-box components. The black-box components are data collectors, statistical distributions, data structures (queues, etc) and visualization tools. They can used without modifications. On the other hand the white-box components are interfaces and abstract classes. These classes must be completed. DesmoJ supports an event orientated and a process orientated modeling style. For the process orientated style, processes, process generators and a simulation model must be implemented. The processes inherit from a class "SimProcess" and must implement a method "lifecycle". This method describe the behavior of its process entity. A process generator is a special process, that generates other processes. Between the generation of two process entities, it waits a interarrival time, that is normally given by a random distribution. The simulation model is an executable class which initializes the black-box components and starts some processes.

The code generator builds all necessary classes from a simulation process model.

The generated classes embrace

- for each epc in the model an Epc_ and Logic_ class. The Epc_ class inherit from the Logic_ class and contains all methods that can be extended by the user. The Logic_ class contains a life cycle method that describes the process logic of the EPC in a procedural formulation.
- a class for each master type. Each process of this type uses the life cycle of the associated EPC.
- a class for each slave type. The slaves wait in a master-slave-wait queue for a master that needs their service. When a service has finished, they walk back into the waiting queue. Each type of slave has qualifications described by one ore more slave rules.
- a class for each slave rule and
- an executable class for the simulation model. This class starts all slaves and lets them go into the waiting queue. Additionally it starts a process generator for each master type. The generator produces a sequence of master processes with inter arrival times described in the simulation model above.

MODEL EXTENSIONS

Not all situations that we are interested in for simulation can be described in a formalized way by an EPC. The generated classes offer a possibility for the controlled extension by the user. The generated classes contain markers for individual code extension. The idea is shown in an excerpt of the class Epc_Consultation.

```
@Generated(value = { "RememberCode", "yes" })
public class Epc_Consultation extends
                              Logic_Consultation{

   //@@_begin of id="_id_26_Function_consultation"
                     generated at 06.02.12 09:29
   /**
    * Type:      epc:Function
    * Name:      consultation
    * Resources: Consultant,
    * Id:        _id_26_Function_consultation
    * EpcFile:
       /Generator_2508/Artikel/Consultation.epc
    */
   protected void _id_26_Function_consultation(
                  EpcProcess proc,
                  List<EpcResource> resources){

       //@@_begin of individual code
       doSomeAdditionalThings(proc);
       //@@_end of individual code
   }
   //@@_end of id="_id_26_Function_consultation"
}
```

When a master entity arrives at a function element in the EPC, the simulator provides the necessary slaves needed to execute the function. In this excerpt the consultation function depends on the master entity (proc) and the provided slave entities (resources). This function describes what the master and slave entities are doing together and not how long they are working together. Usually, this function contains no code, but it can be extended by some individual code.

It is common practice that during the modeling process, simulation code is generated several times and also modified by the user. To account for this, the code generator reads the old version of each class and stores the extensions in memory before generating the new version. At code generation the generated code is extended by the stored extensions. This mechanism can be switched off by the "Generated" annotation of the class Epc_Consultation.

The same mechanism is offered for condition methods of events when they are marked in the "Simulation

Process Model" with a "condition : generated" attribute.

With this approach all properties of the Java language and the DesmoJ framework can be used. It is expected that the extensions contain only a few lines of code to manage additional information.

TRANSFORMATION OF EPC PROCESS LOGIC INTO A PROCEDURALE FORMULATION

To transform a simulation process model into a DesmoJ simulation model the generator builds logic classes from Epc process diagrams. Therefore, it transforms each Epc process diagram into a procedural formulation. The transformation algorithmus works in 2 phases. In the first (preprocessing) phase it is determined whether an Epc node is a

- split connector node (isSplit()) or a
- join connector node (isJoin()) or a
- end node (isEnd()) in the Epc process diagram.

The split connector nodes have normaly multiple and the other nodes only one direct successor. The set of direct successors of a split connector node (elementsOfsplit()) and the single succssor of the other nodes (successor()) are also determined (see Figure 5).

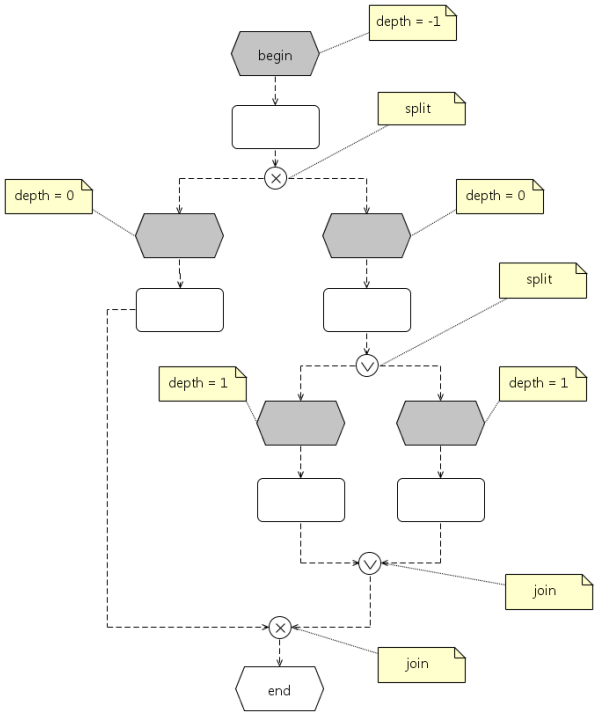

Figure 5:

In the second phase the procedural code of the lifecycle methods of logic classes is generated. Therefor, the begin node and the nodes in the elementsOfSplit() sets (gray nodes in figure 5) are traversed in a fifo order. All nodes of the same elementsOfSplit() set have the same depth and their code is generated together.

```
public void generatorPhase2(EpcNode begin){
   int depth = -1;
   stack.clear();
   stack.push(begin);
   begin.setDepth(depth);
   main: while(! stack.empty()){
      EpcNode a = stack.peek();
      // open if-clause of a
      a.generateCodeIfBegin();
      // run a code sequence
      while(! a.isEnd()){
         if(a.isSplit()){
            depth = stack.peek().getDepth()+1;
            for(EpcNode b: a.elementsOfSplit()){
               stack.push(b);
               b.setDepth(depth);
            }
            continue main;
         }else if(a.isJoin()){
            EpcNode c = stack.pop();
            int d = c.getDepth();
            // close if-clause of c
            c.generateCodeIfEnd();
            if( stack.peek().getDepth() == d)
               continue main;
         }else{
            a.generateCodeFunction();
         }
         a = a.successor();
      }
   }
}
```

This basic algorithm can be extended for processing epc's with loops and multiple end nodes.

ACKNOWLEDGMENTS

My special thanks go to Prof. Dr. Ralf Laue from FH Zwickau, Germany. He developed a Bflow extension for additional attributes. In 2011 we had an intensive discussion about Bflow and useful extensions for storing the simulation process model into Bflow. Only on the basis of his participation, the integration of the code generator into Bflow was possible.

This work was part of a student project at TH Wildau in 2011. My thanks go to B. Schneider, Chr. Thiemich and F. Kropp for writing a specification on the simulation process model, and to M. Till for developing a model validator based on this specification. The team of Chr. Krüger, M. Kannengiesser and N. Herm developed a method to transform the logic of EPC diagrams into the procedural formulation used by the code generator. This method works successfully and is a kernel functionality of the code generator.

REFERENCES

Apache License: Apache License, Version 2.0, 2004
http://www.apache.org/licenses/LICENSE-2.0.html

ARIS Business Simulator: 2012
http://www.softwareag.com/de/products/aris_platform/aris_design/business_simulator/capabilities/default.asp

Böhnlein, C: Simulation in der Betriebswirtschaft 2004 eds: Mertins, K; Rabe,M Experience from the Future – New Methods and Applications in Simulation for

Production and Logistics, Frauenhofer IRB p 1-22

Böhnlein, C: Simulationsunterstützte Spezifikation und Analyse von Geschäftsmodellen und Geschäftsprozessen 2010 eds: Claus, T; Herrmann, F; Simulation als betriebliche Entscheidungshilfe 14.ASIM Fachtagung p.83-104

DesmoJ: A Framework for Discrete-Event Modelling and Simulation 2012 http://desmoj.sourceforge.net/home.html

Eclipse: Eclipse Homepage 2012 http://www.eclipse.org/

Eclipse License: Eclipse Public License - Version 1.0, 2004 http://www.eclipse.org/legal/epl-v10.html

IYOPRO: IYOPRO Premium – Geschäftsmodelle simulieren und optimieren 2012 http://www.iyopro.de/pages/de/produktinformationen/produktuebersicht.html

Freud, J; Rücker, B: BPMN 2.0; 2010 Hanser

Heiko Kern, Stefan Kühne, Ralf Laue, Markus Nüttgens, Frank J Rump, Arian Storch: bflow* Toolbox - an Open-Source Business Process Modelling Tool 2010, Proc. of BPM Demonstration Track 2010, Business Process Management Conference 2010 (BPM'10), Hoboken, USA

Kloos, O; Nissen, V: Vom Prozess zur Simulation – Ein Transformationmodell-Ansatz 2010 eds: Claus, T; Herrmann, F; Simulation als betriebliche Entscheidungshilfe 14.ASIM Fachtagung p.105-119

Kennington, A: Simulation Software Development Frameworks 2012 , http://www.topology.org/soft/sim.html

Müller, C: Ein Ansatz zur Visualisierung von Desmo-J Simulationen 2011 http://www.th-wildau.de/cmueller/Desmo-J/Visualization2d/Visualisierung_DesmoJ_Simulationen.pdf

Müller, C: EPC Simulation Project Homepage 2012 http://www.th-wildau.de/cmueller/SimulationERP/

Nüttgens, M: Bflow Toolbox 2011 http://www.wiso.uni-hamburg.de/professuren/winfo-prof-nuettgens/forschung/projekte/bflow-toolbox/ and http://sourceforge.net/projects/bflowtoolbox/

Oberweis, A; Lenz, K; Gentner, C: Simulation betrieblicher Abläufe 1999 eds: wisu das wirtschaftsstudium 28(1999)02 p 216-223, 245

Object Management Group: Business Process Modeling Notation (BPMN) Version 2.0; 2011; http://www.omg.org/spec/BPMN/2.0/

OR/MS Today: Simulation Software Survey 2012, http://lionhrtpub.com/orms/surveys/Simulation/Simulation.html

Page, B et. al.: The Java Simulation Handbook, Shaker 2005

Rump FJ: Geschäftsprozessmanagement auf der Basis ereignisgesteuerter Prozessketten - Formalisierung, Analyse und Ausführung von EPKs. 1999 Teubner Verlag.

Scheer, AW: ARIS Business Process Modelling. 2000 Springer Verlag.

AUTHORS BIOGRAPHIES

CHRISTIAN MÜLLER has studied mathematics at Free University Berlin. He obtained his PhD in 1989 about network flows with side constraints. From 1990 until 1992 he worked for Schering AG and from 1992 until 1994 for Berlin Public Transport (BVG) in the area of timetable and service schedule optimization. In 1994 he got his professorship for IT Services at Technical University of Applied Sciences Wildau, Germany. His research topics are conception of information systems plus mathematical optimization and simulation of business processes.

His email address is: christian.mueller@th-wildau.de and his web page is http://www.th-wildau.de/cmueller/ .

THE TEMPLATE MODEL APPROACH FOR PLC SIMULATION IN AN AUTOMOTIVE INDUSTRY

Minsuk Ko, Daesoon Chang, Ginam Wang, Sang C. Park
Department of Industrial Engineering
University of Ajou
Suwon, Korea
sebastianminsuk@gmail.com

KEYWORDS
Control Simulation, PLC Program, Virtual model, Simulation.

ABSTRACT

Product systems are quickly and frequently changed because product life cycle is continuously reduced and adopting new product is steadily fast. Thus, various studies are progressed using PLC simulation which is one of control level simulation. The research that is concerning simulation of control verification for shortening the commissioning which has a lot of trial and error is in progress. Also, simulation of control verification has strength that it can catch the errors in advance. However, a virtual device in simulation needs both physical and logical model for representation of control information. For this reason, excessive time and energy is put into constructing virtual models. So, in this paper, we proposed the template model approach for the PLC simulation to cope with this problem. The proposed template model approach provides an efficient construction method for a virtual model based on control information, extracted from the test run procedure of the PLC program. We can minimize the set up time of the PLC simulation environment, as well as cut process time down using our suggestion.

1. INTRODUCTION

As product life cycles are reduced in the continuously changing marketplace, modern manufacturing systems must have sufficient responsiveness to adopt their behaviors efficiently to a wide range of circumstances. To respond to these demands, including high productivity and production flexibility, the use of the concept of a virtual manufacturing (VM) has been widely accepted. VM is a key concept that summarizes computerized manufacturing activities dealing with models and simulations instead of objects and their operations in the real world (B.K. Choi 2000). VM was applied to the small size (cell) manufacturing system in the past. However, recently, with the development of computer technology, it is possible to apply VM technology to the huge size (line, factory) manufacturing system (Hibnio 2006). As part of this revolution, offline programming for robots (Orady 1998) and verification of the control program (David 1998; H. T. Park 2010; S. C. Park 2008) with virtual models have emerged in an automotive industry.

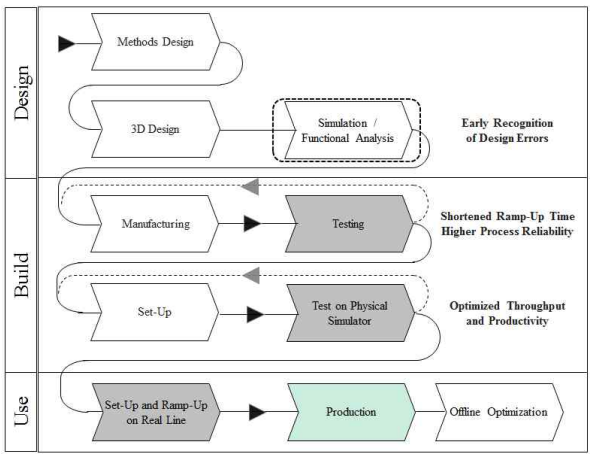

Figure 1. Manufacturing process in production system

Figure 1 shows a manufacturing process that applies to virtual manufacturing technology (VMT). Since early recognition of design errors could be found at the design phase, and design (mechanical & electronic) verification could be done at the build phase, applying VMT to manufacturing process could reduce time for feedback the verified information from the use phase to the design phase. Especially, a simulation based on the VMT has been considered an essential tool in the design and analysis of complex system that cannot be easily described by analytical or mathematical models (Al-Ahmari 1999; Klingstam 1999). Since the implementation of a manufacturing line requires heavy investment, many companies applied VM simulation to the production system design to ensure that a highly automated manufacturing system will successfully achieve the intended benefits.

Automotive manufacturers continuously strive to improve their production system, as well as their products, to remain competitive in this continuously changing market place. Automotive manufacturing is complex task with several automated functions. Machined or purchased components are assembled on sub-systems, and the sub-assemblies are assembled during the final assembly system. Therefore, many engineers in automotive industry want to create much more realistic simulation models, which can forecast not only the production capability of the system but also the logical verification, physical validity, and efficiency of

Proceedings 26th European Conference on Modelling and Simulation ©ECMS Klaus G. Troitzsch, Michael Möhring, Ulf Lotzmann (Editors)
ISBN: 978-0-9564944-4-3 / ISBN: 978-0-9564944-5-0 (CD)

co-working machines.

This demand has resulted in the concept of PLC simulation. PLC simulation can be described as a model executing digital manufacturing processes within a computer simulation. To verify the mechanical and electrical designs of the production system, it provides a realistic effect as a test run for the production system using both the 3D graphic model that appear to the same as real shop floor and the logical model that drives connected a PLC in a real factory.

Considerable work has been undertaken in the field of PLC simulation and validation of the production system. C.M Park (2009) proposed that verifies the controller logic process for the automobile industry via simulation using a state-based model that creates a virtual car body assembly line. Xusong (2006) discussed the concept, the modeling method of building an AS/RS (automatic storage and retrieval system) real time simulation and control integrated system based on the AS/RS control system structure. He proposed key features and the more significant methods used in building simulation models by using virtual reality. S.C Park (2008) proposed the architecture of a PLC program environment that enables a visual verification of PLC program integrated a PLC program with corresponding plant model. The proposed architecture provides a theoretical construction method for a plant model based on the DEVS (Discrete Event Systems Specifications) formalism for the PLC simulation. H.T Park (2010) reports an automated procedure for constructing a plant model for a simple manufacturing cell. Although those researches contributed to construct a theoretical architecture for a control level simulation environment in automobile industry, they remain limited about efficient way to construct an adjusted simulation model. The objective of this paper is to develop an efficient method for constructing models for PLC simulation in an automotive manufacturing system. The proposed model construct method employs a template model consisting of the physical model, and the logical model. The overall structure of the paper is as follow. Section 2 illustrates the architecture of the proposed template based modeling methodology, while Section 3 describes an efficient construction methodology for a template, which can be synchronized with a control program. Section 4 shows an example and illustrations. Finally, concluding remarks are given in Section 5.

2. APPROACH FOR CONTROL LEVEL SIMULATION

Figure 2 shows a conventional implementation procedure of a production system. After the abstract level simulation is performed to verify or optimize the designed process, the mechanical and electrical design phases are performed sequentially. Mechanical design makes layout and physical models (2D, 3D models) that are used for manufacturing devices. It has to be verified with mechanical simulators to inspect motion, kinematic, and assembly errors. On the other hand, we can get control programs as well as logical models through electrical design. To get control programs through the electrical design, usually, electrical engineers manually write control programs by referring to the rough control logic of abstract level simulators. Since control programming is a very tedious and error-prone job, it is essential to verify the control programs offline to reduce the stabilization time of a production system. (Chang Mok Park 2009; David 1998; S.C Park 2008; H.T Park 2010).

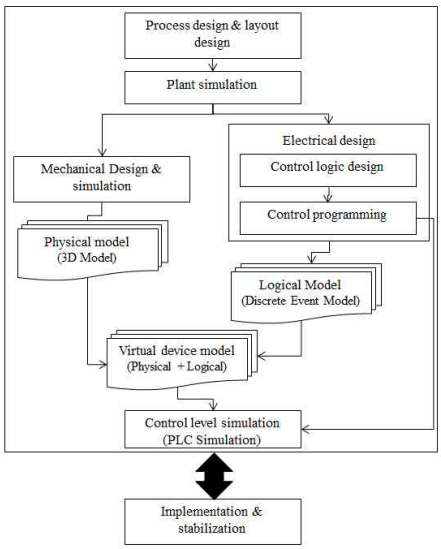

Figure 2. A process for constructing the control level simulation

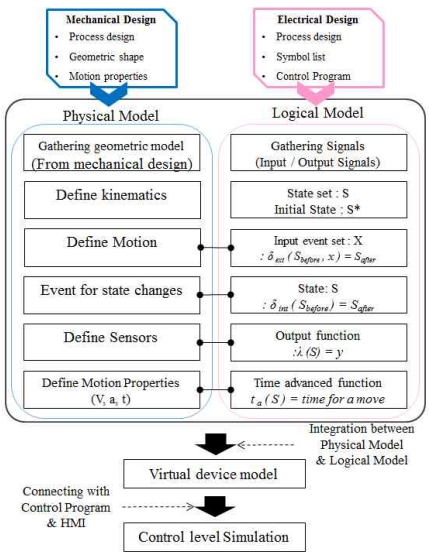

Figure 3. A process for constructing the control level simulation model

Since PLC programs only contain the control information, without device models, it is necessary to build a corresponding virtual model to perform simulation, as shown in Figure 2. However, constructing a virtual device model using for the physical model and the logical model alike requires an excessive amount of

time and effort, because both models are not suitable for the simulation to use immediately. Sometimes, the virtual model construction requires much more time than PLC programming. This serves as the motivation for exploring the possibility of finding a template based modeling methodology for building a virtual model from given both models.

To construct the PLC simulation environment, it is important to understand basic procedure for implementing components used to consist of the PLC simulation. Figure 3 shows general procedure for constructing virtual model in an automotive industry. There are three models, a physical model, a logical model, and a virtual model. A logical model represents the behavioral aspects of a device, while a physical model contains the mechanical aspects of a device. The logical model of a virtual device acts as an interface communicating with PLC programs and determines the behavior of the physical models. Once both physical and logical models are obtained, it becomes possible to make the virtual model, which is a digital model imitating the physical and logical aspects of a real manufacturing device. Because the virtual device model contains the logical core expressed by DEVS formalism and the physical shell shows corresponding motions reflecting the change of states of the logical core during the simulation, it represents such a manufacturing device in the real production system.

Table 1. Four steps for verifying control program based on digital manufacturing technology

#	Topic	Input	Output
1	Control simulation environment	• Symbol list • PLC Program • Process Design	• Logical model (DEVS Model with control signals)
		• 3D Model • Layout	• Physical model (Geometric + Motion + Layout)
		• Logical model • Physical model	• Virtual model (Logical model + Physical model)
2	Manual Mode Simulation	• HMI • Virtual model	• Error report ▪ Device operation error ▪ Error processing
3	Automatic Mode Simulation	• HMI • Robot Program • Product code	• Error report ▪ Entire process ▪ Error processing ▪ Interaction between facilities
4	Control simulation result review	• Error report • Time chart of control signals	• Verified PLC program

To apply the virtual device model to the PLC simulation connected with field environment, we have to proceed sequentially four topics as shown in Table.1. After constructing the simulation environment using virtual models and layout, users have to proceed 'Manual mode simulation' and 'Automatic mode simulation'. Each of both simulation modes has different purpose as shown in Table.1. The input factors of the both modes, HMI means a user interface for the local control console to perform control using a PC. After doing the simulation, users could obtain both the verified control program and the report containing the time chart of the control signals.

In this PLC simulation environment, the behavior of a virtual device model should be the same as the device that of actual system to achieve the control level verification. However, users have to invest so much the time and effort of building the virtual device model suitable for the control level environment, as shown in Figure 4. It is necessary to add virtual sensors and correct motions to achieve the intended task for each task to the physical model when a process design change occurs. Furthermore, the most time-consuming task in developing the logical model is analyzing device behaviors based on the process information, because the process design information contains only the process sequence of the production system not control level information. Therefore, to define the logical model of a device as a DEVS model, the user has to analyze the device behavior specifically according to the signals in control program. Since the logical model has high modeling DOF (Degree Of Freedom), users have to consider how to determine the set of DEVS components to represent device behaviors.

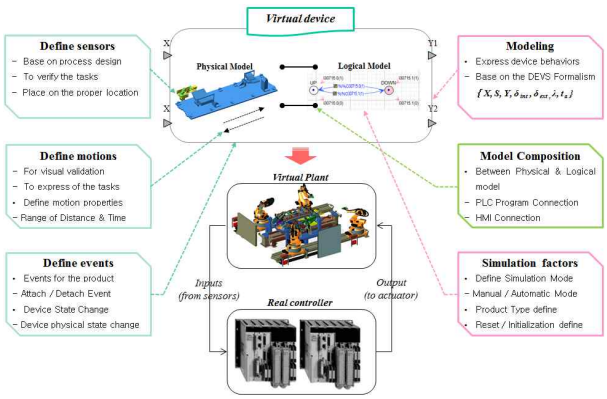

Figure 4. Components of a virtual device model

Once the both model are determined suitable for the simulation, then they have to be connected with one another. The output of this step is usually the virtual device model which becomes a practical guideline for the simulation. Obviously, manufacturer can benefit greatly from PLC simulation using the virtual device model, but there are still many difficulties complicating the full utilization of the virtual device model. One of the main obstacles to build a logical model comes from the understanding device behaviors which are set of tasks that are assigned to the device. Since a logical model interacts with a virtual factory may consist of hundreds of machines and product, it is difficult to find a modeling error of the designed logical model, and physical model during the simulation. Sometimes, finding modeling errors of the virtual device model becomes a bottleneck in the simulation time delay. Therefore, it is necessary to verify both logical model and physical model before the simulation.

We propose a template based modeling approach of the PLC simulation to cope with the problem. The proposed template model has a role for the practical guideline of the virtual device model, since it has

containing process knowledge information in legacy simulation results. In addition that it is possible to verify the validity of the task of the virtual device model and sensor conditions. Therefore, the proposed method can reduce the modeling time and errors of the simulation model instead of reducing the modeling DOF.

3. TEMPLATE MODEL OF THE VIRTUAL DEVICE

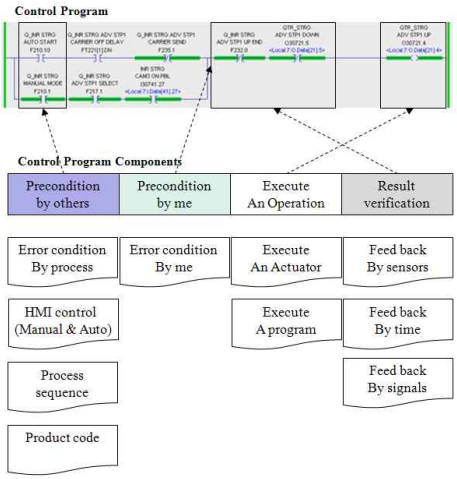

Figure 5. Control program components

To construct a template model of the virtual device, we extracted five major control components from the control program, as shown in Figure 5. PLC program starts with preconditions which are occurred by the others. To proceed this condition, it is necessary to satisfy error conditions caused by the other device, process sequence, HMI signals, and product code. After checking the *precondition by others*, the PLC program checks the self-condition of the device. These preconditions have a role for checking whether the device is located at the proper position to execute the task or not. Once the conditions satisfied, then the device executes an aimed task. The output of the task is usually verified with sensor, timer, or a signal which indicating the task is complete. Since the proposed template model contains these components in the logical model, and physical model, the modeling errors can be avoided. Since signals in the *precondition by others* are occurred by other devices or the controlling process, it is necessary to build a HMI model to send combined signals to the virtual device. If this information is predefined, users can instinctively understand about the controlled device in the control level.

Figure 6 shows a simple template model using a sample of an AGV (Automatic Guided Vehicle) with two tasks, T1 (movement from p1 to p2) and T2 (movement from p2 to p1). As the two tasks should triggered by external events, terms here as *E_X1* and *E_X2*. When the user select this template model, it is possible to instantiate the logical model automatically. And, the physical model is instantiated from the predefined physical model, which has two motions *M1*, *M2*, and two position sensors *S1*, *S2*. And functional relationships will be automatically defined between DEVS components of the logical model and physical activities in the physical model, as shown in Figure 3. Using this template, users can intuitively understand both the logical and the physical aspect of the device. The logical model (DEVS atomic model) of the virtual device, corresponding to the AGV, can be described as follows:

$$M = < X, S, Y, \delta_{int}, \delta_{ext}, \lambda, t_a >$$
$$X:\{ X1, X2 \};$$
$$S:\{ S\_P1, M\_P1\_P1, S\_P2, M\_P2\_P1\}$$
$$Y:\{ Y1, Y2\};$$
$$\delta_{int}(M\_P1\_P2) = S\_P2$$
$$\delta_{int}(M\_P2\_P1) = S\_P1$$
$$\delta_{ext}(S\_P1, X1) = M\_P1\_P2$$
$$\delta_{ext}(S\_P2, X2) = M\_P2\_P1$$
$$\lambda(M\_P1\_P2) = Y1;\ \lambda(M\_P2\_P1) = Y2$$
$$t_a(M\_P1\_P2) = T1\ ;\ t_a(M\_P2\_P1) = T2$$

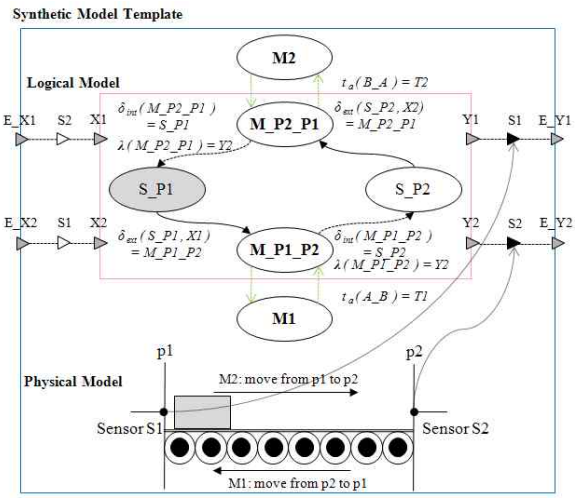

Figure 6. A template model of the virtual device for PLC simulation

This simple template model contained the major components of the PLC program, as mentioned above. Since *S1*, *S2* have a role for sensing the AGV position, the preconditions of the AGV can be verified. And the time to travel between *P1* and *P2* can be used for verifying the AGV motion verification. If the time is not satisfied with the purpose of the motion, the position of sensors or motion properties has to be readjusted. Finally, the external functions have to be verified with the sensors before sending an external signal. To export *E_Y1*, which verifies the task is finishing, it is necessary to satisfy the *S1* and *Y1* simultaneously. When the simulation has to be initialized by the process reset signal, physical model moves to the *P1* position and the state of the logical model set up with initial state *S_P1*.

4. EXAMPLE & ILLUSTRATIONS

As depicted above, we will describe an applying method to the Side Inner Line (called SIL) and Side Quarter Line (called SQL), which have a role for transporting a side inner (side quarter) panel from the AS/RS to the side assembly line, in this chapter. The SIL (SQL) line is typical example of the flow shop. Various types of side sub panels are transported by the handling robot, and conveyor system.

The detailed process of transporting a panel from the pallet in the AS/RS to the side assembly line will be explained with the help of a work cell shown in Figure 7. The work cell consists of three handling robots {ROBOT_1, ROBOT_2, and ROBOT_3}, two conveyor system {CONVEYER_1, CONVEYER_2}, and two idle jigs {JIG_1, JIG_2}. A scenario for this work cell is as follow: If a panel arrives at 'PLT_1', then 'ROBOT_1' moves the panel to 'CONVEY_1'. On the other hand, if a panel arrives at 'PLT_2', then 'ROBOT_2' moves the panel to either 'JIG1' or 'JIG2' by the car type. And 'ROBOT_3' moves the panel from the 'JIG_1 (JIG_2)' to the 'CONVEYOR_2'. When the panel arrived at the conveyor, it moves the carrier which is loading the panel from the front station 'LIFTER_FRT' to the rear station 'LIFTER_RR'. If the carrier arrives at 'LIFTER_RR', it will be removed by the handling robot of the side assembly line, which is the next step production line of the SIL (SQL) line.

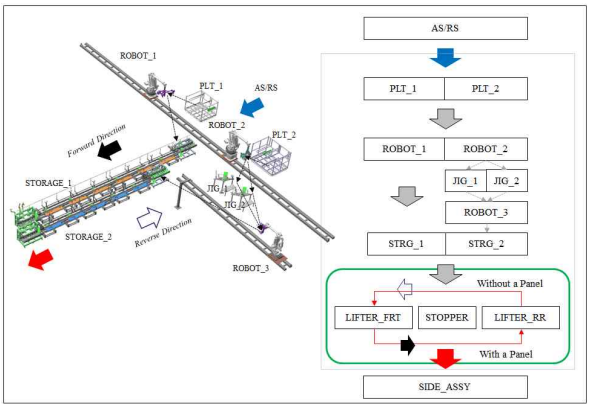

Figure 7. A process flow of Side Quarter and Side Inner line

The proposed template methodology of a virtual device model will be explained with the help of the conveyor system sub-system of the SIL (SQL). It is necessary to identify the behaviors and the tasks assigned to the conveyor to define sub-devices assembled to the conveyor. Although there are various models of the conveyor could be defined by the virtual model, we extracted simple templates for the virtual model, which can explain the behaviors of the conveyor. Figure 8 shows mechanical design of the conveyor system, which consists of ten stoppers and two lifters. To proceed the carrier, the conveyer has used the motor, which continuously running the belt, and stoppers to prevent the carrier to proceed. To describe this system realistically, we have to construct a virtual device model of the motor moving the carrier on the belt. However, it is difficult to describe behaviors of the motor as the virtual device model, since it has continuous behaviors, running continuously until receiving the stop signal. To remedy this problem, we analyzed both mechanical design and PLC program of the conveyor system. Stoppers are attached to the conveyor (top layer: forward direction, bottom layer: reverse direction) to move the carrier circularly, and the distance between stoppers is uniformly defined as *d_stopper*, as shown in Figure 8. And control logic for the conveyor to move the carrier using stoppers could be defined as follow;

IF(STP(N+1) Has NO CARRIER && STP(N+1) is UP){ STP(N) go DOWN; break;}
ELSE IF (STP(N+1) Has a CARRIER && STP(N) is DAWN){ STP(N) go UP; break;}

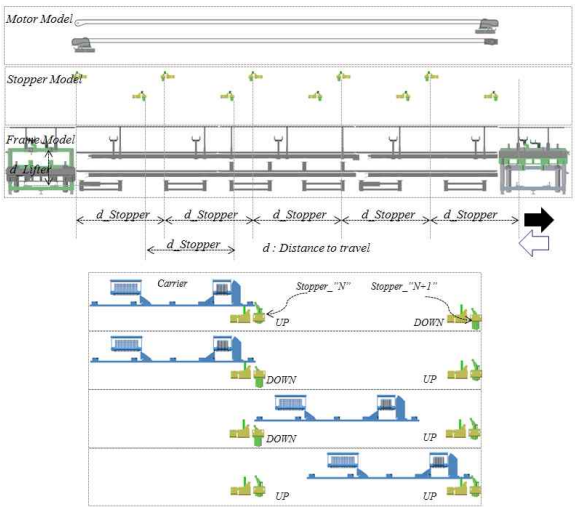

Figure 8. Mechanical design of an automated conveyor

The DEVS atomic model of the virtual device, corresponding to the stopper, can be described as follow;

X:{ STP_UP, STP_DOWN};
S:{UP,MOVE_FORWARD, DOWN, MOVE_REVERSE}
Y:{ STP_UP_DONE, STP_DOWN_DONE};
δ_{int} *(MOVE_FORWARD) = DOWN*
δ_{int} *(MOVE_REVERSE) = UP*
δ_{ext} *(UP, STP_UP) = MOVE_FORWARD*
δ_{ext} *(DOWN, STP_DOWN) = MOVE_REVERSE*
λ*(MOVE_FORWARD) = STP_DOWN_DONE*
λ*(MOVE_REVERSE) = STP_UP_DONE*
t_a*(MOVE_FORWARD)=TIME_TO_TRABEL_FWD*
t_a*(MOVE_REVERSE)=TIME_TO_TRABEL_BWD*

Figure 9 shows a virtual model template of the stopper. To define the physical model of the stopper, which describes the motions for transports the carrier on the belt, we defined the *virtual probe* model obtained physical properties of the belt such as velocity, acceleration, and deceleration. The *virtual probe* has the

predefined motions ‘M_Forward (start to end position)’ and ‘M_Reverse (end to start position)’ and an initial position. When the state ‘UP’ was transited to ‘Move forward’ by the ‘STP_DOWN’, the *virtual prove* attach the nearest carrier and move forward the distance *d_stopper*, then detach it at the destination. Furthermore, a virtual sensor of the virtual model sends a signal to the PLC to indicate whether the carrier is arrived at the proper position or not. This template model of the stopper is applied to all stopper models in the conveyor. Although the signals used in the PLC is different, we used the template model repeatedly according to connect signals to the proper ports of the template. As a results, we can reduce the time for constructing the virtual model, and carry out the ‘manual mode’ simulation efficiently.

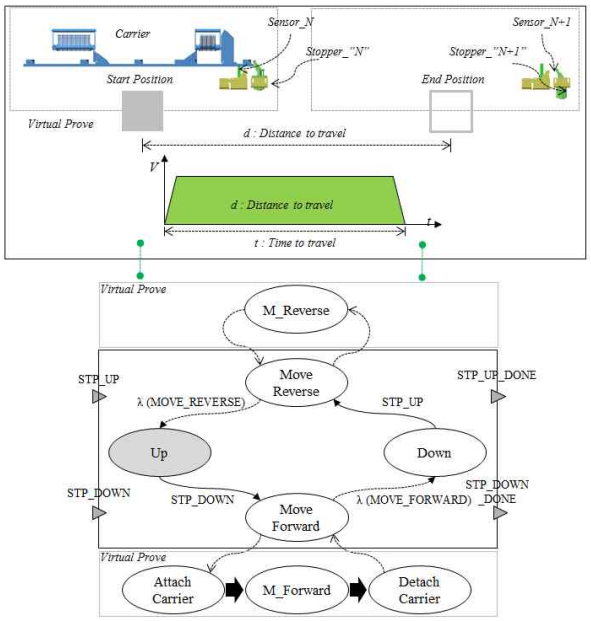

Figure 9. A virtual model template of a stopper

We could obtain the virtual device models from the proposed template model of robot, jig, stopper, and lifter. Since virtual models are built by the template, it could inherit the template properties of each model. Figure 10 shows a virtual model of the stopper and Figure 11 shows a virtual model of the vertical lifter, which consists of ‘PUSHER’, ‘LOCKER’, ‘JIG’, ‘LIFTER’.

We applied the proposed method to the SIL (SQL) line constructed by Korea automaker. The proposed method was implemented in C++ language, and test run were made on a personal computer, as shown in Figure 12. The PLC program was written using RS Emulator of the PLC program provided by AB Corporation.

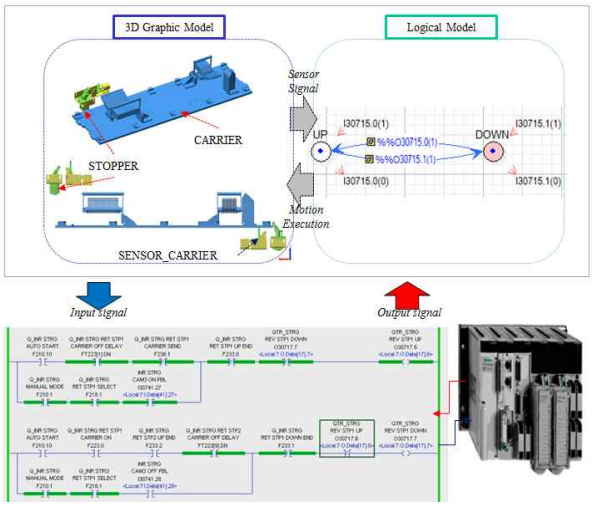

Figure 10. Virtual devices model of the stopper & vertical lifter

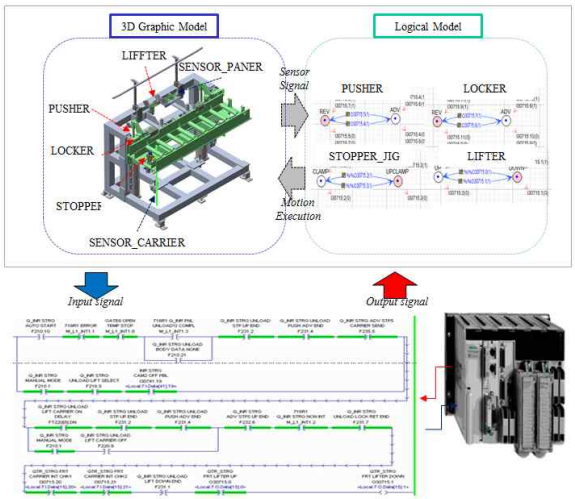

Figure 11. Virtual devices model of the stopper & vertical lifter

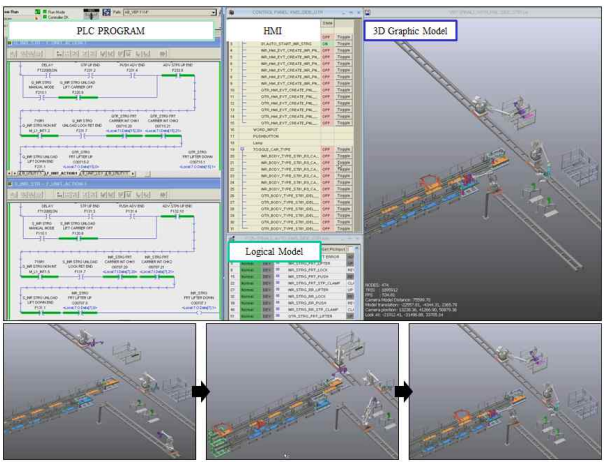

Figure 12. PLC simulation environment of SQ & SIL

5. CONCLUSION

To minimize the stabilization time of a production system to reduce the time to market, it is necessary to carry out the PLC simulation using virtual device

models to fix various errors caused by mechanical devices not being properly adjusted, faults in the PLC program. However, constructing a virtual device model using both physical model and logical model requires an excessive amount of time and effort, because both models are not suitable for the simulation to use immediately. To remedy this problem, this paper proposes an efficient method for constructing the virtual device model for the PLC simulation using template method. The proposed template model contains the logical core expressed by DEVS formalism and the physical shell shows corresponding motions reflecting the change of states of the logical core during the simulation, it represents such a manufacturing device in the real production system. Thus, template could be used as a guild line for the production system, as well as creating the virtual model using given signals. We applied this proposed method for the PLC simulation in the SIL (SQL) line manufactured by Korean automaker. After finishing the project, we stored the template model to use for the next simulation project, since it is possible to reuse the contained physical and logical models repeatedly.

ACKNOWLEDGEMENTS

This work was supported by the Defense Acquisition Program Administration under the Contract No. UD100009DD and the Agency for Defense Development under the Contract No. UD110006MD. This paper was also completed with Ajou University Research Fellowship of 2011. The authors wish to express sincere gratitude for the financial support.

REFERENCES

Al-Ahmari, A.M.A. and Ridgway, K., *An integrated modeling method to support manufacturing system analysis and design*. Computers in Industry, 38 (3), 225–238, 1999.

Anglani, A., et al., *Object-oriented modeling and simulation of flexible manufacturing system: a rule-based procedure*. Simulation Modeling Practice and Theory, 10(3-4), 209-234, 2002.

B.K. Choi, B.H. Kim, *New trends in CIM: virtual manufacturing systems for next generation manufacturing*, in: Current advances in Mechanical Design and Production Seventh Cairo University International MDP Conference, Cairo, February 15-17, 2000, pp. 425-436.

Chang Mok Park, Sang C. Park, and Gi-Nam Wang, Control Logic Verification for an automobile body assembly using simulation, International Journal of Production Research, Vol. 47, No 24, 2009

David, J.D., *Application and benefits of real-time I/O simulation for PLC and PC control system*. ISA Transaction, 36 (4), 305–311, 1998.

Elsayed A. Orady, T. A. Osman, Virtual reality software for robotics and manufacturing cell simulation, Proceedings of the 21st International Conference on Computers and Industrial Engineering, October, 1997, pp. 87-90.

Hibnio, H., Inukai, T., and Fukuda, Y., *Efficient manufacturing system implementation based on combination between real and virtual factory*. International Journal of Production Research,44 (18), 3897–3915, 2006.

H. T. Park, J. G. Kwak, G. N. Wang, and S. C. Park., *Plant model generation for PLC simulation*, International Journal of Production Research, 48(5), 1517-1529, 2010.

Jang, J., Koo, P.H., and Nof, S.Y., *Application of design and control tools in a multirobot cell*. Computers and Industrial Engineering, 32 (1), 89–100, 1997.

Klingstam, P. and Gullander, P., *Overview of simulation tools for computer-aided production engineering*. Computers in Industry, 38 (2), 173–186, 1999.

Sang C. Park, Chang Mok Park, and Gi-Nam Wang, *A PLC programming environment based on a virtual plant*, International Journal of Advanced Manufacturing Technology, 2008, 39(11-12):1262-1270

Xu XuSong, Xiong HongBin, *AS/RS real time simulation and control integrated system research,* International conference on management of logistics and supply chain, 686-693, 2006.

Zeigler, B.P., *Multifaceted modeling and discrete event simulation*. New York: Academic Press, 1984.

AUTHOR BIOGRAPHIES

MIN SUK. KO was born in Korea, and went to the Ajou University of Suwon, where he studied Industrial Information System Engineering. He is a PH.D candidate student in Modeling & Simulation Lab, the Department of IE. His research interests include geometric engineering knowledge management, discrete event system simulation, modeling & simulation. His e-mail address is : sebastianminsuk@gmail.com.

DAE SOON. CHANG was born in Korea, and went to the Ajou University of Suwon, where he studied Industrial Information System Engineering. He is a graduated student in Modeling & Simulation Lab, the Department of IE. His research interests include discrete event system simulation, modeling & simulation. His e-mail address is : webmacome@ajou.ac.kr.

GI NAM. WANG Is a professor in the Department of Industrial and Information System Engineering at Ajou University. His e-mail address is : gnwang@ajou.ac.kr and His Web-Page can be found at: http://udmtek.co.kr.

SANG CHUL. PARK. Is a professor in the Department of Industrial and Information System Engineering at Ajou University. Before joining Ajou, he worked for Daimler- Chrysler Corp. and CubicTek Co., developing commercial and in-house CAD/CAM/CAPP software systems. His research interests include geometric engineering knowledge management, and discrete event system simulation. His e-mail address is : scpark@ajou.ac.kr and his Web-Page can be found at : http://ie.ajou.ac.kr.

ADVICE ON DECISION MAKING IN BUSINESS MODELING BY MEANS OF MICROSOFT SOLUTION FRAMEWORK (MSF) AND THE EXECUTIVE LANGUAGE FOR THE BUSINESS PROCESSES MANAGEMENT (BPM)

Anna Plichta
Faculty of Physics, Mathematics and Computer Science
Cracow University of Technology
ul. Warszawska 24, 31-422 Kraków, Poland
E-mail: aplichta@pk.edu.pl

Szymon Szomiński
Faculty of Electrical Engineering, Automatics, Computer Science and Electronics
AGH University of Science and Technology
Al. A. Mickiewicza 30, 30-059 Kraków, Poland
E-mail: szsz@agh.edu.pl

KEYWORDS
Business modelling, BPM, MSF.

ABSTRACT

The basic aim of business modelling is the qualification of the aim and the range of the project, the qualification of requirements for the created software and the study on the strategy of his implementation. Results of the business modelling for Information Technology (IT) projects are expressed in the specific notation, namely through the general models which concern the business processes, analyzed cases of the use of IT technologies in business, and business objects.

INTRODUCTION

The process of modelling is a technique of describing the functional features of the system. It encompasses flow and the transformations of the data presented with the various processes in the system.

One can divide notations and the methodologies of modelling into two groups:

- modelling purposed for carrying out the analyses and for the optimization of the economic processes and events
- modelling purposed for creating the software

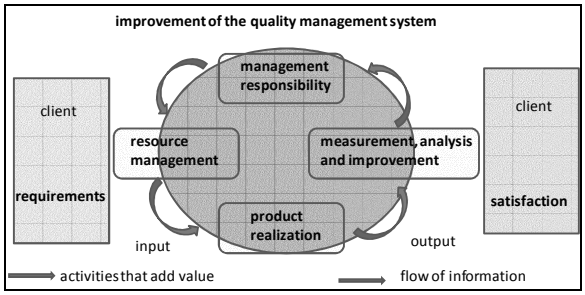

Figure 1: Business project management (Source: http://www.umbrella.org.pl/uslugi/zarz_jakoscia.htm, accessed 03.02.2012)

THE MSF STRATEGY (MICROSOFT SOLUTION FRAMEWORK)

The Microsoft Solution Framework (MSF) strategy used in business modelling is a flexible, integrated set of the models which facilitate accumulating these supplies, human resources and technologies which are necessary to the adaptation of the technical infrastructure to one's aims. During the project of the migration, enterprise or organization can use MSF together with one's own tools and policies.

Every project has its own life cycle, the series of actions which take place from the beginning of the project to its finish.

Proceedings 26th European Conference on Modelling and Simulation ©ECMS Klaus G. Troitzsch, Michael Möhring, Ulf Lotzmann (Editors)
ISBN: 978-0-9564944-4-3 / ISBN: 978-0-9564944-5-0 (CD)

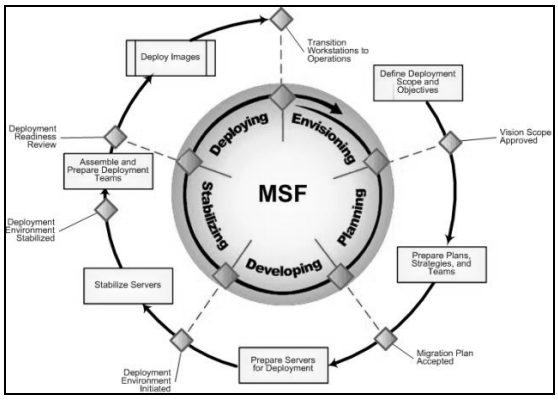

Figure 2: MSF Process Model (Source: http://technet.microsoft.com/en-us/library/bb497060.aspx, accessed 03.02.2012)

MSF Process Model has the advantages of both models of the software production, the traditional and the spiral. It is based on stages and milestones. Stages are the particular periods of time dedicated to the accomplishment of determined actions. Each stage is different and is followed by the change of the focal point of the whole project. Milestones are very particular points, when the synchronization of the stage takes place and the correctness is checked, as well as the level of accomplishment of the stage goals. At each milestone one can adapt the range of the project to meet the customer requirements.

THE PROTOTYPE OF THE SYSTEM

The standards in business modelling and in the executive language of business processes Business Process Management (BPM) have been established in order to facilitate control on the realization of business processes. Through the standardization of the protocols which regard designing, implementation, production, management, service and optimization, BMP leads to the significant improvement of business processes, but all changes are under stringent control of the manager.

The core of the project are Business Process Modelling Notation (BPMN) notation purposed for business process and web-service modelling, and Business Process Execution Language (BPEL), the Extensible Markup Language (XML) based mark-up language which makes use of web services and is purposed for the description of the realization of business processes.

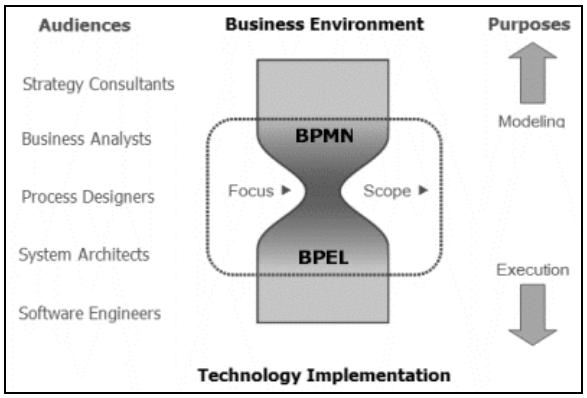

Figure 3: BPMN-Business Process Modelling Notation (Source: own work)

BPMN-BUSINESS PROCESS MODELLING NOTATION

BPMN describes exactly one diagram of business processes: the Business Process Diagram (BPD) diagram. It is easy to grasp and apply, especially for the average users and facilitates and quickens the modelling processes. Moreover, it makes modelling of difficult and complex business processes possible and can be translated into any executive language they use.

BPD diagram insist on taking www services into consideration in these projects which are realized.

BPEL-BUSINESS PROCESS EXECUTION LANGUAGE

BPEL is a perfect example of the Service-Oriented Architecture. It enables a user to design complex business processes, because it is described with the same interface as the typical web service. It means, that the client application can consume it in the same way as a web service (customer's proxy is created in the similar manner) or any other process do. Thus, one can make up services which are very granulated: they can be fused and bound together into final business processes, offered to the client as the end-product. The abundance of constructions and mechanisms provided by BPEL is intended to create complex data flows and to join services of various functionality. It is attractive for corporations, because its language comprises correlation mechanisms, exception service and event-reaction module. These functions, in the hands of experienced user, means coherent business data and complex processes less exposed to breakdowns, able to react to the asynchronic data from other systems.

BPEL, as a tool for business process modelling in SOA, is a kind of 'glue' which links functionalities of many web services together, providing solutions for business

problem. Business process implemented with BPEL is given ability to use many web services and thus to create brand new business application having its own interface for the end-user. Using BPL and web services for the purposes of the systems integration is relatively cheap and convenient, especially for corporations.

BPEL – declarative mark-up XML language

BPEL is a declarative mark-up XML language, purposed for the description of the business process execution by means of web services. Owing to BPEL many simple web services can act as a single service of higher level dedicated to the customer, and SOA can be realized, which is through the various composition and web service coordination techniques.

BPEL language stemmed from two former languages of workflow description: Web Services Flow Language (WSFL) graph modelling language worked out by IBM, and XLANG (block language worked out by Microsoft) The application written in this language is interpreted by the BPEL engine, via the namespaces declared in the language. BPEL process interchangeably order the sequence in which the single services are called out, decides if calling-out is linear or sequential, enables a user to make loops, conditional constructions and variables (and to copy these variables or give them values). Typical BPEL process it is initially given all values by the user, call out the required service (set of ordered services) and gives back the result of the computation. Business process consists of stages (functional blocks, 'activities'). BPEL supports both simple and structural action.

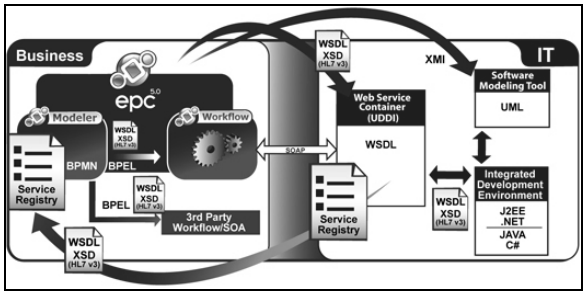

Figure 4: Mapping and dependencies between IT and business (Source: http://www.interfacing.com/ Products/enterprise-bpm/Process-Execution%20/, accessed 03.02.2012)

The composition of complex business processes, by the agency of the BPEL language, is executed either through the so-called orchestration or choreography.

In the orchestration the so-called central unit is required (e.g. the service of Web Services). It coordinates the activation of the individual services which, as a whole, make up the business process. That kind of policy is more flexible. The above-mentioned individual services do not participate in the larger business process 'consciously' so their source code may remain intact. In case of service breakdown alternative protocols may be applied.

In choreography no central unit is used. Instead, it is assumed that each service has a fragmentary knowledge about the structure of the whole business process and communicates with the dependent services on its own. The control flow is maintained through the mutual summoning of the services making up the whole unit.

The features of BPEL:

- The process is introduced as the executable code, independent from the environment of its realization
- The pattern of the representation of the business process is defined
- The language allows for the expression of the co-operation between business objects
- The language can create abstract processes
- Processes can be modified „live"
- the flexibility of the language allows the features taken from the real world to be reflected in the process

Definition of business process in BPEL language orders the sequence in which parallel or serial web services are executed. It is possible to define conditional activities and results of one service can be declared as call arguments of the second one. BPEL offers traditional loop structures, variable declarations, substitution, exception service etc.

BPM-BUSINESS PROCESS MANAGEMENT

BPM provides business processes with easy browsing and detecting and connects them dynamically with administered services. Thus, it facilitates the implementation of business processes into the frame architecture SOA. It allows for separation of the complexity of the system from business processes. As a result, the infrastructure is more flexible.

The business processes management:

- Business processes modelling
- Simulation and optimization of business processes
- Business processes activation
- Monitoring - Business Activity Monitoring (BAM)

Support for popular standards:

- Business Process Execution Language (BPEL)
- Business Process Management Notation (BPMN)

BMP is often combined with SOA (architecture leaning on services), which is the conception concerning the IT systems development which attaches importance to meet exactly the needs of the user.

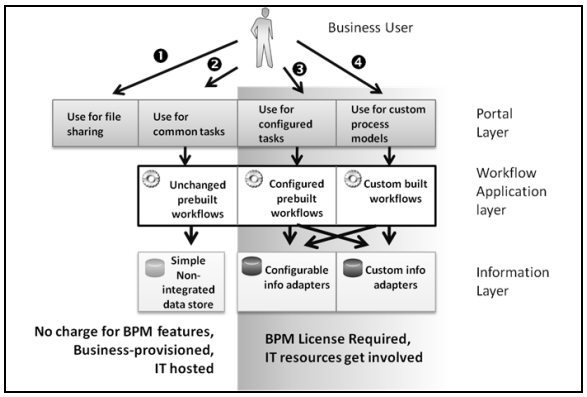

Figure 5: A chart concerning various software used by the customer and mutual relationships between the particular sort of the respective software (Source: http://blogs.msdn.com/ b/nickmalik/archive/ 2010/09/17/a-roadmap-to-bpm-democratization.aspx, (accessed 03.02.2012)

BPMN-BUSINESS PROCESS MODELLING NOTATION

Business Process Modelling Notation (BPMN) is the standard by the BPMI organization which regards www services, modelling the course of business processes and mutual flows between them. It is intended to provide such a description of business processes and business environment which is comprehensible for all users, from business analytics who sketch the initial outlines of processes, to the technical staff responsible for the implementation of technology, which is worked out to serve these processes. It is also intended to uniformly visualize the XML-based executive languages of business processes, by means of using the common notation.

Apart from BPMN, the BPMI worked out:

- the language of business processes modelling Business Process Modelling Language (BPML)
- the query language for business processes Business Process Query Language (BPQL)

They were all grounded on mathematical basis (the Pi calculus, one of the process algebras). As a result, one can directly manipulate the model and the generated executive language of business processes can be executed at once. Roughly speaking, BPD diagram is translated directly into the description in BPML language, in the same manner as diagrams of the data structures translate into the description in the language of definition.

BPMN describes exactly one of the possible diagrams of business processes, namely the Business Process Diagram (BPD) diagram. It is 'digestible' for typical users: easy to grasp and to use in process modeling. Moreover, it can be a tool for modeling much more complex and intricate business processes and translated into any executive language of such processes. Within the BPD diagram the importance is attached to make use of www services in the conducted projects. BPMN can automatically translate itself into BPML or any other standards of the executive languages of business processes e.g., Business Process Execution Language For Web Services (BPEL4WS).

THE SUBJECT OF THE RESEARCH

This article pertains to the notations, elements of the programming languages and models which find application in the decision support systems. At each particular stage decision making starts from defining problem and its possible solutions. Then, the model of the chosen solution is made. When it comes to teams responsible for creating various business applications, the efficiency can be raised e.g., by facilitating procedures concerning business process servicing, by reducing servicing costs, by giving managers monitoring tools, by correction of unfavourable events, by bringing order into data and into data accessing.

Each model type is appropriate to meet a particular need. Business model describes process from the point of view of its business participants. Technical model describes it from the point of view of IT architecture, whereas the executable model – from the point of view of BPEL architecture. Owing to BPM we can integrate business processes into SOA architecture through providing browsing, detecting and dynamic linking to managing services. In other words, it is possible to separate the intricacy of the system form all the business processes and hence to create more flexible architecture.

SUMMARY

Model of the process described by means of BPMN notation is a logical representation of rules and work-manners of the process. One can generate of it a notation in any executive process language. To achieve better results one can use process simulation, which enables him to analyse process models before their implementation. During the simulation model acts as an enterprise, simulating business processes and events at an accelerated rate, and it displays the animation of the simulation. As the simulating application stores the statistical data concerning to the parts of the model, one can define the efficacy on the basis of that data and thus avoid business mistakes before the implementation of processes.

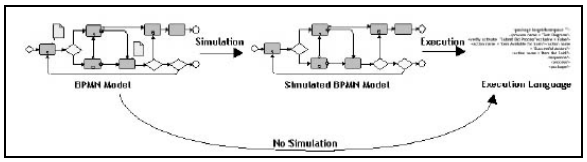

Figure 6: Simulation of the process model in the BPD diagram in BPMN notation (Source: own work)

Process modelling by means of BPMN notation is important if we want to understand how to integrate many business project into one system. BPMN provides a strong support for other modelling techniques (e.g., relational modelling of data, designing systems and applications by means of UML, designing XML schemes and net architecture). Owing to all the above-mentioned modelling methods, it is possible to make up the architecture of an enterprise able to react for the changes more safely and in faster manner.

REFERENCES

Biernacki, P. 2006. *BPMN* (www.mgx.com.pl/bpmn-r10.htm)

Jurij, M.B. 2006. *Business Process Execution Language for Web Services BPEL and BPEL4WS 2nd Edition*

Matuszewski, M. Podkowiński, P. and Kraszewski, K.2007. *Automatyzacja procesów biznesowych: od modelu do realizacji* (www.ids-scheer.com/set/6611/4_Automatyzacja%20procesow%20biznesowych.PDF)

Miers D. and White S.A. 2008. *BPMN Modeling and Reference Guide.*

Olek Ł. 2006. *Wykorzystanie przypadków użycia do opisywania procesów biznesowych* (www.inmost.org.pl/articles/Wykorzystanie_przypadkAw_uAycia_do_opisywania_procesAw_biznesowych www.itp-commerce.com/)

Silver B. 2009. *BPMN Method and Style: A levels-based methodology for BPM process modeling and improvement using BPMN 2.0*

Statuch G. 2006. *Analiza procesów biznesowych (BPEL4WS) za pomocą CWB* (www.mimuw.edu.pl/~sl/teaching/05_06/WZTPW/PREZENTACJE/BPEL4WS_CWB_PPT.pdf)

Zakrzewisz M. 2006. *Tutorial: Implementacja aplikacji biznesowych w technologii WS-BPEL* (www.ploug.org.pl/seminarium/seminarium_XIII/pliki/tutorial.pdf)

Zakrzewisz M. 2008. *Implementacja aplikacji biznesowych w technologii WS-BPEL* (www.cs.put.poznan.pl/mzakrzewicz/bpel.pdf)

www.bcc.com.pl/pad_files/aw_files/385_AW_SAPdlaPM_20080324.pdf

www.bocgroup.com/boc_opendoc.jsp;jsessionid=DC24FC3C2E29C9D1C2EAA729B37976DB?file=WP_3467df26314c0cac.189635d.116a9eaf0e8.-7ffd&lang=pl

www.bpmn.org/Documents/Mapping%20BPMN%20to%20BPEL%20Example.pdf

www.eti.pg.gda.pl/katedry/kask/pracownicy/Tomasz.Boinski//files/PZiTN/05_Workflow_jezyki.pdf

www.rejestracja.software.com.pl/download/3982.html

www.si.pjwstk.edu.pl/dydaktyka/mgr/2006-2007-inter/Narzedzia_Workflow.ppt

www.skutecznyprojekt.pl/artykul.htm?AID=94

www.soa.org.pl/DownloadFile.aspx?AttachmentID=54

www.staff.amu.edu.pl/~ynka/piomaterialy/bpmn.pt

www.visp-project.com/docs/publications/renk_artykul_KSTiT_2006_workflow. pdf

AUTHOR BIOGRAPHIES

ANNA PLICHTA was born in Cracow. She studied comparative literature at the Jagiellonian University and obtained her degree in 2007. She also studied computer science at Cracow University of Technology and obtained her degree in 2010. Currently, she works as a teaching fellow at Cracow University of Technology. Her e-mail address is: `aplichta@pk.edu.pl`

SZYMON SZOMIŃSKI was born in Cracow. He studied computer science at the Cracow University of Technology and obtained her degree in 2010. Currently, he study computer science at the AGH University of Science and Technology. His e-mail address is: `szsz@agh.edu.pl`

AN AGENT-BASED COLLABORATIVE MODEL FOR SUPPLY CHAIN MANAGEMENT SIMULATION

C. M. Vieira
Centre for Management Studies
Technical University of Lisbon
1049-001, Lisbon, Portugal
ESTG
Polytechnic Institute of Leiria
2411-901 Leiria, Portugal
E-mail: carlos.vieira@ipleiria.pt

A. P. Barbosa-Póvoa
Centre for Management Studies
Technical University of Lisbon
1049-001, Lisbon, Portugal
E-mail: apovoa@ist.utl.pt

C. Martinho
Dep. of Computer Science
Technical University of Lisbon
1049-001, Lisbon, Portugal
Email:carlos.martinho@ist.utl.pt

KEYWORDS
Supply Chain Management, Multi-Agent System, Simulation.

ABSTRACT

In traditional supply chain (SC), planning problems are usually considered individually at each SC entity. However, such decisions often influence the other members in the chain and thus an integrated approach should be considered. By modelling system-wide SC networks, different SC problems, like production planning, coordination, order distribution, among others, can be integrated and solved simultaneously so that the solution is beneficial to all entities in a long-term base. In an attempt to make progress in this area, researchers use various methods for modelling the dynamics of SCs. In the literature review, due to their distinctive characteristics, multi-agent-based systems have emerged as one of the most adequate modelling tools for tackling various aspects of SC problems. In this work, a multi-agent supply chain system (MASCS) model that integrates different SC processes is presented. The proposed model allows modelling different SCs with multi-products and different operational policies considering information asymmetry and distributed/decentralized mode of control.
In this article the details of the MASCS model development and implementation are presented. Furthermore, the applicability of the proposed MASCS is briefly demonstrated through the solution of a SC example. The obtained results are discussed and research extensions are outlined.

INTRODUCTION

A supply chain (SC) is a network of trading partners linked through upstream and downstream connections where the main aim is to produce and deliver products/services to the ultimate consumers so as to provide global SC profit. Traditionally, managers have been focusing on the management of their internal operations to improve profitability and thus an internal concern has been the main objective. However, supply chain management (SCM) calls for the integration of the SC operational activities in order to organize/manage the flows between entities as if they form a single organization. Moreover, with the businesses globalization, inter-organizational coordination is becoming strategically important for companies to augment responsiveness while maintaining SC efficiency.
Numerous studies have demonstrated that substantial benefits can be obtained from an integrated SCM. Such integration provides tremendous challenges to managers (Arshinder 2008). Although a completely integrated solution may exist with an optimal system performance, such solution is not always in the best interest of every individual member. As a result, each SC member attempts to optimize a part of the system without giving full consideration to the impact of their myopic decisions on the total system performance. Optimizing the portions of the system yields sub-optimal performance, resulting in an inefficient allocation of scarce resources, higher system costs, compromised customer service, and a weakened strategic position. A key issue in SCM is then how to coordinate the independent players to work together as a whole so as to pursue the common goal of chain profitability.
In an attempt to make progress in this area, researchers use various methods for modelling the dynamics of SCs. The multi-agent system (MAS) approach has appeared as one of the most adequate modelling tool for tackling various aspects of SC coordination problems (Santa-Eulalia et al. 2011). Indeed, considering the fact that most of the SCs involve enterprises with independent ownerships (requiring the ability to model information asymmetry and distributed/decentralized mode of controls), applicability of traditional modelling approaches is limited and unrealistic (Govindu and Chinnam 2010). Additionally, a holistic model is required to explore different coordination mechanisms and their value in SC where different set of combinations of coordination mechanisms can be tried with the help of simulation. Moreover, most of the models describing coordination mechanisms are dealt in two-level SC, which needs to be extended to multi-level SCs (Arshinder 2008).

Proceedings 26th European Conference on Modelling and Simulation ©ECMS Klaus G. Troitzsch, Michael Möhring, Ulf Lotzmann (Editors)
ISBN: 978-0-9564944-4-3 / ISBN: 978-0-9564944-5-0 (CD)

From these considerations, a MASCS model that integrates different SC processes is here presented. The proposed model allows simulating different SCs with multi-products, multi-entity and information asymmetry where different types of decisions are accounted for.
This paper is structured as follows. The first sections describe the proposed MASCS model and the corresponding implementation. Then a SC example is introduced in order to validate the MASCS model. The results are presented and discussed. Finally, the last section summarizes research contributions and identifies some possible extensions.

MASCS MODEL DESCRIPTION

The MASCS model developed is based on a generic process-centered methodological framework (Govindu and Chinnam 2007) Multi-Agent Supply Chain Framework (MASCF), which is a generic methodology that simplifies the SCs modelling through MAS development. MASCF uses the notion of process-centered organization metaphor, and adopts Supply Chain Operations Reference Model (SCOR) (SCC 2010) with Gaia methodology (Zambonelli et al. 2003) focusing on the system analysis and design phases of the MAS development. Given the characteristics to account in our MASCS model, MASCF analysis identifies the number (single/multiple), and the scope of sub organizations that a SC system would comprise along with the services that they have to offer according to the SCOR process definitions. The entire logic of the system dynamics is then split among these SC entities, and is projected into process level logic while determining the role and interaction between these entities. Subsequent analysis and design steps of MASCF resulted in the identification and specification of the agents and services listed in table 1.
The proposed MASCS model is constructed through the definition of five different types of agents (market, sales, inventory, procurement and production). The existence of multiple geographically disperse markets, representing the aggregate demand pattern of customers for different products, are modelled through the creation of Market Agents (MA). The other four agents represent the principal functions that any SC entity possesses that allows them to participate in different SC processes and activities so as to produce value in the form of products/services delivered to the final consumers.
Each MA will be responsible to generate the market demand for each product, send market orders requests to available SC entities, and receive the corresponding products. The market orders can be filled from any SC entity (retailers, manufacturers and suppliers) and will be received by the corresponding sales function. After receiving orders, and in order to fill them, the requested Sales Agent (SA) needs to query the inventory position for the requested items. Based on the inventory position and on the quantity ordered, the SA decides to send all, partial or none of the quantity required.

In case of a total or partial filled order occurrence, the SA depletes inventory and sends the corresponding information to the Inventory Agent (IA). If one or more orders need to be delivered, the SA plans shipment load and delivery, and sends the corresponding shipments to customers.

Table 1: Agents and Services

Agents	Services
Market Agent (MA)	Generate market demand
	Place order
	Receive shipment
Sales Agent (SA)	Receive order
	Query inventory position
	Fill order
	Send deplete inventory information
	Plan shipment load and delivery
	Send shipment
	Compute sales forecast
	Send forecast information
	Receive replenishment information
Inventory Agent (IA)	Receive deplete inventory information
	Receive replenish inventory information
	Update inventory
	Send inventory information
Procurement Agent (PA)	Receive forecast information
	Receive inventory information
	Define order request
	Send order requests
	Receive proposals and refusals
	Analyse proposals
	Send accept/reject proposal notifications
	Receive shipment
	Send replenishment inventory information
	Receive shipment
	Send replenishment inventory information
Production Agent (PrA)	Receive forecast information
	Receive inventory information
	Plan production
	Production
	Send deplete inventory information
	Send replenishment inventory information

Since the Procurement Agent (PA) needs sell forecast information to source products/parts/raw-materials, the SA forecasts sales and sends this information to the PA periodically. Also, whenever there is a product replenishment, the SA receives the corresponding information in order to plan and send a shipment with backorders (BO) that can be satisfied based on the new inventory position.
The IA is responsible to update the stock movements due to deplete and replenish actions performed by the SA and the PA, respectively. Additionally, the IA must inform periodically or continuously the PA on the inventory position of each item based on a periodic or continuous inventory review systems. Based on a

replenishment action, the IA must also inform the SA on new products availability.

The PA is responsible to procure all items required by the SC entity that it represents. As so, the PA must have access to sales forecast and inventory position for each item. The replenishment decision will then be based on a particular replenishment policy method associated. At some instant, if a replenishment quantity is needed then the PA will set an order and send several order requests to potential suppliers of the item under analyse, initiating a negotiation process with the corresponding SAs.

Based on these requests, the PA receives proposals and refusals (one proposal or refusal for each order request) and identifies the proposal that better suits some given criteria. The SA with the winner proposal will then receive an accept proposal information. As for the others, the PA sends a reject proposal notification. Finally, the PA must also receive shipments from their suppliers and send corresponding replenishment inventory information to the IA on the items received.

Due to the negotiation process previously discussed, the SA will additionally need to, in response to a particular order request, send a proposal with his best commercial offer or a refusal signal if the requested item is not available. In case of an accepted proposal the SA performs the services previously discussed.

Finally, the Production Agent (PrA) is responsible to plan production and accordingly produce finished products. In order to perform these actions the PrA must have access to sales forecasts, bill of materials and product/part/raw-material inventory information. The order production will be based on a particular production policy and any production initiation leads PrA to inform IA on parts and raw-materials inventory depletion. Similarly, the PrA must inform the corresponding IA on product inventory replenishment whenever a production order is concluded.

For implementation purposes, the MASCS model will use the notion of reusable and extensible components defined in a software agent-component based framework (Govindu and Chinnam 2010). This framework defines two types of agents – supply chain agents (SCAs) and organizational agents (OAs). Any real-world SC network consists of multiple interacting entities (independent enterprises) at different levels/tiers (e.g., retailer, supplier, manufacturer, and so on). The set of agents representing all such entities constitute the library of SCAs. Also, each of the SC entities in turn consists of multiple functions. The set of all agents representing organizational functions (within the SC entities) constitute the OAs library. The framework by design conceives OAs to be reused in multiple SC entities. Indeed, at a conceptual level the basic functionalities of the sales agent remains the same irrespective of which SC entity it belongs to. Additionally, by design, both SCAs and OAs are only generic shells with communication abilities providing both direct (peer-to-peer between SCAs or between OAs belonging to a particular SCA), and indirect (routed through the corresponding SCAs) modes of communication. As an important feature, the model allows the generation of different SC models and helps the explicit study of SC dynamics (both intra- and inter-organizational) involving Bullwhip-effect and coordination issues in any SC considering information asymmetry. This MAS structures will allow the development of different analysis on any SC network. The MASCS model additionally, as already mentioned, incorporates multiple geographically disperse market entities representing the aggregate demand behaviour of all possible customers for different products through the usage of MAs.

Further additional features have been also added to the MASCS model. SCM spans all movements and storage of raw materials, work-in-process inventory, and finished goods from point of origin to point of consumption. These different products are referenced in the current model with the notion of Stock-Keeping Unit (SKU) in which, different SKU identifications are assigned for each product based on product variants (product form, fit or function) or even package sizes (boxes, pallets or other load unit). As a result, as for real SC, the MASCS model and consequently all the decisions (replenishment, transportation, production and so on) will be based on the SKU notion.

The proposed MASCS model allows to incorporate appropriate operational policies which will support the decision making of the OAs associated with replenishment, procurement, production and distribution processes. Indeed, these policies are defined as generic reusable objects that can be referenced inside agent's behaviours. This model feature allows to conduct studies that will help to understand the impact of such policies in the SC performance.

As a result from the previous model features, it results that the MASCS model will allow to deal simultaneously with multi-products, multi-SKUs and multi-entity SCs where different types of decisions are accounted for. Indeed, the inclusion of any procurement negotiation scheme will support the dynamic formation of SCs over time. Additionally, the MASCS model will provide a way to conduct studies of different information sharing and operational policies scenarios.

MASCS MODEL IMPLEMENTATION

The MASCS model was implemented using the Java Agent Development Framework (JADE™) (Bellifemine et al. 2007). JADE™ is a software development framework aimed at developing MAS and applications conforming to the Foundation for Intelligent Physical Agents (FIPA) standards, which are intended to promote the interoperation of heterogeneous agents and the services that they can represent. The list of services (table 1) that the defined agents have to provide in the proposed MASCS model, are then carried out extending behaviours classes and establishing proper communication schemas between agents.

The JADE™ behaviours classes (Bellifemine et al. 2007) range from simple to composite behaviours with several types within each category. Each behaviour type class has a particular method to insert execution thread within the tasks queue of a specific agent during simulation. The behaviour classes in use are the following: one-shot behaviour that executes only one particular event-based task normally after receiving a given type of message; cyclic behaviour that executes a given task forever during simulation, which is normally associated with the received message service for each agent; waker behaviour that allows to execute a given task only once, just after a given elapsed timeout; and finally ticker behaviour for tasks that must be executed periodically.

As for communication, the messages exchanged by MASCS agents were specified using the Agent Communication Language (ACL) format (FIPA 2001).

In this format, a performative parameter indicates the type of the communicative act which can be among others: REQUEST, if the sender wants the receiver to perform an action as in the query inventory service that the SA must perform; INFORM, if the sender wants the receiver to be aware of a fact as for the send inventory or send forecast information services or; CFP (call for proposal), PROPOSE, ACCEPT PROPOSAL, REJECT PROPOSAL, if the sender and receiver are engaged in a negotiation, which is the case of the procurement negotiation process between SC entities.

The content of the message can be established in JADE™ through the usage of ontology objects. Ontology represents a common vocabulary to share information in a specific domain and includes its terms, their properties and interrelationships. In MASs, the use of an ontology facilitates interaction, coordination, and negotiation among agents. Ontology objects can be transferred as extensions of predefined classes that JADE™ agents can automatically use to encode and decode messages in a standard FIPA format ensuring agent interactions at a semantic-level rather than just pure syntactic-level.

At this point, and before describing the SC ontology adopted, it is important to highlight the messages type needed to be exchanged between agents in the proposed MASCS model. Because the material, money and information flows throughout the entire chain and must be managed in an integrated and holistic manner for the SC to achieve its maximum level of effectiveness and efficiency, it is assumed that the message exchange between MASCS agents represent all the possible material (shipment deliveries, inventory replenishments and so on), money and information (order requests, production orders, order proposals/refusals, inventory and forecast information and so on) exchanges throughout the entire SC.

In technical terms, FIPA/JADE™-compliant ontology (Bellifemine et al. 2007) consists of a set of schemas defining the structure of the predicates, agent's actions, and concepts that are relevant to a domain of interest (Bellifemine et al. 2007). To provide a better idea for the ontology developed, the version of our SC domain ontology includes about 30 concepts and independent slots (in which the mains are: Deplete, Forecast, Inventory, Load, Order, Period, Proposal, Replenish, Ship and SKU) and 10 predicates (Deplete inventory, Inform forecast, Inform inventory, replenish inventory, Send order, send proposal, send accept proposal, send reject proposal, send refusal and send shipment).

At instantiation, the model communication configuration is defined through a MySQL™ table (OAs table in table 2) (Oracle 2011) that allows the establishment of all the acquaintances needed.

At this point, along with JADE™, several toolkits were integrated into the integrated development environment platform: OpenForecast©, Colt© project and Java database connectivity (JDBC). OpenForecast© (Gould 2003) is a package of forecasting models written in Java that can be applied to any data series. It includes a variety of different forecasting models and provides a module for best time series fitting. The provided classes allow to reference any available forecast model into the SA class in order to periodically produce sales forecast. On the other hand, the Colt© project (CERN 2004) provides a set of open source libraries for high performance scientific and technical computing in Java. The Colt library provides fundamental general-purpose data structures optimized for numerical data, such as random number generators and distributions useful for (event) simulations. On the other hand, JDBC (Oracle 2012) is a standard application programming interface that allows Java programs to access database management systems. The need for a database for MASCS variable definitions, parameters initialization and simulation output data is straightforward. For that purpose, MySQL™ database (Oracle 2011) as an open source database was chosen. Diverse tables, see table 2, were created in order to store all the required MASCS information.

Table 2: List of MySQL™ tables

Designation	Description
Behaviour periodicity	Periodicity parameter definition for ticker behaviours for each agent.
Bill of Materials	Materials/parts and quantities of each needed to produce an end product.
Demand	Demand generation process definition between each MA/SCA pair and SKU item.
Inventory	Inventory position /replenishment method definition for each SKU item and SCA.
Inventory details	Inventory movements registered for each SCA and SKU.
OAs	OAs list and interactions needed between each OAs during simulation.
Orders	Registered orders between SCAs.
Procurement	Procurement decisions made by the PAs per simulation period and SKU item.
Production	Production parameters definition for each

parameters	production resource and SKU item.
Production resources	Production resources available for each MfA and availability status.
Proposals	Registered proposals/refusals and output variables between each SCA pair.
Sales	Sales, lost sales and forecasts for each SCA, SKU item and period.
SCAs	SCAs type and number needed for SC structure configuration.
Shipments	Shipments registered and variable values for each SCA pair per simulation period.
Suppliers	SKU supplier entities available.
Timer	Time interval simulation period definition.
Transportation resources	Available resources and associated parameters for each SCA pair and SKU.
Transportation time	Transportation time distribution for each SCA pair and transportation resource.

MASCS APPLICABILITY

The applicability of the proposed MASCS was tested through the resolution of a SC example that will be briefly described (figure 1). The example is composed of two different entities in each SC tier (markets: M1 and M2; retailers: R1 and R2; manufacturers: Mf1 and Mf2; and suppliers: S1 and S2). Products (Products Code (PC): PC111, PC112 and PC232) and parts (PC1111, PC1112, PC2221, PC2222, and PC2321) are handled through several sized function SKUs. For example, PC111 has associated with him 3 different SKU items, each having a different number of units (SKU1: 1 unit; SKU2: 50 units and; SKU3: 20 units).

M1 is responsible for generating the demand for PC111 and PC112 for R1 and the demand of PC232 for R2. M2 is only responsible for generating the demand of PC111 for R1. All market order requests are generated in SKU1 terms and defined through the demand parameters (mean demand: μd [SKU units/period]: demand standard deviation: σd [SKU units/period] and; number of demand events per period NDEP [demand events/period]).

Each time there is an inventory replenishment need, R1 will acquire PC111 according to the best offer received from Mf1 and Mf2. PC112 is only supplied from Mf1, and R2 only procures PC232 from Mf2. Additionally, Mf1 is responsible to produce PC111 and PC112 in SKU2 and SKU3 terms with two dedicated production resources according to a bill of materials. Based on the production needs and on the inventory level Mf1, for example, will procure PC1111 and PC1112 for PC111, and PC2221 and PC2222 for PC112. Finally, the parts needed from Mf1 and Mf2 are procured in 10 PC units SKU size from two suppliers according to figure 1.

Different replenishment policies (RC=1: Periodic Review, Reorder-Up-To-Level System; RC=2: Reorder-Point, Reorder-Quantity (s, Q) System; and RC=3: Reorder-Point, Reorder-Up-To-Level (s, S) System) are associated to each SC entity, PC and SKU item. The on-hand (OH [SKU units]) inventory value for each PC, SKU and SC entity is defined at the beginning of the simulation. The other inventory parameters values (on-order quantity (OO) and BO) are assumed null.

R1 sends Full Truck Load (FTL) shipments for PC111 (18 m^3 and 1 ton truck) and Lot for Lot (LFL) shipments for PC112 (other dispatch rules are illustrated in figure 1). In order to compute a random production time to produce a specified quantity in a specified allocated resource, a normal capacity variable with a mean capacity (μcap[units/time period]) and a standard deviation capacity (σcap[units/time period]) are used. An additional constant setup time parameter (Setup [time period/10]) is used to compute the production order starting time. The corresponding values are shown in figure 1. Other input parameters are used, but are not presented due to space limitation, to allow the full characterization of the SC structure, material and information flows and behaviour periodicity of the SC case study. Finally, it is assumed that sales are known for the ten past simulation period for each PC at each SC entity in order to perform sales forecast.

The current SC example was simulated during 250 periods (each period corresponds to 10 seconds long) and the corresponding results are partially presented in figure 2. Due to the large amount of output data and this paper space limitation, the full example characterization is not possible in this paper. Some illustrative results are discussed, further details are expected to be oulished in an extended paper. Figure 2 shows the decisions and actions made by the OAs from R1 and R2 and by the PAs from the manufacturers in order to respond to the PCs order generation process during the 30 first seconds. Additionally, the PCs inventory level (IL) evolution at the retailers during the entire simulation is also illustrated.

The results show that M1 generates 9 PC111 orders and M2 generates 5 PC111 orders to R1. Additionally, M1 generates 3 PC112 and 3 PC232 orders to R1 and R2 respectively. The PC111 orders are then almost totally sent in two FTL shipments with departure time at 18 and 26 seconds, shipments number 2 and 5 from R1. The first shipment has two different destinations (M1 and M2) in which M1 is the first route destination. PC111 orders 1, 3 and 6, which were requested by M1 at instant time 11, 14 and 17 seconds respectively, were received at instant time 19s. The PC111 order request 1, 2 and 3 from M2 are received one second later. The PC111 orders sent in the first shipment are exclusively filled through PC111 availability in stock. The second PC111 shipment is only sent after a replenishment process due to a procurement need at 20s. Indeed, PC111 orders 11, 14 and 15 from M1 and order 5 from M2 are firstly backordered and then sent in the second shipment due to the FTL shipment condition. As a result from this operational constraint the PC111 order request number 7 which were requested at time instant 18s from M1 is only received at time instant 31s. As illustrated, the retailers IAs identified two PC111, two PC112 and one PC232 inventory replenishment need.

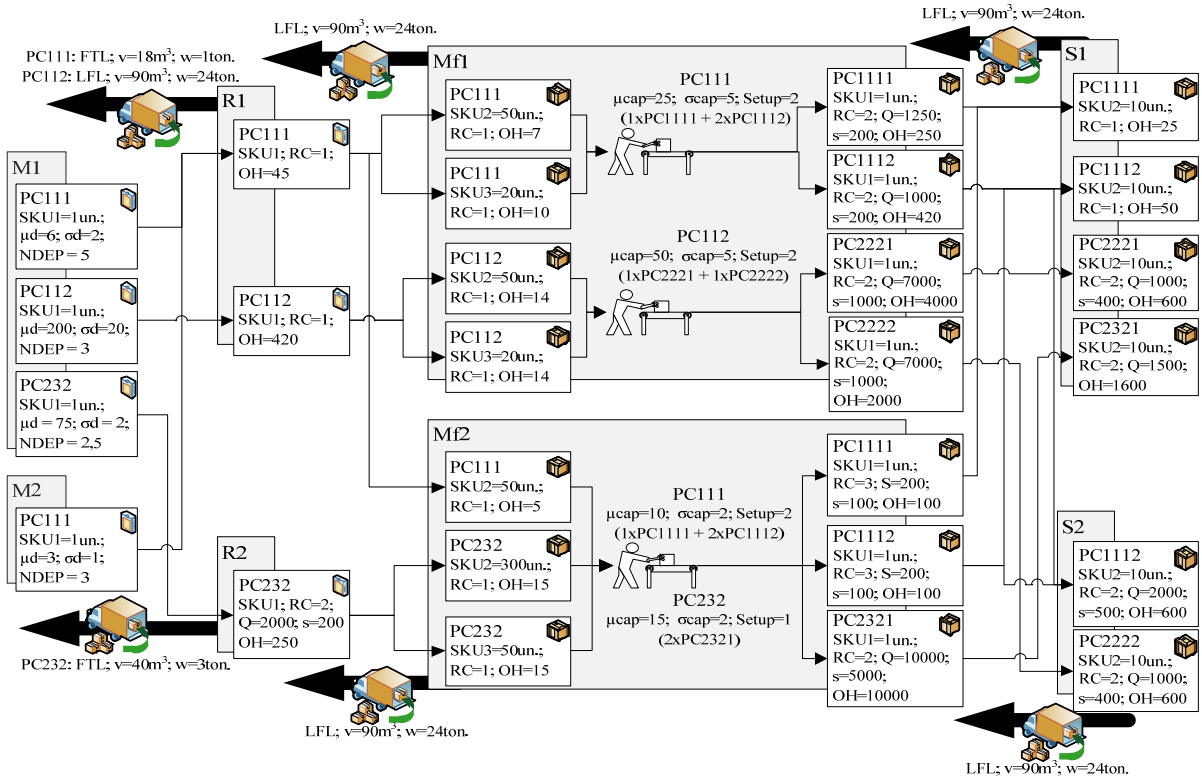

Figure 1: Supply Chain example

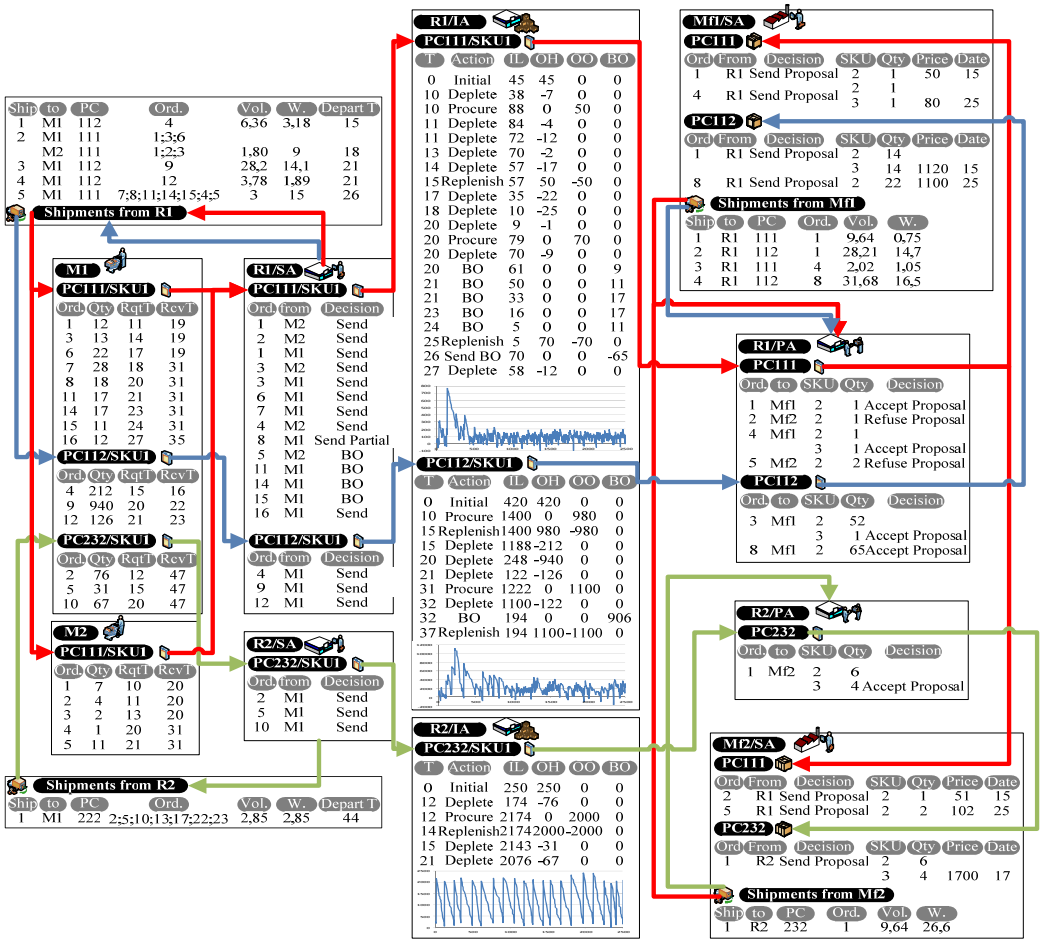

Figure 2: Example results

From these signals, different negotiation process were initialized between the Retailers' PA and the manufacturers. As an example, the first PC111

procurement negotiation, in order to request one SKU2 unit of PC111 at time instant 10s, is initialized from R1'PA sending two order requests (order 1 and 2) to the available suppliers (Mf1 and Mf2). The manufacturers sent back one order proposal with the quantity requested but with different prices. The Mf1 order proposal was then accepted since it presents a lower price (50 against 51 monetary units). The corresponding shipment (ship 1 from Mf1) was then received at time instant 15s allowing the replenishment of 50 units of PC111. Further procurement negotiation process result in the acceptance of a lower quantity then the one requested.

Much more can be said on the obtained results but the most important result is that the current MASCS model act according to the advocated objectives. Indeed, the actions and decisions made by the diverse agents are coherent with the SC example scenario and the MASCS model shows a relative stable behaviour during simulation. This later statement can be highlighted through the inventory level evolution graph illustrated in figure 2 and which were replicated throughout the SC entities of the proposed example.

CONCLUSIONS

A MASCS model has been developed and implemented in JADE™ in order to analyse simultaneously different SC problems, like production planning, inventory management, procurement negotiation, and order distribution. Also it was considered coordination among SC entities considering information asymmetry and distributed/decentralized mode of controls. The proposed model allows to deal additionally with multi-products, multi-SKUs, multi-entity SCs for different SC network configurations. The results show that the MASCS is adequate to analyse coordination issues and the global performance of SC systems under different inventory, production, procurement and shipments policies scenarios. Furthermore it is shown that the developed model can be used as a relevant coordination decision-making tool for SCM.

Further features on the constructed MASCS model can be added to tackle coordination decisions at the interface of the SC. Indeed, the future direction of our work intend to add additional coordination mechanism (SC contracts, information sharing and joint decision making) along as more SC operational and constraints details in order to identify, for different SC scenarios, which set of coordination mechanisms can lead to a better SC performance.

REFERENCES

Arshinder, Arun Kanda and Deshmukh, S.G. 2008. "Supply Chain Coordination: Perspectives, Empirical studies and Research Directions". *International Journal of Production Economics*, 115(2), 316-335.

Bellifemine, F. L., Caire, G., and Greenwood, D. 2007. Developing Multi-Agent Systems with JADE. Wiley.

CERN - European Organization for Nuclear Research. 2004. The Colt© project, version 1.2.0.

FIPA - Foundation for Intelligent Physical Agents. 2001. "*FIPA ACL message structure specification"*. Technical report XC00061.

Gould, S. R. 2003. OpenForecast©, version 0.5. "*The OpenForecast User Guide"*.

Govindu, R. and R. B. Chinnam. 2007. "MASCF: A Generic Process-Centered Methodological Framework for Analysis and Design of Multi-Agent Supply Chain Systems." *Computers & Industrial Engineering*, 53(4), 584-609.

Govindu, R. and R. B. Chinnam. 2010. "A Software Agent-Component Based Framework for Multi-Agent Supply Chain Modelling and Simulation." *International Journal of Modelling and Simulation*, 584-609.

Oracle. 2011. MySQL™, version 5.0. "*MySQL 5.0 Reference Manual*".

Oracle. 2012. JDBC, version 4.0 "MySQL Connector/J".

Santa-Eulalia, L.A., Halladjian, G., D'Amours, S., and Frayret, J.M. 2011. "Integrated Methodological Frameworks for Modeling Agent-Based Advanced Supply Chain Planning Systems: A Systematic Literature Review. *Journal of Industrial Engineering and Management*, 4(4), 624-668.

SCC – The Supply-Chain Council. 2010. *SCOR: Supply Chain Operations Reference Model – Version 10.0*. The Supply Chain Council. August 2010, version 10.0.

Zambonelli, F., Jennings N. R. and Wooldridge M. 2003. "Developing Multiagent Systems: The Gaia Methodology." *ACM Transactions on Software Engineering and Methodology*, 12(3), 317-370.

AUTHOR BIOGRAPHIES

C. M. VIEIRA obtained his Master degree in Technological Innovation and Industrial Engineering from Instituto Superior Técnico (IST), Technical University of Lisbon (UTL). Actually, as a PhD student in Industrial Engineering, his research interests are in the field of SCM/MAS. He is a Professor of Operations and Logistics at the Polytechnic Institute of Leiria.

ANA P. BARBOSA-PÓVOA obtained her PhD in Engineering from Imperial College of Science Technology and Medicine. She is currently a Full Professor of Operations and Logistics at the Department of Management and Engineering of IST, UTL. Ana's research interests are on the SCM, and on the design, planning and scheduling of flexible systems where sustainability is a main topic. Ana has published widely in these areas and supervised several Master and PhD students.

CARLOS MARTINHO received the PhD degree in Computer Science and Engineering from IST, UTL, in 2007. He is an Assistant Professor at the Computer Science and Engineering Department of IST and a Senior Researcher in the Intelligent Agents and Synthetic Character Group (GAIPS) at INESC-ID. His main research interests are in the field of autonomous agents, synthetic characters and social robotics, merging subfields from artificial intelligence into agent based simulation of believable behaviour.

CRISIS MANAGEMENT EVALUATION: FORMALISATION & ANALYSIS OF COMMUNICATION DURING FIRE INCIDENT IN AMSTERDAM AIRPORT TRAIN TUNNEL

Kees Boersma
David Passenier
Department of Organisation Sciences
VU University Amsterdam
De Boelelaan 1081,
1081 HV Amsterdam, The Netherlands
E-mail: {f.k.boersma, d.f.passenier}@vu.nl

Julia Mollee
C. Natalie van der Wal
Department of Artificial Intelligence
VU University Amsterdam
De Boelelaan 1081,
1081 HV Amsterdam, The Netherlands
E-mail: {j.s.mollee, c.n.vander.wal}@vu.nl

KEYWORDS
Crisis management evaluation, communication analysis, fire incident.

ABSTRACT

Communication and inter-organizational coordination in crisis management are of uttermost important for all processes and can lead to fast and effective averting or ending of a crisis situation. In this paper, a real world incident of a fire in the Amsterdam Airport Schiphol train tunnel was formalised, based on a public inquiry report, and subsequently, the emergency response to the incident was analysed by means of automatic property checking. It is shown how this approach is a convenient and effective manner to analyse communication and coordination practices in crisis management and to evaluate what went wrong, where and when.

INTRODUCTION

Fast and effective emergency response is crucial for public safety in critical areas such as tunnels, but the coordination to realise this often fails. In the rare event of a crisis, various parties must be prepared to react in a timely, coordinated manner, which often does not occur. Crisis coordination problems are an international phenomenon. The catastrophic effects of Hurricane Katrina, that hit New Orleans in 2005, showed how fragmented distribution of new information impaired speedy response and how ineffective communication between disciplines incapacitated coherent decision making (Cooper and Block 2006; Comfort 2007). The disaster Hurricane Katrina became iconic because of its scale, but similar problems with crisis coordination occurred during smaller incidents. For example, the crash of a Turkish Airline Boeing 737-800 near Schiphol Amsterdam on 25 February 2009, revealed the problematic communication routines of the first responders (IOOV 2009). These cases illustrate that improved coordination strategies are needed. In the Netherlands, like in other countries, emergency services – fire fighters, police and medical services – are attempting to learn from failures in previous experience during incidents and accidents.

Rigid command and control structures currently in place cannot adapt quickly enough to the unpredictable events as they unfold. Research suggests that the military concept of Network-Centric Capabilities (NCC) could fulfil this need (Houghton et al. 2008; Moynihan 2009; Von Lubitz et al. 2008). These capabilities authorize first responders to decide faster, supported by communication systems that enable shared situational awareness (Gorman et al. 2006; Yang et al. 2009). In order to implement NCC and improve emergency response, coordination processes during crises must be better understood. Methods to analyse crises, however, are costly and time intensive.

This paper shows how a formal analysis, using automatic property checking, can provide a more efficient and practical method to study crisis coordination processes (e.g. Hoogendoorn et al. 2009). In general, empirical data is formalised in so called traces. These traces can be analysed automatically by checking if certain dynamic properties hold in the traces, via a software tool based on the Temporal Trace Language (Bosse et al. 2009). The case to illustrate this method is a dangerous fire incident that occurred on July 2nd 2009 in the train tunnel and underground train station of Amsterdam Airport Schiphol. Different modalities of crisis management could be studied by formal analysis, such as the beliefs and intentions of those involved, as is done in (Bosse et al. 2011). The current research focuses on actions and communications, because by using data from a public inquiry report (IVW and IOOV, 2009), actions and communications are the most accessible and they are essential to the emergency response problem. Others have focussed on the human reasoning process during incident management (Bosse et al. 2008) or on aviation incidents (Bosse and Mogles 2012). Communications relay information that must be shared timely and spread coherently in the overall network of involved parties. Furthermore, they are more reliable than beliefs and intentions, which are not clearly stated in the report.

Our research question is: How can automatic property checking be used in the formal analysis of coordination problems occurring in emergency response during crises? This question is answered by

Proceedings 26th European Conference on Modelling and Simulation ©ECMS Klaus G. Troitzsch, Michael Möhring, Ulf Lotzmann (Editors)
ISBN: 978-0-9564944-4-3 / ISBN: 978-0-9564944-5-0 (CD)

showing how our method indicates the measure of success of several key coordination features. These features refer to the time of response, disciplinary boundaries, and the quality of information sharing in the overall network. Emergency response must be effective in a short, specified period of time after the fire hazard arises. Information must be spread quickly across disciplinary boundaries to facilitate a common operational picture. Overall, the information network must support quick and effective decision making, where for example urgent requests prompt quick and adequate reactions.

The paper proceeds as follows. In Section 2, the Schiphol train tunnel fire case is briefly described on the basis of the public inquiry report (IVW and IOOV 2009). Section 3 details the formalisation process and the resulting formal trace. Section 4 explains the automatic property checking and its results. In the final section, we conclude what value this method has in the field of crisis management research.

SCHIPHOL TUNNEL FIRE

On July 2nd, 2009, an incident took place in the Schiphol train tunnel and station. Around 5:25 PM, dirt collecting in an open case just next to a railway track containing electrical wires began to smoulder, due to a spark released by the braking wheels of a passing train. The case was located in one of the two adjacent tubes on the side of Amsterdam city. Alarm calls went to the Schiphol Coordination Centre that was quick to mobilize airport fire and medical services. The remotely operating Railway Traffic Controller (RTC) also received reports about smoke from train conductors passing through the station, but was hesitant to declare an emergency. When signals and switches began to malfunction, three trains halted in the tunnel tube where the fire was, because of standard procedures in case of such malfunctions. A 'disturbance' emergency scenario was declared by the RTC and his back office. Coordination between the railway and emergency services occurred mostly through the railway Emergency Operations Coordinator (EOC) and the Airport Fire Officer (AFO). As a result of miscommunication, the three trains in the tunnel had to hold for over thirty minutes with increasingly anxious passengers (IVW and IOOV 2009). The AFO asked the regional dispatch room to relay to the Emergency Operations Director (EOD) a request to drive the trains out of the tunnel. This would create a safe space for the fire brigade, holding on the station's platform, to enter the tunnel and find the fire. Instead, the EOD asked the RTC to hold the trains where they were, because he thought the fire fighters were already in the tunnel. The exploring fire fighter crews, who could not find the origin of the fire, were surprised to find the trains standing in the tunnel. They asked for their immediate departure at 6:00 PM through their commanding AFO. He relayed this to the EOC, who was initially unable to pass the order through to the RTC, as he was on the phone with the technical department and had no additional phone lines. After receiving the message, starting at 6:05 PM the RTC ordered the trains out one by one, which took 15 minutes to complete. The fire had already died out by itself, and had not posed a real threat. Yet it had taken far longer than the critical 15 minutes to secure a safe evacuation of the passengers *or* to find and control the fire.

FORMALISATION OF CR ISIS M ANAGEMENT COMMUNICATION

In this section, the process of formalising the available data is addressed. First, the goal and content of the report, from which the data on the calamity in the Schiphol tunnel was extracted, is discussed. Then, the formalisation process and the resulting formal trace of the course of events are described.

The Public Inquiry Report

The public inquiry report on the calamity in the Schiphol tunnel (IVW and IOOV 2009) served as a basis for the analysis of the coordination problems during the emergency response. The investigation is reported for a dual reason: to inform the citizenry on the response to incidents in the public domain, and to advise organisations on measures to prevent similar incidents in the future.

Time	Dutch Railways	ProRail	Emergency Services	Other
17:40		Trdl meldt problemen aan Backoffice ProRail. Trdl besluit gestrande treinen in tunnel aan Amsterdamse zijde terug te sturen. Backoffice ProRail zorgt voor verdere alarmering instanties en hulpdiensten.		RC meldt incident aan MICK. RC meldt incident aan Kmar, AAS Havendienst, AAS DMS en AAS Operations manager.
17:41	Medewerker NS Reizigers meldt brand aan brandweer.		TAS 341 van Post Sloten uitgerukt.	Persoon op perron (medewerker NS Reizigers?) meldt brand aan brandweer via Veiligheidscentrale
17:42	Mcn tr 2169 overlegt met Trdl i.v.m. gedoofd sein.	Trdl geeft mcn tr 2169 opdracht te blijven staan.		KMar en BHV AAS besluiten tot ontruiming alle perrons Schiphol.

Figure 1: Fragment of the Chronology of Events in the IVW & IOOV Report (IVW and IOOV, 2009).

The report consists of several parts. First, factual information on the location, cause and risks of the fire incident is provided. For example, an estimation of the number of passengers that were stuck in the tunnel is provided, and the extent to which the Schiphol train tunnel meets the safety standards is assessed. In addition, an overview of the involved organisations and services and their responsibilities is included, together with a brief description of relevant procedures and protocols. Second, the course of events is described from different perspectives, namely from the perspective of ProRail, the Dutch organisation for maintenance of the national railway network infrastructure, the perspective of the Nationale

Spoorwegen (NS), the Dutch principal passenger railway operator, and from the perspective of the three main emergency services the police, fire fighters and medical services. These descriptions were also summarised in a table with a chronology of the most important events. (See Figure 1 for a fragment of this timeline.) Also, summaries of interviews with people from various organisations involved with the emergency response are provided. By this means, the adequacy of the response of each of the involved parties can be analysed and evaluated separately.

In the formalisation process, the three descriptions of the events during the calamity and the condensed timeline were used to extract the locations, actions and communications of the parties involved. Additionally, screenshots of the screens available to the railway traffic controller were used to determine the locations of the trains inside the tunnel tubes and alongside the platforms at the Schiphol train station.

FORMALISATION

In order to be able to check properties of the emergency response to the incident automatically, first a formal trace must be constructed. This process of formalising the textual description of the events into a computer-readable format equates translating the highly qualitative data into a combination of temporal logical and numerical statements (Bosse et al. 2009). In order to do so, the relevant actors, locations and concepts must be identified, and correspondingly an ontology should be specified. A partial specification of this domain ontology is provided in Table 1.

The main concepts used to formally describe the emergency response to the incident are *world states*, *observations* of information elements by agents, *communications* of information elements by agents to agents, and *actions* by agents. The world states include the locations of actors, the occurrences of signal and railroad switch malfunctions, and the belongs-to relations between actors and organisations. The observations state the information elements that agents perceived, and the communications state how one agent shared a certain information element with another agent. These communicated information elements concern, for example, locations of signs of fire, intentions for actions, requests for information, permission for actions, approvals of permissions, or isolated fragments of information, such as the fact that passengers are panicking or that the fire source is not found yet. Correspondingly, the actions concern, for example, entering and exploring the tunnel tubes by the fire fighter teams, evacuating the platforms, converting the trains in the tunnel tubes and vacating the tunnel.

Table 1: Partial Specification of the Domain Ontology

Predicate Inf	**ormal meaning**
world_state(I:INFO)	The information element I holds in the world.
observation(A:AGENT, I:INFO)	Agent A observes information element I.
communication_from_to(A:AGENT, B:AGENT, I:INFO)	Agent A communicates information element I to agent B.
performed(A:AGENT, ACT:ACTION)	Agent A performs action ACT.

Sort El	**ements**
AGENT	{RTC1, RTC2, CT756, CT3558, AFO, Schiphol_employee, CCS,…}
ORGANISATION	{ProRail, NS, Schiphol, Police, FireFighters, Medics, RMP, …}
LOCATION	{tunnel1A, tunnel2A, platform12, platform34, Schiphol_station, …}
ACTION	{dispatch_to(L:LOCATION), evacuate(L:LOCATION), convert_train…}
INFORMATION ELEMENT	{at_location(weak_signs_of_fire,platform34), request(info(situation), request(permission(enter(tunnel))), request(action(stop_train)), permission(vacate_tunnel), sign_clear(firefighters), panic_in_train, fire_source_not_found, …}

Using the ontology depicted in Table 1, the response to the Schiphol train tunnel incident was formalised in the software tool based on the language Leadsto (Bosse et al. 2005). This language is an extension of order-sorted predicate logic that allows for representation of both quantitative and logical data. Figure 2 is a screenshot of a fragment of the resulting trace, and Figure 3 shows the corresponding visualisation, where the presence of a black bar indicates that the statement is true at the corresponding time point. Each time interval in the trace represents half a minute.

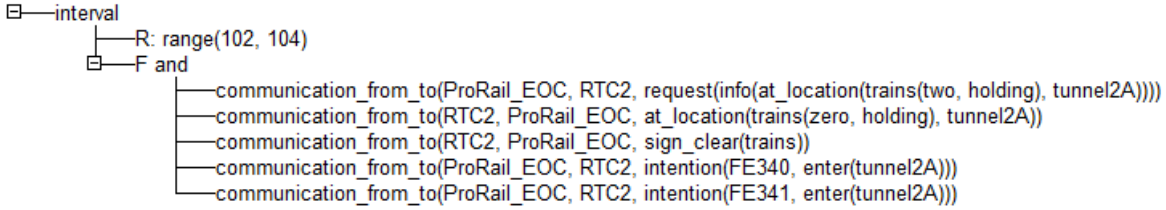

Figure 2: Fragment of Formal Trace

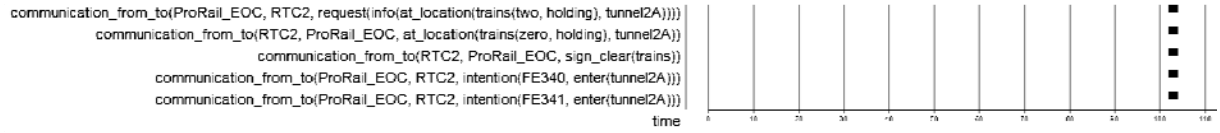

Figure 3: Fragment of Visualisation of Formal Trace.

Automatic Property Checking

This section addresses the analysis of the empirical trace of the fire incident in the Schiphol tunnel, by specification and verification of a number of dynamic properties that have been identified and formalized in the Temporal Trace Language (TTL) and were automatically checked (Bosse et al. 2009). Via a software tool based on TTL, it has been checked whether certain expected (dynamic) properties, expressed as statements in the TTL, hold for a given trace (defined as a time-indexed sequence of states). The purpose of checking the trace for these dynamic properties is to automatically check if important characteristics of net centric incident management hold in the empirical trace and if mistakes were made in communications and actions. This analysis is an innovative way to check for mistakes or find important characteristics of behaviour in the empirical data that is available during or after crisis management.

The TTL software environment includes a dedicated editor supporting specification of dynamic properties to obtain a formally represented temporal predicate logical language TTL formula. In addition, an automated checker is included that takes such a formula and a set of traces as input, and verifies automatically whether the formula holds for the traces. The language TTL is built on atoms referring to states of the world, time points and traces. In addition, dynamic properties are temporal predicate logic statements, that can be formulated with respect to traces based on a state ontology.

Below, a subset of the dynamic properties that were identified for the empirical trace of the fire incident in the Schiphol tunnel are introduced, both in semi-formal and informal notation (where state(γ, t) |= p denotes that state p holds in trace γ at time t). Only a subset of properties is shown, in order to keep the paper concise. Following every property, an evaluation on the empirical trace is discussed. See (Bosse et al. 2009) for more technical details. Properties P1A and B are analysing if the fire was under control on time and the evacuation was performed on time at the correct location. P2A to D are analysing the communications between organisations. P3A and B are analysing the time between requests for permission and the given permissions.

P1A – Fire_Under_Control _Within_15_Minutes

For all time points *t1* and *t2*, all AGENTS *a* and *b* in trace *γ*, if at *t1* there is a fire at location tunnel 2A and there is no earlier time point at which there is a fire at location tunnel2A, and at a later time point *t2*, AGENT *a* communicates to AGENT *b* that the fire is under control, then interval *i* = *t2-t1* and *i* ≤ 30.

P1A_FIRE_UNDER_CONTROL_WITHIN_15MINUTES ≡
∀*γ*:TRACE, ∀*t1*,*t2*:TIME, ∀*a*,*b*: AGENTS
state(*γ*, *t1*) |= world_state(at_location(fire, tunnel2A) &
∀*t0*:TIME < *t1* [state(*γ*,*t0*) |≠ world_state(at_location(fire, tunnel2A)] &
state(γ, *t2*) |= communication_from_to(*a*,*b*, fire_under_control) &
t1 ≤ *t2*
⇒
∃*i*:INTEGER
i = *t2-t1* &
i ≤ 30

Property P1A can be used to check whether the fire was under control within 15 minutes. This is important to check, because as long as it is not clear if it is a big fire or a small (self stopping) fire, the evacuation should be the first priority, in order to safe as many lives as possible. The result of checking this property in the TTL tool is that this property does not hold in the trace; a time gap of 125 intervals = 62.5 minutes was found between the start of the fire and the communication that the fire was under control.

P1B – Evacuation_Performed_Within_15_Minutes_At_Fire_Location

For all time points *t1* and *t2*, all AGENTS *a* and *b* in trace *γ*, if at *t1* there is a fire at location tunnel 2A and there is no earlier time point at which there is a fire at location tunnel 2A, and at a later time point *t2*, AGENT *a* communicates to AGENT *b* that the tunnel is clear of trains, then interval *i* = *t2-t1* and *i* ≤ 30.

P1B_EVACUATION_PERFORMED_WITHIN_15MINUTES_AT_FIRE_LOCATION ≡
∀*γ*:TRACE , ∀*t1*,*t2*:TIME, ∀*a*,*b*: AGENT
state(*γ*, *t1*) |= world_state(at_location(fire, tunnel2A) &
∀*t0*:TIME < *t1* [state(*γ*, *t0*) |≠ world_state(at_location(fire, tunnel2A)] &
state(*γ*, *t2*) |= communication_from_to(*a*,*b*, sign_clear(trains)) &
t1≤*t2*
⇒
∃*i*: INTEGER
i = *t2-t1* &
i ≤ 30

This property can be used to check whether the evacuation of the tunnel (fire location) was performed within 15 minutes. This property was not satisfied in the trace, because the time between the start of the fire and the evacuation of the tunnel was 55.5 minutes, since interval *i* = 111 time steps.

P2A – Communications_Between_Organisations
At time point *t* in trace *γ*, AGENT *a* communicates to another AGENT *b* INFO_ELEMENT *k*, and agent *a* belongs to an ORGANISATION *o1* and agent *b* belongs to an ORGANISATION *o2*, and *o1≠o2*.

P2A_COMMUNICATIONS_BETWEEN_ORGANISATIONS(*γ*:TRACE, *t*:TIME, *a,b*:AGENT, *k*:INFO_ELEMENT) ≡
∃*o1*, *o2*:ORGANISATION
state(*γ*, *t*) |= communication_from_to(*a*, *b*, *k*) &
state(*γ*, *t*) |= world_state(belongs_to(*a*, *o1*)) &
state(*γ*, *t*) |= world_state(belongs_to(*b*, *o2*)) &
o1 ≠ *o2*

P2B – Sum_Communications_Between_Organisations
For all traces *γ*, time points *t*, AGENT *a* and *b* and INFO_ELEMENT *k*, every time P2A holds, add 1 to the sum that starts with 0.

∀*γ*:TRACE, ∀*t*:TIME, ∀*a,b*:AGENT, *k*:INFO_ELEMENT
∃*n*: Σcase(
P2A_COMMUNICATIONS_BETWEEN_ORGANISATION(
γ, *t*, *a*, *b*, *k*), 1, 0) = *n*

P2C – Communications_Within_Organisations
At time point *t* in trace *γ*, AGENT *a* communicates INFO_ELEMENT *k* to another AGENT *b*, and agent *a* belongs to an ORGANISATION *o1* and agent *b* belongs to an ORGANISATION *o2*, and *o1=o2*.

P2C_COMMUNICATIONS_WITHIN_ORGANISATIONS(*γ*:TRACE, *t*:TIME, *a,b*:AGENT, *k*:INFO_ELEMENT) ≡
∃*o1*, *o2*:ORGANISATION
state(*γ*, *t*) |= communication_from_to(*a*, *b*, *k*) &
state(*γ*, *t*) |= world_state(belongs_to(*a*, *o1*)) &
state(*γ*, *t*) |= world_state(belongs_to(*b*, *o2*)) &
o1 = *o2*

P2D – Sum_Communications_Within_Organisations
For all traces *γ*, time points *t*, AGENT *a* and *b* and INFO_ELEMENT *k*, every time P2C holds, add 1 to the sum that starts with 0.

∀*γ*:TRACE, ∀*t*:TIME, ∀*a,b*:AGENT, *k*:INFO_ELEMENT
∃*n*: Σcase(
P2C_COMMUNICATIONS_WITHIN_ORGANISATION(
γ, *t*, *a*, *b*, *k*), 1, 0) = *n*

Properties P2A and P2C check whether there exists a certain communication k between agent a and b. Properties P2B and P2D, respectively count the number of times P2A or P2C hold in the trace. This way, the number of times that there are communications between agents of different organizations and of the same organization, are counted. This is useful information, because the ratio can give an insight in the quality of information sharing between organisations – one of the characteristics of a net centric approach to incident management. The result for the Schiphol trace is that there are 120 communications between organizations and 103 communications within organizations.

P3A – Time_Between_RequestPermission_And_Permission_To_Enter_Tunnel1A
For all time points *t1* and *t2* and all AGENTS *a* and *b* in trace *γ*, if at *t1* agent *a* requests to enter tunnel1A_north to agent *b* and at a later time point *t2*, agent *b* communicates a permission to enter tunnel 1A_north to agent *a*, then interval *i = t2 - t1*.

P3A_TIME_BETWEEN_REQUESTPERMISSION_AND_PERMISSION_TO_ENTER_TUNNEL1A ≡
∀*γ*:TRACE , ∀*t1,t2*:INTEGER, ∀*a,b*: AGENT
state(*γ*, *t1*) |= communication_from_to(*a*, *b*, request(permission(enter(tunnel1A_north)))) &
state(*γ*, *t2*) |= communication_from_to(*b*, *a*, permission(enter(tunnel1A_north))) &
t1 < *t2*
⇒
∃*i*:interval
i = *t2* - *t1*

P3B – Time_Bet ween_RequestPermission_And_Permission_To_Vacate_Tunnel
For all time points *t1* and *t2* and all AGENTS *a* and *b* in trace *γ*, if at *t1* agent *a* requests a permission to vacate the tunnel to agent *b* and at a later time point *t2*, agent *b* communicates a permission to vacate the tunnel to agent *a*, then interval *i = t2 - t1*.

P3B_TIME_BETWEEN_REQUESTPERMISSION_AND_PERMISSION_TO_VACATE_TUNNEL ≡
∀*γ*:TRACE , ∃*t1,t2*:INTEGER, ∀*a,b*: AGENT
state(γ, *t1*) |= communication_from_to(*a*, *b*, request(permission(vacate_tunnel))) &
state(γ, *t2*) |= communication_from_to(*b*, *a*, permission(vacate_tunnel)) &
t1 < *t2*
⇒
∃*i*:interval
i = *t2* - *t1*

The properties P3A en P3B check how much time elapses between a request for permission and the permission. Property P3A holds for 1 time step = 30 seconds and P3B holds for 14 time steps = 7 minutes.

In sum, automatic property checking indicated that the fire was not under control within 15 minutes and that the evacuation was not performed on the correct fire location within 15 minutes. These results show that the fire incident was a near miss situation: if the fire would not have gone out by itself, people stuck in the trains in tunnel 2A could have died. Furthermore, there were more communications between organizations than within organizations in our trace. However, the communications within organizations were partially neglected, because these organizations were black-boxed in the report. Therefore, one should be cautious to draw conclusions upon these numbers. With regard to the permissions, one can see that the permission to evacuate the tunnel was relatively time expensive, due to the fact that this was a next step in the whole procedure, whereas the decision to enter the tunnel already was part of the action and followed immediately after the request.

DISCUSSION

The goal of this paper was to show how automatic property checking can be a more efficient and practical method to study crisis coordination processes. Communications and actions during the fire incident that occurred on July 2nd 2009 in the train tunnel and underground train station of Amsterdam Airport

Schiphol were analysed. Although this fire turned out to be harmless, the organisations involved in the emergency response proved to be ill-prepared for a serious fire that could occur in any tunnel. A serious, explosively growing tunnel fire can be lethal within 15 minutes. Automatic property checking showed that fire was not under control on time and that the evacuation was not performed within 15 minutes on the exact fire location and the permission to evacuate the tunnel was relatively time expensive.

Overall, according to a net centric approach, the information network must support quick and effective decision making, where for example urgent requests prompt quick and adequate reactions. Understanding critical communication processes can then assist in simulating and providing advice about more effective communication strategies that meet currently unfulfilled needs in both practice and research. Research is predominantly focussed on organisational structures, but decision making in crises occurs ad-hoc and under conditions of significant chaos. In such situations, adaptive communication strategies are needed. Current procedures specify rigid communication links within organisational disciplines, where only higher ranking officials coordinate between the parties involved. In practice, this leads to a fragmented spreading of information in the network of people involved in the crisis response. Information travels along lengthy, inefficient communication chains. New information, including requests and permissions to take urgent actions, takes long to travel and often goes lost. The properties in our analysis were designed to indicate where in the formal trace of the events these processes succeed or require the development of alternative communication strategies drawing on NCC. The results show where in the trace of events the communication went wrong and indicate that there is room for improvement, namely following a more net centric communication strategy.

Although the current research shows that automatic property checking can be a more efficient and practical method to study crisis coordination processes, the current formalisation process still requires a lot of hours work. Part of future work is to make this process automated to save time. Other future work concerns planned comparisons of the formalised data of the Schiphol fire incident with agent-based simulations according to a more net centric approach. The (dynamic) properties from Section 4, amongst others, can then be used again. Since the TTL tool can take both simulated and empirical traces as input, it can be used to check (automatically) whether the generated simulation runs show similar patterns to the real world transcripts.

Finally, since there are lots of incidents all over the world, more case studies can be used to validate the proposed approach. This research contributes to previous work mentioned in this area (e.g. Hoogendoorn et.al 2008; Boss et al. 2008; Bosse et al. 2009; Bosse et al. 2011, Bosse and Mogles 2012).

ACKNOWLEDGEMENTS

This research is part of: (1) the interdisciplinary program of the Royal Netherlands Academy of Arts and Sciences (KNAW), in which student assistants conduct innovative research into communication in real-life and virtual social networks. We would like to thank prof. dr. Peter Groenewegen, leader of the program, and dr. Tibor Bosse for their useful comments and guidance. (2) the FP7 ICT Future Enabling Technologies program of the European Commission under grant agreement No. 231288 (SOCIONICAL).

REFERENCES

Bosse, T., Chandra, V., Mitleton-Kelly, E., and Wal, C.N., van der. 2011. *"*Analysis of Beliefs of Survivors of the 7-7 London Bombings: Application of a Formal Model for Contagion of Mental States*"*. In: Lu, B., Zhang, L., and Kwok, J. (eds.), *Proceedings of the 18th International Conference on Neural Information Processing, ICONIP'11, Part I. Lecture Notes in Computer Science*, Vol. 7062, Springer Verlag, 423-434.

Bosse, T., Hoogendoorn, M., Jonker, C.M., and Treur, J. 2008. "A Formal Method to Analyze Human Reasoning and Interpretation in Incident Management". *International Journal of Emergency Management*, Vol. 5, Issue 1/2, 164-192.

Bosse, T., Jonker, C.M., Meij, L. van der, and Treur, J. 2005. "LEADSTO: A Language and Environment for Analysis of Dynamics by SimulaTiOn". *Lecture Notes in Computer Science: Multiagent System Technologies*, Vol.3550, Springer Verlag, 165-178.

Bosse, T., Jonker, C.M., Meij, L. van der, Sharpanskykh, A., and Treur, J. 2009. "Specification and Verification of Dynamics in Agent Models". *Int. Journal of Cooperative Information Systems*, No. 18, 167-1193.

Bosse, T. and Mogles, N. 2012. "Formal Analysis of Aviation Incidents". In: *Proceedings of the 25th International Conference on Industrial, Engineering & Other Applications of Applied Intelligent Systems, IEA/AIE'12*. Springer Verlag, to appear,

Comfort, L.K. 2007. "Crisis management in Hindsight: Cognition, communication, coordination, and control". *Public Administration Review,* No. 67, 189-197.

Cooper, C., Block, R.J. 2006. *Disaster: Hurricane Katrina and the Failure of Homeland Security.* Holt, Henry & Company, Inc.: Times Book.

Gorman, J.C., Cooke, N.J. and Winner, J.L. 2006. "Measuring team situation awareness in decentralized command and control environments". *Ergonomics,* No. 49(12-13), 1312-1325.

Hoogendoorn, M., Jonker, C.M., Treur, J., and Verhaegh, M. 2009. "Agent-Based Analysis and Support for Incident Management". *Safety Science Journal,* Vol. *47*, 1163–1174.

Houghton, R.J., Baber, C. Cowton, M. Walker, G.H. and Stanton, N.A. 2008. "WESTT (workload, error, situational awareness, time and teamwork): an analytical prototyping system for command and control". *Cognition, Technology and Work*, No. 10, 199-207.

IOOV. 2009. *Poldercrash 25 februari 2009. Een onderzoek door de Inspectie Openbare Orde en Veiligheid, in samenwerking met de Inspectie voor de Gezondheidszorg*. Den Haag: Ministerie Binnenlandse Zaken en Koninkrijksrelaties.

IVW and IOOV. 2009. *Calamiteit in de Schiphol spoortunnel. Onderzoek naar de afhandeling van een brandmelding op 2 juli 2009*. Den Haag Ministerie Binnenlandse Zaken en Koninkrijksrelaties.

Moynihan, D.P. 2009. "The network governance of crisis response: case studies of incident command systems" *Journal of Public Administration Research Theory*, No. 19, 895-915.

Von Lubitz, D.K.J.E., Beakley, J.E. and Patricelli, F. 2008. "Disaster Management: The Structure, Function, and Significance of Network-Centric Operations". *Journal of Homeland Security and Emergency Management*, No. 5(2), 1-24.

Yang, L., Prasanna, R. and King, M. 2009. "Situation awareness oriented user interface design for fire emergency response". *Journal of Emergency Management,* No. 7(2), 65-74.

AUTHOR BIOGRAPHIES

KEES BOE RSMA is an Associate Professor of Organization Studies at the Faculty of Social Sciences of the VU University Amsterdam. He is interested in crisis management and safety response, and in surveillance practices. He uses theories from knowledge management, organizational culture, and high reliable organizations. He published in amongst others *Human Relations*, *Business History* and in *Development and Change*. His e-mail address is: `f.k.boersma@vu.nl` and his Webpage can be found at `http://www.keesboersma.com/`.

JULIA MOLLEE studied Artificial Intelligence at the VU University Amsterdam and obtained her Bachelor's degree (cum laude) in 2010. Currently, she is completing her Master's program in Artificial Intelligence in the specialization Human Ambience. Also, she is employed as a research assistant at the interdisciplinary research project of the Royal Netherlands Academy of Arts and Sciences (KNAW), where she investigates methods to combine computer science and social science to study emergency responses to crisis situation. Her e-mail address is: `j.s.mollee@vu.nl`.

DAVID PAS SENIER is currently an Organisation Science graduate student at the VU University Amsterdam. After obtaining his pilot license at the age of 17, he followed several courses in Aerospace Engineering and was subsequently trained as organisational ethnographer. He intends to continue doing research on aviation safety and contribute to resilient systems thinking and practice. He worked as a research assistant in the research project of the Royal Netherlands Academy of Arts and Sciences (KNAW), contributing to an interdisciplinary approach for studying emergency response to crises. His e-mail address is: `d.f.passenier@vu.nl`.

C. NATALIE VA N D ER WAL is a researcher and lecturer in Artificial Intelligence at the VU University Amsterdam. She finished her dissertation on Agent-Based Modelling of Integrated Internal Social Dynamics of Cognitive and Affective Processes in 2012. She received her Master's degree (cum laude) in Artificial Intelligence, graduating on the topic of 'Modeling Agent-Based Support Systems for Group Emotion and Group Development' in 2009. She also received a Bachelor's Degree in Cognitive and Clinical Neuropsychology in 2007 and a Master's Degree in Media and Culture in 2003. Her research interests are modeling dynamics of agent systems in practical application areas, social diffusion of information and emotion, psychological disorders and treatments. Her e-mail address is: `c.n.vander.wal@vu.nl` and her Web-page can be found at `http://www.few.vu.nl/~cwl210/`.

Analysis of Different Search Metrics Used in Multi-Agent-based Identification Environment

Sebastian Bohlmann**, Arne Klauke**, Volkhard Klinger**, Helena Szczerbicka*
*Department of Simulation and Modelling Leibniz University Hannover
30167 Hannover, Germany
Email: {hsz}@sim.uni-hannover.de
**Department of Embedded Systems FHDW Hannover
30173 Hannover, Germany
Email: {sebastian.bohlmann,arne.klauke,volkhard.klinger}@fhdw.de

***Abstract*—Process data-based system identification is one great challenge in technical process modelling and simulation. In this paper we continue our former work presented in [1], [3] and concentrate on the analysis and evaluation of both the data preprocessing and different search metrics used in the multi-agent-based optimization algorithm. This analysis helps to review and benchmark the impact on different preprocessing steps as well as the influence of the selected search metrics. Based on this evaluation we are able to verify the correct and target-oriented identification procedure.**

***Keywords*-system identification, agent-based evolutionary computation, memetic optimization algorithms**

I. Introduction

Modelling and simulating complex process models of manufacturing systems are grand challenges for science and engineering. With regard to the number of influencing variables, like power efficiency, ecological boundary conditions or product quality, process understanding is the key feature for improving the manufacturing process itself. Due to the empiric character of process description, process modelling is one of the fundamental challenges for the profound knowledge of these technical or manufacturing processes. Based on such a model, described by the combination of physical equations and a graph structure, simulation allows the reconstruction of process behaviour and therefore the optimization of the entire process [1]. This identification frame is part of the Hybrid Process Net Simulator-framework (HPNS), described in subsection I-B [2], [4]. The objectives of this framework are to identify models for the simulation and optimization of processes, especially manufacturing and industrial processes. In the following subsections we present our reference process environment and the HPNS framework.

A. The Process Environment: Specific Problems In Industrial Paper Manufacturing

The pulp and paper industry as one application example is a qualified process with regard to large system requirements [9]. There are thousands of continuous and discrete signals describing the behaviour and states of the different subsystems. Hundreds of control loops and relations exist in between these subsystems. There are many backpropagations of state changes and there is almost no separation between the different process steps. For this process no detailed model exists, which could for example provide an evaluation of the process quality. Manufacturing steps have been developed empirically over decades. Therefore up to now techniques able to optimize the manufacturing process have scarcely been used. Two of these techniques are soft sensors and model predictive control [1].

B. HPNS framework including the process identification

Optimization problems are omnipresent in engineering and science. The technical background discussed in this paper, paper manufacturing, is one excellent instance. Instead of a lot of expertise regarding particular process parts, the overall knowledge about the process interrelationship is not sufficient. So, the data-based process model identification with physical equations seems to be the only solution for establishing a precise process model. Based on the constraints and requirements considered, the HPNS framework [1] provides certain functional frames to realize the process identification. The key issue here is the identification frame, represented in Figure 1.

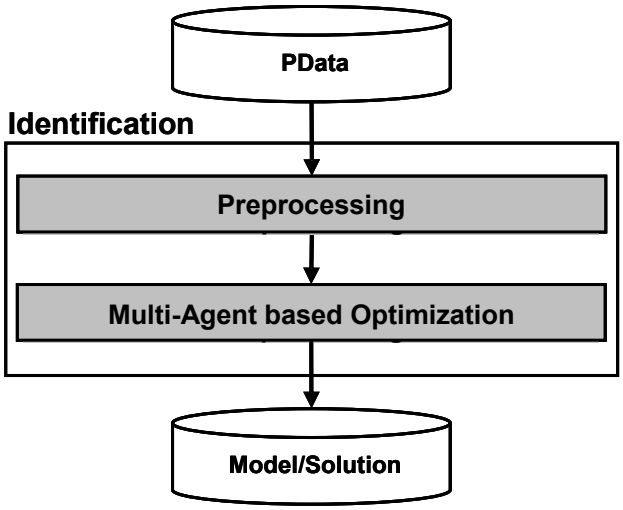

Figure 1. HPNS identification frame

The HPNS framework requires a process model as described above. The identification frame provides a model design flow, based on the historical process data archive

Proceedings 26th European Conference on Modelling and Simulation ©ECMS Klaus G. Troitzsch, Michael Möhring, Ulf Lotzmann (Editors)
ISBN: 978-0-9564944-4-3 / ISBN: 978-0-9564944-5-0 (CD)

on the running manufacturing process. While the interrelationship between the online data and the archive is not under focus here, in the following text we will call the data from all data sources process data (PData).

The data-based process identification is based on evolutionary computation and multi-strategy learning. Formerly, optimization techniques based on linear programming or branch and bound strategies have been used to solve such types of problems. In recent years agent-based computing providing evolutionary algorithms seem to be the most promising approach.

A process model is the basic requirement for successfully modelling and simulation. We are using the manufacturing process data cached by a stream database. It is transformed by an identification step to establish the model for the HPNS-framework [1], [3], [4]. It uses the symbiotic simulation approach to provide an online/offline process simulation to enable forward-looking properties like an online prediction mode.

In figure 1 we have seen the system identification overview. It consists of two basic steps, the preprocessing and the multi-agent based optimization. The PData input is used to generate an appropriate process model [6]. To verify this identification procedure we have to evaluate the different steps very carefully not only to its technically correct function but on its performance behaviour.

Here we focus on the evaluation of the data preprocessing and of different search metrics to compare their impact with regard to the quality and performance of the optimization phase. To be able to allow a meaningful evalution we are working in the following with synthetic data sets. The verification strategy is based on a set of these synthetic data sequences $(x_1)_t, \ldots, (x_m)_t$, $t \in \mathbb{N}$, called *Input Sequences* and sequences $(y_1)_t, \ldots, (y_j)_t$, $t \in \mathbb{N}$, called *Output Sequences*, which are related to the Input Sequences by functional relationships $f\colon \mathbb{R}^m \to \mathbb{R}^j$, illustrated in figure 2:

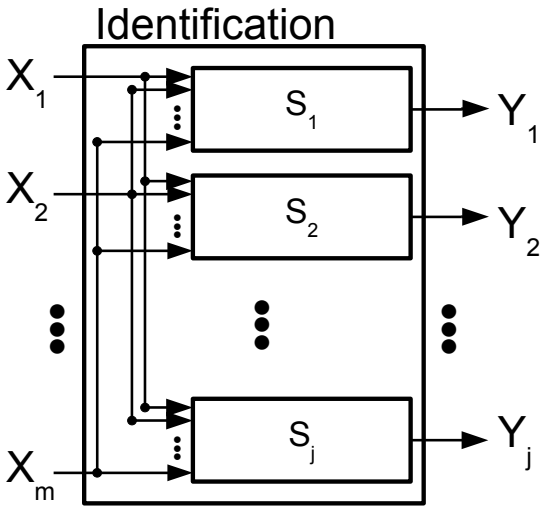

Figure 2. HPNS identification frame

$$f_1\left((x_1)_t, \ldots, (x_m)_t\right) = (y_1)_t,\ t \in \mathbb{N}$$
$$\vdots$$
$$f_j\left((x_1)_t, \ldots, (x_m)_t\right) = (y_j)_t,\ t \in \mathbb{N}$$

In figure 3 an example for $m = 10$ and $j = 1$ is shown. The problem we are solving is to identify this function f, only knowing values of $(x_1)_t, \ldots, (x_m)_t$ (thin lines) and $(y)_t$ (thick line) for a limited set $T \subset \mathbb{N}$ of time indices, which may differ for each sequence. In this paper we are treating only problems with $j = 1$.

Our approach for this challange is formed by the identification framework used for process modell identification and it uses the data management framework presented in [4]. The preprocessing is followed by a Multi-Agent-based Learning Strategy (II-B) using evolutionary-memetic algorithms. In this paper we focus on the so-called *Search Metrics* (III) the agents use to measure the quality of their approximation for f. We will examine different types of metrics, to see which kind is the most suitable for our problem.

II. System Architecture

In this section we give a short overview of our System Architecture with regard to the system verification approach. It consists according to 1 of two main parts: The Data Preprocessing and a Multi-Agent-based Learning Environment.

A. Data Preprocessing

The agents operate on data fields, called planets, of the predetermined size $n = 9^3 = 729$. The objective of the Data Preprocessing is to fill these planets with data samples providing a high average information content, so called data entropy. It splits up in the following steps, shown in the upper half of figure 4.

1) Data Factory: First of all we have to produce the synthetic data sequences described in section I. To do so, we build random data streams for the Input Sequences and choose an appropriate generator function f to calculate the Output Sequence. Then we build the subsets $T \in \mathbb{N}$ for

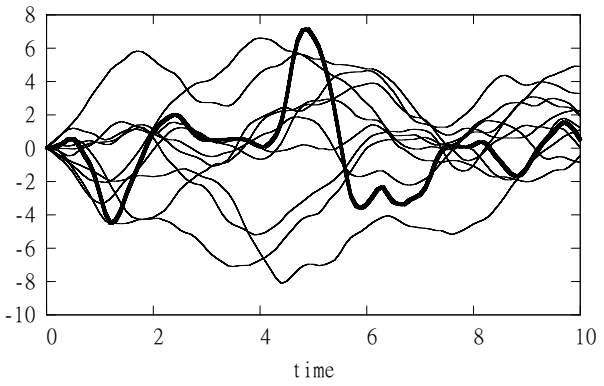

Figure 3. Input and output data series

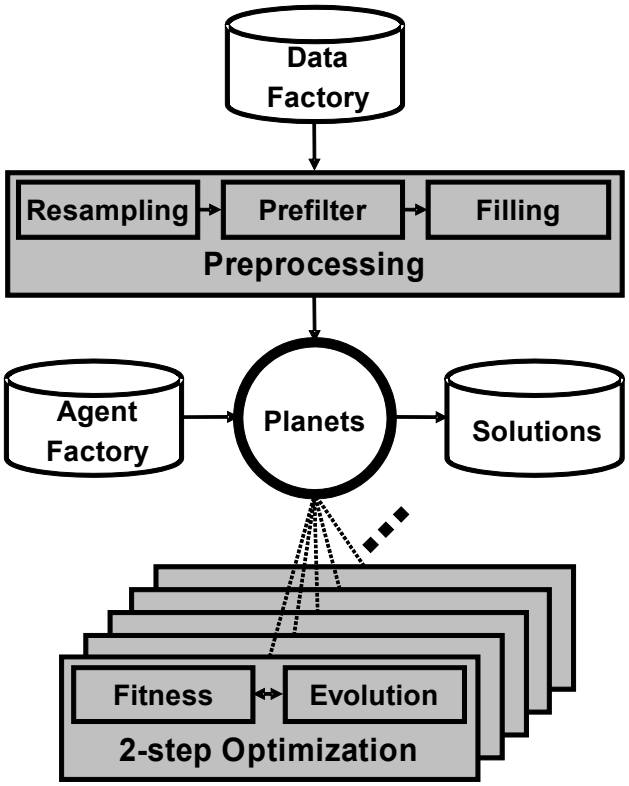

Figure 4. System overview

which we pass the information to our system, in order to imitate the incomplete information one has in real data.

2) Resampling: The data produced in the Data Factory has two main weaknesses: The samples are asynchronous and aperiodic. In order to get a time series of data samples we perform the following steps:

- Interpolation and FIR Filter (finite impulse response)
  For each sequence we interpolate the given values and smooth the result with a convolution.
- Error Correction
  The interpolated data is equalized with the original samples gained from the Data Factory.
- Downsampling
  We pick euklidian equidistant samples from each sequence and combine them to data samples with a timestamp.

During the learning process the data samples will not stay in their chronological ordering. To be able to perform time derivation, it is necessary to save the chronological neighbors for each sample.

After these two initial steps we have build a time series of equidistant data samples p each of which consists of a timestamp p_{time}, a vector $p_{\mathrm{data}} = [p_{\mathrm{out}}, p_{\mathrm{in}}]$, with $p_{\mathrm{out}} \in \mathbb{R}$ and $p_{\mathrm{in}} \in \mathbb{R}^m$, containing the output and input data and its chronological neighbors p^{pre} and p^{post}. With P we denote the set of all such data samples. Furthermore we define $p_{\mathrm{in}}^{\Delta} \in \mathbb{R}^m$ with

$$(p_{\mathrm{in}}^{\Delta})_j := \frac{1}{2}\left(\frac{(p_{\mathrm{in}})_j - (p_{\mathrm{in}}^{\mathrm{pre}})_j}{p_{\mathrm{time}} - p_{\mathrm{time}}^{\mathrm{pre}}} + \frac{(p_{\mathrm{in}})_j - (p_{\mathrm{in}}^{\mathrm{post}})_j}{p_{\mathrm{time}} - p_{\mathrm{time}}^{\mathrm{post}}}\right)$$

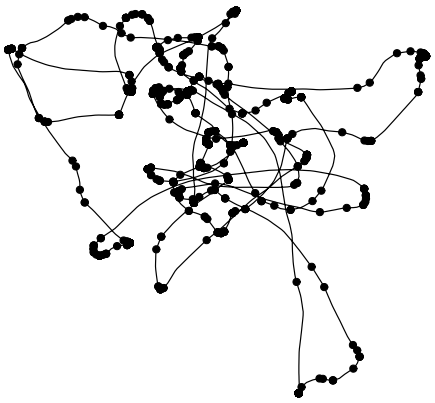

Figure 5. Weighted Random Prefilter: Samples in curved areas are chosen with a higher probability.

$$p_{\mathrm{out}}^{\Delta} := \frac{1}{2}\left(\frac{p_{\mathrm{in}} - p_{\mathrm{in}}^{\mathrm{pre}}}{p_{\mathrm{time}} - p_{\mathrm{time}}^{\mathrm{pre}}} + \frac{p_{\mathrm{in}} - p_{\mathrm{in}}^{\mathrm{post}}}{p_{\mathrm{time}} - p_{\mathrm{time}}^{\mathrm{post}}}\right).$$

3) Data Prefilter: In general the amount of data delivered by the data factory is too large for our framework, that is providing planets of a predetermined size. To choose the samples, which should be passed to the planets, we are using four different techniques.

No Prefilter The last 729 samples are passed to the planets.

Random Prefilter We choose the samples randomly. This approach serves as a reference, the other, more expensive techniques have to compete with.

Weighted Random Prefilter The samples are again chosen randomly, but the samples are chosen with different probabilities. This probability corresponds to the angle between $p_{\mathrm{in}}^{\mathrm{pre}} - p_{\mathrm{in}}$ and $p_{\mathrm{in}}^{\mathrm{post}} - p_{\mathrm{in}}$. The smaller this angle is, the more likely the sample is passed to the planets (figure 5).

k-means Prefilter We are are using a cluster algorithm to chose the samples. We have chosen *k-means* [5] for two reasons. With k-means we are able to determine the number of clusters to be build in a set of data, i.e. the data rate. Moreover the clusters generated by this algorithm are formed spherical, what is more suitable for our purpose, compared to e.g. density based clusters. We subdivided the data from the data factory in blocks. In each of these blocks we build a fixed number of clusters. Only the centers of these clusters were passed on.

4) Data Filling: In the last step of the data preprocessing the data samples are arranged on a 2D surface of a so-called planet (see Figure 6). The surface of the planets is built in a recursive pattern of squares containing nine elements, filled meander like. This method leads to the planet size $9^3 = 729$. This arrangement has the advantage, that the data set used for the local optimization consists of data samples, which may be spread more wideley across the input sequences.

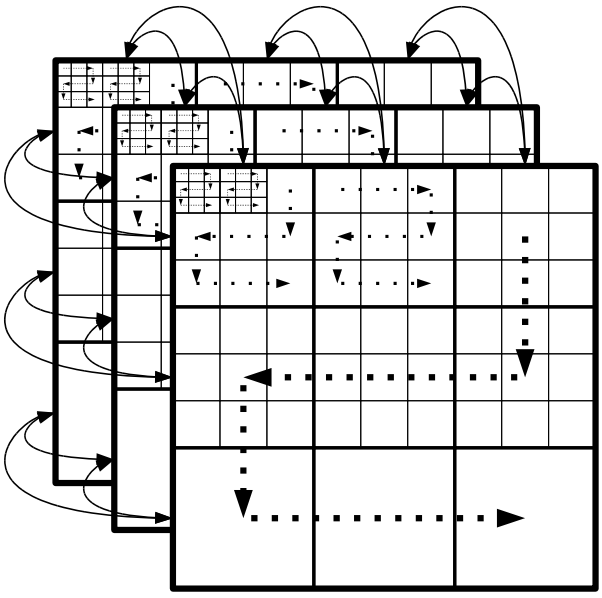

Figure 6. Planet-based data mapping and inter-planet paths

B. Multi-Agent-based Learning Strategy

The lower part of figure 4 contains the planets, the agent factory for filling the planets due to the planet configuration and the 2-step optimization algorithm dedicated to every planet.

1) Agent Description: The agents have 4 essential features: an age, an energy level, an area and their model function mf, approximating f. Moreover a replication mechanism is implemented, meaning the agents are able to produce a child and put it on an area. The age and the energy level are increased after each iteration. All operations an agent can perform, have an energy effort, by which the energy level is lowered, if the operation is executed. The area provides data samples to learn from and calculate the error of the model function. The model function $\mathrm{mf}\colon \mathbb{R}^m \to \mathbb{R}$ is stored in a tree representation (figure 7). This function is composed of elementary operations [8]. In the current test configuration the agents are allowed to use $\sin, +, *, /$ the variables $x_1, \ldots, x_m$ and a set of parameters within their model function. Furthermore the agents have the ability to learn from their local data and improve their model function by executing different *evolutionary operations* to change the structure of the model function, described in II-B2, and a local optimization algorithm to calibrate the parameters.

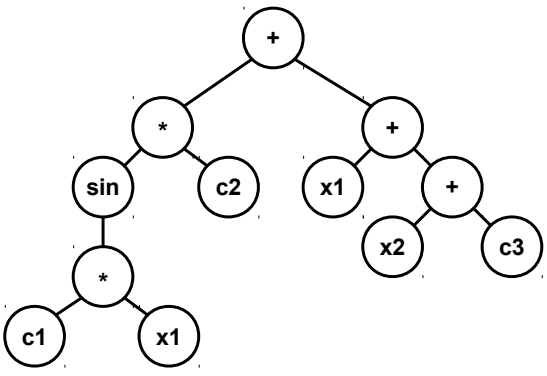

Figure 7. A tree representation of $c_2 \sin(c_1 x_1) + x_1 + x_2 + c_3$

In each iteration the software agents perform the following operations:

- *Calculate Fitness* The individual evaluates the error of his model function with respect to a chosen metric. According to this error the energy level is recalibrated. If it is negative, the agent is removed from the planet and his child, if present, is put on his position.
- *Move* The agent moves to another area, meaning the local test data he uses is modified, so that he can use new data in the next iteration. If the agent carries a child it is set to the former area. Agents in a multi planet system can travel with a small probability to different planets.
- *Local Optimization* The model functions parameters are improved by trying to reduce the error of the current local data with respect to the chosen search metric.
- *Evolutionary Operation* One of the evolutionary operations, explained below, is performed.
- *Nomination* The agents elect a few individuals with the highest fitness values and age on each planet. Next the global fitness value of these agents is calculated. The 25 best agents form the so-called *Elite Population*, containing the best dissimilar agents. The model function of the elite agents are evaluated on the whole data set. If any of these functions has an error below a certain error bound, the algorithm terminates and this function is returned. Copies of these agents are then spread across all planets to distribute their information to other agents.

2) Evolutionary Operations: The agents can perform four different evolutionary operations to produce a child:

- *Mutation* The agents model function gets changed randomly: Either a subtree of the model function is exchanged or new operations are inserted.
- *Crossover* When an agent moves it may happen that the chosen area is allready occupied with another individual. If that is the case, a subtree of the individuals model function is replaced by a randomly chosen, suitable subtree of the other agents model function.
- *Replication* The agent duplicates himself.
- *Global Optimization* The agents, which own enough energy or are not adult yet, optimize the parameters of their model function in the Memetic Coprocessor, explained below.

3) Memetic Coprocessors: The algorithm chosen for the *local* parameter optimization is resource-saving, because it is executed for all agents in every iteration. In

the Memetic Coprocessors, running on an extra processor core, we are executing more sophisticated algorithms for a *global* optimazation. In the current configuration we use a downhill-simplex algorithm [7].

C. Parallelization

Our framework provides the capability of running the evolutionary algorithm described above on several planets at the same time. If this is the case, some of the areas on each planet get marked as so called beam areas. After each iteration copies of all individuals placed on such an area are send to a randomly chosen area on a randomly chosen planet, provided the chosen area is not yet occupied by an agent. In the experiments 3 of the 729 areas on every planet were marked as beam areas. Our implementation associates each planet to one processor core, on an additional processor core a universe supervisor is executed. This supervisor manages the elite population using the data from all planets and controls the termination condition. The information exchange between the cores is implemented via a non-blocking Message Passing Interface.

III. Search Metrics

The agents can use different metrics serving as a measure for the error of their model functions mf. For a single data sample $p \in P$ we can calculate the error of the model function with these functions:

$$\mathrm{Abs}(p, \mathrm{mf}) := |p_{\mathrm{out}} - \mathrm{mf}(p_{\mathrm{in}})|$$

$$\mathrm{Euk}(p, \mathrm{mf}) := (p_{\mathrm{out}} - \mathrm{mf}(p_{\mathrm{in}}))^2$$

$$\mathrm{Log}(p, \mathrm{mf}) := \ln(1 + \mathrm{Abs}(p, \mathrm{mf}))$$

For an indexed subset $F \subset P$ we aggregate these values using

$$\mathrm{Mean}_f(F) := \frac{1}{|F|} \sum_{p \in F} f(\mathrm{mf}, p)$$

$$\mathrm{Max}_f(F) := \max_{p \in F} f(\mathrm{mf}, p)$$

$$\mathrm{PartialMean}_f(F) := \mathrm{Mean}_f(\bar{F})$$

$$\mathrm{PartialMax}_f(F) := \mathrm{Max}_f(\bar{F})$$

where f is one of the three functions described above and $\bar{F} \subset F$ is a set of randomly chosen data samples, with $|\bar{F}| = \lfloor \frac{1}{5}|F| \rfloor$.

For the next metric $\mathrm{CSDelta}(F)$ we choose a small offset $\delta \in \mathbb{R}_{\geq 0}$ and define $\delta_i \in \mathbb{R}^m$ to be the vector containing only zeros except for a δ at the i-th position and set $h = \lfloor \frac{|F|-1}{2} \rfloor$. With that vector we define:

$$K_{d,i}(F) := \left| \frac{(p_h)^{\Delta}_{\mathrm{out}}}{((p_i)^{\Delta}_{\mathrm{in}})_d} - \frac{\mathrm{mf}((p_h)_{\mathrm{in}}) - \mathrm{mf}((p_i)_{\mathrm{in}} + \delta_d)}{\mathrm{mf}((p_h)_{\mathrm{in}}) - \mathrm{mf}((p_h)_{\mathrm{in}} + \delta_d)} \right|$$

In most cases not all of the variables $x_1, \ldots, x_m$ are actually used in the model function. The function u pics the dimensions, which are really of interest:

$$\mathrm{u}(d) := \begin{cases} 1, & \text{if } x_d \text{ is used in } \mathrm{mf} \\ 0, & \text{else} \end{cases}$$

With $K_{d,i}$ and u we can define R:

$$R(F) := \sum_{d=1}^{m} \mathrm{u}(d) \left(\sum_{i=0}^{h-1} (K_{i,d}(F) + \mathrm{Abs}(p_i)) \right)$$

and

$$m := |F| \cdot \mathrm{Mean}_{\mathrm{Abs}}(F).$$

Finally we define CSDelta by:

$$\mathrm{CSDelta}(F) := \frac{R(F)\,(R(F) + m)}{|F|}$$

In the next section we discuss the influence of these metrics.

IV. Experiments

For all experiments we present in the following subsections the hardware configuration, the setup and the specific results.

A. Hardware

All experiments are executed on a Dell PowerEdge R815 with in total 4 AMD Opteron 6174 processors (each providing 12 cores with respectively 128KByte L1-cache, 512 KByte L2-cache and common 12 MByte L3-cache) and an overall RAM configuration of 128 GByte. For the parallelization evaluation this platform provides a scalable hardware environment.

B. Setup

In all experiments we used $f = 8\sin(2x_1) + x_1 + x_2 + 65$ as the generator function and produced 10 data input sequences with 100,000 elements each. We ran 100 iterations of all experiments with 8 Planets. We terminated a run, if the mean error became smaller than 0.001 or the runtime exceeded 15 minutes.

1) Prefilter: Moreover we started experiments in which we exchanged the prefilter module. We ran experiments with all prefilters described in (II-A3). In these experiments we used the $\mathrm{Mean}_{\mathrm{Euk}}$ metric.

2) Metrics: In a first set of experiments we studied the influence of the search metrics listed below.

- $\mathrm{Mean}_{\mathrm{Euk}}$
- $\mathrm{Max}_{\mathrm{Euk}}$
- $\mathrm{Mean}_{\mathrm{Abs}}$
- $\mathrm{Max}_{\mathrm{Abs}}$
- $\mathrm{PartialMean}_{\mathrm{Abs}}$
- $\mathrm{PartialMax}_{\mathrm{Abs}}$
- CSDelta

In these runs the prefilter was set to random.

C. Results

1) Data preprocessing: The results for the prefilters are shown in figure 8 and table I. K-means, the most expensive prefilter, has the highest median runtime and the highest standard deviation as well. So we can conclude that this technique is inappropriate for our problem. The best approach seems to be the weighted random prefilter, though the number of aborts is the highest, it has a median runtime significant smaller than all other prefilters.

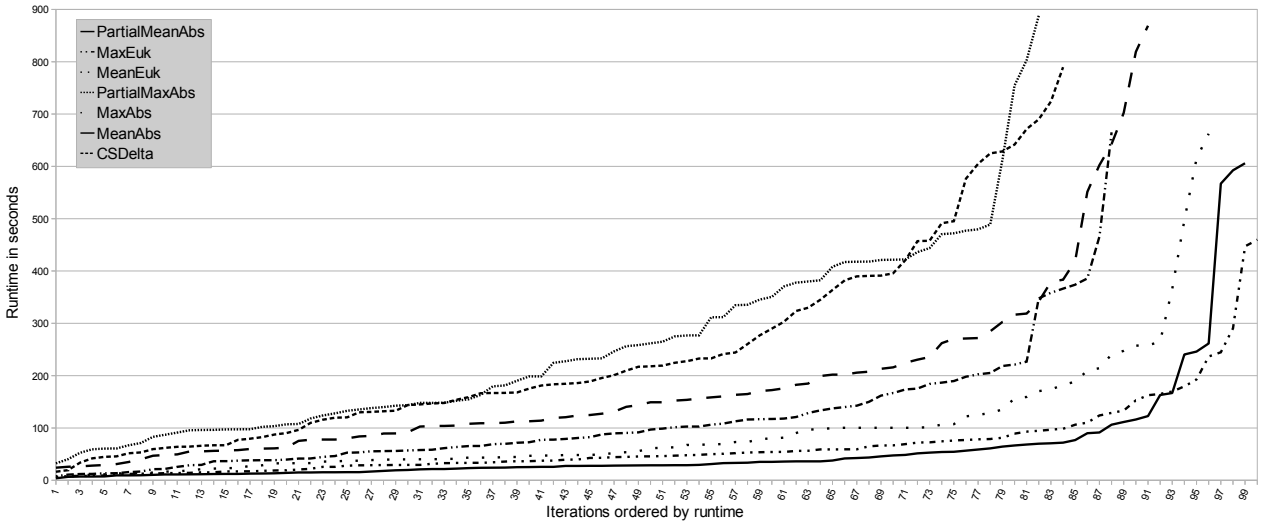

Figure 9. Comparison of the different search metrics

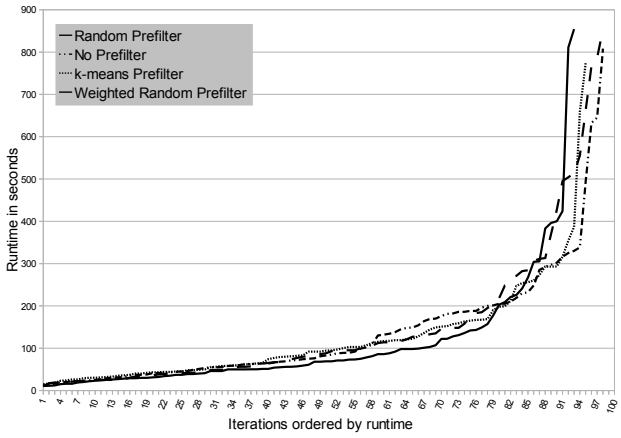

Figure 8. Comparison of the prefilters

Table I
RESULTS FOR THE PREFILTERS

Prefilter	Median	Min	Max	Std. Dev.	Aborts
Wgd. Random	61.07	11.05	854.18	141.44	7
No	82.07	14.10	808.19	137.95	2
Random	87.04	10.08	853.73	175.07	2
k-means	92.06	14.09	773.64	120.95	5

2) Search metrics: The results for the metrics are shown in figure 9 and table II. In figure 9 we combine the runtimes for different search metrics. This figure combines all three criteria: The runtime and its distribution as well as the detection rates. Although the two partial metrics require roughly $1/5$ compute power of the Max/Mean metrics the overall runtime is bad. We attribute this poor performance to the coarseness of the resulting target function. The complex heuristic takes advantage of a locally smoother optimization direction. The most complex metric (CSDelta) is not competitive in this experiment. However

Table II
RESULTS FOR THE METRICS

Metric	Median	Min	Max	Std. Dev.	Aborts
MeanAbs	28.56	3.87	605.92	105.38	1
MeanEuk	45.98	4.87	459.89	77.11	0
MaxAbs	54.64	6.35	662.44	113.73	4
MaxEuk	81.65	7.63	665.09	111.07	12
PartialMeanAbs	127.34	24.13	868.79	166.78	9
CSDelta	184.02	16.38	789.63	188.24	16
PartialMaxAbs	221.44	32.31	888.33	177.29	18

it should be mentioned that this one has a high potential for fine grade parallelization. But in the end the more simple metrics perform best.

V. SUMMARY AND FURTHER WORK

The identification of a process model is the basic requirement for successfully modelling and simulation. This paper presents experimental results for varying approaches within the preprocessing and the multi agent-based optimization steps of the process identifcation algorithm. We analyse and evaluate these results with regard to the overall identification characteristis and the performance behaviour. Furthermore every experimental result verifies the identification results itself and serves as a prove of concept. The preprocessing results emphasize the relevance of efficient data conditioning and show the impact of intelligent data compression like the Weihgted Random Prefilter.

The different metrics used in the optimization step points up the influence of the consideration from neighbourhood correlations.

The further work has two key aspects of activity: Parallelization and multi-metrics.

In the current version the 2-step multi-agent-based algorithm is realized with a modular and scalable architecture providing efficient parallelization of the identification process. To speed-up the run time further we will focus on

special architectures for massively parallelization.
The multi-metric model will realize an automatic switch to other metrics based on the data configuration and the local data condition to improve the benefit of the optimization step.

REFERENCES

[1] Sebastian Bohlmann, Volkhard Klinger, and Helena Szczerbicka. HPNS - a Hybrid Process Net Simulation Environment Executing Online Dynamic Models of Industrial Manufacturing Systems. In *Proceedings of the 2009 Winter Simulation Conference M. D. Rossetti, R. R. Hill, B. Johansson, A. Dunkin, and R. G. Ingalls, eds.*, 2009.

[2] Sebastian Bohlmann, Volkhard Klinger, and Helena Szczerbicka. Co-simulation in large scale environments using the HPNS framework. In *Summer Simulation Multiconference, Grand Challenges in Modeling & Simulation*. The Society for Modeling and Simulation, July 2010.

[3] Sebastian Bohlmann, Volkhard Klinger, and Helena Szczerbicka. System Identification with Multi-Agent-based Evolutionary Computation Using a Local Optimization Kernel. In *Submitted to ICMLA 2010 (International Conference on Machine Learning and Applications)*, 2010.

[4] Sebastian Bohlmann, Volkhard Klinger, Helena Szczerbicka, and Matthias Becker. A data management framework providing online-connectivity in symbiotic simulation. In *24th EUROPEAN Conference on Modelling and Simulation, Simulation meets Global Challenges*, Kuala Lumpur, Malaysia, June 2010.

[5] Tapas Kanungo, David M. Mount, Nathan S. Netanyahu, Christine D. Piatko, Ruth Silverman, and Angela Y. Wu. An efficient k-means clustering algorithm: Analysis and implementation. *IEEE Transactions on Pattern Analysis and Machine Intelligence*, 24:881–892, 2002.

[6] Averill M. Law and W. David Kelton. *Simulation Modeling and Analysis*. McGraw-Hill, 2000.

[7] R. Nelder and J.A. Mead. A simplex method for function minimization. *Computer Journal*, 7(4):308–313, 1965.

[8] Michael Schmidt and Hod Lipson. Comparison of tree and graph encodings as function of problem complexity. In *GECCO '07: Proceedings of the 9th annual conference on Genetic and evolutionary computation*, pages 1674–1679, New York, NY, USA, 2007. ACM.

[9] Paavo Viitamki. *Hybrid modeling of paper machine grade changes*. PhD thesis, Helsinki University of Technology, Espoo, Finland, 2004.

AUTHOR BIOGRAPHIES

SEBASTIAN BOHLMANN is a Ph.D. candidate at Department of Simulation and Modelling - Institute of Systems Engineering at the Leibniz Universität Hannover. He received a Dipl.-Ing. (FH) degree in mechatronics engineering from FHDW university of applied sciences. His research interests are machine learning and heuristic optimization algorithms, complex dynamic systems, control system synthesis and grid computing. His email address is <bohlmann@sim.uni-hannover.de>.

VOLKHARD KLINGER has been a full time professor for embedded systems and computer science at the university of applied sciences FHDW in Hannover and Celle since 2002. After his academic studies at the RWTH Aachen he received his Ph.D. in Electrical Engineering from Technische Universität Hamburg-Harburg. He teaches courses in computer science, embedded systems, electrical engineering and ASIC/system design. His email address is <Volkhard.Klinger@fhdw.de>.

ARNE KLAUKE is a researcher at the university of applied science FHDW in Hannover. He received a Dipl.-Math. from the Gottfried Wilhelm Leibniz Universität Hannover. His email address is <arne.klauke@fhdw.de>.

HELENA SZCZERBICKA is head of the Department of Simulation and Modelling-Institute of Systems Engineering at the Leibniz Universität Hannover. She received her Ph.D. in Engineering and her M.S in Applied Mathematics from the Warsaw University of Technology, Poland. She teaches courses in discrete-event simulation, modelling methodology, queuing theory, stochastic Petri Nets and distributed simulation. Her email address is <hsz@sim.uni-hannover.de>.

3D ALGORITHMS TO IMPROVE DEPLOYMENT OF WIRELESS LOCATION SYSTEMS EFFICIENCY

George Technitis
Department of Geography
University of Zurich - Irchel
Winterthurerstr. 190
CH-8057, Zurich, SWITZERLAND
E-mail: george.technitis@gmail.com

Alexander Sofios
School of Applied Mathematics and Physics
National Technical University of Athens
Zografou, GREECE
E-mail: alx3339@gmail.com

Nikolaos V. Karadimas
Dept of Mathematics and Science Engineering
Hellenic Military Academy
University of Military Education
16673, Vari, GREECE
E-mail: nkaradimas@sse.gr

Kostas Tsergoulas
Nikos Papastamatiou
Omega Technology
4 El. Venizelou
17676, Kallithea, GREECE
E-mail: seikto@gmail.com,
nikos@omegatech.gr

KEYWORDS

Real Time Location Systems, Wireless Networks, 3D Location Algorithms, Locating Assets or People.

ABSTRACT

Real-Time Location Systems (RTLS) have become very popular in recent years. These systems provide a contemporary layer of automation named automatic object location detection. Location measurements involve the transmission and reception of signals between hardware components of a system. A RTLS consists of at least two separate hardware components: a signal transmitter and a measuring unit. The positioning of the components in the monitored area is of great importance (regarding both location accuracy and resources required). This work presents the development of 3D software that can simulate the installation of a RTLS network in a virtual representation of the real world, helping in the decision making for the setup of such a network. The software utilizes a modified site survey algorithm, specifically developed to suit the needs of RTLS. Furthermore, it is capable of identifying the distance between two wireless nodes and the type and size of obstacles between them (walls, furniture, reflecting surfaces) calculating their effect on the formation of the network.

INTRODUCTION

The world is going mobile all the more as technology advances. Wireless communications have reached a degree of maturity that allows development of complex tasks, which were previously unachievable. Indoor location detection has drawn much attention both from researchers and manufacturers, as it constitutes the next step after outdoor position calculation - already achieved with GPS technology. Various solutions are currently under research utilizing different methods for location-tracking, such as Cricket, Mote Track, GPS and RSSI (Erin-Ee-Lin et al., 2008), as well as WiFi and RF fingerprinting. RSSI, as discussed below, is the simplest and least expensive solution, as it depends on RF propagating properties and requires no special hardware manipulation.

Zigbee wireless protocol provides location detection, along with many advantages. Zigbee have been explicitly designed for low consumption and minor radiation levels, making it the best choice for applications involving people tracking. In addition, its long battery life guarantees that infrequent maintenance is required - reducing the cost.

Hardware efficiency, cost effective planning and minimizing logistic operations are some of the many reasons for creating an assistive system; with smart algorithms, user-friendly intuitive interface and high scalability for deploying a Zigbee Real Time Location System (Z-RTLS).

Providing an indoor Real Time Location System (RTLS) solution offers many advantages over other possible approaches, to name a few:

- reduces the time needed for locating assets or people - improving productivity particularly when time critical issues arise
- enhances centralized management and control, as information acquired can be available both locally and remotely
- decreases time required for any statistical calculations over samples of data gathered, as data logging is fully automated
- strengthens security and allows for custom rules definitions over accessibility of certain areas of importance.

Proceedings 26th European Conference on Modelling and Simulation ©ECMS Klaus G. Troitzsch, Michael Möhring, Ulf Lotzmann (Editors)
ISBN: 978-0-9564944-4-3 / ISBN: 978-0-9564944-5-0 (CD)

Implementation of the above contributes for example in asset tracking and cataloging of products stored in warehouses, hospital equipment, finding tagged maintenance tools scattered all over a plant and much more. In addition location detection of people enables for monitoring their situation, providing relative info to them, banning admittance to an area for specific groups by issuing alarms when and where applicable and so forth.

Therefore, software was developed to provide all necessary services for setting up swiftly wireless networks, specializing in location tracking installations. Conclusively, the proposed solution stands apart for taking into consideration variables that are specifically more important in location detection systems that are otherwise mostly ignored, or handled manually in a subjective, insufficient way. Key variables such as the line of sight among network nodes and path loss estimation are estimated based on network topology and the RSSI measurements - the localization method used.

ZIGBEE PRO NETWORK TOPOLOGY

Zigbee Pro, an evolution of Zigbee, features mesh networking topology, which allows link connections between several points of the network structure. That means that each node can communicate with all other nodes in range, providing stable and versatile grid formation with increased resistance to transmission errors. These qualities, along with very low levels of energy consumption and radiation emission, forge a great candidate for indoor location system assembly.

Table 1: Classification of Factors the Affect RSS

Effect on	Factors	Options
Data Collection	1. Proximity of user	User's presence or absence
	2. Orientation of user and terminal	North, East, South, West
	3. Make of Radio	
Statistics	4. Time of measurement	Time of day & days of week
	5. Period of measurement	Second, minute, hour
	7. Interference	Co-channel/ adjacent co-channel
	8. Building environment	Small offices or large hall.

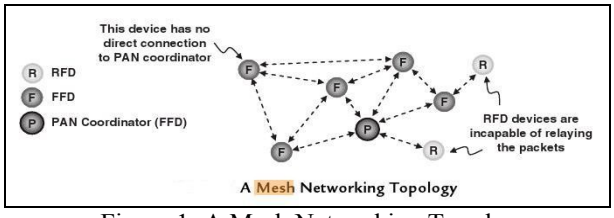

Figure 1: A Mesh Networking Topology

Mesh networking allows nodes to transmit and receive information using the best available path in real time. Such a topology results to an auto repairable wireless network with multiple routes for successful signal propagation. Furthermore, environmental influences on transmissions are greatly reduced.

RSSI AS A DISTANCE CALCULATION METHOD

Several methods exist for measuring the distances between two antennas in a wireless network: RSSI values, signal angle of arrival and time difference of signal arrival using multiple nodes are the most common. The Received Signal Strength Indicator is the simplest and most cost effective way, as it is merely a property of signal propagation. Thus, not requiring specific hardware, it has gained the majority of interest. RSSI is the quantized expression of Received Signal Strength (RSS) (Shahin 2008), which directly refers to the power level of a received packet. Hence, it is greatly affected by many parameters as discussed in (Shashank 2006) and seen in the table below.

What is more; RSSI, being directly affected by the distance the signal has travelled until reaching its destination, can be used to obtain information about the source's location if more measurements from other network nodes are available. The formula proposed and RSS (and thus RSSI) relation to distance is shown in (Aamodt 2008) in the figure that follows.

$$RSSI = -(10n\log_{10} d + A) \quad (1)$$

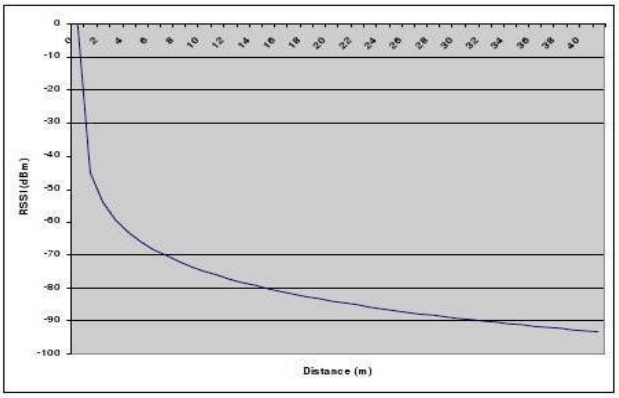

Figure 2: RSSI versus distance for A=40, and n=3

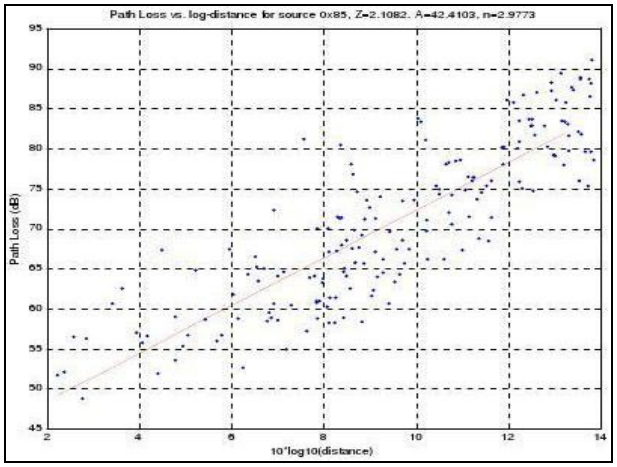

Figure 3: Path Loss vs. Log Distance

Evidently, path loss does have a great role in reducing the power level of the signals recorded. In (Texas instrument CC2431), parameter 'n' is also defined as "the path loss exponent"(although Texas Instruments uses an index analogy for parameter 'n'), highlighting even more the need of a clear line of sight when possible (Chuan-Chin and Hoon-Jae 2011).

METHODOLOGY

Clear Line Of Sight

Wireless transmissions, being waves, decay over distance. The least power loss of signals is usually observed when propagating on a path of what is known as a clear line of sight (Breeze Wireless Communications Ltd). Clear line of sight for radio waves is an imaginary straight line connecting two points of the wireless network, free - at a percentage of 80% minimum (Breeze Wireless Communications Ltd) - of obstacles in the Fresnel Zone of the signal.

Fresnel zone is defined as a circle around the theoretical line that shows the direction of a wave (Breeze Wireless Communications Ltd).

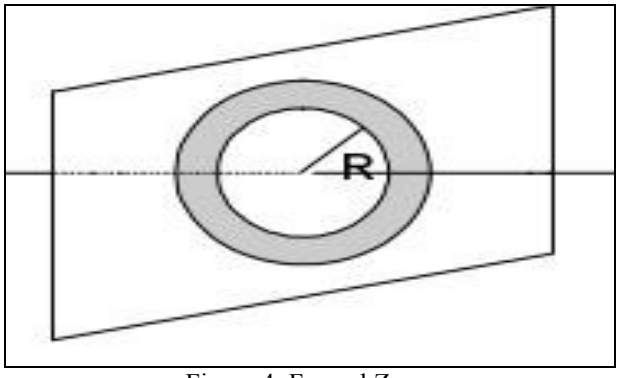

Figure 4: Fresnel Zone

$$\text{Fresnel Zone } R = \tfrac{1}{2}\sqrt{(L * D)} \qquad (2)$$

Where R is the radius of the first Fresnel zone, L is the wavelength and D is the distance between sites.

For example at 2.4GHz the wavelength is around 12cm, thus the radius of the first Fresnel zone is around 1.22 meters at 50 meters distance. Ergo, indoor deployments should avoid placements of nodes closer to ceilings or floors than 1.22 meters to refrain from blocking the clear line of sight from the start.

Being indoors can greatly distort one's view of clear line of sight in many other ways as well; mainly due to reflections, scattering, diffraction which cause, among others, a multi-path fading and shadowing of the frequency band in use. Best practice to take all these into account and minimize data loss later on, is to define the effect these have on wireless transmission on site (Tadeusz and Zepernick 2000; Erin-Ee-Lin et al. 2008).

Experimental setup followed (Tadeusz and Zepernick 2000), but in this case along a corridor with clear line of sight:

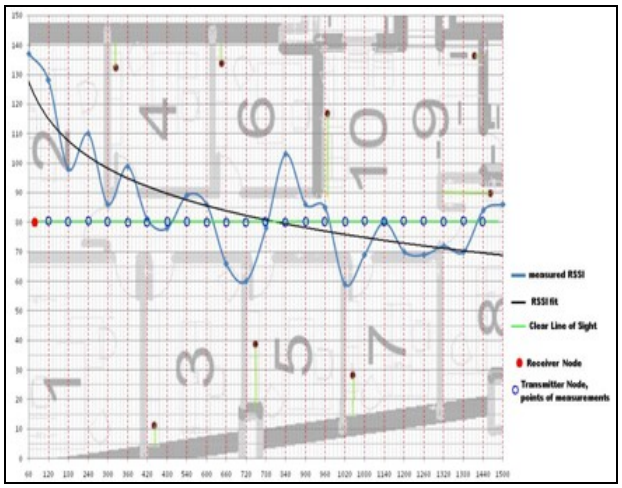

Figure 5: RSSI vs Distance over Clear Line of Sight, Indoor Corridor

Attenuation

Whenever a Radio Frequency (RF) signal loses portion of its original power, it is due to the attenuation that the medium it travels through exhibits under current circumstances. Conditions such as heat and humidity also affect signal absorption, as well as angle of incidence upon joints of different materials. Furthermore, it is evident that space travelled by a transmission may not be of uniform attenuation, hence calculating how much power the signal has in the end is not always trivial.

Attenuation unit is dB, and it is calculated via the expression below.

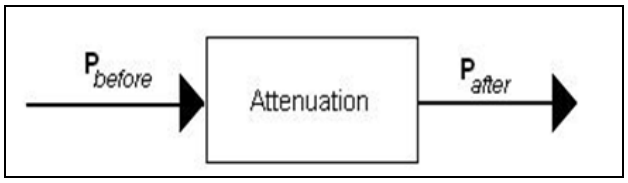

Figure 6: Calculating Attenuation Sample

$$\text{Attenuation} = 10 * \log_{10} * (Pafter / Pbefore)_{dB} \qquad (3)$$

An example of attenuation calculation is demonstrated in (Erin-Ee-Lin et al. 2008) as follows: *"If, due to attenuation, half the power is lost (Pout/Pin = 2), attenuation in dB is 10 x Log (2) = 3dB"*

In supplement to the previous statements, path loss, material absorption as well as any other reason why network link quality suffers, can be attributed to attenuation and is measured in dB.

RESULTS

Path Loss estimation

Deploying wireless networks has always been a challenging task to plan, due to the complexity of the problem. Efficiency of signal propagation depends upon a large set of environmental variables; such as obstacle frequency along signal's path, the diffraction, reflection and scattering of the signal and many more. Path loss is a quantity that describes the overall reduction of signal level which derives from the former reasons. Thus, path loss estimation is necessary as it provides valuable data for predicting when wireless communication is viable between two nodes of the network.

Calculating path loss involves correctly combining mathematical formulas concerning clear line of sight and signal absorption due to attenuation, caused by physical objects. However, one should first define the path followed itself; a difficult problem on its own. Solution to the aforementioned tasks is a tiresome repetitive procedure, given that in addition to network stability, optimal RSSI measurements are needed as well. Hence, an algorithm was developed to transform all available data to something that can be used productively.

Empirical Attenuation Calculation

One of the things that hold a primary role in path loss calculations, are the materials that indoor physical obstacles consist of. This multidimensional variable is introduced by the building structure and indoor environment complexity, cited previously - being mainly responsible for signal attenuation.

Attenuation, as previously noted, relies greatly on the kind of material in question. Obviously, preliminary knowledge of each object's material, and therefore its attenuation is of high importance when planning a wireless network deployment. Attenuation also depends on the thickness of the object, as well as the angle of arrival on the object's surface. The latter is also determined by the type of the antennas being used. Concerning omnidirectional antennas, and their waveform spreading pattern, the importance of the angle of arrival is minimized and thus not taken into consideration. The following figure shows the radiation pattern of an omni – directional antenna with its side lobes in polar form. This antenna radiates and receives in all directions in azimuth, in an isotropic way.

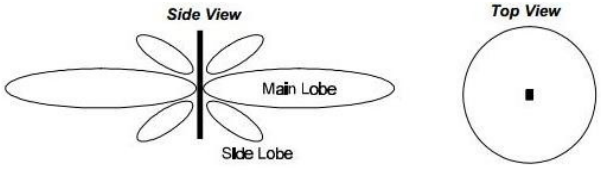

Figure 7: Omni – Directional Antenna

Finally and most importantly; given the material, a specific amount of attenuation is measured. This led to the establishment of databases that list attenuation of many standardized objects with detailed precision. Data can be extracted and used accordingly, forming tables containing data-set addressing certain needs is a common practice to tackle attenuation calculation.

However, mainly due to lacking the ability to correctly identify all materials of interest, experimental values are obtained on site as in (Shahin 2008).

Table 2: Signal Attenuation in Various Objects

Object (at Room Temperature)	Signal Frequency	Signal Attenuation (dB)
Soft cloth partition wall (2 inches)	914 MHz	1.5
Building floor	914 MHz	17
Building floor	1–2 GHz	23
Interior concrete wall (4 inches)	1–2 GHz	6
Interior brick wall (5 inches)	1–2 GHz	2.5
Plaster board	1–2 GHz	1.5
Reinforced glass	1–2 GHz	8

Procedure, known as site survey (Shahin 2008), for collecting attenuation data consists of simple steps:

- properly placing receiver and transmitter nodes at both edges of measured obstacle
- retrieve a satisfactory sample of measurements, reducing errors by using statistical tools
- define object's thickness
- divide attenuation result with object's thickness to find attenuation per length unit
- repeat steps for all kinds of objects of interest

Attenuation per length unit, for example dB per meters, can be applied for sets of obstacles consisting of the same material. Thus, it is most practical and is used by the algorithm mentioned above. It should be noted again, that attenuation does depend on signal frequency - yet it is common when deploying a wireless network to use only one specific RF band.

3D AS A TOOL TO CALCULATE COMMUNICATION STRENGTH

In this work the authors developed a 3D environment as a simulation of the real world, where the wireless nodes can be setup up effectively taking under consideration the real world obstacles (walls, furniture, metallic structures, etc). The achievement is that someone can predict communication losses, density of the network, required resources, before going on site, having only basic infrastructure information of the area.

The procedure consists of selecting the type of wireless nodes you want to add and put them in the 3D software. Then for each node you can see the strength of signal among its neighborhood nodes. The RSSI strength is then calculated with a modified site survey algorithm

based on the obstacles between the node and the losses their materials causes to the signals send.

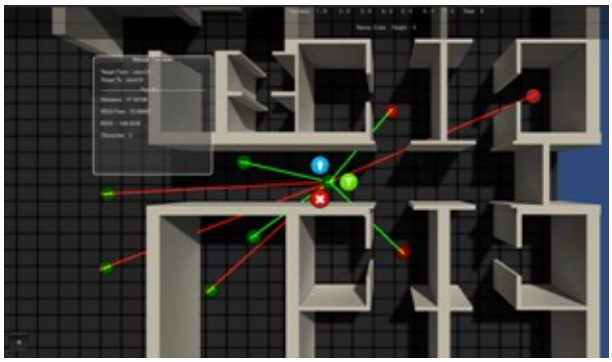

Figure 8: Wireless network with quality of signal between nodes.

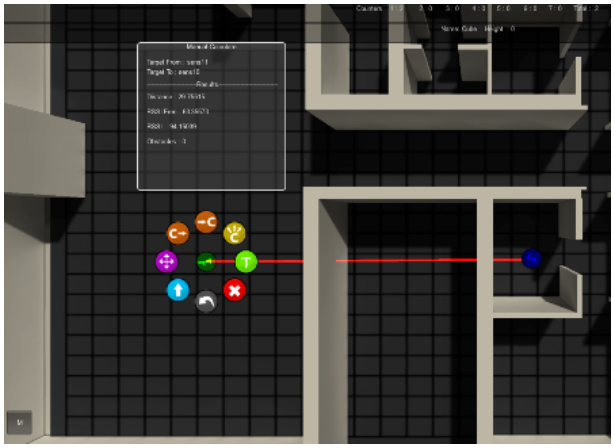

Figure 9: Obstacle identification and signal calculation among two nodes (available options visible)

CONCLUSIONS / DISCUSSION

To begin with, nowadays mainly two categories - asset and people tracking - demand a stable and useful implementation of an indoor Real Time Location System (RTLS).

Information about building structure, indoor environment complexity, quantity of wireless network nodes to be deployed, whether outdoor network coverage is expected and others, are supplied as input to a modified site survey algorithm(like the one described above). Firstly, assuming a grid that is able to cover the area of interest, nodes are assigned coordinates. At this stage the number of available nodes is ignored: the grid is arranged by the theoretical maximum communication points needed. Secondly, attenuation and actual node quantity are taken into account leading to adjustments on how the stationary transmitter will eventually form the network grid. This part utilizes the algorithm developed for path loss calculation, using attenuation data as well. Final results are demonstrated in a 3D building model for evaluation. Further manual adjustment is possible, assisted by presenting link quality in real time.

Highlight of the solution, is its specific design for optimized deployment of Zigbee Real Time Location Systems (RTLS) with minimum planning effort required. Considering particularities of the RTLS which distinctly differentiate such networks, this approach introduces significant insight in the site survey software category.

This research has a limited repository of materials tested and used during the pilot study. In order to cover greater variety, further and more detailed experiments should follow to complete the basic construction materials.

REFERENCES

Erin-Ee-Lin L., L. Boon-Giin, L. Seung-Chul and C. Wan-Young. 2008. “Enhanced Rssi-Based High Accuracy Real-Time User Location Tracking System For Indoor And Outdoor Environments”. *International Journal On Smart Sensing And Intelligent Systems*, Vol.1, No.2, June 2008, 534-548.

Shahin F. 2008. “Zigbee Wireless Networks and Transceivers”. Elsevier Ltd.

Shashank T. 2006. “Indoor Local Positioning System for Zigbee, based on RSSI”. MSc Thesis, Electronics Design in Electrical Engineering.

Aamodt K. 2008. "CC2431 Location Engine, Application Note AN042, Chipcon Products from Texas Instruments". pp. 2-8. http://focus.ti.com/lit/an/swra095/swra095.pdf [Accessed Feb 10, 2012].

Texas instrument CC2431 - System-on-chip for 2.4 GHz Zigbee/IEEE 802.15.4 with Location Engine: Data Sheet.

Chuan-Chin P. and L. Hoon-Jae. 2011. “State and Path Analysis of RSSI in Indoor Environment”. *International Conference on Machine Learning and Computing, IPCSIT.* Vol.3, IACSIT Press, Singapore. 289-293.

Breeze Wireless Communications Ltd. “Radio Signal Propagation”. http://didier.quartier-rural.org/implic/ran/sat_wifi/sigprop.pdf [Accessed Feb 10, 2012].

Tadeusz A. W. and H. J. Zepernick. 2000. "Characterization of the indoor radio propagation channel at 2.4 GHz". *Journal of Telecommunications and Information Technology*.

GEORGE TECHNITIS was born in Athens, Hellas, went to the Harokopio University of Athens where he studied geography and obtained his degree in 2007. He then moved to National Technical University of Athens (NTUA) for a MSc degree in Geoinformatics, 2009, while at same time was conducting research under ESA

scholarship. He worked for three years as technical manager for the Polymechanon Virtual Reality and Robotics Park SA and then as a Solution Product Developer for Omega Technology company working on Wireless Sensors Networks. Since 2011 he is conducting his PhD in the field of Simulation of Moving Objects in University of Zurich, Switzerland.

ALEXANDER SOFIOS was born in Athens, Hellas and went to the National Technical University of Athens (NTUA), where he is studying applied mathematics and physics. He worked for a year (2009-2010) for Polymechanon Virtual Reality and Robotics Park S.A. as a network administrator and programmer, before collaborating with Omega Technology company on a research project concerning wireless networks, sensors and location detection algorithms.

NIKOLAOS V. KARADIMAS was born in Athens and holds a degree in Electronic Engineering and a Master's degree in Computer Science from Glasgow Caledonian University. He also holds a second Master's degree in "Distributed and Multimedia Information Systems" from Heriot-Watt University, Edinburgh. He holds a PhD in Computer Engineering from the National Technical University of Athens (NTUA). He teaches at the Hellenic Military Academy. He has also taught at the Air Force Academy, at the Technological Educational Institute of Chalkis, Technological Educational Institute of Piraeus, Hellenic Air Force Technical NCO Academy and New York College. He is reviewer for many journals and conferences. Finally, Dr. Karadimas has over sixty (60) publications in international journals and conferences. He is a member of IEEE and IET and his research interests are in the area of Databases, Resource Management, Geographical Information Systems, Modeling and Simulation Algorithms and Decision Support Systems.

KOSTAS TSERGOULAS was born in Athens and holds a Bachelor's degree on Graphic and 3D design from Athens Metropolitan College. Since 2006 he is working as a 3D developer/designer in Omega Technology company. His research interests are in the fields on 3D Virtual Worlds, Game developing, 3d/2D animation, motion capture systems, programming for touch devices and web 3D/2D development.

NIKOLAOS P. PAPASTAMATIOU was born in Athens, Greece and he graduated from Aegean University, Samos in 1998 with a Bachelor's degree on Mathematics. He then received a Masters degree in Distributed and Multimedia Information Systems from Heriot-Watt University, Scotland in 1999. From 2002 he is working for Omega Technology company as an analyst/ programmer. He has followed several seminars on web technologies (XML Web services, Programming with XML in the .Net Framework, ASP.NET) and he has participated to many European and National research projects. His research interests are in the fields of Web Development, 3D programming, Mobile Applications, Grid Computing, Natural Language Processing and Semantic Web.

Simulation of Intelligent Systems

EVOLUTIONARY RUIN AND STOCHASTIC RECREATE: A CASE STUDY ON THE EXAM TIMETABLING PROBLEM

Jingpeng Li
Division of Computer Science
The University of Nottingham Ningbo China
Ningbo 315100, China
E-mail: Jingpeng.Li@nottingham.edu.cn

Rong Qu
School of Computer Science
The University of Nottingham
Nottingham NG8 1BB, United Kingdom
E-mail: rxq@cs.nott.ac.uk

Yindong Shen
Department of Control Science & Engineering
Huazhong University of Science & Technology
Wuhan 430074, China
E-mail: yindong@mail.hust.edu.cn

KEYWORDS

Evolutionary algorithm, Intelligent machine learning system, Combinatorial optimisation, Educational timetabling.

ABSTRACT

This paper presents a new class of intelligent systems, called Evolutionary Ruin and Stochastic Recreate, that can learn and adapt to the changing enviroment. It improves the original Ruin and Recreate principle's performance by incorporating an *Evolutionary Ruin* step which implements evolution within a single solution. In the proposed approach, a cycle of *Solution Decomposition, Evolutionary Ruin* and *Stochastic Recreate* continues until stopping conditions are reached. The *Solution Decomposition* step first uses some domain knowledge to break a solution down into its components and assign a score to each. The *Evolutionary Ruin* step then applies two operators (namely *Selection* and *Mutation*) to destroy a certain fraction of the entire solution. After the above steps, an input solution becomes partial and thus the resulting partial solution needs to be repaired. The repair is carried out by using the *Stochastic Recreate* step to reintroduce the removed items in a specific way (somewhat stochastic in order to have a better chance to jump out of the local optima), and then ask the underlying improvement heuristic whether this move will be accepted. These three steps are executed in sequence until a specific stopping condition is reached. Therefore, optimisation is achieved by solution disruption, iterative improvement and a stochastic constructive repair process performed within. Encouraging experimental results on exam timetabling problems are reported.

1 INTRODUCTION

Exam timetabling can be considered as the process of assigning a set of events (i.e. exams) into a limited number of timeslots subject to a set of constraints. The problem has attracted a significant level of research interest since the 1960's. The general timetabling problem comes in many different guises such as nurse rostering (Cheang et al. 2003; Li et al. 2012), sports timetabling (Easton et al. 2004), transportation timetabling (Kwan 2004) and educational timetabling (Carter and Laporte 1996; Schaerf 1999; Petrovic and Burke 2004; Qu et al. 2009). Educational timetabling problems are prob-ably the most widely studied.

Since exam timetabling problems are general NP-hard combinatorial problems which are unlikely to be solved optimally in polynomial time, various methods such as local search-based heuristics (Casey and Thompson 2004; Burke et al. 2004; Burke and Newall 2004), knowledge-based systems (Burke et al. 2006) and hyper-heuristics (Qu and Burke 2009) have been studied. Over the past dec-ade, meta-heuristics have attracted the most attention, including genetic algorithms (Erben 2001; Paquete and Fonseca 2001), ant algorithms (Dowsland and Thompson 2005), tabu search (Burke et al. 2003; White et al. 2004), simulated annealing (Thompson and Dowsland 1998). A number of at-tempts have also been made using other meta-heuristics (Burke et al. 1996; Duong and Lam 2004). The methods and techniques that have been used over the years to tackle exam timetabling problems have tended to draw on problem-specific information and particular heuristics. In this paper, we are trying to deal with the goal of developing a new class of search systems. We use the well-studied exam timetable problem as the test bed.

The work that is presented here is based on the observation that, in most real world problems, the solutions consist of components which are intricately woven together. Each solution component may be a strong candidate in its own right, but it also has to fit well with other components in the enviroment. To deal with these components, Schrimpf et al. (2000) proposed a technique called Ruin and Recreate (R&R) principal,

Proceedings 26th European Conference on Modelling and Simulation ©ECMS Klaus G. Troitzsch, Michael Möhring, Ulf Lotzmann (Editors)
ISBN: 978-0-9564944-4-3 / ISBN: 978-0-9564944-5-0 (CD)

and claimed it could be a general approach for various combinatorial optimisation problems. In this paper, we further extend the idea by incorporating some evolutionary features into the searching process. We term the enhanced version Evolutionary Ruin and Stochastic Recreate (ER&SR). Its general idea is to break a solution down into its components and assign a score to each by an evaluation function working under dynamic environments. The scores are employed as fitness values which determine the chances for the components to survive in the current solution.

2 A GENERAL DESCRIPTION OF THE ER&SR

The Ruin and Recreate (R&R) method uses the concepts of simulated annealing (Kirkpatrick 1983) or threshold accepting (Dueck and Scheuer 1990) with large moves instead of smaller ones. For simple structured problems like the traveling salesman problem, the need of using large moves is not obvious, because algorithms usually generate near optimal solutions with very small moves already. However, for complex problems like exam timetabling problems, difficulties arise if still using such small moves, because complex problems can often be seen as discontinuous: if walking one step from a solution to a neighbouring solution, the qualities of new solutions may be dramatically different, i.e., the landscapes of these problem areas can be very rugged.

Solutions of complex problems usually have many soft and/or hard constraints, which makes it difficult to get just feasible solutions. Neighbouring solutions of complex schedules, for instance, are usually infeasible solutions. It may be very hard to walk in such a complex landscape from one feasible solution to another neighboured feasible solution. The common method of avoiding the infeasibil-ity problem for many forms of the classical algorithms is to impose artificial penalty functions, but this method would typically make the algorithms get stuck in slightly infeasible solutions which might not be allowed at all.

Naturally, one will think in a different paradigm: ruin and recreate. We ruin a quite large portion of the solution and try to rebuild the solution as best as we can, with the hope that the new solution is better than the previous one. The R&R approach is just based on the above idea which has shown an important advantage: if destroying a large part of the previous solution, we have more freedom to generate a new one, and thus it is more likely to find again a feasible solution in this larger solution space. Hence, it is reasonable to believe that problems with many side conditions, or with very complex objective functions, are more tractable using special large moves.

Based on the general R&R principal, this paper presents a more advanced technique called ER&SR which has never been reported in the literature before. The new technique applies two operators of *Selection* and *Mutation* as the ruining strategies, trying to mimic the evolution on single solutions. Each component in the solution has to continuously demonstrate its worthiness to stay in the solution. Hence in each iteration, a number of components will be deemed not worth keeping. The evolutionary strategy adopted may also throw out, with a low probability, some worthy components. Any destroyed component is then reintroduced by using a specific algorithm. Of key importance is that the admittance of a new component is determined by a dynamic evaluation function, which takes into account of how well the prospective component will fit in with others already in the solution. The above processes are iterated together with the remainder of the classical R&R. Thus the global optimisation procedure is based on solution disruption and iterative improvement, while a reconstructive process is performed within.

As outlined, our proposed ER&SR algorithm consists of the following three parts: *Solution Decomposition*, *Evolutionary Ruin* and *Stochastic Recreate*. It executes these parts in a loop on one solution until a stopping condition reached. The first part of *Solution Decomposition* is based on the observation that in most real world combinatorial optimization problems, the solutions consist of components which are intricately woven together in a nonlinear, non-additive fashion. Each solution component may be a strong candidate in its own right, but it also has to fit well with other components. Its general idea is to use some expert's domain knowledge to break a solution down into its components and assign a score to each. The higher the score, the fitter the related component is.

The second part of *Evolutionary Ruin* is based on the consideration that the incumbent solution must be changed not only locally but also over a macroscopic scale, depending on the solution composition defined by the proceeding *Solution Decomposition* part. This part applies two operators of *Selection* and *Mutation* to destroy a certain fraction of the entire solution. The *Selection* operator removes some components based on Darwin's survival of the fitness mechanism, while the *Mutation* operator further removes some components in a totally random manner. Hence, the destroyed part of the solution would sometimes be large enough such that the impact of the "bomb" that is thrown on the solution will be noticeable not only locally but in the whole system. On the other hand, the destroyed part would sometimes be small enough so that at least a main portion of the solution (i.e. a skeleton) remains to facilitate the next solution rebuild.

The third part of *Stochastic Recreate* follows to reintroduce the removed items in a specific way (somewhat stochastic in order to have a better chance to jump out of the local optima), and then ask the underlying improvement heuristic (e.g. hill-climbing,

simulated annealing, or great deluge) whether this move will be accepted. These three parts are executed in sequence until a specific stopping condition is reached.

The above mentioned model is a general framework and many well-known search methods belong to its special case. For example, assume at each iteration x components are removed from an n-component solution, and let p be the acceptance criterion.

- If $x = 0$, then it is a non-iterative method as only one single solution will be generated;
- If $x \leqslant 3$, then it is a local search method that uses small moves to change the configurations;
- If $x = n$, then it is a constructive method with random starting points;
- If (no *Solution Decomposition*) & (no *Selection*), then it equals to the R&R principle.
- If (p = "hill-climbing") & (no *Solution Decomposition*) & (no *Selection*), then is equals to the most basic evolutionary algorithm called "(1+1)EA", in which its population is composed by two individuals only: one being the parent, the other the offspring.

3 EXAM TIMETABLING

Exam timetabling can be considered to be the process of assigning a set of events (i.e. exams) into a limited number of timeslots subject to a set of constraints. Constraints are usually divided into two types: hard and soft. A hard constraint cannot be violated under any circumstances. A typical example is two exams with common students involved cannot be scheduled into the same timeslot. A soft constraint is one that should be satisfied if possible but its satisfaction is not essential. A typical example is exams taken by common students should be spread out over the available timeslots so that students do not have to sit two exams that are too close to each other. Solutions with no violations of hard constraints are called feasible solutions. How much the soft constraints are satisfied gives an indication of how good the solutions (timetables) are.

In a simplified timetabling problem, if we are only concerned with hard constraints, the problem can be represented by a graph colouring model. Vertices in the graph represent exams in the problem, and edges representing the conflicts between exams (i.e. with common students). The problem is to minimise the colours used to colour all vertices, while avoiding the assignment of two adjacent vertices to the same colour. Graph colouring problems are among the most important problems in graph theory and are known to be NP-hard (Karp 1972).

The following objective function is used in (Burke et al. 2007) and many other papers in the literature to calculate the cost of an obtained feasible solution x:

$$\text{Min} \quad f(x) = \sum_{k=1}^{m-1} \sum_{l=k+1}^{m} (w_i \times s_{kl}) \Big/ S, \; i \in \{0,1,2,3,4\}, \quad (1)$$

where

s_{kl} is the number of students involved in both exams e_k and e_l, if $i = |t_l - t_k| < 5$;

$w_i = 2^{4-i}$ is the cost of assigning two conflicted exams e_k and e_l with i timeslots apart, if $i = |t_l - t_k| < 5$ (i.e. $w_1 = 16$, $w_2 = 8$, $w_3 = 4$, $w_4 = 2$, $w_5 = 1$; t_l and t_k as the timeslots of e_l and e_k, respectively);

m is the number of exams in the problem;

S is the number of students in the problem.

4 ER&SR FOR EXAM TIMETABLING

This section presents an ER&SR for exam timetabling. Starting from a randomly generated initial timetable, the steps described in section 4.1 to 4.3 are executed in sequence in a loop until a user specified parameter (e.g. CPU-time or solution quality) is reached or no improvement has been achieved for a certain number of iterations. During each iteration, an unfit portion of the working timetable is removed. Broken timetables are repaired by the constructing heuristic. Throughout the iterations, the best is retained and finally returned as the preserved timetable.

4.1 Solution Decomposition

This step is to evaluate the current arrangement for each event $e_k, k \in \{1,...,m\}$, in a timetable. In this step, the fitness of each event for a generated timetable is computed. The purpose of computing this measure is to determine which events are in positions that contribute more towards the cost reduction for the resulting solution. We can formulate a normalized evaluation function $F_t(e_k), k \in \{1,...,m\}$, at the t-th iteration as

$$F_t(e_k) = \frac{\max(C_t(e_1),...,C_t(e_m)) - C_t(e_k)}{\max(C_t(e_1),...,C_t(e_m)) - \min(C_t(e_1),...,C_t(e_m))}, \quad (2)$$

and

$$C_t(e_k) = \sum_{l=1}^{k-1} (w_i \times s_{kl}) + \sum_{l=k+1}^{m} (w_i \times s_{kl}), \; i \in \{0,1,2,3,4\}, \quad (3)$$

where $C_t(e_k)$ is the cost value brought by event e_k, and w_i uses the same definition as in Equation (1).

4.2 Evolutionary Ruin

This step is to decide whether a component (i.e. an event $e_k, k \in \{1,...,m\}$) in a current timetable should be retained or discarded. The decision is made by implementing two operators of *Selection* and *Mutation*. The *Selection* operator compares its fitness value $F_t(e_k)$ to a random number $p_s^{(t)}$ generated for each iteration t in the range [0, 1]. If $F_t(e_k) \geq p_s^{(t)}$, then e_k will remain in its present allocation, otherwise e_k will be removed from the current timetable. By using *Selection*, an event

e_k with larger fitness value $F_t(e_k)$ has a higher probability to survive in the current timetable. The *Mutation* operator follows to mutate the retained events e_k, i.e. randomly discarding them from the partial timetable at a small rate $p_m^{(t)}$. Compared with the selection rate $p_s^{(t)}$ which is randomly generated for each iteration t, the mutation rate $p_m^{(t)}$ should be much smaller to aid convergence.

4.3 Stochastic Recreate

The *Stochastic Recreate* task is to rebuild a partial timetable by assigning unscheduled events to available timeslots. Once a specific event has been determined, the following two steps will be executed: Step 1 finds all its available timeslots without any conflict exams; Step 2 chooses the timeslot with the smallest increase on the overall cost defined by Equation (1).

Based on the domain knowledge of timetabling, there are many heuristics that can be used to determine the order for the events to be rescheduled. Here we use the following four graph-based heuristics reported in (Qu and Burke 2009): largest degree first (H_1), largest weighted degree first (H_2), largest color degree first (H_3) and least saturation degree first (H_4). Let $p_1^{(k)}$, $p_2^{(k)}$, $p_3^{(k)}$ and $p_4^{(k)}$ be the probabilities of using heuristics H_1, H_2, H_3 and H_4 respectively for the rescheduling of event e_k. These heuristics are alternatively used in each step of recreate, satisfying $\sum_{j=1}^{4} p_j^{(k)} = 1$.

The H_1 heuristic orders events in descending order by the number of conflicts they have with other exams. This heuristic aims to schedule first those events which have the most conflicts. It first goes through the conflict values (which are precalculated) for the unscheduled events, and then proceeds to Steps 1 and 2.

The H_2 heuristic orders events in descending order by the number of conflicts, each of which is weighted by the number of students involved. Among events with the same degree, this heuristic gives higher priority to those with a larger number of students involved. Like H_1, it first goes through the weighted conflict values for the unscheduled exams, and then proceeds to Steps 1 and 2.

The H_3 heuristic orders events in a descending order in terms of the number of conflicts with the other events that have already been placed in the timetable. The degrees of the events not yet scheduled are changed according to the situations encountered at each step of the solution construction. Unlike H_1 and H_2, the conflict value for each exam needs to be firstly updated before scheduling an exam. This involves updating an ancillary matrix that contains the conflict values between any pairs of an unscheduled exam and a scheduled exam. H_3 then goes through the new conflict values for the unscheduled exams, and next proceeds to Steps 1 and 2.

The H_4 heuristic orders events in ascending order in terms of the number of available timeslots that can be selected without violating hard constraints. The priorities of events to be ordered and scheduled are changed dynamically as the solution is constructed. The number of available timeslots for each event needs to be firstly calculated before rescheduling an event. This process can be regarded as executing Step 1 repeatedly for all unscheduled exams. H_4 then goes through the saturation degree numbers for all the unscheduled events, and next proceeds to Steps 1 and 2.

5 EXPERIMENTAL RESULTS

The exam timetabling problems we tested in this paper were first introduced in (Carter et al. 1996), and have been widely tested by a number of approaches during the last ten years. The dataset consists of 13 problems from different institutions, among which 11 have been more heavily investigated because of errors in the other two problems. A more detailed discussion of those datasets (and the difficulties caused by different instances circulating under the same name) was given in (Qu et al. 2009).Our aim with these experiments is not to beat the state-of-the-art approaches in the literature (although the results are competitive with the best results reported), but to present the potential of this more generic methodology to be easily employed and to perform adaptively on a range of different timetabling or optimisation problems.

Table 1 presents the characteristics of the 11 problems in the dataset. Rows 2-5 include the number of exams, the number of students, the number of available time slots and the problem density. The problem size ranges from 81 to 682 exams, from 611 to 18416 students and from 10 to 35 time slots. The "density" (ranged from 0.06 to 0.42) gives the conflict density of elements with value 1 in the conflict matrix, where element C_{ij} = 1 if events i and j conflict, C_{ij} = 0 otherwise. More details about the benchmark dataset can be found at http://www.asap.cs.nott.ac.uk/resources/data.shtml.

Table 2 presents the 20 runs' results on the benchmark exam timetabling problems of the original R&R and the enhanced ER&SR. For comparison, it also lists the results of the state-of-the-art approaches in the literature. The best results among all of the approaches are highlighted. Both algorithms were coded in C++ and implemented on an Intel Core 2 Duo 1.86GHz machine with 2.0GB of RAM under Window XP. The stopping condition is no improvement has been made after 1000 iterations. We can see that the ER&SR outperforms the R&R over all of the problems in terms of best and average results. It is also very consistent on all of the runs with distinct random seeds.

Table 1: Characteristics of the Benchmark Problems

	car91	car92	ear83	hec92	kfu93	lse91	sta83	tre92	uta93	ute92	york83
Exams	682	543	190	81	461	381	139	261	622	184	181
Students	16925	18419	1125	2823	5349	2726	611	4360	21266	2750	941
Timeslots	35	32	24	18	20	18	13	23	35	10	21
Density	0.13	0.14	0.27	0.42	0.06	0.06	0.14	0.18	0.13	0.08	0.29

Table 2: Comparison Results on Benchmark Problems.

	car91	car92	ear83	hec92	kfu93	lse91	sta83	tre92	uta93	ute92	york83
R&R best	5.4	4.9	38.6	12.2	15.3	12.8	161.2	8.8	3.6	30.1	40.7
R&R avg	6.1	5.3	39.9	12.5	15.6	13.2	163.6	9.2	4.2	31.3	43.2
ER&SR best	5.3	4.7	29.7	10.1	13.7	10.2	157.3	8.4	3.3	25.3	37.8
ER&SR avg	5.4	5.2	30.0	11.9	14.1	10.5	157.9	8.7	3.5	26.6	39.0
Abdullah et al. 2007	5.2	4.4	34.9	10.3	**13.5**	10.2	159.2	8.7	3.6	26.0	**36.2**
Asmuni et al. 2005	5.2	4.5	37.0	11.8	15.8	12.1	160.4	8.7	3.6	27.8	40.7
Burke & Newall, 2004	**4.6**	**4.0**	37.1	11.5	13.9	10.8	168.7	8.4	**3.2**	25.8	36.8
Burke et al. 2004	4.8	4.2	35.4	10.8	13.7	10.4	159.1	**8.3**	3.4	25.7	36.7
Caramia et al. 1982	6.6	6.0	**29.3**	**9.2**	13.8	**9.6**	158.2	9.4	3.5	**24.4**	36.2
Carter et al. 1996	7.1	6.2	36.4	10.8	14.0	10.5	161.5	9.6	3.5	25.8	41.7
Gaspero & Schaerf 2001	6.2	5.2	45.7	12.4	18.0	15.5	160.8	10.0	4.2	29.0	42.0
Merlot et al. 2002	5.1	4.3	35.1	10.6	13.5	10.5	**157.3**	8.4	3.5	25.1	37.4

It can be observed that the best results reported in the literature were obtained by different approaches over the years. Among the 8 approaches compared (which have obtained the best results in the literature on the benchmarks), our ER&SR obtained competitive results. However, the most important point to make here is that all of the other approaches were specifically designed for the exam timetabling problem.

6 CONCLUSIONS

This paper presents a new approach to solve timetabling problems based on the original idea of R&R, by incorporating two operators of *Selection* and *Mutation* in its *Evolutionary Ruin* step. In our proposed ERSR, a cycle of *Solution Decomposition*, *Evolutionary Ruin* and *Stochastic Recreate* continues until stopping conditions are reached. Taken as a whole, the ER&SR implements evolution within a single solution and carries out search by solution disruption, iterative improvement and a stochastic constructive process. The experiments have demonstrated that the proposed approach performs very efficiently and competitively.

The architecture of the ER&SR is innovative, and thus there is still some room for further improvement. In the *Solution Decomposition* part, we will study the formulation of domain knowledge for different types of other problems and the influence of different evaluation rules. In the *Evolutionary Ruin* part, we will study the suitable range for the number of components to be destroyed and the condition of applying a large move or a small move. For the *Stochastic Recreate* part, we will study the types of reconstruction methods that are unsuited for generating optimum or near-optimum results. Furthermore, we will evaluate the proposed algorithm with different operators applied in its three parts and the best combination we should try.

REFERENCES

Abdullah S.; S. Ahmadi; E.K. Burke; and M. Dror. 2007. "Investigating Ahuja-Orlin's Large Neighbourhood Search for Examination Timetabling." *OR Spectrum* 29, 351-372.

Asmuni H.; E.K. Burke; and J. Garibaldi. 2005. "*Fuzzy Multiple Ordering Criteria for Examination Timetabling*." *Practice and Theory of Automated Timetabling*. Springer Lecture Notes in Computer Science 3616, 334-353.

Burke E.K.; Y. Bykov; J.P. Newall; and S. Petrovic. 2004. "A Time-Predefined Local Search Approach to Exam Timetabling Problems." *IIE Transactions* 36, 509-528.

Burke E.K.; G. Kendall; and E. Soubeiga. 2003. "A Tabu-search Hyperheuristic for Timetabling and Rostering." *Journal of Heuristics* 9, 451-470.

Burke E.K.; B. McCollum; A. Meisel; S. Petrovic; and R. Qu. 2007. "*A Graph-based Hyper-heuristic for Educational Timetabling Problems*." *European Journal of Operational Research* 176, 177-192.

Burke E.K. and J.P. Newall. 2004. "Enhancing Timetable Solutions with Local Search Methods." *Practice and Theory of Automated Timetabling*. Springer Lecture Notes in Computer Science 2740, 195-206.

Burke E.K. and J. Newall. 2004. “Solving Examination Timetabling Problems through Adaptation of Heuristic Orderings.” *Annals of operations Research* 129, 107-134.

Burke E.K.; J.P. Newalland R.F. Weare. 1996. “A Memetic Algorithm for University Exam Timetabling.” *Practice and Theory of Automated Timetabling*. Springer Lecture Notes in Computer Science 1153, 241-250.

Burke E.K.; S. Petrovic; and R. Qu. 2006. “Case Based Heuristic Selection for Timetabling Problems,” *Journal of Scheduling* 9, 115-132.

Carter M.; G. Laporte; and S. Lee. 1996. “Examination Timetabling: Algorithmic Strategies and Applications.” *Journal of Operations Research Society* 47, 373-383.

Caramia M.; P. DellOlmo; and G. Italiano. 2001. “*New Algorithms for Examination Timetabling*.” *Algorithm Engineering*. Springer Lecture Notes in Computer Science 1982, 230-241.

Casey S. and J. Thompson. 2004. “GRASPing the Examination Scheduling Problem.” *Practice and Theory of Automated Timetabling*. Springer Lecture Notes in Computer Science 2740, 232-244.

Cheang B.; H. Li; A. Lim; and B. Rodrigues. 2003. “Nurse Rostering Problems: a Bibliographic Survey.” *European Journal of Operational Research* 151, 447-460.

Dueck G. and T. Scheuer. 1990. “Threshold Accepting: a General Purpose Optimization Algorithm Appearing Superior to Simulated Annealing.” *Journal of Computational Physics* 90, 161-175.

Duong T.A. and K.H. Lam. 2004. “Combining Constraint Programming and Simulated Annealing on University Exam Timetabling.” In *Proceedings of RIVF 2004 Conference*, 205-210.

Dowsland K. and J. Thompson. 2005. “Ant Colony Optimization for the Examination Scheduling Problem." *Journal of Operations Research Society* 56, 426-438.

Easton K.; G. Nemhauser; and M. Trick. 2004. “Sports Scheduling,” In *Handbook of Scheduling: Algorithms, Models, and Performance Analysis*, J. Leung (ed.). Chapter 52, CRC Press.

Erben W. 2001. “A Grouping Genetic Algorithm for Graph Colouring and Exam Timetabling.” *Practice and Theory of Automated Timetabling*. Springer Lecture Notes in Computer Science 2079, 132-156.

Di Gaspero L. and A. Schaerf. 2001. “Tabu Search Techniques for Examination Timetabling.” *Practice and Theory of Automated Timetabling*. Springer Lecture Notes in Computer Science 2079, 104-117.

Karp R.M. 1983. “Reducibility Among Combinatorial Problems.” *Complexity of Computer Computations* 4, 85-103.

Kirkpatrick S.; C.D. Gelatt; and M.P. Vecchi. 1983. “Optimization by Simulated Annealing.” Science 220, 671-680.

Kwan R.S.K. 2004. “Bus and Train Driver Scheduling.” *Handbook of scheduling: Algorithms, Models, and Performance Analysis*, Chapter 51. CRC Press.

Li J.; E.K. Burke; T. Curtois; S. Petrovic; and R. Qu. 2012. “The Falling Tide Algorithm: a New Multi-objective Approach for Complex Workforce Scheduling.” *OMEGA – The International Journal of Management Science* 40, 283-293.

Merlot L.; N. Boland; B. Hughes; and P. Stuckey. 2002. “A Hybrid Algorithm for the Examination Timetabling Problem.” *Practice and Theory of Automated Timetabling*. Springer Lecture Notes in Computer Science 2740, 207-231.

Paquete L. and C.M. Fonseca. 2001. “A Study of Examination Timetabling with Multiobjective Evolutionary Algorithm.” In *Proceedings of the 4th Meta-heuristics International Conference* (MIC 2001), 149-154.

Petrovic S. and E.K. Burke. 2004. “University Timetabling.” *Handbook of Scheduling: Algorithms, Models, and Performance Analysis*. Chapter 45, CRC Press.

Qu R.; E.K. Burke; B. McCollum; L.T.G. Merlot; and S.Y Lee. 2009. “A Survey of Search Methodologies and Automated System Development for Examination Timetabling.” *Journal of Scheduling*12, 5-89.

Qu R. and E.K. Burke. 2009. “Hybridizations Within a Graph based Hyper-heuristic Framework for University Timetabling Problems.” *Journal of the Operational Research Society* 60, 1273-1285.

Schaerf A. 1999. “A Survey of Automated Timetabling.” *Artificial Intelligence Review* 13, 87-127.

Schrimpf G.; J. Schneider; H. Stamm-Wilbrand; and G. Dueck. 2000. “Record Breaking Optimization Results using the Ruin and Recreate Principle.” *Journal of Computational Physics* 159, 139-171.

Thompson J. and K. Dowsland, 1998. “A Robust Simulated Annealing based Examination Timetabling System.” *Computer & Operations Research* 25, 637-648.

White G.M.; B.S. Xie; and S. Zonjic. 2004. “Using Tabu Search with Longer-Term Memory and Relaxation to Create Examination Timetables.” *European Journal of Operational Research* 153, 80-91.

ACKNOWLEDGEMENTS

The work was supported by Natural Science Foundation of China (NSFC), under grands 70971044 and 71171087.

AUTHOR BIOGRAPHIES

JINGPENG LI received the M.Sc. degree in computational mathematics from Huazhong University of Science and Technology, China, in 1998, and the Ph.D. degree in computer science from University of Leeds, Leeds, U.K., in 2002. He joined the School of Informatics, University of Bradford, U.K., as a Research Associate in 2003. Since 2004, he has been with the School of Computer Science, University of Nottingham (UK campus) as a Research Fellow initially, a permanent Senior Research Fellow later, and currently an Assistant Professor at the University's China campus. His research areas include Intelligent Transport Scheduling, Metaheuristics, Multi-Objective Decision Making, Optimization & Search Methodologies, Machine Learning, Data Mining, Markov Chain Analysis, Fuzzy Logic, and Image Process. He has published over 30 peer-reviewed research papers in a wide variety of world’s leading journals and conference proceedings. Dr. Li has worked on five U.K. government-funded EPSRC projects and three Chinese government-funded NSFC research projects covering the topics of human scheduling, next generation decision support, novel research directions in personnel rostering, general optimization systems, theoretical understanding of

heuristics, ands public transport scheduling. He is a member of the Editorial Board of Wireless Sensor Network. In addition,.he is acting as a referee for more than 20 leading journals, and has served on the program committees for many international conferences. His e-mail address is: Jingpeng.Li@nottingham.edu.cn and his Web-page can be found at http://www.nott.ac.uk/~jpl.

RONG QU received the BSc degree in computer science from XiDian University, Xi'an, China, in 1996, and the Ph.D. degree in computer science from University of Nottingham, Nottingham, U.K., in 2002. She has been working in the School of Computer Science, University of Nottingham as a Lecturer since 2005. Her research areas include Metaheuristics, Constraint Programming, Integer Programming, Data Mining, and Knowledge Based Systems. She has published over 60 peer-reviewed research papers in a wide variety of world's leading journals and conference proceedings. Her e-mail address is: rxq@cs.nott.ac.uk and her Web-page can be found at http://www.nott.ac.uk/~rxq.

YINDONG SHEN received the M.Sc. degree in computer science from Wuhan University, China, in 1989, and the Ph.D. degree in operations research & artificial intelligence from University of Leeds, Leeds, U.K., in 2001. She has been working as a professor at Department of Control Science and Engineering, Huazhong University of Science and Technology, China, since 2006. She is also acting as a council person of Operations Research Society of China (ORSC) and secretary-general and vice-presiding officer of Operations Research Society of Hubei Province. Her major research interests include Modeling and Applications of Operations Research, Optimization in Public Transport Systems, Transit Planning, Vehicle and Crew Scheduling. She was awarded with Runner-Up in the IFORS 2005 OR in Development Prize Competition for her work on scheduling buses and their crew for Beijing Bus Group. Since she returned to China after her productive visit from September 2009 to April 2010 in Massachusetts Institute of Technology (MIT), she has developed a new public transit planning method, which enhances the Chinese traditional one and has been successfully applied in three cities of China. Her e-mail address is: yindong@mail.hust.edu.cn and her Web-page can be found at http://cse.hust.edu.cn/viewnews-666.

WiRKSam: An Approach to Maximize the Functionality of Multi-Factor Systems

Sama Khosravifar
Computer Science, University of Tehran, Tehran, Iran
Email: sama.khosravifar@gmail.com

KEYWORDS

Service Coverage, Satisfaction, Performance Analysis.

ABSTRACT

We introduce in this paper a hospital system as a multi-factor model and concentrate on system's performance. We give a formalization of profit considering service fees and costs and use it to explain the reasoning process of such system that investigates the most efficient setting to to keep a maximal state of profit. The proposed system is domain-specific and considers some relative parameters. However, the approach is general and could be applied to other similar models. The architecture is illustrated in the paper and a discussion on the functionality of this approach in the design is presented.

1 INTRODUCTION

Multi-factor systems are models inspired by decision theory and used to create technological extensions to routine human-designed systems (4). These systems are designed to increase the model's performance in decision makings that yield best profit (3). Obviously, these systems are able to cope with the uncertainty on the environment and increase their individual utility (5). They are important due to bounded nature of human decision making's abilities in complex societies. Consider the following scenario. A big national hospital is known based on its reputation (7). The reputation reflects society's public opinion that is categorized to different factors about the performance of the hospital in serving patients. In general, people prefer highly reputed hospitals, however, some factors like their expenses might prevent vising one and some other factors like their surgery and diagnosis success might encourage one to visit. Preferences are the proactive attitude of individuals, the motor that make the individual patient act, while satisfying his given set of conditions.

In literature, there have been many attempts to address intelligent system designs (6). In the work done by Bhanu and Balasubramanie (2), authors extend the applicability of association rules. They propose a model to investigate the difference between two sets of rules from data-sets in diverse cases. Their result could be applied to generate the rules for a new situation based on available data obtained from the environment. Bastanfard and katebi in (1) consider a multi-agent system that hosts distributed agents with local perceptions that try to achieve a unique goal. Authors provide effective social intelligence and improved performance of individual agents in a cooperative multi-factor system. They obtain their results by decisions made by the agents using reinforcement learning methods. In (8), Rosenfeld applies the principle of Maximum Entropy (ME). Each information source gives rise to a set of constraints, to be imposed on the combined estimate. The intersection of these constraints is the set of probability functions which are consistent with all the information sources. The method is applied in SPHINX-II, Carnegie Mellons speech recognizer and results shows 10 to 14 percent reduction in error rates.

In this paper, we introduce a hospital reputation mechanism that considers some relative parameters to reputation evaluation and study the case where such reputation brings the best profit when serving customers. For simplicity reasons and to achieve a high focus, we discard some non-relevant (or not highly relevant) factors and restrict the reputation model to five crucial parameters: (1) hospital service coverage; (2) hospital satisfaction rate; (3) hospital mean expense value; (4) hospital surgery success rate; and (5) hospital diagnosis success rate. Considering these parameters, we evaluate hospitals reputation value and use it as a means to estimate expected revenue of the hospital. In general, we estimate the hospital's expected profit and investigate cases where optimal profit is achievable. In this mechanism, we use the normal distribution that models the random rates provided for the typical hospital. We aim to theoretically analyze the impacts that parameters have on one another and deduce cases where the hospital vividly expects maximum profit and can accordingly set the controllable parameters. For example, the hospital might invest on adding some service coverage and thus increase the associated factor. This act would bring more patients and thus more revenue that would compensate the investment. Adversely, the hospital might not obtain acceptable results from investing on the surgery success factor. Therefore, some learning and analysis is required to investigate the case where optimal profit is achievable.

The remainder of this paper is as follows. In Section 2, we develop the proposed model and introduce the important factors. In Section 3, we start the discussion about hospitals performance considering the optimal reputation. We base the discussions on the dependency of the optimal case to the involved factors. We elaborate on inter-relation of involved parameters and extract the op-

Proceedings 26th European Conference on Modelling and Simulation ©ECMS Klaus G. Troitzsch, Michael Möhring, Ulf Lotzmann (Editors)
ISBN: 978-0-9564944-4-3 / ISBN: 978-0-9564944-5-0 (CD)

timization problem as a linear program. In Section 4, we discuss some results obtained from theoretical analysis of the reputation parameters. We represent the simulation and outline the properties of our model in the experimental environment, and finally, Section 5 concludes the paper.

2 THE MODEL

2.1 Parameters

Considering the hospital (referred as u) reputation model as a multi-factor system, we extend more details about each one of the considered parameters and their co-relation with optimal profitable case. These factors are listed in the following.

Hospital Service Coverage ($u.cg$): This value represents the extend to which a hospital is able to provide service to customers ($u.cg \in [0,1]$). For example, a well-equipped hospital assigns a better coverage parameters than a small hospital that lacks some equipments and fails to provide some certain services. This value is discretely evaluated for all hospitals and is clear to the community. However, an investment in coverage system would increase this value. Obviously, high coverage factor results in more demand regarding patients. Adversely, high coverage brings more maintenance fee for the hospital and therefore, a rational system would consider reasonable rate before design. The reasonability is inspired by the environment where the system is designed.

Hospital Satisfaction Rate ($u.sf$): This value represents the extent to which a hospital provides satisfactory services ($u.sf \in [0,1]$). This value is computed by accumulating the satisfaction feedback posted by the visiting patients (p). These feedback only extends patients impression about the service. Therefore, could be different considering two different patients. For instance, a patient might post negative feedback only because she felt the service was expensive, whereas the other one posts positive feedback because she is happy with the diagnosis even though she paid a fortune. In satisfaction accumulation, we respect different opinions, but we relax the accumulation by applying the time discount factor to bring up more recent feedback that reflect recent service quality of the hospital. This idea helps up to prevent feedback affect regarding two years ago influence hospital's satisfaction rate in a wrong way.

Consider two types of feedback posted by patient p: $+1$ for positive impression and -1 for negative impression for any reason whatsoever. The posted feedback regarding hospital u by patient p is refereed by $p.f_u$ and the time discount factor associated to this feedback is denoted by $p.f^t$. To evaluate the satisfaction rate, we simply collect all the positive feedback and divide by the sum of all posted feedback. We consider the notion of time to act impartial with respect to time of posting feedback. Equation 1 computed $u.sf$ parameter.

$$u.sf = \frac{\sum_t \sum_{p \in P} (\frac{p.f_u + 1}{2}) \times p.f^t}{\sum_t \sum_{p \in P} |p.f_u| \times p.f^t} \tag{1}$$

Hospital Mean Expense Value ($u.ep$): This value represents the extent to which the hospital is expensive. This value is also ranges between 0 and 1. One can consider $u.ep$ as a factor to predict the cost of her specific service request ($expectedCost = f_1(u.ep, serviceType)$). This value is also assigned by the hospital and is under its control. The hospital would decide about the rate and considers its influence on the satisfaction rate and the customer absorbtion.

Hospital Surgery Success Rate ($u.sg$): This value represents the hospital's success rate in operation. The rate is ranged in $[0,1]$ and inspired by public community's giving rates. This value is out of control of the hospital. However, by investment the hospital expects improvement in this rate. In general, the investment to improve successful surgery rate is quite expensive since it involves research, high salaries, and expensive equipments. Meanwhile, the improvement dramatically influences the satisfaction rate provided by the patients. Like other parameters, the hospital has to balance this parameter to obtain acceptable profit.

Hospital Diagnosis Success Rate ($u.dg$): This value is similar to hospital's surgery success rate in the sense that it also reflects hospital's accuracy in providing the service. However, it is more general compared to surgery in the sense that a big portion of hospital's covered service falls into diagnosis and only a group of patients undergo a surgery treatment. Due to sensitivity of the surgery treatment and its crucial impact on hospital's reputation, we separate surgery success rate from the diagnosis rate to obtain more realistic image about the general reputation of the hospital. But similar to $u.sg$, hospital's diagnosis rate could be expected to improve upon investment. Without an investment, the hospital can compute the relaxed value regarding this parameter over time and keep it unchanged with respect to associated cost of maintenance. In fact, we assume that over time elapse, the hospital obtains an idea how well the diagnosis rate would be and if reasonable, decides to keep it intact.

2.2 Reputation Evaluation

Considering the aforementioned involved parameters, we proceed forward to compute the hospital's general reputation upon which one can use as a means to categorize her choices. For evaluating this value, we associate five different coefficient (c_i, $i = 1, 2, .., 5$) to apply weights that impose importance of the involved factor. Coefficients are ranged in $[0,1]$and sum to 1. The reputation $u.Rep$ is computed (see equation 2) as a dot product of

coefficients and parameters vectors. c_i by default could be considered as 0.2. But inspired by the community, the system could associate variety of values to these coefficients. Logically the hospital will find out about these coefficients upon received periodic (could be annual) reports and accordingly could apply best strategies to the controlled ($u.cg$ and $u.ep$) and expected ($u.sf$, $u.sg$, and $u.dg$) parameters that yield the optimal profit.

$$u.Rep = \overrightarrow{c}.\overrightarrow{u} \quad where \tag{2}$$
$$\overrightarrow{c} = [c_1 \quad c_2 \quad c_3 \quad c_4 \quad c_5]^T \quad and$$
$$\overrightarrow{u} = [u.cg \quad u.sf \quad u.ep \quad u.sg \quad u.dg]^T$$

3 OPTIMAL REPUTATION

In previous Section, we computed the public reputation assigned to the hospital u in equation 2. But this pushes the hospital to a challenge to optimize the reputation to yield the maximum profit. In fact, the hospital is not aware of the exact coefficient values together with some expected parameters. But still, it learns based on experience of serving a number of customers and reports received on coefficients. To clarify the objective of this part, we disregard any non-relevant issue with respect to dynamism of the environment and components distributions. We only concentrate on policy alteration that cause reputation alteration and ends up in a terms we highlight as reputation change R. We compute the reputation change as the percentage of reputation increase (in some cases even decrease) with respect to any sort of policy alteration. Equation 3 computes this value that ranges in $[-1, +1]$. In this equation $u.NRep$ denotes the new reputation computed as a result of any sort of policy alteration such as service coverage increase, surgery or diagnosis success rate improvements, etc.

$$R = \frac{u.NRep - u.Rep}{u.Rep} \tag{3}$$

Now consider the obtained payoff as a result of a policy change. This would be the main challenge for the hospital. We compute the payoff by subtracting the investment (referred as $u.cst$) from the obtained revenue as a result of the policy alteration. The obtained revenue is the product of the reputation change R, mean visiting customer λ_c, and mean customer fee $\beta \times u.ep$. Here β represents a supreme fee and hospital's expense rate would generalize it to its mean charging fee. Equation 4 computes the payoff depending on the reputation change.

$$Pf = R \times \lambda_c \times (\beta u.ep) - u.cst \tag{4}$$

Since the hospital changes the policy, the reputation change would be only expected. Therefore, the obtained payoff is also expected (see equation 5).

$$[Pf] = [R] \times \lambda_c \times (\beta u.ep) - u.cst \quad where, \tag{5}$$
$$[R] = \frac{[u.Rep] - u.Rep}{u.Rep} \quad and$$
$$[u.Rep] = \overrightarrow{c}.[\overrightarrow{u}]$$

We conclude that the policy alteration is emerged by investing on some issues that bring an improvement expectation on some parameters. For simplicity, let the controllable parameters ($u.cg$ and $u.ep$) stay the same. In equation 6, we re-write the parameter vector $\overrightarrow{u}$ with the expected uncontrollable parameters.

$$\overrightarrow{u} = [u.cg \quad [u.sf] \quad u.ep \quad [u.sg] \quad [u.dg]]^T \tag{6}$$

In order to step forward addressing the optimal payoff, we need to compute the expected parameters. Then we can follow computing the best reputation change yielding the maximum obtained payoff. To this end, consider the parameters deviate with respect the applied investment and change by a factor called α. For instance, the expected satisfaction rate would be multiplied by $(1+\alpha_{sf})$. The following Equations substitute the expected parameters.

$$[u.sf] = u.sf(1 + \alpha_{sf}) \tag{7}$$
$$[u.sg] = u.sg(1 + \alpha_{sg}) \tag{8}$$
$$[u.dg] = u.dg(1 + \alpha_{dg}) \tag{9}$$

Combining the previous equations, we can compute the reputation differentials ($d(u.Rep)$) in the following equation. We carry on the assumption that controllable parameters stay intact.

$$d(u.Rep) = c_2\alpha_{sf} + c_4\alpha_{sg} + c_5\alpha_{dg} \tag{10}$$

In order to capture the realistic role of the optimal reputation in optimal payoff, we propose a heuristic function that utilizes an exponential function rather than a normal linear function. The rational behind this idea is the fact that reputation improvement dramatically boosts the profit. This assumption supports the idea that reputation lasts long and brings customers to the hospital. To this end, we believe it is realistic to consider exponential growth rather than linear one. However, the exponent in the heuristic function would not exceed 1 and this way we prevent huge values in profits. Equation 11 introduces a new parameter hospital's obtained payoff ($u.Opf$) and computes the value considering costs regarding satisfaction, surgery, and diagnosis improvements. We assumed so far that the coverage and expense rates stay intact, but we can assume overall service improvements that increase satisfaction factor. This could be simply an alteration in method of payments, or applying some policies that use the same budget, etc. In this Equation, c_{sf}, c_{sg}, and c_{dg} respectively denote costs regarding satisfaction, surgery, and diagnosis improvements.

$$u.Opf = pf(e^{\frac{d(u.Rep)}{u.Rep}} - 1) - (c_{sf} + c_{sg} + c_{dg}) \tag{11}$$

The objective is to maximize the hospitals obtained payoff $u.Opf$. Addressing this approach, first consider the case where the only attempt is to improve the satisfaction, therefore the only cost is c_{sf}. In this case, improving the overall service, the only updated parameter is $u.sf$. Therefore, reputation differential (originally obtained from Equation 10) would be re-computed in Equation 12. In this Equation, ϵ relaxes the unavoidable influences regarding overall service improvement. Accordingly, Equation 13 computes the exponent of the exponential heuristic function that we pointed out earlier.

$$d(u.Rep) = c_2\alpha_{sf} + \epsilon \tag{12}$$

$$\frac{d(u.Rep)}{u.Rep} = \frac{c_2\alpha_{sf} + \epsilon}{c_2\alpha_{sf} + c_4\alpha_{sg} + c_5\alpha_{dg} + \epsilon} \tag{13}$$

We highlight the fact that to be profitable, the alteration strategy would be applied if at the first spot the following condition is held.

$$e^{\frac{d(u.Rep)}{u.Rep}} > \frac{c_{sf} + pf}{pf}$$

Simplifying the inequality, we obtain a new inequality that we use it as a constraint in maximizing the hospital's obtained profit as a linear program.

$$\Rightarrow d(u.Rep) > u.Rep.ln(\frac{c_{sf}}{pf} + 1)$$

Forcing the constraint imposes positive rate of change to the reputation change R (computed in 3) in case of solely satisfaction improvement. Likewise, we obtain other constraints forcing profitable surgery investment, diagnosis improvement, and the package improvement as a whole. Equation 14 represents the $argmax$ of the hospital's obtained payoff as a linear program with respect to the crucial constraints.

$$u.Opf = argmax\ pf(e^{\frac{d(u.Rep)}{u.Rep}} - 1) - (c_{sf} + c_{sg} + c_{dg}) \tag{14}$$

$$subject\ \ to$$

$$d(u.Rep) > u.Rep.ln(\frac{c_{sf}}{pf} + 1)$$

$$d(u.Rep) > u.Rep.ln(\frac{c_{sg}}{pf} + 1)$$

$$d(u.Rep) > u.Rep.ln(\frac{c_{dg}}{pf} + 1)$$

$$d(u.Rep) > u.Rep.ln(\frac{c_{sf} + c_{sg} + c_{dg}}{pf} + 1)$$

Considering the results obtained in Equation 14, the hospital that applies diverse (costly) enhancement strategies needs to consider the obtained linear program with respect to its constraints to achieve the best possible payoff. We believe that using this linear system dramatically increase such hospital's performance in terms of profit.

Table 1: Different objects with diverse parameters and reputation values. In this environment all reputation coefficients c_i are constant and 0.2.

Objects	$u.cg$	$u.sf$	$u.ep$	$u.sg$	$u.dg$	$u.Rep$
u_1	0.60	0.47	0.38	0.31	0.51	**0.45**
u_2	0.64	0.41	0.54	0.11	0.72	**0.48**
u_3	0.72	0.37	0.27	0.19	0.87	**0.48**
u_4	0.43	0.29	0.39	0.45	0.46	**0.40**
u_5	0.28	0.54	0.73	0.27	0.37	**0.44**
u_6	0.58	0.68	0.48	0.38	0.32	**0.49**

In the next Section, we explore more details about the implemented system which its outcome performance is relevant to a multi-factor system. We expand details about different implemented models and their success rate to achieve the objective results.

4 EXPERIMENTAL RESULTS

In this section, we implement a system called $WiRKSam$ to model a multi-factor hospital reputation system. The objective is to maximize one's obtained profit as a result of systematic quality enhancement. To achieve this goal, we discuss in the rest of this chapter the parameters related to different cases that are obtained from different scenarios. We capture the progress pattern and compare it with the results we obtained in the theoretical part.

In the implemented system, entities are implemented as $Java^{©TM}$ objects, i.e. they inherit from the basic class $Java - Simulator^{©TM}\ Entity$. The object of the main class represent a hospital that is capable of applying a range of changes on its associated parameters. This object's reasoning capabilities are implemented as *Java modules* using logic programming techniques. As Java classes, the objects have private data called *Belief Data*. The different enhancement changes are given by a data structure and implemented using tables and the different actions expected by the object in the context of a particular enhancement strategies are given by a table called $data\_representative\_manager$. The different objects' reputation values that an object obtains in the system are recorded in a data structure called $data\_reputation$. In different scenarios, each object has a knowledge base about its improvements in the past scenarios, called $table\_reputation$. Such a knowledge base has the following structure: $Object - name$, $Object - reputation$, $Total - interaction - number$ and $Recent - interaction - time$. We highlight the most important results that is consistent with the results we obtained in the theoretical part.

Table 1 categorizes different objects from the same hospital class that follow different strategies. The parameters associated to these objects are randomly generated and follow a normal distribution. In this Table, the reputation parameter weights are considered as con-

Table 2: Different objects with diverse parameters and reputation values. In this environment the reputation coefficients c_i are random and different where the objects are not aware of them.

Objects	$u.cg$	$u.sf$	$u.ep$	$u.sg$	$u.dg$	$u.Rep$
u_1	0.60	0.47	0.38	0.31	0.51	**0.47**
u_2	0.64	0.41	0.54	0.11	0.72	**0.47**
u_3	0.72	0.37	0.27	0.19	0.87	**0.50**
u_4	0.43	0.29	0.39	0.45	0.46	**0.40**
u_5	0.28	0.54	0.73	0.27	0.37	**0.44**
u_6	0.58	0.68	0.48	0.38	0.32	**0.53**

Table 3: Matrix of coefficients regarding 6 different objects. In this environment the reputation coefficients c_i are random and different where the objects are not aware of them.

Objects	c_1	c_2	c_3	c_4	c_5
u_1	0.30	0.20	0.20	0.15	0.15
u_2	0.20	0.40	0.25	0.10	0.05
u_3	0.25	0.35	0.10	0.15	0.15
u_4	0.20	0.15	0.35	0.20	0.10
u_5	0.35	0.40	0.10	0.05	0.10
u_6	0.20	0.30	0.30	0.10	0.10

sistent portions of 0.2. A more realistic values with randomly generated portions are shown in Table 2. However, in Table 2, the objects are not aware of the intermittent portions and to thus follow more risky strategies in their further enhancement changes. The unknown portion weights regarding 6 different objects are presented in Table 3. Henceforth, we use these coefficients as a reference to compute one's reputation.

We continue the discussions with more details about different strategies that 6 objects could adopt in order to advance their reputation values. To complete this analysis, we categorize objects to three different classes of (1) *random strategy*, which is followed by objects u_1 and u_2; (2) *expense strategy*, which is followed by objects u_3 and u_4; and (3) *efficient strategy*, which is followed by objects u_5 and u_6. In general, we consider that all objects have same amount of budget, but use it by different strategies. The objects following random strategy consume the budget on different sectors and thus enhance the parameter values with no reasoning. These users might increase the coverage, or invest on enhancing the diagnosis, or decreasing the expense fees. Consequently, objects belonging to this category obtain different results based over their random enhancement changes. The objects following the expense strategy mainly concentrate on enhancing the expense factor and obtain results that correlate to their payoffs. To this end, the objects belonging to this group might enhance their reputation to some extent, but mainly focus on the ways to obtain more payoffs. But the objects following the efficient strategy consider the obtained results in their analysis and try a range of enhancement strategies to increase their reputations.

Table 4: Enhanced parameters of different objects following different strategies. This is an independent enhancement of the state represented in Table 2.

Objects	$u.cg$	$u.sf$	$u.ep$	$u.sg$	$u.dg$	$u.Rep$
u_1	0.80	0.49	0.38	0.35	0.55	**0.55**
u_2	0.64	0.45	0.52	0.15	0.75	**0.49**
u_3	0.72	0.50	0.40	0.22	0.85	**0.56**
u_4	0.47	0.50	0.43	0.47	0.50	**0.46**
u_5	0.58	0.62	0.70	0.28	0.40	**0.57**
u_6	0.68	0.69	0.40	0.39	0.35	**0.54**

Table 5: Enhanced parameters of different objects following different strategies. This is another independent (of results shown in Table 4) enhancement of the state represented in Table 2.

Objects	$u.cg$	$u.sf$	$u.ep$	$u.sg$	$u.dg$	$u.Rep$
u_1	0.75	0.52	0.35	0.32	0.59	**0.54**
u_2	0.75	0.50	0.50	0.12	0.72	**0.52**
u_3	0.72	0.40	0.50	0.25	0.87	**0.54**
u_4	0.65	0.32	0.40	0.45	0.46	**0.45**
u_5	0.45	0.60	0.73	0.35	0.40	**0.53**
u_6	0.60	0.70	0.55	0.39	0.35	**0.57**

The objects belonging to this group follow the methodology we represented in this paper. Tables 4 and 5 represent the upgraded parameters obtained from the state corresponding to Table 2. We also show the enhancement percentage of the overall reputation value with respect to the previous case for both of these enhancements in Table6.

The enhancement strategies adopted in Table 4 reflect object u_1's concern about investing on service coverage (0.60 is upgraded to 0.80). In this improvement, the object accordingly obtains higher satisfaction factor (0.47 is upgraded to 0.49). The object u_2 concerns more about the surgery and diagnosis factors and invest on these rates. However, for high investment and their costly enhancements, the improvement is not dramatic (0.11 is upgraded to 0.15 and 0.72 is upgraded to 0.75). Objects u_3 and u_4 mainly concern about the correlated factors with expense issues. The expense factor is highly enhanced by user u_3 (0.27 is upgraded to 0.40) and the satisfaction factor is advanced by u_4 (0.29 is upgraded to 0.50). Objects u_5 and u_6 concern about overall reputation value and investigate the methods that yield the best outcomes. Therefore, these objects start with enhancing the parameters on random basis to comprehend the estimated coefficients with respect to the obtained results. Following this strategy, these objects would have an impression on the fact that how they can effectively use their budget to enhance their reputation values to their optimal cases.

Results shown in Table 5 are also obtained from another independent enhancement over the state corresponding to Table 2. In this Table, objects follow their built-in strategies and therefore, obtain different results. Table 6 compare these two enhancements but their inde-

Table 6: Different reputation improvement results with respect to independent enhancement over state shown in Table 2.

Objects	$Table4$	$Table4$
u_1	17%	15%
u_2	4%	10%
u_3	12%	8%
u_4	15%	12%
u_5	29%	20%
u_6	1%	7%

Table 7: Continuation of different reputation improvement results with respect to independent enhancement over state shown in Table 2.

Objects	Imp_1	Imp_2	Imp_3	Imp_4	Imp_5
u_1	17%	15%	13%	17%	19%
u_2	4%	10%	27%	12%	12%
u_3	12%	8%	10%	9%	3%
u_4	15%	12%	10%	3%	20%
u_5	29%	20%	22%	15%	25%
u_6	1%	7%	8%	15%	19%

pendent enhancement does not show how well these objects act while they follow different strategies. To achieve this result, we carry on independent enhancements over state one (shown in Table 2) in Table 7 and compare over objects' success in improving their reputation values.

Considering the impact of strategic enhancement on the reputation parameters, we continue the first state's results and achieve better results that are compatible with our discussions in the theoretical part of this paper. Table 8 represent the cases that are followed by the first state shown in Table 2. In these cases, the reports obtained from each enhancement could be used in the further enhancement changes. The objects following the random strategies generally ignore the received reports and therefore, the continuous upgrade does not influence their enhancement strategies. However, the received reports mainly influence the objects that seek a specific goal, particularly the ones that use efficient strategy. These objects (u_5 and u_6) obtain best results thanks to strategic enhancement changes that they apply to their reputation parameters.

Table 8: Continuous reputation enhancement of different objects initiated from state one shown in Table 2.

Objects	Imp_2	Imp_3	Imp_4	Imp_5	Imp_6	Imp_7
u_1	7%	4%	3%	4%	7%	9%
u_2	3%	2%	7%	10%	5%	1%
u_3	18%	10%	10%	20%	15%	5%
u_4	15%	15%	12%	21%	12%	21%
u_5	21%	25%	26%	29%	27%	22%
u_6	18%	20%	22%	23%	24%	25%

5 CONCLUSION

In this paper, we proposed a strategic performance analysis that is used for multi-factor systems. We specifically considered a hospital system with its relative reputation parameters and mainly concentrated on the facts and reasons where the reputation of such a system undergoes some changes. The strategic performance analysis mainly aggregates different relative parameters and analyzes their influence directly on the reputation. This process is ended up in a linear programming concept that could be taken into account with the intelligent system once some decisions are made under uncertainty. The proposed model is divided into two parts: (1) theoretical part where we aggregate the relative parameters and compute the reputation of a hospital as a multi-factor system; and (2) the experimental part where we develop such a system and expose to diverse settings with known (and unknown) parameters from the environment. We discuss in details about the progress of the strategic model in different settings. We verify the efficiency of the strategic model in parameter settings with respect to the theoretical results.

For our future work, we have a number of ideas that could be applied to the system. We consider the following as our main future objectives: (1) we would like to apply learning methodologies to enhance the quality and efficiency of the hospital's decision making mechanism. The learning technique enables the system to expand more information from the received reports and therefore, forms a more complete impression about the experiences obtained from the past enhancement changes; (2) we also want to expand the experimental environment and expose the system to vaster settings. Accordingly, we would like to investigate the reasons where a system undergoes some changes or adversely why the final reputation value is constrained the same; (3) we also want to enhance the quality of our theoretical analysis by considering different statistical techniques while using different random distribution functions.

REFERENCES

[1] M. Bastanfard and S. D. katebi. Optimization and mutual information through machine learning technique. ISAST Transactions on Intelligent Systems, No. 1, Vol. 1, 2008.

[2] D. Bhanu, P. Balasubramanie. A Predictive and forecasting model for increased sales a rule mining approach. ISAST Transactions on Intelligent Systems, No. 1, Vol. 1, 2008.

[3] S.Y. Chao, Z. Lee, and A. M. Agogino. Warranty and maintenance decision making for gas turbines. In the Proceedings of the AAAI Spring Symposium on AI in Equipment Service Maintenance and Support, 1999.

[4] S. Gasson. Human-centered vs. user-centered approaches. Journal of Information Technology Theory and Application (JITTA), 5(2):29-46, 2003.

[5] A. Kapoor and E. Horvitz. On discarding, caching, and recalling samples in active learning. Proceedings of the Conference on Uncertainty and Artificial Intelligence 2007, AUAI Press, July 2007.

[6] C. Hayes, A. Goel, I. Tumer, A. Agogino and W. Regli. Intelligent support for product design: looking backwards, looking forwards. To appear in ASME Journal of Computing and Information Science in Engineering, 2011.

[7] K. Regan, P. Poupart, R. Cohen. Bayesian reputation modeling in e-marketplaces sensitive to subjectivity, deception and change. Proceeding of the 20'th AAAI Conference on Artificial Intelligence (AAAI), 2006.

[8] R. Rosenfeld. A maximum entropy approach to adaptive statistical language modelling. In Computer, Speech and Language, 10:187-288, 1996.

ELLIOTT WAVES RECOGNITION VIA NEURAL NETWORKS

Martin Kotyrba
Eva Volna
David Brazina
Robert Jarusek
Department of Informatics and Computers
University of Ostrava
Z70103, Ostrava, Czech Republic
martin.kotyrba@osu.cz
eva.volna@osu.cz
david.brazina@osu.cz
robert.jarusek@osu.cz

KEYWORDS
Elliott wave, neural networks, pattern recognition.

ABSTRACT

In this paper we introduce our method that is able to analyze and recognize Elliott waves in time series. Our method uses an artificial neural network that is adapted by backpropagation. Neural network uses Elliot wave's patterns in order to extract them and recognize. Artificial neural networks are suitable for pattern recognition in time series mainly because of learning only from examples. There is no need to add additional information that could bring more confusion than recognition effect. Neural networks are able to generalize and are resistant to noise. On the other hand, it is generally not possible to determine exactly what a neural network learned and it is also hard to estimate possible recognition error. They are ideal especially when we do not have any other description of the observed series. This paper also includes experimental results of Elliott waves recognition carried out with our method.

INTRODUCTION

Financial data is a set of economic indexes with certain significance in finance. The basic pattern recognition can be classified according to various criteria. Basic criteria of time series pattern recognition are to identify the direction of the trend. The basic step for the future prediction is patterns recognition. The Elliott Wave Principle is a detailed description of how groups of people behave. It reveals that mass psychology swings from pessimism to optimism and back in a natural sequence, creating specific and measurable patterns. One of the easiest places to see the Elliott Wave Principle at work is in the financial markets, where changing investor psychology is recorded in the form of price movements. If we can identify repeating patterns in prices, and figure out where we are in those repeating patterns today, we can predict future trend. This paper introduces our method that allows analysis Elliot wave's patterns in time series for the purpose of their future prediction.

ARTIFICIAL NEURAL NETWORKS

An Artificial Neural Network (ANN) is a connectionist massively parallel system, inspired by the human neural system. Its units, neurons (Fig. 1), are interconnected by connections called synapse. Each neuron, as the main computational unit, performs only a very simple operation: it sums its weighted inputs and applies a certain activation function on the sum. Such a value then represents the output of the neuron. However great such a simplification is (according to the biological neuron), it has been found as plausible enough and is successfully used in many types of ANN, (Fausett 1994).

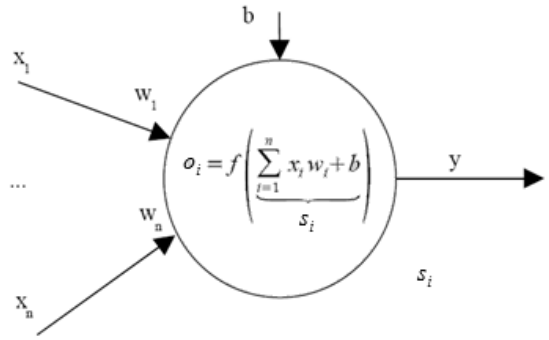

Figures 1: Model of neuron

A neuron X_i obtains input signals $\boldsymbol{x_i}$ and relevant weights of connections $\boldsymbol{w_i}$, optionally a value called bias b_i is added in order to shift the sum relative to the origin. The weighted sum of inputs is computed and the bias is added so that we obtain a value called stimulus or inner potential of the neuron s_i. After that it is transformed by an activation function f into output value o_i that is computed as it is shown in equations (see Fig.1) and may be propagated to other neurons as their input or be considered as an output of the network. Here, the activation function is a sigmoid, (Kondratenko and Kuperin 2003).
The purpose of the activation function is to perform a threshold operation on the potential of the neuron.

Proceedings 26th European Conference on Modelling and Simulation ©ECMS Klaus G. Troitzsch, Michael Möhring, Ulf Lotzmann (Editors)
ISBN: 978-0-9564944-4-3 / ISBN: 978-0-9564944-5-0 (CD)

$$s_i = \sum_{j=1}^{n} w_{ij} x_j + b_i$$
$$o_i = \left(1 + e^{-s_i}\right)^{-1} \quad (1)$$

Many authors agree that multilayer feedforward neural networks belong to the most common ones in practical use. Usually a fully connected variant is used, so that each neuron from the *n-th* layer is connected to all neurons in the *(n+1)-th* layer, but it is not necessary and in general some connections may be missing. There are also no connections between neurons of the same layer. A subset of input units has no input connections from other units; their states are fixed by the problem. Another subset of units is designated as output units; their states are considered the result of the computation. Units that are neither input nor output are known as hidden units, (Hertz and Kogh 1991).
Each problem specifies a training set of associated pairs of vectors for the input units and output units. The full specification of a network to solve a given problem involves enumerating all units, the connections between them, and setting the weights on those connections. The first two tasks are commonly solved in an ad hoc or heuristic manner, while the final task is usually accomplished with the aid of a learning algorithm, such as backpropagation. This algorithm belongs to a group called "gradient descent methods". An intuitive definition is that such an algorithm searches for the global minimum of the weight landscape by descending downhill in the most precipitous direction (Fig. 2).

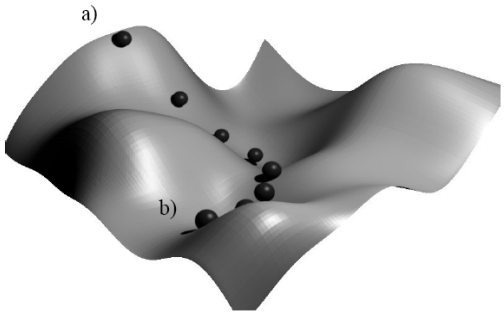

Figures 2: An intuitive approach to the gradient descent method, looking for the global minimum: a) is the starting point, b) is the final one.

The initial position is set at random (note that there is no a priori knowledge about the shape of the landscape) selecting the weights of the network from some range (typically from -1 to 1 or from 0 to 1). It is obvious that the initial position on the weight landscape greatly influences both the length and the path made when seeking the global minimum. In some cases it is even impossible to get to the optimal position due to the occurrence of some deep local minima. Considering the different points, it is clear, that backpropagation using a fully connected neural network is not a deterministic algorithm. Now, a more formal definition of the backpropagation algorithm (for a three layer network) is presented, (Fausett 1994).

- The input vector is presented to the network.
- The feedforward is performed, so that each neuron computes its output following the formula (2) over neurons in previous layer:

$$o_i = \frac{1}{1 + e^{\left(\sum_{j=1}^{n} x_j w_{ij} + b\right)}} \quad (2)$$

- The error on the output layer is computed for each neuron using the desired output (y_j) on the same neuron (3):

$$err_j^0 = o_j(1 - o_j)(y_j = o_j) \quad (3)$$

- The error is propagated back to the hidden layer over all the hidden neurons (hi) and weights between each of them and over all neurons in the output layer (4):

$$err_i^h = h_i(1 - h_i)\sum_{j=1}^{r} err_j^0 w_{ij}^0 \quad (4)$$

- Having values err_j^0 and err_i^h computed, the weights from the hidden to the output layer and from the input to the hidden layer can be adjusted following formulas (5)

$$w_{ij}^0(t+1) = w_{ij}^0(t) + \alpha\, err_j^0 h_i$$
$$w_{ij}^h(t+1) = w_{ij}^h(t) + \alpha\, err_j^h x_i \quad (5)$$

where α is the learning coefficient and x_i is the *i-th* neuron in the input layer.

- All the preceding steps are repeated until the total error (6) of the network over all training pairs does not fall under certain level.

$$E = \frac{1}{2}\sum_{i=1}^{n}(y_i - o_i)^2 \quad (6)$$

The formulas in step three and four are products of derivation of the error function on each node. A detailed explanation of this derivation as well as of the complete algorithm can be found in (Hertz and Kogh 1991).

ELLIOTT WAVE THEORY

Elliott Wave Principle is based on the fact that prices usually move in fives waves in the direction of the larger trend and in three waves contrary to it. In an uptrend a five wave advance will be followed by a three wave decline; in a down trend a five wave decline will be followed by a three wave advance. Five-wave patterns are called impulse waves, three-wave patterns are called corrective waves (see Fig.3). Elliott wave principle works best on markets with the largest public following. The forex market as a result of its enormous size, liquidity and diversity of participants very often displays clear wave patterns which can be used to a trader's advantage - providing him or her with high-reward/low-risk, high-probability entry points in accordance with the prevailing trend. The usefulness of the Elliott wave analysis for the forex trader is also highlighted by the fact that the major waves on the currency markets usually develop in close correspondence with the interest rate cycles specific for the currency pairs that somebody

is trading. Potentially profitable Elliott wave setups occur 50% of the time on the currency markets which makes it important for the forex traders to be at least aware of the basic principles of recognizing them, (Frost and Prechter 2001).

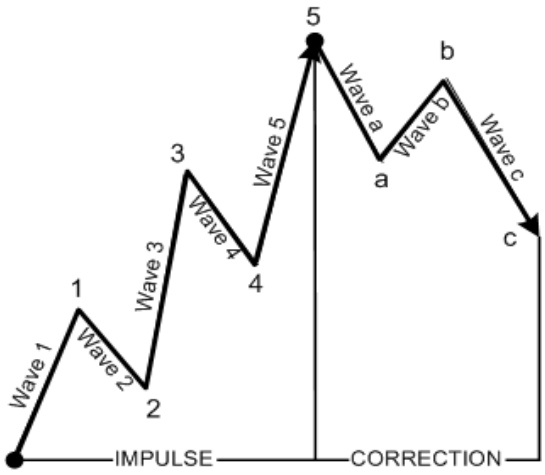

Figures 3: The basic pattern of Elliott wave

Impulse waves are five wave patterns. Impulse waves always unfold in the same direction as the larger trend - the next higher degree impulse or corrective wave. Waves 1, 3 and 5 within an impulse are themselves impulse waves of lower degree which should also subdivide into a five-wave pattern (see Fig.4). One of the impulse waves within an impulse wave will usually be extended or much longer than the other two. Most extensions in the currency markets occur in wave three. When one of the impulse waves extends the other two will frequently be of an equal size. Waves 2 and 4 within an impulse waves are corrective waves. Once an impulse wave is completed it will be followed by a corrective wave. An impulse wave is always followed by a corrective wave of the same degree unless the impulse wave completes a higher degree wave, (Poser 2003).

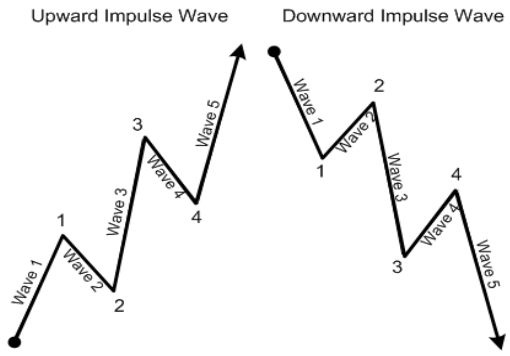

Figures 4: The basic pattern of impulse phase

There are three rules which should hold true for an impulse wave (see fig. 5) to be valid:

- wave two cannot move past the start of wave one;
- wave three cannot be the shortest wave of the three impulse waves (1,3,5);
- wave four cannot move past the end of wave one.

If any of these rules is violated you should try a different wave count. In some cases the wave count can still be considered valid if the currency prices violate any of the above rules but not on a closing basis, (Poser 2003).

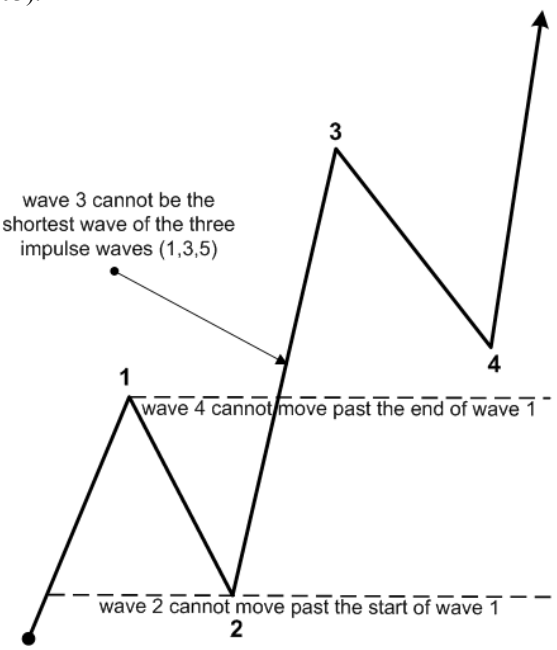

Figures 5: Valid impulse wave

Corrective waves are three wave patterns. Corrective waves always unfold in the opposite direction to the larger trend - the next higher degree impulse or corrective wave. There are two different groups of corrective waves: simple corrective waves (zigzags, flats and irregulars) and complex corrective waves (triangles, double and triple threes). Corrective waves have much more variations than the impulse waves which makes it less easy to identify them while they are still being formed. These corrective waves are broadly called ABC corrections. They differ by the distance their subwaves move in relation to each other and by the way they subdivide. A zigzag consists of a 5-3-5 sequence in which wave B doesn't move past the start of wave A and wave C moves far beyond the end of wave A. A flat is formed by a 3-3-5 sequence in which all the three subwaves are of the same length. An irregular is made up of a 3-3-5 sequence in which wave B exceeds the start of wave A and waves C moves close to or beyond the end of wave A (see fig.6), (Frost and Prechter 2001).

It is useful to know that in all the three ABC corrections wave C subdivides into a five wave pattern, or an impulse wave. This information can be very helpful when making timing decision for entering your trades at the start of the higher impulse waves. ABC corrections

most commonly act as the second subwaves of the impulse waves.

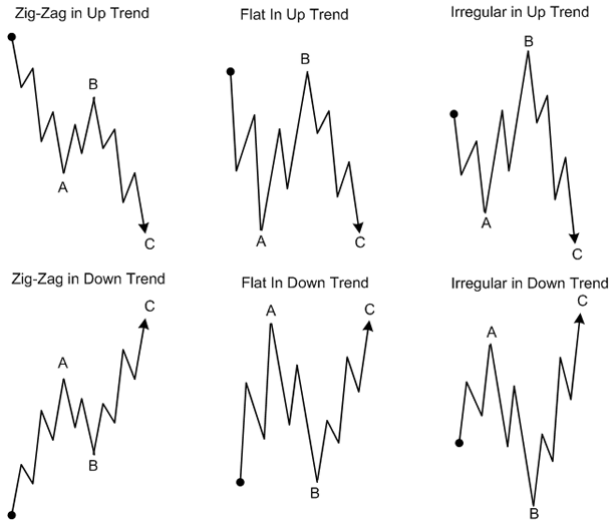

Figures 6: Ideal Zizgaz, Flat and Irregular

FRACTAL STRUCTURE OF ELLIOTT WAVES

One of the basic tenets of Elliott Wave theory is that market structure is fractal in character. The non-scientific explanation of this fractal character is that Elliott Wave patterns that show up on long term charts are identical to, and will also show up on short term charts, albeit with sometimes more complex structures. This property of fractals is called "self-similarity" or "self-affinity" and it is what this writer is referring to when he says that the market is fractal in character. Elliott waves are fractals because fractal is a geometric object that after their division into smaller parts of shape shows similarities with the original motives. Each impulse phase consists of three subwaves upward of five breaks and each correction phase consists of two subwaves downward of three breaks. For a detailed view of the Elliott wave, we can find more and more fractures in each subwave. Just such repeating pattern is a fundamental property of fractals, (see Fig. 7.), (Poser 2003).

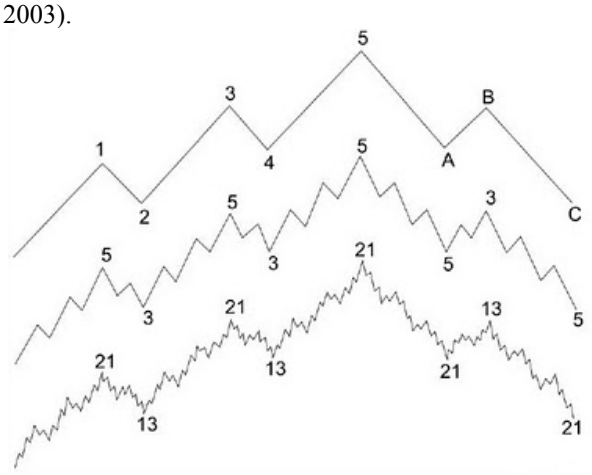

Figure 7: Fractal structure of Elliott wave

Using Elliotts waves for determining the future development of prices is quite simple. If Elliott wave occurs in a stock market trends, we can expect break of a price in the opposite direction after the fifth pulse wave or after the third correction wave. Of course, it is not so simple. Elliott wave is very often distorted differently, and prediction is then very difficult and sometimes impossible. Our use of the word fractal, or Elliott Wave fractal, is not a proper use of the property of self-similarity. When we use the term here we mean a "counting fractal," which is really a description of the relative position of a bar on a high-low bar chart. This may create confusion but we do not want to hijack 'Elliott Wave Fractal' from Dr. Bill Williams, the originator of the expression, (Frost and Prechter 2001).

AN EXPERIMENTAL STUDY

During our experimental work, we made some study included Elliott waves pattern recognition. Our method is based on backpropagation neural network and is able to recognize Elliot wave structures in given time series. In order to test the efficiency of the method, we applied a database from the area of financial forecasting [4]. Artificial neural networks need for their adaptation training sets. In our experimental work, the training set consists of 11 different types of Elliott wave's samples, see Fig. 8.

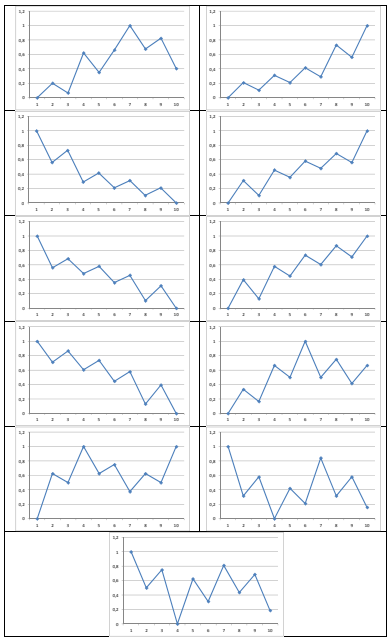

Figure 8: Different types of Elliott wave's samples represented in the training set

Input data are sequences included always *n* consecutive numbers, which are transformed into interval <0,1> by the formula (7). Samples are adjusted for the needs of backpropagation networks with sigmoid activation function in this way.

$$x_i' = \frac{x_i - \min(x_i,...x_{i+n-1})}{\max(x_i,...x_{i+n-1}) - \min(x_i,...x_{i+n-1})} \qquad (7)$$

where x_i' is normalized output value of the *i*-th neuron, and $(x_i,...x_{i+n-1})$ are *n-1* consecutive output values that specify sequences (patterns) from the training set (e.g. training pars of input and corresponding output vectors). The training set for our experimental study is written in Table 1.

Input vector contains 10 components. Output vector has got 11 components and each output unit represents one of 11 different types of Elliott wave's samples. The neural network architecture is 10 - 10 - 11 (e.g. 10 units in the input layer, 10 units in the hidden layer, and 11 units in the output layer), because the pattern recognition is not linearly separable problem and therefore we cannot use neural network without hidden units. The nets are fully connected. Adaptation of the neural network starts with randomly generated weight values. Backpropagation method was used for the adaptation with the following parameters: first 5000 iterations has learning rate value 0.5, and for the next 2000 iterations has learning rate value 0.1, momentum is 0.

Our test set is made from the time series (see Fig. 9) and includes 259 values. We used forex EUR/USD from 11.3.2010. The foreign exchange market (forex) is a global, worldwide-decentralized financial market for trading currencies. Financial centers around the world function as anchors of trading between a wide range of different types of buyers and sellers around the clock, with the exception of weekends. The foreign exchange market determines the relative values of different currencies. The values were downloaded from (Forex databases).

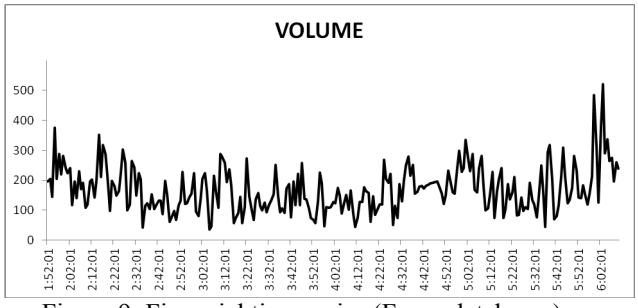

Figure 9: Financial time series (Forex databases)

Our Neural network was able to recognize all given types of Elliott wave's samples represented in the training set (Fig. 8, Table 1). There is shown number of pattern P1-P11 that was recognize from financial time series with several probabilities (grater than 0.9, 0.8, 0.7, 0.6, and 0.5) in Table 2. We can see that pattern P1 was recognized with probability grater then 0.9 quite 6 times, with probability grater then 0.9 quite 2 times etc. Illustration of some recognized patterns that occur in financial time series is shown in Fig. 10. Comparison of the sixth pattern looks, how is learned via neural network versus its present in test set is represented in Fig. 11.

Table 2: Test results

Proba-bility	Number of patterns										
	P 1	P 2	P 3	P 4	P 5	P 6	P 7	P 8	P 9	P10	P11
> 0.9	6	18	19	12	5	3	5	15	22	8	6
> 0.8	2	6	0	2	2	0	6	9	5	1	4
> 0.7	4	2	0	0	1	0	3	5	5	1	3
> 0.6	4	1	1	0	0	0	4	0	1	1	1
> 0.5	0	5	1	0	1	1	3	2	1	0	0

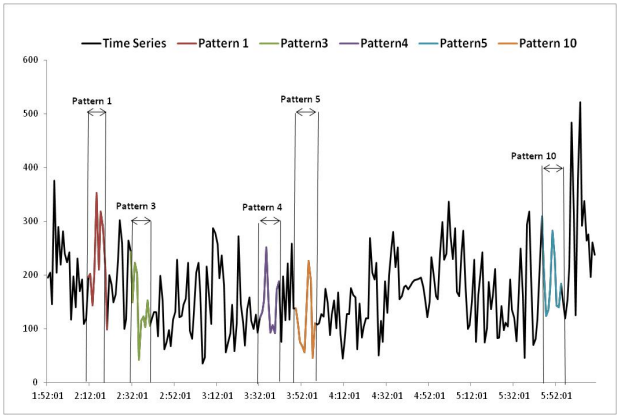

Figure 10: Some recognized patterns that occur in financial time series

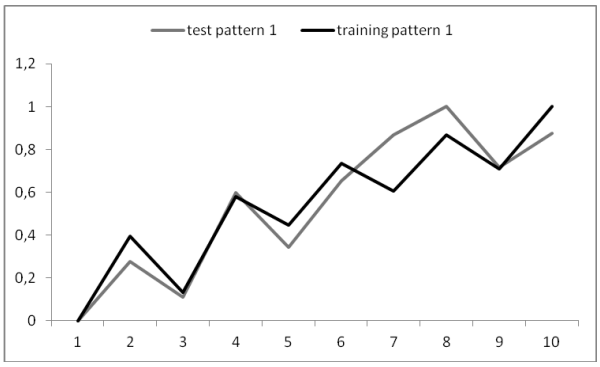

Figure 11: Training pattern 6 and its representation in test set

CONCLUSION

In this paper, a short introduction into the field of time series pattern recognition using artificial intelligence methods has been given. We used method based on backpropagation neural network. According to the results of experimental studies, it can be stated that Elliot wave's patterns were successfully extract in given time series and recognize using suggested method, how as can be seen from figures in result section. The future work will be focused on development of some method, which could be able to recognize a fractal structure in Elliot wave's patterns. It means, that the method should recognize Elliot wave's patterns in a varied time scale. It

might result in better mapping of the time series behavior for better prediction.

ACKNOWLEDGMENT

The research described here has been financially supported by University of Ostrava grant SGS2/PřF/2012.

REFERENCES

Fausett, L., 1994,: "Fundamentals of Neural Network". 1st ed. Prentice Hall, ISBN: 0-13-334186-0.

Hertz, J. and Kogh, A. and Palmer, R G, 1991,: "Introduction to the Theory of Neural Computation", Addison – Wesley.

Kondratenko, V. and Kuperin, Y., 2003. "Using recurrent neural networks to forecasting of Forex. " St. Petersburg State University.

Frost, A.J. and Prechter R.,,2001. "Elliott Wave Principle: Key to Market Behavior" ISBN 0471988499, John Wiley & Sons.

Poser, S. 2003,: "Applying Elliott Wave Theory Profitably" ISBN-10: 0471420077, Publisher: Wiley.

A database from the area of financial forecasting [online], http://www.google.com/finance/forex?=nas:eur/usd:daq 10.11. 2011.

MARTIN KOTYRBA is an Ph.D. student at the Department of Computer Science at University of Ostrava, Czech Republic. His interests include artificial intelligence, formal logic, soft computing methods and fractals. He is an author of more than 15 papers in proceedings of conferences.

EVA VOLNA is an Associative Professor at the Department of Computer Science at University of Ostrava, Czech Republic. Her interests include artificial intelligence, artificial neural networks, evolutionary algorithms, and cognitive science. She is an author of more than 50 papers in technical journals and proceedings of conferences.

DAVID BRAZINA is an doctor at the Department of Computer Science at University of Ostrava, Czech Republic. His interests include computer graphics, neural networks. He is an author of more than 10 papers in technical journals and proceedings of conferences.

ROBERT JARUSEK is an master student at the Department of Computer Science at University of Ostrava, Czech Republic. His interests include artificial intelligence, neural networks, and soft computing. He is an author of more than 5 papers in proceedings of conferences.

SIMULATION OF SURFACES MICROROUGHNESS BY MEANS OF POLYGONAL REPRESENTATION

David Bražina
Martin Kotyrba
Eva Volná
Department of Computer Science
University of Ostrava
Dvoráková 7, Ostrava, 701 03
david.brazina@osu.cz
martin.kotyrba@osu.cz
eva.volna@osu.cz

KEYWORDS
Displacement mapping, bumb mapping, height map, global illumination, AWJ, microroughness.

ABSTRACT

The paper presents a method of visualisation of surface microroughness acquired by hydroabrasive division (AWJ – abrasive water jet), by means of polygon representation. The method stems from theoretical and practical possibilities of so-called global illumination mapping of unevenness using suitable image maps. Based on data interpretation stemming from measurement of the surface roughness, an original method is proposed and realised, which also enables to visualise light interactions in the visualised microsurfaces.

INTRODUCTION

So far, the most used tool to measure surface quality has been a contact profilometer, whose disadvantage is the possibility of only a 2D surface evaluation (i.e. along the selected line), contact with the measured surface (which can lead to destruction of the surface or distortion of the measured data), and finally, to a certain degree, a significant time-shift between the measurement itself and its evaluation. The above-mentioned drawbacks of 2D surface evaluation lead to the necessity of devices of new generation enabling 3D surface evaluation (i.e. on the selected surface) in real time without its possible destruction. Neither of the procedures solves problems of light interaction visualisation on given surfaces (Arola and Ramulu 1997) Current methods of surface evaluation, either 2D (along lines) or 3D (in points on a raster), are limited to monochromatic representation of microroughness without a possibility to compare interaction of various light sources under various angles of incidence and various intensity and wavelength of the used luminous flux, and without an ability to visualise diffusive and reflexive qualities of the examined surface. However, a necessity arises for repeated time-consuming and costly measurements without knowing at least an approximate result. Another disadvantage is the fact that in the case of 3D surface evaluation by non-contact devices, we dispose of a record which does not contain all profile qualities of the examined surface. In the case of optical methods, it depends on the resolution of the used raster where we examine light reflections in the selected network of points. It appears that more demonstrative surface evaluation is still achieved by 2D evaluation methods. Our presented method of visualisation of the observed surfaces, which uses the most modern findings from computer graphics, leads to possibilities of simulation of luminous flux distribution on the examined surfaces and to significantly better possibilities of a subsequent comparative analysis.
Therefore we have created the presented method, which enables to visualise light interactions with microsurfaces from the point of view of reflexive and diffusive qualities using a suitable image mapping combined with selected physical methods of global illumination, their mutual interconnection with consequent visualisation implications.

STATE OF THE ART - SURFACE CREATION

Knowledge of the topography of surfaces created by AWJ and their classification is very important for "machining" techniques (Botak 2009). In the reports published by authors optical methods was used for the investigation of the surface structure cutting of areas (Hloch 2008). Optical methods are based on illuminating by defocused laser beam and white light beams. Measurement of surfaces generated by water jets and abrasive water jets, according to technological conditions is quite difficult (Valíček 2010). It is caused by specific surface structure. In contrast to classical methods, the surface created by water jets and abrasive water jets is rather diffuse (Hlaváček 2009). After testing a few optical methods to study the surface characteristics of several samples prepared by abrasive water jet machining authors (Hloch 2009) decided to apply a newly developed method. It is specially dedicated to measurements on surfaces with a relatively rough surface structure. The method is based on the visualisation of the roughness by oblique angle illumination - shadow method (Valíček 2007). The optical effect caused by light impinging on the surface at an oblique angle is used to visualise the geometrical

Proceedings 26th European Conference on Modelling and Simulation ©ECMS Klaus G. Troitzsch, Michael Möhring, Ulf Lotzmann (Editors)
ISBN: 978-0-9564944-4-3 / ISBN: 978-0-9564944-5-0 (CD)

shapes present at the sample surface. The shapes can thus be displayed in a simulated optical plane. The intensity of the light scattered by the surface treated in this manner contains the information about the frequency and height of the geometrical shapes present on the surface.

Nevertheless, a lot of problems occurred during the investigation of surface structure created by water jet and abrasive water jet machining that is reported in (Hloch, Valíček and Simkuet 2009).

For example scratches made by abrasive particles form small planes with random inclination to the plane tangential to the local surface profile, thus generating micro-mirrors randomly reflecting the incident light. This phenomenon increases the signal noise and it makes proper evaluation of the surface unevenness more difficult. In order to render surfaces acquired by AWJ using image maps, we stem from a consideration. Provided we use a heightmap to create a corresponding relief of the examined surface, a physically exact interpretation needs a corresponding number of reference surfaces (see the reference polygon network). Provided we stem only from the fundamental of displacement mapping, we get to the level of interaction surfaces, whose number is limited by the current visualising tools, particularly concerning rendering speed.

Thus it is necessary to find a solution enabling physically plausible as well as performable visualisation. From physical point of view we presume that those are surface peaks with the highest amplitude that are the most active in light distribution across the visualised surface.

Based on information stored in the corresponding heightmap, we can declare that unevennesses which will be participating most actively in the interaction with luminous fluxes in the scene are surfaces with the highest brightness representing the most significant roughness of the given surface. (Fig.1)

```
HeaderLines=10
ScanMode=3D
XSize=3000
YSize=1000
Depth=32
XRange=0.029999
YRange=0.0100005
ZScale=1.00708e-008

0 0 1
1 0 1
2 0 1
.....
.....
.....
2400 211 64482
2401 211 64264
2402 211 63286
.....
.....
.....
2274 983 1
2275 983 2772
2276 983 3146
```

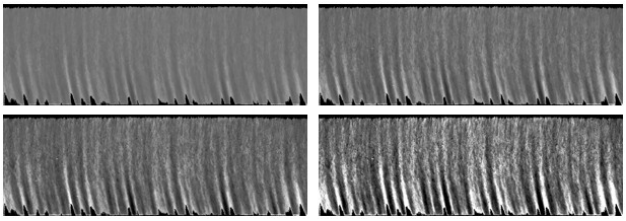

Figure 1: Visualisation of the original heightmap based on the measured unevenness matrix. Contrast marks unevenness of the visualised surface

The number of polygons, and related accuracy of rendering of the visualised surface, is regulated by defining the darkest value of the heightmap for which the given surface will be generated. From implementation point of view, it will concern allocation of the alpha channel to all colour shades which will be below this minimal boundary. The required visualisation accuracy will be then defined by setting the value of the darkest shade (i.e. a concrete value from the data matrix where the values below this boundary will equal 1. Subsequent allocation of a normal map to such created surfaces will define direction normal (Fig.2)

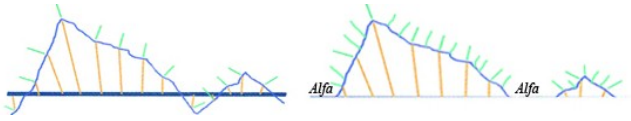

Figure 2: Designated area for primary displacement map

For such a created image map, we introduce a term primary displacement map. Having applied the primary displacement map, the observed relief is segmented while keeping accurate topology of the observed surface. This is the way to physically create a polygon network where the peak of individual polygons are shifted in the direction of the heightmap and reflective qualities of the surfaces defined by those peaks are influenced on the basis of the corresponding normal map. Polygons which have the alpha channel dedicated on the basis of the heightmap are not influenced by this map, therefore we can apply a residual heightmap on them. For this map, we introduce a term secondary displacement map. Despite the fact that the map is more segmented (from the polygon size point of view), there is no conversion of the secondary displacement map into a polygon surface, which will result in a significant reduction of the needed polygons while keeping a physically corresponding value of the given visualisation. In order to specify light simulations more exactly in the secondary displacement map, we will use a virtual displacement mapping with an assigned normal map. A normal map contains information on the angle of incident of the reflected light on the surface of the visualised sample. (Fig 3).

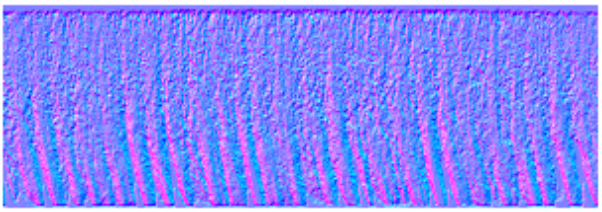

Figure 3: Visualisation of normal map

In fact, it concerns a combination of displacement mapping with normal bump mapping using alpha channel in the displacement map. With respect to the above -described, we have used a term double displacement for this kind of visualisation of a large number of surfaces concentrated into a small area. The network must be chosen in a way that the corresponding visualisation would conform to the information contained in the corresponding image maps. At best, it is necessary to choose such dimensions which would correspond to the dimensions of the visualised surface. The density of such a polygon network is given by the corresponding primary displacement map. (Fig. 4). Depending on the required speed and accuracy of rendering, it is possible to influence this density by changing the relevant attributes with respect to the visualisation software itself. These attributes relate to conversion of the rendered object into triangles designed for subsequent rendering (tessallation).

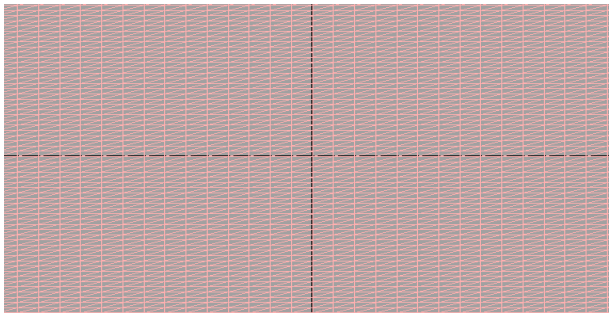

Figure 4: Reference polygon network (zoomed 20x)

It appears that it is not relevant whether the reference polygon network has been created by polygon modelling because in the case of any modelling, rendering itself of any object in the scene is given by this conversion. A reference polygon network thus creates a virtual space (which is possible to be visualised) containing information on the shift of polygon peaks with respect to the primary displacement map. In a reference polygon network, we define only dimensions along axis x and y. the dimension in direction of the x axis is defined by the corresponding primary displacement map on the basis of information contained in the height map. Having applied the primary displacement map on this polygon network, we will use the information contained in this map to generate own polygon surface, where the peaks of individual vertices will be moved (Fig 5).

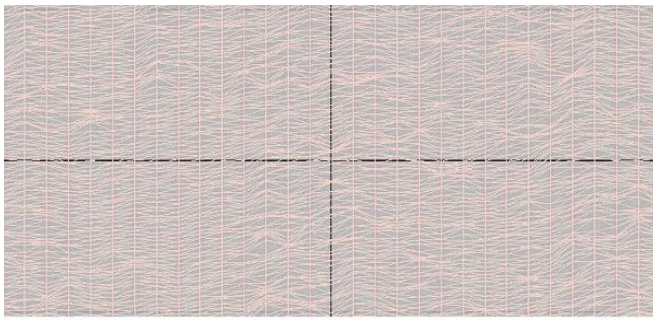

Figure 5: Polygon surface (zoomed 20x)

The places that we define the primary displacement map by alpha channel will keep the original topology of the reference polygon network, which will result in zero change of orientation of the individual polygon peaks with respect to the axis z. We then map in a normal map on such a created object and we assign it corresponding material-optical qualities of the visualised surface of the particular material. It primarily concerns attributes defining reflexive refractive, and diffusive qualities which are related to the distribution of luminous fluxes on given surfaces and which are traceable in material tables. It is then possible to proceed to incorporation of information contained in the secondary displacement map. As this map fills in places which are invisible from the point of view of the primary displacement map it will result in polygon rendering on this part of the surface on the basis of the reference polygon network. Rendering of the secondary displacement map proceeds on the principle of virtual displacement mapping taking into consideration that, with respect to the normal map, there will be a change of orientation of individual normals within the secondary displacement map without changing the typology type of the generated polygon surface. In our proposed conception of visualisation of surfaces by abrasive waterjet, the final visualisation is composed of the primary and secondary displacement map and normal map hand in hand with the corresponding material allocated to the generated polygon surface. The scheme of double displacement applied on aluminium is indicated by a so-called shading network diagram (Fig 6)

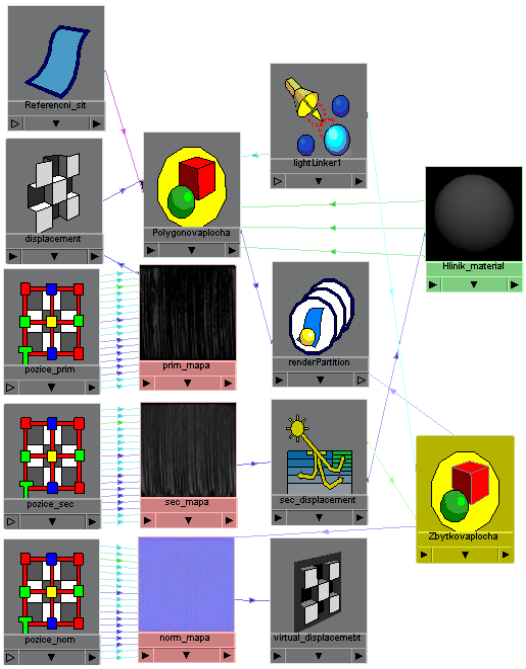

Figure 6: Schematic demonstration of double displacement

To simulate light interactions on surfaces acquired by AWJ, we stem from possibilities of global illumination algorithms, Final Gathering and the method of photon maps, applied on a surface generated by double displacement. Optimal setting of attributes related to rendering algorithms has a crucial influence on the speed of rendering, quality, and usability of the final synthetic image of the simulated surface. We assume that, with respect to theoretical combination presumptions of the photon map method with algorithm Final Gathering, there will be a rapid decrease in the rendering time.

EXPERIMENTAL SET UP

The initial material for experimental purposes was unalloyed titanium with the specification ASTM B265-99, supplied in the annealed condition.
Testing of the rendering speed and image qualities of the visualised surface has been carried out only on the surface generated by the primary displacement.
Table 1 shows that the change of value Global illum radius has a key influence on the speed of rendering, unlike attribute Global illum accuracy, whose influence on the speed of rendering can be neglected. The energy value does not influence the speed of rendering, the same for the exponent expressing attenuation of the light intensity. The energy correspond to energy balance of the emitted photons inside the visualised scene. Value 2 corresponds to a physical model of spreading light in space.

Table 1: Effects of photon map method attributes to the speed of the visualised scene

Photon map method				
Accuracy	Energy	Exponent	Radius	Time(min:sec)
1	8000	2	0	13:34
50	8000	2	0	13:32
100	8000	2	0	13:31
200	8000	2	0	13:32
300	8000	2	0	13:34
100	8000	2	0.1	22:54
200	8000	2	0.2	25:26
300	8000	2	0.5	40:02

The basic disadvantage of using photon maps is a relatively high time-exigency to process synthetic image. Incorporation of algorithm Final Gathering into this process results in reduction in calculation of emitted photons into the scene, which will finally lead to reduction in the rendering time while keeping quantitatively corresponding visualisation. It is given by the algorithm itself, which uses information acquired by the method of photon maps on distribution of photons focused into the visual field of the observer. In the case of visualisation of surfaces acquired by AWJ, the surfaces are rendered in two phases. The first phase sets attributes of the method of photon maps. The next phase carries out implementation of algorithm Final Gathering and testing of influences of corresponding parameters on the speed of rendering. Table 2 shows optimal value setting.

Table 2: Impacts of attributes of method Final Gathering on the speed of rendering of the visualised scene

Final Gathering			
Final gather rays	Min radius	Max radius	Time(min:sec)
100	0	1	15:30
200	0	1	22:12
300	0	1	27:46
400	0	1	30:06
100	0.01	1	12:17
100	0.05	1	05:33
100	0.1	1	04:22
100	0.5	1	02:03
100	0.1	0.1	12:16
100	0.1	0.2	06:38
100	0.1	0.5	04:27
100	0.1	1	04:16

On the basis of the presented data, we can declare that in the case of visualisation of surfaces acquired by AWJ

using our introduced method of double displacement, the interconnection of the method of photon maps with method Final Gathering leads to time-acceptable requirements in the visual device. Implementation of Final Gathering into the algorithm of the method of photon maps leads to a significant reduction of the rendering time while keeping the corresponding information of the synthetic image. Fig. 7 shows realised simulation of an aluminium surface using the method of double displacement.

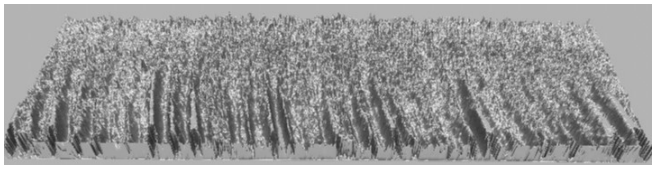

Figure 7: Final visualisation of a titanium microuroughness on the surface acquired by AWJ, using double displacement method.

Another advantage of our introduced method of double displacement for visualising surfaces acquired by AWJ using global illuminating algorithms Final Gathering and the method of photon maps is visualisation of photon maps on relevant surfaces. Classical methods of rendering techniques, stemming from bump mapping, cannot principally simulate distribution of photons on individual parts of the visualised surface. Thanks to creation of a polygon surface on the basis of double displacement, we have at our disposal relevant reference polygon surfaces where photon distribution takes place within the observed scene, which is not possible in the case of rendering bump mapping techniques. Existence of a diffusive surface is a condition for creation of a corresponding photon map. For visualisation of photon maps, we stem from the consequences of creation of photon maps on diffusive surfaces, which participate in the spread of light distribution on the visualised surface and in visualisation of photons participating in caustics phenomenon, which is related to light reflections.

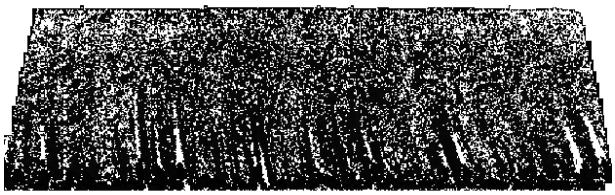

Figure 8: Visualisation of a photon map

According to Fig. 8, white areas correspond to photons participating in caustics phenomenon, which in physical interpretation refers to those surface parts whose division was primarily done by the used abrasive. The other surface parts, rendered in a dark colour, correspond to surfaces which were divided by waterjet almost instantly without a direct influence of the contained abrasive. This visualisation consequence leads to relevant technological conclusions in the choice of a suitable dividing cut. In the case of hard materials, the division itself is rather done by the selected abrasive which leads to creation of surfaces with a high level of reflexive surfaces, which will lead to area visualisation with a high ratio of photons participating in caustics phenomenon. The distribution of photons which simulates diffusive or reflexive reflections in individual areas of the examined surfaces is influences by material-optical qualities stemming from the concrete shading network of the applied material on the object surface and from the corresponding primary displacement map. The size of the area, where is it decided if it concerns a reflexively or diffusively reflecting surface, is done by changing the values stemming from the setting of illuminating algorithms. In the case of the method of photon maps, the value corresponds to the value of Global illum radius.

RESULTS AND DISCUSION

The paper has introduced a method of 3D visualisation of microsurfaces acquired by dividing abrasive waterjet. Based on information stored in image maps using the pre-set method of double displacement, we optimised the combination of global illumination methods of Final gathering and photon maps, which has led to a high level of lifelikeness of the visualised surface in time-acceptable sequences. Such a surface, visualised by distributed luminous fluxes on the surfaces defined by material-optical qualities of particular materials, can be further processed for definition of surface qualities, both from the point of view related to geometric surface qualities of the observed sample and comparison of optical qualities of the light source with respect to wavelength, intensity, or angle of incidence of the light beam. The presented procedures, related to the proposed conception of visualisation solution of unevennesses on surfaces acquired by AWJ, also enable to categorise areas of the visualised surface which are created by primary activity of the used abrasive or primary activity of the waterjet.

Our proposed and realised solution significantly improves the possibilities of comparative analysis against the possibilities of conventional bump mapping techniques, which are dependent on the position of the observer (in certain angles the bump mapping effect fades out) and which do not enable to visualise such phenomena, such as shades, reflections and refractions on the visualised surfaces, related to the change of orientation of the light source in the scene. Moreover, conventional methods of displacement mapping leading to generation of corresponding surfaces on the basis of information stored in height and normal maps fail with respect to unbearable amount of polygon planes necessary to visualise a great number of polygons concentrated in small areas. The presented conception of the solution removes these disadvantages.

APROACH TO THE SOLVED PROBLEMS

The presented method of 3D visualisation of microsurfaces acquired by technological division by abrasive waterjet enables to:

- Render the relief of the visualised sample surface.
- Generate a polygon plane representing significant surface unevennesses.
- Take into consideration material-optical qualities of the observed sample.
- Visualise distribution of luminous fluxes on the visualised surface.
- Take into consideration qualities of the light source with respect to the visualised surface

CONCLUSION

For the following period, we can set tasks related to practical optimisation of our proposed methodology of double displacement in the area of comparative analyses, or selection and implementation of this methodology into various programming tools when using a wide range of global illumination methods in 3D scenes, particularly in cooperation with the staff of the Institute of Geonics, AS CR in Ostrava, company AQUACLEAN in Bratislava, and company REZMAT in Dubnica nad Váhom. Another part of further work is application of the achieved results and pedagogical knowledge when familiarising students with possibilities of 3D graphical visualisation hand in hand with theoretical and practical impacts of the solution in the problem area.
Questions of further research in the following period are formulated in the following lines. It concerns definition of a suitable threshold value for creation of primary displacement maps, stemming from heightmaps, with subsequent definition of nominal parameters. Definition of suitable density of the corresponding reference polygon plane in dependence on the map of unevennesses acquired by optical measuring technological processes defined by requirements on the final visualisation. In addition, possibilities of comparative analyses on the basis of the corresponding photon maps or energy light maps stemming from the possibilities of analysis and image processing. Last but not least, research on impacts of usage of various visualisation algorithms on visualisation of analysed surfaces.

ACKNOWLEDGMENTS

The work has been supported by project SGS23/PRF/2011.

REFERENCES

Arola D, Ramulu M *Material removal in abrasive waterjet machining of metals surface integrity and texture*. In. Wear, vol. (210), pp. 50–8. 1997

Botak Z, Kondic Z, Maderic D. *Waterjet Machining*. Tehnicki Vjesnik-Technical Gazette. Volume: 16 Issue: 3 Pages: 97-101 Published: JUL-SEP 2009

Gombar M, Hloch S, Radvanska A. *Traverse direction influence evaluation on average roughness at AWJ cutting*. Annals of DAAAM for 2006 & Proceedings of the 17th International DAAAM Symposium - Intelligent manufacturing & automation: focus on mechatronics and robotics Pages: 137-138 Published: 2006

Hlavacek P, et al. *Measurement of Fine Grain Copper Surface Texture Created by Abrasive Water Jet Cutting. Strojarstvo*, (2009), Vol. 51, Issue: 4, Pages: 273-279

Hloch S et al. *Experimental study of surface topography created by abrasive waterjet cutting*. In: Strojarstvo. vol. 49, no. 4, (2008), pp. 303-309.

Hloch S., Valíček J., Simkulet, V. *Estimation of the smooth zone maximal depth at surfaces created by Abrasive Waterjet*. International Journal of Surface Science and Engineering 2009 - Vol. 3, No.4 pp. 347 - 359. doi: 10.1504/IJSURFSE.2009.027420

Kusnerova M, et al. *Derivation and Measurement of the Velocity Parameters of Hydrodynamics Oscillating System,* Strojarstvo, (2008) Vol. 50, Issue: 6, Pages: 375-379

Valiček J et al. *An investigation of surfaces generated by abrasive waterjets using optical detection*. In. Strojniski vestnik-Journal of mechanical engineering. vol. 53, no. 4, (2007) pp. 224-232

Valíček J, Hloch S, Kozak D. *Surface geometric parameters proposal for the advanced control of abrasive waterjet technology*. In: The International Journal of Advanced Manufacturing Technology. vol. 41, no. 3-4 (2009), p. 323-328. doi: 10.1007/s00170-008-1489-2

MARTIN KOTYRBA is an Ph.D. student at the Department of Computer Science at University of Ostrava, Czech Republic. His interests include artificial intelligence, formal logic, soft computing methods and fractals. He is an author of more than 15 papers in proceedings of conferences.

EVA VOLNA is an Associative Professor at the Department of Computer Science at University of Ostrava, Czech Republic. Her interests include artificial intelligence, artificial neural networks, evolutionary algorithms, and cognitive science. She is an author of more than 50 papers in technical journals and proceedings of conferences.

DAVID BRAZINA is an professor assistent at the Department of Computer Science at University of Ostrava, Czech Republic. His interests include artificial intelligence, neural networks, and soft computing. He is an author of more than 5 papers in proceedings of conferences.

LEARNING OF AUTONOMOUS AGENT IN VIRTUAL ENVIRONMENT

Pavel Nahodil, Jaroslav Vítků
CTU in Prague, FEE
Department of Cybernetics
Technicka 2, 16627, Prague 6, Czech Rep.
Email: nahodil@fel.cvut.cz, vitkujar@fel.cvut.cz

KEYWORDS

Agent, Creature, Behavior, Artificial Life, Hybrid Architecture, Hierarchical Approaches, Intentions, Planning

ABSTRACT

Presented topic is from area of development of artificial creatures and proposes new architecture of autonomous agent. The work builds on a research of the latest approaches to Artificial Life, realized by the Department of Cybernetics, CTU in Prague in the last twenty years. This architecture design combines knowledge from *Artificial Intelligence* (AI), Ethology, *Artificial Life* (ALife) and Intelligent Robotics. From the field of classical AI, the fusion of reinforcement learning, planning and artificial neural network into one more complex control system was used here. The main principle of its function is inspired by the field of Ethology, this means that life of given agent tries to be similar to life of an animal in the Nature, where animal learns relatively autonomously from simpler principles towards the more complex ones. The architecture supports on-line learning of all knowledge from the scratch, while the core principle is in hierarchical *Reinforcement Learning* (RL), this action hierarchy is created autonomously based solely on agents interaction with an environment. The main key idea behind this approach is in original implementation of a domain independent hierarchical planner. Our planner is able to operate with behaviors learned by the RL. It means that an autonomously gained hierarchy of actions can be used not only by action selection mechanisms based on the reinforcement learning, but also by a planning system. This gives the agent ability to utilize high-level deliberative problem solving based solely on his experiences. In order to deal with higher-level control rather than a sensory system, the life of agent was simulated in a virtual environment.

INTRODUCTION

One of the oldest dreams of scientist and authors of science-fiction, to create an artificial and intelligent living being, still has not been reached and yet, despite the fact that science makes big steps in this field, after many years of research the mankind is still far from reaching this goal.

At the Department of Cybernetics, we're raising a child machine from nowadays infancy to at least pubescence in a near future - thus bringing Turing's vision to fruition - and creating entirely new approaches to machine learning. In our this research is put effort in a strong behaviorist approach, meaning that we work from principle that language is a skill, not simply the output of brain functions, and, therefore, can be learned. Since long time ago, human have always dreamed to create artificial creature. Nowadays, with the help of technology, this dream nearly came true. Our goal is not simply to build machines that are like humans but to alter our perception of the potential capabilities of robots. Our current attitude toward intelligent robots, we assert, is simply a reflection of our own view of ourselves. We are concerned in a part of Artificial Intelligence where more emphasis is put to the behavior of robots and their interaction with their environment. In this research area, intelligence of robots is evaluated as ability to efficiently exploit the environment in order to meet its goals, this research field is called ALife.

As advancement in the research of robotic system continued, it has been shown that in order to create autonomous robots, too much effort has to be put into low-level functions as is processing data from sensory systems and accurate handling the actuators. So the researches that were interested in more complex types behavior consecutively moved from experiments on real robotic systems towards simulation environments, where the word *robot* was replaced by the word *agent*.

Here will be presented the main today's direction and results of our research in this paper. The recent methods used by us to create intelligent machines will be described here. In later sections will be described how these approaches can be combined together, which results in architectures of autonomous creatures. The main accent is put to ability to learn everything that agent needs from an environment.

USED PRINCIPLES

As it can be seen in the Nature on almost all types of organisms, successful life in our highly complex and dynamic environment requires fusion of more than just one selected approach. This is one of the main reasons,

Proceedings 26th European Conference on Modelling and Simulation ©ECMS Klaus G. Troitzsch, Michael Möhring, Ulf Lotzmann (Editors)
ISBN: 978-0-9564944-4-3 / ISBN: 978-0-9564944-5-0 (CD)

why we have focused on hybrid agent architectures, where a several number of different methods of problem solving and learning are connected together. The most important principles will be described here. These principles are used in order to build our artificial creatures, which exhibit behavior and course of learning similar to real living animals (Nahodil, Kadlecek, D. 2008).

Reinforcement Learning

The key and basic principle is the RL, learning method inspired in behaviorist psychology, where an agent learns, which actions should take in the given state in order to maximize its future reward from his environment. The basic idea is the same with a dynamic programming, it is very general approach and the only main disadvantage is fact that an environment formulated as a *Markov Decision Process* (MDP) is required (Bellman, 1957). Interaction with the MDP environment means that each discrete time step t an agent perceives the finite set of states $|S|$ and is able to execute finite set of actions $|A|$. After executing the selected action u_t in the state x_t, the environment responds with a *reward* or *punishment* $r(x_t, u_t)$ and a *new state* $x_{t+1} = T(x_t, u_t)$ is generated. The next-state function T and the reinforcement r function are not known to the agent, the important property of MDP is that the transition function T is based only on the actual state and executed action.

The goal of RL is to choose actions in response to states so that the reinforcement is maximized, this means that an agent is learning policy: a mapping from states to actions. There are several possible ways to implement a learning process; here was chosen a Q-learning. In this form of RL an agent learns to assign values to state-action pairs a Q-value function, the value of this function is sum of all future events. While immediate rewards are more important, hare is used discounted cumulative reinforcement, where future reinforcements are weighted by value $\gamma \in \langle 0, 1\rangle$. The equation (1) represents the optimal Q-value function.

$$Q^*(x_t, u_t) = r(x_t, u_t) + \gamma \max_{u_{t+1}} Q^*(x_{t+1}, u_{t+1}) \quad (1)$$

At each step, the agent executes one action (selected based on the discounted Q-value function) receives reinforcement and updates Q-value of a given state-action pair in the table according to the off policy *Temporal Difference* (TD) control - equation (2), where $\alpha \in \langle 0, 1\rangle$ is the learning rate.

$$Q(x_t, u_t) \leftarrow Q(x_t, u_t) + \\ + \alpha\big[r(x_t, u_t) + \gamma Q(x_{t+1}, u_{t+1}) - Q(x_t, u_t)\big] \quad (2)$$

In order to get a good trade-off between exploration and exploitation, an action selection mechanism uses some kind of randomization, instead of pure greedy method. A system that implements this entire mechanism will be called *return predictor*.

Hierarchical Reinforcement Learning

The classical RL approach has one disadvantage: size of look-up table (matrix) for storing Q-values grows very fast with an environment complexity. This means that in slightly more complex environment the Q-value matrix can have too many dimensions and the learning convergence can be very slow. In order to beat the course of dimensionality, *Hierarchical RL* (HRL) was introduced. We can define *Decision space* (D) as some defined subset of all possible actions and environment states, over this decision space can operate one return predictor. This decision space can be then seen as an *abstract action*. The main idea of hierarchical RL is very simple: in case of the classical "flat" Q-learning algorithm an agent selects among primitive (one-step) actions. Compared to this, in the hierarchical RL the return predictor can select among primitive and abstract actions (decision spaces). The HRL uses *Semi Markov Decision Process* (SMDP), where a waiting time for the next time step $t + 1$ is random variable.

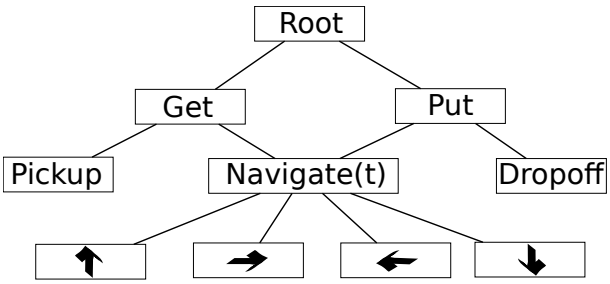

Figure 1: Example of hierarchical task decomposition for well-known taxi problem (Dietterich, 1998)

In our approach is the MAXQ value function decomposition used (Dietterich, 1998), where the received reward can be distributed into a hierarchy of decision spaces D_i using factorization function $\rho(\tilde{r}, D_i)$, where $\tilde{r}$ is the reward generally from the composite behavior. The parameter τ represents positive duration of action, then the Q-learning update formula for decision space D_i is in equation (3).

$$Q_i(x_t, u_t) \leftarrow Q_i(x_t, u_t) + \\ + \alpha\big[\rho(\tilde{r}, D_i) + \gamma^\tau Q_i(x_{t+1}, u_{t+1}) - Q_i(x_t, u_t)\big] \quad (3)$$

Our proposed approach is based on an architecture called *"Hierarchy, Abstraction, Reinforcements, Motivations Agent Architecture"* (HARM) (Kadlecek, 2008). Therefore is used motivation $m(D_i)$ which defines "how much" the agent wants to execute particular action (corresponding to a decision space D_i). The resulting *utility* of action (for a decision space on the top of the hierarchy) is defined in the following equation:

$$\varphi_{D_i}(s,a) = m(D_i)Q_i(s,a). \quad (4)$$

Utilities for the rest of decision spaces in a hierarchy are composed from its own utility and utilities of all parent decision spaces through connection of strength $c_{D_i}^{D_j}(s,a)$ as seen in the equation (5).

$$\varphi_{D_i}(s,a) = m(D_i)Q_i(s,a) \sum_{j \in pars(D_i)} c_{D_i}^{D_j}(s,a)\varphi_{D_j}(s,a) \quad (5)$$

Because of this approach, the motivation to execute a particular behavior (action) can spread through the connection function $c_{D_i}^{D_j}(s,a)$ from the top of a hierarchy towards primitive actions. This means that a selection of concrete primitive action to be executed emerges from various motivations, conditions and dependencies in a whole hierarchy. When a reinforcement/punishment is obtained, this information travels in the opposite direction, from the primitive actions towards the more complex decision spaces on the top of the hierarchy through the factorization function $\rho(\tilde{r}, D_i)$.

Autonomous Creation of RL Hierarchy

Dr. Kadleček, in his Dissertation Thesis, presented HARM system, which is capable of creating such hierarchy of decision spaces autonomously, based on received reinforcements of various types (Kadlecek, 2008). In his architecture, an agent has its own predefined physiology. Agent's physiological state-space, represented by a dynamical system, contains set of agent's internal variables. The physiological state-space contains two important areas: limbo and a purgatory one. Limbo area represents the optimal conditions, if an agent is in this area, no motivation is generated. On the other hand, if an agent is in the purgatory area, an amount of produced motivation increases exponentially. If an agent actively moves some of his physiological variables towards the optimal conditions, a reinforcement is received, if the movement is in another direction, towards the purgatory area, a punishment is received (Kadlecek, Nahodil, P. 2001).

After receiving a reward or a punishment, new decision space D_i in a hierarchy of actions is created and this decision space is connected to a physiological variable through the motivation link $m(D_i)$. Because of this approach, an agent autonomously connects consequences of his behavior with own physiology and learns how to preserve homoeostasis. A set of variables and actions contained in particular decision spaces (and thus also the shape of action hierarchy) is maintained during the agent's life by using four main operations: sub-spacing, behavior associating, variable removing and variable promoting.

PROPOSED NOVEL APPROACH

Later, several improvements in the HARM system were developed, including on-line learning or an intentional state-space. By use of intentions, an agent can autonomously generate its own intentions during his life, this concept will be explained in the following section.

The course of agent's life

At the beginning of the simulation, the agent has no information a priory about world and his regularities and is equipped only with some set of primitive actions and predefined needs, represented as variables in the physiological state-space. These needs can represent for example synonyms for thirst, hunger, or need for recharging a battery.

At first, the agent acts randomly and observes whether something interesting has happened, that is: whether some reward/punishment was received, or whether the agent managed to change some environment variable. In the second case, a new intentional variable (corresponding to the particular ability to influence an environment) is created. In both cases, the new decision space D_i is created and connected to its source of motivation through the motivation link $m(D_i)$.

Later in the simulation, the agent learned some action hierarchy (e.g. he knows how to drink or recharge a battery) and thus exhibits consecutively more and more systematic and stable behavior now.

Compared to agent's predefined physiology, variables in the intentional state-space represent the agent's intention to learn, to "train" some new behavior, autonomously discovered during his interaction with an environment. The intentional state-space has no purgatory area, which causes that the agent learns these behaviors, only in relatively optimal conditions. This concept is similar to learning of young animals by playing with unknown objects.

From Reinforcement Learning towards the Planning

As a latest result of our research in the field of ALife, we have proposed a system that is capable of deliberative "thinking" over this autonomously created hierarchy of abstract actions (decision spaces). This gives the agent whole new dimension of abilities how to use this knowledge.

Compared to the RL, from our point of view, the planning is deliberative approach capable of solving complex tasks, but it requires accurate description of an environment. This requirement can cause problems even in relatively simple environments, where total number of possible states always grows too fast to be handled by a planner. This disadvantage is solved by hierarchical planners, for example *Hierarchical Task Network* (HTN), but these planners are domain dependent, or at least domain configurable. The main advantage of our approach is that our hierarchical planner can beat the course of dimensionality a well as other

hierarchical planners, but moreover maintains its domain independence. In other words our planned is domain self-configurable: by using the autonomous creation of action hierarchy, it can adapt itself to a given domain.

For implementation of planning system was used the world-wide known language, called *Stanford Research Institute Problem Solver* (STRIPS). It is formally represented as a quadruple $\langle P, O, I, G \rangle$. The P is the set of conditions expressed by propositional variables describing the world state, I is the description of initial state and G is description of properties which are fulfilled in a goal state(s). O is the set of operators - actions, each operator consists of the quadruple $\langle \alpha_s, \beta_s, \gamma_s, \delta_s \rangle$. The elements α_s and β_s describe the constraints when the action can be applied, that is: describe which conditions must be true and which false in the given situation. The elements γ_s and δ_s describe action effects after its application, that is: which propositional variables will become true and which false. Roughly speaking, the current state of the world is described by a binary vector, where operators change values of bits on a specified position in a specified manner. The plan is a sequence of applicable operators that consecutively transform the description of initial state towards the state which fulfills the goal conditions.

As a typical planner, STRIPS requires on its input three main things: description of the current state, description of a goal state and a set of possible actions. Our latest architecture, presented in (Vitku, 2011) is able to automatically infers these information from the HARM action hierarchy. This process will be described here in more details.

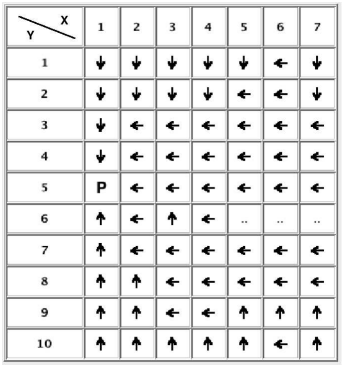

Figure 2: Example of learned behavior which controls the lights. The agent approaches towards the switch and executes action *press* (denoted by P) on the correct position. The successful execution of this behavior switches the value of variable *lights-state* between two possible states: on/off.

In the Fig.2 it can be seen an example of learned decision space represented by a 2D matrix, where each tale corresponds to a position of an agent in the map. Each primitive action (depicted on each tale) represents the learned action, that is the action with the highest Q-value. The agent discovered that by pressing the switch on the left side of the map the light can be switched on/off. It was identified as agent's ability to change some environment property and new intention to learn this behavior was created. The picture represents behavior for turning on/off the lights, which was learned through this motivation. The decision space D_i (matrix of Q-values) contains agent's actual $\langle X, Y \rangle$ position and the variable causing the reinforcement is *lights-state*.

The basic idea is that in order to use this decision space as a primitive action, we need to consider only the "main" variable of a decision space, the variable that **changes during the reinforcement**. In this case, where the decision space consists of three variables: agent's *X* and *Y* position and the *lights-state*, the "main" variable of the decision space is *lights-state*, to the planner will take into account only this variable. Now follows the description of how primitive actions in the STRIPS language are generated: the decision space was created in order to learn the behavior turn on/off the lights. Exactly this does the primitive action in the STRIPS language. In case of a binary variable, this decision space can be represented as two primitive actions in the STRIPS language. The vector describing the problem has one bit **Turn on the lights**, in this simple case only. The action contains precondition: *lights off*, and effect: *lights on*. The action **Turn off the lights** contains precondition: *lights on*, and effect: *lights off*.

The description of entire environment can be automatically generated in form of STRIPS language by use of this principle. The main advantage here (besides the domain independence) is the fact, that only those interesting and potentially important information are passed to the planner. The state description was reduced from 3 variables to one, in the previous example. A hierarchy of RL actions serves here as some kind of filter. This autonomous pre-processor filters information for the deliberative planner, which works over the hierarchy of actions.

SIMULATION RESULTS

For concluding the experiment, the *Massim* simulation environment was used. It was originally created for annual competition called "Multi-agent contest", but for a single-agent case is suitable as well. All information, in both directions agent-environment and environment-agent, is sent through the TCP/IP protocol and coded in the XML format. At each discrete simulation step, the simulator sends all information about an environment to an agent. Agent processes the received data and sends XML with one selected primitive action. Information sent by the environment are in convenient form: for each object in a simulation is send its name and attributes.

In the Fig.3 there is an example of an experiment scenario, the position of lights-switch corresponds to the matrix shown in the Fig.2.

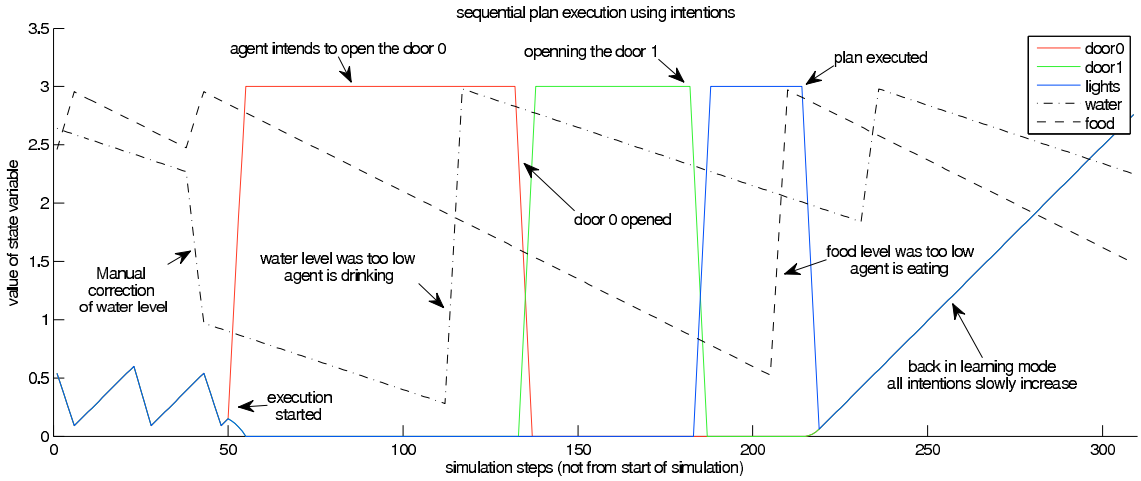

Figure 5: Graph showing the sequential plan execution. The Y axis represents the amount of intention to execute the particular action, the X axis represents time. It can be seen how the planner consequently set the intention to *open the door0*, *open the door1* and *turn on the lights*. The dashed lines represent amounts of *water* and *food* in the agents body. The *water* and *food* levels in the agents body fall towards zero with time, in the picture there are results of *drinking* and *eating* as refilling these amounts towards the maximum.

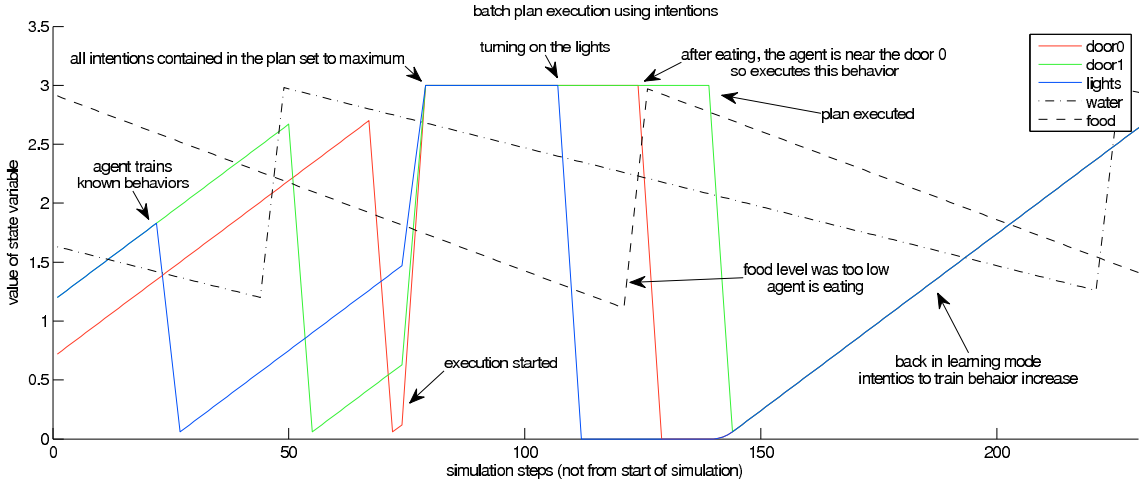

Figure 6: Graph showing the batch plan execution. It can be seen how the planner set intentions corresponding to all actions in the plan to the maximum and waited until all intentions falls towards the zero, which means that the plan was executed. The dashed lines represent amounts of *water* and *food* in the agents body.

Selected Experiment

The agents ability to autonomously identify potentially useful behaviors was tested in our selected experiment. It means, to learn how to open the door and switch the lights. Tested ability to represent these behaviors as a set of primitive actions in the STRIPS language and use them for planning and plan execution was also verified here.

The picture Fig.4 shows three autonomously learned behaviors as decision spaces in form of RL. The meaning of the matrixes is described under this figure. These 3 actions were autonomously represented as 6 primitive actions in the STRIPS language.

Reduction of Decision State Space Size

The original description of the world that contained $10 \times 10 \times 2 \times 2 \times 2 = 800$ states was reduced to the world description for the planning engine to only $2 \times 2 \times 2 = 8$ states, represented as a binary vector with 3 variables. Here can be seen autonomous and effective preprocessing information about the environment to the higher-level decision making system, where the planner does not have to care about the agent's actual position.

The benefit provided by this presented method of state space size reduction dramatically increases with a complexity of given domain. This was tested in other examples where the resulting reduction of decision space was from 64×10^{12} to only 100 states (Vitku, 2011).

For testing agent's ability to create a plan and execute it, the user wants to enable passing through the hallway

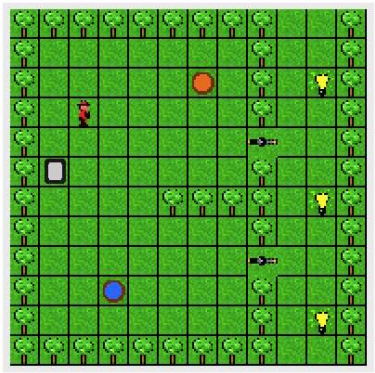

Figure 3: Map of the environment containing one red agent, silver *lights-switch*, blue source of water, orange source of food and two buttons controlling doors. The hallway on the right contains yellow lights and two doors that can be opened/closed. The map corresponds to the learned strategy depicted in the Fig.2

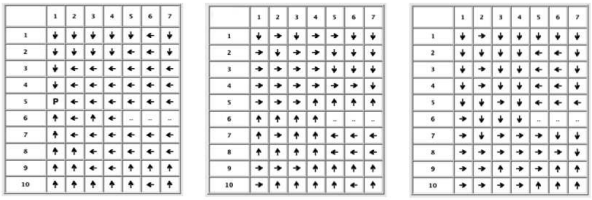

Figure 4: The result of agent's autonomous learning based on the autonomously generated intentions. After discovering that the switch controls lights and the two other switches control the door, these three new decision spaces were created. On the left there is behavior corresponding to lights-control, the center and right matrix represents behaviors corresponding to door control. Note: the door are controlled by approaching to the switch.

on the right side of the map. This requires that the lights are on and both doors are opened (see Fig.3). Actual state is that lights are off and doors are closed. After specifying the goal, the agent was able to create plan containing the sequence of these actions: *open the door0*, *open the door1* and *turn on the lights*. In the following section shows two main ways how a plan can be executed by the planning engine.

Sequential Plan Execution

The first possibility is to execute a given plan sequentially. The Fig.5 depicts this type of plan execution. The planner can influence agent's behavior by manual setting the values of intentions for execution of particular actions. After successful execution of an action, the intention to execute an action falls towards the zero. The planner in this sequential mode sets the intention corresponding to the first action in the plan and waits until it falls towards the zero, after that, the intention to execute next action is set to maximum.

Batch Plan Execution

Now, let's consider simpler problems, where a depth of action hierarchy is not too big and it can be shown that autonomous creation of primitive STRIPS actions can be accurate. Also another type of plan execution can be used here: so called batch mode, after this assumption. This type of plan execution exploits much better the benefits of hierarchical RL. The agent selects an order of actions according to the most efficient strategy, in the current situation. The obvious disadvantage of this type of plan execution requires that the order of actions can be arbitrary.

The Fig.6 depicts how the planner set all intentions contained in the plan to the maximum and waited until all fall towards zero. The main benefit of this approach is in the fact that order of actions to be executed is based on the actual conditions. From the graph it can be seen that the agent was obviously near the *lights-switch* at the beginning, so the maximum utility was produced by the *lights-switch* behavior. After turning on the lights, corresponding utility fell to zero and the next best action was selected.

A good example of exploiting the main benefit of this approach is shown here. After execution of the first action (*turn on the lights*) the *food level* in the agents body was too low and thus the agent had to eat. After eating, the agent was near the water source, which is near the *door0 control*. Obviously the best strategy is to open the *door0*, in this situation.

The Fig.6 also shows that this execution of the same plan was much faster than in the previous-sequential case.

CONCLUSION

We are going to create more sophisticated algorithm with ability to infer preconditions and effects for general problems, in the near future. This includes the ability to infer high-level variables with much more than two states. Also, the algorithm should be used also in domains where effects of particular actions in a hierarchy could interfere. Also, we would like to conclude some experiments in a real environment with some more complicated sensory data. Currently we work on finding of possible real applications of our novel approach in daily praxis.

The most of nowadays similar architectures (which incorporate some hierarchical structures) are domain dependent. This means that some form of domain description has to be specified before the start of any simulation. In case of the commonly used *Belief-Desire Intention Architecture* (BDI) (Sardina, et. al. 2006), the main disadvantage is the plan library. This library describes a causalities in an environment and has to be predefined by user. The another similar idea: an agent architecture which use combination of RL and planning, can be seen in the work called *Reinforcement-Learning Teleo-Operators* (RL-TOPs) (Ryan, Pendrith 1998). In this approach each high-level action (represented by a predicate: e.g. *move(a,b)*) is implemented by some primitive behavior in form of RL. While primitive

behaviors are learned autonomously by the RL engines, the high-level preconditions and effects of actions have to be predefined by the designer.

We believe that, compared to similar ideas found by us, the main advantages of our architecture are:

- The fact that an agent is able of *completely unsupervised adaptation* to a given domain.
- Here, an user does not have to predefine (and therefore he *does not have to know) any part of problem structure*, because our system is able to determine the important knowledge itself, store it and provide it for later reuse.
- The autonomously created hierarchy of actions provides *huge reduction of searched decision space*. In situations where the classical planners fail and hierarchical planners need help of designer, our agent is still able to operate without any problems.

ACKNOWLEDGEMENT

This research has been funded by the Dept. of Cybernetics, Faculty of Electrical Engineering, Czech Technical University in Prague and Centre for Applied Cybernetics under Project 1M0567.

REFERENCES

Bellman, R. (1957), *A Markovian Decision Process*. Indiana Univ. Math. J. 6: pages 679–684.

Dietterich, T.G. (1998), Hierarchical reinforcement learning with the maxq value function decomposition. *Journal of Artificial Intelligence Research 13:* pages 227–303.

Kadleček, D. (2008), *Motivation Driven Reinforcement Learning and Automatic Creation of Behavior Hierarchies*. PhD thesis supervised by Nahodil, P., CTU in Prague, FEE, dept. of Cybernetics, pp. 134, Prague

Kadleček, D., Nahodil, P. (2001), New Hybrid Architecture in Artificial Life Simulation. *In: Proc. of 6th European Conf. of Artificial Life: Advances in Artificial Life*. ECAL 2001, Prague, LNAI Nr. 2159, vol. 1, Printed by Springer, Berlin, vol.1, pages 143-146

Nahodil, P., Kadlecek, D. (2008), Adopting Animal Concepts in Hierarchical Reinforcement Learning and Control of Intelligent Agents. *In Proc. of 2nd IEEE/RAS-EMBS International Conf. on Biomedical Robotics and Biomechatronics,* BioRob 2008, Scottsdale, U.S.A, 2008, pages 122-131

Vítků, J. (2011). *An Artificial Creature Capable of Learning from Experience in Order to Fulfill More Complex Tasks*. Diploma thesis supervised by Nahodil, P., CTU in Prague, FEE, Dept. of Cybernetics, Prague, pp. 123

Ryan M. and Pendrith, M. (1998), RL-TOPs: An Architecture for Modularity and Re-Use in Reinforcement Learning *In Proceedings of the Fifteenth International Conference on Machine Learning,* San Francisco, CA, USA, pages 481-487

Sardina, S., de Silva, L., Padgham, L. (2006), Hierarchical Planning in BDI Agent Programming Language: a Formal Approach. *AAMAS 06 Proceedings of the fifth international joint conference on Autonomous agents and multiagent systems,* ACM New York, pages 1001-1008

AUTHOR BIOGRAPHIES

PAVEL NAHODIL was born in Prague, Czech Republic. Since 1986 he has been a Professor of Technical Cybernetics at the Department of Cybernetics at the Faculty of Electrical Engineering, CTU in Prague. His present professional interest includes artificial intelligence, multi-agent systems, intelligent robotics (control systems of humanoids) and artificial life approaches in general. He is (co-)author of several books, university lecture notes, hundreds of scientific papers and some collection of scientific studies. He is also the international conferences organizer + reviewer (IPC Member) and a member of many Editorial Boards. His e-mail address is: nahodil@fel.cvut.cz

JAROSLAV VÍTKŮ was born in Prague, Czech Republic, graduated in 2011 in Czech Technical University in Prague, Faculty of Electrical Engineering in Artificial Intelligence. His diploma thesis was awarded by Price of Dean. Currently is a PhD student in the CTU, FEE, Department of Cybernetics. His research interest includes behavioral robotics, cognitive science, biologically inspired algorithms and Artificial Life in common. His e-mail address is: vitkujar@fel.cvut.cz

Utilization of Broadcast Methods for detection of the road conditions in VANET

EmadEddin A. Gamati, Evitm Peytchev, Richard Germon, Li, Yueyue
{emadeddin.gamati, evitm.peytchev, richard.germon, Yueyue.li}@ntu.ac.uk
Nottingham Trent University - School of Science and Technology - Computing and Informatics Building,
Clifton Lane, Nottingham, NG11 8NS, UK.

***Abstract*:** *Vehicle to vehicle communication (V2VC) is one of the modern approaches for exchanging and generating traffic information with (yet to be realised) potential to improve road safety, driving comfort and traffic control. In this paper, we present a novel algorithm which is based on V2V communication, uses in-vehicle sensor information and in collaboration with the other vehicles' sensor information can detect road conditions and determine the geographical area where this road condition exists – e.g. geographical area where there is traffic density, unusual traffic behaviour, a range of weather conditions (raining), etc. The built-in automatic geographical restriction of the data collection, aggregation and dissemination mechanisms allows warning messages to be received by other cars, not necessarily sharing the identified road condition, which may then be used to identify the optimum route taken by the vehicle e.g. avoid bottlenecks or dangerous areas including accidents or congestions on their current routes.*

The Traffic Condition Detection Algorithm (TCDA) - which we propose here - is simple, flexible and fast and does not rely on any kind of roadside infrastructure equipment. It will offer live road conditions information channels at - almost - no cost to the drivers and public/private traffic agencies and has the potential to become indispensable part of any future intelligent traffic system (ITS). The benefits from applying this algorithm in traffic networks are identified and quantified through building a simulation model for the widely used Network Simulator II (NS2).

***Index Terms*:** Wireless, Ad hoc network, Vehicular ad-hoc networks (VANET), Mobile ad-hoc networks (MANET), Vehicular Networks, Collaboration, ICT, ITS, collaborative knowledge generation, traffic information systems.

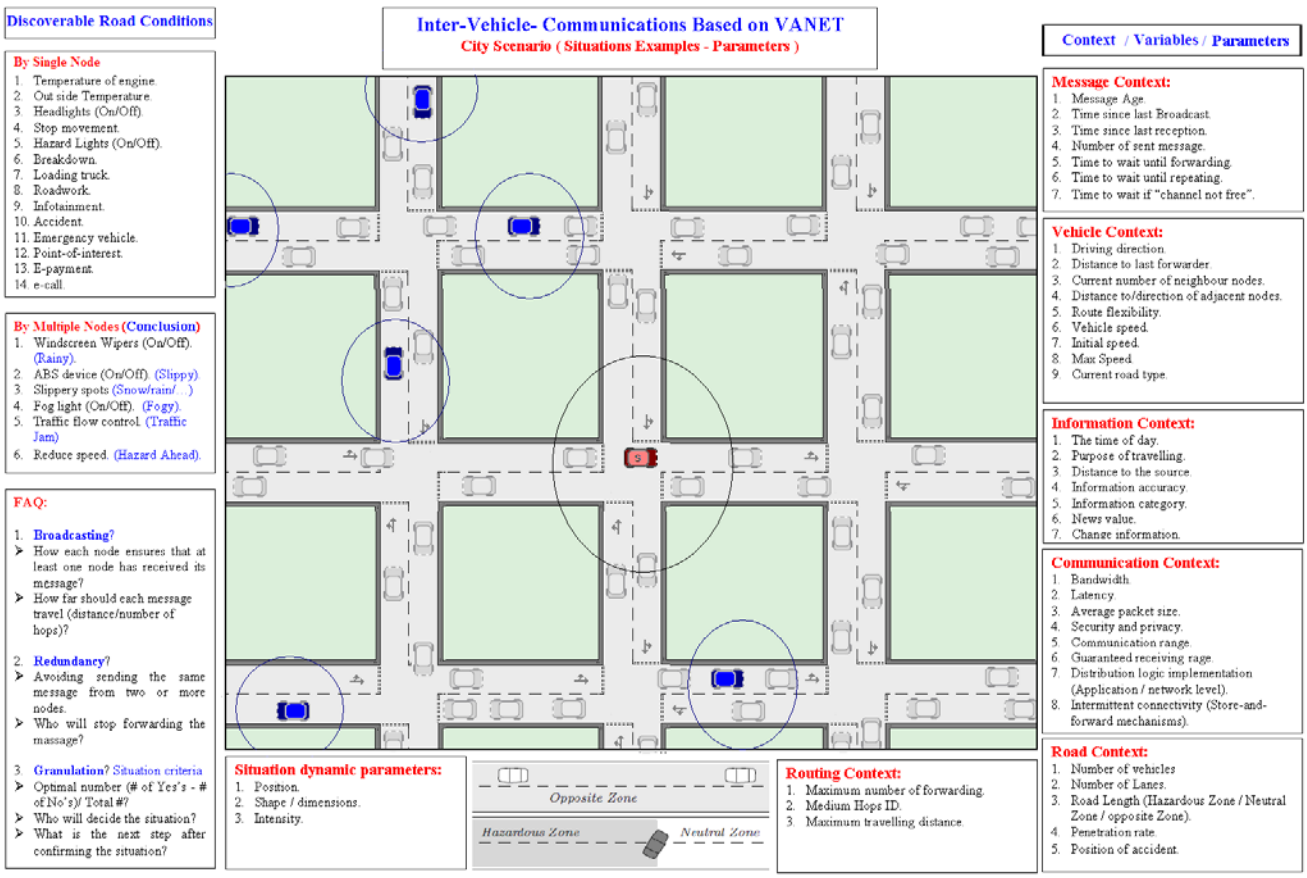

Figure 1: City Scenario (Discoverable Conditions)

Proceedings 26th European Conference on Modelling and Simulation ©ECMS Klaus G. Troitzsch, Michael Möhring, Ulf Lotzmann (Editors)
ISBN: 978-0-9564944-4-3 / ISBN: 978-0-9564944-5-0 (CD)

Introduction

One of the main advantages of the ad-hoc networks is the opportunity to use collaborative effort in connecting and delivering network messages as necessary [1]. This opportunity is under-utilised so far in the area of traffic control and traffic information systems where every car can be considered to be a node in an ad-hoc network [2]. Our aim is to investigate the possibility of bringing ad-hoc collaborative information generation and control into such systems and investigate how the functionality of the ad-hoc node (within the vehicle) affects the quality of the traffic wireless information systems in ITS.
Let us start by classify the discoverable road conditions based on ❶ how many cars needed to discover certain road condition? Also, ❷what kind of parameters and variables needed to put it in its context (determine the road condition)?

Problem definition:

Most of the existing systems in use today work through establishing direct connection between mobile nodes in MANET and pre-existing infrastructure node, which immediately raises questions about the compatibility, required services, updating devices …etc. when we move to collaborative ad-hoc networking and in the same time, the systems already in place have relatively high cost [3][4][5]. The proposed algorithm does not depend on the network topology but the connectivity between the cars can influence the region definitions while identifying traffic conditions. It is clear that the more cars we have on the road the more effective the algorithm will be since the algorithm works on the basis of collaborative data generation and the more cars we have linked in one ad-hoc network the more entities will take part in the collaborative process. Here is small scenario which illustrates the idea:

1) Here is (Figure 3) snapshot of certain area (the lines are roads; the black small points are nodes or vehicles). In urban areas, density of cars in streets is high which make us able to formulate network between cars if we put a small wireless device to enable the communication between the cars.
This will establish direct communication channel between each two cars in the range of each other (Ad-Hoc network). This makes sharing non-valuable individually sensed data among cars more effective, useful and less expensive than any infrastructure communication for generating new knowledge.

Figure 2: Street Map with vehicles in move (Black Dots)

2) The network has been established, the nodes start talking, the exchange messages –called discover message- to share all the data they have (their own sensed data or data they already received about nearby cars). Each node is able to calculate the percentage of cars - within certain area – who got the same situation. If this percentage is big enough to consider this area has

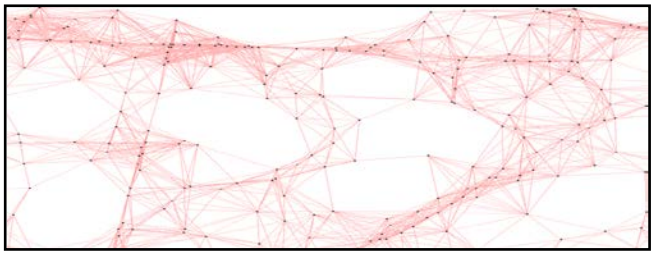

Figure 3: Establishing direct link between Vehicles

that situation (Figure 4), warning message will be generated and broadcast it by that node to inform as much and far cars as possible with the routing feature in each node.

3) Certain areas will be declared as situation zones (Figure 5) for a while, each node or vehicle can know about them by receiving the warning message. This declaration will last for a period of time, if this

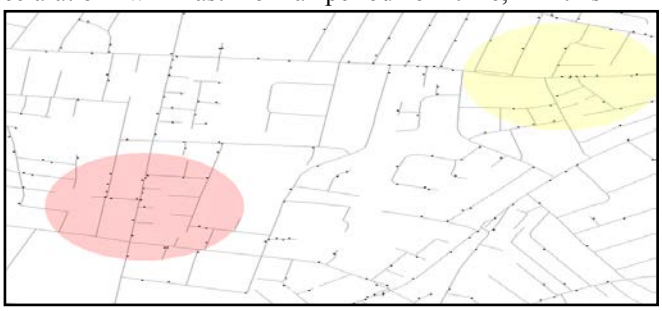

Figure 4: Situation Zones has been identifier

information did not confirmed again– by receiving new message each car will consider the situation has been finished and the normal condition got back to the roads in that area.

4) This will make each GPS or driver itself avoid these zones if it/he was planning to pass through them (Figure 6) to avoid any risk or delay.

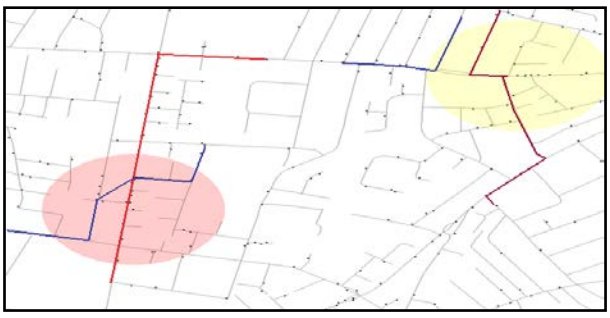

Figure 5: Pre-planned Traveling paths

TRAFFIC CONDITION DETECTION ALGORITHM (TCDA)

TCDA foundation rules:

- TCDA DOES NOT rely on any kind of roadside units or infrastructure, just car to car communication for collaborative data sharing and processing without using any kind of cauterization (processing | storage).
- TCDA DOES NOT rely on central processing, each node in the system DOES have the same functionality (routing messages if needed, processing the received information, generating new messages,…).

Algorithm Overview:

Some road conditions can either be derived (assessed) from the activity of the individual cars' electronic helpers like ESP or ABS, or alternatively, sensors embedded in the individual vehicle may provide this information. The summary in the table below (Table 1) is summary of the most common road situations with the causes of those situations considered as Non-conclusive Individual Car Sensed Data:

Table 1: Possible Road Situations (examples)

Individual Car sensors data	Possible Reasons
Windscreen Wipers (goes ON)	Rain / cleaning / By Accident
ABS Control (Slippery Road)	Snow / Oil spot / bad tires / Bad driving
Fog light (ON).	Fogy / By Accident / Since yesterday
Movement Speed (Slow).	Traffic Jam / Driver using the phone/radio
Reduce Speed (Unexpected)	Hazard Ahead/saw a friend or interesting place

But if we can share this data among all nearby cars, by Combining Individual Car Sensed Data (Table 2), the result will be:

Table 2: Certain Road Situation (examples)

Individual Car sensors data	Optimum Num	The Reason
Wipers	10% of cars = ON	Rainy
ABS Control.	5 cars = ON	Slippery (snow)
Slippery Spot.	2 cars	Slippery spot
Fog light.	50% of cars ON	Fogy
Movement Speed.	(60%) Slow/Stop	Traffic Jam
Reduce Speed	5 cars within 1sec	Hazard Ahead

By comparing the two tables, you will notice that each case in the first table could happen because of many reasons which make it non-conclusive piece of information. But in the second table, if we know the number of neighbouring cars that got the same situation (the numbers quoted in the table are representative rather than conclusive for the condition and represent a matter of future investigation in real-life experiments), we will be certain about the reason for that situation. This mechanism transfer the non-conclusive individual car sensed data into very important (conclusive) data to describe the surrounding road conditions. We should notice that the optimum number in the above table should be predefined and updatable by the system itself.

Algorithm Features:

The algorithm is very flexible and has several variable parameters, which influence the final outcome, and this paper presents our conclusions in determining the optimal set of values:

i) Using Variable Conditions Search Limitation (CSL): Control the searching area by number of hops from source, certain timeout, and/or distance from source.

ii) Multi-zones detection: in case of more than one zone, it can Detect each situation zone boarders separately (even if they are overlapped). Then report them in one or multiple warning messages.

iii) Delay for data collection: Random time slots delay used before forwarding the received messages.

iv) Infrastructure less system.

Definitions of the used Terms:

i) Active Node (AN): refers to any node with sensors indicating that a certain road condition(s) is present and is to be reported to other nearby cars or nodes.

ii) Non-Active Node (NAN): refers to any node with sensors indicating that a certain road condition(s) is NOT present (the node will serve as a router to forward messages coming from nearby nodes).

iii) Situation Discovery Message (SDM): a message generated by AN or - in some cases - by NAN. It has three parts: unique SDM ID (nodeNo:timestamp:Position), SDM limitation conditions (Hops:timeout:distance) and Nodes seen (NodeID:Time:Situations:position). Its purpose is to establish zone identification and contains:

iv) Situation Warning Message (SWM): generated by any node discover a situation zone. It contains the fields: unique SEM ID (SourceNo:timestamp:Position), SWM travel conditions (Hops:timeout:distance) and Zones detected (NodeID:Time:Situations:position).

v) Node behaviour: Node behaviour is the *reaction* of the node when receiving a message. The reaction can be:

a. Forward the message if it is message received for the first time, otherwise discard.
b. Discard the message if it is redundant.
c. Generate new Situation Discovery Message (SDM) if the received message carries new information compared to the existing information, so the generated message will travel in all directions (broadcast).

The Algorithm mechanism:

Pseudo-code of TCDA

Input:
Road situation detection messages (SDM) received. It generated by any node (I called it Active Node) who senses any road problem or certain road situation, each has at least the following information: Message id, Two lists of nodes and its positions: active nodes and non-active nodes.

Initialize:

$i \leftarrow \{ 0 \ldots number\ of\ nodes\ -1 \}$

$B_i \leftarrow$ *neighbor set of current node* N_i

$\boldsymbol{AN_i} \leftarrow$ *detected Active Nodes IDs set by* N_i

$\boldsymbol{NAN_i} \leftarrow$ *detected Non Active Nodes IDs set by* N_i

SDM $\leftarrow$ *road situation Detection Message.*

SWM $\leftarrow$ situation Warning Message.

Event: new situation has been detected in the current node N_i

Add the current node ID to the local $\boldsymbol{AN_i}$ $\{if\ AN_i \neq \emptyset\}$
Generate $\boldsymbol{SDM \leftarrow \{N_i(id), AN_i, NAN_i\}}$
Forward ***SDM*** via 802.11

Event: new $\boldsymbol{SDM_j}$ message has been arrive at the current node N_i

extract from SDM_j data sets : $SDM_j(id)$, AN_j, NAN_j ;
if $\boldsymbol{SDM_j}$ is redundant ***then***
discard $\boldsymbol{SDM_j}$;
else
$\boldsymbol{NAN_i \leftarrow NAN_i \cup NAN_i}$
$\boldsymbol{AN_i \leftarrow AN_i \cup AN_i}$ ***/ update local lists of known AN & NAN***
if $\frac{\text{length}\{AN_i\}}{\text{length}\{AN_j\}+\text{length}\{AN_i\}} \geq$ *optimum Number* ***then***
// all data is Known
Calculate *Zone* ***// identifier zone situation by using AN list (NodeId and Position)***
Generate $\boldsymbol{SWM \leftarrow \{N_i(id), Sl_i, zone, AN_i\}}$ ***// generate new warning Message***
Broadcast *SWM* via 802.11
else-if *(distance between fairest two nodes in* $AN_i \geq$ *Optimum number)* ***OR*** *(timeout)* ***then***
Generate $\boldsymbol{SDM_i \leftarrow \{N_i(id), AN_i, NAN_i\}}$ //
generate new warning Message
Forward $\boldsymbol{SDM_i}$ via 802.11
else
Wait tolerant-time // ***to receive and collect more data to broadcast all in one message***.
update $\boldsymbol{AN_i, NAN_i}$ ***// update lists based on known AN & NAN***
Generate $\boldsymbol{SDM_i \leftarrow \{N_i(id), AN_i, NAN_i\}}$ ***//generate new Discovery Message***
Forward $\boldsymbol{SDM_i}$ via 802.11
end-if
end-if

Event: new $\boldsymbol{SWM_i}$ situation has been received in the current node $\boldsymbol{N_i}$
update $\boldsymbol{AN_i, NAN_i}$ ***// update lists based on known AN & NAN***
Calculate *Zone* // identifier zone situation by using AN list (NodeId and Position)
Generate $\boldsymbol{SDM_i \leftarrow \{N_i(id), AN_i, NAN_i\}}$ //generate new warning Message
Forward $\boldsymbol{SWM_i}$ via 802.11

RESULTS

Results Analysis:

As we are looking for the optimum number of hops to discover the whole local area and, at the same time, the optimum Delay time each node should use before resending any message, we analyse all the available data from the simulation with these two parameters (Num of Hops & Delay Time) as variables separately.

The number of exchange messages needed, message exchange time and number of recognized nodes (AN/NAN) are used as indicators for the best results and are sufficient to detect any Traffic Condition. The results for each are considered in the following:

Number of Exchanged Messages Per Node

Those figures show the number of sent and received messages at each node and indicates how noisy the system is. It also gives an indication of the optimal value for the number of hops parameter.

Number of Sent Messages Per Node

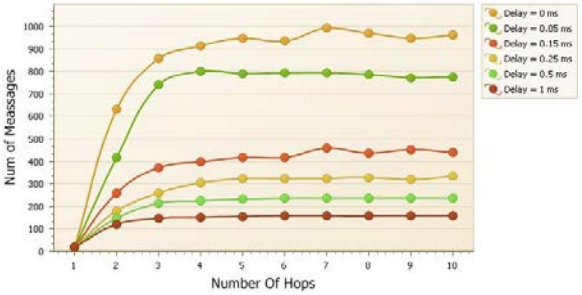

Number of Received Messages Per Node

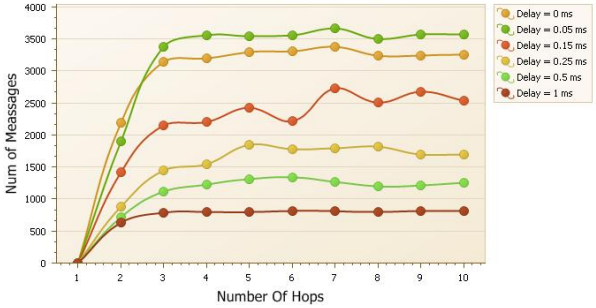

# of Nodes Saw up to 50% of AN

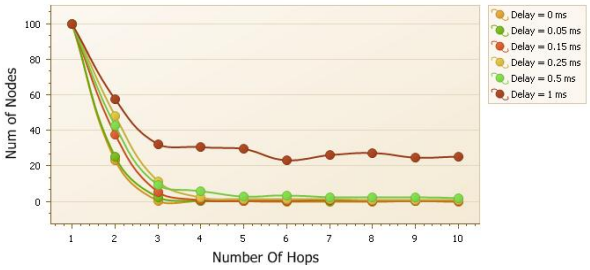

Message Exchange Time Needed to Discover the area

The following Figures shows the total time needed for the algorithm to finish as a function of the number of hops parameter. Choosing the shortest total time needed to exchange all messages to detect a certain situation is important for the speed of detection and also for the timeout required before re-initianting the discovery sequence.

# of Nodes Saw more than 50% of AN

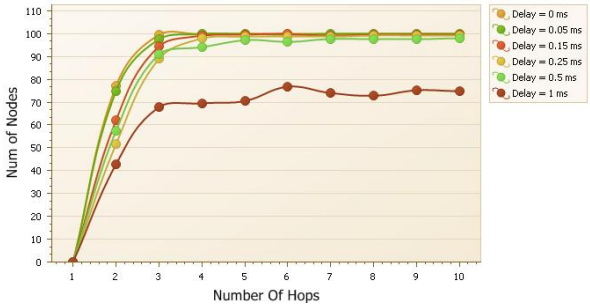

Message Exchange Time (Total Time)

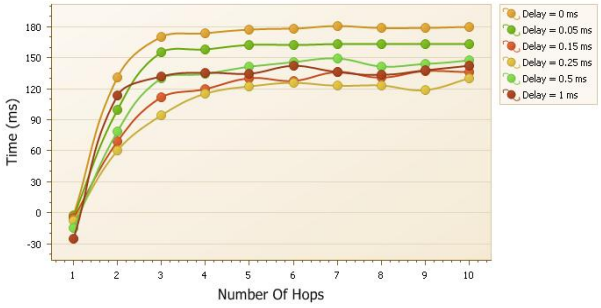

# of Nodes Saw up to 50% of NAN

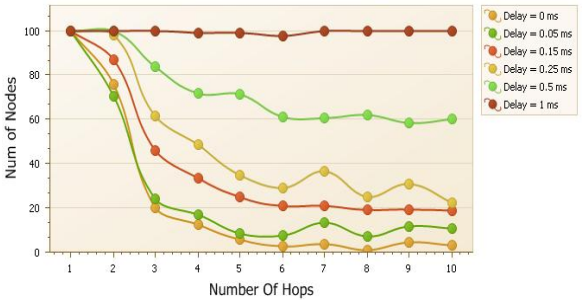

Message Exchange Time (Time / Node)

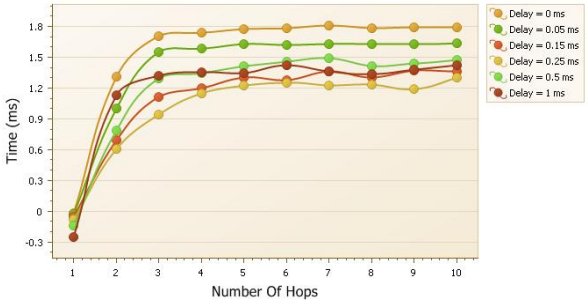

# of Nodes Saw more than 50% of NAN

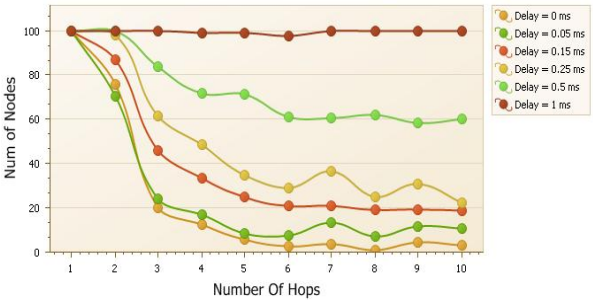

Number of recognized nodes (AN / NAN)

Knowing the ratio between AN and NAN (or simply their numbers) is crucial to detect if the situation is present or not. The results of the experiments presented in the following figures show the number of recognised nodes as a function of the number of hops parameter.

Results outcome

This study attempts to identify the optimum value for two algorithm parameters; number of hops and delay time. The assumption is that different situations are detected by different numbers of recognized AN/NAN (e.g: situation is rainy if 33% of nodes are AN, or a slippery spot can by detected by 3 AN regardless the number of NAN).

Analysis of the graphs presented indicates that there is no fixed optimum number either for delay time or number of hops. Consequently a range of numbers for these two parameters must be considered dependant on the detection cases.. Based on these assumptions, we are looking for the best results which can recognize from 50% up to 100% of active nodes which will be enough to cover all cases.

In the graphs presented the point of saturation i.e. where an increase in the value of the investigated parameter gives relatively small improvement in the quantity of sent/received/discarded messages. The results show clearly that using **from 3 up to 5 hop**s is optimum to detect any Traffic Condition if we consider the mentioned indicators.

The results show that the greatest delay time will reduce the number of exchanged messages, but will increase the total time needed to recognize the biggest possible number of AN/NAN. This is a difficult compromise between Time and noise, though a figure **between 0.01 and 0.1 second** seems to be indicated.

CONCLUSION & FUTURE WORK

An infrastructure-less vehicle-to-vehicle communication system in terms of data sharing and collaborative generation of information, as well as the characterized particular vehicular networks (moved nodes, road constrains mobility and variable communication conditions) is hot issue and research challenge for academics. Several dissemination protocols were proposed in research works. They could be sorted into two classes: (i) protocols for infotainment services (e.g. advertisement applications) that have constraints related to the bandwidth, and (ii) protocols for emergency services (e.g. road safety services) that have end-to-end delay and delivery ratio constraints. Also, Vehicular networks can be considered as the portal of many services, ranging from safety to traffic information and location based services (LBS). These services generally require efficient routing and dissemination protocols.

The proposed TCDA is a highly efficient protocol compared to pure flooding – the only algorithm reported so far capable of discovering reliably the information on an ad-hoc basis. Also, it has been proved that the algorithm can discover traffic conditions within certain areas using both dynamic variable search limitations and an intelligent routing mechanism. Optimal values for recommended number of hops and delay time have been identified and reported.

It is clear that tomorrow's driving assistance systems can go far beyond their present capabilities by implementing co-operation and information exchange in order to collectively and cooperatively perceive the driving environment. Making decisions dependent on the environment can serve car drivers, ITS, environment and people more generally. This paper demonstrates a way of achieving this goal and paves the way for new and improved algorithms which to use car-to-car communication for traffic context identification. In this context the algorithm itself can be improved by identifying dynamically the boundary conditions as well as dynamic change of the traffic conditions for identification and employment of dynamic parameter restrictions.

REFERENCES

[1] L. Krishnamachari, D. Estrin, and S.Wicker. The impact of data aggregation in wireless sensor networks. In ICDCSW '02: Proceedings of the International Conference on Distributed Computing Systems, pages 575–578, 2002.

[2] Thomas, M.; Peytchev E.; Al-Dabass D.; "Auto-sensing and distribution of traffic information in vehicular ad hoc networks", International Journal of Simulation, January 2004, PP 59-63, Volume: 5(3), ISSN: 1473-804X

[3] M. Raya and J.-P. Hubaux. The security of vehicular ad-hoc networks. In SASN '05: Proceedings of the 3rd ACM workshop on Security of ad hoc and sensor networks, pages 11–21, 2005.

[4] C. L. Robinson, L. Caminiti, D. Caveney, and K. Laberteaux. Efficient coordination and transmission of data for cooperative vehicular safety applications. In VANET '06: Proceedings of the 3rd ACM International Workshop on Vehicular Ad Hoc Networks, pages 10–19, 2006.

[5] Xue Yang, Jie Liu, Feng Zhao, and Nitin Vaidya, "A Vehicle-to-Vehicle Communication Protocol for Improving Road Safety," The 1st International Conference on Mobile and Ubiquitous Systems: Networking and Services (Mobiquitous 2004), Boston, MA, Aug. 22-26, 2004.

[6] Agafonov, E., Bargiela, A., Burke, E., Peytchev, E., Mathematical justification of a heuristic for statistical correlation of real-life time series, *European Journal of Operational Research* , 198, 2009, 275-286, doi:10.1016/j.ejor.2008.06.040

[7] Bargiela A., Peytchev E., Intelligent transportation systems: Towards integrated framework for traffic/transport telematics applications, Proc. IEEE Vehicular Technology Conference, Atlantic City, Oct. 6-10, 2001

CRYPTOGRAPHY BASED ON NEURAL NETWORK

Eva Volna
Martin Kotyrba
Vaclav Kocian
Michal Janosek
Department of Informatics and Computers
University of Ostrava
Dvorakova 7, Ostrava, 702 00, Czech Republic
eva.volna@osu.cz
martin.kotyrba@osu.cz
vaclav.kocian@osu.cz
michal.janosek@osu.cz

KEYWORDS
Cryptography key, encryption system, encryption algorithm, artificial neural network.

ABSTRACT

The goal of cryptography is to make it impossible to take a cipher and reproduce the original plain text without the corresponding key. With good cryptography, your messages are encrypted in such a way that brute force attacks against the algorithm or the key are all but impossible. Good cryptography gets its security by using incredibly long keys and using encryption algorithms that are resistant to other form attack. The neural net application represents a way of the next development in good cryptography. This paper deals with using neural network in cryptography, e.g. designing such neural network that would be practically used in the area of cryptography. This paper also includes an experimental demonstration.

INTRODUCTION TO CRYPTOGRAPHY

The cryptography deals with building such systems of security of news that secure any from reading of trespasser. Systems of data privacy are called the cipher systems. The file of rules are made for encryption of every news is called the cipher key. Encryption is a process, in which we transform the open text, e.g. message to cipher text according to rules. Cryptanalysis of the news is the inverse process, in which the receiver of the cipher transforms it to the original text. The cipher key must have several heavy attributes. The best one is the singularity of encryption and cryptanalysis. The open text is usually composed of international alphabet characters, digits and punctuation marks. The cipher text has the same composition as the open text. Very often we find only characters of international alphabet or only digits. The reason for it is the easier transport per media. The next cipher systems are the matter of the historical sequence: transposition ciphers, substitution ciphers, cipher tables and codes.
Simultaneously with secrecy of information the tendency for reading the cipher news without knowing the cipher key was evolved. Cipher keys were watched very closely. The main goal of cryptology is to guess the cipher news and to reconstruct the used keys with the help of good analysis of cipher news. It makes use of mathematical statistics, algebra, mathematical linguistics, etc., as well as known mistakes made by ciphers too. The legality of the open text and the applied cipher key are reflected in every cipher system. Improving the cipher key helps to decrease this legality. The safety of the cipher system lies in its immunity against the decipher.
The goal of cryptanalysis is to make it possible to take a cipher text and reproduce the original plain text without the corresponding key. Two major techniques used in encryption are symmetric and asymmetric encryption. In symmetric encryption, two parties share a single encryption-decryption key (Khaled, Noaman, Jalab 2005). The sender encrypts the original message (P), which is referred to as plain text, using a key (K) to generate apparently random nonsense, referred to as cipher text (C), i.e.:

$$\boldsymbol{C} = \textbf{Encrypt}\ (\boldsymbol{K},\boldsymbol{P}) \tag{1}$$

Once the cipher text is produced, it may be transmitted. Upon receipt, the cipher text can be transformed back to the original plain text by using a decryption algorithm and the same key that was used for encryption, which can be expressed as follows:

$$\boldsymbol{P} = \textbf{Dencrypt}\ (\boldsymbol{K},\boldsymbol{C}) \tag{2}$$

In asymmetric encryption, two keys are used, one key for encryption and another key for decryption.
The length of cryptographic key is almost always measured in bits. The more bits that a particular cryptographic algorithm allows in the key, the more keys are possible and the more secure the algorithm becomes. The following key size recommendations should be considered when reviewing protection (Ferguson, Schneier, Kohno, 2010):
Symmetric key:

- Key sizes of 128 bits (standard for SSL) are sufficient for most applications

Proceedings 26th European Conference on Modelling and Simulation ©ECMS Klaus G. Troitzsch, Michael Möhring, Ulf Lotzmann (Editors)
ISBN: 978-0-9564944-4-3 / ISBN: 978-0-9564944-5-0 (CD)

- Consider 168 or 256 bits for secure systems such as large financial transactions

Asymmetric key:

- Key sizes of 1280 bits are sufficient for most personal applications
- 1536 bits should be acceptable today for most secure applications
- 2048 bits should be considered for highly protected applications.

Hashes:

- Hash sizes of 128 bits (standard for SSL) are sufficient for most applications
- Consider 168 or 256 bits for secure systems, as many hash functions are currently being revised (see above).

NIST and other standards bodies will provide up to date guidance on suggested key sizes.

BACKPROPAGATION NEURAL NETWORKS

An Artificial Neural Network (ANN) is an information processing paradigm that is inspired by the way biological nervous systems, such as the brain, process information. The key element of this paradigm is the structure of the information processing system. It is composed of a large number of highly interconnected processing elements (neurones) working in unison to solve specific problems. ANNs, like people, learn by example. An ANN is configured for a specific application, such as pattern recognition or data classification, through a learning process. Learning in biological systems involves adjustments to the synaptic connections that exist between the neurones. This is true of ANNs as well.

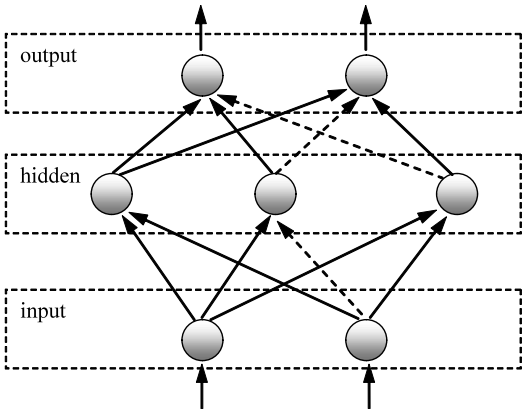

Figures 1: A general three layer neural network

Backpropagation network is one of the most complex neural networks for supervised learning. Regarding topology, the network belongs to a multilayer feedforward neural network. See Fig. 1 (Volna 2000), usually a fully connected variant is used, so that each neuron from the *n-th* layer is connected to all neurons in the *(n+1)-th* layer, but it is not necessary and in general some connections may be missing – see dashed lines, however, there are no connections between neurons of the same layer. A subset of input units has no input connections from other units; their states are fixed by the problem. Another subset of units is designated as output units; their states are considered the result of the computation. Units that are neither input nor output are known as hidden units.

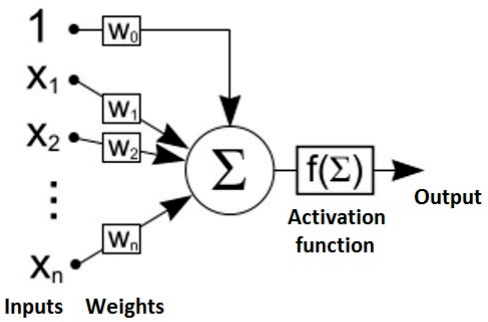

Figures 2: A simple artificial neuron (http://encefalus.com/neurology-biology/neural-networks-real-neurons)

A basic computational element is often called a neuron (Fig. 2), node or unit (Fausett 1994). It receives input from some other units, or perhaps from an external source. Each input has an associated weight ***w***, which can be modified so as to model synaptic learning. The unit computes some function *f* of the weighted sum of its inputs (3):

$$y_i = f\left(\sum_j w_{ij} x_j\right) \tag{3}$$

Its output, in turn, can serve as input to other units. The weighted sum is called the net input to unit *i*. Note that w_{ij} refers to the weight from unit *j* to unit *i* (not the other way around). The function *f* is the unit's activation function. Backpropagation algorithm usually uses a logistic sigmoid activation function (4) for values of *t* in the range of real numbers from $-\infty$ to $+\infty$.

$$f(t) = \frac{1}{1+e^{-t}} \tag{4}$$

Backpropagation algorithm belongs to a group called "gradient descent methods". An intuitive definition is that such an algorithm searches for the global minimum of the weight landscape by descending downhill in the most precipitous direction. The initial position is set at random selecting the weights of the network from some range (typically from -1 to 1 or from 0 to 1). Considering the different points, it is clear, that backpropagation using a fully connected neural network is not a deterministic algorithm. The basic backpropagation algorithm can be summed up in the following equation (the *delta rule*) for the change to the weight w_{ji} from node *i* to node *j* (5):

$$\begin{array}{lcccccc} \text{weight} & & \text{learning} & & \text{local} & & \text{input signal} \\ \text{change} & & \text{rate} & & \text{gradient} & & \text{to node } j \\ \Delta w_{j\,i} & = & \eta & \times & \delta_j & \times & y_i \end{array} \qquad (5)$$

where the local gradient δ_j is defined as follows (Seung 2002):

1. If node j is an output node, then δ_j is the product of $\varphi'(v_j)$ and the error signal e_j, where $\varphi(\_)$ is the logistic function and v_j is the total input to node j (i.e. $\Sigma_i w_{ji} y_i$), and e_j is the error signal for node j (i.e. the difference between the desired output and the actual output);
2. If node j is a hidden node, then δ_j is the product of $\varphi'(v_j)$ and the weighted sum of the δ's computed for the nodes in the next hidden or output layer that are connected to node j.

The actual formula is $\delta_j = \varphi'(v_j)\&\text{Sigma}_k\, \delta_k w_{kj}$ where k ranges over those nodes for which w_{kj} is non-zero (i.e. nodes k that actually have connections from node j. The δ_k values have already been computed as they are in the output layer (or a layer closer to the output layer than node j).

NEURAL CRYPTOGRAPHY

Neural cryptography (Kanter and Kinzel 2002, Kinzel 2002) is based on the effect that two neural networks are able to synchronize by mutual learning (Ruttor *et al*. 2006). In each step of this online procedure they receive a common input pattern and calculate their output. Then, both neural networks use those outputs present by their partner to adjust their own weights. This process leads to fully synchronized weight vectors.

Synchronization of neural networks is, in fact, a complex dynamical process. The weights of the networks perform random walks, which are driven by a competition of attractive and repulsive stochastic forces. Two neural networks can increase the attractive effect of their moves by cooperating with each other. But, a third network which is only trained by the other two clearly has a disadvantage, because it cannot skip some repulsive steps. Therefore, bidirectional synchronization is much faster than unidirectional learning (Ruttor 2004).

Two partners *A* and *B* want to exchange a secret message over a public channel. In order to protect the content against an attacker *T*, who is listening to the communication, *A* encrypts the message, but *B* needs *A*'s secret key over the public channel (Kinzel 2002). This can be achieved by synchronizing two TPMs (Three Parity Machines), one for *A* and one for *B*, respectively. After synchronization, the system generates a pseudorandom bit sequence which passes test on random numbers. When another network is trained on this bit sequence it is not possible to extract some information on the statistical properties of the sequence. The TPMs generate a secret key and also encrypt and decrypt a secret message (Prabakaran, Loganathan and Vivekanandan 2008).

In this paper we present an encryption system based on an Artificial Neural Network (ANN). ANN is used to construct an efficient encryption system by using a permanently changing key. The ANN topology is an important issue, as it depends on the application the system is designed for. Consequently, since our application is a computation problem, we have used a multi-layer topology. In the present paper, Backpropagation network is proposed for the encryption-and-decryption process. Neural networks offer a very powerful and general framework for representing non-linear mapping from several input variables to several output variables. The process to determining the values of these parameters on the basis of a data set is referred to as learning or training, and so the data set is generally referred to as a training set. A neural network can be viewed as suitable choice for the functional forms used for encryption and decryption operations.

DESIGN OF THE PROPOSED ANN-BASED ENCRYPTION SYSTEM

Every practical encryption system consists of four fundamental parts (Garfinger 1998), see Figure 3:

- The message that you wish to encrypt (called the *plain text*).
- The message after it is encrypted (called the *cipher text*).
- The encryption algorithm.
- The key (or keys), which is used by encryption algorithm.

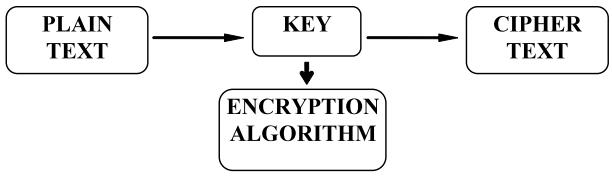

Figures 3: A simple example of the encryption system

In this paper, we conducted an experimental study with using neural network in cryptography. Thus, it means

- to design the topology of the neural network;
- to design the method of training algorithm of the neural network;
- to design the training set for training.

We successfully used neural networks as an encryption and decryption algorithm in cryptography. Parameters of both adapted neural networks were then included into cryptography keys. We used multilayer neural networks, which were adapted by backpropagation. Topology of each neural network is based on their training sets (see Table 1). In the encryption process, the input message is divided into 6-bit data sets and also 6-bit sets are produced after the encryption process. Thus, both systems were designed as follows: 6 units on the input

layer and 6 output units. There is no predetermined number of units in the hidden layer, but we also used 6 units. Both networks were trained on binary representations of symbols. In each training set, chains of numbers of the plain text are equivalent to binary values of their ASCII code, chains of letters of the plain text are equivalent to their binary value, which are 96 less than their ASCII code, each chain of some punctuation symbol of the plain text is equivalent to a binary value of ASCII code of space (e.g. 32), and chains of others chars of the plain text are equivalent to zero. Then, the cipher text is a random chain of 6 bits.
The security for all encryption and decryption systems is based on a cryptographic key. The SIMPLE systems use a single key for both encryption and decryption. The good systems use two keys. A message encrypted with one key can be decrypted only with the other key. If we use the neural network as encryption and also decryption algorithm, their keys have adapted neural networks´ parameters; which are their topologies (architecture) and their configurations (weight values on connections in the given order). Generally, each key is written as follow:

[*Input, Hidden, Output, Weights coming from the input units, Weights coming from the hidden units*]

where
Input is the number of input units;
Hidden is the number of hidden units;
Output is the number of output units;
Weights coming from the input units are weight values coming from the input units to hidden units in a predefined order;
Weights coming from the hidden units are weight values coming from the hidden units to output units in a predefined order

Parameter values of both ANNs in our experimental study are the following:

- each input layer consists of 6 nodes, which represents the 6-bit blocks;
- each hidden layer consists of 6 nodes;
- each output layer consists of 6 nodes, used to define the decrypted output message;
- fully connected networks;
- a sigmoid activate function;
- a learning rate equals 0,3.

History of both Error functions (E) is shown in Fig. 4. There are shown average values of error function, because adaptation with backpropagation algorithm was applied 10 times in each calculation. Other numerical simulations give very similar results.

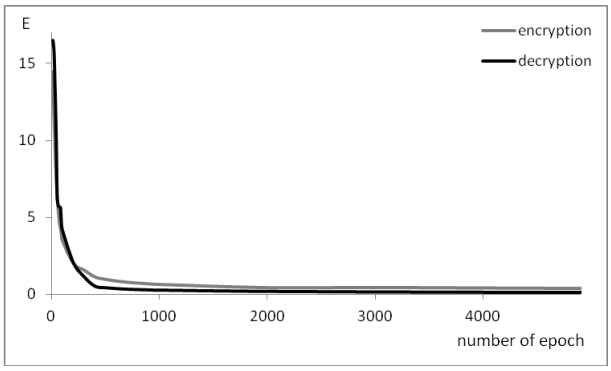

Figures 4: The Error function history

SENDING AND RECEIVING MESSAGES

In this model, a 6-bit plain text is entered ($N = 6$) and a 6-bit cipher text is the output (2^N).

Imagine that we want to send the following message:
"*We are in zoo, call us.*"

The first steps of our encryption process are to convert all uppercase letters to lowercase and to replace all punctuation symbols by a space. After this process, our message is the following:
"*we are in zoo call us*"

Then we replace all two spaces by one space, we get the following plain text:
"*we are in zoo call us*"

The plain text is coded into the chain:
(010111000101100000000001010010000101100000001001001110100000011010001111001111100000000010000000100110000110010000001010101 0011)

Now, we break it down into blocks (N =6), thus:
010111 000101 100000 000001 010010 000101 100000 001001 001110 100000 011010 001111 001111 100000 000010 000001 001100 001100 100000 010101 010011

The corresponding cipher text is the following:
(100100100000101111000010010111100000101111001000011100101111001101101000101000101111001011000010011010111010111101010010011 1)

The encrypted data will then be transmitted to the recipient.

RESULTS AND DISCUSSION

We have tested the behavior of the neural network described in the previous section so that we have generated messages (plain text) that were encrypted via the first adapted neural network. Then we have received some cipher text, which represented some input into the decryption process carried out via the second adapted neural network. Each obtained cipher text was compared with the original message after its pre-

processing. The whole procedure is demonstrated in Fig. 5. We found that:

- the neural network works reliably and absolutely no errors are found in the outputs during encryption;
- the neural network also works reliably during the decryption process, which is the reverse of the encryption process.

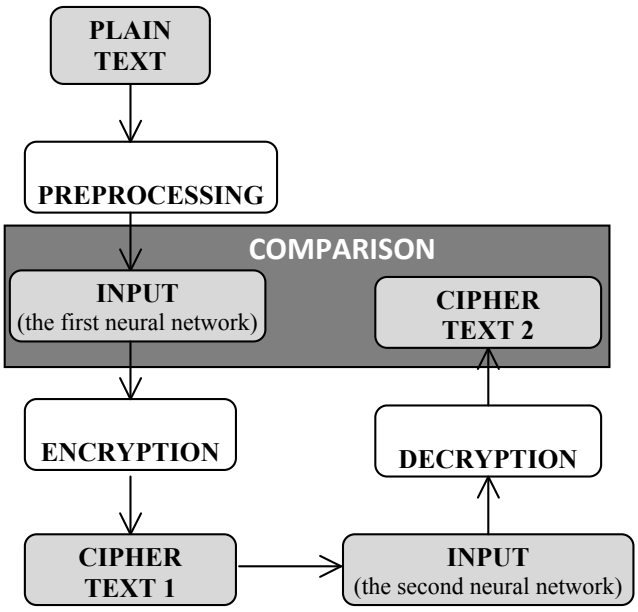

Figures 5: Tested process of a behavior of neural networks

This model presents an attempt to design an encryption system based on artificial neural networks of the backpropagation type. The proposed ANN has been tested for various numbers of plain text. The simulation results have shown very good results.

Table 1: Table of experiment constants

THE PLAIN TEXT			THE CIPHER TEXT
Char	ASCII code (DEC)	The chain of bits	The chain of bits
0	48	110000	111111
1	49	110001	110010
2	50	110010	101100
3	51	110011	111010
4	52	110100	101010
5	53	110101	100011
6	54	110110	111000
7	55	110111	000111
8	56	111000	010101
9	57	111001	110011
punct.	32	100000	101111
others	0	000000	011101
a	97	000001	000010
b	98	000010	100110
c	99	000011	001011
d	100	000100	011010
e	101	000101	100000
f	102	000110	001110
g	103	000111	100101
h	104	001000	010010
i	105	001001	001000
j	106	001010	011110
k	107	001011	001001
l	108	001100	010110
m	109	001101	011000
n	110	001110	011100
o	111	001111	101000
p	112	010000	001010
q	113	010001	010011
r	114	010010	010111
s	115	010011	100111
t	116	010100	001111
u	117	010101	010100
v	118	010110	001100
w	119	010111	100100
x	120	011000	011011
y	121	011001	010001
z	122	011010	001101

CONCLUSION

The neural net application represents a way of the next development in good cryptography, but we can ask question. What are the limitations of the system? The limitations of this type of system are few, but potentially significant. This is effectively a secret-key system, with the key being the weights and architecture of the network. With the weights and the architecture, breaking the encryption becomes trivial. However, both the weights and the architecture are needed for encryption and decryption. Knowing only one or the other is not enough to break it. What are the advantages to this system? The advantages to this system are that it appears to be exceedingly difficult to break without knowledge of the methodology behind it, as shown above. In addition, it is tolerant to noise. Most messages cannot be altered by even one bit in a standard encryption scheme. The system based on neural networks allows the encoded message to fluctuate and still be accurate.

ACKNOWLEDGEMENT

The research described here has been financially supported by University of Ostrava grant SGS2/PřF/2012. Any opinions, findings and conclusions or recommendations expressed in this material are those of the authors and do not necessarily reflect the views of the sponsors.

REFERENCES

Fausett, L.V. 1994 *Fundamentals of Neural Networks*. Prentice-Hall, Inc., Englewood Cliffs, New Jersey

Ferguson, N., Schneier, B., Kohno, T. 2010 *Cryptography Engineering: Design Principles and Practical Applications.* Wiley Publishing ISBN:0470474246 9780470474242

Garfinger, S. 1998. *PGP: Pretty Good Privanci*. Computer Press, Praha.

Kanter, I., Kinzel, W., 2002. Neural cryptography. In: *Proceedings of the 9th International conference on Neural Information Processing*. Singapore.

Khaled, M. Noaman, G., Jalab, H.A. 2005. Data security based On neural networks. *TASK Quarterly* 9 No 4, pp. 409–414

Kinzel, W., 2002 Theory of Interacting Neural Network. Preprint [cont.-mat/020454].

Prabakaran, N., Loganathan, P. and Vivekanandan, P. 2008. Neural Cryptography with Multiple Transfers Functions and Multiple Learning Rule. *International Journal of Soft Computing, 3: 177-181.*

Ruttor, A., Reents, G., Kinzel, W. 2004. Synchronization of random walk with reflecting boundaries. J. Phys. A: Math.Gen, 37: 8609 [cont-mat/0405369].

Seung, S. 2002. Multilayer perceptrons and backpropagation learning. 9.641 Lecture 4. 1-6. Available from: http://hebb.mit.edu/courses/9.641/2002/lectures/lecture04.pdf

Volná, E. 2000. Using Neural network in cryptography. In P. Sinčák, J. Vaščák, V. Kvasnička, R. Mesiar (eds.): *The State of the Art in Computational Intelligence.* Physica-Verlag Heidelberg. pp.262-267. ISBN 3-7908-1322-2, ISSN 1615-3871.

Ruttor, A., Kanter, I., Kinzel, W, 2006. Dynamics of neural cryptography. [cont-mat/061257/21].

AUTHOR BIOGRAPHIES

EVA VOLNA is an Associative Professor at the Department of Computer Science at University of Ostrava, Czech Republic. Her interests include artificial intelligence, artificial neural networks, evolutionary algorithms, and cognitive science. She is an author of more than 50 papers in technical journals and proceedings of conferences.

MARTIN KOTYRBA is a Ph.D. student at the Department of Computer Science at University of Ostrava, Czech Republic. His interests include artificial intelligence, formal logic, soft computing methods and fractals. He is an author of more than 15 papers in proceedings of conferences.

VACLAV KOCIAN is a Ph.D. student at the Department of Computer Science at University of Ostrava, Czech Republic. His interests include artificial intelligence, artificial neural networks, and soft computing methods. He is an author of more than 10 papers in proceedings of conferences.

MICHAL JANOŠEK is a Ph.D. student at the Department of Computer Science at University of Ostrava, Czech Republic. His interests include artificial intelligence, multi-agent systems, modeling and simulations. He is an author of more than 10 papers in proceedings of conferences.

Coastal Ecosystems Simulation: A Decision Tree Analysis for Bivalve's Growth Conditions

João Pedro Reis[1], António Pereira[1,2] and Luís Paulo Reis[2,3]
[1]FEUP - University of Porto, Faculty of Engineering - DEI
Rua Dr. Roberto Frias s/n 4200-465 Porto, Portugal
[2]LIACC - Artificial Intelligence and Computer Science Lab., University of Porto
Rua Dr. Roberto Frias s/n 4200-465 Porto, Portugal
[3]EEUM - School of Engineering, University of Minho - DSI
Campus de Azurem 4800-058 Guimaraes, Portugal
Emails: {ei07119, amcp}@fe.up.pt, lpreis@dsi.uminho.pt

KEYWORDS

Decision Trees, Patterns, Data Preparation, Ecological Behavior.

ABSTRACT

The usage of data mining models has the main purpose of discovering new patterns from dataset analysis by extracting knowledge from data and converting it to information. The most challenging part of problem solving is not the generation of high number of instances in dataset, most often hard to understand, but the interpretation of all those instances to extrapolate information about it. Simulation of coastal ecosystems is used to replicate some real conditions related with physical, chemical and biological processes, and produces large datasets from which it could be deduced some information about attributes behaviors. This paper relates the use of Decision Tree models to analyze the growth of bivalve species in an ecosystem simulation. With a set of attributes that represents the water quality in certain modeled regions, the usage of Decision Tree is intended to identify the most significant attribute conditions, which could justify the growth behavior for each analyzed species. This approach aims the creation of new information about how water conditions should be to promote a healthy and fast growth of the analyzed species, being useful to know in which zones the bivalve should be seeded, and which are the conditions that aquaculture producers should afford to benefit the quality of its crops.

INTRODUCTION

Modeling and simulation processes are intended to provide realistic environment for the analysis of a certain simulation. The simulated area that was used to obtain the final results refers to Sango Bay in China, in which were modeled hydrodynamic and biogeochemical variables (Duarte et al., 2003). All these results were provided by the EcoSimNet framework that is a platform for simulation and support decision-making (Pereira et al., 2009).

The large data set analyzed in this study is the simulation result of a lagoon ecosystem, modeled as two-dimensional vertically integrated. Partial differential equations were used to provide dataset attributes that describes different species, water temperature, water quality, seeded cells position, etc. The simulation is based on a finite difference bathymetric staggered grid with 35 lines by 32 columns, generating 1120 cells, with spatial resolution of 500m (Pereira et al., 2009). The aquaculture doesn't use all the 1120 representative cells of the area model - only 352 cells were chosen to seed - and the simulation covers one year and a half of real-time, the bivalve's growth cycle. All this information results in 800 000 instances for the final simulation dataset, being important the implementation of data preparation phases, first to remove not relevant information, and secondly to choose only the pertinent attributes to the analysis.

The dataset used has several attributes, being a set of them a representation of water quality in aquaculture. The subset selection of these attributes is a common problem in the data mining models, due to its improvement of performance (Quinlan, 1996). In the case of Decision Tree models, that are widely used in data mining and decision support applications (Pach and Abonyi, 2006) and specifically the usage of C4.5 algorithm, allows an efficient analysis of continuous variables, which is a characteristic of simulated environments. With this approach, we could obtain a large spectrum of correlated variables that describe how all the water conditions should be to promote a certain growth behavior.

Initially this paper tells about the *State of the art*, in other words, the developed works and studies related with bivalve's growth behavior and its physiology process. Thereafter it will be presented the C4.5 algorithm, which was the algorithm used for the construction of Decision Tree, and the Section *Dataset Preparation* that sets out the preprocessing phases to prepare the dataset used, describing the different phases that composes it. Section *Implementation* refers to the implementation phase that has the purpose to provide the final dataset used to C4.5 algorithm Decision Tree appliance. Section *Experiments* is the section in which experiments are described seeking the best values to apply in its parameters. Section *Results* shows the obtained results, followed by the Section *Conclusions*, in which the results are discussed

Proceedings 26th European Conference on Modelling and Simulation ©ECMS Klaus G. Troitzsch, Michael Möhring, Ulf Lotzmann (Editors)
ISBN: 978-0-9564944-4-3 / ISBN: 978-0-9564944-5-0 (CD)

reaching some conclusions about the approach used and the attributes relations.

STATE OF THE ART

In the last decades many authors studied the ecosystem properties, aiming a better understanding of how bivalves grow and its physiology could be influenced. Authors like Gilbert (Gilbert, 1973), Bachelet (Bachelet, 1980), Appeldoorn (Appeldoorn, 1983) and Beukema (Beukema and Meehan, 1985) claimed, in the early 80's and 90's, that temperature and food quality are two of the most important factors influencing the bivalve physiology. In the late 90's, Smaal & Haas also contributed proving that seston concentrations and chlorophyll-a levels near the bottom are generally higher than surface values, showing the importance of suspended particulate matter - Boundary SPM concentration (Smaal and Haas, 1997). A review made by Saxby in Western Australia, year 2002, that includes several sites like Seto Inline Sea in Japan and Saldanha Bay in South Africa, proves that phytoplankton - high values affects positively - along with nutrients, water temperature and salinity - prolonged exposure to low salinity mays have depressed all growth parameters - affects the bivalve physiology and food quality (Saxby, 2002).

On the other hand, the technology and tools to reach these conclusions are also significant. The author Michel R. Claereboudt used the GMDH algorithm (Group Method of Data Handling) to achieve some of these results. This algorithm is an inductive process that selects the best solutions for a given problem using the *external criterion* (Claereboudt, 1994). Despite the distinct approach of this algorithm and C4.5 (Quinlan, 1992), both reached good results in this context.

C4.5 ALGORITHM

The most common utilization of Decision Trees (DT) lies in the classification of instances from well-known datasets. There are two types of datasets that are mandatory in classification method, which are the training dataset, and the test dataset. The first one lies about the instances that are already classified, and the second tells about the instances that have to be classified based on the training dataset. For the construction of DT, all the attributes are tested as root nodes using a criterion for split, that can be a binary or a multi-way split, until the most informative attribute is found. The dataset is then divided by the root node split, and recursively subsequent trees are calculated, utilizing the partitioned dataset, until all samples for a given dataset belong to the class.

Decision Trees are attractive in the utilization of data mining models due to its intuitive representation (easy to understand by humans), its relatively fast construction, compared with other models, and its comparable or superior accuracy to other models. The utilization of a Decision Tree implies an algorithm that guides the construction of nodes and leafs. The nodes of DT depicts the attributes of dataset, and leafs represent the labeled instances, being the C4.5 algorithm chosen for its construction (Quinlan, 1992). This algorithm is one of best-known and most widely-used in learning models, allowing the analysis of numeric attributes, which is the case of our problem. The split criterion used in this problem is the Gain Ratio, instead of Information Gain, due to the high levels of entropy (common in continuous variables). The choice of this criterion is well explained in the *Implementation* Section.

In the problem solving method developed, the main purpose was to take advantage of Gain Ratio criterion, knowing the split nodes (conditions of the attributes analyzed) and values of attributes that reach the classified instances. Hence, was only used a set of classified instances to produce a DT based on it, with the intent of capture the Water Conditions of each labeled instance.

DATASET PREPARATION

The analysis of the dataset to be used, is an important phase that could be done by some essential steps. CRISP-DM (Shearer, 2000) is a Data Mining Process that aims in dataset analysis, on a specific domain of problem. For the growth behavior analysis, only the *Data Preparation* phase of this model was used, which is constituted by sub phases like *Data Selection, Data Cleaning, Data Construction, Data Integration and Data Formatting*. Only this phase was used due to the fact of merely clean and construct data phases were needed, making the processed dataset capable of being analyzed, and for further implementation of C4.5 algorithm.

In the first phase of the process, *Data Cleaning*, the treatment is focused on outliers - data that is not common or expected to be different, that in this case represents a non-seeded cell - and missing data. The treatment of these cases is positively important to the final result, in which a consistent analysis couldn't be made due to the corrupted data and miss representation of information. The used dataset from EcoSimNet framework, like previously said, is composed by a 32 lines by 35 columns, but only 352 cells represent the total number of seeded species, due to the existence of land cells and boundaries of the ecosystem. These specific cases of non-seeded cells could be easily found, since a very high number of variables, e.g. shell length, was used. The option was to remove the outlier's cells, being this information not relevant to the final analysis. To the amount of instances produced by the simulation of 731 iterations (days), the removal of missing or corrupted data seems not very harmful. The amount of instances per cells remains sufficient to make a posterior good analysis.

The Subset Selection Problem is a very common problem of attribute selection for dataset analysis. This attribute selection is totally relevant for our solution, since the analysis is focused on the Water Quality, and not in the whole information of the dataset. As we are dealing with continuous variables - Modeling and Simulation

(John et al., 1994) - the appliance of C4.5 algorithm is adequate, and the attribute selection promotes its performance.

The concept of Entropy may be informally defined as the measure of impurity in a group example. It is maximum when we cannot predict nothing from the data - the probability of choosing an example in a group is the same - and it is minimum when we can say for sure that a certain data will be chosen - the probability of choosing an example is 1 (only one type of data in the group). This concept is important, because the several data regarding the dataset have a high level of entropy that is a characteristic of continuous variables. Due to the *Data Cleaning* phase, the value of entropy was significantly reduced, improving the efficiency of the work, being the final result more consistent and credible.

After this step, we have to be aware of the attributes that are important to achieve the main final purpose. The initial dataset has the following attributes, excluding the time step, position, and species information: *Box depth*: depth of the seeded box; *Dynamic height*: height of the water in a determined cell as tide's result; *U Velocity*: velocity of the water in the longitude orientation; *V Velocity*: velocity of the water in the latitude orientation; *Salinity*; *DIN*: Dissolved Inorganic Nitrogen; *Phytoplankton biomass*; *POM*: Particulate Organic Matter; *TPM*: Total Particulate Matter; *Water temperature*; *Zooplankton biomass*; *Boundary NO3 concentration*: nitrate - indicator of water quality; *Boundary POM concentration*: Particulate Organic Matter; *Boundary SPM concentration*: Suspended Particulate Matter; *Boundary Zoo concentration*.

After an analysis phase, in which we select the attributes that are significant to the problem, the final selection attributes are the following: *Boundary NO3 concentration*; *POM*; *Phytoplankton biomass*; *Boundary SPM concentration*. All these attributes represent the quantity of particulate matter and the level of pollution in the water in which the bivalves are seeded.

The last step of this phase, is to separate the species information for a further independent treatment. In the EcoSimNet simulations, it was used three types of species: Chlamys Farreri (scallops), Crassostrea Gigas (oysters) and Laminaria Japonica (algae).

When the *Data Preparation* phase is concluded, the main question that have to be made, regarding the main goal of the problem, is: *how can water quality influence the bivalve's growth?* Firstly we have to analyse the growth behavior of some cells, in order to consider if an improvement of growth could be made. Figure 1 is a representation of Chlamys Farreri growth behavior (Scallop), from seed to harvest season, being each line a single cell of the seeded grid simulated.

As can be seen from Figure 1, not all the cells have the same behavior pattern, or even the same final shell length when the harvest season occurs. This is a great indicator to deduce the water conditions that promotes a good bivalve growth. One of the purposes of this work

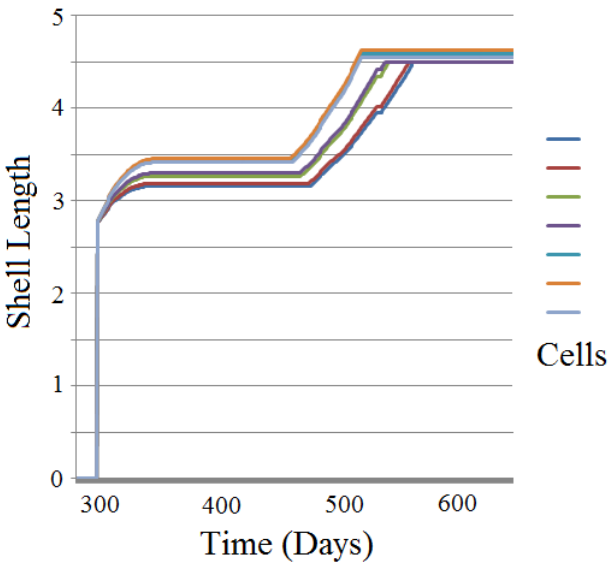

Figure 1: Chlamys Farreri Growth Behavior

is to answer the question above, with information that can be understood by a regular person, provided by very intuitive and easy seen representation methods.

Laminaria Japonica won't be contemplated for further analysis due to the lack of unusual and specific conditions that could be explored to induce a good growth. Hence, only Chlamys Farreri and Crassostrea Gigas will be used to generate its correspondent Decision Tree, with the C4.5 algorithm usage.

Using the derivative of growth species, we could classify the instances of simulation into Good and Bad growth. This *Quality Measure* sub-section is intended to establish a value (*Threshold*) that should separate these two classifiers, in order of being capable to distinguish the attribute circumstances that promote a certain growth, in the final phase of this work. As previously said, the growth derivative was used, represented by Figure 2, being these values a representation of growth registered in a certain time step of the simulation - slope between two neighbor time steps.

Which threshold represents better a quality measure? It is the question that should be answered to reach a high confidence in each species dataset analysis, in which the number of instances per classification Good or Bad has to be considerable and balanced. So, if the number of Good classified instances is significantly low compared with Bad classified ones, we could say that the dataset could be biased due to the unbalanced number of instances, and benefit one of the classifications. Hence, the *Threshold* - value that separates the derivative function of each growth species, into a good or bad label - will be discussed in the following sections.

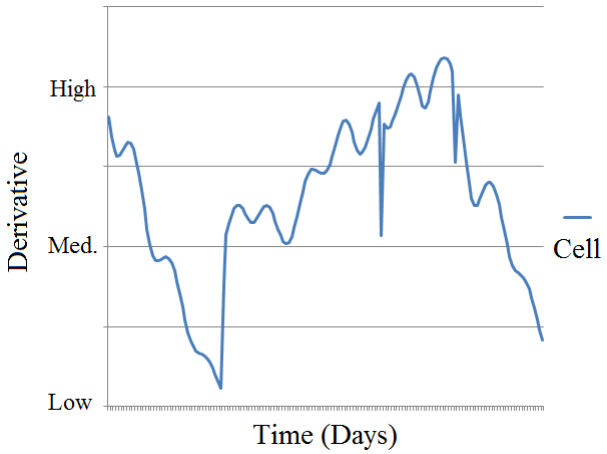

Figure 2: Chlamys Farreri Derivative Growth Behavior

IMPLEMENTATION

The utilization of C4.5 algorithm lies in the fact of dataset attributes generated from the EcoSimNet simulation process being continuous. This algorithm was improved and developed with different versions along time, and now is capable of treat continuous attributes efficiently (Quinlan, 1996).

Relatively to the C4.5 algorithm parameters, the criterion used was the Ratio Gain due to its more adequate appliance, comparing to Information Gain. The fact of dealing with high different values per attribute, normally found in continuous variables (Witten and Frank, 2005), like numeric values, the *Information Gain* approach could be biased, and overfitting could occur - selection of non-optimal attribute for prediction. The *Gain Ratio* is a based *Information Gain* method that takes into account the number of attribute instances, reducing the bias on high-branch attributes. The *Information Gain* is a based *Entropy* method that takes into account the lower value of entropy, high information gain value, to choose the root of the calculated tree.

This type of criterion is used to calculate the root of a tree that maximizes the *Ratio Gain*. Hence, the final tree is the result of an iterative process that calculates the next attribute to use, taking into account the previous one. So, while the tree is constructed, the number of instances is reduced due to the fact of previous attributes limitations and produced leafs. Hence, with this parameters it is possible to modulate a consistent *Decision Tree* that fulfills the goals of this project.

EXPERIMENTS

The *RapidMiner 5* was the framework used to run the experiments with different C4.5 algorithm parameters. It is the most Data Mining framework tool used (KDnuggets, 2010), allowing the creation of Data Mining models, and using the implementations of most relevant algorithms for different types of domains, like classification, clustering and item set mining.

The *Minimal Gain* parameter is the minimum value of Gain Ratio that should occur in an attribute to be chosen for tree expansion, and *Minimal Leaf Size* parameter is the minimum number of instances that a leaf should have in the Decision Tree. These were the two parameters tested to reach a good Decision Tree representation for growth conditions deduction. These parameters variation produces different numbers of nodes and leafs in Decision Trees, and should neither be too high, nor too low, due to the difficult interpretation of its representation.

Chlamys Farreri and Crassostrea Gigas species were tested, and the relation between the Number of Nodes, Minimal Gain and the Minimal Leaf Size will be presented.

Related to Chlamys Farreri species, it can be seen from Figure 3 that best results are provided from the variation of Minimal Leaf Size value between 25 and 100 and Minimal Gain value equal to 0.01 or 0.03. Value of Minimal Leaf Size equal to 10 with Minimal Gain equal to 0.03 and 0.01 produces a very high number of nodes, which is neither a good visual representation, neither easy to deduce the conditions that promote a certain growth.

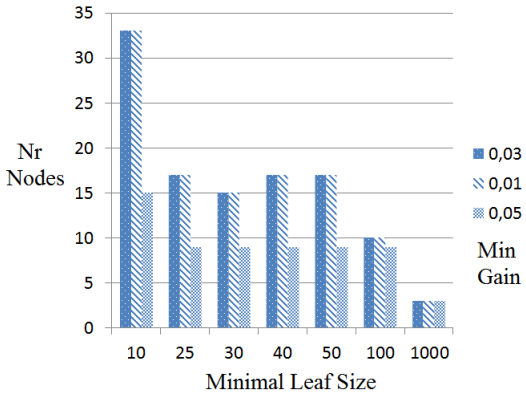

Figure 3: Chlamys Farreri: Number of Nodes

From figure 4 it is easy to see that the best results of Crassostrea Gigas Decision Tree are for Minimal leaf size between 30 and 50, with any value of Minimal Gain. A good result could also be obtained with Minimal Leaf Size value equal to 10, but only with Minimal Gain equal to 0.001.

RESULTS

Each species has its own growth information in separated datasets. For each species analysis, it will be presented the relations of dataset labeled attributes.

An important observation that has to be made before the tables analysis (Tables 1 thru 4), is that low values of instances per conditions (set of rules that satisfy a certain label: Good or Bad), do not discard the confidence inherent to it. The purpose of this paper is to find the circum-

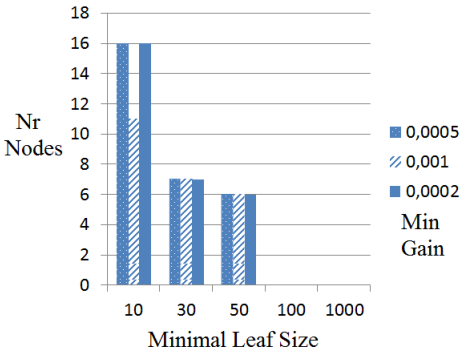

Figure 4: Crassostrea Gigas: Number of Nodes

stances that could determine a certain growth, independently of their number of instances. We are looking for the specificity that water conditions could provide, separating the two labels of associated growth. Another consideration that should be made, is relatively to maximum and minimum values, generated by the simulation framework, from each attribute analyzed. The presented tables will not represent these values, so we assume that when a situation like *NO3* $<$ *4.5* and *NO3* $>$ *4.5*, the NO3 values should variate between its minimum possible value and 4.5, and between 4.5 and its maximum possible value, respectively.

This analysis had two different intentions: Make a qualitative evaluation of most significant attributes, and compare two totally independent analysis: the Decision Tree results, in which could be validated the computer results, with the dataset visual analysis. Due to length restrictions of the paper only the computer analysis will be done.

Chlamys Farreri

As said earlier, a dataset was generated to obtain this type of results. The number of instances that dataset contains is 15 042, being 7724 (51%) labeled as Bad Growth, and 7318 (49%) labeled as Good Growth. This dataset follows the Java implementation metrics, being: Threshold=0.015 and the Derivative Factor=1.

Figure 5 represents the Chlamys Farreri Decision Tree, with the parameters: Minimal Size for Split=2, Minimal Leaf Size=40, Minimal Gain=0.01, Maximal Depth=20 and Confidence=0.25.

From Figure 5 an analysis was made having originated two different tables. One of them tells about a Good growth conditions, Table 1, and the other Bad growth conditions, Table 2.

Regarding Table 1, if Nitrate (NO3) levels are above the 4.586 and Phytoplankton above 0.138 a good growth will occur. To ensure this growth, the POM values should be above 2.218. These water conditions should benefit the Chlamys Farreri species growth.

Regarding Table 2, if NO3 levels are between 1.093 and 4.586, a bad growth will occur. To ensure this

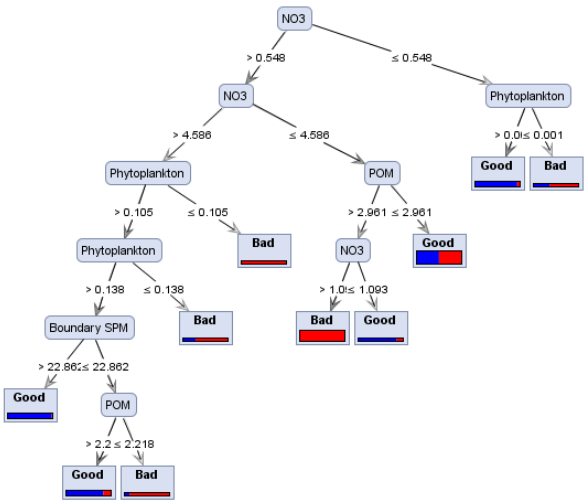

Figure 5: Chlamys Farreri Decision Tree

Table 1: Good Growth: Chlamys Farreri

Leaf	Confidence	Total	Conditions
Good	98.0	1419	$NO3 > 4.586$ $Phytoplankton > 0.138$ $BoundarySPM > 22.862$
Good	94.6	1499	$NO3 \leq 0.548$ $Phytoplankton > 0.001$
Good	84.0	1514	$NO3 > 4.586$ $Phytoplankton > 0.138$ $BoundarySPM < 22.862$ $POM > 2.218$

growth, the POM value should be below 2.218. These water conditions should worsen the growth of Chlamys Farreri species.

Crassostrea Gigas

The next analysis lies in the Crassostrea Gigas species, and dataset description. The number of instances of the dataset is 19 991, being 10 397 (52%) labeled as Bad Growth, and 9594 (48%) labeled as Good Growth. This dataset follows the Java implementation metrics, being: Threshold=0.02 and the Derivative Factor=1.

Figure 6 represents the Crassostrea Gigas Decision

Table 2: Bad Growth: Chlamys Farreri

Leaf	Confidence	Total	Conditions
Bad	99.3	467	$NO3 > 4.586$ $Phytoplankton = 0.138$
Bad	98.6	4006	$1.093 < NO3 < 4.586$ $POM > 2.961$
Bad	87.3	133	$NO3 > 4.586$ $Phytoplankton > 0.138$ $BoundarySPM \leq 22.862$ $POM \leq 2.21$

Table 3: Good Growth: Crassostrea Gigas

Leaf	Conf.	Total	Conditions
Good	83.3	48	$POM = 0.949$ $NO3 \leq 0.336$
Good	64.5	31	$POM = 0.949$ $NO3 > 0.336$ $Phytoplankton > 0.297$ $BoundarySPM > 16.171$
Good	54.6	18787	$0.949 < POM \leq 4.630$

Table 4: Bad Growth: Crassostrea Gigas

Leaf	Conf.	Total	Conditions
Bad	100.0	69	$POM \leq 0.725$
Bad	99.2	258	$POM = 0.949$ $NO3 > 0.336$ $Phytoplankton \leq 0.297$
Bad	88.4	190	$POM > 4.630$

Tree with the parameters: Minimal Size for Split=2, Minimal Leaf Size=10, Minimal Gain=0.001, Maximal Depth=20 and Confidence=0.25.

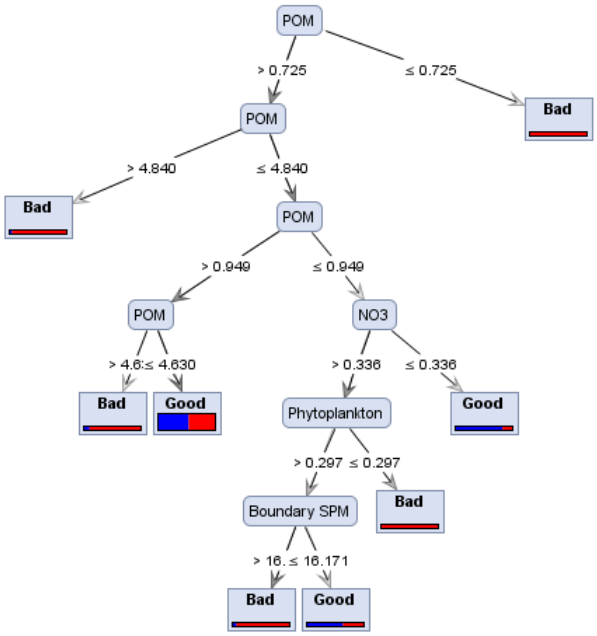

Figure 6: Crassostrea Gigas Decision Tree

Two different tables were generated when analysing Figure 6. One of them tells about a Good growth conditions, Table 3, and the other Bad growth conditions, Table 4.

Regarding Table 3, if POM values are between 0.949 and 4.630 a good growth will occur. To ensure this growth, the SPM values should be below 16.171. These water conditions should benefit the Crassostrea Gigas species growth.

Regarding Table 4, if POM values are higher than 4.630 and lower than 0.725, a bad growth will occur. Low values of phytoplankton reinforce this growth. The reported water conditions will worsen the growth of Crassostrea Gigas species.

CONCLUSIONS

As bivalves are marine and freshwater mollusks, it is obvious that with more pure water - less solid particulates - the bivalves have better conditions to growth healthy and rapidly. By the analysis made previously, it can be deduced that water conditions influence the growth of bivalves.

This approach aims the creation of new information about how water conditions should be to promote a healthy and fast growth of the analyzed species, being useful to know in which zones the bivalve should be seeded, and which are the conditions that aquaculture producers should afford to benefit the quality of its crops.

NO3 levels and POM values are important attributes for the Chlamys Farreri species growth. These two indicators should be controlled to provide guidance to bivalve physiology. High levels of water quality (NO3) and low levels of particulates (water pollution) are needed to produce a beneficial growth. We can see that relatively to the growth of this species, the levels of NO3 are inversely related.

POM and Phytoplankton are the most important attributes for the Crassostrea Gigas species growth. We can conclude that some medium values of POM can benefit its physiology, as much as high values of Phytoplankton. This medium values of POM could be justified by some oyster species life cycle are composed by an attachment to a rocky surfaces, that have some levels of impurity. Phytoplankton describes the environment quality that are important to any species growth, as Crassostrea Gigas.

The results of this study don't accrue only for the bivalve production, but also for the public health. Since the bivalve make part of humans feeding habits, the more quality these species have, the more quality life we are giving to people. With this work, producers can evaluate better the water conditions that promote the species physiology, together with water quality for the ecosystem health and the final consumer.

The application of Decision Tree shown to be a powerful tool to attribute analysis and its behavior and relation with other attributes, and more specifically, the C4.5 algorithm. Also, the Decision Tree is a very intuitive way to deduce the attribute behavior, and representation tool due to its simple and direct presentation. The C4.5 algorithm has demonstrated to be a powerful tool in datasets of continuous attribute, having different flexible parameters that can provide a better solution comparing with different approaches from Decision Tree based.

REFERENCES

Appeldoorn, R. S. (1983), *Variation in the growth rate of Mya arenaria and its relationship to the environment as analyzed through principal components analysis and the omega parameter of the von Bertalanffy equation*. Fishery Bulletin 81: 75-84.

Bachelet, G. (1980), *Growth and recruitment of the tellinid bivalve Macoma balthica at the Southern limit of its geographical distribution, the Gironde estuary (SW France)*. Marine Biology 59: 105-117.

Beukema, J. J. and Meehan, B. W. (1985), *Latitudinal variation in linear growth and other shell characteristics of Macoma balthica*. Marine Biology 90: 27-33.

Chen, Q. and Mynett, A. (2009), *Rule-Based Ecological Model*. In: Handbook of Ecological Modelling and Informatics: 307-324.

Claereboudt, M. R. (1994), *GMDH algorithm as a tool for bivalve growth analysis and prediction*. ICES Journal of Marine Science 51: 439-445.

Debeljak, M. and Deroski, S. (2011), *Decision Trees in Ecological Modelling*. In: Modelling Complex Ecological Dynamics: an Introduction into Ecological Modelling, vol. 2: 197-209.

Duarte, P., Meneses, R., Hawkins, A. J. S., Zhu, M., Fang, J., and Grant, J. (2003), *Mathematical modelling to assess the carrying capacity for multi-species culture within coastal waters*. Ecological Modelling, 168 (1-2): 109-143.

Gilbert, M. A. (1973), *Growth rate, longevity and maximum size of Macoma balthica (L.)*. The Biological Bulletin 145: 119-126.

Hahsler, M., Chelluboina, S., Hornik, K. and Buchta, C. (2011), *The arules R-Package Ecosystem: Analyzing Interesting Patterns from Large Transaction Data Sets*. Journal of Machine Learning Research 12(Jun): 2021-2025.

John, G. H., Kohavi, R. and Pfleger, K. (1994), *Irrelevant Features and the Subset Selection Problem*, MACHINE LEARNING: PROCEEDINGS OF THE ELEVENTH INTERNATIONAL: 121-129.

Jorgensen, S. E. and Bendoricchio, G. (2001), *Fundamentals of Ecological Modelling*.

KDnuggets (2010), *Data Mining/Analytic Tools Used Poll (May 2010)*. Available online: http://www.kdnuggets.com/polls/2010/data-mining-analytics-tools.html.

Pach, F. P. and Abonyi, J. (2006), *Association Rule and Decision Tree based Methods for Fuzzy Rule Base Generation*. Word Academy of Sciences, Engineering and Technology 13: 45-50.

Pereira, A., Reis, L. P. and Duarte, P. (2009) *EcoSimNet: A Multi-Agent System for Ecological Simulation and Optimization*. EPIA 2009, LNAI 5816: 473-484, Springer-Verlag.

Quinlan, J. R. (1992), *C4.5: Programs for Machine Learning*. Morgan Kaufmann.

Quinlan, J. R. (1996), *Improved Use of Continuous Attributes in C4.5*, Journal of Artificial Intelligence Research 4: 77-90.

Saxby, S. A. (2002), *A review of food availability, sea water characteristics and bivalve growth performance at coastal culture sites in temperate and warm temperate regions of the world*. Fisheries Research Report No. 132, Department of Fisheries, Western Australia.

Shearer, C. (2000), *The CRISP-DM Model: The New Blueprint for Data Mining*, Journal of Data Warehousing vol.5, N.4: 13-22.

Smaal, A C and Haas, H A (1997), *Seston Dynamics and Food Availability on Mussel and Cockle Beds*. Estuarine, Coastal and Shelf Science 45: 247-259.

Witten, I. H. and Frank, E. (2005), *Data Mining: Practical Machine Learning Tools and Techniques*. Morgan Kaufmann Series in Data Management Systems, Elsevier.

AUTHOR BIOGRAPHIES

JOÃO PEDRO C. REIS was born in Porto, Portugal, and obtained his degree in Informatics Engineering at the University of Porto. Since 2010 he is dedicated to research in the field of Machine Learning and Multi-agent Systems, and he is a MSc student in Informatics and Computation in the University of Porto. His e-mail address is: `ei07119@fe.up.pt`; `joaoreis.correia@gmail.com` and his personal webpage at `http://www.fe.up.pt/~ei07119`.

ANTÓNIO PEREIRA was born in Porto, Portugal, and has a PhD in Informatics Engineering from University of Porto. Since 2003 he is dedicated to research in the field of Agent-Based Simulation, Distributed Artificial Intelligence, Optimization and Intelligent Systems. His email is `amcp@fe.up.pt` and his personal webpage at `http://www.fe.up.pt/~amcp`.

LUÍS PAULO REIS was born in Porto, Portugal, and has a PhD in Electrical Engineering (Coordination in Multi-Agent Systems) in the University of Porto. He has been researching in the area of (Multi-Agent) intelligent simulation for several years in different projects including FC Portugal simulated robotic soccer team World and European champion of RoboCup in 2000 and 2006. His email is `lpreis@dsi.uminho.pt` and his personal webpage stays at `http://www.fe.up.pt/~lpreis`.

CUDA BASED ENHANCED DIFFERENTIAL EVOLUTION: A COMPUTATIONAL ANALYSIS

Donald Davendra and Jan Gaura,
Department of Computer Science
Faculty of Electrical Engineering and Computer Science
VSB-Technical University of Ostrava
17. listopadu 15, 708 33 Ostrava-Poruba
Czech Republic.
Email: {donald.davendra,jan.gaura}@vsb.cz

Magdalena Bialic-Davendra,
Tomas Bata University in Zlin,
Faculty of Management and Economics,
Nam T.G. Masaryka 5555, 760 01 Zlin,
Czech Republic.
Email: bialic@fame.utb.cz

Roman Senkerik,
Tomas Bata University in Zlin,
Faculty of Applied Informatics,
Nam T.G. Masaryka 5555, 760 01 Zlin,
Czech Republic.
Email: senkerik@fai.utb.cz

KEYWORDS

Differential evolution, flowshop scheduling, CUDA

ABSTRACT

General purpose graphic programming unit (GPGPU) programming is a novel approach for solving parallel variable independent problems. The graphic processor core (GPU) gives the possibility to use multiple blocks, each of which contains hundreds of threads. Each of these threads can be visualized as a core onto itself, and tasks can be simultaneously sent to all the threads for parallel evaluations. This research explores the advantages of applying a evolutionary algorithm (EA) on the GPU in terms of computational speedups. Enhanced Differential Evolution (EDE) is applied to the generic permutative flowshop scheduling (PFSS) problem both using the central processing unit (CPU) and the GPU, and the results in terms of execution time is compared.

INTRODUCTION

During the later part of the past decade, a novel trend emerged where programmers started using the Graphics Processing Unit (GPU) for programming not graphic applications which usually was in the preview of the Central Processing Unit (CPU). The reasoning behind such a move was the possibility to achieving speedups of magnitude compared to optimized CPU implementations.

GPU's have evolved into fast, highly multi-threaded processors, with hundreds of cores and thousands of concurrent threads. These threads which can be invoked simultaneously, provide an excellent platform for parallel execution. A GPU is optimal when a problem has to be executed many times, can be isolated as a function and works independently on different data.

One of the most challenging and computational demanding problems in engineering are the NP-Hard problems. These problems are computationally intractable, and often require the use of optimization algorithms. This research attempts to solve the challenging flowshop scheduling (FSS) problem using a novel Enhanced Differential Evolution (EDE) algorithm utilizing GPU programming.

One of the most widespread programming architectures is the Compute Unified Device Architecture (CUDA) of Nvidia (NVIDIA, 2012). A number of research has been conducted on GPU programming involving evolutionary algorithms and these two architectures. Tabu Search has been used for the evaluating the FSS problem using CUDA by Czapinski and Barnes (2011). Genetic Algorithms (GA) has been been used to solve the traveling salesman problem by Chen et al. (2011), whereas a parallel GA approach has been done by Pospichal et al. (2010). The particle swarm algorithm has also been modified to be used by CUDA Mussi et al. (2011). More interestingly Genetic Programming has also found a niche in GPU programming (Robilliard et al., 2009).

This research utilizes the Nvidia CUDA framework for GPU computation. The enhanced Differential Evolution (EDE) (Davendra and Onwubolu, 2009) is modified to the GPU framework and execution time for both the GPU and CPU variants are compared.

This paper follows the following structure. Section 1 outlines the CUDA framework and syntax. Section 2 describes Differential Evolution (DE) and the EDE algorithms. The problem attempted in this research; flow shop scheduling is given in Section 3. Section 4 describes the code design on the GPU, whereas the experimentation and analysis (Section 5) compares the obtained results. The paper is concluded in Section 6.

Proceedings 26th European Conference on Modelling and Simulation ©ECMS Klaus G. Troitzsch, Michael Möhring, Ulf Lotzmann (Editors)
ISBN: 978-0-9564944-4-3 / ISBN: 978-0-9564944-5-0 (CD)

1 CUDA

The Compute Unified Device Architecture (CUDA) is a propriety parallel computing architecture developed by Nvidia Corporation and released in November 2006. The main objective for this was to introduce general programming to the GPU, in the effort to scale up raw processing power.

The CUDA API (both low level and high level) provides a platform for accessing the Nvidia GPU for processing. This allowed a programmer to bypass the traditional OpenGL or Direct3D techniques which were needed to program the chips. Additionally, and most importantly, C language can now be used to program for CUDA, through the PathScale Open64 C compiler. This has essentially introduced CUDA for mainstream programmers (Sanders and E.Kandrot, 2010).

The general outline of CUDA is given in Fig 1. The CPU is able to communicate with the GPU using the PCIe bus, and therefore the communication speed is limited by the bus speed. A GPU itself has a number of attributes. The GPU is made up of a number of *blocks*. Each *block* is subsequently divided into a number of *threads*. Each block has its own *shared memory* and *registers*, which can be accessed by all the threads residing in that particular *block*. All *blocks* can access the *global memory* and the *shared memory* of the GPU. The minimum applicable amount of *blocks* available is 65,535, and each *block* has 512 *threads* each. CUDA processing cores are referred to as *kernels*, which are launched from the CPU. *Kernels* can be made up of any combinations of *blocks* and *threads*, depending on the application (Kirk and Hwu., 2010).

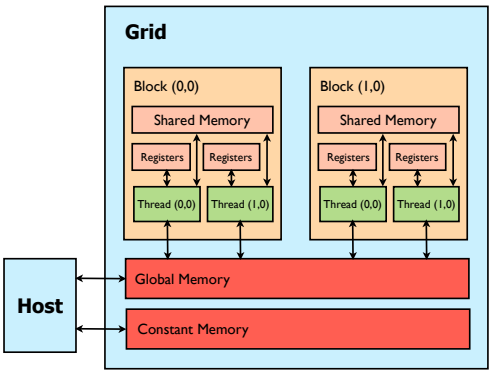

Figure 1: CUDA outline.

There are many types of memory, differing in size, visibility, access time and whether it is cached and writeable. Below is the description of each memory type, its capabilities and purpose.

1. *Global memory* is used for communication between host and device, therefore it is accessible from blocks (directly), and CPU (through API). It is the largest memory space available on GPU, but it is the slowest at the same time.

2. *Shared memory* is a very fast on-chip memory, available for both reading and writing, but only accessible by threads within the same block. Unfortunately, it is also small with a maximum of 16,384 bytes per block.

3. *Constant memory* is accessible as global memory, but it is cached in the case of a cache miss, a read operation takes the same time as reading from global memory, otherwise it is much faster.

4. *Registers* are the fastest on chip memory used for threads automatic variables. The number of 32-bit registers on each multiprocessor is limited up to 16,384, therefore if each thread requires too many registers, the number of blocks executed on each multiprocessor is reduced.

5. *Local memory* is a local per thread memory, used for large automatic variables (e.g. arrays or large structures) that will not fit in registers. It is not cached, and is as slow as global memory.

1.1 CUDA syntax

A brief outline of the CUDA syntax is presented. Memory allocation of dynamic variables is given as: `cudaMalloc((void**)&GPUvarible,(size)*sizeof(type));`, where GPUvariable is the name, type is the datatype and size refers to the total size being allocated.

Data is passed from the CPU to the kernels in the GPU using `cudaMemcpy(GPUvariable,CPUvariable,(size)*sizeof(type),#cudaMemcpyHostToDevice);`. This copies the data from the CPUvariable to the GPUvariable.

The kernel is launched using the following syntax `kernel<<<dim3 grid,dim3 block>>>(...)`, where `dim3` is the built in device variable. `dim3 gridDim` refers to the number of dimension of the grid in blocks whereas `dim3 blockDim` is the dimension of the blocks in threads. Within the kernel, the block index is given by `dim3 blockIdx` and the thread index is given by `dim3 threadIdx`.

After execution on the GPU kernels, the data is read back to the CPU as `cudaMemcpy(CPUvariable,GPUvariable,(size)*sizeof(type),cudaMemcpyDeviceToHost);`. This commands copies the data from the GPUvariable to the CPUvariable. The CUDA procedural outline is shown in Fig 2

2 DIFFERENTIAL EVOLUTION

Developed by Price and Storn (Price, 1999), Differential Evolution (DE) algorithm is a very robust and efficient approach to solve continuous optimization prob-

```
Memory Allocation
    int *GPUvariable
    cudaMalloc((void**)&GPUvariable,(size)*sizeof(type));

Kernel Parameter Passing
    cudaMemcpy(GPUvariable,CPUvaribale,(size)*sizeof(type),
                cudaMemcpyHostToDevice);

GPU kernel Allocation
    dim3 grid, block;

Execution
    kernal<<<dim3 grid,dim3 block>>>(GPUvariable);

Read Back
    cudaMemcpy(CPUvariable,GPUvaribale,(size)*sizeof(type),
                cudaMemcpyDeviceToHost);

Release Memory
    cudaFree(GPUvariable);
```

Figure 2: Generic CUDA template

lems. One of the core features of DE is that it uses a vector perturbation methodology for crossover.

Each solution is visualized as a vector in search space. A new vector is created by the combination of four unique vectors. A schematic of DE is given in Fig. 3.

1. Input: $D, G_{\max}, NP \geq 4, F \in (0,1+), CR \in [0,1]$, and initial bounds: $\vec{x}^{(lo)}, \vec{x}^{(hi)}$.

2. While $G < G_{\max}$

$\forall i \leq NP$

3. Mutate and recombine:

3.1 $r_1, r_2, r_3, r_4 \in \{1,2,....,P_{size}\}$, randomly selected from each cluster

3.2 $j_{rand} \in \{1,2,...,D\}$, randomly selected once each i

3.3 $\forall j \leq D, u_{j,i,G+1} = \begin{cases} x_{best,G} + F \cdot (x_{j,r_1,G} - x_{j,r_2,G} - x_{j,r_3,G} - x_{j,r_4,G}) \\ \quad \text{if } (rand_j[0,1] < CR \vee j = j_{rand}) \\ x_{j,i,G} \quad \text{otherwise} \end{cases}$

4. Select Criteria

$G = G + 1$

Figure 3: DE selection

2.1 Enhanced Differential Evolution outline

Enhanced Differential Evolution (EDE) (Davendra and Onwubolu, 2007), heuristic is an extension of the canonical DE developed for the task of permutative based combinatorial optimization. The basic outline is given in Fig 4.

EDE operates on a permutative set of individuals. These individuals are transformed to a real number using the forward transformation. The DE strategy can then be applied to the real domain values. Once the DE crossover and mutation routines have finished, the resulting vector is transformed back into the permutative individual using the backward transformation. The new trial individual is then randomly repaired, and its objective function calculated. The local search is utilized when stagnation is detected in the population. The detailed description of the EDE approach is given in Davendra and Onwubolu (2009).

1. **Initial Phase**
   (a) *Population Generation*: An initial number of discrete trial solutions are generated for the initial population.
2. **Conversion**
   (a) *Forward transformation*: This conversion schema transforms the parent solution into the required continuous solution.
   (b) *DE Strategy*: The DE strategy transforms the parent solution into the child solution using its inbuilt crossover and mutation schemas.
   (c) *Backward Transformation*: This conversion schema transforms the continuous child solution into a discrete solution.
3. **Mutation**
   (a) *Relative Mutation Schema*: Formulates the child solution into the discrete solution of unique values.
4. ***Local Search**
   (a) *Local Search*: 2 Opt local search is used to explore the neighborhood of the solution.

Figure 4: EDE outline

3 PERMUTATIVE FLOWSHOP SCHEDULING PROBLEM

In many manufacturing and assembly facilities, a number of operations have to be done on every job. Often these operations have to be done on all the jobs in the same order implying the jobs have to follow the same route. The machines are assumed to be set up in series and the environment is referred to as a *flow shop* (Pinedo, 1995).

Flow Shop *Fm*: There are *m* machines in series. Each job has be processed in each one of the *m* machines. All the jobs have to follow the same route (i.e., they have to processed on Machine 1, and then on Machine 2, etc). After completing on one machine, a job joins the queue at the next machine. Usually all jobs are assumed to operate under the *First In First Out (FIFO)* discipline - that is a job cannot "pass" another while waiting in a queue. Under this effect the environment is refereed to as a *permutative* flow shop. the general syntax of this problem as described in the triplet format $\alpha|\beta|\gamma$, is given as

$$Fm\,|Perm\,|C_{\max}$$

The first field denotes the problem being solved, the second field the type of problem (in this case permutative) and the last field denotes the objective being under investigation, which is the makespan (total time taken to

complete the job).

Stating these problem descriptions more elaborately, the minimization of completion time (makespan) for a flow shop schedule is equivalent to minimizing the objective function $\Im$:

$$\Im = \sum_{j=1}^{n} C_{m,j} \tag{1}$$

s.t.

$$C_{i,j} = \max\left(C_{i-1,j}, C_{i,j-1}\right) + P_{i,j} \tag{2}$$

where, $C_{m,j}$ = the completion time of job *j*, $C_{i,j} = k$ (any given value), $C_{i,j} = \sum_{k=1}^{j} C_{1,k}$; $C_{i,j} = \sum_{k=1}^{j} C_{k,1}$ machine number, *j* job in sequence, $P_{i,j}$ processing time of job *j* on machine *i*. For a given sequence, the mean flow time, $MFT = \frac{1}{n}\sum_{i=1}^{m}\sum_{j=1}^{n} c_{ij}$, while the condition for tardiness is $c_{m,j} > d_j$. The constraint of Equation 2 applies to these two problem descriptions.

The value of the makespan under a given permutation schedule can also be computed by determining the *critical path* in a directed graph corresponding to the schedule.

For a given sequence $j_1, .., j_n$, the graph is constructed as follows: For each operation of a specific job j_k on a specific machine *i*, there is a node (i, j_k) with the *processing time* for that job on that machine. Node (i, j_k), $i = 1, ..., m-1$ and $k = 1, ..., n-1$, has arcs going to nodes $(i+1, j_k)$ and (i, j_{k+1}). Nodes corresponding to machine *m* have only one outgoing arc, as do the nodes in job j_n. Node (m, j_n), has no outgoing arcs as it is the terminating node and the total weight of the path from first to last node is the makespan for that particular schedule (Pinedo, 1995). A schematic is given in Fig 5.

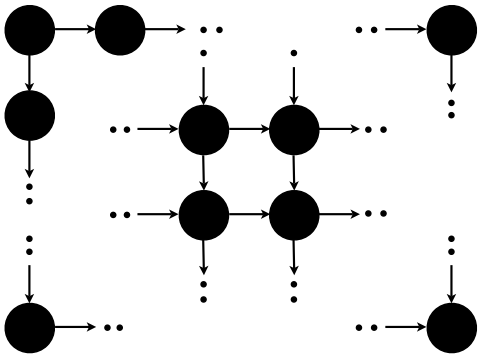

Figure 5: Directed graph representation for $Fm\,|Perm\,|C_{\max}$

The pseudocode of the routine as coded in the GPU kernel is given in Fig 6.

Algorithm for Flow shop scheduling on the GPU

Assume a problem of size n, and a schedule given as $X = \{x_1, .., x_n\}$. Assume the problem matrix as R, which is of size *n* by *m* (job and machine) and the solution array as Y of size *m*.

1. For $i = 1, 2, ..., n$ do the following:
   (a) For $j = 1, 2, ..., m$ do the following:
      i. **IF** *i* = 1
         A. $Y_i = \sum_{i=1}^{i-1} Y_i + R_{X_i,j}$
      ii. **ELSE**
         A. **IF** *i* = 1
            $Y_1 = Y_1 + R_{X_1,1}$
         B. **ELSE**
            $Y_j = \max(Y_j, Y_{j-1}) + R_{X_i,j}$
2. Output Y_m as the objective function.

Figure 6: Pseudocode for Flow shop scheduling

4 CODE DESIGN ON THE GPU

In an evolutionary algorithm, the most time and processor consuming task is the objective function calculation. This amounts to almost 80% of the execution time (Czapinski and Barnes, 2011). Therefore it is logical to utilize the GPU for this task, providing that it can be parallelized.

The major drawback for such a approach is the allocation of memory on the GPU. By rule, the GPU cannot allocate memory dynamically, therefore all dynamically allocated memory has to be assigned in the CPU. This makes all these memories as global memory, which is the slowest. Also, sufficient memory has to be allocated for the calculation itself.

This research uses the GPU only for objective function calculation. The outline is given in Fig 7. A number of parameters have to be passed to the GPU as given in Table 1. These include three individual items; Machine size (*m*), Job size (*n*) and Population size (*p*). The population, problem data and calculation matrix also have to be passed to the GPU. The calculation matrix is required for the calculation of the makespan.

As most of the data is assigned as global memory, and only population size of 100 is used for all simulations, the kernels allocated are to only blocks. All internal memory allocation (loop indexes etc) have been allocated as shared memory. At the first initialization, all the data is

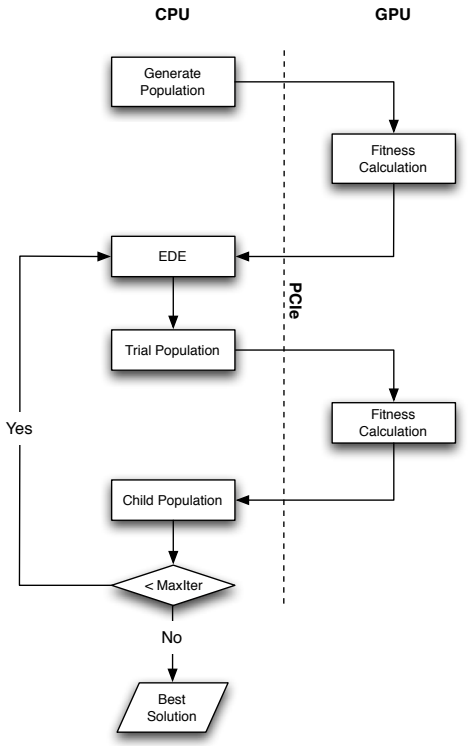

Figure 7: Conceptual outline.

Table 1: Parameters passed to the GPU

Parameters	**Type**	**Size**
Machine size (m)	int	sizeof (int)
Job size (n)	int	sizeof (int)
Population size (p)	int	sizeof (int)
Problem data	int	$(m \cdot n) \cdot$ sizeof (int)
Population	int	$(p \cdot n) \cdot$ sizeof (int)
Calculation matrix	int	$(p \cdot m) \cdot$ sizeof (int)
Objective function	int	$p \cdot$ sizeof (int)

passed to the GPU. After execution of the GPU, only the population and objective function matrix is returned to the CPU. Thereafter, within the generation loop, only the population and objective function matrix are passed to and from the GPU.

The experiment involves the embedding of the 2-opt local search on each trial solution. Therefore the complexity of this routine on each kernel is a minimum of $O\left(n^2\right)$.

5 EXPERIMENTATION

The main objective of this research is to validate the application of using a GPU for general purpose programming. In terms of performance measurement of any algorithm, the execution time is the key indicator, as all other measurement criteria are tied to it.

Table 2: Parameters passed to the GPU

Parameters	**Value**
Population	100
Generations	100
CR	0.9
F	0.5
Strategy	DE/best/2/bin

Table 3: Processing time for CUDA and CPU

Instance	**CUDA**	**CPU**	Δ_{avg}
20 x 5	**1.72**	26.84	1460.46
20 x 10	**2.53**	63.05	2392.09
20 x 20	**4.16**	111.85	2588.7
50 x 5	**19.87**	209.46	954.15
50 x 10	**28.87**	1483.19	5037.47
50 x 20	**50.20**	3483.48	6839.2
100 x 5	**151.31**	4600.52	2940.45
100 x 10	**246.75**	5988.96	2327.14
100 x 20	**387.26**	7545.46	1848.42
200 x 10	**2052.62**	15548.67	657.48
200 x 20	**3237.77**	25572.84	689.82
500 x 20	**8783.75**	44682.3	408.69
Average	**1247.56**	9109.69	2345.34

The experiment design was to apply the EDE code utilizing the local search on each fitness calculation, firstly on the CPU and then on the GPU and measure the time taken to complete the experimentation with fixed operating parameters.

The operating parameters for EDE is given in Table 2.

The operating system utilized for this experiment was a Nvidia Tesla C2050 graphics processing unit. It has 1 GPU core with 3072MB RAM memory, 575MHz core clock speed, version 2 of the CUDA core architecture and supports double precision. This hardware is part of the Media Research Lab (MRL) at the Technical University of Ostrava (MRL, 2012).

The experimentation results are given in Table 3. The average improvement Δ_{avg} of the GPU executed EDE over the CPU version is calculated as given in Equation 3.

$$\Delta_{avg} = \frac{(CPU - GPU) \times 100}{CPU} \tag{3}$$

From the results, it can be easily established that the CUDA based EDE is a faster executing algorithm, however the scale of improvement is quite substantial for medium and larger sized problems. For each problem set, there is a significant improvement for the GPU execution time. The total average improvement of the GPU is 2345.34 over the CPU. The average execution time is 1247.56 sec on the GPU compared to 9109.69 on the CPU. Therefore, we can conclude that the execution is

on a magnitude of eight times faster on the GPU. The results are displayed in Fig 8.

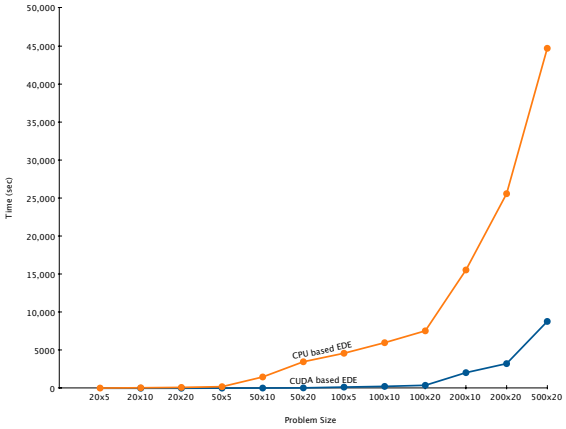

Figure 8: Graph of CUDA vs CPU processing time.

6 CONCLUSION

With the advent of faster processors, it becomes feasible to improve the structure of algorithms in order to harness this new power. With the application of GPGPU based applications gaining a foothold in computational analysis, this research aims to answer the question as to weather it is feasible to spend the necessary resources to convert algorithms to a GPU framework.

From the results obtained during this research, it is very clear that CUDA based EDE is a vast improvement over the CPU based variant in terms of execution time. The improvement is quite substantial, which in turn gives the scope of further optimization of the algorithm based on memory management.

The major fallibility of using the GPU is the time taken to transfer the data using the PCIe bus, which has a fixed bus speed. The next iteration of this research is the porting of the EDE routines to the GPU itself, thus minimizing the transfer time.

REFERENCES

Chen, S., Davis, S., Jiang, H., and Novobilski., A. (2011). Cuda-based genetic algorithm on traveling salesman problem. *Computer and Information Science*, 364:241–252.

Czapinski, M. and Barnes, S. (2011). Tabu search with two approaches to parallel flowshop evaluation on cuda platform. *Journal of Parallel and Distributed Computing*, 71:802–811.

Davendra, D. and Onwubolu, G. (2007). Flow shop scheduling using enhanced differential evolution. In *Proc.21 European Conference on Modeling and Simulation*, pages 259–264, Prague, Czech Rep.

Davendra, D. and Onwubolu, G. (2009). Forward/backward transformation approach. In Onwubolu, G. and D.Davendra, editors, *Differential Evolution: A Handbook for Global Permutation-Based Combinatorial Optimization*. Springer, Germany.

Kirk, D. and Hwu., W., editors (2010). *Programming Massively Parallel Processors: A Hands-on Approach*. Morgan Kaufmann., New York.

MRL (2012). Media research lab. `http://mrl.cs.vsb.cz/`.

Mussi, L., Daolio, F., and S.Cagnoni (2011). Evaluation of parallel particle swarm optimization algorithms within the cudatm architecture. *Information Sciences*, 181:4642 – 4657.

NVIDIA (2012). Cuda webpage. `http://www.nvidia.com/object/cuda$_-$home$_-$new.html`.

Pinedo, M. (1995). *Scheduling: theory, algorithms and systems*. Prentice Hall, New Jersey.

Pospichal, P., Jaros, J., and Schwarz, J. (2010). Parallel genetic algorithm on the cuda architecture. In et.al, D. C. C., editor, *Applications of Evolutionary Computation: Lecture Notes in Computer Science*. Springer, Germany.

Price, K. (1999). An introduction to differential evolution. In Corne, D., Dorigo, M., and Glover, F., editors, *New ideas in Optimisation*. McGraw Hill, UK.

Robilliard, D., Marion-Poty, V., and Fonlupt, C. (2009). Genetic programming on graphics processing units. *Genetic Programming and Evolvable Machines.*, 10:447 – 471.

Sanders, S. and E.Kandrot (2010). *CUDA by Example: An Introduction to General-Purpose GPU Programming*. Addison-Wesley Professional, USA.

AUTHOR BIOGRAPHIES

DONALD DAVENDRA is an Assistant Professor of Computing Science at the Technical University of Ostrava. He has a Ph.D. in Technical Cybernetics from the Tomas Bata University in Zlin. His email address is `donald.davendra@vsb.cz`.

JAN GAURA is an Assistant Professor of Computing Science at the Technical University of Ostrava with a research background is in digital image processing. His email address is `jan.gaura@vsb.cz`.

MAGDALENA BIALIC-DAVENDRA is a postdoctoral researcher at the Center of Applied Economic Research at the Tomas Bata University in Zlin from where she has a Ph.D. in Finance. Her email address is `bialic@fame.utb.cz`.

ROMAN SENKERIK is an Assistant Professor of Informatics at the Faculty of Applied Informatics, Tomas Bata University in Zlin. His email address is `senkerik@fai.utb.cz`.

DESIGNING PID CONTROLLER FOR DC MOTOR SYSTEM BY MEANS OF ENHANCED PSO ALGORITHM WITH DISCRETE CHAOTIC LOZI MAP

[1]Michal Pluhacek, [1]Roman Senkerik, [2]Donald Davendra, [1]Ivan Zelinka

[1]Tomas Bata University in Zlin , Faculty of Applied Informatics
Nam T.G. Masaryka 5555, 760 01 Zlin, Czech Republic
{pluhacek,senkerik,zelinka}@fai.utb.cz

[2]Department of Computer Science, Faculty of Electrical Engineering and Computer Science
VB-TUO, 17.listopadu 15, 708 33 Ostrava-Poruba, Czech Republic

KEYWORDS
PID controller, Optimization, Evolutionary Algorithms, PSO algorithm, Chaos, Lozi map.

ABSTRACT

The main aim of this paper is the utilization of discrete chaotic Lozi map based chaos number generator to enhance the performance of PSO algorithm. This paper presents the results of research, in whichchaos enhanced PSO algorithm is used to design an optimal PID controller for DC motor system. Obtained results are compared with other non-heuristic and heuristic methods.

INTRODUCTION

Optimization started to play a crucial partforalmost every engineering and informatics tasks during recentyears. Optimization problems often representvery complex tasks and non-heuristic methods are very limited in finding of the proper solutions. As the complexity of optimization problems increases, thenon-heuristic methods may not be able to solve them even in very distant future, whereasthe new heuristic methods can solve such tasks.Among these so called "soft-computing" methods belongevolutionary algorithms, which are inspired by evolution theory and natural behavior,and have helped to achieve very impressive results in solving various problems.
Recent study (Davendra et al., 2010) shows that chaos driven evolutionary algorithms might be very promising field of researchwithin evolutionary computation. The main principle is the utilization of chaos based number generator instead of a classic inbuilt computer randomness, which implementation may wary depending on used platform.

Particle swarm optimization algorithm

PSO (Particle swarm optimization algorithm)is the evolutionary optimization algorithm based on the natural behaviorof bird and fish swarms and was firstly introduced by R. EBERHART and J. KENNEDY in 1995 (Kennedy, Eberhart 1995, Eberhart, Kennedy2001). As an alternative to genetic algorithms (Goldbeg, David, 1989) and differential evolution (Storn, Price, 1997), PSO proved itself to be able to find better solutions for many optimization problems. Term "swarm intelligence" (Eberhart,Kennedy, 2001) refers to the capability of particle swarms to exhibit surprising intelligent behavior assuming that some form of communication (even very primitive) can occur among the swarm particles (individuals).
In each generation, a new location of a particle is calculated based on its previous location and velocity, where by velocity is understood "velocity vector" i.e. velocity for each dimension of the problem.
One of the disadvantages of basic PSO algorithm is the rapid acceleration of particles which causes them toabandon the defined area of interest. For this reason, several modifications of PSO were introduced to handle with this problem.
Within this research, chaos driven PSO strategy with inertia weight was used. Default values of all PSO parameters were chosen according to the recommendations given in (Kennedy, Eberhart 1995, Eberhart, Kennedy 2001). Inertia weight is designed to influence the velocity of each particle differently over the time (Nickabadi et al., 2011). In the beginning of the optimization process, the influence of inertia weight factor w is minimal. As the optimization continues, the value of $w$is decreasing, thus the velocity of each particle is decreasing, since w is the number < 1 and it multiplies previous velocity of particle in the process of new velocity value calculation. Inertia weight modification PSO strategy has two control parameters w_{start} and w_{end}. New w for each generation is then given by Eq. 1, where i stand for current generation number and n for total number of generations.

$$w = w_{start} - \frac{\left(\left(w_{start} - w_{end}\right) * i\right)}{n} \quad (1)$$

Chaos driven number generator is used in the main PSO formula (Eq. 2) that determines new "velocity"and thus the position of each particle in next generation (or migration cycle).

Proceedings 26th European Conference on Modelling and Simulation ©ECMS Klaus G. Troitzsch, Michael Möhring, Ulf Lotzmann (Editors)
ISBN: 978-0-9564944-4-3 / ISBN: 978-0-9564944-5-0 (CD)

$$v(t+1) = v(t) + c_1 \cdot Rand \cdot \left(pBest - x(t)\right) + c_2 \cdot Rand \cdot (gBest - x(t)) \quad (2)$$

Where:

v(t+1) – New velocity of particle.
v(t) – Current velocity of particle.
c1,c2 – Priority factors.
pBest – Best solution found by particle.
gBest – Best solution found in population.
x(t) – Current position of particle.
Rand – Random number, interval <0,1>. Within Chaos PSO basic inbuilt computer (simulation software) random generator is replaced with chaotic generator (in this case by using of Lozi map).

New position of particle is then given by Eq. 3, where x(t+1) is the new position:

$$x(t+1) = x(t) + v(t+1) \quad (3)$$

Lozi map

The Lozi map is a simple discrete two-dimensional chaotic map. The Lozi map is depicted in Figure 1. The map equations are given in Eq. 4 and 5.The parameters used in this work are:a = 1.7 and b = 0.5 as suggested in (Sprott 2003).

$$X_{n+1} = 1 - a\left|X_n\right| + bY_n \quad (4)$$

$$Y_{n+1} = X_n \quad (5)$$

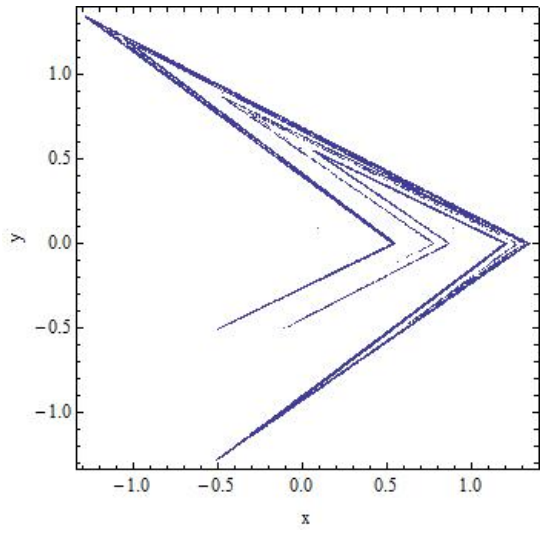

Figure 1: Lozi map

PROBLEM DESIGN

The PID controller contains three unique parts; proportional, integral and derivative controller (Astrom 2002). A simplified form in Laplace domain is given in Eq 6.

$$G(s) = K\left(1 + \frac{1}{sT_i} + sT_d\right) \quad (6)$$

The PID form most suitable for analytical calculations is given in Eq7.

$$G(s) = k_p + \frac{k_i}{s} + k_d s \quad (7)$$

The parameters are related to the standard form through: $k_p = K$, $k_i = K/T_i$ and $k_d = KT_d$. Acquisition of the combination of these three parameters that gives the lowest value of the test criterions was the objective of this research.

The transfer function of used DC motor is given by Eq. 8. [6,7]

$$G(s) = \frac{0.9}{0.00105s^3 + 0.2104s^2 + 0.8913s} \quad (8)$$

Cost function

Test criterion measures properties of output transfer function and can indicate quality of regulation. Following four different integral criterions were used for the test and comparison purposes: IAE (Integral Absolute Error), ITAE (Integral Time Absolute Error), ISE (Integral Square Error) and MSE (Mean Square Error). These test criterions (given by Eq. 9–12) were minimized within the cost functions for the enhanced PSO algorithm.

1. *Integral of Time multiplied by Absolute Error (ITAE)*

$$I_{ITAE} = \int_0^T t\left|e(t)\right|dt \quad (9)$$

2. *Integral of Absolute Magnitude of the Error (IAE)*

$$I_{IAE} = \int_0^T \left|e(t)\right|dt \quad (10)$$

3. *Integral of the Square of the Error (ISE)*

$$I_{ISE} = \int_0^T e^2(t)dt \quad (11)$$

4. *Mean of the Square of the Error (MSE)*

$$I_{MSE} = \frac{1}{n}\sum_{i=1}^{n}\left(e(t)\right)^2 \quad (12)$$

For further details see (Nagraj et al., 2008, Davendra et al., 2010).

RESULTS

All experiments were focused on the optimization of the four different specification functions as given in previous section. The best results of the optimization with corresponding values of k_p, k_i and k_d together with

selected response profile parameters are presented in Table 1.

When tuning a PID controller, generally the aim is to match some preconceived 'ideal' response profile for the closed loop system. The following response profiles are typical (Landau, 2006):

Overshoot: this is the magnitude by which the controlled 'variable swings' past the setpoint. 5 - 10% overshoot is normally acceptable for most loops.

Rise time: the time it takes for the process output to achieve the new desired value. One- third the dominant process time constant would be typical.

Settling time: the time it takes for the process output to die between, say +/- 5% of setpoint.

From the statistical reasons, optimization for each criterion was repeated 30 times. Results of the simple statistical comparison for the optimizations by means of chaos driven PSO algorithm are given in tables 2 and 3. Optimized system responses are depicted in Figures 2a - 2d and compared in Figure 3.

Table 1: The best results for DC motor system

Criterion	CF	Kp	Ki	Kd	Overshoot	Rise Time	Settling time
IAE	0.216732	247.484000	1.651430	58.458400	0.215909	0.010100	0.023300
ITAE	0.006667	271.207000	0.050058	63.790800	0.233985	0.009500	0.031500
ISE	0.018386	143.511000	30.512900	64.054000	0.223480	0.009500	0.032400
MSE	0.000919	146.339000	28.788700	64.040300	0.223686	0.009500	0.032400

Table 2: Average steady state responses for DC motor system

Criterion	Avg. overshoot	Avg. rise time	Avg. settling time
IAE	0.221803	0.009917	0.025920
ITAE	0.228235	0.009810	0.028243
ISE	0.223643	0.009507	0.032380
MSE	0.223739	0.009503	0.032387

Table 3: Statistical overview of the criterion (CF) values for DC motor system

Criterion	Max CF	Min CF	Avg. CF	Median	Std. dev.
IAE	0.307708	0.216732	0.234729	0.232278	0.017130022
ITAE	0.045092	0.006667	0.018588	0.017136	0.008908
ISE	0.018416	0.018386	0.018390	0.018386	0.000007
MSE	0.000920	0.000919	0.000919	0.000919	0

Results obtained for chaos PSO driven PID controller design are compared with previously published result (Nagraj et al., 2008) given by other heuristic and non-heuristic methods in table 4.

Table 4: Comparison of other methods and proposed enhanced PSO

Criterion	Z-N (step response)	Kappa-Tau	Continuous cycling	EP	GA	PSO	PSO Chaos
IAE	0.517600	0.518800	0.560000	0.489100	0.771200	0.916100	0.216732
ITAE	3.380500	3.311300	7.820000	0.072100	0.378100	0.022900	0.006667
ISE	2.346700	2.250300	3.200000	1.027700	1.043500	1.001600	0.018386
MSE	0.011700	0.077778	0.016000	0.005100	0.005200	0.005000	0.000919

Figure 2a

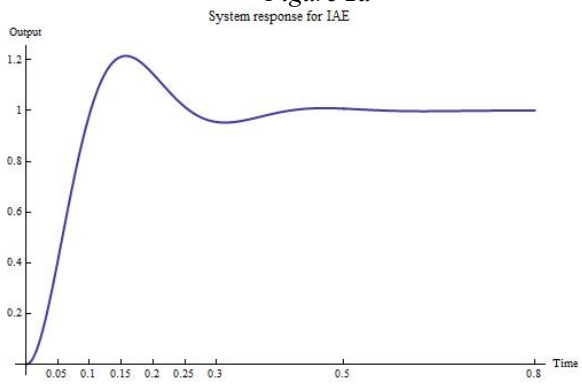

Figure 2b

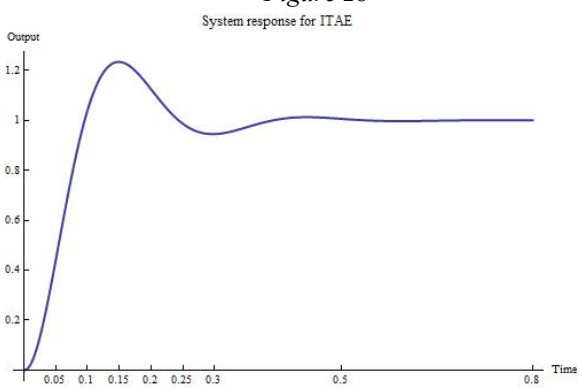

Figure 2c

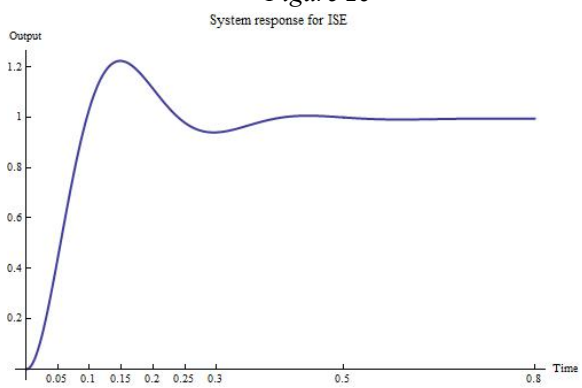

Figure 2d

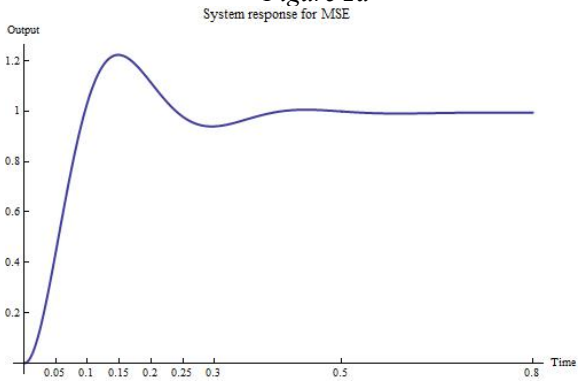

Figure 2: Optimized system responses for K_p, K_i and K_d obtained by four integral criterions.

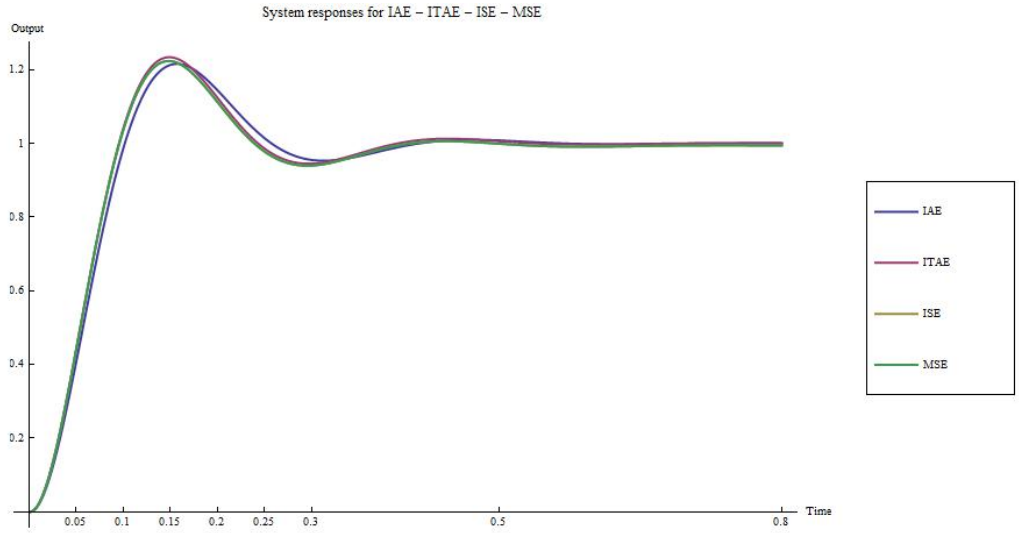

Figure 3: Comparison of optimized system responses for K_p, K_i and K_d obtained by four integral criterions.

CONCLUSION

This research was focused on the utilization of chaos driven PSO with discrete chaotic Lozi map for finding of the PID controller optimal settings for DC motor system.

Presented data and graphical simulation results lend weight to the argument that implementation of chaotic Lozi map as a random number generator into PSO algorithm may significantly improve its performance over other non-heuristic and heuristic methods in the case of solving the problem of optimal PID controller design for DC motor system.

Future research will be aimed to the possibilities of the development and improvement of the enhanced chaos driven PSO algorithm to achieve better results and explore more possible applications for this promising optimization approach.

ACKNOWLEDGEMENT

This work was supported by European Regional Development Fund under the project CEBIA-Tech No. CZ.1.05/2.1.00/03.0089, and by Internal Grant Agency of Tomas Bata University under the project No. IGA/FAI/2012/037.

REFERENCES

Astrom K., “Control System Design”.Santa Barbra, California: University of California, 2002

Davendra D., Zelinka I., Senkerik R., “Chaos driven evolutionary algorithms for the task of PID control”, Computers & Mathematics with Applications, Volume 60, Issue 4, 2010, pp 1088-1104, ISSN 0898-1221.

Dorigo, M., Ant Colony Optimization and Swarm Intelligence, Springer, 2006.

Eberhart, R., Kennedy, J., Swarm Intelligence, The Morgan Kaufmann Series in Artificial Intelligence, Morgan Kaufmann, 2001.

Goldberg, David E. (1989). Genetic Algorithms in Search Optimization and Machine Learning. Addison Wesley. p. 41.ISBN 0201157675.

Kennedy, J.; Eberhart, R. (1995). "Particle Swarm Optimization".Proceedings of IEEE International Conference on Neural Networks. IV. pp. 1942–1948

Landau Y., “Digital Control Systems”. Springer, London, 2006

Nagraj B., Subha S., and Rampriya B., “Tuning algorithms for pid controller using soft computing techniques”, International Journal of Computer Science and Network Security, 2008. 8, pp.278-281.3

Nickabadi A., Mohammad Mehdi Ebadzadeh, Reza Safabakhsh, A novel particle swarm optimization algorithm with adaptive inertia weight, Applied Soft Computing, Volume 11, Issue 4, June 2011, Pages 3658-3670, ISSN 1568-4946

Sprott J. C., “Chaos and Time-Series Analysis“, Oxford University Press, 2003

Storn R., Price K., Differential evolution—a simple and efficient heuristic for global optimization over continuous spaces, Journal of Global Optimization 11 (1997) 341–359.

AUTHOR BIOGRAPHIES

MICHAL PLUHACEK was born in the Czech Republic, and went to the Tomas Bata University in Zlin, where he studied Information Technologiesand obtained his MSc degree in 2011. He is now a doctoral student at the same university. His email address is:pluhacek@fai.utb.cz

ROMAN SENKERIK was born in the Czech Republic, and went to the Tomas Bata University in Zlin, where he studied Technical Cybernetics and obtained his MSc degree in 2004 and Ph.D. degree in Technical Cybernetics in 2008. He is now a lecturer at the same university (Applied Informatics, Cryptology, Artificial Intelligence, Mathematical Informatics). His email address is: senkerik@fai.utb.cz

IVAN ZELINKA was born in the Czech Republic, and went to the Technical University of Brno, where he studied Technical Cybernetics and obtained his degree in 1995. He obtained Ph.D. degree in Technical Cybernetics in 2001 at Tomas Bata University in Zlin. Now he is aprofessor (Artificial Intelligence, Theory of Information).Email address: ivan.zelinka@vsb.cz .

UTILIZATION OF ANALYTIC PROGRAMMING FOR THE STABILIZATION OF HIGH ORDER OSCILLATIONS OF CHAOTIC HÉNON MAP

[1]Zuzana Oplatkova, [1]Roman Senkerik, [2]Ivan Zelinka, [2]Donald Davendra

[1]Tomas Bata University in Zlin , Faculty of Applied Informatics
Nam T.G. Masaryka 5555, 760 01 Zlin, Czech Republic
{senkerik , oplatkova}@fai.utb.cz

[2]Department of Computer Science, Faculty of Electrical Engineering and Computer Science
VB-TUO, 17. listopadu 15, 708 33 Ostrava-Poruba, Czech Republic
{ivan.zelinka , donald.davendra}@vsb.cz

KEYWORDS
Chaos, Control, Hénon map, Evolutionary computation, Analytic programming, SOMA, Differential Evolution.

ABSTRACT

This research deals with a utilization of tool for symbolic regression, which is analytic programming, for the purpose of the synthesis of a new control law. This synthesized chaotic controller secures the stabilization of high periodic orbit – oscillations between several values of discrete chaotic system, which is Hénon map. The paper consists of the descriptions of analytic programming as well as chaotic system, used heuristic and cost function. For experimentation, Self-Organizing Migrating Algorithm (SOMA) and Differential evolution (DE) were used.

INTRODUCTION

During the past five years, usage of new intelligent systems in engineering, technology, modeling, computing and simulations has attracted the attention of researchers worldwide. The most current methods are mostly based on soft computing, which is a discipline tightly bound to computers, representing a set of methods of special algorithms, belonging to the artificial intelligence paradigm. The most popular of these methods are neural networks, evolutionary algorithms, fuzzy logic, and genetic programming. Presently, evolutionary algorithms are known as a powerful set of tools for almost any difficult and complex optimization problem.

The interest about the interconnection between evolutionary techniques and control of chaotic systems is spread daily. First steps were done in (Senkerik et al., 2006; 2010a), (Zelinka et al., 2009), where the control law was based on Pyragas method: Extended delay feedback control – ETDAS (Pyragas, 1995). These papers were concerned to tune several parameters inside the control technique for chaotic system. Compared to previous research, this paper shows a possibility how to generate the whole control law (not only to optimize several parameters) for the purpose of stabilization of a chaotic system. The synthesis of control is inspired by the Pyragas's delayed feedback control technique (Just, 1999), (Pyragas, 1992). Unlike the original OGY control method (Ott et al., 1990), it can be simply considered as a targeting and stabilizing algorithm together in one package (Kwon, 1999). Another big advantage of the Pyragas method for evolutionary computation is the amount of accessible control parameters, which can be easily tuned by means of evolutionary algorithms (EA).

Instead of EA utilization, analytic programming (AP) is used in this research. AP is a superstructure of EAs and is used for synthesis of analytic solution according to the required behaviour. Control law from the proposed system can be viewed as a symbolic structure, which can be synthesized according to the requirements for the stabilization of the chaotic system. The advantage is that it is not necessary to have some "preliminary" control law and to estimate its parameters only. This system will generate the whole structure of the law even with suitable parameter values.

This work is focused on the expansion of AP application for synthesis of a whole control law instead of parameters tuning for existing and commonly used method control law to stabilize desired Unstable Periodic Orbits (UPO) of chaotic systems.

This work is an extension of previous research (Oplatkova et al., 2010a; 2010b), (Senkerik et al., 2010b) focused on stabilization of simple p-1 orbit – stable state and p-2 orbit. In general, this research is concerned to stabilize p-4 UPO – high periodic orbit (oscillations between four values).

Firstly, AP is explained, and then a problem design is proposed. The next sections are focused on the description of used cost function and evolutionary algorithms. Results and conclusion follow afterwards.

PROBLEM DESIGN

The brief description of used chaotic systems and original feedback chaos control method, ETDAS is given. The ETDAS control technique was used in this research as an inspiration for synthesizing a new

Proceedings 26th European Conference on Modelling and Simulation ©ECMS Klaus G. Troitzsch, Michael Möhring, Ulf Lotzmann (Editors)
ISBN: 978-0-9564944-4-3 / ISBN: 978-0-9564944-5-0 (CD)

feedback control law by means of evolutionary techniques.

Selected chaotic system

The chosen example of chaotic system was the two dimensional Hénon map in form (1):

$$\begin{aligned} x_{n+1} &= a - x_n^2 + by_n \\ y_{n+1} &= x_n \end{aligned} \tag{1}$$

This is a model invented with a mathematical motivation to investigate chaos. The Hénon map is a discrete-time dynamical system, which was introduced as a simplified model of the Poincaré map for the Lorenz system. It is one of the most studied examples of dynamical systems that exhibit chaotic behavior. The map depends on two parameters, *a* and *b*, which for the canonical Hénon map have values of $a = 1.4$ and $b = 0.3$. For these canonical values the Hénon map is chaotic (Hilborn 2000). The example of this chaotic behavior can be clearly seen from bifurcation diagram – Figure 1.

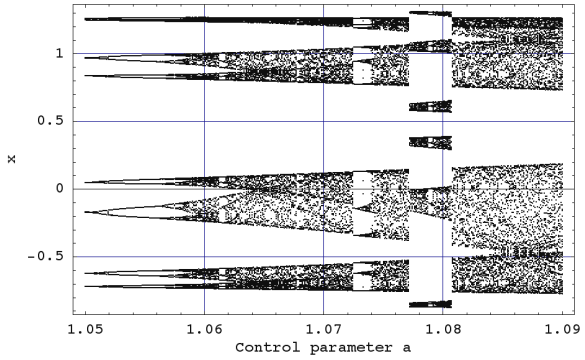

Figure 1: Bifurcation diagram of Hénon Map

Figure 1 shows the bifurcation diagram for the Hénon map created by plotting of a variable *x* as a function of the one control parameter for the fixed second parameter.

ETDAS control method

This work is focused on explanation of application of AP for synthesis of a whole control law instead of demanding tuning of EDTAS method control law to stabilize desired Unstable Periodic Orbits (UPO). In this research desired UPO is only p-2 (higher periodic orbit – oscillation between two values). ETDAS method was obviously an inspiration for preparation of sets of basic functions and operators for AP.

The original control method – ETDAS has form (2).

$$\begin{aligned} F(t) &= K\left[(1-R)S(t-\tau_d) - x(t)\right] \\ S(t) &= x(t) + RS(t-\tau_d) \end{aligned} \tag{2}$$

Where: *K* and *R* are adjustable constants, *F* is the perturbation; *S* is given by a delay equation utilizing previous states of the system and τ_d is a time delay.

The original control method – ETDAS in the discrete form suitable for two-dimensional Hénon map has the form (3).

$$\begin{aligned} x_{n+1} &= a - x_n^2 + by_n + F_n \\ F_n &= K\left[(1-R)S_{n-m} - x_n\right] \qquad (3) \\ S_n &= x_n + RS_{n-m} \qquad (3) \end{aligned}$$

Where: *m* is the period of *m*-periodic orbit to be stabilized. The perturbation F_n in equations (3) may have arbitrarily large value, which can cause diverging of the system outside the interval {0, 1.0}. Therefore, F_n should have a value between $-F_{\max}$, $F_{\max}$. In this preliminary study a suitable $F_{\max}$ value was taken from the previous research. To find the optimal value also for this parameter is in future plans.

Previous research concentrated on synthesis of control law only for p-1 orbit (a fixed point). An inspiration for preparation of sets of basic functions and operators for AP was simpler TDAS control method (4) and its discrete form suitable for logistic equation given in (5).

$$F(t) = K\left[x(t-\tau) - x(t)\right] \tag{4}$$

$$F_n = K\left(x_{n-m} - x_n\right) \tag{5}$$

ANALYTIC PROGRAMMING

Basic principles of the AP were developed in 2001 (Zelinka et al., 2005), (Zelinka et al., 2008), (Oplatkova et al., 2009). Until that time only genetic programming (GP) and grammatical evolution (GE) had existed. GP uses genetic algorithms while AP can be used with any evolutionary algorithm, independently on individual representation. To avoid any confusion, based on use of names according to the used algorithm, the name - Analytic Programming was chosen, since AP represents synthesis of analytical solution by means of evolutionary algorithms.

The core of AP is based on a special set of mathematical objects and operations. The set of mathematical objects is set of functions, operators and so-called terminals (as well as in GP), which are usually constants or independent variables. This set of variables is usually mixed together and consists of functions with different number of arguments. Because of a variability of the content of this set, it is called here "general functional set" – GFS. The structure of GFS is created by subsets of functions according to the number of their arguments. For example GFS_{all} is a set of all functions, operators and terminals, GFS_{3arg} is a subset containing functions with only three arguments, GFS_{0arg} represents only terminals, etc. The subset structure presence in GFS is vitally important for AP. It is used to avoid synthesis of pathological programs, i.e. programs containing functions without arguments, etc. The content of GFS is dependent only on the user. Various functions and terminals can be mixed together (Zelinka et al., 2005), (Zelinka et al., 2008), (Oplatkova et al., 2009).

The second part of the AP core is a sequence of mathematical operations, which are used for the program synthesis. These operations are used to transform an individual of a population into a suitable program. Mathematically stated, it is a mapping from an individual domain into a program domain. This mapping consists of two main parts. The first part is called discrete set handling (DSH) (See Figure 2) (Zelinka et al. 2005, Lampinen and Zelinka, 1999) and the second one stands for security procedures which do not allow synthesizing pathological programs. The method of DSH, when used, allows handling arbitrary objects including nonnumeric objects like linguistic terms {hot, cold, dark…}, logic terms (True, False) or other user defined functions. In the AP DSH is used to map an individual into GFS and together with security procedures creates the above mentioned mapping which transforms arbitrary individual into a program.

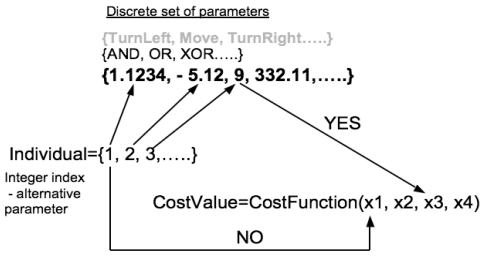

Figure 2: Discrete set handling

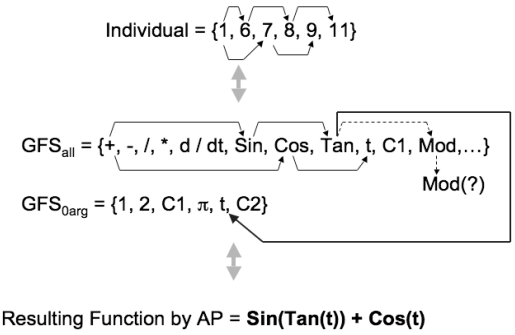

Figure 3: Main principles of AP

AP needs some evolutionary algorithm (Zelinka, 2004) that consists of population of individuals for its run. Individuals in the population consist of integer parameters, i.e. an individual is an integer index pointing into GFS. The creation of the program can be schematically observed in 3. The individual contains numbers which are indices into GFS. The detailed description is represented in (Zelinka et al., 2005), (Zelinka et al., 2008), (Oplatkova et al., 2009).

AP exists in 3 versions – basic without constant estimation, AP_{nf} – estimation by means of nonlinear fitting package in Mathematica environment and AP_{meta} – constant estimation by means of another evolutionary algorithms; meta means metaevolution.

COST FUNCTION

Proposal for the cost function comes from the simplest Cost Function (CF). The core of CF could be used only for the stabilization of p-1 orbit. The idea was to minimize the area created by the difference between the required state and the real system output on the whole simulation interval – τ_i.

But another universal cost function had to be used for stabilizing of higher periodic orbit and having the possibility of adding penalization rules. It was synthesized from the simple CF and other terms were added. In this case, it is not possible to use the simple rule of minimizing the area created by the difference between the required and actual state on the whole simulation interval – τ_i, due to many serious reasons, for example: degrading of the possible best solution by phase shift of periodic orbit.

This CF is in general based on searching for desired stabilized periodic orbit and thereafter calculation of the difference between desired and found actual periodic orbit on the short time interval - τ_s (40 iterations) from the point, where the first min. value of difference between desired and actual system output is found. Such a design of CF should secure the successful stabilization of either p-1 orbit (stable state) or higher periodic orbit anywise phase shifted. The CF_{Basic} has the form (6).

$$CF_{Basic} = pen_1 + \sum_{t=\tau 1}^{\tau 2} \left| TS_t - AS_t \right|, \tag{6}$$

where:
TS - target state, AS - actual state
τ_1 - the first min value of difference between TS and AS
τ_2 – the end of optimization interval ($\tau_1 + \tau_s$)
$pen_1 = 0$ if $\tau_i - \tau_2 \geq \tau_s$;
$pen_1 = 10*(\tau_i - \tau_2)$ if $\tau_i - \tau_2 < \tau_s$ (i.e. late stabilization).

USED EVOLUTIONARY ALGORITHMS

This research used two evolutionary algorithms: Self-Organizing Migrating Algorithm (Zelinka, 2004), Differential Evolution (Price, 2005). Future simulations expect a usage of soft computing GAHC algorithm (modification of HC12) (Matousek, 2007) and a CUDA implementation of HC12 algorithm (Matousek, 2010).

Self Organizing Migrating Algorithm - SOMA

Self Organizing Migrating Algorithm (SOMA) is a stochastic optimization algorithm that is modelled on the social behaviour of cooperating individuals (Zelinka, 2004). It was chosen because it has been proven that the algorithm has the ability to converge towards the global optimum (Zelinka, 2004). SOMA works on a population of candidate solutions in loops called *migration loops*. The population is initialized randomly distributed over the search space at the beginning of the search. In each loop, the population is evaluated and the solution with the highest fitness becomes the leader *L*. Apart from the leader, in one migration loop, all individuals will traverse the input

space in the direction of the leader. Mutation, the random perturbation of individuals, is an important operation for evolutionary strategies (ES). It ensures the diversity amongst the individuals and it also provides the means to restore lost information in a population. Mutation is different in SOMA compared with other ES strategies. SOMA uses a parameter called PRT to achieve perturbation. This parameter has the same effect for SOMA as mutation has for genetic algorithms.

The novelty of this approach is that the PRT Vector is created before an individual starts its journey over the search space. The PRT Vector defines the final movement of an active individual in search space.

The randomly generated binary perturbation vector controls the allowed dimensions for an individual. If an element of the perturbation vector is set to zero, then the individual is not allowed to change its position in the corresponding dimension.

An individual will travel a certain distance (called the PathLength) towards the leader in *n* steps of defined length. If the PathLength is chosen to be greater than one, then the individual will overshoot the leader. This path is perturbed randomly. The main principle is depicted in Figures 4 and 5.

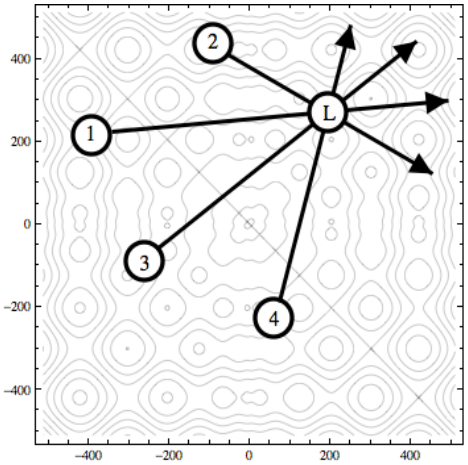

Figure 4: Principle of SOMA, movement in the direction towards the Leader

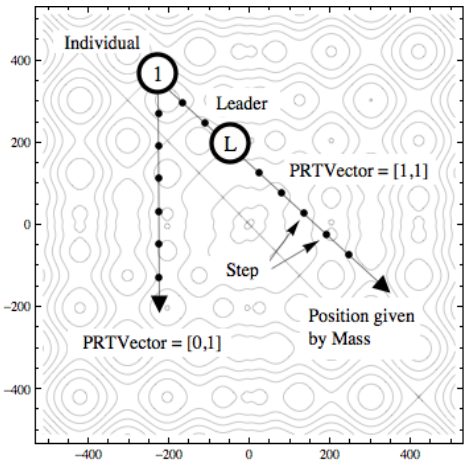

Figure 5: Basic principle of crossover in SOMA, PathLength is replaced here by Mass

Differential evolution

DE is a population-based optimization method that works on real-number-coded individuals (Price, 2005). For each individual $\vec{x}_{i,G}$ in the current generation G, DE generates a new trial individual $\vec{x}'_{i,G}$ by adding the weighted difference between two randomly selected individuals $\vec{x}_{r1,G}$ and $\vec{x}_{r2,G}$ to a randomly selected third individual $\vec{x}_{r3,G}$. The resulting individual $\vec{x}'_{i,G}$ is crossed-over with the original individual $\vec{x}_{i,G}$. The fitness of the resulting individual, referred to as a perturbed vector $\vec{u}_{i,G+1}$, is then compared with the fitness of $\vec{x}_{i,G}$. If the fitness of $\vec{u}_{i,G+1}$ is greater than the fitness of $\vec{x}_{i,G}$, then $\vec{x}_{i,G}$ is replaced with $\vec{u}_{i,G+1}$; otherwise, $\vec{x}_{i,G}$ remains in the population as $\vec{x}_{i,G+1}$. DE is quite robust, fast, and effective, with global optimization ability. It does not require the objective function to be differentiable, and it works well even with noisy and time-dependent objective functions. Description of used DERand1Bin strategy is presented in (7). Please refer to (Price and Storn 2001, Price 2005) for the description of all other strategies.

$$u_{i,G+1} = x_{r1,G} + F \bullet \left(x_{r2,G} - x_{r3,G}\right) \tag{7}$$

RESULTS

As described in section about Analytic Programming, AP requires some EA for its run. In this paper AP_{meta} version was used. Meta-evolutionary approach means usage of one main evolutionary algorithm for AP process and second algorithm for coefficient estimation, thus to find optimal values of constants in the evolutionary synthesized control law.

SOMA algorithm was used for main AP process and DE was used in the second evolutionary process. Settings of EA parameters for both processes were based on performed numerous experiments with chaotic systems and simulations with AP_{meta} (Table 1 and Table 2).

Table 1: SOMA settings for AP

PathLength	3
Step	0.11
PRT	0.1
PopSize	50
Migrations	4
Max. CF Evaluations (CFE)	5345

Table 2: DE settings for meta-evolution

PopSize	40
F	0.8
CR	0.8
Generations	150
Max. CF Evaluations (CFE)	6000

Compared to previous research with stabilization of stable state - p-1 orbit, the data set for AP required only constants, operators like plus, minus, power and output values x_n and x_{n-1}. Due to the recursive attributes of delay equation *S* utilizing previous states of the system in discrete ETDAS (3), the data set for AP had to be expanded and cover longer system output history, thus to imitate inspiring control method for the successful synthesis of control law securing the stabilization of higher periodic orbits.

Basic set of elementary functions for AP:
GFS2arg= +, -, /, *, ^
GFS0arg= $data_{n-11}$ to $data_n$, K

Total number of 30 simulations was carried out. The most simulations were successful and have given new synthesized control law, which was able to stabilize the system at required behaviour (p-4 orbit) within short simulation interval of 200 iterations.
Total number of cost function evaluations for AP was 5345, for the second EA it was 6000, together 32.07 millions per each simulation. See Table 3 for simple CF values statistic.

Table 3: Cost Function values

Min	0.0984
Max	1.0182
Average	0.6130

The novelty of this approach represents the synthesis of feedback control law $F_n(8)$ (perturbation) for the Hénon map inspired by original ETDAS control method.

$$x_{n+1} = a - x_n^2 + by_n + F_n \tag{8}$$

Following Table 4 contains examples of synthesized control laws. Obtained simulation results can be classified into 2 groups, based on the quality and durability of stabilization at real p-4 UPO, which for unperturbed Hénon map has following values: $x_1 = 0.139$, $x_2 = 1.4495$, $x_3 = -0.8595$, $x_4 = 0.8962$. More about this phenomenon is written in conclusion section.

Table 4 covers direct output from AP – synthesized control law without coefficients estimated, further the notation with simplification after estimation by means of second algorithm DE, corresponding CF value, average error between actual and required system output, and identification of figure with simulation results.

Table 4: Simulation results

Control Law	Control Law with coefficients	CF Value	Avg. output error	Figure
$F_n = -K_1 x_{n-8} x_{n-7} x_{n-3}(x_{n-4} - x_n)$	$F_n = -0.527409 x_{n-8} x_{n-7} x_{n-3}(x_{n-4} - x_n)$	0.0984	0.0025	6a
$F_n = \frac{x_{n-2} x_n}{K_1}$	$F_n = 0.011824 x_{n-2} x_n$	0.2230	0.0057	6b
$F_n = \frac{x_{n-5} x_n}{-x_{n-8} - x_{n-4} x_{n-2} + \frac{K_1(-K_3 x_n - K_2)}{\frac{x_{n-1}}{x_{n-3}} - x_{n-8}}}$	$F_n = \frac{x_{n-5} x_n}{-x_{n-8} - x_{n-4} x_{n-2} + \frac{85.45(-65.43 x_n - 58.56)}{\frac{x_{n-1}}{x_{n-3}} - x_{n-8}}}$	0.3052	0.0076	6c
$F_n = \frac{x_{n-7} x_{n-6}(K_2 + x_n)}{K_3 - \frac{x_{n-6}}{K_4}}$ $K_1 + \frac{x_n(K_6 - K_7 + K_8)}{x_{n-3}} - K_5 + x_{n-2}$	$F_n = \frac{x_{n-7} x_{n-6}(10.0667 + x_n)}{59.4863 + \frac{-0.0174 x_{n-6} - 52.191}{\frac{x_n 5.9706}{x_{n-3}} + 39.4742 + x_{n-2}}}$	0.7095	0.0177	6d

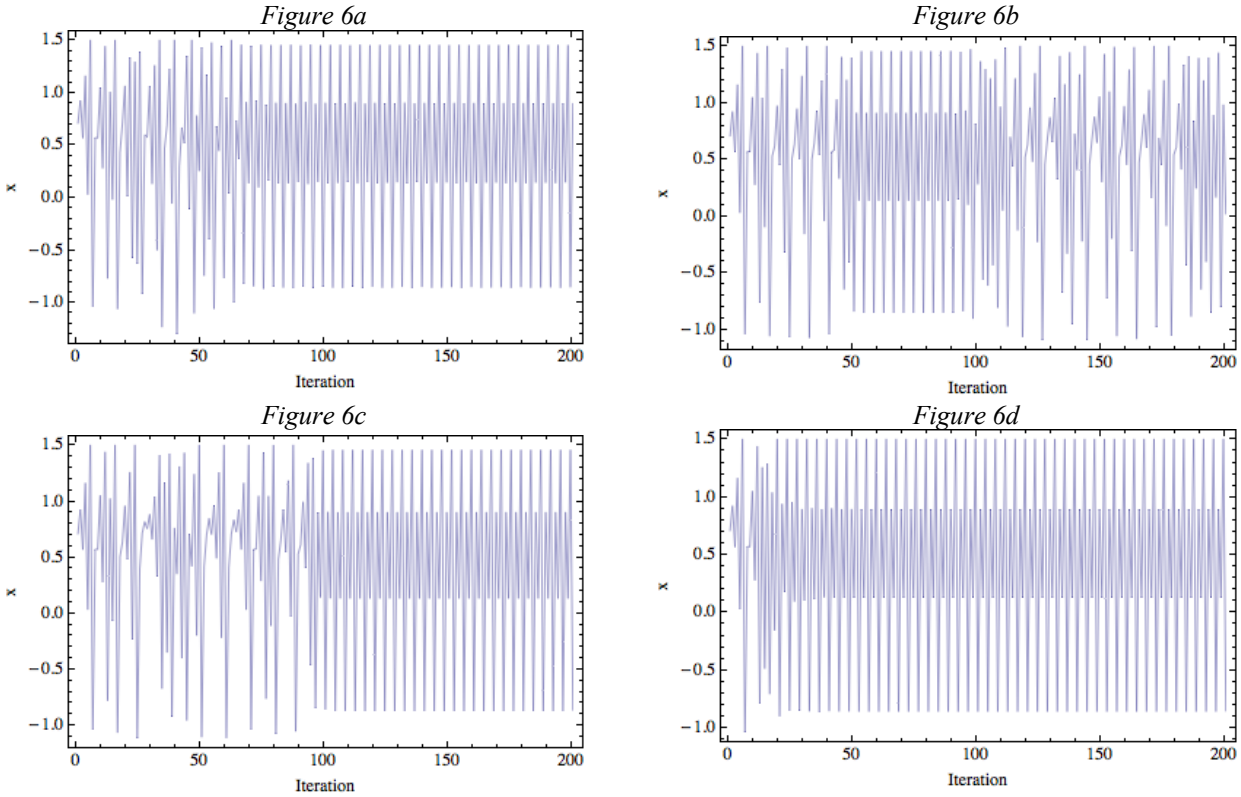

Figure 6: Examples of results – stabilization of p-4 orbit for Hénon map by means of control laws given in Table 4.

CONCLUSION

This paper deals with a synthesis of a control law by means of AP for stabilization of selected chaotic system at high periodic orbit. Hénon map as an example of two-dimensional discrete chaotic system was used in this research.

In this presented approach, the analytic programming was used instead of tuning of parameters for existing control technique by means of EA's as in the previous research.

Obtained results reinforce the argument that AP is able to solve this kind of difficult problems and to produce a new synthesized control law in a symbolic way securing desired behaviour of chaotic system and stabilization.

Presented four simulation examples show two different results. Low CF values indicating precise, but unfortunately slow stabilization and sometimes only temporary, together with simple control law in the first two cases. And according to the higher CF values not very precise, but very fast stabilization and relatively complex notation of chaotic controller in the next two cases. This phenomenon is caused by the design of CF, which was borrowed from the previous research focused on the simpler cases, which were stabilization of stable state and p-2 orbit, and it has given satisfactory results Nevertheless this fact lends weight to the argument, that AP is a powerful symbolic regression tool, which is able to strictly and precisely follow the rules given by cost function and synthesizes any symbolic formula, in the case of this research – the feedback controller for chaotic system. The question of energy costs and more precise and faster stabilization will be included into future research together with development of better cost functions, different AP data set, and performing of numerous simulations to obtain more results and produce better statistics, thus to confirm the robustness of this approach.

ACKNOWLEDGEMENT

This work was supported by the European Regional Development Fund under the project CEBIA-Tech No. CZ.1.05/2.1.00/03.0089 and project IT4Innovations Centre of Excellence No. CZ.1.05/1.1.00/02.0070.

REFERENCES

Hilborn R.C., 2000. Chaos and Nonlinear Dynamics: An Introduction for Scientists and Engineers, Oxford University Press, 2000, ISBN: 0-19-850723-2.

Just W., 1999, "Principles of Time Delayed Feedback Control", In: Schuster H.G., Handbook of Chaos Control, Wiley-Vch, ISBN 3-527-29436-8.

Kwon O. J., 1999. "Targeting and Stabilizing Chaotic Trajectories in the Standard Map", Physics Letters A. vol. 258, 1999, pp. 229-236.

Lampinen J., Zelinka I., 1999, "New Ideas in Optimization – Mechanical Engineering Design Optimization by Differential Evolution", Volume 1, London: McGraw-hill, 1999, 20 p., ISBN 007-709506-5.

Matousek R., 2007, „GAHC: Improved GA with HC station“, In WCECS 2007, San Francisco, pp. 915-920. ISBN: 978-988-98671-6-4.

Matousek R., 2010, „HC12: The Principle of CUDA Implementation“. In MENDEL 2010, Mendel Journal series, pp. 303-308. ISBN: 978-80-214-4120- 0. ISSN: 1803- 3814.

Oplatková, Z., Zelinka, I.: 2009. Investigation on Evolutionary Synthesis of Movement Commands, Modelling and Simulation in Engineering, Volume 2009 (2009), Article ID 845080, 12 pages, Hindawi Publishing Corporation, ISSN: 1687-559.

Oplatkova Z., Senkerik R., Zelinka I., Holoska J., 2010a, Synthesis of Control Law for Chaotic Henon System - Preliminary study, ECMS 2010, Kuala Lumpur, Malaysia, p. 277-282, ISBN 978-0-9564944-0-5.

Oplatkova Z., Senkerik R., Belaskova S., Zelinka I., 2010b, Synthesis of Control Rule for Synthesized Chaotic System by means of Evolutionary Techniques, Mendel 2010, Brno, Czech Republic, p. 91 - 98, ISBN 978-80-214-4120-0.

Ott E., C. Greboki, J.A. Yorke, 1990. “Controlling Chaos”, Phys. Rev. Lett. vol. 64, 1990, pp. 1196-1199.

Price, K. and Storn, R. (2001), *Differential evolution homepage*, [Online]: http://www.icsi.berkeley.edu/~storn/code.html, [Accessed 29/02/2012].

Price K., Storn R. M., Lampinen J. A., 2005, “Differential Evolution : A Practical Approach to Global Optimization”, (Natural Computing Series), Springer; 1 edition.

Pyragas K., 1992, “Continuous control of chaos by self-controlling feedback”, Physics Letters A, 170, 421-428.

Pyragas K., 1995. “Control of chaos via extended delay feedback”, Physics Letters A, vol. 206, 1995, pp. 323-330.

Senkerik R., Zelinka I., Navratil E., 2006, “Optimization of feedback control of chaos by evolutionary algorithms”, in proc 1st IFAC Conference on analysis and control of chaotic systems, Reims, France, pp. 97 - 102.

Senkerik R., Zelinka I., Davendra D., Oplatkova Z., 2010a, “Utilization of SOMA and differential evolution for robust stabilization of chaotic Logistic equation”, Computers & Mathematics with Applications, Volume 60, Issue 4, pp. 1026-1037.

Senkerik R., Oplatkova Z., Zelinka I., Davendra D.,Jasek R., 2010b, “Synthesis Of Feedback Controller For Chaotic Systems By Means Of Evolutionary Techniques,”, Proceeding of Fourth Global Conference on Power Control and Optimization, Sarawak, Borneo, 2010,.

Zelinka I., 2004. “SOMA – Self Organizing Migrating Algorithm”, In: *New Optimization Techniques in Engineering*, (B.V. Babu, G. Onwubolu (eds)), chapter 7, 33, Springer-Verlag, 2004, ISBN 3-540-20167X.

Zelinka I.,Oplatkova Z, Nolle L., 2005. *Boolean Symmetry Function Synthesis by Means of Arbitrary Evolutionary Algorithms-Comparative Study*, International Journal of Simulation Systems, Science and Technology, Volume 6, Number 9, August 2005, pages 44 - 56, ISSN: 1473-8031.

Zelinka I., Senkerik R., Navratil E., 2009, “Investigation on evolutionary optimization of chaos control”, Chaos, Solitons & Fractals, Volume 40, Issue 1, pp. 111-129.

Zelinka, I., Guanrong Ch., Celikovsky S., 2008. Chaos Synthesis by Means of Evolutionary algorithms, International Journal of Bifurcation and Chaos, Vol. 18, No. 4 (2008) 911–942

Modelling, Simulation and Control of Technological Processes

SIMULATION OF ADAPTIVE CONTROL OF A TUBULAR CHEMICAL REACTOR

Petr Dostál, Jiří Vojtěšek, and Vladimír Bobál
Tomas Bata University in Zlin
Department of Process Control, Centre of Polymer Systems
nam. T.G. Masaryka 5555,
760 01 Zlin, Czech Republic
{dostalp, bobal, vojtesek, babik}@fai.utb.cz

KEYWORDS

Tubular chemical reactor, Nonlinear model, External linear model, Parameter identification, Polynomial approach, Pole assignment.

ABSTRACT

The paper deals with continuous-time adaptive control of a tubular chemical reactor with the countercurrent cooling as a nonlinear single input – single output process. The nonlinear model of the reactor is approximated by an external linear model with parameters estimated via corresponding delta model. The control system structure with two feedback controllers is considered. The resulting controllers are derived using the polynomial approach. The method is tested on a mathematical model of the tubular chemical reactor.

INTRODUCTION

Tubular chemical reactor are units frequently used in chemical industry. From the system theory point of view, tubular chemical reactors belong to a class of nonlinear distributed parameter systems with mathematical models described by sets of nonlinear partial differential equations (NPDRs). The methods of modelling and simulation of such processes are described e.g. in (Luyben 1989), (Ingham et al. 1994) and (Dostál et al. 2008).

It is well known that the control of chemical reactors, and, tubular reactors especially, often represents very complex problem. The control problems are due to the process nonlinearity, its distributed nature, and high sensitivity of the state and output variables to input changes. Evidently, the process with such properties is hardly controllable by conventional control methods, and, its effective control requires application some of advanced methods.

One possible method to cope with this problem is using adaptive strategies based on an appropriate choice of a continuous-time external linear model (CT ELM) with recursively estimated parameters. These parameters are consequently used for parallel updating of controller‘s parameters. Some results obtained in this field were presented by authors of this paper e.g. in (Dostál et al. 2004).

For the CT ELM parameter estimation, either the direct method or application of an external delta model with the same structure as the CT model can be used, e.g. (Middleton and Goodwin 1990) or (Mukhopadhyay et al. 1992). Although delta models belong into discrete models, they do not have such disadvantageous properties connected with shortening of a sampling period as discrete *z*-models. In addition, parameters of delta models can directly be estimated from sampled signals. Moreover, it can be easily proved that these parameters converge to parameters of CT models for a sufficiently small sampling period (compared to the dynamics of the controlled process), as shown in (Stericker and Sinha 1993).

This paper deals with continuous-time adaptive control of a tubular chemical reactor with a countercurrent cooling. With respect to practical possibilities of a measurement and control, the mean reactant temperature temperature is chosen as the controlled output, and, the coolant flow rate as the control input. The nonlinear model of the reactor is approximated by a CT external linear model with a structure chosen on the basis of computed controlled output step responses. The control structure with two feedback controllers is considered, e.g. (Dostál et al. 2007). The resulting controllers are derived using the polynomial approach (Kučera 1993) and the pole assignment method, e.g. (Bobál et al. 2005). The method is tested on a mathematical model of a tubular chemical reactor.

MODEL OF THE REACTOR

An ideal plug-flow tubular chemical reactor with a simple exothermic consecutive reaction $A \xrightarrow{k_1} B \xrightarrow{k_2} C$ in the liquid phase and with the countercurrent cooling is considered. Heat losses and heat conduction along the metal walls of tubes are assumed to be negligible, but dynamics of the metal walls of tubes are significant. All densities, heat capacities, and heat transfer coefficients are assumed to be constant. Under above assumptions, the reactor model can be described by five PDRs in the form

$$\frac{\partial c_A}{\partial t} + v_r \frac{\partial c_A}{\partial z} = -k_1 c_A \tag{1}$$

$$\frac{\partial c_B}{\partial t} + v_r \frac{\partial c_B}{\partial z} = k_1 c_A - k_2 c_B \tag{2}$$

$$\frac{\partial T_r}{\partial t} + v_r \frac{\partial T_r}{\partial z} = \frac{Q_r}{(\rho c_p)_r} - \frac{4U_1}{d_1 (\rho c_p)_r}(T_r - T_w) \tag{3}$$

Proceedings 26th European Conference on Modelling and Simulation ©ECMS Klaus G. Troitzsch, Michael Möhring, Ulf Lotzmann (Editors)
ISBN: 978-0-9564944-4-3 / ISBN: 978-0-9564944-5-0 (CD)

$$\frac{\partial T_w}{\partial t} = \frac{4}{(d_2^2 - d_1^2)(\rho c_p)_w}\left[d_1 U_1 (T_r - T_w) + d_2 U_2 (T_c - T_w)\right] \quad (4)$$

$$\frac{\partial T_c}{\partial t} - v_c \frac{\partial T_c}{\partial z} = \frac{4 n_1 d_2 U_2}{(d_3^2 - n_1 d_2^2)(\rho c_p)_c}(T_w - T_c) \quad (5)$$

with initial conditions

$c_A(z,0) = c_A^s(z)$, $c_B(z,0) = c_B^s(z)$, $T_r(z,0) = T_r^s(z)$, $T_w(z,0) = T_w^s(z)$, $T_c(z,0) = T_c^s(z)$

and boundary conditions

$c_A(0,t) = c_{A0}(t)$ (kmol/m^3),

$c_B(0,t) = c_{B0}(t)$ (kmol/m^3), $T_r(0,t) = T_{r0}(t)$ (K),

$T_c(L,t) = T_{cL}(t)$ (K).

Here, t is the time, z is the axial space variable, c are concentrations, T are temperatures, v are fluid velocities, d are diameters, ρ are densities, c_p are specific heat capacities, U are heat transfer coefficients, n_1 is the number of tubes and L is the length of tubes. The subscript $(\cdot)_r$ stands for the reactant mixture, $(\cdot)_w$ for the metal walls of tubes, $(\cdot)_c$ for the coolant, and the superscript $(\cdot)^s$ for steady-state values.

The reaction rates and heat of reactions are nonlinear functions expressed as

$$k_j = k_{j0} \exp\left(\frac{-E_j}{R T_r}\right), \quad j = 1, 2 \quad (6)$$

$$Q_r = (-\Delta H_{r1}) k_1 c_A + (-\Delta H_{r2}) k_2 c_B \quad (7)$$

where k_0 are pre-exponential factors, E are activation energies, $(-\Delta H_r)$ are in the negative considered reaction entalpies, and R is the gas constant.

The fluid velocities are calculated via the reactant and coolant flow rates as

$$v_r = \frac{4 q_r}{\pi n_1 d_1^2}, \quad v_c = \frac{4 q_c}{\pi (d_3^2 - n_1 d_2^2)} \quad (8)$$

The parameter values with correspondent units used for simulations are given in Table 1.

Table 1. Used parameter values

L = 8 m	n_1 = 1200
d_1 = 0.02 m	d_2 = 0.024 m
d_3 = 1 m	
ρ_r = 985 kg/m^3	c_{pr} = 4.05 kJ/kg K
ρ_w = 7800 kg/m^3	c_{pw} = 0.71 kJ/kg K
ρ_c = 998 kg/m^3	c_{pc} = 4.18 kJ/kg K
U_1 = 2.8 kJ/m^{2}s K	U_2 = 2.56 kJ/m^{2}s K
k_{10} = 5.61·10^{16} 1/s	k_{20} = 1.128·10^{18} 1/s
E_1/R = 13477 K	E_2/R = 15290 K
(-ΔH_{r1}) = 5.8·10^4 kJ/kmol	(-ΔH_{r2}) = 1.8·10^4 kJ/kmol

From the system engineering point of view, $c_A(L,t) = c_{A\text{out}}$, $c_B(L,t) = c_{B\text{out}}$, $T_r(L,t) = T_{r\text{out}}$ and $T_c(0,t) = T_{c\text{out}}$ are the output variables, and, $q_r(t)$, $q_c(t)$, $c_{A0}(t)$, $T_{r0}(t)$ and $T_{cL}(t)$ are the input variables. Among them, for the control purposes, mostly the coolant flow rate can be taken into account as the control variable, whereas other inputs entering into the process can be accepted as disturbances. In this paper, the mean reactant temperature given by

$$T_m(t) = \frac{1}{L}\int_0^L T_r(z,t)\,dz \quad (9)$$

is considered as the controlled output.

COMPUTATION MODELS

For computation both steady-state and dynamic characteristics, the finite differences method is employed. The procedure is based on substitution of the space interval $z \in <0, L>$ by a set of discrete node points $\{z_i\}$ for i = 1, … , n , and, subsequently, by approximation of derivatives with respect to the space variable in each node point by finite differences.

Dynamic Model

Using the finite differences method, nonlinear PDEs (1) – (5) are approximated by a set of nonlinear ODEs in the form

$$\frac{dc_A(i)}{dt} = -\left[b_0 + k_1(i)\right] c_A(i) + b_0\, c_A(i-1) \quad (10)$$

$$\frac{dc_B(i)}{dt} = k_1(i)\, c_A(i) - \left[b_0 + k_2(i)\right] c_B(i) + b_0\, c_B(i-1) \quad (11)$$

$$\frac{dT_r(i)}{dt} = b_1 Q_r(i) - (b_0 + b_2)\, T_r(i) + b_0\, T_r(i-1) + b_2\, T_w(i) \quad (12)$$

$$\frac{dT_w(i)}{dt} = b_3\left[T_r(i) - T_w(i)\right] + b_4\left[T_c(i) - T_w(i)\right] \quad (13)$$

$$\frac{dT_c(m)}{dt} = -(b_5 + b_6)\, T_c(m) + b_5\, T_c(m+1) + b_6\, T_w(m) \quad (14)$$

for $i = 1, \ldots, n$ and $m = n - i + 1$, and, with initial conditions

$c_A(i,0) = c_A^s(i)$, $c_B(i,0) = c_B^s(i)$, $T_r(i,0) = T_r^s(i)$, $T_w(i,0) = T_w^s(i)$ and $T_c(i,0) = T_c^s(i)$ for $i = 1, \ldots, n$.

The boundary conditions enter into Eqs. (10) – (12) and (14) for $i = 1$.

Now, nonlinear functions in Eqs. (10) – (14) take the discrete form

$$k_j(i) = k_{j0} \exp\left(\frac{-E_j}{RT_r(i)}\right),\ j = 1, 2 \qquad (15)$$

$$Q_r(i) = (-\Delta H_{r1})\, k_1(i)\, c_A(i) + \\ + (-\Delta H_{r2})\, k_2(i)\, c_B(i) \qquad (16)$$

for $i = 1, \ldots, n$.

The parameters b in Eqs. (10) – (14) are calculated from formulas

$$b_0 = \frac{v_r}{h},\ b_1 = \frac{1}{(\rho c_p)_r},\ b_2 = \frac{4U_1}{d_1(\rho c_p)_r},$$
$$b_3 = \frac{4d_1U_1}{(d_2^2 - d_1^2)(\rho c_p)_w},\ b_4 = \frac{4d_2U_2}{(d_2^2 - d_1^2)(\rho c_p)_w} \qquad (17)$$
$$b_5 = \frac{v_c}{h},\ b_6 = \frac{4n_1 d_2 U_2}{(d_3^2 - n_1 d_2^2)(\rho c_p)_c}.$$

Here, the formula for computation of T_m takes the discrete form

$$T_m(t) = \frac{1}{n}\sum_{i=1}^{n} T_r(z_i, t) \qquad (18)$$

Steady-state Model

Computation of the steady-state characteristics is necessary not only for a steady-state analysis but the steady state values $y^s(i)$ also constitute initial conditions in ODRs (10) – (14) (here, y presents some of the variable in the set (10) – (14)).

The steady-state model can simply be derived equating the time derivatives in (10) – (14) to zero.

Steady-state and Dynamic Characteristics

Typical reactant temperature profiles along the reactor tubes computed for $c_{A0}^s = 2.85$, $c_{B0}^s = 0$, $T_{r0}^s = 323$, $T_{c0}^s = 293$ and $q_r^s = 0.15$ for various coolant flow rates are shown in Fig. 1. A presence of a maximum on the reactant temperature profiles is a common property of many tubular reactors with exothermic reactions.

A dependence of the reactant mean temperature on the coolant flow rate is shown in Fig. 2. The form of the curve documents a nonlinear relation between supposed controlled output and the coolant flow rate which is considered as the control input.

Dynamic charakteristics were computed in the neighbourhood of the chosen operating point $q_c^s = 0.27\ \mathrm{m^3/s}$, $T_m^s = 334.44\,\mathrm{K}$. For the dynamic analysis and subsequent control purposes, the controlled output is defined as a deviation from the steady value

$$y(t) = \Delta T_m(t) = T_m(t) - T_m^s. \qquad (19)$$

Such form is frequently used in the control. The deviation of the coolant flow rate is denoted as

$$\Delta q_c = q_c(t) - q_c^s. \qquad (20)$$

The responses of the output to the coolant flow rate step changes are shown in Fig. 3.

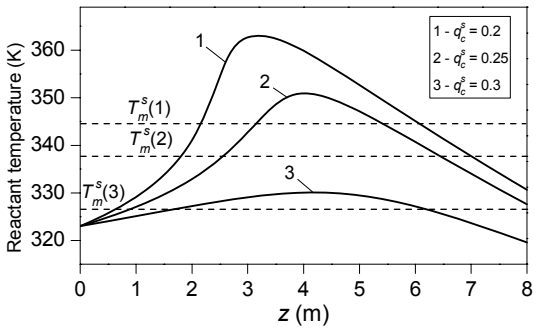

Fig. 1. Reactant temperature profiles for various coolant flow rates.

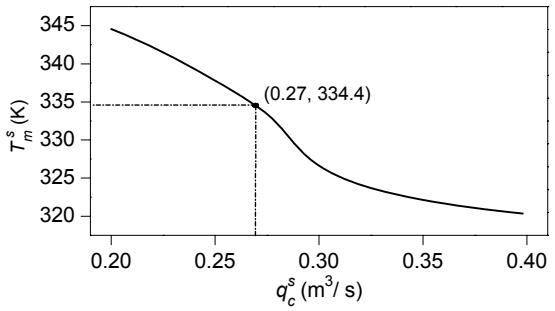

Fig. 2. Dependence of the reactant mean temperature on the coolant flow rates.

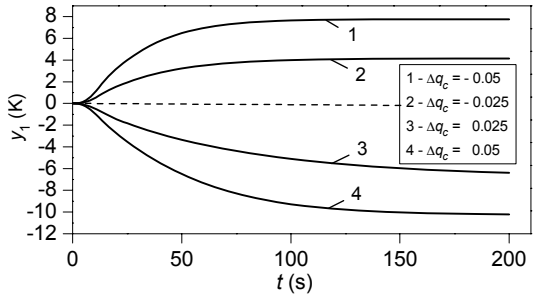

Fig. 3. Reactant mean temperature step responses.

The above shown responses document nonlinear behaviour of the reactant mean temperature.

CT AND DELTA ELM

For the control purposes, the control input variable are considered in the form

$$u(t) = 10\ \frac{q_c(t) - q_c^s}{q_c^s} \qquad (21)$$

This expression enables to obtain control input and controlled output variables of approximately the same magnitude.

A choice of the CT ELM structure does not stem from known structure of the model (1) – (5) but from a character of simulated step responses. It is well known that in adaptive control a controlled process of a higher

order can be approximated by a linear model of a lower order with variable parameters. Taking into account profiles of curves in Fig. 3 with zero derivatives in $t = 0$, the second order CT ELM has been chosen in the form of the second order linear differential equation

$$\ddot{y}(t) + a_1 \dot{y}(t) + a_0 y(t) = b_0 u(t) \tag{22}$$

and, in the complex domain, as the transfer function

$$G(s) = \frac{b_0}{s^2 + a_1 s + a_0} . \tag{23}$$

Establishing the δ operator

$$\delta = \frac{q-1}{T_0} \tag{24}$$

where q is the forward shift operator and T_0 is the sampling period, the delta ELM corresponding to (22) takes the form

$$\delta^2 y(t') + a_1' \delta y(t') + a_0' y(t') = b_0' u(t') \tag{25}$$

where t' is the discrete time. When the sampling period is shortened, the delta operator approaches the derivative operator, and, the estimated parameters a', b' reach the parameters a, b of the CT model (22).

DELTA MODEL PARAMETER ESTIMATION

Substituting $t' = k - 2$, equation (25) can be rewriten to the form

$$\delta^2 y(k-2) + a_1' \delta y(k-2) + a_0' y(k-2) = b_0' u(k-2) . \tag{26}$$

Establishing the regression vector

$$\boldsymbol{\Phi}_\delta^T(k-1) = \begin{pmatrix} -\delta y(k-2) & -y(k-2) & u(k-2) \end{pmatrix} \tag{27}$$

where

$$\delta y(k-2) = \frac{y(k-1) - y(k-2)}{T_0} \tag{28}$$

the vector of delta model parameters

$$\boldsymbol{\Theta}_\delta^T(k) = \begin{pmatrix} a_1' & a_0' & b_0' \end{pmatrix} \tag{29}$$

is recursively estimated using least squares method with exponential and directional forgetting (Bobál et al. 2005) from the ARX model

$$\delta^2 y(k-2) = \boldsymbol{\Theta}_\delta^T(k) \boldsymbol{\Phi}_\delta(k-1) + \varepsilon(k) \tag{30}$$

where

$$\delta^2 y(k-2) = \frac{y(k) - 2y(k-1) + y(k-2)}{T_0^2} \tag{31}$$

CONTROLLER DESIGN

The control system with two feedback controllers is depicted in Fig. 4.

In the scheme, w is the reference signal, v denotes the load disturbance, e the tracking error, u_0 output of controllers, u the control input and y the controlled output. The transfer function $G(s)$ of the CT ELM is given by (23).

The reference w and the disturbance v are considered as

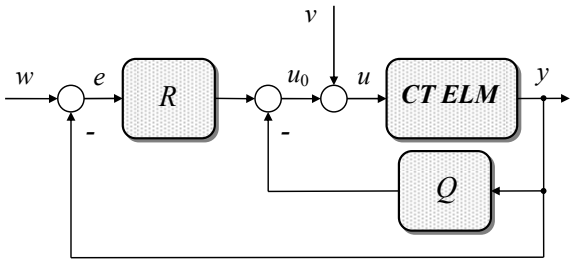

Fig. 4. Control system with two feedback controllers

the step functions with transforms

$$W(s) = \frac{w_0}{s} , \quad V(s) = \frac{v_0}{s} . \tag{32}$$

The transfer functions of both controllers are in forms

$$R(s) = \frac{r(s)}{\tilde{p}(s)} , \quad Q(s) = \frac{\tilde{q}(s)}{\tilde{p}(s)} \tag{33}$$

where $\tilde{q}$, r and $\tilde{p}$ are coprime polynomials in s fulfilling the condition of properness $\deg r \le \deg \tilde{p}$ and $\deg q \le \deg \tilde{p}$.

The controller design described in this section appears from the polynomial approach. The general requirements on the control system are formulated as its internal properness and stability, asymptotic tracking of the reference and load disturbance attenuation. The procedure to derive admissible controllers can briefly be performed as follows:

Let the polynomial t has the form

$$t(s) = r(s) + \tilde{q}(s) . \tag{34}$$

Then, the control system stability is ensured when polynomials $\tilde{p}$ and t are given by a solution of the polynomial equation

$$a(s)\tilde{p}(s) + b(s)t(s) = d(s) \tag{35}$$

with a stable polynomial d on the right side. Evidently, the roots of d determine the closed-loop poles.

Taking into account the transform of the tracking error

$$E(s) = \frac{1}{d}\left[(a\tilde{p} + b\tilde{q}) W(s) - b\tilde{p} V(s) \right] \tag{36}$$

and both transforms (32), the asymptotic tracking and load disturbance attenuation are provided by polynomials $\tilde{p}$ and $\tilde{q}$ having the form

$$\tilde{p}(s) = s\, p(s) , \quad \tilde{q}(s) = s\, q(s) . \tag{37}$$

Subsequently, the transfer functions (33) take forms

$$Q(s) = \frac{q(s)}{p(s)} , \quad R(s) = \frac{r(s)}{s\, p(s)} \tag{38}$$

and, a stable polynomial $p(s)$ in their denominators ensures the stability of controllers.

Now, the polynomial t can be rewritten to the form

$$t(s) = r(s) + s\, q(s) . \tag{39}$$

Taking into account the solvability of (35) and the

condition of internal properness, the degrees of polynomials in (35) and (38) can be easily derived as

$$\deg t = \deg r = \deg a\ ,\ \deg q = \deg a - 1\ ,$$
$$\deg p \geq \deg a - 1\ ,\ \ \deg d \geq 2\deg a\ . \qquad (40)$$

Denoting deg $a = n$, polynomials t, r and q have forms

$$t(s) = \sum_{i=0}^{n} t_i s^i\ ,\ r(s) = \sum_{i=0}^{n} r_i s^i\ ,\ q(s) = \sum_{i=1}^{n} q_i s^{i-1} \qquad (41)$$

and, relations among their coefficients are

$$r_0 = t_0\ ,\ \ r_i + q_i = t_i \ \text{ for } \ i = 1, \ldots, n\ . \qquad (42)$$

Since by a solution of the polynomial equation (35) provides calculation of coefficients t_i, unknown coefficients r_i and q_i can be obtained by a choice of selectable coefficients $\beta_i \in \langle 0,1 \rangle$ such that

$$r_i = \beta_i t_i\ ,\ \ q_i = (1-\beta_i) t_i \ \text{ for } \ i = 1, \ldots, n\ . \qquad (43)$$

The coefficients β_i distribute a weight between numerators of transfer functions Q and R.

Remark: If $\beta_i = 1$ for all i, the control system in Fig. 4 reduces to the 1DOF control configuration (Q = 0). If $\beta_i = 0$ for all i, and, both reference and load disturbance are step functions, the control system corresponds to the 2DOF control configuration.

For the second order model (23) with $\deg a = 2$, the controller's transfer functions take specific forms

$$Q(s) = \frac{q(s)}{p(s)} = \frac{q_2 s + q_1}{s + p_0}$$
$$R(s) = \frac{r(s)}{s\, p(s)} = \frac{r_2 s^2 + r_1 s + r_0}{s(s + p_0)} \qquad (44)$$

where

$$r_0 = t_0\ ,\ r_1 = \beta_1 t_1\ ,\ r_2 = \beta_2 t_2\ ,$$
$$q_1 = (1-\beta_1) t_1\ ,\ q_2 = (1-\beta_2) t_2\ . \qquad (45)$$

The controller parameters then result from a solution of the polynomial equation (35) and depend upon coefficients of the polynomial d. The next problem here is to find a stable polynomial d that enables to obtain acceptable stabilizing controllers.

In this paper, the polynomial d with roots determining the closed-loop poles is chosen as

$$d(s) = n(s)(s+\alpha)^2 \qquad (46)$$

where n is a stable polynomial obtained by spectral factorization

$$a^*(s)\, a(s) = n^*(s)\, n(s) \qquad (47)$$

and α is the selectable parameter.

Note that a choice of d in the form (46) provides the control of a good quality for aperiodic controlled processes.

The coefficients n then are expressed as

$$n_0 = \sqrt{a_0^2}\ ,\ \ n_1 = \sqrt{a_1^2 + 2n_0 - 2a_0} \qquad (48)$$

and, the controller parameters p_0 and t can be obtained from solution of the matrix equation

$$\begin{pmatrix} 1 & 0 & 0 & 0 \\ a_1 & b_0 & 0 & 0 \\ a_0 & 0 & b_0 & 0 \\ 0 & 0 & 0 & b_0 \end{pmatrix} \times \begin{pmatrix} p_0 \\ t_2 \\ t_1 \\ t_0 \end{pmatrix} = \begin{pmatrix} d_3 - a_1 \\ d_2 - a_0 \\ d_1 \\ d_0 \end{pmatrix} \qquad (49)$$

where

$$d_3 = n_1 + 2\alpha,\ d_2 = 2\alpha n_1 + n_0 + \alpha^2$$
$$d_1 = 2\alpha n_0 + \alpha^2 n_1,\ d_0 = \alpha^2 n_0 \qquad (50)$$

Now, it follows from the above introduced procedure that tuning of controllers can be performed by a suitable choice of selectable parameters β and α.

The controller parameters r and q can then be obtained from (45).

The adaptive control system is shown in Fig. 5.

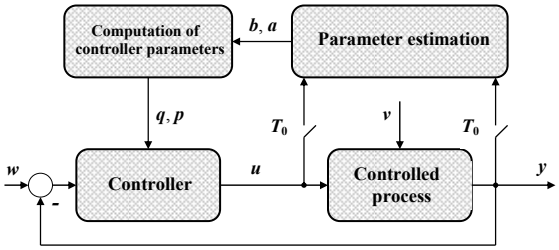

Fig. 5. Adaptive control scheme.

CONTROL SIMULATION

Also the control simulations were performed in a neighbourhood of the operating point $q_c^s = 0.27\ \mathrm{m}^3/\mathrm{s}$, $T_m^s = 334.44\ \mathrm{K}$,. For the start (the adaptation phase), the P controller with a small gain was used in all simulations.

The effect of the pole α on the controlled output responses is transparent from Fig. 6. Here, two values of α were selected. The control simulation shows sensitivity of the controlled output to α. The higher values of this parameter speed the control, however, they provide greater overshoots (undershoots). Other here not shown simulations demonstrated that a careless selection of the parameter α can lead to controlled output responses of a poor quality, to oscillations or even to the control instability. Moreover, an increasing α leads to higher values and changes of the control input as shown in Fig. 7. This fact can be important in control of real technological processes.

The controlled output y response for two values β_2 is shown in Fig. 8. It can be seen that an effect of this parameterer is insignificant.

The controlled output responses documenting an effect of the parameter β_1 are in Fig. 9. There, a higher value of β_1 results in greater overshoots (undershoots) of the controlled output.

Corresponding control input responses can be seen in Fig. 10. It can be seen that an increasing β_1 leads to greater values of inputs.

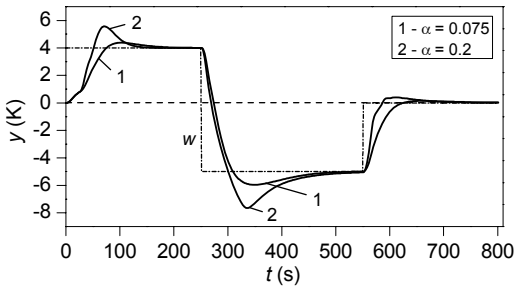

Fig. 6. Controlled output y_1 responses: effect of α ($\beta_1 = 1$, $\beta_2 = 0.5$).

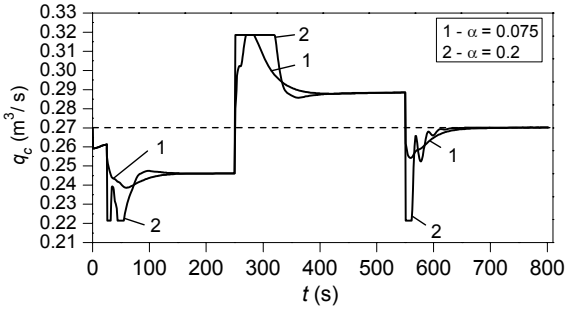

Fig. 7. Coolant flow rate responses in control of reactant mean temperature – effect of α ($\beta_1 = 1$, $\beta_2 = 0.5$).

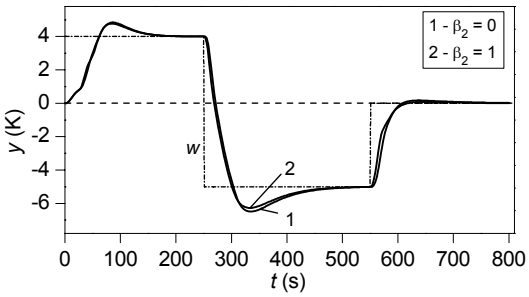

Fig. 8. Controlled output responses: effect of β_2 ($\alpha = 0.1$, $\beta_1 = 1$).

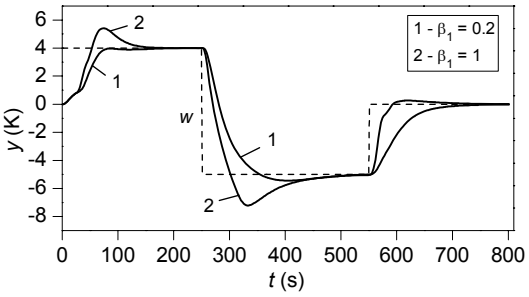

Fig. 9. Controlled output responses: effect of β_1 ($\alpha = 0.15$, $\beta_2 = 0$).

Of interest, the evolution of estimated CT ELM parameters in control of the reactant mean temperature is shown in Fig. 11.

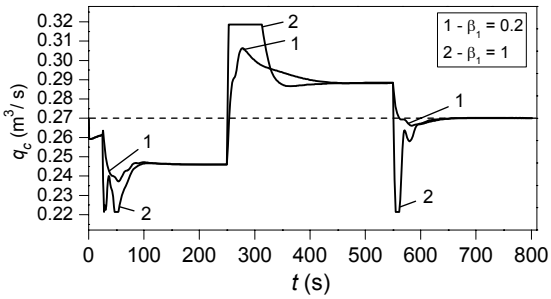

Fig. 10. Coolant flow rate responses in control of reactant mean temperature – effect of β_1 ($\alpha = 0.15$, $\beta_2 = 0$).

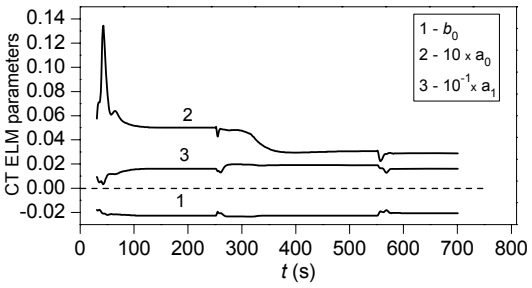

Fig. 11. CT ELM parameter evolution ($\alpha = 0.15$, $\beta_1 = 1$, $\beta_2 = 0$).

A presence of an integrating part in the controller enables rejection of various step disturbances entering into the process. As an example, step disturbances attenuation for the output y is presented. Step disturbances $\Delta c_{A0} = 0.15\,\mathrm{kmol/m^3}$, $\Delta q_r = -0.03\,\mathrm{m^3/s}$ and $\Delta T_{r0} = 2\,\mathrm{K}$ were injected into the nonlinear model of the reactor in times $t_v = 220\,\mathrm{s}$, $t_v = 440\,\mathrm{s}$ and $t_v = 640\,\mathrm{s}$. The controller parameters were estimated only in the first (tracking) interval $t < 200$ s. The authors' experiences proved that an utilization of recursive identification using the delta model after reaching of a constant reference and in presence of step disturbances decreases the control quality. From this reason, during interval $t \geq 200$ s, fixed parameters were used. The controlled output responses y are shown in Fig. 12.

To illustrate an effect of an additive random disturbance, the result of the controlled output y simulation in a presence of the random signal $v(t) = c_{A0}(t) - c_A^s$ is shown in Fig. 13.

CONCLUSIONS

In this paper, one approach to continuous-time adaptive control of the mean reactant temperatures in a tubular chemical reactor was proposed. The control strategy is based on the preliminary steady-state and dynamic analysis of the process and on the assumption of the temperature measurement along the reactor. The proposed algorithm employs an alternative continuous-time external linear model with parameters obtained

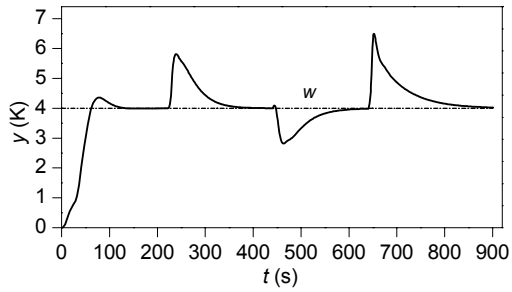

Fig. 12. Controlled output in presence of step disturbances ($\alpha = 0.15$, $\beta_1 = 0.5$, $\beta_2 = 0$).

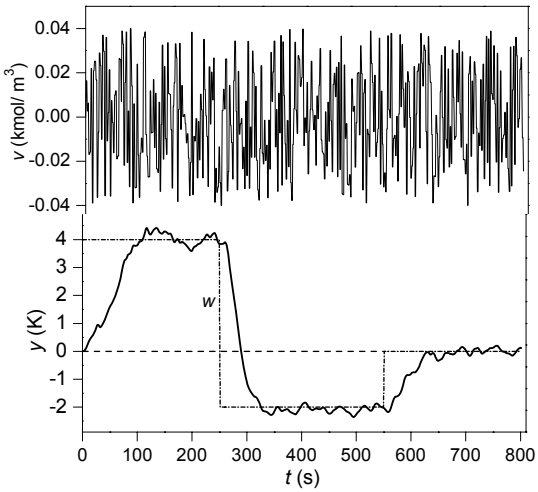

Fig. 13. Controlled output in the presence of random disturbance in c_{A0} ($\alpha = 0.15$).

through recursive parameter estimation of a corresponding delta model. The control system structure with two feedback controllers is considered. Resulting continuous-time controllers are derived using the polynomial approach and given by a solution of the polynomial equation. Tuning of their parameters is possible via closed-loop pole assignment. The presented method has been tested by computer simulation on the nonlinear model of the tubular chemical reactor with a consecutive exothermic reaction. The simulation results demonstrate an applicability of the presented control strategy.

ACKNOWLEDGMENT

This article was created with support of Operational Programme Research and Development for Innovations co-funded by the European Regional Development Fund (ERDF) and national budget of Czech Republic within the framework of the Centre of Polymer Systems project (reg.number: CZ.1.05/2.1.00/03.0111).

REFERENCES

Luyben, W. 1989. *Process modelling, simulation and control for chemical engineers*. McGraw-Hill, New York.

Ingham, J., I.J. Dunn, E. Heinzle, and J. E. Přenosil. 1994. *Chemical Engineering Dynamic: Modelling with PC Simulation*. VCH Verlagsgesellschaft, Weinheim.

Dostál, P., V. Bobál, and J. Vojtěšek. 2008. "Simulation of steady-state and dynamic behaviour of a tubular chemical reactor". In *Proc. 22nd European Conference on Modelling and Simulation*, Nicosia, Cyprus, 487-492.

Dostál, P., V. Bobál and F. Gazdoš, F. 2004. "Adaptive control of nonlinear processes: Continuous-time versus delta model parameter estimation". In *IFAC Workshop on Adaptation and Learning in Control and Signal Processing ALCOSP 04*, Yokohama, Japan, 273-278.

Middleton, R.H. and G.C. Goodwin. 1990. *Digital Control and Estimation - A Unified Approach*. Prentice Hall, Englewood Cliffs.

Mukhopadhyay, S., A.G. Patra and G.P. Rao. 1992. "New class of discrete-time models for continuos-time systems". *International Journal of Control*, 55**,** 1161-1187.

Stericker, D.L. and N.K. Sinha. 1993. "Identification of continuous-time systems from samples of input-output data using the δ-operator". *Control-Theory and Advanced Technology*, 9, 113-125.

Dostál, P., F. Gazdoš, V. Bobál and J. Vojtěšek. 2007. "Adaptive control of a continuous stirred tank reactor by two feedback controllers". In: *9th IFAC Workshop Adaptation and Learning in Control and Signal Processing ALCOSP'2007*, Saint Petersburg, Russia, P5-1 – P5-6.

Kučera, V. 1993. "Diophantine equations in control – A survey". *Automatica*, 29, 1361-1375.

Bobál, V., J. Böhm, J. Fessl, and J. Macháček. 2005. *Digital Self-tuning Controllers*. Springer Verlag, Berlin..

AUTHOR BIOGRAPHIES

PETR DOSTÁL studied at the Technical University of Pardubice, where he obtained his master degree in 1968 and PhD. degree in Technical Cybernetics in 1979. In the year 2000 he became professor in Process Control. He is now Professor in the Department of Process Control, Faculty of Applied Informatics of the Tomas Bata University in Zlín. His research interest are modeling and simulation of continuous-time chemical processes, polynomial methods, optimal and adaptive control.

JIŘÍ VOJTĚŠEK studied at the Tomas Bata University in Zlin, where he got his master degree in chemical and process engineering in 2002 and finished his Ph.D. in Technical Cybernetics in 2007. He works as a senior lecturer in the Department of Process Control, Faculty of Applied Informatics, Tomas Bata University in Zlin.

VLADIMÍR BOBÁL was born in Slavičín, Czech Republic. He graduated in 1966 from the Brno University of Technology. He received his Ph.D. degree in Technical Cybernetics at Institute of Technical Cybernetics, Slovak Academy of Sciences, Bratislava, Slovak Republic. He is now Professor in the Department of Process Control, Faculty of Applied Informatics of the Tomas Bata University in Zlín. His research interests are adaptive control systems, system identification and CAD for self-tuning controllers.

IDENTIFICATION AND DIGITAL CONTROL OF HIGHER-ORDER PROCESSES USING PREDICTIVE STRATEGY

Vladimír Bobál, Marek Kubalčík, Petr Chalupa and Petr Dostál
Tomas Bata University in Zlín
Faculty of Applied Informatics
Nad Stránění 4511
760 05 Zlín
Czech Republic
E-mail: bobal@fai.utb.cz

KEYWORDS
Higher-order processes, Time-delay systems, Digital control, Smith Predictor, Simulation,

ABSTRACT

In technical practice often occur higher order processes when a design of an optimal controller leads to complicated control algorithms. One of possibilities of control of such processes is their approximation by lower-order model with time-delay (dead time). The contribution is focused on a choice of a suitable experimental identification method and a suitable excitation input signals for an estimation of process model parameters with time-delay. The further contribution is design of an algorithm for digital control of high-order processes which are approximated by second-order model of the process with time-delay. The designed control algorithms are based on a predictive control strategy. The controller's algorithm uses the digital modification of the Smith Predictor (SP). The program system MATLAB/SIMULINK was used for simulation verification of these algorithms.

INTRODUCTION

Some technological processes in industry are characterized by high-order dynamic behaviour or large time constants and time-delays. For control engineering, such processes can often be approximated by the FOTD (first-order-time-delay) model. Time-delay in a process increases the difficulty of controlling it. However using the approximation of higher-order process by lower-order model with time-delay provides simplification of the control algorithms.
Let us consider a continuous-time dynamical linear SISO (single input $u(t)$ – single output $y(t)$) system with time-delay T_d. The transfer function of a pure transportation lag is $e^{-T_d s}$ where s is a complex variable. Overall transfer function with time-delay is in the form

$$G_d(s) = G(s)e^{-T_d s} \tag{1}$$

where $G(s)$ is the transfer function without time-delay.

Processes with time-delay are difficult to control using standard feedback controllers. When a high performance of the control process is desired or the relative time-delay is very large, a predictive control strategy must be used. The predictive control strategy includes a model of the process in the structure of the controller. The first time-delay compensation algorithm was proposed by (Smith 1957). This control algorithm known as the Smith Predictor (SP) contained a dynamic model of the time-delay process and it can be considered as the first model predictive algorithm.
Historically first modifications of time-delay algorithms were proposed for continuous-time (analogue) controllers. On the score of implementation problems, only the discrete versions are used in practice in this time.
The digital pole assignment SP was designed using a polynomial approach in (Bobál et al. 2011a). The design of this controller was extended by a method for a choice of a suitable pole assignment of the characteristic polynomial. The designed digital SP was verified by simulation control of the fifth-order system which was identified by a second-order model with time-delay.

IDENTIFICATION OF TIME-DELAY PROCESSES

In this paper, the time-delay is obtained separately from an off-line identification using the least squares method (LSM). The measured process output $y(k)$ is generally influenced by noise. These nonmeasurable disturbances cause errors $\boldsymbol{e}$ in the determination of model parameters and therefore real output vector is in the form

$$\boldsymbol{y} = \boldsymbol{F\Theta} + \boldsymbol{e} \tag{2}$$

It is possible to obtain the LSM expression for calculation of the vector of the parameter estimates

$$\hat{\boldsymbol{\Theta}} = \left(\boldsymbol{F}^T\boldsymbol{F}\right)^{-1}\boldsymbol{F}^T\boldsymbol{y} \tag{3}$$

The matrix $\boldsymbol{F}$ has dimension (N-n-d, 2n), the vector $\boldsymbol{y}$ (N-n-d) and the vector of parameter model estimates

Proceedings 26th European Conference on Modelling and Simulation ©ECMS Klaus G. Troitzsch, Michael Möhring, Ulf Lotzmann (Editors)
ISBN: 978-0-9564944-4-3 / ISBN: 978-0-9564944-5-0 (CD)

$\hat{\boldsymbol{\Theta}}(2n)$. N is the number of samples of measured input and output data, n is the model order.

Equation (3) serves for calculation of the vector of the parameter estimates $\hat{\boldsymbol{\Theta}}$ using N samples of measured input-output data. The individual vectors and matrices in Equations (2) and (3) have the form

$$\boldsymbol{F} = \begin{bmatrix} -y(n+d) & -y(n+d-1) & \cdots & -y(d+1) \\ -y(n+d+1) & -y(n+d) & \cdots & -y(d+2) \\ \vdots & \vdots & \cdots & \vdots \\ -y(N-1) & -y(N-2) & \cdots & -y(N-n) \end{bmatrix}$$

$$\begin{bmatrix} u(n) & u(n-1) & \cdots & u(1) \\ u(n+1) & u(n) & \cdots & u(2) \\ \vdots & \vdots & \cdots & \vdots \\ u(N-d-1) & u(N-d-2) & \cdots & u(N-d-n) \end{bmatrix} \tag{4}$$

$$\boldsymbol{y}^T = \begin{bmatrix} y(n+d+1) & y(n+d+2) & \cdots & y(N) \end{bmatrix} \tag{5}$$

$$\boldsymbol{e}^T = \begin{bmatrix} \hat{e}(n+d+1) & \hat{e}(n+d+2) & \cdots & \hat{e}(N) \end{bmatrix} \tag{6}$$

$$\hat{\boldsymbol{\Theta}}^T = \begin{bmatrix} \hat{a}_1 & \hat{a}_2 & \cdots & \hat{a}_n & \hat{b}_1 & \hat{b}_2 & \cdots & \hat{b}_n \end{bmatrix} \tag{7}$$

Most of higher-order industrial processes can be approximated by a model of reduced order with pure time-delay. Let us consider the following second order linear model with a time-delay

$$G_d\left(z^{-1}\right) = \frac{B\left(z^{-1}\right)}{A\left(z^{-1}\right)} z^{-d} = \frac{b_1 z^{-1} + b_2 z^{-2}}{1 + a_1 z^{-1} + a_2 z^{-2}} z^{-d} \tag{8}$$

The term z^{-d} represents the pure discrete time-delay. The time-delay is equal to dT_0 where T_0 is the sampling period.

Our experience proved that quality of system identification when the higher-order process is identified by the lower-order model is very dependent on the choice of an input excitation signal $u(k)$. The best results were achieved using a Random Gaussian Signal (RGS). The MATLAB code

```
u=idinput(N,'rgs',[0 B],[Umin, Umax])
```

generates an RGS of the length N, where [0 B] determines the frequency passband. Umin, Umax defines the minimum and maximum values of u. The signal level is such that Umin is the mean value of the signal, minus one standard deviation, while Umax is the mean value plus one standard deviation. Gaussian white noise with zero mean and variance one is thus obtained for levels [-1, 1], which are also the default values.

Consider that model (8) is the deterministic part of the stochastic process described by the ARX (regression) model

$$\begin{aligned} y(k) = &-a_1 y(k-1) - a_2 y(k-2) + \\ &+ b_1 y(k-1-d) + b_2 y(k-2-d) + e_s(k) \end{aligned} \tag{9}$$

where $e_s(k)$ is the random nonmeasurable component.

The vector of parameter model estimates is computed by solving equation (3)

$$\hat{\boldsymbol{\Theta}}^T(k) = \begin{bmatrix} \hat{a}_1 & \hat{a}_2 & \hat{b}_1 & \hat{b}_2 \end{bmatrix} \tag{10}$$

and is used for computation of the prediction output.

$$\begin{aligned} \hat{y}(k) = &-\hat{a}_1 y(k-1) - \hat{a}_2 y(k-2) + \\ &\hat{b}_1 u(k-1-d) + \hat{b}_2 u(k-2-d) \end{aligned} \tag{11}$$

The quality of identification can be considered according to error, i.e. the deviation

$$\hat{e}(k) = y(k) - \hat{y}(k) \tag{12}$$

In this paper, the error was used for suitable choice of the time-delay dT_0. The LSM algorithm (3) – (7) is computed for several time-delays dT_0 and the suitable time-delay is chosen according to quality of identification based on the prediction error (12).

Stable process

Consider the following fifth order linear system

$$G_A(s) = \frac{2}{(s+1)^5} = \frac{2}{s^5 + 5s^4 + 10s^3 + 10s^2 + 5s + 1} \tag{13}$$

System (13) was identified by discrete model (11) using off-line LSM (3) – (6) for different time-delay dT_0; $T_0 = 0.5\,\text{s}$. A criterion of the identification quality is based on sum of squares of error

$$J_{\hat{e}^2}(d) = \sum_{k=1}^{N} \hat{e}^2(k) \tag{14}$$

This criterion represents accuracy of process identification. From Fig. 1, it is obvious that value of the criterion (14) decreases when the number of time-delay steps d increases in the interval $d \in [0,4]$ (it is obvious, that criterion (14) has minimum for some higher d). This is caused by the fact that the increase of the number of time-delay steps in the above-mentioned interval improves estimation of the static gain

$$\hat{K}_g = \frac{\hat{b}_1 + \hat{b}_2}{1 + \hat{a}_1 + \hat{a}_2} \tag{15}$$

The difference between estimates of the static gain $\hat{K}_g$ of the discrete model (8) and the continuous-time

model (13) plays important role for the quality of identification because the identification time was relatively long (300 s) with regard to the response time (about 15 s).

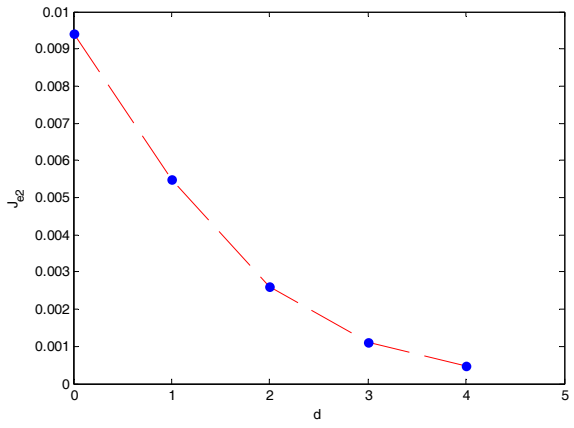

Figure 1: Criterion of Quality Identification for $d \in [0,4]$

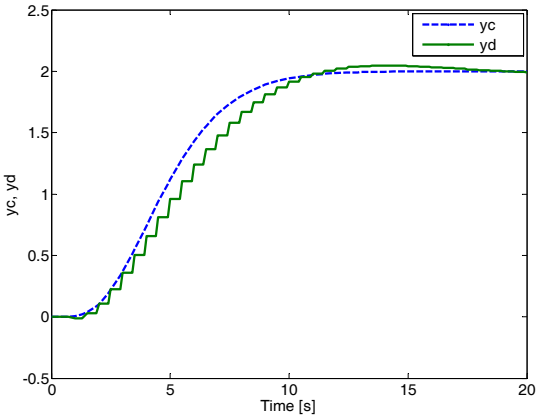

Figure 2: Comparison of step responses yc, yd for $d = 0$ (process (13))

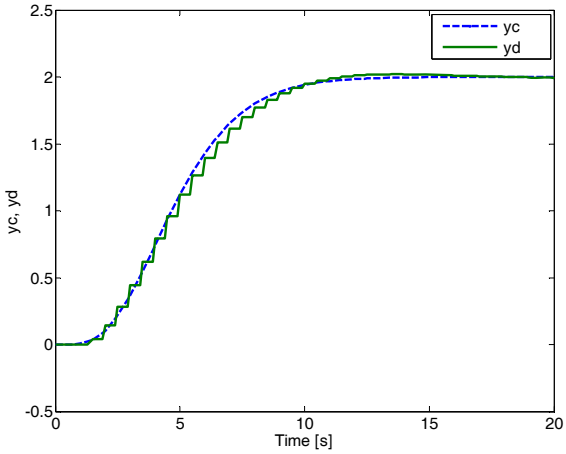

Figure 3: Comparison of step responses yc, yd for $d = 2$ (process (13))

$$G_A\left(z^{-1}\right) = \frac{0.0424z^{-1} + 0.0296z^{-2}}{1 - 1.6836z^{-1} + 0.7199z^{-2}} z^{-d} \qquad (16)$$

for sampling period $T_0 = 0.5$ s (16) with different d are shown in Figs. 2 – 4, where yc is the step response of the model (13) and yd are step responses of the discrete models (16) for individual numbers of time-delay steps d.

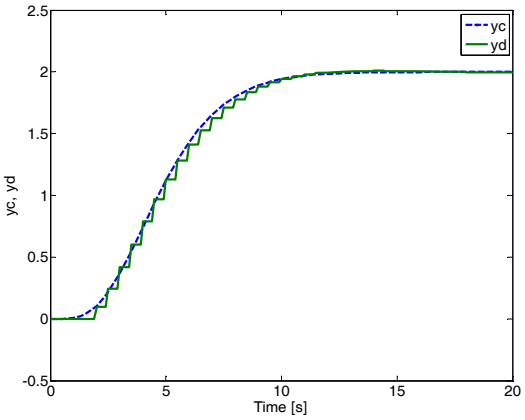

Figure 4: Comparison of step responses yc, yd for $d = 3$ (process (13))

From Figs. 2 – 4 it results that a suitable model (16) for the design of the predictive controller is the model with $d = 2$. Its structure is simple and it relatively well approximates the dynamic behaviour of the continuous-time model (13).

Non-minimum phase process

Consider the following fifth-order linear system with non-minimum phase

$$G_B(s) = \frac{2(1-5s)}{s^5 + 5s^4 + 10s^3 + 10s^2 + 5s + 1} \qquad (17)$$

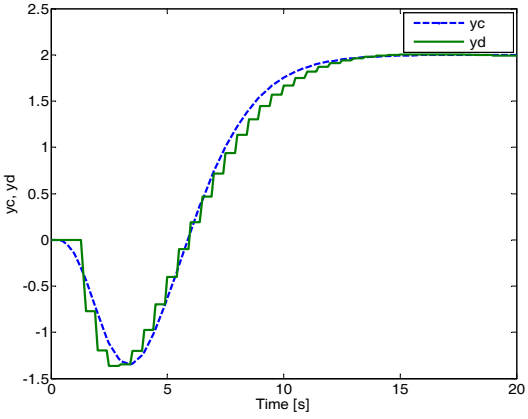

Figure 5: Comparison of step responses yc, yd for $d = 2$ (process (17))

Process (17) was identified by model (8) with a time-delay $d = 2$ and sampling period $T_0 = 0.5$ s . The discrete model is in the following form

$$G_B\left(z^{-1}\right) = \frac{-0.7723z^{-1} + 0.8514z^{-2}}{1 - 1.6521z^{-1} + 0.6920z^{-2}} z^{-2} \qquad (18)$$

The comparison of the step responses of the continuous-time model (17) and the discrete model (18) is shown in Fig. 5.

DIGITAL SMITH PREDICTOR

Although time-delay compensators appeared in the mid 1950s, their implementation with analogue technique was very difficult and these were not used in industry. Since 1980s digital time-delay compensators can be implemented. The digital time-delay compensators are presented e.g. in (Palmor and Halevi 1990, Normey-Rico and Camacho 1998). The discrete versions of the SP and its modifications are suitable for time-delay compensation in industrial practice.

Structure of Digital Smith Predictor

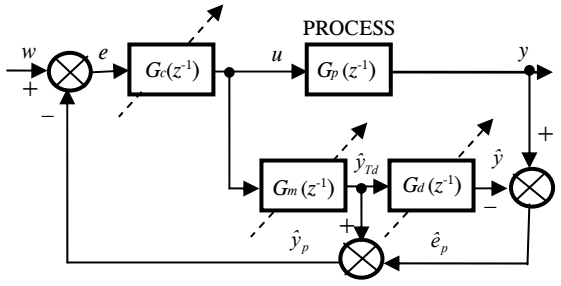

Figure 6: Block Diagram of a Digital Smith Predictor

The block diagram of a digital SP (see Hang et al. 1989, Hang et al. 1993) is shown in Fig. 6. The function of the digital version is similar to the classical analogue version. The block $G_m\left(z^{-1}\right)$ represents process dynamics without the time-delay and is used to compute an open-loop prediction. The difference between the output of the process y and the model including time-delay $\hat{y}$ is the predicted error $\hat{e}_p$ as shown is in Fig. 1 where u, w and e are the control signal, the reference signal and the error. If there are no modelling errors or disturbances, the error between the current process output and the model output will be null and the predictor output signal $\hat{y}_p$ will be the time-delay-free output of the process. Under these conditions, the controller $G_c\left(s\right)$ can be tuned, at least in the nominal case, as if the process had no time-delay. The primary (main) controller $G_c\left(z^{-1}\right)$ can be designed by the different approaches (for example digital PID control or methods based on algebraic approach). The outward feedback-loop through the block $G_d\left(z^{-1}\right)$ in Fig. 1 is used to compensate for load disturbances and modelling errors. The dash arrows indicate the tuned parts of the Smith Predictor.

Digital PID Smith Predictor

Hang *et al.* (1989, 1993) used the Dahlin PID algorithm (Dahlin 1968) for the design of the main controller $G_c\left(z^{-1}\right)$. This algorithm is based on the desired close-loop transfer function in the form

$$G_e\left(z^{-1}\right) = \frac{1 - e^{-\alpha}}{1 - z^{-1}}; \quad \alpha = \frac{T_0}{T_m} \qquad (19)$$

where T_m is a desired time constant of the first order closed-loop response. It is not practical to set T_m to be small since it will demand a large control signal $u(k)$ which may easily exceed the saturation limit of the actuator. Then the individual parts of the controller are described by the transfer functions

$$G_c\left(z^{-1}\right) = \frac{\left(1 - e^{-\alpha}\right)}{\left(1 - z^{-1}\right)} \frac{\hat{A}\left(z^{-1}\right)}{\hat{B}(1)}; \; G_m\left(z^{-1}\right) = \frac{z^{-1}\hat{B}(1)}{\hat{A}\left(z^{-1}\right)}$$

$$G_d\left(z^{-1}\right) = \frac{z^{-d}\hat{B}\left(z^{-1}\right)}{z^{-1}\hat{B}(1)} \qquad (20)$$

where $B(1) = \hat{B}\left(z^{-1}\right)\Big|_{z=1} = \hat{b}_1 + \hat{b}_2$.

Since $G_m\left(z^{-1}\right)$ is the second order transfer function, the main controller $G_c\left(z^{-1}\right)$ becomes a digital PID controller having the following form:

$$G_c\left(z^{-1}\right) = \frac{U(z)}{E(z)} = \frac{q_0 + q_1 z^{-1} + q_2 z^{-2}}{1 - z^{-1}} \qquad (21)$$

where $q_0 = \gamma, q_1 = \hat{a}_1\gamma, q_2 = \hat{a}_2\gamma$ using by the substitution $\gamma = \left(1 - e^{-\alpha}\right) / \hat{B}(1)$. The PID controller output is given by

$$u(k) = q_0 e(k) + q_1 e(k-1) + q_2 e(k-2) + u(k-1) \qquad (22)$$

Some simulation experiments using this digital SP are introduced in (Bobál et al. 2011).

Digital Pole Assignment Smith Predictor

The digital pole assignment SP was designed using a polynomial approach in (Bobál et al. 2011). Polynomial control theory is based on the apparatus and methods of linear algebra (see e.g. Kučera 1991, Kučera 1993). The design of the controller algorithm is based on the general block scheme of a closed-loop with two degrees of freedom (2DOF) according to Fig. 7.

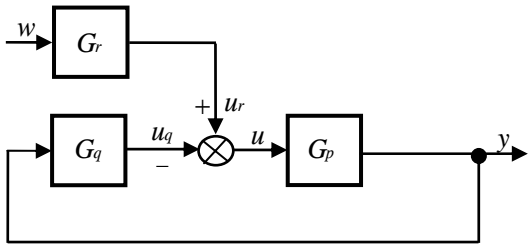

Figure 7: Block Diagram of a Closed Loop 2DOF Control System

The controlled process is given by the transfer function in the form

$$G_p(z^{-1}) = \frac{Y(z)}{U(z)} = \frac{B(z^{-1})}{A(z^{-1})} \tag{23}$$

where A and B are the second order polynomials. The controller contains the feedback part G_q and the feedforward part G_r. Then the digital controllers can be expressed in the form of discrete transfer functions

$$G_r\left(z^{-1}\right) = \frac{R\left(z^{-1}\right)}{P\left(z^{-1}\right)} = \frac{r_0}{1+p_1 z^{-1}} \tag{24}$$

$$G_q\left(z^{-1}\right) = \frac{Q\left(z^{-1}\right)}{P\left(z^{-1}\right)} = \frac{q_0+q_1 z^{-1}+q_2 z^{-2}}{\left(1+p_1 z^{-1}\right)\left(1-z^{-1}\right)} \tag{25}$$

According to the scheme presented in Fig. 7 and Equations (21) – (23) it is possible to derive the characteristic polynomial

$$A(z^{-1})P(z^{-1}) + B(z^{-1})Q(z^{-1}) = D(z^{-1}) \tag{26}$$

where

$$D\left(z^{-1}\right) = 1 + d_1 z^{-1} + d_2 z^{-2} + d_3 z^{-3} + d_4 z^{-4} \tag{27}$$

The feedback part of the controller is given by solution of the polynomial Diophantine equation (26). The procedure leading to determination of controller parameters in polynomials Q, R and P (24) and (25) is in (Bobál et al. 2005). The asymptotic tracking is provided by the feedforward part of the controller given by solution of the polynomial Diophantine equation

$$S(z^{-1})D_w\left(z^{-1}\right) + B(z^{-1})R(z^{-1}) = D(z^{-1}) \tag{28}$$

For a step-changing reference signal value $D_w\left(z^{-1}\right) = 1 - z^{-1}$ holds and S is an auxiliary polynomial which does not enter into controller design. For a step-changing reference signal value it is possible to solve Equation (27) by substituting $z = 1$

$$R\left(z^{-1}\right) = r_0 = \frac{D(1)}{B(1)} = \frac{1+d_1+d_2+d_3+d_4}{b_1+b_2} \tag{29}$$

The 2DOF controller output is given by

$$\begin{aligned} u(k) = {} & r_0 w(k) - q_0 y(k) - q_1 y(k-1) - q_2 y(k-2) + \\ & + (1+p_1)u(k-1) + p_1 u(k-2) \end{aligned} \tag{30}$$

The control quality is very dependent on the pole assignment of the characteristic polynomial

$$D(z) = z^4 + d_1 z^3 + d_2 z^2 + d_3 z + d_4 \tag{31}$$

inside the unit circle. The simple method for choice of individual poles is based on the following approach. Consider 1DOF control loop where controlled process (23) with second-order polynomials A and B is controlled using PID controller which is given by transfer function

$$G_q\left(z^{-1}\right) = \frac{Q\left(z^{-1}\right)}{P\left(z^{-1}\right)} = \frac{q_0\left(1+a_1 z^{-1}+a_2 z^{-2}\right)}{\left(1-z^{-1}\right)} \tag{32}$$

Substitution of polynomials A, B, Q, P into Equation (26) yields the following relation

$$\begin{aligned} & \hat{A}(z^{-1})\left(1-z^{-1}\right) + \hat{B}(z^{-1})q_0\hat{A}(z^{-1}) = \\ & = \hat{A}(z^{-1})\left[\left(1-z^{-1}\right) + \hat{B}(z^{-1})q_0\right] = D(z^{-1}) \end{aligned} \tag{33}$$

where

$$\hat{A}\left(z^{-1}\right) = 1 + \hat{a}_1 z^{-1} + \hat{a}_2 z^{-2}; \quad \hat{B}\left(z^{-1}\right) = \hat{b}_1 z^{-1} + \hat{b}_2 z^{-2} \tag{34}$$

are polynomials with model parameter estimates.
From Equation (33) it is obvious that polynomial $A(z) = z^2 + a_1 z + a_2$ is included in polynomial $D(z)$ (31). Its parameter estimates are known from process identification. The second two poles are dependent on the parameter (see expressions (19, 20))

$$q_0 = \frac{\left(1-e^{-\alpha}\right)}{\hat{b}_1+\hat{b}_2}; \quad \alpha = \frac{T_0}{T_m} \tag{35}$$

which is function of time constant T_m (free setting parameter of the controller). By increasing T_m, the control response is slower (respective without overshoot).

SIMULATION VERIFICATION DIGITAL SP CONTROLLER ALGORITHM

As simulation examples of digital SP controller algorithm, the processes (13) and (17) were chosen. By the identification procedure, the discrete models (16) and (18) for sampling period $T_0 = 0.5$ s were obtained.

A simulation verification of the designed controller was performed in MATLAB/SIMULINK environment. A typical used control scheme is depicted in Fig. 8.

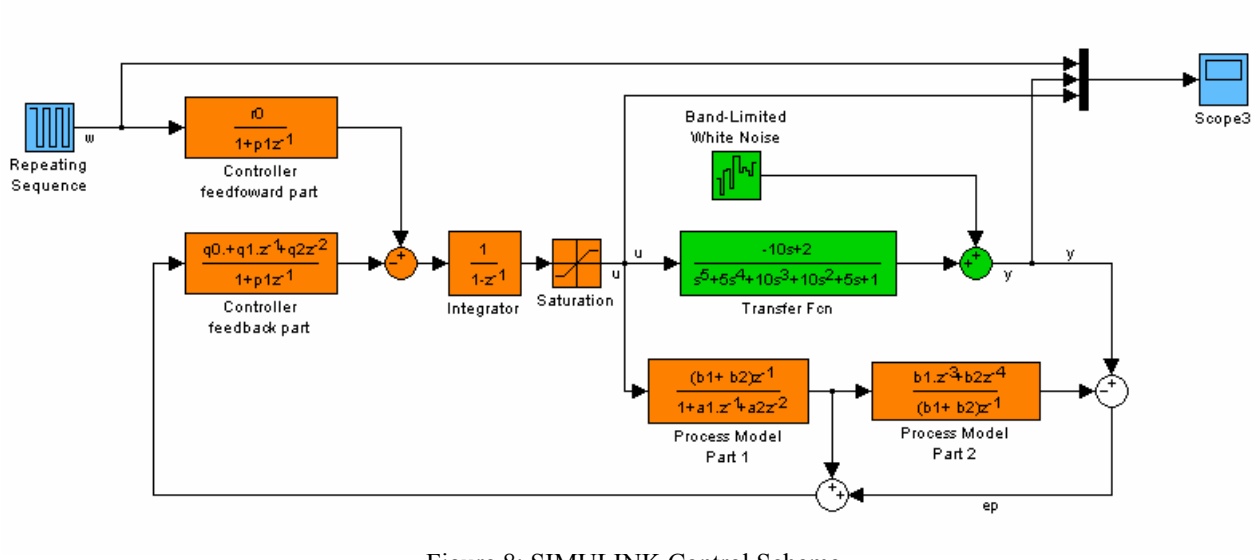

Figure 8: SIMULINK Control Scheme

Control of stable process (13)

1. Simulation conditions:
Time constant $T_m = 1.5$, characteristic polynomial

$$D_{A1}(z) = z^4 - 2.5167z^3 + 2.2390z^2 - 0.7959z + 0.0839$$

Simulation control results of the model $G_A(s)$ with $T_m = 1.5$ are shown in Figs. 9 and 10.

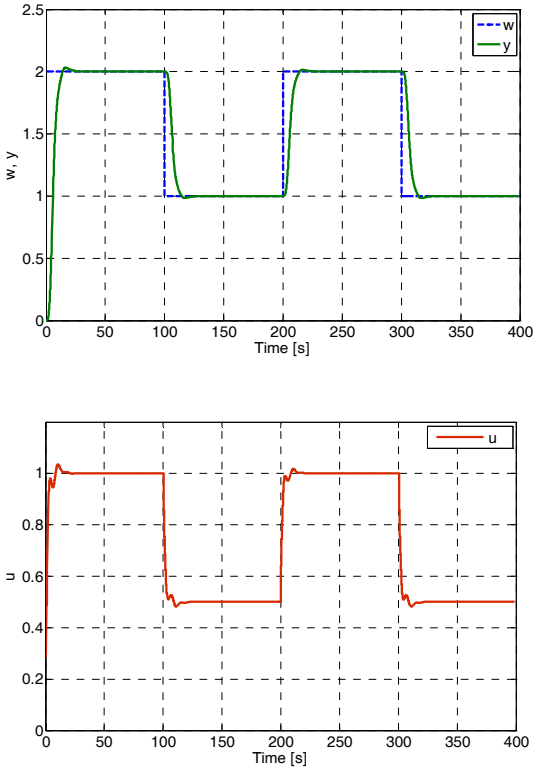

Figure: 9 Control of the Model $G_A(s)$; $T_m = 1.5$

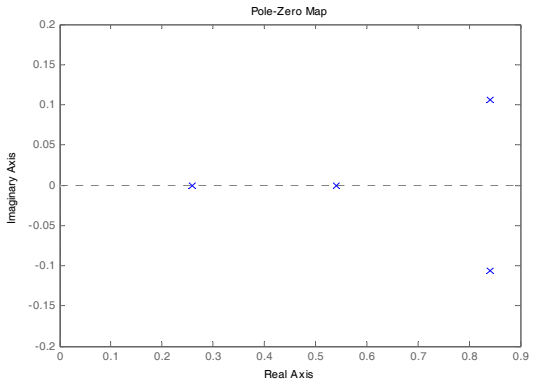

Figure: 10 Pole Map of the Polynomial D_{A1}

2. Simulation conditions:
Time constant $T_m = 3$, characteristic polynomial

$$D_{A2}(z) = z^4 - 2.5932z^3 + 2.3144z^2 - 0.7611z + 0.0454$$

Simulation control results of the model $G_A(s)$ with $T_m = 3$ are shown in Figs. 11 and 12.

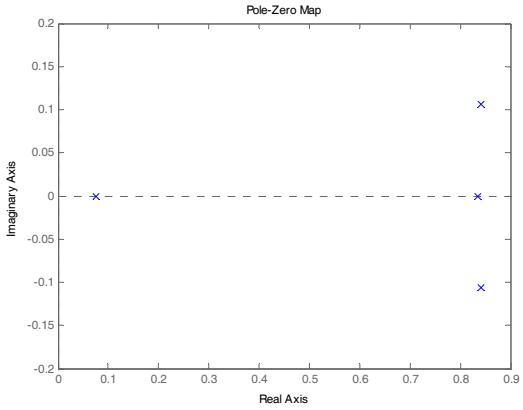

Figure: 11 Pole Map of the Polynomial D_{A2}

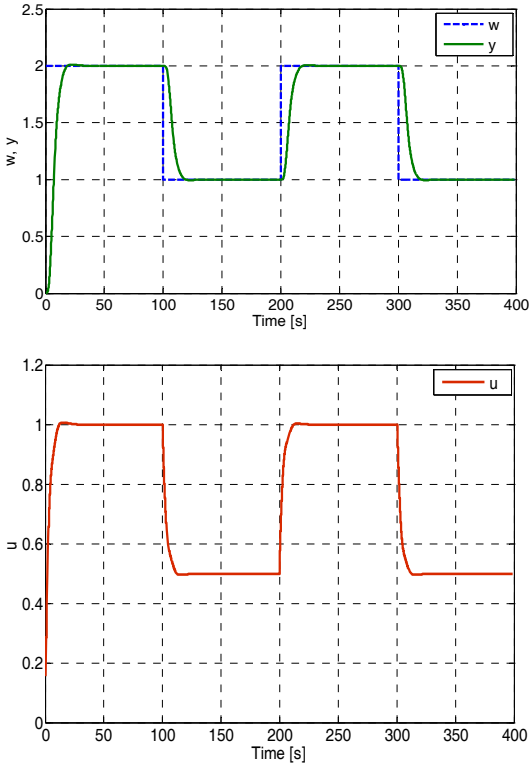

Figure: 12 Control of the Model $G_A(s)$; $T_m = 3$

Control of non-minimum phase process (17)

Simulation conditions:
Time constant $T_m = 7$, characteristic polynomial

$$D_B(z) = z^4 - 3.3252z^3 + 4.1981z^2 - 2.3836z + 0.5135$$

Simulation control results of the model $G_B(s)$ with $T_m = 7$ are shown in Figs. 13 and 14.

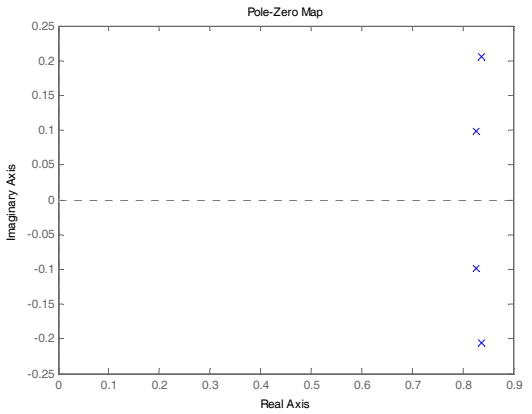

Figure: 13 Pole Map of the Polynomial D_B

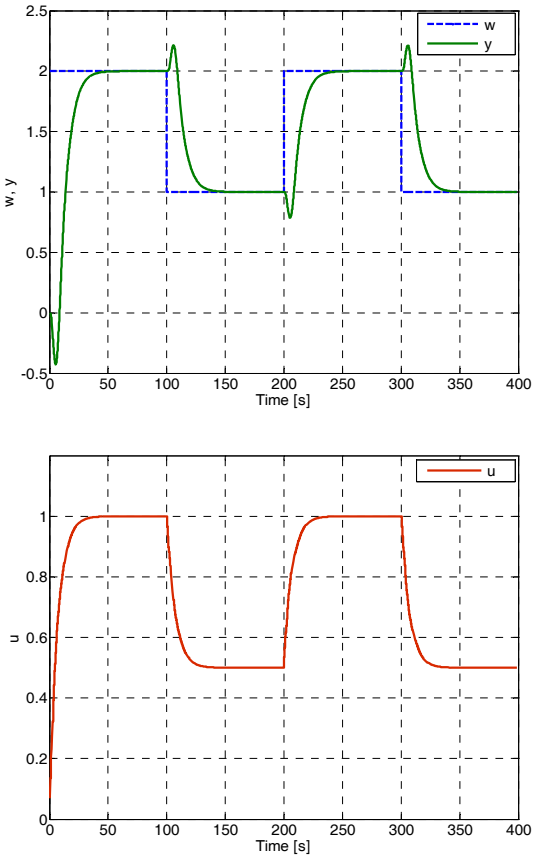

Figure: 14 Control of the Model $G_B(s)$; $T_m = 3$

For small the time constant T_m, the control process could be unstable.

CONCLUSION

Digital Smith Predictor algorithm for control of the higher-order processes was designed. The higher-order process was identified by the second-order model with time delay. For the process identification of the time-delay was used the off-line least squares method, as excitation signal was generated Random Gaussian Signal using MATLAB code idinput( ). The controller algorithm is based on polynomial design (pole assignment approach). The method for a choice of suitable poles of the characteristic polynomial was designed. The polynomial controller was derived purposely by analytical way (without utilization of numerical methods) to obtain algorithm with easy implementability in industrial practice. The control of two modifications of the firth-order processes (stable and non-minimum phase) were verified by simulation. Results of simulation verification in both cases demonstrated very good of control quality. Unfortunately, digital Smith Predictor is not suitable for the control of unstable processes. The proposed digital Smith Predictor will be verified in real-time laboratory conditions for the control of the heat exchanger. Adaptive versions of digital Smith Predictors are designed in (Bobál et al. 2011b).

ACKNOWLEDGMENT

This article was created with support of Operational Programme Research and Development for Innovations co-funded by the European Regional Development Fund (ERDF), national budget of Czech Republic within the framework of the Centre of Polymer Systems project (reg. number: CZ.1.05/2.1.00/03.0111).

REFERENCES

Bobál, V., Böhm, J., Fessl, J. and J. Macháček. 2005. *Digital Self-tuning Controllers: Algrithms, Implementation and Applications.* Springer-Verlag, London.

Bobál, V., Matušů, R. and P. Dostál. 2011a. "Digital Smith Predictors – Design and Simulation Study". In *Proc. of 25th European Conference on Modelling and Simulation*, Krakow, Poland, 480-486.

Bobál, V., Chalupa, P., Dostál, P. and M. Kubalčík. 2011b. "Design and simulation verification of self-tuning Smith Predictors". *International Journal of Mathematics and Computers in Simulation* 5, 342-351.

Dahlin, D.B. 1968. "Designing and tuning digital controllers". *Inst. Control Systems* 42, 77-73.

Hang, C.C., Lim, K. W. and B.W. Chong . 1989. "A dual-rate digital Smith predictor". *Automatica* 20, 1-16.

Hang, C.C., Tong, H.L. and K.H. Weng. 1993. *Adaptive Control.* Instrument Society of America.

Kučera, V. 1991. *Analysis and Design of Discrete Linear Control Systems.* Prentice-Hall, Englewood Cliffs, NJ.

Kučera, V. 1993. "Diophantine equations in control – a survey". *Automatica* 29, 1361-1375.

Normey-Rico, J.E. and E.F. Camacho. 1998. "Dead-time compensators: A unified approach". In *Proceedings of IFAC Workshop on Linear Time Delay Systems (LDTS'98)*, Grenoble, France, 141-146.

Normey-Rico, J. E. and E. F. Camacho. 2007. *Control of Dead-time Processes.* Springer-Verlag, London.

Palmor, Z.J. and Y. Halevi. 1990. "Robustness properties of sampled-data systems with dead time compensators". *Automatica* 26, 637-640.

Smith, O.J. 1957. "Closed control of loops". *Chem. Eng. Progress* 53, 217-219.

AUTHOR BIOGRAPHIES

VLADIMÍR BOBÁL graduated in 1966 from the Brno University of Technology, Czech Republic. He received his Ph.D. degree in Technical Cybernetics at Institute of Technical Cybernetics, Slovak Academy of Sciences, Bratislava, Slovak Republic. He is now Professor at the Department of Process Control, Faculty of Applied Informatics of the Tomas Bata University in Zlín. His research interests are adaptive control and predictive control, system identification and CAD for automatic control systems. You can contact him on email address bobal@fai.utb.cz.

MAREK KUBALČÍK graduated in 1993 from the Brno University of Technology in Automation and Process Control. He received his Ph.D. degree in Technical Cybernetics at Brno University of Technology in 2000. From 1993 to 2007 he worked as senior lecturer at the Faculty of Technology, Brno University of Technology. From 2007 he has been working as an associate professor at the Department of Process Control, Faculty of Applied Infromatics of the Tomas Bata University in Zlín, Czech Republic. Current work cover following areas: control of multivariable systems, self-tuning controllers, predictive control. His e-mail address is: kubalcik@fai.utb.cz.

PETR CHALUPA was born in Zlin, Czech Republic in 1976. He graduated from Brno University of Technology in 1999. He obtained his Ph.D. in Technical Cybernetics at Tomas Bata University in Zlin in 2003. He works as a researcher at Faculty of Applied Informatics at Tomas Bata University in Zlin. His research interests are modeling, adaptive control and predictive control of real-time systems. You can contact him on email address chalupa@fai.utb.cz.

PETR DOSTÁL studied at the Technical University of Pardubice, Czech Republic, where he obtained his master degree in 1968 and PhD. degree in Technical Cybernetics in 1979. In the year 2000 he became professor in Process Control. He is now head of the Department of Process Control, Faculty of Applied Informatics of the Tomas Bata University in Zlín. His research interests are modelling and simulation of continuous-time chemical processes, polynomial methods, optimal and adaptive control. You can contact him on email address dostalp@fai.utb.cz.

MODELING OF ALCOHOL FERMENTATION IN BREWING – SOME PRACTICAL APPROACHES

Ivan Parcunev, Vessela Naydenova, Georgi Kostov, Yanislav Yanakiev, Zhivka Popova, Maria Kaneva, Ivan Ignatov
University of Food Technology
"Technology of wine and brewing"
26 Maritza blvd., Plovdiv, 4033, Bulgaria
E-mail: george_kostov2@abv.bg; vesi_nevelinova@abv.bg; ignatov@bulgariandrinks.com; m_kaneva@abv.bg; zhivkapopova@abv.bg; ivan.parcunev@gmail.com; yanislav.a@abv.bg;

KEYWORD

Brewing, fermentation, immobilized cells, modeling, fermentation kinetics

ABSTRACT

In the present work, a practical method for determination of the basic physicochemical parameters of beer - real extract, alcohol and biomass concentration based on the amount of produced CO_2 during the fermentation is investigated. The method was applied for determination of biomass concentration in immobilized preparations after its approbation with analytical data for beer fermentations with free cells.
The kinetics parameters of the fermentation were determined with 3 of the most used kinetic models. The differences between beer fermentations with free and immobilized cells were investigated. The effect of yeasts immobilization on brewing process was defined.

INTRODUCTION

The beer is made from malt, hops, yeast and water. Non-malting adjuncts such as barley, rice, corn meal, wheat and others are commonly used. They reduce the cost of the product; improve the wort extract and beer flavor and foam. The main stages in the brewing process are: wort production, alcoholic fermentation and maturation, processing and stabilization of the beer (Kunze 2003; Handbook of brewing: Processes, Technology, Markets 2009).
The wort transforms into beer during alcoholic fermentation and maturation, which are the longest processes in brewing. The primary fermentation lasts between 3-6 days and the maturation - up to 2 weeks depending on the fermentation type and the used equipment. The ethanol fermentation occurs as a result of enzymatic activity of the yeast at Embden-Meyerhof-Parnas pathway, which leads to glucose conversion to pyruvate. Under anaerobic conditions the yeasts convert pyruvate to ethanol and CO_2. In aerobic conditions, yeasts consume sugars, mainly for biomass accumulation and CO_2 production (Boulton and Quain, 2001).
Yeasts uptake the carbohydrates of wort in a specific sequence: monosaccharides (glucose and fructose), disaccharides (sucrose and maltose) and trisaccharide maltotriose and ferment them in the same order. Very small amount of maltotriose is used for the formation of reserve polysaccharides (glycogen and trehalose). The amino acids assimilated by yeast are used for the synthesis of proteins, enzymes and new cells. The fermentation by–products: carbonyl compounds, higher alcohols, esters, organic acids and sulfur-containing compounds determine the flavor profile of beer and affect on beer quality. The following processes are carried out during maturation: fermentation of the remaining fermentable extract, saturation with CO_2, removal of unwanted aroma compounds, excretion of flavor-active compounds from yeast to give body and depth to the beer, sedimentation of yeast cells (Kunze 2003; Willaert 2007).
The amount of released CO_2 during fermentation is a direct indicator of fermentation activity of yeast. The ethanol fermentation can be described by the following stoichiometric equation:

$$\underset{1kg}{C_6H_{12}O_6} \xrightarrow{yeast} \underset{0,51kg}{2C_2H_5OH} + \underset{0,49kg}{2CO_2} \qquad (1)$$

The relationship between the original extract (OE), the real extract (RE), the apparent extract (AE) of beer and the produced ethanol A, % w/w ($A_{W/W}$) are presented in tables, produced by Balling (Balling, 1865), Wahl and Henius (Wahl and Henius, 1908), Holtzer (Holtzer,1904) and others. In the work of Cutaia et. al., 2009 the all data used by the authors to find a connection between the operational parameters of pilot plants and industrial breweries are summarized (Cutaia et. al., 2009).
The most well known expression relating OE, RE and Aw/w is the Balling equation, which relates the original extract to the real extract and alcohol (% w/w):

$$\underset{extract}{2,0665\,g} \rightarrow \underset{alcohol}{1,000\,g} + \underset{CO_2}{0,9565\,g} + \underset{biomass}{0,11\,g} \qquad (2a)$$

or:

$$OE = \frac{100*(2,0665*A_{W/W} + RE)}{\left(100 + 1,0665*A_{W/W}\right)} \qquad (2b)$$

The Balling's equation suggests, that from 2.0665 g wort extract, we received 0.11 g yeasts biomass and all sugars in the wort are fermentable monosaccharaides.
The batch fermentation rate on laboratory scale can be easily monitored via measuring the weight of fermentation bottles (flasks). The weight loss is connected with the release of CO_2 and the accumulation of alcohol which leads to reduction in beer specific gravity. The amount of released CO_2 in fermentation on semi-industrial and industrial scale can be easy measured. In both cases, if the relationship between the

Proceedings 26th European Conference on Modelling and Simulation ©ECMS Klaus G. Troitzsch, Michael Möhring, Ulf Lotzmann (Editors)
ISBN: 978-0-9564944-4-3 / ISBN: 978-0-9564944-5-0 (CD)

amounts of released CO_2 (weight loss of samples) and the amounts of fermented sugars and produced alcohol is known, the progress of the fermentation can be easily investigated.

The aim of the present study was to formulate a mathematical model for description of beer fermentation on the basis of the weight loss of fermentation bottles and to find a relationship between the amount of CO_2 and the brewing parameters – OE, AE, RE, $A_{W/W}$. The kinetics parameters of the process were determined on the basis of the received results using our model.

MICROORGANISMS AND FERMENTATION CONDITIONS

The fermentation was carried out with top-fermenting yeasts *Saccharomyces cerevisiae* S-33 and bottom-fermenting yeasts *Saccharomyces cerevisiae* S-23. The wort with 3 different original extracts – 9, 11 and 13% was used for fermentations. All media were sterilized at 121 °C for 20 min before fermentations.

The cells were immobilized in a 3 % calcium alginate gel. After autoclaving the alginate solution for 20 min at 120°C, the solution was mixed with the cell suspension to obtain a cell concentration of 10^7 cells/mL of gel. This suspension was forced through a syringe needle by means of peristaltic pump and dropped into 2 % (w/v) $CaCl_2$ solution. The resulting beads were approximately 2 mm in diameter. The beads were left for 30 min in calcium solution and then number of beads were placed into 0,38 % (w/v) chitosan solution in 1% acetic acid (v/v). Alginate beads stayed in chitosan solution for 60 min. Afterwards, chitosan-alginate beads are washed with physiological solution (saline) to remove the excess of chitosan. Then the beads was transferred in in 0,05 M Na-citrate solution for 30 min for constructing microcapsules with liquid core. Afterwards, chitosan-alginate beads with liquid core were washed with physiological solution (saline) (Willaert 2001).

The fermentation was made with free and immobilized cells. The fermentation was held in bottles, containing 400 ml sterile wort, equipped with fermentation stoppers. Every bottle was inoculated with 0.33 g dry yeasts or 14 g of immobilized beads. The fermentation was carried out in temperature controlled room at 15 °C for 240 h. The fermentation processes were monitored via the amount of released CO_2, which is measured from the weight loss at 24 h. The shown results were average from 3 parallel processes.

The ethanol and extract concentrations are determined by a specialized apparatus type „Anton Paar DMA 4500", Austria. This is a standard method from EBC-analityca (European Brewery Convention, Analytica EBC 2005). The biomass concentration was determined by measuring OD 600 by „Shimatzu UV-VIS 1800". The biomass concentration in immobilized cells was determined using the following methodology: 1.0 g of beads with immobilized cells was put into 1 M solution of magnesium citrate for dissolving of beads; for the control probe 1 g of pure beads were put into 1 M magnesium citrate; after releasing of biomass its concentration was determined spectrophotometrically (Zhou et. al. 1998).

MATHEMATICAL MODELS AND THEIR INTERPREATION

The main relationship, which is used in brewing, is Balling's equation (2a). On the base of this the following coefficients for the process were received:

$$\begin{aligned} Y_{P/S} &= 1{,}0000\ \underset{alcohol}{g} \Big/ 2{,}0665\ \underset{extract}{g} = 0{,}4839\ \text{g/g};\\ Y_{X/S} &= 0{,}11\ \underset{biomass}{g} \Big/ 2{,}0665\ \underset{extract}{g} = 0{,}0532\ \text{g/g};\\ Y_{CO_2/S} &= 0{,}9565\ \underset{CO_2}{g} \Big/ 2{,}0665\ \underset{extract}{g} = 0{,}4628\ \text{g/g} \end{aligned} \tag{2c}$$

The fermentation process was described with the following system of ordinary differential equations:

$$\begin{cases} \dfrac{dX}{dt} = \mu(t)X(t) \\ \dfrac{dP}{dt} = q(t)X(t) \\ \dfrac{dS}{dt} = -\dfrac{1}{Y_{x/s}}\dfrac{dX}{dt} - \dfrac{1}{Y_{p/s}}\dfrac{dP}{dt} \end{cases} \tag{3}$$

where X(t) was biomass' concentration, P(t) is ethanol concentration, S(t) was extract (substrate) concentration; $Y_{X/S}$ and $Y_{P/S}$ were yield coefficients; μ(t) and q(t) were specific growth and product accumulation rates.

Assuming Gay–Lussac relationships, the concentrations of substrate S(t) and ethanol E(t), together with *dS/dt* and *dE/dt*, can be deduced from the amount of carbon dioxide released, $CO_2(t)$, using:

$$\begin{aligned} S(t) &= S_{\text{int}} - aCO_2(t)\\ P(t) &= b(S_{\text{int}} - S(t)) \end{aligned} \tag{4}$$

where ***a*** and ***b*** are coefficients; S_{int}=OE; S(t)=RE(t).

The same approach was used for the control of fermentation process in winemaking (Goelzer et. al. 2009).

The careful consideration of the Balling's equation and the shape of the experimental curves for CO_2 enables us to determine the coefficients ***a*** and ***b*** easily. The coefficient ***b*** came directly from equation (2b) and its value was ***0.4839***. The average value of **b** depended on the yeast strain and fermentation conditions and varies from 0.48 to 0.57 (Cutaia et. al. 2009). But as a first approximation, its value from Balling's equation could be used.

The value of ***a*** could be determined experimentally, if fermentation rates were known. In series of experiments, the amount of released CO_2 and the parameters OE, AE, RE, $A_{W/W}$ were measured during fermentation. It was found that the value of ***a*** varied from 0.49-0.53, i.e. it was closer to 0.4839. Therefore, this value could also be used for determination of the extract dynamics. The determined values of coefficients **a** and **b** were taken into account in equation (4):

$$\begin{aligned} S(t) &= S_{\text{int}} - 0{,}5157CO_2(t)\\ P(t) &= 0{,}5157(S_{\text{int}} - S(t)) \end{aligned} \tag{4a}$$

An important feature of the fermentation process is the biomass concentration in a fermentation medium. The formation of biomass is associated with cell division

process, in which CO_2 also releases. Consequently, the concentration of biomass can also be determined by the amount of released CO_2. The starting point for such calculation will be again the Balling's equation. According to it, 5.32% of the fermentable extract is used by the cells for their vital activity and formation of new cells. It was found in the series of preliminary experiments that the yield coefficient of biomass was higher and it was 10% indeed. Consequently, the concentration of biomass in the medium can be determined by the relationship:

$$X(t) = 0{,}1\left[S(t)_{i-1} - S(t)_i\right] \qquad (4b)$$

where $S(t)_{i-1}$ and $S(t)_I$ are the OE of the wort;

The method was applied for determination of the fermentation parameters in beer production. The results of one of the comparisons are presented in Figure 1. Table 1 shows the statistical analysis of experimental and calculated data presented in Figure 1 (original extract 9%). The data for other investigations are similar.

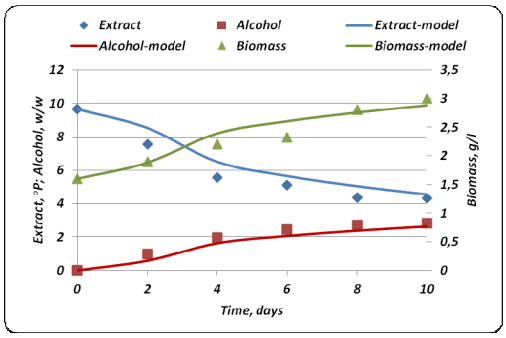

a) free cells *S. cerevisiae* S-23

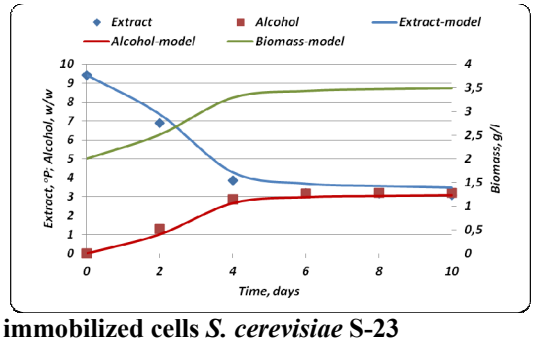

b) immobilized cells *S. cerevisiae* S-23

Figure 1. Comparison between model and experimental results (eq. 4, 4a, 4b); OE=9°P

Table 1

F-test for results on figure 1.

F-Test Two-Sample for Variances (Extract)		
	Experimental	***Model***
Mean	6,1033	6,656
Variance	4,424	4,158
Observations	6	6
df	5	5
F	1,064	
P(F<=f) one-tail	0,473	
F Critical one-tail	5,050	

The statistical analysis showed that the mathematical model gave correct results in calculating the basic parameters of the fermentation process. The conclusion was that the model gave accurate results for the concentration of biomass, slightly underestimated the alcohol formation and respectively, overestimated the final extract in beer. The reason was the initial values of selected parameters. Despite these disadvantages, the proposed model satisfactorily described the course of the fermentation process and it was applicable in practice.

The results for fermentation dynamics, received by equations (4a) and (4b) were used for determination of kinetic parameters of alcoholic fermentation with free and immobilized cells.

KINETICS PARAMETERS OF ALCOHOL FERMENTATION WITH FREE AND IMMOBILIZED CELLS

The fermentation process kinetics was described with the ordinary differential equation (3). The main kinetic parameters are: specific growth rate μ and specific product accumulation rate q. In present investigation three models were used - 5a, 5b, 5c (Birol et. al., 1998; Kostov et. al. 2011). The identification of parameters was made with MatLab. The software minimized the sum of squared errors of the model outputs with respect to the experimental data:

$$e = \left(X(k_1, k_2, \cdots, k_n) - X^e\right)^2 + \left(S(k_1, k_2, \cdots, k_n) - S^e\right)^2 + \left(P(k_1, k_2, \cdots, k_n) - P^e\right)^2$$

For that purpose the function "fmincon" was applied. Here k_i, $i = 1 \div n$ was vector of model parameters to be determined as output of minimization procedure. For that purpose the following complimentary differential equations:

$$dk_i/dt = 0, \quad i = 1 \div n$$

were added to the ordinary differential equations model because k_i, $i = 1 \div n$ were constants. For solving the overall differential equations system based on the explicit Runge-Kutta of 4-5 order formula using MATLAB function "ode45" (Kostov et. al. 2011; Mitev and Popova, 1995; Popova 1997). All parameters are presented on tables 2, 3 and 4.

- **Monod**

$$\mu = \mu_{\max}\frac{S}{K_{sx}+S};\quad q = q_{p\max}\frac{S}{K_{sp}+S} \qquad (5a)$$

- **Aiba**

$$\mu = \mu_{\max}\frac{S}{K_{sx}+S}\exp(-K_{ix}P)X;\qquad q = q_{p\max}\frac{S}{K_{sp}+S}\exp(-K_{ip}P)X \qquad (5b)$$

- **Tiessier**

$$\mu = \mu_{\max}\left(1-\exp\left(-\frac{S}{K_{sx}}\right)\right)\qquad q = q_{p\max}\left(1-\exp\left(-\frac{S}{K_{sp}}\right)\right) \qquad (5c)$$

Table 2

Kinetic parameters for beer fermentation with free and immobilized cells - *ORIGINAL EXTRACT – 9%*

Model parameters								*Efficiency coefficients*		*Model error*
μ_{max}	K_{sx}	q_{pmax}	K_{sp}	$Y_{x/s}$	$Y_{p/s}$	K_{ix}	K_{ip}	η_μ	η_q	
d^{-1}	$g.dm^{-3}$	$g.(g.d)^{-1}$	$g.dm^{-3}$	-	-	$g.dm^{-3}$	$g.dm^{-3}$	-	-	
Saccharomyces cerevisiae S-23 (bottom fermented yeasts)										
Monod										
Free cells										
0.424	***150***	***2.042***	***150***	***0.125***	***0.53***	-	-	***0.708***	***1.350***	***0.306***
Immobilized cells										
0.3	***57.74***	***2.756***	***166.33***	***0.063***	***0.58***	-	-			***0.123***
Tiessier										
Free cells										
0.412	***200***	***1.796***	***100***	***0.167***	***0.6***	-	-	***1.534***	***2.132***	***0.07***
Immobilized cells										
0.633	***200***	***2.292***	***150***	***0.148***	***0.58***	-	-			***0.272***
Aiba										
Free cells										
0.521	***158.672***	***4.07***	***161.419***	***0.125***	***0.56***	***0.155***	***0.06***	***1.741***	***1.954***	***0.224***
Immobilized cells										
0.907	***145.63***	***6.21***	***150.21***	***0.115***	***0.531***	***0.199***	***0.09***			***0.81***
Saccharomyces cerevisiae S-33 (top fermented yeasts)										
Monod										
Free cells										
0.157	***200***	***3.39***	***200***	***0.0597***	***0.521***	-	-	***1.261***	***0.914***	***0.416***
Immobilized cells										
0.196	***226.71***	***3.1***	***216.72***	***0.063***	***0.555***	-	-			***0.382***
Tiessier										
Free cells										
0.181	***200***	***1.754***	***100***	***0.086***	***0.444***	-	-	***0.883***	***0.886***	***0.577***
Immobilized cells										
0.159	***200***	***1.554***	***100***	***0.053***	***0.593***	-	-			***0.382***
Aiba										
Free cells										
0.165	***173.2***	***2.321***	***152.11***	***0.085***	***0.532***	***0.231***	***0.427***	***0.794***	***1.877***	***0.725***
Immobilized cells										
0.131	***232.1***	***4.357***	***183.12***	***0.088***	***0.572***	***0.133***	***0.674***			***0.621***

In the present work, it was accepted that the fermentation with immobilized cells could be modeled using the common relations for free cells. The influence of diffusion resistances in the system was described by the efficiency coefficients, which generalize the influence of internal and external diffusion resistances - η_μ (related to the maximal specific growth rate) and η_q (related to maximal specific ethanol production rate) defined as follows:

$$\eta_\mu = \frac{\mu_{\max}^{free}}{\mu_{\max}^{imm}} \quad \eta_q = \frac{q_{\max}^{imm}}{q_{\max}^{free}}$$

The results from the process kinetics led to interesting conclusions. First, the specific growth rate of the investigated yeasts strains decreased, when the original extract increased.

Second, there were interesting results, when wort with low original extracts was used. Immobilized cells of yeast strain S-23 showed higher specific growth rates than free cells. The main reason was increased concentration of cells in the working volume, which together with low original extract of wort led to higher specific rate of fermentation. The same was observed when wort with 11% OE was used. In contrast to the bottom fermenting yeast, the immobilized cells of top fermenting yeast strain S-33 showed lower specific growth rate than free cells. The difference between specific growth rates of immobilized and free cells was minor at wort with 9% OE, i.e. immobilization did not significantly effect on the cell growth and on the fermentation process. An important indicator of fermentation kinetics is the specific rate of accumulation of ethanol in the medium, which varies between 0.6 and 6 g /(g.d) ethanol. The studied yeast strains showed major differences in this parameter. The fermentation with bottom fermenting yeast ran smooth, without abrupt changes of ethanol content in the medium. The produced beers were with well-formed flavor profile. The fermentation with top fermenting strain S-33 was rapid and the ethanol was accumulated mainly at the first 2-3 days of primary fermentation. At that time larger amounts of secondary metabolites were also accumulated, which had to be reduced in the next

stage of fermentation. At the end of fermentation beers were with well-balanced flavor.

The fermentation rate depends on temperature of fermentation. The optimal fermentation temperatures are: 15-22°C for top-fermenting yeast strain and 8-18°C for bottom-fermenting strains. Therefore, differences in fermentation process were observed.

We can conclude that the fermentation with immobilized cells was faster at the end, which led to higher fermentation degree of produced beers. These beers were characterized by watery taste, because of lower non-fermented extract.

The influence of process immobilization on the investigated yeasts strains was different. The more interesting results were received for the top-fermenting strain – S-33. There was a reduction of the kinetics parameters for the immobilized cells. So, we could conclude that the immobilization had a significant effect on the fermentation process.

Table 3

Kinetic parameters for beer fermentation with free and immobilized cells - *ORIGINAL EXTRACT – 11%*

Model parameters								*Efficiency coefficients*		*Model error*
μ_{max}	K_{sx}	q_{pmax}	K_{sp}	$Y_{x/s}$	$Y_{p/s}$	K_{ix}	K_{ip}	η_u	η_q	
d^{-1}	$g.dm^{-3}$	$g.(g.d)^{-1}$	$g.dm^{-3}$	-	-	$g.dm^{-3}$	$g.dm^{-3}$	-	-	
Saccharomyces cerevisiae S-23 (bottom fermented yeasts)										
Monod										
Free cells										
0.117	*150*	*2.03*	*150*	*0.093*	*0.53*	-	-	*2.564*	*2.724*	*0.725*
Immobilized cells										
0.30	*204.26*	*5.53*	*226.71*	*0.6*	*0.58*	-	-			*0.209*
Tiessier										
Free cells										
0.114	*200*	*0.653*	*0.344*	*0.039*	*0.6*	-	-	*2.228*	*3.987*	*0.747*
Immobilized cells										
0.254	*200*	*2.604*	*100*	*0.06*	*0.6*	-	-			*0.371*
Aiba										
Free cells										
0.348	*173.12*	*3.037*	*143.17*	*0.13*	*0.55*	*0.055*	*0.213*	*2.201*	*2.073*	*0.203*
Immobilized cells										
0.766	*200*	*6.296*	*200*	*0.13*	*0.56*	*0.070*	*0.027*			*0.587*
Saccharomyces cerevisiae S-33 (top fermented yeasts)										
Monod										
Free cells										
0.294	*200*	*6.37*	*197.11*	*0.054*	*0.581*	-	-	*0.918*	*0.695*	*0.202*
Immobilized cells										
0.270	*226.71*	*4.43*	*226.72*	*0063*	*0.57*	-	-			*0.18*
Tiessier										
Free cells										
0.304	*210.13*	*3.010*	*100*	*0.057*	*0.060*	-	-	*0.651*	*0.729*	*0.321*
Immobilized cells										
0.198	*205.7*	*2.195*	*92.11*	*0.0623*	*0.6*	-	-			*0.116*
Aiba										
Free cells										
0.450	*62.68*	*5.907*	*100*	*0.063*	*0.65*	*0.086*	*0.035*	*1.564*	*0.789*	*0.131*
Immobilized cells										
0.704	*200*	*4.662*	*200*	*0.125*	*0.56*	*0.066*	*0.021*			*0.733*

The change in yield coefficients was important for practical application of immobilized cells. The biomass yield coefficient varied between 0.05 and 0.17, which confirmed the initial conclusions – more than 5% of the OE converted to biomass. It can be summarized that the average biomass yield coefficient is 10-11%, i.e. 0.1 to 0.11. The degree of fermentation of all experimental data varied between 55 and 65%. The observed differences were due to the quantity of fermentable extract in the medium and the fermentation rate.

It had to be highlighted that there was no strong substrate or product inhibition. The coefficients in Aiba's model were close to zero and the model was close to the general equation of Monod. It was interesting that Aiba's model gave slightly higher values than the Monod's model. The reason was an additional article, taking into account the substrate or product inhibition. Although this element was negligible, it should not be excluded.

The accuracy of models for description of experimental data was similar. The studies on the accuracy of the models showed that the pattern of Monod and Tissier gave satisfactory accuracy for this stage of work. From the obtained results it is difficult to choose the only one

model. The three mathematical relationships are characterized by their simplicity and good approximating capability. In terms of proper synthesis models of such systems should be characterized by its simplicity as offer the four models. These relationships described very well the fermentation process and gave a clear idea of the process parameters' influence on the kinetic characteristics. In practice the Aiba model could be simplified to the Monod equation because of weak product inhibition.

CONCLUSION

The work presents a method for determining the basic parameters of the alcoholic fermentation process in brewing, based on the amount of produced CO_2. The method is based on the known Balling's equation and the experiment data for the fermentation processes. The developed method is applicable in laboratory and industrial practice and gives reliable results with a good description of the fermentation process. The kinetics of the fermentation process was determined using three mathematical models. There are differences in the course of fermentation with free and immobilized top and bottom fermenting yeast strains. The influence of immobilization on fermentation with two different strains leads to a different taste and flavor profile of the produced beers.

Table 4

Kinetic parameters for beer fermentation with free and immobilized cells - *ORIGINAL EXTRACT – 13%*

Model parameters								*Efficiency coefficients*		*Model error*
μ_{max}	K_{sx}	q_{pmax}	K_{sp}	$Y_{x/s}$	$Y_{p/s}$	K_{ix}	K_{ip}	η_u	η_a	
d^{-1}	$g.dm^{-3}$	$g.(g.d)^{-1}$	$g.dm^{-3}$	-	-	$g.dm^{-3}$	$g.dm^{-3}$	-	-	
Saccharomyces cerevisiae S-23 (bottom fermented yeasts)										
Monod										
Free cells								***1.339***	***1.259***	***0.133***
0.224	***150***	***3.839***	***150***	***0.124***	***0.476***	-	-			
Immobilized cells										
0.300	***221.420***	***4.901***	***226.72***	***0.063***	***0.58***	-	-			***0.370***
Tiessier										
Free cells								***1.092***	***1.02***	***0.691***
0.27	***200***	***2.437***	***100***	***0.0621***	***0.6***	-	-			
Immobilized cells										
0.294	***175***	***2.485***	***12.3***	***0.0527***	***0.7***	-	-			
Aiba										
Free cells								***0.620***	***0.823***	***0.143***
0.527	***200***	***6.665***	***200***	***0.125***	***0.512***	***0.0361***	***0.023***			
Immobilized cells										
0.327	***200***	***5.487***	***200***	***0.081***	***0.56***	***0.009***	***0.009***			***0.102***
Saccharomyces cerevisiae S-33 (top fermented yeasts)										
Monod										
Free cells								***0.559***	***0.879***	***0.192***
0.395	***221.214***	***3.297***	***200***	***0.065***	***0.61***	-	-			
Immobilized cells										
0.221	***158.11***	***2.897***	***200***	***0.071***	***0.59***	-	-			***0.210***
Tiessier										
Free cells								***0.597***	***0.708***	***0.347***
0.307	***178.12***	***2.995***	***150***	***0.074***	***0.597***	-	-			
Immobilized cells										
0.221	***199.78***	***2.123***	***150***	***0.075***	***0.61***	-	-			***0.214***
Aiba										
Free cells								***2.038***	***0.747***	***0.464***
0.321	***124.21***	***6.130***	***100***	***0.054***	***0.59***	***0.123***	***0.065***			
Immobilized cells										
0.654	***200***	***4.578***	***164***	***0.101***	***0.55***	***0.094***	***0.009***			***0.214***

ACKNOWLEDGEMENTS

This work was partially supported by the National Science Fund under the Project No DTK 02/27 "Increasing the efficiency of bio-fuel purpose ethanol production". Our team expresses its sincere thanks to the brewery "Kamenitza"Plc - Plovdiv for supply with wort and conduction of the necessary analyzes.

REFERENCES

Balling C. J. N. 1865. "Die Bierbrauerei" *Verlag von Friedrich Temski*, Prague, CHZ.

Birol G.; P. Doruker; B. Kirdar; Z. Ilsen; K. Ulgen 1998. "Mathematical description of ethanol fermentation by immobilised *Saccharomyces cerevisiae*." *Process*

Biochemistry, vol. 33 (7), 763-771, ISSN 1359-5113, 10.1016/S0032-9592(98)00047-8.

Boulton C. and D. Quain 2001. "Brewing yeast and fermentation." *Blackwell Science*, ISBN 0-632-05475-1

Cutaia J.; A.J. Reid; R.A. Speers. 2009. "Examination of the Relationships Between Original, Real and Apparent Extracts, and Alcohol in Pilot Plant and Commercially Produced Beers." *J. Inst. Brew.* 115(4), 318–327

European Brewery Convention, *Analytica EBC*. 2005, Fachverlag Hans Carl, Nurnberg.

Goelzer A.; B. Charnomordic; S. Colombié; V. Fromion; J.M. Sablayrolles. 2009. "Simulation and optimization software for alcoholic fermentation in winemaking conditions." Food Control, 20(7), 635-642, ISSN 0956-7135, 10.1016/j.foodcont.2008.09.016.

Handbook of brewing: Processes, Technology, Markets. 2009. Hans Michael Esslinger (ed.), ISBN 978-3-527-31674-8, WILEY-VCH Verlag GmbH & Co. KGaA, Weinheim

Holzner G. 1904. "Tabellen zur Berechnung der Ausbeute aus Malze und zur Saccharometririchen Bieranalyze." *Druck und Verlag, von R: Oldenburg*, Munich.

Kostov G.; S. Popova; V. Gochev; P. Kpoprinkova-Hristova; M. Angelov. 2012. "Modeling of batch alcohol fermentation with free and immobilized yeasts *Saccharomyces cerevisiae* 46 EVD." *Biotechnology and Biotechnological equipment*, (in press)

Kunze W. 2003. "Technology of brewing and malting, 3rd edition", ISBN 3-921690-49-8, *VLB-Berlin*

Mitev S.V.; S. B. Popova. 1995. "A model of yeast cultivation based on morphophysiological parameters." *J. Chemical and Biochemical Engineering Quarterly*, 3, Zagreb, 119-121.

Popova S. 1997. "Parameter identification of a model of yeast cultivation process with neural network", Bioprocess and Biosystems Engineering, 16(4), 243-245, DOI: 10.1007/s004490050315

Wahl R. and M. Henius. 1908. "American Handy Book of the Brewing, Malting and Auxiliary Trades". 3rd Ed., vol. II. *Wahl-Henius Institute: Chicago*, *IL*.

Willaert R. 2007. "The Beer Brewing Process: Wort Production and Beer Fermentation." In: Handbook of Food Products Manufacturing. Hui, Y.H. (ed.), *John Wiley & Sons, Inc*.

Willaert R. 2001. "Immobilized cell." *Springer*, Berlin.

Zhou Y.; E. Martins; A. Groboillot; C.P. Champagne; R. Neufeld. 1998. "Cell Release from Alginate Immobilized *Lactococcus lactis* ssp. *lactis* in Chitosan and Alginate Coated Beads" *J. of Appl. Microbiol*., 84, 342-348.

AUTHOR BIOGRAPHIES

GEORGI KOSTOV is an associated professor at the department "Technology of wine and brewery" at University of Food Technologies, Plovdiv. He received his MSc in "Mechanical engineering" in 2007 and PhD on "Mechanical engineering in food and flavor industry (Technological equipment in biotechnology industry)" in 2007 from University of Food Technologies, Plovdiv. His research interests are in the area of bioreactors' construction, biotechnology, microbial populations' investigation and modeling, hydrodynamics and mass transfer problems, fermentation kinetics.

VESSELA NAYDENOVA is a PhD student at the department "Technology of wine and brewery" at University of Food Technologies, Plovdiv. She received her MSc in "Technology of wine and brewing" in 2005 at University of Food Technologies, Plovdiv. Her research interests are in the area of beer fermentation with free and immobilized cells; yeast specification and fermentation activity. The PhD thesis is named "Possibilities for beer production with immobilized yeast cells"

ZHIVKA POPOVA is associated professor at the department "Technology of wine and brewery" at University of Food Technologies, Plovdiv. Her research interests are in the area of brewing microbiology. She has extensive experience in the selection and use of brewing yeast strains. She has participated in the implementation of various microbiological practices in the brewing industry in Bulgaria.

IVAN IGNATOV is assistant professor at the department "Technology of wine and brewery" at University of Food Technologies, Plovdiv. His research interests are in the area of brewing and malting processes, organoleptic analysis of different types of beers. He is constitutor and administrator of the web-site www.bulgariandrinks.com.

MARIA KANEVA is an assistant professor at the department "Technology of wine and brewery" at University of Food Technologies, Plovdiv. Her research interests are in the area on non-alcoholic beverages, herbal extracts for beverages, modeling of extraction processes.

IVAN PARCUNEV is a student at the department "Technology of wine and brewery" at University of Food Technologies, Plovdiv. His bachelor degree thesis is on the subject of "Research in wort fermentation and beers productions with immobilized top-fermenting yeast strains"

YANISLAV YANIKEV is a student at the department "Technology of wine and brewery" at University of Food Technologies, Plovdiv. His bachelor degree thesis is on the subject of "Possibilities for beer production with immobilized yeast cells"

LOCOMOTION ANALYSIS OF A MODULAR PENTAPEDAL WALKING ROBOT

Cong Liu, Filippo Sanfilippo, Houxiang Zhang and Hans Petter Hildre
Faculty of Maritime Technology and Operation
Aalesund University College
Postboks 1517, N-6025 Aalesund, Norway

Chang Liu and Shusheng Bi
Robotics Institute, Beihang University,
Xueyuan Road 37, Haidian Dist., Beijing 100191, China

KEYWORDS
Pentapedal, Five-limbed, Gait.

ABSTRACT

In this paper, the configuration of a five-limbed modular robot is introduced. A specialised locomotion gait is designed to allow for omni-directional mobility. Due to the large diversity resulting from various gait sequences, a criteria for selecting the best gaits based on their stability characteristics is proposed. A series of simulations is then performed to evaluate the various gaits in different walking directions. A gait arrangement scheme toward omni-directional locomotion is finally derived. Lastly, Experiments are also carried out on our pentapedal robot prototype in order to validate the results of simulation. The experiments confirm the gait analysis and selection is highly accurate in the evaluation of gait stability.

I. INTRODUCTION

Legged locomotion offers great advantages due to its discrete foothold resulting in adaptability to uneven terrain, low energy consumption and less environmental destruction. Furthermore, the articulated limbs of legged robots are able to function in both locomotion and manipulation, thereby achieving better mobility and functionality. Therefore, a robot can either eliminate deadlock by properly manipulating its limbs to regulate the centre of gravity of its body, or improve its stability by using an additional limb as a leg (Zhang et al. 1996).

So far, various kinds of walking machines with two, four, six and eight legs have been developed. Systematic studies have been conducted on gait generation, control realization and algorithm implementation. However, most of these studies were concentrated on models with an even number of legs, as research interests in an odd number of legs is much rarer. Beside the research in (Zhang et al. 1996) and (Zhang et al. 1997), Prihastono et al. proposed a five legged mechanism that was inspired by a starfish (phylum echynodermata). The robot is capable of performing autonomous navigation in cluttered environments (Prihastono et al. 2009). However, these studies, for the most part, considered only fixed-shape robots that were designed based on a predefined and set-up environment.

For locomotion in unknown and hostile environments, modular robot platforms are expected to be more flexible and efficient than traditional fixed-shape robots, since such situations demand on-site locomotion adaption, shape adaption and task planning. Moreover, the modular approach also makes the mobile robotic system versatile, robust, cost-effective and fast to prototype, so that new configurations of different robots can be built quickly and easily for exploration. By differing the system architecture, modularity can be recognised in several approaches. Ohira et al. developed multi-legged modular robots, which can be interconnected to achieve multiple locomotion modes via cooperation and accomplish tasks that cannot be done with a single module (Prihastono et al. 2009). In (Aoi et al. 2006), Aoi et al. presented a multi-legged modular robot, consisting of six homogenous modules, which are connected to each other via a 3-degree-of-freedom (3-DoF) joint. The leg joint is driven in such a way that it follows the desired periodic trajectories, and at the same time, acts as a passive shock absorber. Chen et al. proposed a modular method for formulating the dynamics of multi-legged robots with general leg structures. In this approach, each leg is considered as an individual module, while the whole multi-legged system is treated as a free-floating system with the individual leg module coupled to a main body (Chen et al. 1997).

Even though significant progress has been made in this field, the technology of multi-legged robotics is still a challenging topic to be focused on in robotics research. As mentioned above, previous research work either focused on the classic four and six-limbed modular configurations, or on fixed-shape mobile robots, which offered insufficient flexibility in locomotion. In this paper, by combining the multi-legged locomotion techniques with a modular robotic approach, a pentapedal (five-limbed) modular robotic configuration is proposed. The goal of this research is to develop a versatile robotic mobile platform featuring an easy-to-build mechanical structure, various locomotion capabilities and high manipulation flexibility.

Proceedings 26th European Conference on Modelling and Simulation ©ECMS Klaus G. Troitzsch, Michael Möhring, Ulf Lotzmann (Editors)
ISBN: 978-0-9564944-4-3 / ISBN: 978-0-9564944-5-0 (CD)

II. RELATED WORK

A. Modular Robot Research

Modular robotic systems feature extraordinary flexibility, extendibility, robustness and reconfigurability. They are usually composed of multiple building blocks with relatively simple repertoires, together with uniform docking interfaces which enable mechanical junctions and electronic communication throughout the whole system. The last few years have witnessed an increasing interest in modular reconfigurable robotics for education (Daidié et al. 2007), inspired robotic research (Zhang et al. 2007) and space applications (Yim et al. 2007).

Modular robots can be connected in various configurations. Chain-configuration is suitable for locomotion and manipulation since a chain of modules is equivalent to a leg or an arm. Such form is the focus of this paper. In (González-Gómez et al. 2006), 1 dimension (1D), 2D and 3D chain robots are classified according to their topology. A 1D-chain robot, such a snake (Paap et al. 2000), worm (Zimmermann et al. 2004), leg, arm or cord (Kurokawa et al. 2003), can transform its body into different shapes, enabling itself to pass though pipes, grasp objects and move on rough terrain.

In 2004, our group designed a series of low-cost passive modular robots and modular robot locomotion. In cooperation with Dr. Juan González-Gómez, the Y1 modular robot with 1 DoF was designed in 2004 as the first prototype (Gonzalez-Gomez et al. 2007). By using this prototype, the minimal configurations for movement of snake-like robots were studied (Zhang et al. 2008). Then the new modular robot Cube-M with one DoF, an improved version of the Y1 modular robot, was presented (Zhang et al. 2009). It features an easy-to-build mechanical structure, four connecting faces, an onboard micro controller and a friendly programming environment.

B. The Pentapedal Configuration

To the best of the authors' knowledge, limited literature has been found focusing on the pentapedal configuration which has considerable redundancy in locomotion and control. However, the robot could gain auxiliary competence in mobility and functionality if a certain proper control strategy enables the reuse of one or two limbs as manipulator. Our goal is to develop a pentapedal robot platform capable of moving on rough terrain and accomplishing tasks with redundant limbs.

The pentapedal configuration has no corresponding prototype existing in nature, though some quadrupedal animals have certain auxiliary features to enhance their locomotion. For example, primates utilise their tail to keep their balance and improve climbing performance. In addition, it is advisable to implement radial symmetry in the robot's general configuration, inspired by pentamerism in nature. Therefore, the pentapedal robot has the characteristics of omni-directional locomotion. However in special cases, it is able to transform into quadrupedalism while operating one limb as a manipulator.

The design of such a robotic configuration is also inspired by existing multi-legged robots. The omni-directional configuration calls for high equivalence among the legs, in order to satisfy the accessibility of locomotion in various directions. On each leg of the robot, the distribution of articulations adopts the classic layout of insect-mimicking robots. The three Dof are provided by three articulation at the hip, knee and heel.

The control of a pentapedal robot also suggests a novel gait to enable the robot to move in a fluent and efficient manner. Therefore a rational gait should evenly utilise all the legs while maintaining sufficient stability. This paper discusses mainly gait generation and selection towards walking stability and fluency.

Firstly in Section III, this paper outlines the sequential 3+2 gait, which is specifically designed for pentapedal configuration. Due to the large diversity of gait sequences, a series of selections according to locomotion stability criteria is proposed in Section IV. In Section V, simulations are implemented to select the best gait sequences. Finally, the gaits are tested by experiments on our robot prototype.

III. DEFINITION OF PENTAPEDAL LOCOMOTION GAIT

Due to the absence of similar five-limbed creatures in nature, our research aims to introduce a fully artificial gait to be adopted to the robot.

Considering the static stability of the pentapedal configuration, the robot must have a minimum of three supporting feet in order to sustain the body. The remaining two limbs are utilised as striding legs in order to achieve better efficiency. Therefore, the sequential "3+2" gait for the pentapedal robot is defined as follows:

a) The gait cycle is divided into 5 phases. During each phase, a pair of feet stride one pace's length in the walking direction of the robot.

b) The striding foot-pair sequence is indicated by the gait sequence.

c) In every stride phase, the striding foot-pair should not be two adjacent feet.

d) The of robot's torso movement is evenly distributed along the walking direction during each phase. The speed is therefore at 0.4 time of pace length during each stride, in order to follow the movement of feet.

The robot walks with a specified sequence, length and direction. As such, the trajectories of the feet are determined. In Figure 1, the position of robot's torso and feet are illustrated from left to right. The robot starts the gait cycle from a neutral stance, as shown in the left-most picture, and then strides one pair of feet during each state. After a gait cycle, each foot has been involved in striding twice. The robot moves twice the pace length after a whole gait cycle finishes.

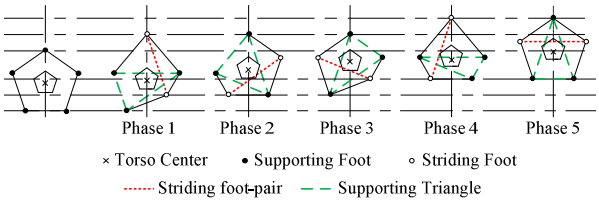

Figure 1: The five phases during a Sequential "3+2" Gait example. The robot strides its legs in pairs according to a certain sequence while the torso moves towards the corresponding direction in fixed speed.

In order to clarify the sequence of the striding feet, the foot-pairs are numbered 1, 2, 3, 4 and 5, as shown in Figure 2. The pole is set at the centre of the body, while the polar axis is defined as 0°. Due to the radial symmetric characteristic of the robot, the characteristics in the range of [54°,126°), [126°,198°), [198°,270°), [270°,342°) and [342°,54°) are identical. In addition, these ranges are axially symmetric with respect to the 90°, 162°, 234°, 306° and 18° axes, which divide their own corresponding range into two symmetric parts. This paper only focuses on the direction between 54° and 90°, which can also represent situations in other ranges by using an appropriate transformation.

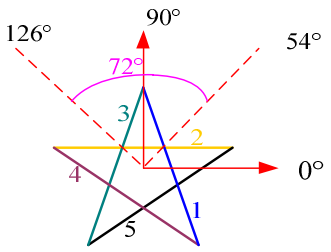

Figure 2: The Numbering of Feet and Foot-pairs

IV. LOCOMOTION GAIT ANALYSIS AND SIMULATION

The Sequential "3+2" Gait can secure at least three supporting feet during the gait cycle, but the robot may eventually fall when some gaits are implemented. The goal of the gait analysis is to select best gaits to apply to the robot.

Since the stride frequency never exceeds 3 Hz due to the speed of the actuator, dynamic effects are not taken into account in the analysis. Hence the analysis of the Sequential "3+2" Gait is based on each state during a gait cycle. Besides the 5 phases during a whole gait cycle, each phase is divided into a pre-stride state and a post-stride state by the stride movement. Each state indicates a situation, recording the positions of all of the feet as well as robot's centre of gravity. Therefore, in 10 states during a gait cycle, the analysis evaluates each gait sequence in terms of its stability, as shown in Figure 3.

The Sequential "3+2" Gait provides an even utilization of striding legs while maintaining the basic stability in locomotion. However, by presenting a sequence permutation between five striding foot-pairs, the number of various gaits reaches the factorial of 5, equals to 120.

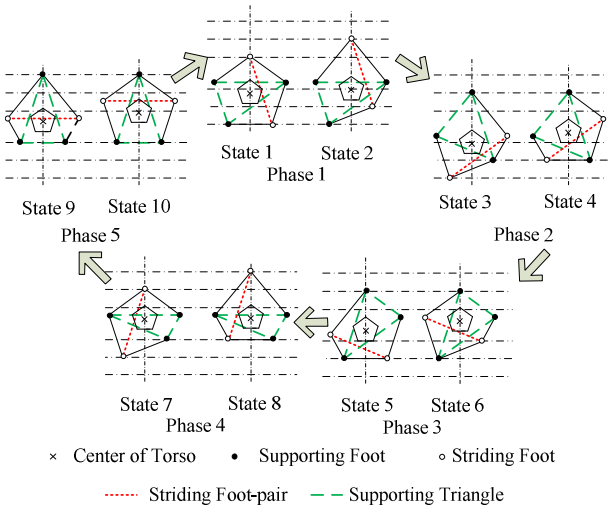

Figure 3: In each phase of a gait cycle, the pre-stride state is numbered with odd numbers while the post-stride state with even numbers. These ten states are sufficient for demonstrating interaction between the centre of gravity and supporting triangle.

Stability Analysis

The stability margin is defined as the minimum distance from the projection of the centre of gravity to one of the edges of the supporting triangle. When the projection of the centre of gravity falls out of the supporting triangle, the robot will be no longer stable to stand on the supporting legs.

The stability margin is investigated as a key value in evaluating the stability of a gait. When the walking direction x is given, a 120×10 matrix $M(x)_{n,s}$ can be derived, where $M(x)_{n,s}$ indicates the stability margin of s^{th} state in No. n gait.

Two indicies are designated as the reference of the stability of a gait. The first is the minimum stability margin $M(x)_{n_{min}}$, which evaluates the most vulnerable

situation to disturbances during the whole period. The summed stability margin $M(x)_{n_{total}}$ is used to investigate the overall stability of a gait.

When the projection of the centre of gravity falls out of the supporting triangle, we deem that $M(x)_{n,s}$ does not exist. Thus the value of $M(x)_{n_{min}}$ and $M(x)_{n_{total}}$ will not be calculated due to its instability.

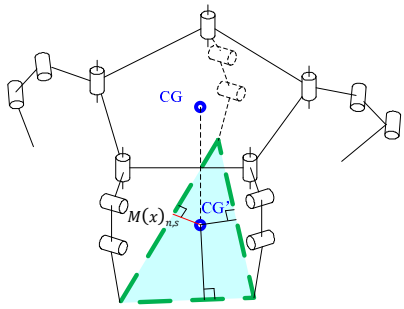

CG- Center of Gravity;
$M(x)_{n,s}$ - Minimum Distance from Projection of Centre of Gravity to Edge of the Supporting Triangle

Figure 4: The Definition of Stability Margin

By investigating the stability margin in each state, any gaits with unstable states are eliminated.

Simulation

A series of parameters derived from the model of our modular pentapedal robot prototype is adopted correspondingly in the simulation.

The robot's five hips are placed at the five corners of a pentagon with a diameter of 188mm, while the feet are set similarly on a pentagon with a diameter of 340mm. The torso is set horizontally at a height of 90mm. The pace length for each stride is 100mm, as shown in Figure 5. Due to the evenness of leg placement, the robot's centre of gravity is supposed to coincide with the centre of the torso.

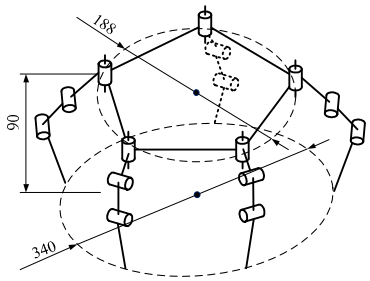

Figure 5: General Set-up of Simulation Model of Pentapedal Robot

The model has five identical legs equally distributed around the torso. Each leg consists of three identical modules, providing three degrees of freedom for transition movement. The kinematic geometry of each leg is shown as Figure 6.

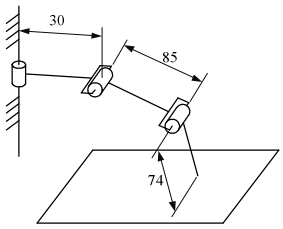

Figure 6: The Kinematic Model of the Robot's Leg

The stability margins of all states are calculated among 120 gaits. The calculation is performed when the walking direction is set at 90°, 84°, 78°, 72°, 66°, 60° and 54°. These 7 directions are selected evenly between 54° and 90° with an interval of 6°, sufficiently showing the distribution of superior gaits in this range of directions.

Stability in the 90° Walking Direction

When the robot moves in the direction of 90°, 52 gaits keep their stability margins above 0 during all the states. The minimum stability margin during the 10 states is calculated as described in (1).

$$M(90)_{n_{min}} = \mathrm{Min}\{M(90)_{n,s}\} \quad (1)$$

Table 1: List of Stable Gaits in 90° Walking Direction

Gaits with Specified Sequences	$M(90)_{n_{min}}$ (mm)
No.79(2-3-4-5-1); No.94(2-1-5-4-3) No.80(2-3-4-1-5); No.93(2-1-5-3-4) No.83(2-3-1-5-4); No.92(2-1-3-4-5) No.84(2-3-1-4-5); No.91(2-1-3-5-4)	20.21
No.49(3-4-5-2-1); No.119(1-5-4-2-3) No.51(3-4-2-5-1); No.118(1-5-2-4-3) No.52(3-4-2-1-5); No.117(1-5-2-3-4) No.63(3-2-4-5-1); No.113(1-2-5-4-3) No.64(3-2-4-1-5); No.114(1-2-5-3-4) No.65(3-2-1-4-5); No.110(1-2-3-5-4) No.66(3-2-1-5-4); No.109(1-2-3-4-5)	12.58
No.15(5-2-4-3-1); No.40(4-2-5-1-3) No.16(5-2-4-1-3); No.39(4-2-5-3-1) No.17(5-2-1-4-3); No.37(4-2-3-5-1) No.18(5-2-1-3-4); No.38(4-2-3-1-5) No.73(2-4-3-5-1); No.89(2-5-1-4-3) No.74(2-4-3-1-5); No.90(2-5-1-3-4) No.75(2-4-5-3-1); No.88(2-5-4-1-3) No.76(2-4-5-1-3); No.87(2-5-4-3-1)	4.54
No.1(5-4-3-2-1); No.29(4-5-1-2-3) No.3(5-4-2-3-1); No.28(4-5-2-1-3) No.4(5-4-2-1-3); No.27(4-5-2-3-1) No.5(5-4-1-2-3); No.25(4-5-3-2-1) No.21(5-1-2-3-4); No.34(4-3-2-1-5) No.22(5-1-2-4-3); No.33(4-3-2-5-1) No.23(5-1-4-2-3); No.31(4-3-5-2-1)	4.03

Secondly, the sum of stability margins in 10 states is also calculated as an alternative reference to evaluate the stability of gaits as described in (2).

$$M(90)_{n_{total}} = \sum_{s=1}^{10} M(90)_{n,s} \quad (2)$$

Table I shows that the minimum stability margins of gaits. All the stable gaits only appear to have 4 values as 20.21, 12.58, 4.54 and 4.03. At the same time, gaits that are symmetric with respect to the 90° axis appear to have the same result since the direction of 90° coincides with the symmetry axis.

Gaits whose first two striding foot-pairs are identical appear to have the same minimum stability margins. In other words, the selection of striding foot-pairs in the first two phases is critical to the total stability of the whole cycle.

Figure 7 shows the total stability margin of 10 states for the 52 gaits in the blue column, together with the minimum stability margins from Table I represented by the red column. The gaits with a higher minimum stability margin also dominate in total stability margin.

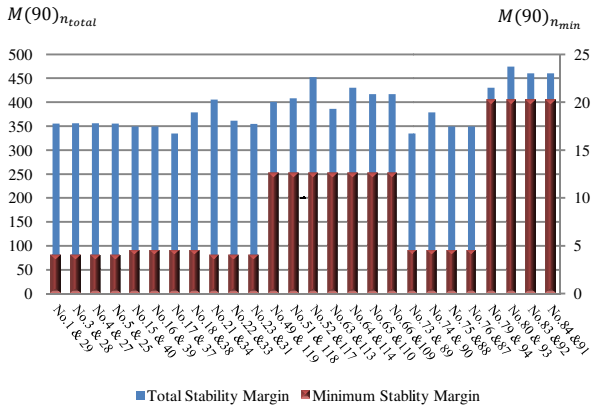

Figure 7: Total and Minimum Stability Margin of All the Stable Gaits in the 90° Walking Direction

Stability in the Range between 54° and 90°

Similar simulations are repeatedly carried out while the walking direction is set to 84°, 78°, 72°, 66°, 60° and 54°.

28 gaits are able to keep their stability margin above zero in these directions. The sets of top-ranking gaits in these walking directions still show great similarity due to the change of direction.

The calculation of the stability margin is performed in a widened range. Equations (3) and (4) show the minimum and total stability margin of a gait in the 7 walking directions.

$$M_{n_{min}} = Min\begin{Bmatrix} M(90)_{n_{min}}, M(84)_{n_{min}}, M(78)_{n_{min}}, \\ M(72)_{n_{min}}, M(66)_{n_{min}}, M(60)_{n_{min}}, \\ M(54)_{n_{min}} \end{Bmatrix} \quad (3)$$

$$M_{n,total} = M(90)_{n_{total}} + M(84)_{n_{total}} + M(78)_{n_{total}} + M(72)_{n_{total}} + M(66)_{n_{total}} + M(60)_{n_{total}} + M(54)_{n_{total}} \quad (4)$$

Figure 8 shows the gaits with dominant minimum stability margins and total stability margins.

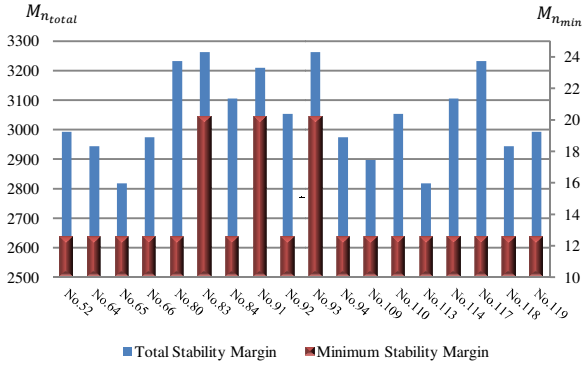

Figure 8: Total and Minimum Stability Margin of Dominant Stable Gaits in 7 Walking Directions

No.83(2-3-1-5-4), No.91(2-1-3-5-4) and No.93(2-1-5-3-4) gaits keep their minimum stability margin above 20mm, and also keep high total stability margins among all the situations.

Gait Transformation for Omni-directional Locomotion

After investigating the stability of the 120 gaits in the range between 54° and 90°, three superior gaits with extraordinary stability emerged from the 120 gaits. By analyzing the axial and radial symmetric characteristics, these three gaits can be transformed appropriately to fit locomotion in directions other than the range between 54° to 90°.

According to the numbering in Figure 2, Foot-pair 1 and 4 is respectively symmetric to Foot-pair 3 and 5 with respect of 90° axis. Therefore, the three best gaits in the range between 90° and 126° are derived as 2-1-3-4-5, 2-3-1-4-5 and 2-3-4-1-5.

Table 2: Optimised Gaits in All Walking Directions

Walking Direction	Selected Gaits
[54°,90°)	2-3-1-5-4; 2-1-3-5-4; 2-1-5-3-4
[90°,126°)	2-1-3-4-5; 2-3-1-4-5; 2-3-4-1-5
[126°,162°)	3-4-2-1-5; 3-2-4-1-5; 3-2-1-4-5
[162°,198°)	3-2-4-5-1; 3-4-2-5-1;3-4-5-2-1
[198°,234°)	4-5-3-2-1; 4-3-5-2-1; 4-3-2-5-1
[234°,270°)	4-3-5-1-2; 4-5-3-1-2; 4-5-1-3-2
[270°,306°)	5-1-4-3-2; 5-4-1-3-2; 5-4-3-1-2
[306°,342°)	5-4-1-2-3; 5-1-4-2-3; 5-1-2-4-3
[342°,18°)	1-2-5-4-3; 1-5-2-4-3; 1-5-4-2-3
[18°,54°)	1-5-2-3-4; 1-2-5-3-4; 1-2-3-5-4

Considering the radial symmetric characteristics, the corresponding gaits in other directions can also be derived by shifting the foot-pairs, as shown in Table 2.

V. EXPERIMENT

The experiment evaluating the sequential "3+2" gait is performed on our pentapedal robot. In fact, all of the geometric parameters and initial set-up in our simulation are inherited from this robot prototype.

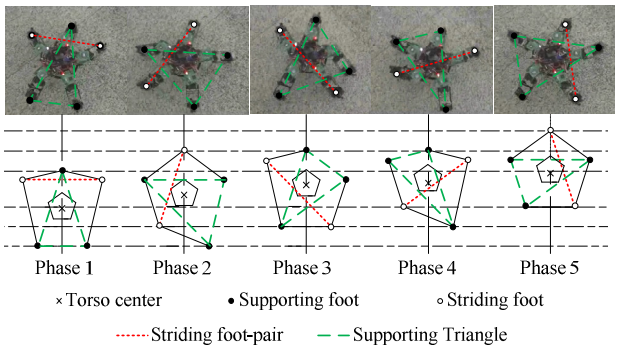

Figure 9: The pentapedal robot succeeds in walking in a stable manner. The picture below shows gait No.79(2-3-4-5-1) in comparison with the snapshots above.

During the experiments, the robot walks on a horizontal even plane, while it performs all of the 120 gaits. The gait parameters are also set identical to the simulation. The walking direction is set to 90°.

Gait stability is judged based on observation. When the robot does not stand on the supporting legs as planned, or any clash of legs appears, the current gait will be deemed instable.

The experimental result shows the 22 gaits which have their minimum stability margin equals to 20.21 and 12.58 in Table I to have satisfying performance. Other gaits, including the ones with minimum stability margins below 10, show the instability in some phases during a gait cycle.

The experiments also show that all these 22 stable gaits do not appear to have any clash between legs. In other words, maintaining sufficient stability margin can, at the same time, guarantee a sparse lay-out of legs, and thus prevent the clash from occurring.

VI. CONCLUSION

The modeling and simulation has greatly reduced the work of testing various gaits, and provided helpful reference to judge the stability of gaits.

The greatest achievement of our research is a locomotion control strategy toward a modular pentapedal robot. First, the modular configuration of an omni-directional pentapedal robot was introduced. A large group of gaits was derived after the Sequential "3+2" Gait had been defined. Following this, a series of analysis and simulation were performed to select the most stable gaits, by calculating and comparing the minimum and total stability margins in various conditions. Lastly, experiments were carried out on our robot prototype, giving evidence that high-ranking gaits provide the robot with sufficient stability in locomotion.

Thus, the research on pentapedal robot is only confined in the locomotion on horizontal and even surface. It is desirable to expand this method to accommodate more complicated environment in future. In addition, the highly pre-defined gaits deprive the possibility which enables the robot to decide the striding strategy according to the current situation. An intelligent algorithm with reversed mechanism will be appreciated to accomplish the gait generation.

REFERENCES

Aoi S, Sasaki H and Tsuchiya K. 2006. "Turning Maneuvers of a Multi-legged Modular Robot Using Its Inherent Dynamic Characteristics". In Proceedings of International Conference on Intelligent Robots and Systems.IEEE. 180-185.

Chen W, Yao S H , Low K H . 1997. "Modular formulation for dynamics of multi-legged robots". In Proceedings of 8th International Conference on Advanced Robotics (Jul.7-9). 279-284.

Daidié D, Barbey O et al..2007. "The DoF-Box Project: An Educational Kit for Configurable Robots". Proceeding of Advanced Intelligent Mechatronics 2007(Zurich, Switzerland, Sep.4-7). 1-6.

González-Gómez J, Zhang H et al..2006. "Locomotion Capabilities of a Modular Robot with Eight Pitch-Yaw-Connecting Modules". In Proceeding of International Conference on Climbing and Walking Robots 2006(Brussels, Belgium, Sep.12-14).

Gonzalez-Gomez J, Zhang H, Boemo E. 2007. "Locomotion Principles of 1D Topology Pitch and Pitch-Yaw-Connecting Modular Robots", In Bioinspiration and Robotics: Walking and Climbing Robots 2007, Maki K. Habib (Ed.), Advanced Robotic System and I-Tech Education and Publishing. Vienna, Austria, 403-428.

Kurokawa H, Kamimura A, Yoshida E et al. 2003. "M-TRAN II: metamorphosis from a four-legged walker to a caterpillar". In Proceedings of International Conference on Intelligent Robots and Systems 2003(Las Vegas, USA, Oct.27-31). IEEE.Vol.3, 2454-2459.

Paap K L, Christaller T, Kirchner F. 2000. "A robot snake to inspect broken buildings". In Proceeding of International Conference on Intelligent Robots and Systems 2000 (Takamatsu, Japan, Oct.30-Nov.5).IEEE. 2079-2082.

Prihastono, Wicaksono H., Anam K. et al. 2009. "Autonomous five legs robot navigation in cluttered environment using fuzzy Q-learning and hybrid coordination node". In Proceeding of International Joint

Conference on Control, Automation and System. ICCAS-SICE. (Fukuoka, Japan, Aug.18-21), 2871-2874.

Ohira M, Chatterjee R, Kamegawa T and Matsuno F. 2007. "Development of Three-legged Modular Robots and Demonstration of Collaborative Task Execution". In Proceeding of International Conference on Robotics and Automation (Apr.10-14). IEEE, 3895-3900.

Yim M, Shen W et al. 2007. "Modular Self-Reconfigurable Robot Systems: Challenges and Opportunities for the Future". IEEE Robotics & Automation Magazine, Vol.14, No.1, March 2007. 2-11.

Zhang H, González-Gómez J, Chen S et al. 2007. "A Novel Modular Climbing Caterpillar Using Low-frequency Vibrating Passive Suckers", In Proceeding of Advanced Intelligent Mechatronics 2007. (Zurich, Switzerland, Sep.4-7). 1-6.

Zhang H, Gonzalez-Gomez J, Xie Z, Cheng S, Zhang J. 2008. "Development of a Low-cost Flexible Modular Robot GZ-I". In Proceeding of 2008 International Conference on Advanced Intelligent Mechatronlics (Xi'an, China, Jul.2-5). 223-228.

Zhang H, Xie Z, González-Gómez J, Zhang J. 2009. "Embedded Intelligent Capability of a Modular Robotic System". In Proceeding of International Conference on Robotics and Biomimetics (Bangkok, Thailand, Feb.22-25). IEEE. 2061 - 2066.

Zhang J, Jinsong W and Bopeng Z. 1996. "The locomotive mode study on five-limbed robots". In Proceedings of International Conference on Systems, Man and Cybernetics. IEEE, Vol. 2, 1595-1600.

Zhang J, Kiantiong Y and Jinsong W. 1997. "A multi-limbed underwater robot and its gait study". In Proceedings of International Conference on Systems, Man, and Cybernetics. IEEE, Vol.1, 755-760

Zimmermann K, Zeidis I, Steigenberger J. 2004. "On artificial worms as chain of mass points". In Proceeding of International Conference on Climbing and Walking Robots 2004. 11-18.

AUTHOR BIOGRAPHIES

CONG LIU works in Aalesund University College as a PhD candidate since October 2011. He received his Master's diploma in Mechanical Electronics Engineering from Beihang University in Beijing.
Email: lico@hials.no.

FILIPPO SANFILIPPO was born in Catania, Italy and obtained his Master's Degree in Computer Engineering at University of Siena in 2011. He worked for six months at Laboratory of Technical Aspects of Multimodal Systems in University of Hamburg, investigating modularity in robotics.
Email: fisa@hials.no.
Web-page:
http://www.hials.no/eng/hials/research/mechatronics/people/filippo_sanfilippo.

HOUXIANG ZHANG received Ph.D. degree in Mechanical and Electronic Engineering in 2003. From 2004, he worked as Postdoctoral Fellow at the Institute of Technical Aspects of Multimodal Systems (TAMS), Department of Informatics, Faculty of Mathematics, Informatics and Natural Sciences, University of Hamburg, Germany. Dr. Zhang joined the Department of Technology and Nautical Sciences, Aalesund University College, Norway in April 2011 where he is a Professor on Robotics and Cybernetics.
Email: hozh@hials.no.

HANS PETTER HILDRE is a Professor on product and system design at the Department of Technology and Nautical Sciences, Aalesund University College, Norway.
Email: hh@hials.no.

CHANG LIU is PhD candidate Robotics Institute, Beihang University, Beijing.
Email: lcyituo0x01@163.com

SHUSHENG BI, born in 1966, is currently a professor at Robotics Institute, Beihang University, China. He received his PhD degree from Beihang University, China, in 2002. His research interests include bionic under water robots, birdlike robots, and flexible microstructure design.
Email: biss_buaa@163.com.

Adjustment of the nonlinear parameters in dynamic simulations of steam generators

Dipl.-Ing. Peter Tusche
Institute of Process Technique, Process Automation and Measuring Technique (IPM)
University of Applied Sciences Zittau/Goerlitz, Germany
Email: ptusche@hs-zigr.de

Prof. Dr.-Ing. habil. Tobias Zschunke
Department of Mechanical Engineering
Chair of Power Plant Technology and Power Engineering
University of Applied Sciences Zittau/Goerlitz, Germany
Email: tzschunke@hs-zigr.de

Prof. em. Dr.-Ing. habil. Rainer Hampel
University of Applied Sciences Zittau/Goerlitz, Germany
Email: r.hampel@hs-zigr.de

KEYWORDS

dynamic simulation, Oxyfuel, load change operation mode, modelling

ABSTRACT

In the long term, due to political decisions and changes in the market of power generation, the position of German coal-fired power plants as base load plants is in question. This fact requires further consideration for the use as highly dynamic power plant in the range of peak load coverage. Dynamic behavior assessment of steam generators related to load change operation, start-up and shut-down processes is in the focus of power plant operators also with regard to possible wear and tear of the components.
Moreover, an innovative technology is being investigated. In the near future, the oxyfuel process, depicting a climate-friendly combustion technology of lignite and hard coal, will be ready for production and applied in large power plants. The use of simulation tools is a low-cost option to gain knowledge from analyses about the behavior of steam generators in dynamic operation or untypical situations without any component damage. The use of dynamic simulations is also reasonable if in addition a new combustion technology is used that is not applied in large power plants yet.
Content of this paper is the modelling of power plant components for the use in complex dynamic systems and the simulation of these highly dynamic processes. The way of modelling is explained by means of an example.

NOMENCLATURE

t	$[s]$	time
m	$[kg]$	mass
p	$[bar]$	pressure
$\dot{m}$	$\left[\frac{kg}{s}\right]$	massflow
h	$\left[\frac{kJ}{kg}\right]$	enthalpy
ξ	$\left[\frac{kg}{kg}\right]$	mass concentration
ϑ	$[^\circ C]$	temperature
ρ	$\left[\frac{kg}{m^3}\right]$	density
v	$\left[\frac{m^3}{kg}\right]$	specific volume
g	$\left[\frac{m}{s^2}\right]$	acceleration of gravity
c	$\left[\frac{J}{kg \cdot K}\right]$	specific heat capacity
V	$[m^3]$	volume
z	$[m]$	heigth
d	$[m]$	diameter
L	$[m]$	length
s	$[m]$	wall thickness
r	$[m]$	radius
A	$[m^2]$	flow cross-section
α	$\left[\frac{W}{m^2 \cdot K}\right]$	heat-transfer coefficient
ζ	$[-]$	pressure loss coefficient
$\dot{Q}$	$[W]$	heat flow
T	$[s]$	time constant
K	$[-]$	amplification factor
x	$[-]$	output data
u	$[-]$	input data

Proceedings 26th European Conference on Modelling and Simulation ©ECMS Klaus G. Troitzsch, Michael Möhring, Ulf Lotzmann (Editors)
ISBN: 978-0-9564944-4-3 / ISBN: 978-0-9564944-5-0 (CD)

in	inlet
out	outlet
W	wall
F	fluid

INTRODUCTION

Dynamic Simulations

The use of dynamic simulations has rapidly increased during the last years in many fields of science and technology. The temporal transient behavior of many instationary processes is analyzed in computer models and used for optimization. Interventions like setpoint controlled operation or process control procedures often provide solutions for transient processes which are economically more efficient and also more sparing for the component. The dynamic behavior of the overall system which consists of a combination or overlap of several instationary sub-processes, can simply be depicted by the application of dynamic simulation tools which was usually impossible in the conventional way by expert knowledge.

In power plant technology the focus is placed on the analysis of accident situations or simulated load changes as well as the start-up and shut-down of complete plants. The analysis may avoid possible destructions of particular plant components by incorrect parameters. Thus, the occurring economic costs caused by the blackout of large plants e.g. power plants can be minimized or even avoided.

Another point is efficiency improvement in power plant operation and the consideration of aspects during the design phase of large plants. Innovative solutions are investigated and tested by means of dynamic simulation models. The low cost option for checking the dynamic behavior during the dimensioning of power plants is indispensable at vast investment costs like new building of large power plants. In the near future, part-load operation will mainly be used in conventional steam generators. For the operators, this change will raise several questions in terms of availability and economic efficiency which can simply be analyzed by dynamic simulations.

Oxyfuel Process

Being an innovative combustion technology, the oxyfuel process can be categorized into the line of combustion processes of lignite and hard coals. Carbon dioxide CO_2, which is harmful for the climate and which arises from the combustion with pure oxygen and from the exhaust gases during distilling separation of water in high concentration, is being prepared and compressed and shall finally be stored in the underground. The oxyfuel process proceeds according to the scheme depicted in figure (fig: 1) and is described as follows: In

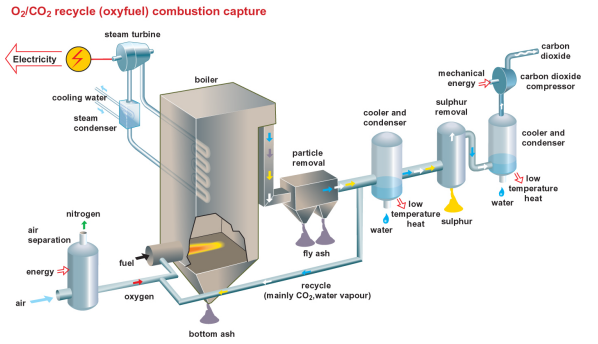

Figure 1: OxyFuel process (6)

the air separation facility, pure oxygen is provided as an oxidant. The coal is combusted with a material mixture of oxidant and recirculating flue gas. Due to the recirculation of dust and ash-less flue gas, the combustion temperature decreases to parameters permitted for steam generators with regard to component wear and tear of the heat transfer heating surfaces. The inert nitrogen missing in the oxidant is replaced by the recirculation of flue gas so that the mass flow of the combustion gas changes only marginally compared to the conventional combustion with air. Here, the composition of flue gas and its associated specific values and properties are determining for the transmission properties in the steam generator. After dust separation the flue gas is partly recirculated. The remaining exhaust gas consists basically of carbon dioxide and is cooled for water separation. It is then compressed and stored underground.

Simulation Software Dynstar

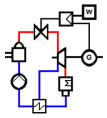

With the help of Dynstar, an in-house developed simulation tool of Zittau/Goerlitz University, simple control sections up to complex systems can be modeled. On a graphical surface, function blocks are placed and interconnected in a way the process simulation becomes possible. The various function block libraries contain many different function blocks which offer multiple possibilities for process modelling. For the simulation of power plant processes plant components like heat exchanger, pump, turbine stage, condenser, tube, valve, mixing or distribution elements are modeled. Special property libraries have been implemented for

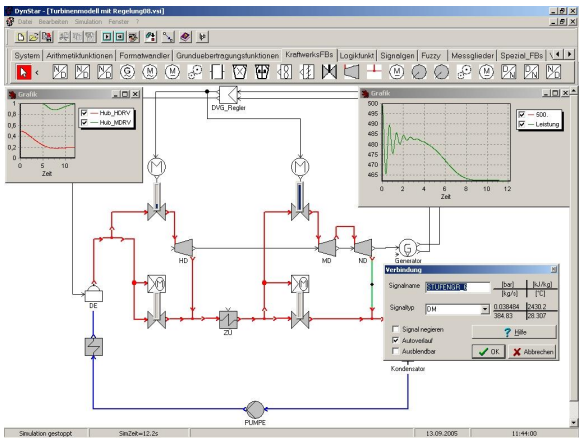

Figure 2: Simulation Software Dynstar (5)

modelling thermodynamic processes and the application of special media like water and combustion gases. Library LibIF97 (1) is applied for water or steam and for ideal gases is used library LibIDGas (2).

MODELLING

Structure Of The Models

For the modelling of a combustion process using a new innovative technology no measuring values are available for the user. ”Black-box” modelling is thus excluded. The lack of expert knowledge or operating point dependent design data of the steam generator components for various load cases and dynamic switching operation of a start-up process of the plant with air and a later switching to oxyfuel process makes the modelling by means of the ”grey box” model impossible as well. Thus, to the modeler must be given complete constructive and geometric data to simulate the physical laws, just as in the ”glass box” model in figure (fig: 3) (3). The function blocks

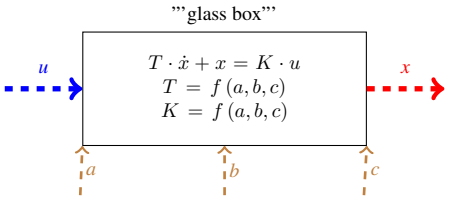

Figure 3: ’glass box’ model

for imaging thermodynamic processes in Dynstar are designed according to the scheme in figure (fig: 4). Flow variables like mass flow, and state variables like pressure, enthalpy and the composition of substances are the input and output data for the model. Constructive data, geometric variables and material data depict the parameters. Related to the modelling of thermodynamic

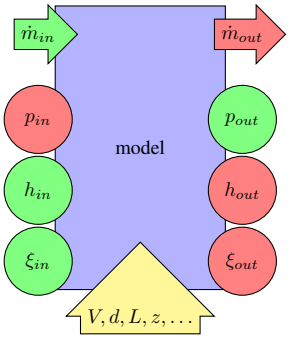

Figure 4: modelling scheme at Dynstar

processes, Dynstar has a special feature in bidirectional processing of input and output data. Contrary to the other variables mass flow, enthalpy and composition of substances, the pressure has a reverse direction of data processing. The reasonable interconnection of function block inputs and outputs as indicated in figure (fig: 5) produces the image of the instationary process which is going to be analyzed.

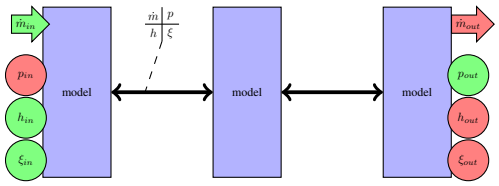

Figure 5: simulation assembly

Model of a tube bundle heat exchanger

As a transfer function, the modelling of a tube bundle heat exchanger (fig: 6) using the given constructive data from a reference power plant of one of the leading German power generating companies, contains an equation system of non-linear differential equations with distributed parameters. The system is reasonably dissected and flow principles are particularly considered. The following figures (fig: 7) depict this subdivision. Due to the different flow course of the hot and cold fluid within the heat exchanger, the submodels are indexed according to a matrix design. The shifting of the flow-specific complex heat exchanger into a circuit of heat exchangers having an ideal flow-through provides advantages for system calculation. The heat exchange without calculating the logarithmic temperature difference by axial discretization allows

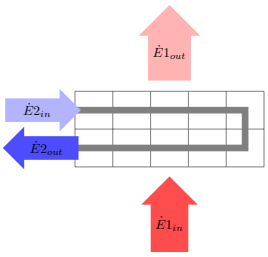

(a) flow scheme of a tube bundle heat exchanger

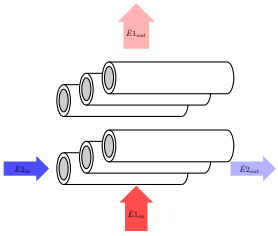

(b) energy flow at the tube bundle

Figure 6: flow scheme of a tube bundle heat exchanger

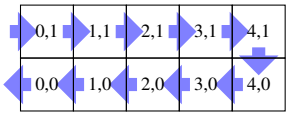

(a) flow scheme of the cold fluid

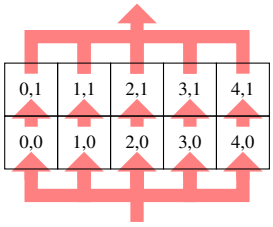

(b) flow scheme of the hot fluid

Figure 7: flow scheme in matrix structure

the calculation with the ideal heat transfer through the superheater tubes, as in figure (fig: 6). The finite volume method is here applied.

Submodel 'Fluid'

A fluid flows through a control volume and releases or absorbs diffusive energy through the outer surfaces in the form of heat, depending on the amount of temperature difference. The thermodynamic state of the fluid at the output is calculated by means of the energy flow balances (eq:2), mass flow balances (eq:1), and material flow balances(eq:3).

$$\dot{m}_{in} - \dot{m}_{out} = V \cdot \frac{d\rho}{dt} = -\frac{V}{v^2} \cdot \frac{dv}{dt} \tag{1}$$

$$\begin{aligned} &\frac{V}{v} \cdot \frac{dh}{dt} - V \cdot \frac{dp}{dt} + h \cdot (\dot{m}_{in} - \dot{m}_{out}) \\ = \; & P + \dot{Q} + \dot{m}_{in} \cdot \left(h_{in} + \frac{\dot{m}_{in}^2 \cdot v_{in}^2}{2 \cdot A_{in}^2} + g \cdot z_{in} \right) \\ & - \dot{m}_{out} \cdot \left(h_{out} + \frac{\dot{m}_{out}^2 \cdot v_{out}^2}{2 \cdot A_{out}^2} + g \cdot z_{out} \right) \end{aligned} \tag{2}$$

$$\begin{aligned} &\frac{d\xi}{dt} \cdot \frac{V}{v} + \xi \cdot (\dot{m}_{in} - \dot{m}_{out}) \\ = \; & \dot{m}_{in} \cdot \xi_{in} - \dot{m}_{out} \cdot \xi_{out} \end{aligned} \tag{3}$$

$$\dot{Q} = \alpha \cdot A_W \cdot (\vartheta_F - \vartheta_W) \tag{4}$$

The flow-caused pressure loss is calculated with the use of Bernoullis Theorem (eq:5) under consideration of fluid friction on the walls (eq:6).

$$\begin{aligned} p_{in} - p_{out} = \; & g \cdot \left(\frac{z_{out}}{v_{out}} - \frac{z_{in}}{v_{in}} \right) + \frac{\dot{m}_{out}^2 \cdot v_{out}}{2 \cdot A_{out}^2} \\ & - \frac{\dot{m}_{in}^2 \cdot v_{in}}{2 \cdot A_{in}^2} + \Delta p_{friction} \end{aligned} \tag{5}$$

$$\Delta p_{friction} = \zeta \cdot \frac{L}{d} \cdot \frac{\dot{m}^2 \cdot v}{2 \cdot A^2} \tag{6}$$

The calculation rules for pressure loss coefficients $\zeta = f\left(\dot{m}, p, h, \xi, \vartheta_W, d, L, R_z\right)$ are calculated according to the VDI-heat atlas (4). The nonlinear system of

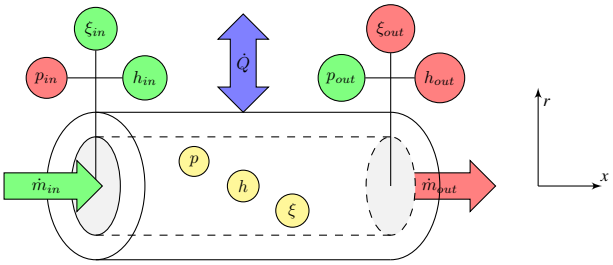

Figure 8: thermodynamic quantities at the pipe section

differential equations requires the description of average values of the control volume. The static energy and material balances for a flow-through system are the calculation basis of yet unknown average state variables (eq:7), (eq:8),(eq:9).

$$p = p_{in} \cdot \frac{A_{in}}{A_{in} + A_{out}} + p_{out} \cdot \frac{A_{out}}{A_{in} + A_{out}} \tag{7}$$

$$h = \frac{A_{in} \cdot v_{out} \cdot h_{in} + A_{out} \cdot v_{in} \cdot h_{out}}{A_{in} \cdot v_{out} + A_{out} \cdot v_{in}} \tag{8}$$

$$\xi = \frac{A_{in} \cdot v_{out} \cdot \xi_{in} + A_{out} \cdot v_{in} \cdot \xi_{out}}{A_{in} \cdot v_{out} + A_{out} \cdot v_{in}} \tag{9}$$

The specific volume can be obtained from the already mentioned specific property tables via functions $v = f\left(p, h, \xi\right)$ (1),(2).
The heat flux over the outer surfaces is the coupling variable with another basic model: Instationary heat conduction through a tube wall.

Submodel 'Wall'

In this submodel also, the energy flow balance (eq:10) is the focus of considerations. Having solid walls, a linear equation system develops which is locally discretized according to the finite volume method and with the linearization of the material constant for the storing effects. Related to average wall temperatures as in figure (fig: 9), the calculation rule for static calculation of temperatures in a cylinder wall is applied (eq:11),(eq:12).

$$\dot{Q}_{in} - \dot{Q}_{out} = \frac{V}{v} \cdot c \cdot \frac{d\vartheta}{dt} \tag{10}$$

$$\vartheta\left(r\right) = (1 - x) \cdot \vartheta_i + x \cdot \vartheta_a \tag{11}$$

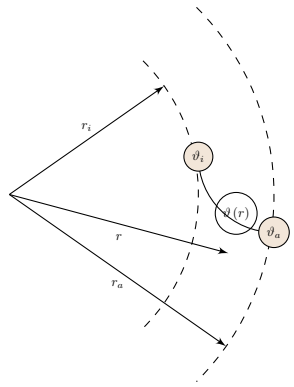

Figure 9: scheme of the nonlinear discretisation method for a cylinder wall

$$x\left(r=\frac{r_i+r_a}{2}\right)=\frac{ln\left(1+\frac{s}{2\cdot r_i}\right)}{ln\left(1+\frac{s}{r_i}\right)} \tag{12}$$

Direct Coupling 'Fluid' with 'Wall'

Both submodels are directly coupled through the diffusive energy flow of the heat transfer, as it is shown in figure (fig: 10). But the energy flow has nonlinear values as in the heat transfer coefficients $\alpha = f\left(\dot{m}, p, h, \xi, \vartheta_W, d, L\right)$ in calculation rule according to (4). The calculation of the coefficient is indirectly back-coupled with the submodels via the temperature of the fluid on one hand and via the wall on the other hand. Flow conditions and substance constants do influence the alpha-value as well. The iterative

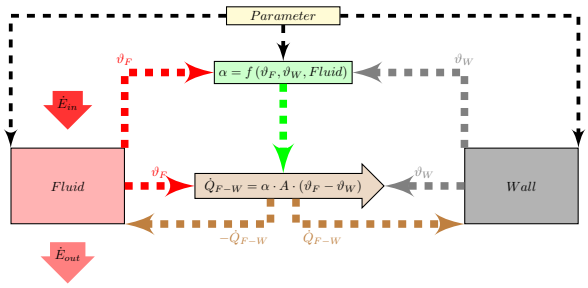

Figure 10: scheme of the direct coupling between 'Fluid' and 'Wall'

adjustment of nonlinear parameters to the current conditions and sequential processing of the submodel calculations require high effort in calculation which, however, provides the topicality of nonlinear parameters. This advantage plays a significant role in load change operation of power plants which will be gone into explicitly in the conclusion.

The following example depicts an instationary transition process of a heat exchanger.

SIMULATION AND RESULTS

A sudden load demand from full-load to 70% also causes a change of the material flow in both fluids (tab: 1). The complexity of such a load change operation is not supposed to be the subject of this simulation. A ramp-shaped reduction of the flue gas flow and steam mass flow in an interval of 10s is sufficient to show how non-linear parameters of the heat transfer coefficient (fig: 14) behave within the model coupling during changes on the inputs of the overall model and which effects does it have on the transferred heat flux (fig: 13) or on the wall (fig: 12) and fluid temperatures (fig: 11).

quantity	unit	value
$\dot{m}_1$	$\left[\frac{kg}{s}\right]$	415(100s) to 290(110s)
$\dot{m}_2$	$\left[\frac{kg}{s}\right]$	226(100s) to 158(110s)
$\vartheta 1_{in}$	$[°C]$	842
$\vartheta 2_{in}$	$[°C]$	491.2
p_1	$[bar]$	1.01325
p_2	$[bar]$	174
ξ_2	$\left[\frac{kg}{kg}\right]$	$N_2 = 0.64, CO_2 = 0.18,$ $H_2O = 0.15, O_2 = 0.04$

Table 1: input values

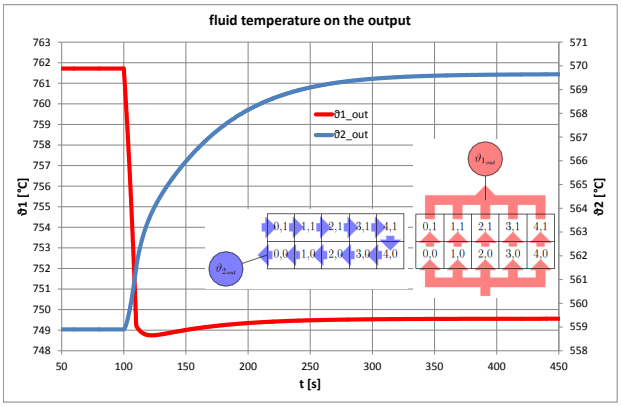

Figure 11: fluid temperature diagramm

DISCUSSIONS

A fast simulated ramp-shaped load change caused by the reduction of mass flow of the cold and hot fluid also has a direct impact on the working point of the superheater.

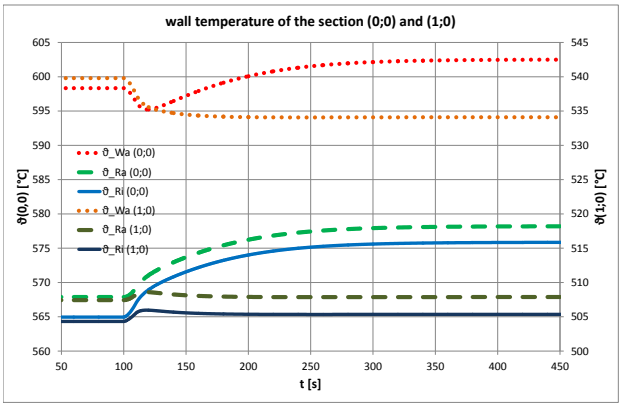

Figure 12: wall temperature diagramm

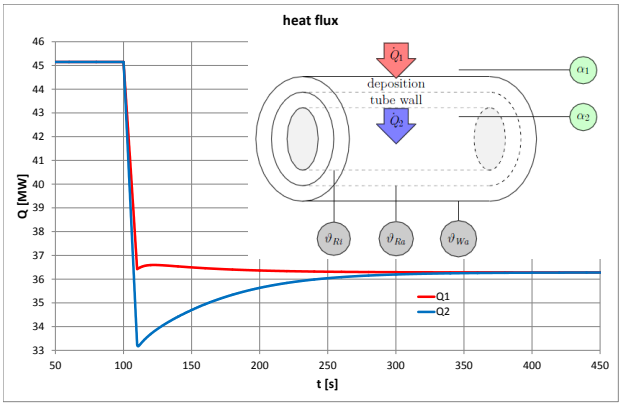

Figure 13: heat flux diagramm

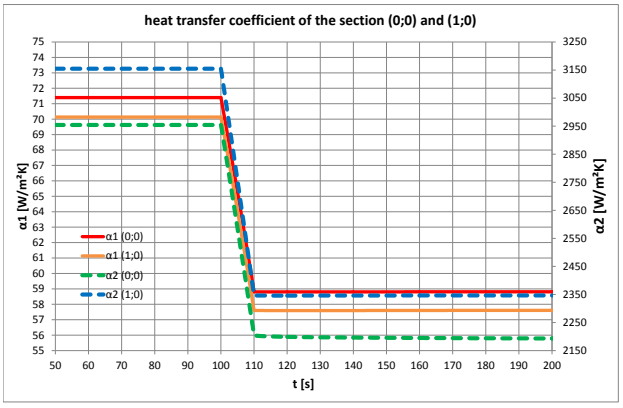

Figure 14: heat transfer coefficient diagramm

The transferred power decreases by ca. 20% as it can be seen in figure (fig: 13). The instationary transition process into the new working point is finished after about 5min. The adjustment of interior (T_{Ri}) and exterior tube temperatures (T_{Ra}) and the temperature of the debris layer on the hot side (T_{Wa}) in (fig: 12) related to matrix structures in (fig: 7) to the new values is finished and no difference between the hot medium onto the wall (Q_1) and the heat flux from the wall onto the cold medium (Q_2) could be found - the energy storing processes in the wall are completed. The change of heat transfer coefficient (fig: 14) is enormously visible in the range of mass flow change but continues marginally due to the change of fluid temperatures (fig: 11). The adjustment process to the new load-change working point requires a similar period of time as the instationary transfer process described before.

CONCLUSION

The system dynamic during load change operation is depicted in the diagrams. The instationary process of the tube bundle heat exchanger during jump-like changes takes several minutes until stationary behavior of the heat transfer does exist in the new working point with new wall temperatures of the tube. In each step of the calculation, the nonlinear coupling functions of the heat transfer are adjusted to the current conditions as well.

OUTLOOK

The topicality of the nonlinear parameters is an essential point in modelling the oxyfuel process. During start-up the steam generator is initially working in air operation.After reaching its operation temperature it is switched to the innovative combustion technology (fig: 15). The inert nitrogen which due to air combustion is yet contained in the recirculated flue gas will be completely replaced by carbon dioxide after some time elapsed. For this process showing permanent changes in material composition and thus also nonlinearities in all thermodynamic state variables, the topicality of the parameters to the current conditions by iterative adjustment and sequential calculation of all submodels is indispensable for correct analysis of the switching process. Linearization is possible only to a limited extent and may lead to distortions. To allow the optimization of the switching process at a later point in time it is essential to act to the process as close as possible. The application of this kind of modelling is thus required.

FUTURE PROSPECTS

Goal of the work is to design a complete steam generator model which is able to simulate the start-up process containing the switching process which has already been referred to. Heat exchangers, tubes for the recirculation line and combustion-specific components have been produced. The interconnection of these components and the function test of the overall model are further

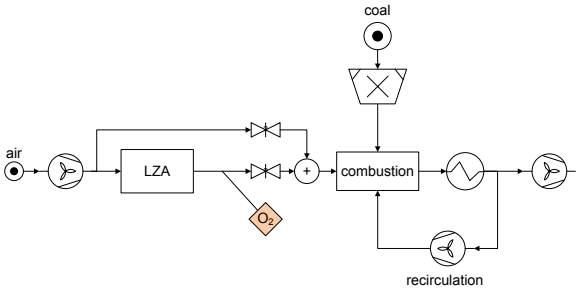

Figure 15: start-up process scheme

actions and the focus of the author. The results offer the opportunity to start the oxyfuel process stable and optimal. Moreover, they help to avoid critical states which may lead to component damage.

ACKNOWLEDGEMENTS

This work is supported by the Free State of Saxony and the European Social fonds ESF.

REFERENCES

[1] University of Applied Sciences Zittau/Goerlitz, Department of Technical Thermodynamic in *Water and steam, calculated from the industrial formulation IAPWS-IF97 and all supplementary standards*, 2007

[2] University of Applied Sciences Zittau/Goerlitz, Department of Technical Thermodynamic in *Combustion gases, calculated as an ideal mixture of ideal gases from the VDI Guideline-4670.* University of Applied Sciences Zittau/Goerlitz, Department of Technical Thermodynamics, 2007

[3] R.Isermann in *Mechatronische Systeme 2.Auflage* Springer Verlag, 2008

[4] Verein Deutscher Ingenieure VDI-Gesellschaft Verfahrenstechnik und Chemieingenieurwesen (GVC) in *VDI-Waermeatlas 10.Auflage* Springer Verlag, 2006

[5] `http://www.hs-zigr.de/~livecms/cmsdocs/IPM/de/data/artikel/Software1/dynstar.html` (06.02.2012)

[6] `http://bayern-innovativ.de/ib/site/documents/media/a6a06fe0-d051-3059-cec5-3553629d3241.pdf/Vortrag_Jentsch.pdf` (06.02.2012)

AUTHOR BIOGRAPHIES

Peter Tusche is working as a PhD student at the Institute of Process Technique, Process Automation and Measuring Technique (IPM) of the University of Applied Sciences Zittau/Goerlitz. The author studied from 1999 until 2003 mechatronics at this university, finishing with the diploma. After graduation he was employed by the RTT GmbH for 3 years in manufacturing automation. Since 2006 he has been involved in research and industry projects in the section 'power plant, boiler and fuel technology' at the IPM. His email is `ptusche@hs-zigr.de`.

Tobias Zschunke was born in Dresden in 1962. The author is married and has three children. At TU Dresden from 1982 to 1990, he completed his studies and his doctorate in the field of thermodynamics and fluid mechanics. From 1990 to 1993 he worked as a project engineer at the engineering company Energietechnik Dresden und Stuttgart (tasks in terms of energy technology and energy economics). He worked as a scientific fellow in the field of combustion and energetic bio-mass utilization as well as on the preparation and execution of national and international research projects at TU Dresden from 1993 to 2007. At TU Dresden from 2007 to 2009, Professor Zschunke completed his post-doctoral dissertation in the field of 'energy process engineering' concerning aspects of coupled energy and heat supply gained from biomass. In 2007 he became professor for power plant and energy technology at Zittau/Goerlitz University of Applied Sciences. Moreover, he became deputy to rector for research at the university in 2010 and he is involved in cooperative research projects with companies from the fields of energy technology and institutes of the Fraunhofer Organization, the organization Biomasseforschungszentrum (DBFZ) in Leipzig and at the TU Dresden. His email is `tzschunke@hs-zigr.de`.

Rainer Hampel was born in 1944. He studied in the field of power engineering at TU Dresden from 1964 to 1970. After his graduation he went to Zittau/Goerlitz University of Applied Sciences. There he finished his doctorate in 1975 and his post-doctoral dissertation in 1984 in the field of 'power plant automation'. In 1987 he became professor for power plant automation at Zittau University of Technology. In 1992 the fields of measuring technology and process automation were added to his chair. From 2003 to 2010 he was the rector of Zittau/Goerlitz University of Applied Sciences. His email is `r.hampel@hs-zigr.de`.

PREDICTIVE CONTROL OF TIME-DELAY PROCESSES

Marek Kubalčík, Vladimír Bobál
Tomas Bata University in Zlín
Faculty of Applied Informatics
Nad Stránění 4511
760 05 Zlín
Czech Republic
E-mail: kubalcikl@fai.utb.cz

KEYWORDS
Predictive control, Time-delay systems, Digital control, Higher order systems, Simulation,

ABSTRACT

In technical practice often occur higher order processes when a design of an optimal controller leads to complicated control algorithms. One of possibilities of control of such processes is their approximation by lower-order model with time-delay (dead time). One of the possible approaches to control of dead-time processes is application of predictive control methods. The paper deals with design of an algorithm for predictive control of high-order processes which are approximated by second-order model of the process with time-delay.

INTRODUCTION

Some technological processes in industry are characterized by high-order dynamic behaviour or large time constants and time-delays. Time-delay in a process increases the difficulty of controlling it. However using the approximation of higher-order process by lower-order model with time-delay provides simplification of the control algorithms.
Let us consider a continuous-time dynamical linear SISO (single input $u(t)$ – single output $y(t)$) system with time-delay T_d. The transfer function of a pure transportation lag is $e^{-T_d s}$ where s is a complex variable. Overall transfer function with time-delay is in the form

$$G_d(s) = G(s)e^{-T_d s} \tag{1}$$

where $G(s)$ is the transfer function without time-delay.

Processes with time-delay are difficult to control using standard feedback controllers. One of the possible approaches to control processes with time delay is predictive control. The predictive control strategy includes a model of the process in the structure of the controller. The first time-delay compensation algorithm was proposed by (Smith 1957). This control algorithm known as the Smith Predictor (SP) contained a dynamic model of the time-delay process and it can be considered as the first model predictive algorithm.

Model Based Predictive Control (MBPC) or only Predictive Control is one of the control methods which have developed considerably over a few past years. Predictive control is essentially based on discrete or sampled models of processes. Computation of appropriate control algorithms is then realized namely in the discrete domain.
The term Model Predictive Control designates a class of control methods which have common particular attributes (Camacho and Bordons 2004, Mikleš and Fikar 2008).

- Mathematical model of a systems control is used for prediction of future control of a systems output.
- The input reference trajectory in the future is known.
- A computation of the future control sequence includes minimization of an appropriate objective function (usually quadratic one) with the future trajectories of control increments and control errors.
- Only the first element of the control sequence is applied and the whole procedure of the objective function minimization is repeated in the next sampling period.

The principle of MBPC is shown in Fig. 1, where $u(t)$ is the manipulated variable, $y(t)$ is the process output and $w(t)$ is the reference signal, N_1, N_2 and N_u are called minimum, maximum and control horizon. This principle is possible to define as follows:

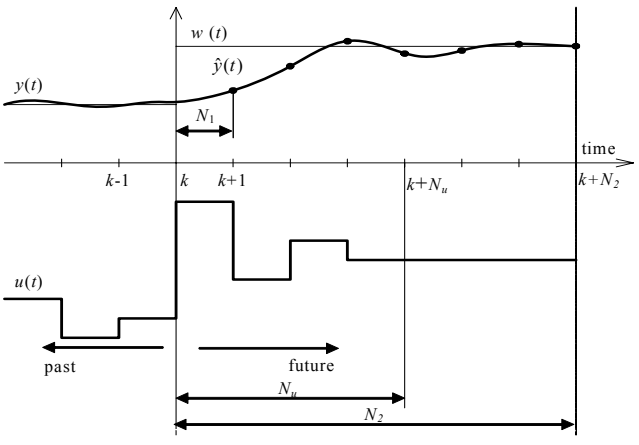

Figure 1: Principle of MBPC

Proceedings 26th European Conference on Modelling and Simulation ©ECMS Klaus G. Troitzsch, Michael Möhring, Ulf Lotzmann (Editors)
ISBN: 978-0-9564944-4-3 / ISBN: 978-0-9564944-5-0 (CD)

1. The process model is used to predict the future outputs $\hat{y}(t)$ over some horizon *N*. The predictions are calculated based on information up to time *k* and on the future control actions that are to be determined.
2. The future control trajectory is calculated as a solution of an optimisation problem consisting of a objective function and possibility some constraints. The cist function comprises future output predictions, future reference trajectory, and future actions.
3. Although the whole future control trajectory was calculated in the previous step, only first element $u(k)$ is actually applied to the process. At the next sampling time the procedure is repeated. This is known as the *Receding Horizon* concept.

Theoretical research in the area of predictive control has a great impact on the industrial world and there are many applications of predictive control in industry. Its development has been significantly influenced by industrial practice. At present, predictive control with a number of real industrial applications belongs among the most often implemented modern industrial process control approaches. First predictive control algorithms were implemented in industry as an effective tool for control of multivariable industrial processes with constraints more than twenty five years ago. The use of predictive control was limited on control of namely rather slow processes due to the amount of computation required. At present, with the computing power available today, this is not an essential problem. A fairly actual and extensive surveys of industrial applications of predictive control are presented in (Morari and Lee 2004, Quin and Bandgwell 1996, 2000, 2003).

The aim of the paper is to design and verify by simulation an algorithm for predictive control of second order linear systems with time delay of two steps. A number of higher order industrial processes can be approximated by this model.

IMPLEMENTATION OF PREDICTIVE CONTROL

In this Section, GPC will be briefly described. The GPC method is in principle applicable to both SISO and MIMO processes and is based on input-output models. The standard cost function used in GPC contains quadratic terms of (possible filtered) control error and control increments on a finite horizon into the future

$$J = \sum_{i=N_1}^{N_2} \delta(i)\left[\hat{y}(k+i) - w(k+i)\right]^2 + \sum_{i=1}^{N_u}\left[\lambda(i)\Delta u(k+i-1)\right]^2 \quad (2)$$

where $\hat{y}(k+i)$ is the process output of *i* steps in the future predicted on the base of information available upon the time *k*, $w(k+1)$ is the sequence of the reference signal and $\Delta u(k+i-1)$ is the sequence of the future control increments that have to be calculated. Implicit constraints on Δu are placed between N_u and N_2 as

$$\Delta u(k+i-1) = 0, \qquad N_u < i \le N_2 \quad (3)$$

The parameters $\delta(i)$ and $\lambda(i)$ are sequences which affect future behaviour of the controlled process. Generally, they are chosen in the form of constants or exponential weights.

Calculation of the Optimal Control

The objective of predictive control is a computation of a sequence of future increments of the manipulated variable $\left[\Delta u(k), \Delta u(k+1), \ldots\right]$ so that the criterion (2) was minimized. For further computation, it is necessary to transform the criterion (2) to a matrix form.

The output of the model (predictor) is computed as the sum of the free response $\boldsymbol{y}_0$ and the forced response of the model $\boldsymbol{y}_n$

$$\hat{\boldsymbol{y}} = \boldsymbol{y}_n + \boldsymbol{y}_0 \quad (4)$$

It is possible to compute the forced response as the multiplication of the matrix $\boldsymbol{G}$ (Jacobian of the model) and the vector of future control increments $\Delta\boldsymbol{u}$, which is generally a priori unknown

$$\boldsymbol{y}_n = \boldsymbol{G}\Delta\boldsymbol{u} \quad (5)$$

where

$$\boldsymbol{G} = \begin{bmatrix} g_1 & 0 & 0 & \cdots & 0 \\ g_2 & g_1 & 0 & \cdots & 0 \\ g_3 & g_2 & g_1 & \cdots & 0 \\ \vdots & \vdots & \vdots & \ddots & \vdots \\ g_{N_2} & g_{N_2-1} & g_{N_2-2} & \cdots & g_{N_2-N_u+1} \end{bmatrix} \quad (6)$$

is matrix containing values of the step sequence.

It follows from equations (4) and (5) that the predictor in a vector form is given by

$$\hat{\boldsymbol{y}} = \boldsymbol{G}\Delta\boldsymbol{u} + \boldsymbol{y}_0 \quad (7)$$

and the cost function (2) can be modified to the form below

$$\begin{aligned} J &= \left(\hat{\boldsymbol{y}} - \boldsymbol{w}\right)^T \left(\hat{\boldsymbol{y}} - \boldsymbol{w}\right) + \lambda\Delta\boldsymbol{u}^T\Delta\boldsymbol{u} = \\ &= \left(\boldsymbol{G}\Delta\boldsymbol{u} + \boldsymbol{y}_0 - \boldsymbol{w}\right)^T \left(\boldsymbol{G}\Delta\boldsymbol{u} + \boldsymbol{y}_0 - \boldsymbol{w}\right) + \lambda\Delta\boldsymbol{u}^T\Delta\boldsymbol{u} \end{aligned} \quad (8)$$

where $\boldsymbol{w}$ is the vector of future reference trajectory.

Minimisation of the cost function (8) now becomes a direct problem of linear algebra. The solution in an unconstrained case can be found by setting partial derivative of *J* with respect to $\Delta\boldsymbol{u}$ to zero and yields

$$\Delta \boldsymbol{u} = -\left(\boldsymbol{G}^T\boldsymbol{G} + \lambda \boldsymbol{I}\right)^{-1}\boldsymbol{G}^T\left(\boldsymbol{y}_0 - \boldsymbol{w}\right) \tag{9}$$

where the gradient $\boldsymbol{g}$ and Hessian $\boldsymbol{H}$ are defined as

$$\boldsymbol{g}^T = \boldsymbol{G}^T\left(\boldsymbol{y}_0 - \boldsymbol{w}\right) \tag{10}$$

$$\boldsymbol{H} = \boldsymbol{G}^T\boldsymbol{G} + \lambda \boldsymbol{I} \tag{11}$$

Equation (9) gives the whole trajectory of the future control increments and such is an open-loop strategy. To close the loop, only the first element $\boldsymbol{u}$, e. g. $\Delta u(k)$ is applied to the system and the whole algorithm is recomputed at time *k*+1. This strategy is called the *Receding Horizon Principle* and is one of the key issues in the MBPC concept.

If we denote the first row of the matrix $\left(\boldsymbol{G}^T\boldsymbol{G} + \lambda \boldsymbol{I}\right)^{-1}\boldsymbol{G}^T$ by $\boldsymbol{K}$ then the actual control increment can be calculated as

$$\Delta u(k) = \boldsymbol{K}\left(\boldsymbol{w} - \boldsymbol{y}_0\right) \tag{12}$$

COMPUTATION OF PREDICTOR

An important task is computation of predictions for arbitrary prediction and control horizons. Dynamics of most of processes requires horizons of length where it is not possible to compute predictions in a simple straightforward way. Recursive expressions for computation of the free response and the matrix $\boldsymbol{G}$ in each sampling period had to be derived. There are several different ways of deriving the prediction equations for transfer function models. Some papers make use of Diophantine equations to form the prediction equations (e.g. (Kwon et. al. 1992)). In (Rossiter, 2003) matrix methods are used to compute predictions. We derived a method for recursive computation of both the free response and the matrix of the dynamics.

Computation of the predictor for the time-delay system can be obtained by modification of the predictor for the corresponding system without a time-delay. At first we will consider the second order system without time-delay and then we will modify the computation of predictions for the time-delay system.

Second Order System without Time-Delay

The model is described by the transfer function

$$G\left(z^{-1}\right) = \frac{b_1 z^{-1} + b_2 z^{-2}}{1 + a_1 z^{-1} + a_2 z^{-2}} = \frac{B\left(z^{-1}\right)}{A\left(z^{-1}\right)} \tag{13}$$

$$A\left(z^{-1}\right) = 1 + a_1 z^{-1} + a_2 z^{-2};\ B\left(z^{-1}\right) = b_1 z^{-1} + b_2 z^{-2} \tag{14}$$

The model can be also written in the form

$$A\left(z^{-1}\right)y(k) = B\left(z^{-1}\right)u(k) \tag{15}$$

A widely used model in general model predictive control is the CARIMA model which we can obtain from the nominal model (15) by adding a disturbance model

$$A\left(z^{-1}\right)y(k) = B\left(z^{-1}\right)u(k) + \frac{C\left(z^{-1}\right)}{\Delta}n_c(k) \tag{16}$$

where $n_c(k)$ is a non-measurable random disturbance that is assumed to have zero mean value and constant covariance and the operator delta is $1 - z^{-1}$. Inverted delta is then an integrator.

The polynomial $C\left(z^{-1}\right)$ will be further considered as $C\left(z^{-1}\right) = 1$. The CARIMA description of the system is then in the form

$$\Delta A\left(z^{-1}\right)y(k) = B\left(z^{-1}\right)\Delta u(k-1) + n_c(k) \tag{17}$$

The difference equation of the CARIMA model without the unknown term $n_c(k)$ can be expressed as:

$$y(k) = (1-a_1)y(k-1) + (a_{1'} - a_2)y(k-2) + a_2 y(k-3) + \\ + b_1\Delta u(k-1) + b_2\Delta u(k-2) \tag{18}$$

It was necessary to compute three step ahead predictions in straightforward way by establishing of lower predictions to higher predictions. The model order defines that computation of one step ahead prediction is based on three past values of the system output. The three step ahead predictions are as follows

$$\hat{y}(k+1) = (1-a_1)y(k) + (a_{1'} - a_2)y(k-1) + a_2 y(k-2) + \\ + b_1\Delta u(k) + b_2\Delta u(k-1)$$
$$\hat{y}(k+2) = (1-a_1)y(k+1) + (a_{1'} - a_2)y(k) + a_2 y(k-1) + \\ + b_1\Delta u(k+1) + b_2\Delta u(k)$$
$$\hat{y}(k+3) = (1-a_1)y(k+2) + (a_{1'} - a_2)y(k+1) + a_2 y(k) + \\ + b_1\Delta u(k+2) + b_2\Delta u(k+1) \tag{19}$$

The predictions after modification can be written in a matrix form

$$\begin{bmatrix}\hat{y}(k+1)\\ \hat{y}(k+2)\\ \hat{y}(k+3)\end{bmatrix} = \begin{bmatrix} g_1 & 0\\ g_2 & g_1\\ g_3 & g_2\end{bmatrix}\begin{bmatrix}\Delta u(k)\\ \Delta u(k+1)\end{bmatrix} + \begin{bmatrix} p_{11} & p_{12} & p_{13} & p_{14}\\ p_{21} & p_{22} & p_{23} & p_{24}\\ p_{31} & p_{32} & p_{33} & p_{34}\end{bmatrix}\begin{bmatrix} y(k)\\ y(k-1)\\ y(k-2)\\ \Delta u(k-1)\end{bmatrix} =$$
$$= \begin{bmatrix} b_1 & 0\\ b_1(1-a_1) + b_2 & b_1\\ (a_1 - a_2)b_1 + (1-a_1)^2 b_1 + (1-a_1)b_2 & b_1(1-a_1) + b_2\end{bmatrix}\begin{bmatrix}\Delta u(k)\\ \Delta u(k+1)\end{bmatrix} +$$
$$+ \begin{bmatrix} (1-a_1) & (a_1 - a_2)\\ (1-a_1)^2 + (a_1 - a_2) & (1-a_1)(a_1 - a_2) + a_2\\ (1-a_1)^3 + 2(1-a_1)(a_1 - a_2) + a_2 & (1-a_1)^2(a_1 - a_2) + a_2(1-a_1) + (a_1 - a_2)^2\end{bmatrix}$$
$$\begin{bmatrix} a_2 & b_2\\ a_2(1-a_1) & b_2(1-a_1)\\ a_2(1-a_1)^2 + (a_1 - a_2)a_2 & b_2(1-a_1)^2 + (a_1 - a_2)b_2\end{bmatrix}\begin{bmatrix} y(k)\\ y(k-1)\\ y(k-2)\\ \Delta u(k-1)\end{bmatrix} \tag{20}$$

It is possible to divide computation of the predictions to recursion of the free response and recursion of the matrix of the dynamics. Based on the three previous predictions it is repeatedly computed the next row of the free response matrix in the following way:

$$\begin{aligned} p_{41} &= (1-a_1)p_{31} + (a_1-a_2)p_{21} + a_2 p_{11} \\ p_{42} &= (1-a_1)p_{32} + (a_1-a_2)p_{22} + a_2 p_{12} \\ p_{43} &= (1-a_1)p_{33} + (a_1-a_2)p_{23} + a_2 p_{13} \\ p_{44} &= (1-a_1)p_{34} + (a_1-a_2)p_{24} + a_2 p_{14} \end{aligned} \quad (21)$$

The first row of the matrix is omitted in the next step and further prediction is computed based on the three last rows including the one computed in the previous step. This procedure is cyclically repeated. It is possible to compute an arbitrary number of rows of the matrix.

The recursion of the dynamics matrix is similar. The next element of the first column is repeatedly computed in the same way as in the previous case and the remaining columns are shifted to form a lower triangular matrix in the way which is obvious from the equation (16). This procedure is performed repeatedly until the prediction horizon is achieved. If the control horizon is lower than the prediction horizon a number of columns in the matrix is reduced. Computation of the new element is performed as follows:

$$g_4 = (1-a_1)g_3 + (a_1-a_2)g_2 + a_2 g_1 \quad (22)$$

Second Order System with Time-Delay

The nominal model with two steps time-delay is considered as

$$G(z^{-1}) = \frac{B(z^{-1})}{A(z^{-1})} z^{-2} = \frac{b_1 z^{-1} + b_2 z^{-2}}{1 + a_1 z^{-1} + a_2 z^{-2}} z^{-2} \quad (23)$$

The CARIMA model for time-delay system takes the form

$$\Delta A(z^{-1}) y(k) = z^{-d} B(z^{-1}) \Delta u(k-1) + n_c(k) \quad (24)$$

where d is the dead time. In our case d is equal to 2. In order to compute the control action it is necessary to determine the predictions from d+1 (2+1 in our case) to d+N_2 (2+N_2).

The predictor (20) is then modified to

$$\begin{aligned} \begin{bmatrix} \hat{y}(k+3) \\ \hat{y}(k+4) \\ \hat{y}(k+5) \end{bmatrix} &= \begin{bmatrix} p_{31} & p_{32} & p_{33} \\ p_{41} & p_{42} & p_{43} \\ p_{51} & p_{52} & p_{53} \end{bmatrix} \begin{bmatrix} y(k) \\ y(k-1) \\ y(k-2) \end{bmatrix} + \\ &+ \begin{bmatrix} g_1 & 0 \\ g_2 & g_1 \\ g_3 & g_2 \end{bmatrix} \begin{bmatrix} \Delta u(k) \\ \Delta u(k+1) \end{bmatrix} + \\ &+ \begin{bmatrix} g_2 & g_3 & p_{34} \\ g_3 & g_4 & p_{44} \\ g_4 & g_5 & p_{54} \end{bmatrix} \begin{bmatrix} \Delta u(k-1) \\ \Delta u(k-2) \\ \Delta u(k-3) \end{bmatrix} \end{aligned} \quad (25)$$

Recursive computation of the matrices is analogical to the recursive computation described in the previous section.

SIMULATION EXAMPLES

As simulation examples were chosen a fifth order linear system described by following transfer function

$$G_A(s) = \frac{2}{(s+1)^5} = \frac{2}{s^5 + 5s^4 + 10s^3 + 10s^2 + 5s + 1} \quad (26)$$

and a fifth-order linear system with non-minimum phase

$$G_B(s) = \frac{2(1-5s)}{s^5 + 5s^4 + 10s^3 + 10s^2 + 5s + 1} \quad (27)$$

The systems were identified by the model (23) using off-line LSM (Bobál et. al., 2012). The system (26) was approximated by

$$G_A(z^{-1}) = \frac{0{,}0424 z^{-1} + 0{,}0296 z^{-2}}{1 - 1{,}6836 z^{-1} + 0{,}7199 z^{-2}} z^{-2} \quad (28)$$

and the system (27) was approximated by

$$G_B(z^{-1}) = \frac{-0{,}7723 z^{-1} + 0{,}8514 z^{-2}}{1 - 1{,}6521 z^{-1} + 0{,}6920 z^{-2}} z^{-2} \quad (29)$$

Both for sampling period $T_0 = 0.5\,\mathrm{s}$. The step responses of the models are in the following figures

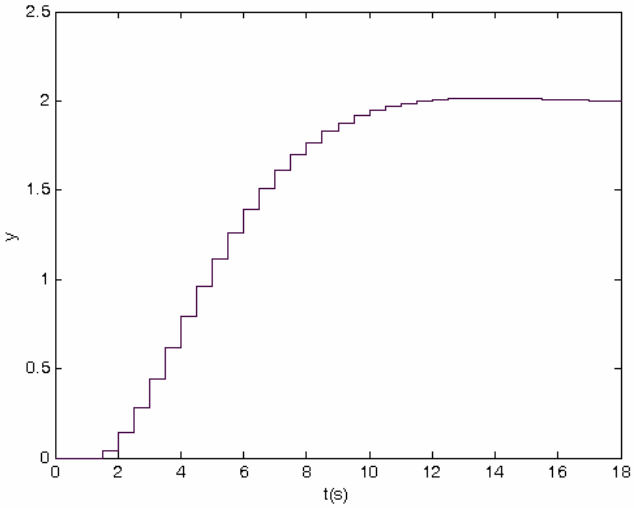

Figure 2: Step response of the model (28)

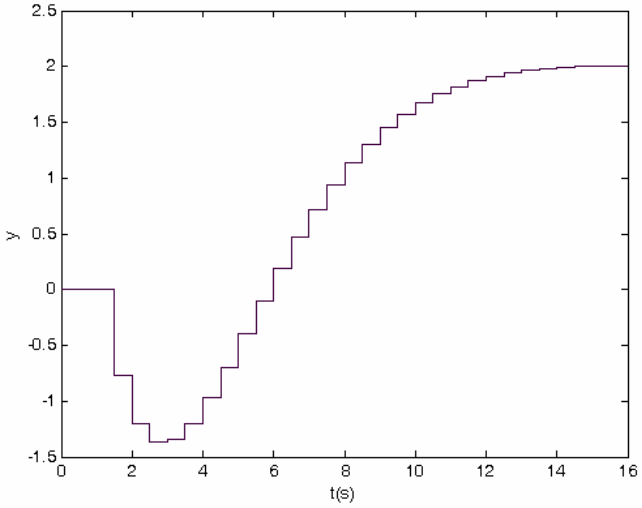

Figure 3: Step response of the model (29)

Control responses are in the figures 4, 5, 6 and 7.

The tuning parameters that are lengths of the prediction and control horizons and the weighting coefficient λ were tuned experimentally. There is a lack of clear theory relating to the closed loop behavior to design parameters. The length of the prediction horizon, which should cover the important part of the step response, was in both cases set to $N = 40$. The length of the control horizon was also set to $N_u = 40$. The coefficient λ was taken as equal to 0,5.

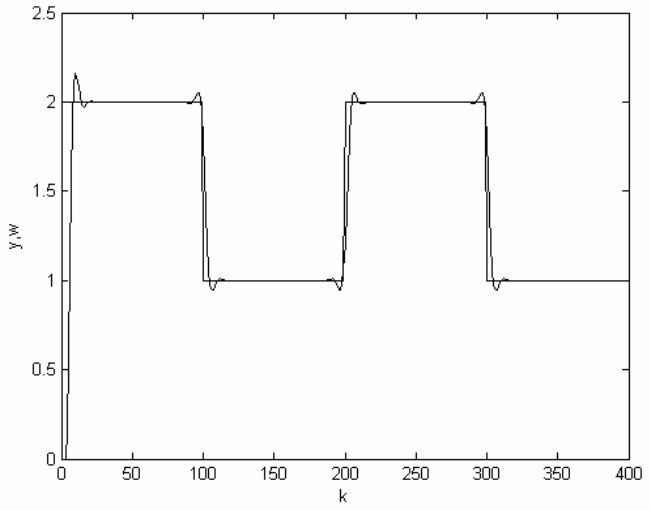

Figure 4: Control of the model (29)

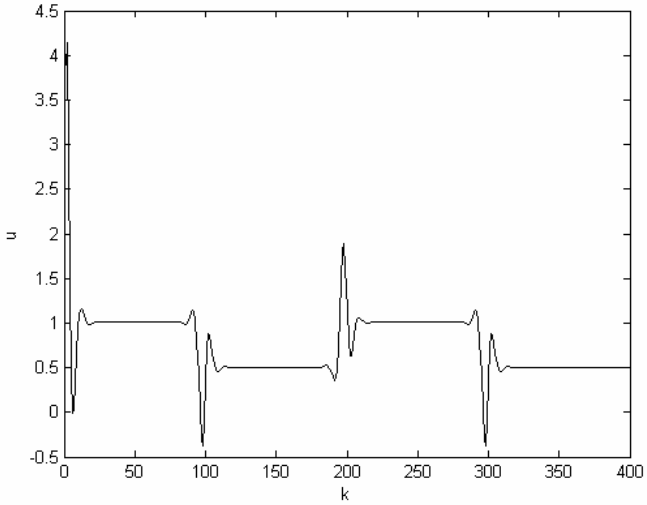

Figure 5: Control of the model (29) –manipulated variable

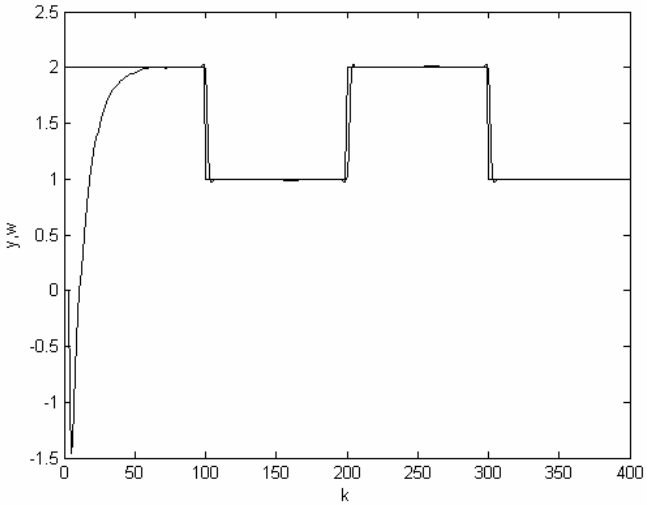

Figure 6: Control of the model (28)

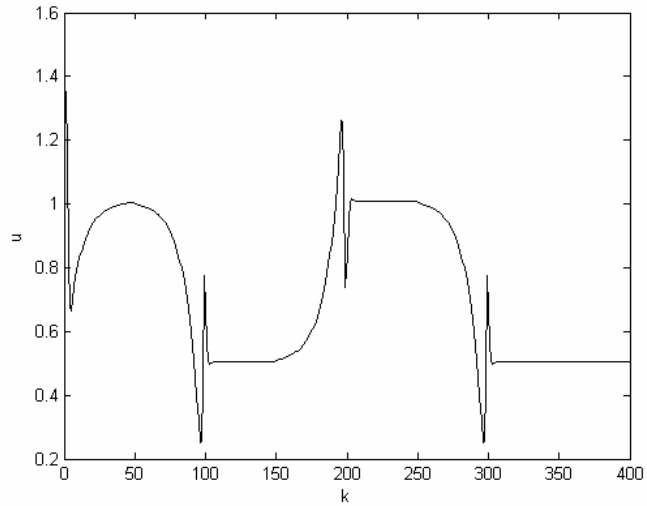

Figure 5: Control of the model (28) –manipulated variable

CONCLUSION

The algorithm for control of the higher-order processes based on model predictive control was designed. The higher-order process was approximated by the second-order model with time delay. The predictive controller is based on the recursive computation of predictions by direct use of the CARIMA model. The computation of predictions was extended for the time-delay system. The control of two modifications of the higher-order processes (stable and non-minimum phase) were verified by simulation. The simulation verification provided good control results. Asymptotic tracking of the reference signal was achieved in both cases. The control of non-minimum phase system was rather sensitive to tuning parameters. Experimental tuning of the controller was more complicated in this case. The algorithm will be tested and verified by real-time control of a heat-exchanger.

ACKNOWLEDGMENTS

This article was created with support of Operational Programme Research and Development for Innovations co-funded by the European Regional Development Fund (ERDF), national budget of Czech Republic within the framework of the Centre of Polymer Systems project (reg. number: CZ.1.05/2.1.00/03.0111).

REFERENCES

Bobál, V., Kubalčík, M., Chalupa, P. and Dostál, P. 2012. "Identification and Digital Control of Highre-Order Processes Using Predictive Strategy". *These proceedings*.

Camacho E. F., Bordons, C. 2004. *Model Predictive Control.* Springer-Verlag, London.

Kwon, W. H., Choj, H., Byun, D.G., Noh, S. 1992. "Recursive solution of generalized predictive control and its equivalence to receding horizon tracking control." *Automatica*, 28(6), 1235–1238.

Mikleš, J., Fikar, M. 2008. *Process Modelling, Optimisation and Control.* Springer-Verlag, Berlín.

Morari, M., Lee, J.H. 1999. "Model predictive control: past, present and future." *Computers and Chemical Engineering, 23*(4), 667-682.

Quin, S.J, Bandgwell, T.A. 1996. "An overview of industrial model predictive control technology." *Proceedings of the Chemical Process Control – V.* Vol. 93 of *AIChE Symposium Series*. CACHE & AIChE. Tahoe City, CA, USA, 232-256.

Quin, S.J, Bandgwell, T.A. 2000. "An overview of nonlinear model predictive control applications." *Nonlinear Model Predictive Control* (F. Allgöwer & A. Zheng, Ed.), (Basel – Boston – Berlin: Birkhäuser Verlag), 369-392.

Quin, S.J, Bandgwell, T.A. 2003. "A survey of industrial model predictive control technology." *Control Engineering Practice*, *11*(7), 733-764.

Rossiter, J.A. 2003. *Model Based Predictive Control: a Practical Approach,* CRC Press.

Smith, O.J. 1957. "Closed control of loops". *Chem. Eng. Progress* 53, 217-219.

AUTHOR BIOGRAPHIES

MAREK KUBALČÍK graduated in 1993 from the Brno University of Technology in Automation and Process Control. He received his Ph.D. degree in Technical Cybernetics at Brno University of Technology in 2000. From 1993 to 2007 he worked as senior lecturer at the Faculty of Technology, Brno University of Technology. From 2007 he has been working as an associate professor at the Department of Process Control, Faculty of Applied Informatics of the Tomas Bata University in Zlín, Czech Republic. Current work cover following areas: control of multivariable systems, self-tuning controllers, predictive control. His e-mail address is: kubalcik@fai.utb.cz.. You can contact him on email address dostalp@fai.utb.cz

VLADIMÍR BOBÁL graduated in 1966 from the Brno University of Technology, Czech Republic. He received his Ph.D. degree in Technical Cybernetics at Institute of Technical Cybernetics, Slovak Academy of Sciences, Bratislava, Slovak Republic. He is now Professor at the Department of Process Control, Faculty of Applied Informatics of the Tomas Bata University in Zlín. His research interests are adaptive control and predictive control, system identification and CAD for automatic control systems. You can contact him on email address bobal@fai.utb.cz.

THE PROCESS OF AN OPTIMIZED HEAT RADIATION INTENSITY CALCULATION ON A MOULD SURFACE

Jaroslav Mlýnek
Department of Mathematics and Didactics of Mathematics
Technical University of Liberec
Studentská 2, 461 17 Liberec,
Czech Republic
E-mail: jaroslav.mlynek@tul.cz

Radek Srb
Institute of Mechatronics and Computer Engineering
Technical University of Liberec
Studentská 2, 461 17 Liberec,
Czech Republic
E-mail: radek.srb@tul.cz

KEYWORDS
Mathematical model, heat radiation, optimization, genetic algorithm.

ABSTRACT

This article is focused on the optimization of heat radiation intensity across the surface of an aluminium mould. The mould is warmed by infrared heaters located above the mould surface, and in this way artificial leathers in the automotive industry are produced (e.g. the artificial leather on a car dashboard). This described model allows us to specify the location of infrared heaters over the mould to obtain approximately the same heat radiation intensity across the whole mould surface. In this way we can obtain a uniform material structure and colour tone across the whole surface of artificial leather. We used a genetic algorithm and the technique of "hill-climbing" during the optimization process. A computational procedure was programmed in the language Matlab.

1. INTRODUCTION

This article is focused on the problems with production technology used for artificial leathers used in car interior equipment (e.g. the artificial leather attached to the plastic surface of a car's interior, or the leather used to upholster the interior of car doors). One successful production method is the heating of the mould surface (usually an aluminium or nickel mould is used) by infrared heaters located above the mould surface at a distance of between 5 and 30[cm]. The inside of the mould is sprinkled with special PVC powder and the outside mould surface is subsequently warmed to a temperature of 250[°C] in a few minutes. Simultaneously, it is necessary to maintain an even temperature across the mould surface at any given time during the warming process, and thereby ensure the same material structure and colour tone across the whole artificial leather surface.
Forms of different size and shape, often very rugged, are applied to production. The mould weight is approximately 300[kg]. The infrared heaters have a tubular form and their length is between 15 and 25[cm]. The infrared heater is equipped with a mirror located above the radiation tube, which reflects heat radiation in a given direction (see Figure 1). Depending on the mould size, the number of heaters is usually between 50 and 200.
It is necessary to ensure the heat radiation intensity within given tolerance on the whole mould surface through the optimization of the heaters' location, and in this way approximately the same temperature is produced across the whole mould surface, which is essential to the production of artificial leathers.

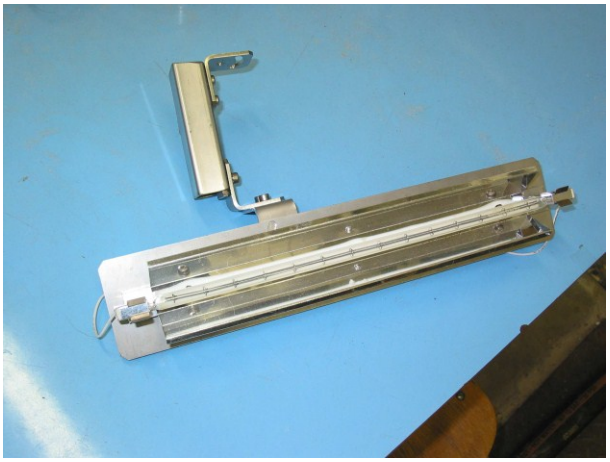

Figure 1: Philips Infrared Heater with 1000W Capacity

In the following chapters are described the heat conduction problem in the mould, the mathematical model of heat radiation on the mould, and the optimization process (a genetic algorithm and the technique "hill-climbing" were used) of the location of infrared heaters. The last chapter contains two examples with solutions. A computational procedure of the optimization process was programmed in the language Matlab.
The producer requires implementing a procedure of the optimization of the heaters' locations at the production line (after its verification in system Matlab). Therefore, we need to know the optimization process in every detail. Hence, in order to solve the respective problem, we have not used any existing commercially available software tool designed for solution of the distributed parameter system problems.

Proceedings 26th European Conference on Modelling and Simulation ©ECMS Klaus G. Troitzsch, Michael Möhring, Ulf Lotzmann (Editors)
ISBN: 978-0-9564944-4-3 / ISBN: 978-0-9564944-5-0 (CD)

2. HEAT CONDUCTION IN THE MOULD

In the following chapters, the technique of optimizing the heaters' locations will be described, as well as the calculation of uniform heat radiation intensity. We are able to calculate temperature T on the mould surface during warming on the basis of knowing the heat radiation intensity I on the mould surface. We will solve the parabolic evolutionary equation of heat conduction

$$\frac{\partial T(x,t)}{\partial t} = \frac{\lambda}{c\rho}\Delta T(x,t) \qquad (1)$$

on the domain $\Omega \subset E_3$, where Ω represents the given mould, E_3 is 3-dimensional Euclidean space. In relation (1) $T(x,t)$ denotes a temperature, point $x = (x_1, x_2, x_3) \in \Omega$, time $t \in (0, \tau)$, where τ is the duration of heat radiation conducted to the mould surface by heaters; the real value λ stands for the heat conductivity of the mould material (we assume an isotropic environment and the independence of λ on x position), and real values c and ρ denote the specific heat capacity and mass density of the mould material. The symbol Δ stands for Laplace operator to space variables, i.e.

$$\Delta T(x,t) = \sum_{i=1}^{3} \frac{\partial^2 T(x,t)}{\partial x_i^2}.$$

We consider the initial condition

$$T(x,0) = T_0 \quad \forall x \in \Omega, \qquad (2)$$

where T_0 denotes the initial temperature of the mould (the mould is preheated before being warmed by the infrared heaters), boundary conditions

$$q^T \eta = -I(x) \qquad (3)$$

on the surface part $P \subset \partial\Omega$ heated by infrared heaters and

$$q^T \eta = \alpha\,(T(x,t) - T_{air}) \qquad (4)$$

on the remaining part of the mould surface $\partial\Omega - P$ (cooling of this part of the mould surface). The symbols in expressions (3) and (4) have the following meaning. The symbol q denotes the thermal flux density and it is true $q = -\lambda\, grad\, T(x,t)$, where

$$grad\, T(x,t) = \left(\frac{\partial T}{\partial x_1}, \frac{\partial T}{\partial x_2}, \frac{\partial T}{\partial x_3} \right)^T.$$

The symbol η denotes unit outward normal vector in point $x \in P$, $I(x)$ is the heat radiation intensity on P (values $I(x)$ are independent of time t), α is heat transfer coefficient, and T_{air} is the temperature of surrounding air. See more detail about the problems of heat conduction e.g. in (Cengel 2007).

The equation (1) with conditions (2) - (4) describes heat conduction in domain Ω (in the mould). No heat sources are inside the domain Ω, only the infrared heaters radiate on surface P. The equation of heat conduction (1) with the aforementioned conditions is possible to solve numerically using the software tool ANSYS through the finite element method. If values of heat radiation intensity $I(x)$ on the surface part P are within specified limit, we will obtain a numerical solution of equation (1) with conditions (2) – (4) with uniform temperature T on the surface $\partial\Omega - P$.

3. MATHEMATICAL MODEL OF HEAT RADIATION ON THE MOULD SURFACE

In this chapter will be described a simplified mathematical model of heat radiation by infrared heaters on the mould surface. The infrared heaters and mould are represented in 3-dimensional Euclidian space by the Cartesian coordinate system (O, x_1, x_2, x_3) with base vectors $e_1 = (1, 0, 0)$, $e_2 = (0, 1, 0)$, $e_3 = (0, 0, 1)$.

3. 1. Representation of a Heater

All heaters are of the same type (i.e. they have the same capacity and shape). A heater is represented by abscissa d in length. The location of heater is described by the following parameters: 1/ coordinates of the heater centre $S = [x_1^S, x_2^S, x_3^S]$, 2/ unit vector $u = (x_1^u, x_2^u, x_3^u)$ of heater radiation direction, component $x_3^u < 0$ (i.e. heater radiates "down"), 3/ the vector of the heater axis $r = (x_1^r, x_2^r, x_3^r)$, where the vectors u and r are orthogonal (see Figure 2).

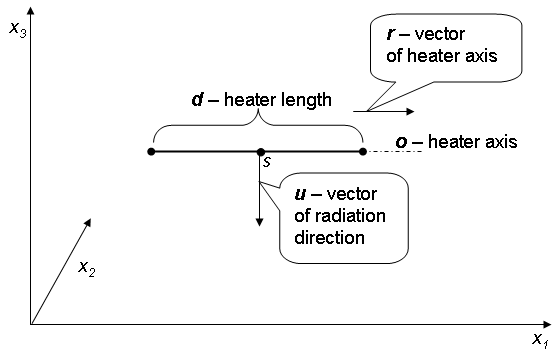

Figure 2: Representation of the Heater in the Model

The other possibility for expressing vector *r* is only by the angle φ (*u* and *r* are orthogonal) that contains the vertical projection of vector *r* to a plane given by the axes x_1 and x_2 (ground plane) and the positive part of axis x_1 ($0 \le \varphi < \pi$). The unambiguous transformation exists between these expressions. We will use the second expression in the following chapters (we need the smallest possible number of parameters to heater location determination in the genetic algorithm). The location of every infrared heater *Z* can be expressed by the following 6 parameters:

$$Z: \left(x_1^S, x_2^S, x_3^S, x_1^u, x_2^u, \varphi\right). \qquad (5)$$

In general, the location of *M* heaters is described by 6*M* parameters.

3. 2. Representation of a Mould

The thickness of an aluminium mould is uniformly 6[mm]. Therefore it suffices to define only total mould surface *P*. We will use elementary surfaces p_j, where $1 \le j \le N$ (i.e. N elementary surfaces) to define the mould surface. It is true $P = \bigcup_{1 \le j \le N} p_j$ and $\operatorname{int} p_i \cap \operatorname{int} p_j = \emptyset$ for $i \ne j$, $1 \le i, j \le N$. Every elementary surface is described by the following parameters: 1/ the centre of gravity $T_j = [x_1^{T_j}, x_2^{T_j}, x_3^{T_j}]$, 2/ the unit outer normal vector $v_j = \left(x_1^{v_j}, x_2^{v_j}, x_3^{v_j}\right)$ in point T_j, 3/ the area of elementary surface s_j. It is possible to unambiguously enter the vector v_j through coordinates $x_1^{v_j}, x_2^{v_j}$ (assuming the outer normal vector does not direct "down").
Every elementary surface p_j is defined therefore by 6 parameters:

$$p_j: \left(x_1^{T_j}, x_2^{T_j}, x_3^{T_j}, x_1^{v_j}, x_2^{v_j}, s_j\right). \qquad (6)$$

3.3. Experimental Measurement of Heater Radiation Intensity

We do not know the distribution function of the heat radiation intensity in the heater surroundings from the heater producer. We realized the experimental measurement of the heat radiation intensity in the surroundings of the heater by sensor. The location of the heater was *Z:* (0, 0, 0, 0, 0, 0) in accordance with relation (5), i.e. the center *S* of the heater lies in the origin, union radiation vector $u = (0, 0, -1)$ and vector of the heater axis $r = (1, 0, 0)$ in Cartesian coordinate system (O, x_1, x_2, x_3).

We will suppose the heat radiation intensity across the elementary surface p_j is the same as at centre of gravity T_j. Heat radiation intensity in T_j depends on the position of this point (determined by the first 3 parameters in relation (6)) and on direction of outer normal vector v_j in point T_j (determined by the fourth and fifth parameters in relation (6)). Thus heat radiation intensity on the elementary surface p_j depends on the first 5 parameters in relation (6). The heat radiation intensity was measured by sensor in chosen points below the heater and various deflections of the sensor (it corresponds to centre of gravity T_j location and direction of outer normal vector v_j of elementary surface p_j). We will use linear interpolation function of 5 variables to determine the heat radiation intensity in the vicinity of heater *Z*. The formula of interpolation function is described in detail e.g. in (Antia 2002).

3. 4. General Case of a Heater Location

In this paragraph will be described the process of calculating the heat radiation intensity of heater *Z* in a general position on an arbitrary elementary surface p_j of the mould. We will suppose the heat radiation intensity is the same on the whole elementary surface p_j as in the centre of gravity T_j. We transformed the previous Cartesian coordinate system (O, e_1, e_2, e_3) into a positively oriented Cartesian system $(S, r, n, -u)$, where point *S* is the centre of heater *Z*, *r* is the heater axis and vector *u* is the vector of radiation direction of heater *Z*. The vector *n* is determined by the vector product of the vectors *–u* and *r* (see more detail in (Budinký 1983)) and is defined by relation

$$n = (-u) \times r = \left(-\begin{vmatrix} x_2^u & x_3^u \\ x_2^r & x_3^r \end{vmatrix}, \begin{vmatrix} x_1^u & x_3^u \\ x_1^r & x_3^r \end{vmatrix}, -\begin{vmatrix} x_1^u & x_2^u \\ x_1^r & x_2^r \end{vmatrix} \right).$$

We assume the unit length of the vectors *r*, *n* and *–u*. Then we can define orthonormal matrix $\mathbf{A}$ (i.e. $\mathbf{A}^T\mathbf{A} = \mathbf{E}$, where $\mathbf{E}$ denotes identity matrix):

$$\mathbf{A} = \begin{pmatrix} x_1^r & x_1^n & -x_1^u \\ x_2^r & x_2^n & -x_2^u \\ x_3^r & x_3^n & -x_3^u \end{pmatrix}.$$

Let us denote $T_j' = [x_1^{T_j'}, x_2^{T_j'}, x_3^{T_j'}]$ the transformation of the centre of gravity $T_j = [x_1^{T_j}, x_2^{T_j}, x_3^{T_j}]$ of an elementary surface p_j in Cartesian coordinate system $(S, r, n, -u)$. Let the vectors $\mathbf{T}_j$, $\mathbf{T}_j'$ and $\mathbf{S}$ represent

coordinates of the points T_j, T_j' and S. Then the transformation of the point T_j is given by relation

$$\left(\mathbf{T}_j'\right)^T = \mathbf{A}^T\left(\mathbf{T}_j - \mathbf{S}\right)^T . \quad (7)$$

An analogy of the transformation of the outer normal vector v_j in the centre of gravity T_j of elementary surface p_j is given by relation

$$\left(\mathbf{V}_j'\right)^T = \mathbf{A}^T\mathbf{V}_j^T . \quad (8)$$

We convert a general case of heater location on the basis of relations (7) and (8) to the case of a heater location with realized experimental measurement of the surrounding heat radiation intensity. It means we are able to calculate the heat radiation intensity of an arbitrarily located heater on centre of gravity T_j of elementary surface p_j.

3. 5. Calculation of Total Heat Radiation Intensity on an Elementary Surface

In this part of the article will be described the numerical calculation of heat radiation intensity on an elementary surface. We denote as L_j the set of all infrared heaters radiating on the j-th elementary surface p_j, $(1 \le j \le N)$ for the defined location of heaters, and I_{jl} for the heat radiation intensity of l-th infrared heater on the p_j elementary surface. Then the total heat radiation intensity I_j on the elementary surface p_j is defined by the following relation (see in more detail in (Cengel 2007))

$$I_j = \sum_{j \in L_j} I_{jl} .$$

We denote as I_{opt} the recommended heat radiation intensity across the whole mould surface by the producer. We define aberration F by relation

$$F = \frac{\sum_{j=1}^{N} \left| I_j - I_{opt} \right| s_j}{\sum_{J=1}^{N} s_j} \quad (9)$$

and aberration $\widetilde{F}$ is determined by relation

$$\widetilde{F} = \left(\sum_{j=1}^{N} (I_j - I_{opt})^2 s_j \right)^{1/2} . \quad (10)$$

We highlight that s_j denotes the area of the elementary surface p_j. We need to find the location of heaters such that value of aberration F (alternatively aberration $\widetilde{F}$) will be within specified tolerance.

4. OPTIMIZATION OF LOCATION OF HEATERS BY GENETIC ALGORITHM AND BY "HILL-CLIMBING" METHOD

In this chapter we will briefly describe a procedure to optimize the location of heaters. Note that we do not know the analytical expression for the function of heat radiation intensity surrounding the heater. During optimization we must test three possible collisions of heaters (one heater radiating on a second heater more than the given limit, one heater having insufficient distance from second heater, a heater has not sufficient distance from mould surface). Hence, optimization process is more complicated.

We will use a genetic algorithm for global optimization (this method is less liable to get stuck in the local minimum) and upon finding a solution we will apply the "hill-climbing" method to locally optimize the heater's location.

4. 1. Use of Genetic Algorithm

We note that the terms and relations used in this paragraph are described in more details e.g. in (Affenzeller et al. 2009). The location of every heater is defined by 6 real parameters according to relation (5). Therefore $6M$ parameters are necessary to define the location of all M heaters. One chromosome will represent one individual (one possible location of the heaters). Particular genes of the chromosome will represent the determining parameters of the heaters' location. The population will include Q individuals. Continuously generated individuals will be saved in the matrix $\mathbf{B}_{Q\times 6M}$. Every row of this matrix represents one individual. Our goal is to find an individual y, such that the radiation intensity on the mould surface for the corresponding location of the heaters approaches the recommended value I_{opt} provided by the producer. Thus, we will seek individual $y_{\min} \in C$ satisfactory condition

$$F(y_{\min}) = \min_{y \in C} F(y) , \quad (11)$$

where $C \subset E_{6M}$ is searched space and function F is defined by relation (9). We often seek minimum of function $\widetilde{F}$ given by relation (10) during the process of optimizing the location (allows us to find location of heaters without extreme difference in radiation intensity from recommended intensity I_{rec} on elementary surfaces p_j, we tested other aberrations too).

4.1.1. Schematic Description of Used Genetic Algorithm

In this part we will describe the schematically particular steps of used genetic algorithm:

begin of algorithm
1/ the creation of the specimen and an initial population of individuals,
2/ the evaluation of all individuals (calculation value $F(y)$ for every individual y), sorting of all individuals y according their evaluation $F(y)$ (from the smallest value to largest value),
3/ *while* a condition of termination is not fulfilled *do*
if operation crossover is randomly chosen *then*
random selection of a pair of parents,
execution of operation crossover and
creation of two new individuals
else
random selection of an individual,
execution of operation mutation and
creation of two new individuals
end if,
integration and evaluation of new calculated individuals, sorting of all individuals in accordance with evaluations, storage of only the first Q individuals with the best evaluation for subsequent calculation
end while,
4/ output of the first row of matrix **B** - the best finding individual
end of algorithm.

The setting of the specimen y_1 (initial individual) is selected in such a way that all the centres of the heaters create nodes in a regular rectangular network, and this network lies over the mould on a plane parallel with the plane defined by axes x_1 and x_2. We generate consequently $Q-1$ remaining individuals of initial generation by random modification of genes with values of y_1. If a collision of any heater exists for any individual y during the genetic algorithm, the individual y is penalized and consequently expelled from the population. Individual selection to operation crossover or to operation mutation is accomplished on the principle of fitness-proportionate selection (see more detail in (Affenzeller at al. 2009)). During the operation crossover we do only one point crossover and modify the variants of crossover and generate two new individuals. During the operation mutation we generate two new individuals, too. This algorithm is described in more detail in (Mlýnek and Srb 2011).

4. 2. Use of "hill-climbing" Method

We will use this method to further locally optimize the solution provided by the genetic algorithm.

4.2.1. Schematic Description of Used "hill- climbing" Method

In this part we will describe the schematically particular steps of the used "hill-climbing" method:
begin of algorithm
1/ let us assign the solution provided by genetic algorithm to $\bar{y}$ and denote $\tilde{y}$ as the individual received by partial increment of $\bar{y}$,
2/ we choose suitable sizes of increments h_i, $1 \le i \le 6M$,
3/ *repeat*
for i:=1 *to* 6*M do begin*
we perform repeatedly an increment of i-th gene of individual $\bar{y}$ by value h_i (we obtain individual $\tilde{y}$) until inequality $F(\bar{y}) > F(\tilde{y})$ is true, $\bar{y} := \tilde{y}$;
$h_i := -\frac{h_i}{2}$
end
until a condition of termination is not fulfilled,
4/ output of optimized solution – individual $\bar{y}$
end of algorithm.

The final optimized solution is individual $\bar{y}$ that includes information about location of every heater in the form (5). "Hill-climbing" method is described in more details e.g. in (Chembers 2001).

5. TESTING EXAMPLE AND PRACTICAL EXAMPLE

We will describe the results of the heat radiation intensity optimisation calculations by using the mentioned methods in Chapter 4. First, we will use the genetic algorithm to globally optimize the location of the heaters and upon received solution we will apply the "hill-climbing" method for local optimization. We will focus on a testing example and a practical example. A software application was programmed in the language Matlab.

5. 1. Testing Example

One of the tested heated surfaces was a section of a spherical surface. The radius of the sphere is 0,4[m], the vertical projection of this part of surface to plane given by axes x_1 and x_2 (ground plane) is square with side length 0,5[m]. This part of the spherical surface is described by 1800 triangular elementary surfaces.
The recommended radiation intensity by a producer I_{opt} we will define as I_{opt} =68[kW/m^2].
We will use 16 heaters to provide radiation across the mould. All heaters are of the same type: producer Philips, capacity 1600W, length 0,15[m], width 0,04[m]. In the first step of genetic algorithm we will construct specimen y_1. We will create a regular rectangular network in the parallel plane ρ with the plane given by axes x_1 and x_2. The centres of the heaters will be located at network nodes. The vector of the heater axis of every heater is parallel with axis x_1. The plane ρ lies over the mould surface at distance 0,1[m] from centre of gravity T_i with the highest value $x_3^{T_i}$ from the all centres of gravity $T_j, 1 \le j \le N$. The aberration $F(y_1)$ given by relation (9) is $F(y_1) = 40{,}46$. The

population will contain 30 individuals (Q =30) and we will construct an initial population of individuals by modifying the parameters of specimen y_1. We will apply the genetic algorithm described in Chapter 4. We will find the optimized individual y_{optga} after 100000 iterations (finding of $y_{\min}$ from relation (11) is not realistic in practice), $F(y_{optga}) = 4{,}00$. Now, we will apply the "hill-climbing" method described in Chapter 4 on y_{optga} and after 5000 iterations we obtain the final optimized solution y_{opt}, value $F(y_{opt}) = 3{,}86$. The values $F(y_{optga})$ and $F(y_{opt})$ depend on the number of iterations of the genetic algorithm and the "hill-climbing" method (see Figure 3).

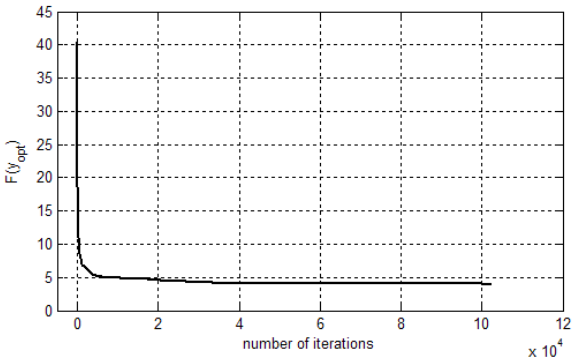

Figure 3: Testing Example - Dependence of $F(y_{optga})$ and $F(y_{opt})$ on Number of Iterations

The graphical representation of heat radiation intensity on the mould surface (levels of radiation intensity in [kW/m^2] correspond to shades of gray colour) and location of heaters corresponding to individual y_{opt} are displayed in Figure 4.

We will make an analogous calculation in the case of replacing function F with function $\widetilde{F}$ given by relation (10); we will execute the same numbers of iterations to the computation of $\widetilde{y}_{optga}$ and $\widetilde{y}_{opt}$. We get the following results:

$\widetilde{F}(y_1) = 25{,}13$; $\widetilde{F}(\widetilde{y}_{optga}) = 3{,}48$; $\widetilde{F}(\widetilde{y}_{opt}) = 3{,}34$. The choice of function $\widetilde{F}$ as the evaluation function in the genetic algorithm and in the „hill-climbing" method allows us to eliminate the parts of the mould surface with extremely high or low heat radiation intensity.

5. 2. Practical Example

Now we will describe a practical example of heat radiation on an aluminium mould surface. The size of the mould is 0,6x0,4x0,12[m^3]. This mould is used to produce the piece of artificial leather that is used to cover a car's passenger-side dashboard. The mould surface is described by 2187 triangular elementary surfaces.

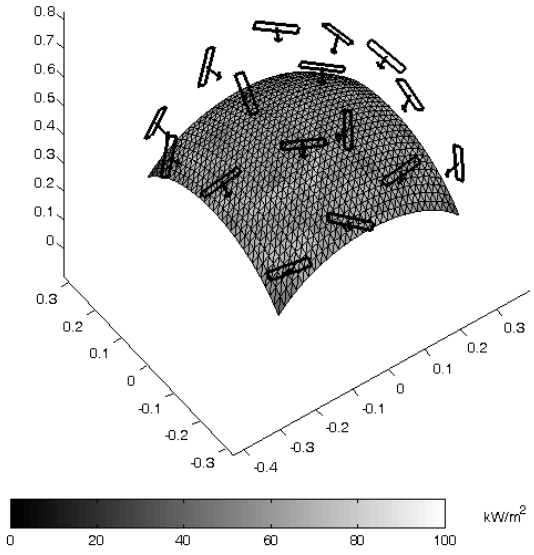

Figure 4: Testing Example - Displaying Heat Radiation Intensity ([kW/m^2]) on the Mould Surface and Location of Heaters Corresponding to Individual y_{opt}

The recommended radiation intensity from the producer is I_{opt} =50[kW/m^2]. We will use 19 heaters to heat the mould. The heaters are of the same type as in the „testing example" and we will use the same determining procedure of specimen y_1 (the distance of plane ρ from the mould surface is again 0,1[m]). Following the computing procedure the population, also analogous to the "testing example", will again contain 30 individuals. We will obtain the following results after 100000 iterations of genetic algorithm, and after 5000 iterations of „hill-climbing":

$F(y_1) = 41{,}11$; $F(y_{optga}) = 5{,}17$; $F(y_{opt}) = 5{,}12$.

The values $F(y_{optga})$ and $F(y_{opt})$ descend in dependence on the number of iterations of the genetic algorithm and the number of iterations of the "hill-climbing" algorithm (see Figure 5). The graphical representations of heat radiation intensity across the mould surface and the locations of heaters corresponding to individual y_{opt} are displayed in Figure 6. Calculation time on PC, CPU 2xAMD Athlon 2,81GHz was 20 hours. When we use function $\widetilde{F}$ given by relation (10) instead of function F during calculation, we obtain the following results:

$\widetilde{F}(y_1) = 28{,}39$, $\widetilde{F}(\widetilde{y}_{optga}) = 4{,}03$, $\widetilde{F}(\widetilde{y}_{opt}) = 3{,}96$.

These two described examples are illustrative. There are often moulds of larger sizes used, with more rugged surfaces and the value of recommended heat radiation

intensity on surface I_{opt} is higher, therefore we apply a higher number of heaters to produce the radiation.

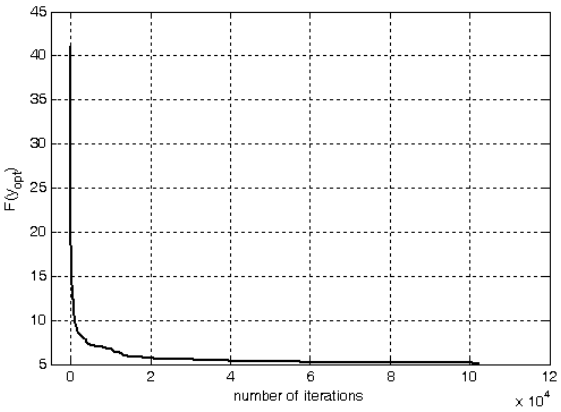

Figure 5: Practical Example - Dependence of $F(y_{optga})$ and $F(y_{opt})$ on Number of Iterations

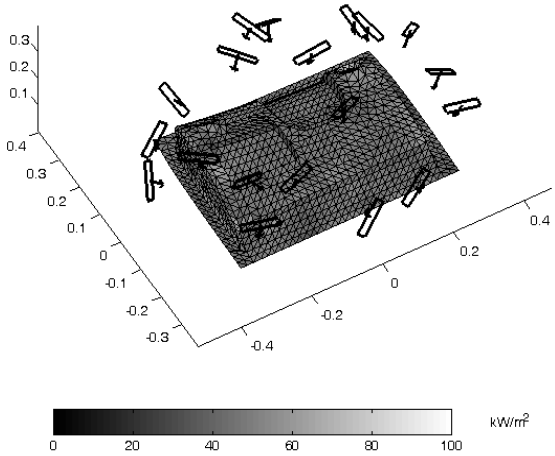

Figure 6: Practical Example - Displaying Heat Radiation Intensity ([kW/m^2]) on the Mould Surface and Location of Heaters Corresponding to Individual y_{opt}

On the basis of practical experience along with finding the optimal location of heaters through use of the genetic algorithm and "hill-climbing" method described in this article we can calculate a sufficiently precise solution for the needs of artificial leathers producer.

6. CONCLUSION

On the basis of numerical tests we get a sufficiently exact solution of the optimized location for heaters over a mould. It is necessary to ensure the temperature differences on the mould surface less than 3[°C] during the mould warming process. Heat conductivity of the mould affects the unification of different temperatures on the mould surface.

Generally, the locations of heaters determined upon the basis of the experience of technicians produce significantly worse results than ours. For various models and, as a result, the process is much more time consuming (approximately 2 week in comparison to our calculation, which usually took from 15 to 30 hours).

ACKNOWLEDGEMENTS

Production of this article was supported by MPO project No. FR-TI1/266.

REFERENCES

Affenzeller, M.; S. Winkler; S.Wagner; and A. Beham. 2009. *Genetic Algorithms and Genetic Programming*. Chapman and Hall/CRC, Boca Raton, 15-120.

Antia, H. M. 2002. *Numerical Methods for Scientists and Engineers*. Birkhäuser Verlag, Berlin, 114-153.

Budinský, B. 1983. *Analytical and Differential Geometry*. SNTL, Prague (in Czech), 57-75.

Cengel, Y. A. 2007. *Heat and Mass Transfer*. McGraw-Hill, New York, 61-130, 663-772.

Chambers, L. 2001. *Genetic Algorithms*. Chapman and Hall/CRC, Boca Raton, 1-56.

Mlýnek, J. and R. Srb. 2011. "Optimization of a Heat Radiation Intensity on a Mould Surface in the Car Industry". In *Proceedings of the Mechatronics 2011 Conference*. Faculty of Mechatronics, Warsaw University of Technology, Warsaw, Springer-Verlag, Berlin, September 2011, 531-540.

AUTHOR BIOGRAPHIES

JAROSLAV MLÝNEK was born in Trnava, Czechoslovakia and went to the Charles University in Prague, where he studied numerical mathematics on Faculty of Mathematics and Physics and he graduated in 1981. He focuses in his work on the computational problems of warming and thermal losses in components of electrical machines and on mathematical models of thermal convection in electric machines. Currently he works as associate professor at the Technical University of Liberec, Czech Republic. His e-mail address is: jaroslav.mlynek@tul.cz.

RADEK SRB was born in Mladá Boleslav, Czech Republic and went to the Technical University in Liberec, Czech Republic, where he studied computer science and programming in the Faculty of Mechatronics. He graduated in 2005. He focuses on problems with automated control of production. He works as a teacher and he is a Ph.D. student. His e-mail address is: radek.srb@tul.cz.

NOVEL MULTIVARIABLE LABORATORY PLANT

Daniel Honc and František Dušek
Department of Process Control
Faculty of Electrical Engineering and Informatics
University of Pardubice
nám. Čs. legií 565, 532 10 Pardubice, Czech Republic
E-mail: daniel.honc@upce.cz

KEYWORDS
Laboratory plant, four water tanks, first principle model, experimental identification.

ABSTRACT

A novel multivariable laboratory plant is presented. The process is a variation of known "four interconnected water tanks". The novelty of the process lies in a way how to ensure multi-variability. Pneumatic volumes above the water levels are connected together and orifices are placed into those circuits. Cross interactions exists only in transient states so the working area is not reduced. First principle nonlinear mathematical model is derived and presented together with its linearized form and experimental identification of unknown parameters.

1. INTRODUCTION

Importance of laboratory experiments in control engineering education is evident. Industrial interest in use of multivariable control techniques (Shinskey 1981; Goodwin et al. 2000; Skogestad and Postlethwaite 2005) is topical problem too. Multivariable laboratory processes are not very common. There exist some commercial products as e.g. Helicopter body on support, Ball&Plate model produced by TecQuipment Ltd, 2 DOF (Degrees of Freedom) Helicopter, Rotary Inverted Pendulum modules from QUANSER Innovative Educate, Four axis Control Moment Gyroscope or Torsional Plant from Educational Control Products, Twin Rotor MIMO from Feedback plc. Some of the multivariable processes are constructed at universities for their own use as various water tank processes, combinations of temperature and flow control of liquids or air, distillation columns, chemical reactors, heat exchangers and other apparatuses. Disadvantage of such systems is usually higher complexity so the systems are more time and money consuming to operate and service. From this point of view water tanks are quite simple – water pumps are cheap and reliable, water level measurement by use of pressure sensors is easy too. Very elegant multivariable process called "quadruple-tank process with an adjustable zero" was developed at Department of Automatic Control in Lund (Johanson and Nunes 1998). We have decided to design and construct our variation of "four tank system". Instead of using three-path valves or connecting water levels we have closed and connected air spaces above water levels. This caused decreasing of original working area so we added air orifices into the air circuits. Novel multivariable process with interesting features arises.
The outline of the paper is as follows. Laboratory plant is presented in section 2. Its nonlinear first principle model is derived in section 3. This model is linearized and state-space representation is given in section 4. In section 5 experimental identification is carried out. Model is verified in section 6. Some conclusions are given in section 7.

2. LABORATORY PROCESS

Laboratory Hydraulic-Pneumatic System (HPS) was designed and realized at Department of Process Control University of Pardubice (Klán et al. 2005; Macháček et al. 2005). It includes a combination of hydraulic and pneumatic components. The pneumatic circuits create cross coupling between both classical double tank sections (Åström and Lundh 1992) and form a multivariable system with non-typical feature. Four cylindrical water tanks are the main parts - see Fig. 1 and 2. Water is pumped by two pumps into upper tanks LH and RH, flows into lower tanks LL and RL and from here back into the reservoir. Water flow rates are controlled by input signal of the pumps u_L, u_R - voltage in the range 0÷10 V, which is amplified and changed into 4÷10 V in pump unit. The levels in lower tanks are measured indirectly by difference pressure sensors.

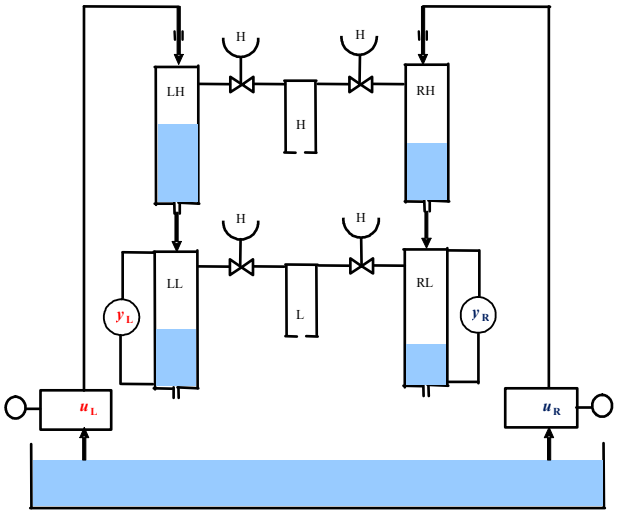

Figure 1: Scheme of HPS

Proceedings 26th European Conference on Modelling and Simulation ©ECMS Klaus G. Troitzsch, Michael Möhring, Ulf Lotzmann (Editors)
ISBN: 978-0-9564944-4-3 / ISBN: 978-0-9564944-5-0 (CD)

Output of the pressure sensors y_L, y_R is given in a form of electric voltage in the range 0÷10 V. Air spaces above the water levels are connected together by pneumatic circuits H and L with manually configurable valves. Orifices in air chambers serve as a connection between pneumatic volumes and atmosphere. The system structure and its behaviour may be changed by the size of orifices and by valves setting in the pneumatic circuits. There is atmospheric pressure in pneumatic circuits in the steady state. If water level is changing pressure in pneumatic volumes changes too and influences adjacent water levels. Air flows into or from air chamber and gradually equilibrates with atmospheric pressure. That means that multivariable cross effect has only dynamic character and after some time disappears – see step responses in Fig. 5 and 6. Diameter of the air orifice influences gain and time life of the effect (effect is stronger but slower for smaller orifice).

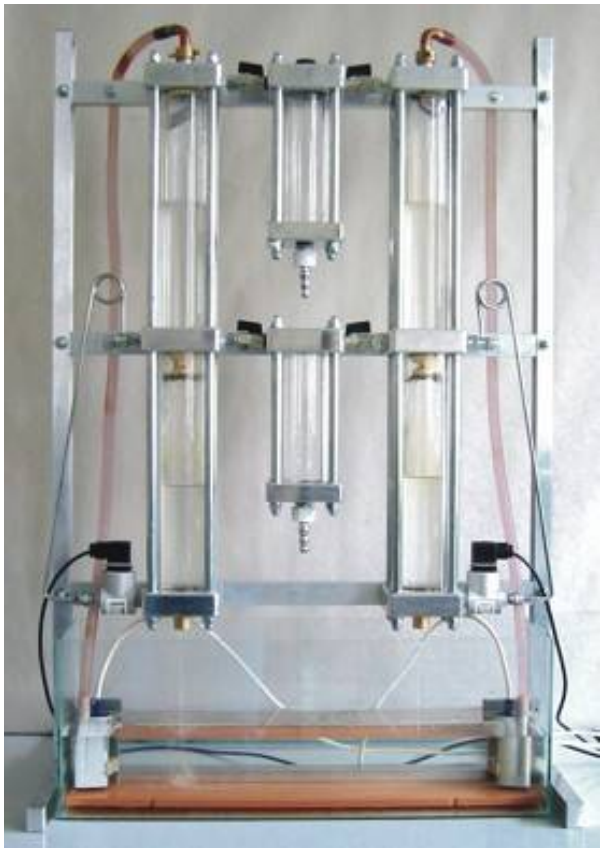

Figure 2: Hydraulic-Pneumatic System

3. NONLINEAR MODEL

Nonlinear model of HPS is derived on the basis of physical laws and system construction. Only the lower pneumatic circuit is considered in this model (upper pneumatic volume C_H is open into atmosphere).

Models of the water tanks can be described by

a) mass balance based on law of mass conservation

$$Q_1 = Q_2 + \rho S \frac{dh}{dt} \tag{1}$$

where Q_1 is water inlet mass flow rate [kg s^{-1}], Q_2 is water outlet mass flow rate [kg s^{-1}], ρ is water density [kg m^{-3}], S is cross-section area of tank [m^2] and h is water level [m].

b) Bernoulli equation - water outlet mass flow rate is given as

$$Q_2 = k\, s\sqrt{2\rho}\sqrt{h\rho g + p_1 - p_2} \tag{2}$$

where k is discharge coefficient [-], s is cross-section area of orifice [m^2], g is acceleration of gravity [m s^{-2}], p_1 is pressure above the water level [Pa] and p_2 is pressure under the orifice [Pa].

In Table 1 variables used in Equations (1) and (2) are specified according to Fig. 1.

Table 1: Notation of variables for tanks nonlinear model

Tank	Q_1	Q_2	S	k	s	h	p_1	p_2
LH	Q_L	Q_{LH}	S_L	k_L	s_L	h_{LH}	p_A	p_L
RH	Q_R	Q_{RH}	S_R	k_R	s_R	h_{RH}	p_A	p_L
LL	Q_{LH}	Q_{LL}	S_L	k_L	s_L	h_{LL}	p_L	p_A
RL	Q_{RH}	Q_{RL}	S_R	k_R	s_R	h_{RL}	p_L	p_A

The lower pneumatic circuit was modelled on the basis of

a) mass balance equivalent of Equation (1)

$$0 = Q_{CL} + \frac{d}{dt}(V_L \rho_L) \tag{3}$$

where Q_{CL} is air outlet mass flow rate [kg s^{-1}], V_L is pneumatic volume (air chamber volume plus volume above water levels) [m^3] and ρ_L is air density [kg m^{-3}].

b) equivalent of Equation (2), which was simplified into the following form

$$Q_{CL} = k_{CL}\, s_{CL}(p_L - p_A) \tag{4}$$

where k_{CL} is air discharge coefficient [$s\ m^{-1}$], s_{CL} is cross-section area of air orifice [m^2], p_L is pressure in the pneumatic loop [Pa] and p_A is atmospheric pressure [Pa].

c) equation of gas state

$$p_L = \rho_L r T \tag{5}$$

where r is air specific gas constant [J K^{-1} kg^{-1}] and T is air temperature [K].

Equations (3), (4) and (5) may be combined together into relationship

$$\frac{d(p_{\mathrm{L}}V_{\mathrm{L}})}{dt} = -k_{\mathrm{CL}}s_{\mathrm{CL}}rT(p_{\mathrm{L}} - p_{\mathrm{A}}) \qquad (6)$$

For pneumatic volume holds

$$V_{\mathrm{L}} = S_{\mathrm{L}}(H - h_{\mathrm{LL}}) + V_{\mathrm{CL}} + S_{\mathrm{R}}(H - h_{\mathrm{RL}}) \qquad (7)$$

where H is tanks height and V_{CL} is volume of the air chamber.

Static characteristic of the pump is considered in the form $Q = a(u - \tilde{u})^b$, where Q is water mass flow rate [kg s^{-1}], u is input signal for the pump unit [V], $\tilde{u}$ is the input signal [V] corresponding to zero mass flow rate, a and b are the pump specific coefficients.

Pressure sensor static characteristic is in the form $y = c \cdot h + d$, where y is output signal from the pressure sensor [V], h is water level [m] c and d are the pressure sensor specific coefficients.

The model has five state variables - four water levels and pressure in the lower pneumatic circuit, two inputs - input signals for pump unit u_{L} and u_{R} and two outputs - output signals from pressure sensors y_{L} and y_{R}.

4. LINEARIZED MODEL

Nonlinear model is analytically linearized for control design purposes. The linearization is realized by the Taylor expansion of the original nonlinear equations - the second and higher order terms are omitted. Symbol Δ denotes deviation of variable from steady state, *e.g.* $\Delta h = h - h_0$, where subscript 0 denotes steady state. The steady state of pressure in lower pneumatic circuit is atmospheric pressure p_{A}.

By linearization of Equation (2) we get

$$\Delta Q_2 = \frac{k^2 s^2 \rho^2 g}{Q_0}\Delta h + \frac{k^2 s^2 \rho}{Q_0}\Delta p_1 - \frac{k^2 s^2 \rho}{Q_0}\Delta p_2 \qquad (8)$$

where Q_0 steady-state mass flow rate.

We can rewrite Equation (1) in deviation form as

$$\Delta Q_1 = \Delta Q_2 + \rho S\frac{d\Delta h}{dt} \qquad (9)$$

If we substitute Equations (8) and (9) and by respecting notation from Table 1 we get two linear differential equations for upper and lower tanks

$$T\frac{d\Delta h_{\mathrm{H}}}{dt} = -\Delta h_{\mathrm{H}} + Z\Delta p_{\mathrm{L}} + Z_{\mathrm{Q}}\Delta Q \qquad (10)$$

$$T\frac{d\Delta h_{\mathrm{L}}}{dt} = \Delta h_{\mathrm{H}} - \Delta h_{\mathrm{L}} - 2Z\Delta p_{\mathrm{L}} \qquad (11)$$

where

$$T = \frac{SQ_0}{k^2 s^2 \rho g}, \quad Z = \frac{1}{\rho g}, \quad Z_{\mathrm{Q}} = \frac{T}{\rho S}.$$

General terms are given. Particular variables for Equations (10) and (11) have to be filled from Tables 1 and 2.

Table 2: Notation of variables for tanks linear model

Tank	Δh_{H}	Δh_{L}	Q_0	ΔQ	T	Z_{Q}
LH	Δh_{LH}	-	Q_{L0}	ΔQ_{L}	T_{L}	Z_{QL}
RH	Δh_{RH}	-	Q_{R0}	ΔQ_{R}	T_{R}	Z_{QR}
LL	Δh_{LH}	Δh_{LL}	Q_{L0}	-	T_{L}	-
RL	Δh_{RH}	Δh_{RL}	Q_{R0}	-	T_{R}	-

Model of the air circuit is nonlinear because of $p_{\mathrm{L}}V_{\mathrm{L}}$ term in Equation (6). We can write its linearization in point [p_{A}, V_{L0}] as

$$p_{\mathrm{L}}V_{\mathrm{L}} = p_{\mathrm{A}}V_{\mathrm{L0}} + p_{\mathrm{A}}\Delta V_{\mathrm{L}} + V_{\mathrm{L0}}\Delta p_L \qquad (12)$$

and calculate left term of Equation (6) as

$$\frac{d(p_{\mathrm{L}}V_{\mathrm{L}})}{dt} = p_{\mathrm{A}}\frac{d\Delta V_{\mathrm{L}}}{dt} + V_{\mathrm{L0}}\frac{d\Delta p_{\mathrm{L}}}{dt} \qquad (13)$$

where V_{L0} is steady-state value of the lower pneumatic volume.

By derivation of (7) and rewriting to deviations we get

$$\frac{d\Delta V_{\mathrm{L}}}{dt} = -S_L\frac{d\Delta h_{\mathrm{LL}}}{dt} - S_R\frac{d\Delta h_{\mathrm{RL}}}{dt} \qquad (14)$$

If we substitute (13) and (14) into (6) (term p_{L}-p_{A} equals to Δp_{L}) we get for dynamic of the lower pneumatic circuit following equation

$$T_{\mathrm{p}}\frac{d\Delta p_{\mathrm{L}}}{dt} + \Delta p_{\mathrm{L}} = Z_{\mathrm{hL}}(\Delta h_{\mathrm{LH}} - \Delta h_{\mathrm{LL}}) + Z_{\mathrm{hR}}(\Delta h_{\mathrm{RH}} - \Delta h_{\mathrm{RL}}) \qquad (15)$$

where

$$T_{\mathrm{p}} = \frac{V_{\mathrm{L0}}Q_{\mathrm{L0}}Q_{\mathrm{R0}}}{2p_{\mathrm{A}}\left(k_{\mathrm{L}}^2 s_{\mathrm{L}}^2 Q_{\mathrm{R0}} + k_{\mathrm{R}}^2 s_{\mathrm{R}}^2 Q_{\mathrm{L0}}\right) + Q_{\mathrm{L0}}Q_{\mathrm{R0}}rTk_{\mathrm{CL}}s_{\mathrm{CL}}},$$

$$Z_{\mathrm{hL}} = \frac{p_{\mathrm{A}}S_{\mathrm{L}}T_{\mathrm{p}}}{V_{\mathrm{L0}}T_{\mathrm{L}}}, \quad Z_{\mathrm{hR}} = \frac{p_{\mathrm{A}}S_{\mathrm{R}}T_{\mathrm{p}}}{V_{\mathrm{L0}}T_{\mathrm{R}}}$$

By linearization of static pump characteristic we get deviation form

$$\Delta Q = ab\left(u_0 - \tilde{u}\right)^{b-1}\Delta u = Z_u \Delta u \tag{16}$$

We can write static characteristic of the pressure sensors in deviation form as

$$\Delta y = c\Delta h \tag{17}$$

Particular variables used in Equations (16) a (17) have to be filled from Tables 1, 2 and 3.

Table 3: Notation of variables for pumps and pressure sensors linear model

Position	ΔQ	Δu	u_0	Z_u	Δy	Δh
L	ΔQ_L	Δu_L	u_{L0}	Z_{uL}	Δy_L	Δh_{LL}
R	ΔQ_R	Δu_R	u_{R0}	Z_{uR}	Δy_R	Δh_{RL}

If we compose appropriate state vector we are able to rewrite linear model into following state space form

$$\underbrace{\begin{bmatrix} \frac{d\Delta h_{LH}}{dt} \\ \frac{d\Delta h_{RH}}{dt} \\ \frac{d\Delta p_L}{dt} \\ \frac{d\Delta h_{LL}}{dt} \\ \frac{d\Delta h_{RL}}{dt} \end{bmatrix}}_{\frac{d\mathbf{x}}{dt}} = \underbrace{\begin{bmatrix} -\frac{1}{T_L} & 0 & \frac{Z}{T_L} & 0 & 0 \\ 0 & -\frac{1}{T_R} & \frac{Z}{T_R} & 0 & 0 \\ \frac{Z_{hL}}{T_p} & \frac{Z_{hR}}{T_p} & -\frac{1}{T_p} & -\frac{Z_{hL}}{T_p} & -\frac{Z_{hR}}{T_p} \\ \frac{1}{T_L} & 0 & -\frac{2Z}{T_L} & -\frac{1}{T_L} & 0 \\ 0 & \frac{1}{T_R} & -\frac{2Z}{T_R} & 0 & -\frac{1}{T_R} \end{bmatrix}}_{\mathbf{A}} \cdot \underbrace{\begin{bmatrix} \Delta h_{LH} \\ \Delta h_{RH} \\ \Delta p_L \\ \Delta h_{LL} \\ \Delta h_{RL} \end{bmatrix}}_{\mathbf{x}}$$

$$+ \underbrace{\begin{bmatrix} \frac{Z_{QL}}{T_L} & 0 \\ 0 & \frac{Z_{QR}}{T_R} \\ 0 & 0 \\ 0 & 0 \\ 0 & 0 \end{bmatrix}}_{\mathbf{B}} \cdot \underbrace{\begin{bmatrix} \Delta u_L \\ \Delta u_R \end{bmatrix}}_{\mathbf{u}} \tag{18}$$

$$\underbrace{\begin{bmatrix} \Delta y_L \\ \Delta y_R \end{bmatrix}}_{\mathbf{y}} = \underbrace{\begin{bmatrix} 0 & 0 & 0 & c_L & 0 \\ 0 & 0 & 0 & 0 & c_R \end{bmatrix}}_{\mathbf{C}} \cdot \underbrace{\begin{bmatrix} \Delta h_{LH} \\ \Delta h_{RH} \\ \Delta p_L \\ \Delta h_{LL} \\ \Delta h_{RL} \end{bmatrix}}_{\mathbf{x}} \tag{19}$$

5. EXPERIMENTAL IDENTIFICATION

The model has 13 unknown parameters beside parameters connected with construction of the plant. Water orifice discharge coefficients k_L, k_R, air orifice discharge coefficient k_{CL} and coefficients for pump and pressure sensor static characteristics (a, b, u_0, c, d) must be estimated experimentally. Except air orifice discharge coefficient k_{CL} all other parameters can be estimated from one experiment. Both air circuits are open to the atmosphere and control voltages for both pumps are changed stepwise gradually. Water flow rate, water levels and pressure sensors outputs are measured after getting into a steady-state. Parameters are calculated by numerical optimization method.

Parameters a and b (for pump static characteristic) are calculated from input voltages for pump unit u and mass flow rates Q – see Table 4.

Table 4: Parameters of pump static characteristics

Position	a	b	$\tilde{u}$
L	$7.98e10^{-3}$	0.552	0.8
R	$8.53e10^{-3}$	0.495	0.9

Parameter $\tilde{u}$ corresponds to a voltage when the liquid starts to flow to the tanks. Parameters k (water orifice discharge coefficients) are calculated from mass flow rates Q and water levels h – see Table 5. Pressures p_1 and p_2 equals to atmospheric pressure p_A.

Table 5: Parameters of tank static characteristics

Position	k
L	0.737
R	0.735

Parameters c a d (for pressure sensors static characteristics) are calculated from water levels h and output from the pressure sensors y – see Table 6.

Table 6: Parameters of sensors static characteristics

Position	c	d
L	32.5	0.12
R	32.2	0.03

It is not possible to estimate air orifice discharge coefficient from static data. Dynamic experiment had to be carried out – to measure response of the water levels for varying pump powers – see solid line in Figure 3. Unknown parameter is estimated by numerical optimization – least square error cost function is used together with simulated response of the dynamic nonlinear model – see dotted line in Figure 3. For the air orifice discharge coefficient see Table 7.

Table 7: Air orifice discharge coefficient

k_{CL}	0.094

Geometric dimensions and physical constants are given in Tables 8 and 9 – this information can be seen as a part of the experimental identification too.

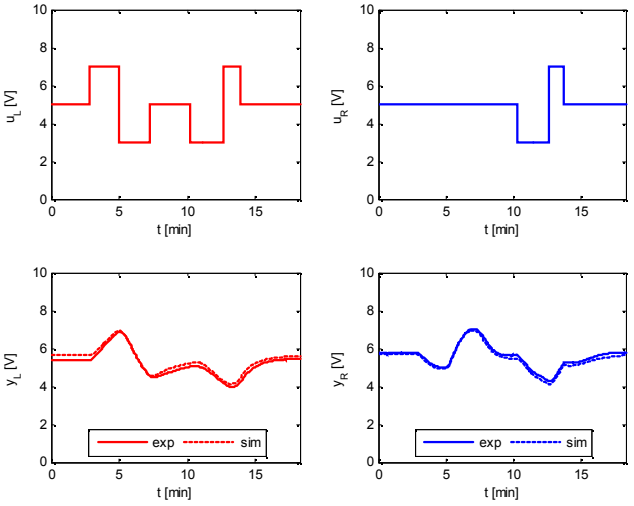

Figure 3: Dynamic experiment for experimental identification

Table 8: Geometric dimensions

Notation	Value	Unit	Meaning
D_L	0.05	m	left tanks diameter
D_R	0.04	m	right tanks diameter
H	0.28	m	tanks height
V_{CL}	$0.45e10^{-3}$	m^3	volume of the lower air chamber
d_L	0.004	m	diameter of the left tanks orifice
d_R	0.004	m	diameter of the right tanks orifice
d_{CL}	$2e10^{-4}$	m	diameter of the lower air orifice

Table 9: Physical constants

Notation	Value	Unit	Meaning
ρ	1000	kg m^{-3}	water density
r	287	J K^{-1} kg^{-1}	air specific gas constant
g	9.81	m s^{-2}	acceleration of gravity
T	293	K	air temperature
p_A	101325	Pa	atmospheric pressure

We can study nonlinearity of the plant by using identified nonlinear process model. If we substitute equations of static characteristics of pumps, water tanks and pressure sensors we get total static characteristic of HPS in a form

$$\Delta y = c\underbrace{\frac{Q_0}{k^2 s^2 \rho^2 g}}_{Z_Q} \underbrace{ab(u_0 - \tilde{u})^{b-1}}_{Z_u} \Delta u \qquad (20)$$

The plant is almost linear in term of steady-state gain. Static characteristic of the tanks is a square function and static characteristic of the pump is close to a square root function. Steady-state gains for whole working area are plotted in upper axes in Figure 4. Time constants of the water tanks in equation (11) are plotted in lower axes in Figure 4. System has smallest time constants for smaller water levels. Dynamic of the process is second order with multiple time constant. Settling time is changing approx. eight times. This holds for the case that the both pneumatic circuits are open.

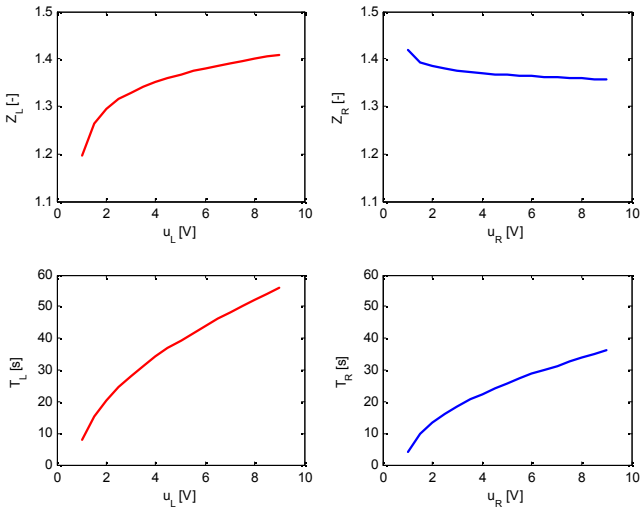

Figure 4: Gains (HPS) and time constants (water tanks)

Situation is different with closed pneumatic circuits. The dynamic of the plant is slowed down and nonlinearity in term of time constants is smaller if the lower pneumatic circuit is closed. This can be observed from step responses. Step responses are calculated for two ultimate cases – for working point close to minimal and maximal water levels – see Fig. 5 and 6.

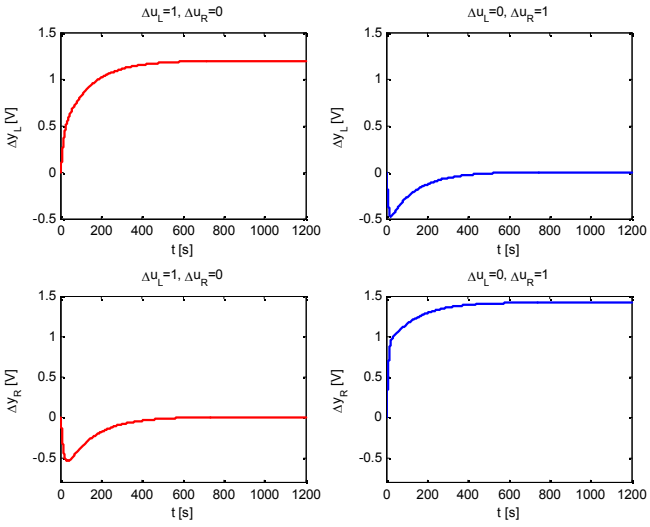

Figure 5: Step responses – u_L = 1 V, u_R = 1 V

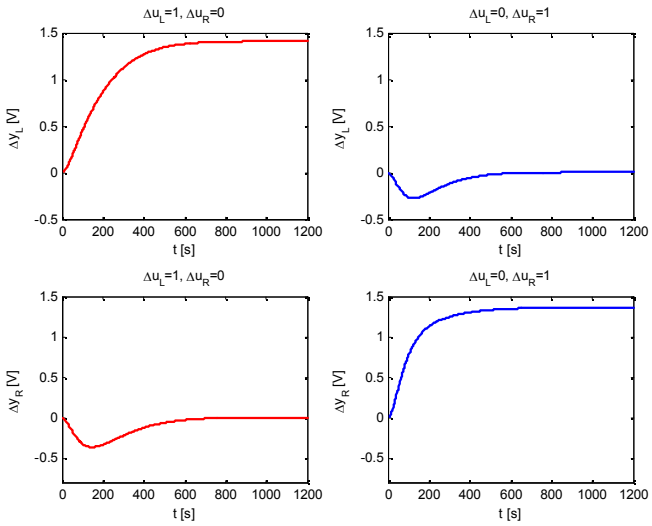

Figure 6: Step responses – u_L = 9 V, u_R = 9 V

Settling time between these two cases is approx. doubled.

6. MODEL VERIFICATION

Step response of HPS is measured – response to a step change in left pump power from 4 to 6 V. Right pump power was kept constant at 5 V. Measured and calculated responses are shown in Figure 7 – measured with the blue and calculated with the red line. Responses are calculated from nonlinear process model. For this particular working point and step change size the linear model would give very similar response.

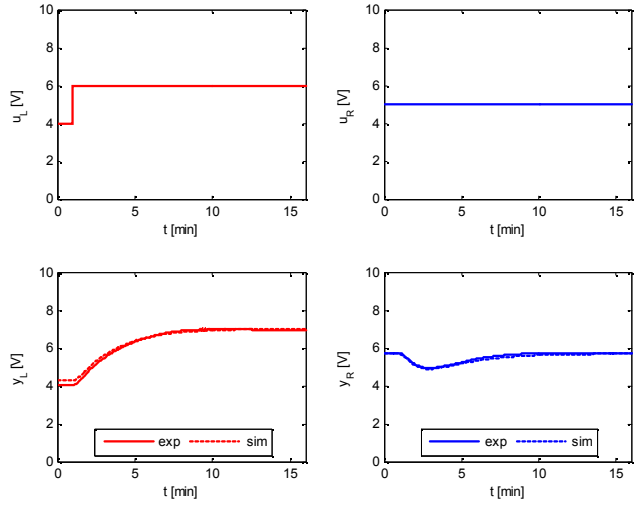

Figure 7: Step response

7. CONCLUSIONS

Novel multivariable laboratory process is introduced. It is a combination of known quadruple water tanks process and pneumatic circuits. Pneumatic volumes are closed and connected instead of water volumes. Air orifice is added to pneumatic circuits and gives arise to a system with interesting features. First principle model is derived. Its linearized state space form can be used for control design. Controllers can be tried and simulated with nonlinear model first and consequently applied to the real laboratory process. From the control point of view the system is interesting because upper water levels are not measured and can easily under- or over-flow. This is hardly to solve with classical controllers but for example state-space predictive controller could be a good choice. State observer would solve the problem of unmeasured upper water levels and controller with respecting state constraints would guarantee that the levels do not cross their limits.

This research was supported by Institutional support of The Ministry of Education, Youth and Sports of the Czech Republic.

REFERENCES

Åström, K. J. and M. Lundh. 1992. Lund control program combines theory with hands-on experience. *IEEE Contr. Syst. ag.*, vol. 12, no. 3, pp. 22–30, 1992.

Goodwin, G.C.; S.F. Graebe and M.E. Salgado. 2000. *Control System Design.* Prentice-Hall 2000. ISBN 0139586539

Johanson, K.H. and J.L.R. Nunes. 1998. "A multivariable laboratory process with an adjustable zero". In *Proceedings of the American Control Conference* (Philadelphia, Pensylvania, June 21-26). 2045-2049.

Klán, P.; M. Hofreiter; J. Macháček; O. Modrlák; L. Smutný and V. Vašek. 2005. "Process Models for a New Control Education Laboratory". *16th World IFAC Congress*, (Prague, Czech Republic, 2005).

Macháček, J.; D. Honc; F. Dušek. 2005. Výukový laboratorní model hydraulicko-pneumatické soustavy. *AUTOMA*, 2005, no. 8 – 9, pp. 108 – 109. ISSN 1210-9592

Shinskey, F.G. 1981. *Controlling Multivariable Processes.* Instrument Society of America, Research Triangle Park, NC, 1981.

Skogestad, S. and I. Postlethwaite. 2005. *Multivariable Feedback Control – Analysis and Design*. Wiley 2005. ISBN 047001167X

DANIEL HONC was born in Pardubice, Czech Republic and went to University of Pardubice, where he studied Process Control and obtained his Ph.D. degree in 2002. He is working at University of Pardubice. His e-mail address is: daniel.honc@upce.cz.

FRANTIŠEK DUŠEK was born in Dačice, Czech Republic and went to Faculty of Chemical Technology Pardubice, where he studied Automation and obtained his MSc. degree in 1980. He worked for pulp and paper research institute IRAPA. Now he is head of Department of Process Control at University of Pardubice. In 2001 he became Ass. professor. His e-mail address is: frantisek.dusek@upce.cz.

NONLINEAR ADAPTIVE CONTROL OF CSTR WITH SPIRAL COOLING IN THE JACKET

Jiri Vojtesek and Petr Dostal
Faculty of Applied Informatics
Tomas Bata University in Zlin
Nam. TGM 5555, 760 01 Zlin, Czech Republic
E-mail: {vojtesek,dostalp}@fai.utb.cz

KEYWORDS
Adaptive control, Polynomial approach, Pole-placement method, Recursive identification, CSTR

ABSTRACT

The most of the processes not only in the industry has nonlinear behavior and control of such processes could be difficult. The controller here consists of linear and nonlinear part where the nonlinear part is derived from the static analysis and the linear part describes nonlinear elements in the loop by the External Linear Model (ELM), parameters of which are estimated recursively with the use of delta (δ-) models. The control synthesis employs polynomial approach with the pole assignment method. The proposed control method satisfies basic control requirements and it was tested by the simulations on the mathematical model of Continuous Stirred Tank Reactor (CSTR) with spiral cooling in the jacket as a typical member of the nonlinear system with lumped parameters.

INTRODUCTION

Chemical reactors are tools widely used not only in the chemical industry for production of various products. Although there are several types from the construction point of view such as batch, semi-bath etc. (Ingham et al. 2000), Continuous Stirred-Tank Reactors (CSTR) and tubular reactors are the most suitable for control purposes.
The Continuous Stirred-Tank Reactor used in this work represents typical nonlinear plant described mathematically by the set of two nonlinear ordinary differential equations (ODE) (Gao et al. 2002). As it is described in (Vojtesek and Dostal 2010), this system has two stable and one unstable steady-state which could lead to very unstable or unoptimal output responses with the use of conventional control methods.
One way how to overcome this inconvience is the use of the adaptive control (Åström and Wittenmark 1989) which adopts parameters of the controller to the actual state of the system via recursive identification of the External Linear Model (ELM) as a linear representation of the originally nonlinear system (Bobal et al. 2005). The results of the adaptive control on this concrete mathematical model can be found for example in (Vojtesek et al. 2011).
The control method used here is based on the combination of the adaptive control and nonlinear control. Theory of nonlinear control (NC) can be found for example in (Astolfi et al. 2008) and (Vincent and Grantham 1997), the factorization of nonlinear models of the plants on linear and nonlinear parts is described in (Nakamura et al. 2002) and (Sung and Lee 2004).
The controller consists of a static nonlinear part (SNP) and a dynamic linear part (DLP). The static part is obtained from the steady-state characteristic of the system, its inversion, suitable approximation and its derivative. As a result of this nonlinear description, the linear part is then described by the external linear model with the use of delta (δ-) models (Middleton and Goodwin 2004) as a special type of discrete-time models which parameters approaches to the continuous ones for the small sampling period (Stericker and Sinha 1993).
The polynomial approach (Kucera 1993) in the control synthesis can be used for systems with negative properties from the control point of view such as nonlinear systems, non-minimum phase systems or systems with time delays. Moreover, the pole-placed method with spectral factorization satisfies basic control requirements such as disturbance attenuation, stability and reference signal tracking.
All graphs shown in this contribution come from the simulation on the mathematical model and they were done on the mathematical simulation software Matlab, version 6.5.1.

CONTINUOUS STIRRED TANK REACTOR

The controlled process under the consideration is the continuous stirred tank reactor (CSTR) with the spiral cooling in the jacket. The scheme of the system can be found in Figure 1.
The complete mathematical description of the process is very complex and we must introduce some simplifications. At first, we expect that reactant is perfectly mixed and reacts to the final product with the concentration $c_A(t)$. The heat produced by the reaction is represented by the temperature of the reactant $T(t)$. Furthermore we also expect that volume, heat capacities and densities are constant during the control.
A mathematical model of this system is derived from the material and heat balances of the reactant and cooling. The resulted model is then a set of two

Proceedings 26th European Conference on Modelling and Simulation ©ECMS Klaus G. Troitzsch, Michael Möhring, Ulf Lotzmann (Editors)
ISBN: 978-0-9564944-4-3 / ISBN: 978-0-9564944-5-0 (CD)

Ordinary Differential Equations (ODEs) (Gao et al. 2002):

$$\frac{dT}{dt} = a_1 \cdot (T_0 - T) + a_2 \cdot k_1 \cdot c_A + a_3 \cdot q_c \cdot \left(1 - e^{\frac{a_4}{q_c}}\right) \cdot (T_0 - T) \quad (1)$$

$$\frac{dc_A}{dt} = a_1 \cdot (c_{A0} - c_A) - k_1 \cdot c_A$$

where $a_{1\text{-}4}$ are constants computed as

$$a_1 = \frac{q}{V};\ a_2 = \frac{-\Delta H}{\rho \cdot c_p};\ a_3 = \frac{\rho_c \cdot c_{pc}}{\rho \cdot c_p \cdot V};\ a_4 = \frac{-h_a}{\rho_c \cdot c_{pc}} \quad (2)$$

variable t in previous equations denotes time, T is used for temperature of the reactant, V is volume of the reactor, c_A represents concentration of the product, q and q_c are volumetric flow rates of the reactant and cooling respectively. Indexes $(\cdot)_0$ denote inlet values of the variables and $(\cdot)_c$ is used for variables related to the cooling.

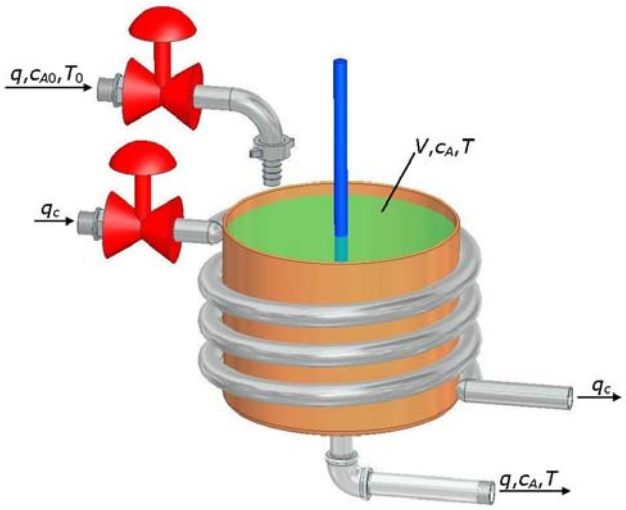

Figure 1: Continuous Stirred Tank Reactor

The fixed values of the system are shown in Table 1 (Gao et al. 2002).

Table 1: Fixed parameters of the reactor

Reactant's flow rate	$q = 100\ l.min^{-1}$
Reactor's volume	$V = 100\ l$
Reaction rate constant	$k_0 = 7.2 \cdot 10^{10}\ min^{-1}$
Activation energy to R	$E/R = 1 \cdot 10^4\ K$
Reactant's feed temperature	$T_0 = 350\ K$
Reaction heat	$\Delta H = -2 \cdot 10^5\ cal.mol^{-1}$
Specific heat of the reactant	$c_p = 1\ cal.g^{-1}.K^{-1}$
Specific heat of the cooling	$c_{pc} = 1\ cal.g^{-1}.K^{-1}$
Density of the reactant	$\rho = 1 \cdot 10^3\ g.l^{-1}$
Density of the cooling	$\rho_c = 1 \cdot 10^3\ g.l^{-1}$
Feed concentration	$c_{A0} = 1\ mol.l^{-1}$
Heat transfer coefficient	$h_a = 7 \cdot 10^5\ cal.min^{-1}.K^{-1}$

The nonlinearity of the model can be found in relation for the reaction rate, k_1, which is computed from Arrhenius law:

$$k_1 = k_0 \cdot e^{\frac{-E}{R \cdot T}} \quad (3)$$

where k_0 is a reaction rate constant, E denotes an activation energy and R is a gas constant.

The static analysis of this system is described in detail for example in (Vojtesek and Dostal 2010). The most important result of the steady-state analysis can be found in the complexity of the system, it has three steady-states – one unstable (N_1) and two stable (S_1 and S_2). This special feature is shown in Figure 2 which represents values of the reactant (Q_r) and cooling (Q_c) heats for the working point represented by the volumetric flow rates $q = 100\ l.min^{-1}$ and $q_c = 80\ l.min^{-1}$ and various values of the temperature $T = <300, 500>\ K$.

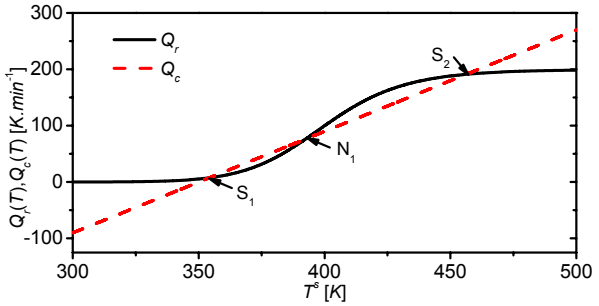

Figure 2: Heat balance inside the reactor

The steady-state values of the state variables in all three steady-states are:

$$\begin{aligned} S_1: &\quad T^s = 354.23\ K &\quad c_A^s = 0.9620\ mol.l^{-1} \\ N_1: &\quad T^s = 392.45\ K &\quad c_A^s = 0.6180\ mol.l^{-1} \\ S_2: &\quad T^s = 456.25\ K &\quad c_A^s = 0.0439\ mol.l^{-1} \end{aligned} \quad (4)$$

It is clear, that the second operating point S_2 has better efficiency (95.6 % reacts) for the same input settings than on the point S_1 (3.8 % reacts). This is the main reason why we have chosen this second steady-state in this work.

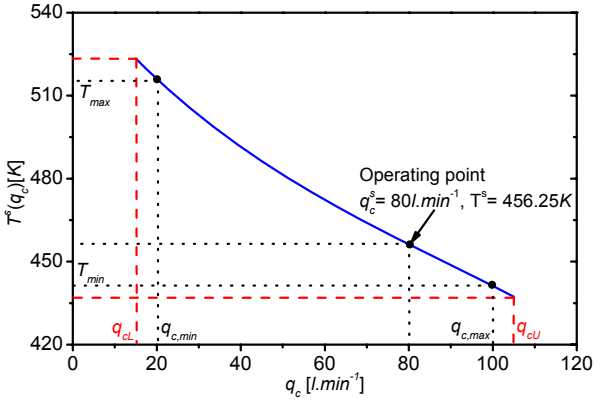

Figure 3: Static analysis of the reactor

The static analysis for the different volumetric flow rate of the coolant

$$q_{c,min} \le q_c \le q_{c,max} \quad (5)$$

was done. The $q_{c,min}$ and $q_{c,max}$ denotes minimal and maximal values of the volumetric flow rate of the coolant and their values are $q_{c,min}$ = 20 $l.min^{-1}$ and $q_{c,max}$ = 100 $l.min^{-1}$. The results are shown in Figure 3.

NONLINEAR CONTROLLER

As it written above, the controller is divided into a static nonlinear part (SNP) and a dynamic linear part (DLP) – see Figure 4.

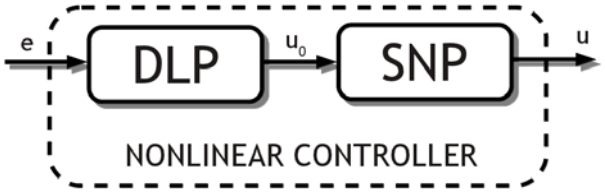

Figure 4: The scheme of the nonlinear controller

The dynamic part DLP defines linear dynamic relation between input to the nonlinear part $u_0(t)$ and the difference between actual and desired reactant temperature $T(t)$, i.e.

$$u_0(t) = \Delta T_w(t) \quad (6)$$

The static part SNP describes nonlinear relation between $u_0(t)$ and corresponding change of the input volumetric flow rate of the coolant $\Delta q_c(t)$.
The interconnection of the controller and the controller plant can be found in the following Figure 5.

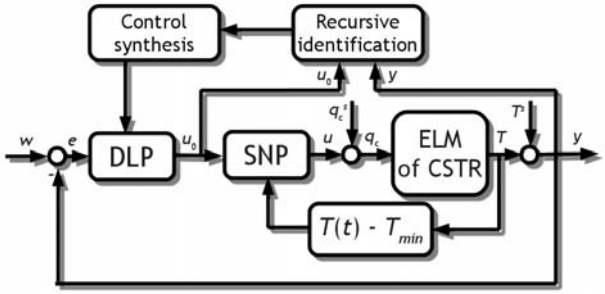

Figure 5: The control scheme

The following chapters will describe individual blocks in the Figure 5.

Static Nonlinear Part (SNP)

The SNP at it is comes from the static analysis displayed in Figure for volumetric flow rate between lower bound q_{cL} = 15 $l.min^{-1}$ and upper bound q_{cU} = 105 $l.min^{-1}$ and we introduce new x- and y-axis coordinates ω and ψ defined as

$$\omega = \frac{q_c^s - q_{cL}}{q_{cL}}[-]; \psi = T^s - T_{min}^s\,[K] \quad (7)$$

where T_{min}^s represents the lowest value of the steady-state reactant temperature, i.e. T^s for the volumetric flow rate in the upper bound, q_{cU}, in this case.
The measured data on the real model are usually affected by the measurement errors. These errors are here simulated by the random white-noise errors. The steady-state characteristic recomputed to the new coordinates ω and ψ is then shown in Figure 6.

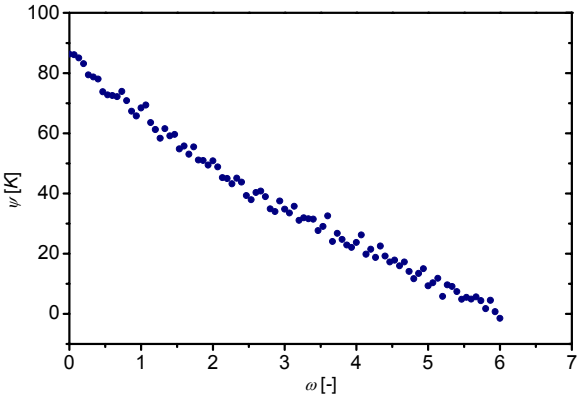

Figure 6: Simulated characteristic $\psi = f(\omega)$

The inverse of this steady-state characteristic is shown in Figure 7 and the resulted simulated data could be approximated by several functions from the ring of polynomial, exponential, rational etc. functions.

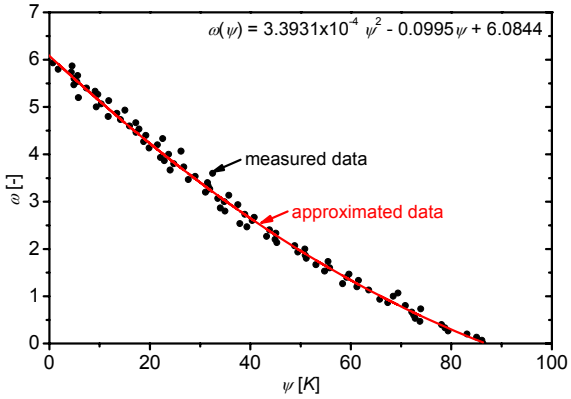

Figure 7: Simulated (dotted) and approximated (line) characteristic $\omega = f(\psi)$

In our case, the second order polynomial was used for the approximation of the noised data. The resulted polynomial has form

$$\omega(\psi) = 3.3931 \times 10^{-4}\psi^2 - 0.0995\psi + 6.0844 \quad (8)$$

and as it can be seen in Figure 7, this function approximates the data in suitable way.
The difference of the input volumetric flow rate of the coolant $u(t)$ = $\Delta q_c(t)$ in the output from the nonlinear part can be computed

$$u(t) = \Delta q_c(t) = q_{cL}\left(\frac{d\gamma}{d\psi}\right)_{\psi(T)} u_0(t) \quad (9)$$

The derivative $d\omega/d\psi$ in the previous equation is computed for each temperature of the reactant T from the derivative of the function (8), i.e.

$$\frac{d\omega}{d\psi} = 6.7861\times10^{-4}\psi - 0.0995 \tag{10}$$

External Linear Model (ELM) of CSTR

The dynamic behavior of the system shows that this system could be represented by the second order transfer function with the relative order one:

$$G(s) = \frac{Y(s)}{U(s)} = \frac{b(s)}{a(s)} = \frac{b_1 s + b_0}{s^2 + a_1 s + a_0} \tag{11}$$

This ELM belongs to the class of continuous-time (CT) models. The identification of such processes is not very easy.

One way, how we can overcome this problem is the use of so called δ–model. This model belongs to the class of discrete models but its parameters are close to the continuous ones for very small sampling period as it proofed in (Stericker and Sinha 1993).

The δ–model introduces a new complex variable γ computed as (see (Mukhopadhyay et al. 1992)):

$$\gamma = \frac{z-1}{\beta \cdot T_v \cdot z + (1-\beta)\cdot T_v} \tag{12}$$

Where β is an optional parameter from the interval $0 \le \beta \le 1$ and T_v denotes a sampling period. It is clear that we can obtain infinite number of δ-models for various β. A so called *forward δ-model* for $\beta = 0$ was used and γ operator is then

$$\gamma = \frac{z-1}{T_v} \tag{13}$$

The continuous model (11) is then rewritten to the form

$$a^{\delta}(\delta)\, y(t') = b^{\delta}(\delta)\, u(t') \tag{14}$$

where polynomials $a^{\delta}(\delta)$ and $b^{\delta}(\delta)$ are discrete polynomials and their coefficients are different from those of the CT model $a(s)$ and $b(s)$. Time t' is discrete time.

Now we can introduce substitution $t' = k - n$ for $k \ge n$ and Equation (14) then will be

$$\begin{aligned}\delta^2 y(k-n) = b_1^{\delta}\delta u(k-n) + b_0^{\delta} u(k-n) - \\ - a_1^{\delta}\delta y(k-n) - a_0^{\delta} y(k-n)\end{aligned} \tag{15}$$

which means that the regression vector $\boldsymbol{\varphi}_{\delta}$ is then

$$\boldsymbol{\varphi}_{\delta}(k-1) = \left[-y_{\delta}(k-1), -y_{\delta}(k-2), u_{\delta}(k-1), u_{\delta}(k-2)\right]^T \tag{16}$$

and the vector of parameters $\boldsymbol{\theta}_{\delta}$ is generally

$$\boldsymbol{\theta}_{\delta}(k) = \left[a_1^{\delta}, a_0^{\delta}, b_1^{\delta}, b_0^{\delta}\right]^T \tag{17}$$

The differential equation (14) has then vector form:

$$y_{\delta}(k) = \boldsymbol{\theta}_{\delta}^T(k)\cdot\boldsymbol{\varphi}_{\delta}(k-1) + e(k) \tag{18}$$

where $e(k)$ is a general random immeasurable component.

Identification of ELM parameters

The Recursive Least-Squares (RLS) method is used for the parameter estimation in this work. The RLS method is well-known and widely used for the parameter estimation. It is usually modified with some kind of forgetting, exponential or directional. Parameters of the identified system can vary during the control which is typical for nonlinear systems and the use of some forgetting factor could result in better output response.

The basic RLS method is described by the set of equations:

$$\begin{aligned}&\varepsilon(k) = y(k) - \boldsymbol{\varphi}_{\delta}^T(k)\cdot\hat{\boldsymbol{\theta}}_{\delta}(k-1)\\ &\xi(k) = \left[1 + \boldsymbol{\varphi}_{\delta}^T(k)\cdot\mathbf{P}(k-1)\cdot\boldsymbol{\varphi}_{\delta}(k)\right]^{-1}\\ &\boldsymbol{L}(k) = \xi(k)\cdot\mathbf{P}(k-1)\cdot\boldsymbol{\varphi}_{\delta}^T(k)\\ &\mathbf{P}(k) = \frac{1}{\lambda_1(k-1)}\left[\mathbf{P}(k-1) - \frac{\mathbf{P}(k-1)\cdot\boldsymbol{\varphi}_{\delta}(k)\cdot\boldsymbol{\varphi}_{\delta}^T(k)\cdot\mathbf{P}(k-1)}{\lambda_1(k-1) + \boldsymbol{\varphi}_{\delta}^T(k)\cdot\mathbf{P}(k-1)\cdot\boldsymbol{\varphi}_{\delta}(k)}\right]\\ &\hat{\boldsymbol{\theta}}(k) = \hat{\boldsymbol{\theta}}_{\delta}(k-1) + \boldsymbol{L}(k)\varepsilon(k)\end{aligned} \tag{19}$$

RLS with the changing exp. forgetting is used for parameter estimation, where the changing forgetting factor λ_1 is computed from the equation

$$\lambda_1(k) = 1 - K\cdot\xi(k)\cdot\varepsilon^2(k) \tag{20}$$

Where K is a small number, in our case $K = 0.001$.

Dynamic Linear Part (DLP)

The DLP is constructed with the use of polynomial approach (Kucera 1993) similarly as it was used in adaptive control described in (Vojtesek et al. 2011).

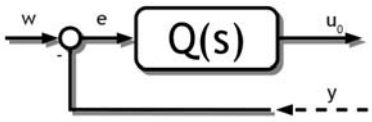

Figure 8: 1DOF control scheme in dynamic linear part

The control system configuration with one degree-of-freedom (1DOF) with controller in the feedback part was used here and it is displayed in Figure 8. The transfer function of the controller $Q(s)$ is designed with the use of polynomial synthesis:

$$\tilde{Q}(s) = \frac{q(s)}{s\cdot\tilde{p}(s)} \tag{21}$$

where degrees of polynomials $\tilde{p}(s)$ and $q(s)$ are computed from:

$$\deg q(s) = \deg a(s);\ \deg\tilde{p}(s) \ge \deg a(s) - 1 \tag{22}$$

and parameters of these polynomials are computed by the Method of uncertain coefficients which compares coefficients of individual s-powers from the Diophantine equation, e.g. (Kucera 1993):

$$a(s)\cdot s\cdot\tilde{p}(s) + b(s)\cdot q(s) = d(s) \tag{23}$$

The polynomial $d(s)$ on the right side of (23) is an optional stable polynomial. It is obvious, that the degree of this polynomial is:

$$\deg d(s) = \deg a(s) + \deg \tilde{p}(s) + 1 \qquad (24)$$

and roots of this polynomial are called poles of the closed-loop and their position affects quality of the control. This polynomial is designed via well-known Pole-placement method. A choice of roots needs some a priory information about the system's behavior. It is good to connect poles with the parameters of the system via spectral factorization. The polynomial $d(s)$ can be then rewritten to the form

$$d(s) = n(s) \cdot (s+\alpha)^{\deg d - \deg n} \qquad (25)$$

where $\alpha > 0$ is an optional coefficient reflecting closed-loop poles and stable polynomial $n(s)$ is obtained from the spectral factorization of the polynomial $a(s)$

$$n^*(s) \cdot n(s) = a^*(s) \cdot a(s) \qquad (26)$$

The Diophantine equation (23), as it is, is valid for step changes of the reference and disturbance signals which means that deg $f(s)$ = 1 in (22). This controller ensures stability, load disturbance attenuation and asymptotic tracking of the reference signal.

The order of the polynomials $q(s)$, $\tilde{p}(s)$ and $d(s)$ for second order transfer transfer function (11) are:

$$\begin{aligned} &\deg q(s) = \deg a(s) = 2 \\ &\deg \tilde{p}(s) \geq \deg a(s) - 1 \Rightarrow \deg \tilde{p}(s) = 1 \\ &\deg d(s) = \deg a(s) + \deg \tilde{p}(s) + 1 = 2 + 1 + 1 = 4 \end{aligned} \qquad (27)$$

The transfer function of the controller is then

$$\tilde{Q}(s) = \frac{q(s)}{s \cdot \tilde{p}(s)} = \frac{q_2 s^2 + q_1 s + q_0}{s \cdot (s + p_0)} \qquad (28)$$

and the polynomial $d(s)$ could be chosen as

$$d(s) = n(s) \cdot (s+\alpha)^2 \qquad (29)$$

Parameters of the polynomial $n(s)$ which are computed from the spectral factorization are defined as:

$$n_0 = \sqrt{a_0^2}, \; n_1 = \sqrt{a_1^2 + 2n_0 - 2a_0} \qquad (30)$$

The control system synthesis is done here in continuous time, but recursive identification uses discrete time steps. The resulted, so called "hybrid", controller works in the continuous time but parameters of the polynomials in the system's transfer function are identified recursively in the sampling period T_v. This assumption results in the condition, that the parameters of the δ-model are close the continuous ones for the small sampling period.

SIMULATION RESULTS

All studies were done in the mathematical software Matlab, version 6.5.1 and the common values for all simulations were: the sampling period was T_v = 0.3 *min*, the simulation time 600 *min* and 6 different step changes were done during this time. The initial vector of parameters used for identification was $\hat{\boldsymbol{\theta}}_\delta^T = [0.1, 0.1, 0.1, 0.1]$ and the initial covariance matrix was $\boldsymbol{P}_{ii} = 1 \cdot 10^7$ for i = 1,..,4.

The goal of the controller is to control the temperature, inside the reactor by the change of the volumetric flow rate of the coolant, i.e. $u(t) = \Delta q_c(t)$, $y(t) = T(t) - T^s$.

The input variable is limited in the bounds ±90 $l.min^{-1}$.

The simulation was done for different values of the position of the parameter α in (29), α = 0.06, 0.1 and 0.18, and the results are shown in Figure 9 and 10.

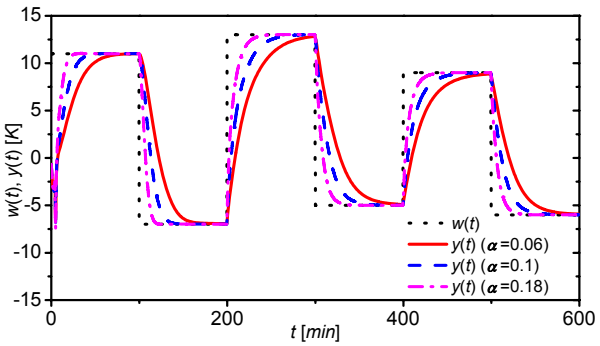

Figure 9: Results of the nonlinear adaptive control - the course of the reference signal $w(t)$ and the output variable $y(t)$ for different values of α

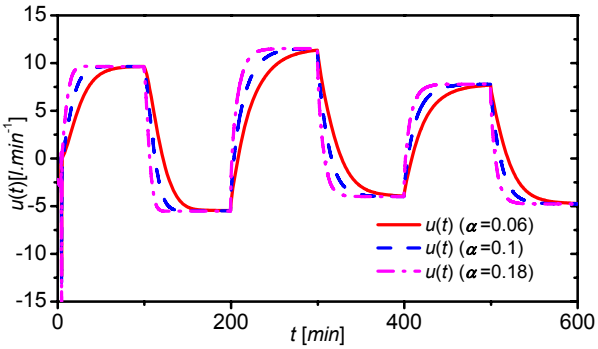

Figure 10: Results of the nonlinear adaptive control - the course of the input variable $u(t)$ for different values of α

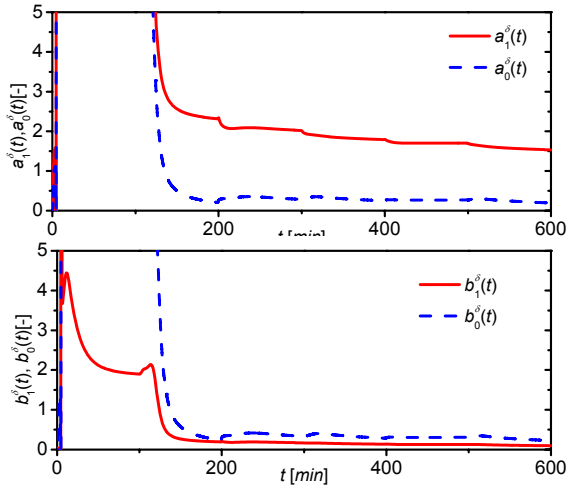

Figure 11: The course of the identified parameters $a_1{}^\delta$, $a_0{}^\delta$, $b_1{}^\delta$ and $b_0{}^\delta$ for α = 0.1

The usability of this control strategy for such type of chemical reactor is obvious. Although the step changes are relatively high (about ±20 *K* in some cases), the controller dealt with it without big trouble. The only problem can be found at the very beginning of the control which was caused by the recursive identification which needs some time for adapting to the right parameters. One sample course of the identified parameters a_1^{δ}, a_0^{δ}, b_1^{δ} and b_0^{δ} for parameter $\alpha = 0.1$ during the control is shown in Figure 11.

Results shown in previous figures clearly shows that the increasing value of the parameter α affects mainly the speed of the output response – increasing value of α results in quicker output response. Very desirable from the practical point of view is also smooth course of the input variable to the system, $u(t)$, which is produced by the controller and represented by e.g. twist of the valve on the input pipe.

CONCLUSION

The paper shows results of nonlinear adaptive control of the continuous stirred-tank reactor with the spiral cooling in the jacket. This system belongs to the class of nonlinear systems with lumped parameters and the mathematical model is described by the set of nonlinear ordinary differential equations. The novelty of this method compared to the pure adaptive control can be found in the factorization of the controller into linear and nonlinear part. The nonlinear part is designed with the use of simulated steady-state characteristic and appropriate modifications. The nonlinearity of the controlled system is approximated via External Linear Model with recursively estimated parameters. The linear part of the controller employs polynomial approach and the output response could be tuned via choice of the poles in closed-loop system. Proposed controller produces smooth course of the action value (input to the system) and consequently also good and accurate course of the controlled output from the system. The future work will be focused on the comparison of this method to the pure adaptive control and application of this control strategy to next types of technological processes such as tubular reactors, batch reactors etc.

REFERENCES

Astolfi, A.; D. Karagiannis; and R. Ortega. 2008. *Nonlinear and adaptive control with applications*. Springer-Verlag, London.

Åström, K.J. and B. Wittenmark. 1989. *Adaptive Control*. Addison Wesley. Reading. MA, ISBN 0-201-09720-6.

Bobal, V.; J. Böhm; J. Fessl; and J. Machacek. 2005. *Digital Self-tuning Controllers: Algorithms. Implementation and Applications*. Advanced Textbooks in Control and Signal Processing. Springer-Verlag London Limited. ISBN 1-85233-980-2.

Gao, R.; A. O'dywer; E. Coyle. 2002. "A Non-linear PID Controller for CSTR Using Local Model Networks". Proc. of *4th World Congress on Intelligent Control and Automation*. Shanghai. P. R. China. 3278-3282

Ingham, J.; I. J. Dunn; E. Heinzle; and J. E. Prenosil. 2000. *Chemical Engineering Dynamics. An Introduction to Modeling and Computer Simulation*. Second. Completely Revised Edition. VCH Verlagsgesellshaft. Weinheim. ISBN 3-527-29776-6

Kucera, V. 1993. "Diophantine equations in control – A survey". *Automatica*. 29. 1361-1375

Middleton, R.H. and G. C. Goodwin. 2004. *Digital Control and Estimation - A Unified Approach*. Prentice Hall. Englewood Cliffs. ISBN 0-13-211798-3

Mukhopadhyay, S.; A. G. Patra; and G. P. Rao. 1992. "New class of discrete-time models for continuos-time systems". *International Journal of Control*. vol.**55**. 1161-1187

Nakamura, M.; T. Sugi and S. Goto. 2002. "Nonlinear separation model and control for a complex process realized by conventional PID controller hardware". In *Proceedings of the 4th Asian Control Conference*, Singapore, 274-279.

Stericker, D.L. and N. K. Sinha. 1993. "Identification of continuous-time systems from samples of input-output data using the δ-operator". *Control-Theory and Advanced Technology*. vol. 9. 113-125

Sung, S. and J. Lee. 2004. "Modeling and control of Wiener-type processes". *Chemical Engineering Science*, 59, 1515-1521.

Vincent,; T.L. and W.J. Grantham. 1997. *Nonlinear and optimal control systems*. John Wiley & Sons, New York. ISBN 0471042358

Vojtesek, J.; P. Dostal. 2010 "Adaptive Control of Continuous-Stirred Tank Reactor in Two Stable Steady-States", In *Proceedings of the IFAC Workshop Adaptation and Learning in Control and Signal Processing 2010*, Antalya, Turkey 2010, ISBN 978-3-902661-85-2.

Vojtesek, J.; J. Novak; P. Dostal. 2011. "Effect of External Linear Model's Order on Adaptive Control of CSTR". In *Proceeding of The 19th IASTED International Conference on Applied Simulation and Modelling (ASM 2011)*, p. 82-87. ISBN 978-0-88986-884-7.

AUTHOR BIOGRAPHIES

JIRI VOJTESEK was born in Zlin. Czech Republic and studied at the Tomas Bata University in Zlin. where he got his master degree in chemical and process engineering in 2002. He has finished his Ph.D. focused on Modern control methods for chemical reactors in 2007. His email contact is `vojtesek@fai.utb.cz.`

PETR DOSTAL studied at the Technical University of Pardubice. He obtained his PhD. degree in Technical Cybernetics in 1979 and he became professor in Process Control in 2000. His research interest are modeling and simulation of continuous-time chemical processes. polynomial methods. optimal. adaptive and robust control. You can contact him on email address `dostalp@fai.utb.cz.`

High Performance Modelling and Simulation

THE MEDIAN RESOURCE FAILURE CHECKPOINTING

Suleman Khan, Khizar Hayat, Sajjad A. Madani
COMSATS Institute of Information Technology (CIIT),
Abbottabad 22060, Pakistan.
Email: sulemankhan1984@yahoo.com, khizarhayat@ciit.net.pk, madani@ciit.net.pk

Samee U. Khan
Department of Electrical and Computer Engineering, North Dakota State University,
Fargo, ND 58108-6050, USA.
Email: samee.khan@ndsu.edu

Joanna Kolodziej
Department of Mathematics and Computer Science, University of Bielsko-Biala,
PL-43300 Bielsko-Biala, Poland.
Email: jkolodziej@ath.bielsko.pl

KEYWORDS

Fault tolerance, Checkpointing, Distributed systems

ABSTRACT

In grid computing, the realization of an enviable fault tolerance ability is linked with the proper utilization of resources and scheduling of jobs. The literature offers two solutions to these two challenging tasks, *viz.* checkpointing and replication. A checkpointing strategy is being proposed that uses the median of failure intervals of the resources in deciding the checkpoint intervals for the given jobs. The strategy shows improved system throughput, job losses and job execution times while eliminating unnecessary checkpoints.

1 INTRODUCTION

It is a usual human tendency to pay little attention to the aspect of fault tolerance, while designing a system. Take, for example, your electronic wrist watch, if it misreports the time costing you some important assignment, the focus of your fury would be the weak battery rather than the watch. The blame is mainly on the watch maker who, for the sack of economy, has ignored the fault tolerance facet and has not put much effort to incorporate any functionality to alert a user in case of low battery. On the other hand, an ordinary car possesses a fault tolerant mechanism against low battery, for the dividends it has for its manufacturer. In a nutshell, a fault tolerance mechanism is generally considered valuable for a system if it adds to the utility of the corresponding system.

When it comes to the distributed grid environments, the concept of fault tolerance becomes rather more important. Due to the heterogeneous nature of the underlying infrastructure, the resources are geographically dispersed in these systems. These resources may be executed under different administrative domains, each of which may behave and deal, even a similar nature of jobs, differently. Handling of such a dynamic and huge environment is a challenging job and requires innovative efforts to minimize the fault incidents. System faults can be variously classified based on their nature, length and cause of occurrence. The nature of a fault in the system can be attributed to the hardware failure, operating system failure, network failure, or IO failure. A system going down due to the aforementioned failures may lead to catastrophic results. The most common causes of occurrence of system fault are incompatibility of various devices, improper software, and external intrusions (Johnson, 1996).

Fault tolerance, in a grid environment, is dependent on the apt utilization of resources as well as on the balanced scheduling of jobs. The grid computing literature offers two solutions to implement proper resource utilization and scheduling, namely the checkpointing (Wong and Franklin, 1996; Cao and Singhal, 2003; Deng and Park, 1994) and replication (Narasimhan et al., 2000; Saito and Levy, 2000; Ratner et al., 1999). Both these approaches have their disadvantages when used in the static mode. With the former, when checkpointing requests are generated, it stops the job and saves its previous state on a stable resource. This may consume a fair amount of time in generating, storing and recovering the checkpoints back. On the other hand, although replication produces its replicas on free available computational resources giving more chance for a job to be executed; the execution of more replicas in a resource-poor distributed environment may lead to low throughput and high job execution times. In this work we focus on the checkpointing aspect and propose a strategy based on our median resource failure checkpointing (MRFCP) algorithm.

The paper is organized as follows: Section 2 explains the related work followed by a discussion on the proposed method in Section 3. The simulation results are presented in Section 4 whereas the conclusion is given in Section 5.

Proceedings 26th European Conference on Modelling and Simulation ©ECMS Klaus G. Troitzsch, Michael Möhring, Ulf Lotzmann (Editors)
ISBN: 978-0-9564944-4-3 / ISBN: 978-0-9564944-5-0 (CD)

2 RELATED WORK

Checkpointing is used to save the executed portion of the jobs running on a resource in case of anticipated resource failure (Pruyne and Livny, 1996). When a checkpoint request is generated, an executable portion of the job states are stored on stable resources (Bouabache et al., 2008). After a resource failure, a job is migrated to the some other available resource(s) for its further execution; it rebuilds the previous states of the job by recalling from the stable resources. The main advantage of using checkpointing is that a job does not start its execution from the start whenever a resource fails. On the other hand, extensive checkpoints requests may lead to overheads in terms of latency, job execution time and system management (Plank et al., 1995).

The scheme, given in (Silva and Silva, 1998), does not save a checkpoint on a disk while using the main memory of its neighboring processors. When a checkpoint request is generated, it saves the states of the jobs in its main memory as well as in its neighbor's. All the resources are arranged in a virtual ring. Each resource has only one connection to it neighboring resource for keeping a record of checkpoints. Each resource should keep two slots of space for the checkpoints; one for its own local states and other for its preceding neighbor resource. The technique is simple and the nature of its failures is not that serious. In addition, it is memory intensive, resulting in high overhead in the shape of system complexity for larger grid environments.

The coordinated checkpointing strategy of (Tamir and Squin, 1984) introduces the concept of a coordinator which stops the processing of a job while taking the image of the job on resource. It also broadcast the message to all the resources to stop their processes and take the checkpoints. Each resource, in return, sends an acknowledgment message to the coordinator telling that the checkpoint process has been successfully completed. Thereupon a success message is broadcast, by the coordinator, to all the resources who then discard the existing checkpoint image and update their individual tables. Due to the involvement latency overheads in the process, de-blocking of the checkpointing is preferred on part of many resources, in practice, thus violating the agreed policy (Elnozahy and Zwaenepoel, 1992). A remedy is therefore inevitably needed to avoid the latency overhead. In (Koo and Toueg, 1987), the overhead is minimized to some extent by adopting a two phase protocol which reduces the coordinated checkpointing. In the first stage, the checkpoint initiator sends a message to those jobs to which it communicated during the last checkpointing process. These jobs, in turn, send the message to all those jobs with which they communicated in their last specified checkpoint stage. This process further continues until all jobs which were involved in the last checkpoint receive a message. In the second stage, all the processes which were identified in the first stage make checkpoints. This results in consistent checkpoints with lesser overhead.

An incremental checkpointing concept has been introduced in (Agarwal et al., 2004), in which the data is stored in a block of memory which has been modified since the last checkpoint wave. A protocol is used which directly distributes the checkpoint images in memory of its computer peers, as in the FT-MPI[1] project or Charm++[2] project. An advantage of this approach is that it does not stop the other processes which were not part of the last checkpointing process. The strategy creates consistency of checkpoint images among those jobs which were part of the last checkpointing process. This reduces lot of overhead and economizes a job's execution time. Bouguerra et al. (2010) propose their "coordinated Checkpoint/Restart mechanism" based on three factors, namely the process failure distribution, the cost to save a global consistent state of processes and the number of computational resources. Relying on a reliability analysis, the authors employ their mechanism to ascertain the optimal interval between checkpoint times while minimizing the average completion time. The authors claim about 20% improvement in the checkpoint rate through the adoption of their proposed model. Another checkpointing scheme is outlined in Bouguerra et al. (2011) that mainly deals in batch jobs under the constraint that failures obey a general probability distribution.

3 THE PROPOSED METHOD

The grid environment scenario considered to elaborate the proposed strategy is shown in Fig. 1. It consists of four distributed heterogeneous sites with 32 computational resources each. The given sites are connected through a wide area network and computational resources within site are connected through a local area network. The users, through a user interface (UI), submit their jobs to the grid transparently. A resource broker is responsible to assign the user jobs to the available and suitable resources. Table 1 describes the symbols used in the explanation of the proposed strategy. The median

Table 1: List of symbols

Symbol	Description
RT_r^J	Remaining time of the job J on resource r
MRF_r	Median failure interval of r
ET_r^J	Execution time of J on r
I	Interval
CI	Checkpoint interval
CI_r^J	Checkpoint interval of J on r
$CI_r^{J^{new}}$	New selected checkpoint interval for J on r
$CI_r^{J^{old}}$	Old checkpoint interval for J on r
CRD	Checkpoint run-time delay
∂	Fraction of J w.r.t. total

resource failure checkpointing (MRFCP) algorithm is being proposed for the modification of the initially specified

[1] http://icl.cs.utk.edu/ftmpi/
[2] http://charm.cs.uiuc.edu

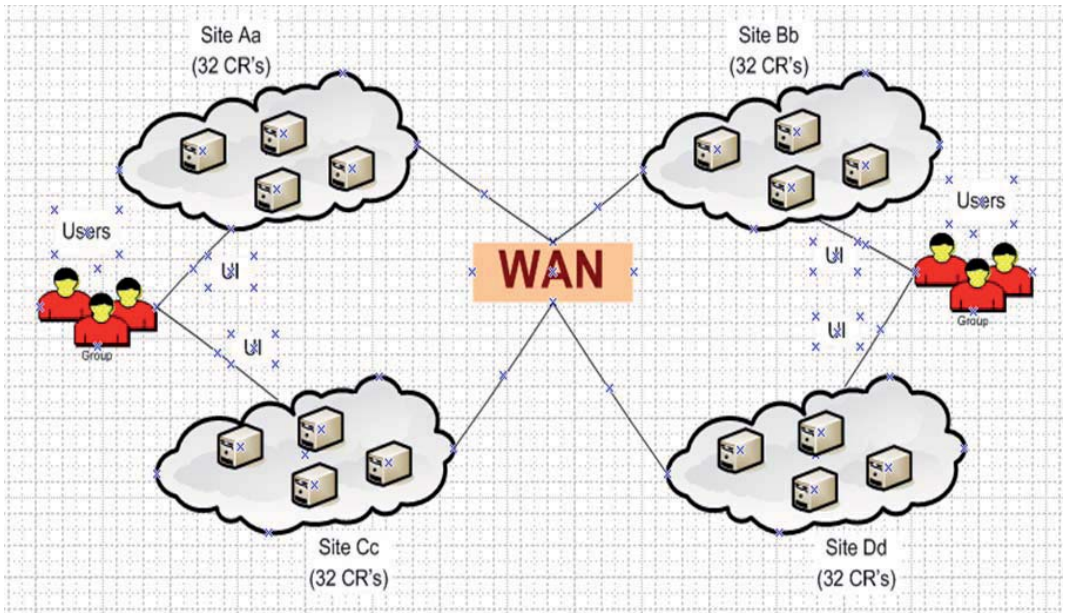

Figure 1: A Grid Computing Scenario for the proposed strategy

Input: Checkpoint request for a resource r, running several jobs
Output: Checkpoint intervals ($CI_r^{J^{new}}$)

```
begin
    if RT_r^J < MRF_r AND CI_r^J < ∂ * ET_r^J then
        /* ∂ < 1                                   */
        set CI_r^{J^new} ← CI_r^{J^old} + CI
    else
        set CI_r^{J^new} ← CI_r^{J^old} − CI
    end
end
```

Algorithm 1: The MRFCP algorithm

static checkpoint intervals. The algorithm is based on the comparison of the remaining time (RT) of the job on a resource and its median resource failure (MRF) interval whereupon it decides on the running time. MRF captures the whole failure event of the resource and whenever the system request for checkpoints, it takes all the failure events time of the resource and take its median value. This median value is then compared with the remaining time of the job to decide the increase/decrease of the checkpoint intervals. A pseudocode description of the proposed MRFCP strategy is given in Algorithm 1.

An instance for the MRFCP algorithm of one job resource execution is depicted in Fig. 2. When RT_r^J is less than MRF_r, it increases the checkpoint interval while decreasing the frequency of the checkpoint. This indicates that resource r is stable enough to execute a job or job J has almost finished its entire execution. The second condition shows that the checkpoint interval should not exceed the job length. This may be important for small jobs. If this condition is not fulfilled the algorithm decreases the checkpoint interval while increasing the frequency of checkpoints.

4 SIMULATION RESULTS

Performance metrics

For the comparison of MRFCP with the existing checkpointing strategies, three standard metrics were employed, namely the average job execution time, Successful job execution and average number of checkpoints.

1. *Average job execution time:* is the total execution time of successful jobs divided by total number of successful jobs. It is also called average turnaround time of the system.

2. *Successful job execution:* it is calculated by subtracting number of failed jobs from total number of submitted jobs in the system. This indicates the system throughput that how much system has successfully executed the jobs.

3. *Average number of checkpoints:* this metric is calculated by dividing total number of successful jobs on total number of checkpoints of successful jobs. Checkpoint requires time to take place, store, and to retrieve.

Simulation setup

For the simulations, the GridSim 5.2 simulator (Buyya and Murshed, 2002) had been employed. Besides being an effective tool to model different heterogeneous resources, schedulers, users and its applications, the GridSim simulator has the facility to simulate scheduler for single and multiple administrative domains in distributed environments. The resources can be scheduled in two modes, namely the space-share mode and the time-share mode. In our simulation we have used space-share mode for resources. Moreover, the resource strength can be

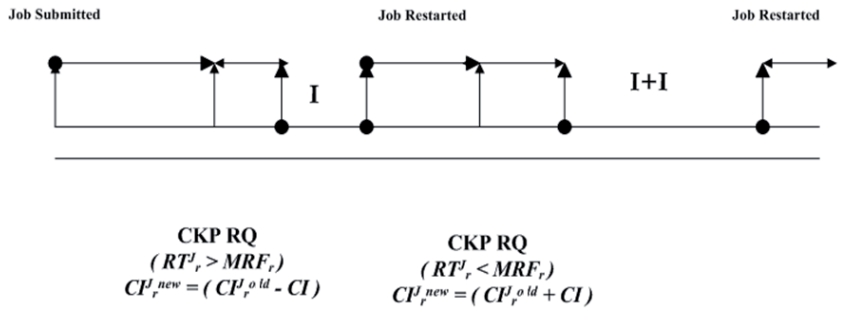

Figure 2: MRFCP running on single job resource

measured in million instructions per second (MIPS). In addition, the resources can not only be mapped into different time zones but weekends and holidays can also be mapped in the GridSim simulation environment.

Table 2: The simulation setup

Type	Parameter	Value
Network	LAN links	
	- Bandwidth	56 $Mbps$
	- Latency	1 ms
	WAN links	
	- Bandwidth	100 $Mbps$
	- Latency	$3 - 10$ ms
	Number of cluster zones	4
	Nodes per zone	32
	Propagation delay for IS	10 min
Host	Speed	10 $MIPS$
	Parallel execution	2 Jobs
	Failure model	LANL
Application	Workload	Lublin model
	Number of jobs	1500
	Jobs I/O	10 MB
	Checkpoint delay	100 $ms - 5$ s

To include the workload for our simulation, the Lublin workload model (Lublin and Feitelson, 2003) had been used that generated 1500 jobs. The Lublin model specifies the number of processor required, arrival time of the jobs and time required (μ) for the job execution. The model correlates between job size, job running time, and job inter-arrival times for daytime cycles. The parameters used for Lublin workload model are given in Table 2. To inject a failure into resources we have used the Los-Alamos National Lab (LANL) failure traces[3]. It is one of the largest high performance computing sites and has a record of the past nine years. Failure frequencies had been modeled according to the Weibull distribution[4] while the mean repair time had been modeled according to a logarithmic distribution. Each site has different failure and repair ranges roughly spanning between an hour and a week.

[3]http://fta.inria.fr/apache2-default/pmwiki/index.php
[4]http://www.weibull.com/AccelTestWeb/weibull_distribution.htm

MRFCP evaluation

In this section, we are comparing three state of the art checkpointing techniques - i.e. PeriodicCP, LastFailureCP (Chtepen et al., 2009) and MeanFailureCP (Chtepen et al., 2009) - with the MRFCP. The PeriodicCP is a static checkpointing technique in which checkpoints are assigned according to a prior selection of time interval. In the LastFailureCP, the difference between the last failure time of a resource and the current system time is compared with the execution time of the job on a resource. While in the MeanFailureCP, the remaining time of a job is compared with the mean failure time of resource.

1. **Average job execution time:** The average job execution time of a job is also called its turnaround time. Fig. 3 plots the average job execution time, under various check-pointing techniques, against five different check-pointing intervals. In general, the average turnaround time increases while decreasing the checkpoint interval and vice versa. This may be attributed to the fact that more frequent checkpointing results in more network delay because of the overheads involved in requesting, storing and retrieving the checkpoints. Among the techniques, the PeriodicCP has the highest average turnaround time due to its static nature as it does not work on finding out the system load and relies on the manual configuration of checkpoint intervals. In comparison, the LastFailureCP omits unnecessary checkpoints and performs better if the system has not worked for more time, lastly. In other words, the LastFailureCP technique is totally dependent on the failure frequency of the resource. With the MeanFailureCP and MRFCP the average turnaround time is lesser, mainly due their dynamicity; the MeanFailureCP remaining, more or less, independent of the checkpoint interval. Not that, like LastFailureCP, the MeanFailureCP strategy also depends on the failure frequency of the resource and the average job execution time escalates, when the failure interval of a resource increases. MRFCP has the least average job execution time because it soaks up

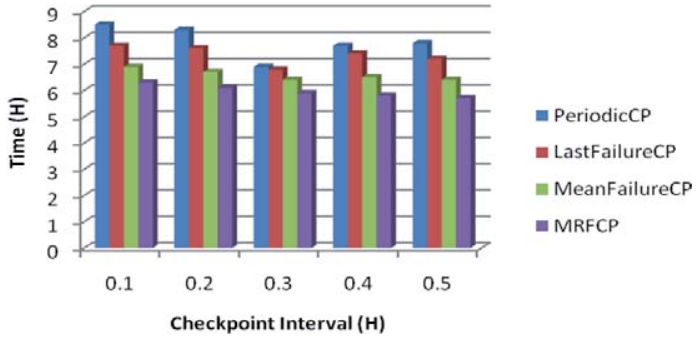

Figure 3: The average turnaround time for various check-pointing intervals

higher failure intervals of the resources. The results are even better for MRFCP at larger checkpoint intervals, a fact that makes it ideal for executing larger jobs. Moreover, it has been observed that MRFCP is a better technique when a resource has random failure intervals.

2. **Successful job execution:**

   This parameter shows us how many jobs was successfully executed by a fault tolerance technique at a given checkpoint interval. It can be readily observed from Fig. 4 that the number of successful jobs varies according to different checkpoint intervals. In the simulation for this comparison, we have injected a fixed number of faults to the system to see the effect of fault tolerance techniques due to varying checkpoint intervals. It can be seen that both MeanFailureCP and MRFCP techniques performs better than the rest of the techniques because both rely on some measure of central tendency to enhance the checkpoint interval depending on the job's remaining time and resource stability. The PeriodicCP and LastFailureCP are independent of system load and while the former only performs checkpointing that has been initially scheduled, the latter looks to the last failure occurrence of the resource. MRFCP starts producing better results as we move further in our checkpoint interval enhancement. This happens because it commences executing longer jobs too after the dilation of the checkpoint intervals thus leading to lower network delay and reduced overhead of the system.

3. **Average number of checkpoints:**

   Fig. 5 plots the average number of checkpoints as a function of varying checkpoint interval for various fault tolerance strategies. Typically, the number of checkpoints increases with decreasing checkpoint interval and vice versa. A better strategy is to consider taking the number of checkpoints dynamically according to the system load. The graph shows that PeriodicCP over-checkpoints at lower intervals, in comparison to the rest of the strategies, resulting in more overhead and escalated execution times. The reason is that the static checkpointing had been carried out in favor of higher intervals; that is why we see its best result at a checkpoint interval of $5\ H$. In such an eventuality the outcome is improved if the number of resource failures is less and the jobs have low execution time intervals. Generally, with MRFCP, the number of checkpoints are reduced as a function of the increasing checkpoint interval because on one hand the elongation of the interval gives more chance of processing to jobs with high execution times and, on the other, it performs processing while looking both at the resource failure occurrence and the remaining time of the jobs.

5 CONCLUSION

The MRFCP has demonstrated interesting results when compared with other state of the art checkpointing techniques. It showed better turnaround time and executed more jobs at any given checkpoint interval. Besides, it exhibited optimal checkpoints with respect to some fixed checkpoint interval. We believe that these results can be ameliorated further if one borrows something from the replication paradigm. The need is to devise a hybrid strategy that can adjust itself between replication and checkpointing. In addition, the simulations need to be conducted with some real experimental data - from Condor, for example, a scheduler that support check-pointing. The ultimate is to test the strategy, in combination with a good replication scheme, in a real environment, such as those briefly outlined in Xhafa et al. (2011).

REFERENCES

Agarwal, S., Garg, R., Gupta, M. S., and Moreira, J. E. (2004). Adaptive incremental checkpointing for massively parallel systems. In *Proceedings of the 18th annual international conference on Supercomputing*, ICS '04, pages 277–286, New York, NY, USA. ACM.

Bouabache, F., Herault, T., Fedak, G., and Cappello, F. (2008). Hierarchical replication techniques to ensure checkpoint storage reliability in grid environment. In *Proceedings of the 2008 Eighth IEEE International Symposium on Cluster*

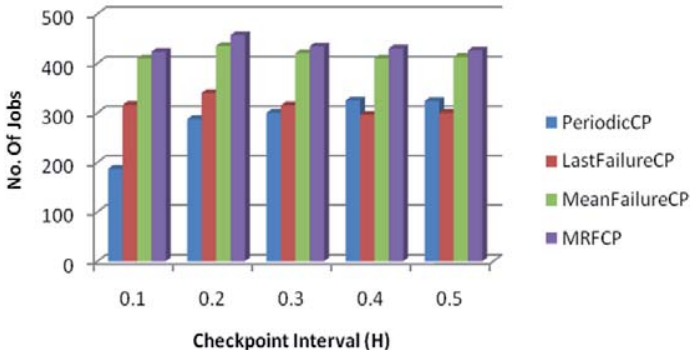

Figure 4: The number of successful job executions

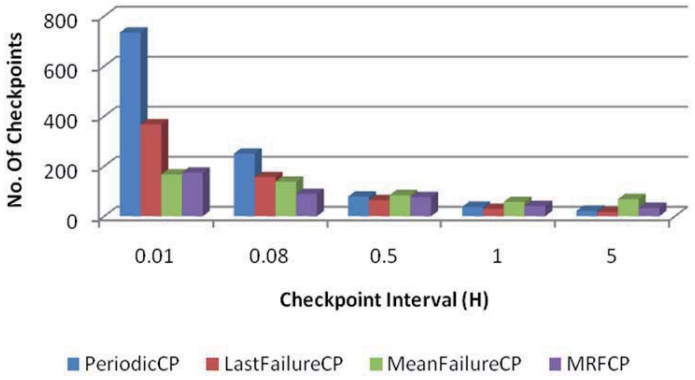

Figure 5: Average checkpoints at various intervals

Computing and the Grid, pages 475–483, Washington, DC, USA. IEEE Computer Society.

Bouguerra, M.-S., Gautier, T., Trystram, D., and Vincent, J.-M. (2010). A Flexible Checkpoint/Restart Model in Distributed Systems. In *Proceedings of the 8th international conference on Parallel processing and applied mathematics: Part I*, PPAM'09, pages 206–215, Berlin, Heidelberg. Springer-Verlag.

Bouguerra, M. S., Kondo, D., and Trystram, D. (2011). On the Scheduling of Checkpoints in Desktop Grids. In *Proceedings of the 2011 11th IEEE/ACM International Symposium on Cluster, Cloud and Grid Computing*, CCGRID '11, pages 305–313, Washington, DC, USA. IEEE Computer Society.

Buyya, R. and Murshed, M. M. (2002). Gridsim: A toolkit for the modeling and simulation of distributed resource management and scheduling for grid computing. *CoRR*, cs.DC/0203019.

Cao, G. and Singhal, M. (2003). Checkpointing with mutable checkpoints. *Theor. Comput. Sci.*, pages 1127–1148.

Chtepen, M., Claeys, F. H. A., Dhoedt, B., De Turck, F., Demeester, P., and Vanrolleghem, P. A. (2009). Adaptive task checkpointing and replication: Toward efficient fault-tolerant grids. *IEEE Trans. Parallel Distrib. Syst.*, 20:180–190.

Deng, Y. and Park, E. (1994). Checkpointing and rollback-recovery algorithms in distributed systems. *Journal of Systems and Software*, 25(1):59 – 71.

Elnozahy, E. and Zwaenepoel, W. (1992). Manetho: transparent roll back-recovery with low overhead, limited rollback, and fast output commit. *Computers, IEEE Transactions on*, 41(5):526 –531.

Johnson, B. W. (1996). *An introduction to the design and analysis of fault-tolerant systems*, pages 1–87. Prentice-Hall, Inc., Upper Saddle River, NJ, USA.

Koo, R. and Toueg, S. (1987). Checkpointing and rollback-recovery for distributed systems. *IEEE Trans. Softw. Eng.*, 13:23–31.

Lublin, U. and Feitelson, D. G. (2003). The workload on parallel supercomputers: modeling the characteristics of rigid jobs. *J. Parallel Distrib. Comput.*, 63:1105–1122.

Narasimhan, N., Moser, L., and Melliar-Smith, P. (2000). Transparent consistent replication of java rmi objects. In *Distributed Objects and Applications, 2000. Proceedings. DOA '00. International Symposium on*, pages 17 –26.

Plank, J. S., Beck, M., and Kingsley, G. (1995). Compiler-assisted memory exclusion for fast checkpointing. *IEEE TECHNICAL COMMITTEE ON OPERATING SYSTEMS AND APPLICATION ENVIRONMENTS*, 7:62–67.

Pruyne, J. and Livny, M. (1996). Managing checkpoints for parallel programs. In *Proceedings of the Workshop on Job Scheduling Strategies for Parallel Processing*, pages 140–154, London, UK. Springer-Verlag.

Ratner, D., Reiher, P., and Popek, G. (1999). Roam: a scalable replication system for mobile computing. In *Database and Expert Systems Applications, 1999. Proceedings. Tenth International Workshop on*, pages 96 –104.

Saito, Y. and Levy, H. M. (2000). Optimistic replication for internet data services. In *Proceedings of the 14th International Conference on Distributed Computing*, DISC '00, pages 297–314, London, UK, UK. Springer-Verlag.

Silva, L. and Silva, J. (1998). An experimental study about diskless checkpointing. In *Euromicro Conference, 1998. Proceedings. 24th*, volume 1, pages 395 –402 vol.1.

Tamir, Y. and Squin, C. H. (1984). Error recovery in multicomputers using global checkpoints. In *In 1984 International Conference on Parallel Processing*, pages 32–41.

Wong, K. F. and Franklin, M. (1996). Checkpointing in distributed computing systems. *Journal of Parallel and Distributed Computing*, 35(1):67 – 75.

Xhafa, F., Pllana, S., Barolli, L., and Spaho, E. (2011). Grid and P2P Middleware for Wide-Area Parallel Processing. *Concurrency and Computation: Practice and Experience*, 23(5):458–476.

AUTHOR BIOGRAPHIES

Suleman Khan is currently working as Senior Officer Network Maintenance in Pakistan International Airlines. He has done MS-Computer Science from CIIT, Abbottabad, Pakistan in 2011. He received his M.Sc computer Science from the Department of Computer Science, University of Peshawar, Pakistan in 2007. His research interests include resource management and job scheduling in grid, parallel and distributed computing as well as the wirelesssensor networks.

Khizar Hayat joined CIIT Abbottabad in Dec. 2009 and currently he is working as Associate Professor in the Computer Science Department. He received his PhD degree from the University of Montpellier II (UM2) in France, while working at the Laboratory of Informatics, Robotics and Microelectronics Montpellier (LIRMM). His areas of interest are image processing and information communication and security.

Sajjad Ahmad Madani works at COMSATS institute of information technology (CIIT) Abbottabad Campus as associate professor. He joined CIIT in August 2008 as Assistant Professor. Previous to that, he was with the institute of computer technology from 2005 to 2008 as guest researcher where he did his PhD research. Prior to joining ICT, he taught at COMSATS institute of Information Technology for a period of two years. He has done MS in Computer Sciences from Lahore University of Management Sciences (LUMS), Pakistan with excellent academic standing. He has already done BSc Civil Engineering from UET Peshawar and was awarded a gold medal for his outstanding performance in academics. His areas of interest include low power wireless sensor network and application of industrial informatics to electrical energy networks. He has published more than 35 papers in international conferences and journals.

Samee Ullah Khan is Assistant Professor of Electrical and Computer Engineering at the North Dakota State University, Fargo, ND, USA. Prof. Khan has extensively worked on the general topic of resource allocation in autonomous heterogeneous distributed computing systems. As of recent, he has been actively conducting cuttingedge research on energy-efficient computations and communications. A total of 111 (journal: 40, conference: 51, book chapter: 12, editorial: 5, technical report: 3) publications are attributed to his name. For more information, please visit: http://sameekhan.org/.

Joanna Kołodziej graduated in Mathematics from the Jagiellonian University in Cracow in 1992, where she also obtained the PhD in Computer Science in 2004. She joined the Department of Mathematics and Computer Science of the University of Bielsko-Biaa as an Assistant Professor in 1997. She has served and is currently serving as PC Co-Chair, General Co-Chair and IPC member of several international conferences and workshops including PPSN 2010, ECMS 2011, CISIS 2011, 3PGCIC 2011, CISSE 2006, CEC 2008, IACS 2008-2009, ICAART 2009-2010. Dr Koodziej is Managing Editor of IJSSC Journal and serves as a EB member and guest editor of several peer-reviewed international journals.

CONTROL FRAMEWORK FOR HIGH PERFORMANCE ENERGY AWARE BACKBONE NETWORK

Ewa Niewiadomska-Szynkiewicz, Andrzej Sikora, Piotr Arabas
Institute of Control and Computation Engineering
Warsaw University of Technology
Nowowiejska 15/19, 00-665 Warsaw, Poland
Research and Academic Computer Network (NASK)
Wawozowa 18, 02-796 Warsaw, Poland
Email: ens@ia.pw.edu.pl, A.Sikora@elka.pw.edu.pl, Piotr.Arabas@nask.pl

Joanna Kołodziej
University of Bielsko Biała
Poland
Email: jkolodziej@ath.bielsko.pl

KEYWORDS

Green Computer Network, Energy-Efficiency, Optimization, Control, Routing, Traffic Engineering

ABSTRACT

Global optimization of the energy consumption in heterogeneous environments has been recently an important research issue in wired and wireless networks. This paper presents a general framework for flexible and cognitive backbone network management which leads to the minimization of the energy utilized by the network. The policy for activity control of all the modules and elements that form a network is introduced and discussed. The idea of the system is to achieve the desired trade-off between energy consumption and network performance according to the traffic load.

INTRODUCTION

Nowadays, information communication technology sector belongs to the group of the big power consumers. Enabling the reduction of energy requirements of wired network is the goal of many research groups in the field of computer networks. There are two main motivations that drive the quest for "green" networking: environmental one, related to the reduction of wastes and impact on CO^2 emissions, and the economic one, stemming from the need of operators to reduce their operational costs. In the last years, large amount of telecoms, Internet service providers and public organizations reported statistics of network energy requirements and the related carbon footprint, showing a growing trend (Bianco et al., 2007; Roy, 2008). For example energy consumption of Telecom Italia network has reached more than 2TWh (1% of the total energy demand in Italy) in 2006, British Telecom 2.6 TWh in 2008, Deutsche Telekom more than 3.5 TWh, and the energy requirement increases every year. Similar trends can be observed in other telecoms and service providers. On the other hand, to support a new generation network infrastructures and related services, telecoms and service providers need a larger number of devices, with sophisticated architectures able to perform more complex operations in a scalable way. Hence, as the Future Internet is taking shape, it is recognized that, about other basic concepts and key aspects, energy awareness is an important part of the network design and management. The main challenge is to design, develop and test novel technologies, integrated control strategies and mechanisms for network equipment enabling energy saving by adapting network capacities and resources to current traffic loads and user requirements, while ensuring end-to-end Quality of Service.

In the recent years various efforts in the green networking field have been undertaken both in the research and industry domain (Bolla et al., 2009, 2010; Chiaraviglio et al., 2009; Coiro et al., 2011; Goma et al., 2011; Zhang et al., 2010). A broad spectrum of green networking activities and scientific projects are carried out. The research focuses on energy aware infrastructures, energy aware applications, energy aware transmission and adaptive control of activity of devices that form a network.

GREEN NETWORKING – RELATED WORKS

Modeling Energy Consumption of Network Devices

The main issue in the design of an efficient power consumption model for wide area networks is the analysis of the multilayer network architecture and classification of all network components based on the power consumption criterion. A significant amount of energy in networks are consumed by all types of IT devices. Physical resources and access points utilize more than 90% of the total power used in the whole network (Chiaraviglio et al., 2009; Goma et al., 2011). The rest of the

Proceedings 26th European Conference on Modelling and Simulation ©ECMS Klaus G. Troitzsch, Michael Möhring, Ulf Lotzmann (Editors)
ISBN: 978-0-9564944-4-3 / ISBN: 978-0-9564944-5-0 (CD)

energy is consumed by the core of the system. The modern power management methodologies must deal with the optimization of the energy utilized at all levels of the network structure. In numerous works on the measurements and modeling of network devices (see. e.g. (Zhang et al., 2010; Coiro et al., 2011; Sivaraman et al., 2011; Chabarek et al., 2008)) the authors propose various formal models for the network management, with power consumption and device load as the main optimization (management) criteria. The load of the data transmission nodes of the network such as routers, is usually defined as a measure of the aggregate traffic transmitted by this device. The loads of physical computational node is usually measured by the amount of processed jobs. The generic model of the power management in such system may be defined as follows: $P(l) = P_0 + f(l)$, where l is a traffic or computation load, P_0 is a power consumption in the idle state (this parameter is constant for a given network) and f is an increasing load function. In the simplest cases, the function $f(l)$ is linear (Qureshi et al., 2009), that is to say:

$$f(l) = \frac{P_{max} - P_0}{l_{max}} \cdot l \tag{1}$$

where: l_{max} indicates the maximal load of the devices in the network, and P_{max} is a power consumption under the maximum load. In complex networks the load function f is usually defined as nonlinear, (Qureshi et al., 2009) polynomial (Bolla et al., 2009) or stepwise function (Vasić and Kostić, 2010).

The main aim of 'green' networking is minimizing the energy required to achieve a given task or service while maintaining the same or similar performance level. Power scaling and standby capabilities are commonly used to decrease energy demands. The *smart standby* capability method assumes putting a device in very low energy mode, in which it can provide only some vital functionalities. Therefore, standby capability can be applied to those devices that will be not used for a longer period of time. The *dynamic power scaling* is the capability of reducing the energy requirement of a network device by scaling its performance. Two main families of power scaling approaches can be distinguished:

- adaptive rate techniques (AR) – scaling the device's processing capacity or the transmission or reception speed of the network interface,
- low power idle techniques (LPI) – exploiting the short inactivity periods by putting a given device into low power state.

Most personal computers follow ACPI (Advanced Configuration and Power Interface) (Intel, 2010) specification defining a number of power-aware states attained via scaling down processor voltage and clock frequency and idle states when processor is in stand-by mode. Similar propositions for network interfaces (Bolla et al., 2010), (Nedevschi et al., 2008) include employing AR and LPI techniques. Partial implementation of these ideas is 802.3az standard (IEEE, 2012), which defines implementation of LPI for Ethernet interfaces.

It must be noted that for typical network devices the correlation of power consumption and load is weak. It is due to the fact that most of currently available network equipment does not implement any energy saving mechanism. The changes in power consumption may be attributed only to e.g. necessity to change state of transistor keys more often when the load is heavier. The detailed analysis of power dissipation in electronic elements building FPGA router may be found in (Sivaraman et al., 2011). Another problem is relatively large fixed part of energy consumed in the idle state (P_0), which in typical router is needed not only by interfaces but also processors, switching fabric, power supplies and cooling fans, some of these elements being doubled or multiplied for redundancy. It is viable that new equipment will be more energy effective both due to introduction of LPI techniques and better electronics or moving more tasks to passive optical devices, however even greater energy savings may be obtained via optimization and control of the whole network.

Network-wide Reduction of Energy Consumption

Energy aware mechanisms mentioned in the previous section, if introduced, can help to reduce the power consumed by single links, e.g. ports of two routers connected via pair of fibers. However, it is not necessarily true, that adoption of such techniques will result in significant reduction of energy needed by the whole network. On the other hand it is obvious that, at least in the periods of low traffic, some links could be switched off or operate at lower rate, as typical telecommunication networks, specifically in the core part, have redundant links. Additional source of redundancy of some sort are bundled links, i.e., links composed of number of fibers to multiply their bandwidth. Such links can be relatively easy and safely scaled down by switching off some of fibers – even without modification of existing equipment (Fisher et al., 2010). The straightforward solution is to formulate a mathematical programming task – namely optimal routing problem with a cost function defined as a sum of energy consumed by all components of the network. The solution of this task can be used, usually in repetitive manner to decide which of network elements can be switched off or operate at lower rate (Idzikowski

et al., 2010) which is often referred as Green Traffic Engineering (Vasić and Kostić, 2010). Therefore, it is possible to build centralized network control system for decreasing the overall energy consumption. Such optimization problem is however much more difficult to solve than typical routing task as selection of paths is not independent, contrary paths should be aggregated allowing to move traffic out of some links and switch them off. The energy consumption functions are often non-convex increasing complexity of the problem which itself cannot be solved by standard methods of convex programming due to presence of integer variables. As the result fully formulated problem is *NP*-complete, while relaxing some constraints introduces sub-optimality or e.g instability (Vasić and Kostić, 2010) of the system. Optimization of energy consumption for large scale networks can be done mainly with heuristics. Various methods are proposed in literature. Simple algorithm which extends single device strategies to network-wide control is presented in (Bianzino et al., 2011). Two stage methods incorporating solving of simpler (usually relaxed) mathematic programming tasks for preselected conditions – usually for a set of active links or paths – are described adequately in (Chiaraviglio et al., 2009; Fisher et al., 2010) and (Zhang et al., 2010; Shen and Tucker, 2009).

Another issue is applicability of such a scheme in the real network where the most common approach is decentralization of control. A complex nature of interconnections that involves many constraints prevents application of direct decomposition (e.g. based on spatial separation) while non-convexity of a cost function makes application of the Lagrange relaxation difficult. Therefore, most of distributed control strategies employ various heuristics that can operate independently or can be used to extend the existing routing protocols – e.g OSPF (Bianzino et al., 2011), (Cuomo et al., 2011), BGP and MPLS. Adoption (and extension) of some signalling infrastructure allows to partially overcome absence of traffic matrix needed to compute flows (Chiaraviglio et al., 2009), and replace this information with observation of the past state of a network (Bianzino et al., 2011).

LOW ENERGY CONSUMPTION NETWORK

We have designed a control framework for high performance energy aware backbone network. The smart standby and dynamic power scaling techniques described in the previous section are employed in our system.

Framework for Power Control

One of the main goals of our project is to design and develop a control framework to reduce the energy requirements of wired network equipment. This framework should provide central and local control strategies and simple internal interface for exchanging data among elements of the network and implementing the decisions of the control units. The architecture of this framework is presented in Fig. 1. It consists of four main components:

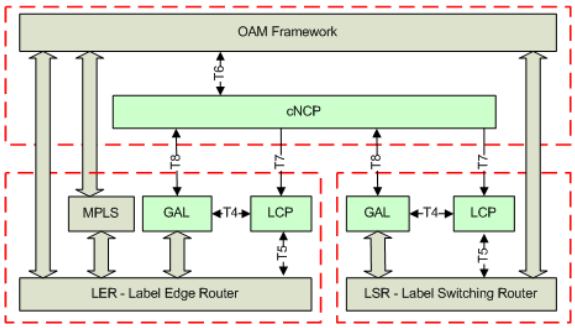

Figure 1: Control framework architecture and data flow.

1. Monitoring and Operation Administration & Management (OAM). The framework that provides monitoring the behavior of the deployed network, and plays a role of middleware between the other components of the system. It should support MPLS TE technology.

2. central Network-wide Control Policy (cNCP). The decision process which goal is to optimize the behavior of the whole network w.r.t. energy consumption. The optimization problem is formulated and solved for a given network topology and expected demands of users. The measurements of current traffic are utilized in calculations. The outcome of cNCP is the routing table for MPLS protocol.

3. Local Control Policy (LCP). The decision process, which objective is to optimize the configuration of the device in order to achieve the desired trade off between energy consumption and performance according to the incoming traffic load measured by OAM framework. The outcome of LCP is calculated based on knowledge about internal architecture of the device, the capability of energy-aware elements and incoming flow. Both cNCP and LCP form control plane layer.

4. Green Abstraction Layer (GAL). The functional abstraction layer – the standard interface between monitoring, control and hardware for exchanging data regarding the power status of the device. The objective is to hide the implementation details of

energy saving approaches, as well as to provide standard interfaces between energy aware technologies and monitoring and control frameworks. The main objective of GAL is to transform the outcome of LCP into power-management configuration of a given device (e.g. shutting off a given card or a given link).

Various control strategies can be applied to manage energy-aware networks. A brief survey of proposed techniques was presented in the previous section. In the next section we formulate the optimization problem that can be applied in cNCP layer of our framework. Our formal statement is similar to the topological design problem for MPLS networks presented in (Pióro et al., 2001). In our approach we assume that the network topology and expected demands are known during the decision calculation.

Network-wide Control Problem Formulation

Let us consider a backbone network formed by the routers labeled with by $r = 1, 2, \ldots, R$. The routers are classified into two groups: transit and edge routers. We provide a hierarchical representation of a router. The router is composed of cards labeled with $c = 1, 2, \ldots, C$, each card can contain a number of ports. All pairs of ports from different routers and cards are linked by direct links labeled with $e = 1, 2, \ldots, E$. Each element can operate in various energy-aware states that are related to the application of standby and power scaling techniques – we distinguish active states of a device, sleeping state and switched off, Fig. 2. The energy-aware states are defined as power settings. These states are labeled with $k = 1, 2, \ldots, K$. We assume that at a given time two ports connected by the link e are in the same energy-aware state k. ξ_{ek} denotes an energy consumption associated with the state k. It depends on a current throughput. Hence, ξ_{ek} implements the power profile model – a stepwise function defining power consumption due to a given throughput. The throughput of the link e in the state k is defined as M_{ek}. Moreover, we assume fixed energy costs associated to routers T_r and cards W_c.

The demands imposed on the network and labeled with $d = 1, 2, \ldots, D$ are transmitted by means of flows allocated to given IP/MPLS path under QoS (Quality of Service) requirements. Two nodes (ports): s_d (the source edge node) and t_d (the destination edge node) are associated with each demand; the volume of demand is equal h_d. The set of paths for each demand d may be defined as the set of all paths between nodes s_d and t_d. We assume that all demands between edge routers are given. The energy aware network management problem can be

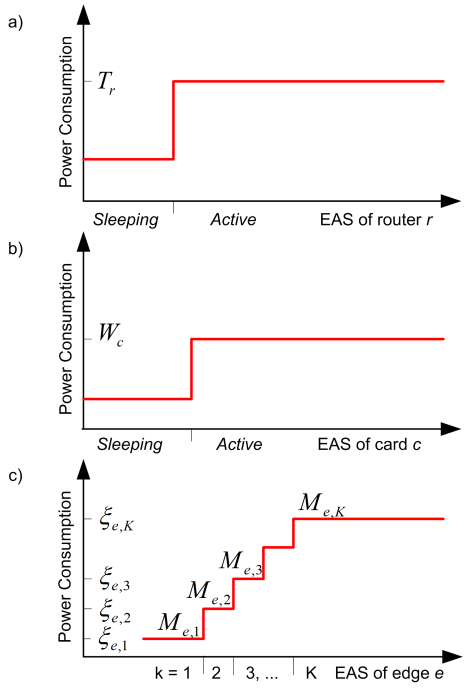

Figure 2: Operating behavior of an Energy Aware States (EAS) – various devices.

formulated as the following mixed-integer optimization problem:.

$$\min_{x,y,z,u_{de}} \{F = \sum_e \sum_k \xi_{ek} y_{ek} + \sum_c W_c x_c + \sum_r T_r z_r\} \tag{2}$$

subject to the following constraints:

$$\forall_e \quad \sum_k y_{ek} \leq 1 \tag{3}$$

$$\forall_{d,c} \quad \sum_p l_{cp} \sum_e a_{ec} u_{dc} \leq x_c \tag{4}$$

$$\forall_{d,c} \quad \sum_p l_{cp} \sum_e b_{ec} u_{de} \leq x_c \tag{5}$$

$$\forall_{r,c} \quad g_{rc} x_c \leq z_r \tag{6}$$

$$\forall_{d,p=s_d} \quad \sum_e a_{ep} u_{de} - \sum_e b_{ep} u_{de} = 1 \tag{7}$$

$$\forall_{d,t_d,p\neq s_d} \quad \sum_e a_{ep} u_{de} - \sum_e b_{ep} u_{de} = 0 \tag{8}$$

$$\forall_{d,p=t_d} \quad \sum_e a_{ep} u_{de} - \sum_e b_{ep} u_{de} = -1 \tag{9}$$

$$\forall_e \quad \alpha_e \sum_d h_d u_{de} \leq \sum_k M_{ek} y_{ek} \tag{10}$$

indices:
$r = 1, \ldots, R$ backbone routers in a network,

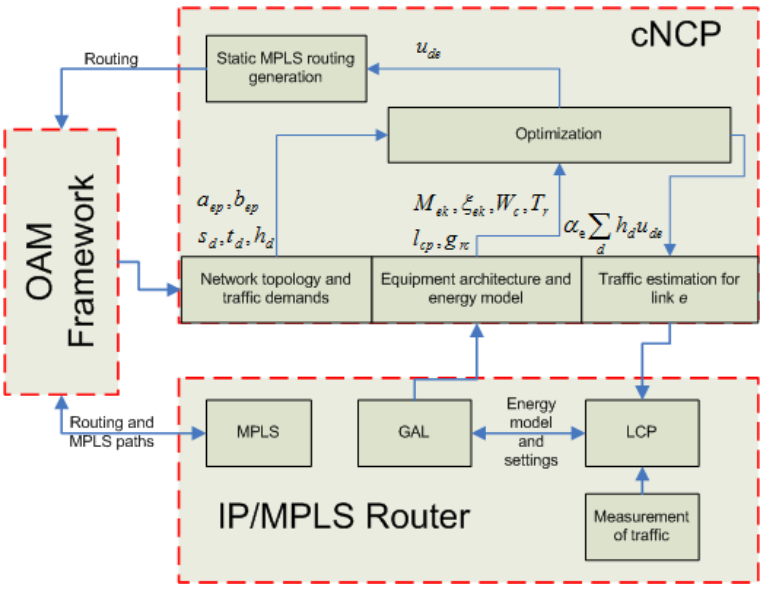

Figure 3: The control plane operation.

$c = 1, \ldots, C$ modules (cards) in a network,
$p = 1, \ldots, P$ ports in a network,
$e = 1, \ldots, E$ links (between two ports),
$d = 1, \ldots, D$ demands,
$k = 1, \ldots, K$ energy-aware states of links.

constants:
g_{rc} = 1 if card c belongs to router r (0 otherwise),
l_{cp} = 1 if port p belongs to card c (0 otherwise),
a_{ep} = 1 if direct link e is outgoing from port p (0 otherwise),
b_{ep} = 1 if direct link e is incoming to port p (0 otherwise),
h_d volume of demand d,
s_d origin edge node (port) for demand d,
t_d destination edge node (port) for demand d,
M_{ek} capacity of link e in energy-aware state k,
ξ_{ek} cost of energy of link e in energy state k (sum of energy costs of two ports connected via link e),
W_c fixed cost of energy of card c,
T_r fixed cost of energy of router r,
$\alpha_e \in < 0, 1 >$ overbooking factor.

variables:
u_{de} =1 if path d belongs to link e,
y_{ek} =1 if link e is in energy-aware state k,
x_c =1 if card c is used to data transmission,
z_r =1 if router r is used to data transmission.

The constraints defined in Eq. (3) assure that each link can be in one energy state, the conditions specified in Eqs. (4), (5) and (6) determine number of cards and routers that have been used to data transmission. The constrains (7), (8) and (9) are defined according to the Kirchhoff's law applied for source node, transit node and destination node. Finally, Eq. (10) assures that the flow does not exceed the capacity of a given link. In this problem the cumulative cost of the energy utilized in the system for finalizing all network operations is assumed to be minimized.

Concluding, as the solution of the problem (2) – (10) we obtain a set of active routers and cards, and the routing table for the MPLS protocol that minimizes the energy consumption in a network and fills all constraints, mainly concerned with expected QoS. Fig. 3 depicts the implementation of the control plane strategy in the control framework defined in this paper. Note that the above optimization problem is known to be *NP*-complete, therefore one can not expect to find time efficient algorithm for exact solving of this problem for large size networks. Techniques based on branch-and-bound approach are proposed for solving smaller size, and similar problems. For more realistic size of networks the formulation (2) – (10) is often relaxed and various heuristics are employed.

Case Study Results

We validated our control framework through simulation We solved the optimization problem (2) – (10) for three network configurations, examples E1 - E3 describing different model size, i.e., E1: r = 6, c = 8,

e = 10, d = 7, k = 5; E2: r = 12, c = 16, e = 20, d = 14, k = 5; E3: r = 18, c = 24, e = 30, d = 15, k = 5; where r, c, e, d, k denote respectively numbers of routers, cards, links, demands and energy-aware states. The branch-and-bound implementation – Lp_solve (http://lpsolve.sourceforge.net/5.5/) was used to calculate the optimal solutions. All tests were performed on Intel Core2 Duo CPU, 2.2 GHz, 2GB RAM. The detailed description of the problems E1 - E3, i.e. their dimensions and complexity are given in Table 1. Moreover, the table presents the execution times for all examples. The results indicate that the calculation time

Task	n_var	n_const	$B\&B\ nodes$	$time$ in [s]
E1	134	182	1608	0,415
E2	408	672	46627	90,820
E3	642	1074	186985	652,575

n_var - number of decision variables, n_const - number of constraints, $B\&B\ nodes$ - number of calculated subtasks generated by the Lp_solve, $time$ - time of calculation in seconds.

Table 1: Problem complexity and results of calculations.

strongly depends on the complexity of the optimization problem. It is obvious that complexity of the problem grows with the size of the network to be considered. It was observed that d (number of demands) is a key parameter that seriously increases the calculation time. From the depicted results, we can see that simplified formulation of the problem and more efficient branch-and-bound implementation supported by efficient heuristics must be considered, especially for medium and large networks. The second approach to speed up calculations is parallel implementation of the optimization task.

SUMMARY AND CONCLUSION

This paper presents the control framework for energy-aware wired networks. We designed hierarchical control structure composed of two decision layers, namely central control layer, which is responsible for the power management in the whole network, and local control layer, which is responsible for the management of the configuration of individual network devices. We formulated a topological design problem for IP/MPLS networks under the assumption of applying standby and power scaling techniques in order to reduce the cumulative energy consumption in a network. This problem is indicated as *NP*-complete challenging optimization task, and very difficult for many conventional optimization methods, such as deterministic branch-and-band algorithms. The simplification of the problem formulation and application of the metaheuristic solvers, and integration of these methods and models with OMNetC++ (http://www.omnetpp.org/) based network simulator is one of the main aims of our recent research. We plan to provide a comprehensive empirical evaluation of the proposed control structure in the testbed network.

Acknowledgment
This work was partially supported by 7 Framework Program UE grant ECONET, No: 258454.

REFERENCES

Bianco, F., Cucchietti, G., and Griffa, G. (2007). Energy consumption trends in the next generation access network – a telco perspective. In *Proc. of 29th Internat. Telecommunication Energy (INTELEC 2007)*, pages 737–742.

Bianzino, A. P., Chiaraviglio, L., and Mellia, M. (2011). GRiDA: a green distributed algorithm for backbone networks. In *Proc. of Online Conf. on Green Communications (GreenCom'11)*, pages 113–119.

Bolla, R., Bruschi, R., Carrega, A., and Davoli, F. (2010). Theoretical and technological limitations of power scaling in network devices (ATNAC). In *Proc. of Australasian Telecommunication Networks and Applications Conference*, pages 37–42.

Bolla, R., Bruschi, R., and Ranieri, A. (2009). Green support for pc-based software router: performance evaluation and modeling. In *Proc. of Communications Int. Conf. (ICC'09)*, pages 1–6.

Chabarek, J., Sommers, J., Barford, P., Estan, C., Tsiang, D., and Wright, S. (2008). Power awerness in network design and routing. In *Proc. of 27th Conf. on Computer Communications (INFOCOM 2008)*, pages 457–465.

Chiaraviglio, L., Mellia, M., and Neri, F. (2009). Energy-aware backbone networks: a case study. In *ICC 2009 Workshop*, pages 1–5.

Coiro, A., Listani, M., and Valenti, A. (2011). Dynamic power-aware and wavelength assignment for green WDM optical networks. In *Proc. of IEEE Int. Conf. on Communications (ICC)*, pages 1–6.

Cuomo, F., Abbagnale, A., Cianfrani, A., and Polverini, M. (2011). Keeping the connectivity and saving the energy in the Internet. In *Proc of. IEEE Workshop on Green Communications and Networking (INFOCOM 2011)*, pages 319–324.

Fisher, W., Suchara, M., and Rexford, J. (2010). Greening backbone networks: reducing energy consumption by shutting off cables in bundled links. In *Proc. of Green Networking 2010*, pages 29–34.

Goma, E., Canini, M., Toledo, A. L., Laoutaris, N., Kosti, D., Rodriguez, P., Stajonevi, R., and Valentin, P. Y. (2011). Insomnia in the access or how to curb access network related energy consumption. In *Proc. of Inter. Conference SIGCOMM'11*, pages 338–349.

Idzikowski, F., Orlowski, S., Raack, C., Rasner, H., and Wolisz, A. (2010). Saving energy in IP-over-WDM networks by switching off line cards in low-demand scenarios. In *Proc. of 14th Conf. on Optical Network Design and Modeling (ONDM'10)*, pages 1–6.

IEEE (2012). Institute of Electrical and Electronics Engineers, IEEE 802.3az Energy Efficient Ethernet Task Force. http://grouper.ieee.org/groups/802/3/az/public/index.html.

Intel (2010). Intel core™ i5 processor datasheet. http://download.intel.com/design/processor/datashts/322164.pdf.

Nedevschi, S., Popa, l., Iannacone, G., Wetherall, D., and Ratnasamy, S. (2008). Reducing network energy consumption via sleeping and rate adaptation. In *Proc. of 5th USENIX Symposium on Networked Systems Design and Implementation*, pages 323–336.

Pióro, M., Mysłek, M., Juttner, A., Harmatos, J., and Szentesi, A. (2001). Topological design of MPLS networks. In *Proc. of GLOBECOM'2001*, volume 1, pages 12–16.

Qureshi, A., R., W., and Balakrishnan, H. (2009). Cutting the electric bill for internet-scale systems. In *Proc. of Inter. Conference SIGCOMM'09*, pages 123–134.

Roy, S. N. (2008). Energy logic: a road map to reducing energy consumption in telecom munications networks. In *Proc. of 30th Int. Telecommunication Energy (INTELEC 2008)*, pages 1–9.

Shen, G. and Tucker, R. S. (2009). Energy-minimized desig for IP over WDM networks. *Journal of Optical Communications and Networking*, 1:176–186.

Sivaraman, V., Vishwanath, A., Zhao, Z., and Russell, C. (2011). Profiling per-packet and per byte energy consumption in the NetFPGA gigabit router. In *Proc. of IEEE Workshop on Green Communications and Networking (INFOCOM)*, pages 331–336.

Vasić, N. and Kostić, D. (2010). Energy-aware traffic engineering. In *Proc. of 1st Int. Conf. on Energy-Efficient Computing and Networking (e-Energy'10)*, pages 1–10.

Zhang, M., Yi, C., Liu, B., and Zhang, B. (2010). GreenTE: power-aware traffic engineering. In *Proc. of 18th IEEE Int. Conf. on Network Protocols (ICNP)*, pages 21–30.

AUTHOR BIOGRAPHIES

EWA NIEWIADOMSKA-SZYNKIEWICZ DSc (2005), PhD (1995), professor of control and information engineering at the Warsaw University of Technology, head of the Complex Systems Group. She is also the Director for Research of Research and Academic Computer Network (NASK). The author and co-author of three books and over 120 journal and conference papers. Her research interests focus on complex systems modeling and control, computer simulation, global optimization, parallel computation and computer networks. She was involved in a number of research projects including EU projects, coordinated the Groups activities, managed organization of a number of national-level and international conferences. Her email is `ens@ia.pw.edu.pl`.

ANDRZEJ SIKORA M.Sc. (2003) in computer science from the Warsaw University of Technology. Currently he is a Ph.D. student at the Institute of Control and Computation Engineering, the Warsaw University of Technology. Since 2005 with Research and Academic Computer Network (NASK). His research area focuses on parallel and distributed simulation, computer networks, ad hoc networks and database systems. His email is `A.Sikora@elka.pw.edu.pl`.

PIOTR ARABAS PhD (2004) in computer science from the Warsaw University of Technology, assistant professor at the Institute of Control and Computation Engineering, the Warsaw University of Technology. Since 2002 with Research and Academic Computer Network (NASK). His research area focuses on computer networks, predictive and hierarchical control. His email is `P.Arabas@elka.pw.edu.pl`.

JOANNA KOŁODZIEJ graduated in Mathematics from the Jagiellonian University in Cracow in 1992, where she also obtained the PhD in Computer Science in 2004. She joined the Department of Mathematics and Computer Science of the University of Bielsko-Biała as an Assistant Professor in 1997. She has served and is currently serving as PC Co-Chair, General Co-Chair and IPC member of several international conferences and workshops including PPSN 2010, ECMS 2011, CISIS 2011, 3PGCIC 2011, CISSE 2006, CEC 2008, IACS 2008-2009, ICAART 2009-2010. Dr Kołodziej is Managing Editor of IJSSC Journal and serves as a EB member and guest editor of several peer-reviewed international journals. Her email is `jkolodziej@ath.bielsko.pl` and webpage is `http://www.joannakolodziej.org`.

A MULTITHREADING LOCAL SEARCH FOR MULTIOBJECTIVE ENERGY-AWARE SCHEDULING IN HETEROGENEOUS COMPUTING SYSTEMS

Santiago Iturriaga, Sergio Nesmachnow
Universidad de la República
Montevideo, Uruguay
Email: {siturria,sergion}@fing.edu.uy

Bernabé Dorronsoro
Interdisciplinary Centre for Security, Reliability, and Trust
Luxembourg
Email: bernabe.dorronsoro@uni.lu

KEYWORDS

multithreading, local search, scheduling, heterogeneous computing

ABSTRACT

This article introduces an efficient multithreading local search algorithm for solving the multiobjective scheduling problem in heterogeneous computing systems considering the makespan and energy consumption objectives. The proposed method follows a fully multiobjective approach using a Pareto-based dominance search executed in parallel. The experimental analysis demonstrates that the new multithreading algorithm outperforms a set of deterministic heuristics based on Min-Min. The new method is able to achieve significant improvements in both objectives in reduced execution times for a broad set of testbed instances.

INTRODUCTION

Nowadays, distributed heterogeneous computing (HC) platforms gather hundreds or thousands of computing resources from different organizations located worldwide. In the last decade, *grid* infrastructures emerged as a useful choice to provide the computing power needed to tackle complex problems in many application domains (e.g. scientific, industrial, commercial, etc.) (Foster and Kesselman, 1998).

The efficient management of the large number of available resources in HC and grid infrastructures poses several challenges, and this can be a problem as complex as the applications to be executed/solved over the infrastructure. The efficient allocation of tasks to be executed in the distributed resources of an HC grid infrastructure is a key problem to solve in order to take full advantage of the computing power of the grid. This kind of task-worker allocation problems, called *scheduling* problems, have been thoroughly studied in the operational research field. However, most of the classic approaches tackle only homogeneous environments (El-Rewini et al., 1994; Leung et al., 2004). The distributed heterogeneous computing systems present a new heterogenity characteristic, and in this scenario the classic aproaches are clearly outperformed by many newly defined methods (Dorronsoro et al., 2010; Nesmachnow et al., 2012).

The goal of the scheduling problem is to assign tasks to the computing resources by satisfying some efficiency criteria, usually related to the total execution time for a bunch of tasks (makespan), but frequently also considering other metrics. Traditional scheduling problems are NP-hard, thus exact methods are not useful in practice to solve large instances. Deterministic heuristics are able to compute accurate results, but in general they do not scale nicely to large dimension instances. Thus, non-deterministic heuristics and metaheuristics are used to tackle scheduling problems, and has been shown that these methods are able to produce efficient schedules in reasonable timespans for both small and large dimension instances (Nesmachnow et al., 2010; Nesmachnow and Iturriaga, 2011).

Energy consumption has become a great challenge in distributed high performance computing, and researchers have focused on developing energy-aware scheduling algorithms for distributed HC infrastructures (Lee and Zomaya, 2009). In this work, we design and evaluate a highly efficient multiobjective local search (LS) metaheuristic to find accurate tradeoff solutions to the multiobjective scheduling problem of minimizing the makespan and the energy consumption in HC and grid systems (ME-HCSP). The proposed method follows a fully multiobjective approach, since it does not optimize an aggregated function of the problem objectives, but uses a Pareto-based dominance analysis instead.

The main contributions of this manuscript are: i) to introduce a fast local search method for energy-aware scheduling in HC grid systems, and ii) to compute accurate schedules in reduced execution times following a truly multiobjective approach. Using only 10 seconds of execution time, the new algorithm is able to outperform the results provided by the compared deterministic heuristics, obtaining improvements of up to **19%** for the makespan objective, and up to **9%** for the energy consumption objective.

The manuscript is organized as follows. Next section introduces the energy-aware scheduling problem in HC systems and a review of related work. After that, the new multiobjective LS proposed in this work is presented. Later, the experimental evaluation of the proposed method over a large set of problem instances is described. Finally, the conclusions of the research are presented and the main lines for future work are formulated.

Proceedings 26th European Conference on Modelling and Simulation ©ECMS Klaus G. Troitzsch, Michael Möhring, Ulf Lotzmann (Editors)
ISBN: 978-0-9564944-4-3 / ISBN: 978-0-9564944-5-0 (CD)

ENERGY-AWARE SCHEDULING IN HC SYSTEMS

Problem Formulation

An HC system is composed of computers (*machines*), with different computing power and energy consumption, depending on the hardware features. In the independent batch scheduling problem, a set of non-dependent tasks with variable computing demands must be scheduled to execute on the system. A task cannot be divided, nor interrupted after it is assigned to a machine (*non-preemptive* scheduling). The execution times of any task and the energy to perform it vary from one machine to another. Thus, there will be competition for using those machines able to execute tasks in short time and with low energy consumption.

In scheduling, the most usual metric to minimize is the *makespan*, defined as the time spent since the first task begins execution to the moment when the last task is completed (Leung et al., 2004). The mathematical model for the ME-HCSP considers the following elements:

- An HC system composed of a set of heterogeneous machines $P = \{m_1, \ldots, m_M\}$; and a collection of tasks $T = \{t_1, \ldots, t_N\}$ to be executed on the system.
- An *execution time function* $ET : T \times P \rightarrow \mathbf{R}^+$, where $ET(t_i, m_j)$ is the time required to execute task t_i on machine m_j.
- An *energy consumption function* $EC : T \times P \rightarrow \mathbf{R}^+$, where $EC(t_i, m_j)$ is the energy required to execute task t_i on machine m_j, and $EC_{IDLE}(m_j)$ is the energy that machine m_j consumes in idle state.

The ME-HCSP proposes to find a schedule $f : T^N \rightarrow P^M$ that simultaneously minimizes the *makespan* (Eq. 1), and the *energy consumption* (Eq. 2), which accounts for both the energy required for the tasks' execution and the energy that each machine spends in idle state. The energy for executing a given task depends on the execution time, but these two objectives are usually in conflict, since fast machines generally consume more energy than the slower ones.

$$\max_{m_j \in P} \sum_{\substack{t_i \in T: \\ (t_i, m_j) \in f}} ET(t_i, m_j) \tag{1}$$

$$\sum_{\substack{t_i \in T: \\ (t_i, m_j) \in f}} EC(t_i, m_j) + \sum_{m_j \in P} EC_{IDLE}(m_j) \tag{2}$$

In the ME-HCSP, all tasks can be performed disregarding the execution order. This kind of programs are frequent in e-Science applications over grid computing, such as Single-Program Multiple-Data applications used for multimedia processing, data mining, parallel domain decomposition of numerical models for physical phenomena, etc.

The independent tasks model also arises when users submit their tasks to execute in a computing service, specially in grid and volunteer-based infrastructures—WLCG, Teragrid, BOINC, Xgrid (Berman et al., 2003)—, where domain decomposition applications are often submitted for execution. Thus, the ME-HCSP faced in this work is relevant in realistic distributed HC and grid environments.

Related Work

The main trend in existing energy-aware schedulers is to apply energy management methods in the computing elements, such as dynamic voltage scaling (DVS), dynamic power management, and slack sharing/reclamation (Kim et al., 2007; Khan and Ahmad, 2009).

Kim et al. (2008) introduced several online/batch dynamic heuristics for scheduling tasks with priorities and deadlines in an ad-hoc grid with limited battery capacity, using DVS for power management. The batch dynamic heuristics based on MinMin (Luo et al., 2007) performed the best, but they required significantly more time. Li et al. (2009) also proposed an energy-aware scheduler based on MinMin to reduce energy consumption using dynamic power management.

Khan and Ahmad (2009) developed an energy-aware grid scheduler based on the concept of Nash Bargaining Solution from cooperative game theory, for DVS-enabled machines. Mezmaz et al. (2011) applied a cooperative parallel biobjective hybrid genetic algorithm (GA), improved with the energy-aware heuristics by Lee and Zomaya (2011). Pecero et al. (2011) applied a biobjective Greedy Randomized Adaptive Search Procedure scheduler, which builds a feasible solution using a greedy evaluation function, and uses a biobjective LS using DVS to improve the solution quality and generate a set of Pareto solutions.

A two-phase energy-aware heuristic for grid scheduling was proposed by Pinel et al. (2011), by first applying MinMin to find good makespan, and a LS in the second phase. Schedules with similar quality to those computed by a cellular GA are found in less time, while significantly improving the MinMin schedules. Kessaci et al. (2011) propose two multiobjective parallel GAs enhanced with energy-aware scheduling heuristics for tasks with dependencies, combining makespan and energy consumption in a unique function and using explicit DVS for energy management.

Kolodziej et al. (2011) developed a GA framework for energy-aware schedulers using DVS for energy reduction, a bag-of-tasks model, and a biobjective scheduling problem minimizing makespan and energy consumption. Recently, Lindberg et al. (2012) introduced a set of eight heuristics, including six list scheduling algorithms and two GAs, for the energy-aware grid scheduling problem subject to deadline constraint and tasks' memory requirements.

The approach in our article does not apply DVS or other energy management methods. Instead, we propose to explicitly compute the energy consumption considering the Max-Min mode, which accounts for hardware-embedded energy saving features (e.g. SpeedStep technology by Intel, or Optimized Power Management by AMD): a working machine is assumed to operate at peak performance, consuming the maximum energy, and when a machine is idle, the embedded energy saving technology keeps the energy consumption at its minimum specified value.

A MULTITHREADING ENERGY-AWARE SCHEDULER FOR HC SYSTEMS

This section describes the multithreading LS algorithm to solve the energy-aware scheduling problem in HC systems.

ME-MLS Design

ME-MLS is a population-based LS algorithm, which maintains a population of non-dominated schedules in order to avoid biasing the search toward one of the objectives of the energy-aware scheduling problem. The algorithm uses a pool of threads in which each thread is a peer, and no thread performs a master role. Algorithm 1 presents the pseudo-code of each thread in ME-MLS.

Algorithm 1 ME-MLS algorithm for each thread.

```
1:  thread_idx ← current thread index
2:  initialize_individual(population, thread_idx)
3:  initialization_barrier()
4:  while not stop_criteria do
5:      lock_population()
6:      s ← draw_random_schedule(population)
7:      s' ← clone(s)
8:      unlock_population()
9:      search_strategy ← random_strategy()
10:     max_iterations ← random(1, THREAD_ITER)
11:     while not search_ready do
12:         for i = 0 → max_iterations do
13:             local_search(search_strategy, s')
14:         end for
15:         trylock_population()
16:         if locked then
17:             check_Pareto_dominance(population, s')
18:             search_ready ← true
19:             unlock_population()
20:         else
21:             rework ← THREAD_ITER / REWORK_FACTOR
22:             max_iterations ← random(1, rework)
23:             search_ready ← false
24:         end if
25:     end while
26: end while
```

Each thread starts by initializing a schedule in the population using a randomized version of the Minimum Completion Time (MCT) heuristic. After that, each thread loops over the schedules in the population searching to improve them. On each loop step, each thread randomly selects a schedule s from the population to perform a LS. To perform the search, the thread clones the selected solution $s' = s$ and then applies a random number of iterations of the LS upon the clone s'. If a given thread finds a non-dominated schedule, it is inserted into the population; otherwise it is discarded. Then, the thread loops and once again randomly selects a schedule to improve from the population of non-dominated schedules.

The population of non-dominated schedules is limited in size, so a replacement policy is applied when the maximum size is reached. Each new non-dominated schedule is always inserted in the population. When the population is full, a schedule currently in the population is selected to be replaced based on a distance function, helping to prevent a stagnation situation. Those schedules that compute the minimum value in the population in at least one of the objectives are never replaced. Figure 1 shows the main activities performed during the execution of the ME-MLS algorithm.

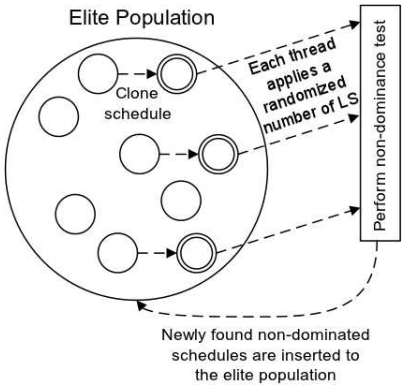

Figure 1: Diagram of the ME-MLS algorithm.

Local search

The energy-aware LS performed by each thread is based on a randomized version of the Problem Aware Local Search proposed by Alba and Luque (2007). Algorithm 2 presents the pseudo-code of the LS performed by each thread.

Algorithm 2 Energy-aware local search.

```
1:  strategy ← current search strategy
2:  s' ← schedule to improve
3:  mach_a ← random_machine(strategy, s')
4:  tasks_x ← random_task_set(mach_a)
5:  mach_b ← random_machine(strategy, s') ≠ mach_a
6:  tasks_y ← random_task_set(mach_b)
7:  best_operation ← none
8:  for all x ∈ tasks_x do
9:      operator ← random(move or swap)
10:     if operator = swap then
11:         for all y ∈ tasks_y do
12:             delta_{x,y} ← improvement(strategy, s', swap_{x,y})
13:             delta_best ← improvement(strategy, s', best_operation)
14:             if delta_{x,y} > delta_best then
15:                 best_operation ← swap_{x,y}
16:             end if
17:         end for
18:     else if operator = move then
19:         dst_set ← random_machine_set() ∪{mach_b}
20:         for all dst ∈ dst_set do
21:             delta_{x,dst} ← improvement(strategy, s', move_{x,dst})
22:             delta_best ← improvement(strategy, s', best_operation)
23:             if delta_{x,dst} > delta_best then
24:                 best_operation ← move_{x,dst}
25:             end if
26:         end for
27:     end if
28: end for
29: if best_operation ≠ none then
30:     apply_operation(best_operation)
31: end if
```

When applied to a schedule s, the energy-aware LS selects one of the following optimization strategies: (1) makespan optimization, (2) energy optimization, or (3) random optimization. Then, the method iterates a randomized number of times trying to improve the schedule s. In each iteration, the method selects a pair of machines m_A and m_B to perform the search. When the makespan optimization strategy is selected, it selects with high probability the makespan defining machine as m_A and the machine with lower computing time as machine m_B. The energy optimization strategy selects with high probability the most energy consuming machine as m_A and the less energy consuming machine as m_B. Finally, the random optimization strategy selects two random machines as m_A and m_B. After that, the method selects a random set of tasks $tasks_X$ from the ones assigned to $machine_A$. For each task $t_X \in tasks_X$, the method randomly selects an operation to perform: (1) a swap operation, or (2) a move operation. If the swap operation is selected for task t_X, the method selects a random set of tasks $tasks_Y$ assigned to $machine_B$ and computes the task t_X swap with each task $t_Y \in tasks_Y$. The method chooses the swap which improves the most the schedule objectives. If the energy and makespan improvements of the computed swap are in conflict (i.e. the swap improves one metric but degrades the other), the method selects the best swap prioritizing one metric according to the selected search strategy. When no swap is found to improve neither of the schedule objectives, no swap is applied.

If the move operation is selected for task t_X, the method selects a set of machines $machines_Y = \{random\ set\ of\ machines\} \cup \{m_B\}$, and computes the variation in the schedule objectives when moving the task t_X to each machine $m_Y \in machines_Y$. The method chooses the move operation which improves the most the schedule objectives prioritizing the currently selected search strategy. Again, if no move is found to improve neither of the schedule objectives, then no move is applied.

Implementation Details

This subsection presents the implementation details of the ME-MLS algorithm proposed in this work.

Implementation language and libraries. The ME-MLS algorithm is implemented in GNU C++ 4.6, but certain C++ constructs where avoided in order to minimize the code execution overhead (e.g.: classes, interfaces, polymorphism, etc.). The multithreading support is provided by the GNU POSIX thread library 2.13. The use of higher level libraries, like OpenMP, were avoided in order to gain fine grain control over the synchronization mechanisms. Finally, the Mersenne Twister (MT) method (Matsumoto and Nishimura, 1998) is used for generating pseudorandom numbers. For this work, the original MT implementation was modified to be thread-safe, to allow the multithreading generation of random numbers.

Problem encoding. To store a schedule, a multi-structure is maintained in memory comprising both a machine-based and a task-based encoding (Nesmachnow et al., 2010) (see Figure 2). This in-memory multi-structure allows to: i) access the tasks assigned to a given machine in $O(1)$ execution time via the machine-based encoding; and ii) given a certain task, locate the machine to which is assigned also in $O(1)$ execution time via the task-based encoding.

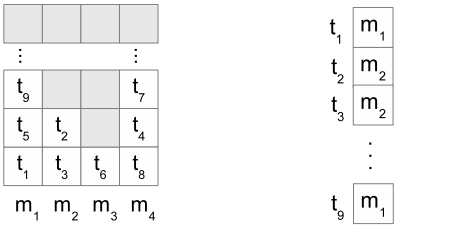

(a) Machine-oriented encoding. (b) Task-oriented encoding.

Figure 2: Problem encodings.

Population initialization. A randomized version of the MCT heuristic is used to initialize the population. The randomized MCT considers the tasks sorted in a random order, thus tasks are scheduled also in a random order, providing some diversity in the initial population.

EXPERIMENTAL ANALYSIS

This section introduces the set of ME-HCSP instances and the hardware platform used in the experimental analysis. After that, the set of Min-Min based heuristics for energy-aware scheduling used as a reference baseline to compare the results computed by the ME-MLS algorithm are introduced. Finally, the experimental results are presented and analyzed, along with a scalability study that evaluates the speedup of the proposed method when using different numbers of threads.

ME-HCSP instances

To evaluate the proposed ME-MLS algorithm a set of **792** ME-HCSP instances were generated. Each instance describes the machines *scenario* and the set of tasks *workloads*. The scenarios were generated using realistic data, gathering for each machine the computational power, the energy consumption in idle state, and the energy consumption in processing state. The workloads were generated following the ETC methodology proposed by Ali et al. (2000).

Three instance dimensions were evaluated (*number of tasks* $\times$ *number of machines*): 512$\times$16, 1024$\times$32, and 2048$\times$64. A number of 11 different scenarios were generated for each dimension, and 24 workloads were generated for each problem dimension, 12 following the parametrization by Ali et al. (2000) and 12 following the parametrization by Braun et al. (2001).

Execution hardware platform
The experimental analysis of the ME-MLS algoritm was performed on a 24-Core AMD Opteron Processor 6172, 2.1GHz, 24 GB RAM, running 64-bits CentOS 5.1 Linux.

Min-Min based heuristics
In order to compare the ME-MLS results, we proposed a set of heuristics based on the Min-Min (Luo et al., 2007) heuristic which is considered to outperform other deterministic heuristics for minimizing the makespan objective (Izakian et al., 2009).

Min-Min uses a two-phase optimization strategy, thus we define four versions of the Min-Min heuristic alternating the minimization objective.The first version minimizes the completion time in both phases; the second version minimizes the energy objective in both phases; in the remaining versions the minimization objectives are alternated to be in the first phase or the second phase. When the completion time is minimized we use the *Min* notation, and when the energy metric is minimized we use the *MIN* notation is used. Thus the four Min-Min versions are: *Min-Min*, *MIN-MIN*, *Min-MIN*, and *MIN-Min*.

Parameter settings
The objective of this work is to *efficiently* solve the ME-HCSP, thus a fixed 10 seconds execution time stopping criterion is used for the ME-MLS algorithm. This time stopping criterion is significantly lower than the execution time of the algorithms in the related literature. A number of 30 independent ME-MLS executions were performed on each instance, considering the stochastic nature of the proposed algorithm. Each execution was performed using 24 threads, the maximum number of cores available.

A configuration analysis was performed using the 512×16 dimension instances in order to find the best values for the population size (POP_SIZE), the number of LS per schedule (THREAD_ITER), the LS neighbourhood size (SRC_TASK_NHOOD, DST_TASK_NHOOD, and DST_MACH_NHOOD), and the re-work factor (REWORK_FACTOR).

The candidate values for the parameter settings study were: POP_SIZE $\in \{30, 35, 40\}$, THREAD_ITER $\in \{500, 650, 800\}$, SRC_TASK_NHOOD $\in \{24, 28, 32\}$, DST_TASK_NHOOD $\in \{16, 20, 24\}$, DST_MACH_NHOOD $\in \{8, 12, 16\}$, and REWORK_FACTOR $\in \{10, 14, 18\}$. The best results were obtained with the following configuration: POP_SIZE $= 30$, THREAD_ITER $= 650$, SRC_TASK_NHOOD $= 28$, DST_TASK_NHOOD $= 16$, DST_MACH_NHOOD $= 16$, and REWORK_FACTOR $= 14$.

Results and discussion
Table 1 presents the average improvements obtained when comparing the ME-MLS algorithm with the Min-Min based heuristic that performs the best for that instance and objective. Figure 3 summarizes the average improvement by dimension compared to each Min-Min based heuristic.

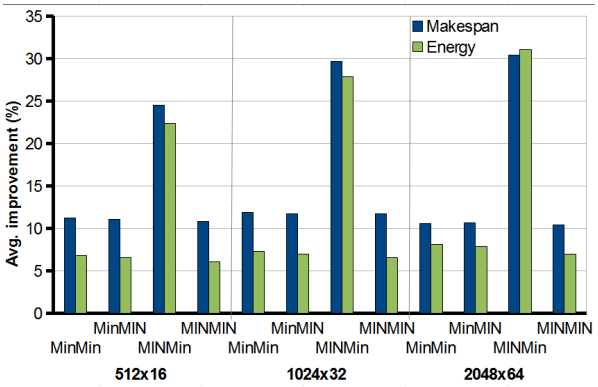

Figure 3: Average ME-MLS improvement over the Min-Min based heuristics.

Table 1 demonstrates that ME-MLS outperforms the best Min-Min based heuristic on the makespan metric with improvements ranging from 3.5% to **19.8%** and on the energy metric with improvements ranging from 2.6% to **9.4%**. Table 1 also shows that ME-MLS produces the best improvements when solving the inconsistent instances, and the second best improvements are produced when solving the semiconsistent instances.

Regarding the energy metric, ME-MLS achieved an acceptable steady improvement ranging from 3.4% to **8.0%** when grouping by type and herogeneity, and ranging from 5.8% to **6.8%** when grouping by dimension. On the other hand, the makespan metric is most sensible to the heterogeneity and type variation, and shows a considerable gap ranging from 4.7% to 16.6% when considering different types and heterogeneities.

Another interesting observation is that the ME-MLS algorithm improvements actually increase with the problem dimension. This performance increase is manly due to the improvements obtained when solving the inconsistent type instances; the improvements when solving this type of instances constantly increase with the dimension increase.

Regarding the computational efficiency of the ME-MLS algorithm, a speedup study was performed. The speedup evaluation was performed using 1024×32 instances, and performing 30 independent executions with a stopping criterion of 6 million iterations. The analysis shows the ME-MLS algorithm has a near linear speedup, achieving a speedup of 19.7 when using 24 threads. Figure 4 shows the results of the speedup analysis.

CONCLUSIONS

This work presented ME-MLS, a multiobjective multithread LS algorithm with strong focus on producing accurate results in short execution times (i.e. less than 10 seconds) for the energy-aware scheduling problem in HC systems. The ME-MLS algorithm uses a population of non-dominated schedules and a Pareto-based search following a fully multiobjective approach.

Table 1: Average ME-MLS improvement over the best Min-Min based heuristic.

type	heterogeneity	dimension						average	
		512×16		1024×32		2048×64			
		makespan	*energy*	*makespan*	*energy*	*makespan*	*energy*	*makespan*	*energy*
consistent	high high	9.2%	5.3%	6.6%	6.3%	5.6%	7.0%	7.1%	6.2%
	high low	6.5%	3.7%	7.1%	5.9%	5.8%	7.4%	6.5%	5.7%
	low high	8.1%	4.7%	7.4%	6.0%	6.0%	8.2%	7.2%	6.3%
	low low	4.5%	5.3%	6.0%	8.7%	3.5%	9.4%	4.7%	7.8%
inconsistent	high high	14.7%	7.4%	16.8%	8.1%	18.4%	7.9%	16.6%	7.8%
	high low	13.2%	6.9%	15.7%	7.2%	19.8%	9.0%	16.2%	7.7%
	low high	14.9%	7.8%	17.2%	8.6%	16.9%	7.5%	16.3%	8.0%
	low low	8.9%	4.9%	13.7%	7.7%	11.7%	6.9%	11.4%	6.5%
semiconsistent	high high	13.4%	6.8%	11.4%	4.0%	8.8%	2.6%	11.2%	4.5%
	high low	8.5%	3.7%	10.9%	3.0%	9.4%	3.5%	9.6%	3.4%
	low high	13.7%	7.6%	11.4%	4.1%	9.3%	4.4%	11.5%	5.4%
	low low	7.3%	5.4%	9.5%	6.1%	5.7%	8.3%	7.5%	6.7%
	average	10.2%	5.8%	11.1%	6.3%	10.0%	6.8%		

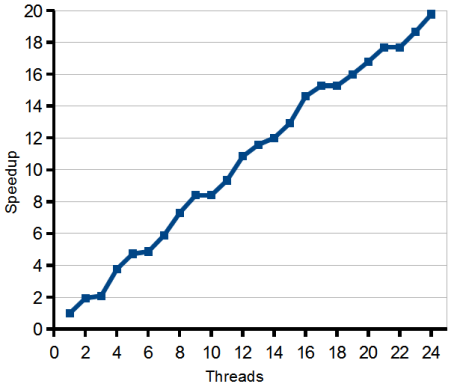

Figure 4: ME-MLS algorithm speedup.

The ME-MLS algorithm was evaluated over a large testbed of 792 instances with dimensions of up to 2048×64. The results were compared to four Min-Min based heuristics which tackle the energy-aware scheduling problem considering both minimization objectives. The experimental analysis showed that the ME-MLS method outperforms the Min-Min based heuristics with average improvements of up to **19.8%** for the makespan objective, and up to **9.4%** in the energy consumption objective. The performance analysis showed that the ME-MLS has a promising scalability behavior.

The main lines for future work include to improve the efficiency of the ME-MLS allowing us to solve larger problem dimensions. We also plan to extend the problem formulation to consider multicore machines and their energy consumption behaviors, this will allow us to model nowadays machine scenarios.

REFERENCES

Alba, E. and Luque, G. (2007). A new local search algorithm for the DNA fragment assembly problem. In *Proc. of 7^{th} European Conference on Evolutionary Computation in Combinatorial Optimization*, pages 1–12.

Ali, S., Siegel, H., Maheswaran, M., Ali, S., and Hensgen, D. (2000). Task execution time modeling for heterogeneous computing systems. In *Proc. of the 9^{th} Heterogeneous Computing Workshop*, page 185, Washington, DC, USA.

Berman, F., Fox, G., and Hey, A. (2003). *Grid Computing: Making the Global Infrastructure a Reality*. Wiley.

Braun, T., Siegel, H., Beck, N., Bölöni, L., Maheswaran, M., Reuther, A., Robertson, J., Theys, M., Yao, B., Hensgen, D., and Freund, R. (2001). A comparison of eleven static heuristics for mapping a class of independent tasks onto heterogeneous distributed computing systems. *J. Parallel Distrib. Comput.*, 61(6):810–837.

Dorronsoro, B., Bouvry, P., Cañero, J., Maciejewski, A., and Siegel, H. (2010). Multi-objective robust static mapping of independent tasks on grids. In *IEEE Congress on Evolutionary Computation*, pages 3389–3396.

El-Rewini, H., Lewis, T., and Ali, H. (1994). *Task scheduling in parallel and distributed systems*. Prentice-Hall, Inc.

Foster, I. and Kesselman, C. (1998). *The Grid: Blueprint for a Future Computing Infrastructure*. Morgan Kaufmann.

Izakian, H., Abraham, A., and Snasel, V. (2009). Comparison of heuristics for scheduling independent tasks on heterogeneous distributed environments. In *Proceedings of the 2009 International Joint Conference on Computational Sciences and Optimization - Volume 01*, CSO '09, pages 8–12, Washington, DC, USA. IEEE Computer Society.

Kessaci, Y., Mezmaz, M., Melab, N., Talbi, E., and Tuyttens, D. (2011). Parallel Evolutionary Algorithms for Energy Aware Scheduling. In *Intelligent Decision Systems in Large-Scale Distributed Environments*. Springer.

Khan, S. and Ahmad, I. (2009). A cooperative game theoretical technique for joint optimization of energy consumption and response time in computational grids. *IEEE Trans. Parallel Distrib. Syst.*, 20:346–360.

Kim, J.-K., Siegel, H., Maciejewski, A., and Eigenmann, R. (2008). Dynamic resource management in energy constrained heterogeneous computing systems using voltage scaling. *IEEE Trans. Parallel Distrib. Syst.*, 19:1445–1457.

Kim, K., Buyya, R., and Kim, J. (2007). Power aware scheduling of bag-of-tasks applications with deadline constraints on DVS-enabled clusters. In *Proc. of the 7^{th} IEEE Int. Symposium on Cluster Computing and the Grid*, pages 541–548.

Kolodziej, J., Khan, S. U., and Xhafa, F. (2011). Genetic algorithms for energy-aware scheduling in computational grids. In *Int. Conf. on P2P, Parallel, Grid, Cloud and Internet Computing*, pages 17–24.

Lee, Y. and Zomaya, A. (2009). Minimizing energy consumption for precedence-constrained applications using dynamic voltage scaling. In *Proc. of the 9^{th} IEEE/ACM Int. Symposium on Cluster Computing and the Grid*, pages 92–99.

Lee, Y. and Zomaya, A. (2011). Energy conscious scheduling for distributed computing systems under different operating conditions. *IEEE Trans. Parallel Distrib. Syst.*, 22:1374–1381.

Leung, J., Kelly, L., and Anderson, J. (2004). *Handbook of Scheduling: Algorithms, Models, and Performance Analysis*. CRC Press.

Li, Y., Liu, Y., and Qian, D. (2009). A heuristic energy-aware scheduling algorithm for heterogeneous clusters. In *Proc. of the 2009 15^{th} Int. Conf. on Parallel and Distributed Systems*, pages 407–413.

Lindberg, P., Leingang, J., Lysaker, D., Khan, S., and Li, J. (2012). Comparison and analysis of eight scheduling heuristics for the optimization of energy consumption and makespan in large-scale distributed systems. *The Journal of Supercomputing*, 59(1):323–360.

Luo, P., Lü, K., and Shi, Z. (2007). A revisit of fast greedy heuristics for mapping a class of independent tasks onto heterogeneous computing systems. *J. Parallel Distrib. Comput.*, 67(6):695–714.

Matsumoto, M. and Nishimura, T. (1998). Mersenne twister: a 623-dimensionally equidistributed uniform pseudo-random number generator. *ACM Trans. Model. Comput. Simul.*, 8(1):3–30.

Mezmaz, M., Melab, N., Kessaci, Y., Lee, Y., Talbi, E. G., Zomaya, A., and Tuyttens, D. (2011). A parallel bi-objective hybrid metaheuristic for energy-aware scheduling for cloud computing systems. *J. Parallel Distrib. Comput.*, 71(11):1497–1508.

Nesmachnow, S., Cancela, H., and Alba, E. (2010). Heterogeneous computing scheduling with evolutionary algorithms. *Soft Computing*, 15(4):685–698.

Nesmachnow, S., Cancela, H., and Alba, E. (2012). A parallel micro evolutionary algorithm for heterogeneous computing and grid scheduling. *Appl. Soft Comput.*, 12(2):626–639.

Nesmachnow, S. and Iturriaga, S. (2011). Multiobjective scheduling on distributed heterogeneous computing and grid environments using a parallel micro-CHC evolutionary algorithm. In *Int. Conf. on P2P, Parallel, Grid, Cloud and Internet Computing*, pages 134–141.

Pecero, J., Bouvry, P., Fraire Huacuja, H. J., and Khan, S. (2011). A multi-objective grasp algorithm for joint optimization of energy consumption and schedule length of precedence-constrained applications. In *Int. Conf. Cloud and Green Computing*, pages 1–8.

Pinel, F., Dorronsoro, B., Pecero, J., Bouvry, P., and Khan, S. (2011). A two-phase heuristic for the energy-efficient scheduling of independent tasks on computational grids. *Journal of Cluster Computing*. Submitted.

AUTHOR BIOGRAPHIES

SANTIAGO ITURRIAGA has a degree on Engineering and is currently a student of the M.Sc. in Computer Science, Universidad de la Republica, Uruguay. He is an Assistant at Engineering Faculty, Universidad de la Republica. His M.Sc. thesis is focused on high performance computing and metaheuristics for scheduling. He has published several conference proceedings in these areas. Email: `siturria@fing.edu.uy`, personal webpage at `http://www.fing.edu.uy/∼siturria`.

SERGIO NESMACHNOW has a degree in Engineering (2000), a M.Sc. in Computer Science (2004), and a Ph.D in Computer Science (2010) from Universidad de la Republica, Uruguay. He is currently an Aggregate Professor at Numerical Computing Center, Engineering Faculty, Universidad de la Republica. His main research areas are scientific computing, high performance computing, and parallel metaheuristics, and their application for solving complex real-world problems. He has published over 50 papers in international journals and conference proceedings. He has also served in several technical program committees of international conferences in related areas, and he serves as reviewer for many journals and conferences. Email: `sergion@fing.edu.uy`, personal webpage at `http://www.fing.edu.uy/∼sergion`.

BERNABÉ DORRONSORO has a degree in Engineering (2002) and the Ph.D. in Computer Science (2007) from University of Málaga, Spain, and he is currently working as research associate at the University of Luxembourg. His main research interests include grid computing, ad hoc networks, the design of efficient metaheuristics, and their application for solving complex real-world problems in logistics, telecommunications, bioinformatics, combinatorial, multiobjective, and global optimization. He has several articles in impact journals and one book, has been member of the organizing committees of several conferences and workshops, and he usually serves as reviewer for leading impact journals and conferences. Email: `beranbe.dorronsoro@uni.lu`, personal webpage at `www.bernabe.dorronsoro.es`.

INTELLIGENT TRAFFIC LIGHTS TO REDUCE VEHICLE EMISSIONS

Ciprian Dobre*, Adriana Szekeres, Florin Pop, Valentin Cristea
Department of Computer Science and Engineering
University POLITEHNICA of Bucharest, Romania
E-mails: ciprian.dobre@cs.pub.ro, adriana.szekeres@gmail.com,
{florin.pop, valentin.cristea}@cs.pub.ro
* Corresponding author

Fatos Xhafa
Universitat Politecnica de Catalunya
Campus Nord - Ed. Omega, C/Jordi
Girona Salgado 1-3, 08034 Barcelona,
Spain
E-mail: fatos@lsi.upc.edu

KEYWORDS
Intelligent traffic light, urban traffic, pollution, wireless communication, modeling and simulation.

ABSTRACT

Cars with petrol-driven internal combustion engines are sources of air pollution. Until alternative car engines will replace petrol-driven engines, road transportation is a major source for emissions of carbon monoxide, carbon dioxide, hydrocarbons, and many other organic compounds into the environment. There is a direct relation between the car's emissions and its acceleration: an accelerating car will pollute more than a non-speeding car. In this paper we present a mobile system capable of guiding the driver's decisions with the goal of reducing vehicle emissions. The system considers parameters ranging from the car's characteristics to human reactions. In this we present results demonstrating the capability of the system to produce decisions that reduce pollution in urban traffic environment.

1. INTRODUCTION

Experts predict that by 2030 the number of cars will reach 2.2 billion (Cars 2011). Today cars are already major sources of emissions, with negative effects on the environment and health (Sovacool 2010). Cars emit tons of pollutants in the air every day: ground level ozone (O3) produces smog (causing visibility and lung medical problems); carbon dioxide is responsible for Global Warming.

To reduce air pollution car manufacturers consider today various alternatives: manufacturing of electrical cars, the creation of new environmentally friendly fuels (Sovacool 2010). Unfortunately, today the reality is that cars do pollute. Even though manufacturers try to reduce this problem, people behind the wheel are also responsible for creating a better future for themselves and their children. The solution to environmental degradations involves unselfish and compassionate behavior, a scarce commodity.

In this we propose a system designed to assist drivers adapt their behavior and take informed decisions to minimize fuel consumption (and, implicitly, air-pollution). We consider the special case of minimizing fuel consumption as drivers approach an intersection. In case of an intersection equipped with traffic lights, previous studies showed that drivers tend to accelerate more than usually to catch the green light (Kuroyanagi et al. 2011). This is also a major cause of the over 5,000 fatal crashes that occur each year in intersections with traffic signals or stop signs.

"Smart" vehicles of the future are envisioned to aid their drivers to reduce fuel consumption and emissions by wirelessly receiving phase-shifting information of the traffic lights in their vicinity, and computing and presenting drivers with suggestions for braking and acceleration decisions. We present models, methods and algorithms to be used in a real-world implementation. In our approach the traffic light periodically broadcasts its scheduling information over the wireless medium to the vehicles in its vicinity. From this information, vehicles compute their required speed in order to hit a green light and offer this information to their drivers who can in turn adapt their speed accordingly.

We also present a methodology for evaluating the impact on the reduction of pollution, using modeling and simulation. While field tests so far have focused on a technical proof of concept, simulation is still the means of choice for an estimation of the achievable large-scale benefits of applications designed for complex vehicular-based scenarios. Our evaluation results provide insights on the positive impact that such a small change in driver's behavior can bring on the environment.

The rest of this paper is organized as follows. Section 2 presents Related Work. In Section 3 we present the theoretical model for predicting fuel consumption, based on the car's characteristics. Section 4 describes the solution, and presents the proposed model to estimate vehicle emissions. We also present the proposed system that uses a prediction algorithm to recommend the cruising speeds to the driver. In Section 5 we present an analysis and experimental results and, finally, in Sections 6 we give conclusions and propose future work.

2. RELATED WORK

A generic solution to reducing air-pollution using vehicular networks was previously presented in (Gradinescu et al. 2007). The authors propose an adaptive traffic light system that uses wireless communication with vehicles and fixed controller nodes deployed in intersections to improve traffic fluency in intersections. They show that traffic fluency has an impact on the

Proceedings 26th European Conference on Modelling and Simulation ©ECMS Klaus G. Troitzsch, Michael Möhring, Ulf Lotzmann (Editors)
ISBN: 978-0-9564944-4-3 / ISBN: 978-0-9564944-5-0 (CD)

pollution caused by cars. A similar solution is presented in (Alsabaan et al. 2010). However, these are generic solutions to the problem of air pollution. We make the steps towards a concrete solution to decrease pollution, and identify key factors on the level of detail and characteristics required for a concrete real-world implementation. We propose the use of "smart" traffic lights to reduce car emissions in the particular situation of an intersection equipped with traffic light.

Regarding the emission model, previous studies that tend to rely on mathematical formulae, calibrated for average personal cars, to compute fuel consumption and emissions (Wegener et al. 2008)(Sanchez et al. 2006). Others use more detailed emission models (Alsabaan et al. 2010), with studies that addressed particular aspects like cold/warm start, gear shifting and different vehicle and emission types. In this we present a more generic model that considers all these aspects combined. Haworth and Symmons (2001) relate speed to fuel consumption and emissions rate. They emphasize on the importance of the driver's behavior on reducing car emissions. Estimating fuel consumption and pollutant emissions is a necessity when evaluating traffic management applications. Similar to our approach, the authors use the method proposed by Akcelik and Besley (2003) to model fuel consumption and emissions (CO2 , CO, HC, N Ox). But, unlike our work, the authors willingly simplified the model to consider only light vehicles. We present a more complex model, similar to the theoretical one, which we believe to more accurately reflect real-world traffic situations.

The authors of (Tielert et al. 2010) show that Traffic-light-to-vehicle communication (TLVC) has the potential to reduce the environmental impact of vehicular traffic by helping drivers avoid braking and accelerating maneuvers at traffic lights. However, the focus is not on the algorithm to be used for speed recommendations, but rather on a methodology to use modeling and simulation to evaluate such solutions. The motivation is that equipping traffic lights with communication technology requires significant financial expenditures. Thereby, credible large-scale simulation studies are an important means to assess the return on investment. In this we propose a complex simulation model to evaluate our solution. Unlike (Tielert et al. 2010), we also propose a concrete solution to use TLVC to disseminate information, and an algorithm to make recommendations considering the characteristics of the car that optimize fuel consumption.

Asadi and Vahidi (2010) find fuel consumption to be lowered by up to 47% for a traffic-light scheduling based cruise control algorithm when evaluating 9 traffic lights in a row and have vehicles consider the phases of the subsequent traffic lights. Richter (2005) states a maximum of 35% and an average of 14% for a single road and traffic light. Providing hard figures on how much fuel/emissions can be saved is difficult, since simulation results depend highly on the simulation setup, models and implementations used as well as on the way of evaluation. For example, when analyzing a single road and traffic light, the ratio of fuel saved depends on the length on the evaluated road segment. Thus, it is not the objective of this paper to provide hard figures, but to identify key influencing factors and quantify the degree of their influence.

3. COMPUTATIONAL MODEL FOR FUEL CONSUMPTION

To estimate fuel consumption we first developed a model that takes as input the car's characteristics, and estimates an optimal cruising speed based on the distance to the traffic light. The prediction of the car's movement is based on a model of the mechanical physics involved. Figure 1 illustrates the forces that act on the car. The force of gravity pulls the car towards the earth. The total normal force, F_N , is the sum of the forces on the front and rear tires and it is equal to the mass of the car multiplied by the acceleration due to gravity and the cosine of the slope angle, θ.

$$F_N = F_{Nf} + F_{Nr} = mg\cos\theta \quad (1)$$

The engine generates torque, which when applied to the wheels causes them to rotate. The force applied to the tires, F_T , is equal to the torque applied to the wheels, T_w , divided by the wheel radius, r_w . When the car is in motion, an aerodynamic drag force develops. This drag force can be modeled as a function of the air density, ρ , frontal area, *A*, the square of the velocity magnitude, *v*, and a drag coefficient, C_D . The last important force in the car diagram (see Figure 1) is due to rolling friction. This force acts on all four wheels and resists the rolling motion of the car. The total rolling friction force, F_R , is equal to the total normal force, F_N , multiplied by the coefficient of rolling friction for the vehicle, μ_r .

The total force that acts on the car parallel to the direction the car is driving, F_{total} , is equal to the sum of the forces due to engine torque, gravity, aerodynamic drag, and rolling friction:

$$F_{total} = \frac{T_W}{r_w} - \mu mg\cos\theta - mg\sin\theta - \frac{1}{2}C_D\rho v^2 A \quad (2)$$

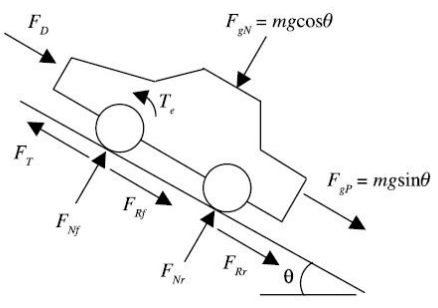

Figure 1. Force balance on a car.

The acceleration of the car at any given time is the net force on the vehicle divided by the mass of the vehicle, *m*:

$$a = \frac{T_W}{r_w m} - \mu g \cos\theta - g \sin\theta - \frac{1}{2}\frac{C_D \rho v^2 A}{m} \quad (3)$$

The engine generates a torque that is used to move the car. The torque generated by the engine is not the same as the torque applied to the wheels (the engine is not coupled directly to the wheels, but to some set of gears). The engine torque is a function of the rate at which the engine is turning over. The engine turnover rate is expressed in revolutions per minute, *rpm*. There is a relation between the engine torque and the engine's turnover rate, which vary from car to car. One characteristic of engine torque is that it does not always increase with the increase of the engine turnover rate.

The torque applied to the wheels of a car determines its acceleration. Generally the torque applied to the wheels is not the same as the engine torque. Before the engine torque is applied to the wheels, it passes through a transmission. The gears inside a transmission change the angular velocity and torque transferred from the engine. This can greatly increase the acceleration of a car. The gear ratio between two gears is the ratio of the gear diameters. Car transmissions will typically have between three and six forward gears and one reverse gear. There is also an additional set of gears between the transmission and the wheels. The gear ratio of this final gearset is known as final drive ratio.

The wheel torque, T_w, is equal to the engine torque, T_e, multiplied by the gear ratio, g_k, of whatever gear the car is in and the final drive ratio, G, of the car. Using the previous equations, the car's acceleration can be computed as:

$$a = \frac{T_e g_k G}{r_w m} - \mu g \cos\theta - g \sin\theta - \frac{1}{2}\frac{C_D \rho v^2 A}{m} \quad (4)$$

Transmission gears also change the angular velocity of the wheel relative to the turnover rate of the engine (the factor "60" is to transform from *rpm* in *revolutions per second*):

$$\omega_w = \frac{2\pi\Omega_c}{60 g_k G} \quad (5)$$

If the tires roll on the ground without slipping (the "burn rubber" effect), the translational velocity of the car, *v*, can be related to the angular velocity of the wheel, and therefore to the engine turnover rate:

$$v = r_w \omega_w = \frac{r_w 2\pi\Omega_e}{60 g_k G} \quad (6)$$

In order to estimate the movement of a car, it is necessary to determine the acceleration and velocity of the car at any point in time. The starting point for this analysis is eq. (4). If the slope angle, frontal area, and air density are known, the only unknown quantity in this equation is the wheel torque, T_w. As explained, the wheel torque is the product of the engine torque, T_e, the current gear ratio, g_k, and the final drive ratio, *G*. The engine torque, T_e, can be obtained from the torque curve of the engine. The torque curve can generally be modeled by three equations. The units for engine torque in all three equations are in N-m.

$$T_e = 220, \quad \Omega_e \le 1000 \quad (7a)$$

$$T_e = 0.025\Omega_e + 195, \quad 1000 < \Omega_e < 4600 \quad (7b)$$

$$T_e = -0.032\Omega_e + 457.2, \quad \Omega_e \ge 4600 \quad (7c)$$

The general equation for the three previous ones is:

$$T_e = b\Omega_e + d \quad (8)$$

Using equations (8), (6), and (4), the expression for the acceleration of the car as a function of the current velocity of the car becomes:

$$a = \frac{60 g_k^2 G^2 b v}{2\pi m r_w^2} + \frac{g_k G d}{m r_w} - \mu g \cos\theta - g \sin\theta - \frac{1}{2}\frac{C_D \rho v^2 A}{m}$$

Knowing this equation that expresses the car motion equation, and some typical parameters for the rolling friction coefficient (0.015), the average frontal area of a car (1.94 m2), the wheel radius (0.3186), etc., we solved this differential equation using the fourth-order Runge-Kutta method.

The relation between speed and fuel consumption and emission rate is given by the Haworth and Symmons model (Haworth and Symmons, 2001). These are results relative to the car's characteristics. However, they clearly show that by accelerating or decelerating a car consumes relatively larger or smaller fuel quantities than it would consume normally (in such a model the normal value is defined depending on the type of car and its characteristics).

A number of curves relating emissions to fuel consumption, and to the average cruising speed have been developed in the related literature (Smith and Cloke, 1999). Emissions of Volatile Organic Compounds (VOCs or HCs) and carbon monoxide (CO) generally decrease as average speed increases and then increase somewhat over 100 km/h. Emissions of nitrogen oxides increase more than proportionally with average speed. The relationship between fuel consumption and average speed is somewhat more complex. It appears to decrease as average speed increases to about 60 km/h to 80 km/, and then it increases. Other authors have presented curves of similar shapes, but with different gradients or minima. For example, Andre and Hammarstrom (2000) report that CO emission reaches a minimum at about 70 km/h, whereas CO emissions decrease monotonically with speed.

These previous studies show a clear relation between acceleration and the car's emissions. Emissions tend to be higher during acceleration, when the fuel to air ratio is higher. The conclusion of this analysis is that the driver can greatly influence the emissions rate through smooth accelerations (i.e., no rapid speed changes), constant speed at cruising, and reduced number of cold starts (by combining several shorter trips into one longer trip).

4. A RECOMMENDING SOLUTION TO DECREASE VEHICLE'S EMISSIONS

We first make the assumption that the intersection is equipped with intelligent traffic lights (ITLs), which are semaphores equipped with sensors and wireless communication capabilities – a concept proposed in (Gradinescu et al. 2007). ITLs can send information to approaching vehicles, to servers, to other traffic lights. In this paper we extend the original ITL approach, and propose a system that uses them to minimize pollution and assist the driver find the optimum cruising speed as he/she approaches the intersection. We consider that messages are constantly exchanged between ITL and vehicles, and also between vehicles. We assume that ITLs and the vehicles are equipped with short range communication devices and computing capabilities. The ITL periodically broadcasts data about the color and the time until it changes, for each segment of road it controls. The broadcasted package contains in addition the local time, which is used for synchronization. The problem of short range communication is resolved by letting cars re-broadcast further all received messages for a limited time period.

The vehicle uses the received information as input for an algorithm that outputs a recommendation speed that optimizes the quantity of car's emissions. To run the algorithm cars are equipped with computational devices. The algorithm is based on the computation of speed, movement, as well as fuel consumption.

4.1. Computing fuel consumption

First we developed a solution to estimate fuel consumption and pollutant emissions. To model fuel consumption and emissions (CO2, CO, HC, NOx), we extended the work of Akcelik and Besley (2003). The qualities of their model are better reflected by the extensive study conducted in (Dia et al. 2007). The method to estimate the value of fuel consumed (mL) or emissions produced (g), in a time interval (Δ_t), is given by:

$$\Delta F = \left(f_i + \beta_1 R_T v + \left[\frac{\beta_2 M_v a^2 v}{1000} \right]_{a>0} \right) \Delta t \quad , \quad R_T > 0 \tag{10}$$

$$\Delta F = f_i \Delta t \ , \ R_T \le 0 \tag{11}$$

where ΔF [mL or g] is the quantity consumed or gas emitted during a time interval, v [m/s] is the vehicle's instantaneous velocity, a [m/s2] the acceleration, M_V [kg] is the mass of the vehicle (1400 kg on average for light vehicles in a city environment), and R_T [kN] represents total force acting on a car, including air drag and rolling resistance. For the values of f_i, β_1, and β_2 we used the results from (Akcelik and Besley, 2003). Figure 2 presents results for fuel consumption for vehicles passing through an intersection.

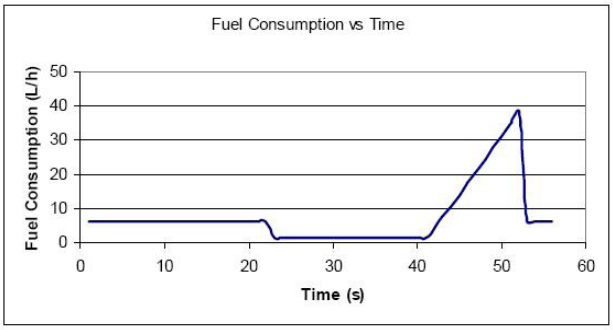

Figure 2. Fuel consumption for vehicles passing through an intersection.

4.2. The decision algorithm

In order to determine the optimal speed when approaching an intersection, we consider that cars are equipped with computational devices. Various experts, in fact, predict this will be a reality on a general-scale in the near future (CARS, 2010). In this section we present the algorithm that runs on the computational device inside a car.

a. Car Movement Prediction

The most important part of the algorithm is the prediction of the movement of the car on a given distance, or in a given amount of time. To make an accurate decision, the algorithm needs to estimate with relatively high precision the future speed and position of the car. For that we use parameters such as the delay to reach a certain speed, the acceleration style of the driver, the characteristics of the road (curves, slopes). The implementation of this part of the algorithm (the content of "*updateSpeedAndLocation*" method in Table 1) is based on the equations for the car's motion previously presented, which consider the forces that act on the car.

b. Green Lights

When the car approaching the intersection is informed that the current traffic light color is green, the device inside the car executes the following algorithm. We consider two scenarios: (1) the driver accelerates to catch the green light, and (2) the driver slowly decelerated to stop at the red light. The first case may not be possible (considering the car's characteristics, the acceleration has an upper limit). If possible, the algorithm will estimate the quantity of emissions for both two cases. If the quantity of gases is smaller in the first case than in the second, it will recommend the accelerating speed to the driver. Otherwise, it will recommend a full stop at the red light.

The application starts by first predicting the movement of the car when we assume the driver will try to catch the green light (case 1). In this case the driver's intention is to

accelerate until the speed he/she anticipates is needed to catch the green light. The pseudocode for this algorithm is:

Algorithm 1. The algorithm for Green Light, case 1.

```
1: car.distance ← 0 // the total distance traveled by the car
2: car.time ←0 // the total time the car traveled
3: timeIncrement ← 0:06 // the time increment to apply runge-kutta
4: car.setMode("accelerate") // the driver accelerates
5: while car.distance < distanceToTrafficLight do
6:     neededSpeed ← (distanceToTrafficLight – car.distance) ÷ (greenTime – car.time)
7:     if neededSpeed > MaxSpeedAllowed then
8:         return // the driver cannot catch the green light
9:     end if
10:    if neededSpeed <= car.speed then
11:        car.setMode("cruise")
12:    end if
13:    car.updateSpeedAndLocation(timeIncrement)
       // this updates car.time, car.speed and car.distance
14:    car.estimateEmissions()
15: end while
```

The application further estimates the emissions of the car, assuming the driver maintains a constant speed, stops at the red color, then accelerates to the speed he/she previously had before stopping (case 2). The pseudocode for this algorithm is:

Algorithm 2. The algorithm for Green Light, case 2.

```
1: car.distance ← 0 // the total distance traveled by the car
2: car.time ← 0 // the total time the car traveled
3: timeIncrement ← 0:06 {the time increment to apply runge-kutta}
4: car.setMode("cruise") // the driver maintains a constant speed
5: while car.distance < distanceToTrafficLight - 100 do
6:     // assume the driver starts to break 100m before the intersection
7:     car.updateSpeedAndLocation(timeIncrement)
8:     car.estimateEmissions()
9: end while
10: car.setMode("break") // the driver breaks to stop at the red light
11: while car.distance < distanceToTrafficLight do
12:     car.updateSpeedAndLocation(timeIncrement)
13:     car.estimateEmissions()
14: end while
15: car.setMode("accelerate") // the driver accelerates to the speed he had before stopping
16: while car.speed < WantedSpeed do
17:     car.updateSpeedAndLocation(timeIncrement)
18:     car.estimateEmissions()
19: end while
```

In the end the application compares the results obtained in these two cases and recommends a speed to the driver that will lead to the least fuel consumption.

c. Red Lights

When the car approaches an intersection and is informed that the current color of the traffic light is red, it executes an algorithm that decides to (1) reduce the speed to enter the intersection when the light color is turning green, or (2) continue to a full stop using the same constant speed. The decision depends on the smaller quantity of emissions when comparing the estimated for these two cases. Again, the algorithm involves two steps.

First the application runs an algorithm to predict the movement of the car, assuming the driver reduces the speed in an attempt to avoid the red light – by the time he/she would reach the intersection the current light will have changed to green in this approach. In this case the algorithm estimate the quantity of emissions. The pseudocode for this case is:

Algorithm 3. The algorithm for Red Light, case 1.

```
1: car.distance ← 0 // the total distance traveled by the car
2: car.time ← 0 // the total time the car traveled
3: timeIncrement ← 0:06 // the time increment to apply runge-kutta
4: car.setMode("accelerate") // the driver accelerates
5: while car.distance < distanceToTrafficLight do
6:     neededSpeed ← (distanceToTrafficLight  - car.distance) ÷ (redTime – car.time)
7:     if neededSpeed < MinSpeedAllowed then
8:         return // the driver cannot avoid stopping at the red light
9:     end if
10:    if neededSpeed >= car.speed then
11:        car.setMode("cruise")
12:    end if
13:    car.updateSpeedAndLocation(timeIncrement)
       // this updates car.time, car.speed and car.distance
14:    car.estimateEmissions()
15: end while
```

Next, it runs an algorithm to predict the movement of the car, assuming the driver maintains constant speed, stops at the red color, then when the color changes he/she accelerates to the speed needed to catch the green light (and possible avoid a new change to red light). The pseudocode for this case is:

Algorithm 4. The algorithm for Red Light, case 2.

```
1:  car.distance ← 0 // the total distance traveled by the car
2:  car.time ← 0 // the total time the car traveled
3:  timeIncrement ← 0:06 // the time increment to apply runge-kuttag
4:  car.setMode("cruise") // the driver maintains a constant speed
5:  while car.distance < distanceToTrafficLight - 100 do
6:      // assume the driver starts to break 100m before the intersection
7:      car.updateSpeedAndLocation(timeIncrement)
8:      car.estimateEmissions()
9:  end while
10: car.setMode("break") // the driver breaks to stop at the red light
11: while car.distance < distanceToTrafficLight do
12:     car.updateSpeedAndLocation(timeIncrement)
13:     car.estimateEmissions()
14: end while
15: car.setMode("accelerate")
    // the driver accelerates to the speed he had before stoppingg
16: while car.speed < NeededSpeed do
17:     car.updateSpeedAndLocation(timeIncrement)
18:     car.estimateEmissions()
19: end while
```

In the end the application compares the results obtained in these two scenarios and recommends the optimal speed to the driver, depending on the least fuel consumption.

5. RESULTS

The evaluation in terms of the environmental impact of the proposed solution was done using modeling and simulation. This cost-effective method of evaluation required us to model at least four components: vehicular traffic, communication from traffic lights to vehicles, driver behavior (speed adaption) and finally fuel consumption and emissions. These and other components were integrated into VNSim (Gradinescu et al. 2007), a VANET simulator which is able to model complex traffic conditions, with real-world mobility assumptions and state-of-the-art networking protocols (Gainaru et al. 2009). Its extensibility allowed us to implement the models for the estimate of fuel consumption and pollutant emissions proposed in the current work.

We were first interested in how acceleration relates to pollutant emissions. These experiments were conducted as a calibration stage, to verify that the simulation model corresponds in known-cases to the expected mathematical results (Section 3). In these experiments we considered the case of an average car - the entry values for these experiments followed the analysis of Smith&Cloke (1999).

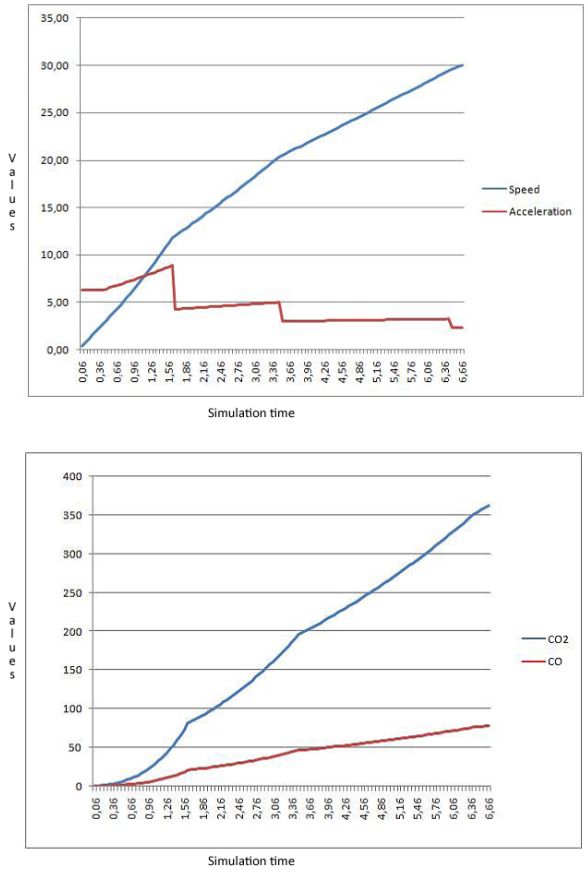

Figure 3. The case of a car that accelerates from 0 km/h to 108 km/h.

We conducted two experiments that evaluate the fuel consumption for the typical driver behaviors. In the first experiment the driver keeps accelerating until the car reaches 30 m/s (or 108 km/h). This speed was chosen based on the theoretical estimated Haworth and Symmons model and ECE 15-04 regulations (a car would not cruise with a higher speed in an urban area – official regulations limit speeds in such situations to much lower values). Figure 3 shows how speed and acceleration change in time. In the second scenario, the driver accelerates until the car reaches 15.22 m/s (or 54.8 km/h, a speed which is more acceptable for urban areas) and then he/she maintains a constant speed (see Figure 4).

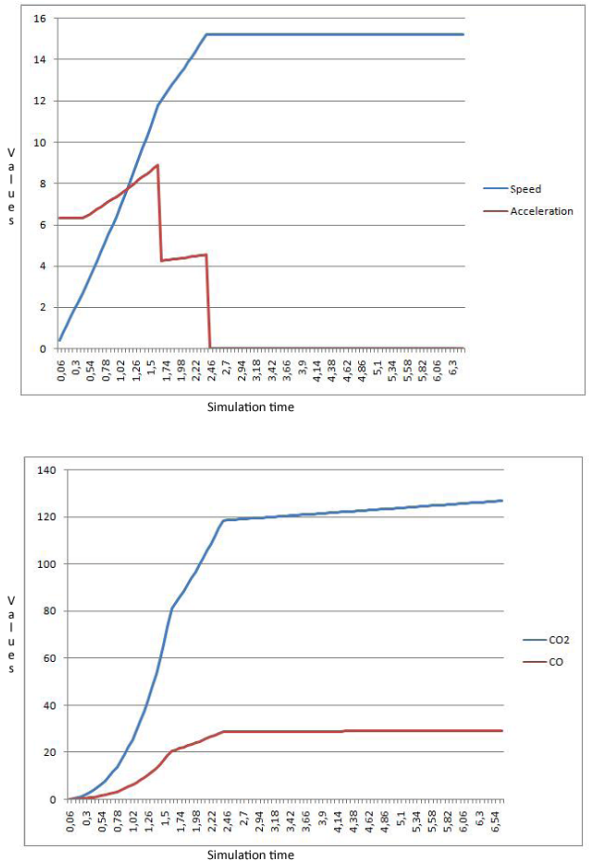

Figure 4. A car that accelerates from 0 km/h to 54.8 km/h and then maintains a constant speed.

Looking at the acceleration curves in Figures 3 and 4, two observations can be made: 1) the very steep slopes (three in Figure 3 and two in 4) are due to gear shifting and 2) acceleration is decreasing in time, due to the gear ratio (and this concurs to the mathematical estimations previously presented, and the increasing drag force). The quantity (in grams) of emitted CO2 and CO in the first scenario is shown in Figure 3 and the results of the second scenario can be visualized in Figure 4 (in which the car traveled for the same amount of time as the one in the first scenario). Comparing the results of the two scenarios, it can be noticed that the quantity of gases emitted by the car in the second scenario ($\approx$ 129g of CO2), is smaller than the one obtained in the first scenario ($\approx$ 360g of CO2). Based on the slope of the emissions curve in Figure 4, we can compute the total distance the car can travel until its emissions reach the ones in Figure 3.

5.1. Case 1 – Green light

We next experimented with the proposed algorithms. We started with the case of the green traffic light. The

algorithm has been used in two relatively different scenarios.

In the first scenario, a car traveling at 40 km/h (~11 m/s) has 15 seconds to catch the green light. This corresponds to the case when a car cruising at a relatively high speed in town approaches the intersection. Also, to avoid potentially dangerous situations, the driver has sufficient time to cross the intersection. The distance between the traffic light and the car is 200 m. According to the proposed algorithm, the car predicts the speed and acceleration of the car until it crosses the intersection, and it estimates the quantity of emissions in the two possible scenarios: 1) the driver tries to catch the green light and accelerates until the needed speed is reached and 2) the driver maintains a constant speed, stops and waits at the red light, and then he/she accelerates until the previous speed is obtained. The quantity of emissions in the first situation was ~54 grams of CO2, and in the second situation ~96 grams of CO2. Based on these results, the system advises the driver to accelerate to catch the green light. By doing this, the driver could reduce the quantity of CO2 by approximately 42 grams (going at high speed, but this higher limit depends on the maximum speed imposed by legislation in that particular location).

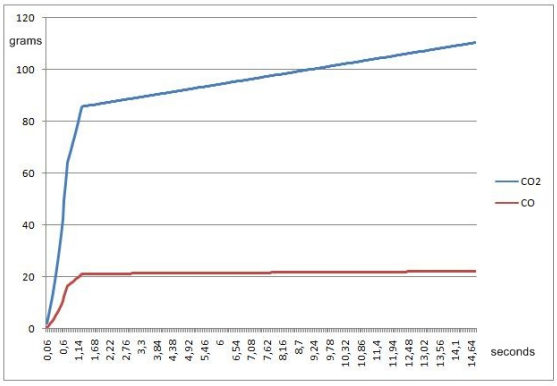

Figure 5. Quantity of emissions in scenario 2, situation 1.

In the second experiment, the same car, now traveling at 22km/h (~6 m/s), has to catch the green light, given the same conditions as in the previous scenario. This corresponds to a slower car approaching the same intersection. As before, the algorithm predicts the speed and acceleration of the car until it passes the intersection, and it estimates the quantity of emissions in the two scenarios previously described. The estimated quantities of emissions are presented in Figure 5 (~110 grams of CO2 emitted). Based on these results the system advises the driver not to accelerate, in the attempt to catch the green light. If the driver complies with this suggestion, he/she would reduce the quantity of CO2 by ~52 grams.

5.2. Case 2 – Red light

This section presents the experimental results obtained with the use of the proposed algorithms applied in case of red traffic light. Again we experimented with two situations.

In the first case, a car traveling at 60 km/h (~16.6 m/s) approaches a traffic light showing a red color, which will change after 20 seconds. This corresponds to a high-speed car approaching the intersection. Again, the distance between the traffic light and the car is 200 m. The algorithm predicts the speed and acceleration of the car until it passes the intersection, and it estimates the quantity of emissions in two possible situations: 1) the driver tries to reduce the speed to avoid the red color and 2) the driver maintains a constant speed, stops waits at the red light, and when the color changes back to green accelerates until the speed needed to avoid the next change to red color is obtained. In the first case the estimated quantity of emissions was ~28 grams of CO2. For the second case ~75 grams of CO2 were emitted. Based on these results, the system advises the driver to reduce the speed until he/she reaches approximately the speed of 34 km/h (~9.47 m/s), such that to avoid waiting at the red light color. By doing this, the driver reduces the quantity of CO2 by ~47 grams.

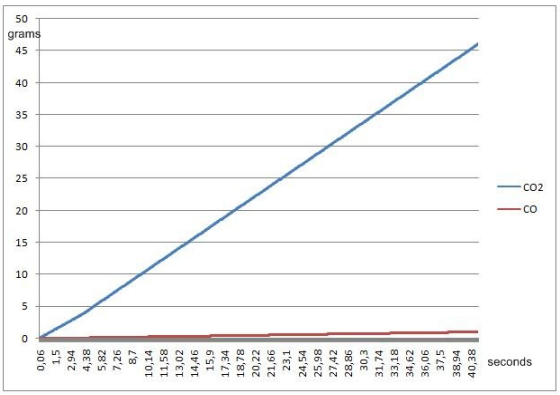

Figure 6. Quantity of emissions in scenario 2, situation 2.

In the second scenario, the same car, traveling at the same speed (60km/h), approaches a red traffic light color which, this time, will last for the next 40 seconds. As before, the algorithm predicts the speed and acceleration of the car until it passes the intersection and estimates the quantity of emissions in the two cases described earlier. The estimated quantities of emissions was ~46 grams of CO2 (first case), and, respectively, ~37 grams of CO2 (second case, see Figure 6). Based on these results the system advises the driver not to reduce the speed, in an attempt to avoid the red light. If the driver complies with this recommendation, he/she will reduce the quantity of CO2 by ~9 grams.

The obtained results show good progress towards decreasing the amount of fuel being consumed. The scenarios consider several parameters which might change depending on the local legislation, characteristics of cars, etc. However, in the different considered scenarios we showed that our recommendations can lead to significant changes in the fuel consumption, with positive results on the environment on the long term.

6. CONCLUSIONS

In this we presented a solution that uses intelligent traffic lights, mobile devices and wireless communication to

reduce car emissions. The solution minimizes the number of stop-starts due to the red light and the accelerations needed to catch the green light (happening quite frequent and having an important influence on the emissions rate). Periodically the traffic lights broadcast information about the status of the current traffic light color. This information is used by a decision algorithm. The role of this algorithm is to assist the driver make informed decisions to 1) avoid the red traffic light and 2) catch the green traffic light, if possible, and reduce the quantity of emitted gases.

In order to decide whether the driver's action of catching the green light leads to less fuel consumption, by recommending accelerate/decelerate, we devised a method to predict the car's movement. For this we use the motion equation of a car to predict its speed and position at any time. The prediction of the movement of the car is among the most challenging part. To estimate a specific driver's behavior and predict how the car is going to move in different situations is a difficult task, because of the number of parameters to be considered: all forces that act on the car, coupled with the human factor. In the end we proposed a solution that was evaluated in an implementation on top of the VNSim simulator. The obtained results are promising and show that the proposed algorithm can recommend speeds that, in fact, lead to a decrease in the emissions of a car.

In the future we plan to further optimize the models and the solution, mainly because of several simplifications made in this current version. They are due mainly to the lack of information: in determining the motion equation, just the x-axis was considered. The weather was also ignored (this means that the slopes and the curves of the roads were ignored - 3D maps are needed to obtain complete information about the roads).

ACKNOWLEDGEMENT

The research presented in this paper is supported by national project: "TRANSYS – Models and Techniques for Traffic Optimizing in Urban Environments", Contract No. 4/28.07.2010, Project CNCSIS-PN-II-RU-PD ID: 238. The work has been co-funded by national project: "SORMSYS - Resource Management Optimization in Self-Organizing Large Scale Distributes Systems", Contract No. 5/28.07.2010, Project CNCSIS-PN-II-RU-PD ID: 201, and by the Sectoral Operational Programme Human Resources Development 2007-2013 of the Romanian Ministry of Labour, Family and Social Protection through the Financial Agreement POSDRU/89/1.5/S/62557.

REFERENCES

CARS 21. "Automotive. Competitive Automotive Regulatory System for the 21st century", October 2010, http://ec.europa.eu/enterprise/sectors/automotive/competitiveness-cars21/cars21/, accessed 14.02.2012.

Gradinescu, V.; C. Gorgorin; R. Diaconescu; V. Cristea; and L. Iftode. Adaptive traffic lights using car-to-car communication, *Proc. of the IEEE 65th Vehicular Technology Conference* (VTC2007-Spring), IEEE Computer Society Press, pp. 21–25, 2007.

Haworth, N.; and M. Symmons. 2001 "Driving to reduce fuel consumption and improve road safety", *Proc. Road Safety Research, Policing and Education Conference*, Melbourne.

Akcelik, R.; and M. Besley. 2003 "Operating cost, fuel consumption, and emission models in aasidra and aamotion", *Proc. of 25th Conference of Australian Institutes of Transport Research*, University of South Australia, Adelaide, Australia.

Smith, L.; and J. Cloke. 1999 "Reducing the environmental impact of driving: Effectiveness of driver trening", *Proc. of EcoDrive Conference*, Graz, Austria, pp.48-55.

Andre, M.; and U. Hammarstrom. 2000 "Driving speeds in Europe for pollutant emissions estimation", *Transportation Research Part D*, 5, pp. 321-335.

Dia, H.; S. Panwai; N. Boongrapue; T. Ton; and N. Smith. 2006 "Comparative Evaluation of Power-Based Environmental Emissions Models", *Proc. of IEEE Intelligent Transportation Systems Conference*, Toronto, Canada, pp. 1251-1256.

Sovacool, B. K. 2010 "A transition to plug-in hybrid electric vehicles (PHEVs): why public health professionals must care", *J. Epidemiol Community Health*, 64:185-187.

Gainaru, A.; C. Dobre; and V. Cristea. 2009 "A Realistic Mobility Model based on Social Networks for the Simulation of VANETs", *Proc. of the 2009 IEEE 69th Vehicular Technology Conference* (VTC2009-Spring), Barcelona, Spain, pp. 1-5.

Tielert, T.; M. Killat; H. Hartenstein; and R. Luz. 2010 "The impact of traffic-light-to-vehicle communication on fuel consumption and emissions", *Proc. of the 2010 Internet of Things (IOT)*, Tokyo, Japan, pp. 1-8.

Alsabaan, M.; K. Naik; T. Khalifa; and A. Nayak. 2010 "Vehicular networks for reduction of fuel consumption and CO2 emission", *Proc. of the 8th IEEE International Conference on Industrial Informatics (INDIN)*, Osaka, pp. 671-676.

Wegener, A.; H. Hellbruck; C. Wewetzer; and A. Lubke. 2008 "VANET simulation environment with feedback loop and its application to traffic light assistance", *Proc. of the 2008 IEEE GLOBECOM Workshops*, New Orleans, LO, pp. 1-7.

Sanchez, M.; J. Cano; and D. Kim. 2006 "Predicting traffic lights to improve urban traffic fuel consumption", *Proc. of the 2006 6th International Conference on ITS Telecommunications Proceedings*, Chengdu, pp. 331-336.

Asadi B.; and A. Vahidi. 2010 "Predictive cruise control: Utilizing upcoming traffic signal information for improving fuel economy and reducing trip time", *IEEE Transactions on Control Systems Technology*, Issue 3, pp. 707-714.

Richter, A. "Geschwindigkeitsvorgabe an Lichtsignalanlagen". *Deutscher Universitatsverlag*, 2005.

Kuroyanagi, Y.; C. Miyajima; N. Kitaoka; and K. Takeda. 2011 "Analysis and Detection of Potentially Hazardous Driving Situations", *ICIC Express Letters, Part B: Applications*, vol. 2, issue 3, pp. 621-626.

AUTHOR BIOGRAPHIES

Dr. Ciprian DOBRE (corresponding author) received his PhD in Computer Science at the University POLITEHNICA of Bucharest in 2008. His main research interests are Modeling and Simulation, Grid Computing, Monitoring and Control of Distributed Systems, Advanced Networking Architectures, Parallel and Distributed Algorithms. His research activities were awarded with the Innovations in Networking Award for Experimental Applications in 2008 by the Corporation for Education Network Initiatives (CENIC).

A CHECKPOINT BASED MESSAGE FORWARDING APPROACH FOR OPPORTUNISTIC COMMUNICATION

Osman Khalid
North Dakota State University
Fargo, ND 58108, USA
osman.khalid@ndsu.edu
North Dakota State University

Samee U. Khan
North Dakota State University
Fargo, ND 58108, USA
samee.khan@ndsu.edu
North Dakota State University

Joanna Kolodziej
Cracow University of
Technology, Cracow, Poland
jkolodziej@uck.pk.edu.pl

Limin Zhang
North Dakota State University
Fargo, ND 58108, USA
limin.zhang@ndsu.edu
North Dakota State University

Juan Li
North Dakota State University
Fargo, ND 58108, USA
j.li@ndsu.edu
North Dakota State University

Khizar Hayat
COMSATS Institute of
Information Technology,
Abbottabad 22060, Pakistan.
khizarhayat@ciit.net.pk

Sajjad A. Madani
COMSATS Institute of
Information Technology,
Abbottabad 22060, Pakistan.
madani@ciit.net.pk

Lizhe Wang
Chinese Academy of Sciences
Beijing, China
lzwang@ceode.ac.cn

Dan Chen
China University of Geosciences
Wuhan, China
Danjj43@gmail.com

KEYWORDS
Mobility, Routing, DTN.

ABSTRACT

In a Delay Tolerant Network (DTN), the nodes have intermittent connectivity and complete path(s) between the source and destination may not exist. The communication takes place opportunistically when any two nodes enter the effective range. One of the major challenges in DTNs is message forwarding when a sender must select a best neighbor that has the highest probability of forwarding the message to the actual destination. However, finding an appropriate route remains an NP-hard problem. This paper presents a concept of Checkpoint (CP) based message forwarding in DTNs. The CPs are autonomous high-end wireless devices with large buffer storage and are responsible for temporarily storing the messages to be forwarded. The CPs are deployed at various places within the city parameter that are covered by bus routes and where human meeting frequencies are higher. For the simulative analysis a synthetic human mobility model in ONE simulator is constructed for the city of Fargo, ND, USA. The model is tested over various DTN routing protocols and the results indicate that using CP overlay over the existing DTN architecture significantly decreases message delivery time as well as buffer usage.

INTRODUCTION

Delay Tolerant Networks (DTNs) are designed to provide delay tolerant communication when there are no end-to-end paths among the nodes and when the network topology changes continuously. The communication of messages takes place in DTNs whenever the nodes opportunistically make contact. Therefore, a node may have to store the messages and wait until the next node is close enough to start the transfer and eventually the message is delivered to the final destination. Due to the lack of end to end connectivity and dynamic topology, the traditional ad hoc routing protocols such as AODV (Johnson and Maltz 1996) and DSR (Perkins and Royer 1999) cannot be applied to DTNs. Therefore, significant research (e.g., Khan *et al.* 2011; Burgess *et al*. 2006; Shinya *et al*. 2011) is carried out in designing routing protocols for DTNs that must tackle unpredictable network environments. Generally, the message forwarding in DTNs is classified as: (a) uninformed and (b) informed forwarding.

In the uninformed approach, nodes do not utilize any existing knowledge and forward messages to neighbors in range, until the messages are finally delivered to their destinations. The aforementioned knowledge can be a meeting probability, mobility pattern, and current direction. To increase message delivery ratio, the nodes in uninformed approach generate and spread the multiple copies of messages. Among popular algorithms, two such techniques are *Epidemic Routing* (Vahdat and Becker 2000) and *Spray and Wait* (Thrasyvoulos *et al*. 2005). As, the uninformed approach uses flooding to propagate maximum messages, the advantage is the higher probability of successful message delivery to destination. A major drawback of uninformed approach is the higher consumption of network resources and buffer. Moreover, there is no guarantee that flooding the network will have messages delivered to the destination.

The nodes in the informed forwarding approach use previous knowledge and heuristics to select suitable nodes to which messages are forwarded for delivering to the destination. The idea is to decrease the number of message flooding in the network, while maintaining an acceptable level of message delivery ratio. Certain

Proceedings 26th European Conference on Modelling and Simulation ©ECMS Klaus G. Troitzsch, Michael Möhring, Ulf Lotzmann (Editors)
ISBN: 978-0-9564944-4-3 / ISBN: 978-0-9564944-5-0 (CD)

parameters may be utilized to make an optimal selection of candidate nodes. Some of the parameters are, but not limited to, node's history of encounters e.g. *PRoPHET* (Lindgren *et al*. 2003), *MaxProp* (Burgess *et al*. 2006), *MV* (Burns *et al*. 2005), mobility pattern (Cacciapuoti, *et al*. 2012; Leguay *et al*. 2005) and frequency of visiting certain places (Ghosh *et al*. 2006), *Message Ferrying* (Zhao *et al*. 2004), and *Data Mules* (Almasaeid and Kamal 2008). All of the aforementioned protocols make use of some kind of available knowledge to improve overall message delivery ratio. However, there is a tradeoff between the improved message delivery and higher consumption of network resources. To make a good choice in selection of forwarding node, a node has to store information of various parameters about other nodes. For example, in (Lindgren *et al*. 2003) each node maintains a history of contacts with all other nodes in the area. When a node encounters more than one node simultaneously, only the node that has maximum number of contacts would be selected for message forwarding. In limited scenarios, the aforementioned protocol(s) may show higher performance. However, in the real-life large scale networks, with the nodes having limited buffer and processing capabilities, the performance of DTN routing protocols may degrade significantly with increasing nodes.

This paper presents an idea of CP based message forwarding approach. Apart from having own memory and processing capabilities, each CP is a node that represents a specific region on the city map and may maintain the information of geographic locations of all the other CPs. However, in contrast to the existing work, the CPs are not communication dependent on any fixed backbone network, and can be easily relocated. The simulation results indicate that the use of CPs reduce the processing overhead and buffer utilization in predicting the locations of the destination nodes in DTNs.

The rest of the paper is organized as follows. First, related work is described with a comparison to the CP approach. Next, the CP architecture is discussed along with simulation scenario. Finally, the simulation results are discussed with conclusion and future work.

RELATED WORK

For many years human mobility has been an active area of research in DTNs. It has been shown through various experiments that human populations follow repeated mobility patterns. Different methods have been applied to collect the human mobility traces. For example (Rhee *et al*. 2011) studied the urban human mobility through GPS traces. The authors in (Cacciapuoti, *et al*. 2012) used the signaling information in cell phones through the AirSage (www.airsage.com) technology to gather the mobility traces, and (Balazinska and Castro 2003) used PDAs and laptops interacting with access points at various locations in an office building to observe the mobility pattern. All the previous studies reveal that humans tend to follow a repetitive schedule of meetings at same places and times, and the human mobility is predictable following a power law distribution. The aforementioned fact is further endorsed by (Song *et al*. 2010) that human mobility is 93% predictable.

Therefore, CP based approach presented in this paper is inspired by the same fact that humans tend to follow schedule of meetings with higher interaction probabilities at commonly visited places such as bus stops/stations and shopping malls where the CPs may be deployed. The aforementioned technique may shift the buffer overheads from nodes to CPs in making the predictions about the destination node's location and next meeting times. In the DTNs context, an approach that involves some sort of location information is categorized as *location-based routing.*

In the past, various techniques have been presented for location-based routing in DTNs. The authors of *MV* (Meeting and Visits) (Burns *et al*. 2005) proposed a message exchange mechanism in pairwise contacts among peers that depends on the history of previous encounters and the visits of nodes to particular geographic locations. *MV* assumes that peers have infinite buffer space. In (Zhao *et al*. 2006), the authors presented algorithms for optimal deployment of *Throw Boxes* that are stationary wireless nodes to relay the messages among the mobile nodes. However, in this paper, we deploy the checkpoints on a real city map to determine the effect of human mobility in DTN based message forwarding. Similarly, Virtual Segment (VS) by (Shinya *et al*. 2011) and TACO-DTN by (Sollazzo *et al*. 2007) are similar techniques that have access points connected with the fixed backbone network installed at various geographic locations and the interconnectivity among the access points is provided through mobile nodes. The aforementioned approach is dissimilar to CP approach presented here as there is no mandatory physical connection of CPs with backbone network and CPs can be easily relocated (e.g. in disaster situations). However, the CPs may be connected with backbone to act as hotspots for Internet. In the next section we discuss the CP architecture.

CHECKPOINT ARCHITECTURE

The major components of the CP architecture include static CP nodes, mobile wireless nodes, buses, and additional components (e.g. Internet connected Access Points) that may be integrated with CP architecture.

CP Nodes

A CP is a wireless node that can be any low cost custom design hardware. The basic components of a CP node are but not limited to processor, memory, solar powered batteries, multiple interfaces (Standard Ethernet, 802.11b/g/n, Bluetooth), GPS, and storage. Each CP may optionally have the record of GPS coordinates of

other CPs in the area. The coordinates are relayed through mobile nodes to the neighboring CPs along with normal data packets. Moreover, we assume that the CPs can be reconfigured with various DTN routing protocols. For example, if routing protocol used by CP is *PRoPHET*, then the CP maintains a database of recent encounters with mobile nodes for certain amount of time *T* after which the old data is overwritten to make space for new records. In addition to message routing, other tasks that may be assigned to CP include content distribution at specific intervals such as travel information, promos, news and information caching. The main fields maintained in the database of each $Checkpoint_i$ are indicated in Table-1.

Table 1: Database fields for a $Checkpoint_i$

Node ID	The ID of a mobile node N_i
Number of contacts	The number of contacts a node made with $Checkpoint_i$
CP ID	CP with which the node made contacts. Here multiple entries are possible. Because, a node may make contacts with more than one CP.
Coordinates	The GPS coordinates of a CP last contacted by a node. This helps in synchronization of location information of CPs throughout the region.
Last Contact Time	Time of last contact with $Checkpoint_i$
Expected Contact Time	This time is predicted based on the node's history of contacts.

Mobile Nodes

The mobile nodes are pedestrians, cars, and buses with each node carrying 802.11b/g/n enabled wireless sets. This assumption makes sense due to a market research report (Technical Report 2009) according to which in year 2009 alone, a total of 144 million mobile phones were shipped with Wi-Fi capability and it is further estimated that such phones may reach 66% of the total shipments till 2015 (Technical Report 2010). In the CP approach, whenever a mobile node interacts with a CP, the mobile node shares database with the CP by sending a light weight summary vector and then the CP updates own database with new information about the node. Any two mobile nodes on encounter, exchange messages for storing, carrying, and forwarding, as well as the metadata of each node's visits to particular CPs. The minimum data structure required at each mobile node is reflected in Table-2.

Table 2: Database fields for a $MobileNode_i$

CPs	The IDs and coordinates of every CP a node has visited in past.
Number of Contacts	The number of contacts a node has made with each $Checkpoint_i$
Last Contact Time	Time of last contact with $Checkpoint_i$

Buses

Buses are the message carriers or relay nodes in CP architecture. Each bus follows a fixed route and schedule and may pass through more than one CP (bus stop) on predefined timings. Moreover, after every scheduled round, every bus returns to a central bus station. The buses may be installed with any custom made wireless hardware having communication and storage ability to store the received messages to be delivered to the destination CPs.

Message

The minimum fields a message may have are source address, destination address, destination CP address, and payload. To find the destination CP address, an online Google based custom map for CPs may be consulted that indicates the specific CPs deployed near a particular geographic location. The aforementioned map can be constructed temporally with the passage of time if the CPs relay their GPS coordinates along with the actual message.

Message Routing

The message forwarding in the presented approach depends on the DTN routing protocol the CP is configured with. If a CP utilizes encounter based routing, then source node uses mobility pattern and schedules of buses, to forward the packet to a CP that is located closer to the destination. As shown in Figure 1, there are four regions A, B, C, and X, each covered by a CP. Buses relay messages between any two regions and each bus also visits a central bus station denoted by X. The time of arrival and departure of buses is predefined. If a source node is within the communication range of CP, the node forwards a single copy of message to CP, to be relayed by bus nodes.

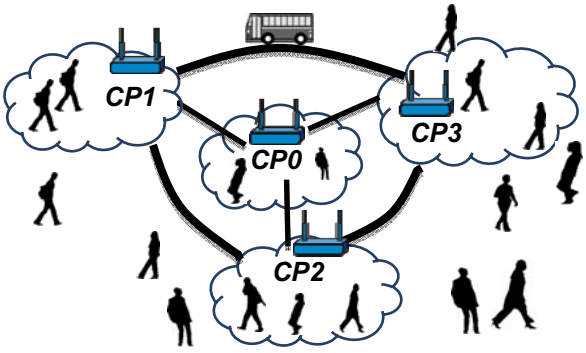

Figure 1: CP architecture with CPs connected through bus nodes.

However, if the source node is outside the communication range of CP, then the source node opportunistically forwards the packets to the neighboring nodes in an attempt to allow at least one copy of message to reach the nearest CP or to the final destination. The aforementioned message forwarding can be accomplished by utilizing any resource efficient

replication based DTN protocol (e.g. *Spray and Wait*). The message copy is stored in a CP until the message is relayed to the next mobile node such as pedestrian, car, or bus. As the CPs are deployed on places where human mobility is higher, this increases the chance of message delivery to the destination. However, if CPs are deployed randomly (e.g. in case of post disaster scenario), then the GPS coordinates may be utilized in the calculation of minimum length routes among the source and destination CPs. There might be the case that a packet's destination information is not present in a CPs database. In that case, the destination is searched on the other CPs until the message TTL expires or all the CPs are searched.

SIMULATION

The simulation tool selected for the evaluation of the proposed CP model is ONE simulator (Keränen *et al.* 2009) which has rich features available for simulating DTNs with numerous mobility models. The map of Fargo city is exported from www.openstreetmap.org. Using open source GIS tool OPENJUMP, the map is post-processed and marked with various locations such as shops, homes, offices, meeting points, NDSU, and GTC bus station. Mobile nodes are divided into several groups and assigned to various locations on the map.

Scenario

For simulation, an area of 4 x 3 KM of the city of Fargo, ND, USA is selected as indicated in Figure 2. The buses are tagged with route numbers and follow various schedules available on the Metro Area Transit website (www.matbus.com). Each bus route has stops at various locations. At some of the stops the CPs are deployed, each identified with an ID and representing a geographic location within 100 meters radius. *CP5* is located in the central bus station where each route bus arrives or departs from. Two main shopping locations (West Acres and Walmart) are covered by *CP9* and *CP10* through which route 15 bus runs. Moreover, *CP1, CP2,* and *CP3* are installed at junctions that are not covered by any bus route and the messages are relayed among the CPs with the help of public automobiles. The human mobile nodes are Wi-Fi/Bluetooth devices that are distributed throughout the simulation area. As an example of the current scenario, if *CP4* receives a message to be relayed, *CP4* stores the message and waits for route 13 bus to arrive. On arrival, bus 13 relays the message to the central bus station where the message is received by *CP5*. *CP5* checks the message destination in database and routes the message to the final destination's CP. If no such entry is found, the message is routed to all the CPs after setting a TTL, on expiry of which, the message is deleted if not delivered (depending on the routing protocol).

Simulation Parameters

For the simulation, various combinations of parameters with range of values are selected. The simulation world is Fargo city map. Table 3 indicates the selected simulation parameters.

Table 3: Simulation parameters used in ONE.

Parameter	Value
World size	4250, 3900 m
Simulation time per run	43200s == 12h
Bluetooth Interface transmit rate	250kbps
Bluetooth interface transmit range	10 m
High speed interface type	Broadcast Interface
High speed interface transmit speed	10Mbps
High speed interface range	100 m
Total number of node groups in the scenario	21
Nodes mobility model	Map based movement
Car / pedestrians nodes buffer size	250Mb
Car / pedestrians wait times	0, 120 s
Car / pedestrians speed range	0.5 to 1.5 m/s
Car / pedestrian node interface	Bluetooth
Message TTL	300 min
Bus nodes buffer size	500Mb
Bus nodes wait time	10, 30 s
Bus nodes speed	7, 10 m/s
Bus nodes interfaces	Bluetooth and High speed
Cars nodes speed range	2.7, 13.9 m/s
Total Checkpoints	11
Checkpoints buffer size	500Mb
Checkpoints interfaces	Bluetooth and High speed
Events interval	45, 55 s
Message size range	500KB – 1MB
Total message generating nodes	78
Warm up period	1000 s

RESULTS

To perform model evaluation, a series of simulations have been performed in ONE Simulator. A single simulation time is 12 hours (43200s). The warm-up period is 1000s that is required for each CP and mobile node to have sufficient information in database. The CP architecture is evaluated for: (a) message delivery ratio, (b) buffer utilization, and (c) average message delay. The number of messages, CPs, buses, mobility pattern, nodes speed, transmission range, number of messages, and buffer sizes are altered in each simulation run to analyze the effect on average message delivery ratio, buffer utilization, and delivery delay.

Effect of CP deployment on average delay and message delivery ratio

One of the most important and challenging task is the selection of ideal places for the deployment of CPs.

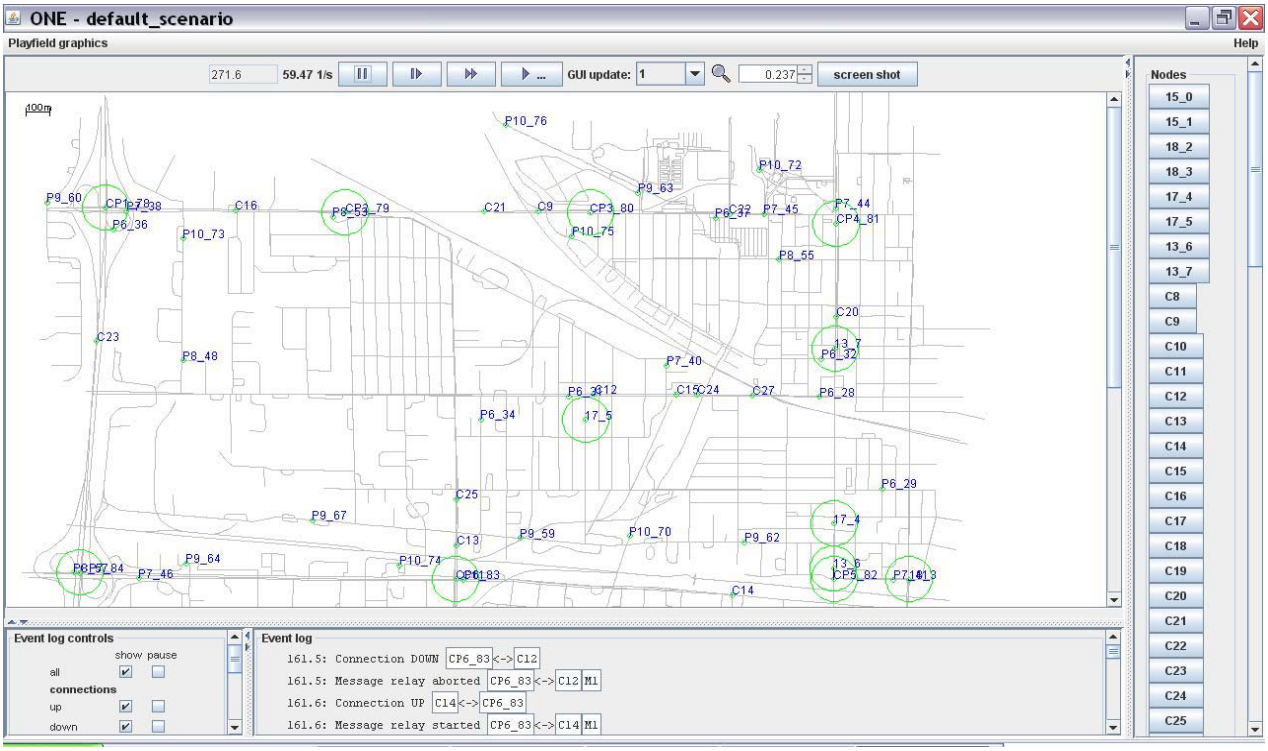

Figure 2: Checkpoint based simulation model in ONE, with circles representing the deployed CPs.

Several factors influence the selection of an ideal location (Khan 2007) and the most important is the human meetings frequency at a particular place. To examine the effect of CPs deployment, *CP1*, *CP7*, and *CP11* are deployed at locations where meeting frequencies are lesser, as compared to *CP4, CP5, CP6, CP9,* and *CP10* that are located at shopping malls, bus stations, and North Dakota State University (NDSU). The simulation is run multiple times to observe the effect of CP deployment on message delivery ratio. The results in Figure 3 indicate that for *CP1*, *CP7*, and *CP11* the message delivery ratio is lesser as compared to *CP5, CP6*, and *CP9* that are deployed considering the higher probability of meetings at these places. Therefore, the CPs would have more desirable outcomes if human mobility and meeting schedules are exploited before deployment.

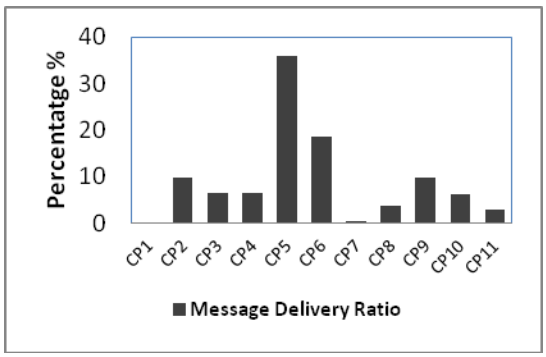

Figure 3: Effect of CP deployment on message delivery ratio.

Effects of the number of CPs on message delivery ratio and average delay

The effect of the number of CPs is observed on message delivery ratio and average delay in Figure 4. The test is run by increasing number of CPs while keeping number of buses and mobile nodes constant.

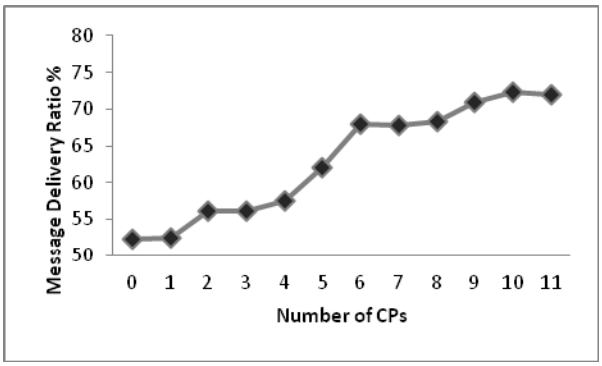

Figure 4(a): Effect of CPs on message delivery ratio.

From Figure 4(a) we can see that message delivery ratio improves by increasing number of checkpoints in the area. In Figure 4(b) we can observe that there is no significant decrease in packet latency until CP 5 is deployed. When CP 5 is deployed on bus station, there is remarkable decrease in packet latency as all the buses visit the common place. Therefore, due to the increase in human meetings at a common point, the packet latency also decreases.

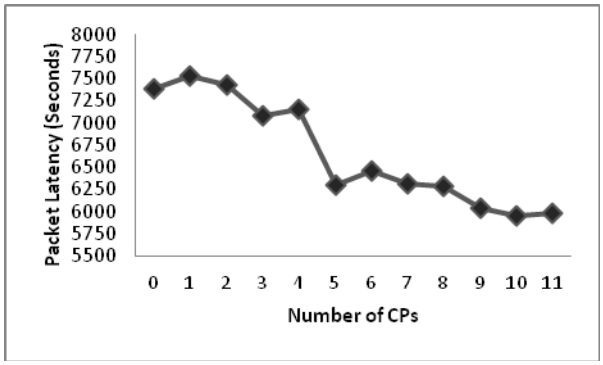

Figure 4(b): Effect of CPs on packet latency.

CP model evaluation with human mobility pattern

A place, where human meeting frequency is higher and repetitive, will be having higher message delivery probability. In such case DTN routing protocol such as *PRoPHET* would be more effective, as compared to the other routing protocols (e.g. *Spray and Wait* and *Epidemic*) that do not consider the node encounters pattern in making routing decisions. To evaluate the effect of human mobility on DTN routing, we identified some areas on the map as meeting points, where people tend to visit more frequently, and deployed a few checkpoints on these locations. Examples of such areas are shopping malls and main bus station GTC. We compared the performance of the three aforementioned routing protocols in terms of message delivery ratio and packet latency to investigate the effect of human mobility on these protocols. The simulation is run with same number of nodes for all three protocols and the results are indicated in Table 4.

Table 4: Performance of DTN protocols for human mobility.

	PRoPHET	Spray and Wait	Epidemic
Delivery Ratio %	71.90	62.39	73.51
Overhead ratio	27.64	7.52	34.77
Latency Avg. (s)	5964.51	5609.17	6163.54
Buffer time Avg. (s)	10249.51	16347.72	10225.18

In Table 4, latency avg. is average message delay from creation to delivery, overhead ratio is assessment of bandwidth efficiency, and buffer time avg. is average time the messages stayed in the buffer at each node. It can be observed that *Epidemic* routing has slightly higher delivery ratio as compared to *PRoPHET.* This is due to the fact that in *Epidemic* routing, the network is flooded with message copies such that each node replicates the message received and forwards to the next node. Therefore, the chances for message to reach the final destination also increase. However, from Table 4 we can see that message flooding increases bandwidth overhead ratio, and latency in *Epidemic* routing as compared to *PRoPHET* and *Spray and Wait* routing protocols. The buffer utilization time of *PRoPHET* is little higher than *Epidemic* as the message has to wait on a checkpoint before being delivered to the next mobile node (e.g. bus and car) towards the destination. The message delivery ratio is minimum for *Spray and Wait* routing due to the limit on number of message copies in the network and that leads to lower bandwidth overhead. Therefore, from Table 4 we can conclude that if human meeting schedules are exploited in message forwarding, then *PRoPHET* routing protocol surpasses the other two protocols in better performance.

CP model evaluation with RWP mobility pattern

To further examine the effect of mobility on DTN routing protocols, simulation is performed with a non-restricted random way point (RWP) mobility pattern. Such mobility pattern may be observed in post disaster scenarios, where people are moving from one relief camp to another and then back to disaster locations not following a specific mobility pattern. The evaluation of the three DTN protocols is performed by randomly placing 11 CPs with fixed number of mobile nodes having various speeds. Simulation is run to study the effect of random mobility on message latency, buffer utilization, and message delivery ratio. Table 5 shows the effect of random waypoint mobility.

Table 5: Performance of DTN protocols for RWP mobility

	PRoPHET	Spray and Wait	Epidemic
Delivery Ratio %	6.53	6.19	7.51
Overhead Ratio	37.42	22.05	44.68
Latency Avg. (s)	8705.82	8426.67	8661.85
Buffer time Avg. (s)	11451.37	14184.71	13090.77

From Table 5, we can observe that in random waypoint mobility, the message delivery ratio is significantly dropped. This is due to the fact that in random way point mobility, the frequency of nodes travel is higher towards the center of the map as compared to the map boundaries.

The aforementioned fact can be further verified by looking at Figure 5, which indicates that the message delivery ratio is higher at CP6 and C8, in all three protocols. Because, both the checkpoints (CP6 and CP8) are placed more closed towards the center of the map.

It can be further observed from Table 5 that there is no significant difference in the performance of the three protocols, as the *PRoPHET* cannot make use of human mobility pattern to forward messages towards the frequently visited points.

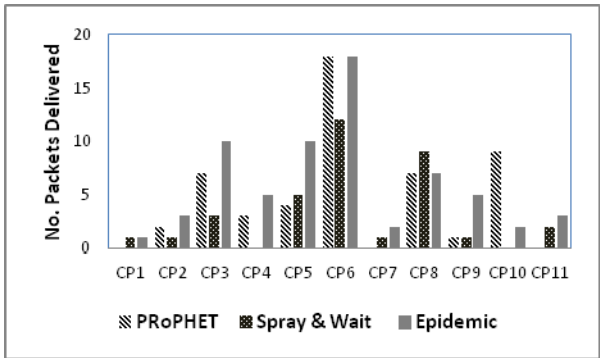

Figure 5: CP6 is located near center of map where nodes mobility is maximum.

CONCLUSIONS AND FUTURE WORK

In this paper, human mobility behavior is exploited to develop a CP based architecture, in which the CPs are deployed on locations where human meetings are more frequent and each CP is covering a specific geographic location in the city of Fargo, ND, USA. The messages are relayed among CPs through buses following fixed schedules. The simulation results indicate that by installing the CPs on locations with higher human interactions increase the predictability of finding the message destination. Therefore, the CP based approach improves message delivery ratio, decreases buffer utilization of nodes and message delivery time.

The future work includes the real test deployment of CP nodes in specific regions to further investigate their usability for message routing and content distribution which is among a few of the future applications of DTNs.

REFERENCES

Almasaeid, H.M. and A.E. Kamal. 2008. "Modeling mobility-assisted data collection in wireless sensor networks". In *Proceedings of Global Telecommunications Conference 2008.* IEEE, 1-5.

Balazinska, M. and P. Castro. 2003. "Characterizing Mobility and Network Usage in a Corporate Wireless Local-Area Network". In *Proceedings of 2003 MobiSys Conference.*

Burns, B.; O. Brock; and B.N. Levine. 2005. "MV routing and capacity building in disruption tolerant networks". In *Proceedings of 2005 Infocom.* IEEE, 398-401.

Burgess, J.; B. Gallagher; D. Jensen; and B. Levine. 2006. "Maxprop: routing for vehicle-based disruption-tolerant networking". In *Proceedings of 2006 infocom Conference.* IEEE*,* 1-11.

Cacciapuoti, A.S.; F. Calabrese; M. Caleffi; G. Di Lorenzo; and L. Paura. 2012. "Human mobility-enabled wireless networks for emergency communications during special events." *Pervasive and Mobile Computing,* 2012*.*

Ghosh, J.; H.Q. Ngo; and C. Qiao. 2006. "Mobility profile based routing within intermittently connected mobile ad hoc networks (icman)". In *Proceedings of the 2006 international conference on Wireless communications and mobile computing*. ACM, 551-556

Johnson, D.B. and D.A. Maltz. 1996. "Dynamic source routing in ad hoc wireless networks". In *Proceedings of 1996 Mobile computing Conference*. 153-181.

Keränen, A.; J. Ott; and T. Kärkkäinen. 2009. "The ONE Simulator for DTN Protocol Evaluation." In *Proceedings of SIMUTools, 2009, Rome, Italy.*

Khan, S.U.; T. Loukopoulos.; and H. Li. 2011. "Advances in Wireless, Mobile and P2P based Internet Protocols, Applications, and Architectures." *International Journal of Internet Protocol Technology.* 6, No.1-2, 1-2.

Khan, S.U. 2007. "Approximate Optimal Sensor Placements in Grid Sensor Fields". In *Proceedings of 65th Semi-annual IEEE Vehicular Technology Conference (VTC),* Dublin, Ireland, April 2007, 248-251.

Leguay, J.; T. Friedman; and V. Conan. 2005. "DTN routing in a mobility pattern space". In *ACM SIGCOMM workshop 2005 on delay tolerant networking and related topics.*

Lindgren, A.; A. Doria; and O. Schelen. 2003. "Probabilistic routing in intermittently connected networks". In *SIGMOBILE mobile computing communications review.* 7, No.3, 19–20.

Perkins, C. and Royer, E. 1999. "Ad hoc on-demand distance vector routing." In *2nd IEEE workshop on mobile computing systems and application.* IEEE. 90-100.

Rhee, I.; M. Shin; S. Hong; K. Lee; S.J. Kim; and S. Chong. 2011. "On the Levy-Walk Nature of Human Mobility Networking." *IEEE/ACM Transaction*s. 19, No.3, 630-643.

Shinya, Y.; A. Nagataa; M. Tsurub; and H. Tamurab. 2011. "Virtual segment: Store–carry–forward relay-based support for wide-area non real-time data exchange." *Simulation Modelling Practice and Theory*, 19, No.1, 30-46.

Sollazzo, G.; M. Musolesi; and C. Mascolo. 2007. "TACO-DTN: a time-aware content-based dissemination system for delay tolerant networks". 2007. *Proceedings of the 1st international MobiSys workshop on Mobile opportunistic networking*, 83-90.

Song, C.; Z. Qu; N. Blumm; and A.L. Barabási. 2010. "Limits of Predictability in Human Mobility." *Science Magzine.,* 327, No. 5968, 1018-1021.

Ionut, A. 2010. "Wi-fi enabled mobile phone handsets in the US, 2010-2015". Technical report. Market research analysis, Coda Research Consultancy.

Ionut, A. 2009. "Wi-fi capable handsets: Residential and enterprise markets for wi-fi and dual-mode handsets". 2009. Technical report, ABI Research.

Thrasyvoulos, S.; K. Psounis; C. S. Raghavendra. 2005. "Spray and wait: an efficient routing scheme for intermittently connected mobile networks" In *Proceedings of the 2005 ACM SIGCOMM workshop on Delay-tolerant networking.* ACM, New York, USA.

Vahdat, A. and D. Becker. 2000. "Epidemic routing for partially connected ad hoc networks". Technical report. Duke University.

Zhao, W.; M. Ammar; and E. Zegura. 2004. "A message ferrying approach for data delivery in sparse mobile ad hoc networks". In *Proceedings of MobiHoc, 2004.*

Zhao, W.; Y. Chen; M. Ammar; M. Corner; B. Levine; and E. Zegura. 2006. "Capacity Enhancement using Throwboxes in DTNs." *International Conference on Mobile Adhoc and Sensor Systems (MASS)*. IEEE. Vancouver, BC, 31-40.

AGENT-BASED SIMULATION OF VOLUNTEER ENVIRONMENT

Aleksander Byrski, Michał Feluś
Jakub Gawlik, Rafał Jasica, Paweł Kobak
Edward Nawarecki
AGH University of Science and Technology
Al. Mickiewicza 30, 30-059 Kraków, Poland
Email: olekb@agh.edu.pl
{felus,jgawlik,jasica,kobak}@student.agh.edu.pl
nawar@agh.edu.pl

Michał Wroczyński, Przemysław Majewski
Tomasz Krupa, Paweł Skorupka
fido intelligence sp. z o.o.
ul. Trzy Lipy 3, 80-172 Gdańsk, Poland
Email: mwroczynski@fidointelligence.pl
pmajewski@fidointelligence.pl
tkrupa@fidointelligence.pl
pskorupka@fidointelligence.pl

KEYWORDS

agent-based simulation, volunteer computing, network traffic simulation

ABSTRACT

Some complex environments require appropriate approach in modelling and simulation. Simulation of network traffic is usually performed using popular tools as NS3 (Carneiro et al., 2011), however, when dealing with dynamic environments, such as volunteer computing, the notion of agency may be leveraged, to ease the implementation of emergent behaviour that is encountered in such cases. In the course of paper two agent-based frameworks for simulation of network traffic are presented. They are implemented using popular agent-based discrete event simulation platforms MASON and RePast. Following the description of the platforms, a case study of server load testing in a volunteer environment in virtual and real world are shown.

INTRODUCTION

Various problems (sociological, biological, etc.) requiring simulation approach there are complex processes observed in populations consisting of a huge number of different, possibly autonomous individuals.

Utilizing the notion of agent (Wooldridge and Jennings, 1995) brings many improvements into the world of simulation, following the idea of decentralisation of control. Each agent may be autonomous, differently configured, utilising different means of discovering the features of the environment and its neighbours, utilising different algorithms and performing different actions in the system.

An interesting example of such problem, that may be simulated using agents is volunteer environment, consisting of a number of computation nodes leased by the users, that are available in random moments of time. Such computations become nowadays quite popular, being a legacy of the well known projects such as SETI@HOME (Korpela, 2012). Such environment may be perceived as a highly dynamical one and characterising by a high notion of autonomy. Thus, the behavioural patterns of certain individuals switching on or off their computers may substantially differ.

Problems arising for computing in such environment, e.g., throughput of the network, load balancing etc. and especially emergent behaviour and autonomy encountered in specific cases (e.g., volunteer environments) may be considered using popular agent-based simulators.

In the course of this paper, a concept of simulation framework for volunteer environment using popular agent-based simulators (MASON and RePast) is presented. The general considerations are illustrated by the experimental results obtained from the implementations using the above mentioned frameworks in monitoring of network traffic during the server load testing in simulated and real volunteer environments.

AGENT-BASED SIMULATION

There exists a plethora of multi-agent frameworks which may be used to support the construction of agent-based simulation systems. Some of them are oriented to specific kinds of simulation (see, Nikolai and Madey (2008); Railsback and Lytinen (2006)): e.g., simulating of movement of entities with 3D visualisation (see, e.g., breve, Klein (2002)), networking (see, e.g, NS3, Carneiro et al. (2011)), possibility of visual programming (see, e.g., SeSam, Ventroux et al. (2010)).

When looking for mature, open-source, agent-based simulation project with universal applicability, supported by the wide society of programmers, two environments seem to especially attract attention, these are MASON and Repast.

MASON is an agent-oriented simulation framework developed at George Mason University. It is advertised as fast, portable, 100% Java based. Multi-layer architecture brings complete independence of the simulation logic from visualisation tools which may be altered anytime. The models are self-contained and may be included in other Java-based programs. Various means for 2D and 3D visualisation, and different means of output are avaiable (PNG snapshots, Quicktime movies, charts and graphs, data streams).

Simulation in MASON consists of a model class `SimState` that composes random number generator

Proceedings 26th European Conference on Modelling and Simulation ©ECMS Klaus G. Troitzsch, Michael Möhring, Ulf Lotzmann (Editors)
ISBN: 978-0-9564944-4-3 / ISBN: 978-0-9564944-5-0 (CD)

and a `Schedule`. An object of `Schedule` class manages many agents, implementing `Steppable` interface, therefore an agent may interact with other ones and the environment by exposing predefined method that will be called by the `Schedule` (Luke et al., 2005). The `SimState` may also manage the spatial structure of the simulation with a concept of `Fields` allocating different objects, thus constructing environment in which the agents may be situated.

Programming model of MASON follows basic principles of object-oriented design. An agent is instantiated as an object of a class, added to a scheduler and its `step` method is called during the simulation. There are no predefined communication nor organisation mechanism, these may be realized using simple method calls. There are neither ready-to-use distributed computing facilities nor component-oriented solutions.

First released in 2003, the environment is still maintained as an open-source project, distributed under Academic Free license (ver. 3.0). The current version (16.0) was released in the end of 2011.

Repast—Recursive Porous Agent Simulation Toolkit—is widely used agent-based modeling and simulation tool. Repast has multiple implementations in several languages and built-in adaptive features such as genetic algorithms and regression (North et al., 2007). The framework utilizes fully concurrent discrete event scheduling, HPC version also exists (Collier and North, 2011). In Repast 3, there are many programming languages interfaces (e.g., Java, Logo dialect, .NET languages, Lisp dialect, Prolog, Python). Logging and graphing tools are built-in. Dynamic access to the models in the runtime (introspection) is possible using graphical user interface. There are predefined libraries for different methods of modelling and analysis available, e.g., neural networks, genetic algorithms, social-network modelling, GIS support.

The implementation of a simulation system in Repast 3 is realized in a similar way as described for MASON. The class suitable for simulation should extend `SimpleModel` class, and contain appropriate implementation of `step()` function that will be called by the scheduler. It is to note that proper construction of the class' attributes allows to edit them using introspection mechanism supported by Repast GUI. The simulation may be even interrupted, available parameters may be changed and the simulation may be carried on.

Repast 3 consists of different implementation of the platform (Repast J—Java-based, Repast.NET—MS .NET and Repast Py—Python). It has been renowned for a long time, however, recently Repast 3 has been superseded by its next stage development called Repast Simphony (Repast S) bringing newly developed GUI, with some significant changes into the programming paradigm.

The latest (Simphony 2.0 beta) version of this open-source project, licensed according to 'new BSD' license, has been released in the late 2010.

VOLUNTEER COMPUTING

Volunteer Computing is a type of distributed computing in which all (or at least some of) the computational resources come from the number of nodes dynamically connecting to a network, with the intent to share their computation power, either altruistically or using some service instead (e.g., gaining access to some resources) (Sarmenta, 1998). A very similar approach to *Volunteer Computing* is called *Sideband Computing*, though it requires a predefined client application installed in a desktop PC and the appropriately prepared server (usually a local gateway) to distribute the tasks (Xu, 1998).

The first Volunteer Computing project was Great Internet Mersenne Prime Search (`http://mersenne.org/`) and was started in 1996. The most famous project, called SETI@Home (`http://setiathome.berkeley.edu/`) (launched in 1999) is dedicated to analysing radio signals, gathered by the radio-telescope located in Arecibo (Puerto Rico), searching for signs of extra-terrestrial intelligence.

Volunteer Computing projects may be implemented using several middlewares, such as Berkeley Open Infrastructure for Network Computing (`http://boinc.berkeley.edu/`) (BOINC) (open-source, base of SETI@Home), Xgrid (`http://www.apple.com/pl/server/macosx/technology/xgrid.html`) (a proprietary software prepared by and for Apple) or Grid MP (`http://www.univa.com/`) (a commercial product).

Besides computation (see, e.g., Byrski et al. (2012)), other tasks may be performed in Volunteer environment. To name a few: web crawling (already attempted by Krupa et al. (2012)), MapReduce (volunteer implementation of MapReduce (Dean and Ghemawat, 2004) is feasible in the opinion of authors), all such approaches may be implemented in volunteer environment, based on flexible delegation of the part of tasks to volunteers. In the next section, the case study of server load testing in volunteer environment is presented.

NETWORK SIMULATION IN AGENT-BASED ENVIRONMENT

There exist many network simulation environments, such as e.g., NS3 (Carneiro et al., 2011) that may be used to extensive simulation of many complex networks (ethernet, WiFi, MANET and others). However implementation of certain phenomena, such as emergent features of volunteer environment, may require more high-level approach, omitting features present in lower layers of ISO/OSI model (Bush and Meyer, 2002) for the sake of abstraction.

The most important notion utilized in RePast and MASON that is taken advantage here of is the one of an agent. Computer networks consist of active (e.g., nodes, routers) and passive (switches, cables) elements.in MASON Therefore, utilizing of the notion of agent in the

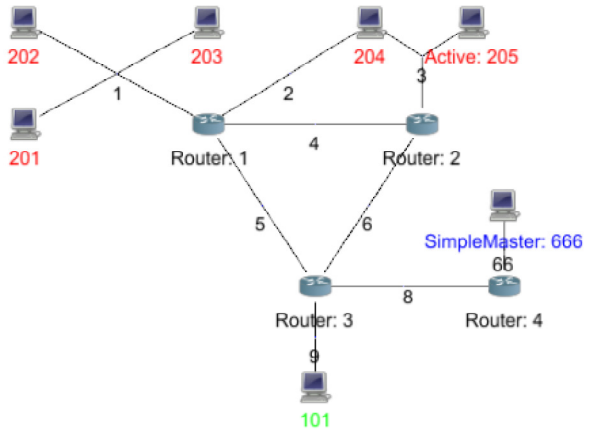

Figure 1: Example network structure with simulated nodes

computer network simulation seems quite straightforward: agents are given capabilities of interacting inside the network environment (by sending and routing packets) while additional technical features supported by the simulation environments will be utilized to link the agents. Two proposed simulator prototypes presented here are implemented using MASON and Repast frameworks.

Network architecture and behaviour The computer network is usually modelled as a connected undirected graph. The nodes of the graph represent devices and the edges represent network connections. All devices should have at least one connection to another node. The active devices utilize the passive ones to communicate by passing the information encapsulated into chunks (packets) (Comer, 2006). Each endpoint has a unique network address. Addresses on the two ends of a link must belong the same subnet. The nodes send the packets to each other. The packets are marshalled by routers according to popular classful routing protocol (Hendrik, 1988).

Network simulation in RePast and MASON The simulation frameworks implemented in RePast and MASON leverage appropriate components supported by these platforms by implementing discrete event-driven entities (agents) and providing means for communication among them. Active entities (routers and nodes) are implemented as agents in both platforms (in MASON as objects implementing the `Steppable` interface and derived from class `Node`, in RePast `@ScheduledMethod` annotation is used), while the communication among them is supported in the following way:

- *connections* are used in RePast, single instance of class `Connection` has references to many adjacent nodes, which allows direct communication between many participants,
- *links* are used in MASON, each link is an object of class `Link` and has exactly two ends, so only two nodes may communicate with each other.

Network nodes can communicate with each other by sending messages (packets). In MASON these are objects of a type derived from a base class `Packet`, delivered by calling the target node's `DeliverPacket` method. In RePast, `Connection` class provides methods for sending objects of type `Packet`. Each node is of type that extends `DTEDevice` class, which offers functionality for receiving packets and routing. Messages meant for a distant node are forwarded by routers using the implemented routing protocol. Each packet has a source and a destination address and may also contain additional data.

Packet processing is implemented using leaky bucket model (Tanenbaum, 2003). The receiving device stores incoming packets in a buffer of limited size. This size is predefined in the network definition and is measured in packets—each packet is assumed to be of the same size. If there is no free space in the buffer overflowing packets are dropped. Sending a packet from a node to its neighbour takes 1 simulation step.

In each step the nodes process a set number of packets from their buffer. This number is called the devices processing power. The action taken depends on the type of node and type of received packet.

Routing is based on static routing tables created before the start of the simulation. Each table entry contains a network subnet address, the interface which should be used for sending packets to that subnet and the value of the metrics (number of nodes to destination).

When processing a packet the router checks a routing table for a subnet address matching the packet's target address and passes the packet to an appropriate next node. If the target address cannot be matched to any entry in the routing table the packet is dropped.

The routing tables are created in the following manner: At the beginning a distance of 1 is assumed to the routers adjacent nodes. The router sends its routing table to all neighbouring routers. Upon receiving a table a router adds all unknown addresses to its own table incrementing metrics values by 1. If a path shorter then the existing entry is received the old entry is replaced by the new one.

Multiple routes with the same distance are stored and used for load distribution. The routers continue to transmit their tables until changes no longer occur.

The exact structure of the network is defined using a text file.

Case study: volunteer-based sever load testing As a case study, server load testing in volunteer environment is considered. In this test, the volunteers are recruited from users browsers (after opening predefined website, e.g., certain portal). The client applications may be implemented using different available technologies, such as Java Applets, Microsoft Silverlight or even Java Script

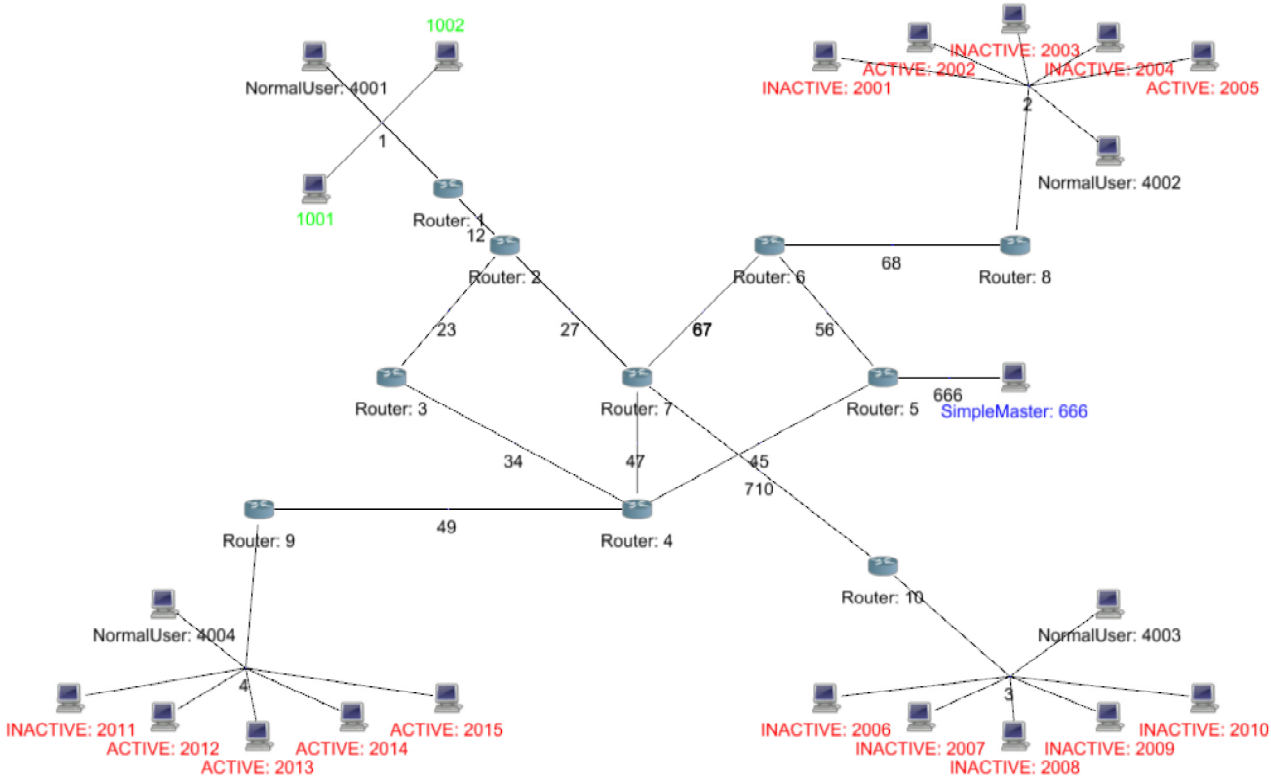

Figure 2: Experimental network setup

(see Byrski et al. (2012) for description of similar environment aimed at solving computing problems). The basic elements of a simulated environment are visualized in Fig. 1.

The network presented there, consists of the following types of nodes, implemented as agents in RePast and MASON:

- Router: as described above, joins two or more subnets and provides packet routing according to RIP protocol.
- Master: The task coordinator. Distributes tasks to nodes, may implement sophisticated planning of distribution including load balancing (e.g., assigning targets to the testers), in order to utilize available computational power of the volunteer environment, at the same time trying to decrease the congestion in the network.
- Tester: A web-browser volunteer participating in the test. Requests (according to possible communication means supported by the technology used) the master for test scenario. A testing node may be in one of two possible states: active or inactive. Depending on the simulation parameters it may change its state during the simulation. During its active status the tester sends packets to the target, however, a pause in test is performed from time to time, in order to make possible communication among the master and the testers (e.g., to adapt change the test strategy).
- Target: Target of the test, a selected node, its address is broadcasted by the master to the testers. There may be more than one target.
- Normal: Neutral device. Exchanges messages with other devices to simulate normal network traffic.

In the simulated network, several types of communication can be performed, each characterized by its own packet type:

- Normal: Packets are sent by testers to targets. These packets are part of the test.
- Master request: Packets send by testers to the master. Contain requests for test scenarios.
- Master reply: Information sent by the master to an tester. Contains the target's address and a test duration.
- Ping/Pong: Packets (and responses) sent by all nodes (with an exception of the routers), used to simulate regular network traffic.

The test is divided into phases of a fixed length, each followed by a period of inactivity called the synchronization period, which is used for communication between the master and testers.

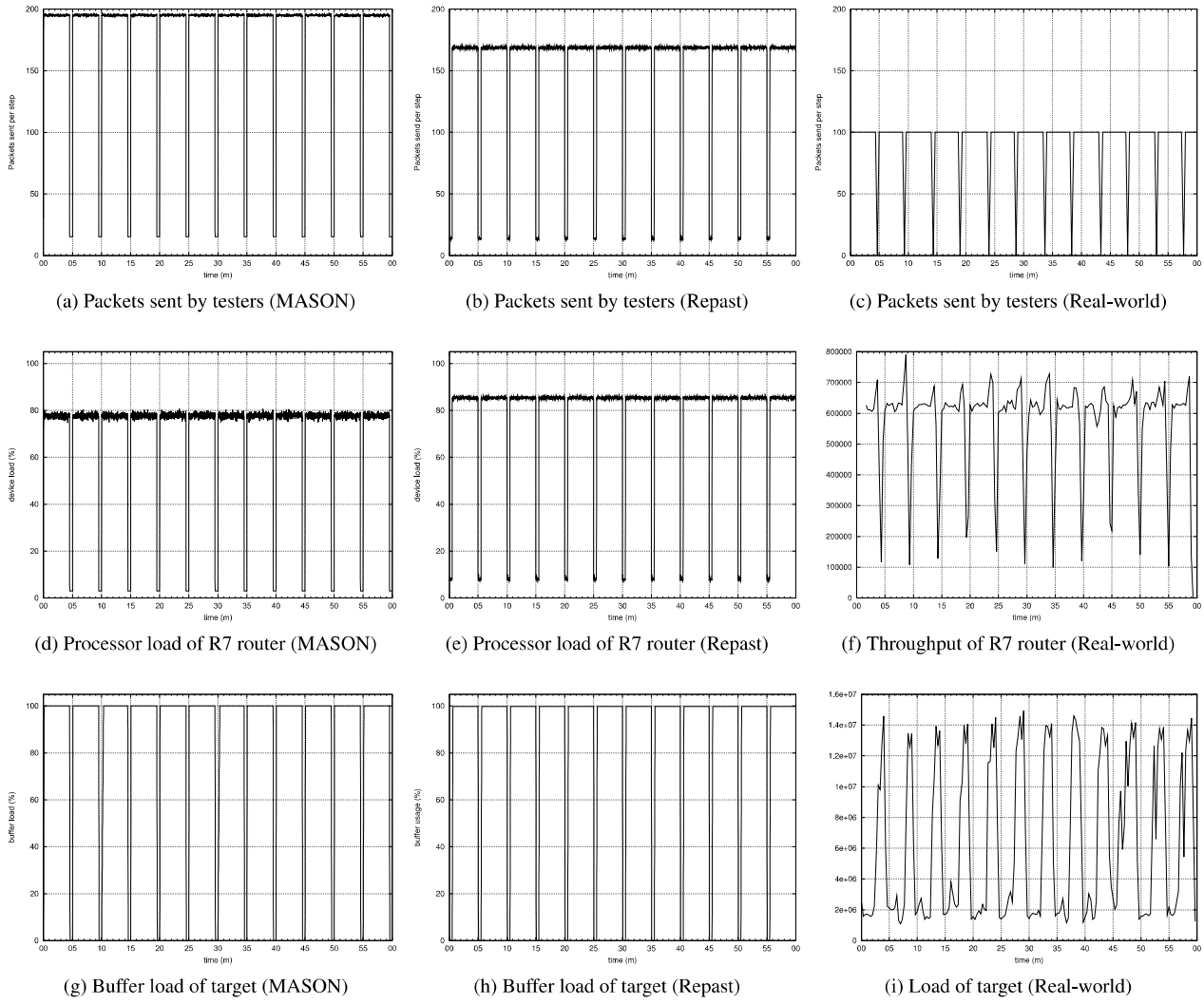

(a) Packets sent by testers (MASON)
(b) Packets sent by testers (Repast)
(c) Packets sent by testers (Real-world)
(d) Processor load of R7 router (MASON)
(e) Processor load of R7 router (Repast)
(f) Throughput of R7 router (Real-world)
(g) Buffer load of target (MASON)
(h) Buffer load of target (Repast)
(i) Load of target (Real-world)

Figure 3: Observation of network activities (simulation and real-world experiment) of testers, one selected router and one selected target

When a tester becomes active, it sends a packet to the master requesting a test scenario. The master responds with the target's IP address and the length of the test.

During the test period active testers send a fixed number of packets to their assigned target. During the synchronization period the master may sends new instructions to all known testers following the possible load balancing scheme etc.

EXPERIMENTAL RESULTS

The experimental configuration of the network is shown in Fig. 2. There are three LANs connected with arbitrarily chosen router structure. Each of LAN contains 5 testers (volunteers) and one neutral node. One of the LANs conains two target nodes. There is also a Master server located in one of the LANs.

Master server assigns the target IP to the testers, and they start transmitting the packets in order to fill-up the buffer of the target, while maintaining pauses from time to time to receive possible management instructions.

Detailed configuration of both MASON- and Repast-based experiments is as follows:

- Simulation time: 1 hour = 360000 simulation steps (1 second = 100 steps).
- Testers Activity: tester changes his state (active/passive) every random number of steps by normal distribution: next_state_change_after = nextGaussian()*360000 + 1080000, measured in simulation steps.
- Synchronization: 4 minutes 30 seconds test, 30 seconds synchronization.
- Devices: Testers, Normals, Masters: buffer size = 20000, packets processed per step = 20.
- Routers: buffer size = 20000, packets processed per step = 200.

- Targets: buffer size = 20000, packets processed per step = 50.

- Background communication: every device (with an exception of Router) sends Ping packet to 2 random devices every 2 steps and awaits an answer—Pong packet.

Figs. 3a, 3b show the number of packets sent by testers in each step. A large difference in traffic volume can be seen between the synchronization period when only tester-master communication and normal network traffic is present, and the test period when the packets are also being transmitted for both simulation frameworks. This situation is repeated on all graphs, showing the results obtained for one of core routers (see Figs. 3d, 3e), and one of the targets (see Figs. 3g, 3h). The differences in observed buffer load and testers activity may be explained by utilizing different simulation platforms, effecting in different means of congestion measurement, however, the main goal is attained, as the buffers of the targets are full between the pause periods. It is to note, that the load of the router is consistently lower than 100%, so this router is still capable of handling all the received packets, even when the test is performed.

Figs. 3c, 3f, 3i show the results obtained in a real-world experiment conducted using a set of nodes and routers deployed in a virtual environment (utilizing VMWare servers run on 5 physical machines Intel Core i7 class connected with gigabit ethernet adapters), configured in a similar structure as displayed in Fig. 2. The relevance between corresponding graphs obtained in the real-world and simulation is easy to see, although some noise occur, that is unavoidable. The main reason is that the real-world environment acting fully in parallel (instead of discrete event driven simulation) is examined. One may also mention, that modelling requires abstraction, so certain features perceivable in a real-world, as e.g. latencies of packet transmission, are be omitted, hence the visible between corresponding graphs differences. Consider original Y-axis scale used in Figs. 3f, 3i. Though these values do not correspond directly with the ones displayed in Figs. 3d, 3g, 3f, 3i, the similarity is visible. Note that of course two different units of measurement are used, RePast and MASON based experiments utilize their own defined packet per second ratio, while the real-world experiment yielded the results displaying actual packets per second value.

CONCLUSION

In the paper two agent-based frameworks for simulation of network traffic were presented. In order to implement these simulation frameworks, popular discrete-event simulation environments RePast and MASON were used. Study of network congestion monitoring in volunteer environment was presented and allowed to compare two approaches to simulation with real-world results. The observation let to state that the prepared frameworks are feasible. Additional features of simulating platforms, such as extensive graphical user interface, possibility of sophisticated visualisation using e.g., animations etc. may be also useful.

In the opinion of the authors, both of the presented environments seem to be well-suited to model different emergent and autonomous features that may occur in volunteer environment. This statement is confirmed by the observation of a real-world experiment's results, performed in a similar network setup, that turned out to be significantly similar to the simulated ones (though the parallel characteristics of the real world were completely simulated in both discrete-event frameworks). Regarding the intrinsic efficiency of the evaluated platforms, rough testing yielded, that MASON-based simulation run about 2 times faster than RePast-based one (considering simulation steps per second), however more sophisticated testing will be required to prove this unquestionably.

It is to note, that though the volunteer simulations may be prepared and run with other popular simulators (e.g. NS3 Carneiro et al. (2011)), the presented approach was implemented very easily (using popular JAVA technology, making the system much easier to develop than NS3, which is based on C++). Moreover, both frameworks that were used (RePast and MASON) have constant support of the developing societies (both projects are open-source) therefore being easily extendable etc.

Future work will consider implementation and testing of different algorithms, such as load balancing, testing the environment in different fault conditions, developing and exploring autonomous and emergent behaviours of the agents applied to self-configuration in dynamic volunteer environment, introduction of hierarchical structure of the agents (middle-agents may be applied to optimize the network traffic and task assignment). Experiments with scaling of the simulations are also envisaged in the future publications.

ACKNOWLEDGMENTS

The research leading to these results has received funding from Polish National Centre for Research and Development with grant agreement number 0108/R/T00/2010/11.

REFERENCES

Bush, R. and Meyer, D. (2002). Some internet architectural guidelines and philosophy. RFC 1058.

Byrski, A., Debski, R., and Kisiel-Dorohinickki, M. (2012). Agent-based computing in augmented cloud environment. *Computer Systems Science & Engineering (In Press)*.

Carneiro, G., Fontes, H., and Ricardo, M. (2011). Fast prototyping of network protocols through ns-3 simulation model reuse. *Simulation Modelling Practice and Theory*, 19(9):2063 – 2075.

Collier, N. and North, M. (2011). *Repast SC++: A Platform for Large-scale Agent-based Modeling*. Wiley.

Comer, D. E. (2006). *Internetworking with TCP/IP - Principles, Protocols and Architecture*. Prentice Hall.

Dean, J. and Ghemawat, S. (2004). Mapreduce: Simplified data processing on large clusters. In *6th Symposium on Operating Systems Design & Implementation*.

Hendrik, C. (1988). Routing information protocol. RFC 1058.

Klein, J. (2002). Breve: a 3d environment for the simulation of decentralized systems and articial life. In *Proc. of Artificial Life VIII, the 8th International Conference on the Simulation and Synthesis of Living Systems*.

Korpela, E. J. (2012). Seti@home, boinc and volunteer distributed computing. *Annual Review of Earch and Planetary Science*, 40(1).

Krupa, T., Majewski, P., Kowalczyk, B., and Turek, W. (2012). On-demand web search using browser-based volunteer computing. In *Proc. of 6th Int. Conf. on Complex, Intelligent and Software Intensive Systems*.

Luke, S., Cioffi-Revilla, C., Panait, L., Sullivan, K., and Balan, G. (2005). MASON: A multi-agent simulation environment. *Simulation: Transactions of the society for Modeling and Simulation International*, 82(7):517–527.

Nikolai, C. and Madey, G. (2008). Tools of the trade: A survey of various agent based modeling platforms. *Journal of Artificial Societies and Social Simulation*, 12(2).

North, M., Howe, T., Collier, N., and Vos, J. (2007). A declarative model assembly infrastructure for verification and validation. In Takahashi, S., Sallach, D., and Rouchier, J., editors, *Advancing Social Simulation: The First World Congress, Springer, Heidelberg, FRG (2007)*.

Railsback, S. and Lytinen, L. (2006). Agent-based simulation platforms: review and development recommendations. *Simulations*, 82:609–623.

Sarmenta, L. (1998). Bayanihan: Web-based volunteer computing using java. In *Proc. of the 2nd International Conference on World-Wide Computing and its Applications (WWCA'98), Tsukuba, Japan, March 3-4, LNCS 1368*.

Tanenbaum, A. S. (2003). *Computer Networks, Fourth Edition*. Prentice Hall.

Ventroux, N., Guerre, A., Sassolas, T., Moutaoukil, L., Blanc, G., Bechara, C., and David, R. (2010). Sesam: An mpsoc simulation environment for dynamic application processing. In *CIT*, pages 1880–1886. IEEE Computer Society.

Wooldridge, M. and Jennings, N. (1995). Intelligent agents: Theory and practice. *Knowledge Engineering Review*, 10(2).

Xu, Y. (1998). Global sideband service distributed computing method. In *Proceedings of the International Conference on Communication Networks and Distributed System Modeling and Simulation (CNDS'98)*.

A Comparative Study of Data Center Network Architectures

Kashif Bilal
North Dakota State University
Fargo, ND 58108, USA
Kashif.Bilal@ndsu.edu

Samee U. Khan
North Dakota State University
Fargo, ND 58108, USA
samee.khan@ndsu.edu

Joanna Kolodziej
Cracow University of
Technology, Cracow, Poland
jkolodziej@uck.pk.edu.pl

Limin Zhang
North Dakota State University
Fargo, ND 58108, USA
limin.zhang@ndsu.edu
North Dakota State University

Khizar Hayat
COMSATS Institute of
Information Technology,
Pakistan.
khizarhayat@ciit.net.pk

Sajjad A. Madani
COMSATS Institute of
Information Technology,
Pakistan.
madani@ciit.net.pk

Nasro Min-Allah
COMSATS Institute of
Information Technology, Pakistan.
nasar@comsats.edu.pk

Lizhe Wang
Chinese Academy of Sciences
Beijing, China
lzwang@ceode.ac.cn

Dan Chen
China University of Geosciences
Wuhan, China
Danjj43@gmail.com

KEYWORDS
Data Center Networks (DCN), Data Center Architecture, Data Center

ABSTRACT

Data Centers (DCs) are experiencing a tremendous growth in the number of hosted servers. Aggregate bandwidth requirement is a major bottleneck to data center performance. New Data Center Network (DCN) architectures are proposed to handle different challenges faced by current DCN architecture. In this paper we have implemented and simulated two promising DCN architectural models, namely switch-based and hybrid models, and compared their effectiveness by monitoring the network throughputs and average packet latencies. The presented analysis may be a background for the further studies on the simulation and implementation of the DCN customized topologies, and customized addressing protocols in the large-scale data centers.

INTRODUCTION

A Data Center (DC) is a pool of computing resources clustered together using communication networks to host applications and store data. Conventional DCs are modeled as a multi-layer hierarchical network with thousands of low cost commodity servers as the network nodes. DCs are experiencing exponential growth in servers. Google, Microsoft, and Yahoo already host hundreds of thousands of servers in their respective data centers (Carter 2007; Rabbe 2006). Google has more than 450,000 servers in 2006 (Arnold 2007, Ho 2007). The number of servers is doubling every 14 months in Microsoft data centers (Snyder 2007). The server portion of data center has experienced enormous commoditization and low cost commodity servers are used in data centers instead of high-end enterprise servers. However, the network part of data center has not seen much commoditization and still uses enterprise-class networking equipment (Sengupta 2011). Increased number of servers demands high end-to-end aggregate bandwidth. The enterprise-class network equipment is expensive and is not designed to accommodate internet-scale services in data centers. Use of enterprise-class equipment therefore experience limited end-to-end network capacity, non-agility, and creation of fragmented server pools (Sengupta 2011).

DC Network is typically based on a three-tier architecture (Kliazovich *et al.* 2012). Three-tier data center architecture is a hierarchical tree based structure comprised of three layers of switching and routing elements having enterprise-class high-end equipment in higher layers of hierarchy. A three-tier DCN architecture is shown in the Figure 1 (Kliazovich *et al.* 2012). Unfortunately, deployment of even highest-end enterprise-class equipment may provide only 50% of end-to-end aggregate bandwidth (Al-Fares *et al.* 2008). To accommodate the growing demands of data center communication, new DCN architectures are required to be designed.

Most of the internet communication in future is expected to take place within the data centers (Mysore *et al.* 2009). Many applications hosted by data center are communication intensive, e.g., more than 1000 server may be touched by a simple web search request. Communication pattern in a data center may be one-to-one, all-to-all, or one-to-all.

Major challenges in the data center network design includes: **(a)** scalability, **(b)** agility, **(c)** fault tolerance, **(d)** maximum end-to-end aggregate bandwidth,

Proceedings 26th European Conference on Modelling and Simulation ©ECMS Klaus G. Troitzsch, Michael Möhring, Ulf Lotzmann (Editors)
ISBN: 978-0-9564944-4-3 / ISBN: 978-0-9564944-5-0 (CD)

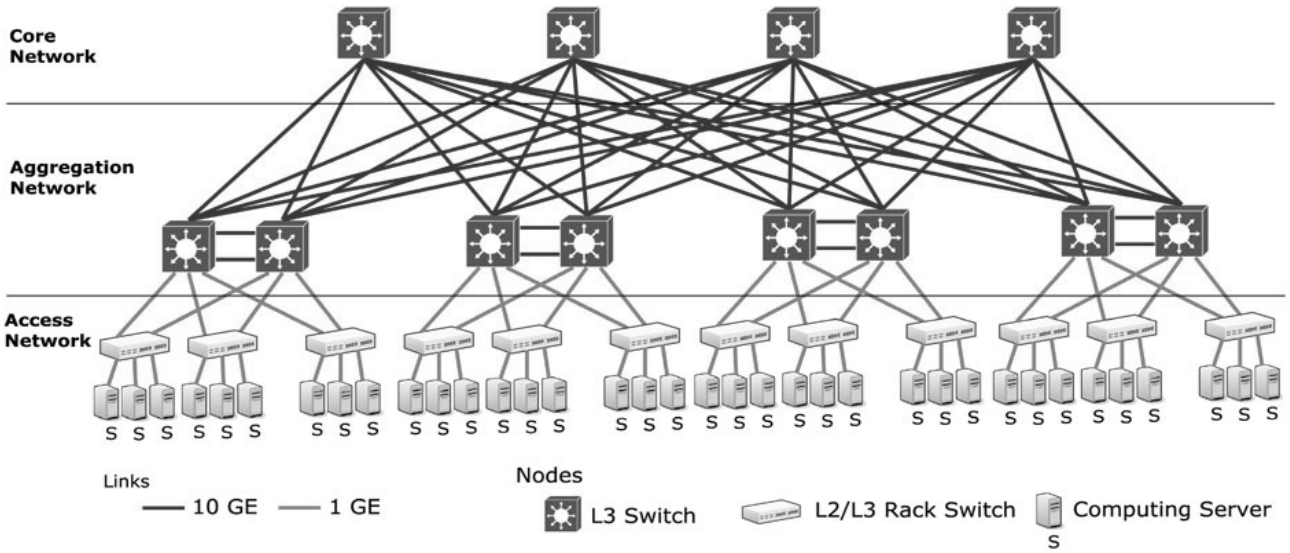

Figure 1: Three-tier Data Center Architecture

(e) automated naming and address allocation, and **(f)** backward compatibility.

DCN architecture is a major part of data center design, acting as a communication backbone, and therefore requires extreme consideration. Numerous DCN architectures have been proposed in recent years (Al-Fares *et al.* 2008; Mysore *et al.* 2009; Guo *et al*. 2008; Guo *et al.* 2009; Greenberg *et al.* 2009; Wang *et al.* 2010; Farrington *et al.* 2010; Abu-Libdeh *et al.* 2010). This paper provides a comparative study of major DCN architectures that are proposed in recent years by implementing: **(a)** proposed network architectures, **(b)** customized addressing scheme, and **(c)** customized routing schemes. We have implemented the fat-tree based architecture (Al-Fares *et al.* 2008) and recursively defined architecture (Guo *et al.* 2008, Guo *et al.* 2009) and compared the performance. To the best of our knowledge, it is the first comparative study of data center network architectures using implementation and simulation.

A simple simulation analysis presented in this paper allows to compare the behavior and performance of the proposed architectures under different workloads and network conditions. The DCN architectures used in the analysis (Al-Fares *et al.* 2008, Guo *et al.* 2008) have been implemented in small-scale system, with 20 servers in the case of DCell model (Guo *et al.* 2008) and 10 machines in the fat-tree model (Al-Fares *et al.* 2008). The simulation analysis may be considered as a general testbed for the realistic networks with large number of hosts and various communication and traffic patterns. The analysis may also be used for the "green data centers'' for designing energy-efficient communication protocols in DCN architectures (Bilal *et al.* 2012; Bianzino *et al.* 2011; Zeadally *et al.* 2012; Khan *et al.* 2012a; Khan *et al.* 2012b;Wang and Khan 2012).

STATE-OF-THE-ART

DCN architecture is an important component of large-scale data centers and has a great impact on the general data center performance and throughput. Numerous empirical and simulation analysis show that almost 70% of network communication takes place within the data center (Mahadevan *et al.* 2009). The cost of the implementation of the conventional two- and Three-tier-like DCN architectures is usually too high and makes the models ineffective in the large-scale dynamic environments (Kliazovich *et al.* 2012). Over the last few years, the fat-tree based and the recursively defined architectures are presented as the promising core structure of the modern scalable data centers. Based on the different types of the routing protocols, the DCN architectures can be classified into the following three basic categories: **(a)** switch-centric models (Al-Fares *et al.* 2008; Greenberg *et al.* 2009), **(b)** hybrid models (using server and switch for packet forwarding (Guo *et al.* 2008, Guo *et al.* 2009)), and **(c)** server-centric models (Abu-Libdeh *et al.* 2010).

The switch centric DCN architectures rely on the network switches to perform routing and communication in the network (e.g., three-tier architecture and the fat-tree based architecture (Al-Fares *et al.* 2008)). Hybrid architectures use a combination of switches and servers (which usually are configured as routers in the network) to accomplish routing and communication (e.g., DCell (Guo *et al.* 2008)). The server- centric architectures do not use switches or routers. The basic components of such models are servers, which are configured as

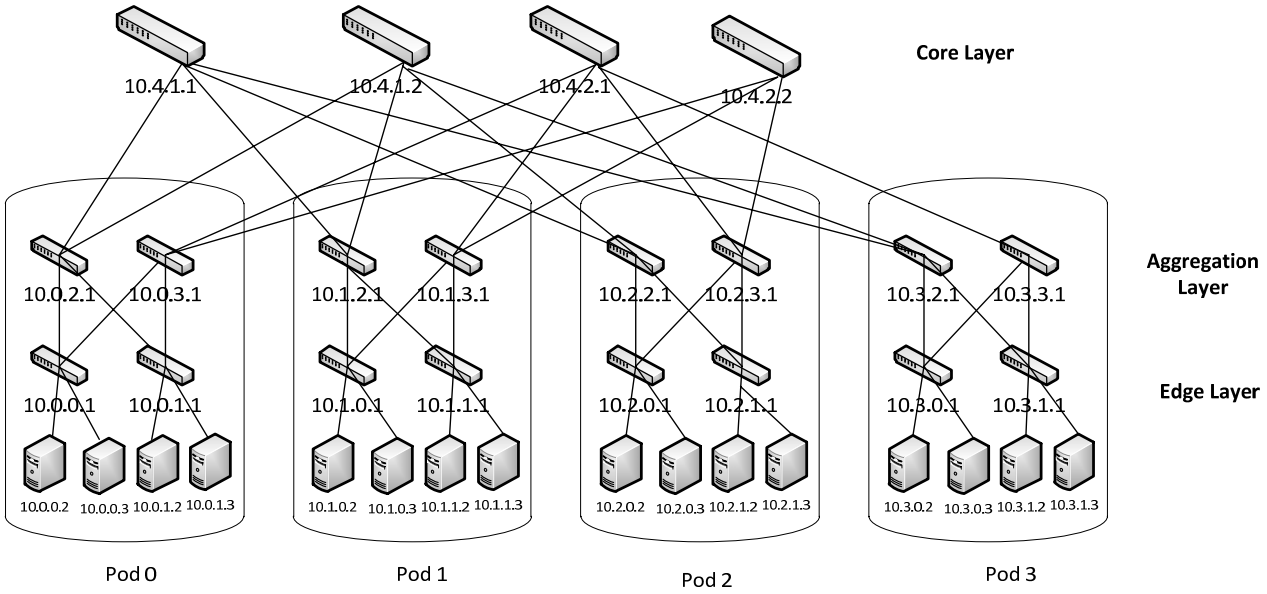

Figure 2: Fat-tree based Architecture

computational devices and data and message processing devices.

The basic model of the fat-tree DCN architecture has been proposed by Al-Fares *et al*. (Al-Fares *et al.* 2008). This model is promoted by the authors as an effective DCN architecture and they have used structured commodity switches to provide more end-to-end bandwidth at much low cost and energy consumption as compared to high-end network switches. Their proposed solution is backward compatible and only makes changes in the switch forwarding functions. The fat-tree based DCN architecture aims to provide 1:1 *oversubscription ratio*. The oversubscription is defined for optimizing the costs of the system design. Oversubscription can be calculated as a ratio of worst-case aggregated bandwidth available to end hosts and the total bisection bandwidth of the network topology (Al-Fares *et al.* 2008). For instance, the oversubscription 4:1 means that the communication pattern may use only 25% of the available bandwidth. The typical oversubscription values are between 2.5:1 and 8:1, and1:80 to 1:240 for the paths near the root at highest level of system hierarchy (Al-Fares *et al.* 2008, Greenberg *et al*. 2009).

Al-Fares *et al.* (Al-Fares *et al.* 2008) adopted a special topology called fat-tree topology (Leiserson 1985). All network structure is composed of *n* pods. Each pod contains *n* servers and *n* switches organized in two layers of *n/2* switches. Every lower layer switch is connected to *n*/*2* hosts in the pod and *n*/*2* upper layer switches (making aggregation layer) of pod. There are $(n/2)^2$ core switches, each connecting to one aggregation layer switch in each of *n* pods. The exemplary interconnection of servers and switches for *n*=4 pods is presented in Figure 2.

The fat-tree based DCN architecture (Al-Fares *et al.* 2008) uses a customized routing protocol, which is based on primary prefix and secondary suffix lookup for next hop. Routing table is divided into two levels. For each incoming packet, destination address prefix entries are matched in primary table. If longest prefix match is found, then the packet is forwarded to the specified port, otherwise the secondary level table is used and the port entry with longest suffix match is used to forward the packet.

A recursively defined DCN architecture, referred to as *DCell model*, has been developed by Guo *et al*. in (Guo *et al.* 2008). In this model the whole system is composed of the cells or pods with *n* servers and a commodity switch. A 0 level cell $DCell_0$ serves as the building block of the whole system. A *level 0* cell ($DCell_0$) comprise of *n* commodity servers and a mini switch. Higher levels of cells are built by connecting multiple lower level ($level_{l-1}$) *DCells*. Each $DCell_{l-1}$ is connected to all other $DCell_{l-1}$ in same $DCell_l$. The DCell provides an extremely scalable architecture and a 3 level DCell having 6 servers in $DCell_0$ can accommodate around 3.26 Million servers. Figure 3 shows a level 2 DCell having 2 servers in each $DCell_0$. Figure shows the connection of only $DCell_{1[0]}$ to all other $DCell_1$.

Unlike the conventional switch based routing used in the hierarchical and fat-tree based DCN architectures, the DCell uses a hybrid routing and data processing protocol. Switches are used to communicate among the servers in same $DCell_0$. The communication with servers in other

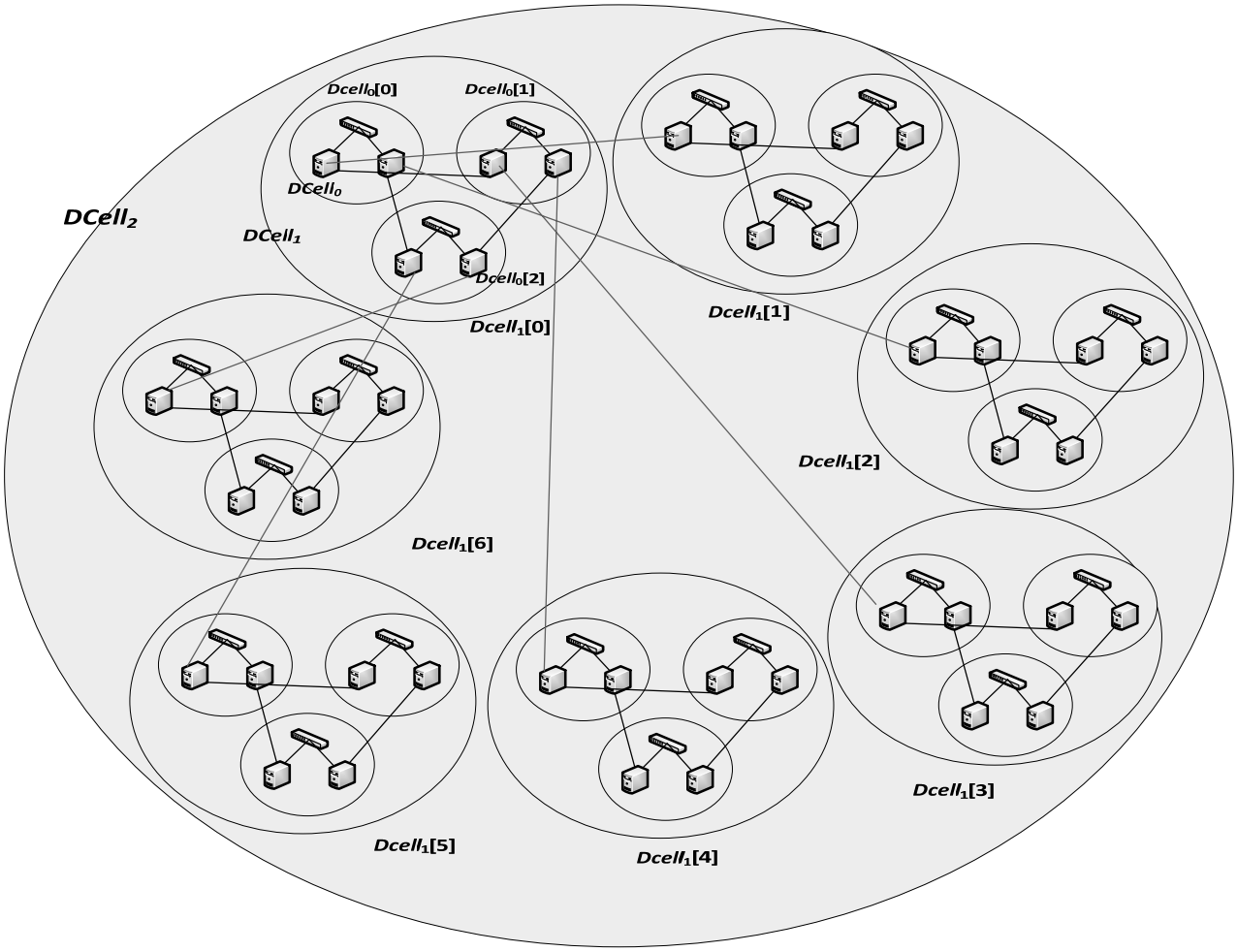

Figure 3: Level 2 DCell ($DCell_2$)

DCells is performed by servers acting as routers. In fact just computational servers are also considered as the routers in the system. The DCellRouting scheme is used in the DCell architecture to compute the path from the source to destination node exploiting divide and conquer approach. Source node (*s*) computes the path from *s* to destination (*d*). The link that interconnects the DCells that contain the *s* and *d* in the same level is calculated first and then sub-paths from *s* to link and from link to *d* is calculated. Combination of both sub-paths gives the path from *s* to *d*. The DCellRouting is not a minimum hop routing scheme therefore, the calculated route has more hops than the shortest path routing.

Popa *et al*. (Popa *et al.* 2010) present a methodology of the theoretical approximation of cost of different DCN architectures by using the system performance metrics, namely network latency and capacity. The authors also presented a cost comparison of different DCN architectures by using current market price of energy and equipment. Gyarmati *et al*. (Gyarmati *et al*. 2010) compared the energy consumption in different DCN architectures. The authors have derived the results from mathematical analysis by considering the number of servers, total number of ports, and switches. They considered the static predefined measurement of energy consumption for devices. Chen *et al.* **(**Chen *et al.* 2010) have surveyed the routing protocols used in the major DCN architecture models and have addressed some open questions and security issues in DCN routing. Implementation of DCN architectures would be discussed in next section.

SIMULATION EXPERIMENTS

Environment

The main aim of a simple empirical simulation analysis presented in this section is to provide the insight of different DCN architectures in a realistic manner. Two

DCN core architectural models, namely the fat-tree based architecture (Al-Fares *et al.* 2008) and recursively build architecture (Guo *et al.* 2008), have been used for the simulation of the multi-level DCN performance. These models have been adapted to illustrate the efficiencies of different routing protocols (Guo *et al.* 2009; Greenberg *et al.* 2009). We used ***ns-3*** discrete-event network simulator for implementing the considered DCN architectures (ns-3 2012). The ***ns-3*** simulator allows to model various realistic scenarios. The most important salient features of ***ns-3*** simulator are: **(a)** an implementation of real IP addresses, **(b)** BSD socket interface, **(c)** multiple installations of interfaces on a single node, **(d)** real network bytes are contained in simulated packets, and **(e)** packet traces can be captured and analyzed using tools like Wireshark. In this work, the DCN architectures uses: **(a)** the customized addressing scheme, **(b)** the customized routing protocols that strongly depend on the applied addressing scheme (e.g., (Al-Fares *et al.* 2008)). Therefore, ***ns-3*** deemed as the most appropriate network simulator for our work. One of the major drawbacks of using the ***ns-3*** simulator is a lack of the switch module in ***ns-3*** library. and conventional Ethernet protocol cannot be implemented. Therefore, we configured Point-To-Point links for the connection of switches and nodes.

Implementation Details

The considered DCN architectures have been implemented using the multiple network interfaces at each node as required. In the case of fat-tree based topology, the primary and secondary routing tables are generated dynamically based on the number of pods. The realistic IP addresses have been generated for all nodes in the system and linked to appropriate lower layer switches. Three layers of switches have been created, interconnected properly and populated with primary and secondary routing tables. We have customized the general simulator model by extending it with an additional routing module for processing two layered based primary and secondary routing tables in ***ns-3***.

In the DCell architecture, the DCellRouting protocol is implemented to generate the end-to-end path at source node. We have specified a scalable addressing protocol for this model. The DCellRouting lacks the generic protocol description and a specific routing scenario is discussed by authors. We have used source based routing to route the packets from the source to destination.

Simulation Results

We have simulated the fat-tree based DCN architecture using its customized routing algorithm. The DCell architecture is implemented with the DCell's customized topology and addressing scheme. However, we have used built-in source based routing module i.e., Nix-Vector routing (Nix-Vector 2012). We have used uniform random distribution and exponential random distribution to compute the communication pattern and traffic generation. The performances of the considered architectural models have been verified by using the following two criteria:

(a) ***Average packet delay***: Average packet delay in the network is calculated using the Eq. (2).

$$D_{agg} = \sum_{j=1}^{n} d^{j}, \quad \textbf{(1)}$$

$$D_{avg} = \frac{D_{agg}}{n}, \quad \textbf{(2)}$$

where D_{agg} calculated in Eq. (1) is the aggregate delay of all the received packets and d_j is the delay of packet *j*. *n* is total number of packets received in the network, whereas D_{avg} is average packet delay.

(b) ***Average network throughput***: Average network throughput is calculated using the Eq. 3.

$$\tau = \frac{\left(\sum_{i=1}^{n} (P_i) \times \delta \right)}{D_{agg}}, \quad \textbf{(3)}$$

where τ is the throughput, P_i is the ith received packet, δ is the size of the packet (in bits), and D_{agg} is the aggregate packets delay.

The parameters used in the simulation of the fat-tree based architecture are given in Table 1.

Table 1: Simulation parameters for the fat-tree

number of pods	4 – 72
number of nodes	16 – 93312
simulation running time	10 – 1000 seconds
Packet size	1024 bytes

The parameters used in the simulation of the the DCell architecture are given in Table 2.

Table 2: Simulation parameters for the DCell

number of levels	1 – 3
number of nodes in $DCell_0$	2 – 8
total nodes in the DCell	20 – 5000
simulation running time	10 – 1000 seconds
routing algorithm	Nix-Vector

Simulations are performed by varying aforementioned parameters to achieve results in respective topologies. A comparison of network throughput and average packet

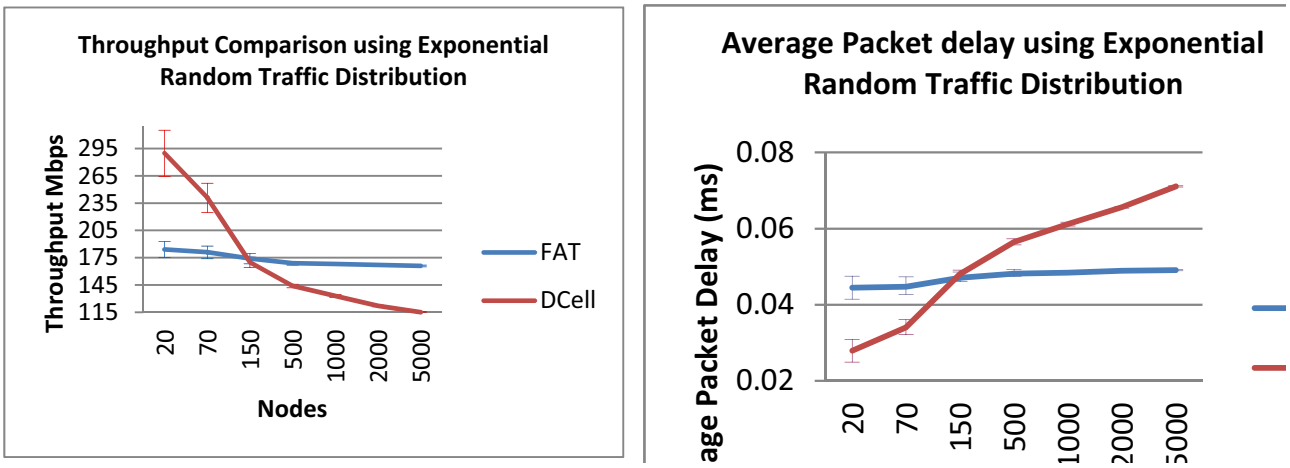

Figure 4: Throughput and average Packet Delay using Exponential Random Traffic distribution

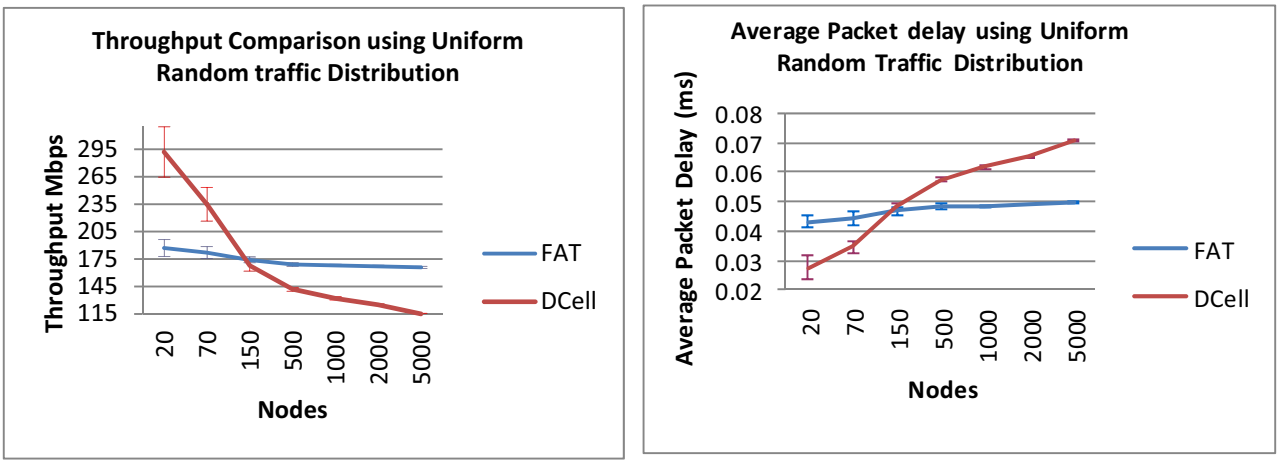

Figure 5: Throughput and average Packet Delay using Uniform Random Traffic distribution

delay for both of the aforementioned architectures is shown in Figure 4. Communication pattern and traffic generation is achieved by using exponential random distribution. Figure 5 shows the comparison of network throughput and average packet delay using uniform random communication pattern and traffic generation.

The simulation results show that the fat-tree topology is consistent in throughput and a slight degradation in throughput is observed when the number of nodes is increased. More than 1 Million packets are exchanged in simulating the fat-tree topology with 72 pods and 93,312 serves in 100 seconds. The average network throughput for 256 to 93,000 nodes was observed in a range from 169Mbps to 165Mbps respectively. The average packet delay in the fat-tree based architecture is also observed to be nearly consistent. The observed average packet delay falls in the range from 0.043 ms to 0.049 ms for 4 pods to 72 pods simulation respectively. The observed results depict that the performance of the fat- tree based architecture is independent of the number of nodes.

In case of the DCell architecture, we have used Nix-Vector source based routing. The observed results show a decline in curve when the number of nodes is increased. The DCell outperforms the fat-tree based architecture for small number of nodes but gradually declines in terms of throughput when number of nodes and *DCell* levels increase. A similar behavior is observed in average packet delay. The results show that the throughput decreases greatly as the number of nodes increase from 20 to 500. However, results show a minor curve declination after the number of nodes reaches 500.

The results show that the fat-tree base architecture outperforms the DCell in terms of average network throughput and packet latency.

CONCLUSIONS

We presented a comparison of the major data center architectures that addresses the issues of network scalability and oversubscription. We simulated the performance of DCN architectures in various realistic scenarios. The simulation results show that the fat-tree based DCN architecture performs better than the DCell DCN architecture in terms of average network throughput and latency. In our future work, we plan to implement the DCell customized routing scheme and compare its performance with shortest path routing and the fat-tree based routing schemes. We will also

implement legacy data center architecture and compare the performance of all major data center architectures in terms of cost and performance.

REFERENCES

Abu-Libdeh, H.; P. Costa; A. Rowstron; G. O'Shea; and A. Donnelly. 2010. "Symbiotic Routing in Future Data Centers". In *Proceedings of the ACM SIGCOMM 2010 conference* (New Delhi, India). 51-62.

Al-Fares, M.; A. Loukissas; and A. Vahdat. 2008. "A scalable, commodity data center network architecture". In *Proceedings of the ACM SIGCOMM 2008 conference on Data communication* (Seattle, WA). 63-74.

Arnold, S. 2007. Google Version 2.0: The Calculating Predator. Infonortics Ltd.

Bianzino, P.; C. Chaudet; D. Rossi; and J. Rougier. 2012. "A Survey of Green Networking Research". *Communications Surveys and Tutorials*, *IEEE* 14, No.1, 3-20.

Bilal K.; S.U. Khan; N. Min-Allah; and S.A. Madani. (Forthcoming). "A Survey on Green Communications using Adaptive Link Rate." *Cloud Computing*.

Carter, A. 2007. Do It Green: Media Interview with Michael Manos. http://edge.technet.com/Media/Doing-IT-Green/, accessed, Feb. 20, 2012.

Chen K.; C.C. Hu; X. Zhang; K. Zheng; Y. Chen; and A.V. Vasilakos. 2011. "Survey on Routing in Data Centers: Insights and Future Directions." *IEEE Network* 25, No.4, 6-10.

Farrington, N.; P. George; R. Sivasankar; B. Hajabdolali; S. Vikram; F. Yeshaiahu; P. George; and A. Vahdat. 2010. "Helios: A Hybrid Electrical/Optical Switch Architecture for Modular Data Centers". In *Proceedings of the ACM SIGCOMM 2010 conference* (New Delhi, India). 339-350.

Greenberg, A.; J. R. Hamilton; N. Jain; S. Kandula; C. Kim; P. Lahiri; D. Maltz; P. Patel; and S. Sengupta. 2009. "VL2: A Scalable and Flexible Data Center Network". In *Proceedings of the ACM SIGCOMM 2009 conference* (Barcelona, Spain). 51-62.

Guo, C.; H. Wu; K. Tan; L. Shi; Y. Zhang; and S. Lu. 2008. "DCell: A Scalable and Fault-tolerant Network Structure for Data Centers." *ACM SIGCOMM Computer Communication Review* 38, No.4, 75-86.

Guo, C.; G. Lu; D. Li; H. Wu; X. Zhang; Y. Shi; C. Tian; Y. Zhang; and S. Lu. 2009. "BCube: A High Performance, Server-centric Network Architecture for Modular Data Centers". In *Proceedings of the ACM SIGCOMM 2009 conference* (Barcelona, Spain). 63-74.

Gyarmati; and T. Trinh. 2010. "How can architecture help to reduce energy consumption in data center networking?". In *Proceedings of the 1st International Conference on Energy-Efficient Computing and Networking* (Passau, Germany), 183-186.

Ho, T. 2007. Google Architecture. http://highscalability.com/google-architecture, accessed February 20, 2012.

Khan S.U.; S. Zeadally ; P. Bouvry; and N. Chilamkurti. (Forthcoming). "Green Networks." *Journal of Supercomputing*.

Khan S.U.; L. Wang; L. Yang; and F. Xia. (Forthcoming). "Green Computing and Communications." *Journal of Supercomputing.*

Kliazovich, D.; P. Bouvry.; and S.U. Khan. (Forthcoming). "GreenCloud: A Packet-level Simulator of Energy-aware Cloud Computing Data Centers". *Journal of Supercomputing*.

Leiserson, C. E. 1985. "Fat-Trees: Universal Networks for Hardware-Efficient Supercomputing," *IEEE Transactions on Computers* 34, No.10, 892–901.

Mahadevan, P.; P. Sharma; S. Banerjee; and P. Ranganathan. 2009. "Energy aware network operations," *INFOCOM Workshops 2009, IEEE*. 1-6.

Mysore, R. N.; A. Pamboris; N. Farrington; N. Huang; P. Miri; S. Radhakrishnan; V. Subramanya; and A. Vahdat. 2009. "Portland: a scalable fault-tolerant layer 2 data center network fabric". In *Proceedings of the ACM SIGCOMM 2009 conference* (Barcelona, Spain). 39-50.

Nix-Vector routing. 2012. http://www.nsnam.org/doxygen-lease/group__nixvectorrouting.html, accessed February 21, 2012.

ns-3. 2012. http://www.nsnam.org/, accessed February 21, 2012.

Popa L.; S. Ratnasamy; G. Iannaccone; A. Krishnamurthy; and I. Stoica. 2010. "A cost comparison of datacenter network architectures". In *Proceedings of the 6th International Conference* (Philadelphia, Pennsylvania
) .1-16.

Rabbe, L. 2006. Powering the Yahoo! Network. http://yodel.yahoo.com/2006/11/27/powering-the-yahoo-network/, accessed February 20, 2012.

Sengupta, S. 2011. "Cloud Data Center Networks: Technologies, Trends, and Challenges.". *ACM SIGMETRICS Performance Evaluation Review* 39,No.1, 355-356.

Snyder, J. 2007. "Microsoft: Datacenter Growth Defies Moore's Law." http://www.pcworld.com/article/id,130921/article.html, accessed February 20, 2012

Wang G.; G. David; M. Kaminsky; K. Papagiannaki; T. Eugene; M. Kozuch; M. Ryan. 2010. "c-Through: Part-time Optics in Data Centers". In *Proceedings of the ACM SIGCOMM 2010 conference* (New Delhi, India). 327-338.

Wang L. and S.U. Khan. (Forthcoming). "Review of Performance Metrics for Green Data Centers: A Taxonomy Study." *Journal of Supercomputing*.

Zeadally, S.; S.U. Khan; and N. Chilamkurti. (Forthcoming). "Energy-Efficient Networking: Past, Present, and Future." *Journal of Supercomputing.*

SIMULATION OF OVERLOAD CONTROL IN SIP SERVER NETWORKS

Pavel O. Abaev (speaker)
Yuliya V. Gaidamaka
Telecommunication Systems Department
Peoples' Friendship University of Russia
Miklukho-Maklaya str., 6,
117198, Moscow, Russia
Email: pabaev@sci.pfu.edu.ru,
ygaidamaka@sci.pfu.edu.ru

Alexander V. Pechinkin
Rostislav V. Razumchik
Sergey Ya. Shorgin
Institute of Informatics Problems of RAS
Vavilova, 44-1,
119333, Moscow, Russia
Email: apechinkin@ipiran.ru,
rrazumchik@ieee.org, sshorgin@ipiran.ru

KEYWORDS

Signalling network, SIP, hop-by-hop overload control, threshold, hysteretic load control.

ABSTRACT

In this study, we investigated a signalling load control mechanism for SIP server networks and developed a corresponding queuing model. The so-called hop-by-hop overload control, known from recent IETF drafts and RFCs, was considered and a similar buffer overload control scheme which was developed for the SS7 signalling link in ITU-T Recommendation Q.704, was proposed. The mechanism is based on hysteretic load control with thresholds for reducing potential oscillations between the control-on and control-off states under certain loading conditions. Adjustment of three types of thresholds – the overload onset threshold, the overload abatement threshold, and the overload discard threshold – makes possible the regulation of signalling traffic to meet blocking requirements. In this study, we built and analyzed the $M|M|1$ queue with bi-level hysteretic input load control. A numerical example illustrating the control mechanism that minimizes the return time from overloading states satisfying the throttling and mean control cycle time constraints is also presented.

INTRODUCTION

Threshold load control is a well-known and reliable tool for preventing SS7 signalling link congestion (ITU-T Recommendation Q.704, 1996). In this paper, it is shown that the same technique (Takshing and Yen, 1983; Takagi, 1985) is applicable to overload control problems in a SIP server signalling network, stated in recent IETF RFCs and drafts (RFC 3261, 2002; RFC 5390, 2008; RFC 6357, 2011; IETF draft SIP Overload Control, 2012; IETF draft SIP Rate Control, 2012) and still not solved. To that end, we analyzed carefully the overloading control mechanism for SIP servers defined in (RFC 3261, 2002). Some variations of the control mechanism studied in numerous documents and papers, e.g. in (ITU-T Recommendation Q.704, 1996; RFC 3261, 2002; RFC 5390, 2008; RFC 6357, 2011; IETF draft SIP Overload Control, 2012; IETF draft SIP Rate Control, 2012; Ohta, 2009; Hilt and Widjaja, 2008; Shen et al., 2008; Montagna and Pignolo, 2008; Garroppo et al., 2009; Montagna and Pignolo, 2008; Homayouni et al., 2010; Abdelal and Matragi, 2010; Montagna and Pignolo, 2010; Garroppo et al., 2011).

We investigated a two-stage server overload processing comprising overload detection and overload mitigation. The total number of messages in the buffer, i.e. buffer occupancy, was monitored to detect overloading. In order to mitigate or eliminate overloading, we restricted or prohibited input signalling load. Three types of thresholds are used to control overloading – overload onset threshold H, overload abatement threshold L, and overload discard threshold R. Overloading occurs when buffer occupancy increases and exceeds the overload onset threshold, H. The input load is then reduced to avoid overloading. However, the load does not return to the normal load value immediately after overloading mitigation, but the buffer occupancy becomes lower than the overload abatement threshold, L, after decreasing. This technique is called hysteretic load control (ITU-T Recommendation Q.704, 1996) by analogy with the terminology of SS7. Two hysteretic thresholds (onset and abatement) are needed to reduce the potential oscillations between the control-on and control-off states under certain loading conditions.

The paper is organized as follows. First, it is shown that overload can be implemented locally, hop-by-hop, and end-to-end according to (RFC 6357, 2011). Queuing models for local overload control have been proposed in (Abaev et al., 2011) and a queuing model for hop-by-hop overload control is built in this study. Second, a queuing system with bi-level hysteretic load control is studied and an analytical solution for steady-state distribution of queue length and mean control cycle time derived. A numerical example is then presented and in conclusion, the main results of the study are summarized.

DEVELOPING SIMULATION MODEL FOR SIP SERVER OVERLOAD CONTROL

In this section, a simulation model for hop-by-hop overload control, which was proposed in (RFC 6357, 2011) is

Proceedings 26th European Conference on Modelling and Simulation ©ECMS Klaus G. Troitzsch, Michael Möhring, Ulf Lotzmann (Editors)
ISBN: 978-0-9564944-4-3 / ISBN: 978-0-9564944-5-0 (CD)

built. Let us briefly describe the main features of the SIP mechanism, which is needed to convey overload feedback from the receiving to the sending SIP server. Three different alternative feedback mechanisms – local, hop-by-hop, and end-to-end – are illustrated in Fig. 1, according to (RFC 6357, 2011).

If overload control is implemented locally, the SIP server measures the current utility of its processor and makes a decision to select the messages that will be affected and determines whether they are rejected or redirected. In case of end-to-end overload control, all the receiving servers along the path of a request should measure the current utility of their processors and notify the sender of a request concerning overloading. All the receiving servers have to cooperate to jointly determine the overall feedback for this path. Each sending server implements the algorithms needed to limit the amount of traffic forwarded to the receiving server. Note that in (IETF draft SIP Overload Control, 2012), the local mechanism was recognized as ineffective and end-to-end mechanism deemed difficult to implement.

Hop-by-hop overload control does not require that all SIP entities in a network support it. It can be used effectively between two adjacent SIP servers if both servers support overload control and does not depend on the support from any other server or user agent. The more SIP servers in a network support hop-by-hop overload control, the better protected the network is against occurrences of overload. Therefore, overload control is best performed hop-by-hop. The receiving SIP server monitors the current utility of its processor and notifies the sending server in case of overloading. The sending server acts on this feedback and reduces the outgoing load, for example, by rejecting messages if needed. According to the loss-based overload control mechanism (IETF draft SIP Overload Control, 2012), a server asks an upstream neighbour to reduce by the desired percentage the number of requests it would normally forward to this server. For example, a server can ask an upstream neighbour to reduce the number of requests by 10%. The upstream neighbour then redirects or rejects the messages that are destined for this server with dropping probability $q = 0.1$. The alternative is a rate-based overload control mechanism (IETF draft SIP Rate Control, 2012). When the rate-based overload control mechanism is used, a server notifies an upstream neighbour to send requests at a rate no greater than or equal to the desired number of requests per second.

The above hop-by-hop overload control principles have been used as the basis of a simulation model and for formulation of the optimization problem of hop-by-hop overload control. In addition, analytical formulae were developed to support the simulation. We considered the interaction between two adjacent SIP servers that use loss-based overload control mechanism and built a simple model with the aim of analyzing the control parameters using the bi-level hysteretic load control idea from (ITU-T Recommendation Q.704, 1996).

Similarly, the example discussed in (IETF draft SIP Rate Control, 2012), we are modeling message processing as a single work queue that contains incoming messages. Fig. 2 shows a single-server queuing system with hysteretic overload control with two thresholds, L and H. In the next section, this is denoted by $M|M|1|\langle L, H\rangle|R$ according to the Kendall classification, where R stands for the overload discard threshold.

Customers arrive at the system and receive service in accordance with the overload control algorithm. The mean processing time is μ^{-1}. The server operates in three modes: normal ($s = 0$), overload ($s = 1$), and discard ($s = 2$), where s is the overload status. When the queue length increases and exceeds the threshold, H, in the normal mode, the system detects the overload and switches to the overload mode. In the overload mode, the system reduces input flow: newly arriving customers are discarded with dropping probability, q. Thereafter, if the queue length decreases and drops below the threshold, L, in the overload mode, the system detects the elimination of overload, turns to normal mode and starts to put all newly arrived customers into the queue. If in the overload mode the queue length continues increasing and reaches threshold, R, the system turns to the discard mode and all newly arrived customers are discarded. After that, the queue length starts decreasing in the discard mode and when it drops below the threshold, H, the system detects mitigation of overloading, turns to the overload mode and starts to put newly arrived customers into the queue with probability $p = 1 - q$.

Let n denote the queue length, $n = 0, ..., R$. Then the state space of the system is of the form $\mathcal{X} = \mathcal{X}_0 \cup \mathcal{X}_1 \cup \mathcal{X}_2$, where $\mathcal{X}_0$ is the set of states of normal load, $\mathcal{X}_1$ is the set of overload states, and $\mathcal{X}_2$ is the set of discard states. These sets are given by following formulae:

$$\mathcal{X}_0 = \{(s, n) : s = 0, 0 \le n \le H - 1\},$$
$$\mathcal{X}_1 = \{(s, n) : s = 1, L \le n \le R - 1\},$$
$$\mathcal{X}_2 = \{(s, n) : s = 2, H + 1 \le n \le R\}.$$

Then the input load function $\lambda(s, n)$ is shown in Fig. 3 and specified by the following relation:

$$\lambda(s, n) = \begin{cases} \lambda, & (s, n) \in \mathcal{X}_0, \\ p\lambda, & (s, n) \in \mathcal{X}_1, \\ 0, & (s, n) \in \mathcal{X}_2. \end{cases}$$

The probability of the system being in the set of normal load states is denoted by $P(\mathcal{X}_0)$, the probability of being in the set of overload states by $P(\mathcal{X}_1)$, and the probability of being in the set of discard states by $P(\mathcal{X}_2)$. Let τ_0 denote the average duration of the system in set $\mathcal{X}_0$. The key performance measures of the system are overload probability $P(\mathcal{X}_1)$, discard probability $P(\mathcal{X}_2)$, and $\overline{\tau}$ as the mean return time from overloading states $\mathcal{X}_1 \cup \mathcal{X}_2$.

Next, we analyze the model developed in this section, and derive formulas for the analysis of its key performance measures.

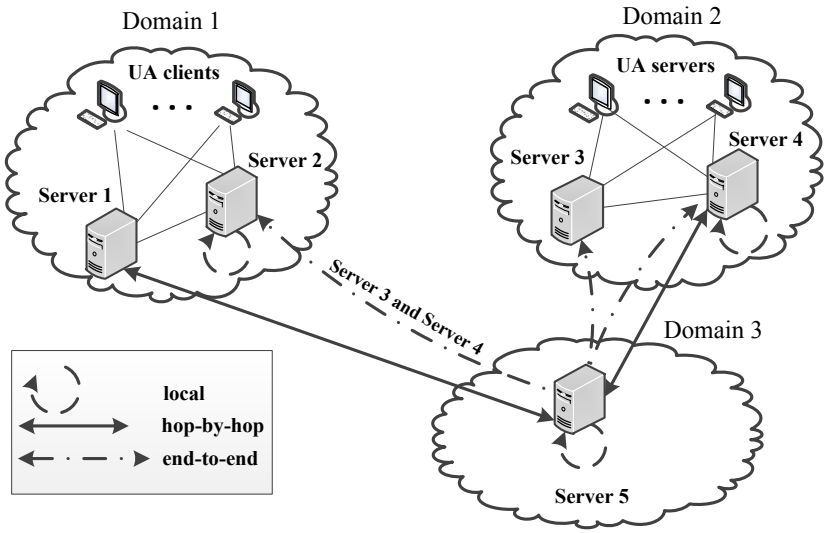

Figure 1: Types of overload control mechanisms

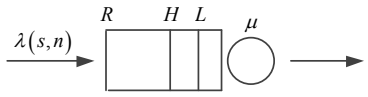

Figure 2: $M|M|1|\langle L,H\rangle|R$ queuing model

QUEUING MODEL AND ITS PERFORMANCE MEASURES

In this section, the queuing model with thresholds L, H, and R, shown in Fig. 2, and with input load function $\lambda(s,n)$, shown in Fig. 3, is considered. The Markov process, $\mathbf{X}(t)=(s,n)$, which completely describes the system over the state space, $\mathcal{X}$, is considered. Our goal is to find stationary probability distribution of the number of customers in the system, $p_{s,n}$, $(s,n)\in\mathcal{X}$, and the mean return time from the states of the set $\mathcal{X}_1\cup\mathcal{X}_2$ to the states of the set $\mathcal{X}_0$, namely to the state $(0,L-1)$. To find the stationary distribution, some auxiliary variables were defined.

Auxiliary variables

Let $\lambda_1=p\lambda$ and denote α_n, $n=L,\dots,R-1,\ \ n\neq H$ the probability that until the first time in the queue remains $n-1$ customers, there will never be R customers. Omitting the intermediate steps, the probabilities, α_n , are represented in the following forms:

$$\alpha_{R-1}=\frac{\mu}{\lambda_1+\mu},\ \ \alpha_{H-1}=\frac{\mu}{\lambda+\mu},$$

$$\alpha_n=\frac{\mu}{\lambda_1+\mu}+\frac{\lambda_1}{\lambda_1+\mu}\alpha_{n+1}\alpha_n,\ \ n=H+1,\dots,R-2,$$

$$\alpha_n=\frac{\mu}{\lambda+\mu}+\frac{\lambda}{\lambda+\mu}\alpha_{n+1}\alpha_n,\ \ n=L,\dots,H-2.$$

The probability that until the first time in the queue remain $n+1$ customers, there will never be less than L customers is denoted by $\beta_n,\ n=L,\dots,H-1$. These probabilities can be calculated using the formula $\beta_L=\lambda_1/(\lambda_1+\mu)$ and, according to the law of total probability, we have

$$\beta_n=\frac{\lambda_1}{\lambda_1+\mu}+\frac{\mu}{\lambda_1+\mu}\beta_{n-1}\beta_n,\ \ n=L+1,\dots,H-1.$$

Equilibrium Equations

It is easy to see that the stationary probabilities satisfy the following system of equilibrium equations:

$$\lambda p_{0,n-1}=\mu p_{0,n},\ \ n=1,\dots,L-1, \tag{1}$$

$$(\mu+\lambda)p_{0,n}=\lambda\alpha_{n+1}p_{0,n}+\lambda p_{0,n-1},\ \ n=L,\dots,H-2, \tag{2}$$

$$(\mu+\lambda)p_{0,H-1}=\lambda p_{0,H-2},\ \ n=H-1, \tag{3}$$

$$(\mu+\lambda_1)p_{1,H}=\lambda p_{0,H-1}+(\mu\beta_{H-1}+\lambda_1)p_{1,H},\ \ n=H, \tag{4}$$

$$(\mu+\lambda_1)p_{1,n}=\lambda_1 p_{1,n-1}+\lambda_1\alpha_{n+1}p_{1,n},\ n=H+1,\dots,R-2, \tag{5}$$

$$(\mu+\lambda_1)p_{1,R-1}=\lambda_1 p_{1,R-2},\ \ n=R-1, \tag{6}$$

$$\mu p_{2,R}=\lambda_1 p_{1,R-1},\ \ n=R, \tag{7}$$

$$\mu p_{2,n}=\mu p_{2,n+1},\ \ n=H+1,\dots,R-1, \tag{8}$$

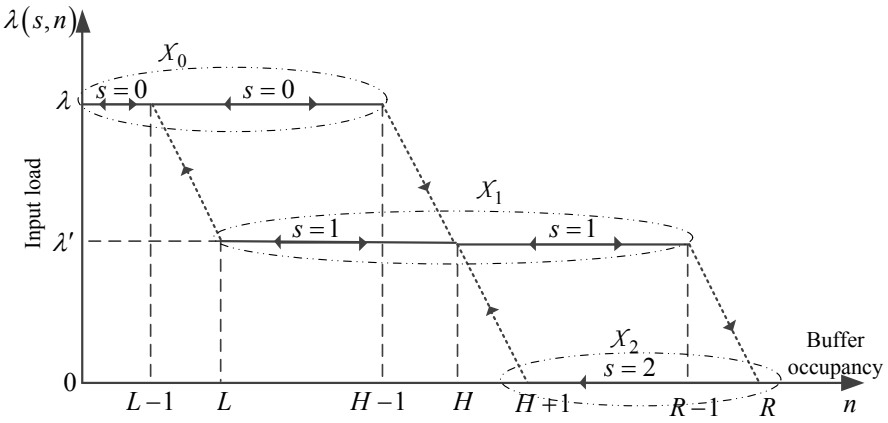

Figure 3: Bi-level hysteretic load control mechanism

$$(\mu+\lambda_1)p_{1,n} = \mu p_{1,n+1} + \mu\beta_{n-1}p_{1,n}, \quad n = L+1,\dots,H-1, \tag{9}$$

$$(\mu+\lambda_1)p_{1,L} = \mu p_{1,L+1}, \quad n = L, \tag{10}$$

$$\sum_{n=0}^{H-1} p_{0,n} + \sum_{n=L}^{R-1} p_{1,n} + \sum_{n=H+1}^{R} p_{2,n} = 1. \tag{11}$$

Equations (1), (3), (6), (7), (8), (10) are the global balance equations. The other equations are obtained using the elimination method found in (Bocharov et al., 2003). Let us explain the derivation of equation (2). For the state $n = L,\dots,H-2$ exclude from consideration states $n+1,\dots,H-1$. Clearly, the probabilistic flow from the state n equals $(\mu+\lambda)p_{0,n}$. The probabilitstic flow to the state n equals the sum of $\lambda p_{0,n-1}$ and $\lambda\alpha_{n+1}p_{0,n}$, because the Markov process with rate λ leaves the state n and with probability α_{n+1} comes back, not reaching state $n = H$. Thus, using the global balance principle yields (2). Equations (5) and (9) are obtained using a similar argument. Now consider the derivation of equation (4). Fix the state $n = H$ and exclude from consideration all other states of sets $\mathcal{X}_1$ and $\mathcal{X}_2$. The probabilistic flow from the state H equals $(\mu+\lambda_1)p_{1,H}$. The Markov process with rate $\lambda_1+\mu$ leaves state H, but, leaving it at rate λ_1, comes back with probability 1 and leaving it at rate μ, comes back not reaching state $L-1$, with probability β_{H-1}. Thus the probabilistic flow to state H equals $\lambda p_{0,H-1} + (\mu\beta_{H-1}+\lambda_1)p_{1,H}$ and using the global balance principle yields (4).

Stationary Distribution

Let us find the solution of the system (1)-(11). Let $p_{0,0} = 1$. From equation (1) $p_{0,n},\ n = 1,\dots,L-1$, is obtained in the form $p_{0,n} = (\lambda/\mu)^n$. From (2), the recursion

$$p_{0,n} = p_{0,n-1}\frac{\lambda}{\mu+\lambda-\lambda\alpha_{n+1}},\ n = L,\dots,H-2$$

is found.

Further, (3) yields the formula for $p_{0,H-1} = \lambda p_{0,H-2}/(\mu+\lambda)$, and (4), the formula for $p_{1,H} = \lambda p_{0,H-1}/(\mu-\mu\beta_{H-1})$. From equation (5), the recursion

$$p_{1,n} = p_{1,n-1}\frac{\lambda_1}{\mu+\lambda_1-\lambda_1\alpha_{n+1}}, n = H+1,\dots,R-2.$$

Using (6) the expression for $p_{1,R-1} = \lambda_1 p_{1,R-2}/(\mu+\lambda_1)$ is obtained; from (7), the expression for $p_{2,R} = \lambda_1 p_{1,R-1}/\mu$; from (8), the expression for $p_{2,n} = p_{2,n+1},\ n = R-1,\dots,H+1$.

Finally, from equation (9), a formula for

$$p_{1,n} = p_{1,n+1}\frac{\mu}{\mu+\lambda_1-\mu\beta_{n-1}}, n = H-1,\dots,L+1$$

is found and equation (10) yields $p_{1,L} = \mu p_{1,L+1}/(\mu+\lambda_1)$.

Using normalization condition (11), the probability $p_{0,0}$ is found and then all other values of $p_{0,n}$, $p_{1,n}$, and $p_{2,n}$ are normalized.

Mean return time

Here, the problem of finding a mean return time from the set of overload and discard states to the set of normal load states is considered.

Let $M_n,\ n = L,\dots,R-1$ be the mean time to reach the moment when the number of customers in the system hits $L-1$ for the first time, given that at some moment there were n customers in the system and newly arriving customers were allowed to enter the system with probability, p. Let $M_n^*,\ n = H+1,\dots,R$, be the mean time to reach the moment when the number of customers in the system hits $L-1$ for the first time, given that at some moment there were n customers in the system and all newly arriving customers were discarded.

Again, in order to find M_n, M_n^* several auxiliary variables are needed. Let:

- $m_n,\ n = L,\dots,H$, be the mean time to the moment when the number of customers in the system

hits $n-1$ for the first time, given that at some moment there were n customers in the system, which accepted newly arriving customers with probability, p;

- $m_n^*,\ n = H+1, \ldots, R$, be the mean time to the moment when the number of customers in the system hits $n-1$ for the first time, given that at some moment there were n customers in the system, which discarded all newly arriving customers;
- $m_n,\ n = H+1, \ldots, R-1$, be the mean time to the moment when the number of customers in the system hits $n-1$ for the first time (if the system always accepted newly arriving customers with probability, p) or hits H (if at some moment the system started to discard all newly arriving customers), given that at some moment there were n customers in the system, which accepted newly arriving customers with probability, p;
- $\tilde{m}_n,\ n = H+1, \ldots, R-1$, be the mean time to the moment when the number of customers in the system hits H for the first time, given that at some moment there were n customers in the system, which accepted new arriving customers with probability, p.

These variables are determined using the following relations:

$$m_n^* = \frac{1}{\mu},\ \ n = H+1, \ldots, R,$$

$$m_{R-1} = \frac{1}{\lambda_1+\mu} + \frac{\lambda_1}{\lambda_1+\mu} \cdot \frac{R-H}{\mu},$$

$$m_n = \frac{1}{\lambda_1+\mu} + \frac{\lambda_1}{\lambda_1+\mu}(m_{n+1} + \alpha_{n+1} m_n),\ \ n = H+1, \ldots, R-2,$$

$$m_n = \frac{1}{\lambda_1+\mu} + \frac{\lambda_1}{\lambda_1+\mu}(m_{n+1} + m_n),\ \ n = L, \ldots, H,$$

$$\tilde{m}_{H+1} = m_{H+1},$$

$$\tilde{m}_n = m_n + \alpha_n \tilde{m}_{n-1},\ \ n = H+2, \ldots, R-1.$$

Now, having expressions for m_n, m_n^*, and $\tilde{m}_n$ computational formulae can be obtained for the mean return times M_n and M_n^*,

$$M_n = \tilde{m}_n + M_H,\ \ n = H+1, \ldots, R-1,$$

$$M_n^* = \frac{n-H}{\mu} + M_H,\ \ n = H+1, \ldots, R,$$

$$M_L = m_L,$$

$$M_n = m_n + M_{n-1},\ \ n = L+1, \ldots, H.$$

The method of computing M_n and M_n^* is obvious from the previous equations, therefore we proceed to the numerical example.

NUMERICAL EXAMPLE

In this section, an illustrative numerical example for solving one of the possible design problems of hysteretic overload control is presented, for which the mean control cycle time, τ, is calculated. The value of the mean control cycle time is obtained in the following form:

$$\tau = \tau_0 + \overline{\tau}.$$

Given that the average number of transitions from the set and to the set should be equal in equilibrium, the value of τ_0 can be obtained from the following relation:

$$\tau_0 = \overline{\tau} \cdot \frac{P(\mathcal{X}_0)}{P(\mathcal{X}_1 \cup \mathcal{X}_2)}.$$

Note that $P(\mathcal{X}_i)$ and $P(\mathcal{X}_1 \cup \mathcal{X}_2)$ can be calculated for $M|M|1|\langle L, H\rangle|R$ queue as folows:

$$P(\mathcal{X}_i) = \sum_{(s,n)\in\mathcal{X}_i} p_{s,n},$$

$$P(\mathcal{X}_1 \cup \mathcal{X}_2) = 1 - P(\mathcal{X}_0).$$

The formula for $\overline{\tau}$ can be obtained in the following form:

$$\overline{\tau} = M_H.$$

The blocking probability $B(\mathcal{X}_i)$ in set $\mathcal{X}_i, i = 1, 2$ are given by the following relations:

$$B(\mathcal{X}_1) = qP(\mathcal{X}_1), B(\mathcal{X}_2) = P(\mathcal{X}_2).$$

The problem is stated as follows: minimise the mean return time needed with respect to the choice of the two thresholds, L and H, such that the requirements $R1$–$R3$ are satisfied

$$\begin{aligned} &\overline{\tau}(L,H) \to \min; \\ R1:&\quad P(\mathcal{X}_1) \le \gamma_1; \\ R2:&\quad P(\mathcal{X}_2) \le \gamma_2; \\ R3:&\quad \tau \ge \gamma_3. \end{aligned}$$

The solution to the problem of the choice of L and H for a given dropping probability $q \in \{0,3; 0,4; 0,5; 0,6\}$, mean service time $\mu^{-1} = 5$ ms, and signalling load $\rho = 1,2$ can now be sought. Let us also consider minimising the mean return time, $\overline{\tau}$, such that the discard threshold $R = 100$, $\gamma_1 = 0,2$, $\gamma_2 = 10^{-4}$, and $\gamma_3 = 450$ ms. Using the above formulae, an algorithm for solving the optimization problem was developed. Note that for the optimum solution obtained by this algorithm, requirements $R1$ and $R2$ are always binding so as to make mean control cycle time as high as possible. The results of calculations with the above-defined input data are presented in Table 1.

The example illustrates the optimum bi-level hysteretic overload control mechanism that minimizes the mean return time from overloading states satisfying the overload $R1$, discard $R2$ and mean control cycle time $R3$ constraints. Let us note that relations for stationary distribution allow computations for large values of the thresholds, e.g. $R = 10^6$ in a reasonable time (less 5 s.).

Table 1: Simulation results

Dropping probability, q	Mean return time, $\overline{\tau}$, ms	Blocking probability in $\mathcal{X}_1$, $B(\mathcal{X}_1)$, %	Blocking probability in $\mathcal{X}_2$, $B(\mathcal{X}_2)$, %	Control cycle time, τ, ms	Optimal threshold set, $\langle L, H\rangle$
0.6	121	16.0	0.0072	455	$\langle 78, 90\rangle$
0.5	146	16.1	0.0079	452	$\langle 74, 85\rangle$
0.4	191	16.2	0.0093	470	$\langle 66, 76\rangle$
0.3	273	16.4	0.0087	500	$\langle 44, 52\rangle$

SUMMARY

In this study, a buffer hysteretic control mechanism was developed to solve the problem of hop-by-hop overload control in SIP server networks. This mechanism, in the case of interaction between two adjacent servers, was modelled as a queue with input traffic throttling depending on bi-level hysteretic overload control. The performance of this queue was determined as a function of input load, ρ, dropping probability, q, onset threshold, H, abatement threshold, L, and discard threshold, R. Using the results of this analysis, an overload control mechanism problem was designed: given the blocking and control cycle time requirements, what is the minimum required mean return time to normal load states and what threshold set $\langle L, H\rangle$ allows this optimum to be attained? The search approach of the solution to the design problem was illustrated with a numerical example. Clearly, the considered problem was only one of the possible formulations. Our further research will be devoted to simulation and construction of a model of SIP server, which interoperates with several clients using hop-by-hop overload control, and to studying SIP server overload control mechanism optimization problems.

Notes and Comments. This work was supported in part by the Russian Foundation for Basic Research (grants 10-07-00487-a and 12-07-00108).

REFERENCES

Abaev, P. O. 2011. Algorithm for Computing Steady-State Probabilities of the Queuing System with Hysteretic Congestion Control and Working Vacations. Bulletin of Peoples Friendship University of Russia, No 3. —Pp.58-62.

Abaev, P., Gaidamaka, Yu., Samouylov, K. 2011. Load Control Technique with Hysteresis in SIP Signalling Server. XXIX International Seminar on Stability Problems for Stochastic Models, the Autumn Session of the V International Seminar on Applied Problems of Probability Theory and Mathematical Statistics related to Modeling of Information Systems. — Pp. 67–69.

Abaev, P. O., Korabelnikov, D. M., Pyatkina, D. A., Razumchik, R. V. 2011. Modeling of SIP-server with hysteric overload control as discrete time queueing system. Bulletin of Central Science Research Telecommunication Institute (ZNIIS). —Pp. 67–69.

Abdelal, A., Matragi, W. 2010. Signal-Based Overload Control for SIP Servers. 7th IEEE Consumer Communications and Networking Conference (CCNC). —Pp. 1–7.

Bocharov, P. P. , DÁpice, C., Pechinkin, A. V., Salerno, S. 2003. Queueing theory. Series "Modern Probability and Statistics". Utrecht: VSP Publishing.

Garroppo, R. G., Giordano, S., Niccolini, S., Spagna, S. 2011. A Prediction-Based Overload Control Algorithm for SIP Servers. IEEE Transactions on Network and Service Management. –Vol. 8, No 1. Pp. 39–51.

Garroppo, R. G., Giordano, S., Spagna, S., Niccolini, S. 2009. Queuing Strategies for Local Overload Control in SIP Server. IEEE Global Telecommunications Conference. — Pp.1–6.

Gurbani, V., Hilt, V., Schulzrinne, H. 2012. Session Initiation Protocol (SIP) Overload Control. draft-ietf-soc-overload-control-08.

Hilt, V., Noel, E., Shen, C., Abdelal, A. 2011. Design Considerations for Session Initiation Protocol (SIP) Overload Control. RFC 6357

Hilt, V., Widjaja, I. 2008. Controlling Overload in Networks of SIP Servers. IEEE International Conference on Network Protocols. —Pp.83–93.

Homayouni, M., Nemati, H., Azhari, V., Akbari, A. 2010. Controlling Overload in SIP Proxies: An Adaptive Window Based Approach Using No Explicit Feedback. IEEE Global Telecom. Conference. — Pp. 1–5.

ITU-T Recommendation Q.704. 1996. Signalling System No.7 – Message Transfer Part, Signalling network functions and messages.

Montagna, S., Pignolo, M. 2008. Performance Evaluation of Load Control Techniques in SIP Signalling Servers. Proceedings of Third International Conference on Systems (ICONS). —Pp. 51–56.

Montagna, S., Pignolo, M. 2008. Load Control techniques in SIP signalling servers using multiple thresholds. 13th International Telecommunications Network Strategy and Planning Symposium, NETWORKS. —Pp. 1–17.

Montagna, S., Pignolo, M. 2010. Comparison between two approaches to overload control in a Real Server: "local" or "hybrid" solutions?. 15th IEEE Mediterranean Electrotechnical Conference. — Pp. 845–849.

Noel, E., Williams, P. M. 2012. Session Initiation Protocol (SIP) Rate Control. draft-ietf-soc-overload-rate-control-01.

Ohta, M. 2009. Overload Control in a SIP Signalling Network. International Journal of Electrical and Electronics Engineering. —Pp. 87–92.

Rosenberg, J., Schulzrinne, H., Camarillo, G. et al. 2002. SIP: Session Initiation Protocol. RFC 3261.

Rosenberg, J. 2008. Requirements for Management of Overload in the Session Initiation Protocol. RFC 5390.

Shen, C., Schulzrinne, H., Nahum, E. 2008. Session Initiation Protocol (SIP) Server Overload Control: Design and Evaluation. Lecture Notes in Computer Science. Springer, Vol. 5310. — Pp.149–173..

Takagi, H. 1985. Analysis of a Finite-Capacity $M|G|1$ Queue with a Resume Level. Performance Evaluation. Vol. 5. —Pp. 197–203.

Takshing, P. Y.,Yen, H.-M. 1983. Design algorithm for a hysteresis buffer congestion control strategy. IEEE International Conference on Communication. —Pp. 499–503.

AUTHOR BIOGRAPHIES

PAVEL O. ABAEV received his Ph.D. in Computer Science from the Peoples' Friendship University of Russia in 2012. He has been a senior lecturer in the Telecommunication Systems department of the Peoples' Friendship University of Russia since 2011. His current research focus is on NGN signalling, QoS analysis of SIP, and mathematical modeling of communication networks. His email address is pabaev@sci.pfu.edu.ru.

YULIYA V. GAIDAMAKA received the Ph.D. in Mathematics from the Peoples' Friendship University of Russia in 2001. Since then, she has been an associate professor in the university's Telecommunication Systems department. She is the author of more than 50 scientific and conference papers. Her research interests include SIP signalling, multiservice and P2P networks performance analysis, and OFDMA based networks. Her email address is ygaidamaka@sci.pfu.edu.ru.

ALEXANDER V. PECHINKIN is a Doctor of Sciences in Physics and Mathematics and principal scientist at the Institute of Informatics Problems of the Russian Academy of Sciences, and a professor at the Peoples' Friendship University of Russia. He is the author of more than 150 papers in the field of applied probability theory. His email address is apechinkin@ipiran.ru.

ROSTISLAV V. RAZUMCHIK received his Ph.D. in Physics and Mathematics in 2011. Since then, he has worked as a senior researcher at the Institute of Informatics Problems of the Russian Academy of Sciences. His current research activities focus on stochastic processes and queuing theory. His email address is rrazumchik@ieee.org

SERGEY YA. SHORGIN received a Doctor of Sciences degree in Physics and Mathematics in 1997. Since 1999, he is a Deputy Director of the Institute of Informatics Problems, Russian Academy of Sciences, since 2003 he is a professor. He is the author of more than 100 scientific and conference papers and coauthor of three monographs. His research interests include probability theory, modeling complex systems, actuarial and financial mathematics. His email address is sshorgin@ipiran.ru.

ENHANCING WSN LOCALIZATION ROBUSTNESS UTILIZING HPC ENVIRONMENT

Michal Marks
Research and Academic Computer Network (NASK)
Wawozowa 18, 02-796 Warsaw, Poland
and
Institute of Control and Computation Engineering,
Warsaw University of Technology
Nowowiejska 15/19, 00-665 Warsaw, Poland
Email: mmarks@elka.pw.edu.pl

KEYWORDS

Wireless Sensor Network, positioning, stochastic optimization, simulated annealing, localization system, distributed computing, HPC.

ABSTRACT

The paper treats the problem of localization in Wireless Sensor Network (WSN). In our work, we present and evaluate *Wireless Sensor Network Localization System*, which offers network models generator along with different localization methods including Trilateration & Simulated Annealing algorithm. The paper describes extension of *WSN Localization System* with modules supporting distributed computing in HPC environment. A provided case study concentrate on improving algorithms robustness through parallel solving a huge number of localization tasks. *WSN Localization System* in distributed version is used for generation a set of test networks with various topology parameters and solving the created localization tasks with very different values of method parameters. Applying distributed computing in our HPC infrastructure allows to speedup calculations by two orders of magnitude.

INTRODUCTION TO WSN LOCALIZATION

The goal of localization is to assign geographic coordinates to each node in the sensor network in the deployment area. Wireless sensor network localization is a complex problem that can be solved in different ways, Karl and Willig (2005). A number of research and commercial location systems for WSNs have been developed. They differ in their assumptions about the network configuration, distribution of calculation processes, mobility and finally the hardware's capabilities, Mao et al. (2007); Awad et al. (2007); Zhang et al. (2010).

Recently proposed localization techniques consist in identification of approximate location of nodes based on merely partial information on the location of the set of nodes in a sensor network. An anchor is defined as a node that is aware of its own location, either through GPS or manual pre-programming during deployment. Identification of the location of other nodes is up to an algorithm locating non-anchors. Considering hardware's capabilities of network nodes we can distinguish two classes of methods: range based (distance-based) methods and range free (connectivity based) methods.

The former is defined by protocols that use absolute point to point distance estimates (ranges) or angle estimates in location calculation. The latter makes no assumption about the availability or validity of such information, and use only connectivity information to locate the entire sensor network. The popular range free solutions are hop-counting techniques. Distance-based methods require the additional equipment but through that much better resolution can be reached than in case of connectivity based ones. In our works we concentrate on range based methods.

The paper is structured as follows: at the beginning we formulate the distance-based localization problem. Next, we provide a short overview of our software environment for WSN localization and an extension applied to our software in order to utilize HPC environment. Finally, we provide a case study results and conclusions.

DISTANCE-BASED LOCALIZATION PROCESS

Distance-based localization is a complex problem and solving it requires to combine two techniques: signal processing and algorithms transforming measurements into the coordinates of the nodes in the network. Hence, distance-based localization schemes operate in two stages.

- *Distance estimation stage* – estimation of inter-node distances based on inter-node transmissions.
- *Position calculation stage* – calculation of geographic coordinates of nodes forming the network.

Distance estimation stage

As it was mentioned in the introduction using range based methods we can reach much better resolution than in case of range free ones. However in order to do that the additional equipment is usually required. Each of popular techniques – widely described in literature, Karl and Willig (2005); Mao et al. (2007), such as Angle of Arrival

Proceedings 26th European Conference on Modelling and Simulation ©ECMS Klaus G. Troitzsch, Michael Möhring, Ulf Lotzmann (Editors)
ISBN: 978-0-9564944-4-3 / ISBN: 978-0-9564944-5-0 (CD)

(AoA), Time of Arrival (ToA), Time Difference of Arrival (TDoA) needs an additional stuff such as antennas or accurately synchronized clocks. The only exception from these requirements is a Received Signal Strength Indicator (RSSI) technique.

RSSI is considered as the simplest and cheapest method amongst the wireless distance estimation techniques, since it does not require additional hardware for distance measurements and is unlikely to significantly impact local power consumption, sensor size and thus cost. Main disadvantage of using RSSI is low accuracy. In respect to wireless channel models provided in literature, Rappapport (2002), received power should be a function of distance. However, the RSSI values have a high variability and they cannot be treated as a good distance estimates, Ramadurai and Sichitiu (2003); Benkic et al. (2008). Nevertheless some authors indicate that new radio transceivers can give RSSI measurements good enough to be a reasonable link estimator, Srinivasan and Levis (2006); Barsocchi et al. (2009).

The signal propagation model outlined in Rappapport (2002); Marks and Niewiadomska-Szynkiewicz (2011) allows to estimate the distance if the strength of received signal is known. The objective of the distance estimation stage is to tune up the parameters of propagation model. It should be underline that the aim of this procedure is obtaining the smallest errors in distances estimations as it is impossible to achieve accurate results due to RSSI inaccuracy. In our previous paper, Marks and Niewiadomska-Szynkiewicz (2011), we provided three methods of distance estimation wrt a given network topology and deployment area – Ordinary Least Square Method (OLS), Weighted Least Square Method (WLS) and Geometric Combined Least Square Method (GCLS).

Position calculation stage

In the position calculation stage the measurements of inter-node distances are used to estimate the coordinates of non-anchor nodes in the network. Let us consider a WSN formed by M sensors (anchor nodes) with known position expressed as l-dimensional coordinates $a_k \in \mathbf{R}^l,\ k = 1, \ldots, M$ and N sensors (non-anchor nodes) $x_i \in \mathbf{R}^l,\ i = 1, \ldots, N$ with unknown locations. Our goal is to estimate the coordinates of non-anchor nodes. We can formulate the optimization problem with the performance measure J considering estimated Euclidean distances of all neighbor nodes:

$$\min_{\hat{x}} \Big\{ J = \sum_{k=1}^{M} \sum_{j \in N_k} (||a_k - \hat{x}_j||_2 - \tilde{d}_{kj})^2 + \sum_{i=1}^{N} \sum_{j \in N_i} (||\hat{x}_i - \hat{x}_j||_2 - \tilde{d}_{ij})^2 \Big\}, \tag{1}$$

where $\hat{x}_i$ and $\hat{x}_j$ denote estimated positions of nodes i and j, $\tilde{d}_{kj}$ and $\tilde{d}_{ij}$ distances between pairs of nodes (k, j) and (i, j) calculated based on radio signal measurements, $N_k = \{(k, j) : d_{kj} \leq r\}$, $N_i = \{(i, j) : d_{ij} \leq r\}$ sets of neighbors of anchor and non-anchor nodes ($j = 1 \ldots, N$), and r maximal transmission range (assessed based on available measurements).

The stochastic optimization algorithms can be used to solve the problem (1). Kannan et al. (2005) present the results of location calculation for simulated annealing method. We propose the hybrid technique that uses a combination of the trilateration method, along with simulated annealing (TSA: Trilateration & Simulated Annealing). TSA was described in details in Marks and Niewiadomska-Szynkiewicz (2007). It operates in two phases:

- *Phase 1* – the auxiliary solution (localization) is provided using the geometry of triangles.
- *Phase 2* – the solution of the phase 1 is improved by applying stochastic optimization.

From the perspective of algorithm robustness especially the second phase is important. It is based on simulated annealing (SA) which is a well known heuristic used to solve the localization problem (1), Kannan et al. (2005); Mao et al. (2007). It is implemented as a computer simulation of a stochastic process. It performs point-to-point transformation. Our implementation of SA algorithm is a classical version of SA with one modification – the cooling process is slowed down. At each value of the coordinating parameter T (temperature), not one but $P \cdot N$ non-anchor nodes are randomly selected for modification (where N denotes the number of sensors with unknown positions in the network and P is a reasonably large number to make the system into thermal equilibrium). The general scheme of SA algorithm is presented in Algorithm 1.

TSA algorithm efficiency and robustness strongly depend on control parameters $\alpha, \beta, \Delta d_0, P, T_0, T_f$ specific to the simulated annealing algorithm used in the second phase of TSA, and depicted in Algorithm 1. All these

Algorithm 1 Simulated annealing algorithm

```
T = T_0, T_0 – initial temperature, T_f – final temperature
Δd = Δd_0, Δd_0 – initial move distance
while T > T_f do
    for i = 1 to P · N do
        select a node to perturb
        generate a random direction and move a node at distance Δd
        evaluate the change in the cost function, ΔJ
        if (ΔJ ≤ 0) then
            //downhill move ⇒ accept it
            accept this perturbation and update the solution
        else
            //uphill move ⇒ accept with probability
            pick a random probability rp = uniform(0,1)
            if (rp ≤ exp(−ΔJ/T)) then
                accept this perturbation and update the solution
            else
                reject this perturbation and keep the old solution
            end if
        end if
    end for
    change the temperature: T_new = α · T, T = T_new
    change the distance Δd_new = β · Δd, Δd = Δd_new
end while
```

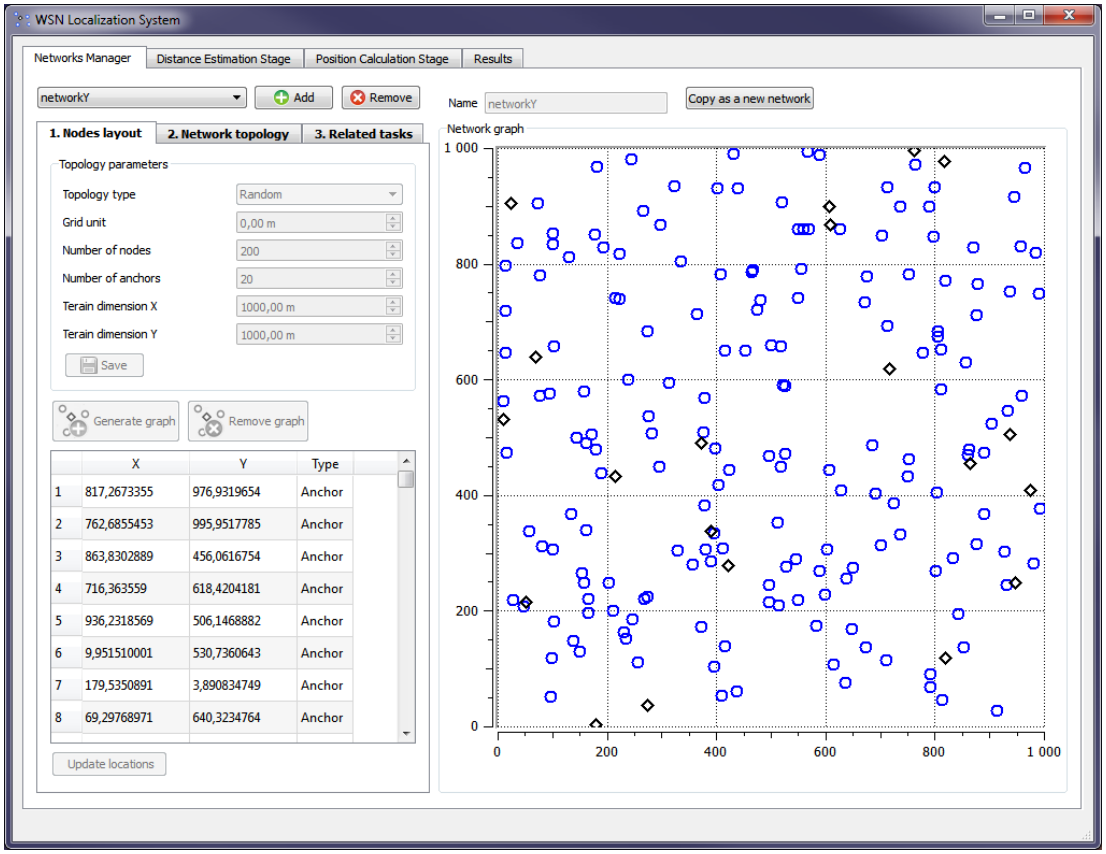

Figure 1: Networks manager in WSN Localization System

parameters influence the speed of convergence and accuracy of the solution. To obtain the general purpose algorithm the values of them should be tuned up for diverse network topologies.

SIMULATION ENVIRONMENT

In order to evaluate our two-phase method new software tool – *WSN Localization System* was created. *WSN Localization System* supports not only the both phases of localization process but it offers also the network models generator. The system architecture is depicted in Figure 2. A user-friendly graphical interface (GUI) for interacting with our system is given. Except the GUI and the database, used for storing all data connected with networks, tasks and localization results, localization system is composed of three main components: *Networks Manager*, *Distance Estimation Module* and *Position Calculation Module*.

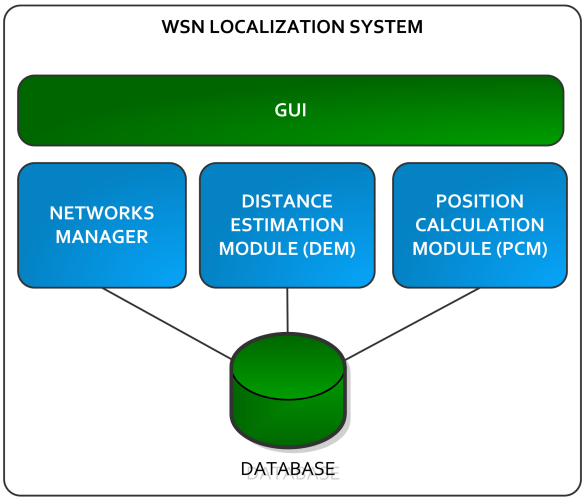

Figure 2: WSN Localization System components

Networks Manager

Networks Manager (Fig. 1) provides an interface for low-power networks modeling. User can add, remove and modify networks by selecting appropriate topology, channel and radio parameters. In general the proper modeling of low-power links is very difficult since the links characterization depends on radio chips (e.g., TR1000, CC1000, CC2420, etc), operational environments (indoor, outdoor) and many other parameters such as traffic load or radio channel – Baccour et al. (2012). In our software we decided to provide models based on *Link Layer Model for MATLAB* provided by Zuniga and Krishnamachari (2004). *Networks Manager* focus on wireless channel modeling and no radio modulation and encoding are considered. In the future *Networks Manager* will be extended to provide data gathering from real-life deployments.

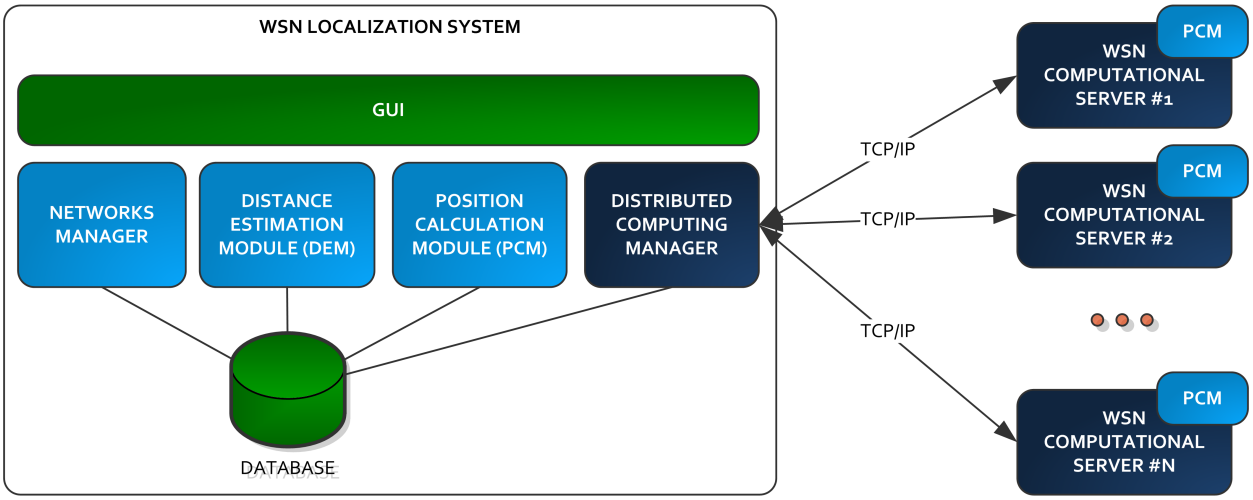

Figure 3: Distributed system architecture

Distance Estimation Module

Distance Estimation Module (DEM) provides optimization methods transforming RSSI measurements into internode distances estimations. At present *DEM* has registered three approaches to distance estimation: Ordinary Least Square Method (OLS), Weighted Least Square Method (WLS) and Geometric Combined Least Square Method (GCLS). More information about distance estimation stage can be found in Marks and Niewiadomska-Szynkiewicz (2011).

Position Calculation Module

Position Calculation Module (PCM) is the main component of our environment as it provides methods for estimating the coordinates of non-anchor nodes in the network using inter-node distances. PCM is realized in the object-oriented way and it can be easily extended with new localization algorithms. Currently TSA (Trilateration & Simulated Annealing) and SA (Simulated Annealing) methods are supported, in the near future TGA (Trilateration & Genetic Algorithm) method will be added. More information about position calculation methods can be found in Niewiadomska-Szynkiewicz and Marks (2009).

DISTRIBUTED COMPUTING EXTENSION

Localization accuracy strongly depends on the measurement errors, network density and anchor nodes location. In paper Niewiadomska-Szynkiewicz and Marks (2009) we provided an extensive analysis of impact of anchor nodes distribution on localization accuracy. However achieving high quality results for very different network topologies in many cases require running localization methods with different values of parameters. For example TSA method can be tuned up by setting up almost a dozen parameters such as: cooling scheme, initial temperature, final temperature, shrinking factors for temperature and movement distances.

On the other hand localization method should guarantee achieving reasonable results for different networks without any tuning, as it is often impossible to select appropriate values in the unknown environment. In order to provide a set of "safety settings" we decided to generate a set of test networks with various topology parameters and to solve the created test tasks with different values of method's parameters. This experiment allows us for improving algorithms robustness but requires solving millions of tasks. Of course this can be done on single machine but it can take a few days to solve all the tasks. Therefore we decided to extend our *WSN Localization System* to include new capabilities connected with distributed computing.

System Architecture

The new capabilities required preparation a new system architecture with *Distributed Computing Manager* module inside simulator and *WSN Computational Server* application. We decided to use client-server communication model as in our system the computational task can be easily decomposed into the set of independent subtasks. The system architecture is presented in Figure 3.

The communication between System and computational server is based on TCP/IP, since we assumed that provided solution shouldn't be bounded up with any special infrastructure such as InfiniBand or protocol like MPI. Of course one System is capable to cooperate with many computational servers.

Distributed Computing Manager

Distributed Computing Manager is the new component in *WSN Localization System* that is responsible for client-server communication and calculation management. The main functionalities of the module are: tasks splitting, displaying results of calculations and presenting current status of each task on computational server. The *Distributed Computing Manager* component manages execution of all tasks assigned to distributed processing,

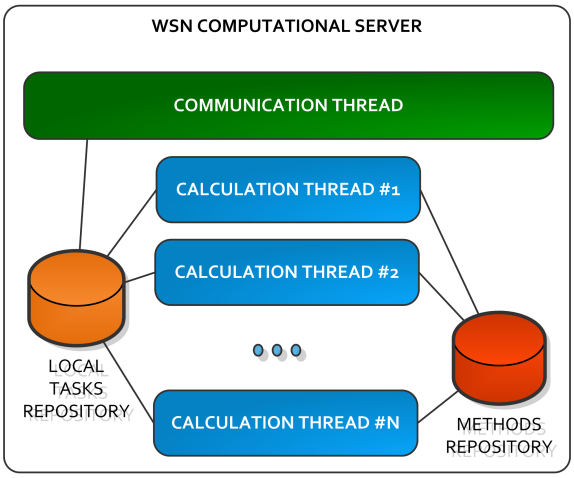

Figure 4: Computational Server Architecture

both in single and batch mode. Moreover, Manager is responsible for computational resources management in order not to overload WSN Computational Servers.

WSN Computational Server

WSN Computational Server is a new application which can be run on remote machines. The role of *WSN Computational Server* is to receive calculation request, realize the experiment and return response to System. The program doesn't have any interface. The computations are done by dedicated calculation threads. The number of threads shouldn't exceed the number of processor cores – the information about available number of cores is stored in XML configuration file. The same configuration file stores also information about port and IP address the communication thread should operate. Each computational server has its own local tasks repository where the network topologies are stored in order to reduce communication – usually only task identifier is sent and there is no need to transfer the whole task descriptor. The task data are transmitted only during running first experiment with appropriate task. It allows not only to reduce communication but also provides a way for new task distribution for running *WSN Computational Servers*. Each computation server has also its own methods repository, so it is possible to add new localization method by providing new *WSN Computational Server* implementation without modifying the running ones. The architecture of computational server is depicted in Figure 4.

Communication Protocol

The communication is done in a master-slave scheme. It is the natural protocol for applications with data decomposition into blocks and iterative calculations. An XML-based communication protocol is proposed to perform communication between System and computational servers. It is based on the TCP/IP protocol and BSD sockets. Our goal was to apply simple mechanism that fulfills the following requirements:

- flexibility – the protocol should be easy to modify and extend with new messages,
- failure resistance – the protocol should be robust as much as possible.

The following messages are supported by communication protocol (see Figure 5):

getServerInfo [DCM ⇒ server] question about server configuration such as number of cores etc,

keepAlive [DCM ⇒ server] link checking,

runExperiment [DCM ⇒ server] order to run computations specifying task, method, its parameters and number of runs,

getExperimentStatus [DCM ⇒ server] question about computation progress,

getTask [server ⇒ DCM] order to download task from System,

uploadResults [server ⇒ DCM] order to upload results to System.

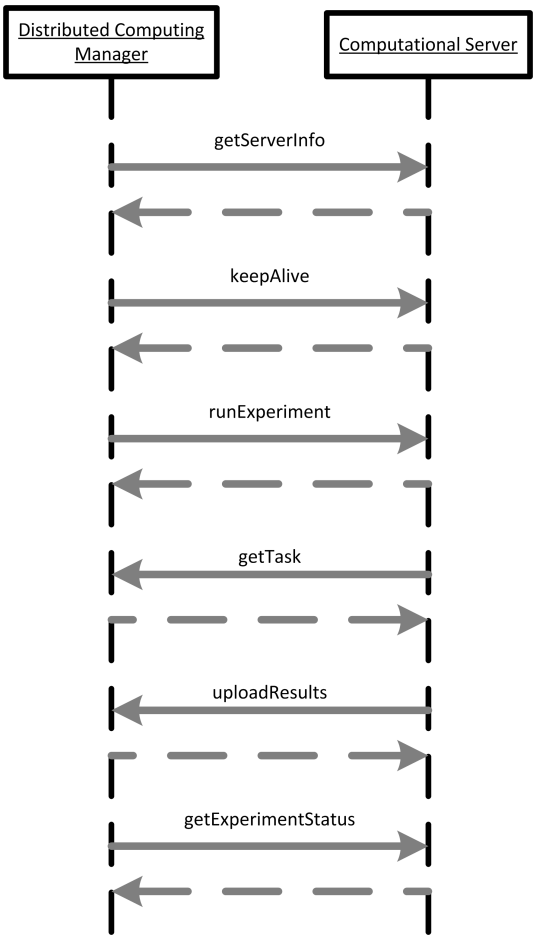

Figure 5: Messages defined in communication protocol.

An example of runExperiment message is presented in Figure 6.

```
<message messageId="00000001">
  <request type="runExperiment">
    <task id="evenly.ols" />
    <method type="TSA">
      <param name="fti" value="4" />
      <param name="alpha" value="0.94" />
      <param name="beta"  value="0.98" />
      <param name="initial_temp" value="0.1" />
    </method>
    <experiment runs="5" />
  </request>
</message>
```

Figure 6: An example of XML message.

NUMERICAL RESULTS

To demonstrate possibilities of our software three tasks connected with three different network topologies were solved with 48000 different values of parameters. The range of tested parameter values is presented in Table 1.

Table 1: Parameters range in batch test

Parameter	Begin	End	Step	Multiply
alpha	0.6	0.98	0.02	
beta	0.6	0.98	0.02	
final temperature	1e-9	1e-14		0.1
distance	0.1	0.29	0.01	

Figures 7 and 8 depict the localization error as a function of alpha and distance parameter. For both charts the values of the rest parameters are constant. In the figure 7 the best solution can be achieved when $alpha = 0.96$. In this experiment $beta$ is equal 0.98. This pair of values forms the optimal set of values which allows to obtain the smallest localization error for considered tasks. This result is in accordance with intuition – it is more safety to change the temperature in SA algorithm slowly, although in some cases it is possible to obtain better accuracy for different values of $alpha$.

Moreover the tests confirmed that better results can be obtained when the distance of node movement is shrunk slower than the coordinating parameter T (temperature) – that is $beta > alpha$. The impact of $distance$ parameter is definitely less significant than $alpha$ and $beta$ parameters, at least for $alpha$ and $beta$ values exceeding 0.9.

CONCLUSIONS AND FUTURE WORKS

We have presented the design and evaluation of our *WSN Localization System* extended with distributed computing feature. The software can be used for creation and solving different WSN localization problems using our TSA or SA methods. The software can be easily extended with another methods utilizing the same software framework. Emphasis was placed on the distributed computation modules which allows us for maximizing the methods robustness for different tasks. In our future research, we would like to add additional methods to our software and improve analytical capabilities – displaying charts with best, worst and average solutions.

ACKNOWLEDGMENT

This work was partially supported by Ministry of Science and Higher Education under grant NN514 672940 and the National Centre for Research and Development (NCBiR) under grant O R00 0091 11.

REFERENCES

Awad, A., Frunzke, T., and Dressler, F. (2007). Adaptive distance estimation and localization in wsn using rssi measures. In *Digital System Design Architectures, Methods and Tools, 2007. DSD 2007. 10th Euromicro Conference on*, pages 471 –478.

Baccour, N., Koubaa, A., Mottola, L., Zuniga, M., Youssef, H., Boano, C. A., and Alves, M. (2012). Radio link quality estimation in wireless sensor networks: a survey. *ACM Transactions on Sensor Networks*, to appear.

Barsocchi, P., Lenzi, S., Chessa, S., and Giunta, G. (2009). Virtual calibration for rssi-based indoor localization with ieee 802.15.4. In *Communications, 2009. ICC '09. IEEE International Conference on*, pages 1 –5.

Benkic, K., Malajner, M., Planinsic, P., and Cucej, Z. (2008). Using rssi value for distance estimation in wireless sensor networks based on zigbee. In *Systems, Signals and Image Processing, 2008. IWSSIP 2008. 15th International Conference on*, pages 303 –306.

Kannan, A. A., Mao, G., and Vucetic, B. (2005). Simulated annealing based localization in wireless sensor network. In *LCN '05: Proceedings of the The IEEE Conference on Local Computer Networks 30th Anniversary*, pages 513–514, Washington, DC, USA. IEEE Computer Society.

Karl, H. and Willig, A. (2005). *Protocols and Architectures for Wireless Sensor Networks*. Wiley.

Mao, G., Fidan, B., and Anderson, B. D. O. (2007). Wireless sensor network localization techniques. *Computer Networks: The International Journal of Computer and Telecommunications Networking*, 51(10):2529–2553.

Marks, M. and Niewiadomska-Szynkiewicz, E. (2007). Two-phase stochastic optimization to sensor network localization. In *SENSORCOMM 2007: Proceedings of the international conference on Sensor Technologies and Applications*, pages 134–139. IEEE Computer Society.

Marks, M. and Niewiadomska-Szynkiewicz, E. (2011). Self-adaptive localization using signal strength measurements. In *SENSORCOMM 2011, the Fifth International Conference on Sensor Technologies and Applications*, pages 73–78, Nice. IARIA.

Niewiadomska-Szynkiewicz, E. and Marks, M. (2009). Optimization schemes for wireless sensor network localization. *International Journal of Applied Mathematics and Computer Science*, 19(2).

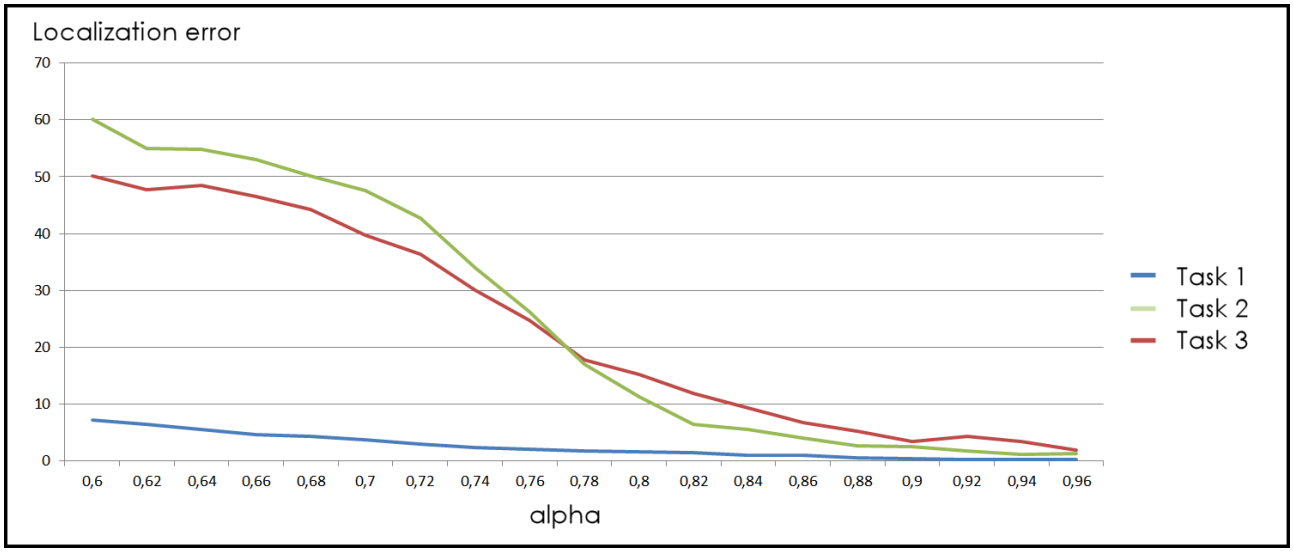

Figure 7: Localization error as a function of alpha parameter.

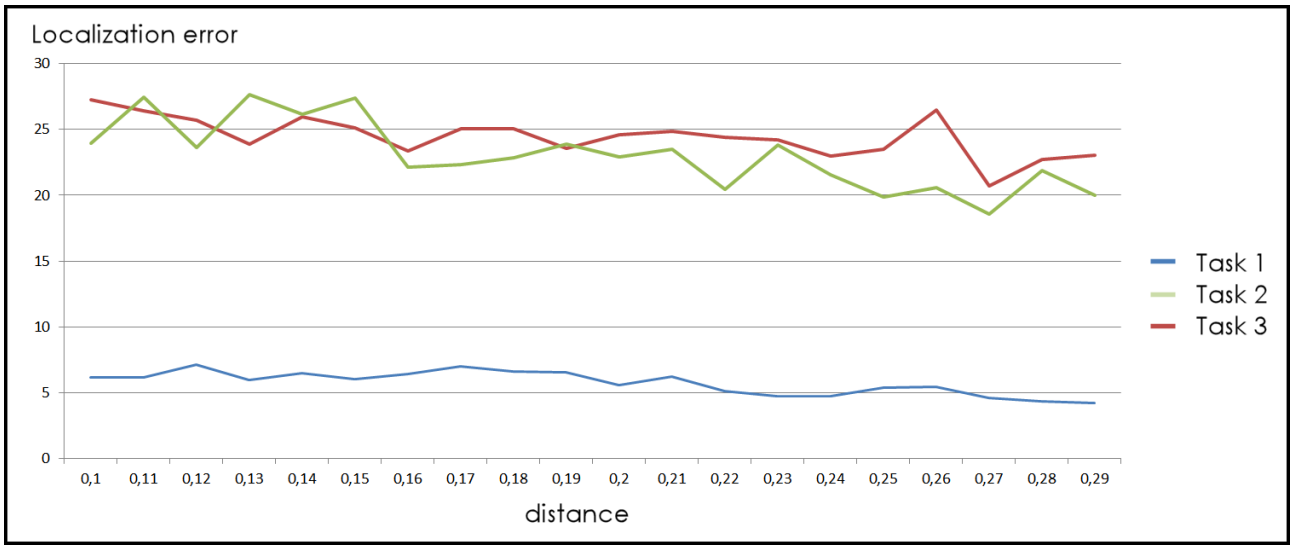

Figure 8: Localization error as a function of distance parameter.

Ramadurai, V. and Sichitiu, M. L. (2003). Localization in wireless sensor networks: A probabilistic approach. In *Proceedings of International Conference on Wireless Networks (ICWN 2003)*, pages 300–305, Las Vegas.

Rappapport, T. (2002). *Wireless communications: principles and practice*. Communications Engineering and Emerging Technologies Series. Prentice Hall, second edition edition.

Srinivasan, K. and Levis, P. (2006). Rssi is under appreciated. In *In Proceedings of the Third Workshop on Embedded Networked Sensors (EmNets*.

Zhang, X., Wu, Y., and Wei, X. (2010). Localization algorithms in wireless sensor networks using nonmetric multidimensional scaling with rssi for precision agriculture. In *Computer and Automation Engineering (ICCAE), 2010 The 2nd International Conference on*, volume 5, pages 556 –559.

Zuniga, M. and Krishnamachari, B. (2004). Analyzing the transitional region in low power wireless links. In *In First IEEE International Conference on Sensor and Ad hoc Communications and Networks (SECON*, pages 517–526, Santa Clara.

AUTHOR BIOGRAPHIES

MICHAŁ MARKS received his M.Sc. in computer science from the Warsaw University of Technology, Poland, in 2007. Currently he is a Ph.D. student in the Institute of Control and Computation Engineering at the Warsaw University of Technology. Since 2007 with Research and Academic Computer Network (NASK). His research area focuses on wireless sensor networks, global optimization, distributed computation in CPU and GPU clusters, decision support and machine learning. His e-mail is `mmarks@ia.pw.edu.pl`

Discrete Event Modelling and Simulation in Logistics, Transport and Supply Chain Management

DEVELOPMENT AND USE OF A GENERIC AS/RS SIZING SIMULATION MODEL

Srinivas Rajanna
Edward Williams
Onur M. Ülgen

PMC
15726 Michigan Avenue
Dearborn, MI 48126 USA

Vaibhav Rothe

PMC India
Nagpur, INDIA

KEYWORDS

Manufacturing simulation, in-process inventory, resequencing, AS/RS [automatic storage and retrieval system], automotive painting and assembly.

ABSTRACT

As usage of simulation analyses becomes steadily more important in the design, operation, and continuous improvement of manufacturing systems (and historically, manufacturing was the sector of the economy first eagerly embracing simulation technology), the incentive to construct generic simulation models amenable to repeated application increases. Such generic models not only make individual simulation studies faster, more reliable, and less expensive, but also help extend awareness of simulation and its capabilities to a wider audience of manufacturing personnel such as shift supervisors, production engineers, and in-plant logistics managers.
In the present study, simulation consultants and client manufacturing personnel worked jointly to develop a generic simulation model to assess in-line storage and retrieval requirements just upstream of typical vehicle final assembly operations, such as adding fluids, installing seats, emplacing the instrument panel, and mounting the tires. Such a final assembly line receives vehicles from the paint line. The generic model permits assessment of both in-line vehicle storage [ILVS] requirements and AS/RS [automatic storage/retrieval system] configuration and performance when designing or reconfiguring vehicle paint and/or final assembly lines. The AS/RS is the physical implementation of the ILVS. These assessments, at the user's option, are based upon current production conditions and anticipated future body and paint complexities.

1. INTRODUCTION

Manufacturing systems represent perhaps both the most frequent and the oldest application areas of simulation, dating to at least the early 1960s (Law and McComas 1998). Questions asked of a simulation model now go far beyond "Will the manufacturing system reach its production quota?" [often expressed as "JPH" = "jobs per hour]. With ever-sharpening competition driving management demand for *lean* efficient operation (2010), simulation analyses are now being called upon to not only achieve production quotas, but also to minimize inventory (both in-line and off-line) and the time and resources to access that inventory whenever necessary.

Furthermore, the accelerating pace of change, often driven by both fickle marketplace demands and by competitive pressures, have increased interest, on the part of both managers and production engineers, in the availability of generic adaptable simulation models. These models, when feasible, represent attractive improvement relative to "We wish the world would stop evolving while we await the building, verification, and validation of a custom-built simulation model for answering our pressing questions." This interest is hardly new – the software tool "GENTLE" [GENeralized Transfer Line Emulation], which allowed quick study of a common type of automotive manufacturing line via a model built in GPSS (Schriber 1974), dates back nearly two decades (Ülgen 1983). As the attractions of such generic models become more widely known, their development is becoming more frequent. For example, (Legato et al. 2008) describes the development and use of a generic model for the study of maritime container terminals. Still more recently, (Zelenka and Hájková 2009) describes the development and use of a generic model for the study of road traffic.

The generic model described here permits examination of the ILVS capacity requirements interposed between the paint line and the final assembly line within vehicle assembly plants. Such examination demands high flexibility relative to volatile production conditions, future market demand, and particularly variations in vehicle resequencing. Vehicles typically exit the paint line in a sequence very different from that anticipated by the final assembly line operators. Perhaps shockingly, occasionally fewer than 5% of the

Proceedings 26th European Conference on Modelling and Simulation ©ECMS Klaus G. Troitzsch, Michael Möhring, Ulf Lotzmann (Editors)
ISBN: 978-0-9564944-4-3 / ISBN: 978-0-9564944-5-0 (CD)

vehicles arriving at final assembly are in "correct" (i.e. expected) sequence. Therefore, the ILVS must be capable of short-term storage so the operator can shunt one vehicle aside to attend to another arriving later but originally expected earlier. We first provide details of the project objectives and the key performance metrics to be tracked each time the generic model is used. Next, we describe the methods of obtaining and cleansing input data for a typical scenario using the model. Next, we describe the structure of the generic simulation model itself. Last, we show the results from a typical application of this model, and indicate directions for future work and enhancements to the model.

2. PROJECT CONTEXT AND OBJECTIVES

The goal of this simulation study was quantitative assessment of the in-line storage requirements between the paint line and the downstream final assembly line in the automotive manufacturing process. Ideally, vehicles exit the paint line in strict accordance with a previously planned production sequence. This ideal sequence is determined by production scheduling engineers using a standard optimization program. This program minimizes (almost always succeeds in setting to zero) the number of violations of long-standing production rules. Examples of these rules are "Avoid scheduling two moonroof-equipped vehicles consecutively" or "Avoid scheduling two vehicles with identical engine-powertrain configurations consecutively." If this optimized sequence could actually be maintained in production practice (veteran production managers in the industry might cynically grumble "Perhaps on some distant planet."), these storage requirements would remain at or near zero – the right parts for the exiting vehicle next in line would themselves be next at the assembly line. For example, the seats poised to be installed in the vehicle would be the correct seats for that vehicle type and paint color. In actuality, due to inevitable production plan changes (such as revisions to the proportions of different models demanded by the marketplace) and other transient problems in the paint shop (and indeed in other operations upstream of the paint shop), vehicles never arrive in the originally planned sequence. This simulation study sought to examine, relative to various performance metrics, the extent of ILVS needed to install the right parts in vehicles at assembly, and the amount of labor needed to access those parts from the storage. The client and consultant managers reached consensus that the model would be generic in that it could accept data from typical automotive plants having body, paint, and final assembly in that order, as almost all such plants do. Such plants, when run at fewer than three shifts per day, will inevitably have non-zero storage requirements even in the limiting case, mentioned above, when no sequence changes occur. Therefore, the model developed is also generic in the sense that it can readily be run with no sequence violations but on one or two shifts, thereby allowing client engineers and managers to assess "background" storage requirements.

To introduce and explain these metrics, let us consider the situation in which vehicles originally scheduled in order 1, 2, 3, 4, 5 leave the paint shop in order 1, 4, 5, 2, 3. A vehicle is considered "in sequence" if its sequence number exceeds that of all vehicles which have preceded it. In this example, the first 3 of the 5 vehicles are in sequence, giving a "percent in sequence" of 60%.

Now, let us consider the actions of the worker, at a specific workstation, responsible for installing the front passenger seat (one of the four seats per vehicle) relative to the stored parts when vehicle 4 arrives. Each front passenger seat comes from a separate storage rack – and these seats arrived from a supplier in a specified sequence. For example, the supplier received advisory "A white seat must be first, then a gray one, then a dark blue one, in accordance with our planned production schedule." When vehicle 4 arrives, the operator must remove the front passenger seat intended for vehicle 2 and the front passenger seat intended for vehicle 3 from the appropriate racks , and set them aside (in the "set-aside rack"). The "set aside" metric is then 2. This incremental work for the operator (an occasion of moving parts around, which is muda [non-value-added activity]) represents one "dig." By contrast, installing the seats in the recently painted vehicle is a value-added activity. Relative to this dig, the operator removed 2 seats from each storage rack (for example, he or she removed front passenger seats for vehicles 2 and 3 to access ("get at") the front passenger seat for vehicle 4. Hence, this dig has a "dig depth" of 2. The set-aside metric and the dig depth metric are closely correlated with the "spread" of the sequence – the maximum difference between sequence numbers of adjacently arriving vehicles. In this arrival sequence 1, 4, 5, 2, 3; the spread is 3 (between vehicles 1 and 4).

In this context, this simulation study sought to specify the proper ILVS size (vehicle capacity) relative to current and anticipated production conditions, particularly the amount of "complexity" – the product of the number of vehicle varieties and the number of paint color choices. Additionally, the study investigated two key in-transit production times:

1. Time-in-system vehicles spend between match-point (the milestone in body-&-assembly (upstream of painting) where a vehicle receives its vehicle identification number [VIN] and all its features are defined, and hang-to-paint (where a vehicle leaving body-&-assembly is suspended from a conveyor-carried hook and carried into the paint shop)
2. Time-in-system vehicles spend between hang-to-paint and entry to the AS/RS constituting the ILVS, at which time they are painted and await final assembly.

3. INPUT DATA – SOURCE AND CLEANSING

One of the most vital, though often unheralded, phases of any analytical simulation project is obtaining (and equally important, checking and cleansing) the input data required (Williams 1996). In this project, the existing process already had equipment installed for extensive data collection. Accordingly, the data necessary to build and validate (after verification) this model came from a database which automatically recorded more than a dozen date/time stamps on each vehicle passing through the process. These data, pertaining to approximately 11,000 vehicles, each identified by its VIN [vehicle identification number], were obtained from the database. The data were uploaded first to a large Microsoft Excel® workbook. There, the data were cleansed by visual inspection, by using Excel®'s data validation techniques, and by inspecting a variety of quickly and easily generated plots. Once ensconced in Excel®, the data could readily be input into the simulation model to control arrival times and/or for use in validating the simulation model against actual production.

As an example of important information obtained from these data, Figure 1 (Appendix) shows the empirical distribution of transit times between the body-&-assembly match point and entry into the ILVS AS/RS system between the painting and final assembly operations. These data are strongly positively skewed (right-skewed): although fewer than one-sixth of the observations are greater than 20 hours (performance goal), the mean time is 17.2 hours and the maximum time 41.1 hours. The 20-hour threshold (elapsed time from match point to completion of painting should not exceed this value), chosen by high-level production management of the client company, represents an attempt to keep the AS/RS inline storage requirements small. When this transit time exceeds 20 hours, excessive AS/RS capacity represents a palliative for inefficiencies in the body and/or the paint operations.

4. SIMULATION MODEL CONSTRUCTION, VERIFICATION, AND VALIDATION

After discussion of alternatives, client personnel and the simulation analysts agreed on the use of the SIMUL8® simulation software tool (Hauge and Paige 2001) to build the model. Like its numerous competitors, SIMUL8® provides built-in constructs for the modeling of buffers and conveyors, both of significant importance to this model. Figure 4 (Appendix) is a screen shot of this model. Furthermore, this tool affords convenient importation of large blocks of data from Excel® workbooks. After examination of sample data, appropriate distributions (usually exponential or Erlang) were chosen for process times using a distribution fitter – a specialized software tool which examines an empirical data set and chooses a suitable statistical distribution for its characterization (Law and McComas 2002).

Verification and validation of this model used traditional techniques. These techniques included informal inspections and walkthroughs among the model developers, step-by-step execution while watching the animation, removing all randomness from the model temporarily, allowing only one entity into the model, and directional testing (Sargent 2004). After errors (e.g., mismatched time units at various points of the model) were corrected, the model achieved agreement within 5% of typical plant experience, and specifically with reference to the key performance metric of "elapsed vehicle time between match point in body & assembly to entry into the AS/RS." Hence, the model achieved credibility among client management.

5. RESULTS

The major usage first made of the model was relative to achievement of the AS/RS performance goals established by plant management. These goals specified that the AS/RS must be of sufficient size (but not unnecessarily large) to achieve the performance metrics summarized in Table 1.

Table 1. AS/RS Performance Metric Goals

% Vehicles in Sequence	No less than	98%
Vehicle set-asides	No more than	10
Dig depth	No more than	5
Digs/100	No more than	2

The model was repeatedly run with the current complexity level (220) and the hypothesized AS/RS capacity increased by one unit at a time, beginning at 350. Runs were made on a steady-state basis with warm-up time 2880 minutes (48 hours, equivalent to one calendar week at the plant)

and simulation time 20,000 minutes (about seven weeks calendar production time). Graphical results of particular importance are shown in the Appendix (Figures 2 and 3). These runs demonstrated that the minimum acceptable capacity for the AS/RS, at current complexity levels, was 365 units. Since the client specified most production parameters (e.g., cycle time, BIW complexity), sensitivity analyses were not performed.

Table 2 below, shows detailed results of 15 distinct replications, with a different random number stream generator used for each replication.

Table 2. Detailed Results of Fifteen Replications

Min. Fill Level	% in Seq. (ASRS Out)	Max. Set Aside	Max. Dig Depth	Digs/ 100
386	98.01%	8	2	1.98
393	98.00%	7	2	1.99
391	98.03%	7	2	1.96
391	98.04%	7	2	1.95
390	98.00%	8	2	1.98
389	98.00%	8	2	1.98
392	98.03%	8	2	1.96
393	98.04%	9	2	1.94
393	98.04%	8	3	1.95
391	98.01%	8	3	1.98
391	98.04%	8	2	1.95
392	98.02%	8	2	1.97
392	98.01%	9	2	1.98
393	98.00%	9	3	1.98
391	98.03%	9	2	1.96

6. CONCLUSIONS AND FUTURE WORK

In the future, the complexity level will surely change periodically. Since this level depends heavily on marketing plans, production managers will have reasonable (several weeks or months) notice, during which operational parameters may be adjusted. Using this model, these managers will be able to insert a new complexity level and determine an updated AS/RS capacity requirement. With this comforting capability in reserve, managers in the client company have come to embrace the "simulate earlier" exhortation as enunciated within (Ball and Love 2009).

ACKNOWLEDGMENTS

The authors gratefully express gratitude to colleague and team leader Ravi Lote for his high-quality guidance of this project. Additionally, collaboration from the client's engineers was most helpful. Comments from anonymous referees have improved the presentation and clarity of this paper.

REFERENCES

Ball, Peter, and Doug Love. 2009. Instructions in Certainty: Rapid Simulation Modeling Now! *Industrial Engineer* 41(7):29-33.

Hauge, Jaret W., and Kerrie N. Paige. 2001. *Learning SIMUL8: The Complete Guide*. Bellingham, Washington: PlainVu Publishers.

Law, Averill M., and Michael G. McComas. 1998. Simulation of Manufacturing Systems. In *Proceedings of the 1998 Winter Simulation Conference*, Volume 1, eds. D. J. Medeiros, Edward F. Watson, John S. Carson, and Mani S. Manivannan, 49-52.

Law, Averill M., and Michael G. McComas. 2002. How the Expertfit Distribution-Fitting Software Can Make Your Simulation Models More Valid. In *Proceedings of the 2002 Winter Simulation Conference*, Volume 1, eds. Enver Yücesan, Chun-Hung Chen, Jane L. Snowdon, and John M. Charnes, 199-204.

Legato, Pasquale, Daniel Gulli, Roberto Trunfio, and Riccardo Simino. 2008. Simulation at a Maritime Container Terminal: Models and Computational Frameworks. In *Proceedings of the 2008 European Conference on Modelling and Simulation*, eds. Loucsas S. Louca, Yiorgos Chrysanthou, Zuzana Oplatková, and Khalid Al-Begain, 261-269.

Sargent, Robert G. 2004. Validation and Verification of Simulation of Simulation Models. In *Proceedings of the 2004 Winter Simulation Conference*, Volume 1, eds. Ricki G. Ingalls, Manuel D. Rossetti, Jeffrey S. Smith, and Brett A. Peters, 17-28.

Schriber, Thomas J. 1974. *Simulation Using GPSS*. New York, New York: John Wiley & Sons, Incorporated.

Suri, Rajan. 2010. Going Beyond Lean. *Industrial Engineer* 42(4):30-35 [April].

Ülgen, Onur M. 1983. GENTLE: GENeralized Transfer Line Emulation. In *Simulation in Inventory and Production Control*, ed. Haluk Bekiroğlu, 25-30.

Williams, Edward J. 1996. Making Simulation a Corporate Norm. In *Proceedings of the 1996 Summer Computer Simulation Conference*, eds. V. Wayne Ingalls, Joseph Cynamon, and Annie Saylor, 627-632.

Zelenka, Petr, and Jana Hájková. 2009. Structural Components in Multiadjustable Road Traffic Models: Their Role and the Means of Generating Their Topology. In Proceedings of the 2009 European Conference on Modelling and Simulation,

eds. Javier Otamendi, Andrzej Bargiela, José Luis Montes, and Luis Miguel Doncel Pedrera, 262-268.

AUTHOR BIOGRAPHIES

SRINIVAS RAJANNA, CPIM, is a Senior Manager with over fourteen years of experience in simulation, lean, production, process improvement, six-sigma, theory of constraints, supply chain, and managing projects. He was graduated from Bangalore University with a Bachelor of Engineering in Mechanical Engineering. He holds a Master's Degree in Industrial Engineering from West Virginia University and an MBA from The Eli Broad Graduate School of Management, Michigan State University.

Srinivas has broad industry experience including automotive, aerospace, semiconductor, consumer, healthcare, and pharmaceutical. He has experience providing solutions that include: developing a throughput improvement roadmap to meet the production target, assessing the operation strategies of a pharmaceutical firm, conducting material flow studies to reduce traffic congestion, optimizing the utilization of staff and equipment, applying lean strategies in manufacturing and service industries, and using analytical techniques such as flow charts, value stream mapping, and process mapping.

VAIBHAV ROTHE is a Technical Lead with interests in the various applications of simulation in the field of Industrial Engineering. Vaibhav has experience in Simul8®, Enterprise Dynamics®, Witness® and Arena®. He received a Master's degree in Industrial Engineering from the University of South Florida and a Bachelor's degree in Mechanical Engineering from Regional College of Engineering, Nagpur, India. Vaibhav's recent projects have spanned a number of industry sectors: aerospace, automotive, steel etc. He has worked as a consultant on projects providing solutions such as capacity planning, scheduling, logistics, six sigma and lean manufacturing. He has had experience in completing several successful simulation-based studies, providing training and customized technical support.

EDWARD J. WILLIAMS holds bachelor's and master's degrees in mathematics (Michigan State University, 1967; University of Wisconsin, 1968). From 1969 to 1971, he did statistical programming and analysis of biomedical data at Walter Reed Army Hospital, Washington, D.C. He joined Ford Motor Company in 1972, where he worked until retirement in December 2001 as a computer software analyst supporting statistical and simulation software. After retirement from Ford, he joined PMC, Dearborn, Michigan, as a senior simulation analyst. Also, since 1980, he has taught classes at the University of Michigan, including both undergraduate and graduate simulation classes using GPSS/H™, SLAM II™, SIMAN™, ProModel®, SIMUL8®, or Arena®. He is a member of the Institute of Industrial Engineers [IIE], the Society for Computer Simulation International [SCS], and the Michigan Simulation Users Group [MSUG]. He serves on the editorial board of the International Journal of Industrial Engineering – Applications and Practice. During the last several years, he has given invited plenary addresses on simulation and statistics at conferences in Monterrey, México; İstanbul, Turkey; Genova, Italy; Rīga, Latvia; and Jyväskylä, Finland. He served as a co-editor of Proceedings of the International Workshop on Harbour, Maritime and Multimodal Logistics Modelling & Simulation 2003, a conference held in Rīga, Latvia. Likewise, he served the Summer Computer Simulation Conferences of 2004, 2005, and 2006 as Proceedings co-editor. He is the Simulation Applications track co-ordinator for the 2011 Winter Simulation Conference. His email address is ewilliams@pmcorp.com.

ONUR M. ÜLGEN is the president and founder of Production Modeling Corporation (PMC), a Dearborn, Michigan, based industrial engineering and software services company as well as a Professor of Industrial and Manufacturing Systems Engineering at the University of Michigan-Dearborn. He received his Ph.D. degree in Industrial Engineering from Texas Tech University in 1979. His present consulting and research interests include simulation and scheduling applications, applications of lean techniques in manufacturing and service industries, supply chain optimization, and product portfolio management. He has published or presented more that 100 papers in his consulting and research areas.

Under his leadership PMC has grown to be the largest independent productivity services company in North America in the use of industrial and operations engineering tools in an integrated fashion. PMC has successfully completed more than 3000 productivity improvement projects for different size companies including General Motors, Ford, DaimlerChrysler, Sara Lee, Johnson Controls, and Whirlpool. The scientific and professional societies of which he is a member include American Production and Inventory Control Society (APICS) and Institute of Industrial Engineers (IIE). He is also a founding member of the MSUG (Michigan Simulation User Group).

APPENDIX

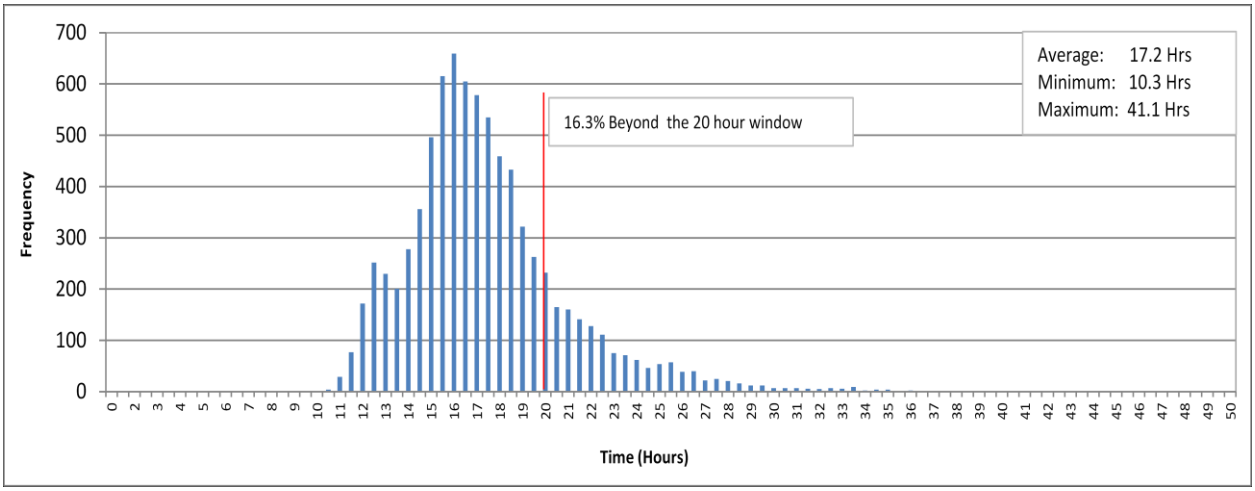

Figure 1. Distribution of In-Process Times Between Match Point (in Body-&-Assembly) and AS/RS Entry

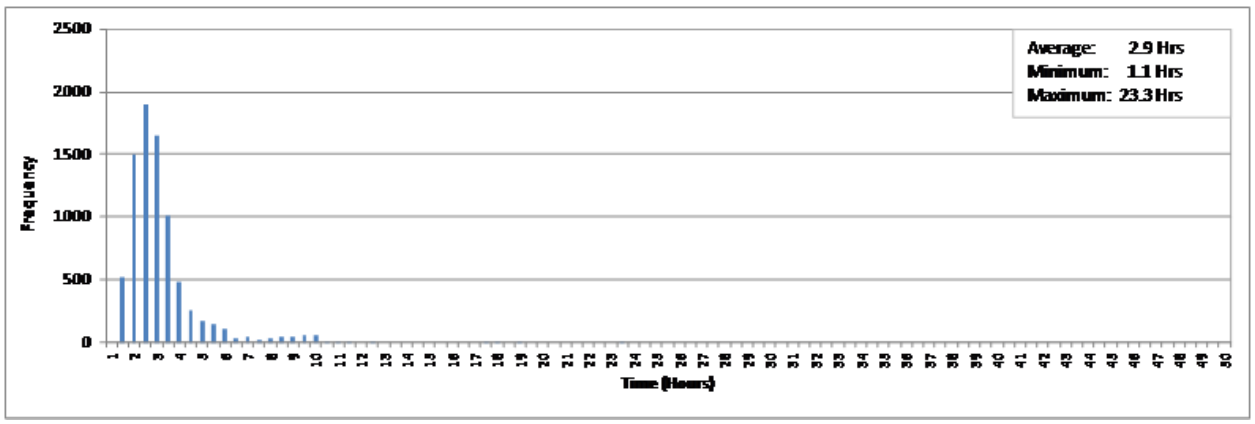

Figure 2. Distribution of Time-in-System from Match Point to Hang-To-Paint

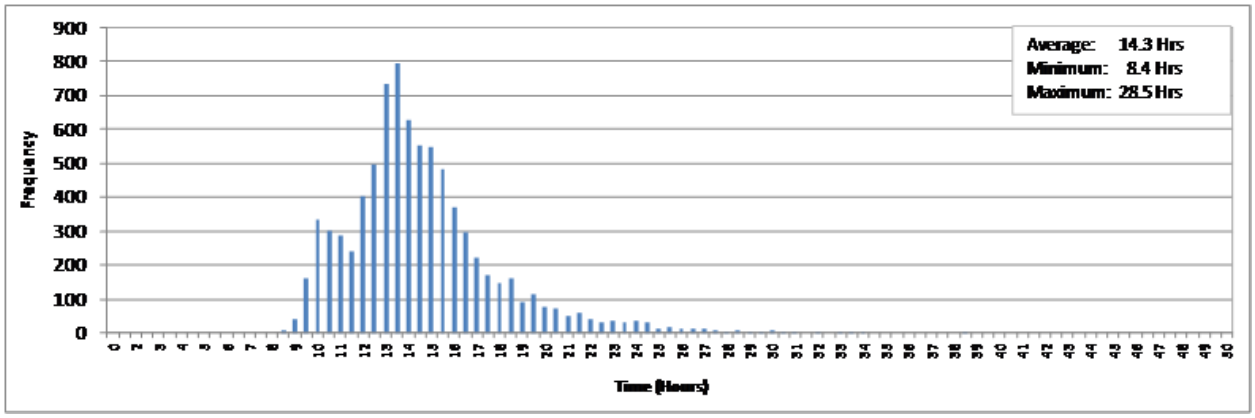

Figure 3. Distribution of Time-in-System from Hang-To-Paint to Entry into AS/RS

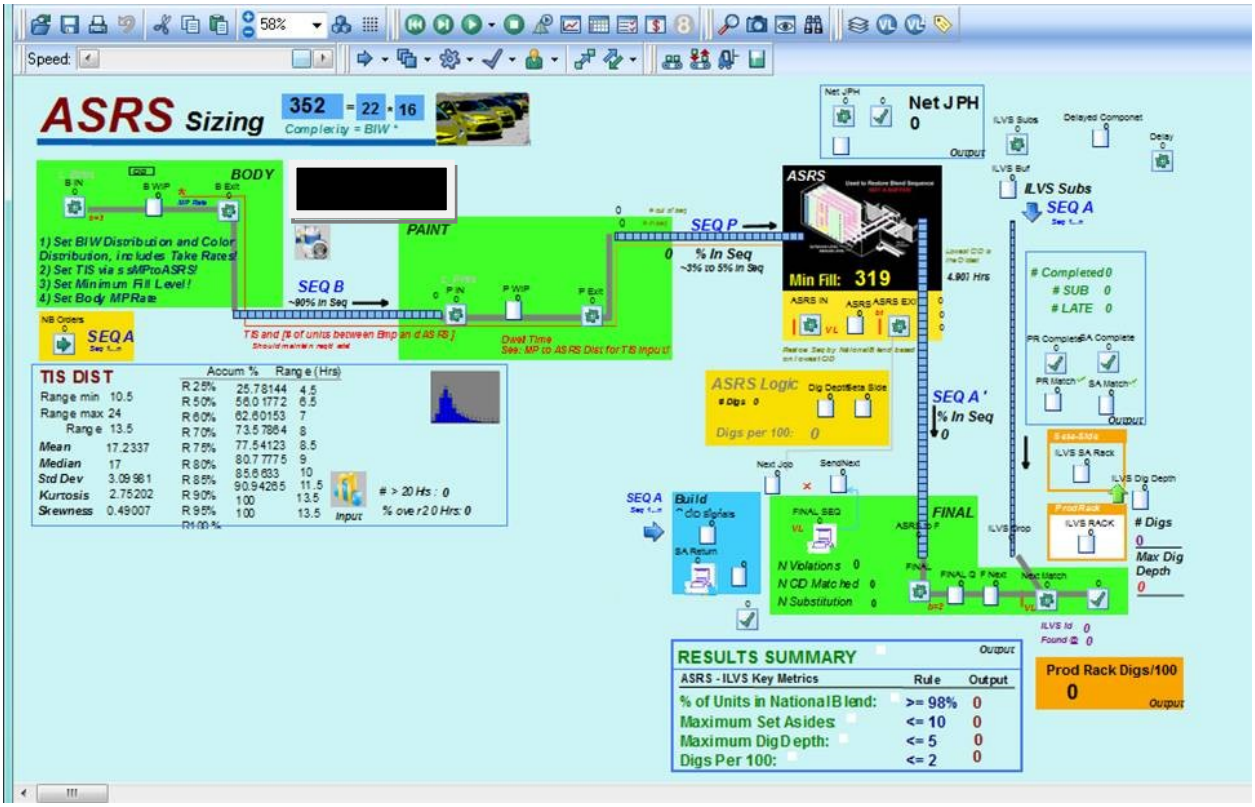

Figure 4. Screen Shot of SIMUL8® Model

DYNAMIC BEHAVIOR OF SUPPLY CHAINS

Hans-Peter Barbey
University of Applied Sciences Bielefeld
Wilhelm-Bertelsmann-Str. 10, 33602 Bielefeld, Germany
Email: hans-peter.barbey@fh-bielefeld.de

KEYWORDS
Supply chain, bullwhip effect, closed-loop control, Smith-predictor, discrete event simulation.

ABSTRACT

The bullwhip effect has been well known since many years and often takes place in supply chains. It is caused by wrong order policy in real systems. The bullwhip effect can be demonstrated easily through a discrete event simulation. It is possible with the application of a Smith-predictor and the limitation of the production rate to eliminate the bullwhip effect in simulations. The difference that it makes on nominal stock can be equalized in a rather short period. With a suitable set of parameters, the oscillation of the stocks of each company, upstream in the supply chain, is nothing more than a variation of the customer's orders at the end of the supply chain. Anyhow, it takes a longer period to compensate the stock differences of the companies upstream. If we deal with a total random order policy, the Smith-predictor can avoid the bullwhip effect, even the variation of stock in the upstream companies is lower than the variation at the end of the supply chain. With application of the Smith-predictor, the companies can equalize their stocks independently.

1 INTRODUCTION

Dynamic behavior of the material flow in a supply chain is influenced by the order policy of each particular company of a supply chain. The interaction of all companies creates the bullwhip effect, which has been described first by (Forrester 1958). It is the increasing of a small variation in the requirements of a customer to an enormous oscillation with the manufacturer at the beginning of a supply chain. In many articles, this phenomenon is only described in general terms without a mathematical definition (i.e. Erlach 2010 and Dickmann 2007). Without any mathematical description, the question is if the bullwhip effect can be avoided at all (Bretzke 2008). The main influences of the bullwhip effect are as follows (Gudehus 2005):

- Independent orders of the particular companies in a supply chain
- Synchronic orders (i.e. subsidiaries of one company)
- Wrong order policy in an emergency case
- Speculative order policy or sale actions

To avoid the bullwhip effect, cooperation between all members in a supply chain is necessary. Basically, information about i.e. orders of customers have to be provided to all subsuppliers in the supply chain. This kind of cooperation is rather difficult in reality. The question is if the bullwhip effect can be avoided without any cooperation and providing of information to all members in a supply chain.

Due to these many influences concerning the combination of the different companies in a supply chain, a mathematical description is rather difficult, even nearly impossible. Therefore, the discrete event simulation is a suitable tool to describe the bullwhip effect. It helps to understand the principle behavior of a supply chain.
It has been shown (Barbey 2008) that production time and storage time are dead times in a closed-loop controlled system. These systems with dead times are nearly impossible to control if a short reaction time is required. If the controller has an unsuitable set of parameters, an oscillation can occur. The unsuitable set of parameters is the reason for the bullwhip effect (Barbey 2011).
To get a short reaction time in a technical process, a Smith-predictor is often applied. The Smith-predictor is a controller, which can compensate the dead time in a system. The Smith-predictor provides a forecast of the control signal with a parallel model included in the controller. Therefore, the model is separated in a part with dead time and in a part without (fig. 1). The controller will be not adjusted at the control signal. It will be adjusted at the forecast without dead time. The forecast will be compared to the real signal and will adjust then the controller. If the model corresponds well to the controlled system, the Smith-controller provides a very good result, because the control variable is calculated without an existing dead time. If there are some changes in the process parameters, the Smith-controller is very sensitive, because these changes are not included in the model.

Proceedings 26th European Conference on Modelling and Simulation ©ECMS Klaus G. Troitzsch, Michael Möhring, Ulf Lotzmann (Editors)
ISBN: 978-0-9564944-4-3 / ISBN: 978-0-9564944-5-0 (CD)

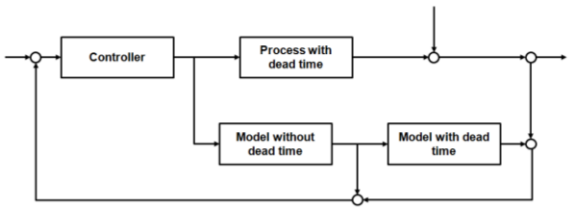

Figure 1: Principle of a Smith-predictor

The following describes the closed-loop control of stocks in a supply chain. Therefore, the production rate is calculated by an algorithm similar to a Smith-predictor or a P-controller. This simulation is a theoretical study of the bullwhip effect and not the copy of a real system.

2 CLOSED-LOOP CONTROL OF A STOCK

To get some information of the quality of a closed-loop controlled stock, the following very simple production system will be calculated (Barbey 2008). It consists of a production unit, stock 1 with definite storage time, i.e. for a cooling process and stock 2 for delivery (fig. 2).

This system has following parameters:

- The production time of one unit is adjustable
- The production time is limited to a definite maximum and minimum
- The storage time in stock 1 is 1 time unit
- The quantity of stock 2 is closed-loop controlled to a nominal stock

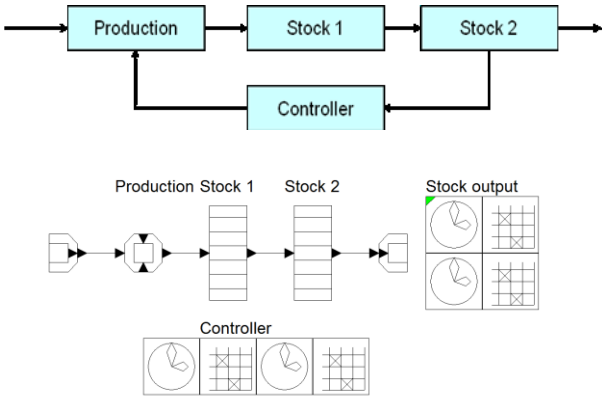

Figure 2: Production system as block model and simulation model designed with DOSIMIS

This production system is closed-loop controlled with three different controllers:

- P-controller with a gain of 1 (the difference of the stock will be produced within the next period)
- P-controller with a gain of 0.5 (half of the difference in the stock will be produced within the next period)
- Smith-predictor with compensation of zero-point deviation

All production parameters of this system are constant. The stock output is constant too. The only deviation is a difference of the nominal stock at the very beginning of the simulation. Additionally, there is an output at two definite times (fig.3). The stock is recorded one time per time unit. Then, the production time for one part is calculated for the next time unit. The controller is acting in a time discrete manner.

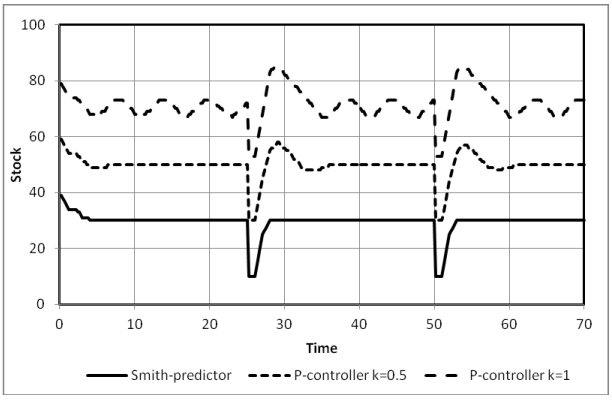

Figure 3: Stock with an additional output

The P-controller with the gain1 is controlling the stock of the nominal stock, briefly after starting the simulation but behaves unstable. There is an oscillation around the nominal stock. The peaks in the stock output create a momentarily increase of the oscillation. The P-controller with the gain 0.5 is controlling the nominal stock too. It obtains the nominal value with a damped oscillation after approx. 10 time units. The Smith-predictor has improved behavior. The difference to the nominal stock is compensated much faster after approx. 3 time units. An oscillation does not occur. The time for the compensation depends only on the difference in the stock. Due to the limitation of the production rate, it takes a definite time to compensate the stock difference. This is the shortest possible time for compensation.

3 SIMULATION OF THE BULLWHIP EFFECT

For the simulation of the bullwhip-effect, the following simulation model of a supply chain will be used:

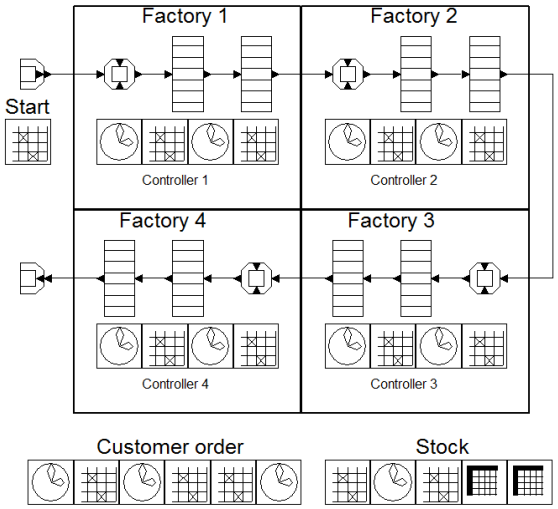

Figure 4: Simulation model of a supply chain designed with DOSI MIS

The basic model is the single production unit (fig. 2). For the supply chain, it will be copied four times (fig. 4). Due to simplification, the parameters of all units are identical, and they are the same as in the first model. To get a small variation in the stock of the first factory, a P-controller with a gain of 0.8 will be used. This small oscillation in the stock of factory 1 increases in the other stocks upstream (fig. 5). The bullwhip effect has been created only with a deviation of the stock at the beginning. Additional disturbances in the stock output are not needed. A P-controller with a large gain is not suitable as a controller in the model of a supply chain.

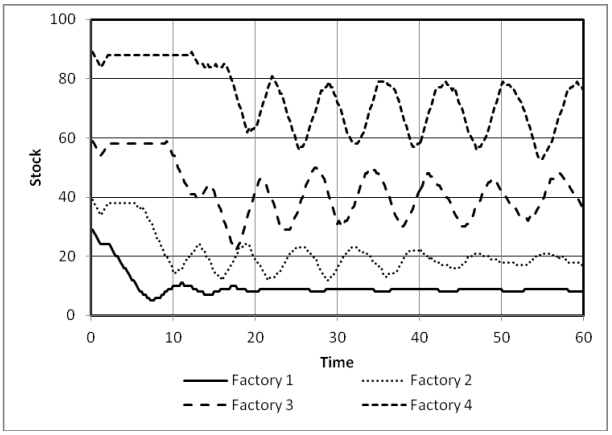

Figure 5: Stock in all factories by application of a P-controller with a gain of 0.8

4 APPLICATION OF A SMITH-PREDICTOR IN A SUPPLY CHAIN

For all factories of the supply chain, a Smith-predictor will be applied to control the stock. The Smith-predictor calculates the amount of the corrective action, the production time in each factory. The production time is limited to maximum and minimum. This limitation helps to reduce the bullwhip effect due to a wrong order strategy in an emergency case (chap.1). As a disturbance, an additional output from the stock of factory1 is applied (fig. 6). The amplitude of this output increases with the time. This additional output simulates a speculative ordering strategy (chap. 1) and the increasing amplitude simulates a trend.

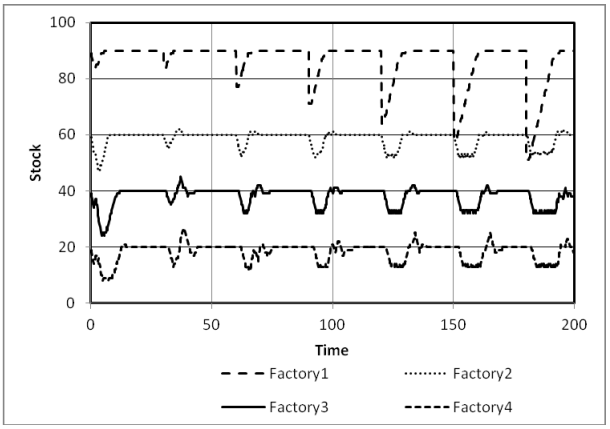

Figure 6: Stocks in a supply chain with additional outputs at definite times

The deviation from the nominal stock is controlled to zero in factory1. The duration for the control depends only from the difference to the nominal stock. The higher the difference, the longer the period. The reason for this increased duration is the limitation of the production rate. This difference in stock takes place in the other factories too. They have increasing stock output with a delay due to dead time. Caused by a newly calculated production rate of the Smith-predictor, an increased stock output takes place in the factories upstream. At the beginning of the simulation, a small bullwhip effect occurs in a oscillation of the stocks. The difference in the stocks upstream is less than at the beginning of the supply chain. The difference in the stock of factory 1 caused by the customer's order is 50 units at the end of the simulation. The difference in the other stocks is 8 units. The reason is a limitation of the production time. On the other hand, this limitation increases the time to compensate this difference and reduces the oscillation of the stock nearly to zero.

In this simulation, the behavior of a supply chain has been shown when only one singular order takes place in a time step of 30 units. This order could be completely controlled. In the following simulation, the order strategy is random as far as the quantity is concerned. The time of ordering is constant. Within an interval of 2 time units, there is a random output between 0 and 13. This time step is not long enough to control the difference completely. In factory1, a high variation in the stock takes place (fig. 7). The variation in the stock take place in the factories upstream too. By comparing the amplitudes in the stock, it will be clearly understood

that they are less in factory1. The bullwhip-effect does not exist here, even if it is reduced. The Smith-predictor is suitable to control stocks in supply chains.

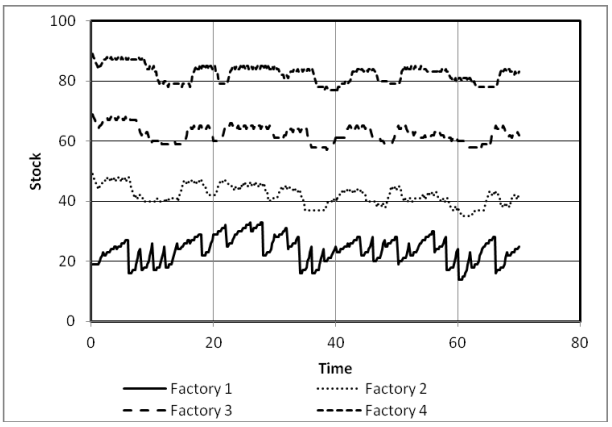

Figure 7: Stock with a random ordering strategy

5 CONCLUSIONS AND FUTURE TASKS

This study is a theoretical view of the bullwhip effect, applying the discrete event simulation. The supply chain model has quite a simple structure. The advantage is to see the main influences of the bullwhip effect. Due to dead times caused by production or storage, it is difficult to get a constant stock through a closed-loop control. In a supply chain, the bullwhip effect is manageable if a Smith-predictor is applied, even if the companies handle their stock independently. Two different order policies for the customer at the end of the supply chain have been studied. The first strategy was a single order, which could be closed-loop controlled in the nominal stock. The second strategy was a random order in a rather short time. In both strategies, with the application of a Smith-predictor and the limitation of the production time for one unit, the bullwhip effect does not exist. In the simulation, the limitation of the production time is a quite simple method to manage the bullwhip effect. Of course, the limitation of the production time can be done in a real system too, however, the knowledge from the orders in the past and the trends for the future define the limitation. This is the reason to create a self-learning model in the next step. Not included in this simulation was the examination of the behavior of a supply chain with a seasonal trend. A seasonal trend is comparable with an oscillation. These oscillations are often very difficult to control. The impact of a seasonal trend to the bullwhip effect has to be exanimated in a next simulation study. Subsequently, it has to be checked if this theoretical knowledge can be transferred to a real supply chain. A real supply chain has to be simulated then.

REFERENCES

Barbey, H.-P.: A New Method for Validation and Optimisation of Unstable Discrete Event Models“, erschienen in den proceedings der 23. European Modeling & Simulation Symposium (EMSS), Rome, 2011.

Barbey, H.-P.: Simulation des Stabiltätsverhalten von Produktionssystemen am Beispiel einer lagerbestandsgeregelten Produktion, Erschienen in: Advances in Simulation for Production and Logistics Application, Hrsg.: Rabe, Markus, Stuttgart, Fraunhofer IRB Verlag, 2008, S.357-366.

Barbey, H.-P.: Application of the Fourier Analysis for the Validation and Optimisation of Discrete Event Models, erschienen in den Proceedings der ASIM 2011, 21. Symposium Simulationstechnik, 7.9.-9.9.2011, Winterthur.

Bobal, V. und R. Matasu, P. Dostal: Digital Smith-predictor-design and simulation study, Proceedings of 25th European conference of Modelling and Simulation (ECMS), Krakow, 2011.

Bretzke, W.-R.: Logistische Netzwerke, Springer Verlag Berlin Heidelberg, 2008.

Dickmann, P.: Schlanker Materialfluss, Springer Verlag Berlin Heidelberg, 2007.

Erlach, K.: Wertstromdesign, Springer Verlag Berlin Heidelberg, 2010.

Forrester, J.W.: Industrial Dynamics: A major breakthrough for decision makers. In: Harvard business review, 36(4), 1958.

Gudehus, T.: Logistik, Springer Verlag Berlin Heidelberg, 2005.

AUTHOR BIOGRAPHIES

HANS-PETER BARBEY was born in Kiel, Germany, and attended the University of Hannover, where he studied mechanical engineering and graduated in 1981. He earned his doctorate from the same university in 1987. Thereafter, he worked for 10 years for different plastic machinery and plastic processing companies before moving in 1997 to Bielefeld and joining the faculty of the University of Applied Sciences Bielefeld, where he teaches transportation technology, plant planning and discrete simulation. His research is focused on the simulation of production processes.

His e-mail address is:
`hans-peter.barbey@fh-bielefeld.de`
And his Web-page can be found at
`http://www.fh-bielefeld.de/fb3/barbey`

Simulation of the control of exponential smoothing by methods used in industrial practice

Professor Dr.-Ing. Frank Herrmann
Hochschule Regensburg - University of Applied Sciences Regensburg
Innovation and Competence Centre for Production Logistics and Factory Planning (IPF)
PO box 120327, 93025 Regensburg, Germany
E-Mail: Frank.Herrmann@HS-Regensburg.de

KEYWORDS
Forecast of demands in industrial practice, simulation experiment, Enterprise Resource Planning (ERP) system, Production Planning and Control (PPS) system, adaptive method, exponential smoothing.

ABSTRACT
Demands of customers for products and of the production for parts are being forecasted quite often in companies. The results are used extensively within the operational production planning and control by IT Systems like the SAP system. Hereby preferably methods based on exponential smoothing are being applied. Especially, in industrial practice it is expected that the pattern of the data change over time in such a way, that the parameters of the exponential smoothing have to be changed. In some companies thousands of items require forecasting, which is very laborious. With an adaptive method the parameters are modified in a controlled manner, as changes in the pattern occur. Two adaptive methods used in industrial practice are explained. Simulation experiments over a huge number of periods show when they should be used.

1. INITIAL SITUATION

Forecasts of demands for quantities of products in subsequent periods are carried out several times in a planning process of a company. The fact that the module "Demand Planning" is the most frequently used module within Enterprise Resource Planning (ERP) or Production Planning and Control (PPS) systems in companies, emphasizes that. Other planning functions within ERP or PPS systems use forecasts as well – one example is the use of "alternative planning types".

In general forecasting methods are chosen for a certain forecasting model. The more accurately a forecasting model describes the actual demand series, the better the forecasting results are. Actual changes in industrial practice can be corrected by adapting the forecasting model and in consequence by changing the forecasting method. Due to the Wold decomposition (Wold 1938) a forecasting model consists – simply speaking – of a linear combination of a sequence of uncorrelated random numbers and a random addend. If there's a level shift within the forecasting model where one (or more) non-zero coefficients (of the linear combination) are being changed to a different non-zero value, the known forecasting methods adapt in time. Their adaption speed is relatively high when using methods based on exponential smoothing. Such (forecasting) methods are preferably used in ERP or PPS systems and therefore generally in companies. Empirical studies (as Armstrong 2001) show that exponential smoothing outperforms on average complex or statistical sophisticated methods and only sometimes they are worse.

If such a level shift is highly significant, there may be a strong manual adaption of the parameters required – depending on the settings of the exponential smoothing. Because of the enormous amount of forecasts in companies, the number of manual settings required might rise quite fast. Furthermore such a change is to be distinguished from a temporal change, especially from an outlier. That is the reason why so called adaptive methods have been developed where the parameters are being adapted automatically. For an overview see (Mertens and Rässler 2005).

For the investigation the behaviour of the forecasting methods are simulated about a huge number of periods. Such simulations at the IPF show that the results occur by exponential smoothing of the first degree. Since the behaviour of this exponential smoothing is easier to understand as the ones for seasonal data or data with a trend, the paper focuses on this method.

Proceedings 26th European Conference on Modelling and Simulation ©ECMS Klaus G. Troitzsch, Michael Möhring, Ulf Lotzmann (Editors)
ISBN: 978-0-9564944-4-3 / ISBN: 978-0-9564944-5-0 (CD)

2. FORECASTING METHODS AND KEY FIGURES

The simplest forecasting method based on exponential smoothing determines the forecast value in period t (p_t) through: $p_t = p_{t-1} + \alpha \cdot e_t$. α is the smoothing parameter and $e_t = y_t - p_t$ the forecasting error. Whereas y_t represents the demand of period t; so: $p_t = \alpha \cdot y_{t-1} + (1-\alpha) \cdot p_{t-1}$.

This exponential smoothing of the first degree is suitable for demands which fluctuate around a mean value. This will be advanced in chapter "Simulations". Before starting with this standard procedure the initial value of the forecast (for the first period) and the smoothing parameter have to be set. That is usually done by analysing a long series of previous demands. This demand series formulates along with a performance criterion an optimization problem. In literature many performance criteria are being proposed; refer to (De Gooijer and Hyndman 2006) for example.

Usually an unbiased forecasting method is required. This means that the expected value of the forecasting errors is zero. The standard deviation of the forecasting errors allows a statement about the safety level with which forecasted demands will occur in the future. That is why it has been examined. In order to achieve steady key figures all forecasting methods are applied on very long demand series – at least over 2500 periods.

3. ADAPTIVE METHODS

Although there is no consensus as to the most useful adaptive method, the most widely-used one was developed by Trigg and Leach (Trigg and Leach 1967). They apply exponential smoothing of the first degree to the forecasting error and to its absolute value. The forecasting error being $SE_t = \phi \cdot e_{t-1} + (1-\phi) \cdot SE_{t-1}$ and the absolute value $SAE_t = \phi \cdot |e_{t-1}| + (1-\phi) \cdot SAE_{t-1}$ with a common smoothing parameter (ϕ). The tracking signal $TS_t = \frac{SE_t}{SAE_t}$ is now used as smoothing parameter α_t for calculating the forecasting value of time period t + 1; this method is called control (of the smoothing parameter). Trigg shows in (Trigg 1964) that the tracking signal recognizes a structural change within a demand series and for this he recommends a smoothing parameter of $\phi = 0{,}1$. The starting values of these two exponential smoothing methods should be low because of the expected mean forecasting errors of nearly zero. In detail $SE_0 = 0{,}05$ and $SAE_0 = 0{,}1$ have been chosen during the investigation for this article.

Since this method delivers sometimes unstable forecasts, α_t is restricted in various ways, s. (Whybark 1973) and (Dennis 1978). In another approach the smoothing parameter is adapted by the Kalman Filter, s. (Bunn 1981), (Enns et al. 1982), (Synder 1988), for weighted least squares s. (Young 1999, Young et al. 1999, Young 2003) and its using for exponential smoothing s. (Harvey 1990). For further approaches s. (Mentzer 1988), (Mentzer and Gomes 1994), (Pantazopoulos and Pappis 1996) and (Taylor 2004). These adaptive methods were investigated empirically, but no method is superior. Gudehus in (Gudehus and Kotzab 2009) presents an adaptive method which he implemented in a number of consulting projects but which is not analysed in research so far.

Gudehus uses an adaptive calculated smoothing parameter $\alpha_\lambda(t)$ which is calculated at the end of each period t in his exponential smoothing of the first degree for the dynamic mean value forecast in period t $\lambda_m(t) = \alpha_\lambda(t) \cdot \lambda(t-1) + (1-\alpha_\lambda(t)) \cdot \lambda_m(t-1)$ and the dynamic variance forecast in period t

$$s_\lambda(t)^2 = \alpha_\lambda(t) \cdot (\lambda(t-1) - \lambda_m(t-1))^2 + (1-\alpha_\lambda(t)) \cdot s_\lambda(t-1)^2$$

With current variation $\upsilon_\lambda(t) = \frac{s_\lambda(t-1)}{\lambda_m(t-1)}$ and maximal acceptable variation υ_{max} $\alpha_\lambda(t)$ is calculated by

$$\alpha_\lambda(t) = \frac{2 \cdot \min(\upsilon_\lambda(t)^2, \upsilon_{max}^2)}{\upsilon_\lambda(t)^2 + \min(\upsilon_\lambda(t)^2, \upsilon_{max}^2)}.$$

Gudehus restricts the effective smoothing range by a lower and an upper limit, i.e. $\alpha_{min} \le \alpha_\lambda(t) \le \alpha_{max}$.

Compared to the aforementioned investigations this paper presents additional types of demand pattern and uses data the IPF received from various companies. There results allow an estimation of the performance of an adaptive method compared to an optimal one.

4. SIMULATIONS

The Wold decomposition mentioned in chapter 1 is a characteristic of so called stationary statistical processes. Within a (weak) stationary statistical process the expected value, the standard deviation and the autocovariance are constant over time and the random variables to the demands in each period are independent of one another; refer to (Tijms 1994) and (Herrmann 2009) for example. Therefore it is not surprising that forecasting methods for stationary statistical processes have been developed.

One such stationary statistical process, called scenario 1 in the following, consists of a constant μ (as mean value) and its the random addend ε_t; i.e. $\mu + \varepsilon_t$ for every period t. Exponential smoothing of the first degree solves the corresponding optimization model with a smoothing parameter close to zero, as shown in (Herrmann 2009) for example.

In scenario 1 the control of the smoothing parameter α provides significantly worse results. Already a constant smoothing parameter of $\alpha = 0.1$ reduces the variance of the forecasting error almost always by at least 9 %. The ideal forecast – hence a very small smoothing parameter – reduces the variance of the forecasting error usually by at least 14%. The mean value of the forecasting error is in the ideal forecast and usually also with a smoothing parameter of 0.1 almost zero. Opposed to the control where admittedly small values exist, but with a high percentage of deviation – typical values are: 0.18, but also values around 1 are possible. That is why the control leads contrary to the standard procedure already with a plausible setting of 0.1 for the smoothing parameter, (which results from a standard recommendation for the smoothing parameter), significantly worse results and should be avoided.

To analyse control, the behaviour of the tracking signal over time is being analysed. At first a smoothing parameter which is small enough to make the forecast equal to the mean value of the demand series, is being considered. An ideal forecasting method has a forecasting error which strongly deviates from zero and an absolute forecasting error which deviates even more from zero. The above-mentioned parameters for the exponential smoothing of the forecasting error and the absolute forecasting error – based on the work of Trigg – do not ensure an ideal forecasting model with the mean value of the forecasting error as a constant value over time. Hence smoothed forecasting errors and smoothed absolute forecasting errors, which differ considerably from zero, occur. Because the forecasting errors and their smoothed values fluctuate around zero, different strong deviations between the smoothed forecasting errors and the smoothed absolute forecasting errors are to be expected in the single periods. Hence it follows that the tracking signal will also fluctuate over time. Empirical investigations with a great number of demand series confirm this analysis.

The development of the tracking signal over 300 periods as shown in figure 1 is representative. The numbers are taken from the periods 1400 to 1699 of a specific demand series. To analyse the degree of the fluctuation, very long demand series – 2500 periods – have been considered. Within these the first 100 periods have not been considered to exclude the influence of less favourable starting parameters for the smoothing of the forecasting error and the absolute forecasting error. Of course the mean values and the standard deviation of the tracking signals of such demand series fluctuate. But due to a high number of demand series the mean values should be 0.2 and the fluctuations 0.15. Figure 2 provides an insight in the rate of the occurring single values by showing the representative percental rate of the tracking signal in left open and right closed intervals of the length 0.1. Although no smoothing parameter is the most frequent, over 70% of the values are greater than 0.1. Hence it is to be expected that when using the control within a great number of periods, a smoothing parameter which is too high will be applied.

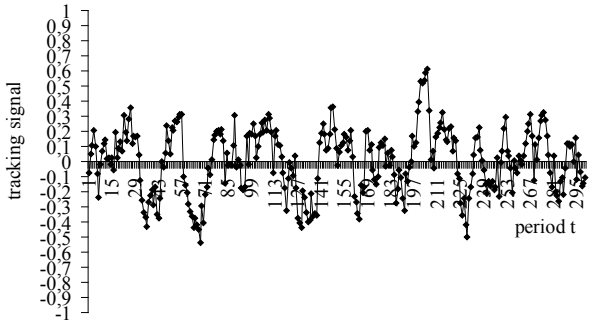

Figure 1: Development of the tracking signal for the periods 1400 – 1699 in an ideal forecast in scenario 1

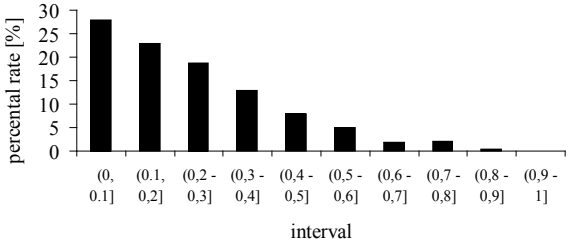

Figure 2: Frequency distribution of the tracking signal in an ideal forecast in scenario 1

A rise of the smoothing parameter in the standard procedure reduces the mean value and also the standard deviation of the tracking signals of such demand series. This explains, that with the control of the tracking signal due to a high number of demand series considered, a similar mean value (0.2) but an around 0.02 lower standard deviation (0.13), occurs. The decrease of the standard deviation which has already been expressed by the reduction of very high and very low tracking signals leads to an modified structure in the representative rate of the tracking signal respectively the control as shown in Figure 3. Because of that the portion of smoothing parameters over 0.1 should be already over 77%. Hence the probability of using a smoothing parameter which is too high even increases. This instability is observed by adaptive methods in general, as said earlier, and they have been criticised for leading to unstable forecasts.

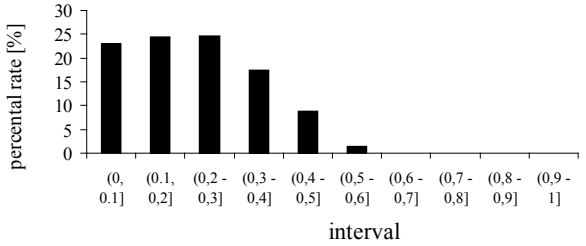

Figure 3: Frequency distribution of the tracking signal in the control in scenario 1

In the procedure of Gudehus the adaptive calculated smoothing parameter $\alpha_\lambda(t)$ has also various values. As Figure 4 shows the highest possible smoothing

parameter of one occurs in 32.32% of the periods. Therefore, the results are significantly worse than the ones obtained by control – the variance increases by 48% compared to the control and 72% compared to the standard procedure with an optimal α. Gudehus recommends an upper limit of 0,33 for $\alpha_\lambda(t)$, which causes a constant $\alpha_\lambda(t)$ in nearly every period. In these cases maximal acceptable variation υ_{max} is equal to the ratio of the variance of the demands and the mean of the demands and around 4,03% which corresponds to the recommendation of Gudehus that the value should be 5%. A significant reduction of the mean demand – the variance of the demand remains unchanged – delivers better values if the maximal acceptable variation υ_{max} is still 5%. So, it can be expected that better results are achieved by a limitation of υ_{max}. Experiments confirm this.

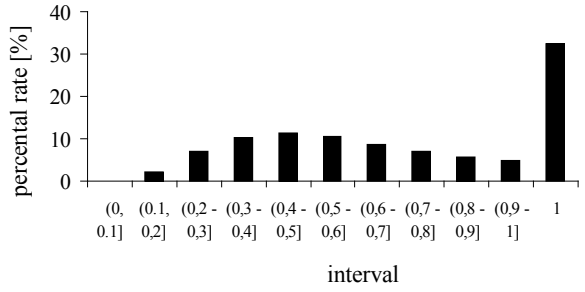

Figure 4: Frequency distribution of the tracking signal in the procedure of Gudehus in scenario 1

In scenario 2 a strong change in the level of the forecasting model occurs at a period T. Due to results in (Trigg 1964) it can be expected that the control delivers nearly immediately values close to the new level. In the standard procedure the speed of adaption increases with an increase of the smoothing parameter (α). So, the adaption speed is in reverse very slow with a α of 0.1 and for very small α the ideal forecast is extremely slow, almost zero. Therefore, the standard procedure delivers after a high number of periods again better values than the control. The results of the procedure of Gudehus are much better than the ones of the standard procedure with a α of 0.1, but still significantly worse than the ones of control. Experiments show that often there exists a α so that the standard procedure delivers the best results.

A reduction of the relative height of the change of the mean value – which has been examined within scenario 3 – reduces this effect. Then the disadvantage of the instability of α is more important, so that a marginal change, especially compared to the standard deviation of the mean value, causes the standard procedure using a smoothing parameter of 0.1 provide better results than the control, but they are a little lower than the improvement of the results in scenario 1. If the standard deviation is high compared to the change of the mean value, a very small smoothing parameter (in the standard procedure) provides even better results, which can often be further improved by a slightly higher smoothing parameter. Whereas this improvement is negligibly small compared to the decline of the key figures when using the control. With a very high smoothing parameter (in the standard procedure) the adaption speed can be increased significantly compared to the control because the tracking signal lies in most cases between 0.7 and 0.8 in some periods after T + 1, which has been proven by a great number of demand series. This approach requires a good recognition of such a strong change in the level of the forecasting model.

According to the research of Trigg (refer to Trigg 1964) the value of the tracking signal should only exceed the threshold of 0.5 when there is a structural change within a demand series which includes a clear level change. Hence the tracking signal in scenario 1 should be between [-0.5, 0.5]. Indeed this did happen during the investigation with the standard procedure the more often, the closer the forecast came to the mean value of the demand series – hence the better the forecast was. With a (very) small smoothing parameter (α) longer fractions of demand series of subsequent demands having a positive or negative forecasting error e_t, compared to a relatively high (α), occur. Or their absolute forecasting errors are higher. This is owing to the fact, that because of the statistical independence of the random values for the single demands, with a rising α it becomes more and more likely, that the forecasting error e_t changes sign and positive and negative forecasting errors balance each other out more often within a relatively short time span. Because of the relatively short memory of exponential smoothing of the first degree, this causes – using a (very) small α compared to a relatively high α – longer sequences with a positive or negative SE_t. Their absolute values are in tendency higher whereas the corresponding SAE_t values are lower. This leads to the occurrence of subsequent demands, which have a higher $|TS_t|$ with a (very) small α than with a high α. That elevates the probability that in one period $|TS_t| > 0,5$ exists. The smallest number of false alarms in the investigations has almost always been with the control. This number has usually already been reached in the standard procedure with a α of 0.2. In reverse the occurrence of a strong level shift has been detected by the control almost as often as by the standard procedure with a very small smoothing parameter during the investigation. The control in scenario 1 rarely provided values of the tracking signal of more than 0.5 in more than two subsequent periods; this could be partly increased quite significantly with a high deviation. For an effective recognition of a significant level shift the tracking signal should be used and its value should be above 0.5 for at least some periods. After that the control should be used

to forecast until the new mean value has been discovered. Then, the ideal forecast should be set. A high number of simulation experiments show, that such a manual intervention should lead to an improvement in the standard procedure opposed to the control, which can be compared to the improvement mentioned in scenario 1.

Responsible for the optimality of the constant forecast in scenario 1 is the stochastic independence of the random values to the single demands. In contrast to this, in industrial practice it is often assumed that subsequent demands are related; this was also confirmed by data the IPF received from various companies. Mathematically this relation can be achieved by an autocorrelation through time. In scenario 4 auto correlated random numbers have been created after the method Willemain and Desautles proposed in (Willemain and Desautles 1993). Here a random value is generated by forming the sum of two uncorrelated uniformly distributed random numbers. This sum is transformed to a uniform distribution with the help of simple formulas for the distribution function of two uniformly distributed random numbers. In the next step this uniform distribution is used as a new addend for the next sum which leads to an auto correlation. Using the inverse method this uniformly distributed random series is transformed to a different distribution. For the investigations a normal distribution, with moments that almost entirely avoid negative demands, has been used. Furthermore the moments are identical in every period. That is why there is again a stationary demand series present (refer to (Herrmann 2009)). The resulting demand series have been additionally classified according to which smoothing parameter of the set R = {0.1, 0.2, 0.3, 0.4, 0.5, 0.6, 0.7, 0.8, 0.9} supplies the best results through the standard procedure.

Even if 0.9 in the standard procedure delivers the best results, control uses only a few high smoothing parameters (α) over 0.5. Figure 5 visualizes an example with many very high smoothing parameters; the mean value is 0.38, the standard deviation is 0.21 and about one third of the α are higher than 0.5. The investigation prooves, that the standard procedure using a α of at least 0.5 (in R) in scenario 4 provides significantly better results than the control. Often the improvements are considerably over 10% of the variance of the forecasting error – a α over 0.7 (in R) provides improvements of over 30%. The other extreme occurs when an α below 0.1 is best. Then the standard procedure usually provides better results with a α of 0.1 than the control, whereas the improvement is typically much smaller than the one mentioned in scenario 1.

Compared to the control the procedure of Gudehus delivers better results. Normally, they are not as good as the ones by the standard procedure. The procedure of Gudehus delivers the best results if the demand follows a curve which is similar to a sinusoidal curve, which is a special case of autocorrelation. Then, the key figures are much better than the ones of control, but the ones of the standard procedure with the best smoothing parameter in R are normally close to ones of the procedure of Gudehus – often they are even slightly better.

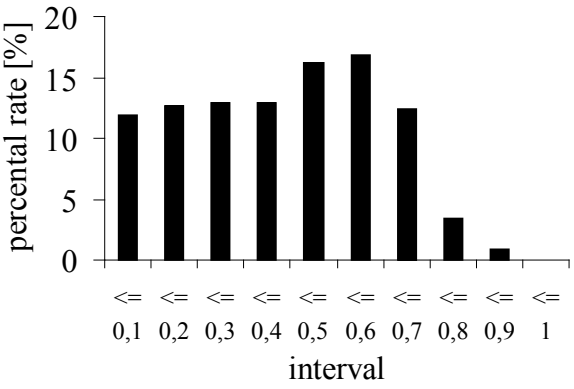

Figure 5: Frequency distribution of the tracking signal with the control – with the standard procedure having a α of the set R α = 0.9 is the best value.

In scenario 4' demand series with α in [0.1; 0.3] as best value in the standard approach are being examined. Such demand series occur when the lag is 1 and the auto correlation coefficient is low. This combination causes the occurrence of several directly succeeding periods, where a high smoothing parameter (greater than 0.5) is suitable (effect 1), because the demands rise or fall in these periods. Or a very low smoothing parameter is suitable (effect 2) because high and low demands alternate in these periods. Figure 6 shows an example. It visualizes the demands of more than 100 subsequent periods. At the beginning and in the middle the first effect occurs and primarily at the end the second one. Within the second effect the short memory of exponential smoothing of the first degree causes the smoothing of the (absolute) forecasting errors to produce small SE_t and relatively high SAE_t values. The control chooses a small smoothing parameter which is preferable. Hence such demand series favor a smoothing parameter which fluctuates over time. The control does not always finds the best parameter over time. Thus the control provides in many cases key figures (primarily the variance of the forecasting error) which are almost as good or even slightly better than the standard procedure with the best possible α. Opposed to any α in [0.1, 0.3] the key figures are usually significantly better; around 10%. Hence the standard procedure should provide increasingly worse results over time, however only with a very high number of periods; this argumentation is confirmed by many simulation experiments. This can be avoided, if the smoothing parameter is adapted periodically according to the last demands. This adaption may happen after a high number of periods. The control is in conclusion especially of advantage, if a manual setting of the smoothing parameter (in the standard approach) is to be

avoided. In this scenario the procedure of Gudehus is not an alternative, because it delivers always the worst results.

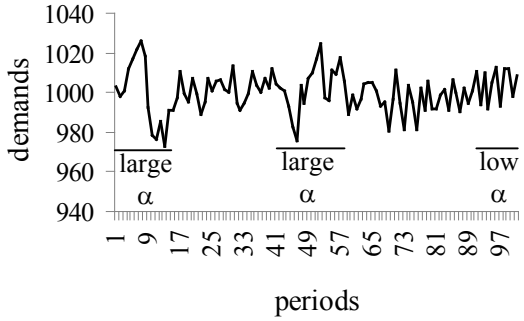

Figure 6: Demand series in scenario 4‘

A rising increase of the autocorrelation coefficient causes a growing occurrence of effect 1 and a growing decline of effect 2, so that a growing increase of α delivers the best results. Opposed to that a higher lag causes a decline of effect 1. With increasing lag, demands like in scenario 1 occur in subsequent periods – in the extreme case it is scenario 1. This favors the standard procedure compared to the control and the smoothing parameter in the standard procedure is rather small, confirmed by extensive simulation experiments. It has to be emphasized, that with a rising lag the value of the autocorrelation coefficient becomes more and more irrelevant. The achieved improvement of the results in this way is usually smaller than in scenario 1 which was measured in a lot of simulation experiments.

Up to this point only stationary demand series have been examined. If the adjustments of scenario 2 and 3 happen not only once, but after a certain number of periods (n), the mean value changes over time. This is scenario 5. Respectively the standard deviation can be altered after n periods as well. The adjustments of n, the mean value and the standard deviation may be constant or they can be produced randomly. Through that further scenarios arise.
According to the considerations above, the following two rules and their reversals are valid:

- a rising mean value favors a rising α and
- a rising number of periods favors a declining α.

If these two factors of influence change radically over time, the two (above) effects yet occur. Control provides the better results for the reasons mentioned above. If one of the factors of influence is being kept constant, a smoothing parameter for the standard approach can be found which provides better results than the control. An autocorrelation in such demand series strengthen the common occurrence of effect 1 and 2. Again, in this scenario the procedure of Gudehus is not an alternative.

The effect of a high variance in the scenarios is studied. The experiments show that a rising increase of the variance causes better key figures for the standard procedure compared to both alternatives. Often the procedure of Gudehus profits by high variance. Then, in the scenarios (in general) in which control delivers better results as the procedure of Gudehus, the difference is reduced by a rising increase of the variance.

Finally, real world data are regarded. There are daily, weekly and monthly demand and the time horizons varies between three and ten years. The data are received from retailers and from companies dealing with spare times. As observed in industrial practice, the demand is normally distributed, typically. This is the case for nearly 70% of the real world data. For them, the standard procedure delivers the best key figures as expected by results for scenario 1. Unfortunately, some data sets consist of just a few periods. In these cases, the number of historical data is too small to calculate an effective start value. So, that in some of these cases, around 35%, control delivers the best results. As also observed in industrial practice, demand is gamma distributed for some products, here for around 10%. With the same reason the standard procedure delivers again the best results; for the same reason as above some exceptions occur. The remaining data sets are unsuccessfully tested for typical distributions with SPSS. Due to the analysis it is plausible, but not proven, that these 20% data sets belong to scenario 5. Responsible for this unusual high portion are the demand for the spare times. In most of these cases, around 80%, control delivers better results than both alternatives. In some cases this is caused by a small number of historical data, as argued above. In the remaining cases the standard procedure is best, but the key figures of control is often just a little bit inferior.

Finally, at the IPF exponential smoothing of the second degree has also been examined where the smoothing parameter α has been set to $|TS_t|$. As in the procedures of Holt and Winters one or more additional smoothing parameters occur. In the studies the additional smoothing in the procedure of Holt is set to 10% of α, as recommended in (Herrmann 2011). In addition the third parameter in the method of Winters is set to $|TS_t|$, where suitable (absolute) forecasting errors for the seasonality have to be calculated. The studies show again a high sensitivity of the tracking signal. So, comparable results can be expected, which is proven by a limited amount of experiments.

5. RESULTS AND RECOMMENDATION

Demand series with correlation of subsequent demands (autocorrelation) or changing structure over time (instationary demand series), for which every smoothing parameter should be smaller than 0.5 in the standard procedure, the standard procedure with any smoothing parameter in G = {0.1, 0.2, 0.3, 0.4, 0.5} often only provides better results than the control or at least just as good results, if the ideal choice of the smoothing parameter in G has been made. A random choice of the

smoothing parameter in G provides in general far worse results. These demand series of type R therefore favor the control, if a manual setting of the smoothing parameter in the standard procedure is to be avoided (because this is too time-consuming). Regarding actual demand series in industrial praxis, forecasting methods based on exponential smoothing usually achieve even better results, if the parameters, including the starting values, are being determined by solving an optimization problem and the parameter settings are being recalculated after a number of periods like 300 for example. This should also apply to a significant number of demands series of type R. Such an approach is especially suitable for premium products, usually A class parts. It should also be mentioned that latest elaborations on exponential smoothing (refer to (Gardner 2006) for example) may offer even better results. Especially concerning an ABC distribution, there are products where such an effort is too high in comparison to the gain of a reduction primarily of the variance of the forecasting errors. Then the control of demand series of type R should be used. As shown by a large number of simulation experiments, for demand series of type R (except for having to choose a high smoothing parameter) the control is less favorable than the standard procedure. It is also the less favorable alternative with stationary demand series which are statistically independent. For such demand series the standard procedure should be applied principally. Finally, the procedure of Gudehus is just in special cases an alternative to the control. Since it is normally unknown if this is the case, the procedure should be avoided.

REFERENCES

Armstrong, J. S. (Editor) 2001. *Principles of Forecasting: A Handbook for Researchers and Practitioners*. Springer Verlag, Boston, USA.

Bunn, D. W. 1981. "Adaptive forecasting using the Kalman filter". *Omega* 9, 323-324.

De Gooijer, J. G., Hyndman, R. J. 2006. "25 years of time series forecasting". *International Journal of Forecasting*, 22, Issue 3, S. 443–473.

Dennis, J. D. 1978. "A performance test of a run-based adaptive exponential smoothing". *Production and Inventory Management* 19, 43-46.

Enns P. G., Machak J. A., Spivey W. A., Wroblesk W. J. 1982. "Forecasting applications of an adaptive multiple exponential smoothing model". *Management Science* 28: 1035-1044.

Gardner, Everette S. 2006. "Exponential smoothing: The state of the art – Part II." *International Journal of Forecasting*, Volume 22, Issue 4, S. 637 – 666.

Gudehus, T. Kotzab, H. 2009: *Comprehensive Logistics*. Springer, Hamburg.

Harvey A. C. 1990. *Forecasting, structural time series models and the Kalman filter*. Cambridge University Press: New York.

Herrmann, F. 2009: *Logik der Produktionslogistik*. Oldenbourg Verlag, Regensburg.

Mentzer J. T. 1988. "Forecasting with adaptive extended exponential smoothing". *Journal of the Academy of Marketing Science* 16, 62-70.

Mentzer J. T, Gomes, R. 1994. "Further extensions of adaptive extended exponential smoothing and comparison with the M-Competition". *Journal of the Academy of Marketing Science* 22, 372-382.

Mertens, P.; Rässler, S. (Editor) 2005. *Prognose-rechnung*. Physica-Verlag, Heidelberg.

Pantazopoulos S. N, Pappis C. P. 1996. "A new adaptive method for extrapolative forecasting algorithms". *European Journal of Operational Research* 94, 106-111.

Snyder R. D. 1988. "Progressive Tuning of Simple Exponential Smoothing Forecasts". *Journal of the Operational Research Society* 39, 393-399.

Taylor J. W. 2004. "Smooth Transition Exponential Smoothing". *Journal of Forecasting*, 23, pp. 385-394

Tijms, H. C. 1994. *Stochastic Models – An Algorithmic Approach*. Wiley, Chichester.

Trigg, D. W. 1964: "Monitoring a forecasting system". *Operations Research Quarterly* 15, 271 ff.

Trigg, D. W., Leach, A. G. 1967. "Exponential smoothing with an adaptive response rate". *Operations Research Quarterly* 18, p. 53 ff.

Whybark D. C. 1973. "Comparison of adaptive forecasting techniques". *Logistics Transportation Review* 8, 13-26.

Willemain, T. R., Desautels, P. A. 1993. „A method to generate autocorrelated uniform random numbers. *Journal of Statistical Computation and Simulation*, 45, pp. 23–31.

Wold, H. 1938. *A study in the analysis of stationary time series*. Verlag Almqvist and Wiksell, Stockholm 1938.

Young P. C. 1999. "Nonstationary time series analysis and forecasting". *Progress in Environmental Science* 1, 3-48.

Young P. C., Pedregal D. J, Tych W. 1999. "Dynamic harmonic regression". *Journal of Forecasting* 18, 369-394.

Young P. C. 2003. "Identification of time varying systems". Forthcoming in Encyclopaedia of Life Support Systems, UNESCO.

AUTHOR BIOGRAPHY

Frank Herrmann was born in Münster, Germany and went to the RWTH Aachen, where he studied computer science and obtained his degree in 1989. During his time with the Fraunhofer Institute IITB in Karlsruhe he obtained his PhD in 1996 about scheduling problems. From 1996 until 2003 he worked for SAP AG on various jobs, at the last as director. In 2003 he became Professor for Production Logistics at the University of Applied Sciences in Regensburg. His research topics are planning algorithms and simulation for operative production planning and control. His e-mail address is: Frank.Herrmann@HS-Regensburg.de and his Web-page can be found at http://homepages.fh-regensburg.de/~hef39451/dr_herrmann/.

APPROXIMATION OF PEDESTRIAN EFFECTS IN URBAN TRAFFIC SIMULATION BY DISTRIBUTION FITTING

Andreas D. Lattner, Jörg Dallmeyer, Dimitrios Paraskevopoulos
Goethe University Frankfurt
P.O. Box 11 19 32, 60054 Frankfurt, Germany
[lattner|dallmeyer|paraskev]@cs.uni-frankfurt.de

Ingo J. Timm
University of Trier
54296 Trier, Germany
ingo.timm@uni-trier.de

KEYWORDS

Multimodal Traffic Simulation, Pedestrian Impact Approximation, Distribution Fitting

ABSTRACT

For a proper simulation of urban traffic scenarios, besides cars other road users, namely bicycles and pedestrians, have to be modeled. In scenarios where a whole city is modeled, a detailed actor-based simulation of pedestrians leads to expensive extra computational load. We investigate to what extent it is possible to capture traffic effects imposed by simulated pedestrians and then perform simulations without pedestrians. We propose to collect information about pedestrian impacts in a simulation with pedestrians, estimate underlying probability distributions and finally, use a simplified model where only these effects are generated probabilistically. We investigate two approaches – a best-fit distribution fitting and a histogram-based distribution approximation – using synthetic data as well as simulated traffic scenarios. The experiments show that using the proposed approximations can lead to similar average cars' travel times.

INTRODUCTION

The continuous increase of traffic has led to the situation that in many areas congestions occur frequently. Traffic as a field of research has been addressed by many researchers and among the goals of such studies are to get insights about traffic effects as well as to investigate strategies to improve the situation. The modeling of traffic dates back to the beginning of the last century (Greenshield, 1935). One famous model that has been widely used for the simulation of traffic – mainly on motorways – has been introduced by Nagel and Schreckenberg. The Nagel-Schreckenberg model (NSM) is a time and space discrete model which has been used to analyze certain traffic effects (Nagel and Schreckenberg, 1992).

For a proper simulation of urban scenarios, besides cars other road users, namely bicycles and pedestrians, have to be modeled. Although there exist some simulation systems which aim at the simulation of urban scenarios, they usually either focus on a detailed reproduction (including visualization) of rather small scenarios or they do not take into account requirements of multimodal traffic with varying behaviors and characteristics (like velocities and acceleration) of different road users.

One particular model for the simulation of multimodal traffic including different cars (passenger cars and trucks), bicycles, and pedestrians has been introduced by (Dallmeyer et al., 2011). In contrast to the NSM, it uses a continuous space model and thus, provides means for the representation of different road users' characteristics. In this work we use and extend this simulation system.

In an earlier study, we have investigated the impact of pedestrians to urban traffic and the results indicated that actually simulating pedestrians has influence to car traffic with a tendency to increase car travel times if more pedestrians are in transit (Dallmeyer et al., 2012b). Therefore, an analysis of the effects including pedestrians in the simulation is out of scope of this paper. Simulating a whole city with potentially one million residents or more leads to a large number of road users including a significant fraction of pedestrians. A detailed actor-based simulation of all these pedestrians leads to expensive computational load.

As in many studies the focus is set on strategies of how to arrange traffic in a way that motorized traffic is more efficient, we investigate in this paper if it is possible to capture effects imposed by pedestrians and then perform simulations without actually simulating pedestrians. We propose to first collect information about pedestrian impacts in a simulation with pedestrians, estimate underlying probability distributions of these impacts and finally, use a simplified simulation model where only these effects are generated probabilistically.

RELATED WORK

Traffic simulation is done for different scenarios ranging from the simulation of whole countries (Voellmy et al., 2001) to high-fidelity simulation of small areas (Bönisch and Kretz, 2009). The simulation of pedestrians has also been addressed by different works including high-fidelity models like the social force model Helbing and Molnár (1995), macroscopic models like Hughes (2003) or microscopic models built on cellular automatons like Blue and Adler (2001). Our work focuses on a level of detail enabling simulation of whole cities and still regarding multi modality (Dallmeyer et al., 2012a).

Techniques of distribution fitting are used to establish a probability distribution function F from a sample (a set of observations) (e.g., (Law, 2007)). Additionally, distri-

Proceedings 26th European Conference on Modelling and Simulation ©ECMS Klaus G. Troitzsch, Michael Möhring, Ulf Lotzmann (Editors)
ISBN: 978-0-9564944-4-3 / ISBN: 978-0-9564944-5-0 (CD)

butions' parameters, e.g., mean and standard deviation of a normal distribution, can be assigned. In Goodness-of-Fit tests, statements as to whether a sample might have been drawn from a certain distribution are made. In these tests, the null hypothesis is that the considered values have been generated by the distribution function F. Common tests are the Chi-Square test, the Kolmogorov-Smirnov test, the Anderson-Darling test and the Poisson-Process test; for more information about these tests see, e.g., (Law, 2007, p. 340-353). Regarding the Chi-Square Test, it is necessary to divide the data in adjacent intervals. In the next step, respecting the specific distribution function, the probability for several values falling into each interval has to be determined. Finally, after computing the test statistic χ^2, the null hypothesis will be rejected, if differences appear to be too large and thus, the probability of a type 1 error is below a threshold α.

Distribution fitting is widely applied to input data in the context of simulation in order to set up probability distributions, e.g., in manufacturing or arrival patterns of patients in healthcare (cf. Kuhl et al. (2007)). To the best of our knowledge the approximation of pedestrian effects in traffic simulation by distribution fitting has not been addressed so far.

TRAFFIC SIMULATION SYSTEM

The traffic simulation system used in this work is MAINS^{2}IM (MultimodAl INnercity SIMulation). It can automatically build up simulation models using cartographical material from *OpenStreetMap*[1] (OSM). A study about OSM map quality can be found, e.g., in Haklay (2010). At first, an arbitrary area is extracted from an OSM file. The included geoinformation is separated into logical layers for different types of geometries. The system generates a graph data structure from a layer representing roads and incorporates information from additional layers like, e.g., the areas of cities. Several analysis and correction steps are performed in order to build a valid graph (e.g., putting nodes at intersections of edges, considering bridges and tunnels and determining roundabouts). The system is built on a geographical information system on the basis of *GeoTools*[2].

Mixed traffic is simulated under usage of models for cars (passenger cars, trucks and buses), as well as bicycles and pedestrians. The models are discrete in time with (default) time steps of 1s per simulation iteration. Movement is modeled continuously in space. Pedestrian movements are simulated using two models: one for sidewalk movements on a graph structure, and one for crossing roads at pedestrian crossings. Interaction of pedestrians with other road users takes place when pedestrians cross roads – either at a pedestrian crossing or at some other position of a road – and other road users need to brake to avoid collisions.

The simulation system is implemented in Java and can be used on an off-the-shelf PC. The system is capable for the simulation of the traffic of whole cities. Further information about MAINS^{2}IM can be found in (Dallmeyer et al., 2012a,b, 2011; Lattner et al., 2011) and on the website `www.mainsim.eu`.

[1] http://www.openstreetmap.org

[2] http://www.geotools.org

PEDESTRIAN EFFECT APPROXIMATION

The pedestrian model used in MAINS^{2}IM is introduced in (Dallmeyer et al., 2012b). This work analyzes the interaction between pedestrians and road traffic. These interactions occur whenever a pedestrian crosses a road or uses a traffic light and a car needs to slow down because of this action. Pedestrians cross roads when a perceptual sufficient gap in traffic exists. The perceptions may be faulty and lead to pedestrians crossing the road without sufficient gaps. Traffic lights and crosswalks are stored in nodes of the simulation graph. A pedestrian crossing a node blocks the affected edges at this position. The impact is measured by capturing how often and how long pedestrians interfere with other road users. This section discusses two methods to approximate the influences of pedestrians on urban traffic. Both approaches use observed data from simulations with pedestrians as input. The approaches are independent of specific data but can be used to generate approximations of probability distributions from provided samples.

Best-fit Distribution Fitting

The first approach is the best-fit distribution fitting. In this approach, the samples are passed to a distribution fitting algorithm based on maximum likelihood estimation for distributions' parameters. We use the *MASS* package of R Project in order to fit the distributions (Venables and Ripley, 2002) (also cf. (Ricci, 2005)). In our approach, we take into account Gaussian, exponential, and uniform distributions. For the latter case, no distribution fitting is used but minimal and maximal values of the sample are taken as parameters for the approximated distribution. Of course, the set of distribution types to be tested can be extended as desired.

In order to decide which distribution to use, a χ^2 test is performed for all distribution types. The range of the sample $s = (s_1, \ldots, s_l)$ is divided into n equidistant intervals with $n = 1 + log_2(l)$ (Sturges' formula). These intervals are used for the performance of the χ^2 tests and the fitted distribution with highest p value is then used as approximation (the lower the p value, the lower the probability having a type 1 error, i.e., selecting the alternative hypothesis assuming that the sample has not been generated by the given distribution although actually the null hypothesis is valid). Figure 1 illustrates the approach where the distribution fitting results for three samples from different distribution types are shown.

Histogram-based Distribution Approximation

As the best-fit distribution fitting approach only takes into account (a selection of) univariate distributions and

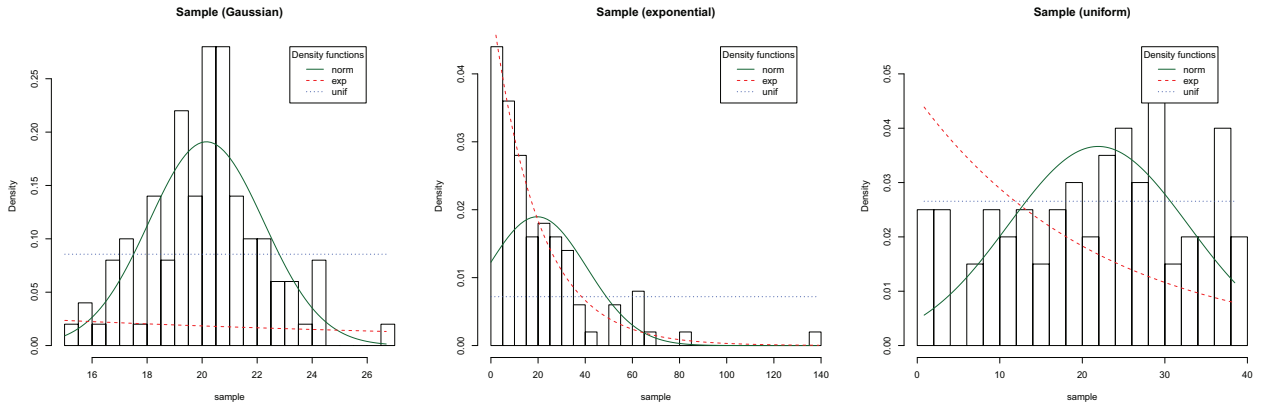

Figure 1: Distribution fitting results for three samples

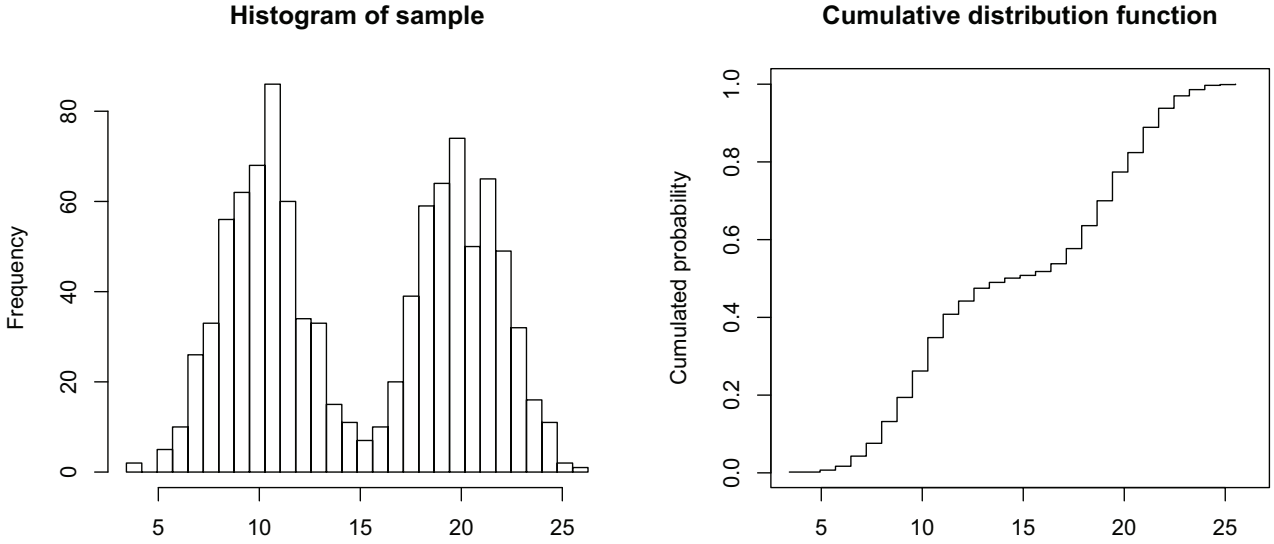

Figure 2: Illustration of histogram-based distribution approximation

as it might be that the probability distributions under consideration exhibit other characteristics, we also analyze a second approach in this paper. In histogram-based distribution approximation, an observed sample $s = (s_1, \ldots, s_l)$ is divided into n categories. While different ways to select n can be chosen, we use the following formula as it leads to a sufficient minimal number of categories and grows logarithmic with the sample size l: $n = max(10, round(10 \times log_{10}(l)))$. The range of the values is split into n intervals and frequencies are measured for each bin. The relative frequency is used to generate a cumulative distribution function (Figure 2). Similar to existing approaches, the inverse of the cumulative distribution function can be used for the generation of random numbers following this distribution. In this case, a uniform random number in the interval $[0, 1]$ is generated and the corresponding x value is identified. A random number is generated using a uniform random number generator in the interval $[x - x_{step}, x]$ with $x_{step} = ((max(s) - min(s))/n)$.

EVALUATION - SYNTHETIC DATA

In the first part of the evaluation, synthetic data using random samples from artificial probability distributions are used in order to evaluate the best-fit distribution fitting approach. An explicit generation of random samples from given distributions has the advantage that the underlying type of probability distribution as well as its parameters are known in advance. Therefore, it is possible to assess if the approach is able to identify the correct type of distribution. Furthermore, using parameter estimation, a statement about the difference of real and estimated values can be performed.

For evaluation, we have generated a number of samples with different sizes and using different probability distributions (Gaussian, exponential, and uniform). For each distribution, we randomly generate parameters and use these parameters to generate random samples of different sizes (20, 50, and 100 values) in order to find out how the approach works in dependence of the size of samples. For each distribution and sample size combina-

	Sample size: 20				Sample size: 50				Sample size: 100			
	Gauss	Exp.	Unif.	Recall	Gauss	Exp.	Unif.	Recall	Gauss	Exp.	Unif.	Recall
Gauss	874	0	126	87.40	983	0	17	98.30	1000	0	0	100
Exp.	155	841	4	84.10	35	965	0	96.50	1	999	0	99.90
Unif.	471	22	507	50.70	263	1	736	73.60	111	0	889	88.90
Prec.	58.27	97.45	79.59		76.74	99.90	97.74		89.93	100	100	

Table 1: Confusion matrices of the best-fit approach using synthetic data

tion, 1000 random values are generated. The generation of parameter values is done as follows (using uniform probabilities within the specified ranges):

- Gaussian distribution: Mean μ is chosen randomly as $\mu = 1 + unif(0.0, 20.0)$ and standard deviation σ is chosen randomly using $\sigma = unif(0.0, 0.2\mu)$.
- Exponential distribution: The rate λ is chosen using the same range for the expected value as in the Gaussian distribution: $\lambda = \frac{1}{1+unif(0.0,20.0)}$.
- Uniform distribution: For the uniform distribution, the minimal value (left limit) min_{unif} is chosen randomly with $min_{unif} = unif(1, 40)$ and the maximal value (right limit) with $max_{unif} = unif(min_{unif}, 40)$.

The function $unif(min, max)$ denotes a random number generator using a uniform probability distribution. For the generation of the samples we have used *R* (R Development Core Team, 2011). Interaction with *R* is done via the *rJava* library (Urbanek, 2011).

For the evaluation with synthetic data, we investigate in how many cases the correct type of distributions has been identified and capture how the actual parameters differ from the estimated ones. Table 1 shows the classification results for the three different sample sizes. The results are presented as confusion matrices where the lines represent the actual distribution and the columns the classification decision. If 20 values are used, the recall values for the Gaussian and exponential samples are above 84% and for the uniform distribution $\sim$ 50%. The precision values using the Gaussian, exponential, and uniform samples are approximately 58%, 97%, and 80%, respectively. It can be observed that the uniform samples are classified as Gaussian distributions in many cases. With increasing sample sizes, the misclassification rates decrease. Using samples with 50 or 100 values leads to recall values above 96% for the Gaussian and the exponential samples and to precision values above 97% for the exponential and uniform samples. Especially, the confusion among Gaussian and uniform distributed values is smaller if more values are used. For sample size 100, only 11.1% of the uniformly distributed samples are misclassified as Gaussian while all but one sample of the other two distribution types are classified correctly.

Table 2 presents the average p values of the χ^2 test and the differences to the original distributions' parameters, subdivided into the samples which have been classified correctly and incorrectly as well as the joint values ("total"). Additionally, it is shown in how many cases the p value of the χ^2 test was below $\alpha = 0.05$ for the different distribution types, indicating that the alternative hypothesis would be chosen, i.e., that it cannot be assumed that the sample was drawn by the corresponding distribution. The results show that on average the p values of the χ^2 test with the (true) distribution type are above 0.5 in all cases and that the average p values are smaller for the misclassified samples in comparison to the correctly classified ones. Average (absolute) differences between fitted and actual distributions' parameters are below 0.22 for Gaussian mean, below 0.16 for Gaussian standard deviation, below 1.88 for the inverse of the exponential rate $(1/\lambda)$, below 0.46 and 0.43 for the minimal and maximal value of the uniform distribution. The α threshold comparisons show that the tests with the correct distribution type reject the null hypothesis in all cases in less than 5%. It also shows that with increasing sample sizes, the rejection rates of the wrong distribution types increase.

EVALUATION - TRAFFIC SIMULATION

In the second part of the evaluation, distribution fitting is applied to the results of simulation runs with simulated pedestrians. The simulation is done in the area of Hanau, shown in figure 3.

Each simulation run starts with a settlement phase of 1,000 iterations, followed by a measurement phase of 50,000 iterations. The amount of road users is held constantly at 2,500 with 33% cars, 7% bicycles and 60% pedestrians. Whenever a pedestrian p crosses a road r, its position, the time period since the last crossing pedestrian on r, and the time duration the crossing took will be stored in an observance object for r. Crossing actions at nodes of the simulation graph are handled similarly. After a simulation run, the measured data is analyzed and probability distributions for crossing time intervals, crossing positions and crossing durations for each node and edge of the graph are estimated.

A second run is performed with identical copies of the used cars and bicycles of the former run, but pedestrians are now approximated by dummy pedestrians, influencing traffic using the estimated probability distributions.

The whole setting is repeated 100 times with different initial seed values for the random number generator. The quantity for a comparison of the different settings in

Sample	correct classif.			incorrect classif.			total			χ^2 test		
	avg. p	avg. diff. mean	avg. diff. sd	avg. p	avg. diff. mean	avg. diff. sd	avg. p	avg. diff. mean	avg. diff. sd	$p_{Gauss} <$ α (in %)	$p_{exp} <$ α (in %)	$p_{unif} <$ α (in %)
Gauss 20	0.69	0.22	0.15	0.56	0.21	0.17	0.68	0.22	0.16	0.60	100.00	15.70
Gauss 50	0.66	0.12	0.09	0.46	0.19	0.10	0.66	0.12	0.09	2.30	100.00	72.20
Gauss 100	0.62	0.09	0.06	n/a	n/a	n/a	0.62	0.09	0.06	3.30	100.00	99.80
	avg. p	avg. diff. $1/\lambda$		avg. p	avg. diff. $1/\lambda$		avg. p	avg. diff. $1/\lambda$		$p_{Gauss} <$ α (in %)	$p_{exp} <$ α (in %)	$p_{unif} <$ α (in %)
Exp. 20	0.62	1.88		0.35	1.70		0.58	1.85		24.40	3.10	77.30
Exp. 50	0.57	1.25		0.20	0.85		0.56	1.24		76.80	4.80	99.90
Exp. 100	0.55	0.86		0.01	0.06		0.55	0.86		98.80	5.00	100.00
	avg. p	avg. diff. min	avg.diff. max	avg. p	avg. diff. min	avg.diff. max	avg. p	avg. diff. min	avg.diff. max	$p_{Gauss} <$ α (in %)	$p_{exp} <$ α (in %)	$p_{unif} <$ α (in %)
Unif. 20	0.61	0.47	0.39	0.40	0.45	0.48	0.51	0.46	0.43	1.10	92.80	3.80
Unif. 50	0.56	0.21	0.21	0.36	0.17	0.19	0.51	0.20	0.20	6.30	99.80	3.90
Unif. 100	0.53	0.09	0.08	0.25	0.09	0.11	0.50	0.09	0.09	21.70	100.00	4.70

Table 2: p-values and differences to original distributions' parameters of the best-fit approach using synthetic data

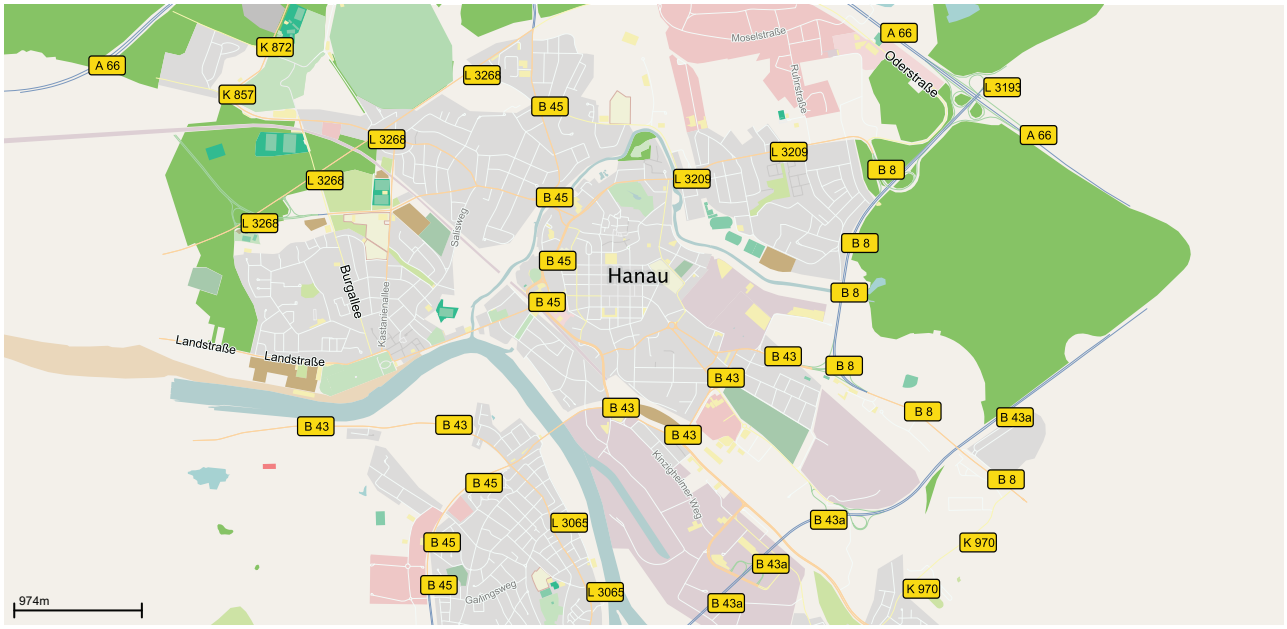

Figure 3: Map area for simulation (4,201 nodes, 5,758 edges, 548km total length of roads)

this experiment is the mean travel time for each setting. Whenever a car or bicycle leaves the simulation, its travel time will be recorded and averaged at the end of the run.

Two methods for estimation of the probability distributions are used: (a) A distribution taking into account all pedestrians crossing roads (blue, rhombus) and (b) one for those pedestrians which are crossing roads and are actually influencing traffic (green, triangle). A pedestrian p influences traffic whenever a road user ru has a distance smaller or equal to its velocity to p, because ru needs to brake in order to avoid a collision with p. Because the pedestrian dummies are set on roads without taking into account the current traffic situation, this might lead to a situation where road users have to brake strongly, because the dummies do not look for sufficient gaps, they just appear. This leads to an overestimation of travel times for road users. Method (b) does not overestimate as much, because the number of dummies is reduced to the number of pedestrians, who have in fact forced road users to brake. The estimated travel times overlap with the original travel times with simulated pedestrians (black, square) in some cases. In comparison to the runs with pedestrians, results of a simulation with no pedestrians and no dummies are shown (red, circle).

Figures 4(a) and 4(b) show the simulation results of the best-fit approach and of the histogram-based approach. It is obvious that pedestrians increase travel times of cars and bicycles. The simple method of calculating probability distributions for each pedestrian crossing roads and then setting dummies without taking care of traffic conditions (a) leads to an overestimation of travel times, as assumed. Method (b) performs better. In a few runs, (b) nearly reproduces the results of the runs with simulated pedestrians. Table 3 shows the mean travel times of cars and bicycles, averaged over all simulation runs. Apparently, method (b) leads to an overestimation of travel times ($\approx 2s$), which is not as great as the underestimation when pedestrians are not respected ($\approx 3s$). Approximations using the best-fit and the histogram-based approaches lead to similar mean travel times.

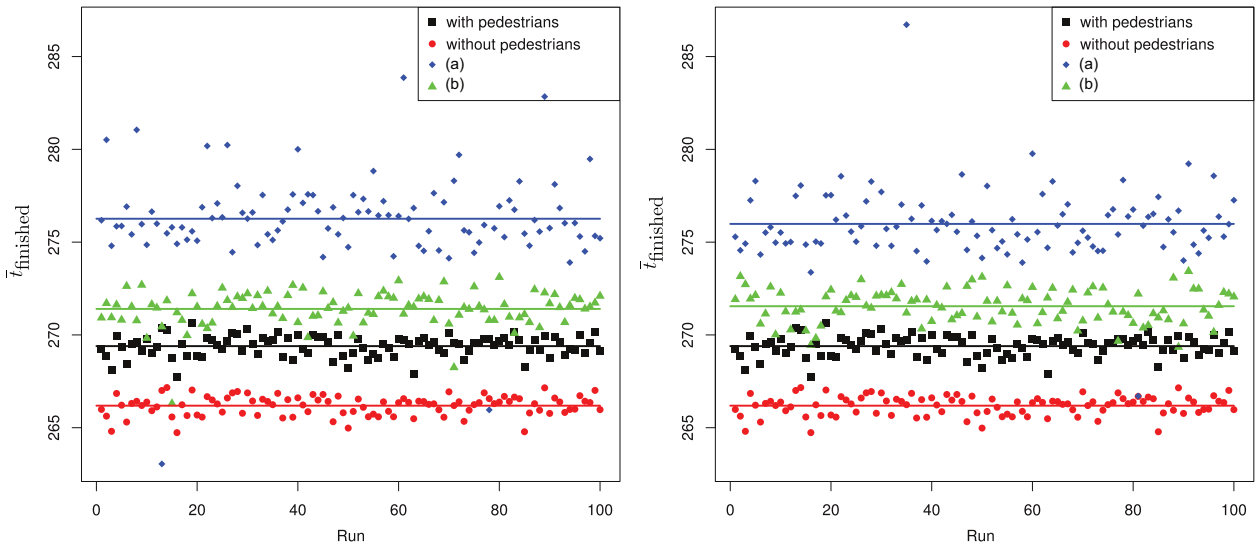

(a) Best-fit (b) Histogram based

Figure 4: Comparison of different setups with average travel times of road users $\bar{t}_{\text{finished}}$ $[s]$. Lines show mean values.

	$\bar{t}_{\text{finished}}$ $[s]$	
	Best-fit	Histogram based
(a)	276.26	275.98
(b)	271.40	271,55
with pedestrians	269.34	
without pedestrians	266.19	

Table 3: Mean travel times for cars and bicycles in different settings.

CONCLUSION

We have investigated two approaches for approximation of pedestrian impacts in urban traffic simulation. The first approach is based on distribution fitting using the distribution with the lowest expected error probability based on a χ^2 test. The second approach is a histogram-based approximation of a probability distribution. The realization of the best-fit approach – if implemented from scratch – needs more effort as specific details about all different distributions have to be taken into account and some technique for parameter estimation needs to be integrated. The histogram-based approach can be implemented with less effort as it is mainly based on counting how many values belong to each of the bins. In some contexts it might be more interesting to get information about what kind of distribution is expected to have generated observed data as provided by the best-fit approach. The histogram-based approach is only reflecting the distribution without providing any additional information.

The best-fit approach has been additionally evaluated using synthetic data. The evaluation has shown that when using sample sizes of 20 that Gaussian and uniform probability distributions are mistaken in many cases, while with increasing sample sizes the distribution types can be distinguished with higher accuracies.

The experiments approximating pedestrian effects in traffic simulation have shown that both approaches, best-fit distribution fitting and the histogram-based approach, exhibit similar mean travel times. The mean differences regarding the observed average travel times in comparison to the simulation with pedestrians are 2.06s and 2.21s. The approximation approaches are overestimating the mean travel times but the differences are smaller than not taking into account pedestrians at all (3.15s).

Using this approximation leads to an about two times faster simulation as detailed pedestrian behavior needs not to be computed. The proposed approach could also be used to extend other traffic simulation systems if the approximated effects of pedestrian travels are integrated.

For future work, it would be interesting to extend the best-fit approach and to take into account further distributions as well as multivariate distributions. Furthermore, a better selection of the "relevant" pedestrians who actually have impact to motorized traffic could lead to even smaller differences in the simulation results. It could also be investigated to what extent different numbers of bins – in the histogram-based approach as well as for the Goodness-of-Fit test – have influence on the results. It would also be interesting to address how more realistic data about pedestrian behavior could be collected – preferably in an automated way.

REFERENCES

Blue, V. J. and Adler, J. L. (2001). Cellular automata microsimulation for modeling bi-directional pedestrian walkways. *Transportation Research Part B: Methodological*, 35(3):293 – 312.

Bönisch, C. and Kretz, T. (2009). Simulation of pedestrians crossing a street. *Proceedings of the Eighth International Conference on Traffic and Granular Flow*, 8.

Dallmeyer, J., Lattner, A. D., and Timm, I. J. (2011). From GIS to Mixed Traffic Simulation in Urban Scenarios. In Liu, J., Quaglia, F., Eidenbenz, S., and Gilmore, S., editors, *4th International ICST Conference on Simulation Tools and Techniques, SIMUTools '11, Barcelona, Spain, March 22 - 24, 2011*, pages 134–143. ICST, Brüssel.

Dallmeyer, J., Lattner, A. D., and Timm, I. J. (2012a). *Data Mining for Geoinformatics: Methods and Applications*, chapter GIS-based Traffic Simulation using OSM. Springer. (accepted).

Dallmeyer, J., Lattner, A. D., and Timm, I. J. (2012b). Pedestrian simulation for urban traffic scenarios. *Proceedings of the 44rd Summer Simulation Multi-Conference (SummerSim'12)*. (submitted).

Greenshield, B. D. (1935). A study of traffic capacity. *Proceedings of the 14th Annual Meeting Highway Research Board 14*, 468:448–477.

Haklay, M. (2010). How good is volunteered geographical information? a comparative study of OpenStreetMap and ordnance survey datasets. *Environment and Planning B: Planning and Design*, 37(4):682–703.

Helbing, D. and Molnár, P. (1995). Social force model for pedestrian dynamics. *Physical Review E*, 51(5):4282–4286.

Hughes, R. L. (2003). The flow of human crowds. *Annual Review of Fluid Mechanics*, 35(1):169–182.

Kuhl, M. E., Lada, E. K., Steiger, N. M., Wagner, M. A., and Wilson, J. R. (2007). Introduction to modeling and generating probabilistic input processes for simulation. In *Proceedings of the 39th Winter Simulation Conference*, WSC '07, pages 63–76, Piscataway, NJ, USA. IEEE Press.

Lattner, A. D., Dallmeyer, J., and Timm, I. J. (2011). Learning dynamic adaptation strategies in agent-based traffic simulation experiments. In *Ninth German Conference on Multi-Agent System Technologies (MATES 2011)*, pages 77–88. Springer: Berlin, LNCS 6973, Klügl, F.; Ossowski, S.

Law, A. M. (2007). *Simulation Modeling & Analysis*. McGraw-Hill, 4th, internat. edition.

Nagel, K. and Schreckenberg, M. (1992). A cellular automaton model for freeway traffic. In *Journal de Physique I*, volume 2, pages 2221–2229. ISSN 1155-4304.

R Development Core Team (2011). *R: A Language and Environment for Statistical Computing*. R Foundation for Statistical Computing, Vienna, Austria. ISBN 3-900051-07-0.

Ricci, V. (2005). Fitting distributions with R. Release 0.4-21, `http://cran.r-project.org/doc/contrib/Ricci-distributions-en.pdf`, accessed: 04/13/2012.

Urbanek, S. (2011). *rJava: Low-level R to Java interface*. R package version 0.9-0.

Venables, W. N. and Ripley, B. D. (2002). *Modern Applied Statistics with S*. Springer, New York, fourth edition.

Voellmy, A., Vrtic, M., Raney, B., Axhausen, K., and Nagel, K. (2001). *Status of a TRANSIMS implementation for Switzerland*. Swiss Federal Institute of Technology. `http://dx.doi.org/10.3929/ethz-a-004339673`.

AUTHOR BIOGRAPHIES

ANDREAS D. LATTNER received the Diploma (2000) and the doctoral degree (2007) in computer science at the University of Bremen, Germany. From 2000-2007 he was working as research scientist at the Center for Computing Technologies (TZI) at the University of Bremen. He works now as a postdoctoral researcher at the chair for "Information Systems and Simulation" at the Goethe University Frankfurt. His research interests include knowledge discovery in simulation experi-ments, temporal pattern mining, and multi-agent systems.

JÖRG DALLMEYER received the bachelor degree (2008) as well as the master degree (2009) in computer science at the Goethe University of Frankfurt am Main, Germany. Since December 2009, he has been a PhD student at the chair for "Information Systems and Simulation" at the Goethe University Frankfurt. His research interests are actor based simulation for the field of traffic simulation under consideration of multi modal traffic and the building of simulation systems from geographical information.

DIMITRIOS PARASKEVOPOULOS received the diploma degree (2010) in computer science at the Goethe University of Frankfurt am Main, Germany. Since February 2011, he has been a PhD student at the chair for "Information Systems and Simulation" at the Goethe University Frankfurt. His research interests are Process Mining and IT Risk Management.

INGO J. TIMM held various positions in research at University of Bremen, Technical University Ilmenau, and Indiana University Purdue University - Indianapolis (IUPUI) from 1998 until 2006 before being appointed full professor for Information Systems and Simulation at Goethe-University Frankfurt/Main. Since 2010, he holds a chair for Business Information Systems at University of Trier. Ingo Timm is speaker of the German SIG on Distributed Artificial Intelligence (FG-VKI) of German Informatics Society. His special interest lies on business information systems, intelligent assistance systems, (actor-based/multiagent-based) simulation, and knowledge-based support to simulation system.

Acknowledgement This work was made possible by the *MainCampus* scholarship of the *Stiftung Polytechnische Gesellschaft Frankfurt am Main*. Parts of this paper are results of the EDASim project (Hessen Agentur Project No.: 260/11-06), funded by the German State Hesse in context of the Hessen ModellProjekte ("LOEWE - Landes-Offensive zur Entwicklung Wissenschaftsökonomischer Exzellenz").

FUEL CONSUMPTION AND EMISSION MODELING FOR URBAN SCENARIOS

Jörg Dallmeyer, Carsten Taubert, Andreas D. Lattner
Goethe University Frankfurt
P.O. Box 11 19 32, 60054 Frankfurt, Germany
[dallmeyer|taubert|lattner]@cs.uni-frankfurt.de

Ingo J. Timm
University of Trier
54296 Trier, Germany
ingo.timm@uni-trier.de

KEYWORDS

Multimodal Traffic Simulation, Fuel Consumption, Emission Simulation

ABSTRACT

Traffic simulation systems are widely used for the prediction of certain effects like traffic jam formation or the analysis of performance for new traffic light systems. Fuel consumption and CO_2 emissions are important measurements. This work integrates a physical model for fuel consumption into a microscopic traffic simulation system for urban scenarios. The parameters of the model are discussed and practical values are given. The model is evaluated on different scenarios with focus on innercity simulation. The results indicate that the simulation of bicycles and pedestrians as well as the usage of a Digital Terrain Model (DTM) increase fuel consumption of simulated cars. A map of CO_2 emissions for the chosen simulation area is calculated and provides an insight on how emissions are distributed in cities.

INTRODUCTION

The increasing amount of road users has led to the situation that road network capacities seem to be exceeded in many areas due to high traffic load. Besides economic disadvantages as well as personal inconveniences of road users being stuck in traffic, the ecological facet has recently gained more attention. Potential effects of air pollution on the Earth's atmosphere like global warming as well as impacts on health are subject of many discussions.

Simulation is widely used to study traffic effects or to get insights on how certain traffic strategies can have influence on a specific situation. However, most studies address consequences regarding the emergence (or avoidance) of congestions or deal with aspects on how to arrange and configure road networks in a way that travel times can be optimized.

Another field of study is the dispersion of gases under certain atmospheric conditions. Using this kind of simulation, it can be estimated how certain gases disperse, e.g., if certain wind directions and wind speeds are present. If information about CO_2 emission of cars was used in combination with such gas dispersal simulations, it would be possible to gain valuable information concerning what regions are likely to have a high pollution due to traffic and atmospheric situations. It could be identified if there are certain regions where it is expected that critical values for toxicity will frequently be exceeded or how high gas concentration is in particular regions of interest.

In this paper, we present a first step towards such a combined simulation. Based on the traffic simulation model presented in (Dallmeyer et al., 2011), we introduce a fuel consumption model and provide means to capture CO_2 emissions at specific positions. With this information at hand, it is possible to generate "emission maps" for different road network configurations. In order to have a more realistic fuel consumption model, the approach also takes into account elevation of the region, i.e., consumption in dependence of the slope can be computed.

The paper is structured as follows. In the next section, we present a selection of related approaches addressing traffic simulation as well as models for fuel consumption. In the subsequent section, we describe the used traffic simulation system. The fuel consumption model and its integration to the simulation system are then presented. The evaluation of the approach is described subsequently. In the final section we draw conclusions and discuss some ideas for future works.

TRAFFIC SIMULATION AND FUEL CONSUMPTION

Traffic simulation systems are used for different purposes like, e.g., traffic jam prediction (Sugiyama et al., 2008) or traffic light optimization (Brockfeld et al., 2001). The range of fidelity differs from macroscopic models (e.g., gas kinetic models) to high fidelity microscopic models (e.g., the Wiedemann model, used in VISSIM (Wiedemann, 1974)).

In order to predict the effects of different influencing actions (e.g., modifications on the course of road or alterations on traffic light circuits) on traffic with respect to fuel consumption and CO_2 emissions, road traffic models need to be extended by a model for fuel consumption. This has been done in several studies (Carten et al., 2010; Karathodorou et al., 2010; Pelkmans et al., 2005; Ahn et al., 2002). To the best of our knowledge, no study investigates the influence of multimodality in urban scenarios on fuel consumption.

Fuel consumption models discussed in literature are

Proceedings 26th European Conference on Modelling and Simulation ©ECMS Klaus G. Troitzsch, Michael Möhring, Ulf Lotzmann (Editors)
ISBN: 978-0-9564944-4-3 / ISBN: 978-0-9564944-5-0 (CD)

based on rolling, aerodynamic, frictional, and acceleration resistance. The physical coherences to calculate the driving resistance and the needed engine power for vehicle movement is discussed in literature, e.g., (Treiber and Kesting, 2010; Heißing et al., 2011). (Ross, 1997) compares an amount of modeled cars with respect to fuel consumption and discusses some strategies for reduction of fuel consumption with new car design strategy or hybrid engine power. The fuel consumptions of four simulated cars are shown to deviate less then 1% from measured data in the study of (An et al., 1997). The functionality of the catalytic converter is analyzed with respect to toxic substances produced by vehicles for the development of an emission model (Cappiello et al., 2002).

The literature shows that the simulation of fuel consumption and emissions is possible. This work focuses on the simulation of the traffic of whole cities with help of MAINS^{2}IM. Thus, the extension by a fuel consumption model based on technologies described in literature will lead to a system being able to undertake innovative simulation studies with respect to multimodality and size of study. We have available a Digital Terrain Model (DTM) with resolution of 10m for our evaluation simulation area and thus, can investigate the influence of downhill-slope force on fuel consumption.

SIMULATION SYSTEM

The model for fuel consumption and CO_2 emissions applied in this work is part of the traffic simulation system MAINS^{2}IM (MultimodAl INnercity SIMulation). Cartographical material from *OpenStreetMap*[1] (OSM) can be used to automatically generate a simulation model from a user defined area. A discussion of map quality of OSM can be found, e.g., in Haklay (2010). The information in this material is split into several logical layers and a simulation graph data structure is calculated. Geographical operations as well as the rendering of the map section are done with help of a geographical information system on basis of *GeoTools*[2]. A number of analysis and correction steps extract information from the map layers and refine the simulation graph.

The simulation system applies microscopic traffic simulation models for cars (passenger cars, trucks and buses), bicycles and pedestrians. The models are continuous in space and discrete in time with simulation time steps of $1s$ real time.

The simulation system is written in Java and can be used on a workstation computer. More detailed information about the basic concept, the developed models and applications for the simulation system can be found in (Dallmeyer et al., 2011; Lattner et al., 2011; Dallmeyer et al., 2012a,b) and on the website `www.mainsim.eu`.

[1] http://www.openstreetmap.org

[2] http://www.geotools.org

MODEL FOR FUEL CONSUMPTION AND CO_2 EMISSIONS

The fuel consumption and emission model is built as a separate simulation extension. In exchange with the new extension only a few parameters are provided by the simulation: position, type, velocity v, acceleration $\dot{v}$ and length l of the vehicle as well as the gradient angle α of the street. Other parameters are defined from the extension itself according to statistical rules.

The physical power P depends on the minimum power demand P_0, instantaneous power F and the velocity v:

$$P = P_0 + \max\left(F \cdot v, 0\right)$$

The value of F may become negative, when the vehicle decelerates or drives downhill. Anyhow, the car spends power P_0 for, e.g., light, radio or the power to overcome friction within the pistons of the motor during idling of the engine.

F depends on the inertial force $m \cdot \dot{v}$, the frictional force $m \cdot g \cdot \mu$, the downhill-slope force $m \cdot g \cdot \sin\left(\alpha\right)$ and the air resistance $\frac{1}{2} \cdot c_w \cdot \rho \cdot A \cdot v^2$. This leads to

$$F = m \cdot \dot{v} + \left[\mu + \sin\left(\alpha\right)\right] \cdot m \cdot g + \frac{1}{2} \cdot c_w \cdot \rho \cdot A \cdot v^2$$

Several parameters for the model need to be defined: The mass of car m, the frictional coefficient μ, the air resistance factor c_w (a measure for aerodynamic), the air density ρ and the cross-section surface A.

Therefore, detailed statistical data of (Kraftfahrt-Bundesamt, 2009) is used that describe the distribution of vehicles and fuel types as well as the loading of trucks in Germany. In order to calculate m, a significant factor for fuel consumption, the defined length of the car l is multiplied with a factor which is measured by a collection of 50 typical cars and their length-mass ratio.

Parameters like the frontal area of a car A and the air drag coefficient c_w are normally distributed on a statistically determined arithmetical mean. Further undefined parameters are supposed constant: the coefficient of rolling resistance of the tires, air density, lower heating value of the gasoline depending on the fuel type and engine efficiency.

Let $\mathcal{N}_a^b\left(\mu, \sigma\right) = \min\left(\max\left(\mathcal{N}\left(\mu, \sigma\right), a\right), b\right)$ be a Gaussian distributed random number with μ and σ bounded to the interval $[a \cdots b]$. Table 1 shows the estimated values for the fuel consumption model. The values of μ, ρ[3] are taken from (Ross, 1997), the values of P_0 from (Treiber and Kesting, 2010).

During initialization of the simulation, the individual car characteristics needed for the fuel consumption and emission model are calculated and assigned to each vehicle. The values for v, $\dot{v}$ and α of the current street are forwarded to the new extension and are used to calculate the consumption and emission during a simulation on every simulation step for every single vehicle. Therewith,

[3] Typical value for normal height null and 20 °C.

$\mu = 0.01$
$P_0^{\text{car}} = 3\text{kW}$ $P_0^{\text{truck}} = 6\text{kW}$
$c_w^{\text{car}} = 0.3$ $c_w^{\text{truck}} = 0.8$
$\rho = 1.2\text{kg} \cdot \text{m}^{-2}$
$m^{\text{car}} = 1000 \cdot l \cdot \mathcal{N}_{0.26}^{0.49}\,(0.339\text{kg}, 0.34)$
$A^{\text{car}} = \mathcal{N}_{2.3}^{2.81}\left(2.5\text{m}^2, 0.1\right)$ $A^{\text{truck}} = \mathcal{N}_{6.0}^{10.0}\left(8.0\text{m}^2, 0.25\right)$

Table 1: Estimated parameters for the fuel consumption model.

it is possible to retrieve the current and overall consumption and emission for every car.

The amount of carbon dioxide is calculated directly proportional to the vehicle's fuel consumption (Treiber and Kesting, 2010; Schreiner, 2011). The emissions vary for diesel (2.68 kg/l) and gasoline-powered vehicles (2.32 kg/l). In order to calculate other emissions like nitrogen and carbon hydride, it would be necessary to take into account dependencies and the functionality and effectiveness of the vehicles catalyst. For that reason only carbon dioxide will discussed in this article.

In order to generate an emission map for a selected area, the simulation map extract is divided in a variable number of subareas. Each subarea cumulates the emissions of all vehicles within in the current simulation step. The emissions are cumulated during the simulation. After finishing a simulation run, the emission module exports a matrix with the summarized emissions of all subareas.

EVALUATION & CASE SCENARIOS

In this section we present the evaluation of the model for fuel consumption and CO_2 emissions. The extended simulation system is applied to a number case studies investigating impacts of multimodal traffic and elevation information.

Evaluation of the Simulation Model

In order to determine the fuel consumption of a new car, the European Union has established the NEDC (New European Driving Cycle). Thereby a car has to pass different traffic situations on a roller dynamometer test bench to log fuel consumption and emissions. Every car manufacturer is obliged to publish these key data.

These data is ideally suitable for comparison with data obtained from simulation. For this purpose some cars are simulated in NEDC-similar conditions in an urban and a mixture of urban and country road scenario. The amount of cars is held constantly at 1. The simulation duration is 86,400 iterations. Whenever the simulated car has reached its destination of travel, a new one gets inserted into the simulation. The vehicle fuel consumptions are protocolled. The experiment is repeated for four

vehicle	NEDC city	NEDC mix	SIM city	SIM mix
Smart ForTwo	4,6 l	4,3 l	5,2 l	4,3 l
Audi A4	8,8 l	7,0 l	9,5 l	7,0 l
Porsche 987	13,8 l	9,4 l	13,5 l	9,8 l
Mercedes C180	6,3 l	4,7 l	6,5 l	4,7 l

Table 2: NEDC and simulated fuel consumption in comparison.

modeled car types. Table 2 shows the results of the simulation in comparison with the NEDC values.

The next step to verify the fuel consumption and emission model described in the preceding section is to simulate scenarios with a typical number of cars in various regions. The first test simulates an urban area with a road network of 150 km and 500 cars. Therefore, the mean fuel consumption for all cars in this simulation run is calculated and compared with the mean NEDC value for urban areas out of 50 reviewed state-of-the-art cars. As there is no interaction and influence between cars in the NEDC, it is expected that the simulated consumption is higher. The simulation results confirm this assumption. While the NEDC calculates about 9 liters per 100 km the simulation computes a consumption of 11,2 liters.

A second test simulates a mixture scenario of urban and non-urban areas on a road network of 65 km and 250 cars. The mean NEDC consumption for mixture areas is 6,7 l. The result of the simulation is 8,1 l.

The comparison to NEDC showed feasible results. The next experiments focus on fuel consumption on motorways under consideration of car-to-car interactions.

Fuel Consumption on Motorways

Fuel consumption on motorways is investigated with periodically boundary conditions on a two-lane motorway with length of 6km. In a first experiment, only cars are simulated. The number of cars is set to 5 and is increased with an increment of 5 for 310 simulation runs. The results of each simulation run are average values over 3 replications. Each replication starts with a settlement phase of 2,000 iterations. Then, each car protocols its fuel consumption during a measurement phase of 20,000 iterations. The result of each replication is the mean fuel consumption in l/100km for all cars. Figure 1 shows the resulting consumptions in relation to the mean velocities driven, with increasing traffic densities.

Low traffic densities lead to low fuel consumptions, because of low interaction between cars. The abrupt rise of fuel consumption with increasing traffic densities is a consequence of the used micro model for car movement. The model is a continuous version of the Nagel-Schreckenberg model (Nagel and Schreckenberg, 1992) extended by a slow-start rule, anticipation and more realistic velocity values. The model has been calibrated for freeway and urban scenarios, leading to realistic density-flow-, density-velocity- and flow-velocity-relations. The

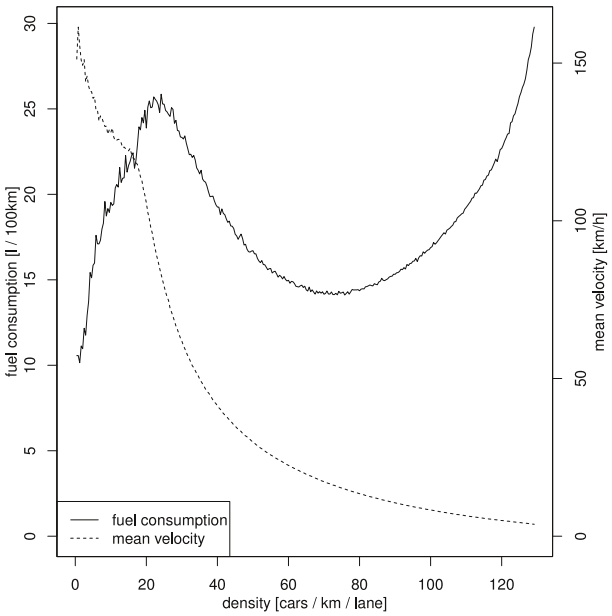

Figure 1: Fuel consumption on a motorway.

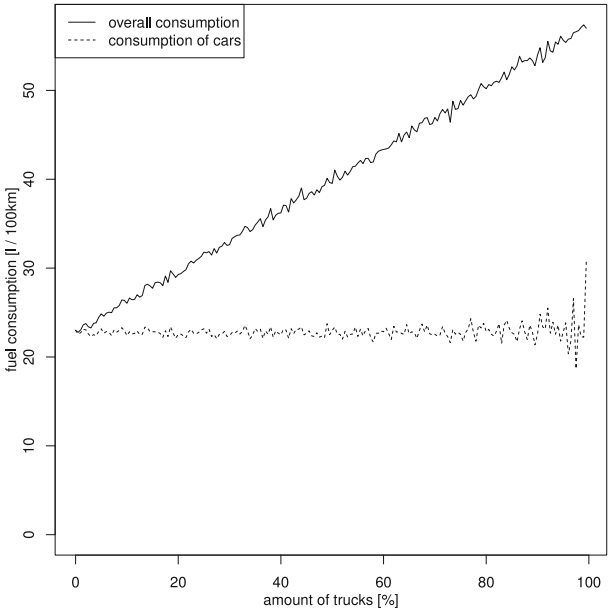

Figure 2: Fuel consumption on a motorway: Influence of trucks.

model gives realistic macroscopic results, but leads to a huge amount of velocity changes, due to lack of a smooth traffic flow.

Nevertheless, the shown maximum value for fuel consumption (in the density area lower than 80 cars/km) is lower than values discussed in literature between 80 l/100km (Yang et al., 2009), 30 l/100km (Madani and Moussa, 2012).

In a second experiment, the number of road users is fixed to 200 ($16.\overline{6}$ cars/km/lane) and the fraction of trucks in the simulation is varied from 0% to 99% with an increment of 1%. The result of each run is the average from 3

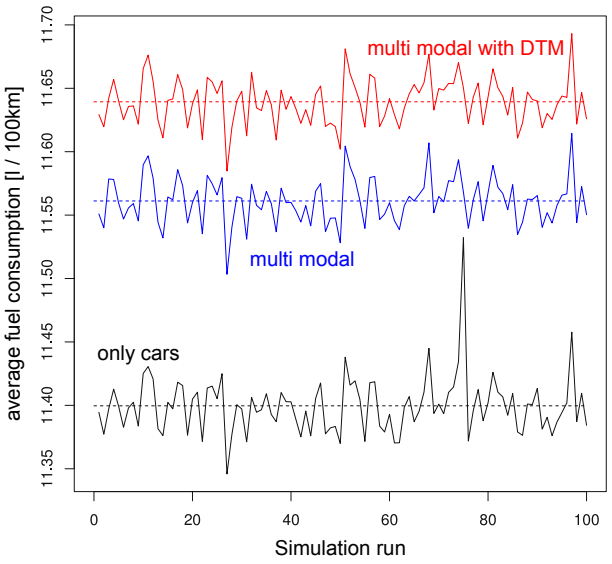

Figure 4: Comparison on fuel consumption in urban traffic. Results shown as lines, in order to simplify comparisons. Dashed lines represent mean values.

replications. The result of each replication is the average fuel consumption of the cars in the simulation and the overall consumption of all road users in the simulation. Figure 2 shows that the influence of the amount of trucks on car fuel consumption is small.

Fuel Consumption in Urban Traffic

MAINS^{2}IM is a simulation system for urban traffic. Thus, the model's evaluation should also be done in a city scenario. Figure 3 (next page) shows the city used. In a first run, 750 cars are simulated on the road map (without DTM). After a settlement phase of 5,000 simulation iterations, a measurement phase of 50,000 iterations estimates the average fuel consumptions of all simulated cars. The simulated cars determine consumptions whenever driving within urban areas.

In the next setting, the simulation is reset and 1,750 bicycles and pedestrians (35% bicycles, 65% pedestrians) are put on the simulation graph. The simulated cars are copies of the cars from the former run, driving identical routes to identical starting times with identical behavior. The measurement is done, analogously.

A third setting uses identical road users of the former setting and enhances the fuel model with a Digital Terrain Model (DTM), enabling cars to determine their height above sea level and thus enabling downhill-slope force.

Every setting is repeated for 100 times in order to estimate the effects. Figure 4 shows the results.

Apparently, fuel consumption is the lowest, when only cars are simulated. Multimodality increases fuel consumption by $0.16\,\mathrm{l} \cdot (100\mathrm{km})^{-1}$ in this scenario. The usage of a DTM additionally increases fuel consumption by $0.08\,\mathrm{l} \cdot (100\mathrm{km})^{-1}$ in comparison to simulation with multimodal traffic and $0.24\,\mathrm{l} \cdot (100\mathrm{km})^{-1}$ overall. Statistical significance tests (t-tests with $\alpha = 0.05$) indicate higher

Figure 3: Extract of simulated map area, representing Hanau am Main (89,000 inhabitants), Germany with the corresponding extract of the DTM. Total length of roads: 548km, number of nodes in simulation graph: 4,201, number of edges: 5,758.

mean values for the multimodal setting against the setting with only cars and for the setting with DTM against the multimodal setting (in each case highly significant, taking into account multiple testing).

CO_2 emissions

The fuel consumption in the simulation system has been discussed in the previous subsections. This subsection analyses how the consumption is allocated in the simulated city. Thus, the popular measure of CO_2 emissions is used and a map layer for visualization of those is created. The map area is separated into 333 rows and 333 columns (110,889 cells). Each cell protocols the amount of CO_2 emitted by cars driving in the cell. This is done for all 100 simulation runs under consideration of multimodality and the DTM. Figure 5 shows the average results over all runs.

As in the urban fuel consumption experiments, only emissions in urban areas are captured. The main routes of travel are charged with CO_2 emissions, the most. The figure highlights two areas. The bridge over the river in the north of the map extract is a crucial point, because the road looses height above sea level to the east and two traffic lights on both sides of the bridge control traffic in this area. This leads to cars braking to standstill and afterwards accelerating against rising course of road and thus a high fuel consumption and high emissions rankings. The second highlighted area in the south is a part of the city with two lane roads with high volumes of traffic and traffic lights at each CO_2 hot spot.

SUMMARY AND PERSPECTIVES

This work has described the integration of a physical model for fuel consumption and CO_2 emissions into the traffic simulation system MAINS^{2}IM. The model parameters are set according to a review of current cars in Germany. An adaptation of these parameters would make the system work in other regions, too.

The model evaluation first compared simulation results without traffic to data from NEDC. Then, traffic on motorways has been examined. The main part of evaluation has been the simulation of an urban scenario in a medium sized city. A comparison between urban car traffic, and simulation runs with added pedestrians and bicycles has shown a significant increase in fuel consumption. The same effect could be observed when a DTM was added.

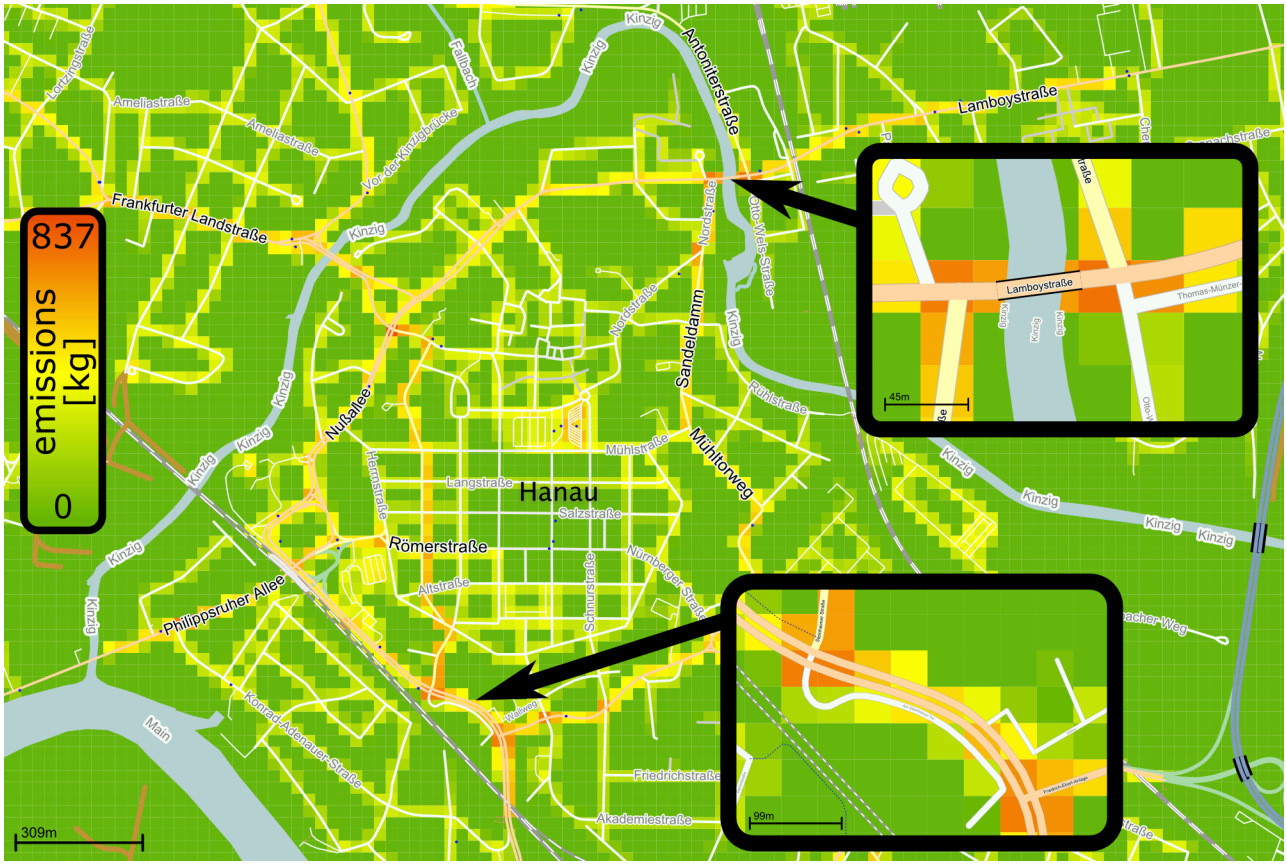

Figure 5: View on CO_2 emissions in case scenario in logarithmic scale.

CO_2 emissions are directly proportional to fuel consumption. A map showing CO_2 emissions in the simulation region was computed. The map shows emission hot spots over the regions of high traffic volumes. The CO_2 map currently assumes that there is no wind in the simulation area. Thus, this information needs to be integrated in the future. In further studies, MAINS^{2}IM has to be attached to a gas dispersion model with realistic wind input from the simulation area. Therefore, a calibration with help of measured origin destination matrices has to be done in order to have realistic traffic volumes. Then, the simulation could be used to determine places within a CO_2 hot spot, which should not have high emission ratios (e.g., positions of playgrounds or kindergartens) and test, which action (e.g., speed limits or other one-way road policies) could lead to an improvement.

Other scenarios like the implementation of a new car model with a certain fuel consumption behavior can be tested for efficiency in motorway, mixed or urban scenarios with help of the presented simulation system.

This could be an interesting problem for the invention of electrically powered cars, e.g., the identification of outstanding road map positions for charging stations or the opportunity to answer questions like “will this car reach its home position from work under given traffic conditions?”. Additionally, the effect of electrically powered cars on the CO_2 map of a city could be tested.

REFERENCES

Ahn, K., Rakha, H., Trani, A., and Van Aerde, M. (2002). Estimating Vehicle Fuel Consumption and Emissions based on Instantaneous Speed and Acceleration Levels. *Journal of Transportation Engineering*, 128(2):182–190.

An, F., Barth, M., Norbeck, J., and Ross, M. (1997). Development of comprehensive modal emissions model operating under hot-stabilized conditionss. *Transportation Research Record*, 1587(1):52–62.

Brockfeld, E., Barlovic, R., Schadschneider, A., and Schreckenberg, M. (2001). Optimizing traffic lights in a cellular automaton model for city traffic. *Physical Review E*, 64(5).

Cappiello, A., Chabini, I., Nam, E. K., Lue, A., and Abou Zeid, M. (2002). A statistical model of vehicle emissions and fuel consumption. *Proceedings of the IEEE 5th International Conference on Intelligent Transportation Systems*, (617):801–809.

Carten, A., Cantarella, G. E., and Luca, S. D. (2010). A methodology for estimating traffic fuel consumption and vehicle emissions for urban planning. *12th World Conference for Transportation Research*, (i).

Dallmeyer, J., Lattner, A. D., and Timm, I. J. (2011). From GIS to Mixed Traffic Simulation in Urban Scenarios. In Liu, J., Quaglia, F., Eidenbenz, S., and Gilmore, S., editors, *4th International ICST Conference on Simulation Tools and Tech-*

niques, SIMUTools '11, Barcelona, Spain, March 22 - 24, 2011, pages 134–143. ICST, Brüssel.

Dallmeyer, J., Lattner, A. D., and Timm, I. J. (2012a). *Data Mining for Geoinformatics: Methods and Applications*, chapter GIS-based Traffic Simulation using OSM. Springer. (accepted).

Dallmeyer, J., Lattner, A. D., and Timm, I. J. (2012b). Pedestrian simulation for urban traffic scenarios. *Proceedings of the 44th Summer Simulation Multi-Conference (SummerSim'12)*. (submitted).

Haklay, M. (2010). How good is volunteered geographical information? a comparative study of openstreetmap and ordnance survey datasets. *Environment and Planning B: Planning and Design*, 37(4):682–703.

Heißing, B., Ersoy, M., and Gies, S. (2011). *Fahrwerkhandbuch: Grundlagen, Fahrdynamik, Komponenten, Systeme, Mechatronik, Perspektiven*. Vieweg+Teubner Verlag, 3rd ed.

Karathodorou, N., Graham, D. J., and Noland, R. B. (2010). Estimating the effect of urban density on fuel demand. *Energy Economics*, 32(1):86–92.

Kraftfahrt-Bundesamt (2009). *Fahrzeugzulassungen, Bestand, Emissionen, Kraftstoff*.

Lattner, A. D., Dallmeyer, J., and Timm, I. J. (2011). Learning dynamic adaptation strategies in agent-based traffic simulation experiments. In *Ninth German Conference on Multi-Agent System Technologies (MATES 2011)*, pages 77–88. Springer: Berlin, LNCS 6973, Klügl, F.; Ossowski, S.

Madani, A. and Moussa, N. (2012). Simulation of fuel consumption and engine pollutant in cellular automaton. In *Journal of Theoretical and Applied Information Technology*, volume 35.

Nagel, K. and Schreckenberg, M. (1992). A cellular automaton model for freeway traffic. In *Journal de Physique I*, volume 2, pages 2221–2229.

Pelkmans, L., Verhaeven, E., Spleesters, G., Kumra, S., and Schaerf, A. (2005). Simulations of fuel consumption and emissions in typical traffic circumstances. *SAE Tech. Paper*.

Ross, M. (1997). Fuel efficiency and the physics of automobiles. *Contemporary Physics*, 38(6):381–394.

Schreiner, K. (2011). *Basiswissen Verbrennungsmotor: Fragen - Rechnen - Verstehen - Bestehen*. Vieweg+teubner Verlag.

Sugiyama, Y., Fukui, M., Kikuchi, M., Hasebe, K., Nakayama, A., Nishinari, K., Tadaki, S., and Yukawa, S. (2008). Traffic jams without bottlenecks - experimental evidence for the physical mechanism of the formation of a jam. *New Journal of Physics*, 10(3).

Treiber and Kesting (2010). *Verkehrsdynamik und -simulation*. Springer, Berlin Heidelberg.

Wiedemann, R. (1974). Simulation des Straßenverkehrsflusses. *Schriftenreihe des IfV*, 8.

Yang, M., Liu, Y., and You, Z. (2009). Investigation of fuel consumption and pollution emissions in cellular automata. In *Chinese Journal of Physics*, volume 47, pages 589–597.

AUTHOR BIOGRAPHIES

JÖRG DALLMEYER received the bachelor degree (2008) as well as the master degree (2009) in Computer Science at the Goethe University of Frankfurt am Main, Germany. Since December 2009, he has been a PhD student at the chair for "Information Systems and Simulation" at the Goethe University Frankfurt. His research interests are actor-based simulation for the field of traffic simulation under consideration of multimodal traffic and the building of simulation systems from geographical information.

CARSTEN TAUBERT received his bachelor degree (2009) in Computer Science at the University of Applied Sciences Wiesbaden, Germany. He is currently enrolled on the MSc course in Computer Science at Goethe University of Frankfurt am Main, Germany. His research interests are in traffic simulation. He has also worked in data mining and software development for financial business applications.

ANDREAS D. LATTNER received the Diploma degree in computer science at the University of Bremen, Germany in 2000. From December 2000 to March 2007 he was working as research scientist at the Center for Computing Technologies (TZI) at the University of Bremen. In 2007 he obtained the doctor's degree for his thesis on "Temporal Pattern Mining in Dynamic Environments". He works now as a postdoctoral researcher at the chair for "Information Systems and Simulation" at the Goethe University Frankfurt. His research interests include knowledge discovery in simulation experiments, temporal pattern mining, and multi-agent systems.

INGO J. TIMM received Diploma degree (1997), PhD (2004) and venia legendi (2006) in computer science from University of Bremen. From 1998 to 2006, he has been PhD student, research assistant, visiting and senior researcher, and managing director at University of Bremen, Technical University Ilmenau, and Indiana University Purdue University - Indianapolis. In 2006, Ingo Timm was appointed full professor for Information Systems and Simulation at Goethe-University Frankfurt. Since 2010, he has held a chair for Business Informatics at University of Trier. He works on information systems, knowledge-based systems in logistics and medicine. His special interests lie on strategic management of autonomous software systems, actor-based simulation and knowledge-based support to simulation systems.

Acknowledgement This work was made possible by the *MainCampus* scholarship of the *Stiftung Polytechnische Gesellschaft Frankfurt am Main*. We want to thank the *Hessisches Landesamt für Bodenmanagement und Geoinformation* for providing the DTM used for evaluation. We also would like to thank Guido Cervone and Sebastian Steinhorst for interesting discussions and fruitful comments in the context of this paper.

Employing simulation to analyze the effects of model incongruence – with examples from airline revenue management

Catherine Cleophas
Freie Universität Berlin
Garystr. 21
14195 Berlin
Email: catherine.cleophas@fu-berlin.de

KEYWORDS

Discrete Event Modelling and Simulation in Logistics, Transport and Supply Chain Management

ABSTRACT

Operations research systems are employed to optimize the performance of logistics, transport and supply chain management through solutions based on mathematical models. The scope of these models is constrained not only by the analysts' knowledge of the system, but also by the computational efficiency of the solution. This restriction can lead to a gap between mathematical models used for solving from conceptual models derived from empirical situations motivating the solutions. This paper claims that simulation models may be employed to analyze and evaluate the effects of the resulting model incongruence. To this end, two types of model incongruence are differentiated, compositional and structural, and two levels of effect are considered separately, short-term and long-term. The concept is illustrated by examples from airline revenue management: A simulation system based on a discrete-event model with multiple agents is used to analyze the effects of parallel flights, competition, and fluctuating demand.

Introduction

According to (Hillier and Lieberman, 2009), operations research "frequently attempts to find a best solution (referred to as an optimal solution) for the problem under consideration". One step toward this solution is to build "a scientific (typically mathematical) model that attempts to abstract the essence of the real problem".

As stated above, the scientific models used to generate operations research solutions cannot represent every detail of the empirical situation that motivated the solution. While some degree of abstraction is a defining characteristic of models, the question of how much abstraction is too much keeps coming up in operations research theory and practice.

In (Bertrand and Fransoo, 2002), the authors differentiate "axiomatic" and "empirical" research and claim that the gap between the two views of operations management problems has grown over time. They call for a "well-defined, shared methodological framework for identifying and measuring the relevant characteristics of real-life operational processes". An approach using simulations to model those characteristics that are known but not included in the axiomatic view of the problem would attempt to link what the authors describe as "axiomatic quantitative research" with what the authors refer to as "empirical model-based quantitative research". While computer simulation is mentioned in (Bertrand and Fransoo, 2002), it is considered exclusively as a – costly – solution approach, not as an opportunity for evaluating mathematical models in a controlled environment based on empirical knowledge.

(Fisher, 2007) also advocates to reduce the gap between theoretical and empirical research in the areas of operations research and operations management: "the way to avoid the risk of separating 'into a multitude of insignificant branches' is to have a healthy injection of empirics". The author defines a taxonomy of empirical research, differentiating prescriptive and descriptive goals as well as highly and less structured approaches to interacting with the world. As data sources that may be used to inform this research, observations as well as laboratory experiments are listed; simulation models are not considered.

This paper suggests the use of simulation models to evaluate models used in operations research by extending their scope. In this way, the range of data sources providing empirical links for operations research may be systematically extended by simulations. As stated by (Gilbert and Troitzsch, 2005), "simulation allows the researcher to conduct experiments in a way that is normally impossible". While the simulation models suggested for evaluation will always be based on abstract and thereby limited models of the real world, their scope is not limited by aspects of solution efficiency. They can include more realistic challenges to those abstract models used for solution generation.

By providing a way to measure the effect of differences between the mathematical model and the empirical problem, this approach offers a new view on the application of operations research techniques. According to (Bertrand and Fransoo, 2002), the fact that operations research solutions are usually based only on parts of empirical problems has traditionally been neglected: "the implicit assumption being that these aspects would not af-

Proceedings 26th European Conference on Modelling and Simulation ©ECMS Klaus G. Troitzsch, Michael Möhring, Ulf Lotzmann (Editors)
ISBN: 978-0-9564944-4-3 / ISBN: 978-0-9564944-5-0 (CD)

fect the effectiveness of the problem solutions". Whether or not this implicit assumption is correct can be tested in a simulation based on a model closer, if not congruent, to reality.

The use of simulation models as suggested here can provide two types of answers. On the one hand, it can indicate which previously neglected aspects of the empirical model contain the greatest potential for improving the current solution. On the other hand, it can indicate whether possibly costly additions to the mathematical models actually are likely to improve the solution. Both statements provide answers to the same question: What is the cost and gain of extending mathematical models?

In the next section, the concept of model incongruence is defined and an approach for implementing mathematical models within simulations is described in more detail. Two types of model incongruence are differentiated and explained: compositional and structural incongruence. With regard to the effect of incongruence, two levels, short-term and long-term, are considered.

Based on previous research, this paper uses a simulation system implemented for airline revenue management to illustrate the concept. Revenue management as described thoroughly in (Talluri and van Ryzin, 2004) represents an interesting operations research problem in that it entails the forecast of uncertain demand driven by customers' choices as well as the mathematical optimization of availabilities and prices. Three aspects of airline revenue management, demand correlation between parallel flights, competing offers, and fluctuating demand are considered.

Finally, the approach presented here, its motivation and its limitations are summarized. The last section offers an outlook both to further research in the general methodology of analysing model incongruence and the applied area of revenue management.

Evaluating the Effects of Model Incongruence

Building a simulation model based on additional information to evaluate a partial mathematical model rather than directly extending the mathematical model may seem superfluous. However, this impression is based on two possibly faulty assumptions: Firstly, that it is feasible to create an extended mathematical model that can be solved efficiently. Secondly, that such an extended model would necessarily lead to better results. Finally the model that is to be evaluated may have been created before awareness or sufficient empirical information about additional aspects existed.

Using simulation modelling, the effects of model incongruence for optimization can be approximated. After presenting the basis, limits and potential of this approach, this section further analyzes different types of model incongruence. Finally, the effect of different types of incongruence and ways of measuring it are introduced.

Model Incongruence in Operations Research

This paper defines considers the gap between partial mathematical models and reality and defines it as *model incongruence*. The term is inspired by the concept of "model congruence" taken from econometric research and explained in (Bontemps and Mizon, 2003): In econometric terms, models aim to statistically represent the process generating observed economic data. In this regard, "congruence is a property of a model that has fully exploited all the information implicitly available once an investigate has chosen a set of variables to be used in modelling". This definition of congruence makes it an unattainable ideal, as the true process that generated the relevant data and all its parameter can usually not be known with certainty.

Model incongruence can be considered while acknowledging that all abstract models are to some extent incongruent to reality in that they are never able to include all variables that actually influence a process or even to parametrize the variables they include with complete accuracy and certainty. However, mathematical models are often more incongruent than strictly necessary: While empirical data may be available on more aspects than those that are included, these are neglected for instance in favor of efficient solutions. If additional data is available, it is possible to create a simulation model that is still incongruent with regard to reality, but less so.

The concept of "enrichment" as described in (Morris, 1967) is an example for a proposed reaction to model incongruence in operations research. Enrichment includes iteratively elaborating simple mathematical models to make them more realistic. The underlying assumption seems to be that a solution based on a model that includes more realistic aspects will provide better results. Given that with the growth of a model comes a growth of complexity and uncertainty – for example if more variables need to be forecasted before an optimization function can be formulated – this is not necessarily true. Incongruence is a feature of abstract models that can be justified if a more realistic model does not provide better solutions.

Analytic Models as Components in Simulation Models

Using a simulation system to evaluate the gap between of a model and the real world extends the process of operations research as described by (Mitroff et al., 1974): The "conceptual model" serves as the basis for not one, but two "scientific models". In this regard, this paper differentiates between a *simulation model* including as much detail from the conceptual model as information is available and relevant and an *analytic model* serving as the basis for the solution. If the simulation model is used to evaluate the performance of the analytic model, the latter can be implemented as a component of the former. For example, a revenue optimization model may be implemented as part of a supply agent in an agent-based simulation.

For the simulation, an extended scientific model including all information about the system considered that is relevant, available and that can be used for calibration and validation has to be implemented. For the solution, a much more parsimonious analytic model is required.

Employing a simulation model for the evaluation of analytic models necessitates the first and possibly the second types of predictions attempted by simulations according to (Troitzsch, 2009). Type 1: If the simulation model can predict the "kinds of behavior [that] can be expected [from a system] under arbitrarily given parameter combinations and initial conditions", it can evaluate the performance of the solution based on the analytic model under arbitrary conditions. This can be sufficient to evaluate the performance of an analytic model given best-case or worst-case parameters. Type 2: If the simulation model can predict the "behavior a given target system (whose parameters and previous states may or may not have been precisely measured) [will] display in the near future", it can evaluate the performance of the solution based on the analytic model under realistic conditions. This provides an opportunity to compare the performance of competing models before implementing one of them in the real world.

A major limitation of this approach is its reliance on the validity of the simulation model. The difficulties of validating complex simulation models have been stated for example in (Windrum et al., 2007). If the simulation model is insufficiently validated, it cannot be used to make statements about the effects of the analytic model's incongruence. With regard to validation and the goal of the evaluation, the differentiation of the two purposes described in the previous paragraph plays a crucial role: Researchers need to be aware of the degree of validation they can provide for the simulation model and the types of predictions they can therefore derive from it.

The approach described here offers a range of opportunities. It provides a way to observe a solution's performance in a situation that corresponds to the analytic model and in one that includes additional aspects. By measuring the difference in outcomes, the potential gain that can be achieved according to any indicator through extending the analytic model becomes measurable. Competing solutions can be implemented and compared under diverse conditions ceteris paribus. Finally, a simulation model provides the opportunity for evaluating heuristic improvements of analytic solutions that are not optimal when all empirical aspects are considered.

Compositional and Structural Model Incongruence

Within the available knowledge of the empirical situation, a simulation model's congruence can be adjusted to be as realistic as possible or closer to that of the analytic model. By implementing the analytic model within the simulation model, researchers gain the opportunity to define not only the *extent* to which an analytic model matches the situation (its congruence to the simulation model) but also the *type of incongruence* it is confronted with.

When considering different types of incongruence, the definition of different types of uncertainty as provided by (Walker et al., 2003) can serve as a template. Uncertainty, defined as "any deviation from the unachievable ideal of completely deterministic knowledge of the relevant system", is a reason for the simulation model's incongruence. If everything about the system (the data generation process) considered could be known and measured, perfect congruence would be achievable. When an analytic model is incongruent to a simulation model incorporating all data available about the empirical situation, this may be described as a type of voluntary uncertainty, self-imposed in order to increase the solution's efficiency.

In (Walker et al., 2003), two types of uncertainty are defined based on location: "context uncertainty" and "model structure uncertainty". Context uncertainty occurs when knowledge about the boundaries of the modeled system is ambiguous; it may result in "the wrong question being answered". Model structure uncertainty occurs when knowledge about the causal relationships within the modelled system is ambiguous, it may result in answers that are plain wrong.

Analogously, two types of incongruence may be defined: *Compositional* and *structural*. Compositional incongruence occurs when parts of empirical an situation that may be relevant to the problem are not included in the model. Structural incongruence occurs when relationships and behaviors between components of the model are not accurately modeled.

An example for compositional incongruence from the area of airline revenue management is the exclusion of competing offers from the model. An example for behavioural incongruence is the exclusion of learning customers – while customer preferences may be considered, the cause-and-effect relationship between experience and expectations with regard to request times is neglected.

Measuring Effects of Model Incongruence

Before measuring the effects of model incongruence, its extent needs to be quantified. This can be achieved by considering the two types of model incongruence introduced in the previous section and checking the components and structural relationships that are known to exist in the empirical situation and are not included in the analytic model. The range of components and the impact of the relationships has to be measured based on empirical data if available. If this can be achieved, a realistic degree of incongruence (or several scenarios thereof) can be implemented in the simulation model.

An analytic model's incongruence can be expected to have both positive and negative effects on the performance of solutions derived from it. As stated before, incongruence between the analytic model and the simulation model may be due not to necessity, but to choice – a partial analytic model may provide a more computationally efficient solution. The effects of model size on computational efficiency, however, are usually explicitly

considered and often stated as a reason for the limitation of analytic models. Examples for this type of discussion can be found in (**?**).

This section focuses on the effects of an analytic model's incongruence on the effectiveness of a solution. A solution's effectiveness may be measured by any indicators taken from the empirical problem that motivated the solution. For example, an approach to optimizing revenue through allocating capacity may aim to increase revenue, but the underlying problem may also consider productivity indicators such as bookings or market share. Both a short-term and a long-term evaluation of the solution's performance according to all indicators that are relevant to the empirical situation are possible.

Short-term evaluations of the indicators that are included in the analytic model are often provided to justify a solution's superiority – short-term evaluations of indicators not included in the analytic model become possible only if the analytic model is evaluated in reality or in a more congruent simulation model.

A simulation model allows one to measure not just the short-term effect of implementing one solution as opposed to another, but also the long-term consequence of applying the solution repeatedly. As stated in (Gilbert and Troitzsch, 2005), the ability to speed up time and thereby model long periods of simulation-time in comparatively little real-time is one of the advantages of simulations.

Long-term evaluations of relevant indicators in a simulation model can expose effects of an analytic model's incongruence that may not be immediately visible when the solution implemented in the real world. In the real world, external factors such as technological progress, market composition or economic activity may change over time and influence or obscure the solution's success. In a simulation model, such external factors can be either kept constant or modulated. Keeping all external factors constant provides a way of evaluating whether the analytic model's incongruence leads to a feedback cycle increasing the gap between the solution and the empirical situation or whether the solution adapts and compensates for the incongruence. Modulating external factors in a controlled environment also provides an opportunity for evaluating the solution's robustness over time.

Finally, if the aim of considering an analytic model through its implementation in a simulation is to improve the current solution, the cost of model incongruence has to be compared to the expected cost of extending the analytic model. This challenge may be supported through simulation modelling, too, as prototypes of a solution based on an extended analytic model may be implemented in a simulation model to test their efficiency and the extent to which they improve the results, that is, their effectiveness.

Examples from Airline Revenue Management

As stated in the introduction, revenue management can be considered to provide interesting examples for the evaluation of model incongruence in operations research models, as it considers a system with uncertain, dynamic aspects due to the inclusion of customer demand in the objective function. The main objective of airline revenue management is maximize revenue by differentiating the availability of booking classes with different sets of restrictions and different prices based on a segmentation of expected demand. This is achieved by computing optimal inventory controls based on a forecast of customer requests. For an introduction to revenue management as well as mathematical methods of demand modeling and optimization, please refer to (Talluri and van Ryzin, 2004).

Analytic revenue management models, used both for the demand forecast and the availability optimization, are mathematical models in the sense of operations research and accordingly subject to model incongruence. In revenue management literature, model aspects that have been identified to be incongruent are often referred to as "challenges". An implicit assumption appears to be that with the extension of the analytic model to meet such challenges and thereby to remove incongruence, revenue management methodology can be continuously improved. Where the extension of the model seems infeasible, an improvement of the solution through human analysts is recommended as in (Mukhopadhyay et al., 2007) or (Isler and Imhof, 2008).

Focusing on indicators of forecast accuracy, the approach introduced here has previously been applied to airline revenue management in (Cleophas et al., 2009). An improved and extended version of the simulation system presented in that paper was employed to generate the results presented here: The system was re-created as a web-based tool for decision support and training as described in (Cleophas, 2012), improving the verification of all components through professional software engineering. Additional revenue management algorithms with regard to forecasting and optimization as well as tools for manipulating availabilities and an improved analysis interface were added.

The simulation system the principles offered in (Frank et al., 2008) with regard to a discrete-event based simulation framework and extends them through the implementation of an agent-based demand model. The demand data as well as the price structure used to parametrize the simulation model were calibrated using data from Lufthansa AG.

This section provides three examples from airline revenue management to illustrate the approach introduced in this paper. In the first example, the independent optimization of parallel flights is considered when customers flexibly decide which flight to book and will choose the one for which cheaper tickets are available. In the second example, the parallel flights are offered by two competing airlines, where one airline applies a pricing structure

that is 5% cheaper than that of the other airline. In the third example, economic cycles are implemented through demand shifts over time, to which the demand forecast has to adapt in order to provide reliant inputs to the availability optimization.

The revenue management system employed for the simulations described here is a hybrid system considering price-sensitive demand as documented in (Fiig et al., 2009). The results shown in this section are based on the bookings generated in 150 simulation runs after 50 initialization runs. All confidence intervals provided are based on a single-sample t-test with error probabilities of at most 5%.

Parallel Flights as Internal Competition

Considered for example by (Zhang and Cooper, 2005), parallel flights are often mentioned as one of the challenges of traditional airline revenue management systems. Customers are indifferent with regard to which of two flights to book if the flights are offered at the same time and by the same carrier, take the same time and follow the same route. Yet, traditional revenue management systems forecast and optimize all flights that are not part of an itinerary independently, not taking that indifference into consideration.

In the case of parallel flights, there is no compositional incongruence: All relevant parts of the system (customer demand, flights offered, booking classes and prices offered) are considered by the analytic model. However, the analytic model is structurally incongruent – the flexible choice behavior of customers that are indifferent to which of two parallel flights to book is not included. Accordingly, one could expect to see revenue diminished when parallel flights are considered independently rather than optimizing them as a unified capacity.

In the example of parallel flights, both short-term and long-term effects of model incongruence are to be expected. In the short-term, revenue may decrease as customers can choose the cheapest ticket available not just on the flight which they are predicted to request, but also on its parallel equivalent. In the long-term, forecast adaptations may lead to a systematic increase of the incongruence or may balance out the effects.

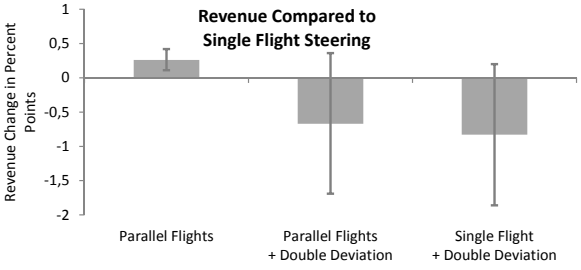

Figure 1: Results of Parallel Flights Compared to Single Flight

Figure 1 shows that this expectation is not necessarily fulfilled. The diagram shows the change in percentage points based on the revenue that is earned when the capacity is offered in one single flight. As illustrated by the diagram, revenue does not actually decrease when capacity is split across two parallel flights and availabilities are optimized separately – instead, it increases significantly. Even when the random demand deviation is doubled, the comparison to the revenue earned through a single flight unifying the capacity does not become negative.

These results advocate the theory that in a hybrid, price-sensitive system, even parallel flights are forecasted in a way that is robust enough to account for customers flexibly choosing between parallel flights. However, this conclusion must come with the limitations of the simulation used – in the case presented here, flights were perfectly parallel and the forecast was initialized well and not disrupted.

Underbidding by External Competition

The idea that competitors' offers may undermine revenue management success when customers buy the cheapest ticket available and are indifferent with regard to carrier brands is described in (Isler and Imhof, 2008). Revenue management models that do not explicitly consider competing offers may be regarded to suffer from compositional incongruence. Even if the existence of cheaper alternatives is regarded as given, structural incongruence may still exist if the model does not consider the fact that the competitor may also implement revenue management. In such a case, causal relationships between the optimized availabilities and observed demand of one carrier and those of a competing carrier is neglected.

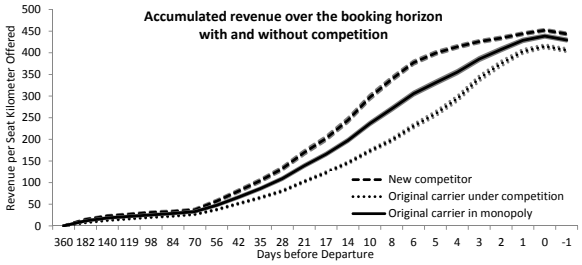

Figure 2: Revenue per Seat Kilometres Offered Under Competition

In the example given by figure 2, only the short-term effects of a situation with competition in a revenue management system that does not consider competition are illustrated. In this simulation, the competing carrier implements a price structure that consistently is 5% lower than that of the original carrier. As a result, the original carrier's revenue per seat kilometer offered is reduced by up to 6%, while the competitor gains 4% more in revenue per seat kilometer offered than what was earned in the monopoly situation. On the long-term, the situation may be even more grave as forecast adaptations and mutual underbidding can lead to a price war.

Forecast Adaptation: Economic Cycles

The final example considers the fact that passenger demand is usually not static but changes over time due to external factors such as economic cycles. An example of research considering the value of human analysts' adjusting passenger demand forecasts is provided by (Mukhopadhyay et al., 2007); most forecast models employed for revenue management adapt to changes in demand as observed through changes in booking numbers. However, lacking a scientific model of demand, these adaptations are usually realized by describing patterns rather than by analyzing causal relationships.

When demand is expected to change over time and the opportunity for adaptation is part of the model, compositional incongruence may not be regarded as given. However, due to the causal relationships between external factors and passenger demand, the external factors (such as for example economic indicators) may be relevant to the model. Ignoring them therefore can lead to compositional incongruence, as ignoring the causes for shifts in demand can constitute structural incongruence.

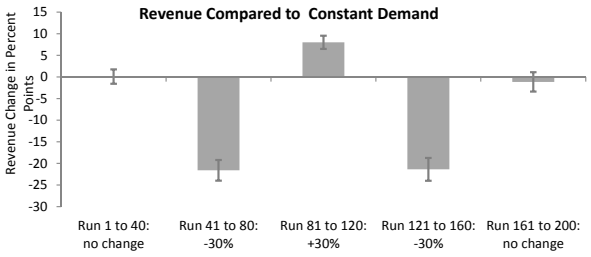

Figure 3: Revenue Changes as Demand Changes

As shifts in demand can only occur over a longer period of time, they may be considered as a long-term phenomenon that is best observed in this time frame. For that reason, short-term effects are not considered in further detail in this example.

Figure 3 shows the change of revenue as demand volume changes over multiple simulation runs. Demand volume is first reduced by 30%, then increased by 30%, reduced by 30% again, and finally set back to the initial status. As illustrated by the diagram, a 30% decrease in overall demand does not necessarily lead to a corresponding decrease in revenue: the system is robust enough to restrict losses to at most 25%. However, a 30% increase in overall demand cannot be translated into a corresponding increase in revenue, either: possibly due to restricted capacity as well as the cost of adapting the forecast, revenue can be increased only by at most 10%. Finally, the demand shifts seem not to diminish the system's performance on the long run: as the demand volume is returned to its initial status, revenue does no longer deviate significantly from what was earned initially.

Conclusion

In this paper, an approach of using simulations to measure the effects of model incongruence has been introduced. Extending the model of operations research as described by (Mitroff et al., 1974), the scientific model differentiated into a simulation model and an analytic model: While the analytic model includes those components and relationships of the conceptual model that allow for a computationally efficient solution, the simulation model may include all relevant components and relationships for which sufficient empirical data is available.

The approach presented here allows one to evaluate and prioritize extensions of the analytic model with regard to their effects on relevant indicators. For the example shown in the previous section, the conclusion may be that the extension of revenue management models with regard to external competition holds greater potential than extensions with regard to internal competition. Of course, such a conclusion is subject to further analysis as well as to considerations of feasibility.

To allow for the analysis and control of model incongruence, two types of incongruence are differentiated. Analogously to the uncertainty that can cause it, incongruence may be compositional or structural. The exclusion of relevant parts of the conceptual model in the analytic model leads to compositional incongruence; the exclusion of relevant causal relationships leads to structural incongruence. The methodological part of the paper concludes that the effects of model incongruence have to be considered on two levels, the short- and the long-term.

The theoretical concept was illustrated using three examples from airline revenue management. Based on simulation results, the short- and long-term effects of different types of model incongruence were illustrated.

The approach suggested here regards the simulation model as being independent of the type of simulation (agent-based, system-dynamic, discrete-event-based) used. This independence of modeling and methodology is intentional: The type of simulation suited for the implementation of the simulation model depends on the conceptual model and the aspects of the system considered. For example, in airline revenue management, customers may be modeled as agents or their requests may be modeled as events depending on the choice-behavior considered. The improvement of analytic models through human analysts may even benefit from participatory agent-based modeling as described in (Guyot and Honiden, 2006).

At this point, the causes for compositional and structural incongruence have not been considered in further detail. The concept may be improved by considering the role of uncertainty with regard to the validity both of analytic and of simulation models. An in-depth treatment of the enrichment approach using the view of evaluation in a simulation model may provide further insight.

REFERENCES

Bertrand, J. and Fransoo, J. (2002). Operations management research methodologies using quantitative modeling. *International Journal of Operations & Production Management*, 22(2):241–264.

Bontemps, C. and Mizon, G. (2003). Congruence and encompassing. In Stigum, B., editor, *Econometrics and the philosophy of economics: theory-data confrontations in economics*, pages 354–378. Princeton University Press.

Cleophas, C. (2012). Assessing multi-agent simulations – inspiration through application. In Prez, J. B., Snchez, M. A., Mathieu, P., Rodrguez, J. M. C., Adam, E., Ortega, A., Moreno, M. N., Navarro, E., Hirsch, B., Lopes-Cardoso, H., and et al., editors, *Advances in Intelligent and Soft Computing 156: Highlights on Practical Applications of Agents and Multi-Agent Systems – 10th International Conference on Practical Applications of Agents and Multi-Agent Systems*, pages 163 – 170. Springer.

Cleophas, C., Frank, M., and Kliewer, N. (2009). Simulation-based key performance indicators for evaluating the quality of airline demand forecasting. *Journal of Revenue and Pricing Management*, 8(4):330–342.

Fiig, T., Isler, K., Hopperstad, C., and Belobaba, P. (2009). Optimization of mixed fare structures: Theory and applications. *Journal of Revenue & Pricing Management*, 9(1):152–170.

Fisher, M. (2007). Strengthening the empirical base of operations management. *Manufacturing & Service Operations Management*, 9(4):368–382.

Frank, M., Friedemann, M., and Schröder, A. (2008). Principles for simulations in revenue management. *Journal of Revenue & Pricing Management*, 7(1):7–16.

Gilbert, G. and Troitzsch, K. (2005). *Simulation for the social scientist*. Open University Press.

Guyot, P. and Honiden, S. (2006). Agent-based participatory simulations: Merging multi-agent systems and role-playing games. *Journal of Artificial Societies and Social Simulation*, 9(4):8.

Hillier, F. and Lieberman, G. (2009). *Introduction to Operations Research*. McGraw Hill, New York, 9th edition.

Isler, K. and Imhof, H. (2008). A game theoretic model for airline revenue management and competitive pricing. *Journal of Revenue & Pricing Management*, 7(4):384–396.

Mitroff, I., Betz, F., Pondy, L., and Sagasti, F. (1974). On managing science in the systems age: two schemas for the study of science as a whole systems phenomenon. *Interfaces*, 4(3):46–58.

Morris, W. (1967). On the art of modeling. *Management Science*, 13(12):707–717.

Mukhopadhyay, S., Samaddar, S., and Colville, G. (2007). Improving revenue management decision making for airlines by evaluating analyst-adjusted passenger demand forecasts. *Decision Sciences*, 38(2):309–327.

Talluri, K. and van Ryzin, G. (2004). *The theory and practice of revenue management*. Springer.

Troitzsch, K. (2009). Not all explanations predict satisfactorily, and not all good predictions explain. *Journal of Artificial Societies and Social Simulation*, 12(1):10.

Walker, W., Harremoes, P., Rotmans, J., Van der Sluijs, J., Van Asselt, M., Janssen, P., and Von Krauss, M. (2003). Defining uncertainty: a conceptual basis for uncertainty management in model-based decision support. *Integrated Assessment*, 4(1):5–17.

Windrum, P., Fagiolo, G., and Moneta, A. (2007). Empirical validation of agent-based models: Alternatives and prospects. *Journal of Artificial Societies and Social Simulation*, 10(2):8.

Zhang, D. and Cooper, W. (2005). Revenue management for parallel flights with customer-choice behavior. *Operations Research*, 53(3):415–431.

AUTHOR BIOGRAPHIES

CATHERINE CLEOPHAS currently holds a position as assistant professor at the Information Systems Department of Freie Universität Berlin. She received her PhD from the University of Paderborn in 2009. Her fields of interest include revenue management, demand modelling and simulation systems. Her email is `catherine.cleophas@fu-berlin.de`.

MODEL-SUPPORTED AND SCENARIO-ORIENTED ANALYSIS OF OPTIMAL DISTRIBUTION PLANS IN SUPPLY NETWORKS

Dmitry Ivanov
Berlin School of Economics and Law,
Chair of International Supply Chain Management,
10825 Berlin, Germany
E-Mail: divanov@hwr-berlin.de

Boris Sokolov, Alexander Pavlov
Institution of the Russian Academy of Sciences,
Saint Petersburg Institute of Informatics and Automation
39, 14 Linia, VO St. Petersburg, 199178, Russia
E-mail: sokol@iias.spb.su, pavlov62@list.ru

KEYWORDS
Supply network, distribution planning, transportation model, scenario, sensitivity analysis.

ABSTRACT

A real case study of distribution planning is considered. An original approach to analysis of multi-stage, multi-commodity distribution network in the multi-period mode with adaptive update of demand, capacity, and supply information is proposed. Optimal distribution plans are calculated for optimistic and pessimistic scenarios. Subsequently, these plans are analyzed subject to different disturbances and regarding distribution network design and sourcing planning decisions. The performed sensitivity and structural analysis reveals some interesting managerial insights into building robust distribution plans and interconnecting decisions on distribution network design, planning, and sourcing.

INTRODUCTION

Distribution network (DN) planning is a referenced research problem that is vital in many supply chains (SC) in order to successfully meet the customer needs while improving the performance efficiency (*Mula et al. 2010*). Given a location structure from facility planning, customer demand from forecasting, and order quantities from inventory management and sourcing planning, the aggregate distribution volumes in the DN and to customers need to be determined for a middle-range period of time (e.g., one month) so that the total costs (e.g., transportation and inventory) and service level (e.g., the relation of the planned and actual product flow) are improved (*Tayur et al. 1999*). The problem is typically constrained by limited capacity of nodes and arcs (*Akkermann et al. 2010*).

Due to increase in complexity of modern supply chains (SC), the multi-stage, multi-period, and multi-commodity DN planning challenges the decision-making in this domain (*Amiri et al. 2006*). Another challenge is uncertainty of demand and supply. This forces the companies to build up inventories, transportation capacities, and use additional distribution centers as alternative distribution channels (*Santoso et al. 2005*). All these counter-measures cause the *excessiveness* of DN which in turn requires additional investments subject to an increase in fixed costs as the price for robustness (*Bertsimas and Sim 2004, Peng et al. 2011*).

Along with the importance of the optimization approaches to DN planning, research community has also recognized importance of the DN analysis.

The research focus of this study is subject to dynamic analysis of (1) the impact of different disturbances on distribution execution and (2) the actual usage of the created robustness excessiveness and nevertheless possible bottlenecks. Such an analysis has a great practical importance since the companies are very interested in the results of those studies which would help them to estimate the investments into different redundancies to mitigate uncertainty or their reduction and the impacts of these investments/reductions on the changes in SC performance (*Craighead et al. 2007*).

STATE OF THE ART

The preliminary analysis of the problem has shown that it could be modelled as stochastic maximal flow model, i.e. as maximal flow models or minimal cost flow models (*Lin 2001, Chou et al. 2011*) and fuzzy-models. However, the existing studies in this research area have not explicitly considered possible structure dynamics and its impact on the flows and cost.

First, deviations or failures in the network structures and operations are possible, but not unrealistic or describable with some probabilistic assumptions. In addition, the DN structural states do not change permanently, but rather in some intervals. Besides, the current execution characteristics of flows (e.g., cross-docking processing) should be considered. The next peculiarity is the necessity to take decisions on operative reconfiguration in case of emergency.

A significant practical challenge is partial information

Proceedings 26th European Conference on Modelling and Simulation ©ECMS Klaus G. Troitzsch, Michael Möhring, Ulf Lotzmann (Editors)
ISBN: 978-0-9564944-4-3 / ISBN: 978-0-9564944-5-0 (CD)

unavailability at the zero point of time as well as information updates during the execution. Finally, some other peculiarities such as return flows, many varying parameters, and multi-objective problem formulation may represent barriers in applying graph-theoretical methods.

Another possibility to model the considered problem can be the mathematical programming (MP)-based implementation (*Melo et al. 2010*). However, due to the above-mentioned peculiarities, the number of variables and constraints became very large and would force us to make some unrealistic assumptions regarding dynamic changes in control and structural parameters.

MATHEMATICAL MODEL

Distribution planning model

We propose to apply an original concept called structure dynamics control (SDC). SDC is a process of producing control inputs and implementing the SC transition from the current macro-state to a planned one (in the planning mode) or any other feasible state (in the disruption-recovery mode) in which the SC adaptation can be performed and the desired performance can be achieved over the given period of time (*Ivanov et al., 2010, Ivanov and Sokolov, 2012*).

The main idea of the SDC-based models is the dynamic interpretation of SC planning and control in accordance with the natural logic of time and the corresponding execution processes (e.g., transportation) with the help of optimal program control (OPC). However, the solution procedure is transferred to other methods (e.g., MP). In this setting, the solution procedure becomes undependable from the continuous optimization and can be of discrete nature, e.g., a linear programming, transportation problem, or integer allocation problem. The planning model has been presented in details in the study by *Ivanov et al. (2011)* and is not included in this paper.

Scenario-oriented analysis

Optimal distribution plans are calculated for optimistic and pessimistic scenarios. The DN is considered as a dynamic non-stationary system. The changes of DN structure (e.g., because of changes in transportation costs, contracts with suppliers, unplanned transportation resource unavailability) are referred as SC structure dynamics (*Ivanov et al. 2010*). With DN structure dynamics, the scenarios of SC execution are set up.

The distinguishing feature of the proposed approach is that the execution scenarios are generated nor randomly, but on the basis of an original approach to network structure reliability assessment developed by authors (*Kopytov et al. 2010*). Based on this method, the nodes 1, 4, and 7 (see Figure 1) have been revealed as critical operations in the considered DN. In Figure 1 corresponding execution scenarios are presented.

In Figure 1, structure dynamics scenarios are depicted. $St_{i_1,i_2,..,i_k}$ denotes the structural state where $i_1, i_2, ..., i_k$ are numbers of missing or disrupted operations (nodes) in the network shown in Figure 1.

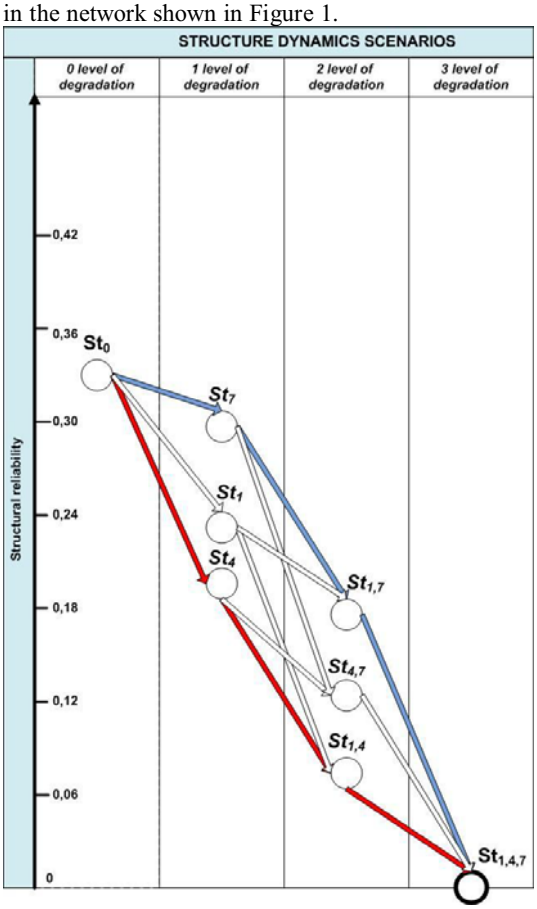

Figure 1. Structural reliability and structure dynamics scenarios

The blue line depicts the optimistic and the red one – the pessimistic scenario.

In order to formalize the above-mentioned dynamic changes, let us introduce a dynamic alternative multi-graph (DAMG):

$$G_\chi(t) = \langle X_\chi(t), E_\chi(t), W_\chi(t) \rangle, \quad (1)$$

where the subscript χ is the number of an execution scenario, the time point t belongs to a given set T, $X_\chi(t) = \{A_{xi}(t), i \in N_\chi\}$ is a set of nodes on the DN, $E_\chi(t) = \{e_{xij}(t),\ i, j \in N_\chi\}$ is a set of arcs in the DN, and $W_\chi(t) = \{w_{\chi ij}(t),\ i, j \in N_\chi\}$ is a set of operation characteristics for the transportation (if $i \neq j$) or processing at warehouse (if $i = j$).

The elements of the time-spatial matrix function $e(t)$ define the links between A_{xi} and A_{xj}, and $e_{xij}(t)$ is equal to 1, if a transportation from A_{xi} to A_{xj} is

possible, 0 – otherwise. In the DN, different products $\rho \in P = \{1,2,...,p\}$ of different importance may be served.

Let us define elements of the set $W_\chi(t) = \{w_{\chi ij}(t),\ i,j \in N_\chi\}$ which describe transportation, processing, and warehouse operations:

- $V_{\chi i}(t)$ is maximal warehouse capacity of the node $A_{\chi l}$;
- $\psi_{\chi i\rho}(t)$ is maximal inbound processing intensity of the product ρ in $A_{\chi l}$;
- $\omega_{\chi ij\rho}(t)$ is maximal transportation intensity of the product ρ between $A_{\chi i}$ and $A_{\chi j}$;
- $\varphi_{\chi i\rho}(t)$ is maximal outbound processing intensity of the product ρ from $A_{\chi i}$.

We assume that each network element within the subintervals (structure constancy intervals) is characterized by these characteristics which do not change within this interval.

CASE STUDY

A DN of an enterprise in the FMCG (fast moving consumer goods) branch is considered. The DN is composed of two mega-hubs (nodes 1 and 6), a central distribution hub (node 4), two intermediate terminals (nodes 2 and 3), an outsourcing terminal (node 7), and a regional distribution center (node 5). The execution in each of the nodes and transportation arcs is limited by maximal warehouse capacity, processing intensity, and transportation intensity correspondingly, see Figure 2.

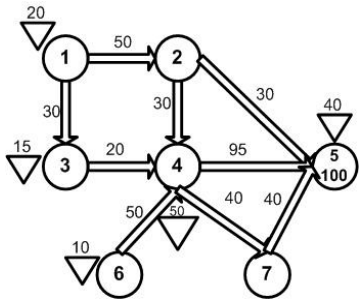

Figure 2. Distribution network structure

In Figure 2, triangles refer to the warehouse capacity and numbers on the arcs refer to maximal transportation intensity. The suppliers first deliver goods to the mega-hubs 1 and 6. Then, the goods shall be processed in the central distribution hub 4 via cross-docking. The goods from the hub 1 should be additionally processed at intermediate terminals 2 and 3. From the hub 4, the goods are moved to the regional distribution center 5 that has a certain demand in each of the periods (i.e., 100 units). In order to take into account possible problems with the channel 4-5, an outsourcing terminal is used as an alternative way for deliveries to the distribution center 5. Besides, it is possible to move small quantities (maximal 30 units) directly from the terminal 2 to the center 5.

The transportation volumes are constraint by maximal transportation intensity (as noted on the arcs in Fig. 1). The stocking volume is constraint by maximal warehouse capacities as shown by triangles in Fig. 2. The processing at terminals and hubs is constrained subject to maximal in- and outbound processing intensities. The suppliers deliver certain order quantities to the nodes 1 and 6 at the beginning of each period, and many periods are involved into the planning horizon. The adaptive planning procedure is applied, i.e., the demand and order quantities become known only shortly before the beginning of the next period, and are known only for this period.

It is assumed, that:

- transportation/processing intensities and warehouse capacities may change in each period,
- the demand of the regional distribution center may change in each period,
- any node or arc in the network may be temporarily unavailable,
- order quantities may vary in each period,
- inventory of the previous periods may be used in the next periods,
- if the processing intensity and warehouse capacity are exceed by the delivered quantity, the unprocessed and unstored goods are sent back to an additional warehouse (not in the main network) subject to additional costs,
- sourcing, transportation and inventory costs are assumed to be a linear function from the quantities,
- inventory costs are count in each of the periods,
- fixed costs are related to both nodes and arcs and are proportionally distributed between them.

The problem consists of the DN optimal plan sensitivity analysis subject to disturbance impact on SC and interconnection with the decisions in capacity and sourcing planning.

EXPERIMENTAL RESULTS

Planning results

Let us consider the optimistic and pessimistic scenarios. We consider three intervals of the structural constancy. The problem is to maximize the service level under the assumption of the demand of 300 units for the planned period of three months (i.e., 100 units each month) whilst minimizing the costs as composed of the storage, transportation, return, sourcing, and fix costs.

In the *optimistic trajectory*, the events for the transition to the second interval are the changes in sourcing volumes at nodes 1 and 6 as well as a failure in the operation of the terminal 7. Analogously, the transition

to the third interval of the structural constancy is launched by the failure in the operation of the mega-hub 1 and terminal 7 along with the change in the sourcing volume in the node 6.

In the *pessimistic trajectory*, the events for the transition to the second interval are the changes in sourcing volumes at nodes 1 and 6 as well as unavailability of the link from the central distribution hub 4 to the regional distribution center 5. Analogously, the transition to the third interval of the structural constancy is launched by the failure in the operation of the mega-hub 1 and further unavailability of the link from the central distribution hub 4 to the regional distribution center 5 along with the change in the sourcing volume in the node 6.

Therefore, the SC structure dynamics considers both the adaptive planning (i.e., changes in the sourcing volumes) and disturbances (i.e., node failures). Note that the demand and supply quantities for the next months become known only shortly before the beginning of this new period and only for this period.

In Figure 3, results of optimal planning subject to the highest priority of the service level component in the goal function for the optimistic and pessimistic scenarios are presented.

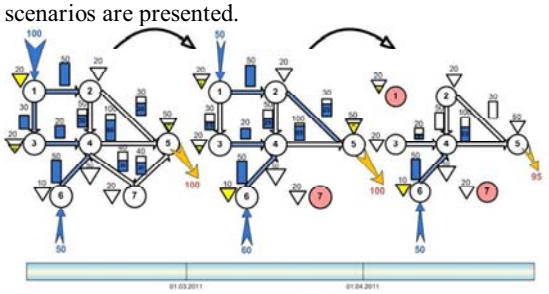

a) Optimistic scenario

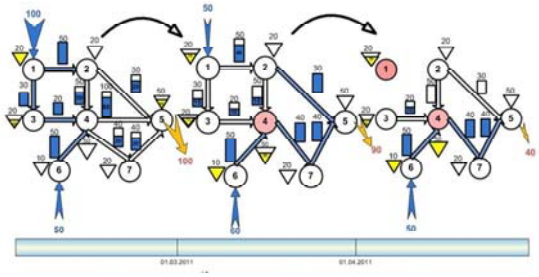

b) Pessimistic scenario

Figure 3. Distribution plans for optimistic (top) and pessimistic (buttom) scenarios

The yellow triangles show the warehouse capacities and their actual utilization. The blue quadrangles represent the transportation channel capacities and the actual transportation quantities.

Through the running of the planning model under the assumption of the high priority of the service level component in the goal function, optimal solution for the optimistic scenario allows to deliver 295 units which is equal to the service level of 98,3% subject to the planned demand of 300 units. Total inventory in all the periods is 125 units with a distribution among periods as 50 units in the first period (caused by excessive sourcing quantities at the nodes 1 and 6), 60 units in the second period, and 15 units in the third period.

Total cost and revenue have been calculated under the following assumptions: transportation cost per unit = 0.1, inventory cost per unit = 0.07, sourcing cost per unit = 0.4, return cost = 0.2, fixed cost for the DN = 90, and selling price = 1. It can be observed that in the optimistic scenario, a profit of 42.75$ can be achieved.

Optimal solution for the pessimistic scenario allows to deliver 230 units which is equal to the service level of 76,7%. Total inventory in all the periods is 200 units with a distribution among periods as 50 units in the first period (caused by excessive sourcing quantities at the nodes 1 and 6), 70 units in the second and 80 units in the third period (caused mainly by the break in deliveries from 4 to 5). The operative reconfiguration in the second period is suggested to increase transportation intensities on the arcs 4-7-5 and 2-5. The operative reconfiguration in the third period is suggested to increase transportation intensities on the arc 4-7-5. It can be observed that in the pessimistic scenario, the selling volume decreases significantly and no profit can be achieved. The losses amount to 21$.

Obviously, if the decision-maker is a pessimistic psychological type, SC design and sourcing decisions should be reconsidered. For example, an alternative link from the node 4 to the node 5 may be introduced along with an additional node on sourcing subject to the mega-hub 1. Warehouse capacities can also be increased. In the optimistic scenario, the failure of the node 7 does practically not influence the flow volume. That is why it can be suggested to analyse a DN structure without this node subject to possible reduction of fixed costs. Subsequently, in both of the scenarios, sourcing decisions may be reconsidered, especially in the first period.

For answering these and many other interesting questions, an analysis of different possible DN structures and execution scenarios is needed.

Scenario-oriented analysis

The further analysis may include two basic decision groups: (1) analysis of DN plans in different scenarios of the SC structure dynamics subject to different disturbances and (2) analysis of SC design excessiveness and flexibility subject to capacity and sourcing planning decisions. In particular, the following questions can be addressed:

- What elements are critical for the SC design and what elements are excessive and can be removed without decreasing the service level?
- Do additional costs in SC design elements pay off

by the increase in the service level subject to mitigating the negative effects of possible operation failures or a large delivery flow volume?

- What are the bottlenecks of the SC structure and where additional elements are needed?
- How sensitive are the SC structures and optimal solutions (i.e., the DN plans) to different execution scenarios?

Disturbance analysis

Let us analyse the plans ($\delta_{optimistic}, \delta_{pessimistic}$) subject to the following disturbances:

- *variant 1* – decrease in transportation intensity on the way $4 \to 7 \to 5$,
- *variant 2* – decrease in warehouse capacity at the node 4,
- *variant 3* – decrease in transportation intensity on the way $4 \to 5$, and
- *variant 4* – influence of all the variants simultaneously.

Plan $\delta_{optimistic}$ turned out to be stable subject to the disturbances of variants 1 and 2. In Figure 4 the analysis of the *optimistic plan* sensitivity to the disturbance of the variant 3 is presented.

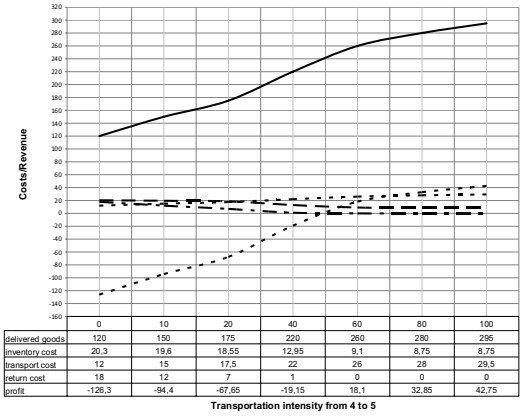

	0	10	20	40	60	80	100
delivered goods	120	150	175	220	260	280	295
inventory cost	20,3	19,6	18,55	12,95	9,1	8,75	8,75
transport cost	12	15	17,5	22	26	28	29,5
return cost	18	12	7	1	0	0	0
profit	-126,3	-94,4	-67,65	-19,15	18,1	32,85	42,75

Figure 3. Analysis of the optimistic plan sensitivity to the disturbance of the variant 3

From the Figure 3 it can be observed that the positive profits may be achieved by the transportation capacity decrease to up to the 50 units. After this point, the number of the delivered goods and, as follows, the revenue fall significantly while the costs increase.

In Figure 4, results of sensitivity analysis for the *pessimistic scenario* plan subject to the disturbances 1-4 are presented.

Corresponding cost- and revenue-based analysis can be performed analogously to the optimistic scenario as shown in Figure 3. An example of such an analysis for the disturbance 3 is presented in Figure 5.

From the Figures 3-5 it can be, e.g., observed that:

- decrease in transportation intensity on the way $4 \to 5$ (disturbance no. 3) does not significantly influence the cost, but considerably impact the volume of delivered goods in optimistic plan. On the contrary, the volume of delivered goods in pessimistic plan is influenced by disturbance no. 3 only to a small extent.
- disturbance no. 1 influences the volume of the delivered goods only in the pessimistic scenario.
- decrease in warehouse capacity at the node 4 (disturbance no. 2) does not influence the volume of the delivered goods neither in the pessimistic not in the optimistic scenario. This is due to reserve warehouse capacities at the other nodes in the DN,
- disturbances of the variants 1 and 2 increase the volume of return flows to 15 and 20 units correspondingly. But their mutual impact (disturbance no.4) increases the volume of return flows to 60 units (see Figure 5).

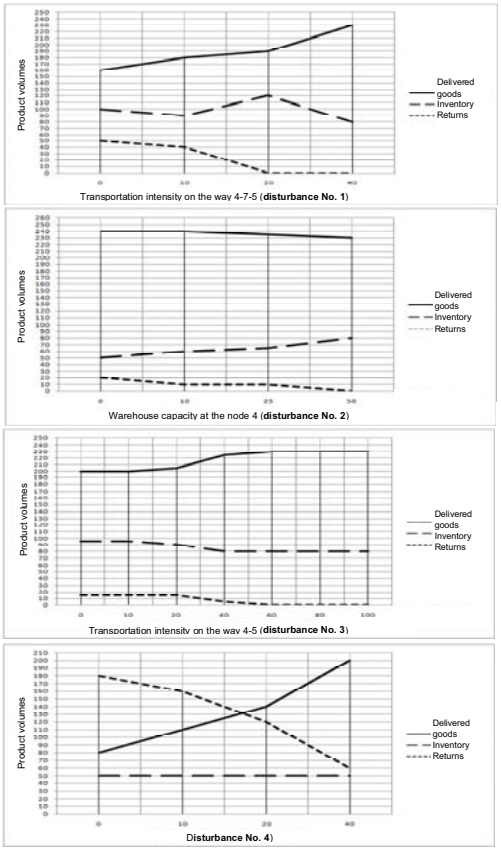

Figure 4. Quantity-based analysis of the pessimistic plan sensitivity to the disturbances of the variants 1-4

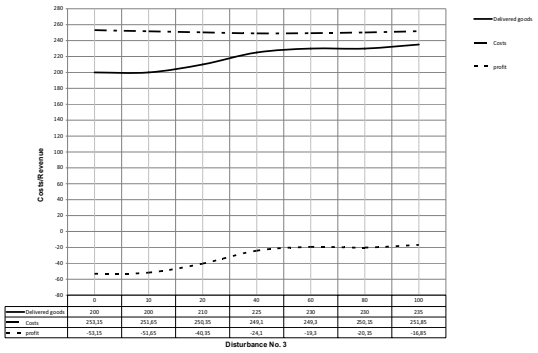

	0	30	20	40	60	80	100
Delivered goods	200	200	210	225	230	230	235
Costs	253,15	251,65	250,35	249,1	249,3	250,35	251,85
profit	-53,15	-51,65	-40,35	-24,1	-19,3	-20,35	-16,85

Figure 5. Cost-based analysis of the pessimistic plan sensitivity to the disturbances of the variant 3

Structural analysis

In this part, in particular, the following questions have be addressed:

- What elements are critical for the SC design and what elements are excessive and can be removed without decreasing the service level?
- Do additional costs in SC design elements pay off by the increase in the service level subject to mitigating the negative effects of possible operation failures or a large delivery flow volume?
- What sourcing quantities can be recommended for different scenarios?

To answer the *first* question, in Figure 6, a re-designed DN structure is presented subject to smaller warehouse capacities at the nodes 3, 7, 2 and 5 as well as smaller intensity of transportation channels 2→4 and 4→5.

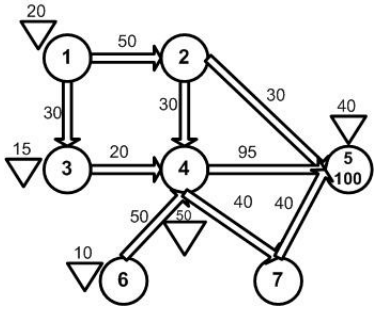

Figure 6. Re-designed DN structure

The smaller capacities result in a decrease of fixed cost of 12$. Both for the optimistic and pessimistic scenarios, the same volume of the delivered goods as in the initial DN structure can be realized. Total cost in the optimistic scenario will be reduced from 252.25 to 240.25$, and the profit increases from 42.75$ to 54.75$. In the pessimistic scenario, total cost will be 239.5 instead of 251.5 and the losses will be reduced from 16.5$ to 4.5$.

CONCLUSIONS

In this study, we extended the planning and control frameworks for supply chains by taking into account the integrated consideration of distribution network planning and analysis. A real case study of distribution planning has been considered. An original approach to analysis of multi-stage, multi-commodity distribution network in the multi-period mode with adaptive update of demand, capacity, and supply information is proposed. Optimal distribution plans are calculated for optimistic and pessimistic scenarios. Subsequently, these plans are analyzed subject to different disturbances and regarding distribution network design and sourcing planning decisions. The performed sensitivity and structural analysis reveals some interesting managerial insights into building robust distribution plans and interconnecting decisions on distribution network design, planning, and sourcing.

ACKNOWLEDGMENTS

This research described in this paper is partially supported by grants of Russian Foundation for Basic Research (RFBR) (10-07-00311, 11-08-01016, 11-08-00767), Saint-Petersburg Scientific Center RAS (SPII RAS project 2011), and the program of fundamental investigation of the department of Nano Technologies and Information Technologies RAS (project 2.3).

REFERENCES

Akkerman R., Farahani, P., Grunow, M. 2010. Quality, safety and sustainability in food distribution: a review of quantitative operations management approaches and challenges. OR Spectrum, 32:863–904.

Amiri A. (2006). Designing a distribution network in a supply chain system: Formulation and efficient solution procedure European Journal of Operational Research, 171, 2, 567-576.

Bertsimas, D., Sim, M. 2004. Price of Robustness. Operations Research, 52(1) 35-53.

Chou, M.C., Chua, G.A., Teo, C.-P., Zheng, H. (2011) Process flexibility revisited: The graph expander and its applications. Operations Research 59 (5), pp. 1090-1105.

Craighead, C., Blackhurst, J., Rungtusanatham, M., & Handfield, R. (2007). The Severity of Supply Chain Disruptions: Design Characteristics and Mitigation Capabilities. Decision Sciences, 38 (1), 131-156.

Ivanov, D., Sokolov B., Käschel J., 2011. Integrated supply chain planning based on a combined application of operations research and optimal control, Central European Journal of Operations Research, 19(3), 219-317.

Ivanov, D., Sokolov, B. (2010), Adaptive Supply Chain Management, Springer, London et al.

Ivanov, D., Sokolov, B. (2012). Dynamic supply chain scheduling. *Journal of Scheduling*, DOI: 10.1007/s10951-010-0189-6.

Ivanov, D., Sokolov, B., Kaeschel, J. (2010). A multi-structural framework for adaptive supply chain planning and operations with structure dynamics

considerations. *European Journal of Operational Research*, 200(2), 409-420.
Kopytov E.A., Pavlov A.N., Zelentsov V.A. New methods of calculating the Genome of structure and the failure criticality of the complex objects' elements. In: Transport and Telecommunication, Vol. 11, No 4, 2010, pp. 4-13. (in Russian)
Lin, YK. (2001). A simple algorithm for reliability evaluation of a stochastic-flow network with node failure. Computers & Operations Research 28, 1271-1285
Mula, J., Peidro, D., Díaz-Madroñero, M., Vicens, E. (2010). Mathematical programming models for supply chain production and transport planning European Journal of Operational Research, 204, 3, 377-390.
Peng, P., Snyder, LV., Lim, A., Liu Z. (2011). Reliable logistics networks design with facility disruptions Transportation Research Part B: Methodological, 45, 8, 1190-1211.
Santoso, T., Ahmed, S., Goetschalckx, G. and Shapiro, A. (2005), "A stochastic programming approach for supply chain network design under uncertainty. European Journal of Operational Research, Vol. 167, pp. 96-115.
Tayur, S., R. Ganeshan and M. Magazine (Eds.). Quantitative Models for Supply Chain Management, Kluwer Academic Publishers, 1999.

AUTHOR BIOGRAPHIES

BORIS V. SOKOLOV is a deputy director at the Russian Academy of Science, Saint Petersburg Institute of Informatics and Automation. Professor Sokolov is the author of a new scientific lead: optimal control theory for structure dynamics of complex systems. Research interests: basic and applied research in mathematical modeling and mathematical methods in scientific research, optimal control theory, mathematical models and methods of support and decision making in complex organization-technical systems under uncertainties and multi- criteria. He is the author and co-author of five books on systems and control theory and of more than 270 scientific papers. Professor B. Sokolov supervised more over 50 research and engineering projects. *Homepage: www.spiiras-grom.ru.*

DMITRY IVANOV is full professor for international supply chain management at Berlin School of Economics and Law, Germany. He is the (co)-author of more than 170 scientific works, including the monograph Adaptive Supply Chain Management. His research interests lie in the area of adaptive supply chains, applied optimal control theory, operations research and business information systems. Member of the IFAC Technical Committee 5.2. His works have been published in various academic journals, including International Journal of Production Research, European Journal of Operational Research, Annual Reviews in Control, Journal of Scheduling, etc. *Homepage: www.ivanov-scm.com*

ALEXANDER N. PAVLOV is a senior researcher at the Russian Academy of Science, Saint Petersburg Institute of Informatics and Automation. Associate Professor Pavlov is the author and co-author of more than 130 scientific papers. His research interests are related to the development of scientific bases of control theory of structural dynamics of complex organizational and technical system.
Homepage: www.spiiras-grom.ru

COMPARATIVE ASSESSMENT OF EXTENDSIM AND ANYLOGIC EFFICIENCY FOR INVENTORY CONTROL SYSTEMS SIMULATION

Eugene Kopytov and Aivars Muravjovs
Transport and Telecommunication Institute
1, Lomonosova Street, Riga, LV-1019, Latvia
E-Mail: kopitov@tsi.lv; aivars.muravjovs@gmail.com

KEYWORDS
Inventory control, simulation tools, ExtendSim, AnyLogic, efficiency index, assessment of efficiency

ABSTRACT

The given research fulfils the evaluation of the efficiency of application of two universal simulation packages ExtendSim 8 and AnyLogic 6.7 for inventory control system simulation. In the study twenty eight evaluating criteria have been developed which are distributed in five groups: general, programming aspects, visualization, simulation and user support. As an object of the simulation the inventory control model with reorder point strategy and stochastic demand has been chosen.

INTRODUCTION

The inventory control problems are very complicated in practice. The search of the effective solutions of stock control in business should be based on a number of economic, social and technical indicators (Kopytov and Greenglaz 2004). In the general case the researches have to investigate the stochastic models for different situations in inventory control systems. At present various models are available to solve the inventory control problem (Chopra and Meindl 2001; Ross 1992). These models can be realized using analytical and simulation methods. As was shown in previous authors' works, the analytical models are fairly complex (Kopytov et al. 2007). The simulation approach gives possibility to find optimum solution of an inventory problem in the case when realization of analytical model is rather difficult. As a result, the number of projects that use simulation models to the problems of inventory management in the last decade has increased significantly. This is due to the following reasons: the complexity of obtaining analytical solutions and the creation of a new generation of modeling, platforms, which have become more friendly for regular users and allow to solve the problem within a reasonable time (Stewart R. 2004).

The existence of a variety of simulation tools makes the issue of choosing the most suitable one rather difficult. There are many studies on the evaluation and comparison of simulation software tools (for example, Seila et al. 2003; Verma et al. 2010), but they do not consider their application for inventory control tasks, which have a number of specific characteristics. For this reason the presented research has been executed.

The authors have evaluated the efficiency of employing simulation tools ExtendSim 8 and AnyLogic 6.7 to solve the inventory control problems. The ExtendSim package is well known in Latvian academic environment versus AnyLogic, which is quite new in this field but is actively used in our university in the last years.

SIMULATION TOOLS UNDER INVESTIGATION

The package ExtendSim (Krahl 2007) is a proven simulation environment capable of modeling a wide range of systems. ExtendSim is used to model continuous, discrete event, discrete rate, and agent based systems. ExtendSim's design facilitates every phase of the simulation project, from creating, validating, and verifying the model, to the construction of a user interface that allows others to analyze the system (Kopytov and Muravjov 2011). Simulation tool developers can use ExtendSim's built-in, compiled language Modl to create reusable modeling components. All of this is done within a single, self-contained software program, which does not require external interfaces, compilers, or code generators.

The package AnyLogic (Marin et al. 2010) is a tool that supports all the most common simulation methodologies in place today: System Dynamics, Process-centric (AKA Discrete Event), and Agent Based modeling (Emrich et al. 2007). The unique flexibility of the modeling language enables the users to capture the complexity and heterogeneity of business, economic and social systems to any desired level of detail. AnyLogic's graphical interface, tools, and library objects allow users to quickly model diverse areas such as manufacturing and logistics, business processes, human resources, consumer and patient behavior. The object-oriented model design paradigm supported by AnyLogic provides for modular, hierarchical, and incremental construction of large models.

METHODOLOGY OF EVALUATION

The procedure for evaluating the effectiveness of the selected simulation tools for inventory control system includes the following stages:

Proceedings 26th European Conference on Modelling and Simulation ©ECMS Klaus G. Troitzsch, Michael Möhring, Ulf Lotzmann (Editors)
ISBN: 978-0-9564944-4-3 / ISBN: 978-0-9564944-5-0 (CD)

- creation of system performance indicators for simulation tools and justification of criteria for evaluating the effectiveness of alternatives;
- choice of methods for estimating indicators of simulation tools;
- implementation of the inventory control models in the ExtendSim and AnyLogic environment;
- performing simulation test;
- assessment of criteria for simulation tools.

The contents of the separate steps are described below.

CRITERIA FORMATION

The problem of simulation tools efficiency evaluation and selecting the most appropriate option was considered by many authors. First of all, we can mention the works (Seila et al. 2003; Verma et al. 2010). It should be noted that in these researches the amount of estimated indicators are significantly different. So, the Seila et al. (2003) have investigated the effectiveness of 20 discrete event simulation tools using a small number of indicators. But Verma et al. (2010) have made an assessment of 4 software tools, estimating more than 200 parameters. Some of the parameters have been evaluated by the expert methods; some parameters were obtained as a result of the experiments.

Taking in account the specificity of inventory control model simulation the authors have formed the system of criteria which includes 28 indicators. These indicators were distributed in five groups shown in the Tab. 1.

Table 1: Groups of criteria of the effectiveness of inventory control simulation tools

Group No	Group Name
1.	General
2.	Programming aspects
3.	Visualization
4.	Simulation
5.	User support

Distributing indicators in the groups allows involving in assessment process various experts: programmers, graphic interface creators, support team, etc.

To evaluate each indicator the authors have selected the numeric scale from 0 to 3, with: 0 – unsatisfactory; 1 – satisfactory; 2 – good; 3 – excellent.

The effectiveness of each simulation tools for the selected groups is characterized by following criteria:

1) *the sum of scores* $S_j^{(i)}$, where $j=1$ for package ExtendSim and $j=2$ for package AnyLogic, where numbers of groups are $i=1,2,..5$;

2) *the priority vector* (local criteria) $p_i=[p_{i,1}, p_{i,2}]$, where the elements of the vector, respectively, define priorities (weights) of ExtendSim 8 and AnyLogic 6.7 calculated for the *i*-th group of indicators as follows:

$$p_{i,j}=\frac{S_j^{(i)}}{S_1^{(i)}+S_2^{(i)}},\quad j=1,2. \qquad (1)$$

It is easy to see that always it is $p_{i,1}+p_{i,2}=1$.

In the final step of the assessment process the vector $P=[p_1,p_2]$ of the *global criteria priorities* can be calculated:

$$P_j=\sum_{i=1}^{5}\beta_i p_{i,j},\quad j=1,2, \qquad (2)$$

where $\beta_i>0, i=1,2,\ldots,5; \sum_{i=1}^{5}\beta_i=1;$ β_i is the weight of criteria of the *i*-th group.

DESCRIPTION OF THE MODEL

To evaluate the efficiency of the selected simulation packages for inventory control tasks there have been selected various models, among them: single- and multiple-product, with random demand, with random and fixed lead time, with different ordering strategies, without restrictions on storage and financing resources.

In this paper we consider a single-product stochastic inventory control model under following conditions. The demand for goods *D* has a normal distribution with known parameters mean *m* and standard deviation σ. In the moment of time, when the stock level $\varphi(t)$ falls till certain level *R*, a new order is placed (see Fig.1). The quantity *R* is called as reorder point. The order quantity *Q* is constant. We suppose that $Q \geq R$. The lead time *L* (time between placing an order and receiving it) is fixed. There is the possible situation of deficit, when demand D_L during lead time *L* exceeds the value of reorder point *R*. We suppose that in case of deficit the last cannot be covered by expected order.

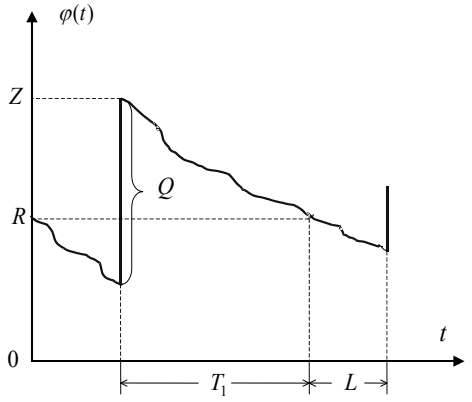

Figure 1: Dynamics of inventory level during one cycle

Denote as Z the quantity of goods in stock in the time moment immediately after order receiving. We can determine this quantity of goods Z as function of demand D_L during lead time L:

$$Z = \begin{cases} R + Q - D_L, & \text{if } D_L < R; \\ Q, & \text{if } D_L \geq R. \end{cases} \quad (3)$$

Expression (3) is basic. It allows expressing different economical indexes of considered process.

Let T be the duration of a cycle. Length of the cycle consists of two parts: time T_1 between receiving the goods and placing a new order and lead time L, i.e. $T = T_1 + L$ (see Fig 1.).

We suppose that next parameters of the model are known:

- the ordering cost C_0 is fixed;
- the holding cost is proportional to quantity of goods in stock and holding time with coefficient of proportionality C_H ;
- the shortage C_{SH} should not exceed 1,5% of demand.

The principal aim of the considered model is to define the optimal values of order quantity Q and reorder point R, which are *control parameters of the model*. A criterion of optimization is the minimum of average total cost in inventory control system per time unit. Denote this average total cost by *E(AC)* which can be found as average total cost during one cycle divided by average cycle time *E(T)* (Ross 1992):

$$E(AC) = \frac{E(TC_H) + E(TC_{SH}) + C_0}{E(T)}, \quad (4)$$

where $E(TC_H)$ and $E(TC_{SH})$ are average holding and average shortage costs within cycle accordantly.

Note that $E(TC_H)$ and $E(TC_{SH})$ depend on control parameters R and Q. Analytical formulas for these economic indicators have been presented in the paper (Kopytov and Greenglaz 2004). For problem solving we have to minimize criteria (4) by R and Q.

The realizations of considered model in ExtendSim 8 and AnyLogic 6.7 environments are presented in the next sections. In examples of simulation presented below we have used the following initial data. The demand for goods D has a normal distribution with parameters mean m =80 and standard deviation σ =18. The lead time L equals 5 days. Starting values for control parameters are: Q=600 and R=500.

SIMULATION MODEL IN EXTENDSIM 8 ENVIRONMENT

For solving the problems considered above we have used discrete events simulation method realized in the package ExtendSim 8 (Strickland 2011). In discrete-event simulation, the operation of a system is represented as a chronological sequence of events (see Fig.2). Each event occurs at an instant in time and marks a change of state in the system (Krahl 2007).
Let us consider the main parts of the simulation model shown in Fig.2. In the area #1 there are placed executive and generation blocks that control model time and transaction generation in the model. Area #2 is responsible for order making decision with equation block results in area #7. Next area #3 represents transportation activity. Demand simulation and decreases in stock are simulated in area #4. Shortage occurrences are represented in area #5. Area #6 is the end of the model and is used for transaction termination.

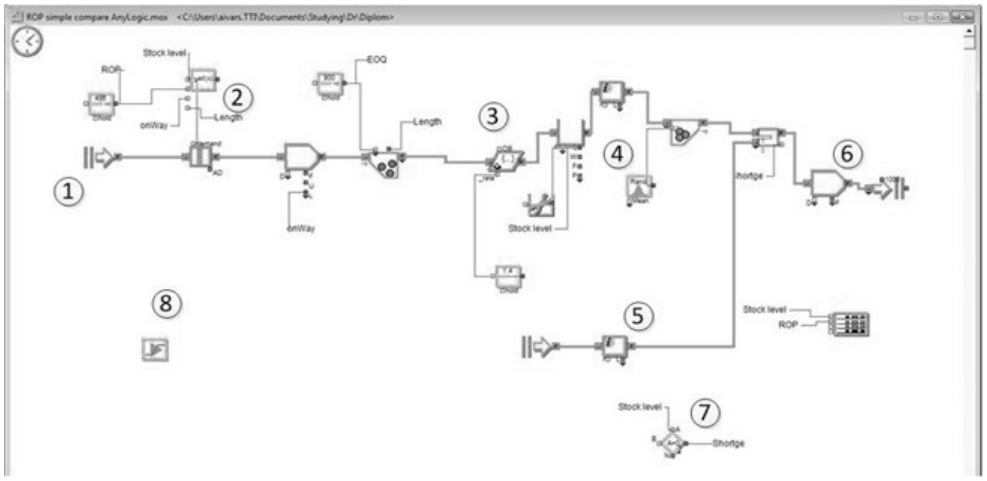

Figure 2: Inventory control model in ExtendSim environment

The example of one realization of inventory control simulation is presented in Fig.3. The plot is showing the stock level for 100 days period simulation.

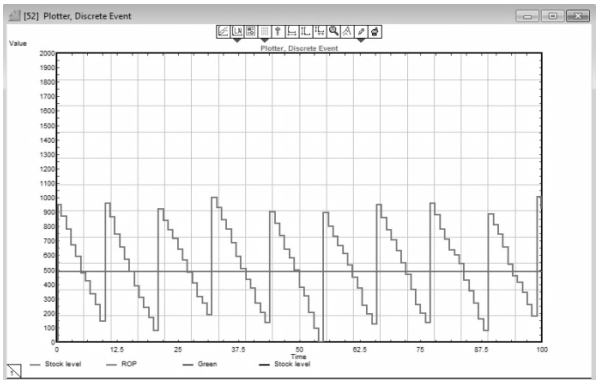

Figure 3: Example of simulation process in ExtendSim

SIMULATION MODEL IN ANYLOGIC 6.7 ENVIRONMENT

The model considered above uses discrete event simulation approach. On the other hand AnyLogic developers promote agent-based modeling (ABM) approach. In ABM the focus is on individual agents, their rules, their behaviors, and their interactions with each other and the environment (Salamon 2011). Collectively agents may exhibit emergent behaviors such as self-organization. Since agents do not follow a pre-scripted flow (as in Discrete Event) and their structure is not pre-specified at the global/aggregate level (as in System Dynamics), they can exhibit novel or surprising behaviors that were not anticipated during design. ABM is a great methodology for exploring non-linear, dynamic environments. ABM is also well suited for situations with no precedent or where past data or experience does not exist. When combined with data and data analytics, ABM forms one of the most powerful predictive analytics / forecasting methodology.

From an architectural viewpoint, a typical AnyLogic agent based model would have at least two active object classes. There would be a main class for a top-level object where agents would be contained and a class for an agent or person. The Person class in most cases would be declared as Agent which is a special subclass of the ActiveObject class that extends the latter with services useful for agent based modeling. A number of agents would be embedded into the Main object, as a replicated object of type Person. One or more Environment constructs may be defined at the level of Main to specify properties shared by the agents.

The suggested inventory model realization is presented in Fig.4. In this figure we can see variable and parameter window that also contains agents for distributer, retailer, truck and events for ordering and transportation tasks. These agents can be used in future more complex models with multiple retailers, distribution point and multiproduct ordering.

In AnyLogic 6.2 are introduced special graphical tolls Action Charts. The designers of AnyLogic have suggested Action Charts as a simple and commonly accepted language, that makes action/decision logic visual, easy to communicate to other people and easier to develop at the same time. Action Charts consist of nested elements, each corresponding to a Java statement: decision-statement, several kinds of loops, local variable declaration, code section, etc. An action chart is straightforwardly mapped to a Java method and therefore is equally efficient. The developers can choose colors and labels of the action chart boxes to further improve its expressiveness. The example of action chart for inventory control model with reorder point is shown in Fig.5.

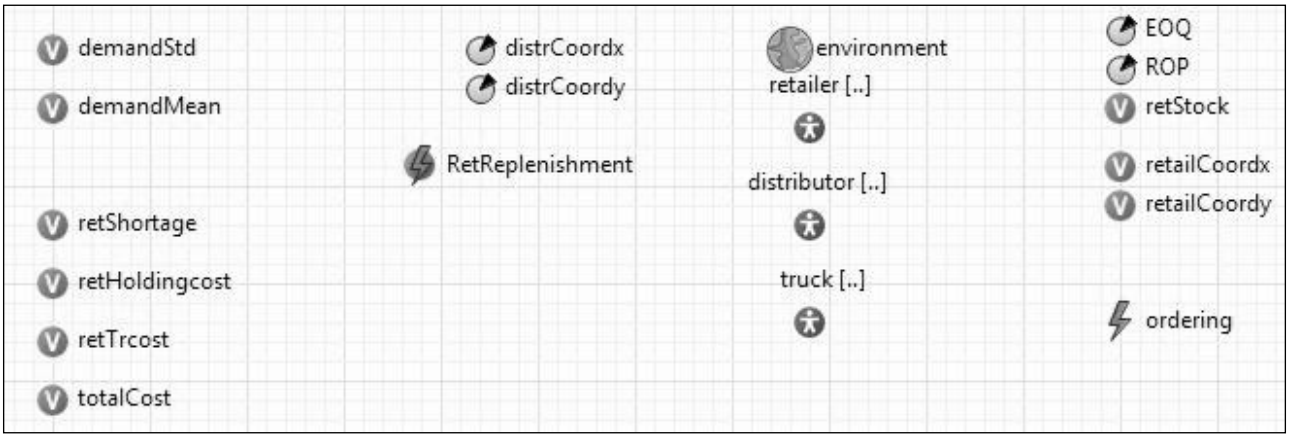

Figure 4: Inventory control model in AnyLogic environment

The example of simulation process realization in AnyLogic environment is presented on Fig.6. As is easily seen, the plots in Fig.3 and Fig.6 are very similar. And this is natural, because the plots show the simulation results of the same task.

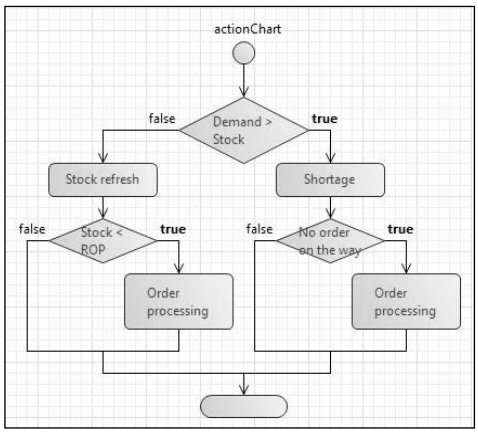

Figure 5: Action chart

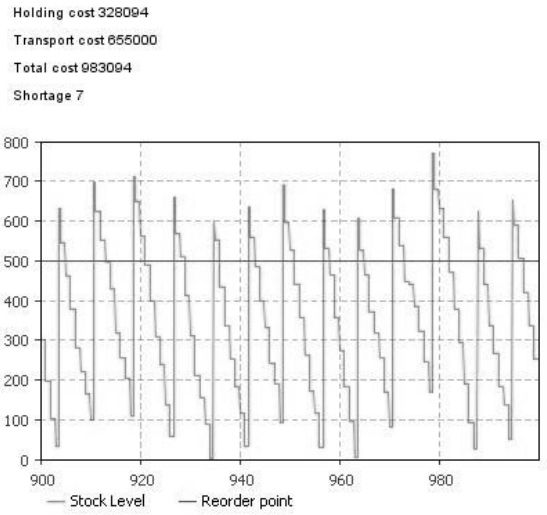

Figure 6: Example of simulation process in AnyLogic

EXAMPLE OF INVENTORY CONTROL SYSTEM OPTIMIZATION

As it was mentioned above the control parameters for presented model are the order quantity Q and reorder point R. In considered example the optimum search of control parameters is carried out in range for $400 \le Q \le 1200$ and $200 \le R \le 800$. Both presented simulation packages have integrated optimization tools that we had used to find optimal result.

At first let's consider optimization process in AnyLogic. To run optimization we should manually create and tune optimization experiment. In tuning process we need to create user interface, define objective function, optimization parameters and constraints. The example of optimization process in AnyLogic environment is presented In Fig.7.

Next let's look at the same procedure in ExtendSim tool, which is a little easier. We can use the same user interface, just putting into model window optimization block, all other steps are similar to AnyLogic except that in ExtendSim we can use optimization parameters only in constraints. The example of optimization process in ExtendSim environment is shown in Fig.8.

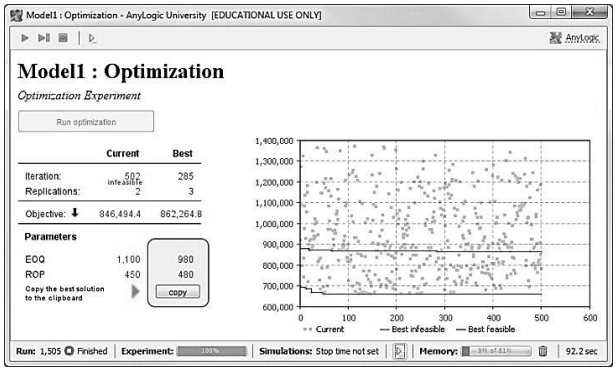

Figure 7: Example of optimization process in AnyLogic

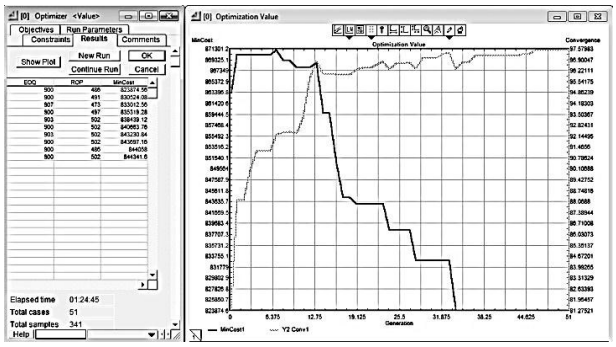

Figure 8: Example of optimization process in ExtendSim

In Tab. 2 final optimization results for both simulation tools are shown. Apparently the obtained results are very similar to each other.

Table 2: Optimization results

	Simulation tools	
Parameter	*AnyLogic*	*ExtendSim*
Reorder point	480	486
Order quantity	980	900
Total cost	862 264 EUR	823 874 EUR

The authors also have investigated more complex models of inventory control systems (for example, see (Kopytov and Muravjov 2011)), which due to the article size limitation are not presented in this paper. The simulation results were used by authors in the comparative assessment of ExtendSim 8 and AnyLogic 6.7 presented below.

ASSESSMENT OF EXTENDSIM AND ANYLOGIC EFFICIENCY

The developed system of criteria described above has been used for comparative assessment of efficiency of the packages ExtendSim 8 and AnyLogic 6.7 for inventory control system simulation. Consequently, the

different groups of criteria have been evaluated by different qualified experts. For instance, the programmers have assessed the general and programming aspects criteria; the experts from the supporting service have evaluated the user support criteria, while the decision makers have estimated the visualization and simulation criteria.

A numerical weight or priority has been derived for each group of criteria (see Tab.3-Tab.7). Each group of criteria has been evaluated by three or more experts then average value of each indicator has been calculated.

Table 3: Simulation tools assessment, group "General"

Indicator	Simulation tools	
	AnyLogic	ExtendSim
Programming language	2,66 (Java)	2 (ModL)
Primary domain	2 (General purpose)	2 (General purpose)
Operating system	3 (Win/Mac/ Linux)	2,66 (Win/Mac 2)
Data connectivity with other applications	2,66 (MS Excel/ Access / SQL ODBC)	2,33 (MS Excel/ Access COM/OLE)
Model packaging	3 (Standalone Java application or embedded to WEB browser)	2,33 (Need ExtendSim player)
Price for universities	2,66 (2600 EUR)	2,66 (1880 EUR)
Optimization	3	2,33
Sum of score	18,98	16,31
Criteria priorities	0,54	0,46

Table 4: Simulation tools assessment, group "Programming aspects"

Indicator	Simulation tools	
	AnyLogic	ExtendSim
Programming flexibility	3	1,33
Support of programming concepts	3	1,66
Built in functions	2,66	2
Debugging	2,66	2,33
Code editor	2	2,33
External code connection	3	1,66
Built-in random numbers generators	2	3
Sum of score	18,32	14,31
Criteria priorities	0,56	0,44

Table 5: Simulation tools assessment, group "Visualization"

Indicator	Simulation tools	
	AnyLogic	ExtendSim
Animation	2,33	3
Logical animation	2	3
Playback mode	3	1.66
3D Animation	1,66	2,33
Graphic library	1,66	1,66
Sum of score	10,65	11,65
Criteria priorities	0,48	0,52

Table 6: Simulation tools assessment, group "Simulation"

Indicator	Simulation tools	
	AnyLogic	ExtendSim
Model execution speed	3	2.66
Simplification of simulation process	2.33	2.66
Variety of simulation approaches	2.66	2.33
Hardware requirements	2	2.66
Sum of score	9.99	10.31
Criteria priorities	0,49	0,51

Table 7: Assessment of ExtendSim and AnyLogic, group "User support"

Indicator	Simulation tools	
	AnyLogic	ExtendSim
Documentation	2.33	2.66
Training courses	3	2
Users forum	2.33	1.33
Knowledge base	2	1.33
Demo models and libraries	3	3
Sum of score	12.66	10.32
Criteria priorities	0.55	0.45

In the final step of the assessment process criteria priorities are calculated using (1), (2) for each of the simulation tools. The weights of relative importance of the various local (group's) criteria suggested by experts are presented in Tab.8.

Table 8: The weights of group's criteria

Group number, i	Group title	Weight, β_i
1	General	0,18
2	Programming aspects	0,30
3	Visualization	0,16
4	Simulation	0,24
5	User support	0,12

The final results of tools assessment are presented in Tab.9. They can be used for choosing simulation package in a particular inventory problem solving. In three groups the criteria weights of AnyLogic are greater (from 8% till 12%) than the weights of ExtendSim. In two groups the AnyLogic yields the ExtendSim by 2-4 %. The global criteria for AnyLogic is greater than global criteria for ExtendSim by 0,06.

Table 9: Evaluations of the vector of the global criteria priorities for ExtendSim and AnyLogic

Group number	Group title	Simulation tools	
		AnyLogic	ExtendSim
1	General	0,54	0,46
2	Programming aspects	0,56	0,44
3	Visualization	0,48	0,52
4	Simulation	0,49	0.51
5	User support	0,55	0,45
Global criteria priorities		0,53	0,47

CONCLUSIONS

This article solves the issue of estimation and choosing the simulating tools for inventory control system modeling. To fulfill the evaluation of the simulating tools, a two-level hierarchy system of criteria has been developed. For investigation two simulation tools ExtendSim 8 and AnyLogic 6.7 were chosen. The assessment was made on the results of the inventory control models implemented in chosen environments. The results indicate the feasibility of the application of ExtendSim 8 and AnyLogic 6.7 in inventory control tasks. Further guidelines of the current research are the following: to apply multiple-criteria decision analysis methods for systems efficiency evaluation; to consider the multi-product inventory control model with certain constraints.

REFERENCES

Chopra, S. and P. Meindl. 2001. *Supply Chain Management*. Prentice Hall, London.

Emrich, Sh.; S. Suslov and J. Florian. 2007. "Fully agent based modellings of epidemic spread using AnyLogic". *EUROSIM 2007*, (Sept. 9-13). Ljubljana, Slovenia, 9-13.

Kopytov, E.; L.Greenglaz; A. Muravjov and E. Puzinkevich. 2007. "Modeling of Two Strategies in Inventory Control System with Random Lead Time and Demand". *Computer Modeling & New Technologies*, Vol. 11(1), Riga: Transport and Telecommunication Institute, 21-30.

Kopytov, E. and L. Greenglaz. 2004. "On a task of optimal inventory control". In *Proceeding of XXIV International Seminar on Stability Problems for Stochastic Models* (Jurmala, Sept. 9-17). Riga, TTI, 247-252.

Kopytov, E. and A. Muravjov. 2011. "Simulation of inventory inventory control system for supply chain "producer – wholesaler – client" in ExtendSim environment". In *Proceedings of the 25th European conference on modeling simulation (ECMS-2011).* (Krakow, June 3-4). Poland, 580-586.

Krahl, D. 2007. "ExtendSim 7". In *Proceedings of the 39th conference on Winter simulation: 40 years!* (Dec. 09-12), S.G. Henderson, B. Biller, M.-H. Hsieh, J. Shortle, J.D. Tew and R.R. Barton (Eds.). Washington D.C., 226-232.

Magableh, G. M. and S. J. Mason. 2009. "An integrated supply chain model with dynamic flow and replenishment requirements". *Journal of Simulation*, Vol. 3, 84–94.

Marin, M.; Zhu, Y.; Andrade, L. Al.; Atencio, E.; Boya, C. and C. Mendizabal. 2010. "Supply chain and hybrid modeling: the Panama Canal operations and it's salinity diffusion". In *Proceedings of the 2010 Winter Simulation Conference.* (Dec. 5-8). American Technologika, Orlando, FL, USA, 2023-2033.

Ross, S. 1992. *Applied Probability Models with Optimization Applications*. Dover Publications, INC, New York.

Salamon, T. 2011. *Design of Agent-Based Models: Developing Computer Simulations for a Better Understanding of Social Processes*, Bruckner Publishing.

Seila, A.F.; V. Ceric and P. Tadikamalla. 2003. *Applied Simulation Modeling,Thomson Learning*, Australia: Thomson Learning.

Stewart, R. 2004. *Simulation – The practice of model development and use*. Wiley.

Strickland, J. 2011. *Discrete Event Simulation using ExtendSim 8*. Lulu.

Verma, R.; A.Gupta and K. Singh. 2009. "A critical evaluation and comparison of four manufacturing simulation software". *Kathmandu university journal of science, Engineering and technology.* Vol. 5(1), 104–120.

ACKNOWLEDGEMENTS

The article is written with the financial assistance of European Social Fund. Project Nr. 2009/0159/1DP/1.1.2.1.2/09/IPIA/VIAA/006 (The Support in Realisation of the Doctoral Programme "Telematics and Logistics" of the Transport and Telecommunication Institute).

AUTHOR BIOGRAPHIES

EUGENE A. KOPYTOV was born in Lignica, Poland and went to the Riga Civil Aviation Engineering Institute, where he studied Computer Maintenance and obtained his engineer diploma in 1971. Candidate of Technical science degree (1984), Kiev Civil Aviation Engineering Institute. Dr.sc.ing. (1992) and Dr.habil.sc.ing. (1997), Riga Aviation University. Professor (1999). Present position: Professor of Computer Science Department. Member of International Telecommunication Academy. Fields of research: statistical recognition and classification, modeling and simulation, modern database technologies. Publication: 270 scientific papers and teaching books, 1 certificate of inventions.

AIVARS MURAVJOVS has graduated at Transport and Telecommunication Institute where he studied Computer Sciences and obtained Master of Natural Sciences in Computer Science in 2009. Present studying PhD student in Telematics and Logistics. Present position: Deputy Head of IT Department.

AN INTEGRATED SIMULATION AND OPTIMIZATION APPROACH FOR SEASIDE TERMINAL OPERATIONS

Daniela Ambrosino
Elena Tànfani
Department of Economics and Quantitative Methods (DIEM)
University of Genova
Via Vivaldi 5, 16126, Genova, Italy
E-mail: ambrosin@economia.unige.it, etanfani@economia.unige.it

,

KEYWORDS

Discrete Event Simulation, 0/1 MIP optimization model, container terminal, seaside operations planning, performance analysis.

ABSTRACT

In this paper we focus our attention on the operational decision problems related to the seaside area of maritime container terminals. In particular, we face the Quay Crane Assignment Problem (QCAP) and Quay Crane Scheduling Problem (QCSP) with an integrated simulation-optimization approach. A 0/1 MIP model is developed in order to determine the optimal assignment, on a shift basis, of QCs to bays of each ship served by the terminal during a given planning horizon, referred as *Bay*_QCAP. The optimization model solutions are used as input parameters for a Discrete Event Simulation (DES) model able to reproduce the system behaviour taking into account its stochastic nature and complexity.
The framework can be used for evaluating the impact on the seaside terminal performance of the optimized solutions and the effects of different operative decisions related to the scheduling of QCs.
The framework is going to be applied to a real case study pertaining to the Southern European Container Hub (SECH), sited in the Port of Genoa, Italy.

INTRODUCTION

The competitiveness of a marine container terminal is based on different factors, such as transhipment time combined with low rates for loading and discharging and fast turnover of containers, which corresponds to a reduction of the berthing time and, consequently, of the cost of the whole transportation process. A marine terminal must be managed in such a way to optimise the flow of containers that arrive and leave it in various ways, as, for instance, by trucks, trains and vessels.
A terminal can be viewed as made up of many interrelated logistic processes as stressed in Vis and De Koster (2003) and Steenken et al. (2004). In these interesting overview papers the authors give a classification of the decision problems at marine container terminal in accordance with the following logistic processes: *i)* arrival of the ship, *ii)* discharging and loading of the ship, *iii)* transport of containers from ship to stack and vice versa, *iv)* stacking of containers, and *v)* inter-terminal transport and other modes of transportation.
In this paper we focus our analysis on the discharging and loading of the ship process. In particular, we are interested in the tactical and operational decision problems related to the organization of the loading and unloading operations.
Gunther and Kim (2006) propose a classification of the problems arising in terminals following the planning level of decisions. In particular, the strategic level refers to long-term decisions pertaining to layout, connections, equipment, berthing and yard capacity, the tactical level regards mid-term decisions pertaining to berth and yard planning and policies, while the operational level refers to short-term decisions pertaining to quay side and land side operations. It is worth mentioning that there are strong relations among strategic, tactical and operations planning at the seaside area, as at the yard and the landside area.
Focusing on the seaside terminal management operations the main problems and their interrelations (see Figure 1) are described in details in a recent survey of Bierwirth and Meisel (2010).

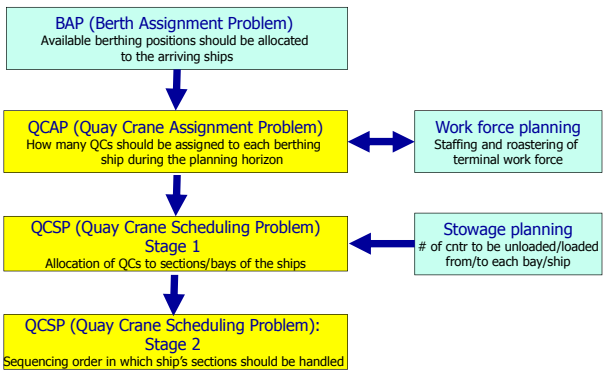

Figure 1: Seaside Decision Problems

The Berth Allocation Problem (BAP) concerns the assignment of quay space to vessels that have to be unload and loaded at the terminal. The Quay Crane Assignment Problem (QCAP) defines how many QCs assigning to each berthing ship, while the Quay Crane Scheduling Problem (QCSP) determines the allocation

Proceedings 26th European Conference on Modelling and Simulation ©ECMS Klaus G. Troitzsch, Michael Möhring, Ulf Lotzmann (Editors)
ISBN: 978-0-9564944-4-3 / ISBN: 978-0-9564944-5-0 (CD)

of tasks to QCs (stage 1) and tasks schedule of each QC (stage 2). Note that tasks can be related to a bay area, a bay, stacks, or group of containers.
Generally, researchers decompose the seaside system into sub-systems and approach the above mentioned problems separately as single decision problem.
Anyway, as pointed out by the recent literature, the interrelations among the decision problems arising in the terminal seaside planning should not be ignored. In fact, only to give an example of these interrelations, we can note the QCSP has a direct connection with the QCAP that defines the exact number of quay cranes operating a vessel; in QCSP tasks must be split and scheduled among the assigned quay cranes.
The main aim of QCSP usually regards the minimization of the makespan of the quay cranes schedule that represents the handling time of a vessel. This time is strictly connected with the number of assigned quay cranes, and finally the BAP depends on the handling time necessary for serving each vessel.
The number of available quay cranes to assign to vessels is directly affected by the quay crane deployment problem (i.e. see Legato et al. 2008) and by the ground crew planning problem (see Legato and Monaco 2004 for details on this problem). Moreover, the tasks to be scheduled in the QCSP are also affected by the stowage plans (see Ambrosino et al. 2004 for details on this problem).
Due to the impact of QCAP on the handling time, in the recent literature it is quite frequent to find integrated approaches for QCAP and BAP. In Bierwirth and Meisel (2010) a classification scheme for integrated seaside operations planning is reported. This scheme follows two different integration concepts proposed by Geoffrion (1999), i.e. deep and functional integration. In the deep integration a whole model includes interrelations among decisions, while in functional integration there is a sequence of solutions of sub-problems and a data exchange between base level and top level.
Approaches based on functional integration between the BAP and QCSP, between BAP and QCAP are reported i.e. in Lee et al (2006), Lokuge and Alahakoon (2007).
Approaches based on deep integration between BAP and QCAP are described, among others, in Giallombardo et al. (2008), Imai et al. (2008), Theofanis et al. (2007) and Park and Kim (2003). In Tavakkoli–Moghaddam et al. (2009) an approach based on deep integration between QCAP and QCSP is presented. Finally, some papers deal with integrated approaches among the three problems arising in the seaside planning (BAP-QCAP-QCSP), and sometimes deep and functional integration are jointly used. The interested readers can see for example Ak and Erera (2006), Liu et al. (2006) and Meisel (2009).
By more holistic point of view, simulation approaches have been quite often used to analyze the seaside terminal operations performance. Nam et al. (2002) examine the optimal number of berths and quay cranes for a terminal in Busan (Korea), while Legato and Mazza (2001) develop a simulation model for the arrival-departure process of vessels at the container terminal of Gioia Tauro (Italy) that is used for optimisation scenario analysis of the berth planning problem. Kia et al. (2002) describe the role of simulation for evaluating the performance of a terminal's seaside equipment and capacity in Melbourne by using interesting performance criteria and model parameters.
In this paper, we start studying the challenging problem of integrating simulation and optimization (Fu 2002; Fu et al. 2005) in order to put together the capability of simulation to describe the dynamics of the system considered and perform scenarios analysis (what-if analysis), with the decisional advantage of optimization, i.e. what-best analysis.
The potentialities of an integrated simulation and optimization approach are herein exploited in order to analyse the performance of the seaside planning at an import/export container terminal.
In particular, we focus our attention on the QCAP and QCSP and propose an integrated simulation-optimization approach to solve in a concise framework the two problems (Figure 1). More precisely, we use a deep integration to solve the QCAP and QCSP (stage 1) by means of an ad hoc optimization model, called *Bay*_QCAP. Afterwards, applying a functional integration, the optimization model solution is used by a Discrete Event Simulation (DES) model designed to reproduce and evaluate alternative scheduling rules and solutions of the QCSP (stage 2) introducing in the analysis some stochastic elements (e.g. QCs' breakdowns).
The paper is organized as follows. Firstly the main characteristics of the modelling approach are described, with particular attention to the performance indexes to be computed. Afterwards, more details on both the optimization model *Bay*_QCAP and the DES model are reported. Finally, the main characteristics of the case study we are going to investigate are presented and some conclusions and further work are given.

PROBLEM ADRESSED AND MODELLING APPROACH

As described in the previous section our analysis is focused on the seaside area at container terminals with particular attention to the operational decisions problems related to the organization of the loading and unloading operations.
In particular, given:

i) the expected time of arrival (ETA) and berthing position of the ships served by the terminal in a given planning horizon, i.e. the solution of the BAP;
ii) the number of import and export containers to be handled and their position on board, i.e. the solution of MBPP;
iii) the staffing and roastering of terminal work force;

we are involved in the QCAP and QCSP, as described in previous section.
In more details, we have to define the assignment of quay cranes to the vessels served by the terminal, and,

more precisely, determine both the assignment of quay cranes to the bays of the vessels (QCAP) and the schedule of tasks of each quay crane (QCSP), in such a way to minimize the berthing time of the ship and the quay crane costs.
The problems herein addressed are solved with an integrated simulation-optimization approach, whose main characteristics are depicted in Figure 2. As optimization is referred, we focus our attention on the QCAP and QCSP (stage 1). A 0/1 MIP model has been developed in order to solve the *Bay*_QCAP and give the optimal number of QCs to be assigned to each ship as well as the assignment of QCs to the bays of the ships.
The optimization model solution is used as input parameter for a Discrete Event Simulation (DES) model designed to simulate the QCSP (stage 2). The DES model is able to manage the non-deterministic and dynamic behaviour of the system and its complexity and can be used to evaluate the impact on the seaside terminal performance of the optimized solutions.
The model can also be used to introduce many causes of variability in the system, such as breakdown and shift set-up times for the QCs and trucks, unplanned delays, meteorological adverse conditions, etc.

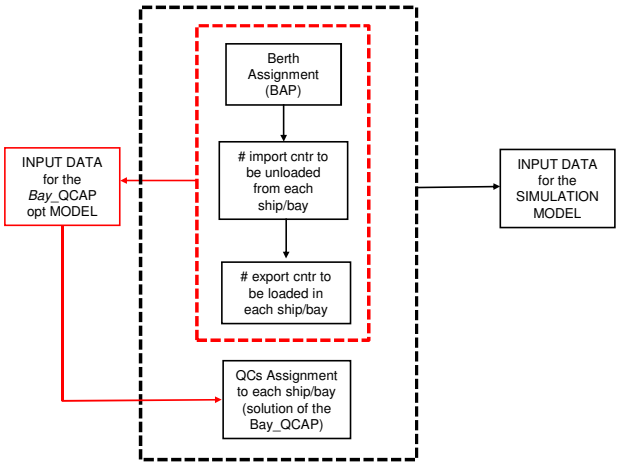

Figure 2: Integration between DES and QCAP opt model

Moreover, the major advantage of the integrated approach herein proposed is its ability to face in a concise and tractable framework both the QCAP and QCSP, using both deep and functional integration.
More details on the *Bay*_QCAP and DES model are given in the following sections.

Performance Indexes

A major characteristic of the framework herein analysed is its ability to perform a very informative bottom-up performance analysis (Figure 3). In particular, we start by the assessment of the productivity of the resources involved in the seaside operations, i.e. gangs and QCs. Note that, a gang is defined as a team of human and associated handling equipment, generally, composed of one quay crane driver, one deck man, one checker, one to three yard crane drivers, three track drivers, two twist handlers (for the entire ship) and three to eight lashing and unlashing operators (for the entire ship). Note that each gang is assigned to one or more working periods (shifts); generally, a shift is 6 hours long.

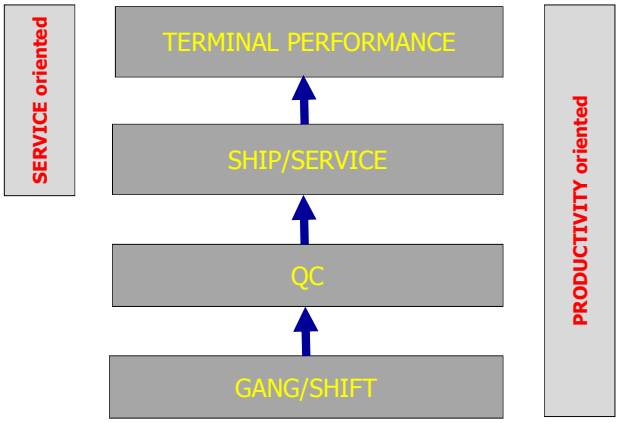

Figure 3: Bottom-up performance analysis

Afterwards, the indexes for each ship/service and for the whole terminal are computed as averages. Moreover, we focus our attention on the evaluation of two series of performance indexes. The first are the so-called productivity-oriented indexes (P) that measure the container traffic volume internal performance of the resources involved, while the second are the service-oriented indexes that measure the service levels (S) provided to clients and are computed for each service/ship and as a macro level terminal point of view.
In Table 1 the whole set of indexes included in the performance analysis is reported.
With reference to the productivity oriented indexes, we decided to use: 1) the berth utilization level, expressed in terms of percentage time of berthing area utilization; 2) the QCs utilization, expressed in terms of percentage of utilization of the QCs involved in the seaside operations; 3) the QC and gang productivity computed as the ratio between the container moves and the berthing time and total shift time, respectively; 4) the "gang" utilisation rate expressed in terms of utilisation (in percentage), i.e. busy time, of the shifts, involved in the loading and unloading operations of each ship; 5) the gang used and related cost. The productivity level indexes should be computed for a macro level/terminal point of view, but more importantly they are also assessed for each ship/service, for each QC and for each gang (i.e. for each shift working period).
The service indexes are usually computed for each ship or service berthing the terminal. Among this group the most important are the berthing time and the so-called terminal performance index, expressed as the ratio between the total number of containers moved and the total berthing time. The above indexes can also be assessed as average, computing the above indexes for

the whole set of ships served by the terminal during a given planning horizon.
The proposed bottom-up performance analysis can allow the terminal to better understand bottlenecks in the seaside process, major costs and productivity gaps in the system.

Table 1. Performance indexes

GANG/shift	*Type*
Shift moves	P
Shift working time	P
Gang productivity=shift moves/shift length	P
Gang utilization= Gang working time/shift length	P
QUAY CRANE	
QC moves	P
Crane working time	P
# gangs (shifts) used	P
Crane productivity=QC moves/Crane working time	P
Crane utilization= Crane working time/Berthing time	P
Gang productivity=QC moves/(# gang used*shift length)	P
Gang utilization= Crane working times/(# gang used*shift length)	P
SHIP/SERVICE	
Ship moves	S
Berthing time	S
Vessel operation time (Gang on - ashore) (=loading time)	S
Terminal performance index=Total moves / Berthing time	S
% of berth utilization = Berthing time / Total time	P
Crane productivity = Ship moves / ∑Crane working times	P
Crane utilization = Avg crane working time/Berthing time	P
Gang productivity=Ship moves/(# gang used*shift length)	P
Gang utilization= ∑gang working times/(# gang used*shift length)	P
# gangs (shift) used	P
Ship gang cost	P
TERMINAL	
Total moves	S
Total Berthing time	S
Vessel operation time (Gang on - ashore) (=loading time)	S
Terminal performance index=Total moves / Berthing time	S
Berth utilization = Total Berthing time / Total time	P
Crane productivity = Total moves / ∑Crane working times	P
Crane utilization = Avg crane working time/Berthing time	P
Gang productivity=Total moves/(# gang used*shift length)	P
Gang utilization= ∑Gang working times/(# gang used*shift length)	P
# gangs (shift) used	P
Total terminal gang cost	P

*Bay*_QCAP MODEL

The model herein developed is designed to determine the amount of resources (gangs) needed to perform the loading and unloading operations of each ship entering the terminal in a given time horizon with the aim of minimizing a multi-objective function that takes into consideration both the overall gang cost (terminal point of view) and the ship cost related to the time the ships spend on berth (maritime company point of view).
As already said, each gang is assigned to one or more working periods (shifts); generally, a shift is 6 hours long. The cost of a gang is different in accordance with the working shift, i.e. shifts at night and on Sunday are more expensive. The assignment of a gang to a shift implies a fixed cost that is charged even if the shift is not completely used.
The maximum number of teams/gangs available in each shift is derived by the solution of the Ground Crew Planning problem. Sometimes it is possible to obtain a higher number of gangs thanks to the possibility of activating some external contracts. In this case it is necessary to distinguish between the maximum number of internal gangs and the maximum number of external ones (i.e. more expensive gangs).
Often, also the minimum and maximum number of QCs to be used for each ship is known in advance. The first is determined by contractual agreement with each maritime company, while the latter is due to physical (i.e. length of the vessel) and logical constraints (interference between crane booms). It is generally required that there are not shifts unworked between the first and the last one (pairing constraints).
Cranes are lined up along the quay and can be moved to every vessel but cannot pass each other (spatial constraints).
More precisely, given: *i*) a planning horizon T, split into a given number of shift periods; ii) the solution of the BAP and MBPP; *iii*) the ETAs of each vessel; *iv*) the number of QCs available in the terminal for each shift; the *Bay*_QCAP herein addressed consists in determining the assignment of QCs to the bays of the vessels and the amount of work executed by each QC. The aim is to minimize the berthing time of the ships and the QCs costs, while satisfying the ships' demand, the QCs' capacity and other operative constraints.
The *Bay*_QCAP differs from the classical QCAP (that defines how many QCs should be assigned to each berthing ship during a given planning horizon) because it also defines which bays must be operated by each QC and the assignment of QCs to the ships in each shift of the berthing period; moreover, QC's costs are also included in *Bay*_QCAP model.
In this first attempt to face this problem, the following assumptions are considered:

- there is a fixed maximum number of gangs available for each shift;
- there is no minimum number of QCs to use for each ship, even if it is required that there are no shifts unworked between the first and the last one (pairing constraints);
- the maximum number of QCs working a ship derives from operational constraints that, in accordance with the type of QCs, require a one-bay or a two-bays distance between QCs working;
- QCs assignment assumptions:
  - a1. a QC should be assigned to more than one ship for each shift;
  - a2. a QC should be assigned to more than one bay for each shift;
  - a3. a bay should not be served by more than one crane in each shift;

A mathematical formulation for the *Bay*_QCAP described above is now introduced.
Let:
S = {1,2,…l} the set of shifts of the given planning horizon T;
V = {1,2,…*m*} the set of vessels of the given BAP;

B = {1,2,…n} the set of bays;
QC = {1,2,…o} the set of quay cranes/gangs;
$d_{v,b}$ the demand, i.e. time necessary for loading/unloading containers in bay b of vessel v, $\forall b \in B$, $\forall v \in V$ (in minutes);
d_v the total demand of vessel v, $\forall v \in V$ (in minutes);
Q_s maximum number of QCs available in shift s;
K_q Shift capacity of QC q, , $\forall q \in$ QC (in minutes);
$cf_{q,s}$ gang fixed cost for using quay crane q in shift s, $\forall q \in QC$, $\forall s \in S$;
$cv_{q,b}$ cost for serving bay b by QC q, $\forall q \in$ QC, $\forall b \in$ B;
$cb_{v,s}$ ship berthing cost for vessel v in shift s, $\forall v \in V$, $\forall s \in S$.

Let us introduce the following decision variables:

$$z_{q,v,b,s} = \begin{cases} 1 \text{ if bay } b \text{ of vessel } v \text{ is assigned to crane } q \text{ in shift } s \\ 0 \text{ otherwise} \end{cases}$$

$$x_{q,v,b,s} \geq 0 \text{ quantity of work executed by crane } q \text{ in bay } b \text{ of vessel } v \text{ in shift } s$$

$$y_{q,s} = \begin{cases} 1 \text{ if crane } q \text{ is used in shift } s \\ 0 \text{ otherwise} \end{cases}$$

$$w_{v,s} = \begin{cases} 1 \text{ if vessel } v \text{ is berthed in shift } s \\ 0 \text{ otherwise} \end{cases}$$

The resulting 0/1 MIP model is the following:

Min

$$\sum_{v \in V} \sum_{s \in S} cb_{v,s} w_{v,s} + \sum_{q \in QC} \sum_{s \in S} cf_{q,s} y_{q,s} + \sum_{q \in QC} \sum_{v \in V} \sum_{b \in B} \sum_{s \in S} cv_{q,b} z_{q,v,b,s} \quad (1)$$

Subject to

$$\sum_{v \in V} \sum_{b \in B} x_{q,v,b,s} \leq K_q y_{q,s} \qquad \forall q \in \text{QC}, \forall s \in \text{S} \quad (2)$$

$$\sum_{q \in Q} \sum_{s \in S} x_{q,v,b,s} = d_{v,b} \qquad \forall b \in \text{B}, \forall v \in \text{V} \quad (3)$$

$$x_{q,v,b,s} - M z_{q,v,b,s} \leq 0 \qquad \forall q \in \text{QC}, \forall b \in \text{B}, \forall v \in \text{V}, \forall s \in \quad (4)$$

$$\sum_{q \in QC} y_{q,s} \leq Q_s \qquad \forall s \in \text{S} \quad (5)$$

$$\sum_{v \in V} z_{q,v,b,s} + \sum_{v \in V} \sum_{q':q' \neq q} z_{q',v,b+1,s} + \sum_{v \in V} \sum_{q':q' \neq q} z_{q',v,b+2,s} \leq 1 \qquad \forall q \in \text{QC}, \forall b \in \text{B}, \forall s \in \text{S} \quad (6)$$

$$d_v - \sum_{q \in Q} \sum_{b \in B} \sum_{s \in S: s' < s} y x_{q,v,b,s} \leq M w_{v,s} \qquad \in \text{V}, \forall s \in \text{S} \quad (7)$$

$$\sum_{q \in Q} \sum_{b \in B} z_{q,v,b,s} \geq w_{v,s} \qquad \forall v \in \text{V}, \forall s \in \text{S} \quad (8)$$

$$\sum_{q \in Q} \sum_{v \in V} z_{q,v,b,s} \leq 1 \qquad \forall b \in \text{B}, \forall s \in \text{S} \quad (9)$$

$$\sum_{v \in V} b \, z_{q,v,b,s} < \sum_{v \in V} (b+i) z_{q+1,v,b+i,s} \qquad \forall s \in \text{S}, \forall b \in \text{B}, \forall i = 1,...|B|-b, \forall q = 1,...o-1. \quad (10)$$

The objective function minimises berthing costs and QCs costs; moreover, it includes a third term aimed at reducing the movements of QCs in the quay. The last term also reduce the possibility of obtaining solutions in which QCs pass other ones, even if for avoiding crossing of cranes spatial constraints are necessary (10).
Berthing costs are computed in accordance with the number of shift vessels are berthed; anyway the minimization of berthing time does not grant that there are no shifts unworked between the first and the last one. For this aim pairing constraints (8) are necessary.
The capacity constraints (2) ensure that the total amount of work executed by a QC in a shift must be less than the maximum shift capacity of the QC. The demand of each vessel, and more precisely of each bay of each vessel, must be satisfied as required by constraints (3).
Constraints (4) are related to the definition of the assignment variables of QC and link variables $z_{q,v,b,s}$ and $x_{q,v,b,s}$. Constraints (5) guarantee not to exceed the maximum number of QCs available for serving vessels in each shift.
Constraints (6) guarantee to have two bays' distance between two quay cranes working a vessel.
Thanks to constraints (7) variables $w_{v,s}$ are fixed to one when the global demand of a vessel is not yet completely satisfied, thus vessel v remains in the port during shift s, while thanks to constraints (8) vessel is worked in shift s. In fact, pairing constraints (8) assign at most one QC to vessel v until the vessel is completely served.
Constraints (9) ensure that in each shift a bay is worked at most by one crane.
If a QC can be assigned to at most one ship in each shift, i.e. the QC assignment assumption a1) does not yet hold, the following constraints should be also included in the model:

$$\sum_{v \in V} a_{q,v,s} \leq 1 \qquad \forall q \in \text{QC}, \forall s \in \text{S} \quad (11)$$

where:

$$a_{q,v,s} = \begin{cases} 1 \text{ if crane } q \text{ is assigned vessel } v \text{ in shift } s \\ 0 \text{ otherwise} \end{cases}$$

and the new set of variables is defined by:

$$\sum_{b \in B} z_{q,v,b,s} \leq |B| a_{q,v,s} \qquad \forall q \in \text{QC}, \forall v \in \text{V}, \forall s \quad (12)$$

If a bay can be served by more than one crane in each shift, i.e. the QC assignment assumption a3) does not yet hold, the following constraints must be included in the model to check that the total amount of work in a bay is less than the length of a shift:

$$\sum_{q \in Q} x_{q,v,b,s} \leq ls \qquad \forall b \in \text{B}, \forall v \in \text{V}, \forall s \in \text{S} \quad (13)$$

where ls represents the length of shifts.
Finally, the model can be easily extended to include external gangs.
This mathematical model has been implemented in MPL and has been solved with the commercial solver Cplex 11.0.

DES MODEL

The DES model is designed to represent the flow of containers related to the unloading and loading operations of the terminal for a given planning horizon.
In Figure 4 the model overview related to the set of operations to be performed for a given ship is reported.
In the operative scenarios herein considered, containers are unloaded (import cntr) and loaded (export cntr) by QCs and internal non-lifting vehicles (trucks) transport containers from the quay to the yard and vice versa.
Note that we assume that QCs move bay to bay in the same direction along the ship (i.e. unidirectional schedule) and after finishing unloading all the bays assigned a QC starts loading bay by bay working the other way round. This means that the unloading and loading processes of each ship are managed in a sequential logic, even if mixed handling techniques can also be analysed.
The model starts at the beginning of the planning horizon (usually a week). As discussed above, the model reads the solution of the BAP that gives the time of arrival and berth position of the set of ship expected to arrive during the period. The number of bays in each ship is known in advance. The number of import and export containers for each ship is generated together with their distribution over the bays of the ship.
Afterwards, the number of QCs assigned to each ship, as well as the set of bays to be handled by each QC, are read by the solution of the *Bay*_QCAP optimization model. The numbers of trucks assigned to each QC/gang are simulation parameters known in advance.
When a ship arrives, the QCs assigned to it start to unload the containers from the first assigned bay following a given sequencing (could be right to left, left to right or other handling techniques).
After unloading a container from its bay position on board the QC drops it to a truck ready on quay. If no trucks are available to transport the unloaded container the QC is blocked and must await a truck to deliver the container and to start another job. These delays must be obviously reduced in order to improve the seaside performance by deciding the right number of trucks to assign to each QC/gang. The trucks transport the containers to the storage area where they will then be stacked by the yard equipment. The trucks' service times include the time needed to transport a container to its yard position and the time needed to RMG or RTG cranes to pick up the container and release the truck to start a new transportation job. This means that we are not interested in what happens to import containers after the internal vehicles have transported them to the yard positions.
After unloading all containers in a given bay the QC must move to the next bay but delays can occur if there is not the security distance of two bays, needed to avoid interference among QCs working.
The QCs unload import containers bay by bay and when they finish unloading start the loading process working the other way round bay by bay. Note that the same pool of internal transport vehicles are devoted to firstly transport import containers to the yard and, afterwards, to deliver the export containers to be loaded under the assigned QC.
The terminating simulation run stops at the end of the planning period (usually a week), when all operations have been performed to the set of ships planned to arrive and all the statistics and performance indexes introduced above are recorded.

APPLICATION TO A REAL CASE STUDY

The proposed framework is going to be applied to a real case study referred as the Southern European Container Hub (SECH) terminal container sited in the Port of Genoa, Italy. The terminal SECH is a medium-sized import export container terminal which covers a 206.000 sqm total surface ground and has a quay length of 526 m. The terminal is based upon the Indirect Transfer System (ITS) in which a fleet of shuttle vehicles (Reach stackers, Fork lifts and Internal trucks) transports the containers from a vessel to the stack area while dedicated cranes (i.e. rail mounted gantry cranes (RMG) or rubber-tired gantry cranes (RTG)) stack containers in the yard slots. In the same way, export containers arriving by road or railway at the terminal are handled within the truck and train operation areas, picked up by the internal transportation equipment and distributed to the respective stacks in the yard by using dedicated equipment. 5 QCs are available for the loading and unloading operations and 27 internal trucks are used to transport the containers from quay to yard and vice versa. Interested readers can refer to the web site http://www.sech.it for getting more information about the terminal SECH.
The DES model presented has been already implemented for the SECH case study using the simulation software environment Witness (Witness, 2010).
At present the main efforts are concentrated on getting the information related to the system parameters to be used in the DES model, with a particular attention to the ship berthing time and number of container movements and to the quay crane and internal transport service times.
As far as the optimization model is considered, preliminary tests for solving real instances of terminal SECH are characterized by a planning horizon of 7 days split into 28 shifts, 5 QCs and a berth 35 bays long. A deeper analysis on the model is under investigation.
Note that, the proposed approach can be easily adapted for being applied to other terminals characterized by different equipment and facilities.

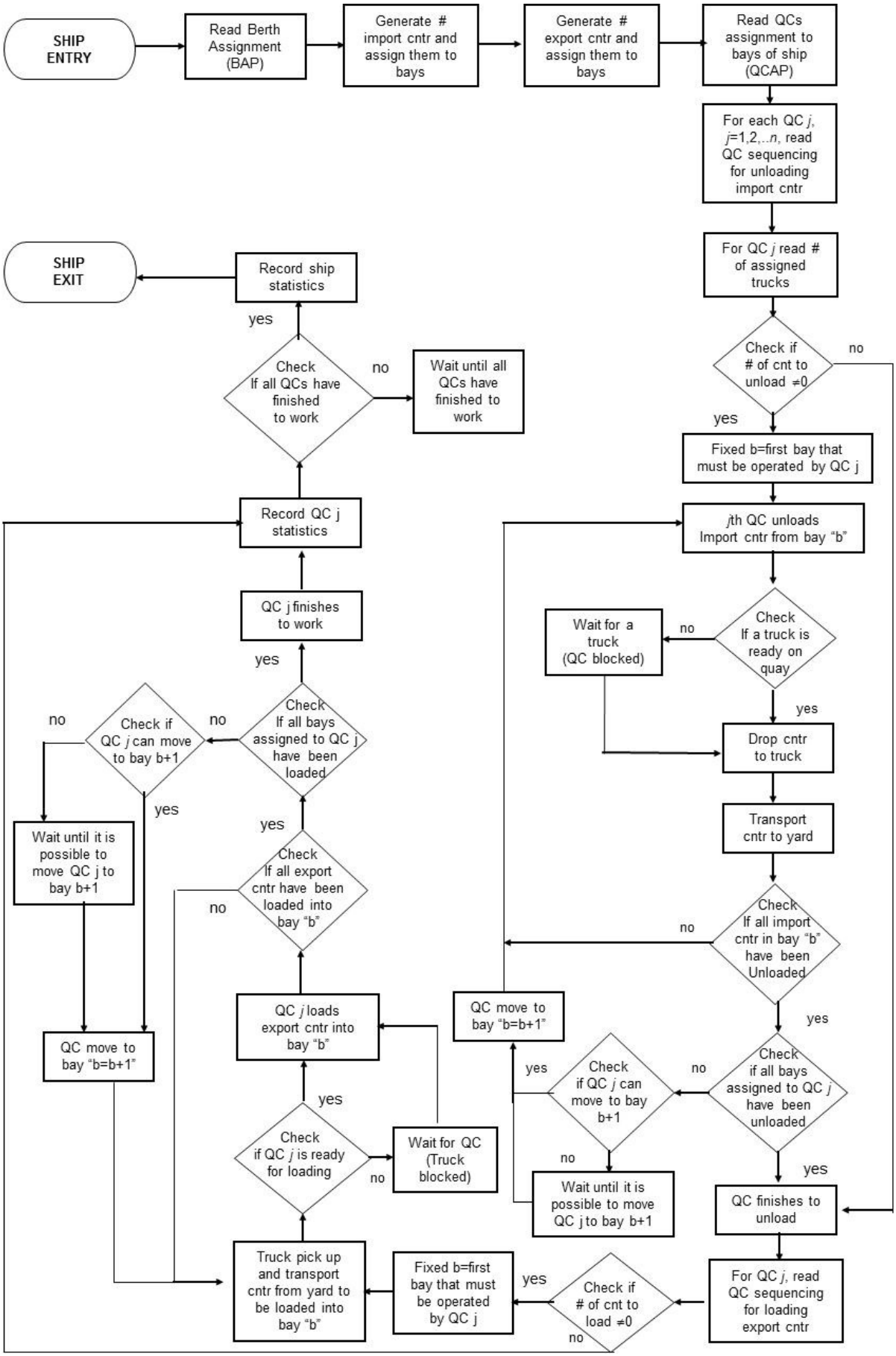

Figure 4. Simulation model overview

CONCLUSIONS AND FURTHER RESEARCH

In this paper we propose an integrated use of optimisation and simulation to study the seaside operations at terminal containers.

In particular, we introduce the *Bay*_QCAP optimization model that generates cranes and gangs allocation plans to be used as input data for a DES model. Afterwards, a simulation model, based on a more realistic representation of the terminal than the one assumed in the *Bay*_QCAP model, is implemented to solve the resource allocation problem and assess the validity of the generated solution.

At present, the main efforts are aimed at collecting the main data, debugging and tuning the model for a real case study. Afterwards, particular attention will be given to the validation of the model comparing the model's output with historical data (parametric tests) and verifying the results together with the terminal operators involved in the data collection (face validity).

We expect to give the first findings of the application of the framework to the SECH terminal during the conference.

Note that, the proposed approach can be easily adapted for being applied to other terminals characterized by different equipment and facilities.

The main expected results regard the possibility to constrain the resources (in particular trucks vehicles and gangs) and compute various performance statistics including: berth and quay utilization, average ship berthing time, QCs delays time, trucks' utilization rate, etc.

The validated model could be used to identify the critical components of the system that represent the process bottlenecks, and perform a scenario analyses aimed at evaluating the impact of organizational changes or alternative operative rules for the quay area, alternative gang work plans for each ship entering the terminal and work sequences on each QC with relevant cost savings.

REFERENCES

Ak, A. and A.L. Erera. 2006. "Simultaneous berth and quay crane scheduling for container ports." Working paper, H. Milton Stewart School of Industrial and Systems Engineering, Georgia, Atlanta.

Ambrosino, D., A. Sciomachen and E. Tanfani. 2004. "Stowing a containership: the master bay plan Problem". *Transportation Research Part A: Policy and Practice*, 38, No.2, 81-99.

Bierwirth, C. and F. Meisel. 2010. "A survey of berth allocation and quay crane scheduling problems in container terminals". *European Journal of Operational Research* 202, No.3, 615-627.

Fu, M.C. 2002. "Optimization for simulation: Theory vs. practice". *INFORMS Journal on Computing* 14, No.3, 192-215.

Fu, M.C., Glover F.W. and J. April. 2005. "Simulation optimization: a review, new developments, and applications". In *Proceedings of the 2005 Winter Simulation Conference*. IEEE, Picataway, N.J., 83-95.

Geoffrion, A. 1999. "Structured modelling: survey and future research directions". *Interactive Transaction s of OR/MS* 1, No.3.

Giallombardo, G., L. Moccia, M. Salani and I. Vacca. 2008. "The tactical berth allocation problem with quay crane assignment and transshipment-related quadratic yard costs". In *Proceedings of European Transport Conference* (ETC), 1-27.

Günther, H.O and K.H. Kim. 2006. "Container Terminals and terminal operations". *OR Spectrum* 28, 437-445.

Imai, A., E. Nishimura and S. Papadimitriou. 2008. "The simultaneous berth and quay crane allocation problem". *Transportation Research Part E: Logistics and Transportation Review*, 44, No.5, 900-920.

Kia, M., E. Shayan and F. Ghotb. 2002. "Investigation of port capacity under a new approach by computer simulation". *Computers & Industrial Engineering* 42, 533-540.

Lee, D.H., L. Song and H. Wang. 2006. "Bilevel programming model and solutions of berth allocation and quay crane scheduling". In *Proceedings of 85 Annual meeting of Transportation Research Board*. Washington DC.

Legato, P., D. Gulli and R. Trunfio. 2008. "The quay crane deployment problem at a maritime container terminal". In *Proceedings of the 22 European Conference of modelling and simulation (ECMS 2008)*, 53-59.

Legato, P. and R.M. Mazza. 2001. "Berth planning and resources optimisation at a container terminal via discrete event simulation". *European Journal of Operational Research* 133, 537-547.

Legato, P. and F. Monaco. 2004. "Human Resource management at a maritime container terminal". *European Journal of Operational Research* 156, 769-781.

Liu, J., Y.W. Wan and L. Wang. 2006. "Quay crane scheduling at container terminals to minimize the maximum relative tardiness of vessel departures". *Naval research logistics* 53, No.1, 60-74.

Lokuge, P. and D. Alahakoon. 2007. "Improving the adaptability in automated vessel scheduling in container ports using intelligent software agents". *European Journal of Operational Research* 177, No.3, 1985-2015.

Meisel, F. 2009. *Seaside operations planning in container terminals*. Physica- Verlag. Berlin.

Nam, K.C., K.S. Kwak and M.S. Yu. 2002. "Simulation study of container terminal performance". *Journal of Waterway, Port, Coastal and Ocean Engineering* 128, No.3, 126-132.

Park, Y.M. and K.H. Kim. 2003. "A scheduling method for berth and quay cranes". *OR Spectrum* 25, No.1, 1-23.

Steenken, D., S. Voss and R. Stahlbock. 2004. "Container terminal operation and operations research - a classification and literature review". *OR Spectrum*, 26, 3-49.

Tavakkoli-Moghaddam R., A. Makui, S. Salahi, M. Bazzazi and F. Taheri. 2009. "An efficient algorithm for solving a new mathematical model for a quay crane scheduling problem in container ports". *Computers & Industrial Engineering* 56, No.1, 241-248.

Theofanis, S., M. Golias and M. Boile. 2007. "Berth and quay crane scheduling: a formulation reflecting service deadlines and productivity agreements". In *Proceedings of the International Conference on Transport Science and Technology (TRANSTEC 2007)*, Prague, 124-140.

Vis, I.F.A. and R. de Koster. 2003. "Transhipment of containers at a container terminal: an overview". *European Journal of Operational Research* 147, 1-16.

Witness Simulation Software (2010 Edition). User Guide, Lanner Group.

Policy Modelling

Demographic and educational projections. Building an event-oriented microsimulation model with CoMICS II

Marc Hannappel

Institut für Soziologie

Universität Koblenz-Landau
56070 Koblenz, Deutschland
Email: MarcHannappel@uni-koblenz.de

Klaus G. Troitzsch
Simone Bauschke
Institut für Wirtschafts- und Verwaltungsinformatik
Universität Koblenz-Landau
56070 Koblenz, Deutschland
kgt@uni-koblenz.de

KEYWORDS

discrete-event-oriented microsimulation, survival function, graduate rates, fertility rates

ABSTRACT

German demographic or educational projections are conventionally based on macrosimulation or period microsimulation models. In this paper we introduce a discrete-event microsimulation model, which we have designed to project the graduate rates of the German population. In this model we use survival functions to calculate different fertility rates by mothers' education. This paper describes how to implement the empirical results into the discrete event microsimulation model CoMICS II and discusses further steps to create a microsimulation model which could demonstrate the development of the German graduate rate considering different strengths of social selectivity mechanisms in the German education system.

INTRODUCTION

Demographic and educational projections are an important basis for policy decisions (Mannion, et.al. 2012). The Australian National Center of Social and Economic Modeling (NATSEM) for example calculates scenarios of the future development of the australian society on the basis of numerous parameters (Kelly & King, 2001). Politicians can then use these projection results to develop political concepts or to reform tax systems or pension schemes. The German Statistical Office (GSO) uses macrosimulation techniques to calculate the development of the German society for the next 50 years. These projections focus on the prediction of the absolute number of the future population and its composition according to age and gender. For instance, the conference of the regional ministers of education uses these results to calculate the educational attainment of the future German population (Kultusministerkonferenz, 2005).

The examples focus on the political fields of application of simulations techniques. However, this view neglects the epistemological gain of simulation models. Conventionally, one assumes microsimulation models are only used to predict social phenomena whereas agent based models are used to explain social phenomena (Spielauer, 2009) (Walker, 2010).

In this paper we present a microsimulation model which will be able to generate theoretical assumptions about interaction effects between demographic processes and social selectivity mechanisms within the German education system. The construction of the model is not finished yet. Therefore, the paper is focused on the presentation of the demographic modules and results.

Correspondingly, we first give an overview of the content frame of our project. This is followed by a method section where we present our microsimulation approach, the database, the survival functions which we use to calculate the biographic events and our model structure. With an example we then show how to implement the empirical results into a simulation module. Finally we present the current simulation results and discuss further steps.

1 DEMOGRAPHIC CHANGE AND SOCIAL SELECTIVITY

Beside the political discussion how to overcome the financial crisis two developments dominate the German scientific and political discourse about the future challenges of German society: the demographic change and the inequality within the German education system. The former is characterized by a successive decrease of the fertility rates during the past decades (Peuckert, 2008). No other country of the western industrial countries has such a low fertility rate as the Federal Republic of Germany. A detailed examination of the development of the birth rates leads to an interesting result. The probability to give birth to a child varies between women with different educational status. The higher the educational level of women the lower the probability to give birth to a child (Peuckert, 2008).

The second development affects the German education system. The PISA-Studie (PISA-Konsortium Deutschland, 2007) shows a relation between the educational status of parents and the educational attainment of their offspring. Also in this issue Germany stands out from

Proceedings 26th European Conference on Modelling and Simulation ©ECMS Klaus G. Troitzsch, Michael Möhring, Ulf Lotzmann (Editors)
ISBN: 978-0-9564944-4-3 / ISBN: 978-0-9564944-5-0 (CD)

other countries. The correlation between the social background and the educational attainment of children is larger in Germany than in any other country.

We summarize: First, the German society is characterized by a negative correlation between the educational status of women and their fertility rates. Second, the German education system is characterized by a positive correlation between the educational status of parents and the educational attainment of their offspring. This leads us to the question: Wich consequences do these developments have on the future social composition of the German society?

To find an answer to this question we developed a dynamic event-oriented microsimulation model which will be described in the following.

2 METHOD

2.1 Event oriented microsimulation

Dynamic micro-analytical simulation models can either be modelled with a period approach or with an event-oriented approach (Gilbert & Troitzsch, 2005). Wheras period-oriented simulations model time as passing between equidistant points of time usually one year apart, in event-oriented microsimulation models time between two events is modeled as a random variable whose distribution is estimated from empirical data. This time interval is calculated by survival functions which parameterise the events.

This method allows to implement different kinds of calculations, which determine time as an interval until an event occurs. In contrast to period-oriented models, which import each individual in every time period into the simulation to examine whether an event will occur or not, event-oriented approaches determine the time when an event will occur (Gilbert & Troitzsch, 2005).

In event-oriented microsimulation models, individuals have to pass a module when all characteristics are available which are necessary to calculate a random value for the time until the next event of a certain type. A random number generator yields a random number from a [0,1] uniform distribution (monte-carlo experiment). A simulation algorithm compares the random number with an empirical value to calculate if an event occurs or not (for more detailed information about the process of event oriented simulation models see section 2.5)

2.2 Discrete-event microsimulation with CoMICS II

The projection of prospective German graduates in CoMICS II is a Java-based event-oriented microsimulation software. Its key elements are a consistent time system and management, a random number generator, various classes of events, an event calendar similar to the crystal ball of DYNAMOD (Abello & King, 2002) and, last but not least an external data base which keeps the model individuals and their attributes. When the simulation is initialised, all model individuals calculate the time when their next events will occur according to the survival functions applicable for these events (see the example below). The event calendar contains these calculated event dates for all individuals, and the event manager accesses this calendar and executes one event after another, and these events will change the state of the respective individual or individuals.

2.3 Data

Micro simulation models are conventionally based on representative data sets with an adequate number of individuals and attributes, so it is necessary to describe the data set which we use in the simulation. The microcensus of the German Statistical Office is the only data set in Germany which satisfies the conditions on microsimulation models: a large number of micro units, variables which include the characteristic of the micro units and a household structure which enables to link the members of a household.

The microscensus is a representative sample (annual 1% census) of the German population which includes questions about socio-economic issues. Whereas the microcensus is focused on information about labour market participation, the data set includes a number of issues about family, education and fertility. For the simulation a 70% subsample of the original microcensus – Scientific Use File (SUF) 2008 – is available, which includes a sufficient number (477,239) of individuals, attributes and dates, so that the SUF can be used for estimating the survival functions.

2.4 Survival functions

Survival functions calculate the probability of individuals to "survive" the time until an event occurs. In this context the special interest of fertility analyses consists in the calculation of the difference between the time from a starting point and the time when a woman gives birth to her first child.

The event "birth of first child" is operationalised by the variable "age at first birth". Conventionally, women are analysed by their age at first birth. The difference between their own year of birth and the age when they give birth to their first children is then used as a parameter for the time until the event "birth of first child" occurs. However, the 2008 microcensus included only information about children living in their parents' household. As a consequence it is not possible to calculate the age of first birth for women whose children have left the household. To avoid this problem, actual results could be achieved by analysing the age of first birth from the children's perspective (Spielauer, 2003), i.e. not the mothers are the subjects of the analysis, but the first born children are analysed by the age of their mothers when they were born.

To do so, we use survival functions to calculate the probability of when a woman will give birth to her first

child.

$$S(t) = P(T > t) \quad (1)$$

$S(t)$ = survival function; probability that a person "survives" (in this case: remains childless) at least until time t
T = random variable (event date)
t = specified time
$P(T > t)$ = probability that the specified time is shorter than the random variable T. The person "survives" the specified time, i.e. the event will not occur.

As mentioned above, the analyses are focused on children cohorts. Therefore the results of the survival function would be zero for 50-year-old mothers. In reality not every woman gives birth to a child, so it is necessary to adjust the survival function by (1- "rate of childlessness").

$$S_i'(t) = S_i(t)(1 - P_i(k)) \quad (2)$$

$S_i'(t)$ =survival function at time t of women with qualification i, reduced by the rate of childlessness by education
$S_i(t)$ = survival function at time T by qualification i of women
$P_i(k)$= probability of childlessness from women with qualification i

Table 1: Age specific risk $h(t)$, cumulative risk $c_{h(t)}$, cumulative survival rate $c_{S(t)}$ and adjusted cumulative survival rate c from 15–50 year-old mothers with a university degree to have a first child.

1	2	3	4	5
age	$h(t)$	$c_{h(t)}$	$c_{S(t)}$	c
15	0	0	100	61000
(...)	(...)	(...)	(...)	(...)
29	7.1	14.02	77.02	46979
30	8.4	19.13	68.64	41871
31	8.3	24.17	60.37	36826
32	9.0	29.66	51.37	31335
33	10.6	36.11	40.81	24984
34	10.0	42.23	30.78	18775
35	8.5	47.42	22.25	13575
36	5.7	50.88	16.58	10116
37	5.0	53.92	11.61	7083
(...)	(...)	(...)	(...)	(...)
50	0.0	61.00	0.00	0
$n = 1639$ weighted (unweighted: 801)				

Source: own calculation based on SUF 2005, cohorts 2002–2005 of first-born children

Table 1 shows the empirical values – risk and survival rates – of women with a university degree by age. The first column lists the age of the women and the second column lists the hazard rates by age. The risk of a first birth for women with a university degree at the age of 30 amounts to 8.4 %. The cumulative risk for these women, which is listed in column 3, amounts to 19.13 %. Compared to columns 2 and 4, columns 3 and 5 include the rate of childlessness. Women aged 50 have a 61 % cumulative risk to have given birth to their first child, unless they remain childless (39 %). The cumulative survival rate ($c_{S(t)}$) for 30-year-old women with a university degree of the analysed cohort amounts to 68.64 %. The adjusted cumulative survival rate is listed in column 5 (c), and these values will be used in the simulation, i.e. the adjusted cumulative survival rate (percentage) multiplied by 1000 – we draw uniformly distributed integer random number between 0 and 100,000. The survival rates have to match with this value range. The values of this column are the survival functions which we have converted according to the life table method and then listed in the event tables. As mentioned below, the event dates of the "age at first birth" are the results of the comparison between the empirically estimated survival function values from column 5 and a number drawn randomly by the random number generator. The idea of microsimulation is that a large number of monte-carlo experiments lead to the result that a certain percentage – in the case of the example 39% – of the random numbers will be larger than a defined "critical" value (61,000). Women with a random number larger than 61,000 will remain childless (for a more detailed description see section 2.5).

2.5 Modules

The simulation of the German graduates includes many different modules (Figure 1) with socio-demographic or socio-cultural tables (Table 1). The module "Death" is the first module the individuals have to pass through. The simulation algorithm calculates the exact time of death for every individual before the simulation starts or when an individual is born during the simulation. The time of death is a result of a comparison between the survival function value which is taken from the life tables of the German Statistical Office, and a random number, which is drawn for every individual (the example of the module "Child 1" will give a detailed overview of the procedure of the simulation algorithm). Within the module "Education" the simulation algorithm decides which kind of educational attainment will be assigned to a child considering his or her parents' education. This module takes into account the different social selectivity mechanisms within the German education system. When a woman gives birth to her first child, a partner will be matched by education and age in the "Partnership" module. As a consequence, fertility is modelled independently of partnership (Spielauer, 2003). The module "Birth" consists of three different submodules ("Child 1", "Child 2" and "Child 3"). As an example we will discuss the module "Child 1": As mentioned above, we model time as a ran-

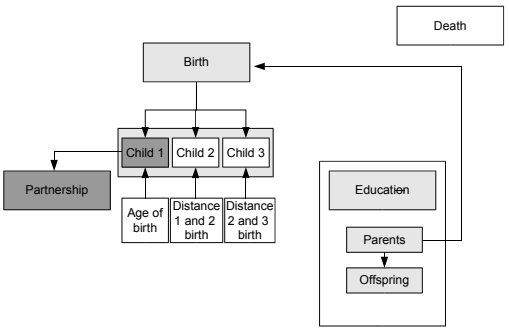

Figure 1: Overview: modules.

dom variable between the simulation start and the time when an event occurs. The module "Child 1" calculates

the day when a certain woman will give birth to her first child. First of all the simulation algorithm selects only female persons from the data set and ascertains the age of the women. Afterward the calculation process is separated in two steps. In the first step the simulation algorithm draws a random number for every woman. This number will then be compared with the first value of the event tables (61,000 for women with a university degree). If the random number is larger than this value the women will remain childless, otherwise the date of her first child's birth will be calculated. In the latter case these women have to pass the second step. A second random number in a range between the age specific value of the women's current age and zero will be drawn for every woman. This number will then be compared to the age specific value of the selected woman. If the random number r is bigger than the age specific value v_x, this woman will stay childless. If $r < v_x$, the simulation algorithm will compare r with the age specific value of women at age $x+1$ (starting age + 1). This process will be repeated until an age specific value is found which is smaller than the random number of the woman. This value represents the "year of her life" in which this woman will give birth to her first child. The year x in which the woman gives birth to her first child is determined by $(v_x > r > v_{x+1})$. The exact date of birth within this year is given by formula 3:

$$D(b)_x = \left(\frac{v_x - r}{v_x - v_{x+1}}\right) \times 365.25 \quad (3)$$

$D(b)_x$ = number of days until birth after the mother's x-th birthday
v_x = cumulative frequency of first children born before a mother's x-th birthday
v_{x+1} = cumulative frequency of first children born before a mother's $(x+1)$-th birthday

r = a uniformly distributed random number

$D(b)_x$ is the number of days after the woman's birthday until the event "birth of first child" occurs. The next step is to calculate the days from the starting age of the woman – the age at the start of the simulation – until the exact day of the event "first birth":

$$D(b) = D(b)_x + [(t_b - t_s) \times 365] \quad (4)$$

$D(b)$ = survival time (number of days until birth since the woman's starting age)
$D(b)_x$ = number of days until birth after the mother's x-th birthday
t_b = age of first birth
t_s = starting age

Finally, the date of first birth is compared to the woman's date of death ($D(d)$) which has been calculated in the module "Death" before. If $D(b) < D(d)$, the event will occur and the date of birth of the first child will be registered in the event calendar. The example in Figure 2 gives an overview of the simulation process:

The calculation processes of all other events is mainly done in the same way. Single events can trigger other events. As a consequence of this not all events will be calculated before the start of the simulation. Following the example, it is not the complete birth biography of women that is calculated at the beginning of the simulation. First, the age of first birth, operationalised as the time until first birth, as mentioned above, will be calculated and afterwards the woman who gives birth to a first

simulation start	1.1.2008	age of the woman =29
first step:		
1. random number	55,321	55,321 < 61,000
	⇒	the woman will give birth to a child
second step:		
2. random number	(age 29)	46,979 → 0
draw		
random number	17,934	$v_{34} > r > v_{35}$
of the woman		$18,775 > 17,934 > 13,575$
Value for age 34	18,775	⇒ *woman has her first*
Value for age 35	13,575	*child at the age of* 34

Calculation of the number of days between the simulation start and the date of the event:
$D(b)_x = \left(\frac{r-v_{34}}{v_{35}-v_{34}}\right) \times 365 = \left(\frac{17,934-18,775}{13,575-18,775}\right) \times 365 = 0,16 \times 365 = 58,4$

$D(b) = D(b)_x + [(t_b - t_x) \times 365] = 58,4 + [34-29] \times 365 = 1,883$

01.01.2008 (simulation start) + 1,883 (days until the event will occur) =27.02.2013

Figure 2: Example

child will pass the module "Child 2", which is operationalised by the time between the first and the second child. All event dates which are calculated this way are registered in the event calendar and executed in the simulation. If an event happens, the program will delete this event from the event list.

The first simulation runs have shown that the results of discrete-event-oriented microsimulation processes are similar to those of period-oriented microsimulation models. Simulations with the full number of 484,422 individuals of the 2008 microcensus will be carried out in the coming weeks.

3 RESULTS

Figure 3 shows our current simulation results and the results of the macrosimulation of the German Statistical Office (GSO) (StaBu, 2006). Although it is not possible to validate projection results, we use the comparison between the results of the GSO and our results to check whether our results are plausible or not. The German Statistical Office calculates 12 different scenarios. The results are taken from a scenario which did not consider migration processes and uses the current fertility and death rates as constant. The assumptions of this scenario are similar to the assumptions within our simulation. The dashed line represents the percentage difference between the different results. The difference between the "official" standard scenario and our simulation is in the range of 3 and -2 percentage points for the population until 80 years. Only for the population older than 80 years, we can observe an increase of the difference up to 7% which is comensated by a negative difference for the population older than 95 years.. The difference shows a very good accordance between both simulation results.

Figure 4 illustrates the number of births between 1951 and 2057. The vertical line separates the real population – the people who really exists before the simulation start – and the simulated population. The result shows a plau-

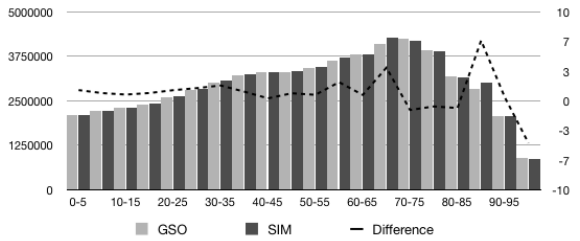

Figure 3: Results for 2057: Difference between the projection of the German Statistical Office and the results of the Simulation

sible development of the birth rates for the next 50 years. The final simulation will only project the population for the next 20 or 30 years. However, to test the simulation algorithm it is necessary to apply a longer simulation time to preclude implausible developments. The decrease of births is caused by the fact that we use a closed microsimulation model, i.e. we don't consider migration processes.

Figure 4: Number of birth between 1951 and 2057

A comparison between the results of the analyses of the age at first birth of the Scientific Use File (SUF) 2008 and the simulation results shows also consistent results (see Figure 5) . We use this comparison to control the simulation algorithm. The parameters of the action decisions which we implemented in the simulation are a result of the analysis of the SUF 2008. Consequently, the frequencies of the variable "age at first birth" of the simulated dataset should be similar to the analyses of the original dataset. The observable small difference is caused

Figure 5: Age of first birth: SUF 2008 vs. simulation results

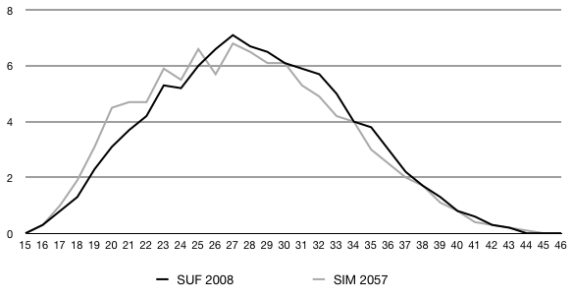

by two reasons. First, we use a 10% subsample of the original dataset to test our simulation algorithm. As a consequence we have a small variance of the simulation results. Second, the results are based on analyses on an aggregate level. However, the survival rates of the age at first birth are calculated depending on the educational status of the women. The graph in Figure 5 shows the age of first birth for all mothers. The average age at first birth is one year smaller for the population of the simulated dataset (the grey line in Figure 5). An explanation of this development is given in Figure 6, which shows the development of the educational attainment of the population. The cohort 1962 - 1982 represents people who had completed their school training before the start of the simulation. Therefore, the development of the educational attainment of people who were born until 1982 shows the so-called "German educational expansion" which is characterised by an increase of the percentage of higher educated people (Becker, 2011). Whereas the percentage of this subpopulation stays constant during the simulation the percentage of the population with a middle secondary degree decreases and the people without a school degree increases dramatically. The development of the

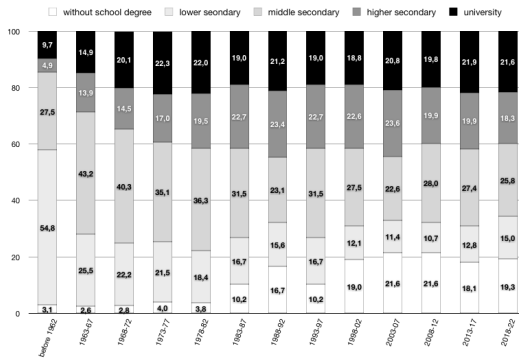

Figure 6: Educational attainment of the cohorts $<$ 1962 to 2022

simulated educational attainment is currently not sufficiently realistic. First, we haven't yet considered transitions between vocational school and university. These transitions are significant for the German education system. Therefore, our model underestimates the development of the people with a university degree. Second, we have a large number of young people without a school degree in the original dataset. These are people who are still in school and listed as "without a school degree". These two issues will be solved in the next weeks. Currently, we are analysing a new dataset which includes information about the transition from high school/ vocational school to a university.

Furthermore, Figure 5 and 6 give an idea how to answer the question of the reciprocal influence of demographic and educational developments on the social composition of the German population. The population without a school degree is characetrised by a high fertility rate and – in contrast to other subgroups – a lower average

age of first birth. The increase of this subpopulation in our current simulation scenario leads to a decrease of the average age of first birth for the entire population. Additionally, the high fertility rate and the low social mobility of this subpopulation leads to an increase of the percentage of people without a school degree (see Figure 6).

For the final results we expect a lower increase of people without a school degree and an higher number of people with a university degree. By the use of different scenarios we are then able to demonstrate the reciprocal influence of the various developments.

4 DISCUSSION

The results are based on a 10 % subsample of the original 2008 data with only 47,000 cases to save computing time during the test phase. Because of the stochastic processes within the simulation, the sample size has an influence on the simulation results: The lower the sample size, the higher the variation of the results. However, the use of a small sample is necessary because the single simulation runs need a lot of time. With the small sample it is possible to test the simulation algorithm in much shorter time. Therefore we assume stabler results with the complete module structure and with the original dataset (484,422 cases).

The advantage of microsimulation models is the flexibility of the model assumptions. The simulated dataset includes all variables of the original empirical dataset and describes the structure of the population in any respect as it can be analysed the same way as the microcensus data set. Instead of the interpretation of the absolute number of simulated cases and very superficial view on the structure of the total population, such as in macromodels, it is possible to analyse the data in many different ways. The dataset includes information about the age at first birth, the educational status of the individuals, and all relations between members of the same family. We can analyse the data to check the particular simulation algorithms and to analyse the interaction between the implemented parameters. It is possible to show the influence of the correlation between fertility processes and the educational attainment of women, and additionally it is possible to analyze the consequences of this correlation on the future social composition of the society. Beside empirical methods, microsimulation models are a specific instrument to analyse the interaction between different strands of development.

REFERENCES

Abello, A.King, A. (2002). Demographic Projections with DYNAMOD-2. *National Centre for Social and Economic Modelling, Canberra*

Becker, R. Hadjar, A. (2011). Erwartete und unerwartete Folgen der Bildungsexpansion in Deutschland. *In Becker, R.: Lehrbuch der Bildungssoziologie. Auflage: 2. VS-Verlag, Wiesbaden. S. 195 - 214.*

Gilbert, N.,Troitzsch, K. G. (2005). Simulation for the Social Scientist. *Open University Press, London*

Kelly, S.,King, A. (2001). Australians over the coming 50 years: providing useful projections.. *National Centre for Social and Economic Modelling, Canberra*

Kultusministerkonferenz (2005). Prognose der Studienanfänger, Studierenden und Hochschulabsolventen bis 2020. *Bonn*

Mannion, O. Lay-Yee, R. Wrapson, W.Davis,P. Pearson, J. (2012). JAMSIM: a Microsimulation Modelling Policy Tool. *Journal of Artificial Societies and Social Simulation 15 (1) 8 http://jasss.soc.surrey.ac.uk/15/1/8.html*

Leim, I. (2008). Die Modellierung der Fertilitätsentwicklung. *Metropolis-Verlag, Marburg*

Peuckert, R. (2008). Familienformen im sozialen Wandel. *VS Verlag, Wiesbaden*

PISA-Konsortium Deutschland, (2007). PISA 2006. *Waxmann, Münster*

Spielauer,M. (2003). Family and Education. *Austrian Institute for Family Studies, Wien*

Spielauer, M. (2009). Microsimulation Approaches. *Statistics Canada*

Statistisches Bundesamt (2006). Bevölkerung Deutschlands bis 2050. *Wiesbaden*

Walker, L. (2010). Modelling inter-ethnic partnerships in New Zealand 1981-2006: a census-based approach. *University of Auckland*

AUTHOR BIOGRAPHIES

Marc Hannappel was born 1980 in Bad Schwalbach, Germany. He studied educational research at the University of Koblenz-Landau and obtained his degree 2006. From 4/2008 to 9/2010 he was a scholarship holder of the Hans-Böckler-Stiftung. Since 10/2010 he has been working at the Institute of Sociology at the University of Koblenz-Landau. His email is `MarcHannappel@uni-koblenz.de`

Simone Bauschke was born 1975 in Cottbus, Germany. Since 2001 she has studied computer science at the University of Koblenz-Landau. She has been working since 2009 as a research assistant at the Institute of Information Systems in Business and Public Management . Her email is `ehrenbsi@uni-koblenz.de`

Klaus G. Troitzsch was born in Lahstedt, Germany, in 1946. He studied sociology and political science at the University of Hamburg from where he received his PhD in 1979. From 1979 until de retired in 2012 he has worked at the University of Koblenz- Landau. In 1986 he was appointed professor of computer applications in the social sciences at the Institute of Information Systems in Business and Public Management where he leads research projects in the field of social simulation. His email is `kgt@uni-koblenz.de`

FRAMING SIMULATIONS FROM A POLICY PERSPECTIVE

Peter De Smedt
SVR Research Centre
Boudewijnlaan 30
B-1000 Brussels
Belgium

KEYWORDS
Reflexive inquiry, Policy simulation practice, Scenarios, Grand Challenges

ABSTRACT

In recent years and accelerated by the economic and financial crisis, complex global issues have moved to the forefront of policy making. These grand challenges require policy makers to address a variety of interrelated issues, which are built upon yet uncoordinated and dispersed bodies of knowledge. Due to the social dynamics of innovation, new socio-technical subsystems are emerging, however there is lack of exploitation of innovative solutions.
In this paper we argue that issues of how knowledge is represented can have a part in this lack of exploitation. For example, when drivers of change are not only multiple but also mutable, it is not sensible to extrapolate the future from data and relationships of the past. This paper investigates ways in which policy simulations can be used as a tool for forward looking approaches addressing the grand challenges. The paper develops a typology of policy simulations and by reviewing simulation practice using scenarios, the authors disclose a variety of policy simulation practice.
To synthesize, we argue that policy simulation practice underpinned by a combination of well-designed modes of futures thinking will provide richer future images that go beyond the probable that is determined by the past and present. This will strengthen the application of policy simulations and enhance the use in a policy context.

INTRODUCTION

Simulations are used in society almost on a daily basis including examples as weather forecast broadcasted by the radio and economic growth forecasts in the daily news. The aim of this paper is to initiate a discussion on how scenario analysis, as a form of policy simulation practice, can help to better cope with the grand challenges our society is facing.

Today's grand challenges, from climate change to unemployment and poverty, go beyond economic and social policies (Boden et al., 2010). The recent economic crisis reminds us of the importance of mobilizing science, technology and innovation not solely for generating economic benefits, but also for anticipating and responding to the grand challenges (OECD, 2011).

Grand challenges are usually interrelated and operating at a global scale (Cagnin et al., 2011). Often it is not clear what the real causes are and different policy options are competing, causing shifts in problem perception and priority setting. One result of the above described complexity is a type of uncertainty about the future, an uncertainty whose distinctive feature is disagreement amongst experts and stakeholders about the long-term consequences of present-day innovations (Webster, 1999). In addition, uncertainty increases as policy targets move progressively further from the present and it is uncomfortable: fear of the unknown generates resistance to change (Linstone, 1973). But also efforts to control, manage, and engineer the future produce increased uncertainties (Adam, 2006). For instance, developments in science and technology have a strong potential to influence social change. There are, however, many reasons why the practical use of scientific knowledge and technology varies widely between countries. Societies differ, economies differ, and governments deal with international scientific developments in different ways through the policies they pursue (Timmermans, 2001). This analysis indicates that policy systems are shaped by social, cultural and political power as well as by technological rationalism and such indeterminism makes systemic approaches to policy far from linear or predictable.

In order to investigate how policy simulations and simulation practice using scenarios can help to better cope with the grand challenges, we first develop a typology of policy simulation techniques. Secondly we explain a reflexive approach how to learn from policy simulation practice. Thirdly we review simulation practice using scenarios to disclose a variety of policy simulation practice. For example, we look how the applied or perceived modes of thinking about the future are initiating enablers or barriers for the policy simulation process. In this paper we argue that this kind of reflexive inquiry can and does provide a sound basis for challenging current practice, for learning from experience and for better articulating our underlying theoretical premises of policy simulations.

Proceedings 26th European Conference on Modelling and Simulation ©ECMS Klaus G. Troitzsch, Michael Möhring, Ulf Lotzmann (Editors)
ISBN: 978-0-9564944-4-3 / ISBN: 978-0-9564944-5-0 (CD)

WHAT ARE POLICY SIMULATIONS?

A wide variety of simulations exist in daily life. Examples can be found in weather forecasts, flight simulators, economic growth forecasts, climate change scenarios, etc. The key element that all the examples have in common is that simulations are mirroring a possible (future) reality to provide additional information for current decision-making.

Using a policy perspective, two elements can be distinguished in simulation practice: the scale and main goal. Table 1 presents a typology of policy simulations based on the two elements. Related with the scale, three levels can be distinguished: (i) the operational, looking at the organization itself; (ii) the tactic, looking at the key actors and stakeholders (network) around the organization; and (iii) the strategic, looking at the external macro drivers influencing the operational environment of the organization.

Related with the second element, i.e. the main goal, three learning dimensions can be distinguished: (i) the analytical, with a focus on learning of possible developments; (ii) the instrumental, with a focus on learning in, i.e. how to respond to potential situations; and (iii) the cognitive, with a focus on learning by doing such as training, envisioning, etc.

Table 1: Typology of policy simulation practice

Policy dimension	Analytical (learning of)	Instrumental (learning in)	Cognitive (learning by)
Operational (organization)	validation of routines	optimization and risk planning	training and assessments
Tactic (network)	planning and impact assessment	collaboration and coordination issues	awareness
Strategic (outlook)	complex adaptive systems	experiencing complexity	envisioning (long term)

The typology highlights the diversity of activities that are (or can be) supported by policy simulation practice. Depending on the goal, simulation practice can support quite different learning processes. Although the diversity can be seen as a strength, i.e. the wide variety of its application areas, it is also part of its weakness.

Policy simulations are practiced across many (Gilbert, and Troitzsch, 2005). Practice can range from strong analytical focused applications such as impact assessment to strong participatory focused applications such as envisioning exercises. However, the disciplines of policy simulation practice are not well articulated or disseminated across domains, leading to miss perceptions between client-developer and weak performing practice that does not make best use of experience in other domains. Clearly developing tools for training is not the same as developing tools for gaining insights in complex adaptive systems.

The fast development of modeling tools induced a shift towards complex models with better dynamic representations and more client-friendly user-interfaces. These fascinating technology driven developments are a clear benefit to better represent reality that is simulated. Still, we argue that equal attention should be given to the theoretical premises underpinning policy simulation models. This is not reflected in the current amount of recent papers published on policy simulations.

LEARNING FROM POLICY SIMULATION PRACTICE

How can we learn from practice? We use the word "practice" to describe the implementation or execution of a concept, plan, methodology or theory. Most practice is based on a set of theories or assumptions. Sometimes those theories are explicit, most often they are implicit. The connection between practice and theory (unlike that between theory and practice) has traditionally been ignored, to the detriment of both (Gunderson et al., 2007).

Reflexive inquiry draws on a social constructionist view of the world and provides a powerful approach that offers insights for academics and practitioners into how we constitute knowledge and realities in our thinking and research practice (Cunliffe, 2003). Reflexivity as a methodology (Alvesson & Sköldberg, 2000), questions representation by suggesting that we are constantly constructing meaning and social realities as we interact with others and talk about our experience. We therefore cannot ignore the situated nature of that experience and the cultural, historical, and linguistic traditions that permeate our work (Cunliffe, 2003). This means that practice, such as policy simulation practice, is rooted in a particular moment and place. In the next section we will look at policy simulation practice using scenarios.

REVIEWING SIMULATION PRACTICE USING SCENARIOS

In the context of this paper, scenarios can be seen as narratives set in the future to explore how the society would change if certain trends were to strengthen or diminish, or various events were to occur. Scenarios substantially differ from predictions, i.e., extrapolations or trends, substituting the criterion of plausibility for probability (Harries, 2003). Although the use of scenarios has gained much adherence, its subjective and heuristic nature leaves many academics and decision-makers uncomfortable (Chermack, 2005). How do we know whether we have credible and salient scenarios? These concerns are legitimate and the use of scenarios would gain in academic standing if more research were

conducted on their comparative performance and underlying theoretical premises (Chermack, 2005). Whilst the scenario literature makes explicit the methodological differences and similarities of various approaches, it tends to pay little attention to the underlying epistemological assumptions (Wilkinson and Eidinow, 2008). For example, scenarios that imaginatively represent plausible futures will meet resistance if they are used as predictions.

The identification of the motivation behind any scenario exercise appears to underpin the scenario typology described by Borjesön et al., (2006) which reviews many other typologies before suggesting an alternative comprising three categories and six types. The categories arise from the kinds of question that a scenario user might use about the future: What will happen? What can happen? How can a specific target be reached? Each of these questions can be seen to evoke the motivation of a particular approach to scenarios. For example, in this typology "What will happen?" scenarios lead to predictive scenarios, in effect, forecasts, which look at what will happen as the likely development occurs. By contrast, "What can happen?" scenarios are normative scenarios - concerned with achieving particular future objectives - which lead to preserving and transforming scenarios. Preserving scenarios are used when the target can be met within an existing structure, while Transforming scenarios feature a form of backcasting, asking what would need to be changed for the target futures to be achieved.

This scenario typology is helpful to understand that policy simulations can be seen as vehicles of our thoughts. Depending and the questions we start with, will lead to different outcomes, i.e. scenarios. In this paper we will use a policy perspective to look at scenario practice. Our analysis is built on (a) a conceptual framework on policy change (De Smedt, 2008) and (b) a recent review of scenario exercises (De Smedt and Borch, 2011). For the context of this paper we will use the conceptual framework and insights and connect it with policy simulation practice.

Instead of framing practice based on theory, policy simulation practice using scenario is deconstructed into seven clusters. This approach is described in detail in De Smedt and Borch (2011). This was the first step and our findings are synthesized in table 2. This table describes for each cluster of simulation practice with scenarios the most common used images of the future and an example of a characteristic technique.

As a second step we focused on the way the future has been represented. Revealing different types of futures and describing how they have been shaped provided insights in some of the theoretical premises, here expressed as modes of futures thinking. So in table 2 these seven clusters of scenario practice are then further linked to the most characteristic theoretical premises, here expressed as modes of futures thinking.

Table 2: Clusters of simulation practice using scenarios from a policy perspective

Policy perspective	Simulation practice	Types of futures	Simulation technique	Modes of futures thinking
Window of opportunity	Using scenarios	Shaped by surprise and confrontation	Uncertainty matrix	Intuitive
	Developing scenarios	Shaped by convention	Consensus (Delphi)	Bounded rationality
Legitimacy for action	Framing boundaries	Shaped by possible futures	Extreme to inform the middle	Eventuality
	Back-casting from targets	Shaped by probable futures	S&T Roadmaps	Predictive
	Back-casting from principles	Shaped by preferable futures	The natural step	Visionary
Empowering stakeholders	Expert driven	Shaped by expertise and discovery	Expert panels	Technocratic
	Stakeholder driven	Shaped by interaction	Future workshops	Evolutionary

For example, looking at 'window of opportunity', we argue that a strong focus on developing scenarios and consensus increases a risk of diluting a sense of urgency. During the scenario exercise, consensus may not be appropriate to promote differences and to stimulate novel ideas. Based on this observation, two clusters of practice can be distinguished: one cluster with using scenarios as the most characteristic feature, and another with developing scenarios as the most characteristic. For the two clusters, the scenario cases have been analyzed to disclose elements of theoretical premises. In the first cluster, we found that the scenarios are used for supporting strategic discussions about futures that are shaped by surprise and confrontation. Examples of supportive techniques are the use of an uncertainty matrix using factors of high-uncertainty and high impact. Based on our reflexive inquiry used to analyze scenario exercises in their context, we can then attribute the most characteristic mode of thinking.

Following this approach we were able to distinguish seven modes of thinking that are underpinning current practice, see De Smedt and Borch (2011) for a more elaborate description of the clusters. In this paper, we want to highlight that acknowledging the theoretical premises, here expressed as modes of future thinking, in current practice is essential for better grounding policy simulations. In addition, using the full spectrum of the

different modes of futures thinking in the design phase will enhance the use of simulations in a policy context.

DISCUSSION AND CONCLUSIONS

In this paper we analyzed the applicability of policy simulations using scenarios as narratives to represent and discuss different perspectives on past, present and future developments. We first developed a policy simulation typology. In developing the framework presented, some relevant questions have been made on the variety of simulation practice and the need for better understanding the policy perspective of simulations. For instance, methodological choice depends on the intention or puzzle to be 'solved'. There are many different aims of policy simulations activities including decision–making, learning, exploration of possibilities, articulation of desirable outcomes, sharing of knowledge, persuasion, encouraging action etc. These aims are set in many different contexts and are concerned with phenomena that behave in many different ways, i.e. have particular ontologies. The commonality is that policy simulations produce knowledge in relation to a simulated (future) time and such instrumental knowledge is generated by social action, e.g. discourse, language, negotiation (Fuller & De Smedt, 2008).

Secondly we used a reflexive methodological approach to review policy simulation practice with a focus on scenarios. Instead of framing practice based on theory, policy simulation practice was deconstructed into several clusters. Following this approach we were able to distinguish seven modes of thinking that are underpinning current practice. In reality, each policy simulation exercise is a mixture of different modes and policy simulation practice is shaped by the image(s) of the future and the techniques applied. Combinations of techniques are possible.

To conclude, we argue that policy simulation practice underpinned by a combination of well-designed modes of futures thinking will provide richer future images that go beyond the probable that is determined by the past and present. Linking practice with theory will enrich the application of policy simulations and enhance the use in a policy context.

ACKNOWLEDGEMENTS

The authors are grateful to Ted Fuller, Kristian Borch and the COST Action A22 network for organizing creative discussion platforms on scenario initiatives.

REFERENCES

Adam, B. 2006. "Futures Transformed." Last accessed on 31/001/12 and available at http://www.cardiff.ac.uk./socsi/futures/wp_ba_futurestransformed231006.pdf

Alvesson, M. and K. Sköldberg. 2000. "Reflexive methodology: New vistas for qualitative research towards a reflexive methodology." Sage, London.

Borjesön, L.; M. Hojer; K-H. Dreborg; T. Ekvall and G. Finnveden. 2006. "Scenario types and techniques: towards a user's guide." *Futures* 38:723-739.

Boden, M.; C. Cagnin; V. Carabias; K. Haegeman and T. Konnola. 2010. "Facing the future: time for the EU to meet global challenges." Luxembourg, Publications Office of the European Union, EUR 24364 EN.

Cagnin, C.; E. Amanatidou and M. Keenan. 2011. "Orienting innovation systems towards grand challenges and the roles that FTA can play." *Proceedings of the Fourth International Seville Conference on Future-Oriented Technology Analysis (FTA), FTA for structural and systemic transformations in response to grand societal challenges: integrating insights, transforming institutions and shaping innovation systems*. IPTS, Seville, 12-13 May.

Chermack, T.J. 2005. "Studying scenario planning: theory, research, suggestions and hypotheses." *Technological Forecasting and Social Change* 72: 59-73.

Cunliffe, A.L. 2003. "Reflexive inquiry in organizational research: questions and possibilities." *Human Relations* 56: 983-1003.

De Smedt, P. 2008. "Strategic intelligence in decision making." In *Future-oriented technology analysis. Strategic intelligence for an innovative economy,* Cagnin et al., (Eds.). Springer, p. 89-102.

De Smedt, P. and K. Borch. 2011. "Future scenarios to inspire innovation." *Proceedings of the Fourth International Seville Conference on Future-Oriented Technology Analysis (FTA), FTA for structural and systemic transformations in response to grand societal challenges: integrating insights, transforming institutions and shaping innovation systems.* IPTS, Seville, 12-13 May.

Fuller, T. and P. De Smedt 2008. Modernization of foresight methodology: Reflexivity and the social construction of knowledge. *Cost Action A22 methodological note*, Brussels.

Gilbert, N. and K. Troitzsch. 2005. Simulation for the Social Scientist. Maidenhead: Open University Press.

Gunderson, L.; C. Folke and M. A. Janssen. 2007. "Reflective practice." *Ecology and Society* 12: 40.

Harries, C. 2003. "Correspondence to what? Coherence to what? What is good scenario-based decision making?" *Technological Forecasting and Social Change* 70: 797-817.

Linstone, H. 1973. "On discounting the future." *Technological Forecasting and Social Change* 4:335-338.

OECD. 2011. "Fostering innovation to address social challenges." *Workshop proceedings.* OECD, Paris.

Timmermans, A. 2001. "Arenas as institutional sites for policymaking: patterns and effects in comparative perspective." *Journal of Comparative Policy Analysis: Research and Practice* 3: 311-337.

Webster, A. 1999. "Technologies in transition, policies in transition: foresight in the risk society." *Technovation* 19: 413-421.

Wilkinson, A. and E. Eidinow. 2008. “Evolving practices in environmental scenarios: a new scenario typology.” *Environ. Res. Lett.* 3.

AUTHOR BIOGRAPHY

Peter De Smedt has a background in ecological system analyses. His professional challenge is connecting science and policy. On a broad range of regional and EU projects, involving foresight and integrated assessment, Peter worked together with experts and stakeholders towards achieving a common understanding on non-sustainable trends, offering scenarios and integrated solutions to support policy-makers. Currently Peter works at the Research Centre of the Flemish Government where he is in charge of foresight and sustainability assessment.

E: peter.desmedt@dar.vlaanderen.be

WHAT-IF ANALYSIS THROUGH SIMULATION-OPTIMIZATION HYBRIDS

Marco Gavanelli
ENDIF University of Ferrara, Italy
marco.gavanelli@unife.it

Michela Milano
DEIS University of Bologna, Italy
michela.milano@unibo.it

Alan Holland and Barry O'Sullivan
Cork Constraint Computation Center, Ireland
{a.holland,b.osullivan}@4c.ucc.ie

ABSTRACT

This paper proposes to improve traditional what-if analysis for policy making by a novel integration of different components. When a simulator is available, a human expert, e.g., a policy maker, might understand the impact of her choices by running a simulator on a set of scenarios of interest. In many cases, when the number of scenarios is exponential in the number of choices, identifying the scenarios of interest might be particularly challenging. We claim that abandoning this *generate and test* approach could greatly enhance the decision process and the quality of political actions undertaken. In this paper we propose and experiment with one approach for combining simulation with a combinatorial optimization and decision making component. In addition, we propose two alternative approaches that can reasonably combine decision making with simulation in a coherent way and avoid the generate and test behaviour.

KEYWORDS

POLICY MODELING SOCIAL SIMULATION COMBINATORIAL OPTIMIZATION

INTRODUCTION

Public policy issues are extremely complex, occur in rapidly changing environments characterized by uncertainty, and involve conflicts among different interests. Our society is ever more complex due to globalisation, enlargement and rapidly changing geo-political situation. This means that political activity and intervention become more widespread. Therefore, the effects of any such interventions become more difficult to assess. Of course, it is becoming ever more important to ensure that actions are effectively tackling the real challenges that this increasing complexity entails. Thus, those responsible for creating, implementing, and enforcing policies must be able to reach decisions about ill-defined problem situations that are not well understood, have no one correct answer, involve many competing interests, and interact with other policies at multiple levels. It is therefore more important to ensure coherence across these complex issues.

The majority of policy models rely on agent-based simulation (Troitzsch et al., 1999; Matthews et al., 2007; Gilbert, 2010) where agents represent the parties involved in the decision-making and implementation process. The hypothesis is that for modelling complex systems, agent-based simulation is a suitable approach to understand such systems in a more natural way. In particular, agent-based models enable the use of computer experiments to support a better understanding of the complexity of economic, environmental and social systems, structural changes, and endogenous adjustment reactions in response to a policy change. In addition to agent-based simulation models, which provide *individual level models*, we claim that the policy planning activity needs a global perspective that faces the problem at a global level and should tightly interact with the individual level model. The policy maker must take decisions by perceiving a set of (possibly conflicting) objectives, and satisfying a set of constraints while at the same time reducing negative impacts and enhancing positive impacts on the environment, society and economy. Simulation could be therefore used to understand the impact of her decisions via what-if analysis or scenario analysis.

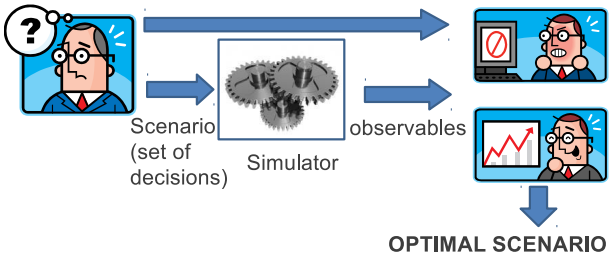

Figure 1: Manual decision making

If a decision maker received no useful feedback regarding the impact of decisions, this would be the worst outcome of all. However, typically at present a policy maker devises a set of scenarios to be simulated and evaluates the impact of the taken decision. The process iterates as soon as the policy maker finds a solution that satisfies her, as depicted in Figure 1. The simplest way to improve this process is to aid the decision maker in the first step of her process, by designing a Decision Support System (DSS) for the selection of (Pareto) optimal points corresponding to specific political actions, as depicted in Figure 2. In brief, the problem components that the policy maker should take into account, namely impacts on

Proceedings 26th European Conference on Modelling and Simulation ©ECMS Klaus G. Troitzsch, Michael Möhring, Ulf Lotzmann (Editors)
ISBN: 978-0-9564944-4-3 / ISBN: 978-0-9564944-5-0 (CD)

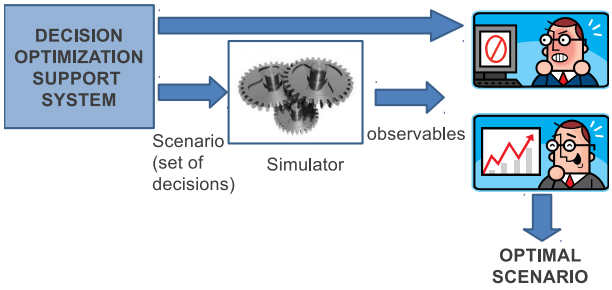

Figure 2: Decision support system for scenario selection

environment, economy, financial aspects, territory-based constraints, and objectives, can be cast as a combinatorial optimization and decision problem and solved using the appropriate techniques, described e.g. in (Gavanelli et al., 2010, 2011). Despite being more sophisticated than the *manual* approach, this secondary process still exhibits a generate-and-test behaviour. In other words, the decision making and optimization component operates within the confines of a limited information set and is not guided toward simulation-reasonable solutions.

In this paper we propose an approach that enables a tight interaction between a simulator and a decision making component based on machine learning. Machine learning is used to synthesize constraints for the decision making component from simulation results. We show an example applied to the Italian Emilia-Romagna region, and in particular on its Regional Energy Plan. The definition of the plans is provided by a decision support system by casting the problem in a mathematical model and solving it through optimization techniques. On the other hand, the implementation strategy, namely the definition of the percentage of incentives to reach the objectives of the regional plan, can be only understood through agent-based simulation. The proper interaction between policy planning and policy implementation should necessarily lead to an integration of decision support and simulation components.

Also, we devise two alternative approaches that maintain close connections between simulation and the decision-making components, and abandon the generate and test behaviour: one is based on Benders' decomposition, while the other is based on the game theoretic principles of Mechanism Design.

The paper is organized as follows: we first describe the considered case study, i.e. the regional energy plan, then we propose the first approach of optimization-simulation hybrids we experimented with, namely the one using machine learning techniques. Then we propose two alternative approaches that would reasonably improve the first integration scheme: one based on problem decomposition and one on mechanism design.

THE REGIONAL ENERGY PLAN CASE STUDY

The Regional Energy Plan defines the strategic regional objectives for the energy production and energy efficiency. The case study is based on data provided by the Italian Emilia-Romagna region. The region has strategic objectives, financial and territorial constraints and environmental impacts. An example of an objective that the region might have is to increase the production of energy while at the same time increasing the share of renewable energy sources in the regional energy balance.

For each energy source, the plan should provide: the installed power, in MW; the total energy produced in a year, in kTOE (TOE stands for Tonne of Oil Equivalent); the total cost, in M€. The ratio between installed power and total produced energy is mainly influenced by the availability of the source: while a biomass plant can, at least in theory, produce energy 24/7, the sun is available only during the day, and the wind only occasionally. For unreliable sources an average for the whole year is taken. The cost of the plant, instead, depends mainly on the installed power: a solar plant has an installation cost that depends on the surface area of installed panels, which on their turn can provide some maximum power (peak power).

The 20-20-20 EU directive imposes that 20% of total energy requirements for 2020 should be provided by renewable sources. Technicians in the region proposed a percentage to be provided during the period 2011-2013 of 177kTOE of electrical energy and 296kTOE of thermal energy. With this premise they developed plans for electrical and thermal energy, respectively. In Table 1 we show the electric plan based only on renewable energy sources. The total private and public investment requirement is 3014M€.

Table 1: Regional Energy plan 2011-2013

Power plants	Power 2010 (MW)	Power 2013 (MW)	Energy 2013 (kTOE)
Hydroelectric	300	310	69.3
Photovoltaic	230	850	87.7
Th.dyn. solar	0	10	1
Wind farms	20	80	10.3
Biomasses	430	600	361.2
Total	980	1850	529.5

In general, after a plan is created, the policy maker defines actions for its implementation. A widely used instrument for supporting the renewable energy market is monetary incentives. For example, in the Emilia-Romagna region, incentives for the photovoltaic energy are distributed to stakeholders by means of auctions that indeed do not result from a specific strategy, but rather from extemporaneous strategies. In these auctions the bids are ranked on the basis of various criteria (including the co-financing percentage), and the first n bids that satisfy the budget constraint are funded. However, this strategy may be far from optimal and further research is required to examine the efficacy of this approach.

Italian law considers four different methods for pro-

viding incentives, while in the auctions developed in the past only one type was used. Finally, one should consider carefully how to spend the limited financial resources available: for example, should we provide higher incentives or spend more money into advertising the availability of incentives? As we can see, the number of possible choices, just for the implementation of the plan, is combinatorial, which makes a hand-made process inapplicable or highly sub-optimal. Moreover, the outcome of a given policy of incentives is not clear or easily foreseeable, and it can only be obtained through a social simulator.

In this paper, we propose to integrate in the planning process a mechanism for defining a proper incentive strategy that achieves the objectives of the plan. For this reason we should devise a methodology for coupling a decision component with a simulator.

INTEGRATING SIMULATION WITH LEARNING

We report on some experiments we have conducted that show how a machine learning system can be integrated with a simulator to assist in the policy-making process associated with a regional energy planning task. In this case, the simulator generates a set of scenarios, relating decisions with observables as depicted in Figure 3. The collected tuples $\langle decision_1, \ldots, decision_n, observable_1, \ldots observable_m \rangle$ are stored as a training set for a learning component which in turn learns a relation between decisions and observables. The relation can be an objective function or a constraint or a cost function, the automated modeling of which can be framed as a regression problem. In any case it should have a form that is compatible with the decision support system model.

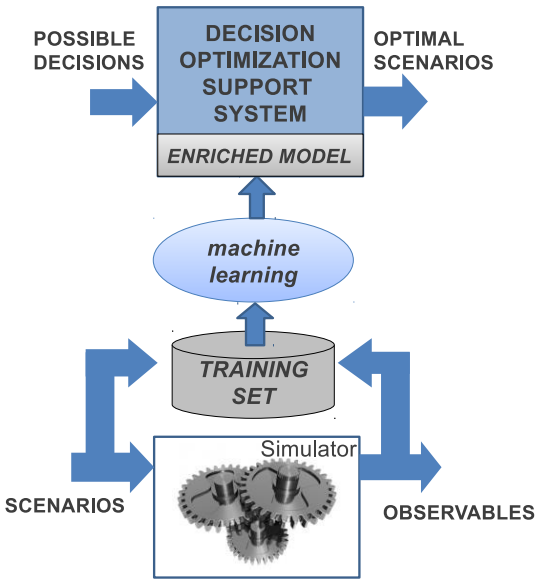

Figure 3: Learning-Based Interaction

We consider now the learning based interaction. What we want to learn is a function that relates the installed power to the percentage of incentives provided by the region. We have performed a large number of simulations (1500) for each value of incentives from 1% to 30% in steps of 1% (for a total of 45,000 simulations). Each simulation has 1000 agents, and we recorded, for each simulation, the total installed power in MW of photo-voltaic plants. A plot of the results is shown in Figure 4 where each point represents an individual simulation.

Of course, an individual simulation does not provide useful information, as can be seen from Figure 4, and one should try to extract some statistics from a significant number of simulations in order to get some insight. In order to learn a model of the dependency of the installed power from the incentives, we average the results of all the simulations with the same amount of incentives. In this way we obtain a point for each value of the incentives from 1% to 30%. Then we learned a function that relates the installed power to the incentives. We tried various regression algorithms, including linear regression (Rousseeuw and Leroy, 1987), Gaussian processes (Mackay, 1998), least median squared linear regression (Rousseeuw and Leroy, 1987), multilayer perceptron (Mitchell, 1997), Gaussian radial basis function networks (Mitchell, 1997) and support vector regression (Smola and Schölkopf, 2004).

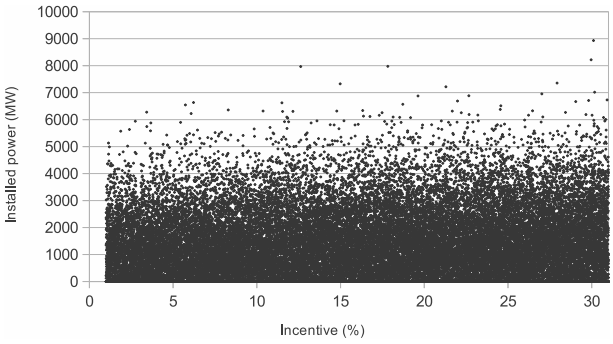

Figure 4: Simulations

We evaluated the mean squared error of each algorithm using ten-fold cross validation. The algorithm that gave the lowest mean squared error was linear regression so we applied it to the whole dataset and we obtained the function

$$G_{PV} = mI^{\%} + q \quad (1)$$

(where PV stands for photovoltaic) that is also shown in Figure 5. The values of the parameters we obtained are $m = 2645MW$ and $q = 405MW$.

We inserted in the model the relationship of Equation 1, in this way we were able to relate the incentives given by the region with the obtained installed power of photovoltaic energy.

The region has a limited budget B_{PV} for the incentives towards photovoltaic plants (PV), so this should be imposed as an upper bound to the total incentive:

$$I^{Tot}{}_{PV} \leq B_{PV} \quad (2)$$

The total incentive is given by the percentage of incentives given by the region multiplied by the total cost of

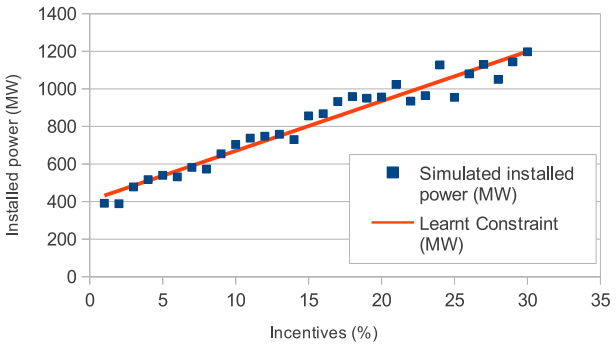

Figure 5: Learned function.

installed photovoltaic panels:

$$I^{Tot}{}_{PV} = I^{\%} c_{PV}^{Tot} \tag{3}$$

the cost is given by the unit cost c_{PV} multiplied by the magnitude of the installed panels:

$$c_{PV}^{Tot} = c_{PV} G_{PV} \tag{4}$$

From the simulations and linear regression, we obtained the relationship between the provided percentage of incentives and the expected magnitude (Eq. 1). Combining equations (1), (3) and (4) we obtain:

$$I^{Tot}{}_{PV} = I^{\%} c_{PV}(mI^{\%} + q) = c_{PV} m (I^{\%})^2 + q I^{\%} \tag{5}$$

The constraint of Eq. (2) can be rewritten (solving Eq. (5) for $I^{\%}$ and excluding a trivial bound, since $I^{\%}$ is non-negative), as:

$$I^{\%} \leq \frac{-q + \sqrt{q^2 + 4mB_{PV}/c_{PV}}}{2m}. \tag{6}$$

By inserting this constraint into the decision support system, we can define regional energy plans whose incentives strategies are compatible with budget constraints.

MORE SOPHISTICATED INTEGRATIONS

In this section we consider how more sophisticated hybrids of optimisation and simulation can be developed. In the first case we consider an approach based on a classic problem decomposition technique from the field of operations research. This technique can be used to link the multiple levels of abstraction needed in a complex policy-making setting. In the second scenario we consider how game theoretic concerns can be considered in the process, by exploiting the utilities of agents to design complex incentive schemes to motivate particular behaviours that maximise overall efficiency of the system.

Benders Decomposition

Benders (1962) decomposition is a method for solving combinatorial optimization problems that can be decomposed into two components: a master problem and a subproblem. Benders Decomposition was originally devised in the field of Integer Linear Programming, but has been extended for dealing with general solvers in the so called Logic-Based Benders Decomposition (Hooker and Ottosson, 2003). In our case, the master problem is the definition of the regional energy plan that partitions the needed energy into renewable sources. The master problem is solved through Constraint Programming as described in (Gavanelli et al., 2012). The subproblem is the definition of the incentive strategy to achieve the required photovoltaic installed power, that is also consistent with the regional budget. The simulator is run to understand which is the proper required incentive to obtain the solution provided by the master problem. In case the incentives are not compatible with the regional budget a Benders cut is generated and another solution is provided by the master.

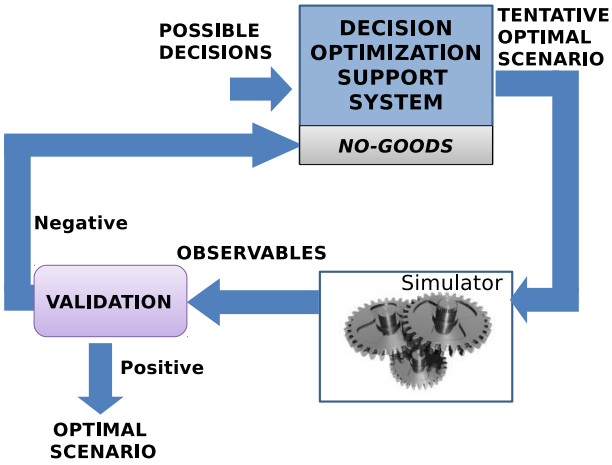

Figure 6: Benders Decomposition Interaction

The learning-based interaction, as described in previous section, requires the execution of a very high number of simulations in order to (1) get significant statistics for each value of the incentives (or, in general, for each possible decision in the policy) and (2) provide a wide set of data for the machine learning.

On the other hand, it may be the case that some values of policy decision variables are not interesting, as they would provide very bad values for the Decision Support System that utilizes optimization. In principle, one would like to simulate only the best values from the DSS viewpoint; unluckily these values are unknown and depend on the constraints provided by the machine learning component. This shows that the architecture in Figure 3, with one-way communication from the simulator to the DSS, should be extended to a cycle, that provides bidirectional communication between the two main components (Figure 6).

The interaction starts from the DSS, that generates an optimal solution of the master problem. This solution contains tentative values for the incentives, and for the required outcome for photovoltaic energy. The tentative values are passed to the simulator, that executes a number of simulations only for those values of the parame-

ters provided by the DSS, and provides the correspondent statistics. These statistics might confirm or not the tentative values proposed by the DSS: if the (average) simulated outcome is higher or equal to the corresponding tentative value, the iteration stops and the result is provably optimal (Benders, 1962). Instead, if the tentative value of the outcome is higher than the simulated value, another iteration is required. So, a constraint (or *nogood*) is communicated from the simulator to the DSS, explaining that one cannot obtain the requested level of photovoltaic power with the proposed value of incentives. The DSS inserts the nogood into the constraint model, solves it to optimality, and provides new tentative values to the simulator.

The main challenge is determining the set of constraints that are communicated between the two systems: if one excludes from the feasible set only the tentative values, the risk is to perform many interactions, leading to exhaustive simulation of all the values of the parameters, while if one excludes further values there is the risk to possibly discard promising solutions. This issue is subject of current research.

INCENTIVE COMPATIBLE MECHANISMS

We now consider an approach that supports What-If Analysis based upon the principles of Economic Theory and, in particular, Game Theory. When one assumes that agents are all self-interested and rational utility maximizers, one can apply the solution concepts of Nash Equilibrium to predict expected outcomes. This is an attractive concept for policy makers because it can aid the predictability of novel economic policies or initiatives.

A seminal result known as the *Revelation Principle* states that, no matter the mechanism, a designer concerned with efficiency need only consider equilibria in which agents truthfully report their "types" that signify their private valuation for an item (Gibbons, 1992). Cleverly designed economic mechanisms (or auctions) can allocate resources and determine payments that are resilient to manipulation. The design of subsidy schemes to support the construction of public goods is particularly challenging (Laffont, 1987). Our setting involves a possibly large number of agents and a set of renewable technologies so tractability concerns must also be borne in mind (Nisan and Ronen, 2001). The key design challenge concerns the *free rider problem* and consequent under provision of public goods. For example, in first price auctions previously conducted in the Emilia-Romagna region, participants that wished to acquire a photovoltaic device without government aid had an incentive to underreport their valuation to receive a subsidy.

Mechanism design is a game of private information in which a single central agent, the "center", chooses the payoff structure. Agents report a type to the center that they may choose strategically so that it is different from their true value. After the reporting phase, the center determines an outcome. The outcome consists of an allocation and a payoff. The center typically wishes to fulfil a *social choice function* to map the true type profile directly to the allocation of goods transferred, whereas a *mechanism* maps the reported type profile to an outcome.

A Subsidy Disbursement Example

Let us consider a more specific example. There are m households whose suitability for receiving a subsidy for a photovoltaic device depends upon the pitch of their roof, orientation, horizon profile and location. We reduce these parameters to a single value describing the worth of a solar device per unit of power to value v^i for agent i. This value reflects the day zero time-discounted value of the expected stream of future cashflows given their circumstances. The *social choice function* is to assign the panels p_j, $j \in \{1, \ldots, J\}$ to agents in a manner that minimizes the maximum cost for any agent. The imposition (or cost) for agent i if panel j is received is the price of the device minus the value per unit of power multiplied by the power output of the device,

$$c_j^i = r_j - v^i \phi_j, \forall i \in \{1, \ldots, I\}, j \in \{1, \ldots, J\}$$

where r_j is the purchase price of an installed panel.

This problem can be transposed to a makespan minimization problem denoted in the scheduling theory literature as $Q||C_{max}$, where C_{max} refers to makespan in scheduling theory. We wish to to allocate device acquisition and hosting responsibility (jobs) across houses (machines) that each perceive a private cost associated with acceptance of that job. The minimization of the maximum time to wait for all jobs to complete is comparable to the minimization of the maximum cost imposed on any house-owner so that inconvenience is bounded as tightly as possible.

Non-monotone Algorithm Consider the following simple algorithm: order the panels from highest to lowest power and greedily assign each device in turn to the household that has received lowest cost imposition thus far in the partial allocation. This algorithm is a 2-approximation that is non-monotone. Consider an example with 3 devices $\{d_1, d_2, d_3\}$ and 2 agents $\{h_1, h_2\}$ that illustrates non-monotonicity. Let the publicly known power ratings for the devices be $\phi_1 = 10W$ and $\phi_2 = \phi_3 = (9 + \epsilon)W$ and all devices cost $r_j = 60$€. This is common to all agents. However, let each house-owner's value per unit of power be $v_1 = 5$€$/W$ and $v_2 = (5 - \epsilon)$€$/W$. This is the private information that we wish to elicit. Our greedy algorithm first assigns: $d_1 \rightarrow h_1$, $d_2 \rightarrow h_2$ and $d_3 \rightarrow h_2$ resulting in costs $c_1 = 60 - 10 \times 5 = 10$€ and $c_2 = 2(60 - (45 - 4\epsilon - \epsilon^2)) \cong (30 + 8\epsilon)$€. But if we increase v_2 so that $v_2 = (5 + \epsilon)$€$/W$ then it receives only the first device. The first (highest power device) will be assigned to the second agent because she now has a higher value per unit of power. The second (lower power) device is assigned to the first agent because this agent has received a lower

cost imposition thus far. The third (lower power) device is also assigned to the first agent because this agent has received a lower cost imposition thus far because the previous lower power device imposed less cost than the high power device did for the agent that values renewable power more. So this algorithm is not monotone and a direct consequence of this is that it cannot be used within any truthful mechanism for allocating devices to agents (Archer and Tardos, 2001).

Monotone Algorithm There exists a *randomized* 3-approximation that is truthful in expectation. Kovács (2005) developed an approximation scheme for scheduling n jobs to m machines of different speeds so that the makespan is minimized. This problem is sometimes referred to as $(Q||C_{max})$ (Kovács, 2005). A fast, deterministic *monotone* 3-approximation algorithm exists for this problem. The importance of monotonicity is very relevant to our setting and the context of truthful mechanisms in general. When each agent knows its own value for hosting a device, it is necessary to design an incentive for declaration of true values to enable efficient allocation. Archer and Tardos (2001) demonstrated that such motivation is possible only if the allocation algorithm within the mechanism is monotone.

RELATED WORK

In the literature, simulation and optimization have been merged mainly in the so-called simulation optimization field. In this case optimization aids simulation for choosing optimal parameters to improve operations (Deng, 2007). The goal of optimization routines is to seek improved settings of system parameters with respect to the performance metrics. Similarly, Neuro-Dynamic Programming (NDP) (Bertsekas and Tsitsiklis, 1996) is an approach to select agent decision making rules (feedback policy) that optimize a certain performance criterion. NDP often relies on simulation, in the so called value function approximation, to tune the parameters of a value function that quantifies the relative desirability of different states in the problem space. Markov decision processes have also been used in Reinforcement Learning (RL) together with simulation, for learning directly the policy parameters (Marbach and Tsitsiklis, 2001). Both NDP and RL are concerned with how a single agent ought to take actions in an environment so as to maximize some form of cumulative reward. On the contrary, in this paper we are interested in understanding how global political actions and interventions impact on a complex systems (namely, the energy market) without changing the agent behavior. We aim to (1) observe/learn the causal link between agents behavior and high level decisions and (2) cast these relations into a model component.

Simulation-aware optimization has been considered in the context of Genetic Algorithms (GAs). The basic integration technique consists in solving a numerical model to evaluate the fitness function (see for example (Obayashi et al., 2000)). Although GAs encode some knowledge of the system behavior through the population individuals, these approaches learn no explicit relation between decision variables and the system observables. As a consequence, analytic properties of the controlled system cannot be discovered and exploited with the typical means of combinatorial optimization.

Finally, the closest approaches to this paper are those related to the governance of a simulated system. The traditional way to cope with combinatorial (global) decision making where a part of the model can be simulated is rather trivial: the decisions are taken and the simulator evaluates their "quality". This is the base of Simulation for Optimization (Fu, 1994) that is strongly based on stochastic programming. The main idea is that candidate solutions are presented to the stochastic discrete-event simulator that, in turn, provides performance estimates of the solutions via statistical analysis. In this case the simulator model is another objective function generator, but the way solutions are presented follows a pure generate-and-test pattern. A similar approach is considered in OptQuest (Glover et al., 1999), a system that integrates in a closed loop simulation and metaheuristics to achieve good quality solutions. In the paper also a primitive form of learning is used, namely a neural network accelerator aimed at avoiding trivially bad solutions. In the same fashion, in (Bartolini et al., 2011), simulation has been used to learn neuron constraints in a thermal aware dispatching application. This last paper is close to the one presented here, with the difference that the learning component aims at tuning parameters of neural constraints, while in this paper we learn a linear function linking decision variables and observables that can be evaluated and validated by domain experts.

CONCLUSION AND FUTURE WORK

In future work we aim to tackle the challenge of devising a mechanism that will facilitate a tractable and budget balanced approach to allocation and payments. We plan to consider alternative social choice functions that takes a more holistic view of agent types that considers both welfare and aggregate renewable energy generated.

We face in this paper the very challenging problem of mixing a regional planning activity with the definition of an implementation strategy. While the planning part can be cast into a combinatorial optimization problem and solved through optimization techniques, the implementation strategy requires a simulator to be understood involving self interested decision making agents. We propose here one technique for integrating optimization and simulation and two alternative solutions to aid this process that are subject of current study in the context of the EU FP7 *ePolicy* Project.

ACKNOWLEDGEMENTS

We would like to thank Fabrizio Riguzzi for his help on the machine learning part.

This work was partially supported by EU project *ePolicy*, FP7-ICT-2011-7, grant agreement 288147. Possible inaccuracies of information are under the responsibility of the project team. The text reflects solely the views of its authors. The European Commission is not liable for any use that may be made of the information contained in this paper.

REFERENCES

Archer, A. and Tardos, Éva. (2001). Truthful mechanisms for one-parameter agents. In *Proceedings of FOCS*.

Bartolini, A., Lombardi, M., Milano, M., and Benini, L. (2011). Neuron constraints to model complex real-world problems. In *Principles and Practice of Constraint Programming*.

Benders, J. F. (1962). Partitioning procedures for solving mixed-variables programming problems. *Numerische Mathematik*, 4:238–252.

Bertsekas, D. and Tsitsiklis, J. (1996). *Neuro-Dynamic Programming*. Athena Scientific.

Deng, G. (2007). *Simulation-based Optimization*. PhD thesis, University of Wisconsin - Madison.

Fu, M. (1994). Optimization via simulation: A review. *Annals of Operations Research*, 53:199–248.

Gavanelli, M., Riguzzi, F., Milano, M., and Cagnoli, P. (2010). Logic-Based Decision Support for Strategic Environmental Assessment. *Theory and Practice of Logic Programming*, 10(4-6):643–658.

Gavanelli, M., Riguzzi, F., Milano, M., and Cagnoli, P. (2012). Constraint and optimization techniques for supporting policy making. In *Computational Intelligent Data Analysis for Sustainable Development*, chapter 16. Taylor & Francis.

Gavanelli, M., Riguzzi, F., Milano, M., Sottara, D., Cangini, A., and Cagnoli, P. (2011). An application of fuzzy logic to strategic environmental assessment. In Pirrone, R. and Sorbello, F., editors, *AI*IA*, volume 6934 of *LNCS*. Springer.

Gibbons, R. (1992). *Game theory for applied economists*. Princeton University Press.

Gilbert, N. (2010). *Computational Social Science*. SAGE.

Glover, F., Kelly, J., and Laguna, M. (1999). New advances for wedding optimization and simulation. In *Proc. of the Winter Simulation Conference*.

Hooker, J. N. and Ottosson, G. (2003). Logic-based benders decomposition. *Mathematical Programming*, 96:33–60.

Kovács, A. (2005). Fast monotone 3-approximation algorithm for scheduling related machines. In *Proceedings of the 13th annual European conference on Algorithms*, ESA'05, pages 616–627, Berlin, Heidelberg. Springer-Verlag.

Laffont, J.-J. (1987). Incentives and the allocation of public goods. *Handbook of public economics*, 2:537–569.

Mackay, D. J. (1998). Introduction to Gaussian processes.

Marbach, P. and Tsitsiklis, J. N. (2001). Simulation-based optimization of markov reward processes. *IEEE Transactions on Automatic Control*, 46(2):191–209.

Matthews, R., Gilbert, N., Roach, A., Polhill, G., and Gotts, N. (2007). Agent-based land-use models: a review of applications. *Landscape Ecology*, 22(10).

Mitchell, T. M. (1997). *Machine Learning*. McGraw-Hill, New York.

Nisan, N. and Ronen, A. (2001). Algorithmic mechanism design. *Games and Economic Behavior*, 35:166–196.

Obayashi, S., Sasaki, D., Takeguchi, Y., and Hirose, N. (2000). Multiobjective evolutionary computation for supersonic wing-shape optimization. *IEEE Transactions on Evolutionary Computation*, 4:182–187.

Rousseeuw, P. J. and Leroy, A. M. (1987). *Robust regression and outlier detection*. Wiley.

Smola, A. J. and Schölkopf, B. (2004). A tutorial on support vector regression. *Statistics and Computing*, 14:199–222.

Troitzsch, K. G., Mueller, U., Gilbert, G. N., and Doran, J. (1999). Social science microsimulation. *J. Artificial Societies and Social Simulation*, 2(1).

AUTHOR BIOGRAPHIES

MARCO GAVANELLI is Ricercatore (Assistant Professor) in Computer Science at the Dartiment of Engineering, University of Ferrara, Italy. His research interests are on Logic Programming and Constraint Programming and their applications. His personal webpage is at `http://www.ing.unife.it/docenti/MarcoGavanelli/`.

BARRY O'SULLIVAN holds the Chair in Constraint Programming at University College Cork and is Director of the Cork Constraint Computation Centre (4C) in the Department of Computer Science. His personal webpage at `http://osullivan.ucc.ie`.

ALAN HOLLAND is a Research Fellow specialising in optimisation and electronic commerce in the Cork Constraint Computation Centre (4C), Department of Computer Science, University College Cork, Ireland. His personal webpage at `http://4c.ucc.ie/~aholland`.

MICHELA MILANO is Associate Professor in Intelligent Systems at the Dartiment of Electronic, Computer Science and Systems, University of Bologna, Italy. Her research interests span from Artificial Intelligence to Operations Research to build hybrid optimization techniques. Her personal webpage at `http://ai.unibo.it/people/MichelaMilano`.

HUMAN DECISION MAKING IN EMPIRICAL AGENT-BASED MODELS: PITFALLS AND CAVEATS FOR LAND-USE CHANGE POLICIES

Grace B. Villamor
Center for Development Research
University of Bonn
53113 Bonn, Germany
Email: gracev@uni-bonn.de

Meine van Noordwijk
World Agroforestry Centre
Southeast Asian Regional Office
Bogor, Indonesia
Email: m.vannoordwijk@cgiar.org

Klaus G. Troitzsch
Institut für Wirtschafts- und Verwaltungsinformatik
Universität Koblenz-Landau
56016 Koblenz, Germany
Email: kgt@uni-koblenz.de

Paul L.G. Vlek
Center for Development Research
University of Bonn
53113 Bonn, Germany
Email: p.vlek@uni-bonn.de

KEYWORDS
Human decision making, empirical agent-based model, process-based, causality, cross-sectional data, decision algorithm

ABSTRACT

This paper describes three fundamental pitfalls or caveats of empirical modeling of land-use decision making in agent-based models for land-use/cover change. A case study in the villages of Jambi Province (Sumatra), Indonesia, is presented to demonstrate the construction of empirical decision-making models using utility functions while taking into account these caveats. Incorporating the decision process as an option to deal with the drawbacks of cross-sectional data is recommended to better specify agents' behavior in the decision-making models.

INTRODUCTION

Decision making in a social, economic and environmentally interacting context is a major research focus in agent-based/multi-agent simulation (AB/MAS) modeling. Indeed, simulating various decision-making processes in their interaction is one of its main advantages (Matthews et al. 2005). Hence, the AB/MAS framework has been increasingly applied for understanding coupled human-natural systems (An 2011), land-use dynamics and policies (Matthews et al. 2007; Parker et al. 2003), and recently in assessing ecosystem services tradeoffs driven by policy interventions (Villamor, 2012). Although there are many ways to explicitly formalize simple to complex human decision making (An 2011), utility-seeking agents using preference functions calibrated with econometric techniques are the most common framework for land-use change studies (Benenson and Torrens 2004; Parker et al. 2008; Villamor et al. 2011). Newer concepts of behavioral economy such as the prospect theory as a step beyond 'utility' have not yet been routinely incorporated (Kahneman and Tversky, 1979). However, one of the fundamental issues is to represent in a statistically consistent way a real-world situation of typically heterogeneous biophysical and socio-economic conditions (Berger and Schreinemachers 2006). This paper presents some challenges of modeling human decision making in the context of land-use change studies. It is subdivided into three main sections. Section 1 describes three often ignored caveats of empirical modeling of human decision making using utility functions, section 2 presents alternative ways to address these caveats, and section 3 demonstrates in a case study, the construction of a process-based decision-making model.

CAVEATS OF MODELING LAND-USE DECISION MAKING

Caveat 1: Causal relationship

Utility functions provide a formal framework for specifying agent-choice behavior (Benenson and Torrens 2004) in which a weight is attached to a particular choice amongst a set of choices or opportunities. In the context of land-use change studies, for instance, a farm household deciding whether to expand its farm plot will consider various factors such as the market price of certain crops and its own labor capital. With a wide range of possible choices, the household will assess each utility of the choices. The utility values are then transformed into choice probabilities. Statistical tools like logistic regression are commonly used to calculate probabilities and correlate particular actor attributes with specific land-use decisions either reported in a survey or observed from remotely sensed imagery (Evan et al. 2006). This approach identifies a statistically significant relationship between actor or

Proceedings 26th European Conference on Modelling and Simulation ©ECMS Klaus G. Troitzsch, Michael Möhring, Ulf Lotzmann (Editors)
ISBN: 978-0-9564944-4-3 / ISBN: 978-0-9564944-5-0 (CD)

landscape attributes and land-cover change. However, the results do not necessarily provide clear insight into actual decision process such as how an agent evaluates the benefits of a land-use change, the risks involved, and time frames considered for decision-making (Evans et al. 2006; Galvin et al. 2006). Even if the results obtained from simulation match those from the target, there may be some aspects of the target that the model cannot reproduce (Gilbert and Troitzsch 2005) and the underlying causes remain unknown (Galvin et al. 2006; Heckbert et al. 2010; Janssen and Ostrom 2006; Windrum et al. 2007).

Missing confounder

In a statistical context, caution should be taken when using observational studies alone to model agents' decision making, i.e., especially when predicting land-use decisions, since these kinds of models (i.e., the mere regress of observed decisions on observed data) "*do not carry the burden in the causal argument nor give much help in controlling for confounding variables*" (Freedman 2010, p.46). According to Rothman et al. (2008), given the observable nature of association measures, it is tempting to substitute them for effect measure and even more natural to give causal explanations for observed associations in terms of obvious differences. It is a well known textbook fact that - outside the realm of experiments - observed associations of variables do not automatically imply causality (Moore and McCabe 2004, p.160) - and therefore cannot establish a law that could predict outcomes. Confounders as defined by Rothman et al. (2008) are the factors (e.g., exposures, interventions, treatment) that explain or produce all or parts of the difference between the measure of association and the measure of effect that would be obtained with counterfactual ideals. The methods of scientific studies therefore need to control these factors to avoid a false positive error or an erroneous conclusion that the dependent variables are in a causal relationship with the independent variable. According to Freedman (2010), it would be better to rely on subject-matter expertise, and to exploit natural variation to mitigate confounding and rule out competing explanations.

Caveat 2: Drawing causal inferences from cross-sectional data

Due to the difficulty of collecting empirical data, the researchers have to rely on the data from cross-sectional surveys. Cross-sectional data are used to estimate parameters of functional forms of agents' decisions or other relations of variables. In most cases, there are no other justifications for the selected variables used in the model as they are available, fairly reasonable and are a good fit with the data.

Generally, cross-sectional data are snapshots, and the decision whether we observed a punctuated equilibrium or a stasis cannot be made by merely using one observation in time. Therefore, using only one point in time, we cannot be sure whether parameters or functional forms are stable in time. The functional form could also be incomplete to produce reliable results from interpolation if relevant confounders are not accounted for. In principle, this unavoidable drawback of using an observational study could only be solved by either using an experimental study or practically by using subject matter's knowledge to justify the functional form. In this case, we would have a model suitable for interpolation. If, at best, the functional form would model a "sufficient cause" then this would justify inter- and extrapolation, as causality solves the matter of confounding, and a modeled causality would be suitable for extrapolation. In fact, models are of little use if they can only be trusted for interpolation in known domains rather than for extrapolation to new conditions. The level of trust in model predictions for extrapolated settings will always require judgment on appropriateness of assumptions rather than proven numerical track records alone.

Caveat 3: Functional form as a compressed description

In using a functional form as a compressed description, initially we have a sample that determines n points in a k-dimensional interval built by the extremes of the k variables (sample intervals). Then we could decide to use either (i) only those points observed as starting values for a new simulation step (bootstrap approach), or (ii) start with points from very small spheres around each observed point (adding noise approach), or (iii) use any point within the sample interval (interpolation). It seems that if we use decent functions in our model and stay in the sample interval in any of the three forms above we should be safe. However, leaving the sample interval and extrapolating might lead to overshooting, heavy oscillations or generally to unrealistic constellations. For example, we might assume that a sample domain has indicated or forced a simple form (e.g., linear) where a sigmoid relation would be more appropriate. In such a case, leaving the sample interval would clearly lead to unrealistic overshoots or lower deviates.

ALTERNATIVE APPROACHES

The best way to address these caveats is through a choice modeling approach using longitudinal data. Longitudinal studies enable one to accurately observe changes or patterns. However, collecting longitudinal data is time consuming and very expensive. Besides, some argue that the power to detect causal relationship in this way is less compared to experiments. A

researcher may decide to use census data, yet the empirical information on the decision-making process of subjects is also often lacking. Some studies employ genetic or evolutionary programming for agent's decision making in which, its computational processes are similar to those in natural selection theory (An 2011). There are few empirical studies on this but nevertheless promising in providing reliable results (Manson and Evans 2007).

Various sources in literature suggest the use of process-based decision making. For example, in dealing with the uncertainty of assumptions in models and data, an accepted way of reducing uncertainty or showing the influence of uncertainty processes on model results is by modeling the actual processes (Barthel et al. 2008). Process-based decision models, accordingly, are those capturing the triggers, options, and temporal and spatial aspects of an actor's reaction in a relatively direct, transparent and realistic way. Thus, substantial efforts should be invested in process-based decision-making mechanisms or models to better understand the socio-ecological systems (An 2011). In the case study below, a process-based decision making model is constructed based on the preferred future land-use choices as part of the decision process of the household agents in the study site. The decision process includes a time element that is pertinent for establishing causal relationships (van Belle 2008) derived from a cross-sectional survey.

CASE STUDY

Study area

The study area is located in Jambi Province (Sumatra), Indonesia. The villages of Lubuk Beringin, Laman Panjang, and Desa Buat, which cover a total area of 157 km^2 - are near the foothills of Kerinci Seblat National Park. Except for Desa Buat, these villages are considered poor and have poor access to market roads and electricity infrastructure due to their distance from the district center. Rubber agroforest is the dominant land use in the province and is the major rural livelihood of the people living there while paddy rice is the main food source. However, due to the low latex productivity from the rubber agroforests, farmers are now forced to convert their farm lands into more profitable land use such as oil palm and monoculture rubber plantations.

Household survey

A household survey was conducted to elicit the agents' characteristics and behavioral responses. The survey was conducted with 95 households (out of 551 households) between February and March 2010. In the survey questionnaires, two main conditions are explored, namely 1) the current condition of the agent, the household profile, and the farm-holding characteristics from which the current land-use choice was generated, and 2) under certain conditions or situations in which the agent will likely perceive and behave as if the condition existed (i.e., if supported by financial investment in the next 5 to 10 years, under payments for ecosystem services or PES through conservation agreement scheme). We also asked the reasons for choosing the land use in order to understand the actual motivations and preferences behind the decision.

Data analysis

The data analysis was in two major steps: 1) household categorization using principal component analysis (PCA) and cluster analysis (i.e., K-means cluster or KCA), and 2) estimation of behavior of household types regarding land-use choices estimated using multinomial and binary logistic regression. We also compared the current land uses derived from the household survey to the land use maps of 1993 and 2002. Only the results of one household type are presented in the land-use choice section.

RESULTS

Household characterization

The summary of results derived from running PCA and KCA show that there are two types of households in the study area (Figure 1). These are rubber-rice households (type 1) as better-off households and rubber-based households (type 2) as relatively poor households, which explicitly shown in Figure 1.

Figure 1: Variation between household type 1 and 2 in terms of land holdings per capita, dependency ratio, and gross income per capita.

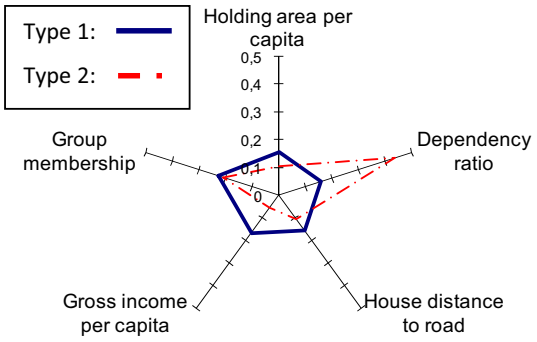

Land-use choices

Current land-use choices

The predictors and probabilities for land-use choices of household agents are summarized in Table 1 and Figure 2. There are 14 variables identified that significantly influence the choices of the household agent (Table 1).

Table 1: M-logit Model Estimation of Land-use Choices by Poor Households (type 2) that have Changed their Land Use between 1993 and 2005 (n = 74 plots); $p = 0.000$ and $R^2 = 0.78$.

Variable	Definition	Rubber agroforest (β)	Paddy rice (β)
constant		36.56*	-271.54
$H_{\_age}$	Age of household head	-0.54**	-0.37
$H_{\_size}$	Household size	1.96	4.52**
$H_{\_dep}$	Household dependency ratio	-7.61**	8.98
$H_{\_edu}$	Education of household head	-4.13*	8.49
$H_{\_mem}$	Household number of memberships	2.26	10.77**
$H_{\_ACT}$	Household activities in regards to conservation agreement	-0.46	2.02*
$H_{\_CA}$	Household participation in conservation agreement	-2.59	-12.29*
$P_{\_wet}$	Plot wetness index	1.01**	4.28**
$P_{\_dt}$	Plot distance to town centre (m)	-2.88	-1.32*
$P_{\_dr}$	Plot distance to road (m)	2.62	-29.05*
$P_{\_F2}$	Neighborhood enrichment factor (NEF) of rubber agroforest	0.017**	0.19**
$P_{\_F45}$	NEF of other land uses	0.02*	0.36*
$P_{\_F6}$	NEF of rice field	0.001*	0.02*
$P_{\_F8}$	NEF of settlement	0.01**	0.09**

Note: ***, **, and * indicate statistical significance at the 0.01, 0.05 and 0.1 level, respectively. Other land uses (e.g., oil palm and rubber monoculture plantation) was selected as the base case for comparison.

Preferred land-use choices under certain condition

The predictors and probabilities for the land-use choice of household agents under the condition of "if supported by financial investment in the next 5 to 10 years" are summarized in Table 2 and Figure 3. There are 5 variables identified that significantly influence the choices of the household agent (Table 2).

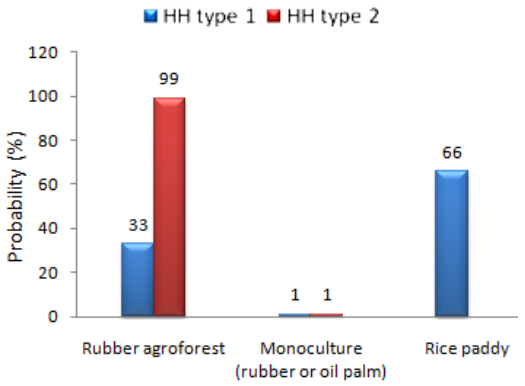

Figure 2: Probabilities for Current Land-use Choices

Table 2: Bi-logit Model Estimation of Land-use Choices by Poor Households (type 2) under Condition of Financial Support (n = 74 plots); $p = 0.003$ and $R^2 = 0.29$.

Variable	Definition	Rubber agroforest (β)
Constant		4.14**
$H_{\_age}$	Age of household head	-0.73*
$H_{\_edu}$	Education of household head	-1.12*
$H_{\_land}$	Household landholdings per person	0.67**
$H_{\_ACT}$	Household activities with regard to conservation agreement	0.17**
$P_{\_F45}$	NEF of other land uses	0.02*

Note: ***, **, and * indicate statistical significance at the 0.01, 0.05 and 0.1 level, respectively. Other land uses (e.g., oil palm and rubber monoculture plantation) was selected as the base case for comparison.

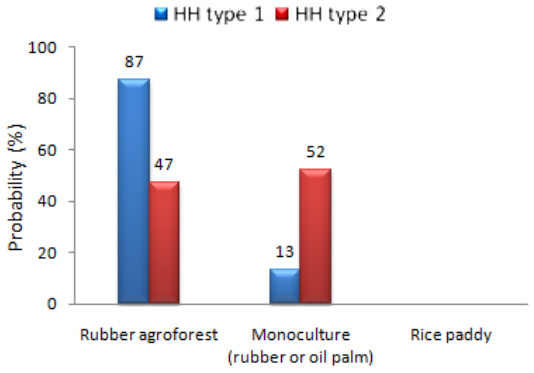

Figure 3: Probabilities of Preferred Land Use under Condition of Financial Support

The results suggest that under the current trend, 99% of the poor households are likely to stay with rubber

agroforest. In terms of future land-use preferences if financial investments are provided, the probability to choose monoculture increases by 50% while the probability that the households will stay with rubber agroforest decreases by almost 50%. This could imply that half of the poor households would risk engaging in more profitable farming. It is also interesting that variables or factors influencing the land-use choice varies from current to future preferences.

It should also be noted that paddy rice was less preferred under condition of financial support (Figure 3) due to the fact that the survey was mainly done with male household heads, who are mainly responsible for rubber and oil palm production; females are solely responsible for rice production. Generally, only one decision maker was interviewed. Thus, the problem arises whether there is a gap between the expressed decision and the implementation of the expressed decision. The expressed intention could be just a wishful thinking, anticipated agreement with the other partner, or a decision that will be implemented without further consulting. In the given cultural environment, we could assume the latter two cases.

DISCUSSION

Choice heuristic algorithms

Based on the calculated choice probabilities, decision algorithms for the household agents were constructed. Using the decision-making routines of the Land Use Dynamic Simulator (LUDAS) model (Le et al. 2008), a decision-making choice algorithm for the current trend is presented in Figure 4. In the static phase, the land-use choice model under the current trend (Table 1) is specified. The same land-use choice model is also specified in the moving phase but with condition that the labor is more than zero and the land holding is equal to zero. If the functional parameters are estimated merely from cross-sectional samples (which is true in this case), we definitely cannot infer causality from the associated parameters (Caveat 1 and 2). At the same time we cannot do extrapolation (Caveat 3). Thus, we can only describe the association within the sample interval; we would otherwise risk unrealistic results. Nonetheless, we need to provide supporting information to justify the inferences from role-playing games, expert knowledge, and to identify missing confounders.

Drawing causal inferences from cross-sectional data can be done by incorporating time and confounding factors. The factors of the decision process itself can be seen as confounding factors between the observed socio-economic data and the production decision. Because such factors are associated with both the socio-economic status and the selected production, these factors could be the risk aversion of the decision maker, long-term decision, and alike. In order to estimate the central decision process more prospectively and so reduce confounding, one could estimate some parameters of the decision process directly. This leads us to the next decision algorithm (Figure 5).

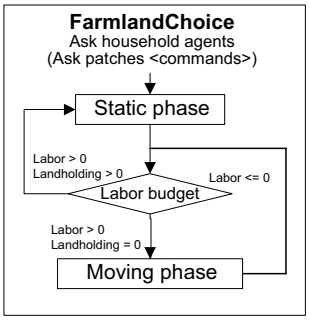

Figure 4: Flow chart of the basic decision-making routine for the farmland choice of the LUDAS model (Le et al. 2008).

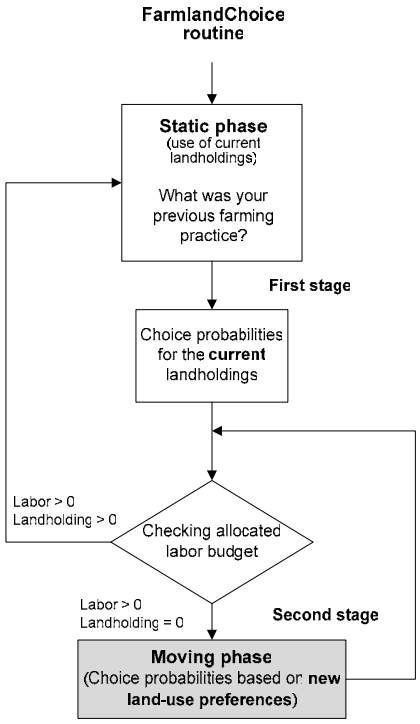

Figure 5: Flow chart of the process-based decision making routine under certain condition

A two-stage (or layered) decision-making routine was constructed to better incorporate the human

behavior component (i.e., decision-making process). In Figure 5, the preferred land use under a certain condition (i.e., if supported by financial investment or subsidies for the next 5 to 10 years) is a new process-based decision-making routine. In the moving phase, the preferred land-use choice model (Table 2) is specified, while the same land-use choice (Table 1) is included in the static phase. In this way, the agents already have available capital (i.e., labor) to open new land as a form of resource-use efficiency (van Noordwijk et al. 2012). In the simulation, in spite of the use of cross-sectional data, inferences regarding the possible land-use change are justified by incorporation of the decision process (i.e., what will you do if supported by financial investment in the next 5 or 10 years). It also allows different decision strategies in different situations, which is consistent with the results in cognitive science (Gigerenzer and Selten, 2001). Although to an unknown extent, the confounding factor "risk aversion" of a given household under certain socio-economic conditions could also be captured.

One of the key issues addressed in the use of process-based decision making (as presented in the case study) is the introduction of a more adequate description of the underlying causal mechanisms, which is crucial in land-use and natural resources management decision making of household agents. By asking what agents will do or choose under certain conditions, including the temporal aspects (e.g., in the next 5 years), we could understand the 'sufficient cause' that would justify future choices. This also allows different decision strategies in different situations to be incorporated in the model. A multi-choice experiment household survey is being developed and designed as a recommended alternative to mend the caveats of using cross-sectional survey in empirical modeling of decision making (Villamor 2012).

CONCLUSIONS

This paper discusses the caveats of decision-making models and lists a number of fallacies (most of which have been discussed for decades in literature). The alternatives offered are experiments and longitudinal studies, which are often much too expensive for most projects. Experiments have their own drawbacks, as they exclude many of the aspects usually considered by decision makers; longitudinal studies might not find the same decision makers in subsequent waves of the study, as decision makers might have moved across the boundaries of the target region.

ACKNOWLEDGEMENTS:

We are grateful for the financial assistance from Federal Ministry for Economic Cooperation and Development (BMZ), German Academic Exchange (DAAD), and the Landscape Mosaic project of ICRAF. We also thank Guido Lüchters for the useful comments on the earlier version of this paper.

REFERENCES

An L. 2011. "Modelling human decisions in coupled human and natural systems: review of agent-based models". *Ecological Modelling* doi:101016/j.ecolmodel.2011.07.010.

Barthel R.; S. Janisch; N. Schwarz; A. Trifkovic; D. Nickel; C. Schulz and W. Mauser. 2008. "An integrated modelling framework for simulating regional-scale actor responses to global change in the water domain". *Environmental Modelling and Software* 23, 1095-1121.

Benenson I. and P. Torrens. 2004. *Geosimulation: automata-based modelling of urban phenomena*. John Willey & Sons New York, USA.

Berger T. and P. Schreinemachers. 2006. "Creating agents and landscapes for multiagent systems from random samples". *Ecology and Society* 11(2).

Evans T.P.; W. Sun and H. Kelley. 2006. "Spatially explicit experiments for the exploration of land-use decision-making dynamics". *International Journal of Geographical Information Science* 20, 1013-1037.

Freedman D.A. 2010. *Statistical models and causal inference*. Cambridge University Press, Cambridge.

Galvin K.A.; P.K. Thornton; J.R. de Pinho; J. Sunderland and R.B. Boone. 2006. "Integrated modeling and its potential for resolving conflicts between conservation and people in the rangelands of East Africa". *Human Ecology* 34, 155-183.

Gigerenzer G. and R. Selten. 2001. *Bounded rationality: the adaptive toolbox*. The MIT Press, Cambridge, MA.

Gilbert N. and K.G. Troitzsch. 2005. *Simulation for social scientists*. Open University Press, Berkshire.

Heckbert S.; T. Baynes and A. Reeson. 2010. "Agent-based modeling in ecological economics". *Annals of the New York Academy of Sciences* 1185, 39-53.

Janssen M. and E. Ostrom. 2006. "Empirically based, agent-based models". *Ecology and Society* 11, No.2 37.

Kahneman D. and A. Tversky. 1979. "Prospect theory: an analysis of decision under risk". *Econometrica* 47 No.2:263-92

Le, Q.B., S.J. Park, P.L.G. Vlek and A.B. Cremers 2008. "Land-use dynamic simulator (LUDAS): a multi-agent system model for simulating spatio-temporal dynamics of coupled human-landscape system. I. Structure and theoretical specification". *Ecological Informatics,* 2:135-153.

Manson S.M. and T. Evans. 2007. "Agent-based modeling of deforestation in southern Yucatán, Mexico, and reforestation in the Midwest United States". Proceedings of the National Academy of Sciences 104: 20678-20683.

Matthews R.; N. Gilbert; A. Roach; G. Polhill; N. Gotts and L. Izquierdo. 2005. "Development of a rural economy and land use simulation modelling strategy". Macaulay Institute Craigiebuckler, Aberdeen, UK.

Matthews R.; N. Gilbert; A. Roach; J. Polhill and N. Gotts. 2007. "Agent-based land-use models: a review of applications". Landscape Ecology 22: 1447-1459.
Moore D.S. and G.P. McCabe. 2004. *Introduction to the practice of statistics.* Freeman, New York.
Parker D.C.; A. Hessl and S. Davis. 2008. "Complexity, land-use modelling, and the human dimension: fundamental challenges for mapping unknown outcome spaces". *Geoforum* 39: 789-804.
Parker D.C.; S.M. Manson; M.A. Janssen; M.J. Hoffmann and P.J. Deadman. 2003. "Multi-Agent Systems for the Simulation of Land-Use and Land-Cover Change: A Review". *Annals of the Association of American Geographers* 93: 314-337.
Rothman K.J.; S. Greenland; C. Poole and T.L. Lash. 2008. Causation and causal inference. *In* Rothman K. J., Greenland S. and Lash T. L. (eds.), *Modern Epidemiology*. Lippincott Williams & Wilkins, Philadelphia.
van Belle G. 2008. *Statistical rules of thumb*. Wiley, New York.
van Noordwijk M.; H.L. Tata; J. Xu; S. Dewi and P. Minang. 2012. Segregate or integrate for multifunctionality and sustained change through landscape agroforestry involving rubber in Indonesia and China. In: *Agroforestry: The Future of Global Landuse*. Nair PKR and Garrity DP (eds.), Springer, The Netherlands (in press)
Villamor, G., 2012. "Flexibility of multi-agent system models for rubber agroforest landscapes and social response to emerging reward mechanisms for ecosystem services in Sumatra, Indonesia". Unpublished manuscript, University of Bonn, Bonn.
Villamor G.B.; M. van Noordwijk; Q.B. Le; B. Lusiana, R. Matthews and Vlek P.L.G. 2011. "Diversity deficits in modelled landscape mosaics". *Ecological Informatics* 6: 73-82.
Windrum P.; G. Fagiolo and Moneta A. 2007. "Empirical validation of agent-based models: alternatives and prospects". *Journal of Artificial Societies and Social Simulations* 10 (2): 8.

AUTHOR BIOGRAPHIES

GRACE B. VILLAMOR was born in Bay, Laguna, Philippines. She is currently a researcher and PhD candidate at the Center for Development Research (ZEF), University of Bonn, Germany, and a research fellow at the World Agroforestry Center (ICRAF) in Indonesia. Prior to that, she was involved in various biodiversity-related research projects in Southeast Asia with the ASEAN Biodiversity Center and ICRAF. She obtained her Master degree at the Technical University in Dresden, Germany, in 2003.

MEINE VAN NOORDWIJK is the Chief Science Advisor of ICRAF. From 2002 to 2008, he was Regional Coordinator for Southeast Asia. Before joining ICRAF, he was a senior research officer at the Root Ecology Section at the DLO Institute for Soil Fertility Research in Haren, The Netherlands, focusing on models of the relationships between soil fertility, nutrient-use efficiency and root development of crops and trees.

KLAUS G. TROITZSCH has been professor of computer applications in the social sciences at the Computer Science Department of the University of Koblenz-Landau, Germany, since 1986. His main focus is on computational social science, in which he has published extensively. He has organized many workshops and conferences.

PAUL L.G. VLEK is the Executive Director of the West African Science Service Center for Climate and Adapted Land Use based in Ghana. He is also Director of the Department of Ecology and Natural Resources Management at ZEF and professor at the University of Bonn. Trained as a tropical soil scientist in The Netherlands and the USA, he conducts research on the sustainable use of natural resources in the tropics and how this is affected by or affects development processes.

EXPLORING TAX COMPLIANCE: AN AGENT-BASED SIMULATION

Francisco J. Miguel
José A. Noguera
Toni Llàcer
Eduardo Tapia
GSADI - Research Group on Analytical Sociology and Institutional Design
Department of Sociology, Autònoma University of Barcelona (UAB)
Fac. Political Sciences & Sociology, Campus Bellaterra, Cerdanyola (Barcelona), 08193 Spain
E-mail: gsadi@uab.cat, Miguel.Quesada@uab.cat

KEYWORDS

Tax Compliance, Decisional mechanisms,
Computational Economics, ABM Simulation.

ABSTRACT

This paper is just a concept presentation to be discussed at the ECMS12, based on preliminary work of a research project funded by the Spanish Institute for Fiscal Studies (Ministry of Economy). This project aims to build an agent-based model (ABM) for the simulation of tax compliance and tax evasion behaviour, and to calibrate it empirically in order to generate some known patterns of tax behaviour among Spanish taxpayers. Here we present the state of the development for the formal model and our present ideas about the implementation methodology, with focus on a new algorithm -based in four different decisional mechanisms- so that it includes not just the usual *expected utility optimization*, but also other sociologically relevant features like social network structure, social influence, decisional heuristics, biases in the perception of the tax system, and heterogeneity of tax motivations and tax morale among the agents. The methodological discussion about this kind of "modularity" in implementing a decisional engine could be completed in Koblenz with some preliminary results based on experimentation with the initial parameters and decisional modules.

INTRODUCTION

Tax evasion, -voluntary reduction of the tax burden by illegal means- is a problem of great social relevance. This is because, (a) it reduces the resources available to the public sector, a fact that is especially hard in the case of Spain, whose "underground" economy is, by some estimates, around 20% of the GDP; and (b) tax fraud, which do not extends homogeneously among all taxpayers, causes that the tax system violates *de facto* the principles of justice, equality and progressiveness. Try to understand the causes and determinants of heterogeneity in tax evasion, both temporal and geographic, appears as a relevant task as long as it should contribute to the design of institutional strategies that ultimately make possible to prosecute such evasion and therefore contribute to improving effective justice system and increase tax revenues without increasing tax rates. This fact is particularly interesting when taking into account the difficulties that governments are experiencing in recent times in maintaining a balanced budget and therefore maintaining welfare-state policies. That is the case of Spain, where the level of tax evasion is, according to different estimations, very high, while the level of tax morale is quite low. This pattern is specially harming in the present context of fiscal crisis and scarcity of public resources.

STATE OF THE ART

Scientific research of tax evasion dates back to the model developed by Allingham and Sandmo (1972), and, in parallel, by Srinivasan (1973), based on neoclassical economic theory. This model is an adaptation of the "crime economics" by G. Becker, an attempt to explain deviant behavior in terms of rational choice: the individual decides how much of their income he should declare in relation to the benefits of hiding (because the tax rate) and the costs of being discovered (given the probability of inspection and the amount of the fine). The main criticism launched against this approach was that predicted a much higher level to the observed tax evasion: given the low probability of inspection and the level of existing sanctions in the real world, the majority behavior should be to evading, which in fact does not happen (Alm et al., 1991). Thus, investigations of the past two decades can be seen as successive attempts to broaden the traditional neoclassical model in order to account for an act, tax compliance, which appears as "quasi-voluntary" (Levi, 1988).

Not surprisingly, in such an enterprise does occupy a prominent place those studies through opinion surveys trying to measure and to explain the tax morality (*tax morale*) of citizens, defined as "intrinsic motivation" or "internalized willingness" to pay taxes (Braithwaite and Ahmed, 2005). Such researches had proliferated recently and have as main figure in Benno Torgler, author of several dozen of these publications in the last decade. Approximation of this kind try to explain the fiscal morale taking as a proxy the *declared tolerance to tax evasion* -often from a single survey question- and including it as a dependent variable in different regression models. Thus, although results are mostly

Proceedings 26th European Conference on Modelling and Simulation ©ECMS Klaus G. Troitzsch, Michael Möhring, Ulf Lotzmann (Editors)
ISBN: 978-0-9564944-4-3 / ISBN: 978-0-9564944-5-0 (CD)

inconclusive, these studies allow us to obtain information about the correlation of fiscal morality with both sociodemographic variables (age, sex, marital status, educational level or income...) and ideological (religion, patriotism, trust in institutions, etc.., see a summary in Torgler, 2007). In Spain there have been a modest number of academic papers of this type, as those of Prieto, Sanzo and Suarez (2006), Alm and Gomez (2008), Alarcon, De Pablos and Carre (2009) and Maria-Dolores, Alarcon and Carre (2010). However, for a country where tax evasion reached alarming proportions, would certainly be desirable to take a greater number of these investigations.

Thanks to all these contributions, researchers have been increasingly assuming that the standard economic approach is insufficient to account for a phenomenon as complex as tax evasion. Therefore, in the last four decades have been publishing an increasing number of studies that try to explain tax evasion incorporating cognitive, cultural, normative, social, and other kinds of variables. These mostly adopt two methodological strategies: first, are the experimental approach of behavioral economists and psychologists, on the other hand, the aforementioned studies about "tax morale" made from opinion surveys.

Against the mainstream of those researches, can be found an incipient and small group of studies using ABM (agent-based models simulation) to explain the tax fraud at the aggregate level. These works contain models that, while assuming that tax evasion depends on the degree of deterrence (inspections and sanctions), have the key advantage of allowing the formalization of other effects, such as social interaction.

Early attempts correspond to Mittone and Patelli (2000), Davis et al. (2003) and the TCS model of Bloomquist (2004). The latter is the first work that uses a NetLogo model and represents an advance over the previous two, since it contains agents with a greater number of attributes; it is more complex in determining the probability of inspections and their effects and further validates the results obtained with real data.

Later we found the excellent EC* series of Antunes et al. (2006a, 2006b, 2007b; Balsa et al. 2006), in which increasingly complex models were developed by introducing progressive modifications over the standard economic model (e.g. adaptive agents with memory, social imitation, etc...). The most remarkable developments of these series of models are the inclusion of tax inspectors with autonomous decision capacity, and especially the proposal for an explanation of unpaid indirect taxes (sales taxes, value added taxes -VAT-, or goods and services taxes -GST-) from the collusion between buyers and sellers.

There is also the NACSM model (Korobow et al., 2007), which analyzes the relationship between tax compliance and the existence of social networks using the Moore neighborhood structure (ie, each agent has eight neighbors surrounding). More recently we find the proposal of Zaklan et al. (2008, 2009a, 2009b), whose peculiarity is to adapt the ISING physical model of the tax research: instead of particles that interact in different ways depending on the temperature, there are individuals who behave depending on behavior of their neighbors.

The TAXSIM model of Szabo et al. (2008, 2009 and 2010) presents a design specially rich in details, it includes four types of agents (employer, employee, government and tax office) and some innovative factors as the degree of satisfaction with public services -depending on previous experiences of individuals, as well as those who are in their social network-.

Finally, Bloomquist (2011) addresses the tax compliance for small business owners and models it as an evolutionary coordination game. The simulation model also is calibrated with data from behavioral experiments.

In short, the social simulation using ABM is a promising approach to a field in which, despite the abundant literature, results have been isolated and often poorly coordinated with each other, to the point of being able to say, as pointed out Kirchler that the investigation of tax evasion is "still in its infancy" (2007: xv).

METHODOLOGY

To build an ABM is a particularly adequate method for construing a model of tax behaviour which includes such parameters as social networks, social influence, heuristics and biases in the perception of the tax system, heterogeneity of tax motivations and tax morale among the agents, and other features that may generate complex social dynamics. Those factors have been traditionally neglected until very recently in the classical econometric models that aimed to explain the observed levels of tax compliance and tax morale -that is, disposition to pay taxes and tolerance towards tax evasion-.

MODEL DESCRIPTION

Parameters

The SimulFIS model presented here is empirically calibrated using the basic features of the Spanish tax system as well as survey data from the *Fiscal Barometer* of the Institute for Fiscal Studies and the *Survey of Public Opinion about Tax Policy* of the Spanish Centre for Sociological Research. We also use for this purpose a survey designed by us on Values and Attitudes on Distributive Justice, Social Benefits, and Taxes -funded by the Catalan Centre for Opinion Studies- (Noguera et al., 2011).

Some relevant setup parameters (see appendix A for the full set) include total population, proportion of workers and employers, proportion of unconditional law-abiders and unconditional evaders.

Agents

Agents are individuals, programmed as posessing certain common attributes such as income level -following a

quasi-exponential distribution-, a labour market position, beliefs about justice principles, perceptions of the tax system, and so on.
Agents are embedded in a rich social network whose characteristics can also be adjusted to different experimental configurations. The links for each agent are generated by a biased random engine to adjust the number of agent-neighbors classed as "workers" or "employers" as a function of the agent-class and the maximum number of links. So each agent is embedded into a social network, with a mix of equal and diverse class links or contacts, which locally became his own source of information about tax evasion behavior, inspections and fines.

Decisional algorithm
The decision algorithm for each agent includes four types of mechanisms -implemented as production rules- that play the role of "decision filters" (Elster, 1979:76; see also 1989:13-14). These elements are constrictions for the action along a deliberative process that generates the decision/action related with tax evasion:
(1) opportunity to evading, due to the economic and labour market position: affecting differently to the 6 typological classes generated by considering employees/(self)employers and socioeconomic level –high/medium/low-.
(2) normative and positive beliefs about the tax system: agents' decision is influenced by the principles of fairness or justice which motivate the agent -and how deeply they do- as well as by his perception of the tax system's factual satisfaction of those principles.
(3) rational choice: the agent maximizes his net income having in mind his knowledge about the tax rates, the probability of being detected if he evades, and the amount of the fines (see parameters table at Appendix A).

$$UE_i(X_i)=(1-p_i)\sqrt{(Y_i - X_i \cdot t_X + Z)} + p_i\sqrt{[Y_i - Y_i \cdot t_Y - \theta(Y_i - X_i) + Z]}$$

(4) social influence: once the decision has been made, the behaviour of the agent is sensitive to the perceived behaviour of the agents in his social network. After an evaluation of the level of fraud, the audit pressure, and the fines imposed in the close neighborhood, each agent adjusted its final behaviour.

Environment
Our model simulates the dynamics in a stylized or simplified virtual environment in which a central authority, each time turn, proceeds to collect taxes and then distributes the tax revenue through public goods (like social benefits, social investment, etc.). The central authority also implements a specific surveillance and inspection policy, and imposes fines on non-compliers. The simulated environment has been modeled with flexibility in mind, so that it could be easy for the simulation users to implement different tax systems and different policies to tackle non-compliance. The very idea of a "virtual tax laboratory" is behind such kind of implementation, considering that the project is commissioned by an end user (the *Spanish Institute for Fiscal Studies*, Ministry of Economy).

System dynamics
The general system dynamics follows this sequence:

System setup: Create agents
For each agent:
-Random Class allocation (workers/employers),
-Random Income allocation (quasi-exponential distribution, with interval probability table).
-Random Network generation (biased and constraint links)

*For each round:
--For each agent:
---Apply opportunity filter (or not)
---Apply normative filter (or not)
---Apply utilitarian filter (or not)
---Apply influence filter (or not)
--- Decision about income statement (X_i)

--For each agent:
---Collection of taxes.
---Inspections and penalties.

--For each agent:
---Payment of benefits.
---Consumption of agents (reference value: no savings, all disposable income is consumed in actual version).
---Update system and agents properties (memory, monitors, plotting, etc…).

*Next round

Outcomes
After running the model for a number of rounds to produce a relatively stable result, it can be analyzed in terms of the aggregate rate of tax evasion and the number of evaders. The simulation model allow to observe how different mechanisms may yield, from given initial conditions, different results in terms of aggregate compliance and tax evasion, by means of plotting and monitoring outcome data series.
By this time, we are still looking for more robust and reliable empirical data about Spanish tax-evasion behaviour, needed to provide validation to SimulFIS, because the final aim is accurately reproduction of actual figures of tax evasion.

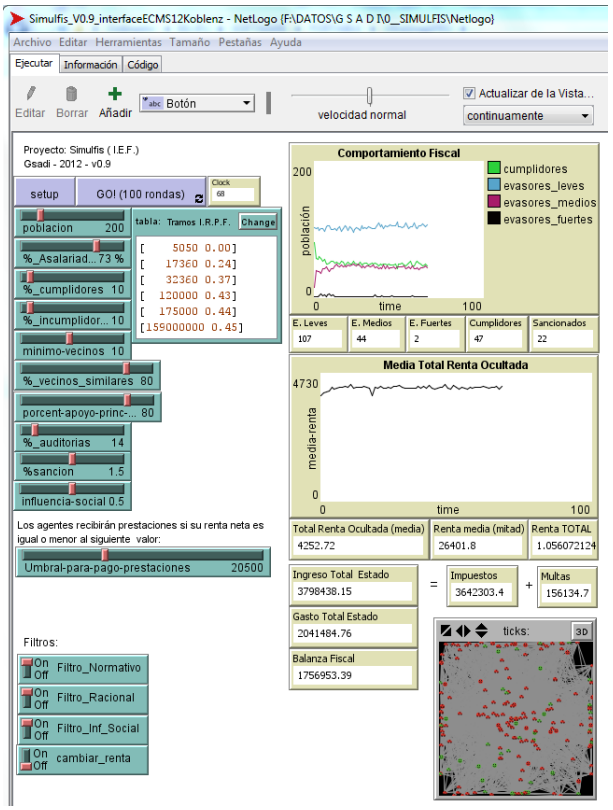

Figure 1: Screen Capture of SimulFIS interface (v0.9)

CONCLUSION AND FURTHER RESEARCH

The SimulFIS model tries to integrate some early model aspects and excellent ideas in a novel way. The "modular" decision mechanisms approach, and the parametrization of many system attributes, allows exploring both different sets of initial conditions –tax policies, tax morale, network topologies- and the relative effect of each filter over the final decision-making outcome.

Each factor, effect and mechanism here implemented has been previously proposed and explored in the relevant literature aforementioned. Added value of SimulFIS could be (1) the aim to embed it into a single model, by means of implementing the "decisional filtering" algorithm, and (2) the relevance of "network position", as the source of local cognitive scope for the decisional agents.

At the present time, the research follows on by systematically performing series of experimental design runs with the real version of the simulation model in order to obtain data to estimate the relative "strength" of each single filter –structural opportunities, normative believes rational utility expectations, and social influence-.

REFERENCES

Allingham, M.G. and Sandmo, A. (1972), "Income tax evasion: a theoretical analysis", *Journal of Public Economics*, 1: 323–338.

Antunes, L.; Balsa, J.; Moniz, L.; Urbano, P.; and Palma, C.R. (2006a), "Tax compliance in a simulated heterogeneous multi-agent society", in J.S. Sichman and L. Antunes (eds.): *MABS 2005*. LNCS (LNAI), vol. 3891. Heidelberg: Springer.

Antunes, L.; Balsa, J.; Respício, A. and Coelho, H. (2006b), "Tactical exploration of tax compliance decisions in multi-agent based simulation". In L. Antunes and K.Takadama (eds.): *Proc. MABS 2006*.

Antunes, L.; Balsa, J. and Coelho, H. (2007a), "Agents that collude to evade taxes". *AAMAS '07 Proceedings of the 6th international joint conference on Autonomous agents and multiagent systems*

Antunes, L.; Balsa, J. and Coelho, H. (2007b), "Tax compliance through MABS: the case of indirect taxes", *EPIA'07 Proceedings of the artificial intelligence 13th Portuguese conference on Progress in artificial intelligence.*

Balsa, J.; Antunes, L.; Respício, A. and Coelho, H. (2006): "Autonomous inspectors in tax compliance simulation". *Proceedings of the 18th European Meeting on Cybernetics and Systems Research.*

Bloomquist, K. M. (2004), "Modeling taxpayers' response to compliance improvement alternatives". Paper presented at the *Annual Conference of the North American Association for Computational Social and Organizational Science* (NAACSOS), Pittsburgh, PA.

Bloomquist, K (2006), "A Comparison of Agent–Based Models of Income Tax Evasion." *Social Science Computer Review* 24 No. 4: 411–25.

Bloomquist, K (2011), "Tax Compliance as an Evolutionary Coordination Game: An Agent-Based Approach", *Public Finance Review*, 39: 25.

Davis, J. S.; Hecht, G.; and Perkins, J. D. (2003). "Social behaviors, enforcement and tax compliance dynamics". *Accounting Review*, 78, 39–69.

Elster, J. (1979). *Ulysses and the Sirens: Studies in Rationality and Irrationality*. Cambridge: Cambridge University Press. Reimp. 1984.

Elster, J. (1989). *Nuts and Bolts for the Social Sciences*. Cambridge: Cambridge University Press.

Kirchler, E. (2007), *The Economic Psychology of Tax Behaviour*. Cambridge: Cambridge University Press.

Korobow, A.; Johnson, C. and Axtell, R. (2007), "An Agent-Based Model of Tax Compliance with Social Networks", *National Tax Journal*, LX (3): 589-610.

Mittone, L. and Patelli, P. (2000). "Imitative behaviour in tax evasion". In B. Stefansson & F. Luna (Eds.), *Economic simulations in swarm: Agent-based modelling and object oriented programming* (pp. 133-158) Amsterdam: Kluwer.

Noguera, J.A.; Guijarro, X.; León Medina, F.J.; Llàcer, A.; Miguel Quesada, F.J.; Tapia, E.; Tena-Sánchez, J. and Vinagre, M. (2011): *Valors i actituds sobre justícia distributiva: prestacions socials i fiscalitat*. Barcelona: Centre d'estudis d'Opinió, Generalitat de Catalunya.

Szabó, A.; Gulyás, L. and Tóth, I. J. (2008), "TAXSIM Agent Based Tax Evasion Simulator", *5th European Social Simulation Association Conference* (ESSA 2008).

Szabó, A.; Gulyás, L. and Tóth, I. J. (2009), "Sensitivity Analysis of a Tax Evasion Model Applying Automated Design of Experiments", Progress in Artificial Intelligence, *Lecture Notes in Artificial Intelligence*, 5816.

Szabó, A.; Gulyás, L. and Tóth, I. J. (2010), "Simulating Tax Evasion with Utilitarian Agents and Social Feedback", *International Journal of Agent Technologies and Systems*, 2 (1): 16-30.

Zaklan, G.; Lima, F. W. S.; and Westerhoff, F. (2008), "Controlling tax evasion fluctuations", *Physica A: Statistical Mechanics and its Applications*, 387: 5857-5861.

Zaklan, G.; Westerhoff, F. and stauffer, D. (2009a), "Analysing tax evasion dynamics via the Ising model", *Journal of Economic of Coordination and Interaction*, 4:1–14.

Zaklan, G.; Westerhoff, F. and Stauffer, D. (2009b), "A multi-agent-based approach to tax morale", *International Journal of Modern Physics* C, eprint 0508.0098 at http://www.arXiv.org.

ACKNOWLEDGEMENTS

This research has been funded by both the Spanish Ministry of Science and Innovation -through Grant CSO2009-09890 (I+D+i project) and CSD 2010-00034 (CONSOLIDER-INGENIO)- and the Institute for Fiscal Studies of the Spanish Ministry of Economy.

APPENDIX A

Table 1. Relevant Model Parameters

Y_i	Agent *i* Total Income
X_i	Agent *i* Declared Income
t_Y	Applicable tax rate (Y)
t_X	Applicable tax rate (X)
N	Population
p_i	Perceived probability of being fined if catch in tax-evasion, for agent *i* .
I_i^i	Tax inspections received by agent *i* in all previous rounds.
I_i^v	Tax inspections received by agent *i* neighborhood (including *i*) in previous round.
R	Total number of previous rounds
V_i	Number of neighbors of *i*
θ	Fines received by tax evasion
ω	Social influence coefficient
$UE_i(X_i)$	Expected utility of tax payment for agent *i*
Z	Public social benefits received
a_i	Rate of loopholes use for agent *i* after its rational choice in period t
a_v	Median of the rate of loopholes use in the neighborhood in the previous round
ψ	Coefficient of *"sucker-feeling"*

AUTHOR BIOGRAPHIES

F. J. Miguel Quesada is Associate Professor at UAB responsible for courses in Methodology for the Social Sciences, Sociology of Consumption and Applied Statistics for Marketing Analysis. He holds a PhD in Sociology from the Universitat Autònoma de Barcelona (UAB) and a University Specialist Degree in Sociology of Consumption from the Universidad Complutense de Madrid. He He has conducted research in sociology of consumption, women situation social indicators, and the school-to-work transitions. At present he mainly works in the domain of computational sociology, as GSADI member and as Director of the "Laboratory for Socio-Historical Dynamics Simulation" (LSDS), he is involved in several projects about the use of agent-based social simulation for the modelling of social networks dynamics and evolution of social behavior. His e-mail address is : Miguel.Quesada@uab.cat and his Web-page can be found at http://gsadi.uab.cat/index.php/members/uab-members/fj-miguel-quesada.

José A. Noguera is Associate Professor in the Department of Sociology at the Universitat Autònoma de Barcelona, and Director of the Analytical Sociology and Institutional Design Group (GSADI). He holds a PhD in Sociology from the Universitat Autònoma de Barcelona and has been visiting researcher at the University of California, Berkeley, and at the London School of Economics and Political Science. His research covers sociological theory, philosophy of social science, social policy, and normative social theory. He is a member of the European Network of Analytical Sociologists, and serves on the Board of the Spanish Basic Income Network (RRB) and on the International Advisory Board of the Basic Income Earth Network (BIEN). He is co-editor of *Papers. Revista de Sociologia*, and an editorial board member of *Revista Española de Investigaciones Sociológicas* and *Basic Income Studies*.
His e-mail address is : jose.noguera@uab.cat and his Web-page can be found at http://gsadi.uab.cat/index.php/members/uab-members/jose-a-noguera.

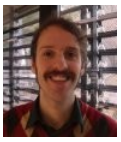

Toni Llàcer holds a FI Research fellowship -granted by Generalitat de Catalunya- to pursue a PhD project on the explanatory factors of tax evasion. He obtained a Bachelor's degree in Economics from Universitat Pompeu Fabra, a Bachelor's degree in Philosophy from Universitat de Barcelona (Academic Excellence Award), and a Master of Science in Applied Social Research from UAB. His e-mail address is : toni.llacer@uab.cat and his Web-page can be found at http://gsadi.uab.cat/index.php/members/uab-members/toni-llacer.

Eduardo Tapia Tejada is a PhD student in Sociology at the Universitat Autònoma de Barcelona and pre-doctoral researcher at GSADI. He is a graduate in Sociology from the Universidad Federico Villarreal of Peru and he holds a Master's degree in Sociological Research from the UAB. He also holds a degree in Design and Evaluation of Social Projects from the Pontificia Universidad Católica del Perú. His research interests are social network analysis, the unintended consequences of social action, the emergent outcomes of social interaction, and social simulation techniques. His e-mail address is : eduardotapiatejada@hotmail.com and his Web-page can be found at http://gsadi.uab.cat/index.php/members/uab-members/eduardo-tapia-tejada.

../

Social Dynamics and Collective Behaviour

OPENING THE BLACK-BOX OF REFEREE BEHAVIOUR. AN AGENT-BASED MODEL OF PEER REVIEW

Flaminio Squazzoni and Claudio Gandelli
Department of Social Sciences
University of Brescia
Via San Faustino 74/B, Brescia, 25122, Italy
E-mail: squazzon@eco.unibs.it

KEYWORDS
Peer review; referees; referee behaviour; reciprocity; agent-based model.

ABSTRACT

This paper investigates the impact of referee behaviour on the quality and efficiency of peer review. We focused especially on the importance of reciprocity motives to ensure cooperation between everyone involved. We modelled peer review as a process based on knowledge asymmetries and subject to evaluation bias. We built various simulation scenarios where we tested interaction conditions and manipulated author and referee behaviour. We found that reciprocity *per se* can have a negative effect on peer review as it tends to increase evaluation bias. It can have a positive impact only when purged by self-interest motivation and accompanied by disinterestedness and fairness standard.

INTRODUCTION

Peer review is the cornerstone of science. It allows scientists to experimentally pursue new lines of research through a continuous, decentralized and socially shared trial and error process and ensure the quality of knowledge produced. It, directly or indirectly, determines how all the resources of the science system, such as funds, careers, and reputation are allocated. Despite its importance, it is dramatically under-investigated and has no "experimental base" (Smith 2006).

One of the main challenges is to understand referee behaviour and increase commitment and reliability for everyone involved in peer review (Squazzoni 2010; Squazzoni and Takács 2011). Indeed, while journal editors and submission authors have clear reputational rewards, understanding incentives and motives of referees is more difficult. This is not trivial as it has been recently acknowledged that referees are dramatically overexploited and this could undermine their commitment (Björk, Roos and Lauri 2009). A survey estimated that peer evaluation is applied to more than 1 million journal articles per year, not to mention conferences, research proposals, fellowships and university/dept/institute productivity evaluation. Serious doubt has been casted by influential journal editors on the possibility that the peer review system could go on efficiently without reform (Alberts, Hanson and Kelner 2008).

Recent cases of misconduct and fraud called for a reconsideration of the potential traps of peer review. For instance, a group of scientists from South Korea published in 2005 an article on stem cell in *Science* that was based on false data. Certain myopic attitudes of editors influenced by "aggressively seeking firsts" and nine referees dazzled by the novelties of the paper implied that reviewing time was dramatically shortened: the referees took just 58 days to recommend the publication against the average of 81 days typical for this influential journal (Couzin 2006). More recently, the Stapel scandal gained public notoriety in the newspapers and the social media, where data for numerous studies conducted over a period of 15 to 20 years and published in many top journals in psychology were found to be fabricated (Crocker and Crooper 2011). It is worth noting first, that these cases can cause a misallocation of reputational credit in the science system with negative externalities on competition. Secondly, they can determine serious consequences on the credibility of science for external stakeholders.

Unfortunately, only a few studies in economics and social sciences tried to understand the behaviour of the figures involved in peer review and its consequences for the quality and efficiency of the evaluation process. One of the few topics studied has been the reviewing rate. For instance, Engers and Gans (1998) suggested a standard economic analytic model that looked at the interaction between editors and referees. They aimed to understand why referees were willing to ensure good quality of reviewing without any material incentives and whether improving these latter could increase the reviewing rate. They showed that payment could potentially motivate more referees to agree to review a submission, but raising the review rate could bring referees to believe that refusing to review a submission could not impose serious costs to the journal, as other referees could happily accept to review. This could cause a decrease of the reviewing rate and bring journals to increase payment to compensate this effect, generating an escalation of compensation unsustainable for journals.

On the other hand, Chang and Lai (2001) studied reviewing rates and came to different conclusions. They suggested that if reciprocity motives were present, which influenced the relationship between journal

Proceedings 26th European Conference on Modelling and Simulation ©ECMS Klaus G. Troitzsch, Michael Möhring, Ulf Lotzmann (Editors)
ISBN: 978-0-9564944-4-3 / ISBN: 978-0-9564944-5-0 (CD)

editors and referees and provided room for reputation building for referees, a possible snowballing effect could emerge that increased the referee recruitment rate. They showed that if accompanied by material incentives, this effect could significantly improve the review quality. This was also confirmed by Azar (2008), who studied the response time of journals. He suggested that shorter response times of journals in specific communities were due to the strength of social norms, towards which referees were extremely sensitive..

The importance of social norms in peer review has also been confirmed by recent experimental findings, where results showed that indirect reciprocity motives more than material incentives provided reasons to expect commitment and reliability by referees (Squazzoni, Bravo and Takács 2011). By manipulating incentives in a repeated investment game, which was modified to mirror peer review mechanisms, they found that adding material incentives to referees undermined pro-social motivations without generating higher evaluation standards. These results are in line with game theory-oriented experimental behavioural studies, where the importance of reciprocity, direct and indirect, for cooperation in situations of asymmetries of information and potential cheating temptations, which could represent a typical situation of peer review, was widely acknowledged (Bowles and Gintis 2011).

Following this perspective, it is possible to argue that referees would cooperate with journal editors in ensuring the quality of evaluation as they are concerned about protecting the prestige of the journal in case of previous publication as a means to protect their own impact. On the other hand, they could also be motivated to cooperate with authors by providing a fair evaluation and constructive feedback, as they are interested to establish good standards of reviewing in prospect of benefiting from other referees when they will be authors. In this respect, looking at referee/author interaction, peer review could be viewed as a "helping game", where referees would act as "donors" who choose whether to give or not a positive benefit to "recipients" (i.e., submission authors) by paying a cost (i.e., time and effort needed to reviewing), which is smaller than the recipients' benefit (i.e., higher impact factor, more citations, higher academic reputation) (Seinen and Schram 2004).

It is worth mentioning that these problems have recently been addressed in *Science*, where Alberts, Hanson and Kelner (2008) suggested the need for seriously reviewing peer review to improve its efficiency and guarantee its sustainability. Unfortunately, all current attempts to reform it, which have insisted especially on the importance of referee reliability and the need for measures to improve it, have followed trial and error approaches not supported by experimental investigation. Although some 'field experiments' on peer review were performed by certain journals or funding agencies, it is widely acknowledged that we lack sound experimental knowledge on essential peer review mechanisms, which can seriously support policy measures (Bornmann 2011).

Our paper is an attempt to contribute on this point by proposing a modeling approach (Martins 2010, Roebber and Schultz 2011; Thurner and Hanel 2011). Indeed, empirical research has serious problems in looking at essential aspects of peer review in general terms and investigating complex mechanisms of interaction such as peer review. We modelled a population of agents interacting as authors and referees in a competitive and selective science system. Our aim was to understand the impact of referee behaviour on the quality and efficiency of peer review and to test the impact of reciprocity strategies between involved agents.

The structure of the paper is as follows. In the second section, we will introduce the model, while in the third we will present various simulation scenarios and the simulation parameters. In the fourth one, we will illustrate our simulation results, while in the concluding section, we will present a summary of results and draw some implications for the current debate on peer review.

THE MODEL

We assumed a population of N scientists (N = 200) randomly selected each tick to play one of two roles: authors or referees. The task of an author was to submit an article and have it published. The task of a referee was to evaluate the quality of submissions by authors. Depending on the referees' opinion, only the best submissions were published (i.e., those exceeding a given quality threshold).

We gave each agent a parameter for individual productivity, which was initially homogeneous. Productivity was a measure of academic status, position, experience and scientific achievement of scientists. The principle was that the more scientists published, the more resource they had and the higher their academic status and position were.

We assumed that resources were needed both to submit and review an article. With each simulation tick, agents were endowed with a fixed amount of resources, equal for all (e.g., common access to research infrastructure and internal funds, availability of PhD. students). Then, they cumulated resources according to their publication score.

We assumed that the quality of submissions was dependent on agent productivity. Each agent had resources $R_a \in N$ from which we derived an expected submission quality as follows:

$$\mu_{ar} = \frac{v \cdot R_a}{v \cdot R_a + 1} \quad (1)$$

We assumed that authors varied in terms of quality output depending on their productivity. More specifically, the quality of submissions by authors followed a standard deviation σ which proportionally varied according to agent productivity and followed a normal distribution $N(R_a, \sigma)$. This means that, with some probability, top scientists could write average or

low quality submissions, and average scientists had some chance to write good submissions.

The chance of being published was determined by evaluation scores assigned by referees (see below). If published, agents earned resources proportionally to the article's quality assigned by referees as follows:

$$P = \frac{Q}{v*(1-Q)} \quad (2)$$

where P was the productivity gained and Q the submission quality score assigned by referees. We assumed that publication multiplied author resources of a M value, which gradually varied between 1 for more productive published authors to 1.5 for less productive published authors each tick. We assigned a heterogeneous value of M, after various explorations of the parameter space, as this mimicked reality where productivity gain from publication is crucial to explain differences in scientists' performance, but is higher for scientists at their initial steps and cannot exponentially increase for top scientists. If not published, following the "winner takes all" rule characterizing science, we assumed that authors lost all the resources invested for submitting. This meant that, at the present stage, we did not consider the presence of a stratified market for publication, where rejected submissions could be submitted elsewhere, as happens in reality (Weller 2001).

Therefore, the value of author submissions was not objectively determined (i.e., it did not perfectly mirror the real quality of submissions), but was dependent on the referees' opinion. When selected as referees, agents needed to invest a given amount of resources (see below) for reviewing but simultaneously lost them as they could not publish in the meantime. We assumed that authors and referees were randomly matched 1 to 1 so that multiple submissions and reviews were not possible and the reviewing effort was equally distributed on the population.

We assumed that reviewing was a resources-demanding activity and that agent productivity determined both the agent's reviewing quality and its cost (i.e., time lost for publishing). The total expense S for any referee was calculated as follows:

$$S = \frac{1}{2} R_r[1 + (Q_a - \mu_r)] \quad (3)$$

where R_r was agent resources, Q_a was the real quality of the submission and μ_r was the referee's expected quality.

We assumed that, if referees were matched with a submission of a quality close to a potential submission of their own, they spent 50% of their resources for reviewing. They spent less when matched with lower quality submissions, more when matched with higher quality submissions. However, reviewing expenses depended proportionally on agent productivity. This means that top-scientists will waste less time for reviewing in general, as they have more experience and ability to evaluate good science than average scientists. However, they will lose more resources than average scientists because their time is more costly than the latter.

We assumed two types of referee behaviour, namely *reliable* and *unreliable*. For reliability, we meant the capacity of referees to provide a consistent and unequivocal opinion that truly reflects the quality of the submission. In case of reliability, referees did the best they could to provide an accurate evaluation and spent resources for reviewing close to their expected quality level. In this case, we assumed a normal distribution of the referees' expected quality, which depended on their productivity, and a narrow standard deviation of their evaluation score from the real value of the submission ($\sigma = R_a/100$). This meant that the evaluation scores by reliable referees were likely to approximate the real value of author submissions. However, we assumed that, also in case of reliability, the evaluation bias increased proportionally to the difference between referees' expected quality and author submission quality. This was to represent the knowledge and information asymmetries between authors and referees that characterize peer review in science.

In case of unreliability, referees fell into type I and type II errors: recommending to publish submissions of low quality or recommending not to publish submissions that should be published (Laband and Piette 1994). More specifically, unreliable referees spent less resources than reliable referees, and under or over estimated author submissions. To avoid that referees eventually assigned the real value by chance to submissions, we assumed that, when they underrated a submission, the evaluation score took a standard deviation around – 90% of the real quality of the submission. The opposite sign was assigned in case of overrating (i.e., + 90%). It is worth noting that certain empirical studies showed that these types of errors were more frequent than expected, especially in grant applications (e.g., van den Besselaar and Leydesdorff 2007; Bornmann and Daniel 2007). For example, Bornamm, Mutz and Daniel (2008) examined EMBO selection decisions and found that between 26 and 48 percent of grant decisions showed these type of errors, underrating being more frequent (2/3 of cases).

Finally, all simulation parameters are shown in Table 1. Agent resources were set at the beginning of the simulation at 0 for all. At the first tick, 50% of agents were published randomly. Subsequently, everyone had a fixed productivity gain each tick. If published, agents had the value of their publication multiplied by the parameter M [1, 1.5] and so their resources grew accordingly. This meant that the quality of their subsequent submission was presumably higher.

Table 1: Simulation parameters.

Parameters	Value
Initial resources	0
Fixed productivity gain	1
Publication selection rate	[0.25, 0.50, 0.75]
Publication productivity gain	[1, 1.5]
Unreliability probability	[0, 1]
Evaluation bias by default	0.1
Author investment for publication	1
Reviewing expenses of unreliable referees	0.5
Underrating by unreliable referees	0.1
Overrating by unreliable referees	1.9

SIMULATION SCENARIOS

We built various simulation scenarios to test the impact of referee behaviour on the quality and efficiency of peer review. For quality, we meant the capability of peer review to ensure that only the best submissions were eventually published (Casati *et al*. 2009). Obviously, this is a restrictive definition of the various functions that peer review covers in science. Here, we only considered the screening function. Neither the role of peer review in helping authors to add value to their submission by referee feedback (Laband 1990), nor its role in deciding the reputation of journals and their respective position in the market were considered (Bornmann 2011). For efficiency, we meant the capability of peer review of achieving quality by minimizing productivity lost by authors and reviewing expenses by referees.

In the first scenario (called "*no reciprocity*"), we assumed that, when selected as referees, agents always had a random probability of behaving unreliably, which was constant over time and not influenced by any past experiences. When selected as authors, agents always invested all their resources for publication, irrespectively of positive or negative past experience with their submission. In this case, there was no room for reciprocity strategies between authors and referees. In the second scenario (called "*indirect reciprocity*"), we assumed that agents, when selected as referees, were influenced by their past experience as authors. In case of previous publication, they reciprocated by providing reliable evaluations in turn when selected as referees. Note that in this case, authors were self-interested and did not consider the pertinence of the referee evaluation, only their publication success or failure in their previous submission. This meant that they reciprocated negatively in case of rejection and positively in case of publication even if they knew that their submission was of a low quality and wasn't worth a publication.

In the third scenario (called "*fairness*"), when selected as authors, agents formulated a pertinent judgment of the referee evaluation of their submission. They measured the fairness of the referee opinion by comparing the real quality of their submission and the evaluation rate received by the referees. If the referee evaluation approximated the real value of their submission (i.e., $\geq$ -10 %), they concluded that referees were reliable and did a good job. In this case, when selected as referees, they reciprocated positively with other authors irrespectively of their past publication or rejection. This meant that now indirect reciprocity was not based on pure self-interest motivation of agents but on normative standards of conducts.

Finally, the last two scenarios (called "*self-interested authors"* and *"fair authors*") extended the previous two. In the "*self-interested authors"* scenario*,* we assumed that, when published, authors reacted positively and continued to invest all their resources for their next submission. In case of rejection, they reacted negatively and invested less in the subsequent round (i.e., only the 10% of their resources). This reaction was independent of the pertinence of the referee evaluation. In the "*fair authors"* scenario, in case of a pertinent referee evaluation received when authors, they reinforced their confidence on the good quality of the evaluation process and continued to invest everything to send good quality submissions irrespectively of the fate of their submission. In case of non-pertinent evaluation (see above), they invested less in the subsequent round (i.e., only the 10% of their resources) and accumulate resources for the subsequent round irrespectively of their previous publication. Therefore, in this case, agents inferred by their experience of authors the overall situation of peer review standards and strategically acted consequently.

To measure the consequences of parameter manipulation under various scenarios, we built the following indexes: (1) evaluation bias, (2) productivity loss, (3) reviewing expenses and (4) career inequality. The first dealt with quality, the second and third with efficiency and the last one with the unequal distribution of resources in the system.

The first measured the percentage of evaluation errors made by referees each tick. We calculated the optimal situation, where submissions were published according to their real value and measured the discrepancy with the actual situation each tick. We did the same with the second index in order to measure how much resources were wasted by (unpublished) authors compared with the optimal solution. The third index measured the resources spent by agents for reviewing compared with authors. The fourth measured inequality in agent resources through a Gini index. Inequality here meant an unequal allocation of science outputs, such as productivity, academic status, and career.

RESULTS

Tab. 2 shows the impact of referee behaviour on the quality and efficiency of peer review in various conditions of the publication rate (weak, medium, and strong selection). Data were averaged on 200 simulation run in any parameter conditions. Results showed, first, that reciprocity motives of referees *per se* had a negative effect on the quality and efficiency of peer review in a strongly selective science environment, while improved only minimally the situation in less

selective environments but at the expenses of referees' resources. Although in general increasing selection implied increasing evaluation bias, as expected, the "*fairness*" scenario implied lower bias and lower productivity loss by authors, although reviewing expenses were generally higher. Furthermore, it ensured higher resilience to changes in competition pressures. On the other hand, indirect reciprocity without fairness by authors implied higher evaluation bias and higher productivity loss when competition increased.

Table 2: The impact of referee behaviour on the quality and efficiency of peer review in various selective environments (values in percentage).

Scenario	Evaluation bias	Productivity loss	Reviewing expenses
Weak selection (75% published submissions)			
No reciprocity	14,10	5,69	23,47
Indirect reciprocity	12,58	6,51	44,16
Fairness	13,14	7,48	40,61
Medium-level selection (50% published submissions)			
No reciprocity	26,32	15,65	30,32
Indirect reciprocity	25,32	12,64	39,88
Fairness	15,68	8,60	38,68
Strong selection (25% published submissions)			
No reciprocity	28,00	15,01	29,47
Indirect reciprocity	43,12	16,92	33,39
Fairness	19,52	8,32	38,29

Tab. 3 shows the impact of reciprocal behaviour of authors in various selection rate environments. Results showed that reciprocity of authors improved peer review only when associated with fair criteria of judgment of the fate of their submission. When authors reacted to referee evaluation only following their self-interest (i.e., being eventually published), the quality and efficiency of peer review drastically declined. Moreover, in case of authors' fairness, peer review dynamics even improved with the increasing competition.

Then, we calculated the system productivity of all the scenarios, by averaging the resources of all agents at the end of the simulation run. Considered the value of the "*no reciprocity*" scenario as a benchmark, "*indirect reciprocity*" implied a loss of 20% of system resources, "*fairness*" showed a loss of 7% while "*self interested authors"* doubled the productivity and "*fair authors*" scenario determined an exponential growth of resources. Figures 1 and 2 compare system productivity accumulation in weakly and strongly selective environments. Results showed that in the "*fair authors*" scenario, stronger competition determined an exponential growth of resources.

Then, we also calculated the inequality of resource distribution in all the scenarios by measuring a Gini index (see Tab. 4). Results showed that, once introduced reciprocity, the best performing scenarios in terms of quality and efficiency of peer review were also the most unequal in terms of resource distribution. When selection was stronger, this trend did not radically change and was only exacerbated. This is coherent with findings of Squazzoni and Gandelli (2012): in a competitive systems where the "winner takes all" principle is the rule, such as in science, well functioning of peer review determines a unequal resource distribution as cumulative advantages for best scientists take place. This is because best published authors gain more resource and more chances to be re-published by taking advantage of fairness and reliability of referees

Table 3: The impact of author reciprocal behaviour on the quality and efficiency of peer review in various selective environments (values in percentage).

	Evaluation bias	Productivity loss	Reviewing expenses
Weak selection (75% published submissions)			
Self-interested	15,30	12,63	46,07
Fair authors	14,85	5,10	29,55
Medium-level selection (50% published submissions)			
Self-interested	30,52	25,63	45,74
Fair authors	14,24	4,00	15,96
Strong selection (25% published submissions)			
Self-interested	45,04	38,31	47,13
Fair authors	14,24	4,00	15,96

.

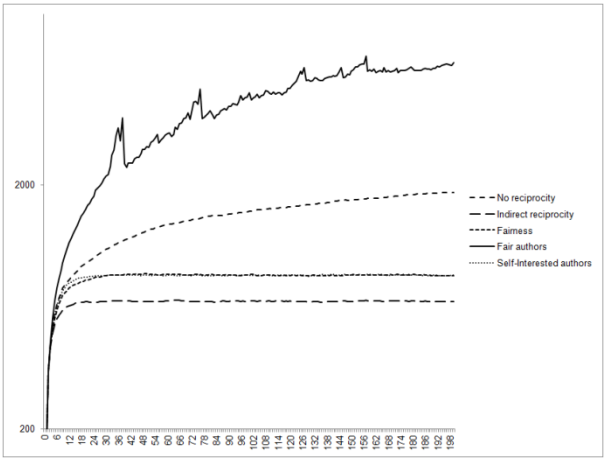

Figure 1: The impact of agent behaviour on system resource accumulation in weakly selective environments. In the x-axis, the number of simulation run.

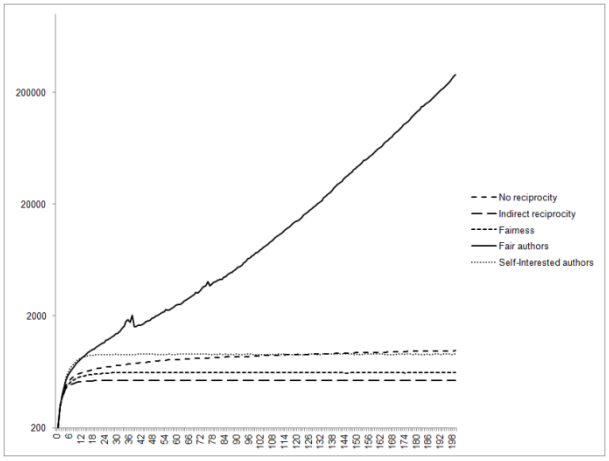

Figure 2: The impact of agent behaviour on system resource accumulation in strongly selective environments. In the x-axis, the number of simulation run.

Table 4: The Gini index in all the scenarios in weakly and strongly selective environments (values calculated at the end of the simulation). The index gave 0 when there was complete equality in resource distribution among agents and 1 when a single agent had everything.

Scenario	Gini index
Weak selection (75% published submissions)	
No reciprocity	0.55
Indirect reciprocity	0.34
Fairness	0.36
Self-interested authors	0.34
Fair authors	0.74
Strong selection (25% of published submissions)	
No reciprocity	0.47
Indirect reciprocity	0.34
Fairness	0.45
Self-interested authors	0.35
Fair authors	0.88

CONCLUSIONS

One of the most convincing explanations of why referees tend to cooperate with editors and authors in ensuring good quality and efficiency of peer review has been reciprocity (Chang and Lai 2001; Squazzoni, Bravo and Takács 2011). By viewing peer review as a cooperation game, we can argue that referees could rationally bear the cost of reviewing so as to establish good standards of reviewing in prospect of benefiting from cooperation by other referees when they are submitting authors. This is a typical mechanism through which reciprocity can sustain cooperation in repeated interaction as it can transform the cost for referees in an investment for potential future benefit.

Recent experimental findings corroborated this view. By comparing experimental treatments where referees were expected to be selected as future authors with treatments where referees could not be also authors in turn, Squazzoni, Bravo and Takács (2011) found that the quality of peer review significantly increased when roles were changing and that this made the introduction of material incentives for referees even superfluous. By alternating roles of referees and authors, indirect reciprocity motives took place that generalised cooperation.

Although highly abstracted and brutally simplified compared to in-depth empirical or experimental research, our simulation results allow us to cast doubt on the strength of reciprocity *per se* to explain the quality and efficiency of peer review. Indeed, our results indicate that if reciprocity is influenced by self-interest motives, its potential positive effect for cooperation in peer review is neutralised. This suggests that reciprocity motives of everyone involved in peer review should associate with fairness to ensure quality and efficiency in the evaluation process. A possible conclusion is that social norms that reflect ethical, cultural and competence-based standards of conduct for scientists could be more important than strategic behaviour to understand peer review and its important contribution for promoting excellence in science (Lamont 2009).

Obviously, neither theoretical generalisation, nor serious policy implications can be drawn from our simulation study. We did not pretend to convey realism here. Our results were based on a highly abstract model and so every conclusion should be taken cautiously. For instance, in reality, reviewing is not equally distributed over the population and also editors are important to provide room for reputation building and reciprocity motives of referees. These are certainly points for future development of our research.

However, one of the most crucial challenges for any future development of our work is to fill the gap between theory and empirical observation. Although it is difficult to obtain empirical data that point to the behaviour of agents involved in peer review, especially at the scale needed to look at general aspects, a possible development could be to empirically test referee behaviour in highly representative journals.

Certain empirical measures have already been developed that could be used to test our findings. For example, Laband (1990) examined referee reliability by measuring the lines of the report text sent to submission authors, assuming that the longer the text, the higher the quality of the referee comments and more reliable the final score assigned to the submissions. This is a brilliant idea to build an *ex-ante* measure that could complete the most common *ex-post* measures of peer review validity, such as published citations or the fate of rejected submissions (Weller 2001).

Let us suppose that we can select a set of representative journals, possibly of different scientific communities and to have access to the list of referees and authors and to the referee reports. Let us suppose to apply the Laband's measure to assess the *ex-ante* validity of peer review and to measure the *ex-post* validity, e.g., by collecting data on citation of published articles or, even better, by analyzing the fate of rejected submissions, so as to build a statistical measure of reliability of referee evaluation. By measuring the link

of referees and authors in these journals, we could test whether room for reciprocity and fairness took place that could influence the quality of the evaluation.

REFERENCES

Alberts, B., B. Hanson, and K. L. Kelner. 2008. "Reviewing Peer Review". *Science,* 321, 15.

Azar, O. H. 2008. "Evolution of Social Norms with Heterogeneous Preferences: A General Model and an Application to the Academic Review Process". *Journal of Economic Behavior and Organization*, 65, 420-435.

Björk, B.-C., Roos, A., M. Lauri. 2009. "Scientific Journal Publishing – Yearly Volume and Open Access Availability". *Information Research*, 14, 1, accessible at: <http://informationr.net/ir/14-1/paper391.html>.

Bornmann, L. 2011 "Scientific Peer Review". *Annual Review of Information Science and Technology*, 45, 199-245.

Bornmann, L. and H.-D Daniel. 2007. "Convergent Validation of Peer Review Decisions Using the *H* Index: Extent of and Reasons for Type I and Type II Errors". *Journal of Informetrics*, 1, 3, 204-213.

Bornamm, L., R. Mut, R. and H.-D. Daniel. 2008. "How to Detect Indications of Potential Sources of Bias in Peer Review: A Generalized Latent Variable Modeling Approach Exemplified by a Gender Study". *Journal of Informetrics*, 2(4), 280-287.

Bowles, S. and H. Gintis. 2011. *A Cooperative Species. Human Reciprocity and Its Evolution*, Princeton, NJ, Princeton University Press.

Campanario, J. M. 1998. "Peer Review for Journals as It Stands Today – Part I". *Science Communication*, 19, 3, 181-211.

Casati, F., M. Marchese, A. Ragone and M. Turrini. 2009. "Is Peer Review Any Good? A Quantitative Analysis of Peer Review". DISI University of Trento, Technical Report # DISI-09-045, accessible at: <http://eprints.biblio.unitn.it/archive/00001654/>.

Chang, J., C. Lai. 2001. "Is it worthwhile to pay referees?" *Southern Economic Journal* 68, 457-463.

Couzin, J. 2006. "…. and how the Problems Eluded Peer Reviewers and Editors". *Science* 311, 614-615.

Crocker, J., M. L. Cooper. 2011. "Addressing Scientific Fraud". *Science,* 334 (6060), 1182.

Engers, M. J. and Gans. 1998. "Why Referees Are Not Paid (Enough)". *American Economic Review*, 88, 1341-1349.

Laband, D. N. 1990 "Is There Value-Added From the Review Process in Economics? Preliminary Evidence from Authors". *The Quarterly Journal of Economics*, 105, 2, 341-252.

Laband, D. N. and J. M. Piette. 1994. "Favoritism Versus Search of Good Papers. Empirical Evidence Regarding the Behavior of Journal Editors". *Journal of Political Economy*, 102, 194-203.

Lamont, M. 2009. *How Professors Think: Inside the Curious World of Academic Judgment*. Cambridge, MA: Harvard University Press.

Martins, A. 2010 "Modeling Scientific Agents for a Better Science". *Advances in Complex Systems*, 13(4), 519-533.

Roebber, P. J. and D. M. Schultz, D. M. 2011. "Peer Review, Program Officers and Science Funding". *Plos One*, 6, 4, e18680, accessible at: http://www.plosone.org/article/info:doi%2F10.1371%2Fjournal.pone.0018680.

Seinen, I. and A. Schram. 2004. "Social Status and Group Norms: Indirect Reciprocity in a Repeated Helping Experiment". *European Economic Review*, 50, 3, 581-602.

Smith, R. 2006. "Peer Review. A Flawed Process at the Heart of Science and Journals". *Journal of the Royal Society of Medicine* 99, 759-760.

Squazzoni, F. 2010. "Peering into Peer Review". *Sociologica*, 3, doi: 10.2383/33640, accessed at: http://www.sociologica.mulino.it/doi/10.2383/33640

Squazzoni, F., G. Bravo and K. Takács. 2011. "Does Incentive Provision Increase the Quality of Peer Review? An Experimental Study". Proceedings of ICORE 2011-International Conference on Reputation, Montpellier, 19th September 2011, accessible at: http://2011.icore.name/

Squazzoni, F. and C. Gandelli. 2012. "Saint Matthews Strikes Again. An Agent-Based Model of Peer Review and the Scientific Community Structures". *Journal of Informetrics*, 6: 265-275.

Squazzoni, F. and K. Takács. 2011. "Social Simulation that 'Peers into Peer Review'". *Journal of Artificial Societies and Social Simulation*, 14(4) 3, accessible at: <http://jasss.soc.surrey.ac.uk/14/4/3.html>.

Thurner, S. and R. Hanel. 2011. "Peer Review in a World with Rational Scientists: Toward Selection of the Average". *The European Physical Journal B*, 84, 707-711.

van den Besselaar, P. and L. Leydesdorff. 2007. "Past Performance as Predictor of Successful Grant Applications. A Case Study". Den Haag, The Netherlands: Rathenau Institute, accessible at: <http://www.leydesdorff.net/magw/magw.pdf>.

Weller, A. C. 2001. *Editorial Peer Review: Its Strengths and Weaknesses*. Medford, NJ: Information Today, Inc.

AUTHOR BIOGRAPHIES

FLAMINIO SQUAZZONI is assistant professor of economic sociology at the University of Brescia, where he leads the GECS-Research Group on Experimental and Computational Sociology (`www.eco.unibs.it/gecs`). He is review editor of *JASSS* and member of the management committee of *ESSA*-The European Social Simulation Association. He is author of the book *Agent-Based Computational Sociology* (Wiley, Chichester, 2012, see: `www.eco.unibs.it/computationalsociology`). His e-mail is: `squazzon@eco.unibs.it` and his web-page can be found at: `http://unibs.academia.edu/FlaminioSquazzoni`.

CLAUDIO GANDELLI is research fellow in the MOSACC-Agent-Based Simulation Models to Support Web Tools for Entrerprise Collaborative Knowledge Management" Research Project, co-funded by the Department of Social Sciences, University of Brescia, Project Group and Regione Lombardia. He received a degree in computer sciences and engineering at the University of Brescia and also works as consultant for web and software applications for business. His e-mail address is: `c.gandelli@gmail.com`.

COMPARING PREDICTION MARKET MECHANISMS USING AN EXPERIMENT-BASED MULTI-AGENT SIMULATION

Frank M. A. Klingert and Matthias Meyer
Institute of Management Control and Accounting
Hamburg University of Technology
Hamburg, Germany
Email: frank.klingert@tu-harburg.de and matthias.meyer@tu-harburg.de

KEYWORDS
Prediction markets, mechanisms, continuous double auction, logarithmic market scoring rule, multi-agent simulation

ABSTRACT

Prediction markets are an interesting instrument to draw on the "wisdom of the crowds", e.g., to forecast sales or project risks. So far, mainly two market mechanisms have been implemented in prediction markets, the continuous double auction and logarithmic market scoring rule. However, the effects of the choice between these two market mechanisms on relevant variables such as prediction market accuracy are not fully understood. These effects are relevant as faulty prediction market outcomes might cause wrong decisions. This work contributes via an experiment-based simulation model to understand the mechanism-related effects and to direct further laboratory experiments. Our results show, that the mechanism decision does matter. Due to the higher amount of trades and the lower standard deviation of the price, the logarithmic market scoring rule seems to have a clear advantage on a first view. Taking the accuracy error as an independent variable, the effects are not as straightforward and depend on the environment and actors.

INTRODUCTION

Prediction markets can be described as markets which are "designed specifically for information aggregation and revelation" (Wolfers and Zitzewitz 2004, p. 108). They are an important example of the use of the "wisdom of the crowds" (Surowiecki 2010). The basic idea is to provide individuals with the possibility to trade their expectations concerning the relevant variable (e.g., the expected number of sales of a product in the next year) on a virtual market and to aggregate this local knowledge of individual actors in form of the market price, which is again visible to all market participants. Thus, these markets can be used to reveal and aggregate the diverse knowledge of even large groups at different locations and they differ considerably from traditional forecasting methods like expert forecasting or statistical methods. They have been successfully applied in research (e.g., Iowa Electronic Markets, e.g., Forsythe et al. 1992) as well as practice. A prominent example is Hewlett Packard's prediction market, which has shown an increased accuracy compared to traditional sales forecasts (Chen and Plott 2002).

A major design question when setting up a prediction market is the choice of a market mechanism (Spann and Skiera 2003, p. 1314), i.e. how trades by individuals on this market can be conducted. Several different market mechanisms have been applied to prediction markets to coordinate the trading interactions between individual actors. This paper focuses on the most commonly used, the continuous double auction (CDA, e.g. used in the Iowa Electronic Market by Forsythe et al. 1992, p. 1144) and the logarithmic market scoring rule (LMSR, invented by Hanson 2003; e.g. used in the Gates Hillman Prediction Market by Othman and Sandholm 2010, p. 368). On average, the performance of prediction markets has been "pretty good" (Wolfers and Zitzewitz 2004, p. 119), while there are cases, where they failed to aggregate information well (e.g., Hansen et al. 2004).

The effects of different market mechanisms on the results are often not intensively discussed in existing research publications, but research does document their importance. In field prediction markets (e.g., Forsythe et al. 1992; Othman and Sandholm 2010; Hansen et al. 2004), the mechanisms are regularly not varied as this would double the effort. Furthermore, they are often chosen without an intensive discussion or at least without documenting it. Some software providers in the area of prediction markets even do not offer alternative mechanisms, e.g., Crowdworx does focus on the LMSR (Ivanov 2008). Nevertheless, some differences are known. From the technical perspective, the LMSR offers constant liquidity and only needs one trader to execute a transaction while the CDA demands at least two.

The possible importance of the choice of an appropriate market mechanism stands, however, in contrast to the current understanding of the effects of different mechanisms on prediction market outcomes (Healy et al. 2010, p. 1995). The existing laboratory results focus on a small selection of aspects, e.g., the influence of knowledge distribution (Healy et al. 2010; Ledyard et al. 2009). Beyond them, especially the influence of the context together with a certain mechanism is unclear (Healy et al. 2010, p. 1995). For instance, the mentioned studies do not vary important aspects, such as the initial money endowment and the trading strategies of their actors. Furthermore, some existing results contradict each other. According to Healy et al. (2010) the

Proceedings 26th European Conference on Modelling and Simulation ©ECMS Klaus G. Troitzsch, Michael Möhring, Ulf Lotzmann (Editors)
ISBN: 978-0-9564944-4-3 / ISBN: 978-0-9564944-5-0 (CD)

accuracy of the LMSR is much worse than the accuracy of the CDA in a simple environment with few traders. This differs to the outcome of an experiment mentioned in a talk of J. O. Ledyard referenced in the same paper (Healy et al. 2010, p. 1995) and another experiment (Ledyard et al. 2009). Finally, the available laboratory experiments (Healy et al. 2010; Ledyard et al. 2009) share a problem as they all have only a very small number of traders starting from 3 up to 6. This number is lower than an average prediction market. It is even lower compared to the average prediction market in a corporate context which generally involves fewer traders than other prediction markets.

This lack of knowledge and the resulting problems are relevant as faulty prediction market outcomes might cause wrong decisions. Due to the increased application of prediction markets in the corporate context (Bray et al. 2008, p. 6), the relevance of differences between mechanism has further increased. Beyond, corporate prediction markets might face different conditions. For example, the amount of traders might be limited in corporate internal markets. As a result, traders who do not have any knowledge on how to trade optimally on a stock market might matter more than in large prediction markets. Therefore, the trading of some traders should rather be represented by a random strategy than by a strategy based on the expected value. A further aspect in the corporate context is that even marginal differences can have a high influence on important corporate decisions, e.g., the acquisition of a company. If there is an effect of the mechanism choice, an intentional decision is therefore necessary. This fact has already been recognized by Spann and Skiera (2003, p. 1314), who include the "choice of [a] trading mechanism" as a crucial step in the design process of a prediction market. But what are the relevant aspects for this mechanism decision?

Against this backdrop, this paper provides a comparative analysis of the CDA and LMSR concerning relevant prediction market output variables such as amount of trades, standard deviation of the price and accuracy error. It contributes by introducing and analyzing an agent-based simulation model to understand the mechanism-related effects and the dynamics of the collective knowledge aggregation of the participants. It aims at strong links with economic laboratory experiments following an iterative process (Klingert and Meyer 2012), as it is based on a laboratory experiment, i.e. the simulation model is constructed, micro and macro validated based on the experimental data and results of Hanson et al. (2006). It also wants to provide input for future laboratory experiments by identifying factors which should further be investigated. Our results show, that the mechanism decision does matter. Due to the higher amount of trades and the lower standard deviation of the price, the LMSR seems to have a clear advantage on a first view. Taking the accuracy error as an independent variable, the effects are less simple and depend on the environment and actors.

The paper is structured as follows. First, the research questions and hypothesis are derived. Second, the simulation model is introduced. Third, this model is validated from several perspectives. Fourth, experiments are conducted, analyzed and tested on robustness. The paper concludes with a discussion of the results.

LITERATURE REVIEW AND HYPOTHESES DEVELOPMENT

In this paper the continuous double auction and the logarithmic market scoring rule (Hanson 2003) are compared. The continuous double auction is the most widely used market mechanism. It allows traders to place asks and bids in an order book and executes a trade when a bid or ask is accepted or an ask or bid are crossing. Contrary in LMSR, the market maker is always the trading partner. This continuously offers to buy and sell for a certain price according to a logarithmic function (see Hanson 2003 for details).

What is the most relevant criterion to measure the quality of prediction market results? Which mechanism is superior to the other one? In this section, these questions will be split up to testable research questions and hypotheses in two steps. First, the dimensions of the evaluation are chosen. These dimensions support the judgment of when a certain prediction market mechanism can be seen as "superior" to another one. Second, along these dimensions, the research questions and hypotheses will be derived based on prior research and the documented differences of both mechanisms.

There are three evaluation criteria used subsequently. The first evaluation criterion is the quantity of trades. For the success of a market, the amount of trades is important. With an increased amount of trades, potentially more pieces of information can be added to the market price. The case of "no trade" does even end without any result and should therefore be avoided. The second evaluation criterion is the accuracy error. This checks the quality of the prediction market consistently with Hanson et al. (2006) and is taken as the central figure. The accuracy error is even more important than the amount of trades as the amount does not always lead to a high quality. The accuracy error is defined as variance of the price from the correct value (Hanson et al. 2006, p. 456). The third evaluation criterion is the standard deviation of the price and ensures the reliability as a good average accuracy might still not be sufficient. The existence of extreme faults might be more important than a slight reduction of the average accuracy as extreme predictions might influence decisions negatively. All three figures are measured at the end of the prediction market.

The accuracy error (hypothesis 2) is consequently used as the most important measure of prediction market quality. As the accuracy seems not to depend on the mechanism only, interaction effects with other factors are considered. Besides, the amount of trades and the standard deviation of the price are explored although the results are expected to be more straightforward.

Therewith, the analysis of these two variables should further contribute to model validation.

Regarding the first criterion, the following question will be analyzed: "Which mechanism shows a higher amount of trades?" This question is relevant as only trades can improve the prediction. It is straightforward, that the LMSR has an advantage in achieving a higher amount of trades as the CDA needs at least two traders to execute a trade. Contrary, the LMSR constantly provides liquidity and therewith is able to act as the second trader. This advantage has also been observed empirically by Ken Kittlitz, a software engineer of Consensus Point: "The number of trades in a market using the market maker is at least an order of magnitude higher than in one not using it." (cited in Hanson 2009, p. 62) Therefore, hypothesis 1 is formulated:

Hypothesis 1: The LMSR leads to a higher amount of trades than the CDA.

The second criterion is analyzed based on the following question: "Which mechanism achieves a better accuracy?" This question is central to prediction markets as the accuracy error measures the quality of the prediction market result. Unlike the first research question, finding a hypothesis for or against one of the mechanisms is more complicated in this case. As the LMSR was introduced after the CDA and specifically tackles its problems, the LMSR might be seen as favorable. However, most of the properties of the mechanisms have two sides. Having a quote-driven market maker (LMSR) might be beneficial, if no trades are expected with very few traders. However, in the absence of no trades and assuming an early end of the market, the traded liquidity in LMSR might be too low to achieve an accurate value. The market maker needs a certain minimum liquidity to move the price. Contrary, the CDA is able to directly change the price with one trade of a single stock. Summarizing, finding a hypothesis is less straightforward compared to the first one. However, considering the increased application due to the enhanced liquidity, the LMSR is supposed to have a slight advantage, leading to our second hypothesis

Hypothesis 2: *The LMSR achieves a better accuracy than the CDA.*

The question linked to the third and last criterion is: "Which mechanism shows a lower standard deviation of the price?" This question is relevant, as it reflects the constancy of a prediction market which might be an important measure for applications. For example, a high probability of a small derivation might be more acceptable than a low probability of a high derivation which results in a disastrous decision. Here, the LMSR seems to have a lower standard deviation as it restricts the action space of traders. Furthermore, the traders constantly only can choose out of exactly three actions, they can accept to buy or sell from or to the market maker or do nothing. Furthermore, the prices of the market maker direct the trading and the liquidity hinders fast price changes. Therefore, extreme trades do not directly result in extreme derivations from the correct value. Summarizing, this leads to our third hypothesis:

Hypothesis 3: *The LMSR has a lower standard deviation of the price than the CDA.*

SIMULATION MODEL

The purpose of the agent-based simulation model is to analyze the effect of the two mechanisms on the number of trades, the accuracy of prediction markets and the standard deviation of the prices. The motivation is to go beyond existing laboratory experiments. In this case, simulation can utilize at least two advantages compared to laboratory experiments (for a more detailed discussion on complementarities of simulation and laboratory experiments see Klingert and Meyer 2012). First, actor strategies can be controlled and therefore varied intentionally. Second, simulation experiments can be executed more efficiently which enables a much broader experimental design including up to 7 factors and 100 simulation runs for each factor combination. Beside its advantages, simulation itself benefits from the strong link to laboratory experiments as outcomes of the default model are validated and strategies are chosen by classification based on experimental data. In this section only an excerpt of the model description and reasoning concerning model design can be given due to space limitations. A more detailed model documentation based on the ODD protocol (Grimm et al. 2010) as well as a comprehensive validation and analysis can be found in Klingert (2012).

As a starting point, the default setting of the simulation model is mostly identical to the laboratory experiment of Hanson et al. (2006, p. 451). Twelve agents are initially endowed with 200 monetary units and 2 stocks. Both stocks give the right to receive an unknown payoff of 0, 40 or 100 with equal probability at the end of the trading period. As private knowledge, the agents know that one value can be excluded with certainty from the possible outcomes. For example, if the true value is 40, half of the agents know it is not 0 and half of the agents know it is not 100. Therefore, an agent which can exclude 0 as true value, knows that the true value is either 40 or 100 and that the stock has an expected value of 70.

Regarding the procedure, there are only few differences to the laboratory experiment of Hanson et al. (2006), e.g., the simulation model is executed in steps instead of a continuous execution. In each step based on CDA, the agents are allowed to place a bid or ask with a limit within the natural numbers between [0, 100]. Alternatively, they can accept an order from the order book. If an offer is accepted, the trade is executed and money and stocks are exchanged. The agent order is determined randomly to align the simulation with the laboratory experiment. The simulation ends after step 60 and then shows a comparable amount of trades (0-41 trades instead of 8-37) as in the laboratory experiment which lasts 5 minutes (Hanson et al. 2006, p. 451). Consistently with other market simulations (Gode and Sunder 1993, p. 122), the agents are limited to trade one

stock per step and the unmatched offers are deleted after a trade to simplify their decision and as the agents are allowed to place the same offers in the next step.

To provide additional contributions, the simulation model goes beyond the laboratory experiment and is varied along its elements, the market institution, the environment and the agents. The market institution is defined by its rules, i.e. the market mechanism. The CDA and the LMSR are used in the simulation experiments. The implementation of the LMSR demands a concrete b-value, which determines the maximum loss of the market maker, for the LMSR. To achieve a comparable result for CDA and LMSR, the b-value of the LMSR should be linked to the CDA setup. It is chosen such as the maximum loss of the market maker and the initial money endowment in LMSR is equal to the maximum value of the initial stocks and the money endowment in CDA.

Finally, the agents trade based on simple rules. The "family" of zero intelligence (ZI) traders is used because these strategies fulfill four criteria. First, the simplicity of the zero intelligence traders allows separating the influence of the market mechanism and the agent strategy. The separation is needed as the analysis should focus on the mechanisms. Second, zero intelligence agents allow cumulative research as they have been used in a variety of simulations. Third, the zero intelligence agents are already validated on the macro level as prior research has recognized similar efficiency of markets with ZI traders compared to markets with human traders (Gode and Sunder 1993, p. 133). Therefore, zero intelligence agents seem to be appropriate to direct subsequent experiments. Fourth, strategies which can be validated on the micro level would be valuable. The zero intelligence strategies have not been micro-validated statistically in their original papers (e.g., Gode and Sunder 1993). However, the simplicity of the zero intelligence strategies allows the statistical micro validation.

As ZI-strategies, ZI.EV, N-ZI, ZIP and two models mixing different strategies are chosen. Fundamental trading is represented by ZI.EV traders. The ZI.EV traders (derivation from ZIC (Gode and Sunder 1993) and N-ZI (Duffy and Ünver 2006)) are selling above and buying below the expected value (exact price is chosen randomly with a uniform distribution as in Gode and Sunder 1993). N-ZI traders (Duffy and Ünver 2006) weight the expected value and the last price to select when to buy and to sell. ZIP traders (Cliff and Bruten 1997) are learning a profit margin and only have a small price span in which they trade. Finally, the Mix 1 (4*ZI.EV, 2*N-ZI) and Mix 2 (2*ZI.EV, 2*N-ZI, 2*ZIU (fully random traders, for details see Gode and Sunder 1993)) are a model with several strategies for different agents.

The strategies (all beside ZIP) have been derived by micro validation similar to Boero et al. (2010). Instead of clustering as in Boero et al. (2010), a classification of experimental actors to the pre-defined ZI-strategies is done based on the data of the laboratory experiment of Hanson et al. (2006). Regarding strategies which are based on one information source only, almost all laboratory actors have been categorized to ZI.EV instead of trading on the trend or last price. After strategies which use more than one information source are added to the classification, the ZI.EV and N-ZI strategy equally fit to the laboratory data. Finally, mixed models have been introduced according to the distribution of these strategies to cover the minimum as well as the maximum amount of traders which are classified as fully random traders (ZIU).

The verification (see Gilbert and Troitzsch 2005, p. 19) of the model relies on three basic procedures: The model has been built based on (semi-) formalized models, it has been tested several times and the code has been inspected with a step-by-step debugging.

EXPERIMENTAL DESIGN, RESULTS AND ROBUSTNESS

In this section, the experimental design and results are described, including tests for robustness. After introducing the simulation results with an exemplary simulation, the results are evaluated along the three evaluation criteria in several steps (cf. Kleijnen et al. 2005; Lorscheid et al. 2012). First, each research hypothesis is evaluated comparing the averages of 100 runs which are based on the default setting. Second, several robustness tests are performed. These include the comparison of the averages over all 3^k-combinations and for each of the 3^k-combinations. Third, an overview of the effect sizes of main and 2-way-interaction effects is given based on a 3^k-experimental design. As effect size measure, partial eta squared is chosen to weight the influence of the factors against the size of the error. Finally, the results are tested for robustness from two further perspectives. They are analyzed in different environments assuming extreme factor levels at the border of all possibilities or assuming different knowledge distributions.

Table 1: Factor levels in experimental design

Scale	Factors	Low	Default	High
Ratio	Steps	30	**60**	90
	Agents	6	**12**	18
	Initial stocks	1	**2**	3
	Initial money	100	**200**	300
Nominal	Mechanism	{**CDA**, LMSR}		
	Strategies	{**ZI.EV**, N-ZI, Mix 1, Mix 2, ZIP}		
	Knowledge distributions	correct value of {0, **40**, 100}		

Table 1 shows the factors which are varied in a 3^k-experimental design. The 3^k- is chosen instead of a 2^k-experimental design. It allows choosing the low and high values linearly around the default value and

therewith systemizes the analysis of the results. As the model is mainly validated based on the experiment of Hanson et al. (2006), the default factor levels are chosen accordingly to the experiment as well. For example, the default number of agents is 12 and is able to reflect the corporate context with few active traders.

Exemplary Simulations

To introduce the simulation results, Figure 1 contains one exemplary simulation run for each mechanism. It depicts the prices achieved in both methods from the step 0 up to 100 within the default setup.
Figure 1 shows clear differences between the price development based on CDA and LMSR. While the price changes are small with LMSR (maximum of 3), the price changes with CDA range up to 42. Furthermore, the number of price changes is higher in LMSR (33) than in CDA (10). Therefore, the two exemplary simulations already give a first indication concerning H1 and H3.

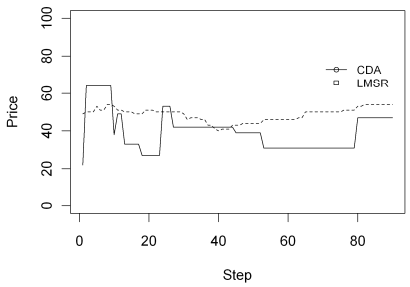

Figure 1: Exemplary simulation based on default model, e.g. a correct value of 40

Amount of trades

Strong support for hypothesis 1 can be found comparing the averages of the default setting, the averages over all 3^k settings and the averages for each 3^k setting in Table 2. Within the default setting, the LMSR achieves on average more than three times the trades than the CDA. Over all 3^k settings, CDA achieves more trades, but still using the LMSR results in nearly twice the amount of trades. It is obvious, that this result is also reflected in the winning settings, i.e. comparing in the 1215 settings the means of 100 runs for each mechanism (1215 times the mean of 100 runs with CDA and 100 runs with LMSR are compared). In 88.07% of the cases the LMSR has more trades. The majority of the cases against the hypothesis are driven by the ZIP-strategy (93 of 243 ZIP settings). Agents applying the ZIP strategy learn a price range. This might be too small to move the given prices of the LMSR, but it can be sufficient to exchange stocks at a constant price over a longer time period. As a reason for the higher amount of trades in LMSR one could argue the fact, that the LMSR steadily provides liquidity and therefore an execution of a trade is always possible. Furthermore, assuming there is just one ask and one bid, the CDA results in a maximum of one trade while the maximum in LMSR is two.

Table 2: Mean and winning settings with independent variable "amount of trades"

	default setting	3^k settings (robustness)	
	Mean trades	Mean trades	Win. settings
CDA	10.70	16.76	107
LMSR	34.95***	32.62***	1108***

Note. Two sided t-test for means and p-value assuming a probability of 50% for winning settings (p < .05. ** p < .01. *** p < .001)*

Summarizing, the effects on the amount of trades are high and the LMSR is superior in achieving a high amount of trades.
To understand the importance of the influence of the market mechanism, an ANOVA is conducted over all 3^k settings. As a result, the main effect "market mechanism" is the third largest effect in an ANOVA including all main and interaction effects. This shows that changing the market mechanism has an important influence on the amount of trades. The agent strategies have an even higher effect size due to the increased amount of trades in the presence of certain traders, e.g., random traders. However, the higher amount of trades due to random traders might not necessarily result in a better accuracy error. Finally, the R^2 of .917 is relatively high. This outlines that the amount of trades can be influenced easily by intentionally adapting the factors, e.g., by choosing LMSR instead of CDA.

Accuracy error

Hypothesis 2 has to be declined, because the expected advantage of LMSR cannot consistently be found in Table 3.

Table 3: Mean and winning settings with fixed factor levels and the independent variable "accuracy error"

		default setting	3^k setting (robustness)	
Fixed values		Mean acc. err.	Mean acc. err.	Win. settings
Default (none)	CDA	224.17	1326.82***	630
	LMSR	110.13***	1361.29	585
Strategy: Mix2	CDA	639.95	1920.93	32
	LMSR	113.90***	1440.95***	211***
Knowl.: CV0	CDA	1321.75***	1732.83***	290***
	LMSR	1792.71	1941.43	115
Knowl.: CV100	CDA	1691.58**	1880.51***	267***
	LMSR	1849.50	2023.47	138
Money: 300	CDA	227.45	1339.36	159
	LMSR	83.35***	1239.65***	246***

Note. Two sided t-test for means and p-value assuming a probability of 50% for winning settings (p < .05. ** p < .01. *** p < .001)*

While the default setting is advantageous for the LMSR, the mean over all settings is slightly documenting an advantage for the CDA. The comparison of the mean accuracy error of LMSR and CDA in all 1215 different settings further underlines the missing clear direction. The difference is not significant assuming each of the mechanisms to be superior with a probability of 50%. This result indicates the need for a more detailed analysis considering the interaction effects.

A selection of interaction effects including the "market mechanism" range upon the most important effects as documented in Table 4. This fact documents the importance of analyzing the interaction effects of the mechanism on the accuracy error as well. However, the knowledge distribution is the most important effect and more than ten times as large as the highest effect size including the "market mechanism". Beyond, the R^2 is lower than regarding the amount of trades. This is caused by two reasons. First, due to the lower R^2 the influence on the accuracy seems to be less straightforward than on the amount of trades. Second, the error is higher compared to the analysis in the prior subsection. As a result, one could argue that the knowledge distribution of Hanson et al. (2006) which has been applied in the simulation is too extreme. Therefore, this main effect can be seen as dominant compared to the other effects, which will be further analyzed in the robustness subsection.

Table 4: The main (on diagonal) and interaction effects with independent variable "accuracy error"

Effect size (accuracy error)	(1)	(2)	(3)	(4)	(5)	(6)	(7)
(1) Steps	.003						
(2) Knowledge distributions	.003	.552					
(3) Mechanisms	.003	.020	.001				
(4) Agents	.000	.002	.002	.000			
(5) Initial stocks	.000	.004	.001	.000	.000		
(6) Strategies	.009	.015	.033	.003	.000	.068	
(7) Initial money	.000	.013	.008	.000	.000	.002	.005

Note. Partial η^2 used as effect size; R^2= .589; 100 runs per 2430 combinations; For all effects >.000: p < .001.

Considering the three biggest interaction effects to analyze the results in more detail, the mechanisms show differing results. With the existence of some fully random traders (Mix 2 which includes ZIU), the LMSR has an advantage, because it lowers the maximum influence of each trader per trade. The LMSR can profit even more with a higher initial endowment of money (300), as the traders in LMSR need certain liquidity to move the price. Contrary, the CDA is advantageous assuming a knowledge distribution at the border of the possible values (correct value of 0 or 100). One reason is the market maker in LMSR which is partly holding the money while in CDA the cumulative money of all traders remains constant. Therefore, the range of possible actions is more restricted to some individual traders in LMSR than in CDA. This especially fits to extreme values, where more money is needed to move the price to the correct value.

Summarizing, the effects of the mechanisms on the accuracy error are less strong and more diverse than the effects on the amount of trades.

Standard deviation of the price

Strong support can be found for hypothesis 3. The standard deviation of the price in the default setting and over all 3^k settings is lower in LMSR as documented in Table 5. Comparing all settings, this holds for 93.09% of all cases which is the highest value of all comparisons. Here, 84 of 84 cases with an advantage for CDA are out of the 243 ZIP cases. Therefore, the learning capabilities of the ZIP traders seem to lower the standard deviation within the CDA. However, even in the ZIP case 65.43% of the cases have a lower standard deviation with the LMSR. The reason is the ability of the LMSR to reduce high price changes (maximum only 5 instead of 47) by determining the price based on all past trades instead of only the last one.

Table 5: Mean and winning settings with independent variable "standard deviation of price"

	default setting	3^k setting (robustness)	
	Std. dev. price	Std. dev. price	Superior settings
CDA	13.79	16.12	84
LMSR	2.17	6.74	***1131

Note. P-value assuming a probability of 50% for winning settings (p < .05. ** p < .01. *** p < .001)*

Robustness of results with different knowledge and extreme factor levels

Finally, at least two further robustness tests seem desirable. First, a robustness test with different knowledge distributions, i.e. less extreme distributions. Second, a robustness test with extreme factor levels as an alternative to the linearly chosen ratio-scaled factor levels. Here, very low factors levels are chosen, e.g., the amount of traders (2 instead of 6 agents) and the end of trading (5 instead of 30 steps) is lower.

Four alternative knowledge distributions are chosen. The first considers a higher diversity of knowledge among the traders and is adapted from a knowledge distribution used by Smith (1962). In this case, each agent has an expected value which differs to all other agents. The expected value of agent 1 is: 25, 2: 35, 3: 20, 4: 40, 5: 15, 6: 45. Here, 30 is assumed as correct value. The second knowledge distribution is a mirrored one with an expected value of 70. The third (fourth) is

adapted from Oprea et al. (2007) and provides 50% of the agents with an expected value of 20 (80) and 40 (60) with a correct value of 30 (70).
The results in Table 6 provide further support for the findings in the prior subsections. While hypothesis 1 and 3 are again supported, the results regarding hypothesis 2 are again ambiguous. The results regarding the interaction effects find further support as well.

Table 6: Summary of all results including the mean of all settings with alternative knowledge and extreme values

Hypothesis	Default	3^k	3^k (settings)	Alt. Knowl.	Extr. values
LMSR: Amount of trades	+	+	++	+	+
LMSR: Accuracy	+	-	o	+	-
LMSR: Mix 2 strategy	+	+	++	+	NA
CDA: CV 0 / CV 100	+	+	++	NA	NA
LMSR: 300 money	+	+	+	+	NA
LMSR: Std. dev.	+	+	+++	+	+

Note. - contrary to hypothesis; o neutral; + support for hypothesis

DISCUSSION AND CONCLUSION

As expected, the CDA and the LMSR result in different outcomes, e.g., the amount of trades is higher and the standard deviation of the price is lower in LMSR. This is due to the fact that the existence of a market maker increases the amount of trades. Two offers can result in a maximum of one trade in CDA, while 2 trades are possible in LMSR. Therefore, the LMSR shows fewer trades only in some exceptional cases. For example, the price movements allowed by LMSR may be too big to cover all possible offers. This might be the case with ZIP learning agents, which negotiate a very small price corridor. Second, the lower volatility is rooted in the fact that the LMSR considers past trades in the price calculation. High price changes in LMSR are not immediately possible and therefore less probable due to noise trading. The maximum price change in LMSR standard setting is 5 compared to 47 in CDA.
Interestingly, the accuracy error which can be seen as the most important evaluation criteria is influenced in a much less straightforward way. Here, the interaction effects with several factors are more important than the main effect. These interaction effects affect the accuracy error in different directions. Here, an important effect is the interaction effect including the strategy of the agent. Adding random traders to a prediction market can decrease the accuracy and decreases it less with LMSR. Another important interaction effect includes the knowledge distribution. While the LMSR has advantages with the default distribution and a correct value in the middle of the possible outcomes, it has problems with the two extreme outcomes. Liquidity issues of traders are one reason as they can prevent them from further participating in trading. Regarding the accuracy error, the mechanism is much less important than the knowledge distribution. This is straightforward as even a prediction market with the best mechanism still will suffer from bad knowledge. However, in a prediction market it is often much harder to influence the knowledge distribution among the participants than to choose a different mechanism.
Overall, the choice of a certain mechanism does clearly matter when drawing on the "wisdom of the crowds" (Surowiecki 2010) in prediction market and a tradeoff has to be considered when setting up such a market. Based on all simulations, the LMSR seems to be advantageous in most of the cases. Limiting the choices of the traders with LMSR seems to enhance the results. The advantage of the flexibility by CDA is only advantageous in the exceptional case of an extreme knowledge distribution. Therefore, the prediction market owner has the option to choose the CDA which gives the full freedom to the traders risking "no trades". In most of the cases this full flexibility seems to be a disadvantage compared to the steady liquidity and cumulative price building process of the LMSR.
Beyond, further factors can be influenced to enhance the accuracy of prediction markets and might direct further valuable laboratory experiments. With LMSR, the initial amount of money has to be decided as well. On the one hand, the cumulative initial money endowment over all participants should be higher than the maximum loss of the market maker. On the other hand, unlimited money endowment would not allow noise or manipulative traders to be sorted out and therefore should be avoided as well. With CDA, random traders can have a major influence. Therefore, an appropriate training of participants in a prediction market with CDA should be ensured.
Finally, limitations of our research have to be considered. A major limitation is caused by the limits of simulation. Therefore, the simulation results should be further validated by subsequent laboratory and field experiments. Furthermore, the mechanisms are compared under the consideration of constant agent strategies. Choosing the best mechanism should also be based on their understandability. If one of the mechanisms is not fully understood by human traders, the quality of the strategies might be lower. The simplicity as a major learning from market design research is also recognized by Roth (2008, p. 306). The LMSR has a smaller freedom in how to trade as only the market maker is allowed to place offers. Therefore, it is the more simple mechanism. Simplifying the options and strategies possibly leads to a simplified strategy choice. This effect might lead to better strategies and should further be considered in subsequent laboratory and simulation experiments.

ACKNOWLEDGEMENTS

We thank Robin Hanson, Ryan Oprea and David Porter for giving us access to the data of their experiment as well as participants of workshops in Groningen and Koblenz for valuable feedback.

REFERENCES

Boero R, Bravo G, Castellani M, Squazzoni F (2010) Why bother with what others tell you? An experimental data-driven agent-based model. *Journal of Artificial Societies and Social Simulation* 13 (3).

Bray D, Croxson K, Dutton W (2008) Information markets: feasibility and performance. Oxford Internet Institute DPSN Working Paper Series No. 10.

Chen K-Y, Plott C (2002) Information aggregation mechanisms: concept, design and implementation for a sales forecasting problem. Social Science Working Paper 1131. California Institute of Technology, Pasadena.

Cliff D, Bruten J (1997) More than zero intelligence needed for continuous double-auction trading. HP Technical Report. HP Laboratories, Bristol.

Duffy J, Ünver MU (2006) Asset price bubbles and crashes with near-zero-intelligence traders. *Economic Theory* 27 (3):537-563.

Forsythe R, Forrest N, George RN, Jack W (1992) Anatomy of an experimental political stock market. *American Economic Review* 82 (5):1142-1161.

Gilbert N, Troitzsch KG (2005) *Simulation for the social scientist*. 2nd edn. Open University Press, Maidenhead.

Gode DK, Sunder S (1993) Allocative efficiency of markets with zero-intelligence traders: market as a partial substitute for individual rationality. *Journal of Political Economy* 101 (1):119-137.

Grimm V, Berger U, DeAngelis DL, Polhill JG, Giske J, Railsback SF (2010) The ODD protocol for describing individual-based and agent-based models: a first update. *Ecological Modelling* 221:2760-2768.

Hansen J, Schmidt C, Strobel M (2004) Manipulation in political stock markets - preconditions and evidence. *Applied Economics Letters* 11 (7):459-463.

Hanson R (2003) Combinatorial information market design. *Information Systems Frontiers* 5 (1):107-119.

Hanson R (2009) On market maker functions. *The Journal of Prediction Markets* 3 (1):61-63.

Hanson R, Oprea R, Porter D (2006) Information aggregation and manipulation in an experimental market. *Journal of Economic Behavior & Organization* 60 (4):449-459.

Healy PJ, Linardi S, Lowery JR, Ledyard JO (2010) Prediction markets: alternative mechanisms for complex environments with few traders. *Management Science* 56 (11):1977-1996.

Ivanov A (2008) Electronic prediction markets, Analyx Reference Information.

Kleijnen J, Sanchez S, Lucas T, Cioppa T (2005) A user's guide to the brave new world of designing simulation experiments. *INFORMS Journal on Computing* 17 (3):263-289.

Klingert FMA (2012) *Prediction market mechanisms and manipulation: a multi-agent simulation based on experimental economics*. PhD thesis, Hamburg University of Technology, Hamburg, forthcoming.

Klingert FMA, Meyer M (2012) Effectively combining experimental economics and multi-agent simulation: suggestions for a procedural integration with an example from prediction markets research. *Computational & Mathematical Organization Theory* 18 (1):63-90.

Ledyard J, Hanson R, Ishikida T (2009) An experimental test of combinatorial information markets. *Journal of Economic Behavior & Organization* 69 (2):182-189.

Lorscheid I, Heine B-O, Meyer M (2012) Opening the 'black box' of simulations: increased transparency and effective communication through the systematic design of experiments. *Computational & Mathematical Organization Theory* 18 (1):22-62.

Oprea R, Porter D, Hibbert C, Hanson R, Tila D (2007) Can manipulators mislead market observers? Working Paper.

Othman A, Sandholm T Automated market-making in the large: the gates hillman prediction market. In: *Cambridge, MA*, 2010. ACM, pp 367-376.

Roth AE (2008) What have we learned from market design? *The Economic Journal* 118 (527):285-310.

Smith VL (1962) An experimental study of competitive market behavior. *The Journal of Political Economy* 70 (2):111-137.

Spann M, Skiera B (2003) Internet-based virtual stock markets for business forecasting. *Management Science* 49 (10):1310-1326.

Surowiecki J (2010) *The wisdom of crowds : why the many are smarter than the few*. Abacus, London.

Wolfers J, Zitzewitz E (2004) Prediction markets. *Journal of Economic Perspectives* 18 (2):107-126.

AUTHOR BIOGRAPHIES

FRANK M. A. KLINGERT is a Ph.D. candidate at the Institute of Management Control and Accounting at Hamburg University of Technology. Previously, he was employed in the enterprise performance management area at SAP headquarters in Walldorf. He studied computer science and information systems at the University of Koblenz-Landau in Germany and at the Leiden University in the Netherlands. His research interests focus on the linkages between computer and business sciences, e.g. multi-agent simulation and prediction markets.

MATTHIAS MEYER is professor of management control and accounting and director of the Institute of Management Control and Accounting at Hamburg University of Technology. He has a habilitation degree from WHU-Otto Beisheim School of Management in Koblenz and received 2003 his Ph.D. from the Ludwig-Maximilians-University in Munich/Germany with a dissertation on principal agent theory and methodology. He studied business administration, economics, philosophy and philosophy of science. His research interests include computer simulation, management control and accounting, institutional economics and methodology.

HIERARCHICAL CONSENSUS FORMATION REDUCES THE INFLUENCE OF OPINION BIAS

Nicolas Perony, René Pfitzner, Ingo Scholtes, Claudio J. Tessone, Frank Schweitzer
Chair of Systems Design
ETH Zurich
Kreuzplatz 5
8032 Zurich
Switzerland
Email: {nperony, rpfitzner, ischoltes, tessonec, fschweitzer}@ethz.ch

KEYWORDS

Opinion dynamics; Consensus formation; Bounded confidence; Hierarchical organisations; Opinion bias

ABSTRACT

We study the role of hierarchical structures in a simple model of collective consensus formation based on the bounded confidence model with continuous individual opinions. For the particular variation of this model considered in this paper, we assume that a bias towards an extreme opinion is introduced whenever two individuals interact and form a common decision. As a simple proxy for hierarchical social structures, we introduce a two-step decision making process in which in the second step groups of like-minded individuals are replaced by representatives once they have reached local consensus, and the representatives in turn form a collective decision in a downstream process. We find that the introduction of such a hierarchical decision making structure can improve consensus formation, in the sense that the eventual collective opinion is closer to the true average of individual opinions than without it. In particular, we numerically study how the size of groups of like-minded individuals being represented by delegate individuals affects the impact of the bias on the final population-wide consensus. These results are of interest for the design of organisational policies and the optimisation of hierarchical structures in the context of group decision making.

INTRODUCTION

Among the problems which apply to the dynamics of social organisations, one of the oldest and best-studied is that of collective decision making (see for example the early work of Black, 1948). The importance and the complexity of this problem become especially clear when considering the many instances in which groups made up of individuals with diverse opinions have to reach a common agreement, or *consensus*, on a particular question. Depending on the distribution of initial opinions and the propensity of individuals to adapt their opinion to that of others, consensus may eventually be reached or opinions within the group may polarise around a restricted number of distinct values, in which case the opinion space is said to be fragmented. The question of *if*, *when* and *where* in the opinion space a consensual agreement may emerge involves the study of the complicated interactions through which members of the group adapt their individual opinions. In other terms, an understanding is needed of the mechanisms by which social interactions between individuals may facilitate collective decision making processes. As argued for instance by Bonabeau (2009), one interesting aspect of such mechanisms is the fact that, under certain circumstances, they can alleviate the cognitive biases of individuals and thus result in better collective decisions. Naturally, depending on the type of individual biases present in the system, *how* consensus is formed strongly affects how pronounced this beneficial effect is. The goal of this paper is to study this question in the context of *hierarchical approaches to consensus formation*, i.e. like-minded individuals gathering and forming a *local* consensus. A single collective decision is then formed in a downstream process.

In order to address this question, we study how a simple proxy for a hierarchical decision process affects the influence of a systemic bias on the collective decision. Our work is applied specifically to a modelling context, based on the well-known bounded-confidence model, which has been widely used as a standard model of opinion dynamics with constrained interactions between agents (Krause, 2000; Deffuant et al., 2000; Dittmer, 2001; Hegselmann and Krause, 2002; Weisbuch et al., 2002; Weisbuch, 2004; Lorenz, 2007). This model posits a population of individuals interacting within a continuous opinion space. In a variation of this model, we introduce a systemic bias which uniformly affects individuals whenever they interact with each other. In the context of social systems, intuitive interpretations of this bias include for example the influence of predominant and highly-biased mass media, or the presence in a decision board of a strongly-opinionated member affecting the debate and inconspicuously steering the discussions. In our model, this influence increases the change in opinions of individuals when interacting with peers whose opinion is consistent with the bias. At the same time, it proportion-

Proceedings 26th European Conference on Modelling and Simulation ©ECMS Klaus G. Troitzsch, Michael Möhring, Ulf Lotzmann (Editors)
ISBN: 978-0-9564944-4-3 / ISBN: 978-0-9564944-5-0 (CD)

ally decreases the change in opinion of those individuals who interact with peers whose opinion is opposed to the bias. In the absence of any interactions, we assume that individual opinions are not affected by the systemic bias, thus resulting in a preservation of their *status quo* as long as no interactions take place.

In this particular setting, we study how a two-step decision process based on the bounded confidence model impacts the eventual consensus reached within the population. For this, we assume that groups of individuals – after they have come to a group-wise, semi-collective decision in a first phase of *bounded confidence* – are represented by an aggregate, *representative* individual which will then interact with all other group representatives during a second phase in an *unbounded confidence* regime. A straightforward interpretation of this two-step decision process is in terms of a delegate system in which like-minded individuals form consensus in groups and then let group representatives negotiate with each other.

A question that arises when considering processes of consensus formation is that of which consensus may be considered the optimal one. Here, we define optimal consensus as the true average of the initial individual opinions, or in other words the collective opinion that cumulatively requires the least change of opinions with respect to the initial state. This can be seen as the simplest democratic optimisation to a problem of finding a common agreement within a population. In this paper, we study in particular under which conditions hierarchical structures – as well as the social interactions bound to them – give rise to a collective decision that is closer to the *optimal consensus* than that of a population lacking such structures.

In the following section, we first provide a detailed description of the bounded confidence model as well as of the extension studied in this paper. We then present numerical results for different strengths of the interaction bias, as well as for different sizes and composition of initial groups forming local consensus in the first step of the two-step process. We finally interpret and discuss our results, and comment on their relevance for the field of collective decision making in scenarios in which it is needed to reach a consensus.

MODEL

The question of how groups or societies collectively reach decisions has recently gained much attention and valuable insights have been obtained, as illustrated for example by the work of Dyer et al. (2008, 2009). Approaches to model such collective phenomena however reach back as far as the early 1990s (Galam and Moscovici, 1991). It is well-known that hierarchical structures play a salient role in such situations and it has been investigated how such structures emerge from the group interactions (see for example the classic Bonabeau model Bonabeau et al., 1995, 1996). Here we do not focus on a study of the mechanisms by which hierarchical structures may emerge, but rather we assume a fixed hierarchical scheme in the decision making process (may it be imposed externally or as a result of social interactions), and study its influence on the eventual consensus decision reached among the individuals of a group.

The Bounded Confidence Model

In this paper we study an extension of the *bounded confidence model*. This agent-based model has been proposed independently by Hegselmann and Krause (Krause, 2000; Hegselmann and Krause, 2002) as well as Deffuant and Weisbuch (Deffuant et al., 2000; Weisbuch et al., 2002). It is suited for studying the dynamics of individual opinions in situations where agents interact to form collective opinions and, in certain cases, consensus (Lorenz (2007) provides a comprehensive review). Let us now introduce the general framework for a continuous bounded confidence model.

We consider a system composed of N individuals, each of which has a *continuous* opinion about a topic $x_i(t)$ defined in the interval $[0, 1]$, i.e. $x_i(t) \in [0, 1]$. Every individual at time t modifies their opinion according to

$$\frac{d}{dt}x_i(t) = \sum_{j=1}^{N} \kappa(x_j(t) - x_i(t))\ (x_j(t) - x_i(t))\,. \quad (1)$$

Here, the function $\kappa(\delta)$ determines the strength of interaction for two individuals whose opinions are at a distance δ. The model assumes that there is exchange of opinion only if the opinions of both individuals depart from each other *at most* a distance ϵ:

$$\kappa(\delta) = \zeta\, H(\epsilon - |\delta|), \quad (2)$$

where H is the Heaviside function, $H(\cdot) = 1$ if its argument is positive, zero otherwise. The parameter ζ is the strength of the interaction. It has been shown that the bounded confidence model displays a stationary state with $\sim\ [1/2\epsilon]$ clusters, if the initial condition is uniform in the unit interval (Deffuant et al., 2000; Ben-Naim et al., 2003).

Opinion Bias and Hierarchical Structure

In public decision making, the individuals may be subject to a bias in the opinion formation process. Such bias may be the result of internal conviction, media influence, or the preservation of their *status quo* (Galam and Moscovici, 1991). In this setting, is it possible that the election of representatives may alleviate the bias and make the population reach a consensus closer to the unbiased result? In order to answer this question, we extend the bounded confidence model to include opinion bias and a hierarchical scheme for the creation of representative agents.

There has been work on the hardening of positions when agents stick to their own opinion (Friedkin and Johnsen, 1990, 1999), and extensions of the bounded confidence model have been proposed to study the influence of heterogeneous confidence thresholds (Weisbuch

et al., 2003; Lorenz, 2007), but to our knowledge no studies have been done on the influence of an opinion bias in the bounded confidence model. Whilst the original Deffuant model (Deffuant et al., 2000) includes a convergence speed μ, or "cautiousness" parameter, and some work (Laguna et al., 2004; Assmann, 2004) showed that the role of this parameter goes beyond a mere time scaling of the convergence, no work has concentrated explicitly on the influence of this convergence speed, especially with regard to a possible asymmetric character for the convergence (which characterises the bias). Likewise, in spite of past empirical studies focusing on the impact of hierarchical structures (compared to egalitarian ones) in decision making processes (Edge and Remus, 1984), to our knowledge there is no analysis linking such considerations to a known opinion dynamics framework.

Our model works as follows: the initial population interacts in a bounded confidence scenario with an interaction threshold ϵ_1. Initially, the individuals opinions are drawn uniformly over the interval $[0, 1]$. There is an internal bias in the population that favours one of the two extreme opinions $\{0, 1\}$. In order to model this behaviour, the interaction term is given by

$$\kappa(\delta) = \begin{cases} \zeta & \text{if } 0 > \delta > \epsilon_1 \\ (\zeta + \sigma) & \text{if } -\epsilon_1 < \delta < 0 \end{cases}, \qquad (3)$$

where σ is the level of bias in the system. Under these conditions, the system is left to evolve for a time T_1, a time constant long enough to allow the system to reach the stationary state.

Then, the clusters of individuals who have reached the consensus internally are replaced by one individual, a *representative*, independently of the group size. The system size at this second stage is equal to the number of groups K formed in the first stage, and each representative has an initial state equal to the (local) consensus reached in the previous round. In this second stage, a new threshold for interaction $\epsilon_2 > \epsilon_1$ is selected. Here we always choose $\epsilon_2 = 1$. This condition is sufficient if one wants to make sure that one single consensus will be reached. This second stage in the dynamics constitutes what can be called *unbounded confidence*. Choosing instead a value of ϵ_2 such that $\epsilon_1 < \epsilon_2 < 1$ would be equivalent to considering a hierarchical decision making process including multiple (more than two) steps. As we concentrate here on the scenario where consensus need be reached eventually, the final value of the interaction threshold (here ϵ_2) has to be 1. In this second stage, the dynamics of the system is driven by the new threshold for interaction ϵ_2, and the model runs for a time T_2 until the final state is reached. It is important to note that the effect of the bias is still present in this level, as the representatives are also individuals, and as such also subject to the same conditions as the initial population. It follows that the dynamics of the representatives is given by

$$\frac{d}{dt} y_i(t) = \sum_{j=1}^{K} \kappa(y_j(t) - y_i(t)) \, (y_j(t) - y_i(t)), \qquad (4)$$

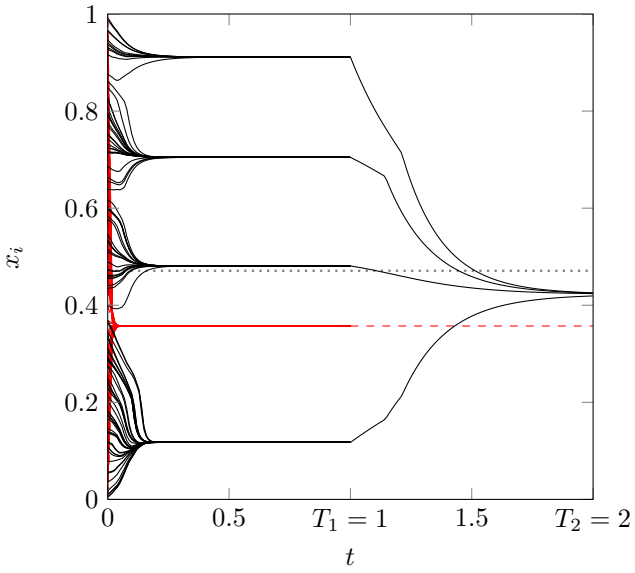

Figure 1: Illustration of the model's dynamics. Black lines represent a typical realisation of the hierarchical decision making model, with $N = 100$, $\epsilon_1 = 0.1, \epsilon_2 = 1$, $\sigma = 1$. These dynamics can be compared to the "best" possible decision, i.e. the initial average opinion X_0 (grey dotted line), and to the output of the non-hierarchical model (classical bounded confidence model, red dasehd lines). In each case, both the hierarchical and non-hierarchical realisations were computed with the same initial distribution $x_i(0)$, so as to avoid stochastic bias.

where the coupling is also given by Eq. 3.

Measures

In order to quantify the behaviour of the system, we first compute the initial average opinion of the population,

$$X_0 = \frac{1}{N} \sum_{i=1}^{N} x_i(0).$$

As developed above, X_0 is the *optimal consensus value*, as it minimises the cumulative opinion deviation of all the agents. We also measure the *final average opinion*, Y_2, computed over the final state of the representatives,

$$Y_2 = \frac{1}{K} \sum_{i=1}^{K} y_i(T_2).$$

Then, a measure for the *final error* $E_2(\epsilon_1, \epsilon_2)$ with respect to the initial opinion of the population is given by

$$E_2(\epsilon_1, \epsilon_2) = |Y_2 - X_0|.$$

In order to be able to assess the benefit of introducing a hierarchical structure (i.e. comparing the two-step with the one-step process), we compute the *quality ratio* of the final consensus state

$$G(\epsilon_1, \epsilon_2) = \frac{E(\epsilon_1, \epsilon_2)}{E(\epsilon_2, \epsilon_2)}.$$

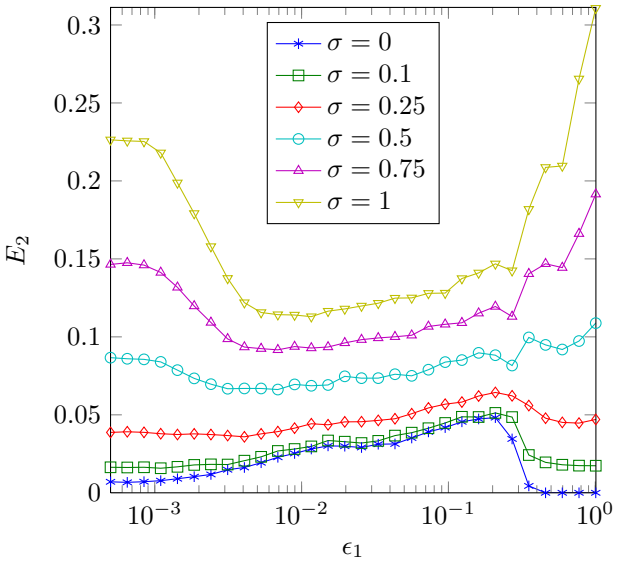

Figure 2: Error of the two-step decision model after the final consensus is reached: $E_2(\epsilon_1, \epsilon_2) = |Y_2 - X_0|$ (with $\epsilon_2 = 1$). Lower values of E_2 correspond to a higher accuracy of the final decision. For large enough values of σ, the error is minimised when local hierarchies are formed in the first phase, i.e. for intermediate values of ϵ_1. We used a population of $N = 100$ agents. In this figure and the following ones, we computed 1000 realisations of the decision process with different initial distributions and plotted the average value of the metric considered over all realisations.

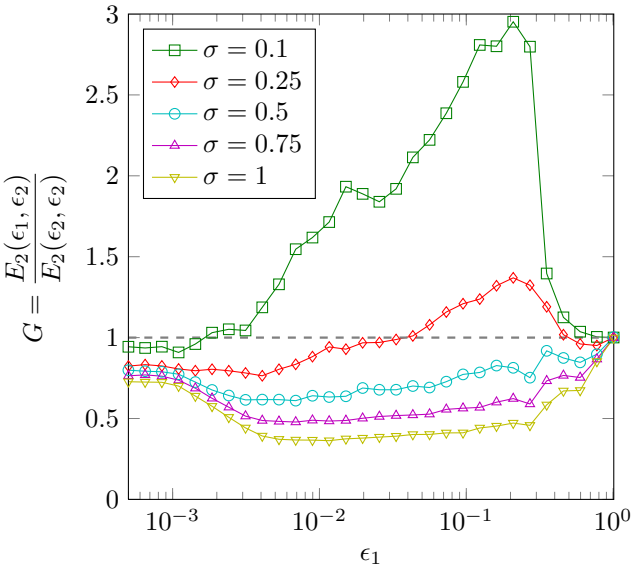

Figure 3: Quality ratio of the two-step decision model compared to the unbounded confidence model with equivalent parameters. The dashed line lies at a value of 1, which would amount to an equal performance (in terms of decision accuracy) of the step-wise and the unbounded confidence model. With $\sigma = 0$ and $\epsilon_1 \to 0$, $E_2 \to 0$ (the unbounded confidence model without opinion bias produces a final consensus that is optimal), and the values of G diverge, which is why $\sigma = 0$ is not included here. We used a population of $N = 100$ agents.

This metric is the ratio between the result achieved by means of the hierarchical process and that which would have been obtained in a fully-unbounded context.

Finally, we compute the total interaction, $\mathcal{H}_1$ and $\mathcal{H}_2$ (for the first and second stages of the process), as a proxy for the amount of opinion exchange. $\mathcal{H}_1$ and $\mathcal{H}_2$ are computed respectively as

$$\mathcal{H}_1 = \int_0^{T_1} dt \sum_{i=1}^{N} \sum_{j=1}^{N} \kappa(x_i(t) - x_j(t)),$$

and

$$\mathcal{H}_2 = \int_{T_1}^{T_2} dt \sum_{j=1}^{K} \sum_{j=1}^{K} \kappa(y_i(t) - y_j(t)).$$

It is worth mentioning that once consensus is reached in each stage, the interaction terms vanish. Hence if T_1 and T_2 are large enough, the final result does not change, and this measure is well-defined. The total exchange of opinion in the population, for the complete process, is then given simply by $\mathcal{H} = \mathcal{H}_1 + \mathcal{H}_2$.

RESULTS

Figure 1 illustrates the time evolution of the reputation of 100 agents, all subject to a strength of interaction $\zeta = 1$ and an opinion biased by the same factor ($\sigma = 1$) towards zero. It can be seen that a two-step decision process may in this case be beneficial, as it produces an eventual consensus that is closer to the optimal consensus X_0 than the one produced by the unbounded confidence model, under the same conditions. The final error, i.e. the distance between the optimal consensus and the final decision reached, is presented in Figure 2. We see that, logically, stronger values of the bias σ produce larger errors. However it is also interesting to note that, for sufficient values of σ, the error due to opinion bias is mitigated by the formation of non-trivial local hierarchies. We call non-trivial hierarchies those formed by a value of $\epsilon_1 \gtrsim \frac{1}{2N}$ (for lower values of ϵ_1 very few to no groups are formed in the first decision phase) and $\epsilon_1 \ll 1$ (if $\epsilon_1 \approx 1$, the step-wise model roughly amounts to the unbounded confidence model). Notwithstanding the positive effect of a hierarchical decision process at high values of σ, we also observe that under weaker opinion bias (e.g., $\sigma = 0.1$), the performance of the system is worse when forming local hierarchies ($\frac{1}{2N} \lesssim \epsilon_1 \ll 1$) than when using the classical unbounded confidence model, where all agents interact with each other.

The exact extent of this gain in decision accuracy (or lack thereof) is considered in Figure 3, where we compute the ratio of the final error E_2 in the two-step decision model over the error obtained from the unbounded confidence model, for the same parameters. An equal

performance of the two models would translate into values of this ratio G around unity. We find however a different picture, with the performance of the two-step decision process varying between consistently worse than the one-step decision process, or unbounded confidence model ($\epsilon_1 = \epsilon_2 = 1$) under low opinion bias, and always better (up to about 2.5 times better for $\sigma = 1$ and $\epsilon_1 \approx 10^{-2}$) under stronger opinion bias. This effect is of course only present for non-trivial hierarchies, and the decisional structure created by such a decision making model can be assessed from Figure 4, where K_1 represents the number of local decision clusters formed at the end of the first phase of decision making; it can also be said that $\frac{K_1}{N}$ is the average number of agents whose opinion is aggregated and represented for by each representative in the second phase. In the population of 100 agents we consider, the optimal gain in decision accuracy is found in the range $10^{-2} \leq \epsilon_1 \leq 10^{-1}$. This amounts to each representative being "elected" by a group of 3 to 30 agents at the end of the first phase.

In the Discussion section, we comment on the importance of the cumulated strength of interaction between agents for the influence of the bias on the eventual consensus reached. Figure 5 shows both $\mathcal{H}_1$, $\mathcal{H}_2$ (see Measures), as well as their sum. We observe that a stronger bias logically results in a higher cumulated strength of interaction, thereby driving the curves of $\mathcal{H}_1$ and $\mathcal{H}_2$ downwards for increasing σ in our example, where the bias drives all opinions toward zero. We observe that for low values of ϵ_1, very few interactions take place in the first decision phase and most happen in the second phase (if few or no clusters are formed before T_1, the second phase will involve most of the convergence toward consensus, hence $\mathcal{H}_1 \ll \mathcal{H}_2$. Conversely, at high values of ϵ_1, a global consensus is found even before T_1 and we observe $\mathcal{H}_1 \gg \mathcal{H}_2$. Of more interest is what happens between those two regimes; as explained in the Measures section, the total exchange of opinion within the population during the decision making process (i.e. the total influence of the opinion bias) is expressed by the sum $\mathcal{H} = \mathcal{H}_1 + \mathcal{H}_2$. We observe that this sum finds its minimum (in absolute value) in the region where ϵ_1 allows for the formation of non-trivial hierarchies. This not only supports our insights on the minimisation of interactions for decision accuracy, but also provides interesting insights into the optimal hierarchical decision structure needed to reach an optimal consensus under strong opinion bias.

DISCUSSION

The results presented in the previous section show that, at least in the situations and under the assumptions considered in this paper, a two-step consensus formation reduces the impact of an opinion bias on the eventual consensus reached by a group through active interaction, and thus improves the overall quality of distributed decision making processes. In the following, we have a deeper look at why this is the case and what conclusions one can

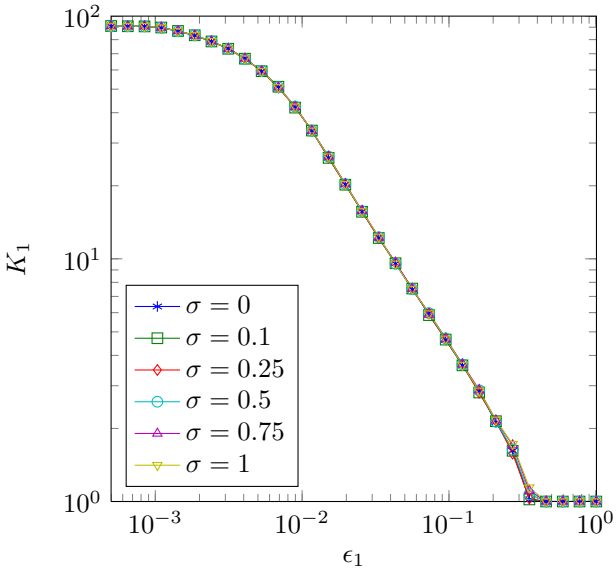

Figure 4: Number of clusters formed at $t = T_1$, the end of the first decision phase. We used a population of $N = 100$ agents. Because the initial distribution of opinions is subject to stochastic fluctuations, even at low values of ϵ_1 a few local clusters form and K_1 never reaches N. $\frac{K_1}{N}$ is also the average number of agents that "elected" a given representative in the second phase.

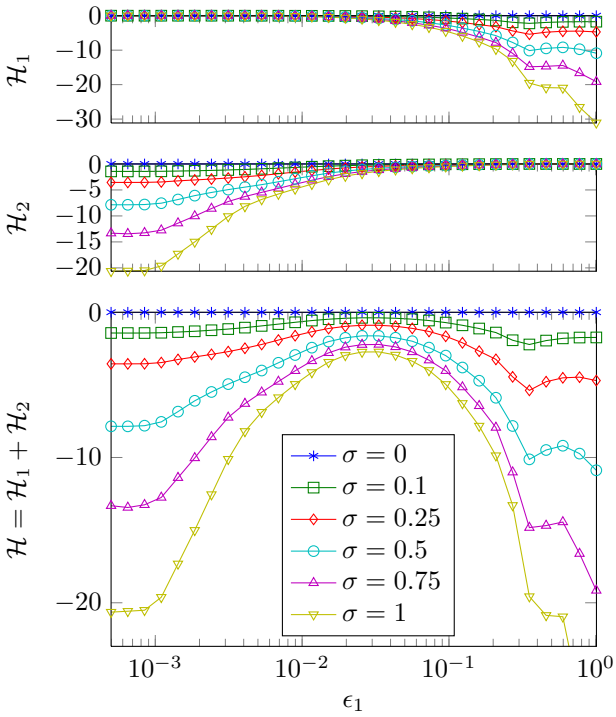

Figure 5: Cumulative integration strength in the first decision phase $\mathcal{H}_1$ (top), in the second decision phase $\mathcal{H}_2$ (middle), and the sum of both (bottom panel). We used a population of $N = 100$ agents.

draw from these results.

We first recall that the systemic bias σ considered in our model only affects opinion convergence when individuals interact, based on their given distance threshold ϵ_1 or ϵ_2 (depending on which phase of the decision process we are in). As such, the total bias present in the eventual collective decision depends on the number of interactions that can take place based on the confidence interval. Due to the fact that – in case an interaction actually takes place – the bias σ is multiplied by the difference of opinions (see Equation 1), the bias present in the eventual decision further depends on the differences in the opinions of interacting agents. In particular, this means that the final bias also depends on the time needed for the opinions to converge. Based on this, an interpretation of our results is that in situations where a bias coupled to interactions negatively affects the quality of the eventual collective decision, a hierarchical decision process as studied in this article provides an optimal tradeoff in terms of the cumulative interaction necessary to reach consensus and the total bias introduced in the process of decision making. This, however, only holds for strong opinion bias, as discussed below.

To underpin this interpretation of our results, we have measured the *cumulative interaction* $\mathcal{H}$ taking place during both steps of the hierarchical consensus formation process. Intuitively, $\mathcal{H}$ integrates the number of interactions as well as the cumulative opinion change subject to the systemic bias over time. In general, since each interaction introduces a bias, a minimisation of $\mathcal{H}$ under the constraint that a single collective decision still emerges should minimise the final deviation from the optimum value. $\mathcal{H}_1$ and $\mathcal{H}_2$ – which measure the cumulative interactions in step one and two of the hierarchical process, respectively –, as well as $\mathcal{H}$ – which sums the interaction in both steps – are shown in Figure 5 for different values of the confidence interval ϵ_1. One observes in the top panel of Figure 5 that, during the first phase of the two-step process, virtually no interaction takes place for small confidence intervals $\epsilon_1 < 10^{-1}$. Figure 4 shows that this results in many small clusters being represented by many representative agents in the second step of the two-step process. As shown in the middle panel of Figure 5, this leads in turn to a large amount of cumulative interactions (in absolute terms) during the second phase of the process, and thus to a large bias in the collective decision. Only for an intermediate regime ($10^{-2} \leq \epsilon_1 \leq 10^{-1}$, bottom panel of Figure 5) are cumulative interactions (and thus the bias introduced) minimised, thus resulting in a low error.

A very important result can be seen in Figure 2, for small values of the opinion bias σ. In this setting, the final error E_2 for intermediate values of the parameter ϵ_1 is actually larger than in the unbounded confidence context. The reason for this effect is that the formation of the hierarchy causes the system to lose part of its averaging power. This can be seen as a mitigation of the "wisdom of crowds" effect (Surowiecki, 2004): indeed, when K groups are formed in the first stage, each group is composed of roughly $\sim N/K$ individuals. If this number is small, the local average of each group is subject to large fluctuations. A similar argument can be used if the number K is small. Interestingly, a strong enough bias can counterbalance this effect, in the sense that the bias introduced by each interaction outweighs these finite-size fluctuations.

CONCLUSIONS

In this paper we have used a standard model of collective opinion dynamics as a basis to study whether hierarchical consensus formation can improve the accuracy of a distributed decision making process, in which each interaction is subject to a bias, which can be seen as the effect of media on the population, or more generally as a common source of polarised influence on all the individuals.

Our findings show that the strength of the bias may lead to different results with respect to whether hierarchical consensus formation leads to better collective decisions in terms of the final deviation from the true average. For a small bias, the reduction of interactions that is due to the hierarchical organisation may turn out to be detrimental in terms of an increased error. For strong biases, we find that a hierarchical decision structure is always better, with an optimum value for the confidence threshold which is independent of the bias strength.

These results foreshadow several possible extensions of this work; one is to study how these results depend on the population size. For larger systems, it is important to address how many levels the hierarchy should comprise in order to maximise the benefits of a hierarchical decision making structure (multiple-level hierarchies can have non-trivial implications, as underlined for example by Galam and Wonczak (2000) in a slightly different context). In this generalised setting, the relation between a level l in the hierarchy and the corresponding ϵ_l should be discussed. Furthermore, in this work we have considered an exogenous bias. It would be interesting to study the role of an endogenously generated bias, by linking the bias with the current average opinion of the population. In this scenario, there would likely be a self-reinforcing dynamics that amplifies small initial opinion fluctuations in the population. Another possible extension could be to consider a non-uniform response to the bias depending on the location of an individual in the opinion space, related to the asymmetric confidence introduced by Hegselmann and Krause (2002). This would allow a more realistic study of opinion dynamics when influenced by an extremist minority, which finds direct applications in voting scenarios. To the best of our knowledge, such extensions have not been considered from the point of view of hierarchical decision making structures. Additionally, a certain level of analytical reduction is possible with the bounded confidence model (Hegselmann and Krause, 2002; Lorenz, 2007); further investigation could focus on an analytical treatment of the model presented here in or-

der to obtain general results on the usefulness of electing representatives in the context of consensus formation under opinion bias.

In summary, we have studied the influence of social interactions and hierarchical structures on the quality of group decision making processes. The problem of consensus formation in heterogeneous populations and under diverse conditions is a very topical, which is the focus of active research at the moment (Conradt and Roper, 2005; Dyer et al., 2008, 2009; Couzin et al., 2011). Whilst in this paper we focused on a very specific scenario and limited the analysis to a single (albeit standard) model, we explored a direction that to our knowledge had remained hitherto uncharted and we expect that future studies on the topic will follow this first step. In general, we think that work along this line of research is crucial for a substantiated understanding of collective decision making.

REFERENCES

Assmann, P. (2004). Monte carlo simulation of deffuant opinion dynamics with quality differences. *International Journal of Modern Physics C*, 15(10):1439–1447.

Ben-Naim, E., Krapivsky, P., and Redner, S. (2003). Bifurcations and patterns in compromise processes. *Physica D: Nonlinear Phenomena*, 183(3-4):190–204.

Black, D. (1948). On the rationale of group decision-making. *The Journal of Political Economy*, 56(1):23–34.

Bonabeau, E. (2009). Decision 2.0: The Power of Collective Intelligence. *MIT Sloan Management Review*, 50(2):45–52.

Bonabeau, E., Theraulaz, G., and Deneubourg, J. (1995). Phase diagram of a model of self-organizing hierarchies. *Physica A: Statistical and Theoretical Physics*, 217(3-4):373–392.

Bonabeau, E., Theraulaz, G., and Deneubourg, J. (1996). Mathematical model of self-organizing hierarchies in animal societies. *Bulletin of mathematical biology*, 58(4):661–717.

Conradt, L. and Roper, T. J. (2005). Consensus decision making in animals. *Trends in ecology & evolution*, 20(8):449–56.

Couzin, I., Ioannou, C., Demirel, G., Gross, T., Torney, C., Hartnett, A., Conradt, L., Levin, S., and Leonard, N. (2011). Uninformed individuals promote democratic consensus in animal groups. *Science*, 334(6062):1578–1580.

Deffuant, G., Neau, D., Amblard, F., and Weisbuch, G. (2000). Mixing beliefs among interacting agents. *Advances in Complex Systems*, 3(1-4):87–98.

Dittmer, J. (2001). Consensus formation under bounded confidence. *Nonlinear Analysis*, 47(7):4615–4622.

Dyer, J. R., Ioannou, C. C., Morrell, L. J., Croft, D. P., Couzin, I. D., Waters, D. a., and Krause, J. (2008). Consensus decision making in human crowds. *Animal Behaviour*, 75(2):461–470.

Dyer, J. R. G., Johansson, A., Helbing, D., Couzin, I. D., and Krause, J. (2009). Leadership, consensus decision making and collective behaviour in humans. *Philosophical transactions of the Royal Society of London. Series B, Biological sciences*, 364(1518):781–9.

Edge, A. and Remus, W. (1984). The impact of hierarchical and egalitarian organization structure on group decision making and attitudes. *Developments in Business Simulation & Experiential Learning*, 11:35–39.

Friedkin, N. and Johnsen, E. (1990). Social influence and opinions. *Journal of Mathematical Sociology*, 15(3-4):193–206.

Friedkin, N. and Johnsen, E. (1999). Social influence networks and opinion change. *Advances in Group Processes*, 16(1):1–29.

Galam, S. and Moscovici, S. (1991). Towards a theory of collective phenomena: consensus and attitude changes in groups. *European Journal of Social Psychology*, 21(1):49–74.

Galam, S. and Wonczak, S. (2000). Dictatorship from majority rule voting. *The European Physical Journal B-Condensed Matter and Complex Systems*, 18(1):183–186.

Hegselmann, R. and Krause, U. (2002). Opinion dynamics and bounded confidence: models, analysis and simulation. *Journal of Artificial Societies and Social Simulation (JASSS)*, 5(3).

Krause, U. (2000). A discrete nonlinear and non-autonomous model of consensus formation. In Elyadi, S., Lada, G., Popenda, J., and Rakowski, J., editors, *Communications in Difference Equations*, pages 227–236. Gordon and Breach.

Laguna, M., Abramson, G., and Zanette, D. (2004). Minorities in a model for opinion formation. *Complexity*, 9(4):31–36.

Lorenz, J. (2007). Continuous opinion dynamics under bounded confidence: a survey. *International Journal of Modern Physics C*, 18(12):1819–1838.

Surowiecki, J. (2004). *The Wisdom of Crowds*. Anchor.

Weisbuch, G. (2004). Bounded confidence and social networks. *The European Physical Journal B-Condensed Matter*, 343:339–343.

Weisbuch, G., Deffuant, G., Amblard, F., and Nadal, J. (2003). Interacting agents and continuous opinions dynamics. *Heterogenous Agents, Interactions and Economic Performance*.

Weisbuch, G., Deffuant, G., Amblard, F., and Nadal, J.-P. (2002). Meet, discuss, and segregate! *Complexity*, 7(3):55–63.

AUTHOR BIOGRAPHIES

NICOLAS PERONY, RENÉ PFITZNER, INGO SCHOLTES, CLAUDIO J. TESSONE, and **FRANK SCHWEITZER** are quantitative scientists with various backgrounds (from engineering to statistical physics via biology and computer science). The personal web page of their group is at `http://www.sg.ethz.ch`.

INVESTIGATION OF COGNITIVE NEIGHBORHOODSIZE BY AGENT-BASED SIMULATION

Jens Steinhoefel
Frauke Anders
Dominik Kalisch
Hermann Koehler
Reinhard Koenig
Chair for Computer Science in Architecture
Bauhaus-University Weimar
Belvederer Allee 1, 99421 Weimar, Germany
E-mail: jens.steinhoefel, frauke.anders, dominik.kalisch, hermann.koehler, reinhard.koenig@uni-weimar.de

KEYWORDS:
urban planning, social sustainability, segregation, neighborhood, agent-based simulation

ABSTRACT

Different social groups tend to settle in different parts of cities leading over time to social segregation. Neighborhood obviously plays an important role in this process – and what constitutes neighborhood is a cognitive notion. In segregation analysis neighborhood borders are often drawn arbitrarily or simple assumptions are used to weight neighbor influences. Some authors have developed ideas to overcome such approaches by more detailed models. In this work we investigate the size of a cognitive neighborhood on the base of a continuous, geographically unlimited definition of neighborhood, using a distance-dependent function as such neighborhood "size" definition. We use agent-based simulation of the choice of residence as our primary investigation tool. Tobler's first law of geography tells us that close things are more related than far ones. Extrapolating this thought and applying it to the question discussed here one could expect that closer neighbors have – on their own and in sum – more influence than those living further apart. The "sum" in the last sentence would lead to a neighborhood weighting of less than the inverse square of distance. The results of this investigation confirm that this is the case.

INTRODUCTION

The population of a city is not equally distributed, but tends to segregate according to the different characteristics of the inhabitants and the areas in the city. That means different inhabitants *tend* to live in different areas. Segregation plays an important role in city planning and in many cases it is deemed negative. Urban planners try to maintain a state of social sustainability in urban areas, which in very short words means that the mixture of different inhabitants should not exceed certain threshold values. In particular, planners try to avoid clusters of socially underprivileged people because the real world has shown that such areas evolve in a negative way in many respects, e.g. crime.

Cities are living and ever-changing entities. Most things to be found in cities are the result of some kind of human-driven process or processes. Urban planners try to control these processes to some degree, but from today's point of view, these will probably never be fully predictable. The work presented in this paper aims to contribute towards a better understanding of segregation as one important process in a city.

RESEARCH QUESTION

We assume that segregation in a city is the result of a long-lasting process of choice of residence by the inhabitants. Every place of residence exists within a neighborhood (a collection of places with relevant characteristics), and the neighborhood plays an important role in the choice of residence. According to Tobler's first law of geography (Tobler 1970) close things are more related than those that are far apart. Accordingly, the far neighborhood should be less important for the choice of residence than the one close by. The question we ask here is how distance-dependent this importance is. In other words we try to find a distance-dependent function that allows us to mathematically weight the distant neighborhood against the one close by for the choice of residence.

STATE OF THE ART

Methods for the numerical measuring of segregation from the 1950s are still significant today (Duncan & Duncan 1955). The corresponding calculations are now a standard procedure used by official statistics in many countries. A next important step was the introduction of entropy-based segregation indices in the 1970s (Theil 1972), which are used in this work.

A milestone in the explanation of the causes of segregation was the work of Schelling in the 1970s (Schelling, 1978), who used agent-based simulations. He demonstrated that feedback effects can play a significant role in segregation. The detection of these effects is naturally difficult using static statistical methods (non-dynamic, not regarding time lapse). Static statistical methods for correlating segregation with other factors are now standard tools in administrative practice.

Proceedings 26th European Conference on Modelling and Simulation ©ECMS Klaus G. Troitzsch, Michael Möhring, Ulf Lotzmann (Editors)
ISBN: 978-0-9564944-4-3 / ISBN: 978-0-9564944-5-0 (CD)

Researchers increasingly use simulations, see e.g. Feitosa et. al. (2007) and Crooks (2010). In this paper we follow the simulation approach of Schelling. Further direct predecessors of this paper, who also follow the basic idea of Schelling, are Benenson (1998), Benenson and Omer (2002) and the Circle City model in Koenig (2010).

Geographic Information Systems (GIS), which allow the provision of high-resolution digital data, are used on a regular basis as a tool in segregation analysis today. Until now, raster-based GIS/raster-based spatial simulation systems are used by researchers, for example in Feitosa et. al. (2007), Laurie and Jaggi (2003), Fosset and Waren (2005). Crooks (2010), however, proposed the application of vector-based systems, which is the method used in the present work.

Various authors have asked questions about the influence of neighborhood size on the outcome of segregation models (Wasserman and Yohe 2001, Laurie and Jaggi 2003, Crooks 2010). They have noted that an increasing neighborhood size (more generally: an increasing weight of far neighbors) results in stronger segregation effects, like the value of a segregation index or the size of segregation cluster areas.

In Benenson & Omer (2002) the authors emphasize that segregation measures are dependent on the settlement unit (city, borough, district, block, etc.) used for their calculation, and can differ significantly according to the selected scale for the same data used. They therefore investigate the question of how large the environment is that people perceive as their neighborhood, which would be best suited for the description of residential segregation. Voronoi polygons are used to define neighborhoods at various levels (level 1: direct neighbors, level 2: direct neighbors of the direct neighbors, etc.). This discrete approach of neighborhood definition is further developed in the present work to a continuous approach.

RESEARCH APPROACH

Segregation is a time-dependent process and there are many decision makers – the people who choose a residence. Using agent-based simulation as an investigation tool is therefore an obvious choice and in this respect we follow Schelling's approach. The nice thing about agent-based simulation is the simplicity of modeling it allows to explain complex phenomena.

These two levels we use here, too. The phenomenon we try to explain is segregation. In the (agent-based) simulation model we need some kind of social submodel for the inhabitants and an infrastructure submodel for the environment they live in (the city) along with status transition rules to run the simulation. These rules involve the social and the infrastructure submodel and need to incorporate the aforementioned distance-dependent weighting function. Using this simulation model we try to reproduce a given segregation scenario by optimizing the weighting function.

SOCIAL SUBMODEL

To measure segregation it is necessary to define certain differences between the inhabitants. A common approach is to divide the inhabitants into groups. We use the sinus milieus of Sinus Sociovision GmbH, Heidelberg, Germany. These milieus divide the inhabitants into ten groups, which serve as the base of the social submodel. An overview of the milieus can be found in figure 1.

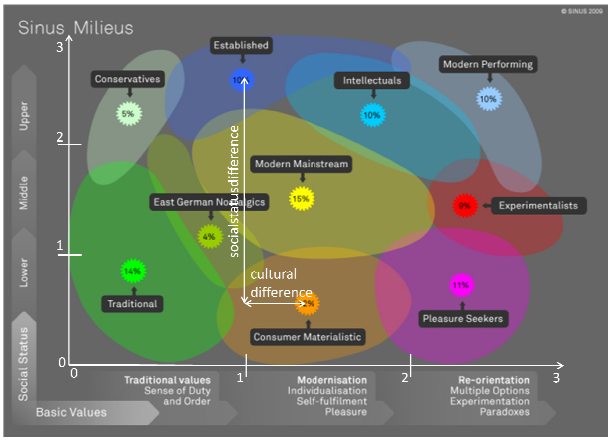

Figure 1: Sinus Milieu Diagram (after a figure by Sinus Sociovision GmbH) / Measuring the Differences of two Milieus

As shown in figure 1 the definition of these groups takes into account the social status (income etc.) and the cultural orientation, visualized by basic values. Each group (=milieu) covers a certain area in the milieu space. The rather small overlapping areas do not play a role in this work as described later.

The basic social entity we care for in the social submodel is the household. Every household belongs to a certain milieu, which never changes in the simulation. For simplicity, a household has no other attributes such as number of members, age etc.

INFRASTRUCTURE SUBMODEL

The infrastructure model consists of the road graph of the city and buildings with a certain number of dwellings. Each building is connected to the road graph as shown in figure 2.

The road graph does not change during the simulation. Again, for simplicity, we use only one feature of the road graph: the distances between every pair of buildings, which are measured along the road graph. These distances are calculated using a variant of the well-known Dijkstra algorithm before the simulation runs.

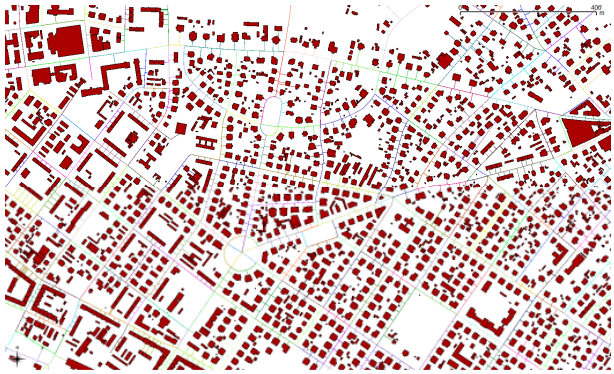

Figure 2: Infrastructure Model: Buildings connected to the Road Graph of the City

TRANSITION RULES

The matter of this work is segregation, which is caused by repeated choice of residence. Because the households themselves don't change during the simulation, transition rules only need to determine the choices of residence and nothing else.

As stated above (see RESEARCH QUESTION), in the approach used here every choice of residence taken by a household is based on the neighborhoods of the potential new residence locations (free dwellings, not occupied by a household). The neighborhood of a dwelling is defined by all the neighbors of that dwelling, and these are all households in the city. The rating of each neighborhood is accordingly based on the ratings of all neighbors.

To be of use for the choice of residence by a household the neighbors need to be rated differently. The phenomenon of segregation as observed in real cities shows that this is the case and that people tend to live with similar people more than they do with different people.

The authors have developed a neighbor rating based on the Sinus milieu diagram in a pragmatic way. This rating is arbitrary and based on nothing else than general rules which in the opinion of the authors feel right and are plausible and, again, the criterion of simplicity.

The general neighbor rating rules are as follows:
(R1) Regarding just the "Basic Values" (cultural axis) of the milieu diagram (see figure 1 above), every household wants to live with neighbors who are as close as possible in the diagram.
(R2) Regarding just the social status axis every household wants to live with neighbors slightly above its own position in the milieu diagram.

To operationalize these rules, the neighbor rating is again broken down into a cultural (neighbor) rating and a social status (neighbor) rating. The milieu diagram was overlaid with a coordinate system with coordinate value ranges of [0..3] for each axis. The cultural and social status differences between the milieus have been measured using this coordinate system. To be able to measure these differences every household needs to have a position in the milieu diagram. In the given segregation scenario, the milieu (group) of a household is known, but not its position in the milieu diagram. Therefore the position of the centroid of each milieu area was used as the position of all the households belonging to this milieu. Figure 1 illustrates the statements of this paragraph.

The differences measured have to be turned into cultural and social status rating values for a neighboring household.

For the cultural rating the following function is used: the rating value is 1 (the maximum) when the cultural difference is 0, and the rating value is 0 (the minimum), when the cultural difference is +3 or -3. For all other cultural differences the values are interpolated piecewise linear as shown in figure 3.

To apply the "slightly above" statement in neighbor rating rule (R2), a different piecewise linear function is used as social status rating. See figure 3. Notably the maximum rating value of 1 is not reached at a social status difference of 0, but for a small positive difference (0.25).

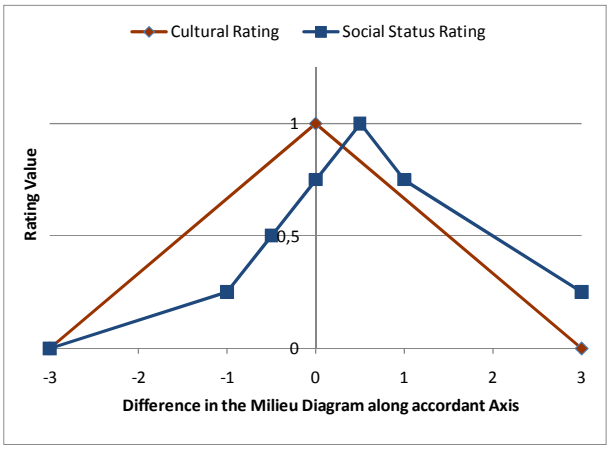

Figure 3: Rating Functions for Cultural and Social Status Differences

The rating value for a neighbor of a certain milieu is calculated by adding the cultural and social status rating values vectorially in a Cartesian coordinate system. The value range of the neighbor rating is therefore [0..1]. Because there are 10 milieus and every milieu is rated by every milieu, a 10 x 10 matrix of possible neighbor rating values results.

To calculate a neighborhood rating, all the neighbor ratings are incorporated into a weighted mean value.

The weight w is the inverse of distance *d* exponentiated by a fixed exponent *E*:

$$w = 1/d^E \text{ (F1).}$$

The final neighborhood rating function is

$$r_{nbh} = \frac{\sum r_{nb}/d^E}{\sum 1/d^E} \text{ (F2)}$$

over all neighbors with r_{nb} as the rating for a single neighbor.

The simulation is run in discrete time steps. The neighborhood ratings for all dwellings are calculated first and then stay fixed for that time step. The agents in the simulation can act in the following ways:
(A1) A household leaves the city. This happens spontaneous by a fixed leave probability.
(A2) A household tries to move to a free dwelling with a better neighborhood rating. If one is available the household moves. All free dwellings in the city are considered.
(A3) New households try to move into the city. A new household occupies the best dwelling it can get, if one is available. If not, the household is withdrawn from the simulation. The number of new households is determined by a truncated Gaussian distributed probability with fixed parameters (derived from an input mean).

A number of parameters such as minimum neighborhood rating of the current dwelling before moving, minimum improvement of the neighborhood rating of the potential new dwelling compared with the current dwelling and others could be removed during the development of the simulation in order to simplify it without damaging the reproduction quality.

SEGREGATION SCENARIO REPRODUCTION

The segregation scenario reproduction quality is measured using a segregation index. The Information Theory Index *H* first published by Theil (1972) has been chosen for this purpose. Other indices could have been employed, but most of them are highly correlated (Massay and Denton 1988), and this one has nice properties. It is widely accepted, well investigated, has a fixed value range of [0..1] and allows for the calculation of a single segregation value for the whole city for any number of groups.

Segregation index values are calculated for the given segregation scenario (target value) and after every step (including the final step) of a simulation run. The reproduction is considered better the smaller the difference to the target value is.

Because segregation indices are fairly dependent on the base unit used for their calculation (Benenson and Omer 2002) we have chosen two quite different ones, the road segment as a quasi one-dimensional base unit and the building block (a couple of buildings surrounded but not divided by a road) as a two-dimensional base unit.

USED DATA

To run the simulation the following data is necessary:

- a dataset containing the building entities including the number of dwellings in each building
- a road graph of the city including geometrical connections to the buildings
- a given segregation scenario containing the milieu of the household for all occupied dwellings

For the simulation runs carried out for this paper we used data from the city of Dresden Town Planning Authority, and from the company Microm GmbH. The building connections have been derived from the road graph and geometrical building data provided by the city of Dresden. The Microm data is the base for the list of buildings, the number of dwellings and the given segregation scenario.

The used dataset contains about 250,000 households living in about 50,000 buildings.

TECHNICAL NOTES

The simulation program was developed using C# in a Windows environment. For the most time-consuming parts of the simulation program native libraries and system functions are used. The main simulation computers were 4- and 8-core Intel XEON machines with 64GB RAM, of which about 40GB are used at program start. Simulation run times were between 1 hour and 10 days for a single run.

THEORETICAL EXPECTATIONS

Extrapolating Tobler's first law of geography and applying it to the question discussed here one could expect that for the choice of residence:
(S1) A close neighbor has more influence than a far one.
(S2) Close neighbors in sum have more influence than the far ones in sum.

The authors of this paper would expect the "sum" statement (S2) to be true from personal and professional experience, considering that everyone in the world has more far than close neighbors.

To express the "more influence" statements (S1) and (S2) in a mathematical way we develop now a continuous city model. This model is derived from the city model used for the simulation by further simplification.

In a first step we assume equally distributed inhabitants living in buildings connected by a uniform grid road graph. Consequently, the city looks the same everywhere. In a second step we abstract further to

obtain a continuous inhabitant distribution with no roads at all. One could imagine such a city as a large plate with the inhabitants like a thin film of water on it, and the inhabitants like water molecules can move in it without any roads. The distance between two dwellings or points is then just the Euclidean distance.

The research aim is to find a distance-dependent weighting function. The approach used is to optimize parameter E in formula (F2). The question in this chapter is what values of E are to be expected. To investigate this we look at the influence of different neighbors on a neighborhood rating calculated by (F2). We use the continuous city model described above.

Looking at (F2) one sees that the denominator $\sum 1/d^E$ is a constant for a given neighborhood and a given distance exponent E. For the influence investigation this is of no interest. In the remaining nominator $\sum r_{nb}/d^E$ we abstract from different r_{nb} (e.g. setting them all to 1). The remaining formula for the influence of a group of neighbors is $\sum 1/d^E$.

The influence of a single neighbor is just the weighting function $w = 1/d^E$. To fulfill influence statement (S1) that a close neighbor should have greater influence than a far one, w must decline as d grows, and therefore E must be chosen to be greater than 0, even if only slightly (e.g. 0.01).

To look at groups of close and far neighbors we can draw virtual distance circles with increasing radii around a dwelling in the continuous city model. The (differentially small) number of neighbors living on the same circle at distance d is $2 \bullet \pi \bullet d$, while their summated influence is $2 \bullet \pi \bullet d/d^E$

Influence statement (S2) applied to these circles means the influence of a close circle has to be greater than that of a far one. For E = 1 the influence of all circles is equal, so E must be chosen to be greater than 1, even if only slightly (e.g. 1.01). The same holds true for laminar rings of constant width instead of the circles. E.g. all neighbors within a distance of 300-600 meters have the same (E=1) / a greater (E > 1) influence than those living at a distance of 600-900 meters.

From influence statement (S2) an even higher requirement can be derived. If one looks at a laminar (filled) circle of reasonable size, the influence of the neighbors inside that circle should be greater than that of all neighbors outside it. To avoid very high and even infinitive influence values of neighbors living close by an inner circle is left neighbor-free. Therefore the inner circle becomes an inner ring from d_{min} to d_{border}. Mathematically the resulting statement can be formulated as:

$$\int_{d_{\min}}^{d_{border}} \frac{2 \bullet \pi \bullet d}{d^E} \partial d > \int_{d_{border}}^{\infty} \frac{2 \bullet \pi \bullet d}{d^E} \partial d \quad \text{(F3)}$$

The smallest neighbor distances along the road graph used have turned out to be about 10 meters, which seems a plausible value to use as the general minimum distance of any two neighbors. Solving the inequation (F3) – strictly spoken the equality border case – for d_{border} one obtains the function $d_{border}(E)$, which is shown as a plot in figure 4. It can be read as "the border distance for E=2.15 is 1,000 meters".

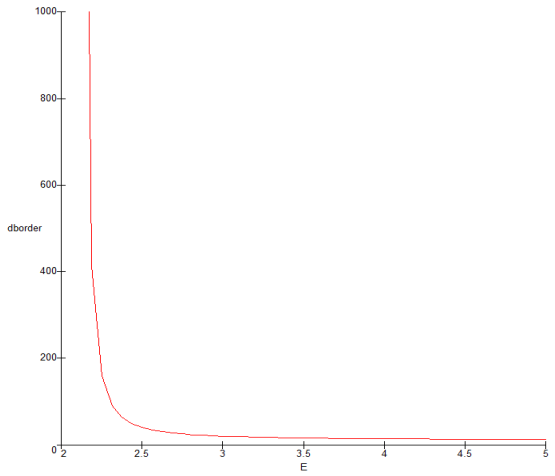

Figure 4: Function $d_{border}(E)$

Other reasonable values for the border distance could be 500 meters (E=2.18) or 50 meters (E=2.39), but not 1 or 10,000 meters. 50 meters is a nearby value that one can derive from Benenson and Omer (2002). These authors use the concept of a home area and determine a mean value of 10,500 square meters for it. A circle of that size has a radius of about 50 meters.

For E=3 the border distance would be 20 meters. Altogether from a theoretical point of view we expect E to be greater than 2, but significantly smaller than 3. This expectation is tested by the experiments that are described in the next section.

SIMULATION EXPERIMENTS

The simulation experiments start with a given data set of buildings, dwellings, the road graph and a segregation scenario (the households). Dwellings are filled randomly with households keeping the percentage of the ten milieus as in the segregation scenario. A percentage of dwellings left free at the beginning can be chosen as a parameter. Two further parameters which impact the simulation at run time are the percentages of households leaving the city spontaneous and the mean of new households moving into the city at one time step. These last two percentages are related to the number of households currently in the city and are used as parameters of accordant random number generators.

They are always kept equal because the city otherwise fills up or is abandoned.

For the main parameter distance exponent *E* a value of 2.0 was chosen as a starting point for the simulation experiments according to chapter THEORETICAL EXPECTATIONS. The other parameters mentioned were set to initial values derived from observed statistical values for the city of Dresden: 11% free dwellings and a percentage of 0.4% for households both moving in and out of the city (thought as monthly movement rates).

Beginning with *E* the parameter values are varied to search the parameter space for an optimal reproduction. The variation was partly done by hand, partly by some parameter production functions in connection with a few reproduction measurement criteria. More automatic parameter optimization approaches have been considered but found not to be necessary in this case. One reason is the long simulation run times.

A simulation run was stopped after several thousand steps when the system either reached a stable status or when there was obviously no chance of reaching the target (segregation index) value. The status is considered stable when the average change per step of the segregation index value is (near) zero or when it oscillates within a value range reached before. Because of the permanent stream of households moving in and out of the city a simulation run never stops by itself.

RESULTS

The simulation experiments have approved that the distance exponent *E* is of major influence on the segregation index, which confirms the findings of other authors (e.g. Laurie and Jaggi 2003). The percentages of free dwellings and moving in/out proved to be much less important.

The free dwellings percentage showed barely any influence. For the moving in/out percentages a positive, but weak correlation with higher segregation index values was observed. Nevertheless, if we set these three parameters to zero nothing ever happens in a simulation run. If we set just the move in/out parameters to zero we change a basic characteristic of our simulation model: being an open system with contact to an environment, and this is an important property of cities (Portugali 2000, p. 75). In our case simulation runs with such a closed system show only little residential move activity after a relatively small number of time steps and leave the city far from what can be observed with the open system model. The in/out flows keep the residential move process running.

The best reproduction is achieved at a distance exponent *E* of about 2.7. This value takes into account the calculated segregation index values based on road segments and on building blocks as shown in figure 5. The road-segment-based Information Theory Index *HRoadSegment* is displayed as the upper curve with a dashed line. The lower curve shows the appropriate building-block-based Index *HBlock*. The grey horizontal lines display the target values for each index. Both indices show a nearly strict dependency on *E*. The target values are reached around $E = 2.7$, for *HBlock* between 2.6 and 2.7 and for *HRoadSegment* between 2.7 and 2.8.

If we use 2.7 as input for the $d_{border}(E)$-function (figure 4), a border distance of about just 27 meters results. In our model a circle of this distance divides the close neighbors that have 50% influence on the neighborhood rating from those neighbors living further away that make up the other 50% influence. Using the same approach one can find a 90%-influence distance of about 270 meters and a 99%-influence distance of about 7200 meters. Because relatively small changes of *E* can lead to significant changes of the aforementioned distance values, one could speak of 30, 300 and 7000 meters, respectively, as approximations.

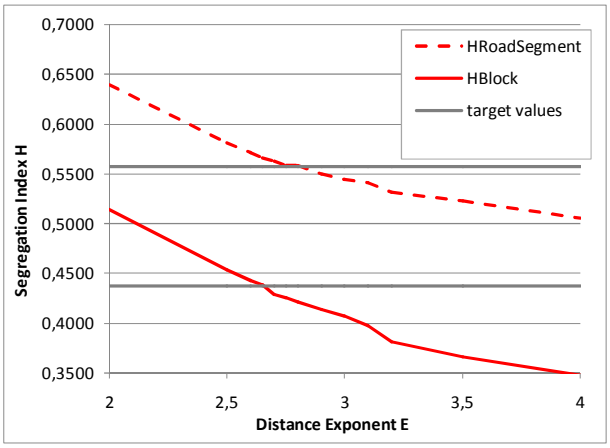

Figure 5: Segregation Index H (the Information Theory Index) Outcomes for Variation of Distance Exponent E

A major input of the simulation is the neighbor rating function as described earlier in chapter TRANSITION RULES, especially figure 3. To assess the influence, tests have been run with an alternative neighbor rating function. The social status rating function was set to be identical to the one used for cultural rating, so that the milieus strongly like living with neighbors from their own milieu (rating value 1). Simulation experiments with this setting result in a distance exponent *E* of about 1.8 for the best reproduction. This result contradicts our theoretical expectations, because for $E = 1.8$ far neighbors have in sum more influence than close ones.

CONCLUSION

Using the agent based simulation model developed here, important segregation characteristics of a given data set for the city of Dresden were successfully reproduced. It has been shown that the milieu approach of social grouping, a small set of neighbor rating rules and a simple distance-dependent weighting function lead to

reasonable results. The results indicate that relatively small neighborhood sizes of about 300 meters are sufficient to cover most cognitive neighborhood effects.

OUTLOOK

The approach presented here can be developed further in many ways. The results from this case study should be proved by using data from other cities. Characteristics of the environment of a dwelling other than social ones should be added. Possible starting points for a more sophisticated cognitive space model include a more detailed and a group-specific weighting function.

REFERENCES

Benenson, I. 1998. "Multi-Agent Simulations of Residential Dynamics in the City". In *Computers, Environment and Urban Systems*, 22(1), 25-42

Crooks, A.T. 2010. "Constructing and implementing an agent-based model of residential segregation through vector GIS". In *International Journal of Geographical Information Science*, 24, No. 5, 661-675

Duncan, O.T. & Duncan, B. 1955. "A Methodological Analysis of Segregation Indexes", In *American Sociological Review*, Vol. 20, No. 2 (Apr., 1955), pp. 210-217

Feitosa F. F; G. Câmara; A. M. V. Monteiro; T. Koschitzki and M. P. S. Silva. 2007. "Global and local spatial indices of urban segregation". In *International Journal of Geographical Information Science,* 21, No. 3, 299-323

Fosset, M. and Waren, W. 2005. "Overlooked Implications of Ethnic Preferences for Residential Segregation in Agent-Based Models". In *Urban Studies*, 42, No. 11, 1893-1917

Gilbert, N. 2008. *Agent-based models*, Sage, Los Angeles

Koenig, R. 2010. *Simulation und Visualisierung der Dynamik räumlicher Prozesse: Eine computergestützte Untersuchung zu den Wechselwirkungen sozialräumlicher Organisation und den baulichen Strukturen städtischer Gesellschaften*. VS Research ed., VS Verlag, Wiesbaden

Landeshauptstadt Dresden. 2009. *Wohnungsmarktbericht der Landeshauptstadt Dresden 2009*. Stadtplanungsamt, Postfach 12 00 20, 01001 Dresden

Laurie, A.J. and N.K. Jaggi. 2003. "Role of "Vision" in Neighborhood Racial Segregation: A Variant of the Schelling Segregation model". In *Urban Studies*, 40, No. 13, 2687-2704

Massay, D. S. and N.A. Denton. 1988. "The dimensions of residential segregation". In *Social Forces*, 67:2, 281-309

Omer, I. & Benenson, I. 2002. "Investigating Fine-Scale Residential Segregation by Means of Local Spatial Statistics". In *Geographical Research Forum*, 12, 41-60

Portugali, J. 2000. *Self-Organization and the City*, Springer, Heidelberg

Schelling, T. 1978. *Micromotives and Macrobehavior*, W.W. Norton, New York, Reissue 2006

Theil, H. 1972. *Statistical Decomposition Analysis*, North Holland, Amsterdam

Tobler, W. R. 1970. "A Computer Movie Simulating Urban Growth in the Detroit Region". In *Economic Geography*, Vol. 46, 234-240

Wasserman, H. and G. Yohe. 2001. "Segregation and the provision of spatially defined local public goods". In *The American Economist*, 45, No 2, 13-24

AUTHOR BIOGRAPHIES

JENS STEINHOEFEL graduated in 1998 in geodesy with a specialization in geoinformatics at the Technical University of Dresden. Since then he has worked in the IT industry. In 2009 he joined the CoMStaR research project at the Chair for Computer Science in Architecture at the Bauhaus-University Weimar. His email-address is jens.steinhoefel@uni-weimar.de.

FRAUKE ANDERS studied geodesy at the Technical University of Berlin, where she obtained her degree in 1997. She worked for a couple of years for rural area development programs and Land Registry before moving in 2002 to the University of Hanover as a research assistant. In her PhD thesis she investigated patterns in road networks. Since 2009 she is working in the CoMStaR research project. Her email-address is frauke.anders@uni-weimar.de.

DOMINIK KALISCH studied social sciences in Bielefeld, Essen and Düsseldorf. He obtained his degree in 2008. In 2009 he joined the CoMStaR research project. His email-address is dominik.kalisch@uni-weimar.de.

HERMANN KOEHLER graduated in 2006 in Sociology with a specialization in Urban Sociology at the Goethe University of Frankfurt/Main. Since then he has worked at the University of Kassel and in the German "Social-City"-Program. In 2009 he joined the CoMStaR research project. In 2011 he started his dissertation on representative mosques in Germany. His email-address is hermann.koehler@uni-weimar.de.

REINHARD KOENIG studied architecture and urban planning and completed his PhD thesis in 2009 at the University of Karlsruhe. He has worked as a research assistant at the Chair for Computer Science in Architecture at the Bauhaus-University Weimar since 2007 and heads research projects on the complexity of urban systems as well as the development of evolutionary design methods. In October 2009 he was appointed Interim Professor of the Chair for Computer Science in Architecture. His email address is reinhard.koenig@uni-weimar.de.

More information about the project, the authors and the Chair for Computer Science in Architecture at the Bauhaus-University Weimar can be found at http://infar.architektur.uni-weimar.de/service/drupal-cms/comstar

ACKNOWLEDGEMENT

This work is supported by Deutsche Forschungsgemeinschaft (DFG, DO 551/18-2). We thank the city of Dresden, especially the town planning office for providing several spatial and social data sets.

A simulation of disagreement for control of rational cheating in peer review

Francisco Grimaldo
Departament d'Informàtica
Universitat de València
Av. Universitat, s/n, Burjassot, Spain, 46100
Email: francisco.grimaldo@uv.es

Mario Paolucci
Institute of Cognitive Sciences and Technologies
Italian National Research Council
Via Palestro 32, Roma, Italy, 00185
Email: mario.paolucci@istc.cnr.it

KEYWORDS

Artificial social systems, Peer Review, Agent-based simulation, Trust reliability and reputation

ABSTRACT

We present an agent-based model of peer review built on three entities - the paper, the scientist and the conference. The systems is implemented on a BDI platform (Jason) that allows us to define a rich model of scoring, evaluating and selecting papers for conferences. Some of the reviewers apply a strategy (called "rational cheating") aimed to prevent papers better than their own to be accepted. We show how a programme committee update based on disagreement control can remove them.

INTRODUCTION

Large scale collaboration endeavors amongst humans are making the headlines of scientific magazines and attracting the attention of the research community. The case of Wikipedia and Amazon's Mechanical Turk are striking examples of what some consider to be the first step in a transition towards collective intelligence (Buecheler et al., 2011), a transition not devoid of risks as averaging effects and isolation (Pariser, 2011). To understand how this transition is happening and what are its consequences, we need to examine carefully the existing social and cultural structures that anticipate this kind of collaboration. The most important of these structures - a social artefact in itself - is the institution known as *peer review*.

Peer review, the process that scrutinizes scientific contributions before they are made available to the community, lies at the core of the social organization of science. Curiously, while the measurement of scientific production, that is, the process that concerns the *citation* of papers - scientometrics - has been an extremely hot research issue in the last years, we can't say the same for what concerns the process of *selection* of papers, although some attention has been focused on its shortcomings. Although being extremely important, the actual effectiveness of peer review in ensuring quality has yet to be fully investigated. In (Neff and Olden, 2006), the review process is found to include a strong "lottery" component, independent of editor and referee integrity. While the heterogeneous review approach to a decision between two options is supported by Condorcet's jury theorem, we move beyond simple accept/reject decisions to a more sophisticated and precise outlook on peer review that considers scoring and ranking. In fact, looking at scoring means looking at the pertinence and reliability of peer evaluation in its current incarnation, which could in turn help to detect kinds of potential failures that are not waived by Condorcet's theorem.

These issues are particularly relevant because peer review should take advantage of the new information publishing approach and technologies created by Web 2.0 and beyond. At the same time, diffuse dissatisfaction of scientists towards the current mechanisms of peer review is perceived - anecdotally, as list of famous papers that were initially rejected and striking fraudulent cases are published, and statistically, as numerical evidence on the failures of peer review (Casati et al., 2009) is starting to appear. To understand and possibly to apply policies to peer review, and in turn, to collective filtering and collective intelligence, we need more evidence coming from both the analysis and review of the process as it is, as well as from the creation of numerical, agent-based models, that could be validated both on the micro and the macro level, and on which we could perform what-if analysis, thus testing "in silico" proposed innovations. In this paper, we propose an agent-based model of peer review and, inspired by the introduction of rational cheaters in (Thurner and Hanel, 2011), we test how a simple mechanism based on disagreement control could help controlling this kind of cheating. The rest of the paper is organized as follows: the next section reviews the (scarce) literature on simulation of peer review. We then outline a general model of peer review endowed with a reviewer disagreement control mechanism, with a few implementation details. In the results section, we show how the mechanism works under two different conditions. In the last section, we present our conclusions and draw the path for future work.

RELATED WORKS

The literature of simulation models about peer review is scarce. We mention (Thurner and Hanel, 2011), where the authors focus on an optimizing view of the reviewer for his or her own advantage. To this purpose, they define a submission/review process that can be exploited by a *rational cheater* (Callahan, 2004) strategy in which the cheaters, acting as reviewers, reject papers whose qual-

Proceedings 26th European Conference on Modelling and Simulation ©ECMS Klaus G. Troitzsch, Michael Möhring, Ulf Lotzmann (Editors)
ISBN: 978-0-9564944-4-3 / ISBN: 978-0-9564944-5-0 (CD)

ity would be better than their own. In that model, the score range for review is very limited (accept or reject) and in case of disagreement (not unlikely because they allow only two reviewers per paper), the result is completely random. They find out that a small number of rational cheaters quickly reduces the process to random selection. The same model is expanded in (Roebber and Schultz, 2011), focusing not on peer review of papers, but of funding requests. Only a limited amount of funding is available, and the main focus is to find conditions in which a flooding strategy is ineffective. The number of cheaters, differently from this study and from (Thurner and Hanel, 2011), is not explored as an independent variable. However, similarly to the present work, the strong dependance of results from the mechanism chosen (number of reviews, unanimity) is evidenced.

In (Squazzoni and Gandelli, 2012), the authors study the impact of referee reliability on the quality and efficiency of the process. Their results emphasize the importance of homogenity of the scientific community and equal distribution of the reviewing effort.

In this work, we will use the score range and programme commitee update defined in (Grimaldo Moreno et al., 2010), and we will apply it to control the effect of rational cheaters as presented in (Thurner and Hanel, 2011), adding also, partly inspired by (Squazzoni and Gandelli, 2012), two different conditions: homogeneous and heterogeneous conferences.

THE PEER REVIEW MODEL

In this section, we define the entities involved in the peer review process, we propose a new model to reproduce its functioning and we present an agent-based implementation of this model.

Peer review entities

The key entities we identify within the peer review process are: the *paper*, the *scientist* and the *conference*.

The *paper* entity is the basic unit of evaluation and it refers to any item subject to evaluation through a peer review process, including papers and project proposals. We assume that the actual value of a paper is difficult to ascertain and that it can only accessible through a procedure implying the possibility of mistakes.

Scientists write papers, submit them to conferences and review papers written by others. Regarding paper creation, the value of a paper will depend on the writing skills of the authors. The submission decision must consider aspects such as the characteristics of the conference (e.g. acceptance rate), those of the authors (e.g. risk taking), etc. Scientists will also be characterized by their reviewing skills, that represent the chance they actually understand the paper they review, thus being the primary cause of reviewing noise. The evaluation process might involve other strategic behaviors possibly adopted by the scientist, such as the competitor eliminating strategy used by rational cheaters in (Thurner and Hanel, 2011).

The *conference* entity refers to any evaluation process using a peer review approach. Hence, it covers most journal or conference selection processes as well as the project evaluations conducted by funding agencies. Every *paper* submitted to a conference is evaluated by a certain number of *scientists* that are part of the programme committee (PC) of the conference. Thus, the conference is where all the process comes together and a number of questions arise. For example, since the number of evaluations a paper receives are just a few (three being a typical case): can the review-conference system ensure quality in the face of variable reviewing skills or strategic behaviors, thanks to some selection process of PC composition that leans on disagreement control? The peer review model presented below is meant to tackle this kind of questions by concretising the different issues introduced for the general entities presented above.

Proposed model

The proposed model represents the peer review problem by a tuple $\langle S, C \rangle$, where S is the set of *scientists* playing both the role of authors that write papers and the role of reviewers that participate in the PC of a set of *conferences* C. *Papers* produced by scientists have an associated value representing their intrinsic value, and receive a review value from each reviewer. These values are expressed as integers in an N-values ordered scale, from strong reject (value 1) to strong accept scores (value N).

Every scientist $s \in S$ is represented by a tuple $s = \langle ap, aq, as, rd, rs, rt \rangle$. Regarding paper production, each scientist has an associated author productivity ap, meaning the number of papers uniformly written per year. Papers are of the form $p = \langle a, iv \rangle$, being $a \in S$ the author of the paper and $iv \in [1, N]$ the intrinsic value (quality) of the paper. This intrinsic value is calculated considering the author quality $aq \in [1, N]$ and the author skill value $as \in [0, 1]$. Whereas aq represents the canonical author quality, as represents the production reliability of scientists. Hence, scientists write papers of value aq with probability as, and of random value with probability $(1 - as)$ in order to produce, occasionally, some paper with outlying quality with respect to their standard. Similarly, as a reviewer, each scientist has an associated reviewer skill value $rs \in [0, 1]$ as well as a reviewing type $rt \in \{\texttt{normal}, \texttt{rational}\}$. In algorithm 1 we show the pseudocode carried out by scientists to review papers. The **if** statement in line 1 models the noisy evaluation of papers, where the result of reviewing is accurate with probability rs, and completely random with probability $(1 - rs)$. Here, `Random` is a function providing a random float number in the range $[0, 1]$ whereas `RandomInt` returns a random integer in $[1, N]$. Furthermore, in line 7 we have incorporated the rational cheating strategy introduced in (Thurner and Hanel, 2011). Hence, $rational$ cheaters punish those papers whose intrinsic value is greater than his own author quality, thus trying to clear the way for his papers - preventing better papers to appear and, for example, collect more citations

than one's own.

Algorithm 1 Pseudocode to review papers

Input: Paper Intrinsic Value (iv), Reviewer Skill (rs), Reviewer's Author Quality (aq), Reviewing Type (rt)
Output: Review Value for the paper ($reviewValue$)

```
1:  if rs > Random() then
2:      estimatedValue ← iv
3:  else
4:      estimatedValue ← RandomInt(1, N)
5:  end if
6:  if rt = rational then
7:      if estimatedValue < aq then
8:          reviewValue ← estimatedValue
9:      else
10:         reviewValue ← 1
11:     end if
12: else
13:     reviewValue ← estimatedValue
14: end if
```

Conferences $c \in C$ are represented by the following tuple: $c = \langle m, PC, rp, pr, av, I, dt, pu \rangle$. Each conference is celebrated every year in a certain month m, in which it sends its call for papers. In algorithm 2 we show the pseudocode executed by scientists when deciding whether to submit a paper to a conference after having received its call for papers. Note how the noisy evaluation of papers also occurs when evaluating the own papers in lines 2 - 6. Scientists decide whether to submit papers or not in accordance with their submission risk degree, expressed through the integer value rd. Hence, the submission happens when the distance between the estimated paper value and the conference acceptance value av is less than or equal to rd (see line 7).

Algorithm 2 Pseudocode to submit papers

Input: Available Papers (AP), Reviewer Skill (rs), Risk Degree (rd), Conference (c), Conference Acceptance Value (av)

```
1:  for all p such that p ∈ AP do
2:      if rs > Random() then
3:          estimatedValue ← iv
4:      else
5:          estimatedValue ← RandomInt(1, N)
6:      end if
7:      if |estimatedValue − av| ≤ rd then
8:          Submit(p, c)
9:      end if
10: end for
```

Conferences employ a subset of scientists $PC \subseteq S$ as their programme committee, whose size depends on the number of reviews received per paper rp and the number of reviews done per PC member pr. Then, they accept those papers whose average review value is greater than the acceptance value av.

Conferences also keep track of disagreements between reviewers, as they might be a signal of low reviewer skill or cheating. One disagreement event is not enough to find out which of the disagreeing parts is to blame. Thus, conferences maintain an image $i \in I$ of each scientist that has ever been a PC member, accounting for the number of disagreements with the other reviewers. Images are of the form $i = \langle s, nd, nr \rangle$, where s is the scientist, nd is the accumulated number of disagreements and nr is the total number of reviews carried out. Disagreements are calculated on a paper basis as the difference between the review value given by the reviewer and the average review value for that paper. When this difference gets higher than a disagreement threshold dt, the reviewer disagreement count grows by one. The dt parameter could also be fine-tuned for the detection of more sophisticated cheating approaches.

Reviewer images are used to update the PC by discarding the $pu\%$ of reviewers with a higher ratio nd/nr and selecting new ones from S. This way, conferences perform a selection process which selects reviewers who provide similar evaluations. Given our choice for reviewers' mistakes (i.e. if they don't understand the paper, the evaluation is random), this mechanism should also select good reviewers.

In algorithm 3 we show the pseudocode executed when celebrating a new edition of a conference. Firstly, function `CallForPapers` in line 3 broadcasts the conference call for papers and receives papers submitted during a fixed period of time (currently, two months). Secondly, function `UpdatePC` in line 4 adjusts the PC to the number of papers received as well as discarding the $pu\%$ of reviewers with the worst image. New members for the PC are selected randomly from the set of scientist S. Thirdly, the **for** statement starting in line 5 is in charge of the evaluation process: function `AskForReviews` returns the reviews from rp reviewers, different to the author and randomly chosen from the PC, in the form of pairs $[s, rValue]$, where s is the reviewer and $rValue$ is the grade given to the paper; function `ComputeAvgReview` computes the average review value for the paper; lines 12 - 16 accept those papers over the acceptance value; and functions `GetImage` and `UpdateImage` in lines 17 - 24 retrieve and update the image of the reviewers after checking for disagreements. Finally, accept and reject notifications are sent to the authors by functions `NotifyAccepts` and `NotifyRejects`.

SCENARIOS

The proposed peer review model has been implemented as a MAS over Jason (Bordini et al., 2007), which allows the definition of both scientists and conferences as BDI agents using an extended version of AgentSpeak(L) (Rao, 1996). In this section, we present the results of a set of simulations involving 1000 scientists and 10 conferences across 50 years. Each scientist writes 2 papers per year ($ap = 2$), so that the overall production amounts to 2000 papers uniformly distributed over the year.

Paper intrinsic values (quality) and review values are expressed in a 10-values ordered scale from 1 to 10 ($N = 10$). Author qualities ($aq \in [1, 10]$) follow a discretized Beta distribution with $\alpha = \beta = 5$. The beta distribution is the obvious choice for a statistic in a fixed interval as the one we are using - the alternative being a normal distribution with cut tails, which is just a less flexible approximation, for example, in terms of central value. We choose this shape, a bell shaped curve with mean 5.5

Algorithm 3 Pseudocode to celebrate a conference

Input: Celebration Year ($year$), Conference Acceptance Value (av), Current Programme Committee (PC), Current Scientists' Images (I), Percentage of PC update (pu), Scientists (S), Reviews Per Paper (rp), Papers Per Reviewer (pr), Disagreement Threshold (dt)
Output: New Programme Committee (PC), New Scientists' Images (I)

$AccPapers \leftarrow \phi$
$RejPapers \leftarrow \phi$
$RcvPapers \leftarrow CallForPapers(year, av)$
$PC \leftarrow UpdatePC(PC, S, I, pu, \lceil |RcvPapers| * rp/pr \rceil)$
for all p such that $p \in RcvPapers$ **do**
  $Reviews \leftarrow AskForReviews(p, rp, PC)$
  $sumOfReviews \leftarrow 0$
  for all $r = [s, rValue]$ such that $r \in Reviews$ **do**
    $sumOfReviews \leftarrow sumOfReviews + rValue$
  end for
  $avgReviewValue \leftarrow sumOfReviews/|Reviews|$
  if $avgReviewValue \geq av$ **then**
    $AccPapers \leftarrow AccPapers \cup \{[p, avgReviewValue]\}$
  else
    $RejPapers \leftarrow RejPapers \cup \{[p, avgReviewValue]\}$
  end if
  for all $r = [s, rValue]$ such that $r \in Reviews$ **do**
    $[nd, nr] \leftarrow GetImage(I, s)$
    if $|avgReviewValue - rValue| > dt$ **then**
      $I \leftarrow UpdateImage(I, s, nd + 1, nr + 1)$
    else
      $I \leftarrow UpdateImage(I, s, nd, nr + 1)$
    end if
  end for
end for
$NotifyAccepts(AccPapers)$
$NotifyRejects(RejPapers)$

and symmetrically distributed between 1 and 10, in the hypothesis that average papers are more common than either excellent or bogus papers. Authors' skills (as) and reviewers' skills (rs) follow instead a Uniform distribution in [0.5,1], that we consider a moderate level of noise in the production and evaluation of papers. With respect to the reviewing type (rt), we show results with rational cheaters up to 30%. We have performed simulations up to 90% of rational cheaters but, when rational cheaters become majority, the probability of having two over three cheating reviews grows enough to turn the system upside down - PCs get filled with rational cheaters and no papers are accepted at all.

Conference parameters have been set to reproduce two different experimental scenarios that we call *homogeneous condition* and *heterogenous condition*. These scenarios are a first step to understand the emergence of quality specialization in the structure of workshops, conferences and papers. To this purpose, we compare a system without specialization with one in which conference differ in the quality they request from a paper.

In the *homogeneous condition* (SR) all the conferences act in the same way and they aim at accepting papers whose quality is just above the average score ($av = 5.5$). Scientists are then configured to submit papers to the first conference available after the moment of production (their risk degree rd is set to 10). In the *heterogeneous condition* (MR) we have one conference for each acceptance value from 1 to 10. In this way, we distinguish high-quality from low-quality conferences. Scientists submit papers to a conference whose av differs at most of 1 score from the estimated paper value ($rd = 1$). For instance, a conference with $av = 7$ would only receive papers of estimated quality from 6 to 8. Conferences are scheduled along the year so as to avoid conferences of similar acceptance value to appear next to each other and reduce contention for the papers.

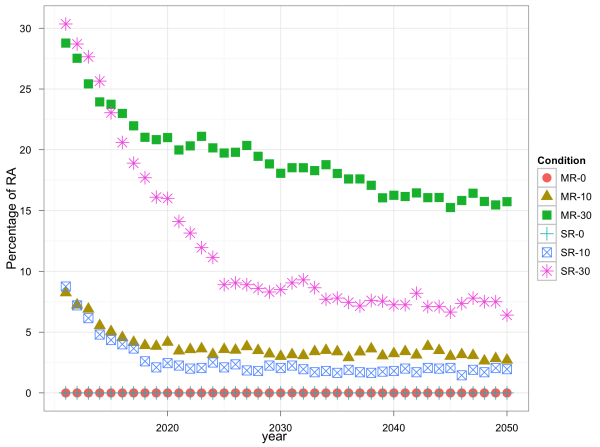

Figure 1: Percentage of rational cheaters (RA) under homogeneous (SR) and heterogeneous (MR) conditions with initial percentages from none to 30%, averaged over 10 runs. The presence of rational cheaters decreases in the first ten years, with the MR being more effective.

Conferences in both the *homogeneous condition* and the *heterogenous condition* ask for 3 reviews per paper (rp) and each PC member carries out a maximum number of 3 reviews (pr). The disagreement threshold (dt) is set to 4 and the percentage of PC members that are updated each year is 10% (pu).

Results

Our research hypothesis is that the PC update mechanism proposed will effectively find out and expel the rational cheater scientists. The argument that rational cheaters will find themselves in disagreement with others every time they act strategically makes sense and, in fact, in figure 1 we can observe how rationals decrease substantially in the conditions where they are more abundant. For the homogeneous condition, averaging removes little information, while in the heterogeneous one, where conferences differ in their acceptance value, this averaging could hide information. We address heterogeneous conferences individually in . The PC update mechanism results significantly more effective in the homogeneous condition than in the heterogeneous one (two-sided t test with p-value of 0.036, comparing MR-30 and SR-30).

Let's now focus on indicators showing the effectiveness of the rational cheating strategy. The purpose of adopting a rational cheating strategy is to remove potential competition from better authors and papers. Thus, the effect of rational cheaters should be seen as an increase in the number of papers that should be accepted, but end up being rejected. We call these "good papers rejected" (GPR). The opposite, that is, the papers that

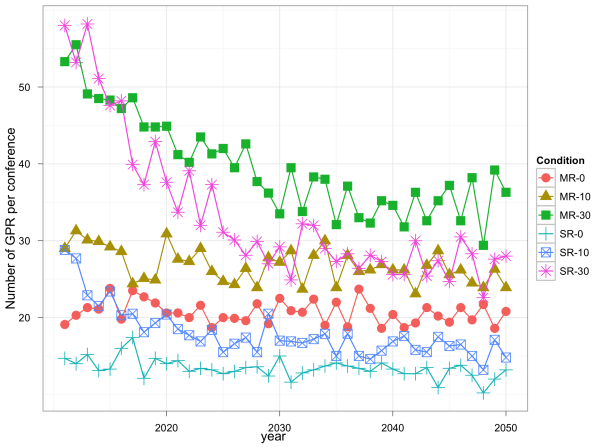

Figure 2: Number of Good Papers Rejected (GPR) under homogeneous (SR) and heterogeneous (MR) conditions with initial percentages of rational cheaters from none to 30%, averaged on ten runs. GPRs decrease significantly for both conditions with 30% of rational cheaters.

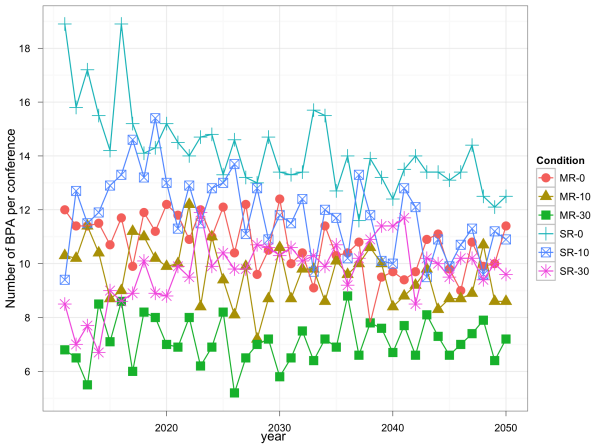

Figure 3: Number of Bad Papers Accepted (BPA) under different conditions: homogeneous (SR) and heterogeneous (MR) conditions with initial percentages of rational cheaters from none to 30%.

should end up rejected but do not, are named as "bad papers accepted" (BPA). They are shown respectively in Figure 2) and Figure 3).

For the simulations starting with more rational cheaters (SR-30 and MR-30 in figure 2), the decrease in the number of GPR , following the removal of rational cheaters from the PC, is already significant after a few years (p-value of 0.02 between 2011 and 2015). However, notwithstanding the very low quantity of rational cheaters at the end of the simulation (consider for example the case of SR-30), the complexive number of GPR remains rather high.

Referring to the number of bad papers accepted, they remain rather stable (Figure 3), and lower than the number of GPRs. Only in the SR-0 condition they seem to decrease in time. But what is more interesting is that the number of BPA at the onset of the simulation and during the first years is inversely proportional to the quantity of rational cheaters at the start. Thus, no rational cheaters bring more BPA than a 30% of rational cheaters, and this is true for both conditions. In figure 4 we show the number of accepted papers, that grows in time for the conditions with rational cheaters. As they are expelled from the PCs, the number of accepted papers grows to approach that of conditions without rational cheaters. This is likely to be happening also because of the reduction in the GPR (i.e. less good papers rejected means more papers accepted).

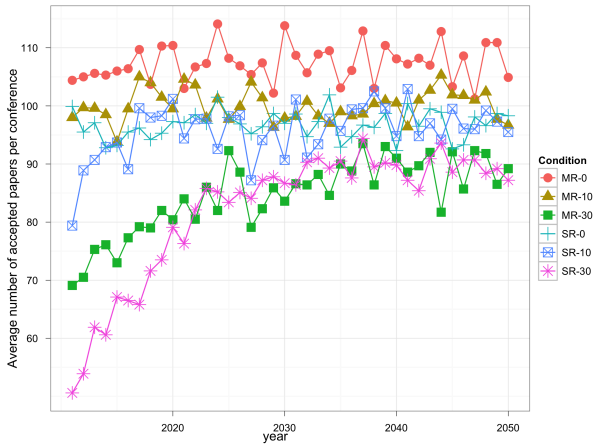

Figure 4: Number of Accepted Papers under homogeneous (SR) and heterogeneous (MR) conditions with initial percentages of Rational Agents (rational cheaters) from none to 30%, averaged over ten runs. Conferences in the heterogeneous condition systematically accept more papers than in the homogeneous condition.

What about quality? Is the removal of rational cheaters from the programme committees going to make a difference in the quality of accepted papers? Surprisingly, in figure 5, we can see that the removal of rational cheaters does not contribute to higher average quality of papers. Only the MR-30 condition shows an initial increase in quality (two-sided t-test between 2011 and 2025 gives a p-value of 0.003).

Looking at heterogeneous conferences

We now open up the box of heterogeneous conferences to see how they contribute to the averages shown previously. From figure 6, where we show the percentage of rational cheaters for each individual conference (characterised by an acceptance value), we see immediately how the PC update mechanism fails in moving rational cheaters away from the PC when the quality of the conference is low. If the acceptance value reaches 4 or lower, there is no decrease at all. This happens due to the paper quality being too near to the lowest possible value used

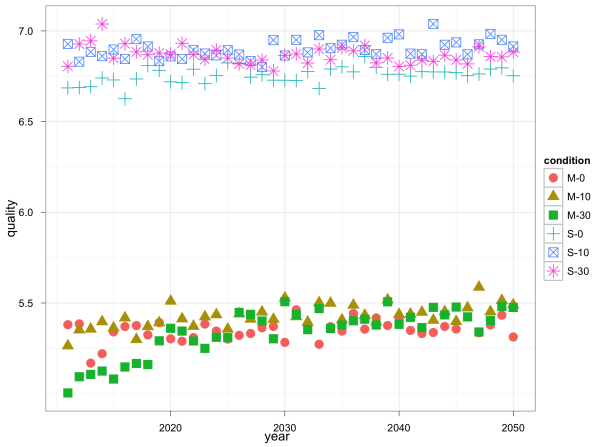

Figure 5: Average paper quality under different conditions: homogeneous (SR) and heterogeneous (MR) conditions with initial percentages or rational cheaters from none to 30%. The quality remains constant notwithstanding the removal of rational cheaters. Only the MR-30 condition shows an initial increase in quality.

by rational cheaters to prevent publication of competitive papers. Consider, for example, a rational cheater with author quality 6. Within a conference of quality 8, it will act as a rational in all cases. But if that same agent ends in a PC for a conference with acceptance value 4, it will never act as a rational because rationals give fair reviews to papers under their author quality. Thus, that conference feels no need to drive it away from the PC.

Finally, we examine the number of accepted papers per conference. As it was foreseeable, more papers are accepted by mid-quality conferences, simply because our distribution of quality is chosen so that more papers of this kind are available. The interesting part of figure 7 is the increasing trend that is distinguishable for conferences with acceptance value greater or equal to 5. The cause here, in accordance with the ratio of rational cheaters seen in figure 6, is the improvement of PC quality thanks to the removal of rational scientist, that increases the number of papers accepted, mainly through the decrease of unfair good papers rejected.

CONCLUSIONS AND FUTURE WORK

This work highlights the importance of adopting more transparent and adaptive policies for conference programme committees. Whereas PC formation is currently more influenced by issues such as path dependency, inertia or self-selection, the application of objective and independent criteria may be beneficial to the quality of science.

Our results show how the mechanism introduced to control disagreement in the PCs is also effective in removing most of the rational cheaters from the process. The benefits can be measured in terms of the growing

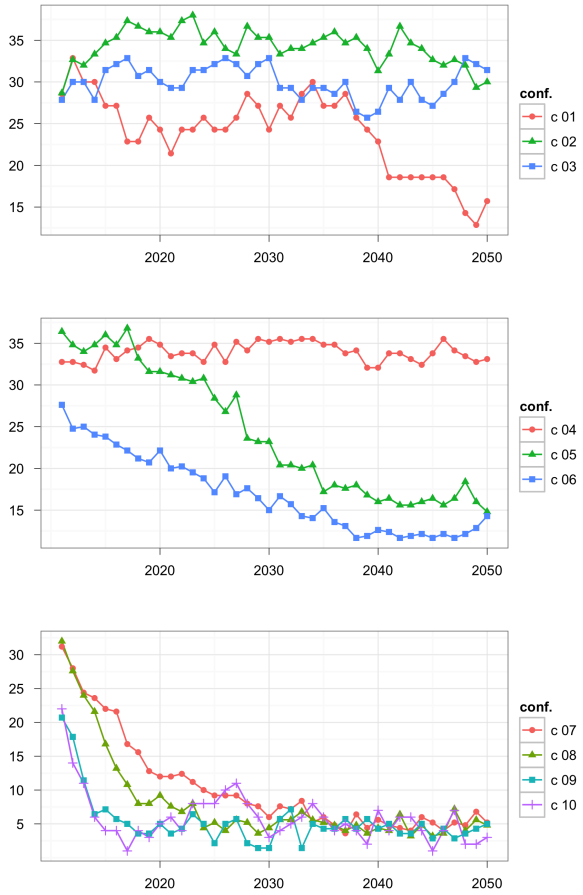

Figure 6: Percentage of rational cheaters in time, condition (MR-30), ten conferences with acceptance threshold from 1 (c01) to 10 (c10). Conferences with higher acceptance threshold push rational cheaters away faster.

number of accepted papers and of the decrease in the number of mistakes (good papers rejected).

When the quality of the conferences is homogeneous, rational cheaters are reduced but at the expenses of the number of accepted papers. It is important to note that neither the homogeneity nor the heterogeneity of conferences determined the sharp transition to random selection shown in (Thurner and Hanel, 2011). We hypothesise that this is due to the fact that our model is based on a larger score range and three, instead than two, reviewers.

A next step in this research would be to ground our model against data extracted from one of the several automated conference review systems. However, this data has proven surprisingly difficult to obtain. Not only our queries to the owners of those systems went unanswered, but we knew that other researchers had the same situation (neither of (Squazzoni and Gandelli, 2012; Thurner and Hanel, 2011) managed to ground their assumption either). The difference between the immediate availability of publication and citation data is especially striking.

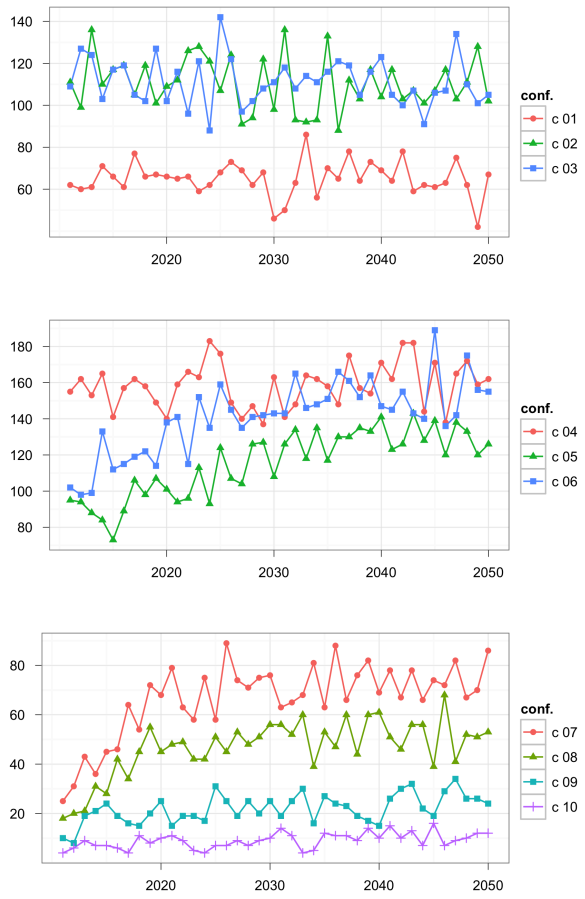

Figure 7: Number of accepted papers in time, , condition (MR-30) with ten conferences with acceptance threshold from 1 (c01) to 10 (c10). Conferences with acceptance threshold over 5 increase the number of papers accepted as a result of the expulsion of rational cheaters.

ACKNOWLEDGEMENTS

Work supported by the Spanish MICINN, Consolider Programme and Plan E funds, European Commission FEDER funds and Universitat de València funds, under Grants CSD2006-00046, TIN2009-14475-C04-04 and UV-INV-AE11-40990.62, as well as under the FuturICT coordination action.

REFERENCES

Bordini, R. H., Hübner, J. F., and Wooldridge, M. (2007). *Programming multi-agent systems in AgentSpeak using Jason*. John Wiley & Sons.

Buecheler, T., Sieg, J. H., Füchslin, R. M., and Pfeifer, R. (2011). *Crowdsourcing, Open Innovation and Collective Intelligence in the Scientific Method: A Research Agenda and Operational Framework*, pages 679–686. MIT Press, Cambridge, Mass.

Callahan, D. (2004). Rational Cheating: Everyone's Doing It. *Journal of Forensic Accounting*, pages 575+.

Casati, F., Marchese, M., Ragone, A., and Turrini, M. (2009). Is peer review any good? A quantitative analysis of peer review. Technical report, Ingegneria e Scienza dell'Informazione, University of Trento.

Grimaldo Moreno, F., Paolucci, M., and Conte, R. (2010). A Proposal for Agent Simulation of Peer Review. *Social Science Research Network Working Paper Series*.

Neff, B. D. and Olden, J. D. (2006). Is Peer Review a Game of Chance? *BioScience*, 56(4):333–340.

Pariser, E. (2011). *The Filter Bubble: What the Internet Is Hiding from You*. Penguin Press HC, The.

Rao, A. S. (1996). AgentSpeak(L): BDI agents speak out in a logical computable language. In Verlag, S., editor, *Proc. of MAAMAW'96*, number 1038 in LNAI, pages 42–55.

Roebber, P. J. and Schultz, D. M. (2011). Peer Review, Program Officers and Science Funding. *PLoS ONE*, 6(4):e18680+.

Squazzoni, F. and Gandelli, C. (2012). Saint Matthew strikes again: An agent-based model of peer review and the scientific community structure. *Journal of Informetrics*, 6(2):265–275.

Thurner, S. and Hanel, R. (2011). Peer-review in a world with rational scientists: Toward selection of the average. *European Physical Journal B-Condensed Matter*, 84(4):707.

AUTHOR BIOGRAPHIES

FRANCISCO GRIMALDO is a lecturer at the Universitat de València, Spain. His research is focused on applied artificial intelligence, agent-based modelling/simulation and social decision making. He is a member of the HiPEAC network of excellence and of the IEEE Systems, Man & Cybernetics Society. His email is `francisco.grimaldo@uv.es` and his personal webpage `http://www.uv.es/grimo`.

MARIO PAOLUCCI is a researcher of the ISTC/CNR (Institute for Cognitive Science and Technology), Rome. He is studying and applying multiagent-based social simulation and agent theory to understand social artefacts, in particular Reputation, Norms, Responsibility, and the cultural evolutionary mechanisms that support them. Mario's publications include a book on reputation with Rosaria Conte and articles on JASSS, ACS and Adaptive Behavior. His email is `mario.paolucci@istc.cnr.it` and his webpage `http://labss.istc.cnr.it/mario-paolucci`.

A simulation model of scientists as utility-driven agents

Melanie Baier
Dresden University of Technology
Faculty of Business and Economics
Chair for Managerial Economics
D-01062 Dresden
Email: Melanie.Baier1@mailbox.tu-dresden.de

KEYWORDS

Agent-based modeling (ABM), coordination, knowledge generation, reputation, scientific advancement, scientific competition, status competition, utility function

ABSTRACT

Agent-based simulations of science that account for the linkage between micro-level behavior of scientists and macro-level results of scientific competition are rather scarce. The approach of this simulation model is to link the motivation and behavior of scientists to knowledge growth and scientific innovations via the emergence of new knowledge fields. A new knowledge field is considered both to be a result of scientific competition and a representation of scientific advancement. This paper takes a closer look at the scientists' motivation and how they coordinate and add to scientific progress as utility-driven agents. Accounting for stylized facts of scientific competition, selected simulation results show how deep the processes of knowledge generation, reputation and scientific innovations are intertwined. As scientists are assumed to be of different utility types and have different aspiration levels, this approach is able to account for adaptive behavior of agents.

INTRODUCTION

The aim of the ABM is to show how scientists as utility-driven agents coordinate scientific competition. Coordination implies that even though science may exhibit biased results as reflected in the Matthew effect, the rules of scientific competition have nevertheless proved to be self-enforcing and well-designed in that they align the individual ambitions with the social purpose of scientific advancement (Vanberg, 2010). Individual scientists may follow the counter-norms of "emotional commitment, particularism, solitariness, interestedness, and organized dogmatism" (Mitroff, 1974), but after all, the *social* system of scientific competition remains robust in Merton's sense (Merton, 1973) as long it enhances the overall stock of knowledge. There is a long-standing debate among philosophers of science on how an individual epistemology can be aligned to a social epistemology. If one adopts the naturalist view that one has to account for the scientists' motivation and behavior in practice (Downes, 2001), it is generally agreed that scientists *are* in fact subject to different individual practices, (non-epistemic) motives and social influences (e.g., Bloor, 1991; Kitcher, 1993; Latour, 1987). The crucial question, however, remains a subject of discussion. How can consensus practices of scientific communities be derived from individual practices? The Naturalists' approach to align a rich cognitive conception of individual scientists with a scientific consensus building that heavily depends on neoclassical microeconomics and Bayesian decision theory has been subject to a lot of criticism (e.g., Downes, 2001; Mirowski, 1996; Sent, 1996).

The approach adopted here is to regard scientists not as utility maximizers of neoclassical economics who consistently base their reasoning on Bayesian decision theory. Rather, scientists are conceptualized as satisficing agents who are occasionally prone to biased reasoning and behavior. Thus, this paper follows a "thick" conception of individual agents, i.e. a claim about a rich psychological makeup of the agent and the relevance of context (Downes, 2001). Recently, research has been carried out in ABMs on science to account for biased behavior of scientists. Thurner and Hanel (2011) discuss biased behavior of agents in the coordination process of science, in particular how self-interested scientists affect the efficiency of the peer review mechanism. They show that referees who tend to reject better papers than their own and accept worse quality considerably reduce the average quality of accepted papers. This result is confirmed in a model by Squazzoni and Gandelli (2012). They also examine the effects of institutional factors on the quality and efficiency of peer-review. For instance, they show that increasing competition in a fragmented scientific community tends to foster evaluation bias and inefficiencies in the peer review process.

While these ABMs focus on the effects of motivational bias and institutional settings on the efficiency of the coordination mechanism, the model presented here intends to explain how individual scientists, who are prone to motivational and cognitive bias, are able via the coordination process of scientific competition to add to scientific advancement. The approach relates to the findings of Solomon (1992), who argues that a cognitive bias of scientists, in particular belief perseverance, leads to a distribution of research effort and thus contributes to the

Proceedings 26th European Conference on Modelling and Simulation ©ECMS Klaus G. Troitzsch, Michael Möhring, Ulf Lotzmann (Editors)
ISBN: 978-0-9564944-4-3 / ISBN: 978-0-9564944-5-0 (CD)

advancement of scientific debate. Especially when scientific problems are "ill-defined", a scientist is expected to support his special community of interest and to "(...) believe in his own findings with utter conviction while doubting those of others (...)" (Mitroff, 1974, p.592).

Scientific advancement is reflected in a growing body of scientific knowledge and its development by means of emerging knowledge fields and scientific innovations. To model this micro-macro-link is the intention of the model. It is an abstract simulation model which is based on plausible micro-level agent behavioral rules (Gilbert, 2008), yields stylized facts of scientific competition at the macro level and feeds back to the behavioral rules of micro-level-agents. To the knowledge of the author, so far there is no such model to link utility-driven micro behavior with the macro level of scientific advancement. This papers thus contributes to research that accounts for micro-macro interdependencies in scientific competition and the social embededdness of science (Edmonds et al., 2011). At first, this paper focuses on the motives and behavior of agents that drive the most important processes on the micro level. The mechanisms are simple, though powerful, and are able to reproduce a number of stylized facts of scientific competition. They are thus considered to be a suitable starting point for modeling the feedback processes between the macro and micro level.

COORDINATION MECHANISMS IN SCIENCE

Stylized facts and characterization of a scientist

Scientists are presumed to gain utility from scientific insight (intrinsic motivation) and scientific reputation (extrinsic, non-monetary motivation). To achieve this, scientists are supposed to produce scientific output, i.e. publications. The distribution of publications per author is approximated by the Lotka distribution, saying that in a specific knowledge field the number of authors generating n scientific papers is proportional to $1/n^2$. This stylized fact has been verified in a number of papers, e.g. for economics (Cox and Chung, 1991). This effect is augmented by the law of decreasing returns, which in the context of scientific progress (Rescher, 1978) states that the more is already known in a scientific field, the smaller the scientific insights that are achievable. It is hypothesized that these two effects may lead to a considerable share of unsatisfied scientists, either in regard to scientific insight or reputation. One solution to the scientist's problem might be to initiate a new knowledge field, publish innovative articles and as the priority rule suggests, achieve disproportionally more credit than before. But a scientist might also choose to stick to one field of knowledge with only small scientific returns. In a nutshell, scientists are considered as heterogeneous as they have differing goals concerning scientific insight and reputation. They do not pursue lifetime utility maximization (Diamond, 1988), but have an aspiration level which they strive to achieve Simon (1955). The aspiration level may be defined in terms of private goals and/or determined by observable properties of other agents. After all, scientific advancement is rooted in the individual disposition of scientists who do not achieve their aspiration level. The concept of satisficing explicitly accounts for adaptive behavior of agents, for instance modeled in Brenner (2006) and Chang and Harrington Jr. (2006).

The present paper concentrates on heterogeneous scientists who are endowed with some basic rules of behavior and who coordinate their behavior in a social process, it abstracts from aspects of *how* scientists create and evalute new ideas (Gilbert, 2007; Watts and Gilbert, 2011), form networks of "invisible colleges" or adjust their lifecycle-productivity (Carayol, 2008; Levin and Stephan, 1991).

The scientist's utility function

As a scientist strives for scientific insight, he gains utility from his accumulated knowledge. The intrinsic utility of a scientist $u_{i,t}^{int}$ is assumed to be a function of his accumulated knowledge w driven by his cumulative productivity pr. The latter is a function of his publication activities pub exhibiting diminishing marginal returns. The function is assumed to have the following properties:

$$\begin{aligned} u_{i,t}^{int} &= f(w(pr(pub))) \\ \partial f/\partial w &> 0 \\ \partial w/\partial pr > 0, \partial^2 w/\partial pr &< 0 \\ \partial pr/\partial pub_i > 0, \partial pr/\partial pub_{-i} &< 0 \end{aligned} \tag{1}$$

The accumulation of knowledge is a private disposition and thus unaffected by the accumulated knowledge of other scientists. However, for scaling purposes in the simulation model, the accumulated knowledge $w_{i,t}$ of scientist i is multiplied with a factor $\gamma = max(w_{-i,t})$. This yields a value $u_{i,t}^{int}$ in the interval $\in [0, 1]$.

$$u_{i,t}^{int} = \gamma * w_{i,t} \tag{2}$$

Utility from reputation $u_{i,t}^{r}$ is considered a social disposition and assumed to decrease with the scientist's position according to his scientific output. Utility $u_{i,t}^{r}$ is defined by the ranking of scientists. The ranks ra are better (i.e. converge to a value of one) for those scientists who have many publications. To account for persistent ranking positions, a parameter of organizational inertia $(1 - \delta) \in (0, 1)$ is added. Rankings do not change if δ yields a value of 0. The closer δ converges to 1, the more ranking positions are proned to change and truly reflect the current publication activities. Utility from reputation is given by

$$\begin{aligned} u_{i,t}^{r} &= f(ra(pub, \delta)) \\ \partial f/\partial ra < 0, \partial^2 f/\partial ra &< 0 \\ \partial ra/\partial pub &< 0 \\ \partial ra/\partial \delta &> 0 \end{aligned} \tag{3}$$

As related works account for an evaluation bias in the review process on the micro-level of scientific competition (e.g., Squazzoni and Gandelli, 2012; Thurner and Hanel, 2011), the parameter δ in this model can be interpreted as an evaluation bias on an aggregate level, i.e. how quick a scientific discipline credits new publications with corresponding ranks. It points to the fact that some disciplines are "tightly knit in terms of their fundamental ideologies, their common values, their shared judgments of quality, (...) and the level of their agreement about what counts as appropriate disciplinary content" (Becher and Trowler, 2001, p.59). Following Loch et al. (2001), utility from reputation yields a value in the interval $\in [0, 1]$ and specifies to:

$$u^r_{i,t} = 1 - \frac{(ra_{i,t} - 1)^2}{n_{j,t}} \tag{4}$$

with $n_{j,t}$ in (4) as the number of rank classes of scientists belonging to one community of scientists. Weighted utility from accumulated knowledge and reputation yields the overall utility function of a scientist. As Equation (5) shows, it is assumed that utility from knowledge and reputation are partial substitutes, with utility becoming zero when one of the terms is zero.

$$u_{i,t} = (u^{int}_{i,t})^{\alpha} * (u^r_{i,t})^{1-\alpha} \tag{5}$$
$$\alpha \in [0, 1]$$

It should be noted that although both utility from accumulated knowledge and from reputation are driven by publication activities, the interpretation is different. Intrinsic utility only aims at utility derived from significantly new findings which increase the stock of knowledge (outcome), whereas utility from reputation may also comprise "normal science" and equivalent types of output (Rescher, 1978).

Types of agents

According to the scientists' motivation reflected in their specific utility weights, it is assumed that scientists can follow three types of individual disposition. Scientists may

- put relatively more emphasis on reputation compared to scientific insight.
- put relatively more emphasis on scientific insight compared to reputation.
- be indifferent between reputation and scientific insight.

Apparently, the assignment of utility weights does not depend on a scientist's actual publication activity. The rationale for this is that there may be scientists who do appreciate knowledge enhancement more than reputational concerns, yet are not successful publishers. It implicitely asssumes that there are scientists who are willing to pay (with a low number of publications) for deviating from the prevailing norm, i.e. the model allows for non-conforming behavior (Brock and Durlauf, 1999). It is argued that scientists who show non-conforming behavior reveal a motivational and cognitive bias. Scientists who deviate from the prevailing scientific paradigm are assumed to constitute a group with a common focus. This common focus allows a new knowledge field to emerge.

Scientists cannot observe the individual disposition of other scientists. However, a scientist takes notice of the output of the scientific coordination process, concretely the number of publications and ranking of other scientists. This is the primary information that influences a scientist's strategy. Moreover, two parameters that reflect the context of a scientific discipline are considered: the degree of organizational inertia and the parameter of half life of scientific knowledge. While scientists can observe both parameters ex-post, they can act upon organizational inertia and adapt their strategies, whereas the parameter of half life is considered to be an exogenous parameter as explained in the next section.

```
initialize scientists and knowledge fields
link scientists to knowledge fields
initialize parameters
while simulation time < termination time
scientists
    publish
    update their knowledge stock
    update their ranks
    calculate utility from knowledge and reputation
if subgroup of scientists does not reach
utility threshold and conditions are met
scientists
    hatch a new knowledge field
    and link to it
end
plot graphics
calculate statistics
```

Table 1: Pseudocode of the simulation model

The scientist in action: outline of the simulation model

The pseudocode in Table 1 summarizes the simulation.

To initialize, n scientists are randomly assigned to one of j knowledge fields. In the current model, a scientist is never assigned to more than one knowledge field. It is assumed that separate knowledge fields may be incommensurable (Brock and Durlauf, 1999). Accordingly, the scientist has to decide which school of thought he wants to belong to, i.e. he makes an "investment" decision. Changing to other fields of knowledge is possible but costly.

All scientists who are assigned to one knowledge field constitute a scientific community. The fundamental activity to attain intrinsic and extrinsic non-monetary utility is to conduct research, i.e. to publish articles in the correspondig field. To model this process, Rauber and Ursprung (2008) used the hurdle model (see also Watts and Gilbert (2011) who used the Weibull distribution for related processes). As this model does not focus on the publication process itself and to keep the simulation as tractable as possible, publication activities are modeled as an adapted version of the lottery example borrowed from the Netlogo Models Library (Wilensky, 2004).

As a convention, a scientist is defined as someone who publishes at least one scientific paper. In the first period, each scientist produces a minimum of 1, and a maximum of 2 publications pub. The accumulated output a scientist produces yields the scientist's cumulative productivity $pr_{i,t}$ and is related to the maximum accumulated output of one of his fellows in his scientific community. In the following periods -according to the lottery example- the propensity to generate additional publications is higher for those scientists who already have a high cumulative productivity. Unless a scientist does not win the lottery, he will maintain his number of publications for the following periods. This assumption can be justified as one simulation run in the model does not intend to reflect a scientist's lifecycle-productivity (Levin and Stephan, 1991) but considers fluctuations within a lifecycle of scientific competition and thus accounts for the fact that no clear evidence exists for an increasing or decreasing overall average publication output per scientist (Wagner-Doebler, 2001). Since only a limited number of scientists will ever win the lottery, the number of publications per author approximates a skewed distribution (Lotka, 1926). Publication activities serves as the intrinsic motivation in that they enhance the scientist's accumulated scientific knowledge. Equation (2) can be specified for the simulation in that knowledge w of a scientist i grows according to

$$w_{i,t+1} = \theta * w_{i,t} + \sqrt{pr_{i,t} * pub_{i,t}} \tag{6}$$

While there is consensus that publications serve as an indicator of scientific output, measuring *knowledge* is not only a problem in ABM models, but it is also a problem in the real world (Payette, 2011). The approach in (6) is justified as follows: The first term accounts for the fact that any scientific knowledge is subject to depreciation. Previous knowledge is thus multiplied with a constant half-life factor $\theta \in (0, 1)$. For instance, a half-life factor of .93 means that after a period of approximately 10 years, the scientific knowledge has lost half of its value in terms of topicality. The specification of θ is subject to the scientific discipline under consideration. As publications can be interpreted as the documentation of knowledge development, the second term describes the effectiveness of a scientist to transform scientific output (publications) into outcome (knowledge). $pr_{i,t}$ is calculated from the cumulated publications of a scientist in field j, normalized for the interval [0,1]. The higher his cumulated productivity $pr_{i,t}$, the higher the propensity to win the lottery in the next period and the more effective output is transferred into outcome. The square-root function represents the assumption that efforts to increase the knowledge stock in a specific knowledge field are subject to diminishing marginal returns (Koelbel, 2001).

Besides knowledge growth, publication activities serve to attain scientific reputation. Following Hopkins and Kornienko (2004) and Loch et al. (2001), ranks are the result of sorting the scientists' status weighted with a factor of organisational memory $(1 - \delta) \in (0, 1)$.

$$ra_{i,t} = (1 - \delta) * st_{i,t-1} + \delta * st_{i,t} \tag{7}$$

Status st in (7) simply counts a scientist's fellows with less or strictly less publications and adds a minimum status value of 1 for each scientist. For each community of scientists, the status values are sorted in ascending order which yields rank $ra = 1$ for the scientist with the highest status. For scientists of one community who may have the same number of publications, it is allowed that they are assigned to the same rank. $(1 - \delta)$ reflects the organisational memory of a scientific *discipline*, i.e. it is defined for all knowledge fields of one discipline. The smaller δ is, the more a scientist benefits from his last period status and the harder it is for other scientists to achieve a higher status respectively.

Selected results on the influence of organizational inertia

Some simulation experiments have been conducted to test how δ influences the distribution of ranks in one specific knowledge field over one lifecycle (run) of scientific competition (35 periods). From the intuition it is sensible to believe that the more successful scientists group to the higher ranks while the scientists who do not stand out constitute the group with the lower ranks.

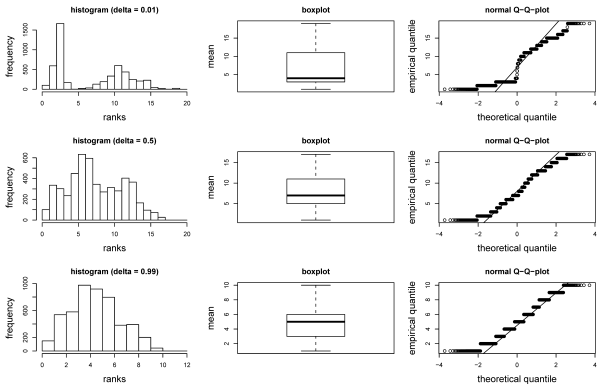

Figure 1: Frequency distribution of ranks for 50 scientists in period 35 based on 100 simulation runs

As can be seen in the upper row of Figure 1, the distribution of ranks is bipolar when there is a high degree of

organizational inertia. In this case, the histogram shows that on the aggregate level, scientists stay pretty separated over the periods of time, and the rank they take at the beginning is rarely prone to change. As δ rises, the frequency disribution converges to a normal distribution, i.e. the ranks change over time and their distance tends to get smaller. However, as the size of a scientific community slightly changes in each simulation run, the results can only show some basic mechanism which prevail on an aggregate level.

The implication of using a factor of organisational inertia $(1-\delta)$ is to show that even though a scientist may achieve a high number of publications, this does not necessarily imply an equivalent ranking value. For instance, if $(1-\delta)$ is close to 1, in the case of two scientists both of whom have a certain number of publications, only the one with the higher rank in previous periods gets rank 1. This was verified in a simple correlation analysis. As the increasing (negative) correlation coefficients show in Table 2, the smaller the parameter for organizational inertia, the closer the ranking reflects the scientists' current publication activities. It should be noted that the negative signs of τ are attributed to the fact that the smallest rank number represents the best rank.

δ	τ	z-value
0.01	-0.6831274	-59.03
0.5	-0.7906952	-69.79
0.99	-0.8133727	-69.86

p-value $<$ 2.2e-16 in all cases

Table 2: Kendall's rank correlations

The aspiration level of scientists and scientific advancement

Looking at the scientists' aspiration level in terms of the knowledge stock, a scientist is said to be satisfied if his knowledge stock grows. In the reference model, the overall amount of publications rises faster than the individual amount of publications, indicating that there is a natural crowding of knowledge fields over time. Thus the cumulated productivity $pr_{i,t}$ decreases for all scientists who do not win the lottery. This again leads to decreasing returns of knowledge growth $\Delta w = \frac{w_{i,t}-w_{i,t-1}}{w_{i,t-1}}$.

In general, knowledge growth becomes zero when the depreciation of the accumulated knowledge stock as defined in the first term of Equation (6) is faster than new output is transferred to knowledge (second term in Equation (6)). This process reflects the fact that the more that is already known in a specific knowledge field, the more effort has to be spent to attain substantially new findings (Rescher, 1978). As mentioned before, unsatisfied agents have the possibility to initiate a new knowledge field. Scientists who engage in a new knowledge field do not necessarily have to stem from the same community of scientists. At first, a new knowledge field is expected to be smaller than existing ones. With a lower number of competitors, they tend to attain a higher cumulated productivity and rank as defined in Equation (6) and Equation (7). As their cumulated productivity and knowledge increases, the propensity to win the lottery for additional publications rises as well. This process reflects two stylized facts of scientific competition: First, when a knowledge field is young, the scientific insights that are achievable are greater (Rescher, 1978) and second, scientists being the first to publish in a specific field attain higher reputation due to the priority rule (Merton, 1957).

For a new knowledge field to emerge, (1) there must be a minimum number of scientists who did not reach their aspiration level in regard to knowledge growth, (2) this state must have lasted for a minimum number of periods, and (3) the agents need a minimum capacity, i.e. knowledge, to engage in scientific search. The rationale for the latter condition results from the fact that scientific innovation is costly in terms of effort and risk and requires a minimum amount of scientific capital to successfully initiate a new field after all.

So far, the simulation model accounts for the first two conditions (see Table 3). The minimum number of unsatisfied agents is set to ten scientists, i.e. 10 per cent of the population of one scientific discipline. This reference value follows a study by Fagerberg and Verspagen on the emergence of the field of innovation studies in the 1960s which finds that the number of influential authors to engage in this new field can be traced back to a group of this size. The rationale for a minimum group size is that some degree of shared knowledge and common focus among unsatisfied scientists has to be developed before a new knowledge field is able to thrive (Fagerberg and Verspagen, 2009). This process takes time and therefore, a number of periods is necessary to let unsatisfied agents adjust their research efforts. In the simulation model, this start-up time is defined as periods with zero growth of knowledge for the scientists under consideration. The number is set to four, spanning a maximum period of two successive scientific evaluations. Taking the values as noted in Table 3 as input parameters for a test run, a simulation has shown that out of 100 runs, 71 times one new knowledge field emerges in a lifecycle of 35 periods. Subsequent analysis will test the sensitivity of the parameters used here.

DISCUSSION AND OUTLOOK

The utility-driven approach presented in this paper is a fruitful approach to unfold the mechanism on the micro and macro level. Two basic processes that drive the scientist's utility have been presented in this paper: At first, the process of knowledge generation that accounts for the depreciation of accumulated knowledge and diminishing marginal returns of efforts, and secondly, the process of how organizational inertia influences the scientists' reputation. Since it is argued that different utility types of

Parameter description	Example values
Initialization	
No. of knowledge fields within one scientific discipline	2
No. of scientists	100
No. of time steps	35
Parameter for half life of scientific knowledge θ	0.93 ($\approx$ 10years)
Parameter for organizational inertia $(1-\delta)$	0.5
Assignment of parameter α in utility function	random $\in [0,1]$
Maximum no. of additional publications for "lottery winner" in each period	2
Emergence of new knowledge field	
Minimum no. of scientists to engage in new knowledge field	10
No. of periods (start-up time) until a new knowledge field can emerge	4
No. of times a new knowledge field emerges within 100 runs	71

Table 3: Parameters for the simulation model

scientists exist, some of them engage in new knowledge fields and add to the advancement of science. This is explicitly accounted for in the simulation model. In the previous section the point was made that the attainment of knowledge growth or reputation is costly since any kind of effort (time, money, etc.) has to be spent on these activities. This effort represents a disutility that has to be accounted for. From what has been said so far, two aspects have to be considered. For some scientists, it may be worth sticking to a specific knowledge field. They are able to take advantage of scale effects in that each additional publication is less costly and reduces the disutility of effort. On the other hand, as a specific knowledge field grows and tends to get more crowded, each additional publication yields smaller returns. Scientists consider this as a trade-off decision. Accordingly, as scientists represent different utility types, they are presumed to differ in their decisions and willingness to take the risk of engaging in new knowledge fields. The extent of disutility is determined by the resources that each scientist is endowed with. On the macro level, the budget allocation is a special representation of the institutional setting within which the process of scientific coordination unfolds. As budget allocation policies have recently been subject to change, enforcing the competitive or market-like character of science, considerable effects are expected concerning the coordination result of scientific competition. In the context of the simulation model, budget allocation policies are interpreted as a selection environment that not only affect the decisions of scientists, but implicitly act on the motives of scientists (utility types). It is hypothesized that a growing share of risk-averse utility types and imitative behavior emerges. This is argued to have a negative effect on the coordination results, in particular the scientists' propensity to engage in innovative research and, by means of emerging knowledge fields, contribution to the stock of scientific knowledge.

REFERENCES

Becher, T. and Trowler, P. (2001). *Academic Tribes and Territories: Intellectual Enquiry and the Culture of Discipline*. Open University Press, Buckingham, 2nd Edition.

Bloor, D. (1991). *Knowledge and social imagery*. University of Chicago Press, Chicago, 2nd Edition.

Brenner, T. (2006). Agent Learning Representation: Advice on Modelling Economic Learning. In: Tesfatsion, L. and Judd, K., Editors, *Handbook of Computational Economics: Agent-Based Computational Economics*, Pages 895–947. Elsevier.

Brock, W. A. and Durlauf, S. N. (1999). A formal model of theory choice in science. *Economic Theory*, 14(1):113–130.

Carayol, N. (2008). An Economic Theory of Academic Competition: Dynamic Incentives and Endogenous Cumulative Advantages. In: Albert, M., Voigt, S., and Schmidtchen, D., Editors, *Conferences on New Political Economy*, Volume 25, Pages 179–203. Mohr Siebeck, Tuebingen, 1st Edition.

Chang, M.-H. and Harrington Jr., J. E. (2006). Agent-Based Models of Organizations. In: Tesfatsion, L. and Judd, K., Editors, *Handbook of Computational Economics: Agent-Based Computational Economics*, Pages 1273–1337. Elsevier.

Cox, R. A. K. and Chung, K. H. (1991). Patterns of Research Output and Author Concentration in the Economics Literature. *The Review of Economics and Statistics*, 73(4):740–747.

Diamond, A. M. (1988). Science as a rational enterprise. *Theory and Decision*, 24:147–167.

Downes, S. M. (2001). Agents and Norms in the New Economics of Science. *Philosophy of the Social Sciences*, 31:224–238.

Edmonds, B., Gilbert, N., Ahrweiler, P., and Scharnhorst, A. (2011). Simulating the Social Processes of Science. *Journal of Artificial Societies and Social Simulation*, 14(4):14.

Fagerberg, J. and Verspagen, B. (2009). Innovation studies - The emerging structure of a new scientific field. *Research Policy*, 38(2):218–233.

Gilbert, N. G. (2007). A generic model of collectivities. *Cybernetics & Systems*, 38(7):695–706.

Gilbert, N. G. (2008). *Agent-based models*. Quantitative applications in the social sciences. Sage Publications, Los Angeles.

Hopkins, E. and Kornienko, T. (2004). Running to keep in the same place: Consumer choice as a game of status. *American Economic Review*, 94(4):1085–1107.

Kitcher, P. (1993). *The Advancement of Science*. Oxford University Press, New York.

Koelbel, M. (2001). Das Wachstum der Wissenschaft in Deutschland 1650-2000. In: Parthey, H. and Spur, G., Editors, *Wissenschaft und Innovation. Wissenschaftsforschung. Jahrbuch 2001*, Pages 113–128. Gesellschaft fuer Wissenschaftsforschung.

Latour, B. (1987). *Science in action*. Harvard University Press, Cambridge.

Levin, S. G. and Stephan, P. E. (1991). Research Productivity over the Life Cycle: Evidence for Academic Scientists. *The American Economic Review*, 81(1):114–132.

Loch, C., Huberman, B., and Uelkue, S. (2001). Status Competition and Group Performance. In: Lomi, A. and Larsen, E. R., Editors, *Dynamics of Organizations*. Cambridge, MA: The M.I.T. Press.

Lotka, A. (1926). The frequency distribution of scientific productivity. *Journal of Washington Academy Sciences*, 16(12):317–324.

Merton, R. K. (1942 (1973)). The Normative Structure of Science. In: *The Sociology of Science: Theoretical and Empirical Investigations.* University of Chicago Press, Chicago.

Merton, R. K. (1957). Priorities in scientific discovery. *American Sociological Review*, 22:635–659.

Mirowski, P. (1996). The economic consequences of Philip Kitcher. *Social Epistemology*, 10:153–169.

Mitroff, I. I. (1974). Norms and Counter-Norms in a Select Group of the Apollo Moon Scientists: A Case Study of the Ambivalence of Scientists. *American Sociological Review*, 39(4):579–595.

Payette, N. (2011). For an Integrated Approach to Agent-Based Modeling of Science. *Journal of Artificial Societies and Social Simulation*, 14(4):9.

Rauber, M. and Ursprung, H. W. (2008). Life Cycle and Cohort Productivity in Economic Research: The Case of Germany. *German Economic Review*, 9(4):431–456.

Rescher, N. (1978). *Scientific Progress*. Pittsburgh University Press. German Edition: Wissenschaftlicher Fortschritt, de Gruyter, Berlin 1982.

Sent, E. (1996). An economists glance at Goldmans economics. *Philosophy of Science*, 64:139–148.

Simon, H. (1955). A Behavioral Model of Rational Choice. *Quarterly Journal of Economics*, 69:99–118.

Solomon, M. (1992). Scientific rationality and human reasoning. *Philosophy of Science*, 59:439–455.

Squazzoni, F. and Gandelli, C. (2012). Saint Matthew Strikes Again: An Agent-based Model of Peer Review and the Scientific Community Structure. *Journal of Informetrics*, 6:265–275.

Thurner, S. and Hanel, R. (2011). Peer-Review in a World with Rational Scientists: Toward Selection of the Average. *The European Physical Journal B*, 84:707–711.

Vanberg, V. (2010). The 'science-as-market' analogy: a constitutional economics perspective. *Constitutional Political Economy*, 21:28–49.

Wagner-Doebler, R. (2001). Rescher's Principle of Decreasing Marginal Returns of Scientific Research. *Scientometrics*, 50:419–436.

Watts, C. and Gilbert, N. (2011). Does cumulative advantage affect collective learning in science? An agent-based simulation. *Scientometrics*, 89:437–463.

Wilensky, U. (2004). Netlogo Lottery Example from Netlogo Library / Code Examples. Online: http://ccl.northwestern.edu/netlogo/.

AUTHOR BIOGRAPHIES

Melanie Baier graduated in economics and is a Ph.D student at Dresden University of Technology. Her email is `Melanie.Baier1@mailbox.tu-dresden.de`.

CHANGING DIMENSIONALITY IN THE POLITICAL ISSUE SPACE: EFFECTS ON POLITICAL PARTY COMPETITION

César García-Díaz
Department of Industrial Engineering
Universidad de los Andes
Cra. 1E 19A-40 (ML-702)
Bogotá, Colombia
E-mail:
ce.garcia392@uniandes.edu.co

Gilmar Zambrana
Department of Management
University of Antwerp
Prinsstraat 13 (Z.108),
Antwerpen, BE-2000, Belgium
E-mail:
gilmar.zambrana@ua.ac.be

Arjen van Witteloostuijn
Department of Organization and Strategy
Tilburg University
K1102A, 5000 LE, Tilburg, The Netherlands
E-mail:
a.vanwitteloostuijn@uvt.nl

KEYWORDS
Political party competition, agent-based modeling, organizational ecology, and dimensionality change.

ABSTRACT

We built an agent-based model of political party competition in order to explore the effect of the decrease in the number of relevant political issues on the number of political parties and the corresponding voter shares. We find that, when the space experiences a *political shock* and suddenly reduces in the number of dimensions, the number of political parties declines. We also observe that, after the shock, (i) the inert parties tend to improve their performance and that (ii) a few of the adaptive large size-seekers cushion their increased mortality hazard by locating in the zone with most intense competition (close to the political space center), which generates strong party size effects.

INTRODUCTION

By and large, the number of political parties in political systems has been associated with both the existence of social cleavages and the features of electoral institutions. On the one hand, political parties are founded to stand for specific social cleavages that represent the regional, religious or ethnic heterogeneity in a political system (Grumm 1958; Lipset and Rokkan 1967; and Rose and Urwin 1970). On the other hand, features of electoral institutions such as the majority rule, proportional representation, district magnitude and ballot structure are important in explaining the number of political parties. The most accepted models propose a direct link between district magnitude, i.e. the number of legislators elected in a district, and the number of political parties (Lijphart 1990; Riker 1982; Taagepera and Shugart 1993; Cox 1997; Neto and Cox, 1997; Ordeshook and Shvetsova 1994; Powell 1986; Taagepera and Grofman 1985). However, there are multiparty systems in which these models fail to predict the number of political parties, especially where district magnitude is high (Lowery et. al. 2011). These models fail to take into account the competition among political parties for voters, especially when a political system is overcrowded with political parties. In this setting, parties need to differentiate themselves in order to attract sufficient number of voters (Lowery et. al. 2010). In modern democracies, the emergence of new sources of political conflict such as environmental protection, women's rights and living standard issues have created new forms of competition among political parties. Nowadays, short term factors such as issues and candidate images are considered by the electorate when they cast their ballot (Dalton, 1996). Lowery et al. (2011) show that, in the Netherlands, the outcome of competition among political parties can be co-explained by the number of relevant issues. The larger the issue agenda space is, the higher the chances that new political parties can develop a distinctive issue configuration that attracts enough voters to survive, and vice versa. Therefore, environmental changes that modify the number of issues affect the density of political parties in a political system, keeping the *resource* availability – i.e., the number of voters – constant. Unlike prior work that focuses on stable environments, we would like to concentrate on the impact of shocks or crises that have the potential to suddenly change the issue agenda space – e.g., terrorist attacks, economic crises or territorial wars. Our aim is to analyze the consequences of a shock that decreases the dimensionality (i.e., number of political issues) of political space. We follow and extend the model developed by Laver and Sergenti (2011), who built an agent-based model to explain how different adaptive party strategies to compete for votes.

AGENT-BASED MODELING OF POLITICAL COMPETITION PROCESSES

Rational choice theory based on mathematical modeling, although elegant, is inadequate to explain complex phenomena in dynamic settings (Laver and Sergenti 2011). Rather, they start from unrealistic assumptions concerning the agents engaged in political competition, particularly perfect rationality of voters and political parties. A realistic model of multiparty competition should consider that politics is *dynamic*, (i.e., does not reach a static equilibrium, but instead evolves over time), *complex*, (i.e., results feedback generate iterative inputs to the system), *diverse*, (i.e., politicians use different strategies to tackle the same

Proceedings 26th European Conference on Modelling and Simulation ©ECMS Klaus G. Troitzsch, Michael Möhring, Ulf Lotzmann (Editors)
ISBN: 978-0-9564944-4-3 / ISBN: 978-0-9564944-5-0 (CD)

problem) and *not random* (i.e., system-level predictions can be made) (Laver and Sergenti 2011). Agent-based modeling (ABM) investigates outcomes from interaction among a diverse set and large number of boundedly rational agents that adapt in an evolving system. ABM is based "on adaptive learning rather than forward looking strategic analysis" (Laver and Sergenti 2011:5). Therefore, ABM constitutes a more realistic approximation when agents – here, political parties – constantly adapt to changing circumstances, interact with other agents and make decisions with limited or partial information.

POLITICAL NICHE THEORY AND CHANGING ISSUE SPACE DIMENSIONALITY

The representation of the political system using a spatial rendering has been used to map voters' policy preferences in a one-dimensional issue space (Dowson 1957). More recently, ABM was applied to analyze political competition in a multidimensional issue space setting. In such a space, a political party selects a position taking into account the relevant political issues in order to attract voters (Muis 2010; Laver 2005; Laver and Schilperoord 2007; Laver and Sergenti 2011; Kollman et al. 1992). The majority of these studies analyze political processes in a context of environmental stability. However, criteria and issues determining whether or not to adhere to a political party may change radically over time. Issues that are initially rather unimportant might become extremely relevant over the course of time, and may reshape voter preferences. Examples include *shock events* that might change the political agenda of parties. A major event can radically redefine strategic positioning in political space. An event like the assassination of Pim Fortuyn in 2002 had a decisive impact on the subsequent political agenda of parties in the Netherlands, triggering high volatility where some parties experienced a surprising defeat while others benefited from an unexpected revival and unprecedented success (Muis 2010). Similarly, the occurrence of terrorist attacks has proved to affect cabinet duration (Gassebner et al. 2008, 2011) and coalition formation (Indridason, 2008).

During the 1990s, a number of Latin American countries witnessed dramatic changes in their political system, either generating an expansion with entry of new parties capturing a large part of the electorate (e.g., Uruguay) or contraction due to the disappearance of many political parties (e.g., Paraguay). In other cases, such as Peru and Venezuela, there was a collapse of the system that involved an electoral decline of incumbent political parties and their subsequent disappearance (Wills-Otero 2009). The reasons for the collapse in Peru and Venezuela were not primarily structural causes or poor economic performance; rather, they are related to internal conflict and crisis of representativeness before the collapse (Mainwaring et. al. 2006).

To analyze the consequences of a collapse in the agenda issue space, we concentrate on systems with a *multidimensional political space* and *multiparty competition*. Many democracies in the world comprise *multiparty settings* (e.g., Continental European and Latin American countries). Another important assumption we adopt is that *a coalition is needed* to form a government. This has implications for the behavior of the voters. When a coalition of parties is part of the government, voters realize that voting sincerely for the preferred party does not harm the possibilities that their preferences are represented in the government coalition formation process (Downs 1957, Lowery et. al. 2010).

There are two factors that affect the opportunities to build a distinctive policy profile. The first involves an increase (reduction) in the number of issues. Having more (fewer) issues, to compete for votes, increases (reduces) the possibilities to differentiate from other political parties (Lowery et. al. 2011). The second relates to increases (decreases) of the span of the issues. When more (less) extreme positions are created regarding an existing issue, more (less) possibilities for a distinguishable political identity emerge (Péli and Witteloostuijn, 2008). In our case, we keep constant the span of the issue space. A political party uses its position to attract specific voters, refered to as the fundamental niche (Hannan and Freeman 1977). These positions may overlap with those of other political parties. The realized voter reflects a political party's realized niche (Péli and Witteloostuijn, 2008). The fundamental niche can be understood as the demand of political representation that a group of voters has, considering a set of issues. Then, the political party is the organization that tries to satisfy such a demand, which can be represented by a location in the *n*-dimensional issue space. The chosen location reflects the party's strategy for *niche differentiation* (Lowery et. al. 2010). Chances for niche differentiation increase with the available issues in the political space. This may happen when a new issue appears (Péli and Nooteboom 1999), which generates extra room for differentiation from which a new party may benefit. If issue space dimensionality collapses, then creating a differentiating issue configuration is harder (Lowery et. al. 2011), with similar parties competing for similar voters under higher *niche overlap*. This collapse or expansion of the issue agenda space affects the birth and mortality rates of political parties.

Conjecture 1: With a constant voter population, the smaller the number of issues on the political agenda, the smaller the number of political parties that survive.

Political parties can use different strategies to attract voters. Some parties are more successful than others in responding to their constituencies; some parties adapt more successfully to challenging changes than others do (Wills-Otero, 2009). Democratic parties that adapt

policies according to the preferences of their constituency are called *aggregators*, ideologically driven parties with an unchangeable policy set are referred to as *stickers*, and parties that constantly modify their policies to increase their size are coined *hunters* (Laver, 2005). *Hunters* and *aggregators* employ adaptive strategies. However, while *hunters* are driven to attract new voters to increase their vote share, *aggregators* move to accommodate preference shifts of their current electorate. *Stickers* never change position. Mass-based populist parties are more successful in adapting to challenging contexts because they have flexible and less institutionalized structures, whereas parties that have highly routinized and more institutionalized structures fact limitations to adapt to those contexts (Wills-Otero, 2009). This argument favors more flexible political parties over their more inert counterparts.

Conjecture 2: A shock that decreases issue space increases the relative mortality hazard of immobile parties (i.e., stickers) vis-à-vis their mobile counterparts (i.e., aggregators and hunters).

However, organizations must be inert to engage in reliable and accountable transactions (Peli et. al. 2000). In a similar vein, political parties can stick to their position to increase their credibility with the aim to attract voters. A political party that changes its policy set frequently cannot build a credible political position, which might affect its voter share negatively. Additionally, party adaptability is restrained by the availability of human and financial resources, as well as by the uncertainty and distrust associated with change (Denemerk 2003). Organizational change studies have revealed that failure increases after changes in organizational core elements (Greve 1999). A sudden change in the political issue space will trigger adaptive behavior of aggregators and hunters. These moves through space are risky, threatening survival chances.

Conjecture 2alt: A shock that decreases issue space increases the relative mortality hazard of mobile parties (i.e., hunters and aggregators) vis-à-vis their immobile counterparts (i.e., stickers).

THE MODEL

Preliminaries

We use a NetLogo implementation in which we assume a population of N voters distributed in a two-dimensional political issue space (Laver 2005; Kollman et al. 1992). We use Laver's model (2005) as a departure point. We introduce four key changes: (i) the voter's utility function measures distances to party policies according to a weighted block distance, as opposed to the traditional Euclidean-based approach; (ii) hunter strategists maximize party size according to the weights of the corresponding dimensions; (iii) issue-related weights are a function of time; and (iv) capabilities that might make a citizen turn into a politician develop endogenously over time. Like Kollman et al. (1992), we assume a political space with discrete positions. We consider two-dimensional uniform, unimodal and bimodal distributions of the voters' ideal preference points.

Political parties decide to take a position in the n-dimensional issue space in order to capture voters. In principle, issue spaces may feature a high number of dimensions. For instance, Kollman et al. (1992) assume a political space with 15 issues. However, Laver (2005) argues that many dimensions can be reduced to a few representative ones, since many of them happen to be highly correlated in real life. Péli and Nooteboom (1999) argue that individuals face a cognitive limitation when trying to decide with reference to more than five or six different criteria. Without loss of generality, we adopt a two-dimensional issue space, but assign different weights to both issues. Adopting ideas from Kollman et al. (1992), we assume that a weight s_i is associated with every issue (i = 1, 2,…, n). Such weights represent the importance of a given issue in citizens' preferences. A weight can range from 1 if the issue is fully active to 0 if the issue is completely inactive. If we define x_{ij} as the voter j's ideal point on issue i, and y_{ik} as party k's positioning on this i-th issue (i = 1, 2,..., n), then voter j's utility is

$$u_j(k) = -(\Sigma^{n}_{i=1} s_i | x_{ij} - y_{ik} |)^2, \quad (1)$$

where |.| stands for "block distance" (see Laver and Sergenti 2011).

Birth and death of parties

Following Laver and Schilperoord (2007), the number of parties in the model is endogenous. We assume that there are two types of citizens: supporters and leaders. Only leaders can form parties, while supporters adopt the role of plain voters. Any citizen has a chance to become a party leader, but past leaders are more likely to become party leaders again. To model this, we assume that every citizen has a capability-related measure at each point in time, Cap_t. The higher the capability measure, the higher the chance this citizen will found a party. The initial condition is $Cap_0 = 10$ for every citizen. When a citizen becomes a party leader, her or his capabilities increase according to the captured voting population: $Cap_{t+1} = Cap_t + CapCoef \cdot PartySize_t$, where $CapCoef$ is a coefficient (we set $CapCoef = 0.5$) and $PartySize$ is realized party size at time t.

Voters compute their utilities associated with the existing parties's positions and become supporters of the party that maximizes their utility (Downs 1957). Every citizen j computes a cumulative dissatisfaction level (Laver and Schilperoord 2007). Since the maximum utility value is zero, each utility value can be interpreted as a deviation from the optimal value – i.e., when the voter's ideal point is perfectly matched by a

party's position in space. Every voter can cumulatively compute a dissatisfaction value according to the cumulative sum of deviations from her or his own ideal point. If individual j computes, at time t, the utilities $u_j(1)$, $u_j(2)$, ..., $u_j(k)$ with respect to k existing parties, then the instantaneous dissatisfaction value (at time t) is defined according to (see Laver and Schilperoord 2007)

$$D_{j,t} = \max_k (u_{j,t}(k)). \quad (2)$$

We denote cumulative dissatisfaction as:

$$D^*_{j,t} = D_{j,t} + \alpha D^*_{j,t-1}, \quad (3)$$

with $\alpha \in [0,1]$ as a cumulative dissatisfaction coefficient (Laver and Schilperoord 2007). The cumulative dissatisfaction value is confronted with a certain threshold or critical point in order to define the likelihood of becoming a party supporter. More specifically, the critical point at time t is defined as (Laver and Schilperoord 2007).

$$D^c_{j,t} = \beta(D^*_{j,t} / \text{mean}(D^*_{j,t})). \quad (4)$$

The coefficient β corresponds to a scale factor. The denominator of the above expression represents the average dissatisfaction value among all voters. The probability to found a party (i.e., to become a party leader) at time t is then

$$(Cap_{j,t} / \Sigma^N_{k=1} Cap_{k,t}) D^c_{j,t} . \quad (5)$$

Each newly born party has an equal probability of picking up any of the above-mentioned strategies. Parties that fall below a certain affiliation share are declared dead, and are dissolved. We take this minimum affiliation value as three per cent of the total vote share. When a party share goes below the minimum affiliation value, the party leader becomes a normal citizen and the voters seek for an alternative affiliation according to the rules described above. In terms of an ecological approach, the party dies due to lack of fitness with its niche.

Party strategies and the role of changing spaces

As introduced above, following the work by Laver (2005), Laver and Schilperoord (2007) and Laver and Sergenti (2011), we define three vote-seeking strategies of parties: *sticker* (the party never changes position), *aggregator* (the party always relocates at the centroid of mean voter support), and *hunter* (the party gradually moves in space toward a perceived size-maximizing position; otherwise the party moves backwards). Since dimensions – or issues – might have different degrees of importance (weights), *hunters* move as to the weights value in each dimension. That is, *hunters* move the farthest in the dimensions that matter the most.

We assume that political issue spaces change due to a transformation of the relative importance of political issues. This means that the coefficients s_i are a function of time. The point at which there is a sudden change of the s_i coefficients, is defined as a *shock*. There are two different types of space change: (ii) *an absolute space collapse* takes place when one of the dimensions absorbs all relevance in the computation of the citizens' utility values; (ii) *a change of relative issue dominance* implies that the relative importance of issues does change (for instance, when an issue that is relatively unimportant becomes highly relevant). Here, we focus on the former.

We introduce a two-dimensional space that runs until time t = 1000 (i.e., the moment of collapse); then, a shock occurs. Following the shock, the simulation continues for another 1000 time steps, reaching a total of 2000 time steps. We set the initial number of parties at five with randomized strategies, and $\alpha = \beta = 1$.

SUMMARY OF RESULTS

We ran our three simulation experiments with a constant voter population of 5,000 voters. Each experiment takes a different voter distribution: uniform, unimodal, and bimodal. We ran 100 simulations for each experiment. We use weights $s_x = s_y = 1$ before the shock, and weights $s_x = 1$, $s_y = 0$ after the shock. In the case of the uniform distribution, the number of political parties declines from 18 to 12. See Figure 1.

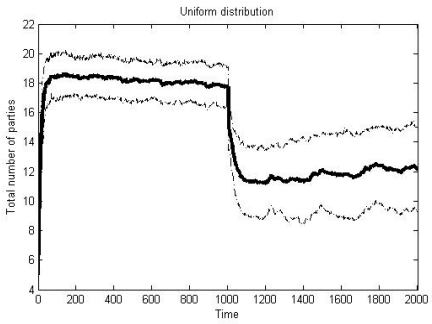

Figure 1. A space collapse shows that the number of parties in the model declines just after the shock at t = 1000. The black central line indicates average behavior and the dotted lines indicate a one standard deviation value range.

Conjecture 1 is confirmed for the uniform distribution. Also, remarkably similar results were observed for the runs with unimodal and bimodal distributions. That is, a collapse in the number of parties always occurs after the shock. The narrower the issue agenda space, the lower the chance that new political parties can develop an issue configuration to attract voters successfully. Similar parties compete for voters with similar preferences. The collapse of the space triggers increased party niche overlap, which leads to increasing competition and the subsequent reduction of the density of political parties in the political system.

Strategy performance in a uniform distribution

A closer look at the performance of different party strategies reveals an effect on the likelihood of survival. *Aggregators* perform best before the shock in terms of

number of parties and aggregated mean vote share (or average party size). See Figure 2. After the shock, the aggregators' performance drops since they are not able to adapt to the post-shock space. A shock reduces opportunities for differentiation and largely hits the aggregators' strategy. Before the shock, each party performs, on average, roughly equal in terms of voter share; after the shock, the average *hunter* party significantly increases performance.

When a sudden decrease in the number of issues occurs, the party niches increase in overlap, boosting competition as now similar parties compete in the same space for voters. The immediate effect is that fewer political parties obtain the support of voters. The *aggregators* exhibit the worst performance in terms of both number of political parties and mean vote share after the shock.

When *aggregators* face other party strategies, especially *hunters,* they do not engage in direct competition but rather seek to protect their current share, leaving room for the advancement of *hunters*. *Aggregators* are pushed out of political space by the *hunters*' large size-seeker behavior. *Stickers* have similar long-run success rates as *hunters* in terms of number of political parties, being able to enlarge their vote share. However, in terms of vote share, *hunters* have a notable advantage over *stickers*, since the former capture a large chunk of the electorate of the *aggregators* after the shock. See Figure 3.

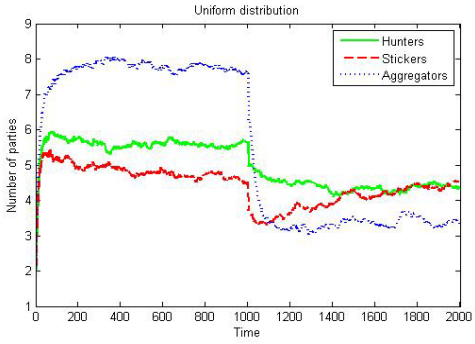

Figure 2. Average performance of party strategies under a uniform distribution of voters. Shock at $t = 1000$.

Strategy competition in a unimodal distribution

Surprisingly, *stickers* are more successful in terms of the number of political parties in a unimodal distribution of voters. See Figure 4.

With respect to the mean vote share, *hunters* are the largest. *Stickers* tend to survive in locations where voters are not densely concentrated; *hunters* steadily locate where the voter mass is more abundant (closer to the electoral space center). However, competition is more intense close to the electoral space center.

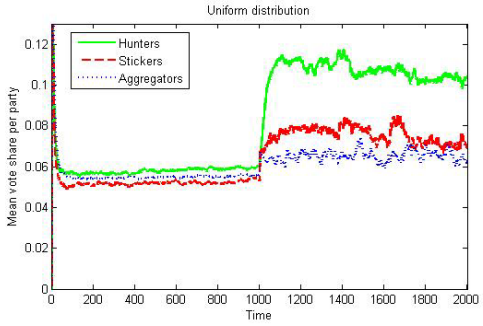

Figure 3. Mean vote share per party under a uniform distribution of voters. Shock at $t = 1000$.

The surviving parties near the center manage to attract more voters than those located further away. Above, we argued that *aggregators* do not perform well in the presence of competition. That it is the reason for their bad performance from the beginning. After the shock, many political parties die. The most affected are *hunters* since they are located in more central positions, when there is a collapse of issue dimensionality; hence, competition increases even more where they are located. Therefore, fewer hunters are able to survive after the shock. *Stickers*, by and large, locate further away from the center, and do not face the same negative impact of space collapse as *hunters* do.

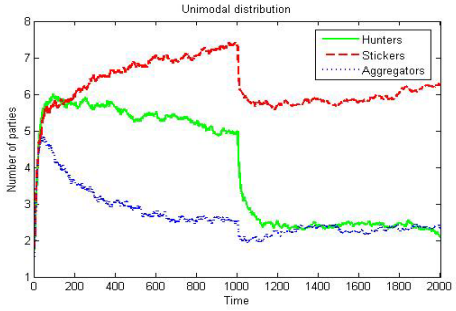

Figure 4. Average performance of party strategies under a unimodal distribution of voters. Shock at $t = 1000$.

The above argument is in line with ecological theories that argue that selection favors inert organizations, as reflected in Conjecture 2alt. This set of results deserves a more detailed analysis. First, our findings reveal how inert organizations can benefit from "standing still", as traditional models in organizational ecology have claimed. In our model, a collapse of resource space means that only a relevant "survivor" dimension sustains the whole set of political issue preferences. In such a space, a party that concentrates on a very specific, fixed voter preference might find itself favored by the reduced set of political preferences. Second, our results exemplify how parties with an inflexible (or perhaps, extremist) position might be hit by luck during a space collapse, gaining subsequent popularity. Nevertheless, surviving *hunters* can expand their vote share in quantities larger than their competitors. In the case of a unimodal distribution, being immobile pays off in terms of survival when the party is located

between the tails and the center. In terms of vote share, however, party size might be able to offset the negative impact of the increased mortality hazard of locating in the area of intense competition (near the center).

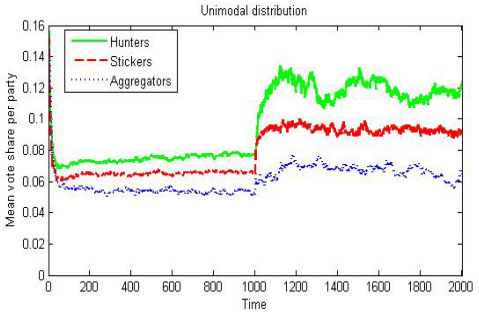

Figure 5. Mean vote share per party in a unimodal distribution of voters. Shock at $t = 1000$.

The bimodal case

In the bimodal case, results as to the behavior of the different strategies are similar to those observed in the case of the unimodal distribution. Worth mentioning is that resources are divided in two different groups of voters, with party competition occurring within these groups because parties cannot easily move across the whole political space. Competition is higher around the space peaks. *Hunters* perform as well as *stickers* before the shock in terms of the number of parties, and maintain a higher aggregated voter share. See Figure 6. After the shock, however, tougher competition increases the mortality hazard of *hunters*. Like in the unimodal case, the increase in the mortality hazard due to intensified competition is offset by the increase in average party size, implying that larger hunter survivors expand their vote share. See Figure 7.

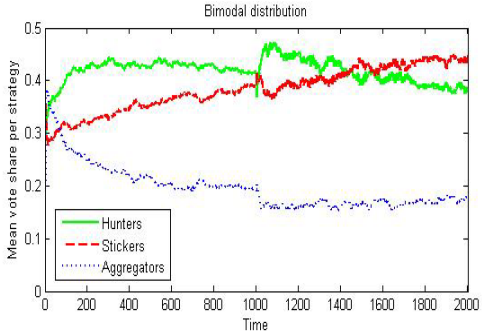

Figure 6. Mean vote share per behavioral strategy in a bimodal distribution of voters. Shock at $t = 1000$.

CONCLUSIONS

The model's results show consistency with the expected outcomes described in the Conjecture 1. Simulation outcomes reveal that the number of political parties after the shock immediately decreases. The results hold independently of the distribution of voters' preferences. Regarding Conjectures 2 and 2alt, we claim that an adaptive strategy does not always guarantee the survival of political parties. *Hunters* and *aggregators* adapt; however, the direction of the adaptation matters. Besides, the location and strategy of the political parties play a role in the survival of a political party. The inert *stickers* are more successful in surviving challenging conditions, when they are not located close to the center. The adaptive *hunters* survive by locating in spots where voters are more densely concentrated. Although fewer *hunters* survive in comparison to *stickers* after the shock, they capture more voters. A smaller distance to the center is associated with a larger mortality rate, but larger party sizes seem to offset the distance effect. For future research, additional explorations include the change of relative dominance of a particular political issue and the study of independent voter distributions per dimension.

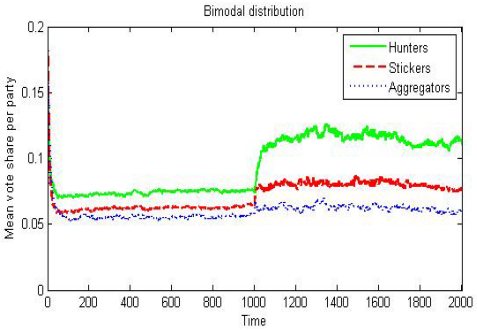

Figure 7. Mean vote share per party in a bimodal distribution of voters. Shock at $t = 1000$.

REFERENCES

Cox, G.W. 1997. *Making Votes Count.* Cambridge University Press, Cambridge.

Dalton, R. 1996. "Political cleavages, issues and electoral change". *Comparing democracies: Elections and Voting in Global Perspective*. Press, Sage: 319-342

Denemerk, D. 2003. "Electoral change, inertia and campaigns in New Zealand: The first Modern FPP campaign in 1987 and the first MPP Campaign in 1996." *Party Politics* 9 (5): 601–18.

Downs, A. 1957. *An Economic Theory of Democracy*. Harper & Row, New York.

Gassebner, M.; R. Jong-A-Pin; and J. O. Mierau. 2008. "Terrorism and electoral accountability: One strike, you're out!" *Economics Letters* 100 (1): 126–29.

Gassebner, M.; R. Jong-A-Pin; and J. O. Mireau. 2011. "Terrorism and cabinet duration." *International Economics Review* 52 (4): 1253–70.

Greeve, H. R. 1999. "The effect of core change on performance: Inertia and regression towards the mean." *Administrative Science Quarterly* 44 (3): 590–614.

Grumm, J. G. 1958. "Theories of electoral systems." *Midwest Journal of political Science* 2(4): 357–76.

Hannan, M. T.; and J. Freeman. 1977. "The population ecology of organizations." *American Journal of Sociology* 82 (5): 929–64.

Indridason I. 2008. "Does terrorism influence domestic politics? Coalition formation and terrorists incidents." *Journal of Peace Research* 45 (2): 241–59.

Kollman, K.; J.H. Miller; and S. E. Page. 1992. "Adaptive parties in spatial elections." *American Political Science Review* 86 (4): 929–37.

Laver, M. 2005. "Policy and the dynamics of political competition." *American Political Science Review* 99 (2): 263–81.

Laver, M.; and M. Schilperoord. 2007. "Spatial models of political competition with endogenous political parties." *Philosophical Transactions of the Royal Society B: Biological Sciences* 362 (1485): 1711–21.
Laver, M.; and E. Sergenti, 2011. *Party Competition: An Agent-Based Model*. Princeton University Press, Princeton.
Lipset, S.; and S. Rokkan, 1967. *Party Systems and Voter Alignments*. Free Press, New York.
Lijphart, A. 1990. "The political consequences of electoral laws, 1945–85." *American Political Science Review* 84 (2): 481–96.
Lowery D.; S. Otjes; S. Gherghina; A. van Witteloostuijn; G. Péli; and H. Brasher. 2011. "Policy agendas, and births and deaths of political parties." *Party Politics,* doi: 10.1177/1354068811407576.
Lowery D.; S. Otjes; S. Gherghina, A. van Witteloostuijn, G. Péli; and H. Brasher. 2010. "Unpacking LogM: Towards a more general theory of party system density." *American Journal of Political Science*, 54 (4): 921–35.
Mainwaring S.; A. M. Bejarano; and E. Pizarro. 2006. *The Crisis of Democratic Representation in the Andes*. Stanford University Press, Stanford CA.
Muis, J. 2010. "Simulating political stability and change in the Netherlands (1998-2002): An agent-based model of party competition with media effects empirically tested." *Journal of Artificial Societies and Social Simulation* 13 (2) 4.
Neto, O.; and G. W. Cox. 1997. "Electoral institutions, cleavage structures, and the number of parties." *American Journal of Political Science* 41 (1): 149–174.
Ordeshook, P. C; and O. V. Shvetsova. 1994. "Ethnic heterogeneity, district magnitude, and the number of parties." *American Journal of Political* Science 38 (1): 100–23.
Péli, G.; L. Pólos; and M. T. Hannan. 2000. "Back to inertia: Theoretical implications of alternative styles of logical formalization." *Sociological Theory* 18: 193–213.
Péli, G. and A. van Witteloostuijn. 2008. "Optimal monopoly area spanning in multidimensional commodity spaces." *Managerial and Decision Economics* 30 (1): 1–14.
Péli, G.; and B. Nooteboom, 1999. "Market partitioning and the geometry of the resource space." *American Journal of Sociology* 104 (4): 1132–53.
Powell, G. B. 1986. "Extremist parties and political turmoil: Two puzzles." *American Journal of Political Science* 30 (2): 357–78.
Riker, W. 1982. "The two-party system and Duverger's law: An essay on the history of political science." *American Political Science Review* 76 (4): 753–66.
Rose, R.; and D. Urwin. 1970. "Persistence and change in western party systems since 1945." *Political Studies* 18 (3): 287–319.
Schilperoord, M.; J. Rotmans; and N. Bergman. 2008. "Modelling societal transitions with agent transformation." *Computational and Mathematical Organization Theory* 14 (4): 283–301.
Taagepera, R.; and B. Grofman. 1985. "Rethinking Duverger's law: Predicting the effective number of parties in plurality and PR systems—parties minus issues equals one." *European Journal of Political Research* 13 (4): 341–52.
Taagepera, R.; and M. S. Shugart. 1993. "Predicting the number of parties: A quantitative model of Duverger's mechanical effect." *American Political Science Review* 87 (2): 455–64.
Wills-Otero L. 2009. "From party systems to party organizations: The adaptation of Latin American parties to changing environments". *Journal of Politics in Latin America* 1 (1): 123–41.

AUTHOR BIOGRAPHIES

CESAR GARCIA-DIAZ is a visiting scholar at the Department of Industrial Engineering at Universidad de los Andes (Colombia) and an affiliated researcher at the Management Department of the University of Antwerp (Belgium). He holds BSc/MSc degrees in Industrial Engineering from Universidad Javeriana (Colombia) and Universidad de los Andes (Colombia), respectively, and a PhD in Economics and Business from the University of Groningen (the Netherlands). His research interests are complex adaptive social systems and agent-based computational modeling in the social sciences. More information about him can be found at http://sites.google.com/site/cesaregarciadiaz/.

GILMAR ZAMBRANA is a PhD student at the Faculty of Applied Economics of the University of Antwerp (Belgium). He holds a MA degree in Development Studies from the Institute of Social Studies (The Hague, the Netherlands) and a BA degree in Economics from the Bolivian Catholic University San Pablo. He has been actively involved in the design and evaluation of public policies in governmental agencies. His professional and research interests are political economy, public economics, development, poverty and inequality, and social mobility.

ARJEN VAN WITTELOOSTUIJN is Professor of Organization and Strategy at Tilburg University (the Netherlands), Research Professor of Economics and Management at the University of Antwerp (Belgium), and Professor of Economics at Utrecht University (the Netherlands). He holds degrees in economics, business and psychology from the University of Groningen (the Netherlands) and a PhD degree in Economics from the University of Maastricht (the Netherlands). He is multidisciplinary social scientist who has published in major journals across a wide variety of disciplines, such as the *Academy of Management Journal, Academy of Management Review, Organization Science, Strategic Management Journal*, *American Journal of Political Science, American Sociological Review* and *Journal of Public Administration Research and Practice*.

Acknowledgements

The authors gratefully acknowledge the financial support through the Odysseus program of the Flemish Science Foundation (FWO).

TOWARDS A SERIOUS GAMES EVACUATION SIMULATOR

João Ribeiro[1], João Emílio Almeida[1†], Rosaldo J. F. Rossetti[1†], António Coelho[1‡], António Leça Coelho[2]
[1]Department of Informatics Engineering
[†]LIACC – Laboratory of Artificial Intelligence and Computer Science
[‡]INESC TEC – INESC Technology and Science
Faculty of Engineering, University of Porto
Rua Roberto Frias, S/N, 4200-465, Porto, Portugal
{joao.pedro.ribeiro, joao.emilio.almeida, rossetti, acoelho}@fe.up.pt

[2]LNEC – National Laboratory of Civil Engineering
Av. Brasil, 101, 1700-066, Lisboa, Portugal
alcoelho@lnec.pt

KEYWORDS
Evacuation simulation, fire drill, modelling and simulation, serious games.

ABSTRACT

The evacuation of complex buildings is a challenge under any circumstances. Fire drills are a way of training and validating evacuation plans. However, sometimes these plans are not taken seriously by their participants. It is also difficult to have the financial and time resources required. In this scenario, serious games can be used as a tool for training, planning and evaluating emergency plans. In this paper a prototype of a serious games evacuation simulator is presented. To make the environment as realistic as possible, 3D models were made using Blender and loaded onto Unity3D, a popular game engine. This framework provided us with the appropriate simulation environment. Some experiences were made and results show that this tool has potential for practitioners and planners to use it for training building occupants.

INTRODUCTION

The problem of evacuation from large facilities during an emergency or disaster has been addressed by researchers and practitioners in recent years. Real-world fire drills lack the realistic atmosphere of the emergency situation. Typically, the scenario is set up with the help of fire consultants and experts in the field, and the evacuation procedures follow some predefined rules and participants are expected to proceed accordingly.

In this paper, Serious Games (SG) are proposed as a means to overcome such drawbacks, since immersion into the emergency scenario artificially created using computer videogames is easier to accomplish. Also, the commitment of players, due to the excitement of using computer digital games, is expected to achieve better results than the traditional approaches.

In this paper the concept of serious games is used to build an evacuation simulator as an attempt to address some of the issues that were identified in real-world fire drills. It is our intention to improve the way people participate in such experiments enhancing their experience in many different ways. We have adapted and customised the environment of a game engine, in this case Unity3D, to support simulation features that enabled users to be tracked and assessed while playing. To test our approach and demonstrate its feasibility, we have carried out preliminary experiences with our prototype, in which subjects using the game environment were asked to evacuate a building in the case of fire.

The remaining part of this paper is organised as follows. We start by briefly presenting some related concepts that concern this project, such as pedestrian simulation and serious games. We then discuss on applying serious games to evacuation training, following the presentation and formalisation of our problem. We propose the approach implemented in this paper and suggest a preliminary experiment using our prototype. Some results are also discussed, after which we finally draw some conclusions and give clues of some further steps in this research.

BACKGROUND AND RELATED WORK

Pedestrian simulators

There are three main reasons for developing pedestrian computer simulations: i) to test scientific theories and hypotheses; ii) to assess design strategies; iii) to recreate the phenomena about which we want to theorize (Pan et al., 2007). Pedestrian flow management demands the correct representation of both the collective as well as the individual (Hoogendoorn et al., 2004). Timmermans et al. (2009) argue that understanding the pedestrian decision-making and movement is of critical importance to develop valid pedestrian models.

According to (Teknomo, 2002), pedestrian studies can be divided in two phases, namely data collection and

Proceedings 26th European Conference on Modelling and Simulation ©ECMS Klaus G. Troitzsch, Michael Möhring, Ulf Lotzmann (Editors)
ISBN: 978-0-9564944-4-3 / ISBN: 978-0-9564944-5-0 (CD)

data analysis. Whereas the former focus on characteristics such as speed, movement and path-planning, the latter is instead related to understanding how pedestrians behave. Predicting the movement of crowds (macroscopic level) or individual pedestrian actions (microscopic level) is the main goal of pedestrian simulation. For the macroscopic level, hydraulic or gas models are used (Santos and Aguirre, 2004). Microscopic models are based on behavioural approaches, in which entities are described individually (Castle et al., 2007). Traditional models, however, are mainly tested and validated through direct observations, techniques based on photography, as well as time-lapse films (Coelho, 1997; Helbing et al., 2001; Qingge et al., 2007) and also by stated preferences questionnaires (Cordeiro et al, 2011).

In such models it is possible to verify certain phenomena such as herding or flocking that happen due to people following other individuals instinctively. However, in conditions of low visibility or little knowledge of the surroundings this can provoke flocks of wandering people, contributing to the panic and confusion of the whole group, which is also a social reaction rather to be avoided if possible (Reynolds, 1987). Kuligowski proposes a model to mimic the human behavioural process during evacuation from buildings. Social science studies are needed to develop these theories, which could then yield more realistic results leading to safer and more efficient building design (Kuligowski, 2008, 2011).

Although many approaches exist to virtually simulate the behaviour of crowds with varying levels of realism, three models seem to be the most used (Heïgeas et al., 2003; Santos and Aguirre, 2004; Pelechano et al., 2007; Pretto, 2011). Cellular Automata Models (Neumann, 1966, Beyer et al., 1985) treat individuals as separate objects in an area divided into the so-called cells. Forces-based Models use mathematical formulaes to calculate the position variations of individual elements through the application of forces (its most explored subtypes consider Magnetic Forces and Social Forces). Finally, in Artificial Intelligence (AI) based Models, the decisions are made by individuals that compose the crowd on an autonomous basis. This sort of structure very much resembles a society of several interacting entities and has inspired much research in the Social Sciences (Kuligowski et al., 2010; Almeida et al., 2011).

The Serious Games Concept

Serious Games has gained a great prominence in the Digital Games field within the last decade, using appealing software with high-definition graphics and state-of-the-art gaming technology. It presents a great potential of application in a wide range of domains, naturally including social simulation.

Contrary to the primary purpose of entertainment in traditional digital games, SG are designed for the purpose of solving a problem. Athough they are indeed expected to be entertaining, their main purpose is rather serious with respect to the outcomes reflected in changes to the player behavior (Frey et al., 2007; McGonigal, 2011).

According to (Hays, 2005), a game is an artificially constructed, competitive activity with a specific goal, a set of rules and constraints that is located in a specific context. Serious Games refer to video games whose application is focused on supporting activities such as education, training, health, advertising, or social change. A few benefits from combining them with other training activities include (Freitas, 2006): the learners' motivation is higher; completion rates are higher; possibility of accepting new learners; possibility of creating collaborative activities; learn through doing and acquiring experience. Other aspects that draw video game players' attention are fantasy elements, challenging situations and the ability to keep them curious about the outcomes of their possible actions (Kirriemuir et al., 2004). Serious Games can be classified in five categories: Edutainment, Advergaming, Edumarket Games, Political Games and Training and Simulation Games (Alvarez et al., 2007).

Bearing in mind the aforementioned characteristics of SG-based frameworks, we expect to contribute to the creation of the next-generation pedestrian simulators.

A SERIOUS GAMES EVACUATION SIMULATOR

The Serious Games Evacuation Simulator proposed in this research is based on the Unity3D game engine, that was selected due to its characteristics, among them: i) powerful graphical interface that allows visual object placement and property changing during runtime (especially useful to rapidly create new scenarios from existing models and assets and quick tweaking of script variables); ii) the ability to develop code in JavaScript, C# or Boo; iii) simple project deployment for multiple platforms without additional configuration, including for instance the Web (which makes it possible to run the game on a Web browser). Detailed characteristics of the implemented environment are presented below.

Combining Simulation and Serious Games

By starting the application the user gains control over the player character. Its aim will be to evacuate the building in the shortest time possible. The User Interface displays the elapsed time, which starts counting as soon as the player presses the "start fire simulation" key (illustrated in Figure 1).

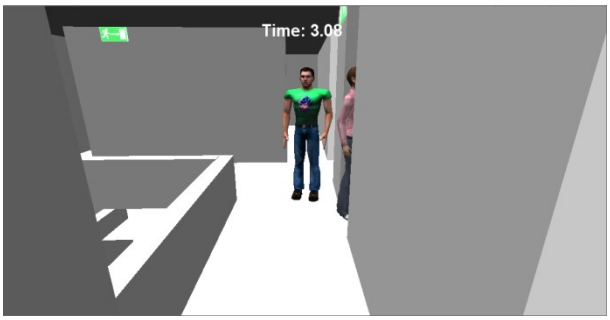

Figures 1: Gameplay example

The game genre – First Person Shooter

First Person Shooters (FPS) are characterised by placing players in a 3D virtual world which is seen through the eyes of an avatar. This attempts to recreate the experience of the user being physically there and exploring their surroundings.

The controls for this game follow the common standards for the FPS genre, using a combination of keyboard and mouse to move the player around the environment. The complete action mapping is as follows:

- **Mouse movement** - camera control, i.e. where the player is looking at;
- **W** - move forward;
- **S** - move backwards;
- **A** - move to the left;
- **D** - move to the right;
- **Space bar** - jump;
- **O** - start fire simulation.

Game scenarios

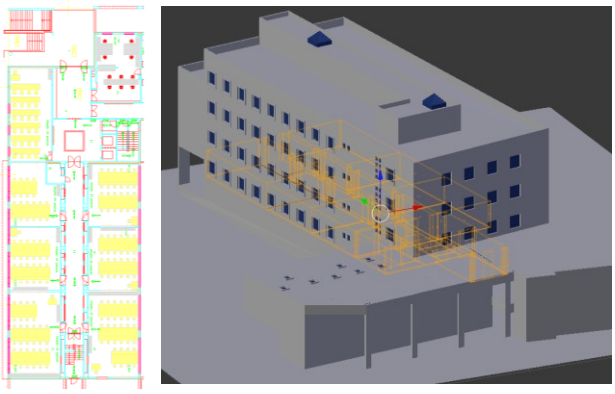

Figure 2 DEI plan and 3D representation

The environment is prepared to support various scenarios modelled in 3D. For the trial described in this paper, a single simulation scenario was considered. It takes place in FEUP's Informatics Engineering Department (DEI). A model of the FEUP campus was used, focusing only on one of the buildings where our research laboratory is located. As a virtual representation of the outside already existed, it was only necessary to create its interiors. This task was handled in Blender and used the official plans in order to recreate it as real as possible in terms of topology, dimensions, scale and proportions. Images of the plans and the 3D model are presented in Figure 2.

The player starts in a predefined room and, upon starting the evacuation event, a fire appears in a random room and the alarm sounds. At this very moment the timer starts. The player must then traverse the building in order to go to the outside as quickly as possible, choosing from one of the two possible exits. Several emergency signs are in place in order to help the player identify the nearest exit.

Challenges, Rules and Scoring Systems

The main challenge involved in the evacuation of a building comes from identifying the exact location of the nearest exit and how to get there. Also to consider is that computer-controlled agents are present and trying to evacuate the building at the same time, possibly clogging the passage and delaying the player.
After starting, fire keeps spreading to adjacent areas in small intervals of time; as fire is not surmountable, this can eventually constitute another obstacle and forces the player to look for a different exit route.
At the current stage, the score given to a player is solely based on the time taken to evacuate the building – meaning that the lower the score, the better. Whether the player picked the nearest exit or not is inherently reflected in the time taken to reach the outside.

Model calibration

Calibration is an important issue to assure the validity of the model. For this purpose, three different paths were considered, named P1, P2 and P3. One in a straight line (P1), two involving taking sets of stairs. Of these latter two, one involved taking the nearest exit from the building (P2) and another the farthest one (P3). These paths were measured using the AutoCAD plans for the building.

The comparison was made between data collected from real evacuations and from the game. The real times were measured with a stopwatch while traversing the paths, whereas for the game times the clock in the interface was used. It is also worth noticing that the adult profile of (1.5 m/s) was used in the game. Subject's speed values were calculated from the measured distance and time taken. Error values were calculated according to the equation:

$$1 - \frac{GameTime}{RealTime} \qquad (1)$$

The values for distances and times are registered in Table 1.

Table 1: Model Validation

	P1	P2	P3
Distance (m)	24	31	72
Real Time (s)	17.53	21.50	55.91
Subject's Speed (m/s)	1.34	1.44	1.29
Game Time (s)	15.86	19.28	48.08
Error (%)	9.53	10.33	14.00

One aspect to notice is that subject's speed is consistent at around 1.3 and 1.4 m/s. Thus, subject's times would always be longer than the ones registered in the game, as the player moves at 1.5 m/s. It is also worth considering that the error is higher for routes involving stairs. This was also expected as the player's speed does not decrease when taking stairs, which in turn is verified in reality.

EXPERIMENTAL SETUP

Description

All subjects were divided according to their previous knowledge of the building. Each had to try to reach a safe exit to the outside as quickly as possible. Besides the time, it was expected that players would select the nearest emergency exit, just outside of the laboratory set as starting point, instead of using the normal way which is longer. Users were tested individually so not to spoil the experience to each other regarding details of their chosen routes. Tests were also performed only once in order to capture first reactions to the game experience and its controls.

Population Sample

A total of 30 subjects were selected as sample to test the developed prototype. These testers can be classified according to the following parameters:

- Regular video game player - Yes or No;
- Familiar with the building -Yes or No.

An attempt was made to equalise these variables, as well as age and gender, so as to receive as many different experiences as possible and maintain a balance among categories. The distribution is shown in Table 2.

Table 2: User Times – Results by Categories

		Regular Video Game Player	
		Yes	No
Previous Knowledge of the Building	Yes	8	6
	No	5	11

Test Setup

Each subject could play only once. Some time was given to the user so as to get acquainted with the keyboard and mouse controls. Players with no previous knowledge of the building were taken to the lab where they had to escape from. The purpose was to show, like a regular visitor (for instance a student or foreign professor) the normal way, from the building entrance, up to the first floor and end of the corridor, where the laboratory is located. After the siren signed, the player was instructed to leave the building following the emergency signs leading to the nearest exit.

Preliminary results

Intuitively it was expected that all subjects would selected the nearest exit available. However, some of the players misbehaved according to these expectations and chose the longer way out. These testers can be classified according to the following parameters, whose distribution is shown in Table 3.

Table 3: Experiment Results

Was the nearest exit chosen?	Y	N
Previous knowledge of the building	11	2
No previous knowledge of the building	6	11

From the analysis of Table 3, it is possible to conclude that users with previous knowledge of the building were aware of the emergency exit and used it. Nevertheless, 2 of them (aprox. 15% - 2 out of 13) missed it and used the longer way out. The remaining players, only 6 out of 17 (aprox. 35%) chose to exit using the emergency way, whilst the remaining 11 of that group followed the same way they were shown initially to get to the starting point of this experience.

CONCLUSION AND FUTURE WORK

This work explores the concept of serious games as an important asset to aid and improve traditional fire drills. The contribution of this work can then be considered two-fold. First we extended a popular game engine to implement a pedestrian simulator to study evacuation dynamics. Second, our approach provided an appropriate environment to test with and influence behaviour of egresses of a building in hazardous situations, such as fires.

It also addresses the common notion that people tend to leave buildings using the same way they use to get into it, unless they are told otherwise. This was highlighted by the experiment in which approximately 65% of players without previous knowledge of the building missed the emergency exit and signage, following the longer but more intuitive path to exit the building.

It is important to bear in mind that this framework does neither completely replace nor avoid the need for in-site

drills to train people for emergency situations, such as with the prospect of fire in an office building or school. Nonetheless, game environments can be very attractive in many different ways, and have proven to be an invaluable tool for training. Additionally, this approach is built upon the potential of such a concept to ease and improve the understanding of human behaviour in such situations, as subjects are monitored during their playing the game and some performance measures are logged to be further analysed later on.

We have implemented our prototype on the basis of a popular game engine, namely Unity3D, which provided us with a customisable framework and allowed us to feature the game virtual environment with characteristics of a serious game platform. We invited some subjects to use the game and collected some preliminary results that demonstrated the viability of the approach. We have then conceived a methodology which is both instrumental as an aid to train people and an invaluable instrument to help practitioners and scientists to better understand group behaviour and the social phenomenon in a vast range of circumstances.

The very next steps in this research include the improvement of the prototype featuring it with tools for rapidly setting up simulation environments from CAD blueprints of buildings. We also intend to include other performance measures to study individual and social behaviour in circumstances other the hazardous scenarios. Ultimately, this framework is also expected to be used as an imperative decision support tool, providing necessary and additional insights into evacuation plans, building layouts, and other design criteria to enhance places where people usually gather and interact rather socially, such as shopping malls, stadiums, airports, and so on.

ACKNOWLEDGMENT

This project has been partially supported by FCT (Fundação para a Ciência e a Tecnologia), the Portuguese Agency for R&D, under grant SFRH/BD/72946/2010.

REFERENCES

Almeida, J. E., Rosseti, R., and Coelho, A. L. 2011. "Crowd Simulation Modeling Applied to Emergency and Evacuation Simulations using Multi-Agent Systems". In *Proceedings of the 6th Doctoral Symposium on Informatics Engineering*, DSIE'11, Porto.

Alvarez, J., Rampnoux, O., Jessel, J.P., and Methel, G. 2007. "Serious Game: Just a Question of Posture? ". In *Artificial & Ambient Inteligence*, AISB'07, pages 420–423.

Beyer, W.; Sellers, P.; Waterman, M. 1985. "Stalinslaw m. Ulam's contributions to theoretical theory". Letter in *Mathematical Physics* 10:231-242.

Castle, Christian J. E. 2007. *Guidelines for Assessing Pedestrian Evacuation Software Applications*. Centre for Advanced Spatial Analysis - UCL University College London. http://eprints.ucl.ac.uk/3471/1/3471.pdf.

Coelho, L. 1997. *Modelação de Evacuação de Edifícios Sujeitos à Acção de um Incêndio* (in Portuguese), Ph.D. Dissertation, FEUP-LNEC, Lisboa.

Cordeiro, E., Coelho, A. L., Rossetti, R. J. F., and Almeida, J. a. E. 2011. "Human Behavior under Fire Situations – A case–study in the Portuguese Society". In the Proceedings of *Advanced Research Workshop: Evacuation and Human Behavior in Emergency Situations*, pages 63–80, Santander, Spain. GIDAI. Universidad de Cantabria.

Freitas, S. (2006). *Using Games and Simulations for Supporting Learning*. Learning, Media and Technology, 31(4):343– 358.

Frey, A., Hartig, J., Ketzel, A., Zinkernagel, A., and Moosbrugger, H. 2007. "The Use of Virtual Environments Based on a Modification of the Computer Game Quake III ArenaR in Psychological Experimenting". *Computers in Human Behavior*, 23(4):2026–2039.

Hays, R. 2005. "The Effectiveness of Instructional Games: a Literature Review and Discussion". Technical report, Naval Air Warfare Center Training Systems Division Orlando, FL.

Heïgeas, L., Luciani, A., Thollot, J., and Castagn´e, N. 2003. "A Physically-Based Particle Model of Emergent Crowd Behaviors". In *Graphicon*.

D. Helbing, I. Farkas, P. Molnar, T. Vicsek. 2001. "Simulating of Pedestrian Crowds in Normal and Evacuation Situations". M.Schreckenberg, S.D. Sharma(ed.) *Pedestrian and Evacuation Dynamics*. Springer Verlag Berlin and Heidelberg, pp. 21-58.

Hoogendoorn, S.P., and P.H.L. Bovy. 2004. "Pedestrian route-choice and activity scheduling theory and models". *Transportation Research Part B: Methodological 38* (2) (February): 169-190.

Kirriemuir, J. and McFarlane, A. 2004. "Literature Review in Games and Learning". Technical report, Futurelab.

Kuligowski, E. D. 2008 "Modeling Human Behavior during Building Fires". NIST Technical Note 1619.

Kuligowski, E. D., Peacock, R., and Hoskins, B. L. 2010. "A Review of Building Evacuation Models, 2nd Edition". NIST Technical Note 1680.

Kuligowski, E. D. 2011. "Predicting Human Behavior During Fires." Fire Technology (November 13). http://www.springerlink.com/index/10.1007/s10694-011-0245-6

McGonigal, J. 2011. *Reality Is Broken: Why Games Make Us Better and How They Can Change the World*, volume 22. The Penguin Press HC.

Neumann, V. 1966. *Theory of self-reproducing automata*. Champaign IL: University of Illinois Press.

Pan, X., Han, C. S., Dauber, K., & Law, K. H. 2007. "A multi-agent based framework for the simulation of human and social behaviors during emergency evacuations". *Ai & Society* 22 (2) (June 29) , 113-132.

Pelechano, N., Allbeck, J., and Badler, N. 2007. "Controlling Individual Agents in High-density Crowd Simulation". In Proceedings of *ACM SIGGRAPH/Eurographics Symposium on Computer Animation*, pages 99–108. Eurographics Association.

Pretto, C. O. 2011. *Desenvolvimento de um Simulador de Pedestres* (in Portuguese). PhD thesis, Universidade Federal do Rio Grande do Sul.

Qingge, J., Can G. 2007. "Simulating Crowd Evacuation with a Leader-Follower Model". *IJCSES International Journal of Computer Sciences and Engineering Systems*, Vol.1, No.4, October 2007.

Reynolds, C. 1987. "Flocks, Herds and Schools: A Distributed Behavioral Model". *ACM SIGGRAPH Computer Graphics*, 21(4):25–34.

Santos, G. and Aguirre, B. E. 2004. A critical review of emergency evacuation simulation models. Critical Review, (1032):25–50.

Teknomo, K. 2002. *Microscopic Pedestrian Flow Characteristics: Development of an Image Processing Data Collection and Simulation Model*. Ph.D. Thesis. Tohoku University, Japan.

Timmermans, H. 2009. *Pedestrian Behavior: Models, Data Collection and Applications*. Emerald Group Publishing Limited.

AUTHOR BIOGRAPHIES

JOAO PEDRO RIBEIRO concluded his MSc in Informatics and Computing Engineering in 2012, from Faculty of Engineering, University of Porto, Portugal. He specialised in Digital Games development and Artificial Intelligence, combining the concepts of multi-agent systems and serious games. He can be reached by e-mail at: joao.pedro.ribeiro@fe.up.pt.

JOAO EMILIO ALMEIDA holds a BSc in Informatics (1988), and MSc in Fire Safety Engineering (2008). He is currently reading for a PhD in Informatics Engineering at the Faculty of Engineering, University of Porto, Portugal, and a researcher at LIACC. He has co-authored many fire safety projects for complex buildings such as schools, hospitals and commercial centres. His areas of interest include Serious Games, Artificial Intelligence, and multi-agent systems; more specifically he is interested in validation methodologies for pedestrian and social simulation models. His e-mail is joao.emilio.almeida@fe.up.pt.

ROSALDO ROSSETTI is an Assistant Professor with the Department of Informatics Engineering at the University of Porto, Portugal. He is also a Research Fellow in the Laboratory of Artificial Intelligence and Computer Science (LIACC) at the same University. Dr. Rossetti is a member of the Board of Governors of IEEE Intelligent Transportation Systems Society (IEEE ITSS) and a co-chair of the Technical Activities sub-committee on Artificial Transportation Systems and Simulation of IEEE ITSS. His areas of interest include Artificial Intelligence and agent-based modelling and simulation for the analysis and engineering of complex systems and optimisation. His e-mail is rossetti@fe.up.pt and his Web page can be found at http://www.fe.up.pt.com/~rossetti/.

ANTONIO COELHO was born in 1971, in Porto, Portugal, and is currently an Assistant Professor at the Informatics Engineering Department of the Faculty of Engineering, University of Porto, where he teaches in the areas of Computer Graphics, Programming and Digital Games. He is also a Research Fellow at INESC TEC (INESC Technology and Science). His e-mail is acoelho@fe.up.pt.

A. LEÇA COELHO holds both the Electrotechnical and Civil Engineering degrees, as well as a Master's and PhD in Civil Engineering. He is currently a Principal Researcher with Habilitation at LNEC. His areas of interest include fire safety and risk analysis. He can be reached by e-mail at alcoelho@lnec.pt.

SOCIODYNAMIC DISCRETE CHOICE APPLIED TO TRAVEL DEMAND: MULTI-AGENT BASED SIMULATION AND ISSUES IN ESTIMATION

Elenna R. Dugundji
Universiteit van Amsterdam
P.O. Box 16697, 1001 RD Amsterdam, Netherlands
Email: e.r.dugundji@gmail.com

László Gulyás
AITIA International Inc.
Czetz János u. 48-50, 1039 Budapest, Hungary
Email: lgulyas@aitia.ai

KEYWORDS
Multi-agent based social simulation, Social influence, Heterogeneity, Choice behavior, Network density.

ABSTRACT

This paper discusses a multi-agent based model of binary choice behavior with interdependence of decision-makers' choices. Analytical results established by other authors are briefly summarized where agent heterogeneity is not explicitly treated. Next the well-known Erdős-Rényi network class is considered to introduce agent heterogeneity via an explicit local interaction structure. Then the model is applied in an example of intercity travel demand using empirical data to introduce individual agent heterogeneity beyond that induced by the local interaction structure. Studying the long run behavior of more than 120,000 multi-agent based simulation runs reveals that the initial estimation process can be highly sensitive to small variations in network instantiations. We show that this is an artifact of two issues in estimation, and highlight particular attention that is due at low network density and at high network density. Limitations in the present work are summarized and suggestions for future research efforts are outlined.

1 INTRODUCTION

Pioneered in the domain of travel demand by Ben-Akiva (1973), Domencich and McFadden (1975), and others, discrete choice analysis has become an industry standard in land use and transportation planning models. An outstanding methodological challenge remains however in the treatment of the interdependence of various decision-makers' choices. There is growing awareness and interest in the influence that social factors have on transportation and land use behaviors (Dugundji, Páez and Arentze 2008; Dugundji et al. 2011).

While there exists a substantial stream of research in *identifiable* intra-household interactions and explicit inter-household interactions of extended family, friends and colleagues in travel demand modeling such as coordination of individual daily activity patterns, joint participation in activities and travel, mechanisms for allocation of maintenance activities, and activity location and residential location choice behavior, the topic of *aggregate* or collective social interactions between individuals in different households at a market level in travel demand has only recently begun to attract attention. Some examples of the empirical estimation of a discrete choice model with aggregate social interactions with application to transportation include Dugundji and Walker (2005), Goetzke (2008), Goetzke and Andrade (2009), Goetzke and Rave (2010), Goetzke and Weinberger (2012). Some explorations of the dynamical behavior of such a model with application to transportation include Fukuda and Morichi (2007), Páez and Scott (2007), Páez, Scott and Volz (2008), Arentze and Timmermans (2008), and Dugundji and Gulyás (2008). This paper continues this line of research, exploring a multi-agent based model of binary choice behavior with interdependence of decision-makers' choices.

Discrete-choice estimation results controlling overall mechanisms related to individual heterogeneous preferences are embedded in a multi-agent based model to be able to observe the simulated evolution of choice behavior over time with socio-dynamic feedback due to network effects. Studying the long run behavior of more than 120,000 multi-agent based simulation runs reveals that the initial estimation process can be highly sensitive to small variations in network instantiations. We show that this is an artifact of two issues in estimation, and highlight particular attention that is due at low network density and at high network density. This finding is an important warning with respect to empirical application of agent-based models.

2 MODEL

Discrete choice theory allows prediction based on computed individual choice probabilities for heterogeneous agents' evaluation of alternatives. In accordance with the notation and convention in Ben-Akiva and Lerman (1985), the so-called binary logit model is specified as follows. Assume a population of N decision-making entities indexed $(1,...,n,...,N)$ each faced with a choice among two alternatives of some universal choice set $C = \{i,j\}$, say, choice of travel by car versus by railway, which we assume to be available to all agents. The choice alternatives are further assumed to be mutually exclusive (a choice for one alternative excludes the simultaneous choice for another alternative, that is, an agent cannot choose two

Proceedings 26th European Conference on Modelling and Simulation ©ECMS Klaus G. Troitzsch, Michael Möhring, Ulf Lotzmann (Editors)
ISBN: 978-0-9564944-4-3 / ISBN: 978-0-9564944-5-0 (CD)

alternatives at the same moment in time) and collectively exhaustive within C (an agent must make a choice for one of the options in the choice set).

Let $U_{in} = V_{in} + \varepsilon_{in}$ be the utility that a given decision-making entity n is presumed to associate with elemental alternative i in its choice set, where V_{in} is the deterministic (to the modeler) or so-called "systematic" utility and ε_{in} is an error term. The error term represents unobserved heterogeneity. Such unobserved heterogeneity may arise due to unobserved attributes of the choice alternatives, unobserved characteristics of the decision-making entities or simply measurement errors in observed attributes and/or characteristics. Also in the case where instrumental variables are used as a proxy for variables which are not observable, the error term is relevant for capturing unobserved heterogeneity. Under the assumption of Gumbel distributed disturbances ε_{in}, the probability P_{in} that agent n chooses alternative i has a convenient closed form expression, given by:

$$P_{in} = \frac{e^{\mu V_{in}}}{e^{\mu V_{in}} + e^{\mu V_{jn}}} = \frac{e^{\mu\left(V_{in} - V_{jn}\right)}}{e^{\mu\left(V_{in} - V_{jn}\right)} + 1} \qquad (1)$$

where μ is a strictly positive scale parameter which we generally normalize to 1. The assumption that the disturbances are Gumbel distributed can be defended as an approximation to the normal density.

2.1 Global Social Influence: The Field Effect Model

The classical discrete choice framework discussed so far assumes independent individuals. Aoki (1995), Brock and Durlauf (2001) and Blume and Durlauf (2003) relax this assumption. Their approach is to assume that the otherwise independent individuals are influenced by an aggregate of all other choices in the community. There is an inherent dynamic because each individual re-evaluates its choice based on the choices made by other individuals. This implies an implicit time-trajectory of repeated choices that defines the dynamics of the system. It is in this sense that we call this a "socio-dynamic" model: the dynamics are driven by social influence, albeit global social influence at this stage. The steady states of this dynamic process are reviewed below.

Let N_i and N_j be the total numbers of decision-making entities who have chosen respectively alternative i and alternative j at time t. Since we assume the choice set to be mutually exclusive and collectively exhaustive, for the binary case we have $N = N_i + N_j$. Now let $x_i = N_i / N$ and $x_j = N_j / N = (1 - x_i)$ be the global proportions of decision-making entities who have made each choice, and define the field variable:

$$x \equiv x_i - x_j = x_i - (1 - x_i) = 2x_i - 1 \qquad (2)$$

Note that the field variable x varies on the range -1 to 1. In the limit where x = -1, none of the decision-making entities in the sample have chosen alternative i, that is, all have chosen alternative j. In the limiting case where x = 1, all of the decision-making entities in the sample have chosen alternative i, and none have chosen alternative j. In the case where x = 0, half of the decision-making entities in the sample have chosen alternative i, and half have chosen alternative j.

Global social dynamics are introduced by allowing the term $V_{in} - V_{jn}$ in equation (1) to be a linear-in-parameter β function of the proportions x_i and x_j of decision-making entities who have made each choice:

$$V_{in} - V_{jn} \equiv \beta f\left(x_i - x_j\right) = \beta f\left(x\right) \qquad (3)$$

The function $f(x)$ is an arbitrary function of x. In our application we consider $f(x)$ linear in x, however the analytical results apply more generally. Substituting equation (3) into (1) and normalizing the scale parameter μ =1, we have:

$$P_{in}\left(x\right) = \frac{e^{\beta f(x)}}{e^{\beta f(x)} + 1} \qquad (4)$$

Aoki (1995) shows that the mean φ of the field variable x is governed by the deterministic differential equation:

$$\frac{d\varphi}{dt} = \kappa \frac{1-\varphi}{2} P_{in}\left(\varphi\right) - \lambda \frac{1+\varphi}{2} P_{jn}\left(\varphi\right) \qquad (5)$$

Substituting (4) into (5) and normalizing κ =1 and λ =1, we have:

$$\frac{d\varphi}{dt} = \frac{1}{2}\left(\tanh \frac{1}{2} \beta f\left(\varphi\right) \right) - \frac{\varphi}{2} \qquad (6)$$

Stationary points are zeros of $d\varphi / dt$. Thus the key equation to determine local equilibria is:

$$\frac{d\varphi}{dt} = 0: \quad \varphi = \tanh \frac{1}{2} \beta f\left(\varphi\right) \qquad (7)$$

This equation can be solved conveniently by plotting the left-hand-side and the right-hand-side on a graph, and finding their intersection. Depending on the specification of $f(\varphi)$ and the value of β, this equation may have more than one solution.

2.2 Local Social Influence: Erdős-Rényi Networks

The model described in the previous section assumes uniform, global and perfect information access. The very fact that certain influences are transferred via social interactions, and thus via social networks implies heterogeneous local information. Therefore, in the following we extend the model to explicitly model interaction networks.

Each decision-making entity n is assigned a set of "reference" decision-making entities influencing its choice. At each time step during the iteration phase, the

decision-making entities look at the choices their particular reference entities made in the previous round, plus their own choice, and calculate *localized* values of the difference in systematic utility between the alternatives:

$$V_{in} - V_{jn} \equiv \beta f\left(x_{in} - x_{jn}\right) = \beta f\left(x_n\right) \qquad (8)$$

The critical difference between equations (8) and (3) is that subscript n now becomes important in determining $x_n = x_{in} - x_{jn}$. The "reference" relationships introduced here define a graph or network.

It is hypothesized that different network structures yield different system behavior. In practice however, it can be difficult to reveal the exact details of the relevant network(s) of reference entities influencing the choice of each decision-making entity. Moreover, the actual reference entities for a given decision-making entity may not be among those in the data sample. One way to test the above hypothesis theoretically even without reliable empirical information about the social influence network is by studying abstract classes of networks in the hope of identifying classes of networks that yield similar results.

An early abstract model of social interaction is due to Erdős and Rényi (1959). Their random network consists of a number of nodes and set of random edges between them, such that the probability of the existence of a given link is uniform across all possible edges. The actual number of the links is determined by the density p of the network, which is usually perceived as a parameter of the Erdős-Rényi graph. Here network density p is defined as the ratio of the number of actual existing links to the number of all theoretically possible links in a fully connected network with the given number of nodes. Otherwise said, p is the "link probability," the probability that a link exists.

One advantage of studying random networks is that they are perhaps the simplest possible networks that are general enough to describe a wide range of graphs, from unconnected nodes to a fully connected network (ie. a graph that contains all possible links). In addition, they accomplish this without introducing any explicit bias into the structure of the network. Moreover, results are known about important properties such as at approximately what value of p will the network become connected (ie. when each node is "reachable" along the edges from any other node), or otherwise said, when a so-called "giant component" will emerge. Finally, an important feature of random networks which is observed in real-life social networks is the so-called "small-world" property: the average path length l (the average number of "hops" between an arbitrary pair of nodes) is less than or of the order ln(N), where N is the number of nodes.

3 EMPIRICAL DEMONSTRATION

In the next step of our model development process we now turn our attention to an empirical application of intercity transportation mode choice behavior. Here we include individual level heterogeneity in two ways. We use revealed preference survey data collected by the Hague Consulting Group for the Netherlands Railways to assess factors which influence the binary choice between car versus rail for intercity travel (Ben-Akiva and Morikawa, 1990). We also test the role of the social influence, modeled as an Erdős-Rényi graph over a full sweep of link probabilities from zero to one. In the limit that the link probability approaches zero, we have a classical binary logit model without social interaction. In the limit that the link probability approaches one, we recover a fully-connected network. For the special case of very high link probabilities, we can therefore apply approximate theoretical benchmark results in section 2.1 to verify our agent-based model implementation.

At the outset of section 2, we discussed the notion of a "systematic" utility V_{in} that a given decision-making entity n is presumed to associate with a particular alternative i. We have considered until now the interaction effect as the only term in the systematic utility. In typical transportation applications, the systematic utility is commonly assumed to be defined by a function of observable characteristics $\mathbf{S}_n$ of the decision-making entity and observable attributes $\mathbf{z}_{in}$ of the choice alternative for a given decision-making entity. We will consider the term $V_{in} - V_{jn}$ in equation (1) to have the general form:

$$\begin{aligned} V_{in} - V_{jn} &\equiv \beta f\left(x_{in} - x_{jn}\right) = \beta f\left(x_n\right) \\ &= \beta x_n + h + \boldsymbol{\gamma}'\mathbf{S}_n + \boldsymbol{\zeta}_i'\mathbf{z}_{in} - \boldsymbol{\zeta}_j'\mathbf{z}_{jn} \end{aligned} \qquad (9)$$

where $\boldsymbol{\gamma} = [\gamma_1, \gamma_2, \ldots]'$, $\boldsymbol{\zeta}_i = [\zeta_{i1}, \zeta_{i2}, \ldots]'$ and $\boldsymbol{\zeta}_j = [\zeta_{j1}, \zeta_{j2}, \ldots]'$ are vectors of unknown utility parameters respectively corresponding to the relevant observable agent characteristics $\mathbf{S}_n$, and observable agent-specific attributes $\mathbf{z}_{in}$ of the choice alternative such that:

$$\begin{aligned} \boldsymbol{\gamma}'\mathbf{S}_n &= \gamma_1 S_{n1} + \gamma_2 S_{n2} + \ldots \\ \boldsymbol{\zeta}_i'\mathbf{z}_{in} &= \zeta_{i1} z_{in1} + \zeta_{i2} z_{in2} + \ldots \\ \boldsymbol{\zeta}_j'\mathbf{z}_{jn} &= \zeta_{j1} z_{jn1} + \zeta_{j2} z_{jn2} + \ldots \end{aligned} \qquad (10)$$

The term h is a so-called "alternative specific constant" (ASC); it is included as good practice to explicitly account for any underlying bias for one alternative over another alternative. In other words, h reflects the mean of $\varepsilon_{jn} - \varepsilon_{in}$, that is, the difference in the utility of alternative i from that of j when all else is equal. In general the utility parameters $\boldsymbol{\zeta}_i$ and $\boldsymbol{\zeta}_j$ may take alternative specific values, however in this paper we will consider only "generic" values of the utility parameters $\boldsymbol{\zeta} \equiv \boldsymbol{\zeta}_j = \boldsymbol{\zeta}_j$ and define $\mathbf{z}_n \equiv \mathbf{z}_{in} - \mathbf{z}_{jn}$ so that we have the further simplification:

$$V_{in} - V_{jn} = \beta x_n + h + \boldsymbol{\gamma}' \mathbf{S}_n + \boldsymbol{\zeta}' \mathbf{z}_n \qquad (11)$$

The travel behavior data available to us is cross-sectional. Due to the expense and logistical aspects of data collection, it is common that a transportation agency or other commissioning party will use cross-sectional data to estimate a model, and then make forecasts about how variables will change over time and use the revised variables to make forecasts (Ben-Akiva and Lerman, 1985). This is the approach taken in this paper. This said, it would be better to have estimated a panel model and use the panel estimates within our agent-based model if we had had panel data available. We hope this paper may serve as a call to the community for the relevance of network panel data in improving modelling efforts. Descriptions of the survey variables available for use in our modeling endeavor are given in Table 1. There are no reported missing values.

Table 1: Description of Variables in Survey Data

Name	Type of variable	Description
choice	y_n	Travel mode choice indicator: 1 if rail; 0 if car
gender	S_n	Gender of the respondent: 1 if female; 0 if male
business	S_n	Business trip indicator
shoprec	S_n	Shopping/recreation trip indicator
ttcar	z_{in}, i = car	In-vehicle travel time for the car alternative (minutes)
tccar	z_{in}, i = car	Travel cost for the car alternative (NLG)
ovtcar	z_{in}, i = car	Out-of-vehicle time to walk from parking place to destination (minutes)
ttrail	z_{jn}, j = rail	In-vehicle travel time for the rail alternative (minutes)
tcrail	z_{jn}, j = rail	Travel cost for the rail alternative (NLG)
ovtrail	z_{jn}, j = rail	Out-of-vehicle time for access and egress for rail (minutes)

As in section 2.2, in our agent-based model each decision-making entity n is assigned a set of "reference" decision-making entities influencing its choice. At each time step, the decision-making entities look at the choices their particular reference entities made in the previous round, plus their own choice, and calculate localized values of the difference in systematic utility between the alternatives:

$$\begin{aligned} V_{in} - V_{jn} &= \beta x_n + h + \gamma_1 * \text{gender}_n \\ &+ \gamma_2 * \text{business}_n + \gamma_3 * \text{shoprec}_n \\ &+ \zeta_1 * (\text{tt}_{\text{car}} - \text{tt}_{\text{rail}})_n + \zeta_2 * (\text{tc}_{\text{car}} - \text{tc}_{\text{rail}})_n \\ &+ \zeta_3 * (\text{ovt}_{\text{car}} - \text{ovt}_{\text{rail}})_n \end{aligned} \qquad (12)$$

We are interested in how the dynamics of the discrete choices of these heterogeneous individuals depend on the structure of the underlying social influence network. We vary the network density p on the parameter range (0,1) ranging from a non-connected to a fully-connected graph, excluding endpoints. We select the following 30 values of p to sample: 0.005 to 0.100 at increment 0.005 (20 network density values), 0.200 to 0.600 at increment 0.100 (5 network density values), 0.700 to 0.900 at increment 0.050 (5 network density values). In each case, we repeatedly situate the agents in 20 distinct instantiations of an Erdős-Rényi graph per network density value.

For these 600 networks (30 network density values times 20 network instantiations per density value), we repeatedly compute the local interaction field variable x_n for each of the 235 agents in the sample in two ways, one with counting the agent's own choice in its reference group (that is, with so-called "self loops"), and one without counting the agent's own choice in its reference group (that is, without self loops). From a theoretical perspective, the model with self-loops is interesting because in the limiting case of network density $p = 1$ (a fully-connected network), we recover Aoki's original model if there were no other explanatory variables in the utility function. Likewise from a theoretical perspective, the model without self-loops is interesting because in the limiting case of network density $p = 0$ (a non-connected network), we have pure random behavior if there were no other explanatory variables in the utility function. From a multi-agent based simulation perspective, the model with self-loops at low network density might logically provide inertia in the behavior, damping down the volatility of switching from one choice to another. At high network density, when the number of agents is large, there is not likely to be discernible difference in the multi-agent based simulation behavior between the model with self-loops and without self-loops.

After preliminary model specification testing, we proceed to repeatedly estimate sets of the utility parameters β, h, γ_1, γ_2, γ_3, ζ_1, ζ_2, ζ_3 in equation (12) via maximum likelihood estimation for each of the 1200 network scenarios described above, with two different binary logit utility specifications: with the alternative specific constant h freely estimated, and with the alternative specific constant constrained to zero. Using the distinct sets of coefficients for each of the 2400 estimated models, we then run 50 multi-agent based simulations with distinct pseudo-random number

sequences for 2000 iterations per each run, per each model. The value of x representing the difference between the aggregate mode shares x_i and x_j in the sample at the last time step of each run is counted in histograms, one per each network instantiation. We group these histograms by network density in each of the four experimental settings (with or without self-loops and with and without an alternative specific constant). Figure 1 shows aggregate histograms from each experimental setting at low and high network density values.

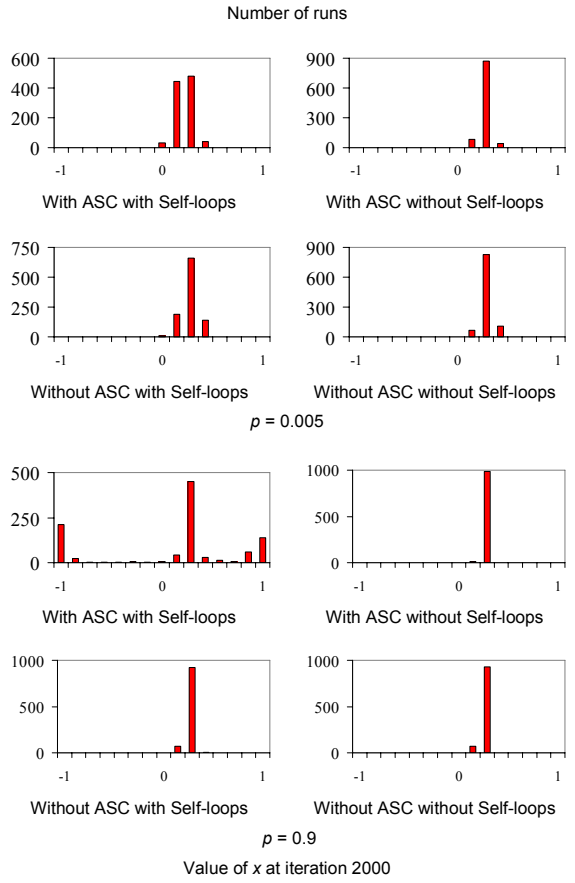

Figure 1: Aggregate histograms for four model specifications with and without an alternative specific constant and with and without self loops, at network density p = 0.005 and p = 0.9; for each histogram there are 20 Erdős-Rényi network instantiations per density value, 50 multi-agent based simulation runs per network instantiation, and 2000 iterations per simulation run; the values of the set of utility parameters are re-estimated per each network instantiation; the bins of the histogram encompass a range from -1 to 1

Molloy and Reed (1998) have shown that the critical point when a giant component emerges, occurs around $p = 1/N + \varepsilon$, where N is the number of nodes and $\varepsilon > 0$ is a small value. In our case of 235 agents this formula gives $p \sim 0.005$ as a critical point when, in practical terms, the graph becomes connected. We therefore might potentially expect to see behavioral transitions occurring somewhere in the low network densities. However, the most striking result is that only with the model with the alternative specific constant and with self loops do we ever get the signature bimodal histogram. Thus we can conclude that adding additional agent-specific heterogeneity in our model beyond the heterogeneity automatically induced by the localized interactions does indeed seem to matter.

A closer analysis of the histograms reveals a significant insight: not all of the network instantiations for the models with the alternative specific constant and with self loops give the signature bimodal histogram. In fact at higher network densities we see both the single sharply-peaked distribution and the signature bimodal histogram co-existing as outcomes with the alternative specific constant and with self loops, giving a hint at some kind of instability in the model. See Figure 2. This insight motivates a further analysis of the estimated coefficient values which we will undertake in section 4.

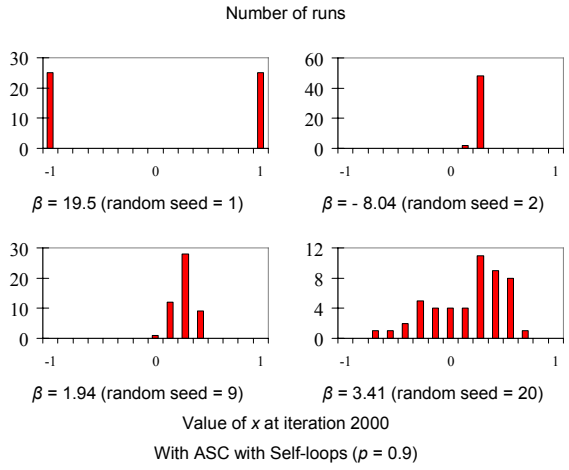

Figure 2: Individual histograms for four Erdős-Rényi network instantiations with different network generator random seeds for the model specification with an alternative specific constant and with self loops at network density $p = 0.9$; there are 50 multi-agent based simulation runs per network instantiation, and 2000 iterations per run; the value of the model coefficients are re-estimated per each network instantiation; the bins of the histogram encompass a range from -1 to 1

For the case shown in Figure 2 with $p = 0.9$, we may suppose that the network density is close enough to approaching unity that the mean field analytical results in section 2.1 may be relevant as an approximate guidepost. Using the mean values of variables given in Table 1 and the estimated utility parameters β, h, γ_1, γ_2, γ_3, ζ_1, ζ_2, ζ_3 for each of the network instantiations with random seeds shown in Figure 2, we plot the left-hand-side and the right-hand-side of equation (7) on a graph, and find their intersection for $\beta f(x_n) = V_{in} - V_{jn} = \beta xn + h + \boldsymbol{\gamma}'\mathbf{S}n + \boldsymbol{\zeta}'\mathbf{z}n$ as given in equation (12). In Figure 3, we can see that the effect of adding the alternative

specific constant, the agent characteristics and the agent-specific attributes of choice alternatives to the model is to shift the tanh curve horizontally so that the curve no longer crosses the line $y = \varphi$ at $\varphi = 0$. A larger value of the certainty parameter β is accordingly necessary to achieve the signature bimodal behavior.

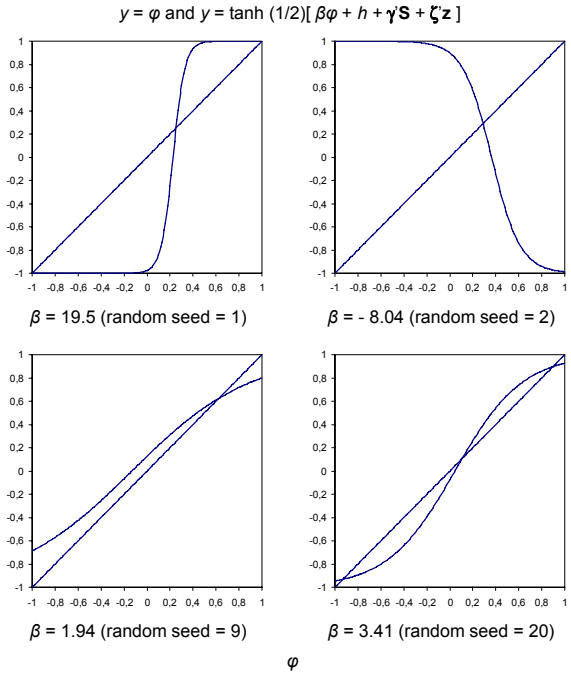

Figure 3: Plots of $y = \tanh(1/2)\,[\beta x_n + h + \boldsymbol{\gamma}'\mathbf{S}_n + \boldsymbol{\zeta}'\mathbf{z}_n]$ and $y = \varphi$ versus φ for values of estimated utility parameters β, h, γ_1, γ_2, γ_3, ζ_1, ζ_2, ζ_3 in the individual network instantiations with the same network generator random seeds shown in Figure 2; stable equilibria are seen where the tanh curves the line y = φ "from above," and unstable equilibrium are seen where the tanh curves the line y = φ "from below"; both the y-axis and φ are shown in the range from -1 to 1

4 ISSUES IN ESTIMATION

We plot the sets of estimated coefficient values for the same 30 network density values swept in section 3. Figure 4 shows the four model specifications with and without an alternative specific constant and with and without self loops (20 network instantiations per density value). Analyzing the plots, the clue to our puzzling behavior in section 3 becomes obvious in light of the analytical results in section 2.1. Far from being constant across all estimated models, we see instead systematic variation in the estimated coefficient values. From the analytical benchmark in section 2.1, we know that the coefficient on the interaction variable must be sufficiently large and positive relative to the other contributions in the utility in order to trigger the signature bimodal histogram long-run behavior. What we see is that for many of the models, this coefficient on the local interaction variable is in fact negative. In such case we can never expect to see the signature bimodal histogram.

There are two subtle issues to understand about the estimation. One issue has to do with correlation of explanatory variables. The other issue has to do with an explanatory variable or linear combination thereof being (almost) a perfect predictor for the dependent variable.

A key aspect to recognize about the local interaction variable is that in networks with a large number of agents and at high network density, the "local" interaction variable will become effectively "global", ie. constant across agents in the network - whereby this variable will become highly correlated with the value of unity included in the model when estimating an alternative specific constant. This leads to a violation in the estimation process. In fact the local interaction variable will be perfectly correlated with unity at network density $p = 1$ (a fully-connected network) when the model includes self loops. In Figure 4, we can visually track the increasing correlation as the network density increases, between the coefficient on the local interaction variable and the alternative specific constant (ASC) for rail in the models with the ASC.

When the model does not include an alternative specific constant, the local interaction variable takes on this role at high densities. Since the alternative specific constant happened to be positive for this case study in a baseline model without any interaction, simple calculation can show that the coefficient on the local interaction variable will be negative for this case study in models without an alternative specific constant for high network density, since the "local" interaction variable itself will be negative (the sample mode share for rail is less than the sample mode share for car). This is the reason why we never saw the signature bimodal histogram in section 3 for the models without an alternative specific constant at high network density.

At low network densities in models with self loops, we have a problem in that the local interaction variable will be almost a perfect predictor for the dependent variable, particularly if we do not have time series data. At high network density in models without self loops and with an alternative specific constant, we are confronted with a double effect: the local interaction variable is almost perfectly correlated with unity whereby we have a violation in estimation due to the correlation between explanatory variables, and additionally a linear combination of the local interaction variable and unity is highly correlated with the choice variable itself, leading to the second violation in estimation. This linear combination is a perfect predictor for the model without self loops and with an alternative specific constant when network density $p = 1$.

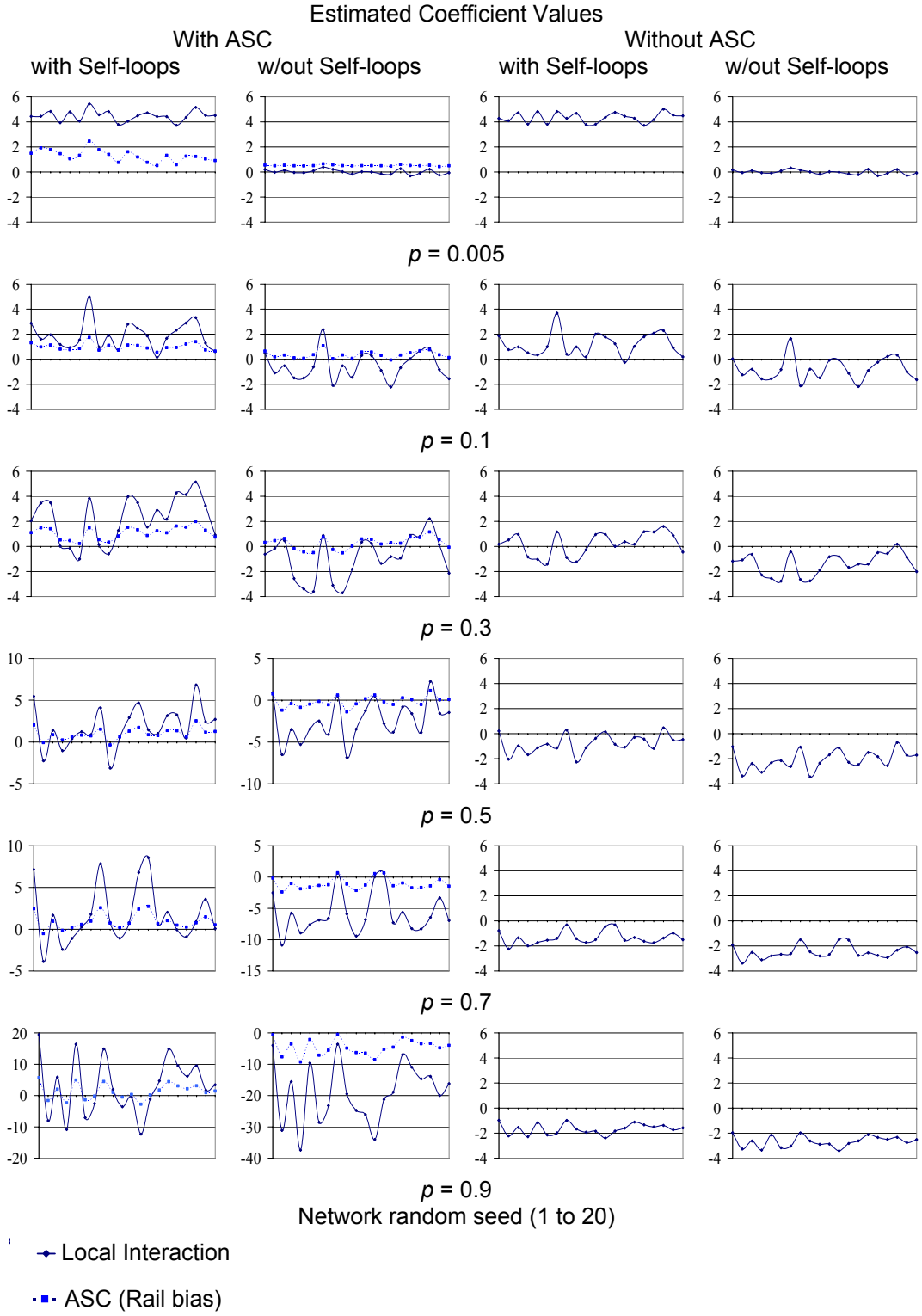

Figure 4: Estimated coefficient values for the four model specifications with and without an alternative specific constant, and with and without self loops; there are 20 network instantiations per density value for the sweep of network density from $p = 0.005$ to 0.9

5 CONCLUSIONS

In this paper, we have explored a multi-agent based model of discrete choices with interdependence of decision-makers' choices. By applying the model to an example of intercity travel demand using empirical data, we introduced individual agent heterogeneity beyond that induced by the local interaction structure. We found that the model's characteristic phase transition is dependent on network density in an example with Erdős-Rényi graphs, as well as on the importance of the estimated value of the coefficient for the local interaction variable relative to other coefficients in the binary model. Furthermore, we find that the estimation process to determine the set of coefficients can be highly sensitive to the small variations in the different instantiations, particularly in models including an alternative specific constant.

Special care must be taken in estimation of empirical models with networks with:

- very low network densities when the model includes self loops;
- very high network densities when the model includes an alternative specific constant (ASC),, especially in a model without self loops.

In general, preference goes to models with an ASC in order to ensure the error terms in the utility function have zero mean and the estimated coefficients are unbiased. Whether self-loops are implemented or not in an empirical model depends on the rationale of the system, and ideally on availability of panel data over multiple time periods.

In addition to this central contribution, we hope that our work also serves a secondary function to highlight good practice with multi-agent based social simulation. A key feature of agent-based modelling is internal verification, or otherwise said, how can the researcher be confident that the agent-based model is performing the actions that it is expected to do? What is the evidence that the programming implementation of the abstract or conceptual model is correct? To address this fact, we began our modelling endeavor with a very simplified model studied previously by others as a cornerstone, and built up our multi-agent based model step by step, and adding different layers of complexity one at a time. In our case, this meant adding different kinds of heterogeneity. In section 2.1, the dynamics of the model are driven by choices made by agents with global information. For this simple model, there is an analytical solution. The analytical benchmark gives us behavioral insights for corner solutions in parameter space, and also serve as a cross-check that the subtleties of scheduling, event simulation and sequences of random draws in our model behave as expected. In section 2.2, there is additional heterogeneity due to the network structure and the fact that agents have local information, rather than global information. We experiment with a well-known abstract class of networks to see the effect of density, and drawn on established results about connectivity in such graphs to guide behavioral hypotheses. Finally, in the empirical demonstration, we add heterogeneity due to individual characteristics of agents (gender, travel purpose) as well as agent-specific attributes of choice alternatives (travel time, travel cost).

6 RECOMMENDATIONS

In order to be able to apply the agent-based model for policy purposes, more extensive data would be desirable than what was available to us for this exploratory methodological study applying abstract classes of networks. Manski (1995) highlights three hypotheses in his classic monograph "to explain the common observation that individuals belonging to the same group tend to behave similarly... endogenous effects, wherein the propensity of an individual to behave in some way varies with the prevalence of that behavior in the group; contextual effects, wherein the propensity of an individual to behave in some way varies with the distribution of background characteristics in the group; and correlated effects, wherein individuals in the same group tend to behave similarly because they face similar institutional environments or have similar individual characteristics." The first two hypotheses express inter-agent causality in a model. The third hypothesis does not. The important distinction between the two inter-agent causal effects is that the first involves feedback that can be reinforcing over the course of time depending on the strength of the certainty parameter in relation to the rest of the utility function as we have seen in our agent-based model. The policy implications of the approaches are widely different, especially if there exists a case of an inherent dynamic with feedback. Access to temporal panel data is highly desirable in order to better empirically distinguish the effects during the estimation of the utility parameters.

In addition to the availability of empirical data on the change in the choice distribution over time, as well as changes in agent characteristics and agent-specific attributes of the choice alternatives over time, another consideration in applying the agent-based model for policy purposes is the availability of data on the possible change in the population itself, both its size and its network structure. In the agent-based model in this study, we have fixed the population in the initialization phase of the model and this population continues at each time step throughout all iterations of a simulation run until time T. In a policy application however, the links in the base population may change among existing agents, and furthermore perhaps some agents may leave and other new agents may enter.

ACKNOWLEDGEMENTS

We would like to thank Harry Timmermans, Cars Hommes, Loek Kapoen, Frank le Clercq, George Kampis, József Váncza and András Márkus for fruitful discussions. Simulations were performed at SARA Computing and Networking Services, Science Park Amsterdam, with special thanks to Willem Vermin and the High Performance Computing team.

REFERENCES

Aoki M. 1995. "Economic fluctuations with interactive agents: Dynamic and stochastic externalities." *Japanese Economic Review* 46, No.2, 148-165.

Arentze TA, Timmermans HJP. 2008. "Social networks, social interactions, and activity-travel behavior: A framework for microsimulation." *Environment and Planning B* 35, No.6, 1012-1027.

Ben-Akiva M. 1973. "Structure of passenger travel demand models." Dissertation, Department of Civil Engineering, Massachusetts Institute of Technology.

Ben-Akiva M, Lerman SR. 1985. *Discrete choice analysis: Theory and application to travel demand*. MIT Press, Cambridge, MA.

Ben-Akiva M, Morikawa T. 1990. "Estimation of travel demand models from multiple data sources." *Transportation and Traffic Theory* 461-476.

Blume L, Durlauf SN. 2003. "Equilibrium concepts for social interaction models." *International Game Theory Review* 5, No.3, 193-209.

Brock WA, Durlauf SN. 2001. "Discrete choice with social interactions." *Review of Economic Studies* 68: 235-260.

Domencich T, McFadden D. 1975. *Urban travel demand*. North Holland Press, Amsterdam.

Dugundji ER, Gulyás L. 2008. "Socio-dynamic discrete choice on networks: Impacts of agent heterogeneity on emergent equilibrium outcomes." *Environment and Planning B* 35, No.6, 1028-1054.

Dugundji ER, Páez A, Arentze TA. 2008. "Social networks, choices, mobility and travel." *Environment and Planning B* 35, No.6, 956- 960.

Dugundji, ER, Páez A, Arentze TA, Walker JL, Carrasco JA, Marchal F, Nakanishi H. 2011. "Transportation and social interactions." *Transportation Research Part A* 45, No.4, 239-247.

Dugundji ER, Walker JL. 2005. "Discrete choice with social and spatial network interdependencies: An empirical example using mixed generalized extreme value models with field and panel effects." *Transportation Research Record* 1921: 70-78.

Erdős P, Rényi A. 1959. "On random graphs." *Publicationes Mathematicae* 6: 290-297.

Fukuda D, Morichi S. 2007. "Incorporating aggregate behavior in an individual's discrete choice: An application to analyzing illegal bicycle parking behavior." *Transportation Research Part A* 41: 313-325.

Goetzke F. 2008. "Network effects in public transit use: Evidence from a spatially autoregressive mode choice model." *Urban Studies* 45, No.2, 407-417.

Goetzke F, Andrade PM. 2010. "Walkability as a summary measure in a spatially autoregressive mode choice model: An instrumental variable approach. In *Progress in spatial analysis: Methods and applications*, Páez A, Buliung RN, Le Gallo J, Dall'erba S (Eds.). Springer-Verlag, Berlin Heidelberg, 217-229.

Goetzke F, Rave T. 2011. "Bicycle use in Germany: Explaining differences between municipalities with social network effects." *Urban Studies* 48, No. 2, 427-437.

Goetzke F, Weinberger R. 2012. "Separating contextual from endogenous effects in automobile ownership models." *Environment and Planning A*, forthcoming.

Manksi CF. 1995. *Identification problems in the social sciences*. Harvard University Press, Cambridge, MA.

Molloy M, Reed B. 1998. "The size of the largest component of a random graph on a fixed degree sequence." *Combinatorics, Probability and Computing* 7, 295-306.

Páez A, Scott DM. 2007. "Social influence on travel behavior: A simulation example of the decision to telecommute." *Environment and Planning A* 39, 647-665.

Páez A, Scott DM, Volz E. 2008. "A discrete-choice approach to modeling social influence on individual decision making." *Environment and Planning B* 35, No. 6, 1055-1069.

AUTHOR BIOGRAPHIES

ELENNA R. DUGUNDJI is research affiliate at the Department of Quantitative Economics of the Amsterdam School of Economics, Universiteit van Amsterdam. Her research addresses diffusion of innovation and social influence in dynamic networks and develops methodologies to study self-consistent behavior with interacting consumers, drawing on techniques in bifurcation theory, statistical physics, multi-agent social simulation, econometrics and geographical information systems. She is co-founder of the international workshop series: *Frontiers in Transportation: Social Interactions*. She is guest editor of special issues in Environment and Planning B (2008), Transportation Research Part A (2011), Environment and Planning A (2012), and Journal of Transportation Geography (forthcoming). http://www.e-du.nl/frontiers

LÁSZLÓ GULYÁS is assistant professor at the Department of History and Philosophy of Science, Lorand Eotvos University, Budapest. He is also a research partner at AITIA International Inc and a fellow at Collegium Budapest (Institute for Advanced Study). He has been doing research on agent-based modeling and multi-agent systems since 1996. His main research interests are computational multi-agent systems where he has worked on "engineering" desired emergent phenomena. He is a member of the Scientific Advisory Board of the Simulation Center of the Informatics Cooperative Research and Education Center of the Eötvös Loránd University. He participated in several international research consortia under the European Commission's Framework Programme and has been project leader or participant in numerous research and development projects funded by the Hungarian Government. http://www.aitia.ai

Simulation-Based Business Research

A NEW RESEARCH ARCHITECTURE FOR THE SIMULATION ERA

Martin Ihrig
The Sol C. Snider Entrepreneurial Research Center
The Wharton School of the University of Pennsylvania
418 Vance Hall, 3733 Spruce Street, Philadelphia, PA 19104

KEYWORDS
Simulation, modeling, research, methodology, business, management, theory, social sciences.

ABSTRACT
This paper proposes a novel research architecture for social scientists that want to employ simulation methods. The new framework gives an integrated view of a research process that involves simulation modeling. It highlights the importance of the theoretical foundation of a simulation model and shows how new theory-driven hypotheses can be derived that are empirically testable. The paper describes the different aspects of the framework in detail and shows how it can help structure the research efforts of scholars interested in using simulations.

INTRODUCTION

Business and management researchers are increasingly interested in exploring phenomena that are emergent and/or one of a kind and in studying complex and non-repeatable processes. Simulation modeling is the appropriate methodological approach for this kind of research. Harrison, Lin, Carroll and Carley (2007: 1229) consider simulation modeling to be a "powerful methodology for advancing theory and research on complex behaviors and systems", while Davis, Eisenhardt and Bingham (2007: 480) point out that "the primary value of simulation occurs in creative and systematic experimentation to produce novel theory". Simulation research results in theory-driven frameworks and hypotheses that would be difficult to obtain from empirical analyses alone. In this paper, we propose a novel research architecture, a framework that gives an integrated view of a research process that involves simulation modeling. In what follows, we describe the different aspects of the framework and show how it can help structure the research efforts of scholars interested in using simulations.

AN 'EXTENDED' LOGIC OF SIMULATION AS A METHOD

Carley (2002: 254) gives a detailed explanation for "why so many social and organizational scientists and practitioners are turning to computational modeling and analysis as a way of developing theory and addressing policy issues". Among the many reasons she advances is that "social and organizational systems are complex non-linear dynamic systems; hence, computational analysis is an appropriate technology as models can have these same features." (Carley, 2002: 254) Harrison, Lin, Carroll and Carley note that "the academic field of management has been slow to take advantage of simulation methods" (2007: 1229). But looking at the increased number of recent articles based on simulation research in management journals and of simulation-specific workshops and papers at management conferences, it seems that management theorists are finally discovering the benefits of simulation methods. Davis, Eisenhardt and Bingham (2007) and Harrison, Lin, Carroll and Carley (2007) give guidelines for simulation research in the field of management. Gilbert and Troitzsch (2005) put forward the following framework (Figure 1) to explain the logic of simulation as a method in their authoritative book on simulation for the social scientist.

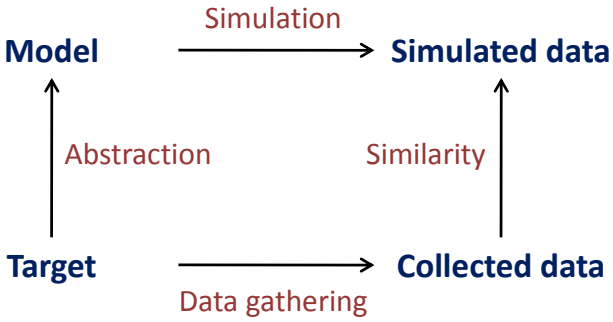

Figure 1: The logic of simulation as a method (Gilbert & Troitzsch, 2005: 17)

Starting at the bottom left, the real world 'target' under study is modeled by abstracting characteristics from it, and then a computer model is used to run simulations in order to produce simulated data. This data can then be compared with data collected in the 'real' social world.

This framework nicely illustrates the core logic of simulation as a method that underlies all the different kinds of simulation approaches that Gilbert and Troitzsch (2005) review in their book. But does it capture the entire simulation research process that scholars encounter, especially for complex agent-based modeling approaches? What is the role of existing theory, insights and frameworks from the literature, when it comes to modeling? Where do simulation environments, software toolkits that help researchers create, run, and analyze simulation models, come into play? To account for those questions and provide a more detailed picture of the simulation research life-cycle, we constructed an expanded framework (Figure

Proceedings 26th European Conference on Modelling and Simulation ©ECMS Klaus G. Troitzsch, Michael Möhring, Ulf Lotzmann (Editors)
ISBN: 978-0-9564944-4-3 / ISBN: 978-0-9564944-5-0 (CD)

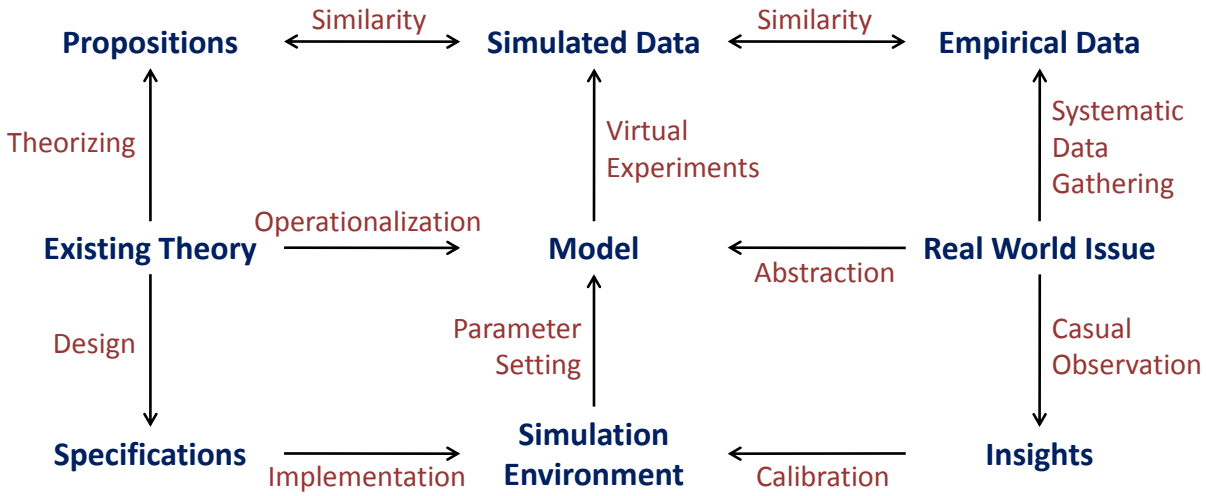

Figure 2: A new research architecture

2) to extend the logic of Gilbert and Troitzsch's (2005) basic model. This framework is meant to provide future simulation researchers with a research architecture that can assist them in their modeling efforts. Simulation methods are used for studying complex processes; simulation research, being a complex process itself, should therefore be described by an appropriately complex process model that depicts all the relationships between its building blocks. The following sections explain the different components of this research architecture.

FROM THEORY TO SIMULATION MODEL

In contrast to Gilbert and Troitzsch (2005), we propose to start the simulation research 'adventure' in the bottom half of the framework (Figure 3) on the left with a particular *theory*. The bottom left square describes the process of implementing theory with software, whereas the bottom right square depicts the real world grounding of the model.

Implementing Theory with Software. In a very general definition, a theory is "a statement of what causes what, and why" (Christensen, Carlile, & Sundahl, 2003). In order to build simulation software, one has to *design* and write a detailed document with *specifications* that mirror the theory in computer algorithms. This is both a conceptual and technical task, and requires the simulation researcher to be very specific about how "what causes what" is based on theoretical considerations ("why"). The next step is to *implement* the concrete specifications in computer code, and program the *simulation environment* as executable software. With the software up and running, finding the right *parameter settings* for the generic simulation environment can allow an application specific *model* to be created. The resulting model will *operationalize* the specific theory on which the simulation environment is based.

Real World Grounding. The purpose of simulation research is not necessarily to model a theory in the

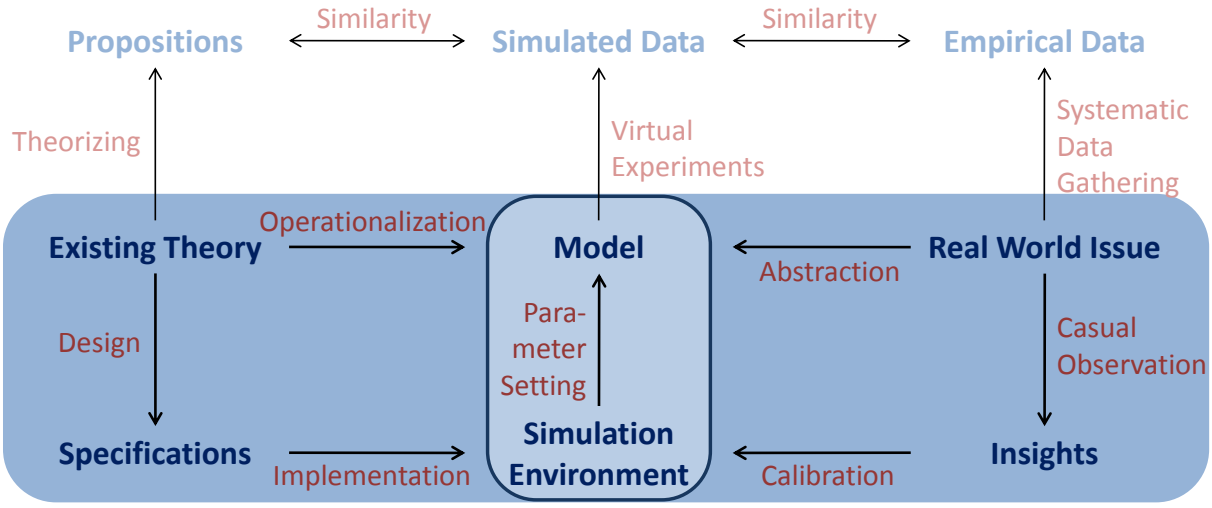

Figure 3: From theory to simulation model

abstract. The researcher wants to study a *real world issue* (what Gilbert and Troitzsch (2005) call a 'target') so as to produce new theory. *Casual observations* of the social world will yield helpful *insights* about the real world issue that will help *calibrate* the parameter space in the simulation environment: thus the final model will be an *abstraction* of the real world issue under study.

What distinguishes the simulation approach described here from many other simulation exercises is that a fully-fledged theory lies behind the simulation environment that is built. In the case of agent-based models and simulations (Gilbert, 2008), most modelers endow their virtual agents with only a couple of simple rules as an abstraction from real social agents (individuals, companies, etc.). Therefore, the entire bottom half of our research framework (and especially the left side) disappears, because the modeling lacks a theoretical underpinning. This is reflected in Gilbert and Troitzsch's (2005) simpler framework shown above. More simulation models are needed that have a stronger theoretical foundation, because "the advance of multi-agent techniques provides social scientists, who are used to thinking about agency, the ability to reason in the terms of their theories" (Carley, 2002).

SIMULATION RESEARCH IN ACTION

Once the researcher has built an application-specific model informed by the real world and grounded in some theory, the actual simulation research can start – the top part of our framework (Figure 4). The top left quadrant describes the process of new theory generation, and the top right links the simulation work to empirical follow-up studies.

The basic component of simulation research concerns running the simulation *model* and conducting many *virtual experiments* by varying the parameter space. The resulting *simulated data* can then be compared to both theoretical and empirical assessments, which is the first step in generating novel theory. The researcher will have *theorized* about the subject under study and will have come up with *propositions* based on the underlying *theory* used in the simulation effort. The simulated data can be evaluated in the light of these theoretical analyses and propositions, and the researcher can learn from studying *similarities* and *differences*. This exercise will result in theory-driven hypotheses that are empirically testable. Subsequently, the simulated data can be compared to *empirical data*. In an empirical follow-up study, the *real world issue* that is being investigated can be further examined by obtaining empirical data through *systematic data gathering* on a basis that is informed by the previous simulation research.

CONVENTIONAL RESEARCH APPROACH

The research architecture described above is more comprehensive than conventional approaches that do not employ simulation tools, and so is better suited for studying complex phenomena and obtaining new theoretical insights.

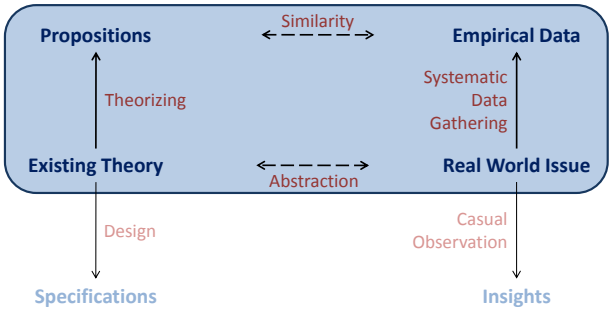

Figure 5: Conventional research approach

The conventional research approach can be depicted by connecting the left- and right-hand ends of our framework (Figure 5). Predictions and analyses are made based on existing theories, and the empirical data gathered on real world issues is compared to these theoretical accounts or propositions. What is lacking is

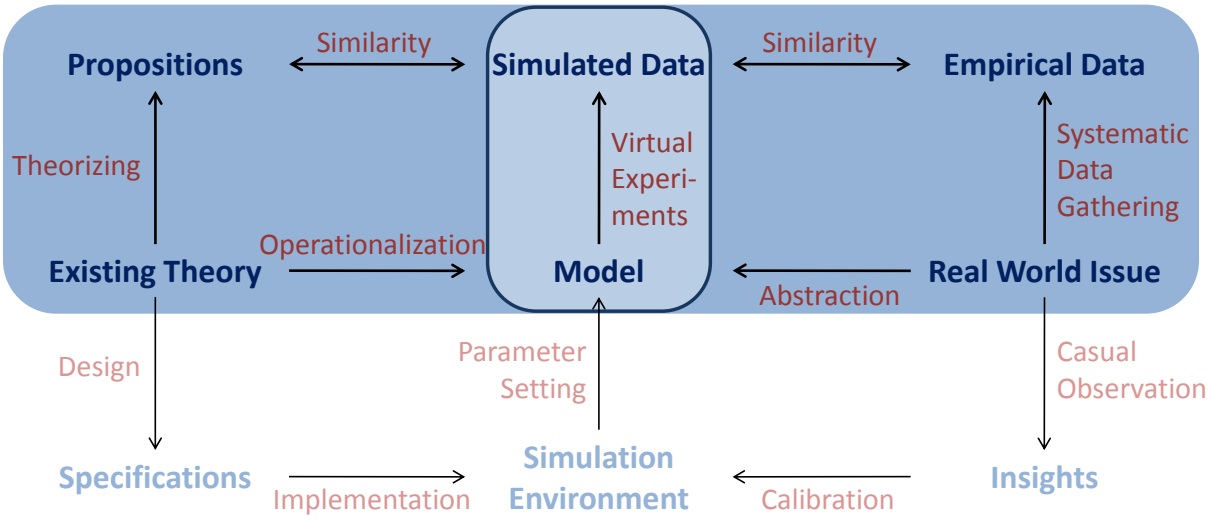

Figure 4: Simulation research in action

the power of computer tools that enable us to study more complex processes by modeling micro behaviors that individually might be straightforward, but may result in unpredictable outcomes when considered together.

VERIFICATION AND VALIDATION

Our framework can also be used to illustrate the important processes of verification and validation, both of which have been explained in detail in the literature (Carley, 2002; Davis, et al., 2007; Gilbert, 2008; Gilbert & Troitzsch, 2005; Harrison, et al., 2007). Gilbert and Troitzsch (2005: 23) give a concise definition:

> While verification concerns whether the program is working as the researcher expects it to, validation concerns whether the simulation is a good model of the target.

Our framework allows us to identify multiple instances where verification and validation come into play (Figure 6). There are three layers of interest: verification, validation, and ascertaining the two.

Verification. Starting at the bottom left, the obvious area where the model needs verifying is in the building of the software, where the researcher has to ensure that the program's technical specifications have been properly implemented. The simulation environment has to perform exactly as described in the technical document, without errors or 'bugs'. The simulation processes, in their abstracted form, also have to work like and be consistent with the real world social processes they represent.

Validation. The middle layer of the framework depicts the areas of interest in validation terms. Most researchers will look to the right, and ensure that the application-specific model fully represents the real world issue or target under study. But there is another important area: since the simulation environment is underpinned by a theory, they also have to make sure the model is a fair representation of the theoretical constructs.

Ascertaining Verification and Validation. The factors noted above will be difficult to ascertain without comparing the simulated data to either empirical data or theoretical predictions, or both. Therefore, simulation researchers have to pay attention to the top layer of the framework. They have to infer and draw conclusions from the actual results of the simulation runs to assess whether the program is working as intended, and represents the actual phenomenon studied. Great care must be taken here because - as Gilbert and Troitzsch (2005) point out - mistakes can occur at any step in the research process.

SIMULATION CAPABILITIES BEYOND A SINGLE RESEARCH PROJECT

Considering our research framework further, the top half of Figure 7 (shaded area, blue) maps the area usually covered by research employing simulation methods. The core research activities classically conducted in scholarly work based on simulation modeling as described by Gilbert and Troitzsch (2005) are those depicted in the top right quadrant. Many recent simulation studies also base their modeling on existing theories, represented by the top left quadrant (a fine example of this would be Csaszar & Siggelkow, 2010). Generally however, simple simulation models are programmed that can only be used for and applied to the particular research topic of the study. For this, an increasing number of researchers turn to preexisting modeling and simulation tools (environments) that support the construction of simulations (e.g., RePast for

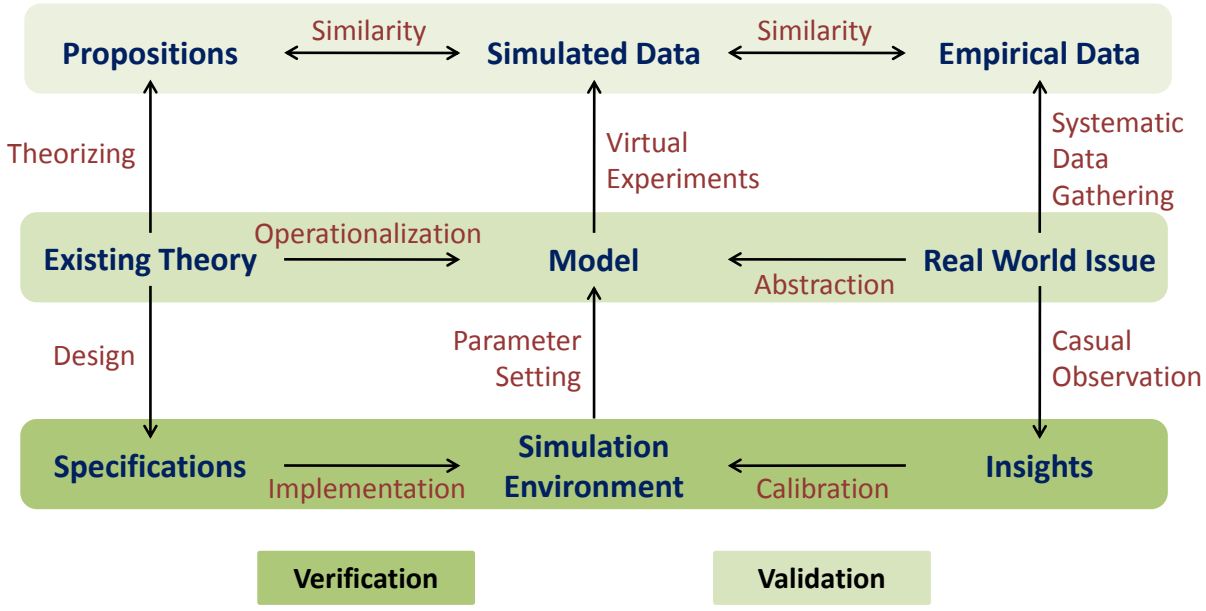

Figure 6: Verification and Validation

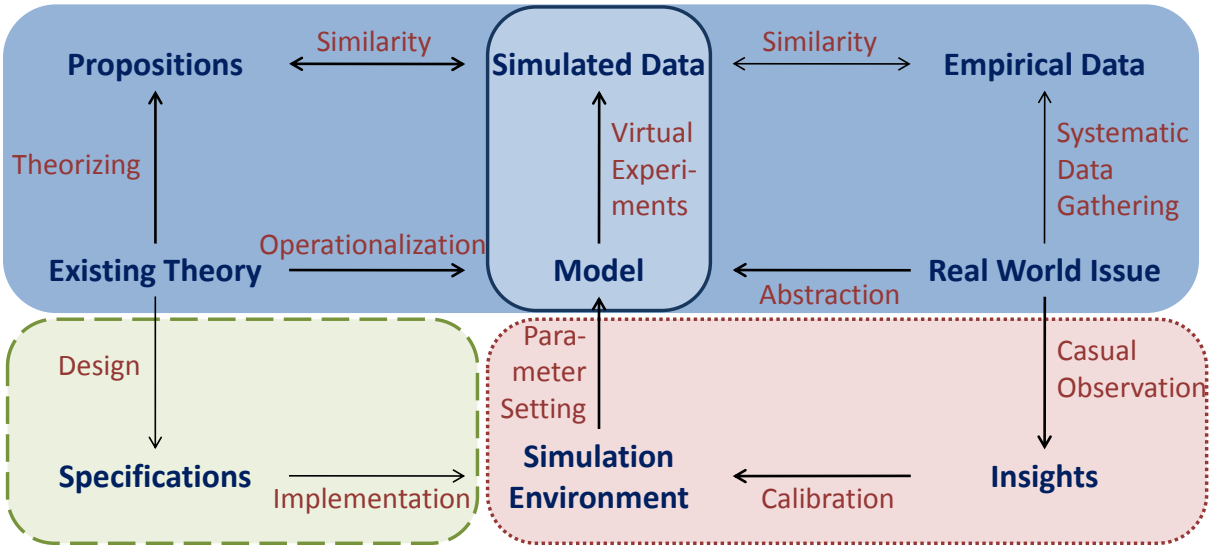

Figure 7: Simulation research activities

agent-based systems (North, Collier, & Vos, 2006)), which is represented by the bottom right quadrant (round dots, red). Very few simulation research projects cover the additional area marked in the dotted line in the bottom left (long dashes, green). Most researchers do not build an entire simulation environment that can be used for many different research topics and purposes, far beyond the subject of the immediate research needs. This is a pity because future research projects studying different topics could also employ the simulation environment created to derive new theory-driven hypotheses that are empirically testable and which range across numerous applications.

Designing and implementing a full simulation environment or platform (including a simulation execution and reporting suite) that can be used for a variety of research projects is a difficult and laborious process (Figure 8). This probably explains why many people shy away from developing them. Problems can occur at various places, especially if researchers are not able to write the actual software code themselves, but have to rely on software engineers who may not necessarily understand the theory fully. In fact, completely debugging a simulation environment can take several years. However, once developed, it benefits the many researchers who are interested in simulation methods but lack the computer science skills that are necessary to build the software. They can use the graphical user interface to easily set up, run, and analyze simulations that model their particular research questions.

To help build a simulation environment, some of the lessons learned from difficulties the author encountered during this effort are listed below. Attending to these four points will help simulation researchers to get closer to the proper computational representation of the theory they want to model and avoid losing too much time on software development.

1. If the software development project is inherited, or there are multiple authors, the researcher will have to revisit the specifications thoroughly and check whether they are all correct and appropriate, a process which involves uncovering and repairing inconsistencies, errors and omission in the spec.
2. If the researcher has to work with successive generations of programmers, and proper documentation is not in place, coherent knowledge about what has been implemented and how it has been implemented may be lacking. The software development process must be either very closely monitored over its entire development cycle, or rigorously and consistently documented.
3. Software bugs are an inevitable part of the development process, but having the program properly designed by a good software architect can at least avoid faulty code and inappropriate architecture.
4. Misrepresenting theory is dangerous: a researcher who is not their own software architect must attend to the specifications and technical document closely to ensure the computer algorithms really implement the theory the researcher wants to model.

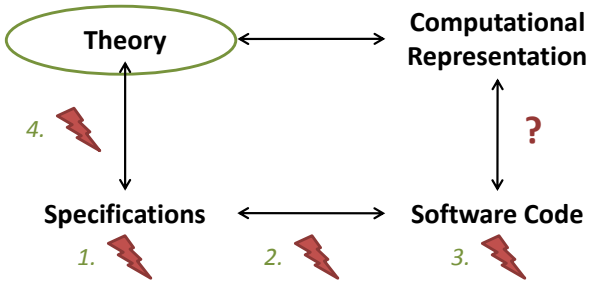

Figure 8: The long road to a simulation environment

CONCLUSION

This paper describes our unique research architecture and discusses the applicability of its framework, and looks ahead to many future research projects that could be structured using this approach. Being able to navigate the research space presented by this framework is a first step in using simulation methods to produce novel theory. We hope that the framework will help other researchers conceptualize the different tasks required to realize good simulation studies.

REFERENCES

Carley, K. M. (2002). Computational organizational science and organizational engineering. *Simulation Modelling Practice and Theory, 10*(5-7), 253-269.

Christensen, C. M., Carlile, P., & Sundahl, D. (2003). The process of theory-building. Retrieved 01.06.2004, 2004, from http://www.innosight.com./template.php?page=research#Theory%20Building.pdf

Csaszar, F. A., & Siggelkow, N. (2010). How Much to Copy? Determinants of Effective Imitation Breadth. *Organization Science, 21*(3), 661-676.

Davis, J. P., Eisenhardt, K. M., & Bingham, C. B. (2007). Developing theory through simulation methods. *Academy of Management Review, 32*(2), 480-499.

Gilbert, N. (2008). *Agent-based models*. London: Sage Publications.

Gilbert, N., & Troitzsch, K. G. (2005). *Simulation for the social scientist*. Maidenhead: Open University Press.

Harrison, J. R., Lin, Z., Carroll, G. R., & Carley, K. M. (2007). Simulation modeling in organizational and management research. *Academy of Management Review, 32*(4), 1229-1245.

North, M. J., Collier, N. T., & Vos, J. R. (2006). Experiences Creating Three Implementations of the Repast Agent Modeling Toolkit. *ACM Transactions on Modeling and Computer Simulation, 16*(1), 1–25.

AUTHOR BIOGRAPHY

MARTIN IHRIG is President of *I-Space Institute, LLC* (USA) and Adjunct Assistant Professor at the *Wharton School* of the *University of Pennsylvania* (USA). He holds a Master of Business Studies from *UCD Michael Smurfit School of Business* (Ireland) and a Doctor of Business Administration (PhD) from *Technische Universität Berlin* (Germany).

The research initiative he manages at Wharton's *Snider Entrepreneurial Research Center* focuses on the strategic and entrepreneurial management of knowledge. In his simulation research, he is studying entrepreneurial opportunity recognition strategies with the help of agent-based models.

His e-mail address is ihrig@wharton.upenn.edu.

Organizational Path Dependence: The Prevalence of Positive Feedback Economics in Hierarchical Organizations

Arne Petermann
Deutsche Universität für Weiterbildung
email: arne.petermann@duw-berlin.de

Stefan Klaußner
Freie Universität Berlin
email: stefan.klaussner@fu-berlin.de

Natalie Senf
Europa Universität Viadrina
email: nsenf@europa-uni.de

ABSTRACT

We focus on the application of path dependence logic in organizations, particularly on the role of self reinforcing mechanisms in the evolution of institutions in business firms. Path dependence theory suggests that self reinforcing mechanisms may lead to very high persistence of inefficient institutional solutions. The so called lock-in can create a growing threat to an organization's viability. While path dependence theory is developed as a market based approach and widely accepted in economics, some critics doubt its application to organizations science. They argue that asymmetric power structures in organizations contradict with the basic assumptions of perfect markets and thereby models of path dependence cannot properly be applied to organizations. Attempts to incorporate asymmetric power structures to formal models of path dependence are difficult because they create process-oriented, complex models of interaction on different levels that become mathematically intractable. With the use of computer simulation, institutional change in organizations can be modeled as an interdependent multilevel-process and analyzed numerically. The results allow predictions of institutional long-term states of the system and the conditions, which result in a lock-in situation. By varying the magnitude of the complementary effects and organizational structure as the two independent variables, the institutional evolution in social systems prone to positive feedback can be examined. The results of this work in progress will add to both path dependence theory and the discussion about optimal organizational design.

Keywords: path dependence; institutional change; complementarity, simulation

INTRODUCTION

The role of institutional arrangements in organizations cannot be overestimated: *"Institutional change determines the development of social systems over time and thus is the key in the understanding of historic change. (...) The differences in economic performance over time depend heavily on how the institutions evolve." (North, 1990)* Complementary effects are at the heart of positive feedback-loops that drive the process of institutional development. Path dependence theory suggests that under these conditions inefficient institutions may become

Proceedings 26th European Conference on Modelling and Simulation ©ECMS Klaus G. Troitzsch, Michael Möhring, Ulf Lotzmann (Editors)
ISBN: 978-0-9564944-4-3 / ISBN: 978-0-9564944-5-0 (CD)

locked-in, meaning that it is not possible to abandon them by actions undertaken from within the system (Sydow, Schreyögg, & Koch, 2009).

First we present an overview of path dependence literature and the main arguments. We focus on the process of adopting new institutional solutions. A simple simulation model of institutional evolution in a social system with self reinforcing mechanisms is presented. Applying the building block method suggested by Davis, Eisenhardt, and Bingham (2007) we developed an advanced model that includes organizational structure as independent variable. The advanced model will enable us to test the predictions of path dependence theory for different types of organizational hierarchy and different degrees of hierarchical power. Although the work on the advanced model is still in progress, we provide some insights from the first test runs.

PATH DEPENDENCE THEORY

As a dynamic theory path dependence theory basically assumes that initial decisions may increasingly restrain present and future choices. Paul David initiated the discussion on path dependence from an economic perspective (David, 1985). Within his historical studies he explored the development of the QWERTY keyboard technology and describes how this inferior standard was diffused and maintained although superior technological innovations were available at some point. Similar studies were carried out by others on the technologically surprising dominance of inferior technologies (Cusumano, Mylonadis, & Rosenbloom, 1992; Katz & Shapiro, 1986). As already noted, path dependence theory is based on the fact that history matters (Teece, Pisano, & Shuen, 1997; Nooteboom, 1997). Brian Arthur (1989; 1994) has formalized and to a minor extent also simulated path-dependent processes by highlighting the additional importance of self-reinforcing mechanisms.

From that perspective, path dependent processes are generally described as self reinforcing processes characterized by non-predictability, non-ergodicity, inflexibility, and potential inefficiency (Arthur, 1989, 1990; David, 2001; Pierson, 2000). In other words, the path's final outcome among possible different alternatives is not predictable and might become a dysfunctional trap, inhibiting the organization to deviate from it. Thus, path dependence is conceptualized as the outcome of a dynamic process that is ruled by one or more self-reinforcing mechanisms which lead to a narrowing of the variation and range of (managerial) discretion (Sydow, Schreyögg, & Koch, 2009). Path dependence describes a tapering process. Thus, a path constitutes a restriction of choice for a social or psychic decision-making system. While choice is not restricted to start with, it becomes restricted in the process of following that path. Figure 1 illustrates all three stages. The degree of path dependence increases with the duration of Phase II and is full-blown in Phase III (lock-in).

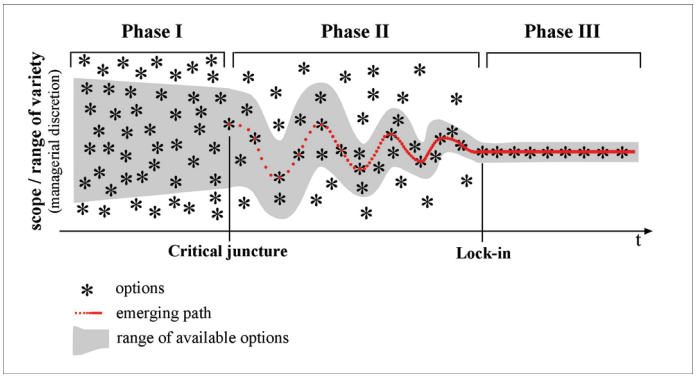

FIGURE 1:
The three stage model of path dependence
(Sydow, Schreyögg & Koch, 2009)

Phase I is characterized by contingency, although certain choices and events may already have a slight narrowing impact, illustrating that history already matters in

that early phase (Teece et al., 1997; David, 1994). In Phase II, self-reinforcing mechanisms increasingly limit the scope of choice and thereby facilitate the evolvement of an organizational path (Sydow et al., 2009; Stieglitz & Heine, 2007; North, 1990). With the transition to Phase III, the diminishing window of opportunity finally closes, leaving the organization strategically trapped in an unalterable state.

The idea of self-reinforcing mechanisms implies a positive feedback. A self-reinforcing mechanism is a necessary precondition for what is defined as a path. That presumes that agents act (consciously or unconsciously) upon these mechanisms and by doing so they reinforce the path-building effects. The diminishing variety and the rising limitations of choices are collateral effects of this process. Hence, the hallmark of path dependence theory is its focus on self-reinforcing effects (Arthur, 1994; David, 1993; Bassanini & Dosi, 2000). These effects are understood as the central triggering elements that drive path dependence (Sydow et al., 2009). Up to now, path dependence research has hallmarked the crucial elements that drive path emerging processes and finally lead to a lock-in in phase II (see Figure 2) of the model. At least six different forms of self-reinforcing mechanisms (Sydow, Schreyögg, & Koch, 2005) can be distinguished from a technological and from an institutional perspective: (1) economies of scale and scope, (2) direct and indirect network externalities, (3) learning effects, (4) adaptive expectations, (5) coordination effects and (6) complementary effects.

The first three mechanisms particularly apply to diffusion processes of technological standards. Economies of scale and scope refer to the market's supply-side and cost advantages due to production expansion as well as synergy effects of adjunctive product variety. Direct and indirect network externalities refer to the demand-side and cover the single agent's additional utility stemming from the technologies diffusion rate. Learning effects build on a rather individual level of the demand-side with illuminating experiences agents gain with their adoption of a specific technology. Learning effects also play an important role from an institutional perspective. Here the implementation and the repeated appliance of institutions lead to learning effects and the internalization of these institutions, resulting in a declining attractiveness of deviation. Adaptive expectations relate to the agents' interaction and their co-building of preferences. The more an agent expects others to prefer a particular product or standard, the more attractive it becomes.

From the institutional perspective of this paper the final two mechanisms are of most relevance. The coordination effect was introduced by North (1990) and refers to the general benefit of coordinated behavior. The more agents adopt a specific institution the more efficient the interaction among these agents becomes. In other words, shared rules contribute to the anticipation of other agents' behavior; reactions can be foreseen and uncertainty as well as coordination costs will be reduced. From a single adopter's point of view it the attractiveness of adopting an institution rises with its spread.
The well-known traffic-rule example illustrates this (Arthur, 1994: 14): Imagine an island having roads but neither cars nor any traffic rule. Once cars are introduced, drivers have to decide for left-hand or right-hand driving in order to prevent unwanted collisions. Oncoming indifferent drivers coordinate their behavior, others accordingly adapt and at some point one alternative dominates the other, with the obvious benefit of coordinated interaction.

Complementarity effects on the other hand result from plurality and

connectivity between different institutions (Stieglitz & Heine, 2007). Essentially, complementarities mean synergy resulting from the interaction of two or more separate and different institutions, where the institutions' advantages do not just add up but create a surplus based on complementarity: $F_{(x+y)} > F_{(x)} + F_{(y)}$ (Sydow et al., 2009). In other words: an institution is reinforced by another one and vice versa. Referring to the traffic-rule example, introducing the institution of giving way at crossroads to drivers coming from the right reinforces right-hand driving.

At this point it should be stated that these effects can only be differentiated on an analytically level, empirically they are rather jointly at work than acting separately.

Conceptual argument of complementarity feedback

In our study we focus on one of the mechanisms: complementarity. Complementary effects form positive feedback loops that may pave the way for path dependence and lock-in. We adopt the understanding of David (1994) arguing that two (or more) institutions are complementary to one another when the existence (or more precise: a higher diffusion rate) of the focal institution makes the adoption of the other institution(s) more attractive for the relevant decision makers in the system and vice versa. David argues that in dynamic and complex environments new problems emerge all the time, creating the necessity of adopting new institutional solutions. In the process of finding new institutional arrangements capable of solving the problem at hand decision makers favor those institutions that are more compatible with already existing institutions over those which are less compatible. The main argument here is the desire of decision makers to avoid so called misfit-costs. Those include time and resources needed to solve conflicts resulting from the installation of less-compatible institutions. The tendency to avoid misfit-costs favors the emergence of a set of institutions that are highly compatible with each other (in the sense of having very low misfit-costs when existing together with the other institutions in the set). Such a set is called an institutional cluster (North, 1990). Whenever a new institutional arrangement is highly compatible with the existing institutional cluster, the cluster becomes denser. This means that future misfit costs will significantly rise for institutions that are not compatible with the already established institutions in that cluster. Thereby chances increase for forthcoming institutional arrangements to be again in line with the institutional cluster – forming an even denser cluster. This conceptual argument of institutional complementarity is illustrated in figure 2.

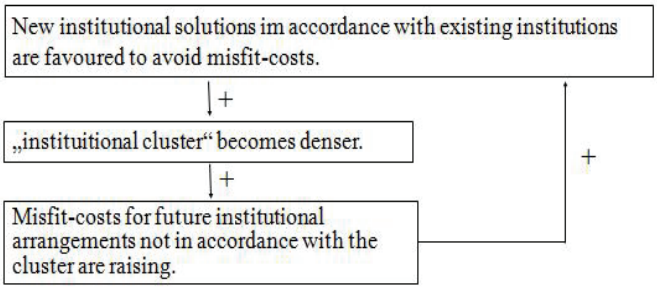

FIGURE 2:
The conceptual argument of positive feedback created through complementary effects

SIMULATING COMPLEMENTARY EFFECTS

Because of the interdependency of the macro variables (density of the institutional cluster, diffusion rate of institutions) with the variable on the micro-level process (decision of members of the social system who adopt one institutional rule or the other), an analytical approach applying solely mathematical deduction is not promising, as the differential equations that describe the systems behavior become intractable even with very restrictive assumptions and number of variables (see the work of

Arthur, 1989). Davis, Eisenhardt, and Bingham (2007) suggest a numerical solution when nonlinear, multilevel and longitudinal processes need to be modeled, and call for the application of computer simulations.

Computer simulations as scientific method

Besides logical deduction and empirical research computer simulations have become a third way of doing research in social sciences. When interdependencies between variables in complex and dynamic systems make the problem mathematically intractable, computer simulation offers a numerical solution to many problems. "Simulation is particularly useful when the theoretical focus is longitudinal, nonlinear, or processual, or when empirical data are challenging to obtain." (Davis et al., 2007) In simulation research a formal model is implemented into computer codes and often run numerous times to uncover the system's behavior. When examining the development of institutions in organizations and disclosing path dependencies we face most of the difficulties mentioned by Davis et al. Thereby computer simulation seems a very promising method.

A Simple Model

In a simple model we examine the process of institutional evolution in a multi-level, interdependent system. Our goal is to concentrate on the implications of complementary effects that trigger positive feedback loops. Here we put aside the influence of organizational hierarchy which will be included later on in the advanced model.

We adopt the idea of the netlogo implementation of the opinion formation model and look at a very simple social system consisting of a number of agents (i.e. 1000 agents) who decide whether to comply with one of two possible institutional solutions. In accordance with that simple traffic-rule example given above, the two institutional solutions are exclusive, meaning that they offer incongruous solutions to the same problem. In the simulation model colors are assigned to each solution, so for simplification it is possible to speak of a red and a blue institutional solution. The system contains a set of agents while each agent has exactly one attribute which is the behavior regarding the two contradicting institutional solutions red and blue. We applied a discrete timeline where time is counted in so called "ticks". For every tick, each agent decides whether he complies with the blue or red institutional solution. The decision function that defines the agent's decision is at the heart of the model. Deriving from path dependence theory, random small events (Arthur, 1990) are present and potentially influencing the process with earlier occurring events being potentially more influential than later ones. Due to complementary feedback, decision makers favor an institutional solution that is compatible to a denser cluster (David, 1994). In the modeled system two institutional clusters exist, one containing the blue and one containing the red institution. (Note: Arthur (1989) showed analytically that in cases where the diffusion of only one technology (respectively institution A) enjoys positive feedback while the other one (B) does not, the domination of A is inevitable.) The independent variable is the magnitude of complementary feedback. The initial density of the two institutional clusters can be varied in different simulation runs. The results stated in this paper are obtained with equal initial density for each cluster at the beginning of each simulation run.

Implementation of simulation model

The formal model was implemented using netlogo 4.0 implementation environment. At every tick, all agents adopt red or blue behaviors according to the actual diffusion of institutional rules and the density of

each cluster, taking into account the misfit costs arising from a choice that is incompatible to the denser cluster. The corresponding variables implemented in the simulation model are called 'pop-state' and 'complementarity'. 'pop-state' varies from -1 to 1 and shows whether agents actually favor the red institutional solution over the blue (pop-state < 0) or the blue institutional solution over the red (pop-state > 0). When 'pop-state' reaches the value of 1 (-1), the corresponding system behavior shows a diffusion rate of 100% of the blue (red) institution, meaning that all individuals have fallen in line with the institutional solution compatible to the denser cluster. 'Complementarity' is the strength of the complementary feedback. It is the independent variable of the model. It regulates the impact of a higher diffusion rate of the focal institution on the institutional cluster's density. 'Complementarity' ranges from 0 to +1. A value of 0 means that an additional highly compatible institutional solution does not change the clusters density at all while a value of +1 means that an additional highly compatible institutional increases the clusters density dramatically. Also at every tick a random number is drawn for every agent, incorporating personal preferences and random small events into the decision process. In the netlogo implementation the corresponding variable is called 'random-number' which is a random number between 0 and +1. A value of close to 0 is associated with a very strong random tendency to choose red behavior. A value close to 1 is associated with the very strong tendency to choose blue.

Adopting the logic of the motivational theory formed by Vroom (at first 1964) for this context, agents experience a *force to act* in accordance with A (FTA_A) or B (FTA_B) depending on random events describing their personal preferences at time t (α,β), the density of the institutional cluster (x), and the strength of complementay effects (c) inherent in the system. With every tick, one agent after another chooses to adopt the red or the blue institutional solution corresponding to the following decision rule: Behave in accordance with A if and only if FTA_A (x) > FTA_B (x) and B if and only if FTA_B (x) > FTA_A (x) and if FTA_A (x) = FTA_B (x) do not alter the previous behavior. FTA_A (x) and FTA_B (x) are specified as follows: FTA_A (x) = α * $f_{A,c}(x)$ and FTA_B (x) = β * $f_{B,c}(x)$ with $f_{M,c}(x) := e^{m*c*x*1.5}$ and fixed c ϵ [0,1]; α,β randomly ϵ [0,1]; M ϵ {A, B}and m=1 for $f_{A,c}(x)$ and m=-1 for $f_{B,c}(x)$ (for a detailed introduction of the formal model logic see Petermann 2010:140).

Figure 3 shows the netlogo interface and a sample run of the simulation model.

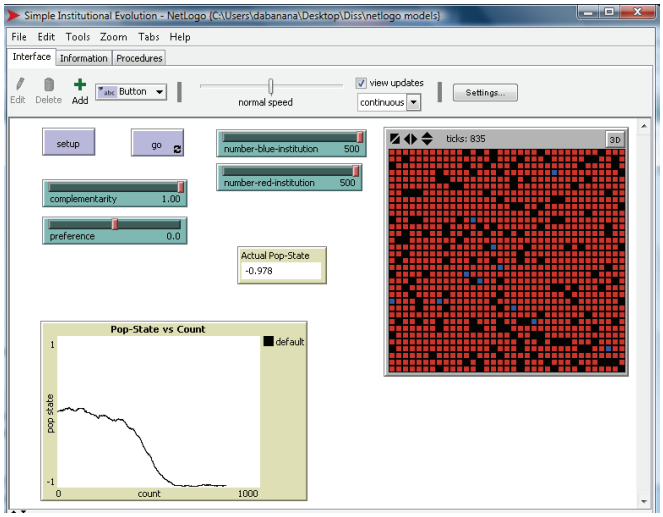

FIGURE 3:
A Sample run of the simulation model

Results

Applying the Monte-Carlo method, the system behavior can be examined over time for different degrees of complementary feedback strength. Figure 4 shows the results for complementarity c = 0 and c = +1. When there are no complementary effects at work (complementary c = 0), random small events govern the process. Because of 1.000 agents making simultaneous decisions every tick, the law of large numbers applies: In the long run both institutions persist with significant

diffusion rates. Decision makers are not bound to a dominant behaviors rule but can choose dependent on their personal preferences and actual circumstances (small events).

In contrast if strong complementary feedback applies, the probability of finding a system with significant diffusion rates for both institutional solutions decreases with time, approaching zero in the long run. Dependent on the random small events governing the process in the early stage, one of the two institutional solutions becomes dominant and locked-in, being the only alternative for decision makers at some point.

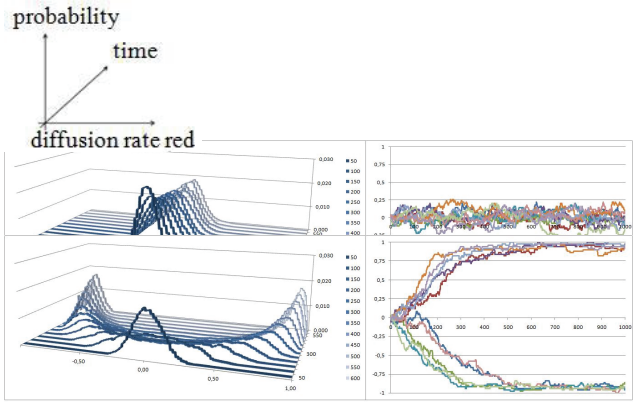

horizontal x-axis: diffusion of red institution in %
diagonal z-axis: time
vertikal y- axis: probality to find a diffusion rate x at time z

FIGURE 4
Results of the simple model: high complementarity necessarily leads to a lock-in situation

The results shown in figure 4 are consistent with the results of Arthur's deductive analysis of positive feedback processes. With the application of computer simulation it was possible to model the process much more realistically and with less restrictive assumptions compared to Arthurs polya urn model (Arthur, 1989).

Towards an advanced model: implementing organizational hierarchy

Path dependence theory is a market based approach (David, 1985, Arthur, 1989). The application to social systems like a firm is often criticized because a firm lacks some basic constituents of a perfect market, especially the absence of power. While scholars of market-based approaches at least theoretically argue that total competition and the absence of power do exist, management scholars cannot negate one of the fundamentals of a firm, namely the organizational structure that explicitly creates power inequalities among the members of the organization. Thereby it seems necessary to include hierarchy into the model to address the fact that power structures and maybe the specific organizational design might impact the evolutional diffusion processes of institutions (and technologies) within organizations.

In an attempt to embrace this argument, the notion of organizational hierarchy has been added to the simple model. A formal organizational structure is introduced by assigning a superior to every agent in the system. In the simple model, agents decide exclusively on the basis of small events and mis-fit costs arising from dense institutional clusters. Now a third variable influencing the individual decision making process is introduced, which is called 'leadership impact' (li). This variable includes explicit orders from superiors as well as more implicit elements, as individuals in organizations try to meet the expectations of their superiors. The individual's decisions are now dependent on random small events, complementary feedback *and* hierarchical influence of their superiors.

At every tick, one agent after another chooses to adopt rather the red or the blue institutional solution corresponding to the following decision rule: Behave in accordance with A if and only if FTA_A (x,y) > FTA_B (x,y) and B if and only if FTA_B (x,y) > FTA_A (x,y) and if FTA_A (x,y) = FTA_B (x,y) do not alter the previous behavior. FTA_A (x,y) and FTA_B (x,y) are specified as follows: FTA_A (x,y) = α * [$f_{A,c}(x)$ + i (y) * li]and FTA_B (x,y) = β * [$f_{B,c}(x)$ + i (y) * li] with $f_{M,c}(x)$:=

$e^{m*c*x*1.5}$ and fixed c ϵ [0,1]; α,β randomly ϵ [0,1]; M ϵ {A, B}; m=1 for $f_{A,c}(x)$; m=-1 for $f_{B,c}(x)$; li fixed ϵ R^+ and i(y) ϵ {-1,1} depending on the adoption behavior of the superior which determines the order to adopt A or B that the agents receives from his superior (for a more detailed introduction of the formal model logic see Petermann 2010:186).

Advancing the simple model with the assigning of superiors who influence the decisions of their subordinates is our research agenda. A typical hierarchical organizational design has been implemented. The netlogo implementation is shown in figure 5.

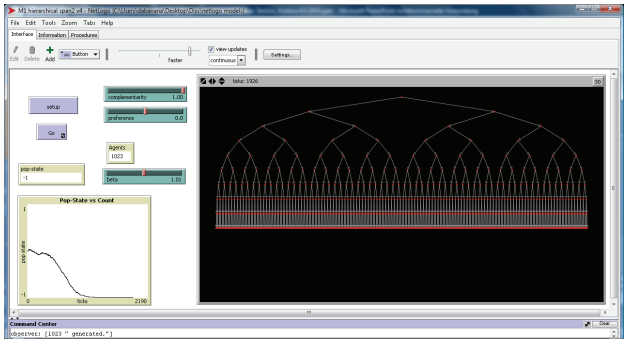

FIGURE 5:
The Advanced model with hierarchical organizational design

Future prospects

The advanced model is modified for different types of organizational designs and run with different values for complementary feedback and hierarchy influence. The analysis of this data is not yet presented in this paper. Detailed insights from the results will be presented during the conference indicating that the path dependence logic holds also for systems with hierarchic structure. It can be shown that hierarchy in organizations seems to influence the process of complementary feedback in degree, but not in kind. When complementary feedback is strong path dependent logic leads to a lock-in, a close to 100% diffusion rate for on institutional solution. Which of the competing institutional solutions will prevail and dominate the systems in the long run seems to depend on random events and leadership influence in the beginning of the process, while the influence of those at the hierarchical top fades away as time goes by and institutional clusters become more and more dense.

CONCLUSIONS AND DIRECTIONS

We formally modeled the impact of complementarity effects in the process of institutional development. By means of computer simulation we technically validated the predictions made by scholars of path dependence theory about the importance of positive feedback in institutional evolution. Our simple model is much more sophisticated (i.e. agents can revoke their decision as time goes by) than the polya urn model introduced by Arthur (1989). The consistency of our results with Arthur's mathematical deduced solution to the polya urn model is a good means of validation for our work. The latest results of the advanced model will be presented during the presentation for different organizational designs. This approach enables us to clarify if and to what extend the predictions of path dependence theory hold when asymmetric power structures are incorporated in the social system observed. The results provide insight to the questions, which organizational designs are more or less prone to the dangers of path dependence and lock-in. The results will thereby add to path dependence research and to the ongoing discussion about optimal organizational design.

REFERENCES

Arthur, W. B. 1989. Competing technologies, increasing returns, and lock-in by historical events. ***Economic Journal***, 99(394): 116-131.

Arthur, W. B. 1990. Positive feedbacks in the economy. ***Scientific American***, February: 80-85.

Arthur, W. B. (Ed.). 1994. ***Increasing returns and path dependency in the economy***. Ann Arbor: University of Michigan Press.

Bassanini, A. P., & Dosi, G. 2000. Heterogeneous agents, complementarities, and diffusion. Do increasing returns imply convergence to international technological monopolies? In D. Dalli Gatti (Ed.), ***Market structures, aggregation an heterogeneity***: 185-206. Berlin, New York: Springer Verlag.

Cohen, M. D., March, J. G., & Olsen, J. P. 1972. A garbage can model of organizational choice. ***Administrative Science Quarterly***, 17: 1-25.

Cusumano, M. A., Mylonadis, Y., & Rosenbloom, R. S. 1992. Strategic maneuvering and mass-market dynamics: The triumph of VHS over Beta. ***Business History Review***, 66(1): 51-94.

David, P. A. 1985. Clio and the economics of QWERTY. ***The American Economic Review***, 75(2): 332-337.

David, P. A. 1993. Path-dependence and predictability in dynamic systems with local network externalities: A paradigm for historical economics. In D. Foray, & C. Freeman (Eds.), ***Technology and the wealth of nations: The dynamics of constructed advantage***: 208-231. London: Printer Publishers.

David, P. A. 1994. Why are institutions the "carriers of history"? Path dependence and the evolution of conventions, organizations and institutions. ***Structural Change and Economic Dynamics***, 5(2): 205-220.

David, P. A. 2001. Path dependence, its critics and the quest for "historical economics". In P. Garrouste (Ed.), ***Evolution and path dependence in economic ideas: Past and present***: 15-40. Cheltenham UK und Northampton USA: Edgar Elgar Publishing limited.

Davis, J. P., Eisenhardt, K. M., & Bingham, C. B. 2007. Developing theory through simulation methods. ***Academy of Management Review***, 32(2): 480-499.

Katz, M., & Shapiro, C. 1986. Technology adoption in the presence of network externalties. ***Journal of Political Economy***, 94: 822-841.

Nooteboom, B. 1997. Path dependence of knowledge: Implications for the theory of the firm. In L. Magnusson, & J. Ottosson (Eds.), ***Evolutionary economics and path dependence***: 57-78. Cheltenham: Edward Elgar Publishing Ltd.

North, D. C. 1990. ***Institutions, institutional change and economic performance***. Cambridge: Cambridge University Press.

Petermann, A. (2010): „Pfadabhängigkeit und Hierarchie: Zur Durchsetzungskraft von selbstverstärkenden Effekten in hierarchischen Organisationen“, Berlin, S.1-321

Pierson, P. 2000. Increasing returns, path dependence, and the study of politics. ***American Political Science Review***, 94(2): 251-267.

Stieglitz, N., & Heine, K. 2007. Innovations and the role of complementaries in a strategic

theory of the firm. ***Strategic Management Journal***, 28(1): 1-15.

Sydow, J., Schreyögg, G., & Koch, J. 2005. Organizational paths: Path dependency and beyond. Free University of Berlin.

Sydow, J., Schreyögg, G., & Koch, J. 2009. Organizational path dependence: Opening the black box. ***Academy of Management Review***, 34(4): 689-709.

Teece, D. J., Pisano, G., & Shuen, A. 1997. Dynamic capabilities and strategic management. ***Strategic Management Journal***, 18(7): 509-533.

Vroom, V. H. 1964. ***Work and motivation***. New York.

SOCIAL SIMULATION WITHIN CONSUMER GOODS INDUSTRY: THE WAY FORWARD

Abhijit Sengupta
Unilever Research & Development
Colworth Science Park
Sharnbrook, UK MK44 1LQ
Email: sengupta.abhijit@gmail.com

KEYWORDS

consumer behaviour, market dynamics, marketing, validation

ABSTRACT

Simulation based research, especially for social systems have grown in size and matured in the last two decades. But in spite of high potential impact, adoption and applicability within businesses is relatively low, especially so in the consumer goods industry. This paper indicates some key focus areas in research which, if pursued consistently, are most likely to have the highest impact. These areas are: providing complementary predictive capability to standard market mix models, modelling disruptive changes in the market, increased partnership with the automated personalized algorithms research community and focussing on toolkits which can be directly used by businesses for training and research purposes. It goes on to point out strategies which can be adopted by the research community which will increase the chances of effectively focussing research onto the areas mentioned above.

INTRODUCTION

Simulations have been widely used across multiple functions within industries over the years – be it in product design, process optimization or in general business simulations used for training purposes (Summers, 2004; Faria et al., 2008). However, it is only recently that simulations have entered the arena of organizational, market and consumer research, mostly as a complement to more traditional statistical and econometric techniques (Garcia, 2005; Delre et al., 2007; North and Macal, 2007). This can only be attributed to the growing awareness of the fact that markets, consumer groups, supply chains, and even whole organizations can be treated as complex systems, as they have unique characteristics which lend themselves to bottom-up analysis (Bonabeau, 2002; Robertson, 2004; Jager, 2007).

However, in spite of its growing popularity, the use of simulation based approaches such as Agent Based Modelling and Simulation (ABMS), have made only rudimentary in-roads into traditional business oriented applications such as marketing, supply chain optimization, optimization of organizational complexity etc. This paper discusses some of the recent developments in simulation based research relevant to applications within industry – focussing primarily on research within social and behavioral sciences, rather than on the use of simulations from the technology and organizational focus. This paper argues that the state of ABMS research and applications is at an important juncture and would require a sustained and focussed effort from both researchers and practitioners in order to reach similar levels of success as traditional quantitative methodologies of analysis. This paper takes the lead on presenting some of the key issues that researchers in both academia and industry need to focus on, if the science of complex adaptive systems and social simulations has to be established as a standard within businesses.

It is well known within the research community that ABMS and other bottom-up simulation based methods have a number of advantages over traditional methods in analyzing large networked systems which exhibit typical characteristics of complex adaptive systems – *emergence, heterogeneity, connectedness and evolution* (Bonabeau, 2002). Consumers are generally heterogenous in tastes and preferences and competition leads businesses/firms intervene through pricing and promotions, packaging, advertising campaigns etc. very regularly. Additionally, markets may be subject to exogenous shocks such as new product launches, evolving nature of consumer preferences and even lateral non-linear interactions through word of mouth and social networks. All of the above, acting on individual constituents or subsets of constituents give rise to various interesting macro level phenomena, such as high volatility, crashes or even exponential growth (Adebanjo and Mann, 2000; Ailawadi et al., 2001).

It needs to be noted that businesses differ from each other a great deal, not just across industries but even within a particular industry. Companies generally embody their own product portfolio, market focus, internal management structure, R&D philosophy and ways of working etc. Hence, the motivation behind adoption of new techniques both in research and applications will be different from business to business – and a meta study such as this may not be applicable in all respects to every business under its purview. However, the aim is to

Proceedings 26th European Conference on Modelling and Simulation ©ECMS Klaus G. Troitzsch, Michael Möhring, Ulf Lotzmann (Editors)
ISBN: 978-0-9564944-4-3 / ISBN: 978-0-9564944-5-0 (CD)

pick up general trends and identify overarching patterns governing the use of simulation based modelling within specific industries. This paper focusses on the fast moving consumer goods (FMCG) industry in particular but also touches upon issues related to consumer goods in general. Social simulation and complexity is relevant for most other industrial sectors, but a more general analysis is beyond the scope of this paper.

This paper is organized as follows. The next section provides a brief review of the state of the literature which is relevant to industrial applications of social simulation research. Next, we present the main focus areas for research, which in the opinion of this author, will have the biggest impact on encouraging businesses to adopt social simulation techniques on a more regular basis. Following that, we present some broad strategic directions within the research community, which are likely to maximize the chances of success in the focus areas mentioned in the previous section. We conclude in the following section.

BACKGROUND

We start by reviewing a sample of the simulation based literature dealing with topics relevant to industry with particular emphasis to consumer goods markets. A substantial number of high quality papers have been published in the literature relevant but lack of space prevents us from providing an exhaustive review. Hence, we shall touch upon a few ones which seem to have the most relevance.

One of the core areas where simulations and simulation based research is likely to have direct impact is around optimization of marketing spends. Consumer goods businesses in partnership with retailers and supermarkets are usually involved in heavy marketing interventions – pricing, promotions, product placement, advertisement to name a few – all of which involve large marketing budgets (Blattenberg and Wisniewski, 1989; Ailawadi et al., 2001). Additionally, with the advent of social media and online networks, radical new possibilities have opened up in reaching out to their consumers.

As mentioned by (Gilbert et al., 2007) and (Jager, 2007), consumer goods markets exhibit complex behaviour at multiple levels. The role of traditional modelling paradigms is highly restricted in many cases where markets undergo exogenous disturbances, either through disruptive innovations or through exogenous shocks (Bonabeau, 2002). Even during normal steady states, forecasting and analysis is only possible of aggregate phenomena, for instance market specific demand forecasting, price elasticity estimation etc. But actual examination of micro-level dynamic properties such as product take up, diffusion of information and shocks are difficult to undertake using these traditional techniques. As will be shown subsequently, this is where agent based modelling shows a lot of promise, given the focus on agent level phenomena and interactions (Adebanjo and Mann, 2000; Garcia, 2005; Delre et al., 2007).

Whereas traditional marketing models, based on general linear models, logistic regression etc. are able to provide a lot of good insights on the overall structure and macro level dynamics of markets, micro level characteristics such as product switching, lock-ins, loyalty and other psychologically motivated behavioral traits can only be studied through more disaggregated techniques such as ABMS and micro-simulations etc. (Janssen and Jager, 1999, 2003; Adjali et al., 2005). ABMS in particular can model social influences, peer pressure, dynamic feedbacks etc., which traditional top down modeling paradigms fail to capture robustly (Tesfatsion, 2006). Additionally, ABMS is not restricted to strong assumptions regarding distributions and error terms in any model and hence provides the flexibility of addressing the "natural" description system in a more complete manner (Bonabeau, 2002).

Any modelling paradigm for social systems has to be reliable and robust in order to address real world phenomena. In fact, the modelling paradigm should itself inculcate and internalize the principles of validating those models. This assumes far greater importance in the context of real world applications within any sphere. A large amount of literature within the agent based modelling community has addressed this issue at many levels. A number of authors, (Fagiolo et al., 2005; Windrum et al., 2007; Garcia et al., 2007; Midgley et al., 2007) stress the fact that validation in agent based models should be key, and should possess a "satisfactory range of accuracy" matching the simulated model to the real world. They also point out that the validation methodologies should address model accuracy at multiple levels – macro and micro and possibly at intermediate levels as well. The importance of verification and validation can never be overstated in the context of using ABMS in industry. This is a topic we shall revisit in the subsequent sections.

Although ABMS has been popularized over the last two decades, it is only recently that consumer goods industry specific research and case studies have made an appearance in the literature. The important aspect of acceptability has been addressed by (Midgley et al., 2007), (Marks, 2007) and more recently by (Rand and Rust, 2011). Midgley and Marks provide a framework within which rigorous testing of models created using agent based technologies is possible. They stress the modelling of "complete systems" instead of parts, and to do it, take into account the heterogeneity that exists within *different players* of the same system (for instance, different firms, different supermarkets and of course, different consumers). Rand and Rust addresses similar issues on the acceptability of agent based modelling in marketing research, and provide directions towards further rigor in the analysis via the example of product diffusion through an agent based version of the well known Bass Model (Bass, 1969).

Heterogeneity within a system can reduce predictive

power within traditional top-down methods as has been shown in (Sengupta and Glavin, 2010). The authors build a simulation of a consumer goods market within a multi-agent framework, set out a rigorous validation methodology at multiple levels using individual purchase data and show that a simple single parameter multi-agent model can achieve significantly higher *shopper level* as well as *market level* predictive accuracy on out of sample data, compared to a market share based probabilistic choice model. In a recent paper (Sengupta and Glavin, 2012), the authors extend the above rational choice based consumer model by incorporating psychological drivers explicitly into the behavior of agents. This extension is shown to improve prediction accuracy further at both micro and macro levels as compared to the earlier work. In an illuminating article on the use of simulations within an industrial context, (North et al., 2010) examines how ABMS technology has been used within consumer goods companies for building market simulations for actual decision making. The retail sector, through which the majority of consumer goods industry supply their products to consumers, has also seen a rise in the use of ABMS for analysis and decision making (Siebers and Aickelin, 2011; Siebers et al., 2011).

FOCUS AREAS FOR ABMS

ABMS holds a lot of promise in the fields of marketing and consumer science. However, in spite of its exponential growth within the research community, it is yet to have a significant presence in marketing and the consumer goods industry. Over the last two decades, the number of start-ups and consulting agencies who employ ABMS technology have been rising dramatically, but how much of the available expertise is actually used to embed ABMS systems within businesses is questionable as well. There are definitely some documented cases where ABMS is being used, most notably in the areas of supply chain optimization, distribution networks etc. (Siebel and Kellam, 2003; North and Macal, 2007; North et al., 2010). But the use of *social* simulation is still in its infancy. In this author's own experience, convincing senior stakeholders in businesses, of the immediate impact of ABMS in their daily operations when standard analytical techniques have been considered as best practise for many years, is an uphill task.

However, with growing awareness about the usefulness of computational modelling techniques, with increasing availability of advanced computational resources, and with a large body of high quality research to draw from, it is the author's contention that the ABMS technology is uniquely positioned to deliver high impact solutions to a myriad of issues which the consumer goods industry is facing. We discuss a few challenging areas where ABMS research can and should focus on in the near future and which carries a high probability of capturing attention from stakeholders within businesses.

Complementary Predictive Capability

One of most widely used quantitative techniques for market analysis within the consumer goods sector is Market Mix Modelling (MMM). This uses various types of multivariate regression techniques to identify effects of primary marketing variables (such as price, promotions, distributions and media spend) on market shares and sales of products. MMM typically uses aggregated sales data to build these models, and in general, have found wide acceptability as a marketing tool in many companies.

Standard MMM models are usually highly sophisticated and uses advanced econometric techniques. However, partly because of the analytical rigor involved and partly because of the top-down nature of these models, they are not suitable for making targeted predictions at levels below the one at which the models have been constructed. ABMS seems to be just the right technology to fulfill this gap and provide a more complete picture of the market. One way is to use ABMS as standard predictive technology *a lá* (Sengupta and Glavin, 2010) and (Sengupta and Glavin, 2012). However, a more fruitful way of using this technology is to *explore the space* of possible models at the micro level, which give rise to the appropriate MMM model at the macro level. Appropriate micro level data is certainly available nowadays, in the form of point of sale records and loyalty card based transactions data from retailers and shopping panel data collected by various agencies.

Modelling Disruptive Changes

Consumer goods markets are usually in a state of flux, with a constant stream of new products being launched, old ones being re-packaged and/or re-branded or being taken off the market completely. Standard quantitative techniques being used today to model markets require two to three years of data for identifying seasonal patterns and effects of market interventions. This is normally not an issue with established products and categories, but products launched in the near past cannot be modeled this way. This can and does create problems for practitioners when deciding on the optimum marketing mix, both at the time of the launch and for a significant time afterwards as witnessed in the unreasonably low rate of new product take up in the consumer goods sector (Schneider and Hall, 2011).

ABMS once again, can prove to be useful if practical toolkits can be built which helps a practitioner to handle this issue. These potential toolkits have to embody a number of different aspects of a product launch – for instance, appropriate market mix supporting the launch, characteristics of the target market, competition and its response, dynamics of information diffusion, market reactions to new launches and corresponding feedback effects as well as non-linear interactions. Depending on the category and nature of the new launch involved, a number of other idiosyncratic issues may have to be addressed within the same toolkit. The challenge is not only to be able to build repeatable models incorporating all of the

above, but to be able to verify and validate them to a high degree of accuracy using retrospective data. One may refer to (Marks, 2007) in order gauge the level of challenge facing the modeler in such situations – especially with respect to the issue of *sufficiency versus necessity* in model validation. According to (Marks, 2007), one of the reasons why ABMS has not been fully accepted by the economics profession, is because "simulation can, in general, only demonstrate sufficiency, not necessity" and that "simulation can disprove a proposition...but cannot prove it...", unless the degrees of freedom in the model are low and hence, it is possible to exhaustively explore all possibilities.

Solution Space for Automated Algorithms

With the advent of online shopping and retail, the use of automated (often personalized or customized) algorithms have become very popular (Dias et al., 2008). Such algorithms cluster consumers based on past history and demographics, make product recommendations to the consumers based on similar information and often link consumers based on shopping profile in order to improve take up of recommendations.

These algorithms have so far been purely within the domain of online retailers selling durable consumer goods such as books, DVD/CDs of movies and music albums, consumer electronics etc. However, online grocery and FMCG is becoming increasingly popular and major retailers are pushing to have an online presence, followed closely by the manufacturers themselves. With fast changing shopping habits, the use of automated algorithms will become more widespread as an important driver of shopper behaviour. Moreover, such algorithms are becoming more and more ubiquitous given the increased access of potential consumers to the internet, using a large variety of mobile devices.

While the applied mathematics and data mining research community has been at the forefront of popularizing these algorithms, the ABMS research community seems to have largely ignored this area. This is puzzling at first glance as there seems to be some significant overlap within both the areas – at least as far as addressing individual choice and behaviour is concerned. The main reason behind this divide is probably methodological as well as philosophical. Yet both areas would benefit from using an inter-disciplinary approach in a number of ways – improving prediction accuracy and hence adding to validation methods, providing the ability to test algorithms speedily and realistically without resorting to expensive live tests, as well as providing insights on behaviour where there were previously none. At the very least, algorithms embedded in mobile systems would provide a rich source of social network data, which currently is difficult to obtain. Additionally, it would allow the ABMS community direct access to the online shopping business – a small market currently, but one which is growing at a fast rate.

Market Simulation Toolkits and Validation

This is an area where a number of researchers and practitioners have already been active, as evidenced in the number of market simulators available off the shelf. For instance, AnyLogic (`http://www.xjtek.com/`), MarkStrat (`www.stratxsimulations.com/`), ThinkVine (`http://thinkvine.com`) to name a few. Some of these in fact incorporate ABMS as part of the modelling toolkit under the hood. However, these are often general pieces of software which need to tailored for specific markets using data provided by clients – hence may miss out on capturing some key market specific artifacts within the simulation engine. Additionally, one of the biggest drawbacks of using off the shelf solutions is that they tend to be implemented as "black boxes". As a result, the verification and validation methodology is hidden from the final user and which also points toward the reason why these simulation platforms are not part of standard practise as yet.

However the contribution of the ABMS research community should not just be in building the underlying simulation engine involving consumers, products and retailers. This should be tied with modelling disruptive changes in the market place as well, and should enable the user to examine non-standard market phenomena.

More quantitative research is necessary in the area of verification and validation of ABMS based models. This is challenging problem to overcome, as validation of ABMS models is inherently difficult – usually due to the nature of the data, presence of non-linear interactions and hidden complexities within the system under study. However, this is definitely one area where the social simulation research community needs to invest more resources into, given the potential benefits in the future. Important lessons on the needs and requirements of any business, when implementing advanced decision tools, can be found in the excellent article (Divakar et al., 2005).

THE WAY FORWARD

In the preceding paragraphs, we discussed the status of social simulation research with particular emphasis on consumer goods industry. We briefly covered the state of the literature on this topic which directly impacts the needs of this industry and then examined a few key areas where more focus ought to be given by the research community in order to embed this technology more solidly with businesses. Currently, interest within industry is definitely present, but is at a nascent and experimental stage. Yet the promise of this technology and what it can achieve in terms of impact is easily visible to *researchers* active in this field. This author proposes that the best set of strategies at this point in time, for the ABMS community, are those which focus more on achieving the same for the *potential practitioners* within the industrial sector. The list of potential practitioners include experts in consumer analytics, brand and marketing managers and

executives.

An important step in this direction will be taken if the fields of economics/econometrics, behavioral economics and marketing are willing to accept social simulation more readily than is done currently. This has not been easy traditionally, as is pointed out in (Marks, 2007), but important steps have been taken already in many areas of social systems modelling and economics. However, marketing as it is practised within industry, is still dominated by top-down quantitative techniques such as time series analysis, different flavours of multi-variate regression including Bayesian methods, discrete choice modelling, Markov Chain Monte Carlo (MCMC) etc. See (Frances and Montgomery, 2002) for more details. While these techniques are no doubt rigorous and proven to work well within their own domains, they lack the flexibility, reach and usability provided by the bottom up methodologies. The attempt from the ABMS research community should be to provide an important compliment to such techniques – with solid evidence of how ABMS can extend and improve the reach and usability from the point of view of managers and practitioners.

The key point at this stage is to encourage more and more empirical work in the field of ABMS led social science research, focussing on the verification and validation aspects of model building. There is strong evidence to show that such empirical research is possible and potentially useful to businesses and practitioners (Marks, 2007; Midgley et al., 2007; Sengupta and Glavin, 2010; Rand and Rust, 2011; Sengupta and Glavin, 2012). Constraint in space prevents a more detailed exploration of the models and modelling paradigms in these papers, but it is sufficient to say that a strong verification and validation methodology coupled with relevant business application centric approach, makes them useful examples to follow in the future. If the aim is to embed this technology within industry as a standard complement to existing toolkits, the evidence has to be forthcoming on the usefulness of this technique to add value over and above that provided by the existing ones. The nature of this evidence and the areas where they may be best explored has been specified above. However, to carry out this exercise on a suitably large scale, a few primary requirements have to be satisfied: availability of data of sufficient level of granularity and enough information (in order to identify not just agent level characteristics but also the complex inter-relationships), comparable models built on the same or similar data using standard techniques (to be used as benchmark to determine the value addition made by ABMS) and suitable questions and problems forthcoming from the practitioners in the field and not just what a researcher might think is relevant for practitioners.

Organizations often partner with specialized external firms in order to carry out their quantitative market research on the vast amounts of data that they possess. Some of the large and well known global firms in this sphere such as AC Nielsen, the SymphonyIRI Group etc. are well entrenched as part of the marketing philosophy in many, if not all, marketing and consumer goods businesses. Apart from these well known ones, a vast number of medium sized and smaller consulting firms offer a range of quantitative research assistance in many domains. The ABMS research community will be hugely benefitted if a sizable proportion of these consulting firms embody ABMS as part of their service offerings in a similar manner as other quantitative techniques. A change of mind set is required within this service industry so that adoption of ABMS technology happens organically – with the demand for agent based solutions going up on one hand, and solutions become increasingly available on the other. Hence, the research community should engage both sides of the market in a sustained manner – the consumer goods industry as well as the crucial service providers.

Two important qualifications to the points made above need to be made here. Firstly, this author is not advocating empirical methods *at the cost of* theoretical and interdisciplinary approaches – in fact quite the opposite. Robust empirical research is a *necessary* but not a sufficient precondition towards acceptability of ABMS within industries, businesses and quantitative practitioners. As pointed out succinctly in (Axelrod, 2006), agent based modelling acts as "bridge" between disciplines, is able to tackle problems intractable through other methods and in spite of all its advantages, is more difficult to sell. Empirical research can be used to show that ABMS can not only tackle the same problems which have been normally addressed by traditional methodologies, efficiently, but can also extend the frontier by addressing issues fundamental to many disciplines and not tractable through traditional means. The state of the ABMS discipline has advanced very quickly where theoretical methods and addressing theoretical questions are concerned (and which is absolutely necessary in a nascent field), but it is now become necessary to address more empirical questions for broader acceptability of this area.

Secondly, there is no doubt that more and more data sets containing high quality disaggregated information are being made available and also will be available in the future. Computational data analysis/mining techniques such as machine learning, genetic algorithms etc. have improved and are able to search for complicated patterns and micro level relationships within data sets very efficiently. Hence, the question of the role of ABMS naturally arises in relation to these new methods of data analysis – and not just its position with regard to the traditional top down methods as has been discussed above. Most of these data intensive techniques tend to "dive into the data" blindly and are able to find interesting insights – they usually fall short of providing causal explanations behind the emergence of these patterns. It is here that ABMS has to play a crucial role – once again acting as bridge between the theory and the data – to provide an explanation of the patterns themselves. In fact, validation methodologies presented in (Sengupta and Glavin, 2010,

2012), involving agent specific parameter searches can be effectively achieved through optimization techniques – particularly, where large complicated parameter spaces have to be searched.

CONCLUSION

The ABMS paradigm has grown rapidly in the past decade within the research community and has just started making inroads into the business community as well. But the growth rate of the latter has been relatively low and thinly distributed. In particular, the inroads made into the mainstream marketing community in terms of actual implementation have been marginal. However, given the current practises in the industrial sector and the complexity seen in markets, it is here that ABMS can make the biggest impact in the future.

This paper sets out a few key areas where the social simulation community ought to invest more resources in the near future in order to encourage businesses to adopt this technology, side by side with the existing ones. These are: (a) improving the predictive capacity of ABMS technology within social systems, (b) build modelling capability to handle disruptive events for which past data is lacking or fragmentary, (c) engage the applied mathematics and computer science communities active in developing automated personalized algorithms for online markets and (d) help build more sophisticated but usable toolkits for the practitioners within businesses. At the same time, it specifies some strategies to adopt which would help researchers to align with the focus areas mentioned above. A lot more of empirically rooted modelling needs to forthcoming within research, concentrating on the verification and validation methodologies in ABMS. The underlying aim should be to bring the mainstream econometric modelling community within its fold. It is this research community which has the biggest impact in marketing and quantitative market research. These traditional modelling practises are driven forward, not only within the consumer goods businesses themselves, but also through the vast service industry which has grown up around it in the form of data providers and consultants. Hence to capture the attention of the practitioners within the industry, one would have to influence the big players in this sector as well.

Neither is the list of focus areas and strategies specified above exhaustive, nor does it claim to address all the requirements of researchers and practitioners in the field of ABMS. However, it is the author's belief that it is in these areas specified above, that a start can be made and which will maximize the chances of embedding social simulation methodologies within industry.

REFERENCES

Adebanjo, D. and Mann, R. (2000). Identifying problems in forecasting consumer demand in the fast moving consumer goods sector. *Benchmarking: An International Journal*, 7(3):223–230.

Adjali, I., Dias, B., and Hurling, R. (2005). Agent based modeling of consumer behavior. In *Proceedings of the 2005 North American Association for Computational Social and Organizational Science Annual Conference*, University of Notre Dame, Notre Dame, Indiana.

Ailawadi, K., Lehmann, D., and Neslin, S. (2001). Market response to a major policy change in the marketing mix: Learning from procter and gamble's value pricing strategy. *Journal of Marketing*, 65(January):44–61.

Axelrod, R. (2006). Agent-based modeling as a bridge between disciplines. In Tesfatsion, L. and Judd, K. L., editors, *Handbook of Computational Economics*, volume 2 of *Handbook of Computational Economics*, chapter 33, pages 1565–1584. Elsevier.

Bass, F. (1969). A new product growth model for consumer durables. *Management Science*, 36(9):1057–1079.

Blattenberg, R. and Wisniewski, K. J. (1989). Price induced patterns of competition. *Marketing Science*, 8(4):291–309.

Bonabeau, E. (2002). Agent-based modeling: Methods and techniques for simulating human systems. *PNAS*, 99(3):7280–7287.

Delre, S., Jager, W., Bijmolt, R., and Janssen, M. (2007). Targeting and timing promotional activities: An agent-based model for the takeoff of new products. *Journal of Business Research*, 60(8):826–835.

Dias, B., Locher, D., Li, M., El-Deredy, W., and Lisboa, P. (2008). The value of personalised recommender systems to e-business: a case study. In *Proceedings of the 2008 ACM conference on Recommender systems*, RecSys '08, pages 291–294, New York, NY, USA. ACM.

Divakar, S., Ratchford, B., and Shankar, V. (2005). Chan4cast: A multichannel, multiregion, sales forecasting model and decision support system for consumer packaged goods. *Marketing Science*, 24(3):334–350.

Fagiolo, G., A., M., and Windrum, P. (2005). Empirical validation of agent-based models: A critical survey. In *International Workshop on Agent-Based Modeling and Economic Policy Design*, University of Bielefeld, Germany.

Faria, A., Hutchinson, D., Wellington, W., and Gold, S. (2008). Developments in business gaming - a review of the past 40 years. *Simulation and Gaming*, 40(4):464–487.

Frances, P. and Montgomery, A. (2002). *Econometric Models in Marketing*, volume 16 of *Advances in Econometrics*. JAI Press.

Garcia, R. (2005). Uses of agent-based modeling in innovation/new product development research. *The Journal of Product Innovation Management*, 22(5):380–398.

Garcia, R., Rummel, P., and Hauser, J. (2007). Validating agent-based marketing models through conjoint analysis. *Journal of Business Research*, 60:848–857.

Gilbert, N., Jager, W., Deffuant, G., and Adjali, I. (2007). Complexities in markets: Introduction to the special issue. *Journal of Business Research*, 60(8):813–815.

Jager, W. (2007). The four p's in social simulation, a perspective on how marketing could benefit from the use of social simulation. *Journal of Business Research*, 60:868–875.

Janssen, M. and Jager, W. (1999). An integrated approach to simulating behavioural processes: A case study of the lock-in of consumption patterns. *Journal of Artificial Societies and Social Simulation*, 2(2).

Janssen, M. A. and Jager, W. (2003). Simulating market dynamics: Interactions between consumer psychology and social networks. *Artificial Life*, 9:343–356.

Marks, R. (2007). Validating simulation models: A general framework and four applied examples. *Computational Economics*, 30(3):265–290.

Midgley, D., Marks, R., and Kumchamwar, D. (2007). Building and assurance of agent-based models: An example and challenge to the field. *Journal of Business Research*, 60(8):884–893.

North, M. J. and Macal, C. M. (2007). *Managing business complexity: Discovering strategic solutions with agent-based modeling and simulation*. Oxford University Press, New York, NY.

North, M. J., Macal, C. M., Aubin, J. S., Thimmapuram, P., Bragen, M., Hahn, J., Karr, J., Brigham, N., Lacy, M. E., and Hampton, D. (2010). Mulitscale agent-based consumer market modelling. *Complexity*, 15(5):37–47.

Rand, W. and Rust, R. T. (2011). Agent-based modeling in marketing: Guidelines for rigor. *International Journal of Research in Marketing*. doi:10.1016/j.ijresmar.2011.04.002.

Robertson, D. (2004). The complexity of the corporation. *Human Systems Management*, 23:71–78.

Schneider, J. and Hall, J. (2011). Why most product launches fail. *Harvard Business Review*.

Sengupta, A. and Glavin, S. (2012). Predicting volatile consumer markets using multi-agent methods: Theory and validation. In Martinez-Jaramillo, S., Alexandrova-Kabadjova, B., Garcia-Almanza, A. L., and Tsang, E., editors, *Simulation in Computational Finance and Economics: Tools and Emerging Applications*. IGI Global. Forthcoming.

Sengupta, A. and Glavin, S. E. (2010). Volatility in a consumer packaged goods market: A simulation based study. *Advances in Complex Systems*, 13(4):579–605.

Siebel, F. and Kellam, L. (2003). The virtual world of agent-based modeling: Proctor & gamble's dynamic supply chain. *Perspectives on Business Innovation*, 9:22–27.

Siebers, P. and Aickelin, U. (2011). A first approach on modelling staff proactiveness in retail simulation models. *Journal of Artificial Societies and Social Simulation*, 14(2).

Siebers, P., Aickelin, U., Celia, H., and Clegg, C. (2011). Towards the development of a simulator for investigating the impact of people management practices on retail performance. *Journal of Simulation*, 5:247–265.

Summers, G. (2004). Today's business simulation industry. *Simulation and Gaming*, 35(2):208–241.

Tesfatsion, L. (2006). Agent based computational economics: A constructive approach to economic theory. In Tesfatsion, L. and Judd, K. L., editors, *Handbook of Computational Economics, Volume 2: Agent-Based Computational Economics*. North-Holland, Amsterdam.

Windrum, P., Fagiolo, G., and Monneta, A. (2007). Empirical validation of agent-based models: Alternatives and prospects. *Journal of Artificial Societies and Social Simulation*, 10(2):8.

AUTHOR BIOGRAPHIES

ABHIJIT SENGUPTA joined Unilever R&D in 2005, after completing a PhD. in Economics from Stony Brook University in New York, specializing in applied game theory and industrial organization. Since joining Unilever, he has been increasingly drawn into modelling complex systems and analyzing markets and behaviour using agent based simulation methods. Abhijit enjoys working at the intersection of different disciplines like economics, psychology and mathematics to build holistic models of behaviour. He is also involved with exploring verification and validation methodologies for agent based systems using both computational methods and experimental setups. More information on his research can be found in his personal webpage at `http://sites.google.com/site/abhisgsite`. He can be reached at his email address `sengupta.abhijit@gmail.com`.

AUTHOR INDEX